THE

LONDON, EDINBURGH, AND DUBLIN

PHILOSOPHICAL MAGAZINE

AND

JOURNAL OF SCIENCE.

CONDUCTED BY

SIR OLIVER JOSEPH LODGE, D.Sc., LL.D., F.R.S.
SIR JOSEPH JOHN THOMSON, O.M., M.A., Sc.D., LL.D., F.R.S.
ALFRED W. PORTER, D.Sc., F.R.S.

AND

ALLAN FERGUSON, M.A., D.Sc.

"Nec aranearum sane textus ideo melior quia ex se fila gignunt, nec noster vilior quia ex allenis libamus ut apes."

JUST. LIPS. *Polit.* lib. i. cap. 1. Not.

VOL. XXVI.—SEVENTH SERIES.

JULY—DECEMBER 1938.

LONDON:

TAYLOR AND FRANCIS, LTD., RED LION COURT, FLEET ST.

Agents: WM. DAWSON AND SONS, LTD., CANNON HOUSE, PILGRIM ST., E.C. 4.

" Meditationis est perscrutari occulta ; contemplationis est admirari perspicua . . . . Admiratio generat quæstionem, quæstio investigationem, investigatio inventionem."—*Hugo de S. Victore.*

—— " Cur spirent venti, cur terra dehiscat,
Cur mare turgescat, pelago cur tantus amaror,
Cur caput obscura Phœbus ferrugine condat,
Quid toties diros cogat flagrare cometas,
Quid pariat nubes, veniant cur fulmina cœlo,
Quo micet igne Iris, superos quis conciat orbes
Tam vario motu."

J. B. Pinelli ad Mazonium.

CONTENTS OF VOL. XXVI.

(SEVENTH SERIES).

NUMBER CLXXIII.—JULY.

Page

Prof. V. A. Bailey and Mr. J. M. Somerville on the Graphical Solution of Ordinary Differential Equations 1

Dr. R. Roscoe on the Calculation of the Elastic Scattering of Electrons by Molecular Hydrogen 32

Dr. Allan Ferguson and Mr. S. J. Kennedy on the Surface Tensions of Liquid Crystals 41

Dr. Paul White on the Theory of Electrosmotic Circulation in Varying Fields 49

Mr. G. D. Preston on the Parabolic Law of Oxidation 65

Prof. T. M. MacRobert on Proofs of some Formulæ for the Generalized Hypergeometric Function and certain related Functions. 82

Dr. J. Frederick J. Dippy on the Limiting Conductivities of Organic Acids in Aqueous Solutions 93

Prof. Bibhutibhusan Sen on Direct Determination of Stresses from the Stress Equations in some Two-Dimensional Problems of Elasticity.—I. 98

Prof. J. A. Crowther, Dr. H. Liebmann, and Mr. R. Jones on a Study of the Action of Ionizing Radiations on Colloidal Graphite 120

Dr. William Hume-Rothery and Mr. Geoffrey Vincent Raynor on Atomic and Ionic Radii.—I. Numerical Values and their Bearing on the Compressibilities of Metals 129

Dr. William Hume-Rothery and Mr. Geoffrey Vincent Raynor on Atomic and Ionic Radii.—II. Application to the Theory of Solid Solubility in Alloys 143

Mr. Geoffrey Vincent Raynor on Atomic and Ionic Radii.—III. Polarization Effects in Alloys 152

Mr. D. V. Gogate on a Relativistic Study of the Joule-Thomson Effect and Adiabatic Processes in a Gas.—Part II. 166

Mr. S. P. Chakravarti on Band-pass Effect in Wave-filters terminated in Negative Resistances 173

Prof. F. H. Newman: Note on the Oxidation of the Arc Cathode 187

Notices respecting New Books:—

Mr. E. C. Kemble's Fundamental Principles of Quantum Mechanics 188

Prof. Edward W. Strong's Procedures and Metaphysics 189

Prof. E. C. Titchmarsh's Introduction to the Theory of Fourier Integrals 191

Dr. C. H. Douglas Clark's The Fine Structure of Matter.—Part I. X-Rays and the Structure of Matter 192

NUMBER CLXXIV.—AUGUST.

Mr. G. F. Herrenden Harker on the Mechanism of Synchronization in the Linear Time Base 193

Prof. Bhagawati Charan Guha on X-ray Analysis of the Structure of Anthraquinone 213

Page

Dr. Ludwik Silberstein on Short Derivation of a Fundamental Probability Formula 223
Mr. Weng Wen-Po on Molecular Force and Imperfect Gases 225
Mr. B. N. Singh on Effect of a Longitudinal Magnetic Field on the Conductivity and Refractive Index of Ionized Air 244
Dr. J. E. R. Constable on Acoustical Insulation afforded by Double Partitions constructed from Dissimilar Components .. 253
Mr. A. R. Ubbelohde on the Nernst Heat Theorem and Irreversible Processes at Low Temperatures..... 260
Mr. W. H. Ingram on Kirchhoff Constraints and Sagittal Graphs. 268
Mr. C. Salter on Sensitivity of the Immersed Venturi-Pitot Head at Low Speeds 272
Prof. J. S. Townsend and Mr. E. W. B. Gill on Generalization of the Theory of Electrical Discharges 290
Notices respecting New Books :—
Dr. C. H. Douglas Clark's The Fine Structure of Matter.—Part II. Molecular Polarization. Part III. The Quantum Theory and Line Spectra.. 311

NUMBER CLXXV.—SEPTEMBER.

Dr. D. M. Wrinch on the Molecular Weights of the Globular Proteins 313
Dr. Louis A. Pipes on Operational Solution of the Wave Equation. 333
Dr. Arnold N. Lowan on Wave-motion for Infinite Domains..... 340
Mr. R. J. Clark on the Measurement of the Velocity of Light over a Single Journey..... 361
Messrs. K. Mendelssohn and J. G. Daunt on Co-existence of Normal and Supra-conductive Regions 376
Mr. R. V. Thosar on the Fluorescent Ion of Chromium in Ruby. 380
Prof. V. V. Narlikar : a Note on Riemannian Tensors 390
Dr. N. W. McLachlan on Operational Forms and Contour Integrals for Bessel Functions with Argument $a\sqrt{t^2-b^2}$ 394
Dr. W. Fabian on Generalized Fractional Integration and Differentiation 408
Mr. Albert Eagle : a Criticism of the Special Theory of Relativity. 410
Mr. W. J. Archibald on the Complete Solution of the Differential Equation for the Confluent Hypergeometric Function 415
Notices respecting New Books :—
Perspectives in Biochemistry (edited by Messrs. Joseph Needham and David E. Green) 419
Mr. Bernard Lewis and Herr Guenther von Elbe's Combustion, Flames, and Explosions of Gases 421
Mr. W. A. Wooster's A Text Book on Crystal Physics 422
Messrs. Albert Einstein and Leopold Infeld's The Evolution of Physics 423

NUMBER CLXXVI.—OCTOBER.

Prof. V. A. Bailey on some Effects caused in the Ionosphere by Electric Waves.—Part II. 425
Dr. H. Löwy on Electrodynamic Volume and Porosity of Metallic Particles 453

Page

Dr. N. W. McLachlan on Operational Forms and Contour Integrals for Struve and other Functions 457
Prof. H. S. Carslaw and Mr. J. C. Jaeger on some Problems in the Mathematical Theory of the Conduction of Heat 473
Prof. J. K. Robertson and Mr. R. H. Hay on Optical Resolution and the Visual Examination of two Overlapping Photographic Images 495
Dr. D. B. McNeill and Miss K. F. Harvey on some Aspects of Nitrogen Afterglows 502
Mr. N. F. Astbury on the Effects of Stray Admittances in Four-Arm Bridge Networks 507
Prof. Alfred W. Porter on Capillary Ascent in Cylindrical Tubes. 519
Dr. W. Vaughan on an Original Method of Comparison of Capacities at Radio Frequencies 521
Mr. S. T. Newing and Dr. W. M. Shepherd on Finite Strain: Dislocation Solutions 557
Mr. L. Jacob on Field Distribution and Graphical Ray Tracing in Electron Optical Systems 570
Mr. L. Jacob on the Equation to the Axial Potential Distribution in Electron Optical Systems 601
Dr. G. E. Allan: Note on Velocity of Sound in Copper 609
Notices respecting New Books:—
Mr. C. E. Weatherburn's An Introduction to Riemannian Geometry and the Tensor Calculus 615

NUMBER CLXXVII.—NOVEMBER.

Dr. D. Williams on the Relations between the Energy Theorems applicable in Structural Theory 617
Mr. J. W. Hughes on a new Method for determining the Uniaural Differential Threshold 635
Mr. J. J. Hermans on Surface Phenomena with Charged Spherical Particles when moving in a Solvent 650
Mr. J. J. Hermans on Charged Colloid Particles in an Ultrasonic Field.—II. Particles surrounded by a Thin Double Layer 674
Prof. E. L. E. Wheatcroft and Dr. T. G. Hammerton on Pre-striking Conditions in a Thyratron 684
Dr. N. W. McLachlan on Operational Form of $f(t)$ for a Finite Interval, with Application to Impulses 695
Dr. A. J. Ockleston on the Damping of the Lateral Vibration of a Mild Steel Bar 705
Dr. Raymond D. Mindlin on Stresses in an Eccentrically Rotating Disk 713
Prof. F. H. Newman: Note on the Electrical Discharge in Argon. 719
Prof. D. N. Sen on Mean-Value Theorem in Riemann-Stieltje's Integral 722
Notices respecting New Books:—
Messrs. Russell A. Dodge and Milton J. Thompson's Fluid Mechanics 724
Messrs. M. Muskat and R. D. Wickoff's The Flow of Homogeneous Fluids through Porous Media 725
Dr. Edwin Hubble's The Observational Approach to Cosmology 726
Mr. W. H. Watson's On Understanding Physics 727

Page

NUMBER CLXXVIII.—NOVEMBER (SUPPLEMENT).

Mr. W. A. Tuplin on Torsional Vibration in certain Mechanical Systems 729
Dr. A. E. Bate and Mr. E. T. Wilson on Resonance in Truncated Cones 752
Prof. D. M. Bose and Mr. P. C. Mukherji on the Origin of Colour of Paramagnetic Ions in Solution 757
Mr. J. H. Awbery on the Latent Heat of Fusion of Aluminium.. 776
Mr. A. C. Walshaw : Note on Thermodynamics of Energy Balance Sheets of Internal Combustion Engines 784
Drs. N. A. V. Piercy and J. H. Preston and Mr. L. G. Whitehead on the Approximate Prediction of Skin Friction and Lift 791
Mr. D. H. Landon and Dr. R. M. Davies on the Determination of the Rigidity Modulus of Nickel and some of its Alloys in the Annealed and Unannealed States 816
Mr. N. Kürti and Prof. F. Simon : Remarks on the Thermodynamic Scale of Temperature 840
Mr. N. Kürti and Prof. F. Simon : Remarks on the " Curie " Scale of Temperature 849
Mr. G. D. Preston on the Diffraction of X-rays by an Age-hardening Alloy of Aluminium and Copper. The Structure of an Intermediate Phase 855
Dr. A. Erdelyi on Integral Representations for Products of Whittaker Functions 871
Mr. B. V. Thosar on the Fluorescent Chromium Ion in Ruby ... 878
Prof. V. A. Bailey and Mr. J. M. Somerville on Study of the Magneto-Ionic Theory of Wave Propagation by Means of Simple Formulæ, Linkages, and Graphical Devices 888
Dr. Arne Eld Sandström on the Action of Soft X-rays upon Selenium Barrier-Layer Cells 906

NUMBER CLXXIX.—DECEMBER.

Dr. Balth. van der Pol : Application of the Operational or Symbolic Calculus to the Theory of Prime Numbers 921
Mr. R. H. Healey on the Behaviour of Electrons in Iodine Vapour 940
Prof. B. Dasannacharya and Mr. Amar Chand Seth on Optical Silvering on Glass 953
Dr. T. E. W. Schumann : a General Graduation Formula for the Smoothing of Time Series 970
Sir S. M. Sulaiman on the Solution of Einstein's Orbital Equation. 983
Dr. Ernst Fredlund on Absolute Measurements of Radiometric Action in Gases 987
Dr. V. Voss on Arcs of Various Metals in Capillary Tubes 1000
Mr. R. A. Fairthorne on the Large Deflexions of a Thin Circular Ring 1006
Dr. S. Ramachandra Rao and Mr. A. S. Narayanaswami on the Crystalline Diamagnetism of Thallium 1018
Mr. W. E. Benham on Classical Wave Functions for Moving Corpuscles 1031
Drs. M. Benjamin and R. O. Jenkins on the Surface Migration of Barium 1049
Dr. H. Bateman on Paraboloidal Coordinates 1063
Mr. B. C. Mukerji on Gravitational Waves in Linearized Fields.. 1068
Mr. W. E. Hoare on Calculation of the Area of Basis Metal exposed at Discontinuities in the Tin Coating of Tinplate 1077

Page

Mr. Harish Chandra Gupta on the Flow of a Viscous Fluid past a Circular Cylinder 1085

Notices respecting New Books :—

Dr. H. S. W. Massey's Negative Ions 1110

Mr. W. R. Westropp Roberts's Elliptic and Hyperelliptic Integrals and Allied Theory 1111

Prof. E. L. E. Wheatcroft's Gaseous Electrical Conductors.. 1112

Dr. J. R. Ashworth's Ferromagnetism 1113

Prof. E. F. Burton's The Physical Properties of Colloidal Solutions 1114

Index 1115

PLATES.

I. & II. Illustrative of Dr. D. M. Wrinch's Paper on the Molecular Weights of the Globular Proteins.
III. Illustrative of Prof. J. K. Robertson and Mr. R. H. Hay's Paper on Optical Resolution and the Visual Examination of two Overlapping Photographic Images.
IV. Illustrative of Dr. D. B. McNeill and Miss K. F. Harvey's Paper on Some Aspects of Nitrogen Afterglows.
V. Illustrative of Mr. L. Jacob's Paper on Field Distribution and Graphical Ray Tracing in Electron Optical Systems.
VI.–VIII. Illustrative of Mr. G. D. Preston's Paper on the Diffraction of X-rays by an Age-hardening Alloy of Aluminium and Copper. The Structure of an Intermediate Phase.
IX. Illustrative of Mr. B. V. Thosar's Paper on the Fluorescent Chromium Ion in Ruby.
X. Illustrative of Dr. V. Voss's Paper on Arcs of Various Metals in Capillary Tubes.
XI.–XV. Illustrative of Drs. M. Benjamin and R. O. Jenkins's Paper on the Surface Migration of Barium.

THE

LONDON, EDINBURGH, AND DUBLIN

PHILOSOPHICAL MAGAZINE

AND

JOURNAL OF SCIENCE.

[SEVENTH SERIES.]

JULY 1938.

I. *The Graphical Solution of Ordinary Differential Equations.*

By V. A. BAILEY, *M.A., D.Phil.* (*Oxon*), *F.Inst.P., Professor of Experimental Physics, University of Sydney, and* J. M. SOMERVILLE, *B.Sc.* (*Sydney*), *B.A.* (*Cantab*), *Carnegie Research Assistant in Physics, University of Sydney* *.

Introduction.

IN all branches of applied mathematics there occur problems which require the solution of a differential equation which satisfies given "initial" conditions. The object of this paper is to give an outline of certain simple graphical methods for the solution of a large class of differential equations. This work has its origin in an investigation of the influence of an electric wave on the atmosphere †.

The problem of the graphical solution of ordinary differential equations has received considerable attention. A number of methods have been given for solving particular equations: for instance, Kelvin's ‡ graphical treatment of the general second order equation, and Le Corbellier's § excellent treatment of non-linear oscilla-

* Communicated by the Authors.

† *Vide* V. A. Bailey, Phil. Mag. xxiii. p. 774 (April 1937).

‡ Phil. Mag. xxxiv. p. 443 (1892).

§ Ph. Le Corbellier, I. E. E. Journal, lxxix. no. 477, p. 361 (1936).

tions. References to a number of such special methods may be found in Runge and Willer's article in the 'Encyklopädie d. Math. Wissench.' vol. xi. In addition, Runge * has considered the problem generally, and gives a method of solving the general first and second order equations and an indication of the possible extension of the method to cover the general nth order equation. In the present communication we consider a differential equation of the nth order which, while not completely general, is sufficiently so to include the great majority of those equations which occur in practical problems. By the introduction of a transparent sliding graph and other devices we are able to simplify considerably the necessary graphical manipulations.

The curve or curves which represent the solution are constructed in small segments, the slope of each segment being obtained from the differential equation by what is simply a geometrical or graphical method of performing numerical calculations—a method which is generally much speedier than actual arithmetical computation. The process is thus one of building up a solution from a set of initial values; it is not directly applicable to problems in which we are given "terminal" instead of initial conditions—*e. g.*, if we have a second order equation and are given two points through which the solution must pass, or one point and the differential coefficient at another point. Solutions determined by such conditions can be obtained only by trial and error. As the methods are entirely graphical, they are particularly suited to equations involving functions of one or more of the variables which are given only in graphical form and have no analytic formulation. Completely arbitrary functions thus fall within the scope of the methods.

Although methods are given which are applicable to a very general type of equation, it is to be emphasized that a particular equation will often have special properties (*e. g.*, one or more constant coefficients or a relation between coefficients) which will enable considerable simplifications to be made to the general method. Each equation should therefore be considered on its own merits and advantage taken of any opportunity for simplifications.

* 'Graphische Methoden' (1928).

The unambiguous verbal description of procedures which in practice are very simple often proves disproportionately long and tedious. With the object of shortening such descriptions the following conventions are used.

The independent variable x occurs in every equation discussed, and a line is said to be "horizontal" if it is parallel to the axis of x and "vertical" if it is perpendicular to that axis.

The "slope" of a line means the tangent of the angle between the line and the axis of x.

A curve is described as "the $f(x)$ curve," "the $\chi(y)$ curve" etc. when it is considered that there is no ambiguity in so doing.

§1. *Ordinary Equations of the First Degree* (*a*).

The general ordinary differential equation of the nth order and the first degree is of the form

$$f\left(x, y, \frac{dy}{dx}, \ldots \frac{d^{n-1}y}{dx^{n-1}}, \frac{d^n y}{dx^n}\right) = 0. \quad \ldots \quad (1)$$

In this section we consider equations which may be written in the form

$$A_n(x, y)\frac{d^n y}{dx^n} + A_{n-1}(x, y)\frac{d^{n-1}}{dx^{n-1}} + \ldots + A_1(x, y)\frac{dy}{dx} + A_0(x, y)y = 0, \quad (2)$$

where $A_0, A_1, \ldots A_n$ are functions of x and y,

In §2 we extend the discussion to equations in which $A_0, A_1, \ldots A_n$ are functions of any two of $x, y, \frac{dy}{dx}, \ldots \frac{d^{n-1}y}{dx^{n-1}}$, and in §3 we consider equations from which the restriction that the nth differential coefficient shall occur in the first degree is removed.

We consider first the equation

$$\phi_n(y)\frac{d^n y}{dx^n} + \phi_{n-1}(y)\frac{d^{n-1}y}{dx^{n-1}} + \ldots + \phi_1(y)\frac{dy}{dx} + \phi_0(y)y = f(x). \quad \ldots \quad (3)$$

It will subsequently be shown that the equation

$$\psi_n(x)\frac{d^n y}{dx^n} + \psi_{n-1}(x)\frac{d^{n-1}y}{dx^{n-1}} + \ldots + \psi_1(x)\frac{dy}{dx} + \psi_0(x)y = f(x) \quad \ldots \quad (4)$$

may be solved by a process almost identical with that which serves for equation (3), and that the more general equation (2) may be solved by a similar method. The simplicity of the first and second order equations renders them capable of special treatment, and as they afford a good introduction to the methods used throughout this paper, we discuss them first, leaving the more general case (2) till later (Method 1.3).

First Order.

The first order equation of the type (3) takes the form

$$\phi_1(y')\frac{dy'}{dx}+\phi_0(y')y'=f(x),$$

Fig. 1.

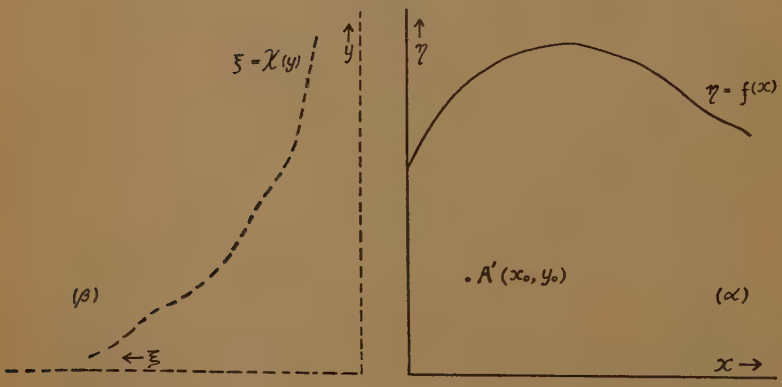

or, by writing $y=y'\phi_0(y')$,

$$\chi(y)\frac{dy}{dx}+y=f(x). \quad \ldots\ldots \quad (5)$$

and we take as our initial conditions

$$\left.\begin{aligned} x&=x_0\\ y&=y_0 \end{aligned}\right\}.$$

The solution we seek is thus, in general, a curve giving y for all values of x in the range under consideration, and passing through the " initial " point (x_0, y_0).

Method 1.0.—On a sheet of squared paper (α), as in fig. 1, draw rectangular axes (x, η) and the curve $\eta=f(x)$

and mark the initial point $A'(x_0, y_0)$. On a sheet of transparent paper (β) draw left-handed rectangular axes (ξ, y), the scales of ξ and y being the same as those of x and η respectively. Draw the curve $\xi = \chi(y)$. (The same notation is used throughout the paper—i. e. (x, η) axes on the opaque sheet (α) ; (ξ, y) axes on the transparent sheet (β) ; plain letters denote points on (β) and accented letters points on (α) ; curves and axes on the transparent sheet are indicated by broken lines.)

Place (β) over (α) so that the x and ξ axes coincide and the y axis passes through A′. On (β) mark the point B where the y axis cuts the $f(x)$ curve.

Fig. 2.

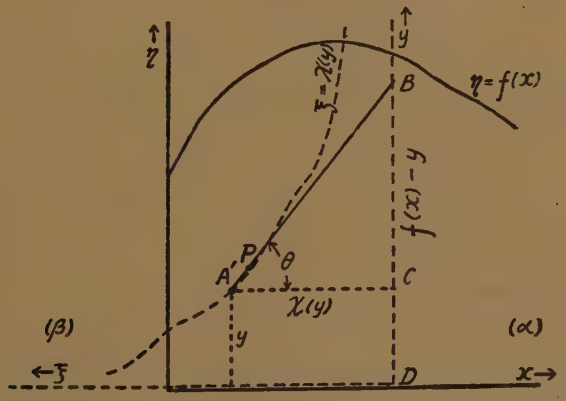

Now, keeping the x and ξ axes coincident, move (β) until A′ lies under the $\chi(y)$ curve as in fig. 2.

Then in this position the line A′B is the tangent to the curve $(\eta = y)$ at A′, for

$$CB = DB - DC = f(x) - y.$$

Hence
$$\tan\theta = \frac{CB}{AC} = \frac{f(x)-y}{\chi(y)}$$
$$= \frac{dy}{dx} \text{ from equation (5).}$$

Thus, if we take any point P on the line A′B close to A′ and prick through to the sheet (α) we will get a point P′ which may be taken as a consecutive point to A′ on the curve $(\eta = y)$, and A′P′ may be taken as a small segment

of the curve being constructed. By repeating the process with P′ as initial point we obtain another consecutive point and segment, and so on until we have a series of such points and segments, and thus we construct an approximation to the curve $(\eta=y)$, which is the solution required.

Method 1.01.—When $\chi(y)$ is a constant C a specially simple method is possible.

Plot on squared paper the curve $\eta=f(x-C)$ and place a strip of paper of width C as shown in fig. 3.

Fig. 3.

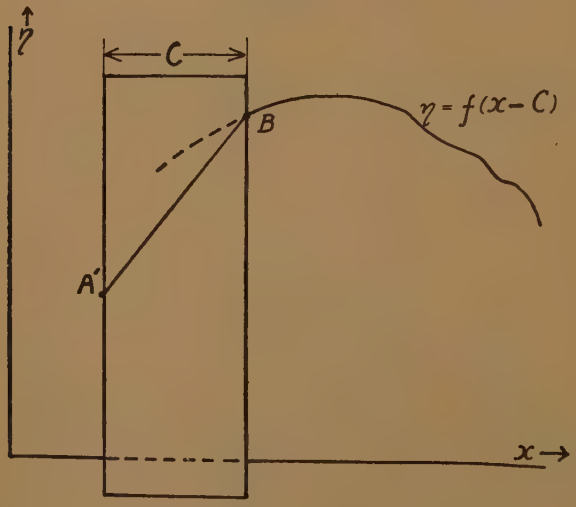

Then it is clear that the line A′B is tangential to the solution of

$$C\frac{dy}{dx}+y=f(x)$$

which passes through A′.

Method 1.1.—We give an alternative method of solving equation (5), in which the transparent sheet moves always with its origin on the y curve—the curve which is being constructed.

As before, draw the $f(x)$ curve on the sheet (α). On the transparent sheet (β) draw the curve $\xi=\chi(y)$ as shown

dotted in fig. 4 (it is the same curve as used in Method 1·0, turned through an angle of 180° about the origin).

Place the origin of the (ξ, y) axes on the initial point A′, the ξ, x axes being parallel, as in fig. 4.

If B is the point where the horizontal through the intersection C of the y axis and the $f(x)$ curve meets the vertical through the intersection D of the x axis and the $\chi(y)$ curve, then AB is the tangent at A′ to the required

Fig. 4.

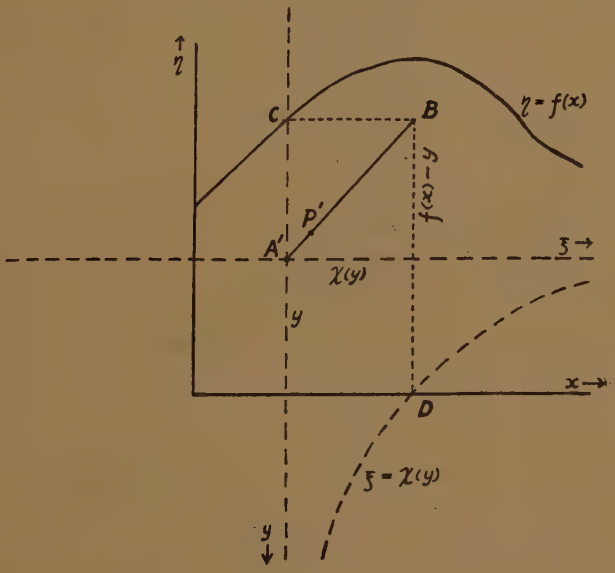

solution of equation (5). A consecutive point P′ may be pricked through and the process repeated as before.

Example A.

As an example of either of the methods 1.0 or 1.1 consider the following equation :

$$\left.\begin{array}{lll} \dfrac{1}{(1-y^2)^{\frac{1}{2}}}\dfrac{dy}{dx}+y=1\cdot 2 & 0<x\leqq \mathrm{T} \\ =0 & >\mathrm{T}, \end{array}\right\} \quad . \quad . \quad . \quad (6)$$

$$\left.\begin{array}{l} \text{given} \quad x=0, \\ \qquad\quad y=0, \end{array}\right\}$$

which will be recognized as the relativistic equation of motion of a particle of unit rest mass moving for a time T under a force of 1·2 units, and a retardation equal to the velocity y, x being the time.

The continuous curve I in fig. 5 (a) is the solution of equation (6), with T=3·5. For comparison we give the broken curve II, which is the solution when relativity is neglected and the mass is taken as constant. This solution was obtained by a method similar to method 1·01.

Fig. 5 (a).

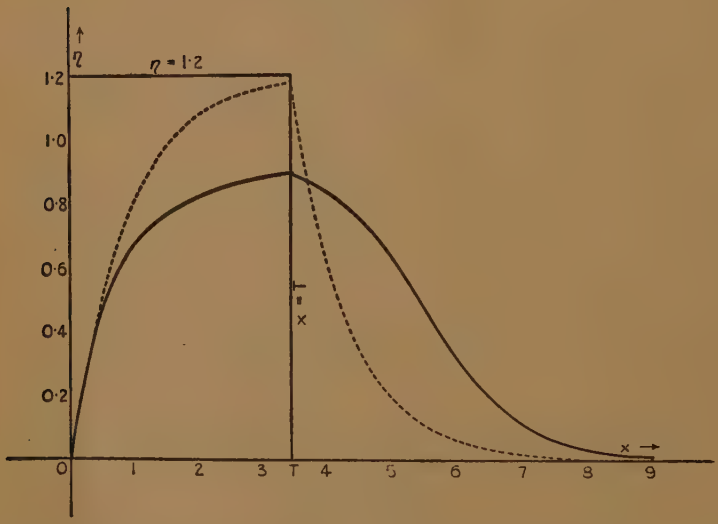

The curve $\xi = \dfrac{1}{(1-y^2)^{\frac{3}{2}}}$, used to solve equation (6) by method 1.0, is shown in fig. 5 (b). The same curve rotated through 180° serves for the solution by method 1.1.

Second Order.

$$\chi_2(y)\frac{d^2y}{dx^2}+\chi_1(y)\frac{dy}{dx}+y=f(x). \quad . \quad . \quad . \quad (7)$$

In general the solutions of this equation form a doubly infinite family of curves—one in every direction through every point. Given an initial point and direction, the

solution is in general unique. We take as our initial conditions

$$\left.\begin{aligned} y &= y_0, \\ \frac{dy}{dx} &= \left(\frac{dy}{dx}\right)_0, \\ x &= x_0. \end{aligned}\right\}$$

We give now a method which is of special nature—*i. e.*, it is not a particular case of the general method given in 1·3. The particular case of method 1.3 which applies to equation (7) will be indicated later, and it is just as satisfactory in practice as that now given.

Fig. 5 (*b*).

Method 1.2.—On the squared paper (α) draw as before the curve $\eta = f(x)$, and mark the initial points $A'(x_0, y_0)$ and $B'\left(x_0, \left(\frac{dy}{dx}\right)_0\right)$, and also draw a line through A′ with slope equal to $\left(\frac{dy}{dx}\right)_0$ as in fig. 6. On a transparent sheet (β) draw the curves $\xi = \chi_1(y)$, $\xi = -\chi_2(y)$, as shown dotted in fig. 6.

Now place (β) on (α) so that the origin of the (ξ, y) axes is over A′ and the ξ and x axes are parallel, as shown in fig. 6.

The χ_1 and χ_2 curves cut the x axis in D and E respectively and the y axis cuts the $f(x)$ curve in G. The point C, which is the intersection of the tangent at A′ to the y curve and the vertical through D, is noted, and F is the point of intersection of the horizontal through C and the vertical through E.

Then from the figure

$$HA' = y,$$

$$HD = \chi_1(y) = A'I,$$

$$IC = A'I\left(\frac{dy}{dx}\right) = A'J;$$

Fig. 6.

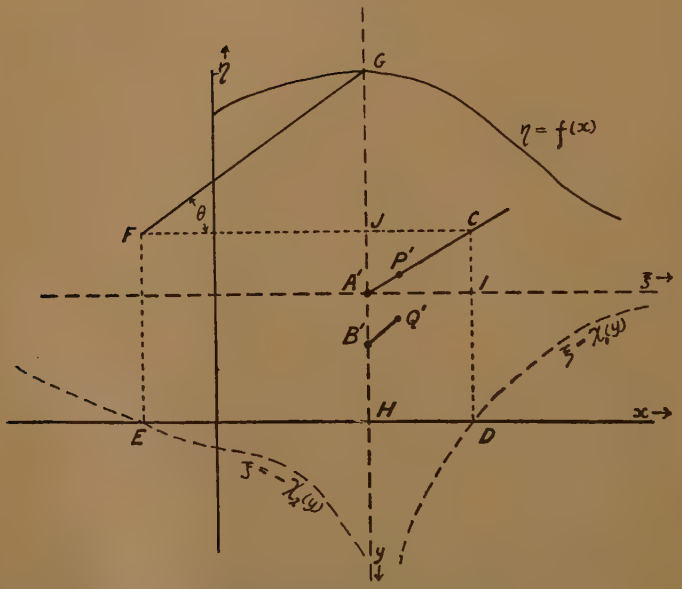

$$\therefore \quad HJ = \chi_1(y)\left(\frac{dy}{dx}\right) + y;$$

$$\therefore \quad JG = f(x) - y - \chi_1(y)\frac{dy}{dx},$$

and

$$\tan\theta = \frac{JG}{FJ} = \frac{f(x) - y - \chi_1(y)\dfrac{dy}{dx}}{\chi_2(y)}$$

$$= \frac{d^2y}{dx^2} \quad \text{from equation (7),}$$

so that the line FG is parallel to the tangent to the curve $\left(\eta=\frac{dy}{dx}\right)$ at B′. Thus, by transferring F to B′ or by the use of a parallel ruler, a consecutive point Q′ on the $\frac{dy}{dx}$ curve may be obtained. If P′ is the corresponding consecutive point to A′ on the y curve, then using P′ and Q′ in place of A′ and B′ and a line through P′ with a slope equal to the mean ordinate between B′ and Q′ in place of the line A′C, we may repeat the process, and continue until as much as is desired of both the curves $\eta=y$ and $\eta=\frac{dy}{dx}$ has been constructed.

When $\chi_1(y)$ and $\chi_2(y)$ are constants, equation (7) takes the form

$$A\frac{d^2y}{dx'^2}+B\frac{dy}{dx'}+y=\phi(x'),$$

an equation of frequent occurrence in applied mathematics.

By the simple transformation $x'=Bx$ we obtain the equation

$$C\frac{d^2y}{dx^2}+\frac{dy}{dx}+y=f(x), \quad . \quad . \quad . \quad . \quad . \quad (8)$$

where $C=\frac{A}{B^2}$.

Method 1.21.—Mr. D. Myers has suggested the following method of solving equation (8) without the use of transparent paper.

On a sheet of squared paper draw axes OA, OB, and let x be measured along OA and $f(x)$ along OB, O being the initial x point. (See fig. 7.)

Draw the $(x, f(x))$ curve and let it cut OB in P. Through P draw a line PK parallel to OA. Let D be a point on AO produced such that DO=C. Draw DE parallel to OB.

We use P for the zero of y and measure y downwards in the direction BO, and we use D for the zero of $\frac{dy}{dx}$ and measure $\frac{dy}{dx}$ in the direction DE with the same scale as

y and $f(x)$. We measure x in the direction OA with O as initial point for the y curve and D as initial point for the $\frac{dy}{dx}$ curve.

Mark Q such that $PQ = y_0$, the initial value of y and R such that $DR = \left(\frac{dy}{dx}\right)_0$ the initial value of $\frac{dy}{dx}$. Then clearly the line RQ has the slope

$$\frac{f(x) - y - \frac{dy}{dx}}{C},$$

Fig. 7.

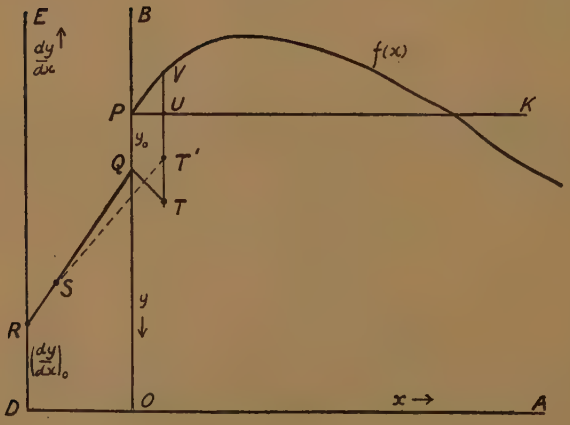

i. e., it is tangential to the $\frac{dy}{dx}$ curve at R. Take a neighbouring point T to Q, the downward slope of the line QT being equal to the mean ordinate between R and S.

Let the vertical through T cut PK in U and the $f(x)$ curve in V. Mark T′ on TU so that TT′ = UV (this is readily done on squared paper). Then ST′ is tangential to the $\frac{dy}{dx}$ curve at S. Thus we obtain another neighbouring point, and so on.

Although somewhat lengthy to describe, this method is very simple and rapid in practice.

Example B.

As an example of the use of Method 1.21 we give in fig. 8 the solution of the equation

$$3\frac{d^2y}{dx^2}+\frac{dy}{dx}+y=4+2\sin\frac{\pi x}{3} \quad . \quad . \quad . \quad (9)$$

with

$$\left.\begin{aligned} x&=0,\\ y&=0,\\ \frac{dy}{dx}&=9. \end{aligned}\right\} \quad . \quad . \quad . \quad . \quad . \quad . \quad . \quad (10)$$

Fig. 8.

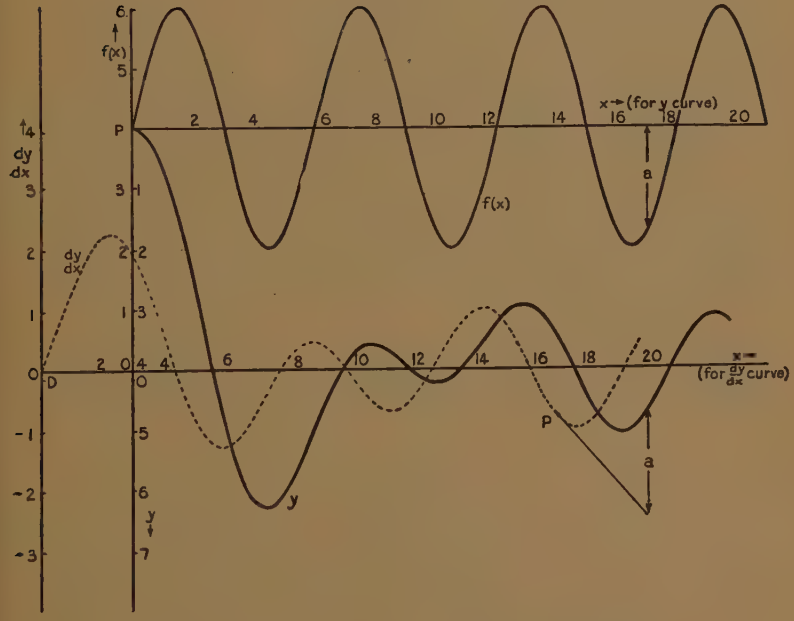

The construction of the tangent to the $\frac{dy}{dx}$ curve at the point P is shown in the figure.

The solution of this equation may be written down in analytic form and it is, for the initial conditions (10),

$$y=4+3\cdot7e^{-\frac{x}{6}}\sin(0\cdot55x-1\cdot5)-0\cdot79\sin\left(\frac{\pi x}{3}+0\cdot42\right). \quad (11)$$

It may thus be verified that the curve in fig. 8 represents this function very closely. The graphical method is more rapid and less laborious than plotting the curve from the solution (11).

Equations of any Order.

We now consider the equation

$$\chi_n(y)\frac{d^n y}{dx^n}+\chi_{n-1}(y)\frac{d^{n-1}y}{dx^{n-1}}+\ldots+\chi_1(y)\frac{dy}{dx}+\chi_0(y).y=f(x), \quad \ldots \quad (12)$$

reintroducing the coefficient $\chi_0(y)$ for the sake of more complete symmetry.

As it is desirable to avoid unnecessary and confusing movement of the transparent sheet, it is advisable, at this stage, to introduce some device for adding together a number of vertical lengths. The simplest device for this purpose is a strip of paper along the edge of which the lengths are marked; a slide with a movable pointer which can be attached to the drawing board is better. With such an "adder" most of the vertical movements of the transparent sheet may be eliminated, and in the following discussion we shall assume that some such device is being used.

Method 1.3.—Given equation (12) and the initial conditions

$$x=x_0,$$

$$y=y_0,$$

$$\frac{dy}{dx}=\left(\frac{dy}{dx}\right)_0,$$

$$\ldots\ldots\ldots$$

$$\frac{d^{n-1}y}{dx^{n-1}}=\left(\frac{d^{n-1}y}{dx^{n-1}}\right)_0,$$

we proceed as follows:—

On the squared paper (α) draw axes O′P′, O′Q′. Let O′Q′ serve as axis for both η and y, and let O′P′ serve as axis for x and ξ, x being measured in the direction O′P′, ξ in the direction P′O′, and the x and ξ scales being the same. Let O′ be the origin of all coordinates.

Now draw the curves

$$\eta = f(x),$$

$$\xi = \chi_0(y),$$

Fig. 9 (*a*).

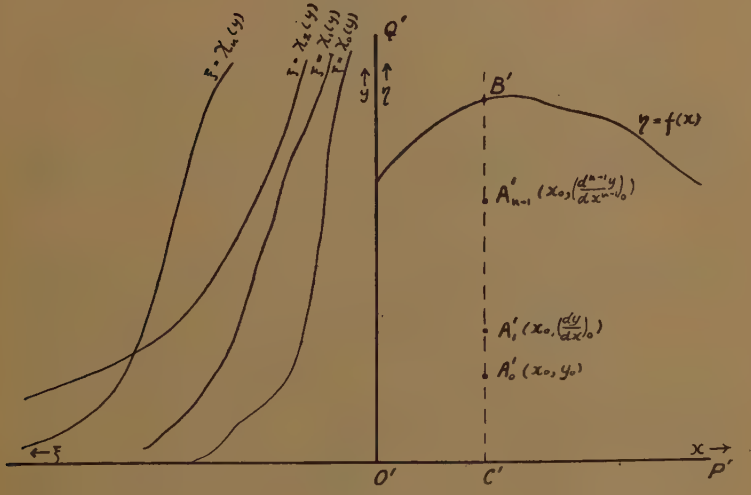

Fig. 9 (*b*).

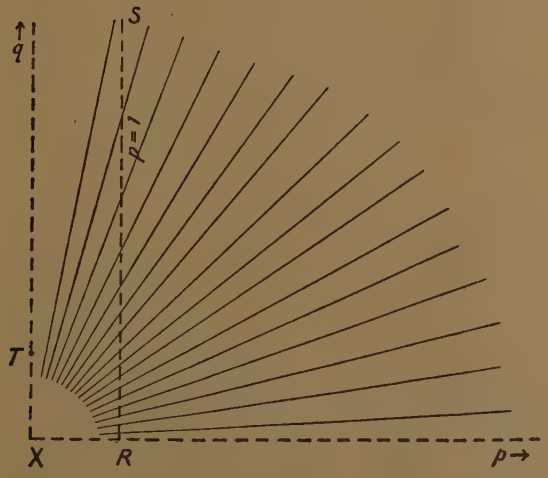

$$\xi = \chi_1(y),$$

. . . .

$$\xi = \chi_n(y),$$

and mark the initial points

$$A_0'(x_0, y_0),$$

$$A_1'\left(x_0, \left(\frac{dy}{dx}\right)_0\right),$$

. . . . . .

$$A_{n-1}'\left(x_0, \left(\frac{d^{n-1}y}{dx^{n-1}}\right)_0\right),$$

as in fig. 9 (*a*).

On the transparent sheet (β) draw two axes (p, q), the line $p=1$ (to the scale of ξ) and a set of faint radial lines passing through the origin X, as in fig. 9 (*b*).

Part I.

Place (β) on (α) so that the p and x axes coincide and the line RS is over the points $A_0', \ldots A_{n-1}', B$. Mark the points $A_0, \ldots A_{n-1}$ over the points $A_0', \ldots A_{n-1}'$. Now place X on A_0' with the q axis coinciding with the line $x=x_0$. Then $A_0'A_1$ is the tangent to the curve $\eta=y$ at A_0', and a consecutive point may be marked.

Move (β) vertically until X is on A_1'. Then $A_1'\,A_2$ is the tangent to the curve $\eta=\dfrac{dy}{dx}$ at A_1'. Continue this process until X is on A_{n-2}' and $A_{n-2}'A_{n-1}$ is the tangent to the curve $\eta=\dfrac{d^{n-2}y}{dx^{n-2}}$ at A_{n-2}'.

Thus we obtain neighbouring points to $A_0' \ldots A_{n-2}'$.

Part II.

To obtain the tangent to the curve $\eta=\dfrac{d^{n-1}y}{dx^{n-1}}$ at A_{n-1}' we proceed as follows :—

Place X over C′ with the q axis over the line $x=x_0$ and mark T over A_0'. Thus $XT=y$. With the p and x axes coincident, move (β) until T lies over the curve $\eta=\chi_0(y)$. Note the radial line from X which passes through the point A_0 and let it cut the η axis in the point K_0. Then clearly $XK_0=\chi_0(y).y$. Record this length on the adding device. Now move (β) until T is over the curve χ_1, note the radial line passing through A_1 and the point K_1 where it cuts the η axis. Then $XK_1=\chi_1(y)\dfrac{dy}{dx}$. Add this to XK_0, already recorded. Repeat the process with

T successively over the $\chi_2, \ldots \chi_{n-1}$ curves, recording the sum of all the lengths $XK_0 \ldots XK_{n-1}$. Then

$$XK_0+XK_1+XK_2+\ldots+XK_{n-1} = \chi_0 y+\chi_1\frac{dy}{dx}+\ldots\chi_{n-1}\frac{d^{n-1}y}{dx^{n-1}},$$

and this length is recorded on the adder and is available for further manipulation. Subtract this length from C'B', giving the length B'Y' say. Move (β) until T is over the curve χ_n and mark U on (β) so that $A'_{n-1}U=Y'B'$. Now move (β) until the q axis is over the line $x=x_0$, and then the line $A'_{n-1}U$ will be the tangent to the curve $\eta=\dfrac{d^{n-1}y}{dx^{n-1}}$ at A'_{n-1} and a consecutive point to A'_{n-1} is thus obtained.

If the order n of equation (12) is high it may be advisable to draw the curves $\eta=y$, $\eta=\dfrac{dy}{dx}$ ... in different colours and the curves $\chi_0, \chi_1, \ldots \chi_{n-1}$ in corresponding colours in order to avoid confusion.

We have assumed that the scales of x and ξ are the same. It is often desirable to alter the scale of one or more of the curves, and this will be discussed and illustrated in example C.

Method 1.31.—As a particular case of method 1.3 we may take $n=2$, thus obtaining a method for the solution of the second-order equation which is just as satisfactory as that already given in method 1.2.

Method 1.32. *Funicular Method.*—Although it does not appear to be quite so convenient in actual use as method 1.3, an interesting mode of approach to the solution of the general equation (12) is afforded by what might be called the "funicular method."

The equation

$$\chi_n(y)\frac{d^ny}{dx^n}+\chi_{n-1}(y)\frac{d^{n-1}y}{dx^{n-1}}+\ldots+\chi_1(y)\frac{dy}{dx}+\chi_0(y)y=f(x)$$

may be regarded as an expression of equilibrium between parallel "forces" $\chi_0, \chi_1, \ldots \chi_n$ acting at distances $y, \dfrac{dy}{dx}, \ldots \dfrac{d^ny}{dx^n}$ from a fulcrum, and a force of unit magnitude acting in the opposite direction at a distance $f(x)$ from the fulcrum.

Our initial conditions give us x, y, $\frac{dy}{dx} \ldots \frac{d^{n-1}y}{dx^{n-1}}$, $\chi_0, \ldots \chi_n$, and the unknown quantity is $\frac{d^ny}{dx^n}$. Thus, if we construct a "force polygon" of the "forces" $\chi_0, \chi_1, \ldots \chi_n, -1$, and apply the usual graphical funicular method employed in statics, we obtain the point of application $\frac{d^ny}{dx^n}$ of the force χ_n.

Method 1.4.—We now consider the equation

$$\psi_n(x)\frac{d^ny}{dx^n}+\psi^{n-1}(x)\frac{d^{n-1}y}{dx^{n-1}}+\ldots+\psi_1(x)\frac{dy}{dx}+\psi_0(x)y=f(x). \quad \ldots \quad (13)$$

This may be solved by a method almost identical with method 1.3.

On squared paper (α) draw the curve $\eta=f(x)$ and mark the initial points A_0', A_1', $\ldots$ A_{n-1}' as before. To avoid confusion we replace the y axis in method 1.3 by a z axis and plot the curves

$$\xi=\psi_0(z),$$
$$\xi=\psi_1(z),$$
$$\ldots\ldots$$
$$\xi=\psi_n(z).$$

On the transparent sheet (β) draw axes (p, q) and radial lines as in fig. 9 (b).

Consecutive points to A_1', $A_1 \ldots A_{n-2}'$ may be found by exactly the same procedure as outlined in Part I. of method 1.3, and it is clear that the only modification necessary in order to make Part II. applicable to equation (13) is that the point T on (β) should be taken so that

$$XT=x_0,$$

instead of y_0 as before. With such a point T the procedure is exactly as in Part II. The z scale is of course quite arbitrary.

Example C.

As an example of methods 1.3 and 1.4 and also as an illustration of the adjustment of scales to suit a particular

problem, we give a solution of Legendre's Associated Equation :

$$(1-x^2)\frac{d^2y}{dx^2}-2x\frac{dy}{dx}+\left\{n(n+1)-\frac{m^2}{1-x^2}\right\}y=0$$

for the values $n=7$, $m=2$.

We choose our initial conditions so that the solution will be the normalized associated Legendre function $\overline{P_7^2}(x)$. This choice of initial conditions and integral values of n and m is made solely with the object of comparing the solution obtained with the well-known function $\overline{P_7^2}(x)$. The method employed would apply equally well to any initial conditions, any values of m and n, integral or otherwise, and to the case where we have an arbitrary function of x on the right-hand side of the equation.

Thus our problem is to find, in the range $0\leqq x\leqq 1$, a solution of

$$(1-x^2)\frac{d^2y}{dx^2}-2x\frac{dy}{dx}+\left(56-\frac{4}{1-x^2}\right)y=0 \quad . \quad (14)$$

satisfying the initial conditions

$$\left.\begin{aligned} x&=0,\\ y&=0,\\ \frac{dy}{dx}&=5{\cdot}85. \end{aligned}\right\} \quad . \quad . \quad . \quad . \quad . \quad . \quad . \quad (15)$$

A preliminary survey of the problem shows that :

(*a*) We have to deal with the rather large factor 56 : 1 ;

(*b*) $\frac{dy}{dx}$ is on the whole considerably larger than y.

With the object of dealing in terms of $\frac{1}{10}\frac{dy}{dx}$ rather than $\frac{dy}{dx}$, we write (14) in the form

$$10(1-x^2)\frac{d}{dx}\left(\frac{1}{10}\frac{dy}{dx}\right)-20x.\frac{1}{10}\frac{dy}{dx}+\left(56-\frac{4}{1-x^2}\right)y=0.$$

$$. \quad . \quad . \quad (14a)$$

This also has the effect of making the two coefficients $20x$ and $\left(56-\frac{4}{1-x^2}\right)$ more of the same order over most of the range.

As y is of the order of 1, $\left(56-\frac{4}{1-x^2}\right)y$ will be of the order of 50, which is too large for convenience. We reduce this product by a factor of 30, by using the line $p=30$ on the transparent sheet instead of the line $p=1$ as in method 1·4. This will also reduce the product $-2x\frac{dy}{dx}$ by the same factor. Before the final "division" the length $10(1-x^2)$ must also be reduced by the same factor, and this is best done in the original plotting, by plotting $\frac{1}{3}(1-x^2)$ in place of $10(1-x^2)$, and we must plot this to the same scale as x; but, p, $-20x$, and $\left(56-\frac{4}{1-x^2}\right)$ may be plotted to any common convenient scale.

Thus, finally, with, for convenience,

$$1 \text{ unit of } \eta = \frac{1}{4} \text{ unit of } x,$$

$$1 \text{ ,, ,, } z = \frac{1}{2} \text{ ,, ,,}$$

$$1 \text{ ,, ,, } \xi = \frac{1}{100} \text{ ,, ,,}$$

$$1 \text{ ,, ,, } p = \frac{1}{100} \text{ ,, ,,}$$

we draw on (α) the curves

$$\xi = -20z,$$

$$\xi = \left(56-\frac{4}{1-z^2}\right),$$

$$\xi = \frac{100}{3}(1-z^2),$$

(*i. e.*, $\frac{1}{3}(1-z^2)$ in the scale of x) and on (β) we draw the line $p=30$.

Proceeding as in 1·4 we obtain the two curves :

$$\eta = y,$$

$$\eta = \frac{1}{10}\frac{dy}{dx}.$$

All of these curves are shown in fig. 10. A comparison with the curve given by Jahnke-Emde * shows an agreement to within 2 per cent. A short discussion of the accuracy to be expected for different sizes of step will be given in 5.2.

Method 1.41.—A combination of methods 1.3 and 1.4 serves for the solution of an equation of the form

$$\{\chi_n(y)+\psi_n(x)\}\frac{d^2y}{dx^2}+\ldots+\{\chi_1(y)+\psi_1(x)\}\frac{dy}{dx}+\{\chi_0(y)+\psi_0(x)\}y=f(x). \qquad (16)$$

Fig. 10.

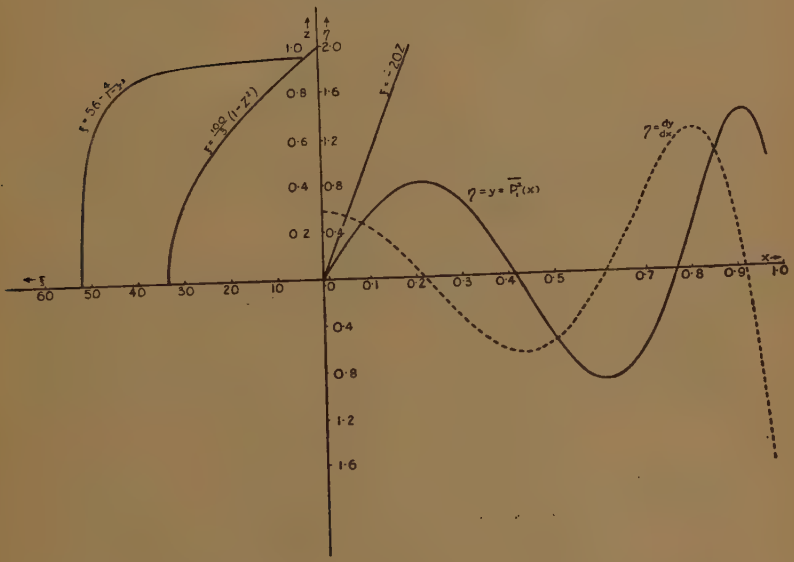

On (α) all the curves

$$\xi=\chi_k(y), \quad k=0, 1, \ldots n,$$
$$\xi=\psi_k(z),$$

are plotted, and on (β) two points T and T_1 are marked, such that

$$XT=y_0,$$
$$XT_1=x_0.$$

* Jahnke-Emde, ' Funktionentafeln ' (Teubner, 2nd Revised Edition, p. 179, fig. 87).

The sum of the products $\chi_k(y)\frac{d^k y}{dx^k}\ldots$ and $\psi_k(x)\frac{d^k y}{dx^k}\ldots$ is obtained by methods similar to those of 1.3 and 1.4, and we must remember that the final "division" is by the sum of the two terms

$$\chi_n(y) \quad \text{and} \quad \psi_n(x).$$

It may be noted that the equation

$$\psi_n(x)\frac{d^n y}{dx^n}+\ldots+\psi_1(x)\frac{dy}{dx}+\psi_0(x)y=g(y)$$

is a particular case of equation (16).

Method 1.5.—We now come to the most general equation involving the differential coefficients in the first power only, namely,

$$\phi_n(x, y)\frac{d^n y}{dx^n}+\ldots+\phi_1(x, y)\frac{dy}{dx}+\phi_0(x, y)y=0. \quad (17)$$

For the solution of this equation we must be given the functions $\phi_0(x, y)\ldots\phi_n(x, y)$ in graphical form. A convenient method of representing a function $\phi(x, y)$ of two variables is to plot a series of curves

$$X=\phi(c, Y)$$

for a series of values of c, the values of c for each curve being written beside it.

Thus in place of the curves $\xi=\chi_0(y), \ldots \xi=\chi_n(y)$ drawn on (α) in fig. 9 (a) we draw a series of curves :

$$\xi=\phi_0(c_1, y), \ldots \xi=\phi_n(c_1, y),$$
$$\xi=\phi_0(c_2, y), \ldots \xi=\phi_n(c_2, y),$$
$$\cdots\cdots\cdots\cdots$$
$$\xi=\phi_0(c_k, y), \ldots \xi=\phi_n(c_k, y),$$

and in place of the curve $\eta=f(x)$ we have in this case simply the axis $\eta=0$.

Then, with the transparent sheet (β) as in fig. 9 (b), and using the curves for which $c=x_0$, *i. e.*, the curves

$$\xi=\phi_0(x_0, y), \ldots \xi=\phi_n(x_0, y),$$

we proceed exactly as in method 1.3, and obtain consecutive points on all the curves. Then, using the curves for which $c=x_0+\Delta x$ (interpolation may be necessary) we repeat the process to obtain the next set of consecutive points.

Method 1.51.—The first-order equation

$$\frac{dy}{dx}=\phi(x, y). \quad . \quad . \quad . \quad . \quad . \quad . \quad (17\,a)$$

deserves special consideration and may be solved much more simply than by method 1.5.

Take axes (x, y) with origin 0 and plot he set of curves

$$x=\frac{y}{\phi(c, y)}$$

for various values of c.

Let the horizontal through the initial point $A(x_0, y_0)$ cut the curve for which $c=x_0$ in P. Then the line OP has the slope

$$\frac{y_0}{y_0/\phi(x_0, y_0)}=\phi(x_0, y_0),$$

so that OP is parallel to the tangent at A to the solution of equation (17. a) passing through A. With a parallel ruler we may transfer this direction to the point A. Alternatively we might plot the curves

$$\mathrm{X}=\frac{\mathrm{Y}}{\phi(c, \mathrm{Y})}$$

on transparent paper with axes X, Y, and origin Ω, and, keeping the X and x axes coincident, move the transparent sheet till the curve

$$\mathrm{X}=\frac{\mathrm{Y}}{\phi(x_0, y)}$$

lies over A, when the line Ω A would be the tangent at A.

We may clearly take P as the intersection of the vertical through A and the curve

$$y=x\phi(x, y_0),$$

if for any reason it is more convenient to plot the curves $y=x\phi(x, c)$ than the curves $x=y/\phi(c, y)$.

§ 2. *Ordinary Equations of the First Order* (b).

Hitherto we have considered only equations in which all the differential coefficients occur in the first power. We now consider first degree equations which do not possess this property.

Method 2.0.—It is clear that a very large class of such equations may be solved by methods very similar to methods 1.3–1.5.

For instance, an equation of the form

$$\chi_n\left(\frac{dy}{dx}\right)\frac{d^ny}{dx^n}+\chi_{n-1}\left(\frac{dy}{dx}\right)\frac{d^{n-1}y}{dx^{n-1}}+\cdots$$
$$+\chi_1\left(\frac{dy}{dx}\right)\frac{dy}{dx}+\chi_0\left(\frac{dy}{dx}\right)y=f(x)$$

may be solved by a method identical with that given in 1.3, if the point T be taken so that $XT=\left(\frac{dy}{dx}\right)_0$.

An equation of the more general type

$$\left\{\chi_{n,n-1}\left(\frac{d^{n-1}y}{dx^{n-1}}\right)+\chi_{n,n-2}\left(\frac{d^{n-2}y}{dx^{n-2}}\right)+\cdots\right.$$
$$\left.+\chi_{n,1}\left(\frac{dy}{dx}\right)+\chi_{n,0}(y)\right\}\frac{d^ny}{dx^n}+\cdots$$
$$+\left\{\chi_{1,n-1}\left(\frac{d^{n-1}y}{dx^{n-1}}\right)+\cdots+\chi_{11}\left(\frac{dy}{dx}\right)+\chi_{10}(y)\right\}\frac{dy}{dx}$$
$$+\left\{\chi_{0,n-1}\left(\frac{d^{n-1}y}{dx^{n-1}}\right)+\cdots+\chi_{01}\left(\frac{dy}{dx}\right)+\chi_{00}(y)\right\}y=f(x)$$
$$\ldots \quad (18)$$

may be solved by an extended method similar to 1.41.

We do not pursue this line of approach, initiated in 1.3, any further in detail. It is clear that if necessary, method 1.5 can be extended to cover the case in which the χ's of equation (18) are functions of any two of x, y, $\frac{dy}{dx}$, $\ldots$ $\frac{d^{n-1}y}{dx^{n-1}}$. However, with equations of such a complicated nature it is better to consider each equation on its own merits and employ such simplifying devices as suggest themselves, rather than to adhere strictly to a general procedure.

§ 3. *Ordinary Equations not of the First Degree.*

We now consider equations in which the differential coefficient of highest order does not appear in the first power.

Method 3.0.—Suppose that we have an equation

$$\mathrm{PF}\left(\frac{d^n y}{dx^n}\right) - \mathrm{Q} = 0, \quad . \quad . \quad . \quad . \quad . \quad (19)$$

where P and Q are such functions of the two variables and the derivatives up to the $(n-1)th$ as can be dealt with by methods 1.3–2.0, and F is an arbitrary function. Then, by one of those methods, we can obtain $\mathrm{F}\left(\frac{d^n y}{dx}\right)$ as a geometrical quotient—*i. e.*, we obtain Q as a vertical distance and P as a horizontal distance.

By the use of biangular coordinates, $\frac{d^n y}{dx^n}$ may be readily obtained directly as a slope.

Fig. 11.

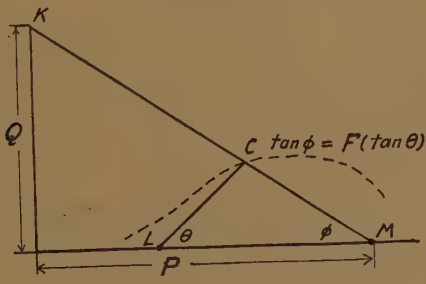

Suppose we have biangular coordinates θ and ϕ with origins L and M.

Plot the curve

$$\tan \phi = \mathrm{F}(\tan \theta),$$

as in fig. 11.

Now, if we measure a distance P from M in the direction ML, and then measure Q vertically, we reach the point K, as in fig. 11.

Let MK cut the curve $\tan \phi = \mathrm{F}(\tan \theta)$ in C. Then clearly $\tan \theta = \frac{d^n y}{dx^n}$, and the line LC is parallel to the tangent to the $\frac{d^{n-1} y}{dx^{n-1}}$ curve.

We do not attempt to give an actual procedure for the application of this method, since the most appropriate procedure will depend on the particular problem in hand.

Method 3.01.—The first-order equation

$$\chi(y)\mathrm{F}\left(\frac{dy}{dx}\right)+y=f(x) \quad . \quad . \quad . \quad . \quad (20)$$

may be solved very simply by the use of biangular co-ordinates.

On squared paper (α) with axes (x, η), draw the curve $\eta=f(x)$, and on a transparent sheet (β) with axes (ξ, y) and origin L, draw the curve $\xi=\chi(y)$, as shown in fig. 12; also, with L as the origin of the biangular coordinate θ

Fig. 12.

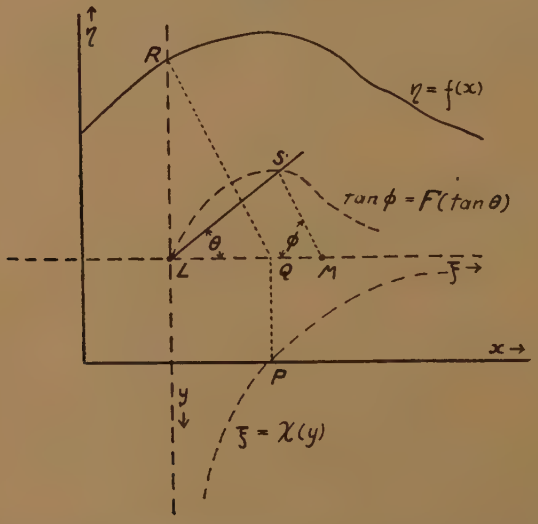

and some convenient point M on the ξ axis as origin of ϕ, draw the curve

$$\tan\phi=\mathrm{F}(\tan\theta).$$

Place (β) on (α) with L over the initial point A and the x axes parallel, as in fig. 12.

Let P be the intersection of the curve $\xi=\chi(y)$ and the axis $\eta=0$, and let Q be vertically above P on the axis $y=0$. Then if $\xi=0$ cuts $\eta=g(x)$ in R

$$\tan\angle\mathrm{LQR}=\frac{f(x)-y}{\chi(y)}=\mathrm{F}\left(\frac{dy}{dx}\right).$$

Draw MS parallel to QR cutting the curve $\tan\phi=\mathrm{F}(\tan\theta)$ in S.

Then clearly LS is the tangent at L to the curve $\eta=y$.

Example D.

To illustrate methods 3·0 and 3·01 we consider the following equation :

$$3 \sin 2\pi y \cdot \frac{4\frac{dy}{dx}}{\left(\frac{dy}{dx}\right)^2 - 3} + y = \cos\frac{\pi x}{4} \quad . \quad . \quad . \quad (21)$$

Following method 3·01, we plot on the transparent sheet the curve $\xi = 3 \sin 2\pi y$, and we need the curve

$$\tan\phi = \frac{4\tan\theta}{\tan^2\theta - 3} \quad . \quad . \quad . \quad . \quad (22)$$

referred to biangular coordinates θ and ϕ, with origins L and M respectively. It is readily seen that this curve is a circle of radius 2LM, with centre C on the line LM, such that MC=LM. We draw this curve, taking LM arbitrarily=1 unit on the x scale.

Since any line through M cuts the circle in two points we see that there are two values of the differential coefficient at each point. To obtain a unique solution we must adopt some arbitrary convention for eliminating this ambiguity. We adopt the following convention :— With the notation of fig. 12, we take the point S, such that the vector MS is parallel to the vector QR, and then S is defined unambiguously since the other intersection S′ is always on the opposite side of M. This convention is, of course, only one of an infinite number which might equally well be adopted.

In fig. 13 we give three solutions of equation (21) (curves I, I, and III) corresponding to three different initial conditions. The dotted lines represent the transparent sheet in the position for determining the tangent LS to the curve I and L. The notation of fig. 12 is used. (The coincidence of Q with the curve III is, of course, accidental.)

§ 4. *Simultaneous Equations.*

A certain class of simultaneous differential equations may be solved by methods similar to methods 1.3–3.0. In these methods we have shown how an equation of the form

$$F\left(\frac{d^n y}{dx^n}\right) = \frac{P}{Q} \quad . \quad . \quad . \quad . \quad . \quad . \quad (23)$$

may be solved when P and Q are functions of x, y, $\frac{dy}{dx}$, .., $\frac{d^{n-1}y}{dx^{n-1}}$ of certain types.

Suppose, then, that we have a set of simultaneous equations

$$F_1\left(\frac{d^n y_1}{dx^n}\right) = \frac{P_1}{Q_1}, \quad . \quad . \quad . \quad . \quad . \quad (24.1)$$

Fig. 13.

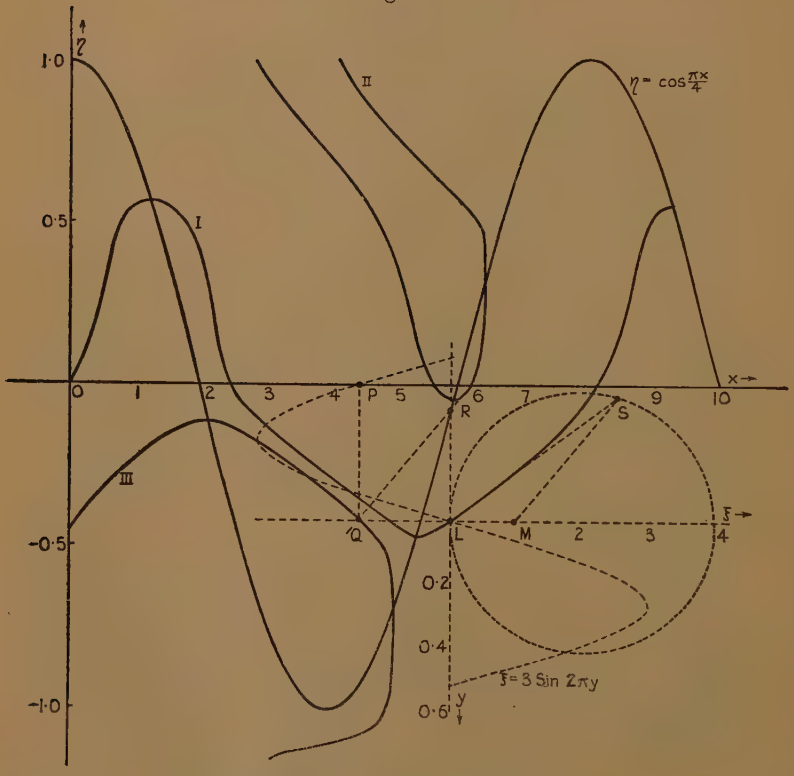

$$F_2\left(\frac{d^n y_2}{dx^n}\right) = \frac{P_2}{Q_2}, \quad . \quad . \quad . \quad . \quad . \quad (24.2)$$

. . . . . .

$$F\left(\frac{d^n y_k}{dx^n}\right) = \frac{P_k}{Q_k}, \quad . \quad . \quad . \quad . \quad . \quad (24.k)$$

where $P_1 \ldots P_k$; $Q_1 \ldots Q_k$ are functions of x; $y_1, y_2, \ldots y_k$; $\frac{dy_1}{dx}, \ldots \frac{dy}{dx}$; $\ldots \frac{d^{n-1}y_1}{dx^{n-1}}, \ldots \frac{d^{n-1}y_k}{dx^{n-1}}$ similar to the functions P, Q of equation (23). Then, given the initial values of x; $y, \ldots y_k$; $\ldots \frac{d^{n-1}y_1}{dx^{n-1}}, \ldots \frac{d^{n-1}y_k}{dx^{n-1}}$, from (24.1), we may find $\frac{d^n y_1}{dx^n}$, and hence a consecutive point on the $\frac{d^{n-1}y_1}{dx^{n-1}}$ curve, and so on, each equation (24.m) giving a consecutive point on the $\frac{d^{n-1}y_m}{dx^{n-1}}$ curve. The process may then be repeated.

Some sets of simultaneous differential equations which are not in the form (24) may be put into that form by solving them algebraically for $\frac{d^n y_1}{dx^n}$, $\frac{d^n y_2}{dx^n}$, $\ldots \frac{d^n y_k}{dx^n}$. In particular, the general set of linear simultaneous equations may always be given the form (24).

§ 5. *Practical Considerations.*

5.1 *Scale.*—In all preceding discussion, with the exception of example C, we have assumed a uniformity of scale which is not likely to be either convenient or desirable in practice; the introduction of scale factors would have complicated the discussion unduly. However, in many problems a manipulation of scales will be necessary, and some idea of what may be done in this way may be gained from example C. A transformation may sometimes be advisable; for example, the equation

$$1000\frac{d^2y}{dx'^2}+50\frac{dy}{dx'}+y=f(x')$$

may be transformed by $x'=10k$ to

$$10\frac{d^2y}{dx^2}+5\frac{dy}{dx}+y=\phi(x)$$

and the large factor 1000 : 1 avoided. Other devices such as a temporary change in scale in order to negotiate a peak will suggest themselves where necessary.

5.2 *Accuracy.*—A curve constructed by small segments is liable to both random and systematic errors. The random errors occur in the evaluation of the slope of each segment and in the drawing. The systematic errors are due to the finite length of the segments of which the curve is constructed; these errors are usually more important than the random errors which tend to balance out over a large number of steps. A full discussion of these " step " errors is difficult when we are constructing more than one curve, since errors in one curve may either compensate or aggravate errors in another. However, by considering the construction of a single curve we may get some idea of the order of the error to be expected for a certain size of step.

Throughout this paper it has been assumed that the curve is constructed as follows :—

Procedure A.

Starting at a point P_0 (x_0, y_0) the slope of the solution which passes through P_0 is found and a line of that slope is drawn from P_0 to P_1 $(x_0+\delta, y_1)$. The appropriate slope at P_1 is then found and a line drawn to P_2 $(x_0+2\delta, y_2)$, and so on to $P_n(x_0+n\delta, y_n)$.

This procedure is sufficient for a rapid approximation, but when accuracy of the order of say 1 per cent. is desired, the following procedure is much better.

Procedure B.

Starting from P_0 (x_0, y_0) determine the slope of the solution through P_0 and draw the line $P_0Q_0(x_0+\delta/2, y_1')$ with that slope. Now determine the slope at Q_0 and, returning to P_0, draw another line with this slope through P_0 to P_1 $(x_0+\delta, y_1)$. Similarly we obtain a point $Q_1(x_0+3\delta/2, y_2')$, find the slope there, and by drawing a line with that slope through P_1, obtain a point P_2 and so on.

Though this procedure involves twice as many operations as Procedure A it is nevertheless speedier, as is shown by actual calculation for the case of a sine wave. If we construct the portion of the curve $y=a \sin x$ between $x=0$ and $x=\pi/2$ in n steps (*i. e.*, $\delta=\pi/2n$), then the

percentage by which the maximum obtained will exceed a is as follows :—

	$n=5$	10	20	50
	Per cent.	Per cent.	Per cent.	Per cent.
Procedure A.....	20	11	4	1
Procedure B.....	2	1		

Although these figures have been calculated for the particular case of a sine curve they nevertheless give an indication of the superiority to be expected from Procedure B in the construction of curves which have maxima not widely differing from the sinusoidal type.

§ 6. *Conclusion.*

We have shown how a number of simple and inexpensive graphical devices may be applied to the solution of a large class of ordinary differential equations such as are frequently met with in applied mathematics *. The treatment is general and emphasis is laid on the method of attack rather than on the solution of particular equations. In a subsequent paper, the application of these methods to particular equations of importance in various branches of applied mathematics will be given in greater detail.

We wish to acknowledge the benefit of discussions with and suggestions by Mr. D. M. Myers who has also undertaken the design and construction of a simple machine to solve the second-order linear equation with constant coefficients, *i. e.*,

$$A\frac{d^2y}{dx^2}+B\frac{dy}{dx}+C=f(x),$$

where $f(x)$ is an arbitrary function given graphically.

We would draw attention to the fact that the work of one of the authors has been made possible by a grant from the Carnegie Corporation.

* The relatively high cost of machines like Bush's Differential Analyser leaves room for methods like ours when an accuracy of the order of 1 per cent. is sufficient.

II. *The Calculation of the Elastic Scattering of Electrons by Molecular Hydrogen.* *By* R. Roscoe, *Ph.D., Physics Laboratories, University of Leeds* *.

THE problem of the scattering of electrons by simple atomic systems such as hydrogen and helium has been thoroughly investigated by mathematical means [1], but relatively little work has been done on scattering by molecules. The only published calculations on the elastic collision of electrons with molecular hydrogen are those of Massey and Mohr [2], [3], who used the simple Born theory [4] in conjunction with the wave function for the ground state of the molecule given by Wang [5]. Large errors in the scattering at small angles may result from the use of approximate formulæ of this type to represent the wave function, so the present work has been undertaken with the object of improving the results by using better forms of the wave function, many of which have become available since the publication of Massey and Mohr's papers. Further improvements could be made by taking into account electron exchange, distortion, etc. (effects which are neglected in the simple Born theory), but a consideration of these factors is deferred for the present, as their neglect can only produce considerable errors for low velocities of the impacting electrons.

The elastic cross-section $I(\delta)$ is defined so that $2\pi I(\delta)\sin\delta d\delta$ represents the fraction of electrons scattered through the small solid angle between angles δ and $\delta+d\delta$ in passing through unit length of gas containing one molecule per unit volume. With this definition the Born scattering formula is

$$I(\delta)=\frac{4\pi^2m^2}{h^2}\mathbf{A}\left|\iiint V\psi_0\psi_0^* e^{i\mathbf{K}\cdot\mathbf{R}_1}\,d\tau_1\,d\tau_2\,d\tau_3\right|^2, \quad . \quad (1)$$

where

A denotes averaging over all orientations of the molecular axis ;

V is the scattering potential ;

ψ_0 is the wave function of the ground state of the molecule ;

* Communicated by Professor Whiddington, F.R.S.

$\mathbf{R}$ is the radius vector from the centre of the molecule ; $\frac{\mathbf{K}h}{2\pi m}$ is the vector difference between the initial and final velocities of the scattered electron, and the suffix 1 denotes the coordinates of the scattered electron, while 2 and 3 refer to the bound electrons.

The scattering potential is given by

$$V=-e^2\left(\frac{1}{r_1}+\frac{1}{p_1}-\frac{1}{r_{12}}-\frac{1}{r_{13}}\right),$$

where r_1 denotes the distance of electron 1 from one nucleus, p_1 its distance from the other, and r_{12} stands for the distance between electrons 1 and 2. By making use of the relation

$$\int\left(\frac{1}{r_1}-\frac{1}{r_{12}}\right)e^{i\mathbf{K}\cdot\mathbf{r}_1}\,d\tau_1=\frac{4\pi}{K^2}(1-e^{i\mathbf{K}\cdot\mathbf{r}_2})$$

and the vector equations

$$\mathbf{R}=\mathbf{r}+\tfrac{1}{2}\mathbf{d}=\mathbf{p}-\tfrac{1}{2}\mathbf{d}, \quad \ldots\ldots \quad (2)$$

where $\mathbf{d}$ is the nuclear separation, equation (1) may be reduced to the form

$$I(\delta)=\frac{16}{(Ka_0)^4}A\left|\cos(\tfrac{1}{2}\mathbf{K}.\mathbf{d})-\int\int e^{i\mathbf{K}\cdot\mathbf{R}_2}\psi_0{}^2 d\tau_2\,d\tau_3\right|^2, \quad (3)$$

where $a_0=\frac{h^2}{4\pi^2me^2}$ and $I(\delta)$ is expressed in units of $a_0{}^2$.

Wave Functions of the Ground State of the Molecule.

In order to obtain the elastic cross-section by equation (3) it is necessary to assume some approximate analytic form for the wave function of the ground state which is close to the true wave function at the equilibrium separation of the nuclei. Several such approximate forms have been obtained by variational methods, the simplest being that due to Wang :

$$\psi_0=N\{e^{-Z(r_2+p_3)}+e^{-Z(p_2+r_3)}\}.$$

This has been improved by Rosen [6], who added a "polar" term, and by Weinbaum [7], who introduced

an "ionic" term as well. All these functions may be represented by the general form

$$\psi_0 = N\{e^{-Z(r_2+p_3)}.(1+\sigma r_2\cos\theta_2)(1+\sigma p_3\cos\theta_3')$$
$$+e^{-Z(p_2+r_3)}.(1+\sigma p_2\cos\theta_2')(1+\sigma r_3\cos\theta_3)$$
$$+\frac{1}{c}e^{-Z(r_2+r_3)}(1+\sigma r_2\cos\theta_2)(1+\sigma r_3\cos\theta_3)$$
$$+\frac{1}{c}e^{-Z(p_2+p_3)}(1+\sigma p_2\cos\theta_2')(1+\sigma p_3\cos\theta_3')\},$$
$$\ldots \quad (4)$$

where θ is the angle between $\mathbf{r}$ and $\mathbf{d}$, θ' is the angle between $\mathbf{p}$ and $-\mathbf{d}$, and N is the normalizing factor. The constants were all determined by variational methods, and the values given by the authors are as follows :

	Za_0.	c.	σa_0.
Wang function	1·166	∞	0
Weinbaum (ionic)	1·193	3·9	0
Rosen (polar)	1·166	∞	0·1
Weinbaum (polar-ionic).....	1·190	5·7	0·07

The energy values calculated from these functions are increasingly good in the order in which they are set forth above. The best energy value is obtained from the function given by James and Coolidge [8], and this consequently represents the nearest approach to the correct wave function so far obtained, but unfortunately it contains such a large number of terms that its use would make the calculation of the cross-section extremely difficult. The present work is therefore restricted to the use of the four wave functions given above, of which Weinbaum's "polar-ionic" form probably gives the best results.

Calculations with Wang and "Ionic" Wave Functions.

The calculation of the elastic cross-section using Wang's function is closely similar to that using Weinbaum's "ionic" function, so in the following work the latter function is used, the result for the Wang function being obtained by putting c equal to infinity in the final expression for the cross-section. By putting σ equal

to zero in equation (4) the normalizing factor for the "ionic" function is obtained as

$$2\pi^2 N^2 = \frac{Z^6}{(A+B)},$$

where

$$A = \left(1+\frac{1}{c^2}\right)+\frac{2}{c}\sqrt{S},$$

$$B = \left(1+\frac{1}{c^2}\right)S+\frac{2}{c}\sqrt{S},$$

$$S = (1+Zd+\tfrac{1}{3}Z^2d^2)^2 e^{-2Zd}.$$

Also

$$\int \psi_0^2 d\tau_3 = \frac{\pi N^2}{Z^3}\left\{ Ae^{-2Zr_2}+Ae^{-2Zp_2}+\frac{2B}{\sqrt{S}}e^{-Z(r_2+p_2)}\right\}.$$

Using the vector relation (2), this gives the following expression for the integral occurring in (3):

$$\iint e^{i\mathbf{K}.\mathbf{R}_2}\psi_0^2 d\tau_2 d\tau_3 = \frac{2\pi N^2}{Z^3}\left\{ A\cos(\tfrac{1}{2}\mathbf{K}.\mathbf{d})\int e^{i\mathbf{K}.\mathbf{r}_2}e^{-2Zr_2}d\tau_2 + \frac{B}{\sqrt{S}}\int e^{i\mathbf{K}.\mathbf{R}_2}e^{-Z(r_2+p_2)}d\tau_2\right\}$$

$$= \frac{2\pi N^2}{Z^3}\left\{ \frac{16\pi AZ}{(4Z^2+K^2)^2}.\cos(\tfrac{1}{2}\mathbf{K}.\mathbf{d}) + \frac{B}{\sqrt{S}}\int e^{i\mathbf{K}.\mathbf{R}_2}e^{-Z(r_2+p_2)}d\tau_2\right\}$$

$$= \frac{16Z^4}{(4Z^2+K^2)^2}\cos(\tfrac{1}{2}\mathbf{K}.\mathbf{d})-\frac{BZ^4}{A+B}.T,$$

where

$$T = \frac{16}{(4Z^2+K^2)^2}\cos(\tfrac{1}{2}\mathbf{K}.\mathbf{d}) - \frac{1}{Z\pi\sqrt{S}}\int e^{i\mathbf{K}.\mathbf{R}}e^{-Z(r+p)}d\tau.$$

This gives for the cross-section

$$I(\delta) = \frac{16}{a_0^4}A\left[\frac{8Z^2+K^2}{(4Z^2+K^2)^2}\cos(\tfrac{1}{2}\mathbf{K}.\mathbf{d})+\frac{BZ^4}{A+B}\frac{T}{K^2}\right]^2. \quad (5)$$

The advantage of this form lies in the fact that both terms are finite throughout the whole range of K, and the only integral which cannot be evaluated in algebraic form is contained in the second term, which is always

found to be small compared with the first. When K is large, the integral falls off inversely as K^4, consequently the second term vanishes more rapidly than the first as K approaches infinity.

Averaging over all orientations of the nuclear axis, the vector **K** being kept fixed, may be accomplished by integration with respect to $\sin\chi \,.\, d\chi$ between 0 and π and dividing by 2, where χ denotes the angle between the axis of the molecule **d** and the vector **K**. It is to be noted that

$$\tfrac{1}{2}\mathbf{K}\,.\,\mathbf{d}=\tfrac{1}{2}\mathrm{K}d\,.\,\cos\chi$$

and

$$\mathrm{K}=2k\,.\,\sin\frac{\delta}{2},$$

where $\dfrac{hk}{2\pi m}$ is the magnitude of the velocity of the incident electrons. Thus the cross-section is given approximately by the relation

$$\mathrm{I}(\delta)=\frac{8}{a_0{}^4}\frac{(8\mathrm{Z}^2+\mathrm{K}^2)^2}{(4\mathrm{Z}^2+\mathrm{K}^2)^4}\left\{1+\frac{\sin\mathrm{K}d}{\mathrm{K}d}\right\}\quad\ldots\quad(6)$$

The exact value is obtained by taking into account the terms containing $\int \mathrm{T}\cos(\tfrac{1}{2}\,\mathbf{K}\,.\,\mathbf{d})\sin\chi\,d\chi$ and $\int \mathrm{T}^2\sin\chi\,d\chi$. The first of these is obtainable in trigonometric form, since it can be shown that

$$\iint e^{i\mathbf{K}\,.\,\mathbf{R}}\,e^{-\mathrm{Z}(r+p}\,.\,d\tau\,.\cos(\tfrac{1}{2}\,\mathbf{K}\,.\,\mathbf{d})\sin\chi\,.\,d\chi$$
$$=\frac{64\pi\mathrm{Z}^3e^{-\mathrm{Z}d}}{\mathrm{K}^2(4\mathrm{Z}^2+\mathrm{K}^2)^2}\left\{\left(\frac{\mathrm{K}^2}{4\mathrm{Z}^2}-1\right)\left(1+\frac{\sin\mathrm{K}d}{\mathrm{K}d}\right)+\frac{1}{\mathrm{Z}d}(1-\cos\mathrm{K}d)+2\right\}.$$

The remaining term, which is very small, is more difficult to evaluate and cannot be obtained in trigonometric form. It is found best to expand T in this term as a series of Legendre polynomials $\mathrm{P}_n(\cos\chi)$, so that after squaring and integrating with respect to $\sin\chi\,d\chi$ the third term is obtained as a simple series. This series is found to be convergent, and its sum decreases rapidly as K increases.

The resulting expression for the cross-section enables calculations to be carried out quite easily, since the only term which has to be evaluated numerically is

extremely small (less than 0·8 per cent. of the total). Neglect of both the small terms, *i. e.* taking expression (6) to represent the cross-section, only leads to errors of 4 per cent. in the result. The expression obtained by Massey and Mohr (who used only the Wang function) is in the form of an infinite series, of which a large number of terms must be taken even for small values of K, and the higher terms are very difficult to evaluate.

Calculations with the "Polar" Wave Functions.

The introduction of a "polar" term into the wave function complicates the problem to some extent, but the method of attack is similar to that outlined above for the Wang and simple "ionic" wave functions. The effect of the "polar" term is to modify the integral occurring in T to a slight extent, and two more trigonometric terms are introduced in the squared bracket in equation (5). Most important of these is the term

$$\frac{256}{Z^2}\frac{\pi^2 N_0^2 A\sigma}{(4Z^2+K^2)^3}\frac{\sin(\frac{1}{2}\mathbf{K}.\mathbf{d})}{K}.\cos\chi,$$

where A is now given by a more complicated expression, which involves σ as well as c.

Discussion of the Results.

The elastic cross-sections calculated for zero scattering angle (K equal to 0), expressed in units of a_0^2, are as follows :—

Wang function	2·107
Weinbaum (ionic)	1·910
Rosen (polar)	2·464
Weinbaum (polar-ionic)	2·140

On account of the very rapid decrease of $I(\delta)$ with K, it is very difficult to give an accurate representation of the calculated results for other scattering angles on a graph. So the approximate form for the cross-section given by (6) is taken, with Za_0 equal to 1·190, and the percentage excess of the calculated values above this is plotted against $ka_0 \sin\delta/2$ (fig. 1).

The introduction of the "ionic" term into the simple Wang function is seen to reduce the small angle scattering, chiefly because of the higher value of Za_0. The "polar"

term, on the other hand, produces an increase in the small angle scattering as a result of the introduction of the additional terms inside the bracket of equation (5). When the wave function containing both "polar" and "ionic" terms is used, the two effects nearly balance

Fig. 1.

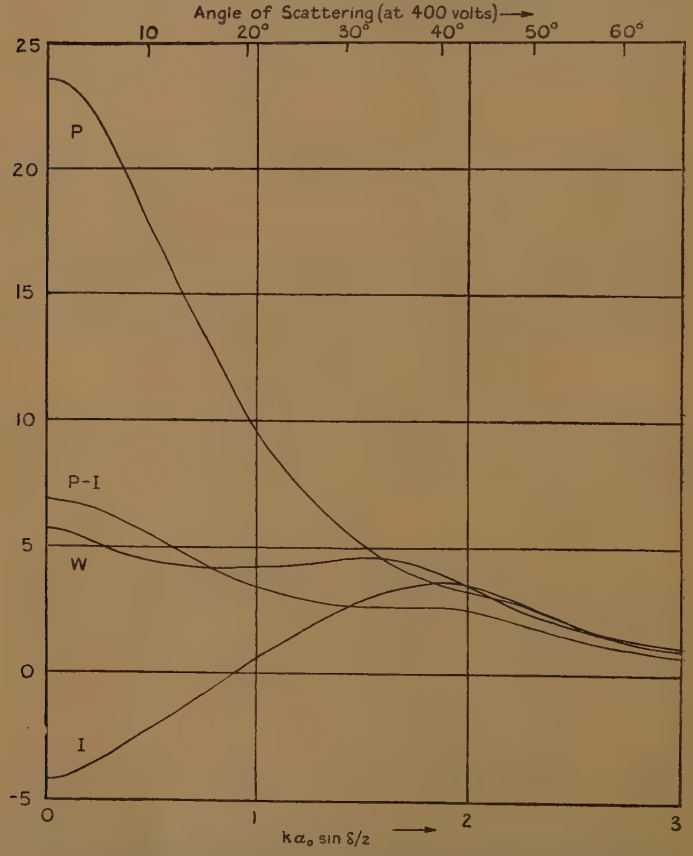

Ordinates represent percentage excess of scattering above that given by equation (6) with $Za_0 = 1{\cdot}190$. Wang's function gives curve W, Weinbaum's "ionic" function gives curve I, Rosen's polar function gives curve P, and Weinbaum's "polar-ionic" function gives curve P–I.

each other, and the scattering is quite close to that given by use of the simple Wang function. All four wave functions give close results when $ka_0 \sin \delta/2$ is greater

than 2, and when it is very large the scattering becomes in all cases equal to the Rutherford scattering from two heavy masses of charge e.

Fig. 2 shows the ratio of the cross-sections of molecular and atomic hydrogen plotted against the same variable. This method was adopted by Massey and Mohr to bring out the oscillatory effect produced by the " diffraction factor " $\left(1+\frac{\sin Kd}{Kd}\right)$. The results plotted in this case are those obtained from the " polar-ionic " wave function.

Fig. 2.

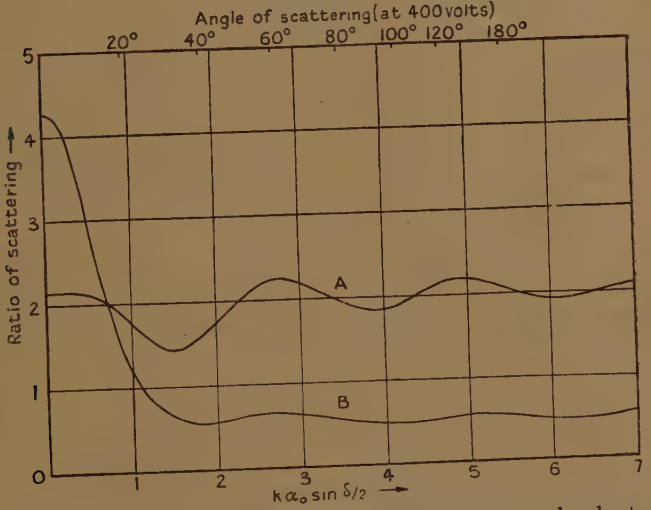

Curve A shows the ratio of scattering by hydrogen molecules to the scattering by *single* hydrogen atoms.
Curve B shows the ratio of scattering by hydrogen molecules to the scattering by helium atoms.

It is to be noted that this curve differs, especially near the origin, from that published by the previous authors. This is not so much due to the difference between the Wang and " polar-ionic " results as to an error in the previous paper. (The author is indebted to Dr. Massey for confirmation of the fact that in fig. 2 of their second paper the ordinate at the origin should be 1·05 instead of 1·4.) Although oscillatory scattering curves have been obtained for heavy atoms, this particular type of diffraction, due to interference of waves scattered by the two nuclei,

has not yet been confirmed by experiment. Harnwell [9] found that the scattering by hydrogen molecules is approximately equal to scattering by double the same number of hydrogen atoms, and Webb [10] obtained results which agree with the calculations over a certain range. At large and small values of $ka_0 \sin \delta/2$ Webb's figures give a greater value of the ratio of molecular to atomic scattering than the theory. His results in the intermediate region seem to fit the oscillatory curve, but the figures are not sufficiently accurate to prove the existence of maxima and minima definitely. At very small scattering angles close agreement is not to be expected between the experimental results and calculations based upon the simple Born formula, as a more comprehensive treatment of the problem is probably necessary in this instance. It is unfortunate that the ratio of scattering by molecular hydrogen to scattering by helium (also shown in fig. 2) does not show the diffraction effect so clearly, as this ratio might be more easily determined by experiment.

In conclusion, the Author wishes to thank Dr. J. McDougall for his advice on this research, and Dr. H. S. W. Massey and Prof. R. Whiddington for their very helpful suggestions.

Summary.

It is shown that the simple Born theory applied to the problem of the elastic scattering of electrons by molecular hydrogen gives an expression for the elastic cross-section which is approximately equal to

$$\frac{8}{a_0^4}\frac{(8Z^2+K^2)^2}{(4Z^2+K^2)^4}\left(1+\frac{\sin Kd}{Kd}\right),$$

where Za_0e is the effective nuclear charge occurring in the wave function of the ground state of the molecule.

Calculations of the elastic cross-section are made using the four different types of wave function due to Wang, Rosen, and Weinbaum. It is found that the introduction of Weinbaum's "ionic" term into the simple wave function due to Wang decreases the small angle scattering, while Rosen's "polar" term increases it considerably, The function which contains both ionic and polar terms

(also due to Weinbaum) gives scattering very close to that obtained from the simple Wang function.

References.

(1) Mott and Massey, ' The Theory of Atomic Collisions,' Oxford, 1933.
(2) Massey, Proc. Roy. Soc. A, cxxix. p. 616 (1930).
(3) Massey and Mohr, Proc. Roy. Soc. A, cxxxv. p. 258 (1932).
(4) Born, *Z. f. Physik*, xxxviii. p. 803 (1926).
(5) Wang, Phys. Rev. xxxi. p. 579 (1928).
(6) Rosen, Phys. Rev. xxxviii. p. 2099 (1931).
(7) Weinbaum, Journ. of Chem. Physics, i. p. 593 (1933).
(8) James and Coolidge, J. Chem. Physics, i. p. 825 (1933).
(9) Harnwell, Phys. Rev. xxxiv. p. 661 (1929).
(10) Webb, Phys. Rev. xlvii. p. 384 (1935).

III. *On the Surface Tensions of Liquid Crystals.* *By* Allan Ferguson, *M.A.*, *D.Sc.*, *and* S. J. Kennedy, *M.Sc.* (*Queen Mary College*) *.

Abstract.

In this communication is described a method for the measurement of surface tension over a wide range of temperature, in which a furnace of simple design is used. The method, which does not demand the use of more than a few cubic millimetres of liquid is applied to the determination of the surface tensions of anisaldazine, *p*-azoxyanisol, and *p*-azoxyphenetol. The results obtained cover the region which contains the transition temperatures.

DESPITE the mass of literature which has accumulated on the measurement of surface tensions very little attention has been paid to the determination of the surface tensions of liquid crystals. There are a few determinations by Schenck(1) at one or two isolated temperatures, and there is a systematic set of determinations by E. M. Jaeger(2), who used the maximum bubble-pressure method usually described as Jaeger's method(3), and determined the surface tension against an atmosphere of *nitrogen*. His observations, which cover a wide range of temperature, were specially concerned with the determination of the magnitude of the Eötvös constant,

* Communicated by the Authors.

and are taken at fairly wide temperature intervals. They do not therefore show, as do the results to be described, the details of the interesting changes of surface tension which occur in the neighbourhood of the transition point.

The method has been fully described by us in a previous paper[4], and need only be outlined here.

Briefly, it consists in forcing a thread of liquid along a horizontal capillary tube, and adjusting the pressure on one end of the liquid column until the surface of the liquid at the open end of the tube is plane. When this is the case (fig. 1) we easily see that if h_1 is the pressure head in a U-tube manometer containing liquid of density ρ_1—the manometer indicating the pressure excess at A—we have, the atmospheric pressure being Π,

$$\Pi = P_D = P_C = P_B$$

and

$$P_A = \Pi + g\rho_1 h_1.$$

Fig. 1.

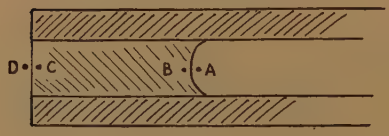

Also $P_A - P_B = 2\gamma/R$, where R is the radius of curvature of the meniscus at its vertex. Hence

$$\gamma = \tfrac{1}{2}.Rg\rho_1 h_1.$$

This equation is exact if the meniscus may be considered as a figure of revolution.

If now we assume a zero contact angle, and neglect any gravitational distortion of the meniscus, we may identify R with r, the radius of the capillary tube, and we have

$$\gamma = \tfrac{1}{2}.rg.\rho_1 h_1, \quad . \quad . \quad . \quad . \quad . \quad . \quad (1)$$

showing that no knowledge of the density of the liquid under test is needed for the determination of γ.

The question of any distortion of the meniscus is important. If we imagine the tube in fig. 1 to be vertical, a similar argument, taking into account first-order corrections, shows that

$$\gamma = \tfrac{1}{2}rg[\rho_1 h_1 + \rho_2(h_2 + \tfrac{1}{3}r)], \quad . \quad . \quad . \quad . \quad (2)$$

where ρ_2 is the density of the liquid under test and h_2 the length of the liquid column in the capillary. We can test the limits of applicability of equation (1) by comparing the value of γ calculated therefrom by observations made using any particular tube, with the value of γ obtained with the tube in a vertical position and calculated from equation (2).

With the same liquid in the manometer and capillary this amounts to a comparison of the value of h_1' (say), the tube being horizontal, with the value of $h_1+h_2+\frac{1}{3}r$ obtained with the tube vertical. Thus, using a capillary

Fig. 2.

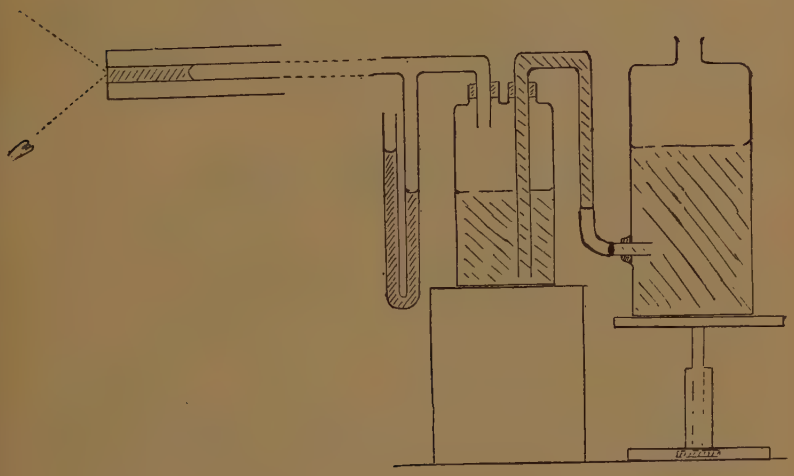

of diameter 0·9 mm., and with aniline for the test- and manometer-liquid, a number of settings gave

h_1' cm. (tube horizontal) : 1·936, 1·938, 1·937, 1·933, 1·933.
$h_1+h_2+\frac{1}{3}r$ cm.
(tube vertical) : 1·938, 1·938, 1·938, 1·935, 1·935, 1·934.
Mean h_1' =1·935 cm.
Mean $h_1+h_2+\frac{1}{3}\gamma$ =1·936 cm.

A number of such observations with tubes of different radii showed clearly that, for liquids of the densities and surface tensions commonly encountered, it was quite safe to use a capillary tube of not greater than 1 millimetre bore. The arrangement of the apparatus is shown

in fig. 2, which is self-explanatory. It need only be remarked that the drawing is not all on the same scale, the horizontal capillary tube being shown, for convenience, much enlarged.

The planeness of the meniscus is tested by illuminating the meniscus by means of a 12 v. lamp and watching it through a pocket-lens. The illumination appears uniform when the meniscus is plane, and the setting, as shown by the figures quoted for h_1' and $(h_1+h_2+\frac{1}{3}r)$, is very sharp and consistent.

Experiments with Liquid Crystals.

The substances used all melted at temperatures above 100° C., and it was therefore necessary to devise some form of furnace in which to place the capillary. The simple design used is shown in fig. 3.

Fig. 3.

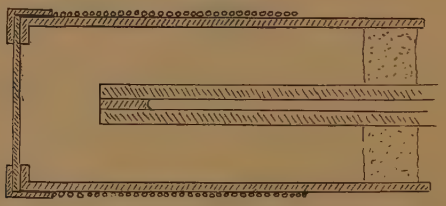

The furnace is supported on a tripod base not shown in the figure.

The furnace consists of a copper tube, asbestos covered, and closed at one end by a brass cap fitted with a window of optical glass. The capillary was clamped horizontally and passed into the tube, the gap at the back being loosely plugged with slag wool. The furnace tube was wound with a double layer of No. 26 S.W.G. nichrome wire, the total resistance being of the order of 100 ohms. Temperatures were read by means of a chromel-alumel thermocouple which had been calibrated using a standardized Black mercury thermometer. The couple was sensitive enough to made it possible to read to 0·2° C., and preliminary experiments showed that no sensible temperature gradient existed either along or perpendicular to the axis of the furnace over the region occupied by the liquid and the portion of the capillary in that immediate neighbourhood.

Previous experiments had also been made to determine the steady temperatures reached in the interior of the furnace in the vicinity of the tube when certain known currents were passing. Thus it was possible to obtain any required temperature in the furnace by passing the appropriate current through the furnace coils. The exact value of the temperature was, of course, obtained from the readings of the thermocouple.

The substances used were carefully purified and packed into the end of the capillary. The temperature was raised until the crystals melted, when observations were begun, and were continued until the temperature was well past the transition temperatures.

1. *Anisaldazine.*

The authors are indebted to Dr. Patterson, of Queen Mary College, who kindly provided a specimen of this

TABLE I.—Anisaldazine.

Transition temperature 180·5° C.
Manometer liquid aniline, density 1·026 gr./c.c.

Authors' figures.		Jaeger's figures.	
Temp. °C.	γ dynes/cm.	Temp. °C.	γ dynes/cm.
169·0	32·97	171·0	32·10
170·0	32·24	176·5	30·5
170·5	32·02	178·0	29·9
171·5	31·74	179·0	29·4
172·0	30·82	180·5	31·2
173·0	30·18	185·0	30·4
174·0	30·04	195·0	29·2
176·0	29·34	204·5	28·3
178·0	29·65	219·0	27·4
179·0	29·90		
179·5	30·23		
180·0	30·50		
181·5	30·38		
183·5	30·03		
186·0	30·09		
189·0	29·75		
190·5	29·61		
194·0	29·25		
199·0	28·85		
203·0	28·45		
204·0	28·42		

substance, and also recrystallized it from benzene and ligroin. The crystals were well formed, of a light yellow colour, and melted at 168·5° C.

These results are shown graphically in fig. 4.

Fig. 4.

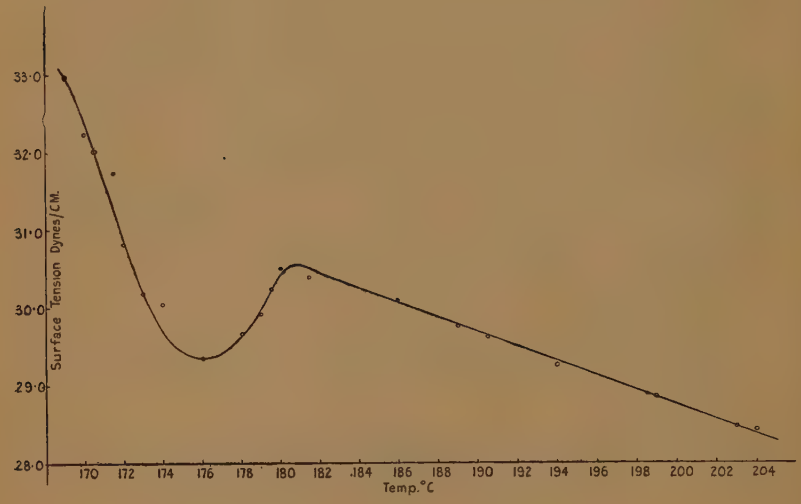

2. *p-azoxyanisol.*

This substance was obtained from Kahlbaum, and was purified by successive recrystallization from absolute alcohol. These crystals were very pale yellow in colour, well formed, and melted at 117° C.

TABLE II.—*p*-azoxyanisol.

Transition temperature 135° C.

Manometer liquid aniline, density 1·026 gr./c.c.

Temp. °C.	γ dynes/cm.	Temp. °C.	γ dynes/cm.
117·5	39·28	134·0	36·23
119·5	39·00	135·0	36·43
120·5	38·74	136·0	37·10
122·0	38·43	137·0	37·40
123·0	38·26	138·0	37·36
124·0	38·21	140·0	37·03
125·0	37·97	142·0	36·71
127·0	37·50	144·0	36·55
128·0	37·40	148·0	35·99
130·0	37·10	151·0	35·69
131·0	36·86	154·0	35·51
132·0	36·60	158	35·08
133·0	36·51	165·5	34·66

These results are shown graphically in fig. 5.

Fig. 5.

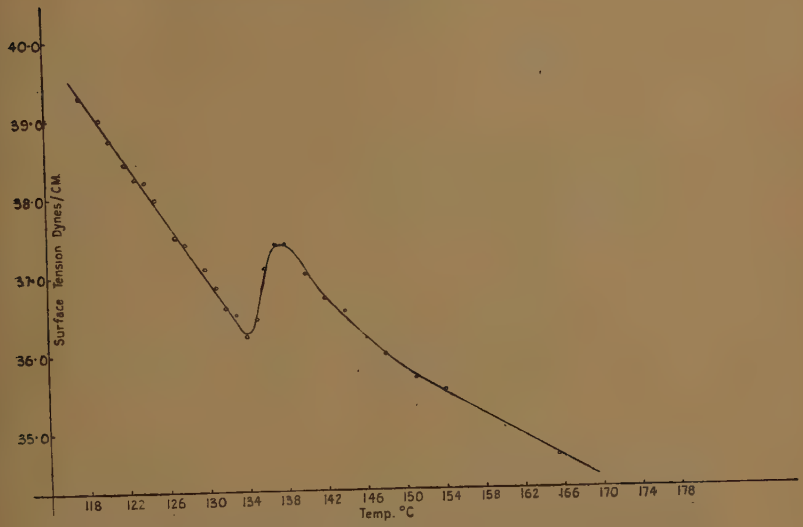

3. *p-azoxyphenetol.* Sample A.

This also was obtained from Kahlbaum and recrystallized in the same manner as for *p*-azoxyanisol. The purification was not so successful, the crystals not being so well formed, and eventually after several attempts the best that could be obtained were used. The melting-point was 141° C.

TABLE III.—*p*-azoxyphenetol. Sample A.
Transition temperature 162° C.
Manometer liquid aniline, density 1·026 gr./c.c.

Temp. °C.	γ dynes/cm.	Temp. °C.	γ dynes/cm.
145·0	31·17	168·0	28·70
146·0	31·09	169·0	28·77
147·0	30·70	170·0	28·77
150·0	30·45	172·5	28·37
152·0	30·10	173·0	28·25
154·0	29·98	181·5	27·65
156·0	29·38	188·0	27·49
158·0	29·06	189·0	27·41
160·0	28·85	195·5	26·75
162·0	28·59	200·0	26·28
164·0	28·41	205·0	26·20
166·5	28·55		

The results are shown graphically in fig. 6.

Fig. 6.

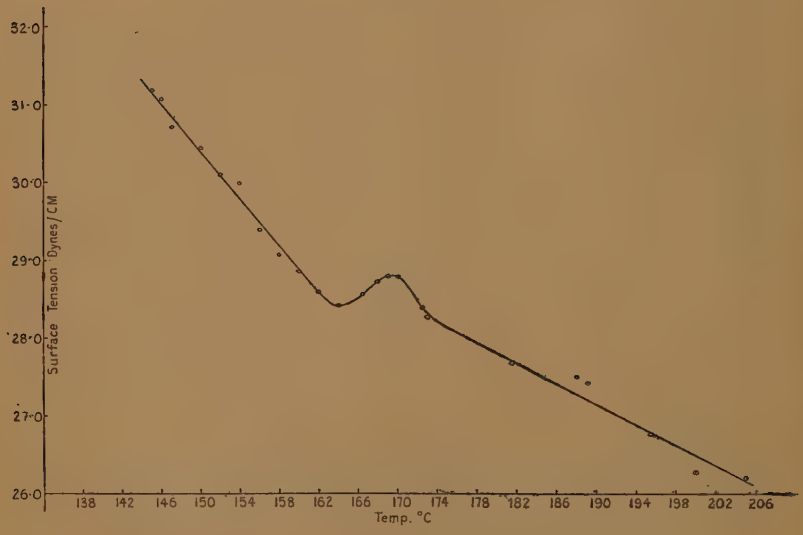

4. *p-azoxyphenetol.* Sample B.

This specimen was obtained through the kindness of Sir William Bragg, and was used without any further purification. The melting-point was 136·5° C.

TABLE IV.—*p*-azoxyphenetol. Sample B.

Transition temperature 165·5° C.

Manometer liquid aniline, density 1·026 gr./c.c.

Temp. °C.	γ dynes/cm.	Temp. °C.	γ dynes/cm.
137·5	31·95	160·0	29·20
138·0	31·73	162·0	29·14
139·0	31·62	162·5	29·00
143·0	31·26	164·0	28·90
145·5	31·05	165·5	28·85
146·0	30·93	166·0	28·84
147·0	30·88	168·0	28·59
151·0	30·14	169·0	28·77
154·0	29·88	171·0	28·70
155·0	29·75	172·0	28·54
157·0	29·60	174·0	28·04
158·0	29·38	183·0	27·45

It will be seen that in general the curves connecting surface tension and temperature have a " van der Waals " shape. The upward branches of these curves, which have been obtained again and again, are the only examples with which we are acquainted in which surface tension increases with temperature.

This work has been made possible by a grant from the Department of Scientific and Industrial Research to one of us (A. F.), who desires to express his thanks to the Advisory Council of the Department for their assistance.

References.

(1) Schenck, *Zeit. für phys. Chem.* xxv. p. 337 (1898).
(2) E. M. Jaeger, *Zs. für. anorg. u. allg. Chem.* ci. p. 1 (1917).
(3) G. Jaeger, *Wien. Ber.* ci. (20), pp. 158, 954 (1892).
(4) Ferguson and Kennedy, Proc. Phys. Soc. xliv. p. 511 (1932).

IV. *The Theory of Electrosmotic Circulation in Varying Fields.* *By* Paul White, *M.A., Ph.D.(Cantab.), Lecturer in Physics in the University of Reading* *.

THE electrosmotic circulation set up in a mass of liquid by the application of a constant electric field has been investigated by many workers both experimentally and theoretically and is now fairly well understood for simple cases. Very little information is available, however, concerning the motion set up by a varying field.

Svedberg and Andersson †, using an alternating E.M.F. of square wave-form at 11 cycles per sec., found that the distribution of amplitude of the periodic electrosmotic motion through the thickness (50 to 70 μ) of a laminar cell was not detectably different from the distribution of velocity which would have been set up by a constant field. Blüh ‡, on the other hand, measuring electrophoresis at higher frequencies (50 to 308 cycles per sec.) in a cell 6 μ deep, obtained indirect evidence from which he concluded that electrosmosis was entirely absent. Pugh and Swartz § found that in a cell 10 μ deep the

* Communicated by the Author.
† Svedberg, T., and Andersson, H., *Koll.-Zeit.* xxiv. p. 156 (1919).
‡ Blüh, O., *Ann. d. Phys.* lxxviii. p. 177 (1925) ; lxxix. p. 143 (1926) ; lxxx. p. 181 (1926).
§ Pugh, E. M., and Swartz, C. A., Phys. Rev. xxxvi. p. 1496 (1930).

electrosmotic motion was reduced, but not entirely eliminated. Beyond this there appears to be no experimental investigation for varying fields.

The great practical advantages of using either an alternating field or a very brief application of direct field in electrophoretic measurements and the necessity of then allowing for the electrosmotic motion make it desirable to investigate this motion for non-constant fields. In the present paper the distribution of electrosmotic velocity in laminar and cylindrical cells is examined theoretically for the case in which the field-strength varies with time in any manner. An account is also given of an experimental verification of the equations obtained for a particular frequency.

A theoretical treatment for alternating fields has recently been given by Rosenhead and Miller * in a form applicable to surface-conductivity measurements. This treatment is restricted to the case in which the liquid is free to move bodily along the cell, and thus there is no return current of the type to which v. Smoluchowski drew attention. The majority of electrophoretic experiments are, however, carried out in closed (or partly closed) cells where the return current is an important feature. It is therefore impossible to interpret the results of such experiments in terms of Rosenhead and Miller's theory, unless it can be established that the cells used were operating as truly " open " cells.

The treatment given here differs from that of Rosenhead and Miller in two respects. In the first place we neglect the finite thickness of the ionic cloud near the wall. This is justifiable in the case of the relatively deep cells ($>10^{-4}$ cm.) used in electrophoretic measurements with the ultramicroscope, since the net charge density of the cloud layer falls to $1/e$ of its maximum value in distances of the order of 10^{-6} cm. (*cf.* the quantity α^{-1} used by Rosenhead and Miller). On the other hand, the effect of closure or of partial closure of the cell in setting up v. Smoluchowski's return currents is taken into account, and a criterion is given for determining whether a given cell will behave as a closed, partly closed, or open cell at a given frequency.

* Rosenhead, L., and Miller, J. C. P., Proc. Roy. Soc A, clxiii. p. 298 (1937).

In order to deal with any type of variation of field-strength with time which can occur in practice, it is clearly sufficient to solve the problem for sinusoidal variation. Since the equations governing the electrosmotic motion are linear, a non-sinusoidal field can then be subjected to Fourier analysis, and the motions due to the component sinusoidal fields can be summed or integrated to give the motion due to the resultant field.

For convenience of reference the mathematical notation is indexed here.

A = cross-sectional area of a side tube.

$a = \sqrt{\frac{1}{2}kv}$.

b = breadth of a laminar cell.

c = radius of a cylindrical cell.

$f = \sqrt{-ikv}$.

g = acceleration of gravity.

h = height of a laminar cell.

$k = \rho/\eta$ = reciprocal of kinematic viscosity of sol.

l = length of a laminar cell between electrodes.

m is defined and used in equation (5) and the preceding equation only.

p = pressure-gradient along cell (instantaneous value).

p_0 = amplitude of p.

$Q = 1 - \frac{\nu^2 q \rho}{2h}$ for laminar cells; $= 1 - \frac{2\nu^2 q \rho}{c^2}$ for cylindrical cells.

q = net volume of liquid passing along cell per unit breadth per unit pressure-gradient set up.

r = radius vector in a cylindrical cell.

u = velocity of liquid.

v is defined by equation (2).

v_0, v_1, v_2 are defined by equation (6) and the preceding equation.

w = amplitude of electrosmotic velocity at a face of a cell.

= peak-value of applied field × electrosmotic mobility.

w_+, w_- are the values of w at the upper and lower faces respectively.

z = ordinate measured from the mid-point of a laminar cell.

$\alpha = (1+i)\, ah$.

$\beta = (1+i)\, az$.

η = viscosity of sol.

ν=frequency of applied field.
ρ=density of sol.
ϕ is the parameter of figs. 1, 2, and 3 and may equal ah or az.

§1. *Closed Laminar Cell.*

We consider first the case in which the cell is of rectangular section and its depth $2h$ is much smaller than either its length parallel to the field or its breadth. If we restrict our attention to the parts of the cell near the middle of it in plan, the effect of the end and side faces on the motion may then be neglected. Further, we suppose the cell to be staunch and to be completely filled with liquid (so-called " closed " cell) so that the net rate of transport of liquid across any section is nil at every instant.

The primary effect of the applied field is to set in motion the layer of liquid in immediate contact with the walls. This motion is then communicated to the interior by viscosity and at the same time establishes a pressure-gradient along the cell. Since there is no vertical motion except in the neighbourhood of the electrodes, there can be no vertical pressure-gradient in the middle of the cell other than the constant gradient due to gravity: the horizontal gradient, (pt) say, due to electrosmotic flow, must therefore be the same at all levels. It must also be of such magnitude that the return current caused by it in the middle levels just balances the primary current near the walls in order to satisfy the condition of no net transport.

The equation of motion in the part of the cell under consideration is clearly

$$\eta \frac{\partial^2 u}{\partial z^2} = \rho \frac{\partial u}{\partial t} + p(t), \quad . \quad . \quad . \quad . \quad . \quad (1)$$

where z is measured vertically from the mid-point of the cell, η is the viscosity, ρ the density, and $u\ (z, t)$ the horizontal velocity of the liquid.

If we write

$$v(z, t) = u(z, t) + \frac{1}{\rho}\int p(t)\, dt \quad . \quad . \quad . \quad . \quad (2)$$

and

$$k = \rho/\eta \quad . \quad . \quad . \quad . \quad . \quad . \quad . \quad (3)$$

this equation becomes

$$\frac{\partial^2 v}{\partial z^2} = k\frac{\partial v}{\partial t}. \quad . \quad . \quad . \quad . \quad . \quad . \quad . \quad (4)$$

Since the system contains a dissipative force (viscosity) and is maintained in motion solely by the action of an external simple-harmonic agency of frequency $\nu/2\pi$, say, every variable linearly describing the motion must have the same frequency, and we may set

$$p = p_0 e^{i\nu t}$$

and take as a trial solution

$$v = v_0 \exp\{(a+im)z + i\nu t\}.$$

We immediately find that

$$a = m = \pm\sqrt{\tfrac{1}{2}k\nu}. \quad . \quad . \quad . \quad . \quad . \quad . \quad (5)$$

The solution therefore consists of terms of the form

$$v = v_1 \exp\{(1+i)az + 2ia^2 t/k\}$$

and

$$v = v_2 \exp\{(-1-i)az + 2ia^2 t/k\}.$$

If the electrosmotic mobility is the same at both upper and lower faces of the cell *, the solution must be an even function of z and hence must be

$$\left.\begin{aligned} v &= v_0 e^{i\nu t}\cosh(1+i)az, \\ \text{and hence} \quad u &= v_0 e^{i\nu t}\cosh(1+i)az + ip_0 e^{i\nu t}/\rho\nu. \end{aligned}\right\} \quad . \quad . \quad . \quad (6)$$

The values of v_0 and p_0 are fixed by the boundary conditions and by the condition of no net transport of fluid. The boundary conditions require that at the upper and lower faces of the cell ($z = \pm h$) the velocity u should be the product of the electrosmotic mobility and the instantaneous value of the applied field-strength and therefore equal to $we^{i\nu t}$, say. We have, accordingly,

$$w = v_0\cosh(1+i)ah + ip_0/\rho\nu. \quad . \quad . \quad . \quad (7)$$

The condition of no net transport requires that

$$\int_{-h}^{h} u\,dz = 0 \quad \text{for all } t, \quad . \quad . \quad . \quad . \quad . \quad (8)$$

or

$$v_0 e^{i\nu t}\cdot\frac{\sinh(1+i)ah}{(1+i)ah} = -ip_0 e^{i\nu t}/\rho\nu. \quad . \quad . \quad . \quad (9)$$

* This is by no means always the case in practice. See, for example, Lane, T. B., and White, P., Phil. Mag. xxiii. p. 824 (1937). The possibility of unequal mobility is taken into account in the present treatment below, p. 58.

Combining equations (6), (7), and (8) and writing for brevity

$$\alpha=(1+i)ah,$$
$$\beta=(1+i)az,$$

we have

$$v_0=w/\{\cosh\alpha-\alpha^{-1}\sinh\alpha\}, \quad . \quad . \quad . \quad . \quad (10)$$
$$p_0=i\rho vw\sinh\alpha/\{\alpha\cosh\alpha-\sinh\alpha\}. \quad . \quad (11)$$
$$u=we^{ivt}\frac{\alpha\cosh\beta-\sinh\alpha}{\alpha\cosh\alpha-\sinh\alpha}. \quad . \quad . \quad . \quad . \quad (12)$$

Fig. 1.

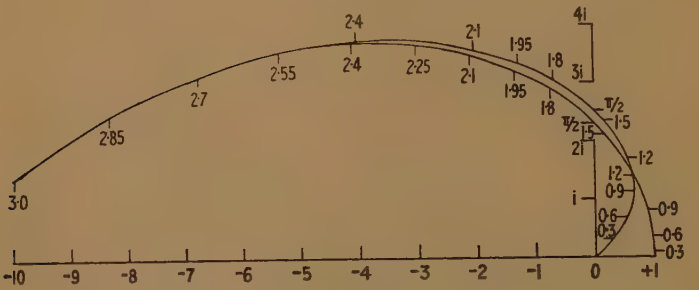

Argand diagrams for cosh and sinh of $(1+i)\phi$ for $0\leqslant\phi\leqslant3$.

Fig. 2.

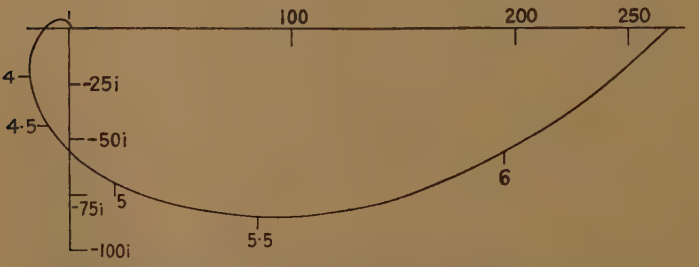

Argand diagrams for cosh and sinh of $(1+i)\phi$ for $0\leqslant\phi\leqslant2\pi$. The part of the curve above the real axis is shown on 26 times this scale in fig. 1.

In order to visualize the physical significance of these results and to obtain numerical values rapidly, it is convenient to use Argand diagrams of the functions cosh $(1+i)\phi$ and sinh $(1+i)\phi$, where ϕ is real. Such diagrams are given for $0\leqslant\phi\leqslant3$ in fig. 1, and on a smaller scale for $0\leqslant\phi\leqslant2\pi$ in fig. 2. The two functions are indistinguishable on this scale beyond $\phi=$about 2·5.

As an illustration of the use of these figures we may take the practical case arising in the verification described below (p. 62). A cell 3 mm. deep ($h=0{\cdot}15$ cm.) was filled with a hydrosol ($k=100$ gm. per c.c. per poise) and subjected to an alternating field of 1·3 cycles per sec. ($\nu=2{\cdot}6\,\pi$ sec.$^{-1}$); thus $ah=3{\cdot}03$. To find, for example, the motion at the levels $z=\pm 0{\cdot}0866$ cm. (these levels are of particular interest, as with a steady field they would be v. Smoluchowski's levels of no motion), we plot (fig. 3) the points A ($\phi=ah=3{\cdot}03$) and B ($\phi=az=1{\cdot}75$) on the curve for cosh $(1+i)\phi$ and the point C representing

Fig. 3.

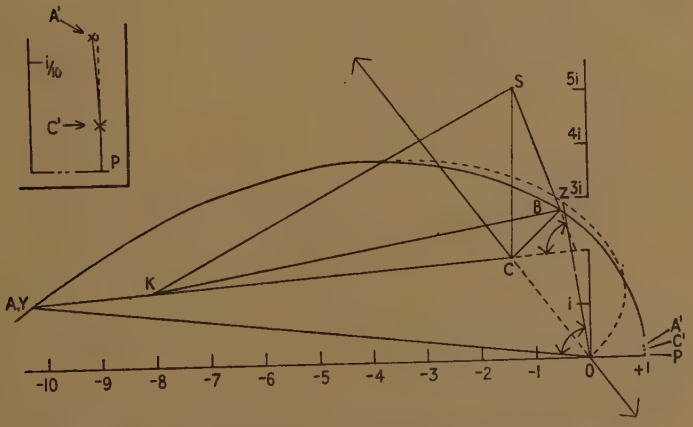

Graphical construction for velocities of liquid and particles.
Continuous line :— $^1\cosh\,(1+i)\phi$; broken line :— $^2\sinh\,(1+i)\phi$.
Inset.—Region of the curves for very small values of ϕ with scale × 20.
Phase of applied field and of oscillations of both liquid and particles at walls given by direction AKC.
Scale adjusted to make CA represent amplitude of liquid motion at wall (electrosmotic mobility × field strength).
CB represents amplitude and phase of oscillation of liquid at level corresponding to B ($\phi=az$) when $w_+=w_-$. KB represents oscillation of particle at same level. If $w_+\neq w_-$, CS and KS represent liquid- and particle-oscillations respectively.

the quantity $\dfrac{\sinh\{3{\cdot}03(1+i)\}}{3{\cdot}03(1+i)}$. The vectors CA and CB then represent respectively α^{-1} times the denominator and numerator in the expression for u. If CA be taken as representing in magnitude and phase the motion at the wall (electrosmotic mobility × field-strength), CB

will represent the *liquid* motion at the level in question. The amplitude and phase of the oscillation at any other level can be found by transferring B to the appropriate point on the cosh curve between A and P. The points C and A remain fixed for a given depth of cell, frequency, and kinematic viscosity (k^{-1}).

What is frequently of more interest than the electrosmotic motion of the liquid (CB) is the oscillation of a suspended colloid particle at the given level. If we assume that the adjustment of the pure electrophoretic motion (relative velocity of particle and adjacent liquid) to the applied field-strength is instantaneous *, we can represent this relative motion by a vector CK plotted off along CA of such a length that CK/CA equals the ratio of the electrophoretic to the electrosmotic mobility, which we assume to be known. K is thus fixed independently of the level for which the calculation is to be carried out, KB represents the amplitude of the resultant oscillation of the colloid particle and $\angle$ BKA its phase-lag on the applied field. In fig. 5 the distribution of amplitude through the cell is shown for an actual case.

In order to apply the present theory to the experiments of Svedberg and Andersson it would strictly be necessary to carry out a Fourier analysis of the wave-form of the voltage they used. A considerable insight into the behaviour of the particles can, however, be gained by neglecting all the harmonics except the fundamental and treating the case as if alternating current of sine wave-form at 11 cycles per sec. had been applied. Taking h as $60\,\mu$, we find $ah = 0{\cdot}36$. The points C and A are therefore situated at C′ and A′ in fig. 3 (see inset). It might appear at first sight that, since C′A′ is so much shorter than CA in the main diagram, very little movement were to be expected. The *scale*, however, is controlled by the length of C′A′ and, in fact, the distribution of amplitude through the cell, in this case as in every case where ah comes out to be about unity or less, is predicted by the diagram to be scarcely distinguishable from the distribution of velocity in the case of a steady field. This is what Svedberg and Andersson found.

The condition that an alternating-current experiment should give results corresponding closely to those given

* The experiments of Pugh and Swartz (*loc. cit.*) indicate that this is so, at least, for moderate frequencies.

by a direct-current experiment is, as we have seen, that ah should not exceed unity. Where the dispersion medium is water ($k=100$) this implies that the square of the total depth of the cell in centimetres multiplied by the frequency of the current must not exceed 0·013. If ah is greater than unity it will still be possible to measure the electrokinetic phenomena by the ultramicroscope, but it will be necessary to evaluate the results by means of the present theory and not in terms of the theory for steady fields.

In Blüh's experiments ah was never greater than 0·1, and the electrosmosis must therefore be presumed to have been of the typical steady-field kind. His criterion for the total absence of electrosmosis (undistorted linear particle-tracks) appears to be quite illusory in the light of the better understanding of the phenomenon possible of recent years. The marked scatter of his results, though in part due to observational difficulties, as he was aware, must also have been caused to a great extent by the particles being at a variety of levels and their motion consisting of electrosmotic and electrophoretic components in different proportions, as Pugh and Swartz pointed out.

In both Blüh's experiments and those of Pugh and Swartz with single phase current, we probably have to do also with cells which were not staunch in the sense in which the word is used here. The presence of drainage channels modifies the motion considerably, and the good agreement of Svedberg and Andersson's results with the present theory is largely due to the design of their cell, which was directed specially to preventing the escape of liquid. The question of incompletely closed cells is further treated below (p. 58).

The brilliant work of Pugh and Swartz with two phase alternating current requires separate treatment, as the results obtained in the present paper are not applicable to three-dimensional motion without further consideration.

It is a matter of some interest to compute the magnitude of the pressure gradient set up along the cell. The amplitude of this oscillatory gradient is given on the Argand diagram by $\rho\nu \times \mathrm{CO}$ and its phase by $\mathrm{O\hat{C}A} - 90°$. In the experiment made to check the present theory (p. 61) the electrosmotic mobility was about $2{\cdot}2 \times 10^{-4}$ cm.^{2}/volt. sec., a figure which gives a peak value of $5{\cdot}4 \times 10^{-3}$ dynes/sq. cm. for the total pressure difference between

the ends of the cell per volt applied at the electrodes. The smallness of this quantity explains the experimental fact, frequently observed with surprise, that cells constructed with quite large openings (*e. g.*, the Tuorila type *) can behave as " closed " cells.

§ 2. *Unequal Mobilities at Opposite Faces.*

We have hitherto supposed that the electrosmotic mobilities at the upper and lower faces were equal. Lane and the author (*loc. cit.*) have, however, shown that this condition is not necessarily fulfilled in practice. The foregoing treatment can easily be modified to take account of a possible difference between w_+ and w_-, the mobilities at the upper and lower faces respectively. Equation (12) of page 54 then becomes

$$u=e^{i\,t}\left[\tfrac{1}{2}(w_+ + w_-)\,\frac{\alpha\cosh\beta-\sinh\alpha}{\alpha\cosh\alpha-\sinh\alpha}+\tfrac{1}{2}(w_+ - w_-)\,\frac{\sinh\beta}{\sinh\alpha}\right].$$

while in equation (11) for p_0 it is sufficient to replace w by $\frac{1}{2}(w_+ + w_-)$.

These results can be represented graphically by a slight adjustment of fig. 3. The scale has now to be taken so that CA represents $\frac{1}{2}(w_+ + w_-)$. S is then plotted off from B so that BS is equal to $\dfrac{w_+ - w_-}{w_+ + w_-}\cdot\dfrac{\sinh\beta}{\sinh\alpha}$ on this scale, while the angle between BS and CA is equal to the angle between OY and OZ, Y and Z being the points on the *sinh* curve for which $\phi = ah$ and az respectively. KS is then the resultant motion of the particle, CS that of the liquid.

§ 3. *" Closed " and " Open " Cells.*

If the cell is so designed that the liquid fills it entirely and no liquid escapes, the net flow across any surface within it must be zero at every instant. We call such a cell a " closed " cell and take account of this property mathematically by means of equations (8) or (9). It is often convenient to construct " open " cells and to rely on surface tension forces and/or gravity to retain the liquid. In such cases a small net amount of liquid passes along the cell in the direction of the electrosmosis

* Tuorila, P., *Koll.-Zeit.* xliv. p. 15 1928)

and by distorting the meniscus and/or altering the levels of the free surfaces, establishes the pressure-gradient responsible for the return current, if any. As we have seen above (p. 57) the gradients necessary are very small, and we may therefore take them to be proportional to the net volume of liquid transported along the cell. If q is the net volume (per unit breadth of cell) which must be moved to set up unit pressure-gradient, we may replace equation (8) by

$$q.p(t) = \int dt . \int_{-h}^{h} u\, dz$$

$$= \frac{2he^{ivt}}{iv}\left[v_0 \frac{\sinh \alpha}{\alpha} + \frac{ip_0}{\rho\nu} \right].$$

Combining this equation with equations (6) and (7) and writing for brevity

$$Q = 1 - \frac{\nu^2 q \rho}{2h},$$

we have

$$p_0 = \tfrac{1}{2}(w_+ + w_-) \frac{i\rho\nu \sinh \alpha}{Q\alpha \cosh \alpha - \sinh \alpha},$$

$$u = e^{ivt}\left[\tfrac{1}{2}(w_+ + w_-) \frac{Q\alpha \cosh \beta - \sinh \alpha}{Q\alpha \cosh \alpha - \sinh \alpha} + \tfrac{1}{2}(w_+ - w_-) \frac{\sinh \beta}{\sinh \alpha} \right].$$

For a closed cell $q = 0$; $Q = 1$.

For an open cell $0 < q < +8$; $1 > Q > -\infty$.

The behaviour of an open cell may be represented graphically by substituting for the point C of fig. 3, the point C″ on the line OC, such that $OC = Q . OC''$. C″ may lie anywhere on the line OC produced indefinitely either way, but not between O and C. An interesting condition arises when Q is zero and thus C″ at infinity. Both the amplitude and the phase of the liquid motion are then uniform through the cell and the liquid moves as a rigid body. The same is true of the assembly of the colloid particles. This case occurs when $\nu^2 = 2h/q\rho$, that is, when the applied field is in resonance with the natural frequency of oscillation of the contents of the cell under the action of the surface tension or gravity forces. It is usually impossible to determine this natural frequency

directly by displacing the liquid and timing its oscillations with the electrodes disconnected as the movement is heavily damped by viscosity. If an A.C. supply of variable frequency is available the simplest method of measuring Q, and hence q, is to find that frequency for which the track of the particles is of the same length at all depths in the cell.

The quantity q, which we might call the *absolute staunchness*, is of fundamental significance for the behaviour of a given design of cell at various frequencies. The behaviour at a given frequency is best expressed in terms of Q, which varies with frequency and which might be called the *coefficient of staunchness*. In order to form a clearer picture of the physical meaning of Q and q, and

Fig. 4.

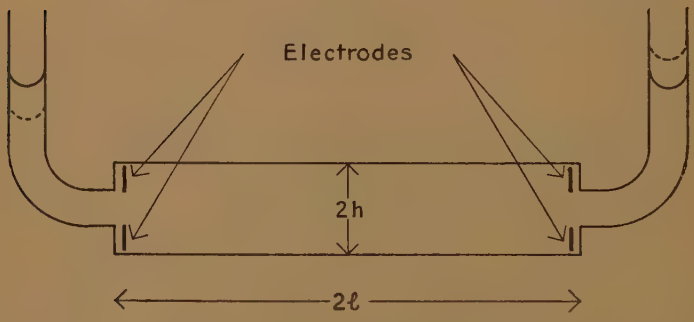

to gain some idea of their magnitude in an actual case, consider the cell illustrated in fig. 4, of height $2h$, breadth $2b$, and length $2l$ between the electrodes. For filling it is fitted behind the (pierced) electrodes with two similar tubes of cross-sectional area A, bent upwards to retain the liquid. The tubes are sufficiently short and wide for the inertia and viscous drag of the fluid in them to be negligible compared with the corresponding quantities for the main body. The transport of unit volume per unit breadth will alter the level of the free surface in each tube by b/A and hence induce a pressure-gradient of $2\rho gb/\mathrm{A}l$. The absolute staunchness is therefore $\mathrm{A}l/2\rho gb$, and the coefficient of staunchness at frequency ν is

$$1-\frac{\nu^2}{4g}\cdot\frac{\mathrm{A}l}{hb}.$$

The critical frequency at which Q=O is that of a simple pendulum whose length is four times the length of the cell between electrodes multiplied by the ratio of the cross-sectional area of the cell to that of either side-tube.

§ 4. *Cylindrical Cells.*

The problem for a cylindrical cell is similar to that for a rectangular one, and it will be sufficient to indicate the main points of difference and to quote the final results. The question of unequal mobility at opposite faces does not arise, but that of open construction must still be considered in this case. Let the radius be c.

Equation (1) is now to be replaced by

$$\frac{\eta}{r}\cdot\frac{\partial}{\partial r}\left(r\frac{\partial u}{\partial r}\right)=\rho\frac{\partial u}{\partial t}+p(t),$$

with a corresponding change in (4).

The solution for v becomes

$$v=v_0e^{ivt}\mathrm{J}_0(r\sqrt{-ikv}),$$

where J_0 is the Bessel function of order zero. This leads to

$$p_0=\frac{i\rho vw\mathrm{J}_1(cf)}{\frac{1}{2}\mathrm{Q}cf\mathrm{J}_0(cf)-\mathrm{J}_1(cf)},$$

$$u=we^{ivt}\cdot\frac{\frac{1}{2}\mathrm{Q}cf\mathrm{J}_0(rf)-\mathrm{J}_1(cf)}{\frac{1}{2}\mathrm{Q}cf\mathrm{J}_0(cf)-\mathrm{J}_1(cf)},$$

where $\mathrm{Q}=1-\frac{2\nu^2\rho q}{c^2}$ and $f=\sqrt{-ikv}$.

Numerical values can easily be obtained from tables of the ber and bei functions since

$$\mathrm{J}_0(rf)=\mathrm{ber}(r\sqrt{kv})+i\,\mathrm{bei}(r\sqrt{kv}).$$

$$\mathrm{J}_1(rf)=-\frac{1+i}{\sqrt{2}}\{\mathrm{ber}'(r\sqrt{kv})+i\,\mathrm{bei}'(r\sqrt{kv})\}.$$

The graphical technique of pages 55 *et seq.* can be used in an exactly analogous fashion if the Argand diagrams for cosh and sinh are replaced by those for J_0 and J_1 respectively and ϕ is taken as rf or cf.

§ 5. *Experimental Test.*

In view of the wide range of values through which each of the three independent variables ν, h, and q can

pass, it was out of the question to attempt an exhaustive test of the theory. It seemed best, in fact, to concentrate on one set of conditions in a region where the peculiar predictions were most striking and to avoid, as far as possible, the conditions used by previous workers. The results of these workers, using in every case very shallow cells ($<1/10$ mm. deep) and moderate frequencies (>10 sec.$^{-1}$), were certainly consistent with theory. An experiment with a deeper cell and a lower frequency was therefore desirable, the more so as by keeping ah greater than unity it was possible to test just those predictions of the theory which are in marked contrast with the theory for steady fields.

A cell of the Tuorila type (*loc. cit.*), 3 mm. deep, was available for the work. At this depth a frequency of the order of one alternation per second is sufficient to ensure that ah is well above unity for an aqueous dispersion ($k=100$). It is, of course, desirable to keep the frequency as low as possible, since the length of the particle-tracks is inversely proportional to the frequency for a given peak-velocity in any periodic oscillation.

It was impossible to explore the whole depth of the cell with a high power objective on account of the long working distance required with a deep cell. A 2/3 inch objective was the highest power which could be used, and the consequent rather low magnification necessitated a high voltage.

An A.C. supply of 300 volts peak value at $1{\cdot}3\sim$ was obtained by applying 600 volts D.C. to the terminals of a 1200 ohm rheostat and driving a light sliding contact over it by means of a long connecting rod actuated from a gramophone turn-table (78 r.p.m.).

The sol used was a gold hydrosol obtained by reduction with hydrogen peroxide and having a particle diameter of about 9×10^{-6} cm. This sol was prepared by Dr. H. Liebmann, who also kindly undertook the whole of the very trying visual observations with the ultra-microscope. I should like to express here my sincere gratitude to Dr. Liebmann for his help, without which the experimental tests would have presented great difficulties.

The procedure was first to measure the particle velocity with D.C. in the ordinary way at the two levels given by v. Smoluchowski and at the middle of the cell. From these readings the electrophoretic mobility of the particles

and the electrosmotic mobilities of the medium at the upper and lower faces could be calculated *. A.C. was then applied and the voltage adjusted by means of a series resistance in the rheostat circuit until the range of the oscillatory motion of the images of particles in sharp focus just equalled the distance between two fine parallel wires mounted in place of an eye-piece scale. This voltage was measured by a D.C. voltmeter across the rheostat and the corresponding value of KS calculated from the equation:

$$\text{Track length} \times \nu = \text{KS} \times \text{voltage} \times \text{electrophoretic mobility.}$$

Fig. 5.

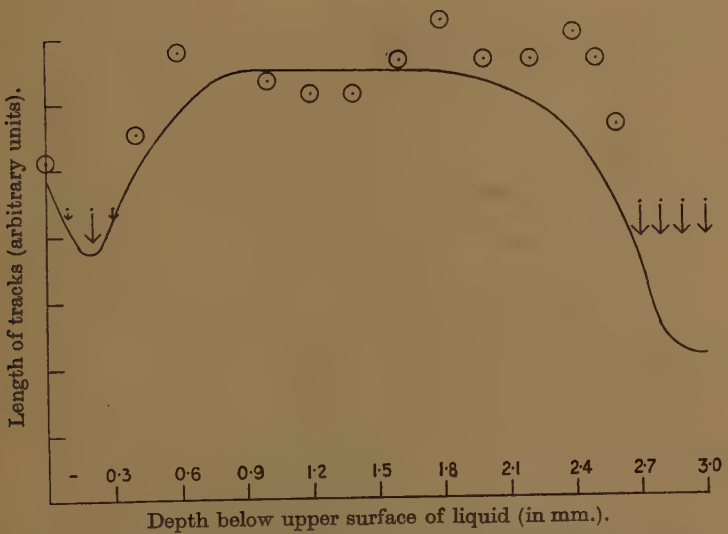

Some difficulty was experienced in securing readings at a sufficient number of different levels before convection currents caused by heating and by products of electrolysis became detectable.

In fig. 5 the results of a typical series of measurements under good conditions are shown together with the theoretical curve calculated from the mobilities found with D.C. and a value of $-\frac{1}{2}$ for Q. Arrows indicate that the mobility at the level in question was slightly too small to bring the range of motion of the images

* White, P., Phil. Mag. xxiii. p. 811 (1937).

of the particles out to the wires with the whole voltage available. In view of the fact that owing to electrolysis a series of readings cannot be repeated without changing the sample of sol the agreement is good. The error of a typical single measurement was estimated at the time as being possibly as great as 10 per cent., due to the finite size of the diffraction images and the difficulty of observing on a moving object. The median percentage deviation of the points from the curve in the figure is, however, only 5 per cent. There is some evidence on the right of the diagram (later readings) that a progressive increase in electrosmotic mobility has taken place during the experiment—an effect which was not altogether unexpected in the light of the observation of Lane and the author (*loc. cit.*) that the difference between the electrosmotic mobilities at the two faces of a cell increases with continual use. The main features of the curve—a flat central portion and distinct minima much greater than zero—are, however, well confirmed and are in marked contrast with the parabolic distribution given by steady voltages. They were observed in all cases where the motion was reasonably free from convection.

An attempt to measure the distribution of phase of the motion through the cell gave results which were in general agreement with theory, but could not be made accurate enough to bear much weight.

The value of $-\frac{1}{2}$ for Q was found by trial so as to give the best fit to the measurements. As the liquid is retained in cells of the Tuorila type purely by surface tension it is impossible to make a theoretical estimate of the value to be expected for this constant without an extended investigation of the distortion of the meniscus by the pressure-gradient.

It is a pleasure to have this opportunity of thanking Professor J. A. Crowther for his sympathetic interest in this work.

Summary.

The electrosmotic motion set up in a liquid by an alternating electric field is examined theoretically for laminar and cylindrical cells. In an experiment with a cell 3 mm. deep and alternating current of $1{\cdot}3\sim$ results were obtained which were not in accordance with the

usual theory of electrosmosis for steady fields, but which agreed well with the present theory. Results of previous experiments by other workers with A.C. also agree with the present theory.

The behaviour of open cells (*e. g.*, of Tuorila's type) is examined and a criterion is given for determining whether a given cell will operate as a closed, partly closed, or open cell at a given frequency.

A method is described whereby the theory can be extended from alternating fields to apply to fields varying with time in any manner.

The University of Reading.
April 7th, 1938.

V. *The Parabolic Law of Oxidation.* *By* G. D. Preston, *M.A.** (From the National Physical Laboratory.)

Summary.

The type of pressure-time relation which will be observed when oxidation experiments are carried out at constant volume is discussed. Certain very accurate observations on copper by Wilkins and Rideal are shown to conform to the parabolic law of oxidation provided the constant occurring in the law is assumed to be proportional to the oxygen pressure. It is pointed out that the occurrence of a logarithmic pressure-time relation is consistent with the parabolic law if the constant is a quadratic function of the pressure; experimental evidence for molten lead is cited as indicating that such a relation has been observed. Attention is directed to the large rate of oxidation observed by Wilkins when the oxygen pressure over a copper specimen is suddenly increased; it is suggested that this observation may have a bearing on the problem of corrosion fatigue.

---

(1) The parabolic law of oxidation, associated with the names of Tammann [1] and of Pilling and Bedworth [2], which is obeyed by a large number of metals is usually stated in the form

$$w^2 = 2kt, \quad . \quad . \quad . \quad . \quad . \quad . \quad . \quad (1)$$

* Communicated by C. H. Desch, F.R.S.

where w is the weight of oxygen combined on unit area of the metal surface at time t, the initial weight at $t=0$ being zero. The equation is supposed to be derived by integration of the expression

$$w\frac{dw}{dt}=k, \quad . \quad . \quad . \quad . \quad . \quad . \quad . \quad (2)$$

which expresses the fact that the rate of oxidation is inversely proportional to the thickness of the oxide film, the film being supposed to be uniform, so that w is proportional to the thickness. When experimental determinations of w and t are made at constant temperature and constant pressure the parameter k in (2) is treated as constant, and integration yields equation (1) with an added constant, w_0^2, representing the square of the weight of oxygen per unit area already combined at the instant $t=0$. In certain circumstances, when, for instance, it is desired to study the process of oxidation at elevated temperatures and low pressures, it is convenient to carry out the experiments at constant volume and to utilize the observed pressure changes to measure the quantity of oxygen absorbed by the oxidation of the metal. In this case if the reaction is carried out in a vessel of volume v c.c. at a temperature T° K. we will have

$$p_0v=m_0\mathrm{RT}$$

and

$$pv=m\mathrm{RT},$$

p_0, m_0 being the pressure and the mass of oxygen present at time $t=0$, and p, m the same quantities at some subsequent instant, t. R is the gas constant per gramme. The mass of gas absorbed in the interval t is m_0-m, so that

$$w=(p_0-p)\frac{v}{\mathrm{RTA}}+w_0, \quad . \quad . \quad . \quad . \quad . \quad (3)$$

w_0 representing the mass of oxygen per unit area already on the surface when the first pressure reading, p_0, is recorded at the instant $t=0$, and A being the total area exposed. To interpret the results of experiments made at constant volume this value of w is substituted in (2), and some assumption is then made regarding the dependence of k on pressure. Integration of the resulting equation leads to an expression of p as a function of t which can be compared with the observational data.

In a recent investigation of the oxidation of molten lead [3] it was found that the results could, in the early stages of oxidation, be quite satisfactorily accounted for on the assumption that k of equation (2) is proportional to the pressure. The dependence of k on pressure has not received very much attention, although it was investigated by Pilling and Bedworth in the case of copper; but certain observations on copper by Wilkins and Rideal [4] appeared to provide suitable data for a further test of the relation found to hold in the case of molten lead. Although the authors (Wilkins and Rideal) give another interpretation, the accuracy of their observational data is exceptional, and it is for this reason that they have been chosen for investigation.

(2) In this section I propose to consider the results obtained by Wilkins [5] on the oxidation of copper. The figures given in Tables I., II., and III. are taken from his paper. They form a series of observations of the pressure changes during the oxidation of the same specimen at 183° C., fresh oxygen being admitted to the apparatus in the intervals between the three sets of observations. Wilkins interprets the results on the assumption that k of equation (2) is constant (*i. e.*, independent of the pressure), and concludes that there is a critical pressure below which the parabolic law is not obeyed, on the grounds that the data of Tables II. and III. agree with that law when k is a constant while those of Table I. do not. In the sequel it will be shown that all the data are consistent with the parabolic law if k is assumed to be proportional to the pressure, but before proceeding to this there are one or two points to which it is desirable to draw attention when the condition k=constant is assumed.

Following Wilkins, we assume that k is constant, and making the substitution (3) in (2) we have

$$\frac{d}{dt}(w^2)=2k,$$

giving on integration

$$\left\{p-\left(p_0+\frac{\mathrm{RTA}w_0}{v}\right)\right\}^2=2\left(\frac{\mathrm{RTA}}{v}\right)^2 kt+\left(\frac{\mathrm{W}_0\mathrm{RTA}}{v}\right)^2,$$

which is of the type

$$(p-a)^2=bt+c, \quad \ldots\ldots\ldots \quad (4)$$

where
$$a = p + \frac{\mathrm{RTA}w_0}{v},$$
$$b = 2\left(\frac{\mathrm{RTA}}{v}\right)^2 k,$$
$$c = (a - p_0)^2.$$

The parameters a, b, c have been calculated for the data of Tables II. and III., with the results :—

	Table II.	Table III.
a	45·68	72·07
b	0·01595	0·00747
c	1·72	0·98
p_0	44·37	71·08

TABLE I.

(i.)	(ii.)	(iii.)	(iv.)	(v.)
t.	τ sec.	p mm.	τ calc. (4)	τ calc. (6).
50′ 39″ ..	0	26·40	—	0
	16	23·80	—	13
	32	22·22	—	32
	49	20·94	—	53
	86	19·34	—	90
	108	18·43	—	116
	128	17·93	—	133
	154	17·26	—	159
	174	16·86	—	172
	216	16·22	—	200
	258	15·88	—	—
55′ 36″ ..	297	15·58	—	—

TABLE II.

(i.)	(ii.)	(iii.)	(iv.)	(v.)
t.	τ sec.	p mm.	τ calc. (4).	τ calc. (6).
57′ 20″ ..	0	44·37	0	0
	43	44·13	43	43
	100	43·85	102	98
	160	43·64	153	152
	220	43·41	215	211
	340	43·00	343	341
65′ 0″ ..	460	42·67	460	466

There are two points to which attention is drawn: (1) the values of b are not equal, so that although we have assumed k to be independent of p we must still suppose it to be a function of the initial pressure p_0. It is assumed that the introduction of oxygen was effected without changing the volume of the reaction vessel; (2) corresponding to each of the parabolæ (4) we can find a time t_0, preceding the instant $t=0$, at which the tangent to the curve is parallel to the pressure axis. This point corresponds to an infinite rate of oxidation, and cannot be realized physically, but if the surface were initially

TABLE III.

(i.)	(ii.)	(iii.)	(iv.)	(v.)
t.	τ sec.	p mm.	τ calc. (4).	τ calc. (6).
67′ 0″ ..	0	71·08	0	0
	120	70·70	120	120
	240	70·50*	—	—
	—	70·40	242	241
	360	70·15	362	361
	480	69·96	464	463
	660	69·66	646	644
	900	69·27	919	917
	1140	68·96	1163	1162
	1380	68·71	1380	1380

clean a very large oxidation rate might be observed. Leaving this question aside it will be seen from (4) that $t_0=-c/b$ when $p=a$. For Table II. $t_0=-108$ secs., for Table III. $t_0=-131$ secs., figures which are very close to the intervals between the times at which observations stopped in one table and started in the next. For Tables I. and II. this interval is 104 secs., for Tables II. and III. it is 120 secs. The difference between these figures and the values of t_0 could no doubt be reduced by small adjustments of the constants without altering the agreement of the calculated pressure-time curve with the observations. In both cases the agreement is sufficiently close to show that when fresh oxygen is admitted the rate of oxidation is very large and approximately

* It has been assumed that this is a misprint, and should be 70·40.

equal to that which would have been observed if the surface had been free from oxide, although the surface is in each case covered by the layer of oxide produced in the earlier experiments. This can be quite clearly seen in fig. 1, where the circles represent the data. The ordinates are $(a-p)$ for curves II and III, which correspond to Tables II. and III. For curve I the ordinate is p_0-p, p_0 being the first value (26·4) of Table I.; the scale for this curve is one-fifth of that for the other two. The vertical lines at the last observed points on curves

Fig. 1.

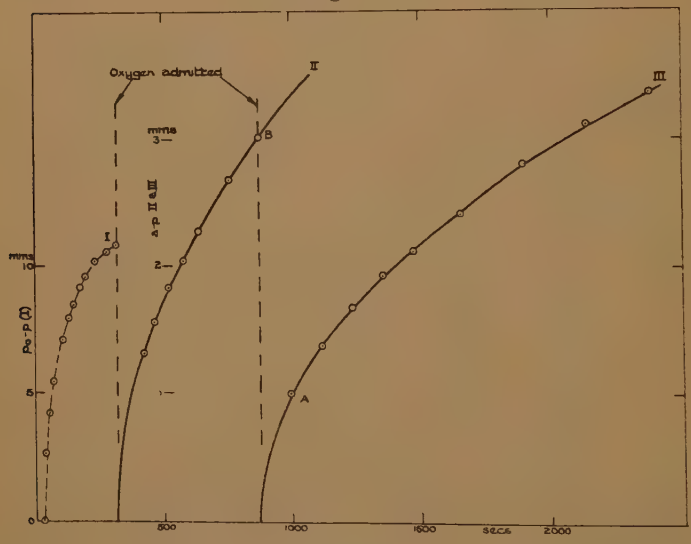

I and II are seen to correspond roughly with the tangents to the apsides of the calculated curves II and III. It will also be seen that the experimental points lie on the calculated curves very exactly. At the point B on II the rate of oxidation $dp/dt = \cdot 0026$ mm./sec., while at A, the first observation on III, the rate is ·0037 mm./sec., nearly 50 per cent. larger. These rates are proportional to the rate of weight increment. The introduction of oxygen has thus caused a rise in the rate of oxidation, but a fall in the value of the parameter b of equation (4).

(3) The experimental data given in Table I. do not fit on a parabolic pressure-time curve of the type (4). Wilkins

interpreted this as indicating that below a certain critical pressure the parabolic oxidation law (2) ceased to be obeyed. This would be true if we were sure that k was independent of pressure, but if k is a function of the pressure then the pressure-time relation is not of the form (4). Actually all the results are very well represented by the assumption that k in (2) is proportional to the pressure. With this assumption we have, using (3),

$$-\frac{v}{\mathrm{RTA}}\left((p_0-p)\frac{v}{\mathrm{RTA}}+w_0\right)\frac{dp}{dt}=kp,$$

where k has now a different significance but is still supposed to be independent of p. On integrating, setting $p=p_0$ when $t=0$, this leads to

$$\frac{p-p_0}{p_0}-\left(1+\frac{w_0\mathrm{RTA}}{v}\right)\log_e\frac{p}{p_0}=\frac{(\mathrm{RTA})^2}{p_0v^2}kt, \quad . \quad (5)$$

an equation which has been used by Hinshelwood [6] in the simpler form when $w_0=0$. For purposes of computation it is simpler to write this in the form

$$\left.\begin{aligned} &\frac{p-p_0}{p_0}-a\log_{10}\frac{p}{p_0}=bt,\\ \text{with}\quad &a=\left(1+\frac{w_0\mathrm{RTA}}{p_0v}\right)\log_e 10,\\ \text{and}\quad &b=\frac{(\mathrm{RTA})^2}{p_0v^2}\mathrm{K}. \end{aligned}\right\} \quad . \quad . \quad . \quad (6)$$

This formula represents a pressure-time relation which over a limited range is very nearly identical with the parabolic expression (4). Taking the simple case in which $w_0=0$, and expanding $\log p/p_0$, we find

$$\begin{aligned}\log_e\frac{p}{p_0}&\equiv\log_e\left(1+\frac{p-p_0}{p_0}\right)\\ &\equiv\frac{p-p_0}{p_0}-\frac{1}{2}\left(\frac{p-p_0}{p_0}\right)^2+\frac{1}{3}\left(\frac{p-p_0}{p_0}\right)^3\end{aligned}$$

—substituting in (5) the first term cancels out, and we are left with

$$\frac{1}{2}\left(\frac{p-p_0}{p_0}\right)^2-\frac{1}{3}\left(\frac{p-p_0}{p_0}\right)^3+\ldots=\frac{(\mathrm{RTA})^2}{p_0v^2}kt.$$

Provided $(p-p_0)/p_0$ is so small that its cube can be neglected in comparison with its square, this expression will be

experimentally indistinguishable from (4). This condition is satisfied for the figures given in Tables II. and III. In the middle of each of these tables the value of $(p-p_0)/p_0$ is less than $-\cdot 02$ and the value of $p-p_0$ is about 1 mm. To distinguish experimentally between (6) and (4) an accuracy of at least 2 per cent., *i.e.*, $\cdot 02$ mm., would be necessary. Accurate though the observations are they can hardly be expected to show this small difference. The agreement between formula (6) and the

Fig. 2.

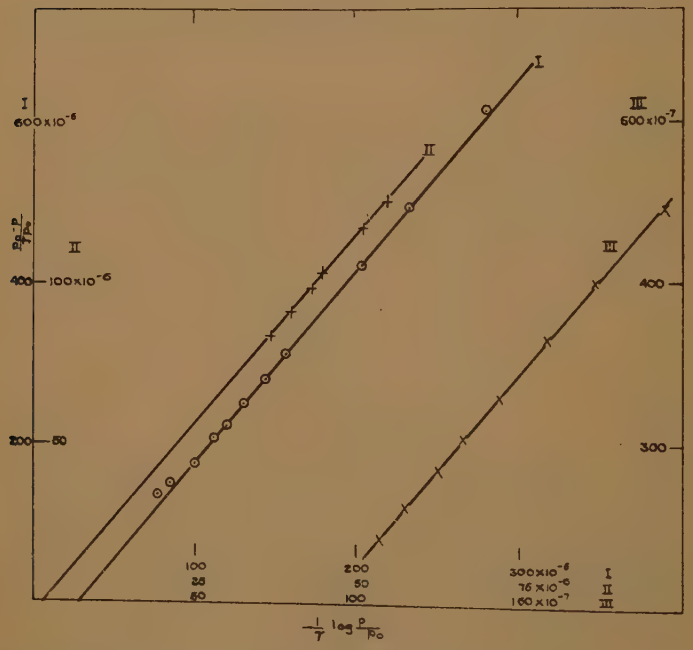

observations of Wilkins is shown graphically in fig. 2. Here $-(p-p_0)/tp$ is plotted against $-1/t \log_{10} p/p_0$, the result being three straight lines. The slope of the lines is a measure of the value of a in (6): with the scales used in the diagram the approximate parallelism of the lines indicates that a is nearly the same in each case. With the exception of two points at the end of I nearest the origin, corresponding to the last two observations, it will be seen that very good agreement is shown. The

values of the parameters a and b of equation (6) are as follows :—

TABLE (a).

	a.	$b \times 10^6$.	p_0.	$bp_0 \times 10^5$.
I.	2·352	560	26·4	148
II.	2·362	3·80	44·37	16·9
III.	2·336	0·769	71·08	5·47

The values of p_0 and bp_0 have been added, as comparison of (5) and (6) shows that bp_0 is now proportional to k. The numerical values obtained from equations (4) and (6) are given in columns (iv.) and (v.) of Tables I.–III. The values of the times, t, corresponding to the observed pressures have been calculated, as (6) cannot be conveniently used to calculate the pressure at a given time. So far as II and III are concerned, the two formulæ give results which differ very little ; either formula gives an adequate description of the process over the very limited range of p/p_0 covered by the observations. The figures given in Table I. cannot be described at all by a formula of the type (4), but it will be seen that the calculated times are in very fair agreement with those observed when formula (6) is used, the agreement extending over a range of p/p_0 from 1 to 0·6.

This shows that Wilkins's case for departure from the parabolic law of oxidation is not proved by his figures. The pressure-time relation (6) is consistent with the parabolic law at constant pressure provided the parameter k of (2) is assumed to be proportional to the pressure.

The values of a and b given above present the same two points of interest referred to in section (2). The values of b or bp_0 differ greatly in the three experiments, and the values of a are nearly equal to $\log_e 10$ (2·3025 . . .), which would correspond to $w_0 = 0$ in (6). The effect of introducing oxygen into the system is to start the process anew, almost as if the previously formed film were absent.

(4) Further confirmation of the view that k of equation (2) is proportional to the pressure can be obtained from the results of Wilkins and Rideal on the oxidation of

activated copper. The authors interpret the data as proving that a law

$$\log \frac{p}{p_0} = -kt \quad . \quad . \quad . \quad . \quad . \quad . \quad (7)$$

expresses the oxidation process. Now, if in (6) the parameter a becomes large the term $(p-p_0)/p_0$, which always lies between 0 and -1 if p_0 is the initial pressure observation, becomes relatively unimportant, and it would be difficult to distinguish experimentally between (6) and (7). In view of the accuracy of the experiments of Wilkins and Rideal it appeared to be worth while examining the data to see whether there were any systematic deviations from (7) which could be interpreted by means of (6). Tables IV.–IX. contain the figures, in columns (i.) and (ii.) taken from Wilkins and Rideal's paper. The third column under the heading τ gives the value of the time of each observation reckoning from $\tau=0$ when the first pressure observation p_0 is made. If (7) describes the process, then $-1/\tau \log p/p_0$ should be constant. The values are given in column (iv.) of the table, and it will be seen that in all cases there is a tendency for this quantity to diminish as the experiment proceeds. This gradual decrease must mean that either (7) is not an accurate representation or that in every case the initial pressure reading p_0 is in error. The latter seems highly improbable, as the error would in every case have to be assumed to be in the same direction, the observed value being always too large. It is much more likely that the observations are correct in indicating that $\log p/p_0$ is not a linear function of t, but is a curve concave to the time axis. The figures have been analyzed to find if they agree with a formula of the type (6), and the values in Table X. of the coefficients a and b have been found to give a good account of the pressure-time observations. The values refer to the equation

$$\frac{p-p_0}{p_0} - a \log_{10} \frac{p}{p_0} = b\tau,$$

τ replacing the t of equation (6).

The values of the times corresponding to the observed pressures are given in the fifth column of Tables IV. to IX. The agreement with the observed values is quite good. In the experiments at 209° C. and 218° C.,

TABLE IV.

142° C.

t sec.	p mm.	τ sec.	$-\frac{1}{\tau}\log_{10} p/p_0$.	τ calc.
71	8·88	0	—	0
148	8·12	77	$5{\cdot}04\times10^{-4}$	85
234	7·68	163	3·87	159
298	7·40	227	3·49	215
358	7·14	287	3·30	275
418	6·88	347	3·19	342
508	6·56	437	3·01	436

TABLE V.

183° C.

t sec.	p mm.	τ sec.	$-\frac{1}{\tau}\log_{10} p/p_0$.	τ calc.
18	7·42	0	—	0
37	7·03	19	$1{\cdot}23\times10^{-3}$	19
61	6·63	43	1·14	41
83	6·24	65	1·18	64
103	5·90	85	1·17	85
128	5·55	110	1·15	110
160	5·12	142	1·13	142
187	4·80	169	1·12	169
221	4·41	203	1·11	206
254	4·08	236	1·10	240

TABLE VI.

209° C.

t sec.	p mm.	τ sec.	$-\frac{1}{\tau}\log_{10} p/p_0$.	τ calc.
11	10·38	0	—	0
22	9·88	11	$1{\cdot}95\times10^{-3}$	11
32	9·46	21	1·92	21
53	8·62	42	1·92	42
69	7·98	58	1·97	60
86	7·46	75	1·91	77
100	7·08	89	1·86	89
116	6·60	105	1·87	107
139	6·06	128	1·82	128

TABLE VII.

218° C.

t sec.	p mm.	τ sec.	$-\frac{1}{\tau}\log_{10}p/p_0$.	τ calc.
22	5·96	0	—	0
34	4·81	12	$7{\cdot}76\times10^{-3}$	12
43	4·08	21	7·84	21
56	3·34	34	7·40	32
61	—	—	—	—
71	2·60	49	7·35	47
84	2·18	62	7·05	58
99	1·62	77	7·35	75
113	1·24	91	7·49	91

TABLE VIII.

249° C.

t sec.	p mm.	τ sec.	$-\frac{1}{\tau}\log_{10}p/p_0$.	τ calc.
12	4·82	0	—	0
20	4·02	8	$9{\cdot}85\times10^{-3}$	8
31	3·42	19	7·85	16
41	2·84	29	7·92	27
51	2·38	39	7·86	38
63	1·96	51	7·66	51
75	1·60	63	7·60	65
93	1·26	83	7·02	83

TABLE IX.

300° C.

t sec.	p mm.	τ sec.	$-\frac{1}{\tau}\log_{10}p/p_0$.	τ calc.
14	5·14	0	—	0
24	3·24	10	$2{\cdot}00\times10^{-2}$	10
33	2·46	19	1·68	18
42	1·78	28	1·64	30
53	1·34	39	1·50	41
65	1·04	51	1·36	51

Tables VI. and VII., the values of a are so large that the effect of the term $(p-p_0)/p_0$ in (6) is hardly appreciable, but in the remaining cases the evidence is all in favour of the view that the pressure-time relation is given by (6).

It is, perhaps, worth while pointing out that even if the relation (7) had been accurately obeyed it would still not have been necessary to assume that the oxidation process was different in character from that which leads to the parabolic law when observations are carried out at constant pressure. It is evident that if in equation (2) we write

$$k=k_1pw=k_1p(\alpha(p-p_0)+w_0)$$

we will obtain a relation of the type (7) at once. We can, however, derive a law of this type in the following more general way. In equation (2) we assume that $k=pf(p)$, where $f(p)$ is a function of the pressure p, so that putting

$$w=\alpha(p_0-p)+w_0,$$

where $\alpha=\dfrac{v}{\mathrm{RTA}}$ as in (3), (2) now becomes

$$\left(p-p_0-\frac{w_0}{\alpha}\right)\frac{dp}{dt}=pf(p)/\alpha^2,$$

or

$$\left\{\frac{1}{f(p)}-\frac{p_0+w_0\alpha}{pf(p)}\right\}\frac{dp}{dt}=\frac{1}{\alpha^2}. \quad . \quad . \quad . \quad (8)$$

Integration can be effected by use of the expansion theorem

$$\frac{\mathrm{F}(p)}{pf(p)}=\frac{\mathrm{F}(0)}{pf(0)}+\Sigma_n\frac{\mathrm{F}(p_n)}{p_nf'(p_n)}\frac{1}{p-p_n}, \quad . \quad . \quad . \quad (9)$$

where the summation extends over the roots $p_1, p_2, \ldots p_n$ of the equation $f(p)=0$, the roots being all supposed unequal, and $f'(p_n)$ is the value of $\dfrac{\partial f(p)}{\partial p}$ when $p=p_n$. By use of (9) (8) now becomes, on integration with the initial conditions $p=p_0$ when $t=0$,

$$\frac{1}{f(0)}\left\{p-p_0-\frac{(p_0+w_0)}{\alpha}\log_e\frac{p_0}{p}\right\}$$
$$+\Sigma\frac{1}{p_nf'(p_n)}\left\{p-p_0+\left(p_n-p_0-\frac{w_0}{\alpha}\right)\log_e\frac{p-p_n}{p_0-p_n}\right\}=\frac{t}{\alpha^2}.$$
$$. \quad . \quad . \quad (10)$$

When $f(p)$ is a constant equal to k, say, there are no terms under the summation sign, and the first term of (10) is identical with (6). If, however, $f(p)$ is of the first or higher order in p, then the linear term, $p-p_0$, disappears from (10). Because if in (9) we write $F(p)=p-p_0$ we have

$$\frac{p-p_0}{pf(p)} \equiv \frac{-p_0}{pf(0)} + \Sigma \frac{p_n-p_0}{p_n f'(p_n)} \frac{1}{p-p_n},$$

so that putting $p=p_0$, and provided p_0 is not a root of $f(p)=0$,

$$\frac{1}{f(0)} + \Sigma \frac{1}{p_n f'(p_n)} \equiv 0.$$

The left-hand side of this identity is the coefficient of $(p-p_0)$ in (10), which therefore becomes, provided $f(p)$ is not simply a constant,

$$-\frac{1}{f(0)}\left(p_0+\frac{w_0}{\alpha}\right)\log_e \frac{p}{p_0} + \sum_n \frac{p_n-p_0-\dfrac{w_0}{\alpha}}{p_n f'(p_n)} \log_e \frac{p-p_n}{p_0-p_n} = \frac{t}{\alpha^2}. \quad . \quad (11)$$

If $f(p)$ happens to be of such a nature that the terms under the summation sign are small compared with the first term, then the expression will approximate to (7), and may be experimentally indistinguishable from it. The occurrence of a logarithmic pressure-time relation is an analytical consequence of the original differential equation (2) combined with (3) which arises from the experimental method.

The simplest form in which (11) can appear is obtained when $f(p)=p-p_1$, p_1 being a constant and the only root of $f(p)=0$. When this condition is satisfied (11) simplifies to an equation of the type

$$\log_e \frac{p}{p_0} - a \log_e \frac{p-p_1}{p_0-p_1} = bt. \quad . \quad . \quad . \quad (11a)$$

Quite recently I have met with some results which can be accurately represented by an equation of this form. The data were obtained by Bircumshaw [3] in an investigation of the oxidation of molten lead; with the exception of two sets of observations taken at 700° C. all the results were in agreement with either (6) or (7), the former relation holding during the early stages of oxidation.

The results recorded at 700° C. could also be represented by (6) in the beginning, but the later stages could not be accounted for in terms of (7). It now appears that the whole of these two series of observations are in complete agreement with a relation of the type (11 *a*). The results are shown graphically in fig. 3, where the experimental points are shown by circles. The curves are calculated

Fig. 3.

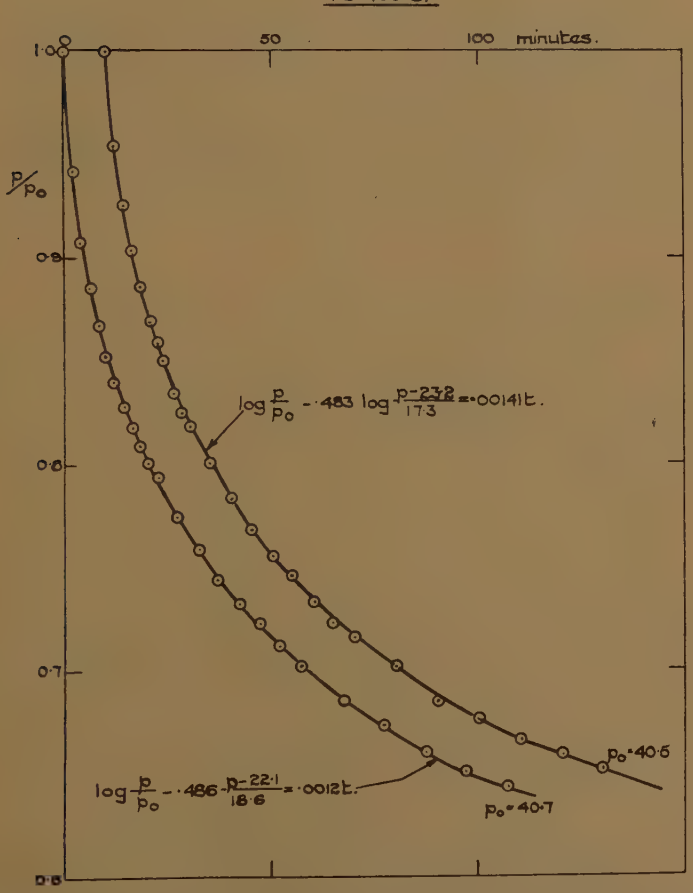

from (11 *a*), with the following values of the constants *a* and *b* :—

p_0.	*a*.	*b*.	p_1.
40·7	0·486	0·0012	22·1
40·5	0·483	0·00141	23·2

The agreement with experiment is quite accurate over the whole period of the observations extending to over 100 minutes in each case. It will be observed that p_1 is a limiting pressure attained after the lapse of an infinite time. The values of the quantities a, b, and p_1 in the two cases are nearly the same, one experiment being intended to be a repetition of the other. Reference to the paper quoted will show that in this respect this pair of experiments is rather better than the others reported, a fact which suggests that the agreement with (11 a) is not a coincidence. The gradual approach of the pressure to a steady final value might be the effect of a leak in the apparatus, but it is improbable that a leak of the same magnitude should have developed in these two runs and in no others. The experiment suggests that in certain circumstances the constant k in the parabolic law may be a quadratic function of the pressure.

TABLE X.

	T° C.	a.	$b \times 10^3$.	p_0.	$bp_0 \times 10^2$.
IV. ...	142	2·631	0·194	8·88	0·172
V. ...	183	6·347	5·06	7·42	3·71
VI. ...	209	9·22	13·6	10·38	14·1
VII. ...	218	27·76	195·0	5·96	116·0
VIII. ...	249	4·18	20·5	4·82	9·9
IX. ...	305	3·32	29·5	5·14	15·1

(5) The values of the parameters a and b of equation (6), tabulated in Table X., present certain features which suggest that although (6) gives an accurate description of the pressure-time relation the interpretation put upon the symbols may not be correct. The quantity bp_0 in the last column of the table should be proportional to the k of equation (2), and might be expected to increase with rising temperature. Up to 218° C. this is the case, but then a sudden fall ensues. The values of a follow the course of those of b and bp_0. From the way in which the experiments were carried out we should have expected a not to differ greatly from $\log_e 10 = 2{\cdot}302$, the amount by which $a/2{\cdot}302$ exceeds unity being a measure of w_0 the weight of oxide per cm.^{2} of the surface when the first pressure reading is recorded. The large values of a recorded in Table X. suggest that some modification

of (6) is required in which the symbols have a different significance. This change can be effected by making use of a relation due to Evans ('Metallic Corrosion and Passivity,' p. 89) in which the rate of increase of film thickness, x, is expressed by

$$\frac{dx}{dt} = \frac{k_D k_c C_0}{k_D + x k_c}. \quad \ldots\ldots \quad (12)$$

Here k_D is a constant connected with the diffusivity of either the metal or oxygen ion in the oxide film, k_c is a measure of the velocity of chemical reaction, and C_0 is the excess concentration of oxygen in the oxide film at the oxygen-oxide interface. C_0 will be dependent on pressure and temperature, but if these are both constant integration of (12) gives

$$x^2 + 2\frac{k_D}{k_c}x = 2k_D C_0 t + \text{a constant},$$

an expression of the same form as (4). When the pressure varies during an experiment some assumption as to the variation of C_0 with pressure must be made before integrating (12). Evans (*loc. cit.*), discussing the formation of films of silver iodide on silver in solutions of iodine, states that C_0 is found to be nearly proportional to the concentration of iodine in the solution. We make an equivalent assumption here, namely, $C_0 = \beta p$, where β is a constant. Putting

$$x = \alpha(p_0 - p) + x_0,$$

where α is a constant depending on the dimensions of the apparatus and the density of the film, (12) gives on integration, with the condition $p = p_0$ when $t = 0$,

$$\frac{p - p_0}{p_0} - \left\{1 + \frac{k_D^2 + x_0 k_c}{k_c \alpha p_0}\right\} \log_e \frac{p}{p_0} = \frac{\beta k_D}{\alpha^2 p_0} t.$$

This equation is of the same form as (6), but a, the coefficient of $\log_e p/p_0$, now includes the term $k_D/k_c\alpha p_0$, so that even if x_0 is very small we do not have to expect a value of the parameter a in the neighbourhood of unity. The objection to (6) is thus removed, and the experimental results may be accepted as conforming to Evans's equation (12), with the additional condition that C_0 is proportional to the pressure.

In sections (2) and (3) attention was drawn to certain peculiarities in Wilkins's experiments on copper, which are illustrated in fig. 1. The increase of rate of oxidation immediately, or very soon, after the admission of fresh oxygen is inexplicable if the k of equation (2) is assumed independent of pressure. When k is taken to be proportional to p an increase in $\frac{dw}{dt}$ would be expected if p is suddenly increased, but the reason for the simultaneous decrease of the quantity bp_0 in Table (*a*) is not obvious. Whatever the explanation may be the increase in rate of oxidation which accompanies increase of pressure, if confirmed, would seem to have some bearing on the process of corrosion fatigue. If alternating strains produce increases of pressure of any gas trapped in fissures near the surface the rate of corrosion will increase to a value above that found for the same material in an unstressed state.

References.

(1) Tamman, G., *Z. anorg. Chem.* cxi. p. 83 (1920).
(2) Pilling, N. B., and Bedworth, R. E., J. Inst. Met. (i.) xxix. p. 529 (1923).
(3) Bircumshaw, L. L., and Preston, G. D., Phil. Mag. xxv. p. (1938).
(4) Wilkins, F. J., and Rideal, E. K., Proc. Roy. Soc. cxxviii. p. 394 (1930).
(5) Wilkins, F. J., Proc. Roy. Soc. cxxviii. p. 407 (1930).
(6) Hinshelwood, C. N., Proc. Roy. Soc. cii. p. 318 (1922).
(7) Evans, U. R., ' Metallic Corrosion and Passivity,' p. 89.

VI. *Proofs of some Formulæ for the Generalized Hypergeometric Function and certain related Functions.* By T. M. MacRobert, *Professor of Mathematics, University of Glasgow* *.

§1. *Introductory.*

THIS paper contains proofs of various formulæ for the Hypergeometric, Generalized Hypergeometric, and other related functions. The formulæ in sections 2, 3, 4, which were originally given by Kummer and Gauss, are here proved by transforming the integrals which

* Communicated by the Author.

represent the functions. Section 5 contains a proof of a formula due to Whipple. In section 6 it is shown that certain formulæ for the Confluent Hypergeometric and Bessel Functions are particular cases of the expression for a function, which may be called the E-function, in terms of Generalized Hypergeometric Functions. In section 7 a relation, due to Macdonald, between the Bessel and Legendre Functions is discussed, some new formulæ being obtained.

§2. *Two Formulæ due to Kummer.*

The first of these formulæ (*Journal für Math.* xv. pp. 138, 139, 140 (1835)) is

$$ {}_1F_1(\alpha\,;\ \rho\,;\ z)=e^z\,{}_1F_1(\rho-\alpha\,;\ \rho\,;\ -z), \quad . \quad . \quad (1) $$

where ρ is not zero or a negative integer.

It can be proved as follows. If $R(\alpha)>0$, $R(\rho-\alpha)>0$,

$$ {}_1F_1(\alpha\,;\ \rho\,;\ z)=\frac{1}{B(\alpha,\ \rho-\alpha)}\int_0^1 e^{zt}t^{\alpha-1}(1-t)^{\rho-\alpha-1}\,dt\,; \quad (2) $$

this can be seen by expanding the exponential function in powers of t and integrating term by term. On replacing t by $1-t$ in the integral it is found that the R.H.S. of (2) becomes

$$ e^z\,\frac{1}{B(\rho-\alpha,\ \alpha)}\int_0^1 e^{-zt}t^{\rho-\alpha-1}(1-t)^{\alpha-1}\,dt, $$

from which (1) follows. The restrictions on α and ρ may now be removed by applying the method of analytical continuation.

The second formula is

$$ {}_1F_1(\alpha\,;\ 2\alpha\,;\ 2z)=e^z\,{}_0F_1(\alpha+\tfrac{1}{2}\,;\ \tfrac{1}{4}z^2), \quad . \quad . \quad (3) $$

where α is not half an odd negative integer.

In (2) put $\rho=2\alpha$, $t=\frac{1}{2}(1+\lambda)$, and replace z by $2z$; then, if $R(\alpha)>0$,

$$ {}_1F_1(\alpha\,;\ 2\alpha\,;\ 2z)=\frac{e\ 2^{1-2\alpha}}{B(\alpha,\ \alpha)}\int_{-1}^1 e^{z\lambda}(1-\lambda^2)^{\alpha-1}\,d\lambda $$

$$ =e^z\,\Gamma(\alpha+\tfrac{1}{2})\left(\frac{2}{z}\right)^{\alpha-\frac{1}{2}}I_{\alpha-\frac{1}{2}}(z), $$

since

$$ \Gamma(\tfrac{1}{2})\,\Gamma(2\alpha)=2^{2\alpha-1}\,\Gamma(\alpha)\,\Gamma(\alpha+\tfrac{1}{2}). $$

From this (3) follows. If α is replaced by $n+\frac{1}{2}$, the formula just obtained can be written

$$I_n(z)=e^{-z}\frac{1}{\Gamma(n+1)}\left(\frac{z}{2}\right)^n {}_1F_1(\tfrac{1}{2}+n\,;\,1+2n\,;\,2z). \quad (4)$$

On applying (1) to the R.H.S. of (4) we obtain the equivalent formula

$$I_n(z)=e^{z}\frac{1}{\Gamma(n+1)}\left(\frac{z}{2}\right)^n {}_1F_1(\tfrac{1}{2}+n\,;\,1+2n\,;\,-2z). \quad (5)$$

The formulæ above were discussed by Barnes (Trans. Camb. Phil. Soc. xx. pp. 253–279 (1907)).

From (4) it follows that, if $R(z)>1$, $R(m+n)>-1$,

$$\int_0^\infty e^{-\lambda z} I_{n+\frac{1}{2}}(\lambda)\lambda^{m-\frac{1}{2}}\,d\lambda = \frac{1}{2^{n+\frac{1}{2}}\Gamma(n+\frac{3}{2})}\int_0^\infty e^{-\lambda(z+1)}\lambda^{n+m}\,{}_1F_1(1+n\,;\,2+2n\,;\,2\lambda)\,d\lambda.$$

On expanding the Bessel and Hypergeometric Functions in powers of λ and integrating term by term we obtain the formula

$$F\left(\frac{n+m+1}{2},\ \frac{n+m+2}{2}\,;\ n+\tfrac{3}{2}\,;\ \frac{1}{z^2}\right) = \left(\frac{z}{1+z}\right)^{n+m+1} F\left(n+m+1,\ n+1\,;\ 2n+2\,;\ \frac{2}{1+z}\right), \quad (6)$$

where $|z+1|>2$. From this it follows that

$$Q_n^m(z) = \frac{\Gamma(n+m+1)\,\Gamma(\frac{1}{2})}{2^{n+1}\Gamma(n+\frac{3}{2})}\frac{(z^2-1)^{\frac{1}{2}m}}{(z+1)^{n+m+1}} \times F\left(n+m+1,\ n+1\,;\ 2n+2\,;\ \frac{2}{z+1}\right), \quad (7)$$

where $|z+1|>2$. This formula was given by Hobson ('Spherical and Ellipsoidal Harmonics,' p. 203); see also Barnes (Quart. Journ. of Math. xxxix. p. 107 (1908)) and Phil. Mag. xiv. p. 654 (1932).

The derivation of (7) from (5) is an example of the method of deducing Legendre Function formulæ from corresponding Bessel Function formulæ, developed in a previous paper (Phil. Mag. xxi. pp. 697–703 (1936)). Another application of this method will be found in section 7.

§ 3. *A Formula, due to Kummer, for the Hypergeometric Function.*

The formula (*Journal für Math.* xv. p. 78 (1835)) is

$$\mathrm{F}(\alpha, \beta; 2\beta; z) = \left(1-\frac{z}{2}\right)^{-\alpha} \mathrm{F}\left\{\frac{\alpha}{2}, \frac{\alpha+1}{2}; \beta+\tfrac{1}{2}; \left(\frac{z}{2-z}\right)^2\right\}, \quad \ldots \quad (8)$$

where $|z|<1$ and β is not half a negative odd integer.

If $\mathrm{R}(\beta)>0$,

$$\mathrm{F}(\alpha, \beta; 2\beta; z)$$

$$= \frac{2}{\mathrm{B}(\beta, \beta)} \int_0^{\frac{\pi}{2}} (\sin\theta\cos\theta)^{2\beta-1} (1-z\sin^2\theta)^{-\alpha}\, d\theta$$

$$= \frac{2^{1-2\beta}}{\mathrm{B}(\beta, \beta)} \int_0^{\pi} (\sin\phi)^{2\beta-1} \left(1-\frac{z}{2}+\frac{z}{2}\cos\phi\right)^{-\alpha} d\phi$$

$$= \frac{2^{1-2\beta}}{\mathrm{B}(\beta, \beta)} \int_0^{\frac{\pi}{2}} (\sin\phi)^{2\beta-1} \left\{ \begin{array}{c} \left(1-\frac{z}{2}+\frac{z}{2}\cos\phi\right)^{-\alpha} \\ +\left(1-\frac{z}{2}-\frac{z}{2}\cos\phi\right)^{-\alpha} \end{array} \right\} d\phi$$

$$= \frac{2^{2-2\beta}}{\mathrm{B}(\beta, \beta)} \left(1-\frac{z}{2}\right)^{-\alpha}$$

$$\times \int_0^{\frac{\pi}{2}} (\sin\phi)^{2\beta-1} \left\{1+\frac{\alpha(\alpha+1)}{2\,!} \left(\frac{z}{2-z}\right)^2 \cos^2\phi + \ldots\right\} d\phi$$

$$= \frac{\mathrm{B}(\beta, \frac{1}{2})}{\mathrm{B}(\beta, \beta)} 2^{1-2\beta} \left(1-\frac{z}{2}\right)^{-\alpha}$$

$$\times \mathrm{F}\left\{\frac{\alpha}{2}, \frac{\alpha+1}{2}; \beta+\tfrac{1}{2}; \left(\frac{z}{2-z}\right)^2\right\}.$$

An application of the formula

$$\Gamma(\tfrac{1}{2})\,\Gamma(2\beta) = 2^{2\beta-1}\,\Gamma(\beta)\,\Gamma(\beta+\tfrac{1}{2})$$

then gives (8). The restriction $\mathrm{R}(\beta)>0$ may now be removed.

Alternatively the formula may be deduced from (6) by replacing $n+m+1$, $n+1$ and $2/(z+1)$ by α, β, and z respectively.

§ 4 *A Formula, due to Gauss, for the Hypergeometric Function.*

In proving the formula (Gauss, *Ges. Werke*, iii. p. 225 (1866))

$$\mathrm{F}\left(\begin{matrix}\alpha,\ \beta\ ;\ z\\ 1+\alpha-\beta\end{matrix}\right)=(1-z)^{-\alpha}\mathrm{F}\left\{\begin{matrix}\frac{1}{2}\alpha,\ \frac{1}{2}+\frac{1}{2}\alpha-\beta\ ;\\ 1+\alpha-\beta\end{matrix}\ \frac{-4z}{(1-z)^2}\right\} \qquad (9)$$

use is made of the expansion

$$\frac{1}{\sqrt{(1-z)}}\left\{\frac{2}{1+\sqrt{(1-z)}}\right\}^{\alpha-1}=\mathrm{F}(\tfrac{1}{2}\alpha+\tfrac{1}{2},\ \tfrac{1}{2}\alpha\ ;\ \alpha\ ;\ z). \qquad (10)$$

This may be obtained by differentiating the expansion

$$\left\{\frac{1+\sqrt{(1-z)}}{2}\right\}^{-2a}=\mathrm{F}(a,\ a+\tfrac{1}{2}\ ;\ 2a+1\ ;\ z), \qquad (11)$$

which can be established by means of Lagrange's Expansion, and then putting $a=\frac{1}{2}\alpha-1$. Alternatively (10) can be deduced from the formula

$$e^{-nx}=(2\cosh x)^{-n}\tanh x\,\mathrm{F}\left(1+\frac{n}{2},\ \frac{1+n}{2}\ ;\ 1+n\ ;\ \operatorname{sech}^2 x\right) \qquad (12)$$

(Phil. Mag. xiv. p. 651 (1932)) by putting $\operatorname{sech}^2 x=z$, $n=\alpha-1$.

Now, if $\mathrm{R}(\alpha)>0$, $\mathrm{R}(1-\beta)>0$,

$$\mathrm{F}\left(\begin{matrix}\alpha,\ \beta\ ;\ z\\ \alpha-\beta+1\end{matrix}\right)=\frac{1}{\mathrm{B}(\alpha,\ 1-\beta)}\int_0^1 t^{\alpha-1}\{(1-t)(1-zt)\}^{-\beta}\,dt.$$

Here put $(1-t)(1-zt)=1-\lambda$,

so that $$t=\frac{2\lambda}{1+z+\sqrt{\{(1+z)^2-4z\lambda\}}}.$$

Then

$$\mathrm{F}\left(\begin{matrix}\alpha,\ \beta\ ;\ z\\ \alpha-\beta+1\end{matrix}\right)=\frac{1}{\mathrm{B}(\alpha,\ 1-\beta)}$$

$$\times\int_0^1\left[\frac{2\lambda}{1+z+\sqrt{\{(1+z)^2-4z\lambda\}}}\right]^{\alpha-1}\frac{(1-\lambda)^{-\beta}\,d\lambda}{\sqrt{\{(1+z)^2-4z\lambda\}}}.$$

Hence, from (10),

$$\mathrm{F}\left(\begin{matrix}\alpha, \beta\,; z\\ \alpha-\beta+1\end{matrix}\right) = \frac{(1+z)^{-\alpha}}{\mathrm{B}(\alpha,\ 1-\beta)} \times \int_0^1 \lambda^{\alpha-1}(1-\lambda)^{-\beta}\mathrm{F}\left\{\tfrac{1}{2}\alpha+\tfrac{1}{2}, \tfrac{1}{2}\alpha\,;\ \alpha;\frac{4z\lambda}{(1+z)^2}\right\}d\lambda$$

$$= (1+z)^{-\alpha}\,\mathrm{F}\left\{\tfrac{1}{2}\alpha, \tfrac{1}{2}\alpha+\tfrac{1}{2}\,;\ 1+\alpha-\beta\,;\frac{4z}{(1+z)^2}\right\}. \quad . \ . \ . \quad (13)$$

From this formula (9) is derived by applying the transformation

$$\mathrm{F}(\alpha, \beta\,;\ \gamma;\ x)=(1-x)^{-\alpha}\,\mathrm{F}\left(\ (\alpha,\ \gamma-\beta\,;\ \gamma\,;\frac{x}{x-1}\right).$$

§ 5. *A Formula, due to Whipple, for a Generalized Hypergeometric Function.*

The formula

$${}_3\mathrm{F}_2\left(\begin{matrix}\alpha, \beta, \gamma\,; z\\ \alpha-\beta+1,\ \alpha-\gamma+1\end{matrix}\right) = (1-z)^{-\alpha}\,{}_3\mathrm{F}_2\left[\begin{matrix}\frac{\alpha}{2}, \frac{1+\alpha}{2}, 1+\alpha-\beta-\gamma;\\ \alpha-\beta+1,\ \alpha-\gamma+1\end{matrix}\ \frac{-4z}{(1-z)^2}\right] \quad (14)$$

was discovered by Whipple (Proc. Lond. Math. Soc. xxvi. p. 267 (1926)). It is a generalization of (9), as can be seen by putting $\gamma=\frac{1}{2}(\alpha+1)$, and it may be derived from (9) as follows :

$${}_3\mathrm{F}_2\left(\begin{matrix}\alpha, \beta, \gamma\,; z\\ \alpha-\beta+1,\ \alpha-\gamma+1\end{matrix}\right)$$

$$= \frac{1}{\mathrm{B}(\gamma,\ \alpha-2\gamma+1)}\int_0^1 t^{\gamma-1}(1-t)^{\alpha-2\gamma}\mathrm{F}\left(\begin{matrix}\alpha, \beta\,; zt\\ \alpha-\beta+1\end{matrix}\right)dt$$

$$= \frac{1}{\mathrm{B}(\gamma,\ \alpha-2\gamma+1)}\int_0^1 t^{\gamma-1}(1-t)^{\alpha-2\gamma} \times (1-zt)^{-\alpha}\mathrm{F}\left[\begin{matrix}\frac{\alpha}{2}, \frac{1+\alpha}{2}-\beta\,;\\ \alpha-\beta+1\end{matrix}\ \frac{-4zt}{(1-zt)^2}\right]dt,$$

by (9). Now, keeping z small, expand the hypergeometric series and integrate term by term : the expression is then equal to

$$\mathrm{F}\left(\begin{matrix}\alpha, \gamma ; z\\ \alpha-\gamma+1\end{matrix}\right)$$

$$+\frac{\left(\frac{\alpha}{2}\right)\left(\frac{1+\alpha}{2}-\beta\right)(\gamma)}{1!\,(\alpha-\beta+1)(\alpha-\gamma+1)}(-4z)\mathrm{F}\left(\begin{matrix}\alpha+2, \gamma+1 ; z\\ \alpha-\gamma+2\end{matrix}\right)$$

$$+ \quad . \quad . \quad . \quad . \quad . \quad . \quad . \quad . \quad . \quad . \quad . \quad . \quad . \quad . \quad .$$

$$=(1-z)^{-\alpha}\mathrm{F}\left(\begin{matrix}\frac{\alpha}{2}, \frac{1+\alpha}{2}-\gamma ; \lambda\\ \alpha-\gamma+1\end{matrix}\right)$$

$$+(1-z)^{-\alpha}\frac{\left(\frac{\alpha}{2}\right)\left(\frac{1+\alpha}{2}-\beta\right)(\gamma)}{1!\,(\alpha-\beta+1)(\alpha-\gamma+1)}\lambda\mathrm{F}\left(\begin{matrix}\frac{\alpha}{2}+1, \frac{1+\alpha}{2}-\gamma ; \lambda\\ \alpha-\gamma+2\end{matrix}\right)$$

$$+ \quad . \quad . \quad . \quad . \quad . \quad . \quad . \quad . \quad . \quad . \quad . \quad . \quad . \quad . \quad . \quad . \quad . \quad . \quad .,$$

by (9), where $\lambda=-4z/(1-z)^2$ This is equal to

$$\frac{(1-z)^{-\alpha}}{\mathrm{B}(\frac{1}{2}\alpha,\ 1+\frac{1}{2}\alpha-\gamma)}$$

$$\times\left\{\begin{aligned}&\int_0^1 t^{\frac{1}{2}\alpha-1}(1-t)^{\frac{1}{2}\alpha-\gamma}(1-t\lambda)^{\gamma-\frac{1}{2}-\frac{1}{2}\alpha}\,dt\\ &\quad+\frac{\left(\frac{1+\alpha}{2}-\beta\right)(\gamma)}{1!\,(\alpha-\beta+1)}\lambda\int_0^1 t^{\frac{1}{2}\alpha}(1-t)^{\frac{1}{2}\alpha-\gamma}(1-t\lambda)^{\gamma-\frac{1}{2}-\frac{1}{2}\alpha}\,dt\\ &\quad+ \quad . \quad . \quad . \quad . \quad . \quad . \quad . \quad . \quad . \quad . \quad . \quad . \quad . \quad . \quad .\end{aligned}\right\}$$

$$=\frac{(1-z)^{-\alpha}}{\mathrm{B}(\frac{1}{2}\alpha,\ 1+\frac{1}{2}\alpha-\gamma)}\int_0^1 t^{\frac{1}{2}\alpha-1}(1-z)^{\frac{1}{2}\alpha-\gamma}$$

$$\times(1-t\lambda)^{\gamma-\frac{1}{2}-\frac{1}{2}\alpha}\mathrm{F}\left(\begin{matrix}\frac{1+\alpha}{2}-\beta, \gamma ; t\lambda\\ \alpha-\beta+1\end{matrix}\right)dt.$$

By applying the formula

$$\mathrm{F}(\alpha, \beta ; \rho ; x)=(1-x)^{\rho-\alpha-\beta}\mathrm{F}(\rho-\alpha, \rho-\beta ; \rho ; x)$$

we see that this is equal to

$$\frac{(1-z)^{-\alpha}}{\mathrm{B}(\frac{1}{2}\alpha,\ 1+\frac{1}{2}\alpha-\gamma)}\int_0^1 t^{\frac{1}{2}\alpha-1}(1-t)^{\frac{1}{2}\alpha-\gamma} \times \mathrm{F}\left(\begin{matrix}\frac{1+\alpha}{2},\ 1+\alpha-\beta-\gamma\ ;\ t\lambda \\ \alpha-\beta+1\end{matrix}\right) dt,$$

from which (14) at once follows.

§ 6. *Some Simple Cases of the* E*-function.*

In a recent paper (Proc. Roy. Soc. Edin. lviii. pp. 1–13 (1937)) a function denoted by $\mathrm{E}(p,\ \alpha_r : q,\ \rho_s : z)$ was defined as a multiple integral, and it was proved that

$$\mathrm{E}(p,\ \alpha_r : q,\ \rho_s : z) = \sum_{r=1}^{p} \mathrm{P}(\alpha_r\ ;\ p-1,\ \alpha_s : q,\ \rho_t : z), \quad (15)$$

where the P-functions are multiples of certain Generalized Hypergeometric Functions.

One special case of the formula (15) is

$$\begin{aligned}&\mathrm{E}(\tfrac{1}{2}-k-m,\ \tfrac{1}{2}-k+m : 0 : z)\\ &\quad = \Gamma(2m)\,\Gamma(\tfrac{1}{2}-k-m)z^{\frac{1}{2}-k-m}{}_1\mathrm{F}_1(\tfrac{1}{2}-k-m\ ;\ 1-2m\ ;\ z)\\ &\qquad + \Gamma(-2m)\,\Gamma(\tfrac{1}{2}-k+m)z^{\frac{1}{2}-k+m}{}_1\mathrm{F}_1(\tfrac{1}{2}-k+m\ ;\ 1+2m\ ;\ z),\end{aligned} \quad \ldots \quad (16)$$

where

$$\mathrm{E}(\tfrac{1}{2}-k-m,\ \tfrac{1}{2}-k+m : 0 : z) = \Gamma(\tfrac{1}{2}-k-m)\int_0^\infty e^{-\lambda}\lambda^{-\frac{1}{2}-k+m}\left(1+\frac{\lambda}{z}\right)^{-\frac{1}{2}+k+m} d\lambda. \quad (17)$$

If Whittaker's notation for the Confluent Hypergeometric Function (Whittaker and Watson's 'Analysis,' chapter xvi.) is employed, this is seen to be the well-known formula

$$\mathrm{W}_{k,\,m}(z) = \frac{\Gamma(-2m)}{\Gamma(\frac{1}{2}-k-m)}\mathrm{M}_{k,\,m}(z) + \frac{\Gamma(2m)}{\Gamma(\frac{1}{2}-k+m)}\mathrm{M}_{k,\,-m}(z). \quad \ldots \quad (18)$$

Again,

$$K_n(z)=\frac{\cos n\pi}{\sqrt{(2\pi z)}}e^{-z}E(\tfrac{1}{2}+n,\ \tfrac{1}{2}-n : 0 : 2z)$$

$$=\frac{\cos n\pi}{\sqrt{(2\pi)}}e^{-z}\left\{\begin{array}{l}\Gamma(-2n)\,\Gamma(\tfrac{1}{2}+n)2^{\frac{1}{2}+n}z^n \\ \qquad\qquad \times {}_1F_1(\tfrac{1}{2}+n\ ;\ 1+2n\ ;\ 2z) \\ +\,\Gamma(2n)\,\Gamma(\tfrac{1}{2}-n)2^{\frac{1}{2}-n}z^{-n} \\ \qquad\qquad \times {}_1F_1(\tfrac{1}{2}-n\ ;\ 1-2n\ ;\ 2z)\end{array}\right\};$$

and, on comparing this with the formula

$$K_n(z)=\frac{\pi}{2\sin n\pi}\{I_{-n}(z)-I_n(z)\},$$

we see that

$$I_n(z)=e^{-z}\frac{1}{\Gamma(n+1)}\left(\frac{z}{2}\right)^n {}_1F_1(\tfrac{1}{2}+n\ ;\ 1+2n\ ;\ 2z),$$

which is formula (4).

§ 7. *A Relation between the Legendre and the Bessel Functions.*

Macdonald's formula (21) below was also, in the paper referred to in section 6, derived from the properties of the E-function. The following is an alternative proof.

If C denotes a contour starting from $-\infty$ on the real axis, passing positively round the point $+1$, and returning to $-\infty$ on the real axis,

$$I_{n+\frac{1}{2}}(z)=\frac{z^{m+\frac{1}{2}}}{2\pi i}\sqrt{\left(\frac{2}{\pi}\right)}\int_C e^{z\zeta}(\zeta^2-1)^{\frac{1}{2}m}Q_n^{-m}(\zeta)\,d\zeta, \quad (19)$$

where $R(z)>0$ and amp (ζ), amp (ζ^2-1) are both zero at the point of C on the real axis to the right of $+1$. This can be verified by expanding the Q-function in descending powers of ζ and integrating term by term. The contour can be deformed to ensure that $|\zeta|>1$ at all points on it.

Now, if $R(m)>-1$, the contour can be deformed into the real axis between $-\infty$ and $+1$, described both ways and indented at -1 and $+1$. Hence, making use of the formula

$$e^{\frac{1}{2}m\pi i}Q_n^{-m}(\zeta)-e^{-\frac{1}{2}m\pi i}Q_n^{-m}(\zeta,\ +1-)=\frac{\pi}{i}T_n^{-m}(\zeta) \quad (20)$$

(given in the author's ' Complex Variable,' second edition, p. 306), we see that

$$I_{n+\frac{1}{2}}(z) = \frac{z^{m+\frac{1}{2}}}{\sqrt{(2\pi)}} \int_{-1}^{1} e^{z\xi}(1-\xi^2)^{\frac{1}{2}m} T_n^{-m}(\xi)\, d\xi$$

$$+ \frac{z^{m+\frac{1}{2}}}{\pi} \sqrt{\left(\frac{2}{\pi}\right)} \sin(m-n)\pi \int_{1}^{\infty} e^{-z\lambda}(\lambda^2-1)^{\frac{1}{2}m} Q_n^{-m}(\lambda) d\lambda, \quad . \quad . \quad . \quad (21)$$

where $R(z)>0$, $R(m)>-1$.

In particular, if m is replaced by $m-\frac{1}{2}$ and n by $m+r-\frac{1}{2}$, where r is zero or a positive integer,

$$I_{m+r}(z) = \frac{z^m}{\sqrt{(2\pi)}} \int_{-1}^{1} e^{z\xi}(1-\xi^2)^{\frac{1}{2}(m-\frac{1}{2})} T_{m+r-\frac{1}{2}}^{\frac{1}{2}-m}(\xi)\, d\xi, \quad (22)$$

where $R(m)>-\frac{1}{2}$. This is equivalent to a formula of Gegenbauer's (Watson, ' Bessel Functions,' p. 50).

Also, since

$$T_{-n-1}^{-m}(\xi) = T_n^{-m}(\xi), \quad . \quad . \quad . \quad . \quad . \quad (23)$$

$$Q_{-n-1}^{-m}(\lambda) \sin(m+n)\pi + Q_n^{-m}(\lambda) \sin(m-n)\pi$$

$$= -\pi \cos n\pi P_n^{-m}(\lambda) \quad (24)$$

(' Complex Variable,' p. 265), and

$$K_{n+\frac{1}{2}}(z) = \frac{\pi}{2\cos n\pi} \{I_{-n-\frac{1}{2}}(z) - I_{n+\frac{1}{2}}(z)\},$$

it follows from (21) that

$$K_{n+\frac{1}{2}}(z) = \sqrt{\left(\frac{\pi}{2}\right)} z^{m+\frac{1}{2}} \int_{1}^{\infty} e^{-z\lambda}(\lambda^2-1)^{\frac{1}{2}m} P_n^{-m}(\lambda)\, d\lambda, \quad (25)$$

where $R(z)>0$, $R(m)>-1$.

Again, in (21) put $m=-\frac{1}{2}$ and replace n by $n-\frac{1}{2}$; then, since

$$\sqrt{(\sin\theta)} T_{n-\frac{1}{2}}^{\frac{1}{2}}(\cos\theta) = \sqrt{\left(\frac{2}{\pi}\right)} \cos n\theta,$$

$$\sqrt{(\sinh u)} Q_{n-\frac{1}{2}}^{\frac{1}{2}}(\cosh u) = \sqrt{\left(\frac{\pi}{2}\right)} e^{-nu},$$

$$I_n(z) = \frac{1}{\pi} \int_0^{\pi} e^{z\cos\theta} \cos n\theta\, d\theta - \frac{\sin n\pi}{\pi} \int_0^{\infty} e^{-z\cosh u - nu}\, du, \quad (26)$$

where $\mathrm{R}(z)>0$. Thus (21) may be regarded as a generalization of this well-known formula.

A formula involving Legendre Functions only can be deduced from (21) as follows :—

If $\mathrm{R}(z)>1$, $\mathrm{R}(m+n+1)>0$, $\mathrm{R}(p)>-1$,

$$\int_0^\infty e^{-zx}\mathrm{I}_{n+\frac{1}{2}}(x)x^{m-\frac{1}{2}}\,dx$$

$$=\frac{1}{\sqrt{(2\pi)}}\int_{-1}^{1}(1-\xi^2)^{\frac{1}{2}p}\mathrm{T}_n^{-p}(\xi)\,d\xi\int_0^\infty e^{-(z-\xi)x}x^{m+p}\,dx$$

$$+\sqrt{\left(\frac{2}{\pi}\right)}\frac{\sin(p-n)\pi}{\pi}\int_1^\infty(\lambda^2-1)^{\frac{1}{2}p}\mathrm{Q}_n^{-p}(\lambda)\,d\lambda$$

$$\times\int_0^\infty e^{-(z+\lambda)x}x^{m+p}\,dx.$$

Hence, as in the proof of formula (7),

$$(z^2-1)^{-\frac{1}{2}m}\mathrm{Q}_n^m(z)=\tfrac{1}{2}\,\Gamma(m+p+1)\int_{-1}^{1}\frac{(1-\xi^2)^{\frac{1}{2}p}\mathrm{T}_n^{-p}(\xi)}{(z-\xi)^{m+p+1}}\,d\xi$$

$$+\frac{\sin(p-n)\pi}{\pi}\,\Gamma(m+p+1)\int_1^\infty\frac{(\lambda^2-1)^{\frac{1}{2}p}\mathrm{Q}_n^{-p}(\lambda)}{(z+\lambda)^{m+p+1}}\,d\lambda, \quad (27)$$

where $\mathrm{R}(z)>1$, $\mathrm{R}(m+n+1)>0$, $\mathrm{R}(p)>-1$.

In particular, if $p=n$, since

$$\mathrm{T}_n^{-n}(\xi)=(1-\xi^2)^{\frac{1}{2}n}/\{2^n\,\Gamma(n+1)\}, \quad . \quad . \quad . \quad (28)$$

$$(z^2-1)^{-\frac{1}{2}m}\mathrm{Q}_n^m(z)=\frac{\Gamma(n+m+1)}{2^{n+1}\,\Gamma(n+1)}\int_{-1}^{1}\frac{(1-\xi^2)^n}{(z-\xi)^{n+m+1}}\,d\xi, \quad (29)$$

where $\mathrm{R}(n)>-1$, $|\,z\,|>1$. This formula was given by Hobson (' Spherical and Ellipsoidal Harmonics,' p. 195).

Again, from (23) and (24), with p in place of m, and (27) we have

$$(z^2-1)^{-\frac{1}{2}m}\{\mathrm{Q}_n^m(z)-\mathrm{Q}_{-n-1}^m(z)\}$$

$$=-\,\Gamma(m+p+1)\cos n\pi\int_1^\infty\frac{(\lambda^2-1)^{\frac{1}{2}p}}{(z+\lambda)^{m+p+1}}\,\mathrm{P}_n^{-p}(\lambda)\,d\lambda.$$

But (' Complex Variable,' p. 276)

$$\mathrm{P}_n^{-m}(z)=\frac{\sin(n-m)\pi}{\pi\cos n\pi}\,\frac{\Gamma(n-m+1)}{\Gamma(n+m+1)}\{\mathrm{Q}_n^m(z)-\mathrm{Q}_{-n-1}^m(z)\}. \quad (30)$$

Hence

$$(z^2-1)^{-\frac{1}{2}m}\mathrm{P}_n^{-m}(z)=\frac{\Gamma(m+p+1)}{\Gamma(m+n+1)\,\Gamma(m-n)}\times\int_1^\infty\frac{(\lambda^2-1)^{\frac{1}{2}p}\mathrm{P}_n^{-p}(\lambda)}{(z+\lambda)^{m+p+1}}\,d\lambda, \quad (31)$$

where $\mathrm{R}(z)>1$, $\mathrm{R}(m+n+1)>0$, $\mathrm{R}(m-n)>0$, $\mathrm{R}(p)>-1$.

Finally, in (27) put $p=-\frac{1}{2}$ and $n-\frac{1}{2}$ for n; then, as in the proof of (26),

$$(z^2-1)^{-\frac{1}{2}m}\mathrm{Q}_{n-\frac{1}{2}}^m(z)=\frac{\Gamma(m+\frac{1}{2})}{\sqrt{(2\pi)}}\int_0^\pi\frac{\cos n\theta\,d\theta}{(z-\cos\theta)^{m+\frac{1}{2}}}-\frac{\Gamma(m+\frac{1}{2})}{\sqrt{(2\pi)}}\sin n\pi\int_0^\infty\frac{e^{-nu}\,du}{(z+\cosh u)^{m+\frac{1}{2}}}, \quad (32)$$

where $\mathrm{R}(z)>1$, $\mathrm{R}(m+n+\frac{1}{2})>0$ (Proc. Roy. Soc. Edin. lvii. p. 20 (1936)).

VII. *The Limiting Conductivities of Organic Acids in Aqueous Solutions.* *By* J. Frederick J. Dippy, *Ph.D., F.I.C.**

WORKING on the assumption that Onsager's Equation holds for dilute aqueous solutions of sodium salts of organic acids the author has employed a method of determining, with reasonable accuracy, the equivalent conductivity at infinite dilution (Λ_0) which eliminates the necessity of making the modified solvent correction appertaining to salts undergoing partial hydrolysis (for full account see J. Chem. Soc. pp. 161, 1888 (1934)). The procedure seems to be justified in view of the agreement with determinations of other workers employing the more laborious calculations (see J. Chem. Soc. *loc. cit.* p. 343 (1935)), and it can be claimed that the method is actually less empirical than that based on the "n" equation of Ferguson and Vogel (Phil. Mag. l. p. 971 (1925); *cf.* J. Chem. Soc. p. 1605 (1937)) in which arbitrary constants are introduced.

In order to obtain Λ_0 (acid) a knowledge of the limiting mobilities of sodium and hydrogen ions in water is necessary, and having regard to the possible sources of error

* Communicated by the Author.

it is not surprising to find that even the most modern data are somewhat at variance. The values employed for the whole of the present author's work have been those of MacInnes, Shedlovsky, and Longsworth (J. Amer. Chem. Soc. liv. p. 2758 (1932)), viz., Na 50·1, and H 349·7 (temp. 25°). It should be noted that when the mobilities of Jeffery and Vogel (J. Chem. Soc. p. 1715 (1931), p. 400 (1932)) are employed the values of Λ_0 (acid) are smaller by 1·4 units. In the case of acrylic acid German, Jeffery, and Vogel (J. Chem. Soc. p. 1604 (1937)) point out that $K_{therm.} \times 10^5$ recorded by them (5·501) differs from that published by Dippy and Lewis (*ibid.* p. 1008), viz., 5·56, and suggest that this is largely due to the difference in the mobilities used in the calculations. This assertion is incorrect, however, since, on the contrary, a *higher* constant would inevitably result from the use of their mobility data. Consequently the lack of agreement is even greater than hitherto supposed, and the reason must be sought in the experimentally determined Λ_0(salt) data.

German, Jeffery, and Vogel give a value of 90·62 for sodium acrylate, determined with solutions made from the isolated solid salt, whilst Dippy and Lewis found 87·5, with solutions made directly from the acid by neutralization; if these equivalent conductivities had been in harmony the recorded strengths would have been very close. Dippy and Lewis found that the values of Λ_0 (salt) fell very gradually in going from acrylic through vinylacetic to allylacetic acid, and involved a total fall of 4·4 units. It was also pointed out at the time that unsatisfactory data were obtained when solutions were made from isolated salts; the mean values of Λ_0 actually obtained in this way for the foregoing salts were 91·0, 90·1, and 89·6 respectively. This apparent value of 91·0 for sodium acrylate approximates to that derived by German, Jeffery, and Vogel (90·6). It is likely that Λ_0 for sodium acrylate will be appreciably less than that for sodium acetate (91·2, Dippy and Williams, J. Chem. Soc. p. 1888 (1934); and 90·7, Jeffery, Vogel, and Lowry, *ibid.* p. 1637 (1933)), and also that the conductivities of the vinylacetic and allylacetic salts will show a considerable decrease, similar to that observed in the fatty acid series (Bredig, *Z. physikal Chem.* xiii. p. 191 (1894); unpublished work of the author has confirmed this). Therefore it seems that

where the acid is of unsaturated aliphatic type the data derived from salt solutions made directly from the acid are more acceptable. It is well known that olefinic acids undergo isomeric change on prolonged action of alkali, but it is very doubtful if isomerization of an ion would account for such marked changes in mobility as those observed above.

It is also noteworthy that German, Jeffery, and Vogel's potentiometric $K_{therm.}$ data are higher than those obtained

TABLE I.

	Acetic acid.		Benzoic acid.	
	Λ_0(acid).	10^5 $K_{therm.}$	Λ_0 (acid).	10^5 $K_{therm.}$
MacInnes and Shedlovsky, J. Amer. Chem. Soc. liv. p. 1429 (1932) ..	390·6	1·753	..	..
Brockman and Kilpatrick, *ibid.* lvi. p. 1483 (1934) ..	..	..	382·1	6·312
Saxton and Meier, *ibid.* p. 1918 ...	..	..	381·96	6·295
Dippy and Williams, *loc. cit.**	390·6	1·756	383·1	6·273
Jeffery, Vogel, and Lowry, *loc. cit.*, and Vogel and Jeffery, Chem. and Ind. liii. p. 779 (1934) : Phil. Mag. (7) xviii. p. 901 (1934)	388·6	1·764	381·3	6·373
Ives, J. Chem. Soc. p. 731 (1933) ...	391·6	1·759	379·7	6·527

Comparable values for the limiting ion mobilities were employed in the first four series of investigations mentioned above.

conductometrically in all but one of the five monobasic acids studied. This also seems to signify that the value of $5{\cdot}501 \times 10^{-5}$ for acrylic acid is probably low.

In the case of acetic and benzoic acids, however, discordant ion mobilities (and possibly differences in the fundamental equations used for computing Λ_0 (salt)) *are* largely responsible for divergences in the various published constants ; this is seen from Table I.

* The dissociation constants given here to four significant figures are calculated from the original tables of figures.

Experimental.

Aqueous solutions and solid specimens of the sodium salts of acrylic, vinylacetic, and allylacetic acids were prepared in the manner already described elsewhere (J. Chem. Soc. p. 161 (1934)). The conductivity procedure has also been given before. The purity of the acids is described by Dippy and Lewis (*loc. cit.*), who published the acid measurements in detail.

In Table II. the mean values of the Λ_0 (salt) are given; series A refers to measurements made on solutions derived from isolated solid, and series B refers to solutions obtained directly by titration. In the case of every salt two runs

TABLE II.

	A.	B.
Sodium acrylate	91·0	87·5
Sodium vinylacetate	90·1	84·9
Sodium allylacetate	89·6	83·1

TABLE III.

Sodium acrylate.

A.

10^3 C.	Λ.	Λ'.	10^3 C.	Λ.	Λ'.
6·368	85·02	84·87	1·584	88·47	87·94
3·746	86·31	86·06	1·421	89·13	88·47
2·479	87·30	86·94	0·8121	89·78	88·67
2·190	87·72	87·30			

Λ_0=91·3. Water=0·9 gemmho.
Value of Λ_0 determined in second run 90·7.

B.

10^3 C.	Λ.	Λ'.	10^3 C.	Λ.	Λ'.
7·570	81·86	81·68	1·892	84·49	83·99
4·844	82·29	82·12	1·361	85·30	84·61
3·720	82·86	82·52	0·6101	86·38	84·74
2·279	84·12	83·66			

Λ_0=87·5. Water=1·0 gemmho.
Value of Λ_0 determined in second run 87·5.

Sodium vinylacetate.

A.

10^3 C.	Λ.	Λ'.	10^3 C.	Λ.	Λ'.
2·830	85·60	85·29	0·9858	88·13	87·20
2·238	86·23	85·84	0·7841	88·40	87·28
1·537	87·18	86·66	0·6969	88·72	87·42
1·310	87·52	87·06	0·4840	89·36	87·50

Λ_0=90·2. Water=0·9 gemmho.
Value of Λ_0 determined in second run 90·0.

B.

10^3 C.	Λ.	Λ'.	10^3 C.	Λ.	Λ'.
5·776	79·10	78·94	2·116	81·61	81·23
4·624	79·97	79·79	1·421	82·28	81·64
3·481	80·59	80·34	1·030	82·95	82·12
2·787	81·05	80·79	0·6400	83·75	82·33

Λ_0=84·9. Water=0·9 gemmho.
Value of Λ_0 determined in second run 84·9.

Sodium allylacetate.

A.

10^3 C.	Λ.	Λ'.	10^3 C.	Λ.	Λ'.
4·225	84·70	84·53	2·256	86·42	85·96
3·330	85·02	84·74	1·474	86·77	86·14
2·916	85·31	85·02	1·156	87·36	86·58
2·352	85·88	85·47	0·9519	88·22	87·30

Λ_0=89·6. Water=0·9 gemmho.

B.

10^3 C.	Λ.	Λ'.	10^3 C.	Λ.	Λ'.
5·808	77·58	77·45	1·043	81·02	80·17
3·504	78·87	78·61	0·6969	81·83	80·58
2·134	79·59	79·14	0·4840	82·60	80·74
1·522	80·27	79·68			

Λ_0=83·1. Water=0·9 gemmho.

were conducted in each series, and details of one run (in each instance) are recorded in Table III. Λ denotes the uncorrected equivalent conductivity, and Λ' the "normal" solvent-corrected equivalent conductivity; c is in terms of g equivalents/litre. The two cells possessed constants of 0·1252 and 0·07716 respectively; the cell of lower constant was used for the more dilute solutions. All measurements were made at 25° C.

Department of Chemistry,
Technical College, Cardiff.

VIII. *Direct Determination of Stresses from the Stress Equations in some Two-Dimensional Problems of Elasticity.*—Part I. *By* Bibhutibhusan Sen, *Krishnagar College, Bengal* *.

Introduction.

In two-dimensional problems of elasticity, stresses are usually derived from Airy's stress function which satisfies a differential equation of the fourth degree. Attempts have seldom been made for determining stresses from the stress equations of equilibrium and compatibility without the use of this function. In a noteworthy contribution † on the subject, S. D. Carothers has obtained, in terms of plane harmonic functions, certain expressions for stresses which satisfy the equations of equilibrium in an elastic solid having plane deformation. He has used these results for finding stresses in a semi-infinite solid subjected to different distribution of normal pressures on the plane boundary. It is shown in this paper how for certain plane strain problems of solids with curved as well as plane boundaries, stresses can be directly deduced without using Airy's function. Values of stresses on the boundaries being prescribed, problems are reduced to boundary value problems of the theory of potential, and as such the results are expressed either in infinite series or definite integrals. The use of complex variables occasionally makes the solution easier and simpler.

* Communicated by the Author.

† "Plane Strain. The Direct Determination of Stresses," Proc. Roy. Soc. A, London, xcvii. p. 110. See also 'The Mathematical Theory of Elasticity,' by A. E. H. Love, 4th edition, chapter ix.

It is found that the methods developed in this paper can be applied to a wide range of problems, some of which, though solvable by other methods, have been incorporated in this paper as illustrations. Since the equations satisfied by average stresses in problems of "generalized plane stress" are of the same type as those in plane strain problems, the results obtained here can be utilized in finding stresses in thin plates under different edge conditions. (The only modification to be made in the cases of thin plates is the substitution of $\frac{2\lambda\mu}{\lambda+2\mu}$ for the elastic constant λ.)

1 (a). *Solution suitable for a Semi-infinite Solid having a Plane Boundary.*

Supposing that the problem is one of deformation in the x-y plane, we have, in the absence of body forces, the following relations satisfied by the stresses, namely,

$$\left.\begin{aligned} \frac{\partial \widehat{xx}}{\partial x}+\frac{\partial \widehat{xy}}{\partial y}&=0,\\ \frac{\partial \widehat{xy}}{\partial x}+\frac{\partial \widehat{yy}}{\partial y}&=0,\\ \widehat{zz}&=\sigma(\widehat{xx}+\widehat{yy}), \end{aligned}\right\} \quad \ldots\ldots \quad (1.1)$$

while the equation of compatibility stands as

$$\frac{\partial^2}{\partial y^2}[(1-\sigma)\widehat{xx}-\sigma\widehat{yy}]+\frac{\partial^2}{\partial x^2}[(1-\sigma)\widehat{yy}-\sigma\widehat{xx}]=2\frac{\partial^2 \widehat{xy}}{\partial x\,\partial y}. \quad (1.2)$$

From these stresses we can deduce the consistency equations

$$\left.\begin{aligned} \nabla_1^2\widehat{xy}+\frac{\partial^2\odot}{\partial x^2}&=0,\\ \nabla_1^2\widehat{xy}+\frac{\partial^2\odot}{\partial x\,\partial y}&=0,\\ \nabla_1^2\widehat{yy}+\frac{\partial^2\odot}{\partial y^2}&=0,\\ \nabla_1^2\odot&=0, \end{aligned}\right\} \quad \ldots\ldots \quad (1.3)$$

where

$$\odot=\widehat{xx}+\widehat{yy}, \quad \ldots\ldots \quad (1.4)$$

and

$$\nabla_1^2=\frac{\partial^2}{\partial x^2}+\frac{\partial^2}{\partial y^2}. \quad \ldots\ldots \quad (1.5)$$

As the solution of equation (1.3), we can put

$$\left.\begin{aligned}\widehat{xx}&=-\tfrac{1}{2}x\frac{\partial\odot}{\partial x}+\phi_1(x,y),\\ \widehat{xy}&=-\tfrac{1}{2}x\frac{\partial\odot}{\partial y}+\phi_2(x,y),\\ \widehat{yy}&=\odot+\tfrac{1}{2}x\frac{\partial\odot}{\partial x}-\phi_1(x,y),\end{aligned}\right\}\quad\ldots\quad(1.6)$$

in which the expressions $\phi_1(x, y)$ and $\phi_2(x, y)$ are plane harmonic functions satisfying the conditions

$$\left.\begin{aligned}(\widehat{xx})_{x=0}&=[\phi_1(x,y)]_{x=0}=p(y),\\ (\widehat{xy})_{x=0}&=[\phi_2(x,y)]_{x=0}=q(y).\end{aligned}\right\}\quad\ldots\quad(1.7)$$

Since

$$\frac{\partial\widehat{xx}}{\partial x}+\frac{\partial\widehat{xy}}{\partial y}=0,$$

we have from (1.6)

$$\frac{1}{2}\frac{\partial\odot}{\partial x}=\frac{\partial\phi_1(x,y)}{\partial x}+\frac{\partial\phi_2(x,y)}{\partial y}.\quad\ldots\quad(1.8)$$

Expressions for $\phi_1(x, y)$ and $\phi_2(x, y)$ which satisfy Laplace's equation in two dimensions and assume the boundary values (1.7) are usually written as

$$\left.\begin{aligned}\phi_1(x,y)&=\frac{1}{\pi}\int_0^\infty da\int_{-\infty}^{\infty}e^{-ax}p(\lambda)\cos a(\lambda-y)\,d\lambda,\\ \phi_2(x,y)&=\frac{1}{\pi}\int_0^\infty da\int_{-\infty}^{\infty}e^{-ax}q(\lambda)\cos a(\lambda-y)\,d\lambda.\end{aligned}\right\}\quad(1.9)$$

Alternative forms that can be deduced by Green's theorem are

$$\left.\begin{aligned}\phi_1(x,y)&=\frac{1}{\pi}\frac{\partial}{\partial x}\int_{-\infty}^{\infty}p(\lambda)\log R\,d\lambda,\\ \phi_2(x,y)&=\frac{1}{\pi}\frac{\partial}{\partial x}\int_{-\infty}^{\infty}q(\lambda)\log R\,d\lambda,\end{aligned}\right\}\quad\ldots\quad(1.10)$$

where

$$R^2=(\lambda-y)^2+x^2.$$

Putting

$$\left.\begin{aligned}\int_{-\infty}^{\infty}p(\lambda)\log R\,d\lambda&=V_1,\\ \int_{-\infty}^{\infty}q(\lambda)\log R\,d\lambda&=V_2,\end{aligned}\right\}\quad\ldots\quad(1.11)$$

we get

$$\odot = \frac{2}{\pi}\left[\frac{\partial V_1}{\partial x} + \frac{\partial V_2}{\partial y}\right]. \quad . \quad . \quad . \quad (1.12)$$

If $p(y)$ and $q(y)$ are known on the plane boundary $x=0$, we can find from (1.11) the functions V_1 and V_2, whence the value of $\odot$, can be obtained with the help of (1.12). Values of $\phi_1(x\,y)$ and $\phi_2(x, y)$ can be deduced from (1.10), and then the stresses can be completely determined from equations (1.6).

1 (b). *Use of Complex Variables.*

(i.) When the boundary $x=0$ is acted on by normal stress only, we shall have $\phi_2(x, y)=0$, and we shall get at once from (1.8)

$$\odot = 2\phi_1(x, y). \quad . \quad . \quad . \quad . \quad . \quad (1.13)$$

Let $\psi_1(x, y)$ be the function conjugate to $\phi_1(x, y)$, so that

$$\left.\begin{aligned} \phi_1(x, y) + i\psi_1(x, y) &= f_1(z), \\ z &= x + iy. \end{aligned}\right\} \quad . \quad . \quad (1.14)$$

where

Then we can write

$$\phi_1(x, y) = \mathrm{Re}[f_1(z)], \quad . \quad . \quad . \quad . \quad (1.15)$$

Re denoting the real part of the function.

Hence from (1.6) we get

$$\left.\begin{aligned} \widehat{xx} &= \mathrm{Re}[-xf_1{}^1(z) + f_1(z)], \\ \widehat{xy} &= \mathrm{Re}[-ixf_1{}^1(z)], \\ \widehat{yy} &= \mathrm{Re}[f_1(z) + xf_1{}^1(z)]. \end{aligned}\right\} \quad . \quad . \quad (1.16)$$

(ii.) In the case of the straight boundary $x=0$ having a shear load only, we shall have $\phi_1(x, y)=0$, and hence from (1.8)

$$\frac{1}{2}\frac{\partial \odot}{\partial x} = \frac{\partial \phi_2(x, y)}{\partial y}.$$

Putting now

$$\phi_2(x, y) = \mathrm{Re}[f_2(z)], \quad . \quad . \quad . \quad . \quad (1.17)$$

where

$$f_2(z) = \phi_2(x, y) + i\psi_2(x, y). \quad . \quad . \quad . \quad (1.18)$$

we get from (1.6)

$$\left.\begin{aligned} \widehat{xx} &= \mathrm{Re}[-ixf_2{}^1(z)], \\ \widehat{xy} &= \mathrm{Re}[xf_2{}^1(z) + f_2(z)], \\ \widehat{yy} &= \mathrm{Re}[2if_2(z) + ixf_2{}^1(z)]. \end{aligned}\right\} \quad . \quad . \quad . \quad (1.19)$$

1 (c). *Illustrative Examples.*

I. *Concentrated Normal Load on the Plane Boundary.*

We shall begin with the simple case of a concentrated normal load of intensity p_0 acting on the plane boundary at the point $x=0$, $y=0$. From (1.10) we get

$$\left.\begin{aligned} \phi_1(x, y) &= -\frac{p_0}{\pi}\frac{x}{r^2}, \\ r^2 &= x^2+y^2. \end{aligned}\right\} \quad \ldots \quad (1.20)$$

where

There being no shear load on the boundary, we have

$$\odot = -\frac{2p_0}{\pi}\frac{x}{r^2}, \quad \ldots \quad (1.21)$$

whence we obtain, with the help of the formulæ (1.6),

$$\left.\begin{aligned} \widehat{xx} &= -\frac{2p_0}{\pi}\frac{x^3}{r^4}, \\ \widehat{xy} &= -\frac{2p_0}{\pi}\frac{x^2y}{r^4}, \\ \widehat{yy} &= -\frac{2p_0}{\pi}\frac{xy^2}{r^4}. \end{aligned}\right\} \quad \ldots \quad (1.22)$$

II. *Concentrated Shear Load on the Boundary.*

Let us now suppose that the boundary $x=0$ has got only a shear load q_0 at the origin. Then

$$\phi_2(x, y) = -\frac{q_0 x}{\pi r^2} = \mathrm{Re}\left[-\frac{q_0}{\pi z}\right]. \quad \ldots \quad (1.23)$$

Hence, putting $f_2(z) = -\dfrac{q_0}{\pi z}$ in (1.19),

we get

$$\left.\begin{aligned} \widehat{xx} &= -\frac{2q_0}{\pi}\frac{x^2y}{r^4}, \\ \widehat{xy} &= -\frac{2q_0}{\pi}\frac{xy^2}{r^4}, \\ \widehat{yy} &= -\frac{2q_0}{\pi}\frac{y^3}{r^4}. \end{aligned}\right\} \quad \ldots \quad (1.24)$$

III. *Uniform Normal Load over a certain Portion of the Boundary.*

Let there be a distribution of normal pressure on the boundary $x=0$ such that

$$\left.\begin{aligned} \widehat{xx}&=0 \quad \text{if} \quad y<-h \quad \text{and if} \quad y>h, \\ \widehat{xx}&=-p_0 \quad \text{if} \quad -h<y<h. \end{aligned}\right\} \quad . \quad (1.25)$$

Then from (1.9) we obtain

$$\phi_1(x, y)=-\frac{p_0}{\pi}\left[\tan^{-1}\frac{h+y}{x}+\tan^{-1}\frac{h-y}{x}\right], \quad (1.26)$$

which gives, in the absence of any shear load on the boundary,

$$\left.\begin{aligned} \widehat{xx}&=-\frac{p_0}{\pi}\left[x\left\{\frac{h-y}{x^2+(h-y)^2}+\frac{h+y}{x^2+(h+y)^2}\right\}\right. \\ &\qquad \left.+\tan^{-1}\frac{h+y}{x}+\tan^{-1}\frac{h-y}{x}\right], \\ \widehat{yy}&=-\frac{p_0}{\pi}\left[\tan^{-1}\frac{h+y}{x}+\tan^{-1}\frac{h-y}{x}\right. \\ &\qquad \left.-x\left\{\frac{h-y}{x^2+(h-y)^2}+\frac{h+y}{x^2+(h+y)^2}\right\}\right], \\ \widehat{xy}&=\frac{p_0}{\pi}x^2\left[\frac{1}{x^2+(h+y)^2}-\frac{1}{x^2+(h-y)^2}\right]. \end{aligned}\right\} \quad . \quad . \quad . \quad (1.27)$$

IV. *Uniform Shear Load over a certain Portion of the Boundary.*

We shall now discuss the case when the boundary $x=0$ has no normal load, but has the shear load as given below.

$$\left.\begin{aligned} \widehat{xy}&=0 \quad \text{when} \quad y<-h \quad \text{and} \quad y>h, \quad \text{and} \\ \widehat{xy}&=-q_0 \quad \text{when} \quad -h<y<h. \end{aligned}\right\} \quad . \quad (1.28)$$

The value of $\phi_2(x, y)$ is then given by

$$\begin{aligned} \phi_2(x, y)&=-\frac{q_0}{\pi}\left[\tan^{-1}\frac{h+y}{x}+\tan^{-1}\frac{h-y}{x}\right] \\ &=\mathrm{Re}[f_2(z)], \quad . \quad . \quad . \quad . \quad . \quad . \quad . \quad . \quad (1.29) \end{aligned}$$

where

$$f_2(z)=\frac{q_0}{\pi}i\log\frac{z+ih}{z-ih}. \quad . \quad . \quad . \quad . \quad (1.30)$$

Hence from (1.19) we get

$$\left.\begin{aligned}
\widehat{xx} &= -\frac{q_0 x^2}{\pi}\left[\frac{1}{x^2+(h-y)^2} - \frac{1}{x^2+(h+y)^2}\right], \\
\widehat{xy} &= -\frac{q_0}{\pi}\left[\tan^{-1}\frac{h+y}{x} + \tan^{-1}\frac{h-y}{x}\right. \\
&\qquad \left. -x\left\{\frac{h-y}{x^2+(h-y)^2} + \frac{h+y}{x^2+(h+y)^2}\right\}\right], \\
\widehat{yy} &= -\frac{q_0}{\pi}\left[\log\frac{x^2+(h+y)^2}{x^2+(h-y)^2}\right. \\
&\qquad \left. -x^2\left\{\frac{1}{x^2+(h-y)^2} - \frac{1}{x^2+(h+y)^2}\right\}\right].
\end{aligned}\right\} \quad . \quad . \quad . \quad (1.31)$$

V. *Pressures given in the Form of an Infinite Series.*

When the boundary values of the stresses are given in the form of an infinite series the problem becomes extremely simple. As, for example, if

$$\left.\begin{aligned}
\phi_1(x, y) &= \sum_{m=0}^{\infty} A_m e^{-mx}\cos my, \\
\text{and} \qquad \phi_2(x, y) &= 0,
\end{aligned}\right\}, \quad . \quad . \quad (1.32)$$

we have $\quad . \quad . \quad \widehat{xx} = \sum_{m=0}^{\infty} A_m \cos my,$

and $\widehat{xy} = 0,$

on the boundary $x = 0$.

We shall obtain in this case

$$\odot = 2\sum_{m=0}^{\infty} A_m e^{-mx}\cos my, \quad . \quad . \quad . \quad (1.33)$$

which gives

$$\left.\begin{aligned}
\widehat{xx} &= \sum_{m=0}^{\infty} A_m(mx+1)e^{-mx}\cos my, \\
\widehat{xy} &= \sum_{m=1}^{\infty} A_m\, mx\, e^{-mx}\sin my, \\
\widehat{yy} &= -\sum_{m=0}^{\infty} A_m(mx-1)e^{-mx}\cos my.
\end{aligned}\right\} \quad . \quad . \quad (1.34)$$

VI. *A Case of Variable Pressure on a Portion of the Boundary.*

If we assume that

$$\left.\begin{aligned} \phi_1(x, y) &= -p_0 \operatorname{Re}[\sqrt{b^2+z^2}-z], \\ \text{and} \qquad \phi_2(x, y) &= 0, \end{aligned}\right\} \quad . \quad . \quad (1.35)$$

we find the following distribution :

$$\left.\begin{aligned} (\widehat{xy})_{x=0} &= 0 \quad \text{for all values of } y, \\ (\widehat{xx})_{x=0} &= -p_0\sqrt{b^2-y^2} \quad \text{when} \quad -b \leqq y \leqq b, \\ &= 0 \quad \text{for other values of } y. \end{aligned}\right\} \quad (1.36)$$

Applying (1.16) we get

$$\left.\begin{aligned} \widehat{xx} &= -p_0 \operatorname{Re}\left[\frac{-xz}{\sqrt{b^2+z^2}} + \sqrt{b^2+z^2}\right], \\ \widehat{xy} &= p_0 \operatorname{Re}\left[\frac{ixz}{\sqrt{b^2+z^2}}\right], \\ \widehat{yy} &= -p_0 \operatorname{Re}\left[\frac{xz}{\sqrt{b^2+z^2}} - 2z + \sqrt{b^2+z^2}\right]. \end{aligned}\right\} \quad (1.37)$$

1 (d). *Expressions for the Displacement.*

In this section the method of deducing expressions for displacement in some cases discussed above will be given. From the stress-strain relations we have in the case of plane deformation

$$\left.\begin{aligned} \frac{\partial u}{\partial x} &= \frac{1}{2\mu}[\widehat{xx}(1-\sigma)-\sigma\widehat{yy}], \\ \frac{\partial v}{\partial y} &= \frac{1}{2\mu}[\widehat{yy}(1-\sigma)-\sigma\widehat{xx}], \\ \frac{\partial v}{\partial x} + \frac{\partial u}{\partial y} &= \frac{1}{\mu}\widehat{xy}. \end{aligned}\right\} \quad . \quad . \quad . \quad (1.38)$$

(i.) Let the normal load be given by the function $[f_1(x, y)]_{x=0}$, and let $\psi_1(x, y)$ be the function conjugate to it, so that

$$\phi_1(x, y) + i\psi_1(x, y) = f_1(z).$$

Then the shear load being absent, we have

$$\left.\begin{aligned}\frac{\partial u}{\partial x}&=\frac{1}{2\mu}\left[(1-2\sigma)\phi_1-x\frac{\partial\phi_1}{\partial x}\right],\\ \frac{\partial v}{\partial y}&=\frac{1}{2\mu}\left[(1-2\sigma)\phi_1+x\frac{\partial\phi_1}{\partial x}\right],\\ \frac{\partial u}{\partial y}&+\frac{\partial v}{\partial x}=-\frac{x}{\mu}\frac{\partial\phi_1}{\partial y}.\end{aligned}\right\}\quad\ldots\quad(1.39)$$

Putting $\int f_1(z)\,dz=\mathrm{F}_1(z)=\Phi_1(x,y)+i\Psi_1(x,y)$, . (1.40)

we obtain

$$\left.\begin{aligned}u&=\frac{1}{2\mu}[2(1-\sigma)\Phi_1-x\phi_1]-\alpha_1 y+\beta_1,\\ v&=\frac{1}{2\mu}[(1-2\sigma)\Psi_1+x\psi_1]+\alpha_1 x+\gamma_1,\end{aligned}\right\}\quad\ldots\quad(1.41)$$

or

$$\left.\begin{aligned}u&=\frac{1}{2\mu}\mathrm{Re}[2(1-\sigma)\mathrm{F}_1(z)-xf_1(z)]-\alpha_1 y+\beta_1,\\ v&=\frac{1}{2\mu}\mathrm{Re}[-i(1-2\sigma)\mathrm{F}_1(z)-ixf_1(z)]+\alpha_1 x+\gamma_1.\end{aligned}\right\}\quad(1.42)$$

In the case of a concentrated normal load acting at the origin we have

$$\left.\begin{aligned}f_1(z)&=-\frac{p_0}{\pi z},\\ \text{and}\qquad \mathrm{F}_1(z)&=-\frac{p_0}{\pi}\log z.\end{aligned}\right\}\quad\ldots\quad(1.43)$$

Therefore, neglecting the rigid body displacements, we get

$$\left.\begin{aligned}u&=-\frac{p_0}{2\pi\mu}\left[2(1-\sigma)\log r-\frac{x^2}{r^2}\right],\\ v&=-\frac{p_0}{2\pi\mu}\left[(1-2\sigma)\theta-\frac{xy}{r^2}\right].\end{aligned}\right\}\quad\ldots\quad(1.44)$$

(ii.) When there is only the shear load $[\phi_2(x,y)]_{x=0}$ on the boundary, we can put

$$f_2(z)=\phi_2(x,y)+i\psi_2(x,y),\quad\ldots\quad(1.45)$$

and $$\int f_2(z)\,dz=\mathrm{F}_2(z)=\Phi_2(x,y)+i\Psi_2(x,y).\quad\ldots\quad(1.46)$$

Hence we get from (1.6) and (1.38)

$$\left.\begin{aligned} u&=\frac{1}{2\mu}[-(1-2\sigma)\Psi_2+x\psi_2]-\alpha_2 y+\beta_2,\\ v&=\frac{1}{2\mu}[2(1-\sigma)\Phi_2+x\phi_2]+\alpha_2 x+\gamma_2, \end{aligned}\right\}, \quad (1.47)$$

or

$$\left.\begin{aligned} u&=\frac{1}{2\mu}\mathrm{Re}[(1-2\sigma)i\mathrm{F}_2(z)-ixf_2(z)]-\alpha_2 y+\beta_2,\\ v&=\frac{1}{2\mu}\mathrm{Re}[2(1-\sigma)\mathrm{F}_2(z)+xf_2(z)]+\alpha_2 x+\gamma_2. \end{aligned}\right\}. \quad (1.48)$$

For instance, let us consider the case of a concentrated shear load q_0 at the origin. Then

$$\left.\begin{aligned} f_2(z)&=-\frac{q_0}{\pi z},\\ \text{and}\qquad \mathrm{F}_2(z)&=-\frac{q_0}{\pi}\log z, \end{aligned}\right\}. \quad . \quad . \quad . \quad . \quad (1.49)$$

which give, on neglecting the rigid body displacements,

$$\left.\begin{aligned} u&=-\frac{q_0}{2\pi\mu}\left[-(1-2\sigma)\theta-\frac{xy}{r^2}\right],\\ v&=-\frac{q_0}{2\pi\mu}\left[2(1-\sigma)\log r+\frac{x^2}{r^2}\right]. \end{aligned}\right\}. \quad . \quad (1.50)$$

2. (a). *Solution suitable for a Solid Cylinder having a Circular Boundary.*

From the first two equations of (1.3), we get

$$(x\nabla_1^2\widehat{xx}+y\nabla_1^2\widehat{xy})+\left(x\frac{\partial^2\odot}{\partial x^2}+y\frac{\partial^2\odot}{\partial x\,\partial y}\right)=0,$$

or

$$\nabla_1^2(x\widehat{xx}+y\widehat{xy})+r\frac{\partial}{\partial r}\left(\frac{\partial\odot}{\partial x}\right)-2\left(\frac{\partial\widehat{xx}}{\partial x}+\frac{\partial\widehat{xy}}{\partial y}\right)=0.$$

By virtue of the equations of equilibrium, this equation reduces to

$$\nabla_1^2(r\mathrm{X}_r)+\frac{\partial}{\partial x}\left(r\frac{\partial\odot}{\partial r}-\odot\right)=0, \quad . \quad . \quad (2.1)$$

where $r^2=x^2+y^2$,

and X_r=x-component of the stresses at a point (r, θ) on the circle of radius r.

Similarly, taking the second and the third of equations (1.3), we have

$$\nabla_1^2(rY_r)+\frac{\partial}{\partial y}\left(r\frac{\partial\odot}{\partial r}-\odot\right)=0, \quad . \quad . \quad (2.2)$$

Y_r being the y-component of the stresses at the point (r,θ) on the circle of radius r.

Putting $$\odot=\Sigma\odot_n, \quad . \quad . \quad . \quad . \quad . \quad . \quad (2.3)$$

where $\odot_n$ is a homogeneous plane harmonic function of the nth degree, we have

$$\left(r\frac{\partial\odot}{\partial r}-\odot\right)=\Sigma(n-1)\odot_n. \quad . \quad . \quad . \quad (2.4)$$

Hence we can write (2.1) and (2.2) in the forms

$$\left.\begin{aligned}\nabla_1^2(rX_r)+\Sigma(n-1)\frac{\partial\odot_n}{\partial x}&=0.\\ \nabla_1^2(rY_r)+\Sigma(n-1)\frac{\partial\odot_n}{\partial y}&=0.\end{aligned}\right\}. \quad . \quad . \quad (2.5)$$

By solving the above equations we get

$$\left.\begin{aligned}rX_r&=-\tfrac{1}{4}\Sigma\frac{n-1}{n}(r^2-a^2)\frac{\partial\odot_n}{\partial x}+a\Sigma L_n(x,y),\\ rY_r&=-\tfrac{1}{4}\Sigma\frac{n-1}{n}(r^2-a^2)\frac{\partial\odot_n}{\partial y}+a\Sigma M_n(x,y),\end{aligned}\right\}. \quad (2.6)$$

in which $L_n(x,y)$ and $M_n(x,y)$ are homogeneous plane harmonic functions of the nth degree such that

$$\left.\begin{aligned}(X_r)_{r=a}&=[\Sigma L_n(x,y)]_{r=a},\\ (Y_r)_{r=a}&=[\Sigma M_n(x,y)]_{r=a}.\end{aligned}\right\}. \quad . \quad . \quad . \quad (2.7)$$

Since

$$\frac{\partial}{\partial x}(rX_r)+\frac{\partial}{\partial y}(rY_r)=\frac{\partial}{\partial x}(x\widehat{xx}+y\widehat{xy})+\frac{\partial}{\partial y}(x\widehat{xy}+y\widehat{yy})=\odot,$$

we have from (2.6)

$$\Sigma\odot_n=-\tfrac{1}{4}\Sigma\frac{n-1}{n}\left[2x\frac{\partial\odot_n}{\partial x}+2y\frac{\partial\odot_n}{\partial y}\right]+a\Sigma\left[\frac{\partial L_n}{\partial x}+\frac{\partial M_n}{\partial y}\right],$$

which gives

$$\Sigma\frac{\odot_n(n+1)}{2}=a\Sigma\left[\frac{\partial L_n}{\partial x}+\frac{\partial M_n}{\partial y}\right]. \quad . \quad . \quad . \quad (2.8)$$

Hence, unless* $n=-1$, we have

$$\odot_n=\frac{2a}{n+1}\,S_n(x, y), \quad . \quad . \quad . \quad . \quad (2.9)$$

where
$$S_n(x, y)=\frac{\partial L_{n+1}}{\partial x}+\frac{\partial M_{n+1}}{\partial y}. \quad . \quad . \quad (2.10)$$

It is thus apparent that when the values of X_r and Y_r are prescribed on the boundary $r=a$ we can determine from the known solutions of the boundary value problems in the theory of potential, the functions $\Sigma L_n(x, y)$ and $\Sigma M_n(x, y)$ which satisfy Laplace's equation in two dimensions within the circle and assume the prescribed values on the boundary. These functions being known we can find from (2.9) the value of $\odot_n$ (except when $n=-1$), and hence from (2.6) the values of X_r and Y_r at any point within the circle can be determined.

2. (b). *Use of Complex Variables.*

By using complex functions the results (2.6) can be put in a more compact form. Let us suppose that when expressed in convergent power series

$$\left.\begin{aligned}\Sigma L_n(x, y)&=\Sigma A_n z^n,\\ \Sigma M_n(x, y)&=\Sigma B_n z^n,\end{aligned}\right\}, \quad . \quad . \quad . \quad (2.11)$$

where A_n's and B_n's are real constants and $z=x+iy$. Then, assuming

$$\Sigma\odot_n=\Sigma C_n z^n, \quad . \quad . \quad . \quad . \quad . \quad (2.12)$$

we get from (2.8) for all positive values of n

$$C_n=2a[A_{n+1}+iB_{n+1}]. \quad . \quad . \quad . \quad (2.13)$$

Hence we can write

$$\left.\begin{aligned}rX_r&=-a\mathrm{Re}\Big[\sum_{n=2}^{\infty}\frac{n-1}{2}(r^2-a^2)(A_{n+1}+iB_{n+1})z^{n-1}\\ &\qquad -\sum_{n=0}^{\infty}A_n z^n\Big],\\ rY_r&=-a\mathrm{Re}\Big[\sum_{n=2}^{\infty}\frac{n-1}{2}(r^2-a^2)(iA_{n+1}-B_{n+1})z^{n-1}\\ &\qquad -\sum_{n=0}^{\infty}B_n z^n\Big].\end{aligned}\right\} \quad (2.14)$$

* The case $n=-1$ is treated separately in a later section [*vide* 3 (*b*)].

The constants A_n's and B_n's are to be determined from the prescribed values of X_r and Y_r on the boundary, which can be put as

$$\left.\begin{aligned}(X_r)_{r=a}&=\mathrm{Re}\left[\sum_{n=0}^{\infty} A_n z^n\right]_{|z|=a},\\ (Y^r)_{r=a}&=\mathrm{Re}\left[\sum_{n=0}^{\infty} B_n z^n\right]_{|z|=a}.\end{aligned}\right\} \quad . \quad . \quad . \quad (2.15)$$

2 (c). *Boundary Value Problems of the Circle.*

We have seen in section 2 (a) that the solution of the main problem depends on the determination of the plane harmonic functions $\Sigma L_n(x, y)$ and $\Sigma M_n(x, y)$ which satisfy definite boundary conditions. For the circular region we introduce polar coordinates (r, θ) and assume that

$$\left.\begin{aligned}&[\Sigma L_n(x, y)]_{r=a}=f_1(\theta)\\ \text{and}\quad&[\Sigma M_n(x, y)]_{r=a}=f_2(\theta),\end{aligned}\right\} \quad . \quad . \quad . \quad (2.16)$$

where $f_1(\theta)$ and $f_2(\theta)$ are continuous periodic functions of θ with sectionally continuous first derivatives. Then in terms of polar coordinates, the expressions for the functions are

$$\left.\begin{aligned}\Sigma L_n(x, y)&=\frac{a^2-r^2}{2\pi}\int_0^{2\pi}\frac{f_1(\alpha)}{a^2-2ar\cos(\theta-\alpha)+r^2}d\alpha,\\ \Sigma M_n(x, y)&=\frac{a^2-r^2}{2\pi}\int_0^{2\pi}\frac{f_2(\alpha)}{a^2-2ar\cos(\theta-\alpha)+r^2}d\alpha.\end{aligned}\right\} \quad (2.17)$$

It will, however, be more convenient in many examples to express these functions in series. Let the prescribed boundary functions $f_1(\theta)$ and $f_2(\theta)$ expanded in Fourier series be given by

$$\left.\begin{aligned}f_1(\theta)&=\frac{A_0}{2}+\sum_{n=1}^{\infty}(A_n\cos n\theta+B_n\sin n\theta),\\ f_2(\theta)&=\frac{A_0'}{2}+\sum_{n=1}^{\infty}(A_n'\cos n\theta+B_n'\sin n\theta).\end{aligned}\right\} \quad (2.18)$$

Then the required functions suitable for the interior region of the circle can be put as

$$\left.\begin{aligned}\Sigma L_n(x, y)&=\frac{A_0}{2}+\sum_{n=1}^{\infty}\frac{r^n}{a^n}(A_n\cos n\theta+B_n\sin n\theta),\\ \Sigma M_n(x, y)&=\frac{A_0'}{2}+\sum_{n=1}^{\infty}\frac{r^n}{a^n}(A_n'\cos n\theta+B_n'\sin n\theta).\end{aligned}\right\} \quad (2.19)$$

If the series assumed for $f_1(\theta)$ and $f_2(\theta)$ converge absolutely and uniformly, the series given in (2.19) also converge uniformly and absolutely in the interior of the circle. Since the convergence is uniform we can interchange integration and summation and obtain

$$\left.\begin{aligned} \mathrm{L}_n(x, y) &= \frac{1}{\pi}\int_0^{2\pi}\left[\tfrac{1}{2}+\sum_{n=1}^{\infty}\frac{r^n}{a^n}\cos n(\theta-\alpha)\right] f_1(\alpha)\, d\alpha, \\ \mathrm{M}_n(x, y) &= \frac{1}{\pi}\int_0^{2\pi}\left[\tfrac{1}{2}+\sum_{n=1}^{\infty}\frac{r^n}{a^n}\cos n(\theta-\alpha)\right] f_2(\alpha)\, d\alpha. \end{aligned}\right\} \quad (2.20)$$

2 (d). *Illustrative Examples.*

It is evident from what has been stated above that the values of X_r and Y_r can be obtained at once from the expression (2.6) by expressing their boundary values in series or integrals. In this section some particular examples will be discussed in which, instead of X_r and Y_r, the stress components $\widehat{rr}$ and $\widehat{r\theta}$ are prescribed on the boundary.

I. We shall begin with a simple case in which the given distribution on the boundary $r=a$ is

$$\left.\begin{aligned} \widehat{rr} &= \mathrm{P}_n \cos\theta, \\ \widehat{\theta r} &= 0, \end{aligned}\right\} \quad \ldots\ldots \quad (2.21)$$

P_n being a constant.

Then we have

$$\left.\begin{aligned} (\mathrm{X}_r)_{r=a} &= \frac{\mathrm{P}_n}{2}[\cos(n+1)\theta+\cos(n-1)\theta], \\ (\mathrm{Y}_r)_{r=a} &= \frac{\mathrm{P}_n}{2}[\sin(n+1)\theta-\sin(n-1)\theta]. \end{aligned}\right\} \quad (2.22)$$

To satisfy these relations we may take

$$\left.\begin{aligned} \Sigma\mathrm{L}_n(x, y) = \mathrm{L}(x, y) &= \frac{\mathrm{P}_n}{2}\left[\frac{r^{n+1}}{a^{n+1}}\cos(n+1)\theta\right. \\ &\qquad \left.+\frac{r^{n-1}}{a^{n-1}}\cos(n-1)\theta\right], \\ \Sigma\mathrm{M}_n(x, y) = \mathrm{M}(x, y) &= \frac{\mathrm{P}_n}{2}\left[\frac{r^{n+1}}{a^{n+1}}\sin(n+1)\theta\right. \\ &\qquad \left.-\frac{r^{n-1}}{a^{n-1}}\sin(n-1)\theta\right]. \end{aligned}\right\} \quad (2.23)$$

Since

$$\left.\begin{aligned}\frac{\partial}{\partial x}&=\cos\theta\frac{\partial}{\partial r}-\frac{\sin\theta}{r}\frac{\partial}{\partial\theta},\\ \frac{\partial}{\partial y}&=\sin\theta\frac{\partial}{\partial r}+\frac{\cos\theta}{r}\frac{\partial}{\partial\theta},\end{aligned}\right\}\quad\ldots\quad(2.24)$$

we have from (2.8)

$$a\left[\frac{\partial \mathrm{L}}{\partial x}+\frac{\partial \mathrm{M}}{\partial y}\right]=(n+1)\mathrm{P}_n\frac{r^n}{a^n}\cos n\theta=\frac{n+1}{2}\odot_n,$$

which gives

$$\odot_n=2\mathrm{P}_n\frac{r^n}{a^n}\cos n\theta,\quad\ldots\quad(2.25)$$

(except when $n=-1$), and

$$\left.\begin{aligned}r\mathrm{X}_r=\frac{\mathrm{P}_n a}{2}\Big[&-(n-1)\frac{r^{n-1}}{a^{n+1}}(r^2-a^2)\cos(n-1)\theta\\&+\frac{r^{n+1}}{a^{n+1}}\cos(n+1)\theta+\frac{r^{n-1}}{a^{n-1}}\cos(n-1)\theta\Big],\\ r\mathrm{Y}_r=\frac{\mathrm{P}_n a}{2}\Big[&(n-1)\frac{r^{n-1}}{a^{n+1}}(r^2-a^2)\sin(n-1)\theta\\&+\frac{r^{n+1}}{a^{n+1}}\sin(n+1)\theta-\frac{r^{n-1}}{a^{n-1}}\sin(n-1)\theta\Big].\end{aligned}\right\}\quad(2.26)$$

Moreover, if on the boundary $r=a$,

$$\left.\begin{aligned}\widehat{rr}&=\frac{\mathrm{P}_0}{2},\\ \widehat{r\theta}&=0,\end{aligned}\right\}\quad\ldots\quad(2.27)$$

we have simply

$$\left.\begin{aligned}r\mathrm{X}_r&=\frac{\mathrm{P}_0}{2}r\cos\theta,\\ r\mathrm{Y}_r&=\frac{\mathrm{P}_0}{2}r\sin\theta.\end{aligned}\right\}\quad\ldots\quad(2.28)$$

II. Thus, if we have on the boundary $r=a$,

$$\left.\begin{aligned}\widehat{rr}&=\frac{\mathrm{P}_0}{2}+\sum_{n=1}^{\infty}\mathrm{P}_n\cos n\theta,\\ \widehat{r\theta}&=0,\end{aligned}\right\}\quad\ldots\quad(2.29)$$

we can write

$$\left.\begin{aligned} rX_r &= \frac{P_0}{2} r\cos\theta + \frac{a}{2}\sum_{n=1}^{\infty} P_n\left[-(n-1)\frac{r^{n-1}}{a^{n+1}}(r^2-a^2)\cos(n-1)\theta\right. \\ &\qquad \left. + \frac{r^{n+1}}{a^{n+1}}\cos(n+1)\theta + \frac{r^{n-1}}{a^{n-1}}\cos(n-1)\theta\right], \\ rY_r &= \frac{P_0}{2} r\sin\theta + \frac{a}{2}\sum_{n+1}^{\infty} P_n\left[(n-1)\frac{r^{n-1}}{a^{n+1}}(r^2-a^2)\sin(n-1)\theta\right. \\ &\qquad \left. + \frac{r^{n+1}}{a^{n+1}}\sin(n+1)\theta - \frac{r^{n-1}}{a^{n-1}}\sin(n-1)\theta\right]. \end{aligned}\right\} \quad . \quad . \quad . \quad (2.30)$$

It is to be noted that when the forces applied on the boundary are self-equilibrating, we must have the relations

$$\left.\begin{aligned} \left[\int_0^{2\pi} rX_r\, d\theta\right]_{r=a} &= 0, \\ \left[\int_0^{2\pi} rY_r\, d\theta\right]_{r=a} &= 0, \end{aligned}\right\} \quad . \quad . \quad . \quad (2.31)$$

which make $P_1=0$.

III. *A Diametrically Compressed Circle.*

Let us now take the instance of a diametrically compressed cylindrical roller. The boundary conditions in this case are

$$\left.\begin{aligned} \widehat{r\theta} &= 0, \\ \widehat{rr} &= -F \quad \text{when } \theta = \pm\frac{\pi}{2}, \\ \widehat{rr} &= 0 \quad \text{for other values of } \theta, \end{aligned}\right\} \quad \text{when } r=a. \quad (2.32)$$

By Fourier's theorem we get *

$$\left.\begin{aligned} P_0 &= -\frac{2F}{a\pi}, \\ P_{2n+1} &= 0, \\ P_{2n} &= (-1)^{n-1}\frac{2F}{a\pi}. \end{aligned}\right\} \quad . \quad . \quad . \quad . \quad (2.33)$$

* To avoid mathematically infinite stresses the load may be supposed to be uniformly distributed over the small arcs

$$\frac{\pi}{2}-\alpha<\theta<\frac{\pi}{2}+\alpha \quad \text{and} \quad -\left(\frac{\pi}{2}+\alpha\right)<\theta<-\left(\frac{\pi}{2}-\alpha\right).$$

Hence

$$\left.\begin{aligned} rX_r &= -\frac{F}{a\pi} r\cos\theta \\ &\quad + \frac{F}{\pi}\sum_{n=1}^{\infty}(-1)^{n-1}\left[-(2n-1)\frac{r^{2n-1}}{a^{2n+1}}(r^2-a^2)\cos(2n-1)\theta\right. \\ &\quad \left. + \frac{r^{2n+1}}{a^{2n+1}}\cos(2n+1)\theta + \frac{r^{2n-1}}{a^{2n-1}}\cos(2n-1)\theta\right], \\ rY_r &= -\frac{F}{a\pi} r\sin\theta \\ &\quad + \frac{F}{\pi}\sum_{n=1}^{\infty}(-1)^{n-1}\left[(2n-1)\frac{r^{2n-1}}{a^{2n+1}}(r^2-a^2)\sin(2n-1)\theta\right. \\ &\quad \left. + \frac{r^{2n+1}}{a^{2n+1}}\sin(2n+1)\theta - \frac{r^{2n-1}}{a^{2n-1}}\sin(2n-1)\theta\right]. \end{aligned}\right\} \quad . \quad . \quad . \quad (2.34)$$

These results give

$$\left.\begin{aligned} \widehat{rr} &= -\frac{2F}{\pi}\left[\tfrac{1}{2} - \sum_{n=1}^{\infty}(-1)^{n-1}\left\{n\frac{r^{2n-2}}{a^{2n-2}} - (n-1)\frac{r^{2n}}{a^{2n}}\right\}\cos 2n\theta,\right. \\ \widehat{r\theta} &= -\frac{2F}{a\pi}\sum_{n=1}^{\infty} n(-1)^{n-1}\left\{\frac{r^{2n}}{a^{2n}} - \frac{r^{2n-2}}{a^{2n-2}}\right\}\sin 2n\theta. \end{aligned}\right\} \quad . \quad . \quad . \quad (2.35)$$

3 (a). *Solution suitable for an Infinite Solid having a Circular Hole* *.

Let us first consider the case of a distribution of stresses which vanish at infinity and satisfy the boundary conditions

$$\left.\begin{aligned} \widehat{rr} &= Q_m\cos m\theta, \\ \widehat{r\theta} &= 0, \end{aligned}\right\} \text{ when } r=a, \quad . \quad . \quad . \quad (3.1)$$

Q_m being a constant.

Then we have

$$\left.\begin{aligned} (X)_{r=a} &= \frac{Q_m}{2}[\cos(m+1)\theta + \cos(m-1)\theta], \\ (Y_r)_{r=a} &= \frac{Q_m}{2}[\sin(m+1)\theta - \sin(m-1)\theta]. \end{aligned}\right\} \quad . \quad (3.2)$$

* These results have been obtained by W. G. Bickley, by a different method, *vide* " The Distribution of Stress round a Circular Hole," in Phil. Trans. Roy. Soc. A, London, ccxxvii.

Hence we can write in this case

$$\left.\begin{aligned}\Sigma L_n(x, y) = L'(x, y) &= \frac{Q_m}{2}\left[\frac{a^{m+1}}{r^{m+1}}\cos(m+1)\theta\right.\\ &\qquad \left.+\frac{a^{m-1}}{r^{m-1}}\cos(m-1)\theta\right],\\ \Sigma M_n(x, y) = M'(x, y) &= \frac{Q_m}{2}\left[\frac{a^{m+1}}{r^{m+1}}\sin(m+1)\theta\right.\\ &\qquad \left.-\frac{a^{m-1}}{r^{m-1}}\sin(m-1)\theta\right].\end{aligned}\right\} \quad (3.3)$$

Writing $-m$ for n, we have from (2.6) and (2.8) for all values of $m \neq 1$

$$\odot_{-m} = 2Q_m \frac{a^m}{r^m}\cos m\theta. \quad . \quad . \quad . \quad . \quad (3.4)$$

Hence for these values we get from (2.6)

$$\left.\begin{aligned}rX_r &= \frac{Q_m a}{2}\left[(m+1)\left(1-\frac{a^2}{r^2}\right)\frac{a^{m-1}}{r^{m-1}}\cos(m+1)\theta\right.\\ &\qquad \left.+\frac{a^{m+1}}{r^{m+1}}\cos(m+1)\theta+\frac{a^{m-1}}{r^{m-1}}\cos(m-1)\theta\right],\\ rY_r &= \frac{Q_m a}{2}\left[(m+1)\left(1-\frac{a^2}{r^2}\right)\frac{a^{m-1}}{r^{m-1}}\sin(m+1)\theta\right.\\ &\qquad \left.+\frac{a^{m+1}}{r^{m+1}}\sin(m+1)\theta-\frac{a^{m-1}}{r^{m-1}}\sin(m-1)\theta\right],\end{aligned}\right\} \quad (3.5)$$

3 (b). *Solution for the Case $n=-1$ or $m=1$.*

When $m=1$, we have

$$\left.\begin{aligned}(X_r)_{r=a} &= \frac{Q_1}{2}[1+\cos 2\theta],\\ (Y_r)_{r=a} &= \frac{Q_1}{2}\sin 2\theta,\end{aligned}\right\}$$

which are obtained by the assumption

$$\left.\begin{aligned}L_1(x, y) &= \frac{Q_1}{2}\left[1+\frac{a^2}{r^2}\cos 2\theta\right],\\ M_1(x, y) &= \frac{Q_1}{2}\frac{a^2}{r^2}\sin 2\theta.\end{aligned}\right\} \quad . \quad . \quad (3.6)$$

Putting $m=1$ or $n=-1$ in (2.8) we find that both sides identically vanish. Hence $\odot_{-1}$ cannot be directly obtained from this relation. Let us put

$$\odot_{-1}=\frac{A\cos\theta}{r}, \quad . \quad . \quad . \quad . \quad . \quad (3.7)$$

where A is a constant to be determined.

With this assumption we have from (2.6)

$$\left.\begin{aligned} rX_r&=\frac{A}{2}\left(1-\frac{a^2}{r^2}\right)\cos 2\theta+\frac{Q_1 a}{2}\left[1+\frac{a^2}{r^2}\cos 2\theta\right],\\ rY_r&=\frac{A}{2}\left(1-\frac{a^2}{r^2}\right)\sin 2\theta+\frac{Q_1 a}{2}\frac{a^2}{r^2}\sin 2\theta, \end{aligned}\right\} \quad . \quad (3.8)$$

or

$$\left.\begin{aligned} X_r&=\frac{A\cos^2\theta}{r}+\tfrac{1}{2}\frac{Q_1 a-A}{r}+\tfrac{1}{2}(Q_1 a-A)\frac{a^2}{r^3}\cos 2\theta,\\ Y_r&=\frac{A\sin\theta\cos\theta}{r}+\tfrac{1}{2}(Q_1 a-A)\frac{a^2}{r^3}\sin 2\theta, \end{aligned}\right\} \quad (3.8')$$

which give the stresses

$$\left.\begin{aligned} \widehat{xx}&=\frac{A\cos^3\theta}{r}+\tfrac{1}{2}(Q_1 a-A)\frac{\cos\theta}{r}+\tfrac{1}{2}(Q_1 a-A)\frac{a^2}{r^3}\cos 3\theta,\\ \widehat{xy}&=\frac{A\cos^2\theta\sin\theta}{r}+\tfrac{1}{2}(Q_1 a-A)\frac{\sin\theta}{r}+\tfrac{1}{2}(Q_1 a-A)\frac{a^2}{r^3}\sin 3\theta,\\ \widehat{yy}&=\frac{A\cos\theta\sin^2\theta}{r}-\tfrac{1}{2}(Q_1 a-A)\frac{\cos\theta}{r}-\tfrac{1}{2}(Q_1 a-A)\frac{a^2}{r^3}\cos 3\theta. \end{aligned}\right\} \quad . \quad . \quad . \quad (3.9)$$

The displacement system (u_1, v_1) due to the terms

$$\frac{A\cos^3\theta}{r}, \quad \frac{A\cos^2\theta\sin\theta}{r}, \quad \frac{A\cos\theta\sin^2\theta}{r},$$

in the stress components $\widehat{xx}$, $\widehat{xy}$, and $\widehat{yy}$ respectively is given by (1.22) and (1.44) in the form

$$\left.\begin{aligned} u_1&=\frac{A}{4\mu}\left[2(1-\sigma)\log r-\frac{x^2}{r^2}\right],\\ v_1&=\frac{A}{4\mu}\left[(1-2\sigma)\theta-\frac{xy}{r^2}\right]. \end{aligned}\right\} \quad . \quad . \quad (3.10)$$

Terms

$$\tfrac{1}{2}(Q_1 a-A)\frac{\cos\theta}{r}, \quad \tfrac{1}{2}(Q_1 a-A)\frac{\sin\theta}{r}, \quad -\tfrac{1}{2}(Q_1 a-A)\frac{\cos\theta}{r},$$

in the stress components $\widehat{xx}$, $\widehat{xy}$, and $\widehat{yy}$ are such that their contribution to $\odot$ $(=\widehat{xx}+\widehat{yy})$ is zero.

Since the stress equations are of the forms

$$\frac{\partial \widehat{xx}}{\partial x}+\frac{\partial \widehat{xy}}{\partial y}=0 \quad \text{and} \quad \frac{\partial \widehat{xy}}{\partial x}+\frac{\partial}{\partial y}(\odot-\widehat{xx})=0,$$

we obtain when $\odot=0$

$$x\hat{x}-i\widehat{xy} \quad \text{as a function of } x+iy.$$

Let

$$\widehat{xx}-i\widehat{xy}=\chi(z) \quad . \quad . \quad . \quad . \quad . \quad (3.11)$$

Then expressing the corresponding displacements (u_2, v_2) in the form

$$u_2-iv_2=\Omega(z),$$

we find that

$$(u_2-iv_2)=\frac{1}{2\mu}\int \chi(z)\,dz.$$

Hence putting

$$\chi(z)=\frac{Q_1a-A}{2z},$$

we get

$$\left.\begin{aligned} u_2&=\frac{Q_1a-A}{4\mu}\log r,\\ v_2&=-\frac{Q_1a-A}{4\mu}\theta. \end{aligned}\right\} \quad . \quad . \quad . \quad . \quad (3.12)$$

The remaining terms of $\widehat{xx}$, $\widehat{xy}$, and $\widehat{yy}$ in (3.9), namely

$$\tfrac{1}{2}(Q_1a-A)\frac{a^2\cos 3\theta}{r^3}, \quad \tfrac{1}{2}(Q_1a-A)\frac{a^2\sin 3\theta}{r^3},$$

$$-\tfrac{1}{2}(Q_1a-A)\frac{a^2\cos 3\theta}{r^3},$$

also make $\odot=0$. The expression $\widehat{xx}-i\widehat{xy}$ evaluated from these terms

$$=\frac{1}{2}\frac{Q_1a-A}{z^3}a^2.$$

Hence the displacements (u_3, v_3) are given by

$$u_3-iv_3=\frac{1}{4\mu}(Q_1a-A)a^2\int\frac{dz}{z^3}=-\frac{1}{8\mu}\frac{Q_1a-A}{z^2}a^2,$$

which gives

$$\left.\begin{aligned} u_3 &= -\frac{1}{8\mu}(Q_1 a - A)\frac{a^2\cos 2\theta}{r^2}, \\ v_3 &= -\frac{1}{8\mu}(Q_1 a = A)\frac{a^2\sin 2\theta}{r^2}. \end{aligned}\right\} \quad . \quad . \quad (3.13)$$

Since the resultant displacement must be single-valued we must have from (3.10) and (3.12)

$$A(1-2\sigma) = Q_1 a - A,$$

or

$$A = \frac{Q_1 a}{2(1-\sigma)}. \quad . \quad . \quad . \quad . \quad . \quad (3.14)$$

3 (c). *Illustrative Examples.*

I. *Stresses due to Normal Pressure* $Q_1 \cos\theta$ *on the Internal Boundary* $r=a$.

Substituting the value of A from (3.14) in (3.8) we have

$$\left.\begin{aligned} rX_r &= \frac{Q_1 a}{4(1-\sigma)}\left[2(1-\sigma)+\left\{1+(1-2\sigma)\frac{a^2}{r^2}\right\}\cos 2\theta\right], \\ rY_r &= \frac{Q_1 a}{4(1-\sigma)}\left[1+\frac{a^2}{r^2}(1-2\sigma)\right]\sin 2\theta. \end{aligned}\right\} \quad (3.15)$$

II. *Effect of a small Cylindrical Cavity in an Infinite Solid subjected to Uniform Tension.*

In the case of an infinite solid with an inner cylindrical hole of radius a, the solid being in a state of tension T at a great distance from the cavity, we have the conditions

$$(X_r)_{r=a}=0, \qquad (Y_r)_{r=a}=0,$$

and

$$\left.\begin{aligned} (X_r)_{r\to\infty} &= Tr\cos\theta, \\ (Y_r)_{r\to\infty} &= 0. \end{aligned}\right\} \quad . \quad . \quad . \quad . \quad (3.16)$$

Hence we can take

$$L(x, y) = Tr\left(1-\frac{a^2}{r^2}\right)\cos\theta = T.Re\left(z-\frac{a^2}{z}\right). \quad (3.17)$$

From (2.8) we know that

$$\Sigma\odot_n = \Sigma\frac{2a}{n+1}TRe\left[\frac{\partial L}{\partial z}\right].$$

$$\left.\begin{aligned} &\therefore \qquad \odot_1 = \mathrm{T}, \\ &\text{and} \qquad \odot_{-2} = -2\mathrm{T}a^2\mathrm{Re}\left[\frac{1}{z^2}\right]. \end{aligned}\right\} \quad . \quad . \quad . \quad . \quad (3.18)$$

Substituting these values in (2.6) we get

$$\left.\begin{aligned} \mathrm{X}_r &= \mathrm{T}\left(1-\frac{a^2}{r^2}\right)\left[\cos\theta - \frac{3}{2}\frac{a^2}{r^2}\cos 3\theta\right], \\ \mathrm{Y}_r &= -\frac{3}{2}\mathrm{T}\left(1-\frac{a^2}{r^2}\right)\frac{a^2}{r^2}\sin 3\theta. \end{aligned}\right\} \quad . \quad (3.19)$$

Since

$$\odot = \odot_1 + \odot_{-2} = \mathrm{T}\left[1 - \frac{2a^2\cos 2\theta}{r^2}\right],$$

we have on the boundary $r=a$, where $\widehat{rr}=0$,

$$\widehat{\theta\theta} = [\odot]_{r=a} = \mathrm{T}(1-2\cos 2\theta). \quad . \quad . \quad . \quad (3.20)$$

Conclusion.

In this paper some problems of plane deformation have been solved without the help of Airy's stress function. The solutions of corresponding plane stress problems can be deduced by substituting $(1+\sigma)^{-1}$ for $(1-\sigma)$ in the results obtained. It is found that, except in some special cases (as, for instance, in the case of a circular hole with normal stresses varying as $\cos\theta$), the knowledge of the displacement is not essential. In these special cases stresses cannot be directly determined from the stress equations, but the complete solution is obtained on making the displacement single-valued with the addition of extra terms (see 3 (b)). The method given here has this advantage, that the prescribed boundary values of the stresses being known, in most cases stresses can be very easily determined from the stress equations; and since, in every case, the value of $\odot$ is found out first, the values of the principal stresses on the boundary can at once be written down when one of these stresses is zero or has a given value on the boundary. An illustration of this will be found in the second example of section 3 (c).

Krishnagar College,
Bengal.

IX. *A Study of the Action of Ionizing Radiations on Colloidal Graphite.* *By* J. A. Crowther, *M.A., Sc.D., Professor of Physics in the University of Reading,* H. Liebmann, *Ph.D., and* R. Jones, *B.Sc.**

Introduction.

In previous communications [1], [2] we have given some account of a phenomenon, not previously recorded, in connexion with the action of X-radiation on colloidal solutions. In brief, if a suitable colloid is subjected to a uniformly increasing dose of X-radiation the ζ potential of its particles alternately increases and decreases in a regular manner. The fluctuations are not large (they are of the order of ± 10 per cent.), but their origin presents some interesting problems, and, in addition, they occur for comparatively trifling doses of radiation, well within what is usually termed the therapeutic region. Except for the ionization produced in gases few physical or chemical changes have been demonstrated with doses of this order of magnitude, though biological changes are often quite striking. In the present paper we record the results of a further study of the phenomenon.

As previously described, the fluctuations in potential have been observed for ferric hydroxide and for colloidal solutions of sugar carbon and of graphite. We have more recently observed the phenomenon with gold sols and with suspensions of quartz, and hope to report more fully on these in a further communication. In the present paper we confine ourselves to a more detailed study of colloidal graphite.

Experimental Details.

The methods employed for preparing and exposing the sol and for measuring the electrophoretic velocity of its particles (from which the ζ potential is deduced) have been fully described elsewhere [2], [3]. In an attempt to improve the precision in timing an electrically driven and operated timepiece has been substituted for the usual stop-watch. It was also observed that the variance in the twenty separate observations of velocity which

* Communicated by Prof. J. A. Crowther, M.A., Sc.D.

constitute an " observation " was considerably reduced if the liquid was allowed to remain in the cataphoresis chamber for ten minutes before measurement began. Apparently the currents set up in the liquid when the cell is filled continue to affect the motion of the particles for some minutes after filling. With these improvements the variance is of the order to be expected from the Brownian movement of the particles. The standard error of a single observation of electrophoretic velocity is 2 per cent.

The sol employed throughout the experiments described in the present communication was a solution of colloidal graphite (Aquadag) in conductivity water with a concentration of 2·6 gm. per litre. Its specific conductivity was $14{\cdot}1\times10^{5}$ cm.$^{-1}$ ohm^{-1}, and its normal ζ potential $-2{\cdot}88\times10^{-2}$ volts. The particle number was 8×10^{13} particles per litre. The energy of the beam of X-rays was measured by allowing the rays to pass through an ionization chamber of the type described in the previous paper, the charge liberated in the chamber being measured by allowing it to collect on a standard condenser and subsequently discharging the condenser through a ballistic galvanometer. The measurements should be accurate to about 2 per cent. In all cases the width of the beam was so adjusted that it passed freely through the ionization chamber and just filled the dish which contained the sol. From the dimensions of the ionization chamber and the surface area of the sol the actual dose in rontgen received at the surface of the sol was calculated.

Effect of the Intensity of the Radiation.

In order to investigate the effect of varying the intensity of the radiation on the colloid the dish in which the colloid was to be exposed was mounted on a sliding carrier of a vertical cathetometer, so that it could be placed at different known distances from the target of the X-ray tube. In this way it was possible to alter the intensity of the radiation at the surface of the sol by as much as 20 to 1 without changing the working conditions of the tube. A change in the latter might conceivably affect not only the output but also the quality of the radiation, and thus introduce complications which it was eminently desirable to avoid. In most of the experiments

an aluminium filter 0·7 mm. in thickness was placed over the window of the X-ray tube in order to increase both the penetrating power and the homogeneity of the issuing beam. The mean wave-length of this filtered radiation as deduced from its mean absorption coefficient was about $0{\cdot}7 \times 10^{-8}$ cm.

Using the filtered radiation a series of observations were made with intensities of 0·022, 0·15, and 0·43 rontgen per sec. The results obtained from these three sets of experiments are shown by the points in fig. 1. It will be seen that the three sets of points are in satisfactory agree-

Fig. 1.

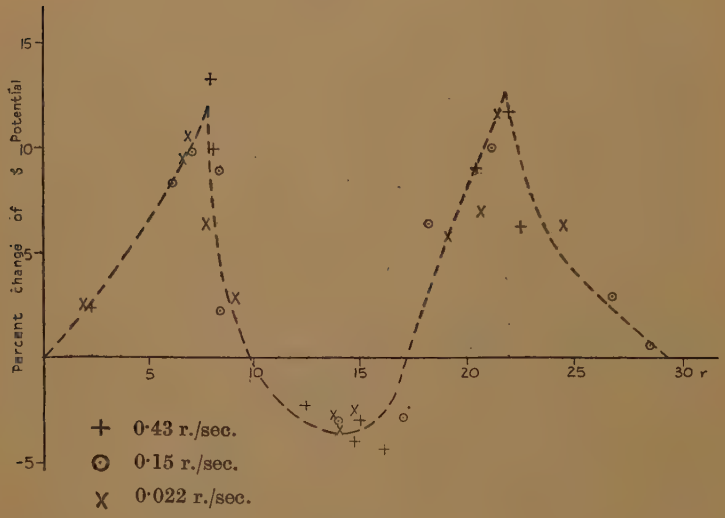

ment and can all be represented by the single graph which has been drawn through them. Only two of the thirty points depart by more than would be expected from the standard error of experiment.

In order to extend the range of the experiment the aluminium filter was removed and two further sets of observations made, one with an intensity of 0·53 r. per sec. and the other with an intensity of 2·57 r. per sec. The results obtained are shown by the two sets of points in fig. 2. Here again the points lie reasonably well on a single curve. As pointed out below the doses of the two sets of experiments are not directly comparable. It

appears, however, that for a given type of radiation a variation of the intensity of the radiation is of no influence on its effect on the sol.

Permanency of the Change.

As reported in the earlier paper the particles after irradiation remain permanently affected. Measurements of the ζ potential made a week after irradiation give precisely the same value as those made immediately. To test the matter further three samples of the sol were each given a dose of 28 r. of unfiltered radiation, which leaves the ζ potential unchanged (fig. 2). After a lapse of

Figs. 2.

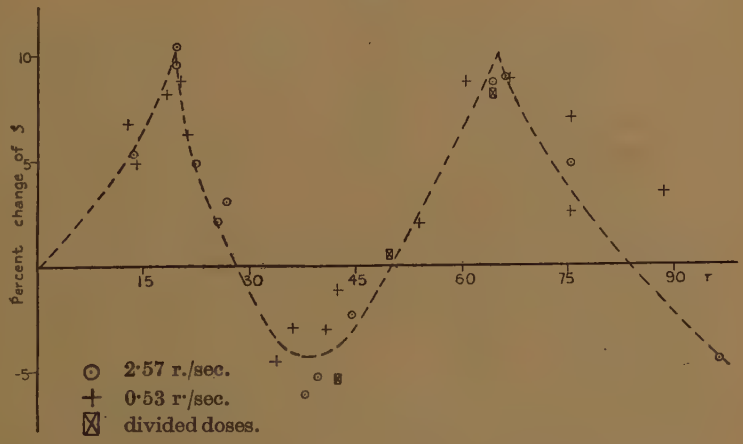

twenty-four hours they were given additional doses of 14·7 r., 20·2 r., and 36·6 r. respectively. The results are shown by the points within the square brackets in fig. 2, the change of ζ potential being plotted against the total dose received by each sample. It will be seen that the points lie quite well on the curve. The effect produced is therefore the same whether the total dose is delivered at one exposure or divided between two exposures with an interval of twenty-four hours between them.

The experiments, however, have a further interest. Particles in a sol which has received a dose of 28 r. have exactly the same electrophoretic mobility as those in the untreated sol, and are indistinguishable from them physically. If, however, each is given a dose of 14·7 r.

the ζ potential of the latter increases by 7 per cent., while that of the former decreases by 5 per cent. The two sets of particles must, therefore, differ in some way or other in spite of the identity of their electrokinetic potential.

The Effect of Temperature.

The experiments described in the previous sections were carried out at the normal laboratory temperature of about 17° C. It was thought possible that the temperature of the sol during exposure might have some effect on the result of irradiation, and experiments were made

Fig. 3.

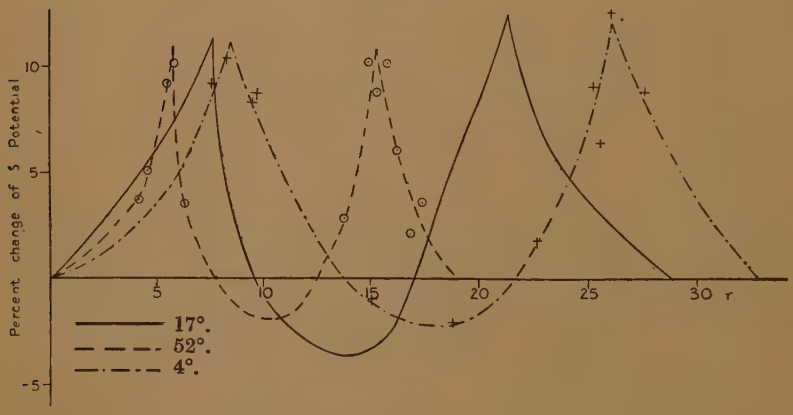

at two different temperatures, 4° C. and 52° C., to test this point. Preliminary experiments showed that the electrokinetic potential of the unirradiated sol was not affected by these temperatures. After irradiation the sol was allowed to attain room-temperature, and the measurements on the sol were made, as usual, at the normal laboratory temperature. The experiments were carried out using the filtered radiation.

The results are shown in fig. 3. The crosses represent the readings obtained when the sol was exposed at 4° C., the circles the values obtained when the irradiation was carried out at 52° C. The curve of fig. 1, representing the result of exposing at 17° C., is also reproduced for purposes of comparison. It will be seen that, while the

maximum change in ζ potential is unaltered by the temperature of irradiation, the quantity of radiation required to produce this maximum variation shows a very marked dependence on the temperature. Raising the temperature of the sol from 4° C. to 52° C. increases the efficiency of irradiation in the ratio of about 5 to 3. In other words, to produce a given change in the ζ potential at 52° C. requires only about 3/5th of the radiation which would be necessary at a temperature of 4° C. As will be seen from the table, in which the results are collected, the ratio of the doses required to produce the first and second maximum is the same, within the limits of experimental error, at all temperatures.

Type of radiation.	Temp.	Dose required for first max.	Dose required for second max.	Maximum change in ζ potential.
50 k.v. X-rays, 0·7 mm. al. filter.	4° C.	9·4 r.	26·0 r.	11·5 per cent.
	17° C.	7·9 r.	22·0 r.	
	52° C.	5·7 r.	15·0 r.	
50 k.v. X-rays, unfiltered.	17° C.	20 r.	65 r.	9·5 per cent.
γ-rays	17° C.	9½ mins. (24 r.)	31 mins. (77 r.)	14 per cent.

As an appendix to this section we may mention some experiments in which the sol was exposed to radiation in the frozen state at a temperature of about −5° C. The graphite sol is a very stable system, and survives the process of freezing and thawing out with little change in its electrokinetic potential, although there is a marked decrease in the number of particles in solution. Measurements of the ζ potential after the sol had been exposed in the solid state to varying doses of X-rays showed significant variations from the normal. Doses of from 6 r. to 9 r. increased the potential by about 6 per cent., an exposure of 13 r. reduced the potential by 3 per cent. The drastic treatment of the sol seemed to impair the accuracy of the observations to some extent. There is no doubt, however, that the fluctuations which are the subject of this communication can be produced (possibly with diminished amplitude) with the sol in the solid state.

The Action of Gamma-Radiation.

Experiments have also been made on the effect of exposing the sol to increasing doses of γ-radiation. The sol was exposed in a quartz dish at a fixed distance from a 56 mgm. source of radium contained in a silver tube of 1 mm. wall thickness for varying times. After exposure the ζ potential of the particles in the sol was measured by the standard technique. The dose in rontgen was not measured directly. It can, however, be calculated roughly from a knowledge of the geometrical disposition of the apparatus and the value of the Sievert unit. (The Sievert unit measures the ionization produced in 1 hour by a point source of 1 mgm. of radium surrounded by 0·5 mm. Pt in 1 c.cm. of air at a distance of 1 cm. Its value is approximately 8·3 rontgen.)

The effects produced by γ-radiation were found to be similar to those already described for X-radiation. The ζ potential rose to a maximum for an exposure of about 11 minutes, fell to a minimum after an exposure of $18\frac{1}{2}$ minutes, and gave a second maximum with an exposure of 31 minutes. The fluctuation seemed to be distinctly greater with the γ-radiation than with X-radiation, the maxima corresponding to an increase of 15 per cent. and the minima to a decrease of 9 per cent. of the normal ζ potential of the sol.

The Form of the Relation between Dosage and ζ Potential.

The series of experiments described in the present and in previous papers demonstrates clearly that the ζ potential of a colloid exposed to a uniformly increasing dose of ionizing radiation passes through a series of maxima and minima. In the present paper we have confined our observations entirely to the first two of these. It may be pointed out, however, that, as we showed in a previous paper, these fluctuations are not confined to small exposures, but continue with undiminished amplitude to exposures as high as 2000 r., and possibly 20,000 r. The effect is shown not only with the graphite sol, with which we have been concerned in the present series of experiments, but also with positive and negative sugar carbon sols and with a comparatively simple system as finely ground quartz in conductivity water.

All the curves obtained in the present research are clearly of the same type. In particular the ratio of the exposures required to produce the first and second maxima of the curve are practically the same for each type of radiation used, and for different temperatures. The fluctuations are therefore far from being random.

Mainly for convenience in representation, and with some diffidence, we have drawn a smooth curve through the points relating to each complete set of observations. It should be borne in mind, however, that the standard error of a single observation is about 2 per cent., so that, apart from the position of the peaks of the curve, which are well established, it would be possible to modify the curves considerably without overpassing the limits of error in the experiments.

Taking them as a whole they seem to indicate that the effect of the radiation is first to produce a steady increase in the ζ potential of the particles up to some critical value. With further irradiation there is a steep drop in the potential to some value slightly but definitely below the normal potential. This portion of the curve is strongly reminiscent of a relaxation phenomenon. After reaching a rather flat minimum the phenomena repeat themselves, apparently indefinitely.

The peaks are distinctly sharp, and correspond to an increase of from 10 to 14 per cent. above the normal value. There is some indication that the value for the unfiltered radiation is rather less and for γ-radiation distinctly greater than that for the filtered radiation. If the effect is real it may possibly be due to a partial screening of the lower layers by the upper layers of the sol during exposure, which would obviously be more effective with the more absorbable radiation.

The first maximum is reached for a dose of 7·9 r. of filtered X-radiation, 20 r. for the unfiltered radiation, and 24 r. for the γ-radiation. At first sight this might be supposed to indicate that the phenomenon is a function of the wave-length of the radiation. This, however, is by no means certain. The effective dose received by the sol is clearly to be measured by the energy absorbed from the radiation per unit volume of the sol. The measurement in rontgen, on the other hand, gives the energy absorbed in unit volume of air. The relation between the effective dose and the dose in rontgen is thus a function of the

coefficients of absorption of the radiation in the two substances, and varies with the wave-length of the radiation. For strictly homogeneous beams of radiation a suitable correction can be calculated. For inhomogeneous beams, such as have been used in the present experiments, this is not possible, owing to the change in composition of the beam in passing through the absorbing medium. As far as the present experiments go, the question of a possible wave-length effect must be regarded as entirely open.

In conclusion, we wish to express our thanks to the British Empire Cancer Campaign, whose generous support has alone made it possible to continue this work. One of us (R. J.) has been in receipt of a training grant from the Department of Scientific and Industrial Research, and takes this opportunity of expressing his thanks to the Department. For the slit ultra-microscope used in the experiments our thanks are due to the Research Board of the University of Reading.

Summary.

Continuous irradiation of colloidal graphite with X-rays produces alternate increases and decreases in the potential of the particles, the maximum change being of the order of 12 per cent. The change of ζ potential for radiation of a given type depends only on the total dose administered, and is independent of the intensity of the radiation. The change is permanent unless the sol is subjected to further irradiation. For a given total dose the change in ζ potential is the same whether the whole dose is given in one exposure or in two partial doses, separated by a time interval of twenty-four hours.

The phenomenon shows a marked temperature effect, the efficiency of the radiation increasing by 70 per cent. if the temperature at which the sol is exposed is raised from 4° C. to 52° C. Significant changes in ζ potential can be produced if the sol is irradiated in the frozen state.

Similar effects are caused by γ-radiation. The dose as measured in rontgen necessary to produce a maximum change in the potential of the sol varies with the quality of the radiation employed. There is insufficient evidence to show whether this indicates a real dependence of the phenomenon on the wave-length of radiation.

References.

(1) Crowther, Liebmann, and Mill, Brit. Journal of Radiology, ix. (new series) p. 631 (1936).
(2) Crowther, Liebmann, and Lane, Phil. Mag. ser. 7, xxiv. p. 654 (1937).
(3) White, Phil. Mag. ser. 7, xxiii. p. 811 (1937); Lane and White, Phil. Mag. ser. 7, xxiii. p. 824 (1937).

The University of Reading.
May 24, 1938.

X. *Atomic and Ionic Radii.*—I. *Numerical Values and their Bearing on the Compressibilities of Metals.* *By* WILLIAM HUME-ROTHERY, *D.Sc., F.R.S., Royal Society Warren Research Fellow, and* GEOFFREY VINCENT RAYNOR, *B.A., B.Sc., Keble College, Oxford.**

[Received June 8, 1938.]

I.

MANY papers have dealt with the atomic radii of the elements and the interatomic distances in metallic crystals, and their connexion with various properties, but a number of points still remain obscure. The work of Goldschmidt has led to the conceptions of atomic radii which apply to certain metallic crystal structures. For certain properties, such as the lattice parameters of intermediate alloy phases, the Goldschmidt atomic radii are of great value, but when other properties are considered it is clear that the Goldschmidt values by themselves do not give a complete picture of the sizes of the atoms. A general relation has, for example, been traced (1) between the power of one metal to dissolve another and the relative sizes of the two atoms, but for this purpose the atomic radii, defined by one-half of the closest distances of approach in the crystals of the elements, give a much better correlation than the atomic radii of Goldschmidt. It is the purpose of the present paper to discuss more closely what constitutes the size of an atom in a metallic structure, and to suggest that when two factors are considered, many properties of metals and alloys can be understood in a general way.

From the point of view of modern theory, a metal is to be regarded as an array of positive ions held together by the valency electrons which are free to move through

* Communicated by W. Hume-Rothery, D.Sc., F.R.S.

the crystal. In the different metals, the valency electrons differ in number and in the firmness of their binding, whilst the ions differ as regards their electron cloud distributions in space, and the extent to which the electron clouds of adjacent ions overlap. In the alkali metals for example, the electron clouds of the ions have almost vanished at a point midway between adjacent atoms, whilst in copper, silver and gold, the *d* shells of the ions of adjacent atoms overlap considerably, so that, as pointed out by Mott and Jones[2], these metals may be regarded almost as hard spheres held in contact by the attraction of the valency electrons. The alkalis and the copper group thus represent two extreme types, and any complete theory of metals must, of course, involve the accurate determination of the electron cloud density of the ions and the valency electrons. We suggest, however, that for many purposes, a rough indication of the nature of a metal or alloy may be obtained by comparing the interatomic distances in the crystal with the suitably defined *ionic radii* of the atoms concerned. In brief, if the ionic radius is small compared with the interatomic distance, we shall have a metal of what may be called the " open " type, whilst if the ionic radii are nearly equal to the interatomic distances we shall have a metal of the " full " type, with many different properties. The term ionic radius has been used with several different meanings, and it is therefore necessary to explain which set of constants is being used.

In the theory of ionic crystals developed by Born and others, it is customary to regard the ions as attracted by a Coulomb force varying as the inverse square of the distance, and balanced by a repulsive force varying as a high inverse power of the distance. The potential energy of the crystal may be written in the form

$$\Phi = -\frac{AZ_1Z_2}{d} + \frac{B}{d^n}, \quad . \quad . \quad . \quad . \quad . \quad (1)$$

where Z_1 and Z_2 are the charges on the positive and negative ions, A a numerical constant depending on the crystal structure, and d is the distance between the ions. Evidence from a number of sources indicates that the exponent n is of the order 5, 7, 9, 10, and 12 for ions with electronic configurations similar to those of He, Ne, A, Kr, and Xe atoms respectively. This theory has been

further developed from the viewpoint of modern electron theory, and alternative forms of the repulsion term have been proposed, but the general picture remains unaltered, and the high values of n indicate that at the distances concerned the ions behave as moderately hard spheres, the repulsion being due to the overlapping of the electron clouds of adjacent ions. Concurrently with these developments, the work on crystal structures of salts has led to the conception of *ionic radii*, by means of which the inter-ionic distances in salts can be expressed approximately by assigning to each ion a characteristic radius. Extensive tables of ionic radii have been given by Goldschmidt[3], but it is important to realize that these empirical ionic radii involve the charges of the ions, and are not absolute measurements of the sizes of the ions, if by the term "size" we mean the extent and density of the electron clouds. We may imagine, for example, a univalent A^+, and a divalent B^{2+} ion each having, in the free state, exactly the same electron cloud distribution in space. In an actual ionic crystal, the double charge on the B^{2+} ion will result in its being pulled more strongly to a given anion than the univalent A^+ ion would be at the same distance. The electron cloud of the B^{2+} ion will therefore be overlapped more than that of the A^+ ion, and in order to account for the interionic distances in salts it will be necessary to assign the B^{2+} ion a smaller radius than that of the A^+ ion, even though their actual electron cloud density distributions in space are the same. Attempts to express the sizes of ions free from this complication were first made by Pauling[4], who gave a series of so-called "univalent ionic radii." This expression is in some ways rather unfortunate, since by the univalent radius of, for example, a calcium ion, is meant not the radius of a Ca^+ ion, but the radius which would have to be assigned to the actual Ca^{2+} ion in order to account for the distances if it were present in a hypothetical salt in which it was attracted to the anions by a force equal to that which would be exerted if both ions were univalent. This conception was later developed with greater attention to detail * by Zachariasen [5] for ions of the inert gas type. The actual distances in ionic salts can then be expressed in terms of Zachariasen's "univalent radii" by

* Zachariasen considers co-ordination effects which are not dealt with by Pauling.

applying corrections for the charges on the anion and cation, the values of n in equation (1), and the co-ordination number. It is of course obvious that the variation of the electron cloud density of an ion in space cannot really be expressed by a single constant, but in so far as one constant may be used in order to express the size of an ion the values of Zachariasen appear to be the most suitable. Where these are not available we use the univalent radii of Pauling, and in some other cases we use the empirical radii of Goldschmidt with an indication of the direction in which these must be corrected in order to give univalent radii analogous to those of Zachariasen. The difference

Fig. 1.

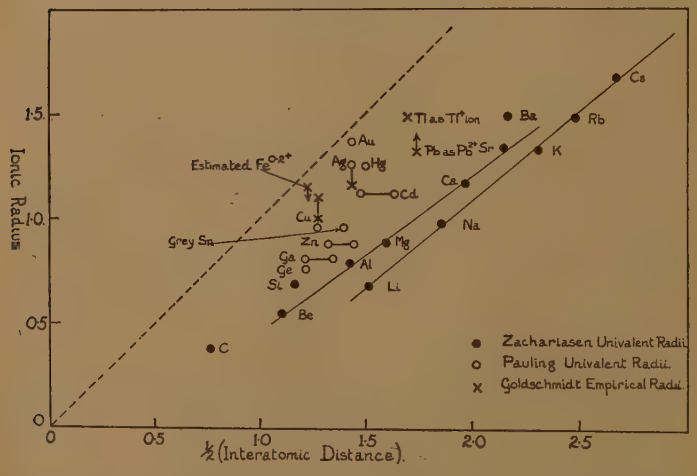

between the univalent ionic radius and the ionic radius of Goldschmidt naturally increases with the valency.

In fig. 1 we have plotted the ionic radii against one half of the interatomic distances in the crystals of the elements, and have drawn a line through the origin at 45° to the axes ; this line represents the limit at which the inter-atomic distances are equal to twice the ionic radii. For the alkali metals, which all crystallize in the body-centred cubic structure, an approximately linear relation exists between the ionic and atomic radii, if by the latter term we mean one half the closest distances of approach of the atoms in the metallic crystal. A similar linear relation exists for the alkaline earth metals beryllium,

magnesium, calcium, and strontium which crystallize in cubic or hexagonal close-packed structures with co-ordination number 12. Barium crystallizes in the body-centred cubic structure with co-ordination number 8, and does not agree with the linear relation. The difference is greater than that to be expected from the change in co-ordination number according to Goldschmidt*[6], and it is possible that the high point for barium in fig. 1, which suggests an unduly large ionic radius, is a preliminary indication of the approaching internal rearrangement which takes place in the rare earth group. The alkaline earth metals thus form comparatively open crystals. In contrast to these, the points for copper, silver, and gold indicate crystals of a much more full type. It is unfortunate that the data for the radii of univalent Cu^+, Ag^+, and Au^+ ions are only approximate. Pauling's theoretical value for the Cu^+ ion (0·96 Å.) is less than the empirical value (1·0–1·1 Å.) of Goldschmidt, although the two should be equal for univalent ions, but for silver the position is reversed, and Pauling's value (1·26 Å) is greater than the empirical value (1·13 Å). For gold, only Pauling's theoretical value is available, since the Au^+ ion is unstable in crystals, and always changes to a co-valent linkage. The points for these elements are only approximate, but clearly indicate a very full type of crystal, in agreement with the views of Mott and Jones.

With zinc and cadmium the crystal structures are such that each atom has six close neighbours in one plane and six others at a greater distance, and the radii corresponding to both distances are shown in fig. 1. It will be seen that even for the greater of the two distances the structure is of a less open type than for the alkaline earths, and the same applies to mercury which crystallizes in a simple rhombohedral structure in which each atom has six close neighbours. Zinc, cadmium, and mercury all form considerably more open structures than the preceding univalent elements copper, silver and gold, since not only are the interatomic distances of the former slightly greater, but their ionic radii are smaller. In

* Goldschmidt's work indicated a contraction of about 3 per cent. on passing from co-ordination number 12 to 8, but it must be admitted that this was deduced from a study of elements the crystals of which were of a less open type than barium.

order to appreciate the structures of the remaining elements it is necessary to consider what may occur in the crystal of the element as the valency increases.

It is well known that for the elements of Groups IV B to VII B, there is a tendency for the elements to crystallize so that each atom has (8 −N) neighbours where N is the number of the Group. In this way each atom satisfies its normal valency by what are equivalent to co-valent bonds *. The simplest example of these is the diamond type of structure formed by carbon, silicon, germanium, and grey tin, where each atom has four valency electrons and four close neighbours. As will be seen from fig. 1, these structures are slightly less open than those of the alkaline earths, but much more open than the structures of copper, silver, and gold. For the remaining elements obeying the (8 −N) rule, the position is less clear. In antimony for example, each atom has five valency electrons and forms co-valent bonds with three close neighbours, so that there are two unshared electrons per atom. In so far as these two unshared electrons are distributed uniformly through the crystal, the ionic radius required is the " univalent " radius of the Sb^{5+} ion ; in this case the structure is comparatively open, but with a high concentration of valency electrons in the extra-ionic space †. But in so far as the two electrons are concentrated round the individual atoms, to form a sub-group of two, the ionic radius required is the univalent radius of the Sb^{3+} ion, and the structure will be of a more full type. The true condition is probably intermediate between these two extremes, and the same considerations apply to the selenium group, but ionic radii are not yet available for ions such as Sb^{3+}.

The second characteristic of the B-Group elements is a tendency towards incomplete ionization in the elements

* It may be emphasized that this view is complementary to, rather than antagonistic to the Brillouin Zone theories of those structures, each conception being imperfect. The co-valent theory gives the more correct picture of the probable cloud density of the valency electrons in the crystal, indicating that this is greater in the directions of the co-valent bonds. This conception by itself ignores the fact that the valency electrons are free to move throughout the crystal. The Brillouin Zone theory takes into account the fact that the electrons are free to move throughout the crystal, but in its turn ignores the varying density of the electron cloud in space. Both conceptions are therefore required to express the whole truth.

† The term extra-ionic volume or space may be used to denote the volume of a unit cell less the volume of the ions.

of Groups III and IV. The interatomic distances in thallium (3·40 Å.) and lead (3·49 Å.) are much greater than in gold (2·88 Å.), and in view of the well-known stability of the Tl^{+} and Pb^{2+} ions, it seems highly probable that although a continuous interchange of valency electrons takes place, each atom is building up a relatively dense electron cloud equivalent to a sub-group of two electrons, which are thus responsible for repulsion rather than attraction. In fig. 1 we have therefore plotted the atomic radius of thallium against the ionic radius of the Tl^{+} ion, and the point corresponds with a rather full type of structure. For lead we can only give the empirical Goldschmidt value for the Pb^{2+} ion; by analogy the univalent radius of the Pb^{2+} ion would be about 0·1–0·2 Å. larger, and the structure is of a moderately full type. If the much smaller ionic radii of the fully ionized Tl^{3+} and Pb^{4+} ions had been used, the structures would have been of an open type, and as we shall show later the compressibilities do not support this view.

In the previous Period, the same kind of increase in the interatomic distances is shown to a lesser degree on passing from silver (2·88 Å.) to indium (3·24 and 3·36 Å.) and white tin (3·01 and 3·18 Å.), and it is probable that in the crystals of the elements, indium and white tin represent not so much the fully ionized tri-valent and tetra-valent elements as the uni- and di-valent elements respectively, or to some intermediate stage in which the sub-group of two electrons is beginning to build up round each atom. In alloys, however, indium and tin often exert their normal valencies of three and four, and as we shall show in the following paper the ionic radii of the In^{3+} and Sn^{4+} ions are here of great interest. There are, unfortunately, no means of estimating the ionic radii of the In^{1+} and Sn^{2+} ion, and these elements are not included in fig. 1.

In the First Long Period, gallium and germanium do not show this behaviour, and their interatomic distances (Ga. 2·43 Å., Ge. 2·44 Å.) are less than in copper (2·54 Å.). We have therefore included in fig. 1 the points for the Ga^{3+} and Ge^{4+} ionic radii, which indicate that the metals are of a moderately open type.

In the Second Short Period we have plotted the atomic radius of aluminium against the univalent ionic radius of the Al^{3+} ion, and the resulting point corresponds with

a fairly open structure. The abnormalities in the sequence of melting points, and some other properties, suggest that this metal may not be of the normal tri-valent type, and if incomplete ionization exists this point will not be correct.

In the transitional elements the transition process results in the expansion of the *d*-shells of the ions, and as the electronic state in the solid element is usually not known, the points cannot be plotted in fig. 1. In the case of iron, Mott and Jones[7] show that there are probably 0·2 electrons per atom in the solid. From the empirical values of Goldschmidt for the radii of Fe^{2+} and Fe^{3+} ions, we can by linear extrapolation obtain a rough estimate for the radius of an ion of the type $Fe^{0\cdot2+}$, and this is

Fig. 2.

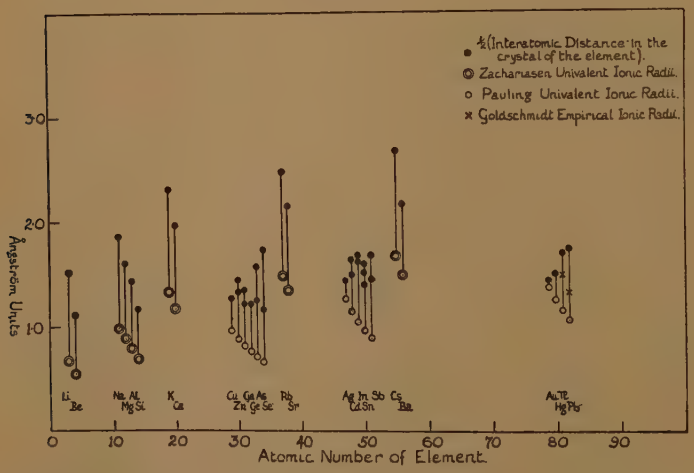
½(Interatomic Distance in the crystal of the element).
Zachariasen Univalent Ionic Radii.
Pauling Univalent Ionic Radii.
Goldschmidt Empirical Ionic Radii.
30
20
10
Ångström Units
Li Be
Na Al Mg Si
K Ca
Cu Ga Zn Ge As Se Rb Sr
Ag In Sb Cd Sn Cs Ba
Au Tl Hg Pb
0 10 20 30 40 50 60 70 80 90
Atomic Number of Element.

included in fig. 1 and clearly represents a very full type of structure; the univalent radius of the $Fe^{0\cdot2+}$ ion would be slightly lower. So far as they can be estimated, the transitional elements of Group VIII all correspond with very full structures, and this is reflected in their properties.

Fig. 1 shows some characteristics of the atomic and ionic radii relationships, but for other purposes it is more convenient to redraw this in the form of fig. 2, where the atomic numbers as abscissæ are plotted against both the ionic radii and one half the interatomic distances in the crystals of the elements. This diagram shows very clearly the distinction between the elements following

the alkali metals and those following copper, silver and gold. After each alkali metal both interatomic distances and ionic radii decrease, but the latter decrease less rapidly, so that the structures become less open. With the elements following copper and silver the ionic radii decrease more rapidly than the interatomic distances, and it is this fact which is responsible for many of the anomalies discussed later.

II.

In discussing the compressibilities of the elements, only the results of Bridgman[8] are of sufficient accuracy for detailed comparison. For some elements only data from earlier work by Richards are available, but it does not seem justifiable to use these since comparison by Bridgman[9] has shown that in several cases the results of Richards differ considerably from the accepted results.

If the ideas of the previous section are correct, we shall expect a difference between the compressibilities of elements of the "open" and "full" types. In the elements of the open type the properties are controlled essentially by the valency electrons, and it is known that, for many purposes, these may to a first approximation be treated as particles of an electron gas. The pressure, p, of an electron gas is proportional to $\left(\frac{N}{V}\right)^{5/3}$, where N is the number of electrons in volume V, and hence the compressibility $\frac{1}{V} \cdot \frac{dV}{dp}$ is proportional to $\left(\frac{V}{N}\right)^{5/3}$. In an actual metallic crystal part of the volume is occupied by the ions, and when a valency electron is so close to the atom as to be within the ionic radius its resemblance to a gas particle will be comparatively small, and no simple theory can be developed. Since, however, a valency electron spends most of its time outside the ion *, we may for the open type of crystal expect an approximate proportionality between the compressibility and the function $\left(\frac{V_{ex}}{N}\right)^{5/3}$, where V_{ex} is the extra-ionic volume in the unit cell of the crystal, and N the number of valency electrons

* In the free atom, for example, electrons in penetrating orbits, to use the older terminology, spent most of their time outside the inner shells.

in the unit cell (*i. e.*, N equals the number of atoms in the unit cell multiplied by the valency). We have tentatively estimated the function $\left(\frac{V_{ex}}{N}\right)^{5/3}$ by assuming the ions to be spheres of radius equal to the univalent radii of Zachariasen and Pauling, so that V_{ex} is obtained by subtracting the volume of the spherical ions from the volumes of the unit cells of the different crystal structures. Fig. 3 shows the compressibilities of the open type of crystal plotted against $\left(\frac{V_{ex}}{N}\right)^{5/3}$ calculated as described

Fig. 3.

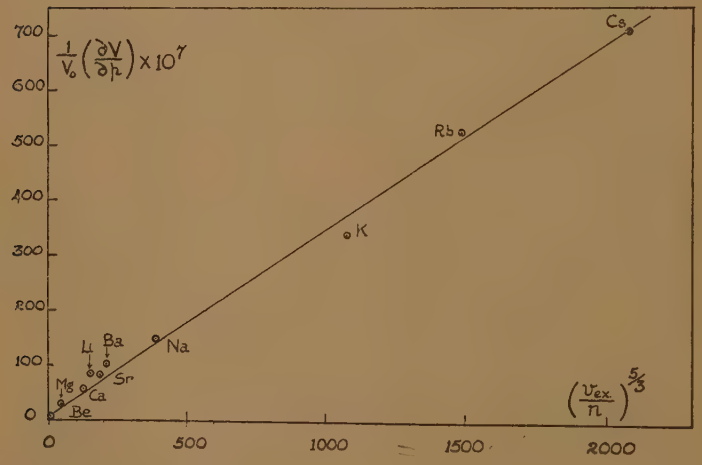

above, and the general proportionality between the compressibility and the function $\left(\frac{V_{ex}}{N}\right)^{5/3}$ is evident. An exact agreement is not to be expected from so crude a method of approach *, but the general proportionality is sufficiently striking to suggest that our underlying picture of the phenomenon may be correct, even though

* We are ignoring the fact that the number of electrons in the extra-ionic space is slightly less than the total number of electrons. The effect of the type of crystal structure is also being ignored. The selection of one temperature for the compressibility measurement is, of course, arbitrary, but is to some extent counterbalanced by the effect of temperature on the lattice spacing.

the expression of the value of an ion by means of a single radius is admittedly a crude approximation.

In order to discuss the compressibilities of the remaining elements, it is necessary to plot the extreme left hand lower corner of fig. 3 on a much larger scale, and this has been done in fig. 4. It will be seen that the points for lithium and barium are relatively high, and since these elements crystallize in the body-centred cubic structure it is possible that this is a structure effect.

Fig. 4.

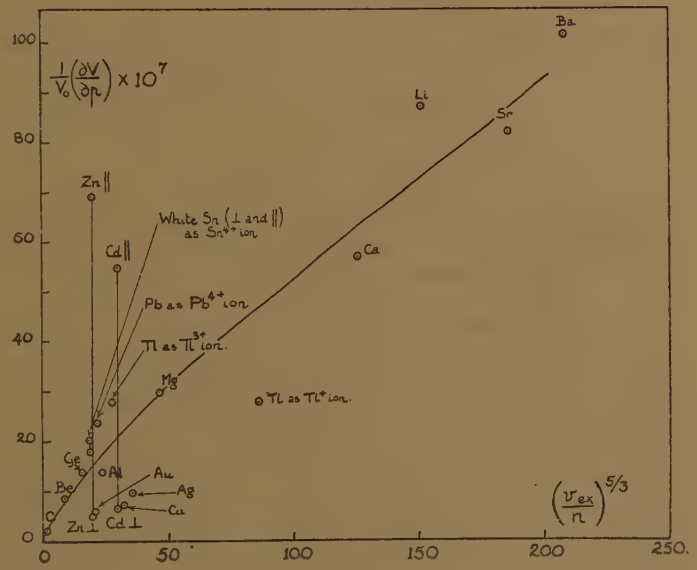

In general the open type of crystals for which $\left(\frac{V_{ex}}{N}\right)^{5/3}$ is small have rather higher compressibilities than would be given by the straight line through the heavier alkali metals in fig. 3.

The points for copper, silver, and gold in fig. 4 lie very much lower than those for open metals of the same values of $\left(\frac{V_{ex}}{N}\right)^{5/3}$, and their undoubtedly low position is not affected by the doubt as to the exact values of the ionic radii (see page 133) used to estimate V_{ex}. In other words,

the compressibilities of copper, silver, and gold are not merely much less than those of the open type of metals with comparable *atomic volumes*, but are less than would be expected if the compressibility were determined by all the valency electrons being concentrated in the small *extra-ionic volumes*. The conclusion thus appears inevitable that in copper, silver and gold the compressibility is no longer determined mainly by the valency electrons, but depends to a great extent on the overlapping of the ions.

In contrast to copper, silver and gold, it will be seen that the point for germanium agrees with that for the open type of metal. This can be understood by reference to fig. 2, which shows that although the interatomic distances in germanium are slightly less than those in copper, the ion has shrunk away considerably, so that the structure of germanium is comparatively open.

With zinc and cadmium the position is complicated by the abnormal crystal structures, in which each atom has six close neighbours in the basal plane and six at a larger distance (three above and three below). Bridgman [10] has by indirect methods determined the coefficients of *linear* compressibility in different directions in the crystal, and in order to make the results comparable with the remaining points in fig. 4, we have multiplied the linear coefficients by three so as to give the volume compressibilities which these metals would have if the whole crystal contracted uniformly with the coefficients observed for the parallel or perpendicular directions. It will be seen that the compressibility perpendicular to the hexagonal axis corresponds with a fairly full type of structure, as would be expected from the close packed array, whilst the compressibility parallel to the axis is very much greater, and may suggest that the valency electrons are less densely packed in this direction.

In any one Period, the lowest compressibilities among the metals are shown by the transitional elements of Groups VI, VII, and VIII, the crystals of which are very full structures, so that the low compressibilities are readily understood as being due to the overlapping of the ions.

With thallium and lead, the values of $\left(\frac{V_{ex}}{N}\right)^{5/3}$, based on the assumption of the fully ionized Tl^{3+} and Pb^{4+} ions

are shown below, together with the compressibilities; the compressibility for thallium is due to Richards, and must be accepted with caution, but as the numerical value is large

Tl.	Pb.
$\left(\frac{V_{ex}}{N}\right)^{5/3}$ based on Pauling's "univalent" Tl^{3+} ionic radius=27·85	$\left(\frac{V_{ex}}{N}\right)^{5/3}$ based on Pauling's "univalent" Pb^{4+} ionic radius=21·38
$\left(\frac{V_{ex}}{N}\right)^{5/3}$ based on Goldschmidt's Tl^{+} (thallous) ionic radius=86·3	
Compressibility=$27{\cdot}7\times10^{-7}$ (Richards).	Compressibility=23·73 (Bridgman).

the error may not be so great as in the examples previously quoted (p. 137). If these values are plotted in fig. 4 the compressibilities are definitely greater than those expected from the curve through the points for the open metals beryllium, germanium, aluminium, and magnesium. As the crystal structures are of the close-packed (cubic or hexagonal) type, there seems no reason for this anomaly *. We have previously shown that the interatomic distances suggest that thallium may be based on univalent Tl^{+} ions rather than on Tl^{3+} ions. The Tl^{+} ion is of course much larger than the Tl^{3+} ion, so that the extra-ionic volume V_{ex} is considerably less for the full Tl^{+} structure than for the relatively empty Tl^{3+} structure. But at the same time the change from a trivalent to a univalent metal reduces the value of N by a factor of three. This more than counteracts the decrease in V_{ex}, and the value of $\left(\frac{V_{ex}}{N}\right)^{5/3}$ is greater for univalent than for trivalent thallium. The point for thallium as a univalent metal is included in fig. 4, and corresponds with a compressibility

* The value for the compressibility of thallium quoted by Bridgman ('The Physics of High Pressure,' p. 161) as $2{\cdot}77\times10^{-7}$ appears to be a misprint for $27{\cdot}7\times10^{-7}$.

It will be appreciated that it is very improbable that in fig. 4 a point really lies above the curve for the metals of the open type, since this would imply a compressibility greater than that for metals such as the alkalis for which it is known that the electron clouds of the ions have almost vanished at a point mid-way between adjacent nuclei.

lower than that for an open type of structure of equivalent $\left(\frac{V_{ex}}{N}\right)^{5/3}$ value, but higher than those for copper, silver and gold. Other things being equal we should expect the compressibility to be somewhat greater for overlapping thallous Tl^{+} ions than for overlapping gold Au^{+} or silver Ag^{+} ions, since the outermost shell of the Tl^{+} ion contains only two electrons spread over a large volume, so that the density of the electron cloud will be less than in ions with $10\,d$ electrons in the outermost shell. There is unfortunately no accurate figure for the univalent radius of a Pb^{2+} ion.

In the preceding Period both indium and white tin have abnormal crystal structures, so that each atom has neighbours at slightly different distances. As will be seen from fig. 4, the points for white tin *, calculated on the assumption of a stannic Sn^{4+} ion, are slightly higher than those for the open metals beryllium, germanium, aluminium, and magnesium, although not to the same extent as the points for lead and thallium based on the assumption of Pb^{4+} and Tl^{3+} ions. But in view of the abnormal crystal structure, this can only be taken as a suggestion that in white tin a sub-group of two electrons is being built up; there is, unfortunately, no way of estimating the univalent radius of an Sn^{2+} ion.

In general, therefore, it may be claimed that the compressibilities agree with the picture of metals given by considering the ionic radii and the extra ionic volumes. Where the ionic radii are relatively large, so that the ions overlap, the compressibilities are small. Where the ions are relatively small and the extra-ionic volumes relatively large, the compressibilities show a general correspondence with the function $\left(\frac{V_{ex}}{N}\right)^{5/3}$. If it is considered justifiable to argue from the diagram involving this function, there is then some indication that lead and thallium in the metallic crystal correspond with Pb^{2+} and Tl^{1+} ions rather than with the fully ionized forms. It may be also noted that for the open type of metal, although

* As with zinc and cadmium, the values given for white tin are three times the linear coefficients of compressibility in the two directions. They thus represent the hypothetical volume compressibilities if the whole crystal contracted with the constants referring to each direction respectively.

the exact agreement is not good, the slope of the line in fig. 3 gives the correct order of magnitude for the effect of temperature on compressibility if this is regarded as due to the expansion of the extra-ionic volume, the volumes of the ions remaining constant.

References.

1) Hume-Rothery, Mabbott, and Channel Evans, Phil. Trans. Roy. Soc. A, ccxxxiii. p. 1 (1934).
(2) Mott and Jones, 'The Theory of the Properties of Metals and Alloys,' p. 144.
(3) Goldschmidt, *Ber.* lx. p. 1263 (1927).
(4) Pauling, J. Amer. Chem. Soc. xlix. p. 765 (1927).
(5) Zachariasen, *Zeit. Krist.* lxxx. p. 137 (1931).
(6) Goldschmidt, *Zeit. phys. chem.* cxxxiii. p. 397 (1928).
(7) Mott and Jones, 'The Theory of the Properties of Metals and Alloys,' p. 222.
(8) Bridgman, 'The Physics of High Pressure.' It should be noted that numerical mistakes exist in some of the earlier data of Bridgman, and have been corrected (Bridgman, Proc. Amer. Acad. Arts. Sci. lxx. p. 71 (1934).
(9) Bridgman, 'The Physics of High Pressure,' p. 152.
(10) Bridgman, 'The Physics of High Pressure,' p. 161.

The Old Chemistry Department,
The University Museum,
Oxford.
May 1938.

XI. *Atomic and Ionic Radii.*—II. *Application to the Theory of Solid Solubility in Alloys.* *By* WILLIAM HUME-ROTHERY, *D.Sc., F.R.S., Royal Society Warren Research Fellow, and* GEOFFREY VINCENT RAYNOR, *B.A., B.Sc., Keble College, Oxford* *.

[Received June 8, 1938.]

I.

IN the preceding paper, the atomic and ionic radii have been discussed, and the general distinction between the "full" and "open" types of metal has been indicated. The formation of a substitutional solid solution involves the fitting of different atoms on to a common lattice, and we shall therefore expect to find the difference between the full and open types of metal exerting an influence on the formation of solid solutions. Two metals may, for example, have the same atomic radius

* Communicated by W. Hume-Rothery, D.Sc., F.R.S.

as defined by one half of the closest distances of approach in the crystals of the elements, or the same Goldschmidt radius, but their ionic radii may be quite different, and in such a case it may be possible to fit together atoms of the open type, but not those of the full type. The following examples may be discussed as illustrating either general principles or systems which have previously proved difficult to understand.

II.

The Solubility of Silver, Cadmium, Indium, Tin and Antimony in Solid Copper, Nickel, Cobalt, and Iron.

It is well known that with copper or silver as solvents, the solubilities of B—Subgroup Elements of favourable

TABLE I.

In this Table, solubilities are given in atomic percentages. The temperature 549° C. is that of the peritectic involving the α-solid solution in the copper-cadmium system.

Solvent.	Group I.	Group II.		Group III.			Group IV.			Group V.	
	Ag.	Zn.	Cd.	Al.	Ga.	In.	Si.	Ge.	Sn.	As.	Sb.
Ag. Max solubility.	—	37·8	42·5	20·4	19·0	20·0	—	6	12·2	6	7
Cu. Max. solubility.	5	38·4	1·7	20·4	20·3	11·0	14·0	12·0	9·3	6·2	5·6
Solubility at 549° C.	1	37·5	1·7	20·3	20·1	9·4	10·9	10·5	9·2	6·2	5·6
Solubility at 300° C.	0·2	37·5	0·35	20·3	19·0	4·5	7·5	10·2	5·5	6·2	3·0

size-factor correspond with an approximately constant electron concentration of the order 1·4, and this has been explained theoretically by H. Jones [1]. The solubility thus decreases with increasing valency of the solute, as can be seen from Table I. In contrast to this general principle, the elements silver and cadmium are comparatively slightly soluble in copper, whilst indium, tin, and antimony show solubilities which approach more and more nearly to those expected from the normal valency

values (see Table I.). This at first appears very puzzling in view of the fact that the atomic diameters of Goldschmidt, and hence the lattice distortion * of copper produced by equiatomic percentages of solute *increase* in passing from silver to antimony, so that we should at first expect the solubility to become increasingly less than the normal value. This apparent anomaly is readily explained by reference to fig. 1. Copper forms a fairly full type of structure in which the *d* shells of the ions overlap considerably. Silver has not merely a larger atomic radius in the Goldschmidt sense, but it has also

Fig. 1.

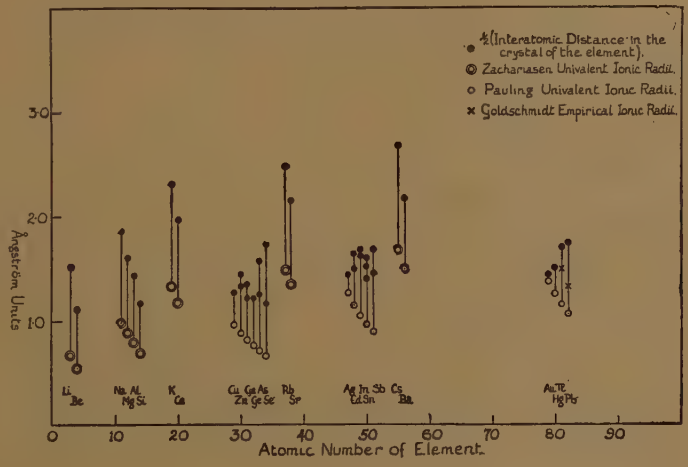

a larger *ionic radius*. Consequently, in so far as copper may be regarded as composed of ions in contact, it will clearly be difficult to insert a larger ion, since this will produce an even greater overlapping of the ions. With cadmium, the atomic radius in the Goldschmidt sense is larger than that of silver, but the ionic radius is smaller, although still a little larger than that of copper. It is therefore still difficult to fit a cadmium atom on to the lattice of copper, although not so difficult as to introduce an atom of silver, and, as will be seen from Table I., the

* The term " lattice distortion " is employed in its usual sense to denote the increase in lattice parameter as measured by ordinary X-ray methods.

solubility of cadmium at a given temperature is greater than that of silver. With indium, tin and antimony the atomic radii of Goldschmidt increase, but, as shown in fig. 1, the ions become smaller, and consequently the maximum solubility values begin to approach the normal, since at each step it is more easy to introduce the ions. It will be noted that in all these systems the solid solubility decreases markedly with falling temperature, and this can readily be understood since the electronic structure of the ions will not be affected by the temperature, but

TABLE II.

In this Table solubilities are given in atomic percentages.

Solvent.	Solutes.				
	Ag.	Cd.	In.	Sn.	Sb.
Ni	<3 (immiscible liquids).	No data.	No data.	11 at 1,100° C. 1 at 500° C.	4 approx.
Co	No solutions in liquid or solid state.	No data.	No data.	Small.	5–6.
Fe	No solution.	No solution.	No data.	Maximum of 9 at 760°, falling at lower temperatures.	4 approx.

as the metal expands it will become increasingly easy to accommodate the larger ions.

If the above explanation is correct we shall expect to find the same relations for the solubilities of the above elements in solid iron, nickel, or cobalt. As shown in Table II. this is confirmed experimentally in those systems for which data are available, the solubilities of silver and cadmium being small and those of tin and antimony greater. The decrease in solubility at low temperatures is again very marked, and this may be a general characteristic of solid solutions in which a larger *ion* is being introduced into a crystal which is already of the "full" type.

III.

The Mutual Solid Solubilities of Pairs of Metals of the Full Type, and the Relative Stabilities of Superlattices of the Types A_3B and AB_3.

The mutual solid solubilities of a given pair of metals depend on many factors, such as their valencies, the types of crystal structure with their accompanying electronic energy characteristics, the tendency to form compounds, etc. In so far as we can separate the effects due to the sizes of the atoms or ions, we may extend the arguments of the preceding section and say that, other things being equal, for a given pair of metals of the full type with an appreciable difference in the sizes of the two kinds of atoms and ions, we shall expect the solid solution in the metal of the larger ionic diameter to be the greater *. For, if a metal of the " full " type is already an assembly of ions " in contact," it will be more difficult to introduce a larger ion than a smaller one †. When, however, the two ionic radii are nearly the same and the metals are of the full type, the mutual solid solubilities depend more on the densities and deformabilities of the electron clouds, and this is discussed later.

It is well known that in many cases alloys form solid solutions with a random crystal structure at high temperatures, but with an ordered or superlattice structure at low temperatures, the phenomenon being particularly common when the two kinds of atoms, although still sufficiently similar in size to form a solid solution, are nearing the limits of the zone of favourable size-factor. In such cases the strain caused by fitting atoms of different sizes on to a common lattice is relieved by a regular arrangement of the atoms, and the most common types of superlattice are based on compositions A_3B, AB, and AB_3, where A and B are the two kinds of atoms. Extending the above argument we shall expect, for metals of the full type, the random solid solution to be greater on the side of the metal with the larger atom and ion, and if this

* All references to solubility values are, of course, to atomic percentages.

† The fact that elements of a very open type, such as magnesium or aluminium, can dissolve in a metal of the full type, such as silver, shows that the formation of a metallic solid solution is not prevented by unequal sizes of the *ions*, provided that the size factors deduced from the atomic radii are favourable.

metal is called A we shall expect superlattices of the type AB_3 to be more common than those of the type A_3B, since the strain to be relieved is greater when the larger A ion is being fitted into the B lattice than for the reverse case.

The following systems may be taken as illustrating these general principles :—

Copper-Silver.—This is a simple eutectic system in which both metals are of the full type and of the same valency. At a given temperature the solubility of copper in silver is always greater than that of silver in copper, in agreement with the conclusion reached above.

Copper-Gold.—Both metals are of the full type and of the same valency, and the diagram is one in which a continuous solid solution is formed at high temperatures, and at low temperatures the lattice strain is relieved by the formation of superlattices. The disordered solid solution has a wider range on the gold side of the equilibrium diagram than on the copper side, thus confirming that it is more easy to introduce smaller ions into a lattice of the full type than to introduce larger ions. This effect is so great that a superlattice of the type Au_3Cu is not formed on the side of the relatively large gold atom, although a superlattice of the type Cu_3Au is formed on the copper side.

Copper-Palladium and Copper-Platinum.—Copper and nickel form a continuous solid solution, but in the systems copper-palladium and copper-platinum the size factors are sufficiently different for superlattices to be formed at lower temperatures. Superlattices of the types Cu_3Pt Cu_3Pd, CuPt, and CuPd are formed, but not those of the type $CuPt_3$ or $CuPd_3$, thus confirming the general principle that it is easier to introduce smaller ions into a lattice of the full type than to introduce larger ions.

Gold-Nickel, Gold-Cobalt, Gold-Iron, Gold-Manganese and Gold-Chromium.—In the system gold-nickel a continuous solid solution is formed at high temperatures, but at low temperatures this splits up into two solid solutions, of which the gold-rich solid solution is of the wider extent, in agreement with the above principle. In the alloys of gold with cobalt, iron, manganese and chromium, the diagrams are of different types and not always known in detail, but from the diagrams given by Hansen[2] it

appears that the gold-rich solid solution is always the wider, which is what we should expect from the above principle, since the gold ion is larger than the ions of the series chromium to copper.

Zinc-Cadmium.—As previously explained[3], zinc and cadmium form more open structures than copper and silver, but are still much more of a full type than the aklali or alkaline earth metals. The same general principle is found in the system zinc-cadmium, the solid solution in cadmium with the larger atomic and ionic diameter being greater than that in zinc.

IV.

The System Silver-Beryllium.—In the system silver-beryllium, beryllium dissolves approximately 11 atomic per cent. of silver, whilst silver dissolves only 3·5 atomic per cent. of beryllium. The atomic diameters of silver and beryllium are 2·88 Å. and 2·28 Å. respectively, so that the beryllium-rich solid solution is remarkable, not only in view of the comparatively large difference in the atomic diameters (26 per cent.), but also as an exception to the general valency principle (relative valency effect), according to which in an alloy of copper, silver or gold with an element of higher valency the solid solution in the univalent element is nearly always the greater. Reference to fig. 1 may provide an explanation of this apparent anomaly. The metallic radius of beryllium is considerably smaller than that of silver, but whereas silver is a structure of the full type, the ionic radius of beryllium is so small that beryllium contains a large amount of extra-ionic space. We can understand therefore how it may be possible to insert a silver atom on the beryllium lattice, since the latter has a large amount of extra-ionic space.

V.

The preceding considerations should make it clear that solid solubility relations in detail are not likely to be explained by any single series of atomic diameters, since we must always consider how much of the atomic diameter is occupied by the underlying ion. Provided that allowance for a change from the incompletely ionized to the fully ionized state is made for the later elements of Groups III. B. and IV. B, the best correlation between

solid solubility and atomic diameter is given by using the atomic diameters defined as the closest distance between the atoms in the crystals of the elements * [4]. This, however, must be regarded as an empirical approximation only, and for any detailed examination we must consider the atom and the ion in greater detail. We have already [3] emphasized the crude approximation involved in attempting to express the size of an ion by a single radius, and for greater accuracy we require the full curve showing the variation of the electron cloud density surrounding each ion. It seems probable, however, that even detailed considerations of the sizes of atoms and ions alone are not sufficient to explain the solid solubility relations in some alloy systems. We have already seen how consideration of the atomic and ionic diameters enables us to understand the mutual solubilities in the systems copper-silver and copper-gold. But it seems improbable that consideration of atomic and ionic diameters will explain why the one system (CuAu) forms a continuous series of solid solutions and the other (CuAg) comparatively restricted solid solutions. In particular, since silver and gold have nearly equal atomic and ionic radii, it is difficult to understand from considerations of size alone why gold can dissolve copper and silver cannot, except to a very limited extent. The conclusion appears inevitable that other factors exert an influence, and we suggest that of these one of the most important is the mutual deformation or polarisation of the ions in each other's fields. That is to say, the ion must not be looked upon as a hard sphere of definite radius, but as a positively charged nucleus embedded in a cloud of negative electricity. The charge distribution at the outside of this electron cloud can be deformed or polarized by the effect of neighbouring ions, and this polarization may determine whether atoms of different kinds can fit together upon a lattice.

When a foreign atom enters into solid solution in a given solvent there must always be some local disturbance of charge distribution, since no two ions have identical electron clouds. With metals of the full type, in which

* We have attempted to correlate the solubility data with the Goldschmidt *atomic* radii using the *ionic* radii as an additional complicating factor, but this appears to give rise to more anomalies than when using the atomic diameters as defined above.

the ions overlap considerably, we shall expect that a solid solution will be formed more readily if this local disturbance can be "smoothed out" or adjusted so as to fit the lattice of the solvent, and hence, other things being equal, we shall expect a metal with an easily polarisable ion to dissolve more readily than one whose ion is difficult to polarize. Similarly, when metals are compared as solvents, other things being equal, we shall expect those whose ions are strong polarizers to take up metals into solid solution most readily, since the stronger the polarizing power of the solvent ions the more they can deform the charge distribution of the solute ions, and so permit the latter to fit into the lattice. It has also been pointed out to us by Professor Mott, that with metals of the full type, increasing polarizability of the solute ion will not only facilitate the fitting together of different kinds of ions but will also favour the existence of attractive forces of the van der Waals type. For the more the ions are polarizable, the more easily they can give rise to a "sympathetic vibration" or dynamic polarization, which is the cause of the van der Waals forces. These two conceptions may be different aspects of one general process, since the polarization which deforms the different kinds of ions so that they fit together may bring them into the condition in which the sympathetic vibration is favoured.

With copper, silver and gold the polarizing powers of the ions * are in the order

$$Cu^+ > Au^+ > Ag^+.$$

The polarizabilities of these ions are given by van Vleck[5] as in the order

$$Au^+ > Ag^+ > Cu^+.$$

The figures of van Vleck are based upon work by Pauling, and the order is confirmed indirectly by the work of Heydweiller [6] on ionic refractivities in aqueous solution. Heydweiller does not give values for copper or gold, but he places the polarizability † of zinc, cadmium, and

* The copper and gold halides are covalent. With silver, the chloride and bromide are ionic in the crystals, whilst the iodide exists in both ionic and covalent forms, the iodide ion being the most polarizable of the halogen ions. The silver ion has therefore the least polarizing power. Since both copper and gold have the same outer electronic structure, the smaller copper ion is almost certainly the better polarizer.

† The values given include the effect of the ions upon the water molecules, but this is unlikely to affect the orders.

mercury ions in the order $Hg^{2+}>Cd^{2+}>Zn^{2+}$, and it may reasonably be assumed that the order for the preceding univalent elements is the same.

The solubility relations may now be understood in terms of these sequences. *With copper as solvent*, both gold and silver have larger ions, but the gold ion is more easily polarizable, and its charge distribution can therefore be deformed or modified so as to fit the copper lattice, whereas the less easily polarizable silver ions cannot. The van der Waals attractive forces are also favoured in the case of gold. *With copper as solute*, the atomic diameters of silver and gold are almost identical. Copper can dissolve in gold but not to any great extent in silver, because the gold ion is both a better polarizer and more polarizable than the silver ion, so that in the system copper-gold everything is more favourable for the mutual adjustment of the electron charge distribution in such a way that the two kinds of atoms fit together. In the third paper of this series one of us (G. V. R.) has examined the polarization of ions in greater detail.

References.

(1) H. Jones, Proc. Phys. Soc. xlix. p. 250 (1937).
(2) M. Hansen, ' Der Aufbau der Zweistofflegierungen,' 1936.
(3) W. Hume-Rothery and G. V. Raynor, Phil. Mag. xxvi. p. 129 (1938).
(4) W. Hume-Rothery, ' The Structure of Metals and Alloys,' London, The Institute of Metals (1936).
(5) van Vleck, ' The Theory of Electric and Magnetic Susceptibilities,' p. 225. Oxford (1932).
(6) A. Heydweiller, *Phys. Zeits.* xxvi. p. 526 (1925).

The Old Chemistry Department,
The University Museum,
Oxford.
May 1938.

XII. *Atomic and Ionic Radii.*—III. *Polarization Effects in Alloys.*

By Geoffrey Vincent Raynor, *B.A., B.Sc., Keble College, Oxford* *.

[Received June 8, 1938.]

I.

In the preceding papers [1], [2] it was shown that metals may in general be classified into two main types, the "full" type in which the ionic and atomic radii differ

* Communicated by W. Hume-Rothery, D.Sc., F.R.S.

very little, and the " open " type, in which the ionic and atomic radii may differ considerably, and that, for a given pair of metals of the full type, the relative extents of the primary solid solutions formed depend upon the relative sizes of the ions of the two metals. It was indicated that, although in many cases simple considerations of ionic sizes give an adequate interpretation of the solubility effects, there are complicating factors, one of the most important of which is the mutual deformation of the ions of the constituent metals ; this effect is discussed in detail in the present paper.

The evidence from crystallography and from many other sources shows clearly that ions are not be be considered as hard spheres carrying a certain number of positive or negative units of charge, although it is necessary to make this assumption in order to obtain an estimate of their relative sizes. The most convenient conception of an ion for our present purpose is that of a minute positively charged nucleus embedded in a cloud of negative electricity, which is to be regarded as the " smoothed out " resultant charge of the individual electrons. The electron clouds of ions of the inert gas configurations and of ions having an outermost group of 18 electrons are spherically symmetrical ; for certain ions of the transitional metals (and for ions of lower valency than the group valency *e. g.*, Pb^{2+}, Sb^{3+}) the electron clouds may no longer be spherically symmetrical. Such an electron cloud as we have visualized is not rigid but may be deformed by the action of an electric field, as is demonstrated by the production of a dipole when a neutral atom or an ion is introduced into a homogeneous electric field such as that between the plates of a condenser. The dipole is due to the relative displacement of the centres of gravity of the positive and negative charges. The conditions when an ion is subjected to an inhomogeneous field due to other ions are somewhat different. Considering a free molecule composed of a positive and a negative ion, the positive charge of the cation repels the nucleus of the anion but will attract the whole of the electron cloud of the anion towards it. The anion is thus polarized as a whole ; the portions of the cloud lying nearest to the cation are more strongly attracted than those more distant, and the electron cloud loses its spherical symmetry. When the anion is situated on a crystal lattice in which it is sur-

rounded symmetrically by cations, there can be no relative displacement of the centres of gravity of the positive and negative charges, and the ion is not polarized as a whole. There is frequently considerable distortion, however, the portions of the electron cloud lying nearest to a cation being attracted outwards. The behaviour of cations under the deforming influence of the field of anions is analogous, the electron clouds of the cations being repelled.

Similar considerations may clearly apply in a crystal lattice composed entirely of cations, as in the normal metal. In this connexion it must be realized that we must not expect the effects to be as definite and as well defined in metallic systems as in the study of salts. The polarizability of a cation is much less than that of an anion, since the electron cloud of a cation is more firmly bound together by reason of the excess positive charge under the influence of which the electrons are moving. It is for this reason that, in the study of salts, the deformation of the cations may in general be neglected in comparison with that of the anions ; most of the observed polarization phenomena with salts are due to the deformation of the anion. An additional factor which militates against the manifestation of well-defined polarization phenomena in metals is the magnitude of the interatomic distance, which is in general greater in the case of metals than in salts.

From a study of the salts of metals having ions of the inert gas configurations it has been shown [3], [4], [5] that the polarizing power of a cation of the inert gas type is greater the higher its charge and the smaller its radius, while for an anion, the higher the charge and the larger its radius the more easily may it be deformed. The striking regularities obtained by Fajans for this type of ion enable us to compare polarizing powers satisfactorily to a first approximation. Although it is difficult to obtain satisfactory numerical estimates of the polarizing powers of positive ions, we may express them approximately in terms of the " field strengths " of the ions concerned, *i. e.*, $\frac{\text{Ionic Charge}}{(\text{Radius})^2}$. There is definite evidence that cations whose outer shell contains 18 electrons (*i. e.*, ions of metals of the B subgroups) are more efficient as polarizers than cations having the inert gas configurations. Attempts

to work this out in detail by methods which are successful with the inert gas type of ion, however, lead to anomalies. The expression given above for the "field strength" is no longer even approximately valid, and it is necessary to assume the operation of factors of a specific nature which have not yet been worked out. Very approximate information may be obtained from chemical evidence.

The effect of the polarizability of the copper, gold and silver ions on the binary alloys of these metals has been discussed in the preceding paper[2]. The metals considered were of the "full" type, and the position is more complex when we consider systems in which both constituents are of the "open" type. In these cases we may expect the primary effect of the sizes of the ions to be of relatively less importance than in the cases of the copper, silver and gold alloys and other systems where one constituent at least is of the full type. Experience shows, however, that the mutual solubility relations in some alloy systems may be interpreted in terms of the relative polarizing powers and polarizabilities of the ions concerned.

When the ion of a solute element is introduced into the solvent lattice a considerable disturbance of the charge distribution characteristic of the lattice occurs. If this is allowed to remain localized at the point of substitution, the effect on the solubility, *i. e.*, the further introduction of solute ions, is likely to be marked, since the resultant strain in the lattice will be high. If, however, the charge disturbance may be *distributed* so that it does not remain intensely localized, the effect may be expected to be less serious; in general, the consequences of a distributed strain in any structure are less serious than those of a localized strain. It is probable that the ability of one ion to polarize another affords a mechanism for the distribution of the charge disturbance consequent on solution. Consider, for example, the introduction of an ion with a dense electron cloud into the lattice of a metal whose ions possess a less dense electron cloud. The charge disturbance at the point of introduction will be considerable. If, however, the solvent ions, which will, in a dilute solution, in most cases be distributed symmetrically around the introduced ion, are strongly deforming, and if the introduced ion is easily polarizable, the dense electron cloud of the solute ion will be drawn

out, mainly in the directions of its symmetrically situated nearest neighbours. Effectively, a certain amount of the electron cloud of the solute ion will come under the control of the positive charges of the neighbouring deforming ions; this amounts to a sharing of the disturbance, which would otherwise be confined to the point of introduction, between the solute ion and its nearest neighbours on the solvent lattice. The extension in space of the solute ion would be increased in certain directions by a process of this type, but this would be compensated for by the decrease in density of the electron cloud.

It is probable that effects of this nature are responsible for the invalidity in metallic solid solutions of Vegard's Law [9], according to which the lattice parameters of a primary solid solution vary linearly with the atomic percentage of the solute element. The great majority of alloys deviate from this law and the deviation usually corresponds to a contraction compared with the parameters to be expected from a linear relation. If some of the electron cloud of the solute ion is coming partially under the control of the positive fields of neighbouring solvent ions, we have a condition which represents a slight tendency towards the formation of a linkage in which electrons are shared between atoms, *i. e.*, a covalency. Although it is not, of course, suggested that we have anything more than a slight tendency in this direction, we might expect a slight diminution of the internuclear distances as a result of the deformation processes, and this is what is in most cases observed. This effect may be reinforced by the existence of attractive forces of the van der Waals type, which will also depend upon the polarizabilities of the ions, as explained previously [2].

If our ideas are correct we should in general expect, for a given pair of metals of the open type, that if one ion is a powerfully deforming ion and the other is capable of being easily deformed, the more powerfully polarizing ion would give rise to the wider range of solid solutions. For ions of the inert gas type the polarizability decreases with increasing polarizing power in general, so that the better polarizer of two ions will also be the less easily polarized or deformed.

The simple relation between the polarization effects

and solid solubilities may, of course, be obscured by other factors. If, for instance, the metals are of different valencies, purely electronic effects may be dominant, as shown by the work of H. Jones[7] and by Hume-Rothery and Raynor[8]. In the alloys of the univalent metals copper, silver and gold there is a well-marked relative valency effect, the solid solubility of the metal of higher valency in the univalent metal being greater than the reverse. There is, however, little justification for the rigid extension of this rule to the alloys of other metals, and especially to those systems in which both constituents have valencies higher than unity.

If we consider the alloys of metals of the A subgroups, we find that our expectations are fulfilled wherever accurate data are available, even though the character of the metals is such that at points midway between the nuclei the electron clouds of the ions have died away almost completely.

In the system aluminium-beryllium, of the simple eutectic type[9], restricted solid solutions are formed in both metals, but the solubility of aluminium in the more strongly deforming beryllium lattice is greater than the reverse. The trivalent aluminium ion is also the more easily deformable of the two[10], and everything is favourable for the polarization effect. The system aluminium-calcium is of a more complex type with two intermetallic compounds; of the two ions the aluminium ion is the more powerfully deforming ion, and here again the solubility of the calcium ion in the more strongly deforming aluminium is greater than the reverse. Of the two ions calcium is the more easily deformable[10]. In the system aluminium-lithium, lithium dissolves in aluminium to an extent of approximately 10 atomic per cent. In the work of Müller it is stated that an alloy containing 10 atomic per cent. aluminium gave a primary liquidus arrest and a second arrest at the melting-point of lithium[11]. Thus it is extremely probable that the solubility of lithium in the more strongly deforming aluminium lattice exceeds that of aluminium in lithium, in agreement with the principle. The solid solubilities in the system magnesium-aluminium are nearly reciprocal, but the more strongly polarizing and less easily polarized aluminium gives rise to the wider solution of the two.

In general, systems containing silicon introduce compli-

cating factors due to the formation of very stable intermetallic compounds. The aluminium-silicon system, however, is free from this complication, the two metals forming a simple eutectic, but unfortunately the diagram has not been very completely studied at the silicon-rich end. From the data at present available, however, it seems probable that the solubility of silicon in aluminium is less than that of aluminium in silicon. Of the two ions, silicon, which has a high charge and a very small size, is undoubtedly the more powerfully deforming and less easily deformable ion.

In this discussion we have considered the trivalent Al^{3+} ion. It has been suggested, from certain physical properties[12] that aluminium is incompletely ionized in the crystal of the element, like indium, thallium, tin and lead, but the evidence is not conclusive. In the cases of indium, thallium, tin and lead there is ample chemical evidence of the stability of ions having valencies other than the group valency; such ions, however, are extremely unstable in the case of gallium, and as their stability decreases with the lighter elements of the particular group in the Periodic Table, it is not certain that the irregularities in the physical properties of aluminium are due to this cause. There is, on the other hand, evidence which suggests that aluminium behaves as a trivalent element in alloys[13] and, as we shall see later, this can be accounted for even if the element is considered to be incompletely ionized in the metallic crystal.

In the magnesium-calcium system, where magnesium gives the more strongly polarizing ion and is the less easily deformed, we expect magnesium to give rise to the wider solid solution. There is definitely a solid solution of calcium in magnesium, but the calcium-rich alloys have not yet been carefully examined.

The magnesium-lithium system is at present in dispute, and is of great interest. Since magnesium gives the more strongly polarizing of the two ions we again expect it to give rise to the wider solid solution; the diagram of Saldau and Schamray is in agreement with this[14], but those of other workers[15], [16] do not agree with the principle.

Thus it becomes evident that, whereas for pairs of metals of the full type the metal with the smaller ion tends to dissolve to the greater extent, for metals of the open type the reverse may be the case, the mutual solu-

bility relations depending more upon the relative polarizing powers and polarizabilities.

When the systems containing metals of the B subgroups are considered two separate difficulties are encountered. In the first place many of the B subgroup metals are approaching the full type of structure, for which the relative sizes of the ions assume greater importance; and secondly, it is difficult to assess the polarizing powers of these ions satisfactorily, either relative to each other or to the metals of the A subgroups. In some cases evidence may be drawn from their general chemistry and the same general tendency is shown, though the complicating factors prevent any detailed comparison. This is particularly so where we have definite evidence that the metal is incompletely ionized in the solid crystal, since it is extremely difficult to arrive at any estimate of the polarizing powers.

The system silver-beryllium has been discussed[2] as an example of the effect of the ionic sizes on solubility relations. It is probable that the wide solubility range of silver in beryllium, although primarily due to the size effect, is also due in part to the fact that silver is much more easily polarized or deformed than beryllium, and can be deformed under the action of the strongly deforming field of the ions of the beryllium lattice.

The possibility of the operation of polarization effects in metallic systems enables certain puzzling phenomena to be interpreted in a general way. We have referred above to the evidence suggesting that aluminium may be incompletely ionized in the crystal. When dissolved in copper, silver, gold, and possibly magnesium, however, the experimental data suggest clearly that its behaviour is that of a normal trivalent metal *. This may be understood when we consider that the introduced ion of aluminium is brought under the deforming influence of the positively charged ions of the solvent lattice. The deforming field to some extent frees the outer electrons from the control of the aluminium nucleus, so that conditions would be favourable for complete ionization, leading to dissolution in the trivalent state.

The same type of process may be at work in intermediate phases of certain alloy systems. In the aluminium-gold

* In the copper-aluminium system the initial depression of freezing-point for the α-solid solution is abnormally small.

system, according to Coffinberry and Hultgren[17], there is an intermediate phase of the composition corresponding to Al_2Au, which is a brilliant purple in colour and has the fluorspar type of crystal structure. These authors suggest that this is an electron-compound characterized by the electron concentration 8/3[18], formed as a result of the assumption by the gold ion of a divalency under the action of the concentrated field of force due to the small highly charged aluminium ions. This may be regarded as an extreme case of our conception of the polarization effect. The "competition" between the gold and aluminium nuclei for the outer electrons of the larger gold ion results in a greater portion of the electrons originally attached to the gold ion becoming effectively "free." The absence of this phenomenon in the copper-aluminium and silver-aluminium systems may be explained in terms of the inferior polarizabilities of the copper and silver ions, as compared with the gold ion[19].

In certain alloys of copper, silver and gold the β-phase, an electron compound characterized by the ratio of electrons to atoms of 3 : 2, possesses a maximum melting-point at which the solidus and liquidus curves meet. This is an approximate indication of the enhanced stability of these β-phases as compared with those which possess a liquidus curve falling gradually from a peritectic at which $\alpha+\text{Liquid}\rightarrow\beta$ to a peritectic or eutectic involving the formation of the γ-phase, and separate from the solidus curve throughout. If our conception that the ease of building up structures of ions of different sizes depends upon the ease with which the ions can be deformed is correct, we should expect to find significant differences between the copper, silver, and gold systems. This is fully borne out in practice. In the systems copper-zinc and silver-zinc the liquidus of the β-phase falls very gradually from the $\alpha+\text{Liquid}\rightarrow\beta$ peritectic and the solidus and liquidus curves are very close together. In the system gold-zinc, however, the liquidus curve of the β-phase rises to a definite maximum. We suggest that this is due to the greater polarizability of the gold ion under the influence of the deforming fields of the zinc ions. Similarly, in the system silver-cadmium, the β-phase liquidus falls throughout, but there is a pronounced maximum in the β-phase liquidus of the gold-cadmium system *.

* The copper-cadmium system does not form a typical β-phase, as the atomic size-factor is unfavourable.

It is significant the maximum in the gold-zinc system occurs at 725° C. as compared with 627° C. for the gold-cadmium system, since there is distinct evidence that the zinc ion is a more efficient polarizing ion than that of cadmium. Cadmium oxide is *ionic* in the crystal (NaCl type of crystal structure), whereas zinc oxide forms a covalent crystal of the wurtzite type. A similar sequence to those described above occurs in the β-phases of the systems silver-magnesium and gold-magnesium (copper and magnesium do not form a typical β-phase on account of unfavourable size-factors). The maxima in the β-phase liquidi are here so much higher than those in the corresponding zinc and cadmium systems, however, that the predominant factor may be the highly electropositive character of magnesium.

In a paper by Hume-Rothery and Reynolds[20] dealing with the lattice expansion in the α-solid solutions of alloys of silver and copper with the elements of the B-sub-groups, it was found that equal atomic per cents. of zinc, gallium and germanium expand the lattice of copper by amounts proportional to the factors 3 : 4 : 4·8, while the corresponding factors for cadmium, indium, tin and antimony in silver were 2 : 3 : 4 : 6. It will be noticed that the relative increase in passing from solutes of Group II to Group III is less marked in the copper series, where the ratio is 3 : 4, than in the silver series, where it is 2 : 3. Also the increase on passing to Group IV is no longer regular for the copper alloys. Clearly the copper lattice is more difficult to expand than the silver lattice. It is possible that this behaviour is connected with the difference in the polarizabilities of the ions of copper and silver. The less polarizable copper ion will presumably give rise to the less flexible metallic lattice structure ; so that the effects which cause a regular expansion of the more flexible silver lattice are to some extent restrained in the copper alloys. The copper lattice may be regarded as possessing more resistance to distortion. The reason for the agreement of the factors with whole numbers is difficult to interpret.

In general, therefore, it may be said that, although the sizes of the ions of the metals, considered in conjunction with the interatomic distances in the crystals of the elements, give a general guide to the behaviour of metals in binary systems, it is necessary also to consider the

effects of the deforming powers and deformabilities of the ions. The present knowledge of the polarization of ions does not, however, permit the considerations to be expanded into a general law for metallic systems.

II.

It is clear from the above discussion that, owing to the lack of accurate estimates of the polarizing powers of ions, no really trustworthy guide to the relative solubilities of two metals in each other can yet be sought in this connexion ; particularly is this so in the case of the B-sub-

Fig. 1.

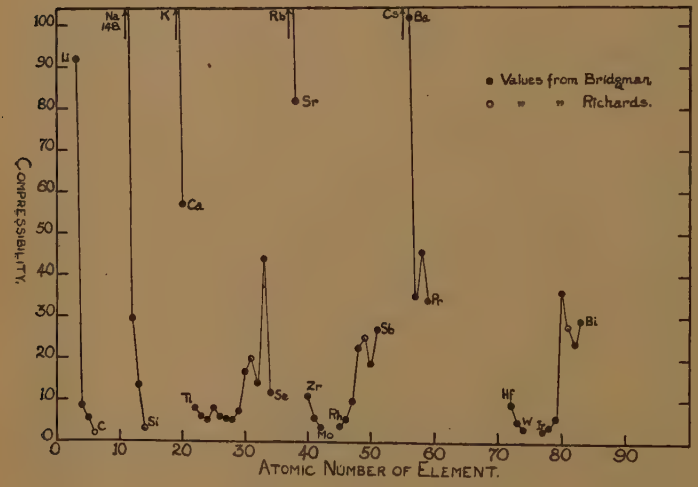

group and transitional metals, which are important constituents of many alloys in practical use.

An examination of the published data suggests, however, that a correlation exists between the *compressibilities* of the metals and the extent to which they may form primary solid solutions with each other. In general, the less compressible of a given pair of metals tends to dissolve more of the metal with the higher compressibility than the reverse. This is especially true for metals of the full type. It is probable that this is connected with the polarization effect. The polarizability of an ion measures its capacity for deformation under the action of electrical forces, while the compressibility of metals of the full type,

where the outer shells of the ions are overlapping, measures the capacity of the ions for deformation under the action of mechanical forces §.

Table I. shows how general the relation between compressibility and mutual solid solubility is. The metallurgical data are taken from Hansen ('Der Aufbau der Zweistofflegierungen') and the compressibilities, which are plotted in fig. 1, are taken mainly from Bridgman's work [21]; other sources, where used, are indicated. In the figure, the points for elements of consecutive atomic numbers in the periodic table are joined by a line, and the symbols for the elements which lie at the beginnings and ends of these sequences are given. The compressibilities are given as $\frac{1}{V_0} \cdot \left(\frac{\partial V}{\partial p}\right) \times 10^7$.

Systems in which no primary solid solutions have been discovered, or in which the solid solutions are continuous, are omitted from Table I., but certain systems containing superlattices are included in a separate section. The extents of the primary solid solutions are compared wherever possible at room temperature, on account of the magnitude of the temperature coefficients of compressibility for most metals. Cases of systems in which the present knowledge is very incomplete or untrustworthy have also been omitted from the Table.

From Table I. it will be seen that the agreement with the rule is very general where accurate data are available.

There are, however, certain systems which are in disagreement if the present accepted equilibrium diagrams are considered. These systems are the following :—

NiCr*, CdPb*, CdZn†, MgPb †, MgSn †, MgBi †, GaIn ‡, MgCd, MgTl, MgZn, AgCu, AgPt, CaCd, PbSn, and TlSn.

[*Notes* :—* In these systems the compressibility values are very close together.

† In these systems the pronounced age-hardening effect at both ends of the equilibrium diagram makes it very difficult to assess the solubilities at low temperatures. Careful work might indicate that these systems really agreed with the rule.

‡ The metallurgical data for this system are very incomplete.]

It seems clear that some additional factor is operative, of which the nature is not clear. It will be noticed that

§ The more powerfully polarizing ions are in general, though not necessarily, the less easily polarized.

TABLE I.

The alloy systems shown in this Table agree with the principle that the less compressible metal of a given pair of metals gives rise to the wider solid solution. The symbol for the less compressible metal is given first.

1.	2.	3.	4.	5.	6.
AgAl.	CuMn.	AuAl.	FeCe.	AlCa.	PbHg.
AgAs.	CuCd.	AuBi.	FeAl.	AlGa.	PbLi.
AgBi.	CuGa.	AuCd.	FeSb.	AlHg.	PbNa.
AgCd.	CuGe.	AuHg.	FeSn.	AlLi.	PbBi.
AgGe.	CuHg.	AuMg.	FeZn.	AlMg.	*PdSb.
AgHg.	CuIn.	AuSn.	MoFe.	AlZn.	PbTl.
AgIn.	CuMg.	AuZn.	CrCo.	BeAl.	PbIn.
AgMg.	CuSb.	AuMn.	CrSb.	MnAl.	CdHg.
AgPb.	CuSn.	AuFe.	CrSn.	SiAl.	CdLi.
AgSb.	CuZn.	CoSb.	NiPb.	*MnSb.	ZnHg.
AgSn.	CuAl.	CoAl.	NiSb.	MnSn.	SnSb.
AgTl.	*FeCu.	MoCo.	NiSn.	TlHg.	SnCd.
AgZn.	CoCu.	PdSb.	NiZn.	TlLi.	
BeAg.	PtSb.	PdPb.	NiAl.	TlBi.	
SiAg.	PtSn.		NiBi.	InTl.	
NiAg.					

Notes :—Column 1.—In the system AgNi immiscible liquids are formed, but the evidence that nickel dissolves more silver than the reverse seems satisfactory.

Column 2.—The data for the system CoCu at the cobalt end of the diagram are very scanty, but it is probable that the cobalt-rich solid solution exceeds the copper-rich solution in extent, since alloys with 10 atomic per cent. of copper may be cooled slowly from 1,100° C., at which temperature they are homogeneous, without change in microstructure (see Hansen, p. 483).

Column 4.—The system CrSn forms immiscible liquids ; there appears, however, to be satisfactory evidence that tin dissolves in chromium to a greater extent than the reverse.

Column 5.—The AlGa equilibrium diagram is at present in dispute, but from the work of Jenckel [22] it is probable that the solubility of gallium in aluminium is greater than the reverse.

the exceptions tend to occur in cases where one metal is comparatively highly compressible ; the exceptions among the " full " type of metal are remarkably few.

It is possible that the non-agreement with the rule of the systems MgCd, CdPb, MgZn, and MgBi is connected with the fact that the linear compressibilities of Zn, Cd and Bi are not equal in all directions. Although the bulk com-

* In these systems the rapid decrease in solubility with falling temperature makes it difficult to estimate the relative values at lower temperatures.

pressibilities of cadmium, zinc, and bismuth are less than that of magnesium, and the bulk compressibility of cadmium less than lead, the *linear* compressibilities of magnesium and lead are somewhat less than the linear compressibilities of zinc and cadmium parallel to the hexagonal axis of the crystal.

In the systems copper-gold, copper-platinum and copper-palladium, a continuous series of solid solutions is formed at high temperatures but superlattices are formed at low temperatures. In each case the superlattice of the type Cu_3X is formed, but no corresponding CuX_3, indicating that the range of solid solution in the copper-rich alloys before a superlattice intervenes is less than that of the gold, platinum, or palladium-rich alloys. This has been discussed [2] in relation to the sizes of the ions, but it is noteworthy also that each of these three metals has a compressibility lower than that of copper. This may be taken as an extension of the general compressibility rule.

References.

(1) W. Hume-Rothery and G. V. Raynor, Phil. Mag. xxvi. p. 129 (1938).
(2) W. Hume-Rothery and G. V. Raynor, Phil. Mag. xxvi. p. 143 (1938).
(3) Fajans and Joos, *Z. Physik.* xxiii. p. 1 (1924).
(4) Fajans, *Z. Phys. Chem.* cxxx. p. 729 (1927).
(5) Fajans, *Z. Elecktrochem.* xxxiv. p. 502 (1928).
(6) L. Vegard and H. Dale, *Z. Krist.* lxvii. p. 148 (1928).
(7) H. Jones, Proc. Phys. Soc. xlix. p. 250 (1937).
(8) W. Hume-Rothery and G. V. Raynor, J. Inst. Metals, lxiii (1938). Advance copy.
(9) M. Hansen. ' Der Aufbau der Zweistofflegierungen,' p. 83.
(10) A. Heydweiller, *Phys. Zeits.* xxvi. p. 526 (1925).
(11) A. Müller, *Z. Metallkde,* xviii. p. 231 (1926).
(12) W. Hume-Rothery, Phil. Mag. [vii.] x. p. 217 (1930).
(13) W. Hume-Rothery. ' The Structure of Metals and Alloys,' London, The Institute of Metals, p. 98 (1936).
(14) P. Saldau and F. Schamray, *Z. Anorg. Chem.* ccxxiv. p. 388 (1935).
(15) O. H. Henry and H. V. Cordiano, Trans. Amer. Inst. Min. Met. Eng. iii. p. 319 (1934).
(16) G. Grube, H. v. Zeppelin, and H. Bumm, *Z. Elekrochem.* xl. p. 160. (1934).
(17) A. S. Coffinberry and R. Hultgren, ' Metals Technology,' v. p. 1 (1938).
(18) N. F. Mott and H. Jones, ' The Theory of Metals and Alloys,' Oxford, p. 170 (1936).
(19) van Vleck, ' The Theory of Electric and Magnetic Susceptibilities,' Oxford, p. 225 (1932).
(20) W. Hume-Rothery and P. W. Reynolds, Proc. Roy. Soc. A, clvii. p. 167 (1936).
(21) P. Bridgman, ' The Physics of High Pressure.'
(22) E. Jenckel, *Z. Metallkde,* xxvi. p. 249 (1934).

The Old Chemistry Department,
The University Museum,
Oxford.
May 1938.

XIII. *A Relativistic Study of the Joule-Thomson Effect and Adiabatic Processes in a Gas.*—Part II. *By* D. V. Gogate, *M.Sc., Physics Department, King's College, London* †.

[Received April 1, 1938.]

Introduction.

In a previous paper [1] (referred to hereafter as Part I.) the author has discussed the Joule-Thomson effect and adiabatic transformations in a relativistic non-degenerate gas obeying Fermi-Dirac statistics. It was shown that for such a gas a Joule-Thomson expansion results in a rise of temperature, while for a gas obeying Bose-Einstein statistics a fall of temperature occurs during a Joule-Thomson expansion, the change in temperature in either case being proportional to the value of A_0^r, which is known as the degeneracy-discriminant and is given by the relation

$$A_0^r = \frac{n}{8\pi g}\left(\frac{ch}{kT}\right)^3,$$

where n is the number of free electrons per unit volume, g the weight factor equal to two for electrons, c the velocity of light, and k and h are Boltzmann's and Planck's constants respectively. The object of this paper is to study the Joule-Thomson effect and adiabatic processes in a relativistic degenerate gas, degenerate in the sense of Fermi-Dirac statistics. In the first section we shall give briefly, in an elementary way and in a form suited to our present purpose, a derivation of the expressions ‡ for $E^r_{deg.}$, $p^r_{deg.}$, etc. (the suffix r in these symbols indicates that the latter refer to the relativistic case) which would be used subsequently in the evaluation of the Joule-Thomson effect discussed in section 2. Section 3 deals with the adiabatic changes occurring in a degenerate gas, and in section 4 the results obtained so far for the limiting states of a Fermi-Dirac gas, with and without [2] the use of relativity mechanics, are compared.

† Communicated by Prof. O. W. Richardson.

‡ These expressions are implicitly contained in the results of investigations of Fowler, Majumdar, and others (see R. H. Fowler, 'Statistical Mechanics, 2nd edition, p. 650; also R. C. Majumdar, *Astro. Nachr.* Dec. 1932, p. 246. They have, however, not been so far explicitly given in the form in which they appear in this paper.

1. *An Elementary Derivation of the Expressions for* $E_{deg.}^{r}$, $p_{deg.}^{r}$ etc.

We know that in the case of degeneracy $A \gg 1$. Now following Sommerfeld [3] we write, if for $A \gg 1$

$$U_\rho = \frac{1}{\Gamma(\rho+1)} \int_0^\infty \frac{u^\rho \, du}{1/A . e^u + 1},$$

then

$$\Gamma(\rho+2)U_\rho = u_0^{\rho+1}\left[1+2\left\{\binom{\rho+1}{2}\frac{2!\,c_2}{u_0^2}+\binom{\rho+1}{4}\frac{4!\,c_4}{u_0^4}+\cdots\right\}\right], \quad \ldots (1)$$

where $u_0 = (\log A)$, the notation

$$\binom{\rho+1}{2} = \frac{(\rho+1).\rho}{2!}, \quad \binom{\rho+1}{4} = \frac{(\rho+1)\rho(\rho-1)(\rho-2)}{4!},$$

and the constants C_2, C_4, etc., are given by the series :—

$$C_\nu = 1 - \frac{1}{2^\nu} + \frac{1}{3^\nu} - \frac{1}{4^\nu} + \cdots$$

Hence

$$U_\rho = \frac{u_0^{\rho+1}}{(\rho+1)\Gamma(\rho+1)}\left[1+2\frac{(\rho+1).\rho}{2!}.\frac{2!}{u_0^2}.\frac{\pi^2}{12}+\cdots\right]$$

$$= \frac{u_0^{\rho+1}}{(\rho+1)\Gamma(\rho+1)}\left[1+(\rho+1).\rho.\frac{\pi^2}{6u_0^2}+\cdots\right]$$

and

$$\int_0^\infty \frac{u^\rho \, du}{1/A . e^u + 1} = \frac{u^{\rho+1}}{\rho+1}\left[1+\frac{\pi^2}{6u_0^2}(\rho+1).\rho\right]. \quad \ldots (2)$$

We then get from equation (16) of Part I.,

$$n = \frac{D}{V}\int_0^\infty \frac{u^2 \, du}{1/A . e^u + 1} = 4\pi g\left(\frac{kT}{ch}\right)^3 \frac{u_0^3}{3}\left(1+\frac{\pi^2}{u_0^2}\right). \quad \ldots (3)$$

(here we have put $\beta = +1$ because, in the case of degeneracy ($A \gg 1$) β cannot be equal to -1, for otherwise the value of $N(\epsilon)d\epsilon$ in the expression (6) of Part I. becomes negative for some values of ϵ), where

$$D = 4\pi g V\left(\frac{kT}{ch}\right)^3 \quad \text{and} \quad u = \frac{\epsilon}{kT},$$

see equation (10), of Part I.

Hence

$$u_0 = \left(\frac{3n}{4\pi g}\right)^{1/3} \frac{ch}{kT}\left(1+\frac{\pi^2}{u_0^2}\right)^{-1/3}$$

$$= \left(\frac{3n}{4\pi g}\right)^{1/3} \frac{ch}{kT}\left[1-\frac{\pi^2}{3}\left\{\frac{ch}{kT}\left(\frac{3n}{4\pi g}\right)^{1/3}\right\}^{-2}\right], \quad . \quad (4)$$

approximately.

If now we put

$$A_0^r = \frac{n}{8\pi g}\left(\frac{ch}{kT}\right)^3,$$

we get

$$u_0 = (6A_0^r)^{1/3}\left[1-\frac{\pi^2}{3}\cdot\frac{1}{(6A_0^r)^{2/3}}\right],$$

or

$$u_0 \equiv \log A = (6A_0^r)^{1/3}\left[1-\frac{\pi^2}{2^2\,3\,.\,3^{5/3}\,.\,A_0^{r\,2/3}}\right]. \quad . \quad (5)$$

When the temperature $T \to 0$, *i. e.*, in the case of complete degeneracy,

$$u_0 = \log A \sim (6A_0^r)^{1/3},$$

and in this case the Fermi-Dirac distribution law shows that all energy states below an energy ϵ^* are completely filled and that above ϵ^* no state is occupied.

$$\epsilon^* = (u_0 kT)_{\text{when } u_0 \to \infty} = ch\left(\frac{3n}{4\pi g}\right)^{1/3}. \quad . \quad . \quad (6)$$

Even when T does not approach zero and the degeneracy is not so complete, still ϵ^* will have a physical significance[4] in that the number of electrons having energy exceeding ϵ^* will bear a very small ratio to the total number of electrons—in fact, this ratio will approximately be $\sim kT/\epsilon^* -$.

Let us now derive an expression for $E^r_{\text{deg.}}$. From equation (17) of Part I., we have

$$E^r_{\text{deg.}} = DkT\int_0^\infty \frac{u^3\,du}{1/A\,.\,e^u+1}$$

(the case of $\beta=-1$ does not occur in a degenerate gas to which only Fermi-Dirac statistics are applicable). Hence from (2) we have

$$E^r_{\text{deg.}} = DkT\,\frac{u_0^4}{4}\left(1+\frac{\pi^2}{6u_0^2}\,.\,4\,.\,3\right). \quad . \quad . \quad . \quad (7)$$

Substituting the value of u_0 from (5) we have. to the approximation we are considering,

$$E^r_{deg.}=V\pi g\left(\frac{kT}{ch}\right)^3 . kT\left(\frac{ch}{kT}\right)^4\left(\frac{3n}{4\pi g}\right)^{4/3}\left[1-\frac{\pi^2}{2^{2/3}.3^{5/3}(A^r_0)^{2/3}}\right]^4 \cdot\left[1+\frac{2\pi^2}{6^{2/3}(A^r_0)^{2/3}}\right],$$

which after a little reduction yields

$$E^r_{deg.}=\pi gV . ch\left(\frac{3n}{4\pi g}\right)^{4/3}\left[1+\frac{2}{3}\frac{\pi^2}{(6A^r_0)^{2/3}}\right]$$

$$=\tfrac{3}{4}chN\left(\frac{3n}{4\pi g}\right)^{1/3}\left[1+\frac{2}{3}\frac{\pi^2}{(6A^r_0)^{2/3}}\right] \quad . \quad . \quad (8)$$

$$=\tfrac{3}{4}\epsilon^*N\left[1+\frac{2}{3}\frac{\pi^2}{(6A^r_0)^{2/3}}\right], \quad . \quad . \quad . \quad . \quad . \quad (9)$$

where ϵ^* is the maximum energy of the Fermi-Dirac distribution. ϵ^* represents the maximum kinetic energy of any electron in an assembly of electron concentration n and at absolute zero of temperature. Similarly,

$$p^r_{deg.}=\frac{1}{3V}\cdot E^r_{deg.}=\frac{\epsilon^* n}{4}\left[1+\frac{2}{3}\frac{\pi^2}{(6A^r_0)^{2/3}}\right]. \quad . \quad (10)$$

2. *Joule-Thomson Effect in a Degenerate Gas.*

We know that the Joule-Thomson effect is given by the expression

$$\Delta T=\frac{T(dV/dT)_p-V}{C_p}\cdot\Delta p, \quad . \quad . \quad . \quad . \quad (11)$$

where ΔT is the fall in temperature of a gas when its pressure is diminished by Δp, and C_p is the specific heat per Avogadro-number (N) at constant pressure. From the relativistic expression (8) for the internal energy of a degenerate gas we get the specific heat per Avogadro number of free electrons at constant volume

$$C_V=\left(\frac{dE^r}{dT}\right)_V=\frac{\pi^2 RkT}{\epsilon^*}=\frac{\pi^2 R}{(6A^r_0)^{1/3}} \quad . \quad . \quad . \quad . \quad (12)$$

As is well known, the difference between the two specific heats of a gas is given by

$$C_p-C_V=T\left(\frac{dp}{dT}\right)_V\left(\frac{dV}{dT}\right)_p \quad . \quad . \quad . \quad . \quad . \quad (13)$$

Now from (10) we get

$$\left(\frac{dp^r}{d\mathrm{T}}\right)_{\mathrm{V}} = \frac{1}{3}\frac{\pi^2 k^2 n \mathrm{T}}{\epsilon^*} = \frac{1}{3}\frac{\pi^2 k n}{(6\mathrm{A}_0^r)^{1/3}} \quad . \quad . \quad . \quad (14)$$

and

$$-\mathrm{V}\left(\frac{dp^r}{d\mathrm{V}}\right)_{\mathrm{T}} = \tfrac{1}{3}\epsilon^* n\left[1+\frac{1}{3}\frac{\pi^2 k^2 \mathrm{T}^2}{\epsilon^{*2}}\right]$$

$$= \frac{nk\mathrm{T}}{3}(6\mathrm{A}_0^r)^{1/3}\left[1+\frac{\pi^2}{3}\cdot\frac{1}{(6\mathrm{A}_0^r)^{2/3}}\right]. \quad (15)$$

Hence

$$\left(\frac{d\mathrm{V}}{d\mathrm{T}}\right)_p = -\frac{(dp^r/d\mathrm{T})_{\mathrm{V}}}{(dp^r/d\mathrm{V})_{\mathrm{T}}} = \frac{\pi^2/(6\mathrm{A}_0^r)^{2/3}}{1+\frac{\pi^2}{3}\cdot\frac{1}{(6\mathrm{A}_0^r)^{2/3}}}\cdot\frac{\mathrm{V}}{\mathrm{T}} \quad . \quad (16)$$

Substituting the values of $\left(\frac{dp^r}{d\mathrm{T}}\right)_{\mathrm{V}}$ and $\left(\frac{d\mathrm{V}}{d\mathrm{T}}\right)_p$ from the above equations in (13), we get

$$\mathrm{C}_p - \mathrm{C}_{\mathrm{V}} = \frac{\pi^2 \mathrm{R}}{(6\mathrm{A}_0^r)^{1/3}}\left[\frac{1}{1+\frac{3}{\pi^2}\frac{1}{(6\mathrm{A}_0^r)^{2/3}}}\right] \quad . \quad . \quad . \quad (17)$$

This equation shows that the difference between C_p and C_{V} for a degenerate gas is very small, since in this case $\mathrm{A}_0^r \gg 1$. This difference becomes smaller and smaller as the degeneracy of the gas (A_0^r) increases. We now have

$$\mathrm{C}_p = \frac{\pi^2 \mathrm{R}}{(6\mathrm{A}_0^r)^{1/3}}\left[1+\frac{\frac{\pi^2}{3(6\mathrm{A}_0^r)^{2/3}}}{1+\frac{\pi^2}{3(6\mathrm{A}_0^r)^{2/3}}}\right] \quad . \quad . \quad . \quad (18)$$

Substituting the values of $(d\mathrm{V}/d\mathrm{T})_p$ and C_p from (16) and (18) respectively in equation (11) we get, after a little algebraical simplification,

$$\Delta\mathrm{T} = -\frac{(6\mathrm{A}_0^r)^{1/3}}{\pi^2 kn}\left[\frac{1-\frac{2}{3}\frac{\pi^2}{(6\mathrm{A}_0^r)^{2/3}}}{1+\frac{2}{3}\frac{\pi^2}{(6\mathrm{A}_0^r)^{2/3}}}\right]\Delta p \quad . \quad . \quad (19)$$

$$\doteq -\frac{(6\mathrm{A}_0^r)^{1/3}}{\pi^2 kn}\Delta p = -\frac{1}{\pi^2 kn}\left(\frac{\epsilon^*}{k\mathrm{T}}\right) \quad . \quad . \quad . \quad (20)$$

Equation (20) clearly shows that during a Joule-Thomson expansion a relativistic degenerate gas is heated (not cooled), and the amount of heating per unit fall of pressure increases as the gas becomes more and more degenerate, *i. e.*, as the value of A_0^r increases.

3. *Adiabatic Changes.*

The relativistic expression for the entropy of a degenerate gas assumes the form

$$S = \frac{R\pi^2 kT}{ch}\left(\frac{4\pi g}{3n}\right)^{1/3}, \quad \ldots \ldots \quad (21)$$

and since entropy remains constant during an adiabatic transformation

$$n^{1/3}/T = \text{constant}.$$

From this it follows that a degenerate gas continues to remain degenerate during any adiabatic change, for the degree of degeneracy is given by

$$A_0^r = \frac{n}{8\pi g}\left(\frac{ch}{kT}\right)^3.$$

The pressure of a relativistic degenerate gas is given by

$$p^r_{\text{deg.}} = \frac{chn}{4}\left(\frac{3n}{4\pi g}\right)^{1/3},$$

and since, as shown above, $n^{1/3}/T$ remains constant during an adiabatic process, we have $(p^r/T^4) = \text{constant}$.

Again we know that in the case of an adiabatic process,

$$T\,dS = dE + p\,dV = 0,$$

and since in the relativistic case we are considering,

$$p^r = \frac{1}{3}\cdot\frac{E^r}{V},$$

we get, by eliminating E from the above two equations,

$$p^r V^{4/3} = \text{constant}.$$

We may note in passing that these adiabatic relations for a degenerate gas come out to be exactly the same as those for a non-degenerate gas discussed in Part I.

4. *A Comparison of the Expressions for the Joule-Thomson Effect in the Limiting States of a Fermi-Dirac gas.*

Joule-Thomson Effect in a Gas.

Non-relativistic [5].

i. The kinetic energy per particle is $<<$ the rest-mass energy mc^2, where m is the mass of the particle and c is the velocity of light.

ii. $$A_0 = \frac{nh^3}{g(2\pi mk\mathrm{T})^{3/2}} = \text{Degeneracy-discriminant},$$

where n is the free electron concentration, g the weight factor ($g=2$ for electrons), T the temperature, m the electron mass, and k and h are Boltzmann's and Planck's constants respectively.

Non-degenerate.

$$\Delta\mathrm{T} = \text{J.T. effect} \doteqdot -\frac{\beta A_0}{2^{5/2}nk}.\Delta p,$$

where $\beta = +1$ or -1 according as the gas obeys F.D. statistics or B.E. statistics.

$$\frac{\Delta\mathrm{T}}{\Delta p} \doteqdot -\frac{\beta h^3}{2^{5/2}g(2\pi m)^{3/2}k^{5/2}\mathrm{T}^{3/2}}.$$

Here the Joule Thomson effect is independent of pressure and vanishes only when $\mathrm{T}\to\infty$.

Degenerate.

$$\Delta\mathrm{T} \doteqdot -\frac{g}{\pi kn}\left(\frac{3A_0}{4\pi}\right)^{2/3}.\Delta p.$$

$$\frac{\Delta\mathrm{T}}{\Delta p} \doteqdot -\frac{3}{8\pi^3}\left(\frac{4\pi}{15}\frac{gh^2}{m}\right)^{1/5}\frac{h^2}{mk^2}\frac{1}{\mathrm{T}p^{1/5}}.$$

$$\frac{(\Delta\mathrm{T}/\Delta p)_{\text{non-deg.}}}{(\Delta\mathrm{T}/\Delta p)_{\text{deg.}}} \doteqdot \frac{\pi^{5/3}}{2^{3/2}.6^{2/3}}.A_0^{1/3}.$$

Relativistic.

i. The kinetic energy per particle is $>>mc^2$.

ii. $$A_0^r = \frac{n}{8\pi g}\left(\frac{ch}{k\mathrm{T}}\right)^3 = \text{Degeneracy-discriminant}.$$

Non-degenerate.

$$\Delta\mathrm{T} = \text{J.T. effect} \doteqdot -\frac{\beta A_0^r}{16kn}.\Delta p,$$

$$\frac{\Delta\mathrm{T}}{\Delta p} \doteqdot -\frac{\beta c^3h^3}{2^7.\pi gk^4\mathrm{T}^3}.$$

Here the Joule-Thomson effect is independent of pressure and vanishes only when $\mathrm{T}\to\infty$.

Degenerate.

$$\Delta\mathrm{T} \doteqdot -\frac{(6A_0^r)^{1/3}}{\pi^2kn}.\Delta p.$$

$$\frac{\Delta\mathrm{T}}{\Delta p} \doteqdot -\frac{1}{2\pi^2}\left(\frac{3ch}{4\pi g}\right)^{1/2}\frac{ch}{k^2}\frac{1}{\mathrm{T}p^{1/2}}.$$

$$\frac{(\Delta\mathrm{T}/\Delta p)_{\text{non-deg.}}}{(\Delta\mathrm{T}/\Delta p)_{\text{deg.}}} \doteqdot \frac{\pi^2}{16.6^{1/3}}.(A_0^r)^{2/3}.$$

My best thanks are due to Prof. O. W. Richardson, D.Sc., F.R.S., for his kind interest and advice in the course of this work.

References.

(1) D. V. Gogate, Phil. Mag. xxv. p. 694 (1938).
(2) D. S. Kothari, Proc. Nat. Inst. Sci. (India), vol. iv. no. 1 (1938).
(3) A Sommerfeld, *Zeits. f. Phys.* vol. xlvii. (1928).
(4) ' Magnetism and Matter,' by E. C. Stoner, 1934 edition, p. 182.
(5) Kothari, *loc. cit.*; Kothari and Srivastava, ' Nature,' vol. cxl. Dec. 1937.

King's College,
London.

XIV. *Band-pass Effect in Wave-filters terminated in Negative Resistances.* *By* S. P. Chakravarti, *M.Sc. (London), D.I.C., A.M.I.E.E., University Lecturer, University of Calcutta* *.

[Received April 28, 1938.]

Summary.

The paper relates to the " band-pass effect " obtained when symmetrical low-pass and high-pass filter sections of simple type are terminated by stable negative resistances of magnitude equal to their maximum characteristic impedances in the transmission band. The cut-off frequencies of the resulting band-pass arrangement depend upon the values of elements in the original filter section.

Amplitude and non-linear distortions are inappreciable in the resulting band-pass arrangement. Effect of increasing the number of original filter sections on the resulting arrangement is to shift the position of the transmission band in the frequency spectrum, to reduce the band-width, and to increase gain in the band.

Since, in addition, gain is obtained in the transmission band, this method of obtaining band-pass arrangement has distinct advantages on account of lower cost, better characteristics, and simpler design over a composite band-pass filter and an associated amplifier to give the same gain in the transmission band.

---

* Communicated by the Author.

1. *Introduction.*

AN ideal wave-filter of purely reactive elements (in series and shunt arms) and non-reactive characteristic impedance (in the transmission band) terminated in its characteristic impedance will produce no attenuation in the transmission band and infinite attenuation at frequencies outside the band. Commercial filters, however, fall short of this ideal, The coils are equivalent to inductances with resistances in series and the condensers to capacitances with resistances in series or parallel to them. In such cases characteristic impedance in the transmission band cannot be regarded as purely non-reactive, and there is some attenuation in the transmission band.

It has been shown elsewhere [12], [13] by the present writer that an electric wave-filter of (more or less) non-reactive characteristic impedance Z_0 in the transmission band, fed from a source of non-reactive impedance Z_0 and terminated in negative resistance $-Z_0$ gives large gain for frequencies in the transmission band instead of attenuation obtained with positive resistance termination. The total insertion loss thus changes into total insertion gain due to large negative reflexion loss obtained on account of negative resistance termination.

The present paper shows that simple types of low-pass and high-pass filter sections when terminated by negative resistances equal in magnitude to their (maximum) characteristic impedances in the transmission band give " band-pass effect " in addition to " gain-effect " already found. Gain-frequency characteristic has been found to be better than that given by a composite band-pass filter, composed of several sections and designed to give sharp cut-offs at the edges and an amplifier. These two effects will enable the designer to obtain band-pass filters by simpler means from low-pass or high-pass filter sections and negative resistance elements at less than half the cost.

2. *Formation and Stability of the Negative Resistance Termination.*

The internal resistance of a screen-grid tube under secondary emission condition in series with positive

resistance has been employed to obtain negative resistance termination. The circuit diagram is shown in fig. 1.

The capacitance C has been used to block the d.c. from flowing into the circuit to which negative resistance may be connected. Its value is large, so that at frequencies involved its impedance can be neglected, and the resultant resistance between T_1 and T_2 may be $R-R_a=-R'$. The choke L is one of large impedance at frequencies involved to prevent alternating currents from taking the parallel path through H.T. battery. Experiments with additional chokes in screen and control-grid connexions have shown that they are unnecessary. The difficulty encountered with negative resistance is the instability of the device.

Fig. 1.

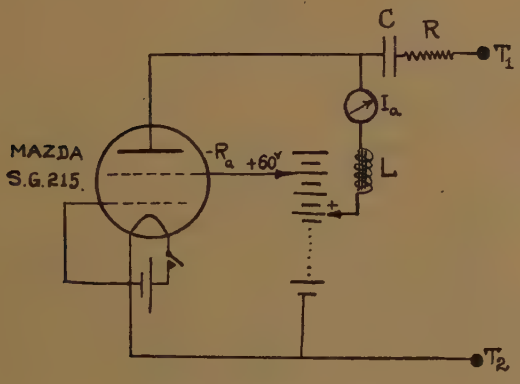

Negative resistance circuit.

Instability of negative resistance can result from the following :—(1) Variation of filament current, plate voltage and screen-grid voltage ; (2) variation of the degree of contamination and mechanical nature of the surface emitting secondary electrons ; and (3) oscillations set up in the negative resistance circuit on switching. Stability studies have been carried on Mazda S.G. 215.

(1) *Variation of Filament Current, Plate Voltage and Screen-grid Voltage.*

Normal filament current and screen-grid voltage of the tube are about 0·22 amperes and 60 volts respectively.

Measurements of V_a and I_a have shown that minimum filament current and screen-grid voltage that can be allowed without appreciably altering the negative resistance portion of the characteristic are 0·21 amperes and 58 volts respectively.

Similarly, the plate voltage can be allowed to fluctuate ± 2 volts between 20–50 volts without appreciably altering the negative resistance portion of the characteristic provided the screen-grid voltage is constant.

(2) *Variation of the Degree of Contamination and Mechanical Nature of the Surface emitting Secondary Electrons.*

The condition and the mechanical nature of the surface emitting secondary electrons can alter with age and use

TABLE I.

($V_s = 60$ volts.)

V_a volts.	I_a (m.a.) for old Mazda S.G. 215.			I_a (m.a.) for new Mazda S.G. 215.		
	0 hour.	4 hours later.	8 hours later.	0 hour.	4 hours later.	8 hours later.
6	1·50	1·43	1·43	1·70	1·65	1·64
10	2·30	2·28	2·27	2·48	2·47	2·45
16	1·54	1·54	1·53	1·80	1·82	1·83
20	1·49	1·475	1·475	1·78	1·80	1·80
30	1·375	1·37	1·365	1·73	1·77	1·77
40	1·30	1·30	1·30	1·70	1·73	1·73
50	1·20	1·20	1·20	1·68	1·70	1·70
60	1·65	1·68	1·66	2·23	2·23	2·23

of the tube. Two Mazda S.G. 215 tubes have been selected for observation—one which has been in use for over eighteen months and another quite new. Observations have been taken at intervals on both these tubes for a considerable length of time with voltages and current strictly the same. Table I. gives typical values recorded during a day at intervals of four hours, power being on all the time in the circuit.

Observations show that between 16–50 volts over the negative portion of the characteristic the stability is sufficiently good for both tubes to justify their use in circuit.

(3) *Oscillation set up in the Negative Resistance Circuit on Switching.*

If the negative resistance circuit be switched on with terminals T_1—T_2 open audible oscillations are set up as observed by a pair of headphones connected to the secondary winding of an observation transformer con-

Fig. 2.

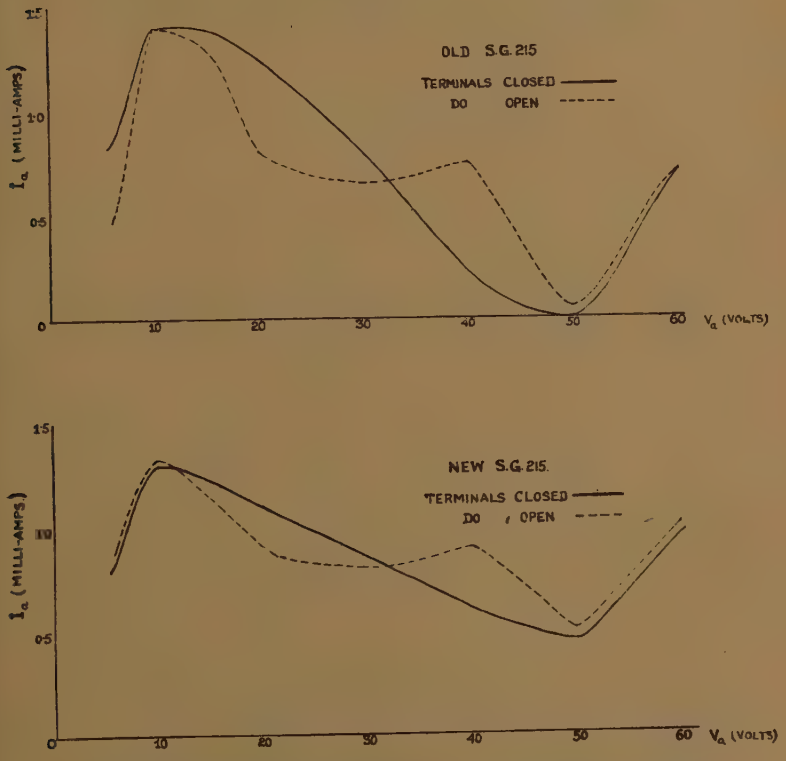

V_a–I_a characteristics under closed and open terminal condition.

nected in series with the choke. This may be due to positive inductance in choke and transformer primary (with stray capacitances) being connected in series with the negative resistance. The effect of this oscillation is to make the negative resistance portion of the characteristic wavy.

It has been found, however, that on closing the terminals

T_1—T_2 by a circuit the oscillations stop and the negative resistance portion of the characteristic becomes almost a straight line, coinciding more or less with the static characteristic. This resulting characteristic has further been found to be independent of the type of network connected across T_1—T_2.

Fig. 2 shows the V_a—I_a characteristics of old and new Mazda S.G. 215 under open and closed terminal conditions. Table II. shows the observations when terminals are closed through various types of circuits and networks.

TABLE II.

(Old Mazda S.G. 215.)

V_a volts.	I_a (m.a.).				
	Terminals open (static characteristic).	Terminals open (with choke in anode circuit).	Terminals closed through high resistance and inductance.	Terminals closed by high-pass filter.	Terminals closed by low-pass filter.
6	1·68	1·44	1·44	1·46	1·44
10	2·40	2·28	2·28	2·30	2·33
16	2·30	1·54	2·30	2·31	2·40
20	2·20	1·475	2·20	2·20	2·30
30	1·67	1·375	1·66	1·70	1·80
40	0·84	1·30	0·79	0·78	0·82
50	0·40	1·20	0·34	0·38	0·40
60	2·18	1·65	1·68	1·66	1·68

3. *Low-pass Filter Section terminated in Negative Resistance.*

Two symmetrical low-pass filter sections of T type (L—total inductance in series and C—total capacitance in shunt) have been used for the experiment. (1) Low-pass filter section (L=14·4 mH., R=12 Ω ; C=1·0 μF.) of cut-off frequency f_c=2·7 KC/S and characteristic impedance (at zero frequency)=120 Ω. (2) Low-pass filter section (L=300 mH., R=272 Ω ; C=·012 μF.) of cut-off frequency f_c=6·6 KC/S and Z_0=4000 Ω.

Transmission loss and gain characteristics measured for positive and negative terminations respectively for two filters are shown in fig. 3.

Filter no. (1) gives a band-pass characteristic for the range 1·0—2·5 KC/S. The sharpness of cut-off at the edges are 8 dB in 0·5 KC/S and 10 dB in 0·5 KC/S respectively.

Filter no. (2) gives a band-pass characteristic for the range 4·1–5·9 KC/S. The sharpness of cut-off at the edges are 4 dB in 0·1 KC/S and 6·5 dB in 0·1 KC/S respectively.

Fig. 3.

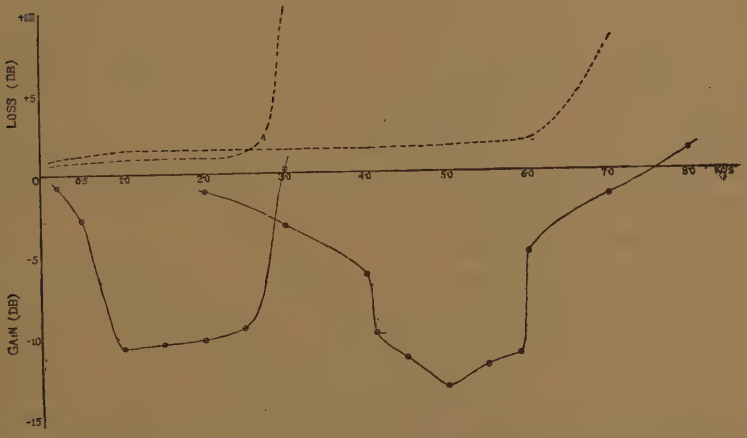

Characteristics of low-pass filters with positive and negative terminations. (With positive termination dotted; with negative termination full curves.)

Amplitude Distortion.

For filter no. (1) gain in the band 1·0–2·5 KC/S varies from —10·7 dB to —9·6 dB. Variations at the extreme frequencies with respect to the geometric mean frequency of 1·5 KC/S are —0·2 and +0·9 dB respectively. It can be said that there is no appreciable amplitude distortion.

For filter no. (2) gain in the band 4·1–5·9 KC/S varies from —13·4 dB to —10 dB. Variations at the extreme frequencies with respect to the geometric mean frequency of 4·9 KC/S are +3·2 and +1·9 dB respectively. Amplitude distortion is still within limits as laid down by the C.C.I.F.

Non-linear Distortion.

Filter no. (2) has been examined for non-linear distortion. Three sets of readings have been taken with input voltages of 0·6, 1·2, and 4·8 volts. Gain characteristics for three cases shown in fig. 4 are almost coincident, thereby indicating that there is no non-linear distortion. Gain is therefore independent of the input voltage.

Fig. 4.

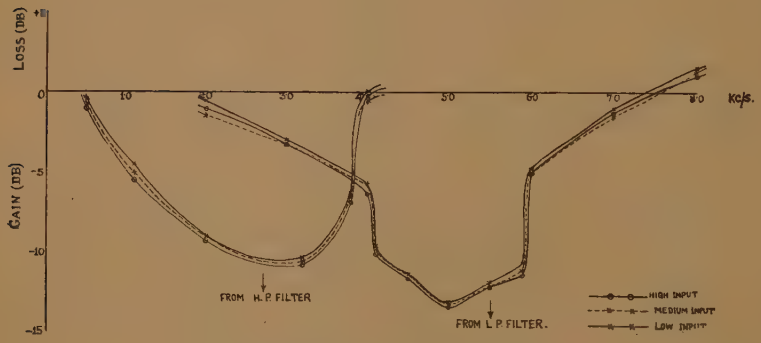

Gain characteristics with different inputs.

4. *High-Pass Filter terminated in Negative Resistance.*

Two symmetrical high-pass filter sections of T type (C—total capacitance in series and L—total inductance in shunt) have been used for the experiment. (1) High-pass filter ($C=0{\cdot}5\,\mu F$.; $L=78{\cdot}9$ *m*H., $R=4\Omega$) of cut-off frequency $f_c=0{\cdot}4$ KC/S and characteristic impedance (at infinite frequency) $Z_0=400\ \Omega$. (2) High-pass filter ($C={\cdot}00025\,\mu F$; $L=90\,\mu H.$, $R=0{\cdot}2\ \Omega$) of $f_c=532$ KC/S and $Z_0=600\ \Omega$.

Transmission characteristics measured for two filters are shown in figs. 5 (*a*) and 5 (*b*) respectively.

Filter no. (1) gives a band-pass characteristic for the range 1·0–3·8 KC/S. The sharpness of cut-off at the edges is 12 dB in 0·8 KC/S and 5·5 dB in 0·1 KC/S respectively.

Filter no. (2) gives a band-pass characteristic for the range 740–769 KC/S. The sharpness of cut-off at the edges are 14 dB in 5 KC/S and 28 dB in 10 KC/S respectively.

Fig. 5 (*a*).

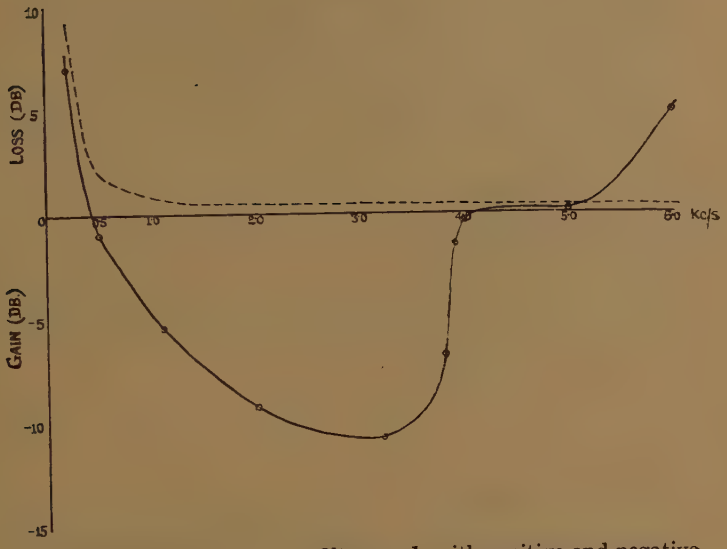

Characteristics of high-pass filter no. 1, with positive and negative terminations.

Fig. 5 (*b*).

Character!stics of high-pass filter no. 2, with positive and negative terminations.

Amplitude Distortion.

For filter no. (1) the gain in the band 1·0–3·8 KC/S varies from −5 dB to −11 dB. Variations at the extreme frequencies with respect to the geometric mean frequency of 1·95 KC/S are +4 and +1·8 dB respectively.

For filter no. (2) the gain varies from 34·6 to 35 dB over a frequency band of 29 KC/S. It can be said in both the cases that there is no appreciable amplitude distortion.

Non-linear Distortion.

Filter no. (1) has been examined for non-linear distortion. Three sets of readings have been taken with

Fig. 6.

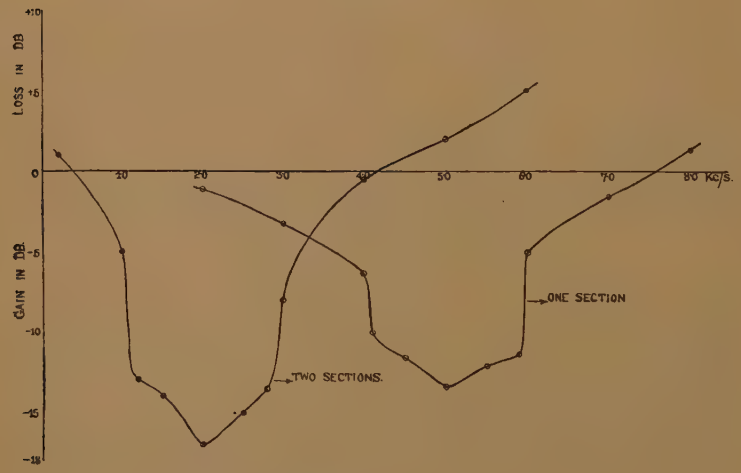

Effect of increasing the number of sections.

input voltages of 0·6, 1·2, and 4·8 volts. Characteristics for all three cases shown in fig. 4 appear to be almost coincident, indicating that there is no non-linear distortion. Gain is therefore independent of the input voltage in this case also.

5. *Effect of a number of Sections.*

The low-pass filter no. (2) in section 3 has been used for this experiment. Gain characteristics for one and two sections are shown in fig. 6. Effect of increased number

of sections is (1) to increase the gain in the transmission band of the resulting band-pass arrangement; (2) to decrease the width of the transmission band; and (3) to lower the value of cut-off frequencies.

Table III. shows the results of observation in the present case.

TABLE III.

No. of sections.	Variation of gain in transmission band.	Width of transmission band.	Cut-off frequencies.
One....	−10 to −13·2 dB	4·1–5·9 KC/S (1·8 KC/S)	4·1 and 5·9 KC/S
Two ...	−13 to −17 dB	1·2–2·8 KC/S (1·6 KC/S)	1·2 and 2·8 KC/S

6. *Results.*

The experiments described above have given the following results :—

(1) A symmetrical low-pass or high-pass filter section of simple type of cut-off frequency "f_c" when terminated by a negative resistance of magnitude equal to maximum value of characteristic impedance in the transmission band gives a "band-pass characteristic" of sharpness to the extent of 6·5 dB in 100 c.p.s. at the edges.

(2) The cut-off frequencies of the resulting band-pass arrangement depend on the values of elements composing the original filter section.

(3) A gain of −10 to −32 decibels has been obtained by using the same tube for negative resistance element with various filter sections.

(4) Amplitude and non-linear distortions are inappreciable in the resulting band-pass arrangement.

(5) Effect of increasing the number of sections has been (*a*) to reduce the band-width obtained from a single section; (*b*) to shift the transmission band lower and higher in the frequency spectrum for low-pass and high-pass sections respectively; and (*c*) to increase the gain in the transmission band.

7. *Application of the effect on design of Band-pass Filters.*

The results obtained above are of great value in designing band-pass filters. It is much easier first to design a low-pass filter section of the type considered, and then to obtain the band-pass characteristic by terminating it with the proper negative resistance. A specific case

Fig. 7.

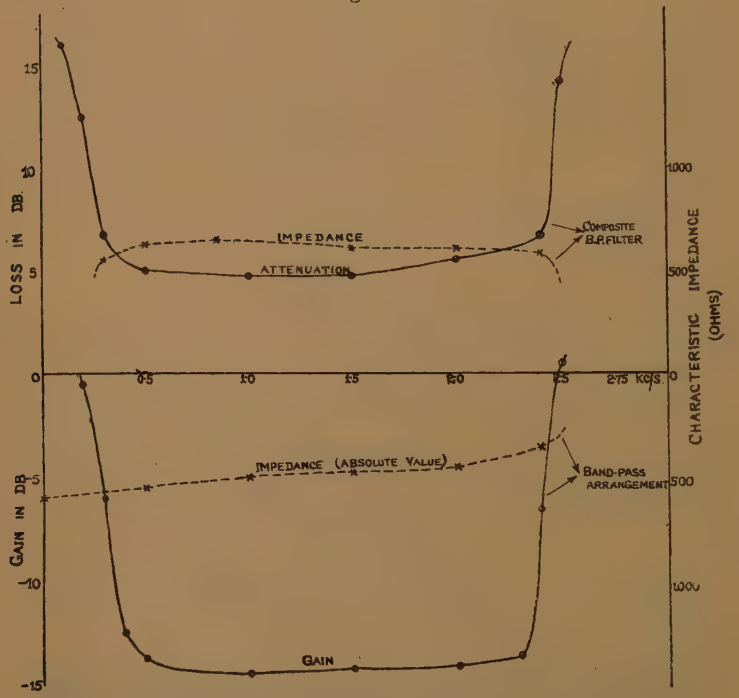

Characteristics of composite B.P. filter and band-pass arrangement.

of the design of a band-pass filter by this and the usual method has been taken to compare characteristics and cost.

Suppose it is desired to design a band-pass filter having cut-off frequencies of 0·3 and 2·4 KC/S and characteristic impedance at mid-frequency of 600 ohms.

(1) *Using "band-pass effect."*

First design a low-pass filter section of cut-off frequency 3 KC/S, say, and characteristic impedance 600 ohms.

Total inductance in series arm works out to be 63·7 millihenries and total capacitance in shunt arm 0·2 microfarads for each section. Two sections of this filter are taken. Three coils required (31·8, 63·7, and 31·8 millihenries) were made air-core coils.

The sections are then terminated by a negative resistance of −600 ohms to obtain gain-frequency characteristic as shown in fig. 7. The cut-off frequencies are observed to be 0·4 and 2·3 KC/S, and there is obtained a uniform gain of about 14 decibels in the transmission band.

Fig. 8.

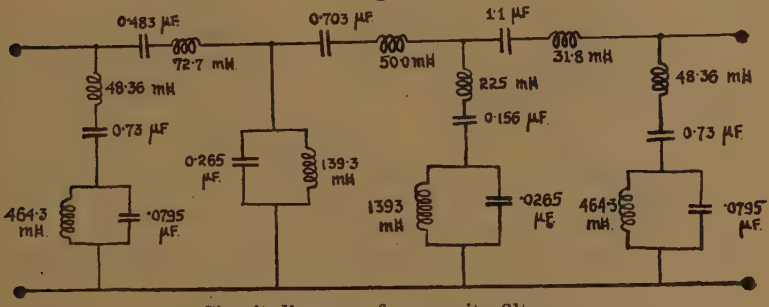

Circuit diagram of composite filter.

(2) *By usual method of designing a composite band-pass filter.*

The composite structure consists of (*a*) the prototype section ($m=1$), (*b*) a m-derived section $m=0{\cdot}1$, and (*c*) two half m-derived sections when $m=0{\cdot}6$. The circuit designed is shown in fig. 8.

In order to build this filter ten capacitance and ten inductance elements are required. Twenty-one mica condensers have been used to give ten capacitance elements. Four coils of lower inductance values (31·8, 48·4, 50, and 72·7 millihenries) have been made air-core multilayer coils, and four others of higher value have been made single layer toroidal coils on stalloy stampings.

The measured transmission loss in the transmission band is about 5 dB, as shown in fig. 7. In order to introduce a gain of 14 to 15 dB a two-stage amplifier, giving roughly a uniform gain of 20 dB in the transmission band, has been inserted. In addition to the difficulties of designing the composite filter and auxiliary amplifier, cost in this case is over twice that in the writer's

method, leaving aside cost of low-tension and high-tension batteries, which are the same in both cases. Table IV. shows the various items required and cost in both cases.

TABLE IV.

By usual method and amplifier.	By " band-pass effect."
(1) Mica condensers—21.	(1) Mica condensers—2.
(2) Coils (air-core)—5.	(2) Coils (air-core)—3.
,, (stalloy stamping core)—5.	
(3) Two-stage amplifier.	(3) Negative resistance element.
Tubes—2.	Screen-grid tube—1.
Blocking condenser—1.	Choke—1.
Anode resistance—1.	Blocking condenser—1.
Leak resistance—1.	Positive resistance spool—1.
Output transformer—1.	
Total cost.. £7 14*s.* 0*d.*	Total cost.. £3 8*s.* 0*d.*

References.

(1) A. W. Hull, " Dynatron—A Tube possessing Negative Resistance." Proc. Inst. R. E. vi. (5 February, 1918).
(2) J. Scott-Taggart, 'Radio Review,' xi. p. 598 (1921).
(3) A. C. Bartlett, " Boucherot's Constant Current Networks and their Relation to Electric Wave Filter," J. I. E. E. lxv. p. 373 (1927).
(4) Van der Pol, " A new Transformation in Alternating Current Theory and an Application to the Theory of Audition," Proc. I. R. E. xviii. p. 221 (February 1930).
(5) Hajime Ilinuma, " A Method of Measuring the Radio-frequency Resistance of an Oscillatory Circuit," Proc. I. R. E. xviii. p. 537 (March 1930).
(6) C. E. Worthen, " The Dynatron," ' General Radio Experimenter ' (4 May, 1930).
(7) L. C. Verman, " Negative Circuit Constants," Proc. I. R. E. (April 1931).
(8) George Crisson, " Negative Impedances and the Twin 21-Type Repeater," B. S. T. J. (July 1931).
(9) L. C. Verman, " Transients in Negative Constant Series Circuits," J. Ind. Inst. Sc. (1932).
(10) H. S. Black, " Stabilized Feedback Amplifiers," B. S. T. J. (January 1934).
(11) S. Cabot, " Resistance Tuning," Proc. I. R. E. (June 1934).
(12) S. P. Chakravarti, " Voltage Amplification by Electric Wave Filters terminated in Negative Resistances," Proc. Indian Academy of Science (1934).
(13) S. P. Chakravarti, " Sur les Filtres se terminant par des resistances negatives," *L'Onde Electrique* (March 1936).
(14) S. P. Chakravarti, " On Negative Resistance Equalizers for Telephone Transmission System," Phil. Mag. xxiii. (May 1937).

Kanodia Electrical Communication
Engineering Laboratories,
University of Calcutta.

XV. *Note on the Oxidation of the Arc Cathode.* By Prof. F. H. Newman, *D.Sc., F.Inst.P., University College, Exeter* *.

[Received May 25, 1938.]

Suits and Hocker † have recently pointed out that an oxide film on the cathode of arcs in the atmospheric pressure range may play an important part in the arc mechanism. Their results indicate that it is impossible to strike an arc between copper or silver electrodes in hydrogen or nitrogen provided that the gas is quite free from oxygen. Their interpretation of these results is that the cathode cannot supply sufficient emission without an oxide mechanism.

Doan and Myer ‡ had found previously that an arc between very pure iron electrodes in argon, rigorously purified, could not strike even with moderate potentials, and suggested that the normal arc discharge depends upon the presence of chemically active atoms or molecules either in the gas or on the electrodes.

Doan and Thorne § also investigated arcs in pure inert gases between electrodes of pure metals. Their experiments showed that such arcs are impossible to maintain under ordinary conditions, whereas they are easy to maintain if the gas is slightly contaminated. For highly purified iron in argon, helium, and neon, and highly purified silver and zinc in argon, the arc discharge is inherently unstable, the cathode spot darting rapidly up and down the electrode, and finally disappearing under conditions at which a stable arc is ordinarily obtained when slightly less pure elements are used.

In previous work the author ‖ has shown that the existence of films on the electrodes plays an important part in the striking and maintenance of an arc at very low gaseous pressures. The technique employed differs from that used by the other workers in that, while they actually brought the two electrodes into contact in order to strike the arc, the author started the arc by passing a momentary discharge across one of the arc electrodes

* Communicated by the Author.
† Phys. Rev. liii. p. 670 (1938).
‡ Phys. Rev. xl. p. 36 (1932).
§ Phys. Rev. xlvi. p. 49 (1934).
‖ Phil. Mag. ii. p. 796 (1926); vi. pp. 807 & 811 (1928); vii. p. 1085 (1929); xiv. pp. 712–718 (1932).

and a third one, the potential difference across the two arc electrodes being applied while this discharge passed. With patches of various fused salts, *e. g.*, potash, soda, sodium chloride, and sodium carbonate, on the ends of iron electrodes the arc struck readily and consistently in air at very low pressures, whereas when the ends of the electrodes were completely covered with an oxide film it was impossible to start the arc. If the oxide film were removed the arc could be produced. On the other hand, when pure tungsten electrodes were used it was extremely difficult to strike and maintain the arc, but by fusing a little salt on the ends of the electrodes the arc was readily produced and maintained.

The experiments of Suits and Hocker confirm these results. The author attributed his results to the existence of cathode spots rather than to a complete film on the cathode. Electrons are freed from these spots and produce ionization which is localized near the spots. Due to the high mobilities of the electrons a dense space-charge results which increases the electric field near the active spots and consequently the number of electrons emitted therefrom. This process is cumulative and proceeds rapidly until the field at the spot increases sufficiently to produce field electrons from the cathode, and an arc results.

XVI. *Notices respecting New Books.*

Fundamental Principles of Quantum Mechanics. By E. C. Kemble. [Pp. 611+xviii.] (McGraw Hill Publishing Co., Ltd. Price 36*s.* 0*d.* net.)

IN compiling this volume the author has borne in mind the requirements of graduate students of physics, and the introduction of basic mathematical notions is always accompanied by suitable applications of the theory. Readers will appreciate the attempt which has been made to give a treatment possessed of some rigour and yet to avoid tedious complexity. In starred sections and appendices appear those portions of the subject which may well be omitted on first reading.

Discussions of the dualistic theory of matter and the relations between classical and wave mechanics are followed by

a chapter devoted to mathematical theory, and by succeeding chapters on the two-particle central field problem and the many-particle problem. Dynamical variables, commutation rules, matrix theory, and the theory of perturbations are then considered, and the methods are exemplified by applications. The concluding chapters deal with quantum statistical mechanics and problems of atomic structure.

This book will be welcomed by prospective research students for its comprehensive account of fundamental ideas in modern quantum theory, and by experienced research workers as a useful book of reference.

Procedures and Metaphysics. By Edward W. Strong. (University of California Press. Price 11*s.* 6*d.*)

Professor Strong calls this very learned work "a Study in the Philosophy of Mathematical-Physical Science in the Sixteenth and Seventeenth Centuries." In two respects this sub-title is slightly misleading. First, the historical survey really stops before the middle of the seventeenth century with the great figure of Galileo. There is no mention of so great a mathematical genius as Pascal, and though there is a page together with some incidental references to Descartes such a perfunctory treatment of the chief modern influence in the "mathematicising" of philosophy would be grotesque if the sub-title were to be taken literally. And, in the second place, it is really the author's purpose to show that the mathematical-physical science of what he aptly enough calls the "early modern" period did not, in fact, involve a "Philosophy" at all in the sense maintained, for instance, by Professor Burtt in his book 'The Metaphysical Foundations of Modern Physical Science,' against the argument of which Professor Strong's discussion is, in fact, mainly directed

It is Burtt's contention that the profound difference between the world-view of mediæval and of modern thought is to be explained in terms of a change in the "metaphysical foundations accepted by the great pioneers of modern physical science." The Aristotelianism which dominated the middle ages came to be replaced by a view of the universe as fundamentally geometrical in structure, which was in essence derived from the tradition of Pythagorean and Platonist philosophy. Thus, of Galileo, Burtt wrote (the quotation is given by Strong): "The Neo-Platonic background of the mathematical and astronomical development of the time has strongly penetrated the mind of the Italian scientist, as in the case of so many lesser figures." Strong's book may be called an extended and adverse comment upon this sentence, in which he seeks to show that both in the greater and in the

lesser figures of Renaissance science there was far less " penetration " by metaphysical presuppositions than Burtt's view implies. Metaphysical tradition then and since has been largely irrelevant to Science, which has always had its own " operational autonomy," and adopts conceptions and procedures (mathematical, metrical, geometrical) because of their methodological efficacy rather than because they are corollaries of any metaphysic or cosmology.

After a general statement of his problem and point of view, the author proceeds to give an account of how the mathematical tradition in the ancient world became, in the hands of the Neo-Platonists and their successors, a sort of " numerological mysticism," in which numbers assumed a status and a significance that has, or had, very little to do with the requirements of science. The Platonic tradition really—though the author does not put in in this way—prostituted mathematics rather than advanced it. I do not feel that there is here a clear enough distinction drawn between the genuine scientific spirit of Platonism and the far less scientific tradition of the later neo-Platonists. Did not Renaissance science perhaps owe more to the former than is here admitted, while certainly being totally opposed to the spirit of the latter ?

The author gives detailed and most erudite summaries of the scientific ideas of the Italian mathematicians of the sixteenth century, of Tartaglia and Cardan and Cataneo, as well as of others. Then he turns to mechanical science in the precursors of Kepler and Galileo, and then to these two great figures themselves. The last chapter deals with " the metamathematical tradition in the early-modern period " (Ficino, Pico, Reuchlin, Zamberti, Domenico, Henrion, and John Dee). The conclusion he draws from his wide and laborious survey reinforce those of his earlier chapters. " To suit a metaphysical purpose, mathematics was thrown into a status and assigned a rôle divorced from mathematical conception and meaningless for procedure . . . Modern mathematical-physical science established its method and achieved its results in spite of, rather than because of, this kind of metamathematical tradition " (p. 217). His final paragraph gives a very wholesome admonition addressed to ourselves, his contemporaries, that we should be wary of assuming too readily that the conclusions of physical science either substantiate or are dependent upon the metaphysical doctrines with which they may seem to have a clear affinity.

It may, perhaps, be questioned whether Professor Strong has not in some degree overstated his case. Probably " metaphysical " ideas neither are so irrelevant to the working scientist as he seems to maintain (and as many scientists

would certainly agree with him in maintaining) nor yet form the " basis " of the scientist's procedures to the extent sometimes assumed, especially by philosophers. But whether or no the author's argument is wholly conclusive at every point, there can be no question that he has given us a most interesting as well as a most erudite piece of criticism, which will be of the greatest value to students of sixteenth and seventeenth century science.

Introduction to the Theory of Fourier Integrals. By E. C. Titchmarsh. [Pp. 390.] (Humphrey Milford: Oxford University Press. Price 17*s.* 6*d.*)

Only during the last decade has the Fourier Integral come to be regarded as a first-class weapon in the higher flights of pure mathematics. Professor Titchmarsh was doubtless one of the first to realize its powers, and, judging by the careful production of this volume, he has also realized the neglect from which the subject has suffered in the past and the serious need of a book upon the Fourier Integral written from the point of view of the mathematical analyst. He has clearly set himself the task of exhibiting the analytical substance of the very wide range of application of these integrals. This has been done before, but never from the point of view of pure mathematics and with full analytical rigour. The result is a book monumental in character and yet eminently readable.

The work assumes no previous knowledge of the Fourier Integral, though, as the author says in his preface, an acquaintance with Fourier's Series is demanded of the reader. The outlook in which the book is framed certainly assumes a knowledge of the processes of mathematical analysis and an analytical interest. Nevertheless the work is never allowed to become a mass of general theory, the structure of the theory is never obscured by the demands of rigorous argument, and heaviness of treatment is avoided by frequent excursions into particular matters.

The opening chapters develop the Fourier Integral theory up to that concerning the class L^p, a considerable degree of variety being happily achieved by dealing with special topics on the way—Mellin's Integrals, Poisson's Formula, Hermite's Polynomials, to name a few. Chapters upon Hilbert Transforms and uniqueness theorems follow. After a well-chosen set of applications and examples the book proceeds to the higher levels of general transforms, self-reciprocal functions and integral equations, and at the end comes a most comprehensive bibliography, naming papers and memoirs from all sources, both pure and applied.

The author has wisely excluded the most recent developments of the Fourier Transform (Wiener's amongst them), which have taken place in the field of pure mathematics His book is encyclopedic as it stands, for it collects together a vast body of important material, and presents it for the first time in a truly systematic manner. The book is a complete foundation for study of the more recent and more advanced type of work. The author must be well satisfied with his achievement.

The printing and arrangement of the work is of the excellent kind to be expected from Oxford.

The Fine Structure of Matter.—Part I. *X-Rays and the Structure of Matter.* By C. H. Douglas Clark. [Pp. lxxii+216.] (London : Chapman and Hall, 1937. Price 15*s.* net.)

This volume, though in a sense complete in itself, forms one section only of a comprehensive treatise on atomic and molecular structure, the first volume of which, serving as a general introduction to the work, has already appeared. The present work is the first section of the second volume, and is devoted to a discussion of crystal and allied structures as determined by methods of X-ray diffraction. After a brief introduction on space-lattices in general, the work is mainly a summary of facts. The author seems to have made it his aim to make at least a passing reference to every structure of importance which has been determined by X-ray analysis, and has succeeded in compressing an immense amount of information into an incredibly short space. Brevity, however, has not led to any lack of clarity, and many excellent diagrams assist the understanding of the various types of structure described. A research worker about to enter this field of investigation will find it profitable to read the book through from cover to cover. As a work of reference it is almost indispensable. The text is supplemented by unusually extensive lists of references to original sources, and excellent indices make it comparatively easy to find any required piece of information. Dr. Clark may be congratulated on the completion of another stage in an arduous, but valuable, compilation.

[*The Editors do not hold themselves responsible for the views expressed by their correspondents.*]

THE

LONDON, EDINBURGH, AND DUBLIN

PHILOSOPHICAL MAGAZINE

AND

JOURNAL OF SCIENCE.

[SEVENTH SERIES.]

AUGUST 1938.

XVII. *The Mechanism of Synchronization in the Linear Time Base.*

By G. F. HERRENDEN HARKER, *M.A.*, *University College, Cardiff* *.

[Received April 26, 1938.]

THOUGH the thyratron time base is well known the property upon which its usefulness so largely depends—its aptitude for synchronization—has received much less detailed discussion.

This short note is devoted to a general consideration of this important aspect of the problem.

1. The simplest version of the fundamental circuit competent to provide a time base of adequate amplitude, linearity, and frequency response is illustrated in fig. 1. It consists of a diode D, working under voltage saturation conditions, in the anode circuit of which is interposed a condenser of appropriate capacity, C, and, in parallel with this, a thyratron G in association with a suitable protective series resistance R. These two branches function alternately, the thyratron behaving as an infinite resistance while the condenser is being charged, and providing a conducting path when the condenser discharges.

* Communicated by the Author.

The thyratron is a hot cathode triode of special design, containing mercury vapour, or an inert gas, at a suitable low pressure, which becomes conducting, as a result of cumulative ionization, only when its anode potential reaches a certain critical value, which, in turn, is determined by the potential setting of its grid. Thus, for example, it is not until the grid voltage attains the value $-V_g$, or the anode voltage has reached the value $+KV_g$, that cancellation of the repulsive field at the cathode permits ionization to occur. The factor K, which is a constant characteristic of the thyratron, termed its grid control ratio, may have a value between 10 and 20. The discharge through the thyratron being luminous,

Fig. 1.

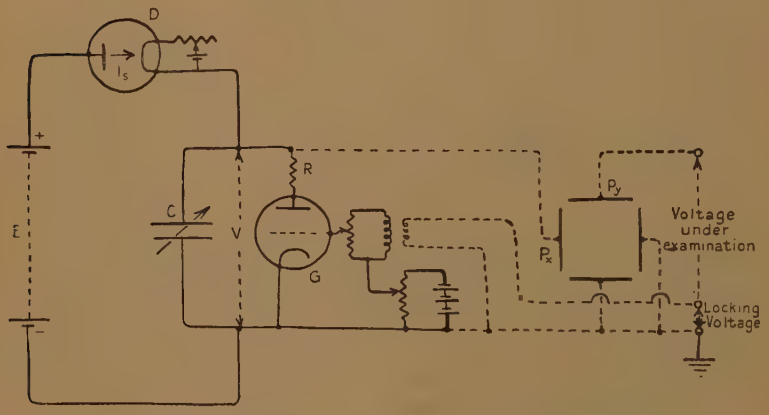

this critical anode potential, KV_g, is usually referred to as its ignition voltage *.

The grid is only competent to serve as control element during the predischarge stage. The positive ions, which are generated as soon as ionization sets in, nullify the space charge and render the grid completely ineffective. The interval between the instant at which the grid surrenders control and that at which the anode current

* This definition of the grid control ratio, due to A. W. Hull (' General Electric Review,' xxxii. p. 390, 1929), implies that the linear portion of the plot of positive anode voltage against negative grid voltage that will just allow current to start would, if produced, pass through the origin. This is confirmed experimentally for the type of thyratron under consideration in which the grid effectively envelops the cathode, though it does not necessarily hold for all other types.

assumes its full value is very short—of the order of two microseconds. Not unless the anode voltage falls to a limiting extinction value, and not until a sufficient interval has elapsed to allow the ions present to disperse, can the grid again take charge. The time needed to reduce the potential applied across the thyratron from its ignition to its extinction value is governed by the effective resistance of the discharge path, which is practically that of the safety resistance R. By cutting down the latter this time can be decreased, though it cannot usefully be made shorter than the deionization time, which is between 10 and 100 microseconds, since the correspondingly increased discharge current would materially lessen the life of the thyratron. Subject to this proviso both the ignition and extinction voltages are definite and stable as long as a condition of temperature equilibrium is maintained. The former is the more sensitive to temperature fluctuations, and the latter has a value ranging from 15 to 20 volts for the mercury vapour thyratrons normally employed in the present connexion. Moreover, in view of the fact that the former can be predetermined by an appropriate selection of the negative grid bias (imposed by means of the potentiometer arrangement indicated in fig. 1), the difference between these two critical voltages admits of considerable variation.

2. Provided the temperature of the diode filament is kept constant and the steady battery voltage, E, is sufficiently high to ensure that voltage excursions throughout the ignition–extinction range of the thyratron do not bring the point of functioning on the diode characteristic outside the region of saturation, the space-charge current traversing the diode will remain independent of V. In the predischarge stage, when the conduction across the thyratron is negligible, this constant current, I_s, will, accordingly, charge up the condenser at a uniform rate and cause the difference of potential between its plates to rise linearly with time. The time occupied in increasing this difference of potential from V_0, the thyratron extinction voltage, to V_1, its ignition voltage, will be given by

$$_cT=\frac{C}{I_s}(V_1-V_0).$$

But, in virtue of the circuit connexions, this potential difference is applied between the anode and cathode

of the thyratron, and, as soon as its value has risen to V_1, the thyratron starts to discharge. This discharge will be localized in the condenser–thyratron loop, in which the charged condenser constitutes the sole source of energy. As E consistently exceeds V, the valve action of the diode will block any inverse circulation of the discharge current through the main branch of the circuit, though it is still possible for the charging current to traverse the thyratron in its conducting state. However, if the effective resistance, R, opposing the discharge is reasonably small, so that I_s is insignificant in comparison with V/R, the time taken for the difference of potential to fall to V_0 will be given, to a sufficiently close approximation, by

$$_dT = RC \ln \frac{V_1}{V_0} *.$$

It will be observed that both these expressions depend essentially on time constants, $_cT$ on that pertaining to the charging circuit, $_dT$ on that characterizing the discharge circuit.

Provided $_dT$ exceeds the small, but finite, deionization time the thyratron will become non-conducting, and again subject to grid control, by the time V has fallen to V_0. The charging phase then recommences, and the alternation between it and the discharging phase continues, the complete period, T, being equal to $_cT + _dT$.

The parameters V_0, V_1, and C occur in the expressions for both $_cT$ and $_dT$, while of the remaining pair I_s enters into that for $_cT$ alone and R into that for $_dT$ alone. Of the former set V_0 is fixed, but, as V_1 and C are chiefly employed for varying the period, $_cT$ and $_dT$ are normally interdependent, though $_cT$ is usually, and preferably, large in comparison with $_dT$. Thus, if we take as typical figures $V_0 = 20$ volts, $V_1 = 100$ volts, $I_s = 5 \times 10^{-3}$ amp., $R = 100$ ohms, and assume the thyratron is designed to pass a maximum discharge current of 1 amp., in comparison with which I_s is certainly small,

$$_cT = \frac{C}{5 \times 10^{-3}} \cdot 80 = 1{\cdot}6 \times 10^4 \, C$$

* The complete expression is

$$_dT = RC \ln \frac{V_1 - RI_s}{V_0 - RI_s}.$$

and $$_dT = 100\ C \ln \frac{100}{20} = 1{\cdot}6 \times 10^2\ C.$$

The fly-back ratio $\frac{_cT}{_dT}$, being 100, the main portion of the period will be occupied in charging the condenser and only the small remainder in discharging it.

Now this type of recurrent cycle drawing its energy supply from a direct current source, having an amplitude defined in terms of an upper critical voltage initiating a discharge and a lower critical voltage terminating it, and a period specified by the parameters defining the time constants appropriate to the respective circuits involved in the charging and discharging phases, is characteristic of a relaxation oscillation.

Fig. 2.

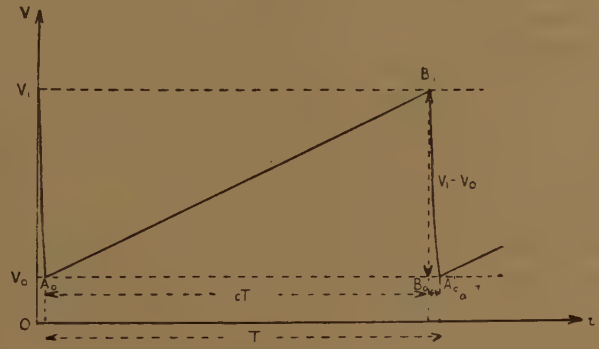

The wave profile of the relaxation oscillation under consideration will be of the " saw tooth " form depicted in fig. 2. Allocation of the rate of charging of the condenser, by assigning definite values to C and I_g, fixes the slope of the line $A_0\ B_1$, and the intersection of the line itself with the horizontal line drawn at the ignition voltage level V_1 determines not only the amplitude, B_0B_1, but also the period, A_0A_0', of the relaxation oscillation when the value of R is specified. V_0, as has been pointed out, does not admit of variation, but V_1, being equal to KV_g, depends upon the bias voltage imposed on the grid of the thyratron, and the value allotted to V_1 will obviously influence the amplitude as well as the

period of the relaxation oscillation. Thus, reducing V_1 will decrease the amplitude, B_0B_1, and, by proportionately diminishing both A_0B_0 and B_0A_0', shorten the period A_0A_0'; and *vice versa*.

If V_1 is kept constant the effect of variations in C and I_s will be confined exclusively to the period, and, if R is invariable, it may be noted that when the slope of the charging line is controlled by varying C the fly-back ratio $\left(\frac{A_0B_0}{B_0A_0'}\right.$ in fig. 2$\left.\right)$ remains constant, whereas control by means of I_s alters ${}_cT$, leaving ${}_dT$ unchanged, and thus modifies the fly-back ratio. A change in the capacity of the condenser, in fact, affects the time constants of both the charge and discharge circuits in the same proportion, whereas a change in the charging current affects the former alone.

It has also been pointed out that the deionization time imposes a lower limit on the permissible value of ${}_dT$, and so indirectly determines the minimum period and maximum frequency at which the thyratron time base can profitably be operated. This upper frequency limit lies between 5000 and 10,000 sec.$^{-1}$, though it can only be reached at the cost of a certain contraction in amplitude and some sacrifice of stability.

To ensure stable functioning at much higher frequencies recourse must be had to time base circuits incorporating hard valves.

3. The linear time base circuit is coupled up to the cathode ray tube in the manner indicated in fig. 1, so that the voltage variations developed across the condenser are applied across one pair of the oscillograph plates. The luminous spot, resulting from the impact of the focused beam of cathode rays on the fluorescent target, is thus made to travel across the viewing screen at a uniform speed in one direction, occupying an interval ${}_cT$, and to fly back much faster in the reverse direction in the interval ${}_dT$. On account of this high return velocity of the electron beam the return track is very faint in comparison with the forward sweep. As the vertical pair of plates is normally chosen for this purpose the forward and return strokes will (in the absence of any voltage across the horizontal pair of plates) be superposed and horizontal.

The length of this base line varies as the voltage amplitude of the corresponding relaxation oscillation, and depends also on the stiffness of the cathode ray beam. Thus, for example, if $K=10$ and $V_g=-10$ volts, so that $V_1=100$ volts, then, taking $V_0=20$ volts, so that $V_1-V_0=80$ volts, and the electrostatic deflexion sensitivity of the cathode ray tube as 1 mm. per volt, the length of the base line on the screen will be 8 cm. Similarly when $V_g=-11$ volts, $V_1=110$ volts, the voltage amplitude of the time base relaxation oscillation will be 90, and the base line length 9 cm.; while if $V_g=-9$ volts, $V_1=90$ volts, the voltage amplitude of the time base relaxation oscillation will be 70, and the base line length 7 cm.

To employ the apparatus depicted in fig. 1 to delineate on the fluorescent screen the displacement time curve characterizing some particular periodic phenomenon, the latter, translated into corresponding voltage variations of appropriate amplitude by some suitable means, is applied across the horizontal pair of oscillograph plates. The electron beam will then be subjected to the joint action of the stated voltages simultaneously imposed across the two mutually perpendicular pairs of electrostatic deflecting plates.

As, however, the frequency of the linear time base will not, except by chance, coincide with that of the periodic phenomenon under investigation, or with any integral submultiple thereof, successive forward sweeps of the tracing beam will, in general, commence at different points on the cycle representative of the phenomenon. This progressive phase shift will cause the trace to drift bodily from left to right or from right to left across the viewing screen, the rate of drift depending on the extent of departure from integral relationship.

The ability to hold the pattern stationary on the screen, obviously convenient for visual study and practically indispensable for photographic recording, is rendered possible by the extent to which, and the ease with which, the time base frequency can be controlled by the operator. Alteration of a single parameter in the time base circuit (that most conveniently accessible being the capacity of the condenser) will usually suffice to bring the frequency of its relaxation oscillations into coincidence with the fundamental frequency of the periodic phenomenon.

Failing this, any necessary final adjustment can be carried out by means of the diode filament rheostat.

Successive traces will then be accurately superimposed, and their resultant repetition will delineate on the screen very nearly one complete cycle of the phenomenon against the linear portion of the time base cycle, the remainder being accomplished during the much more rapid non-linear fly-back, and only faintly visible on that account.

When the fundamental frequency, η, of the phenomenon in question exceeds the upper frequency limit, $N_{max.}$, that can be handled satisfactorily by the time base, the frequency, N, of the latter can be set equal to η/p (where p is an integer), in which case (as long as $\eta/p < N_{max.}$) $p-1$ complete periods and the major part of the succeeding period of the phenomenon will appear immobilized along the same length of the linear time axis, provided the requisite adjustment in the frequency of the time base has been made independently of its amplitude.

This frequency demultiplication, which is a characteristic property of a relaxation oscillator, can thus be turned to practical account in the study on the oscillograph of phenomena whose fundamental frequencies lie considerably above those which could otherwise be dealt with. It supplies what is virtually the equivalent of an upward extension of the frequency limit with which the time base can cope.

4. Manual adjustment of the time base frequency can only be relied upon temporarily to hold the pattern stationary when the two voltages applied across the oscillograph plates are completely independent, unless the frequencies of both can be maintained rigorously constant.

Synchronization can, however, be rendered automatic without any very exacting restrictions as to frequency uniformity, or any very precise preliminary tuning, by the simple expedient of feeding back a fraction of the voltage developed by this periodic phenomenon to the relaxation oscillator furnishing the time base. This may be accomplished, as indicated in fig. 1, by electromagnetic linkage between adjacent portions of the respective circuits. The control is particularly sensitive if the voltage variations picked up in this way are applied

to the grid of the thyratron (already suitably biassed to furnish a base line of appropriate length), where an amplitude of a volt, or under, usually serves to lock the time base in step provided its frequency has been roughly tuned to that of the fundamental, or some selected sub-harmonic, of the periodic phenomenon under investigation. As it is preferable to employ the minimum degree of interaction consistent with synchronization, the amplitude of this subsidiary voltage is arranged to be varied by means of the potentiometer shown.

Let us now consider how this synchronization is brought about. Assume, for simplicity, that the voltage fed back to the grid is given by $v \sin \frac{2\pi t}{\tau}$, where τ represents the period of the phenomenon to be recorded against the linear time base on the oscillograph screen. Then if, in the absence of this auxiliary voltage, the thyratron grid bias is set at $-V_g$, this auxiliary voltage will, when present, cause the grid bias to vary sinusoidally with time between the extreme values $-(V_g-v)$ and $-(V_g+v)$ with period τ.

But, as we have seen, it is permissible to imagine this periodic voltage variation transferred from the grid to the anode of the thyratron provided its period is conserved, its phase reversed, and its amplitude multiplied by the grid control ratio, K. In other words, assuming its grid voltage to be given by $-\left(V_g - v \sin \frac{2\pi t}{\tau}\right)$, the corresponding ignition voltage will be given by $V_1 = K\left(V_g - v \sin \frac{2\pi t}{\tau}\right)$.

We can, therefore, confine our attention exclusively to the anode, and regard the ignition voltage of the thyratron as varying sinusoidally between the extreme values $K(V_g-v)$ and $K(V_g+v)$ with the same period τ, in the manner indicated in fig. 3. Thus, using the previous data, and taking $v=1$ volt, $K(V_g-v)=90$ volts, while $K(V_g+v)=110$ volts.

The firing of the thyratron will no longer be restricted to the single voltage level, $K V_g$, defined by the static grid bias, $-V_g$, but can now take place within a belt bounded by a pair of voltage levels, symmetrically situated with respect to the mean ignition voltage KV_g,

and separated by double the amplitude, Kv, of the periodic variation imposed on the anode.

Assuming the rate of rise of potential $\left(\frac{dV}{dt} = \frac{I_s}{C}\right)$ between the terminals of the condenser in the time base unit to be fixed, we can, using the previous data and assuming successive discharges of the thyratron to be all initiated at exactly the assigned voltage level, calculate the relaxation period corresponding to any value of V_1 between the above limits $K(V_g+v)$ and $K(V_g-v)$.

Thus, for example (Table, p. 203).

Fig. 3.

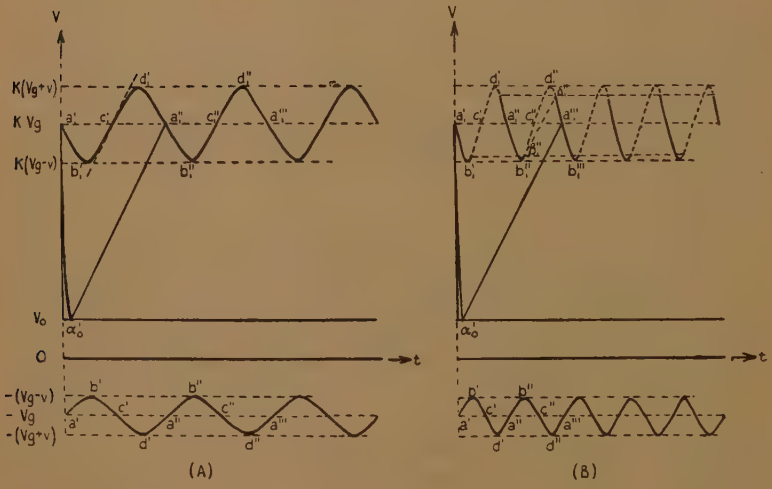

Obviously, if the amplitude of the periodic variation imposed on V_1 is increased the resulting extension of the firing zone will permit of the accommodation of a still wider range of relaxation periods.

Conversely, having plotted V_1 against T, it will be possible to read off from the graph the value of V_1 corresponding to any prescribed value of T.

5. Now suppose the value of the forcing period, τ, is such that some integral multiple of it, say $p\tau$, satisfies the inequality $T_{max.} > p\tau > T_{min.}$. It follows from the above that an ignition voltage V_1 can be found, such that $V_{1\,max.} > V_1 > V_{1\,min.}$, corresponding to which T_{v_1} will have

V_1 (volts).	Voltage amplitude of relaxation oscillation ($=V_1-V_0$).	Length of time base on screen (cm.) *.	Duration of discharge $\left({}_dT=100\ln\frac{V_1}{V_0}C\right)$.	Duration of charge $\left({}_cT=\frac{V_1-V_0}{5\times10^{-3}}C\right)$.	T ($={}_cT+{}_dT$).	Period (secs.) when $C=1$ *mfd.*
110 (V_1 max.) ..	90	9	$0{\cdot}17\times10^3$ C.	18×10^3 C.	$18{\cdot}17\times10^3$ C.	$18{\cdot}17\times10^{-3}$ ($T_{max.}$).
100 ($\bar{V}_1$)	80	8	$0{\cdot}16\times10^3$ C.	16×10^3 C.	$16{\cdot}16\times10^3$ C.	$16{\cdot}16\times10^{-3}$ ($\bar{T}$).
90 (V_1 min.) ..	70	7	$0{\cdot}15\times10^3$ C.	14×10^3 C.	$14{\cdot}15\times10^3$ C.	$14{\cdot}15\times10^{-3}$ ($T_{min.}$).

* Assuming an electrostatic deflexion sensitivity of 1 mm. per volt.

precisely the value $p\tau$. It turns out to be the special attribute of a relaxation oscillator that, when such a forcing oscillation is imposed on one of the factors determining its period, and this period happens to approximate to some integral multiple of the forcing period, the period of the relaxation oscillator is capable of assuming automatically a value which coincides exactly with this particular multiple of the forcing period. It is in virtue of this property that a relaxation oscillator can be locked into synchronism, not only with the applied forcing frequency, but also with the several members of the set of integral submultiples thereof, or, if it is permissible so to phrase it, with its various subharmonic undertones.

Once the appropriate phase relation has been secured between the relaxation oscillation and the feed-back forcing oscillation to allow successive discharges of the thyratron always to occur at this particular voltage level V_1, locking of these two oscillations in synchronism is manifestly possible. Assuming that interlocking does actually follow, a stationary pattern, comprising almost exactly p complete cycles of the periodic phenomenon, will appear on the viewing screen. The point on the cycle at which recording commences will be determined by the phase relation that must be established as a prelude to synchronization.

The existence of a theoretically feasible interlocking level does not, however, necessarily imply that it is practically realizable. The slope of the line $\alpha_0' a_1''$ in fig. 3 A (or $\alpha_0' a_1'''$ in fig. 3 B), representing the building up of the potential across the condenser with time, is given by $\frac{I_s}{C}$, and is constant as long as neither of the two parameters involved is altered. The slope of the tangent to the sinusoid, representing the manner in which the thyratron ignition voltage varies with time, is given by

$$\frac{dV_1}{dt} = -\frac{2\pi K v}{\tau} \cos \frac{2\pi t}{\tau},$$

which likewise varies with t/τ, increasing from zero at b_1' $\left(\frac{t}{\tau} = \frac{1}{4}\right)$ to $\frac{2\pi K v}{\tau}$ at c_1' $\left(\frac{t}{\tau} = \frac{1}{2}\right)$, subsequently decreasing to zero again at $d_1'\left(\frac{t}{\tau} = \frac{3}{4}\right)$. The line representing the

rise in voltage across the condenser can only intersect the sinusoid defining the ignition voltage of the thyratron throughout its whole arc when $\frac{I_s}{C} > \frac{2\pi K v}{\tau}$. This applies to the case illustrated in fig. 3 A, where we suppose $p=1$ and $\tau=16{\cdot}16\times10^{-3}$ sec., so that

$$\frac{I_s}{C} = \frac{5\times10^{-3}}{1\times10^{-6}} = 5\times10^{3},$$

while $$\frac{2\pi K v}{\tau} = \frac{2\pi.10.1}{16{\cdot}16\times10^{-3}} = 3{\cdot}9\times10^{3}.$$

If, however, instead of the single cycle of the periodic phenomenon that would be delineated along the length of the linear time base in fig. 3 A we arrange matters so that two cycles are inscribed along the same time base length, by taking $\tau' = \frac{\tau}{2} = \frac{16.16}{2} \times10^{-3}$ sec., the conditions obtaining will be as illustrated in fig. 3 B. Here the maximum slope of the tangent to the sinusoid, given by $2\frac{2\pi K v}{\tau} = 7{\cdot}8\times10^{3}$, is greater than $\frac{I_s}{C}$. Hence if we draw, parallel to the charging line $\alpha_0' a_1'''$, a line touching the sinusoid at β_1'' just past the trough b_1'' on its ascending arc $b_1'' c_1'' d_1''$, this line will intersect the sinusoid somewhat beyond the crest d_1'' in the point δ_1'' on its descending arc $d_1'' a_1''' b_1'''$. Interlocking will clearly be precluded at all points above this line, *i. e.*, throughout the arc $\beta_1'' c_1'' d_1'' \delta_1''$ shown dotted in fig. 3 B.

The extent of the arc of the sinusoid over which interlocking is prohibited will obviously increase with the number of cycles of the periodic phenomenon recorded along the length of the linear time base.

6. We have been assuming in the above that the period, or some multiple of the period, of the phenomenon under investigation coincides with the period of the time base when successive firings of the thyratron occur at the mean ignition level V_1, and that the two are so intercoupled that the initial firing of the thyratron takes place as the descending arc of the sinusoid crosses this mean ignition level.

As, however, even over the available sections of the sinusoid, it will not normally prove possible to couple up the relaxation oscillation in precisely the proper phase relation to the feed-back forcing oscillation, an interval of transition must, in general, precede synchronization.

Suppose, for example, that $p=1$ and $\tau=15\times10^{-3}$ sec., so that, since $\overline{T}>p\tau>T_{min.}$, the interlocking level will be located below the mean ignition voltage level $\overline{V}_1$ (its actual value V_1 being 94·2 volts), and suppose further that, at the instant of intercoupling (arbitrarily reckoned as the

Fig. 4.

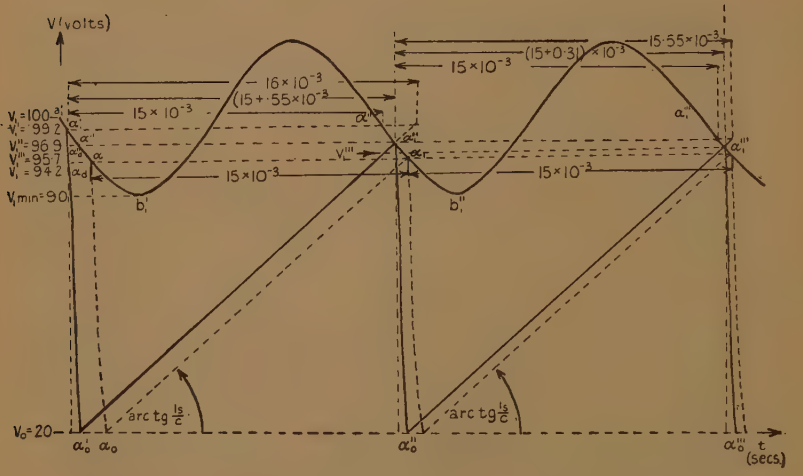

origin of time), the thyratron fires just as the descending arc of the sinusoid crosses the voltage level V_1', corresponding to which the natural period, $T_{v_1'}$, of the time base would be 16×10^{-3} sec. It is clear then from fig. 4 that, when the descending arc of the sinusoid next crosses the level V_1' (at the epoch 15×10^{-3} sec.), the potential across the condenser will still be below V_1', so that the second firing of the thyratron will be postponed until the charging line intersects the firing curve at the lower voltage level V_1'' at an interval after the first firing which is greater than τ and less than $T_{v_1'}$.

Let the V_1'', V_1 voltage levels intersect the consecutive descending arcs $a_1'\,b_1'$, $a_1''\,b_1''$ of the firing curve in

α'', α_1'' and α, α_1 respectively. Further, let these same voltage levels intersect the descending arc which represents the discharge through the thyratron initiated at α_1' and terminating at α_0' in α_d'', α_d respectively. Then the descending arc $\alpha\alpha_0$, representing a discharge through the thyratron initiated at α and terminating at α_0, will run parallel to the portion $\alpha_d\alpha_0'$ of the descending discharge arc $\alpha_1'\,\alpha_0'$. Hence if α lies to the right of α_d, α_0 will lie to the right of α_0', *i. e.*, the discharge from α will terminate at a later epoch than that from α_1' (the interval being represented, on the abscissa time scale, by $\alpha_0'\alpha_0$). But since the lines representing the subsequent charging up of the condenser run parallel to one another, $\alpha_0'\,\alpha_1''$ will lie above $\alpha_0\alpha_1$, so that the second firing will take place at a level V_1'' which, since $V_1'>V_1''>V_1$, will be intermediate between the first firing and interlocking levels.

This is what happens in the example illustrated in fig. 4. The equation denoting the discharge initiated at α_1' being given approximately by $V_1=V_1'\exp.\left(-\frac{t}{RC}\right)$, the slope of the tangent to the corresponding curve at α_1' will be $\left(\frac{dV}{dt}\right)_{t=0}=-\frac{V_1'}{RC}$, and its value $-\frac{99{\cdot}2}{10^2.10^{-6}}$, *i. e.*, $-99{\cdot}2\times10^4$. The slope of the tangent to the descending arc of the sinusoid at this same point can be written $-\frac{2\pi Kv}{\tau}\lambda'$, the value of which (since $1>\lambda'>0$)* cannot exceed $-\frac{2\pi 10.1}{15\times10^{-3}}.1$, *i. e.*, $-4{\cdot}2\times10^3$. It will be apparent, therefore, that the firing arc $\alpha_1'\,b_1'$ must lie consistently to the right of the discharge arc $\alpha_1'\,\alpha_0'$.

It is not difficult to calculate the voltage levels at which the successive firings of the thyratron occur. The first firing level being $V_1'=99{\cdot}2$ volts, the second is $V_1''=96{\cdot}9$ volts, and is therefore, as already stated, such that $V_1'>V_1''>V_1$, while the interval between the first and second firing is $15{\cdot}55\times10^{-3}$ sec. The third firing level is $V_1'''=95{\cdot}7$ volts, again such that $V_1''>V_1'''>V_1$, while the interval between the second and third firings is $15{\cdot}31\times10^{-3}$ sec., and so on.

* The value of λ' is actually 0·997.

It may be noted that the interval between the first and second firing must approximate very closely to the time base relaxation period appropriate to the second firing level, since the difference between them is represented by the difference in the times of discharge from these two firing levels, which will be given by $RC \ln \frac{V_1'}{V_1''}$ and have the value $10^{-4} \ln \frac{99{\cdot}2}{96{\cdot}9}$, *i. e.*, $0{\cdot}002_3 \times 10^{-3}$ sec. Moreover, as the difference in voltage between consecutive firing levels diminishes progressively as the interlocking level is approached, so also will the magnitude of this interval steadily decrease.

Thus, subject to the condition stated and starting from a voltage level V_1' ($>V_1$) the interlocking level V_1 will be approached asymptotically from above. Similarly, starting from a voltage level V_2' ($<V_1$) the interlocking level V_1 will be approached asymptotically from below.

After a comparatively few periods have elapsed the approximation to the interlocking level can, for all practical purposes, be deemed complete.

If under these circumstances some chance perturbation should cause the thyratron to fire above the interlocking level (*i. e.*, slightly prematurely), it will next fire at a lower level, located between the previous firing and the interlocking level; while if the chance perturbation causes the thyratron to fire below the interlocking level (*i. e.*, a trifle late) it will next fire at a higher level, likewise located between the previous firing and the interlocking level.

But when any small stray disturbance of a system in the vicinity of a prescribed regime of functioning brings into operation conditions which result in a reversion of the system to its predisturbed state, the prescribed regime is one of stable equilibrium. This criterion being respected, it follows that synchronization, once established, will persist.

The more nearly comparable the slopes of the respective tangents to the discharge curve and the firing curve at the point of firing the more rapidly will the consecutive firing levels converge on the interlocking level. The initial slope of the discharge curve is fixed for a specified firing level, while that of the firing curve at this same level

will depend upon the character of the periodic variation imposed on V_1, which need not necessarily be sinusoidal. Even assuming the latter still to be sinusoidal its slope can be increased p-fold by the inclusion of p-cycles of the periodic phenomenon along the length of the time base. It is apparent, however, that not until p is of the order of 240 will the slopes of the two tangents become equal, thus introducing an element of indetermination into the problem, so that all practically useful values of p will be definitely subcritical as long as the periodic variation imposed on V_1 remains sinusoidal.

The same is likely to be true of the majority of the non-sinusoidal wave profiles encountered in practice which admit of Fourier resolution into a finite number of component terms. The descending arc α_1' α_0' of the discharge curve would, in fact, only be likely to pass through, or lie to the left of, α if the discharge time were considerably prolonged and the fly-back ratio unduly reduced.

7. The ideas developed above enable an interpretation to be given of certain observations familiar to those who have had occasion to employ the cathode ray oscillograph for the delineation of wave profiles.

Let us assume that the voltage applied across the horizontal plates consists of the suitably amplified output from a pure tone oscillator, and suppose that, under the particular operating conditions in force and as a consequence of the feed-back of a fixed fraction of this periodic voltage to the thyratron grid, a stationary pattern comprising p-cycles, or its effective equivalent, is visible on the viewing screen.

Without modifying the time base parameters in any way, let the period of the sinusoidal oscillation be increased, keeping its amplitude constant. In order to preserve the p-cycle stationary pattern the period of the time base relaxation oscillation must automatically lengthen to conform with the variation imposed on the feed-back forcing period. The requisite adjustment of the relaxation period necessitates a rise in the interlocking voltage level, which, in turn, results in an increase in the relaxation amplitude and leads to a corresponding expansion of the base length along which these p-cycles are inscribed.

More often than not a definite limit will be imposed

on the continued rise of the locking level in response to a progressive increase in the forcing period, owing to the existence of a portion of the sinusoidal arc over which interlocking is prohibited for the reason already given. If, when this upper available locking level is reached, it happens that the lowest permissible locking level is so located that the corresponding relaxation period, $T_{min.}$, is equal to, or less than, $(p-1)\tau$, an abrupt transition will occur, the p-cycle stationary pattern giving place to a $(p-1)$-cycle stationary pattern delineated along a correspondingly contracted base length. Should $T_{min.}$ be greater than $(p-1)\tau$ the pattern on the screen will "run wild" until τ has been sufficiently increased to convert this condition of inequality into one of equality, when interlocking will become possible for a pattern including $(p-1)$-cycles.

It has been tacitly assumed so far that only a single integral value of p can be found to satisfy the essential condition upon which the existence of an interlocking level depends, namely, $T_{max.} > p\tau > T_{min.}$. Should it happen that p and τ can be so chosen that $T_{max.} > p\tau$, while $(p-1)\tau > T_{min.}$, two interlocking levels will be theoretically possible. Thus, again reverting to our original data and taking $\tau = 3 \times 10^{-3}$ sec., $T_{max.}$ $(= 18{\cdot}17 \times 10^{-3}$ sec.$) > (6).3 \times 10^{-3}$ sec. and $(6-1).3 \times 10^{-3}$ sec. $> T_{min.}$ $(= 14{\cdot}15 \times 10^{-3}$ sec.$)$. Here, therefore, in addition to the interlocking level at $V_1 = 94{\cdot}2$ volts, already discussed, the possibility of another interlocking level above the mean ignition voltage level arises for consideration, and this, corresponding to a relaxation period of 18×10^{-3} sec., would occur between 109·1 and 109·2 volts. Since it is, in point of fact, situated upon the prohibited portion of the arc of the sinusoid, this latter level will be unrealizable in practice. The actual presence of such supernumerary locking levels is, however, by no means always ruled out by this criterion.

These considerations are illustrated diagrammatically in fig. 5. Fig. 5 A represents a close approximation to the lower limit for a stationary pattern comprising three cycles of the phenomenon concerned. In fig. 5 B the forcing period has been increased to the upper limit for which a stable three-cycle pattern is possible. In fig. 5 C the forcing period has been still further increased, resulting in a stationary pattern comprising two cycles of the periodic

phenomenon under investigation. In order to restore the three-cycle pattern along the same length of base the time base parameters would need to be so altered as to give the charging line the gentler gradient indicated by the dotted line. The appearances on the viewing screen (shown in the adjacent circles) correspond to the connexions in fig. 1, on the assumption that the target end of the cathode-ray tube is located in front of the plane of the diagram.

Fig. 5.

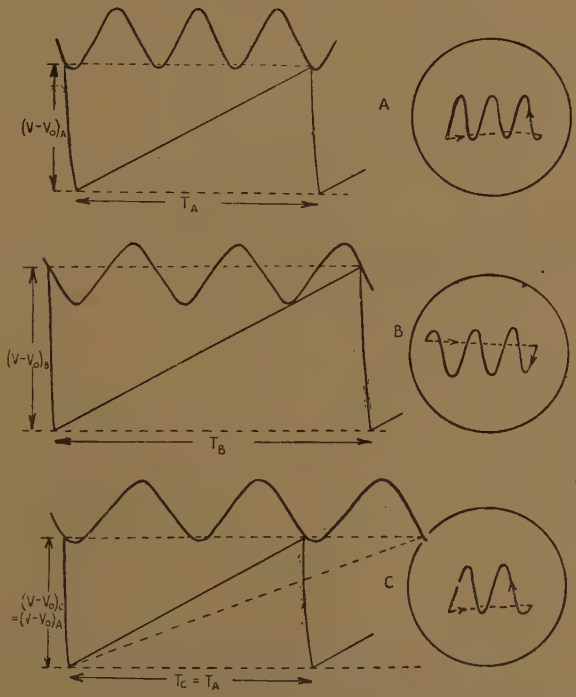

The direction in which the spot traverses the sinusoid is indicated by the arrow on the trace, while the fly-back is shown dotted. The location of the right-hand edge of the pattern, corresponding to the thyratron extinction voltage, is more or less fixed, that of the left-hand edge, corresponding to the thyratron ignition voltage, is variable, their separation being proportional to $V_1 - V_0$.

It is fascinating to observe the manner in which the extremities of the visible arc move up as the applied

period is slowly increased, the pattern meantime experiencing a shift and undergoing an expansion in a horizontal direction towards the right, this being succeeded, either at once or after an interval of instability, by a pattern from which one cycle has been lopped off. The progressive reduction in the rise permitted to the extremities of the visible arc as the number of cycles under observation is augmented (which follows as a consequence of the fact, already alluded to, that as p increases the arc of exclusion occupies a proportionately larger fraction of the whole arc of the sinusoid) is likewise evident even on cursory examination.

Fig. 6.

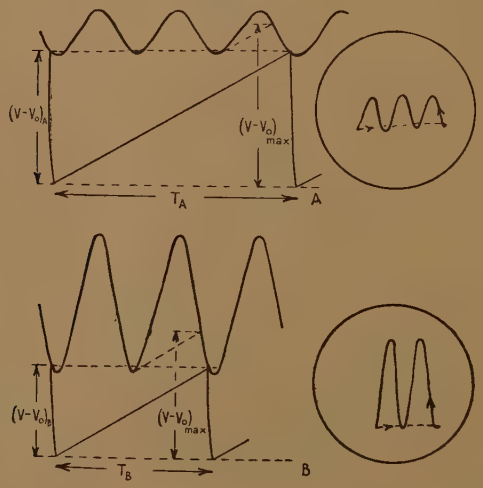

Still without altering the time base parameters, suppose now that, keeping the period of the oscillation furnished by the pure tone oscillator fixed, its amplitude is progressively increased by means of the volume control on the amplifier. An effect analogous to the above is obtained in that, starting from the extreme left of the pattern, one after another of the cycles visible on the screen is suppressed until only a solitary cycle survives. The manner in which this is brought about, and the shortening of the base line length which accompanies it, is sufficiently obvious from a diagram. Fig. 6 A corresponds to a

reasonably small amplitude and fig. 6 B to a fairly large one. As before, the appearances on the viewing screen are represented in the adjacent circles.

An alternative manner of securing an equivalent result consists in tightening up the coupling, which in effect feeds back to the grid of the thyratron a larger fraction of the fixed input voltage instead of applying to it a fixed fraction of an increased input voltage. The only difference is that, since the amplitude of the deflecting voltage is fixed, so also will be the amplitude of the trace on the viewing screen.

I wish to take this opportunity of thanking Dr. J. H. Shaxby for his kindness in reading through the above in manuscript.

XVIII. *X-ray Analysis of the Structure of Anthraquinone.*

By Bhagawati Charan Guha, *Professor of Physics, Midnapore College, Midnapore, Bengal* *.

[Received October 5, 1937.]

Introduction.

IN a previous paper † K. Banerjee and the author determined the space group of anthraquinone crystal. In the present communication the arrangements of the atoms in the crystal lattice will be discussed. In the above-mentioned paper it was found that the anthraquinone molecule does not possess any symmetry, and so we are to determine the positions of fourteen carbon atoms and two oxygen atoms, *i. e.*, forty-eight unknown parameters. This apparently shows the complicated nature of the problem ; but, in view of the structure of anthracene as determined by K. Banerjee ‡, and later confirmed by the Fourier analysis method by Robertson §, we may make a beginning by assuming that, similar to anthracene, the carbon skeleton of anthraquinone has also a plane structure with regular hexagons, and then by trial we can find the correct orientation of the molecule in the lattice as well as any distortion that might be present.

* Communicated by the Author.
† K. Banerjee and B. C. Guha, Ind. J. Phys. ix. pt. iii. p. 287 (1934).
‡ K. Banerjee, Ind. J. Phys. iv. pt, vii. p. 557.
§ J. M. Robertson, Proc. Roy. Soc. A, cxl. p. 79 (1933).

Robertson * found in the case of the simpler compound of benzoquinone, that the benzene ring was appreciably distorted from a regular hexagon. The double bonds are shorter than the single bonds, the length being 1·32 Å. and 1·5 Å. respectively. The internal ring angle between the single carbon bonds is 109° and between double and single bonds 125° approximately. The C=O distance is 1·14 Å., and the oxygen atoms are placed symmetrically with respect to the carbon ring. The chemical viewpoint, that the benzene ring in benzoquinone has four single bonds in fixed positions, is thus substantiated.

Fig. 1.

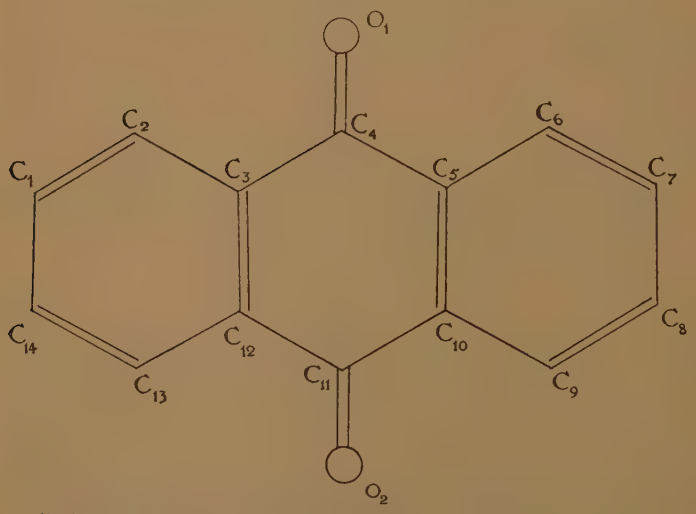

Carbo-oxygen skeleton of anthraquinone molecule, showing the chemical bonds.

Such a fixing up of bonds occurs also in anthraquinone (fig. 1); but here in the two outer rings the alternate bonds are double and single. So a difference might arise, and it is not possible to say *à priori* whether there is any distortion in the anthracene skeleton in anthraquinone similar to the benzene ring in benzoquinone.

Crystal Data—Space Group.

Anthraquinone, having the chemical formula $C_{14}H_8O_2$, belongs to the orthorhombic class. Needle-shaped crystals

* J. M. Robertson, Proc. Roy. Soc. A, cl. p. 106 (1935).

elongated along the *c*-axis, were obtained from benzene. The (110), (011), and (001) faces are generally well-developed. The axial ratios are given in Groth's 'Chemische Krystallographie':—$a : b : c = 0{\cdot}8004 : 1 : 0{\cdot}1607$. The melting-point is 273° C. The space group was found to be D_{2h}^{13} *Pmmn*. The unit cell, having the dimension $a = 19{\cdot}7$ Å., $b = 24{\cdot}6$ Å., and C = 3·95 Å., contains eight molecules. The volume of the unit cell is 1914 Å^3., the density, as calculated from X-ray data, is 1·434, which is approximately the same as the upper limit to the range of the values (1·419–1·438) mentioned by Groth.

Experimental.

Well-developed tiny crystals were mounted on the goniometric head of an oscillation camera with high dispersion in order to avoid overlapping of the spots. Photographs about the "*b*" and "*c*" axes were taken with range of oscillation of 10°. The small crystal was completely immersed in the X-ray beam during the exposures. Care was taken to give the same time of exposure in each photograph, and the films were developed under conditions as far identical as possible, viz., as regards the strength of the developing and fixing baths, their temperature, and duration of developing and fixing. The intensities of the X-ray beam could not, however, be kept absolutely constant, but for estimates of intensity this variation, as well as that due to variations of sensitivities of different films, were neglected. The spots were identified in the usual way after Bernal, and classified under different categories according to the intensity of reflexion.

Analysis of the Structure by Trial.

For the determination of the atomic parameters the method of trial and error was adopted. Two atomic structure factor curves—one for the aromatic carbon (fig. 2) and the other for oxygen (fig. 3)—from the data given in Table I. were drawn.

The atomic structure factors for different planes were obtained from these two curves. Regarding the atomic structure factors for carbon, the values which are adopted are those given by Robertson * for aromatic hydrocarbons

* J. M. Robertson, Proc. Roy. Soc. A, cxl. p. 79 (1933).

based on his measurements on anthracene. For the atomic structure factor of oxygen the values are taken from Wollan's * paper on magnesium oxide. Robertson †, in his work on benzoquinone, assumed that the structure factor of oxygen was proportional to the corresponding values for aromatic carbon atoms for equal scattering angles ; but the assumption seems to be too artificial,

Fig. 2.

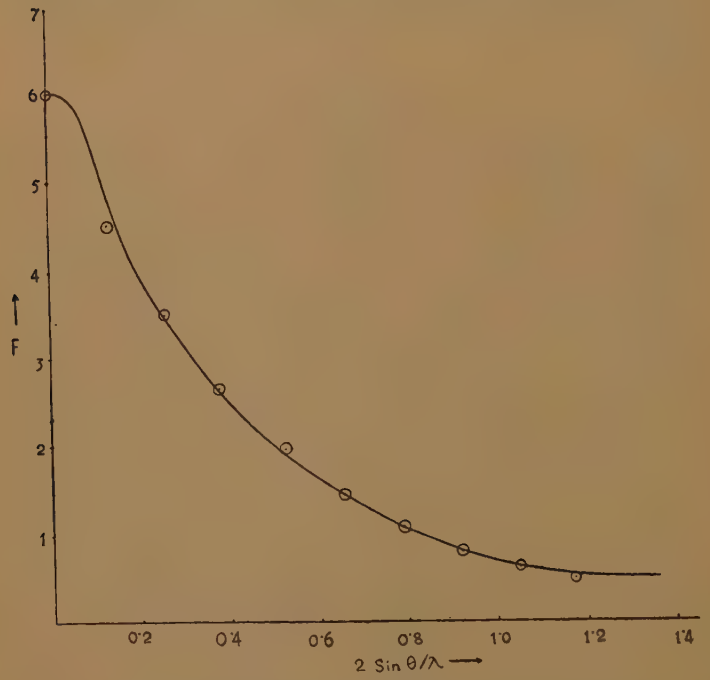

Atomic structure factor curve for aromatic carbon.

and hence Wollan's experimental values have been adopted here.

For the trials a molecule was supposed to be placed parallel to the "*ab*" face, with centre having the parameters $\frac{1}{4}$, $\frac{1}{8}$, and 0, the positions of the other seven molecules being obtained from the equivalent positions ‡ corre-

* E. C. Wollan, Phys. Rev. xxxv. p. 1019 (1930).
† J. M. Robertson, Proc. Roy. Soc. A, cl. p. 106 (1935).
‡ W. A. G. Wycoff, 'Analytical Expressions of the Theory of Space Groups,' p. 64.

sponding to the space group D_{2h}^{13} P*mmn*. Different tilts and displacements were then tried for the first molecule. The best agreement was obtained when the plane of this molecule was tilted by 6° about all the three axes x, y, and z. The centre of this molecule was

Fig. 3.

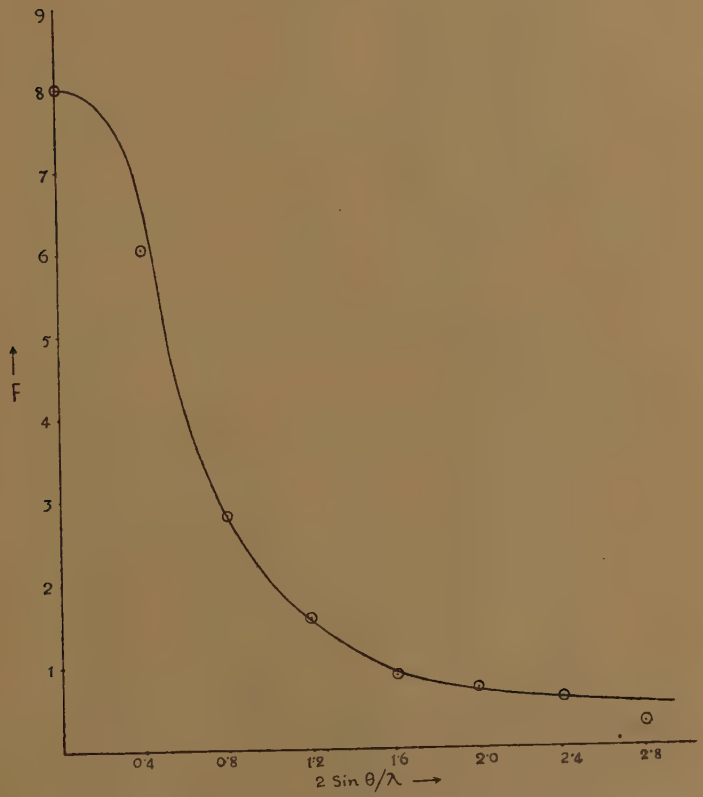

Atomic structure factor curve for oxygen.

found for the best agreement to have the parameters $x/a=0{\cdot}275$, $y/b=0{\cdot}125$, and $z/c=0{\cdot}194$. The final values of the parameters of the different atoms (expressed as fractions of the sides of the unit cell) are given in Table II.

The C—C and the C=C bonds are respectively 1·46 Å. and 1·35 Å. The C=O distances calculated from the

TABLE I.

Atomic Structure Factors for Aromatic Carbon and Oxygen.

Aromatic carbon.		Oxygen.	
$2 \sin \theta/\lambda$.	F_c	$2 \sin \theta/\lambda$.	F_o
0·1320	4·5	0·4	6·04
0·2632	3·1	0·8	2·82
0·3944	2·64	1·19	1·60
0·5264	1·95	1·6	0·90
0·6578	1·44	2·0	0·75
0·7906	1·08	2·38	0·6
0·9220	0·78	2·85	0·30
1·052	0·60		
1·176	0·46		

TABLE II.

Coordinates of the different Atoms.

Kind of atom.	x.	y.	z.
C_1	1·645	3·277	0·461
C_2	2·772	4·209	0·670
C_3	4·127	3·602	0·719
C_4	5·315	4·715	0·928
C_5	6·606	4·009	0·978
C_6	7·857	5·018	1·186
C_7	9·086	4·489	1·234
C_8	9·187	2·872	1·075
C_9	8·063	1·940	0·866
C_{10}	6·710	2·546	0·818
C_{11}	5·521	1·433	0·608
C_{12}	4·230	2·140	0·560
C_{13}	2·979	1·132	0·350
C_{14}	1·749	1·661	0·301
O_1	6·074	5·535	0·768
O_2	5·199	0·615	—0·099

above values come out on both sides to be equal to 1·13 Å.—almost the same as that obtained by Robertson for benzoquinone ; but the oxygen atoms are placed unsymmetrically on the opposite sides of the rings, and the

inclinations of the C=O bonds to the C_4C_{11} line are both approximately equal to 132°. The reflecting planes

TABLE III.

Estimated Intensities and Calculated Values of Structure Factors.

Plane.	$\frac{2 \sin \theta}{\lambda}$.	F_c	F_o	Intensity estimated.	F calculated.
400	0·203	3·87	7·48	Moderate.	16·0
600	0·305	3·12	7·1	Strong.	−64·0
800	0·406	2·5	6·0	Moderate.	−23·7
10, 00	0·508	2·02	4·8	Weak.	8·6
12, 00	0·609	1·6	3·85	Moderate.	13·6
040	0·163	4·2	7·7	Strong.	−64·0
060	0·244	3·57	7·38	Absent.	0
080	0·325	2·98	6·9	Strong*.	−72·8
010, 0	0·407	2·5	5·4	Absent.	0
0120	0·488	2·13	4·95	Weak †.	−15·7
0140	0·569	1·77	4·15	Absent.	0
0160	0·650	1·47	3·7	Weak.	−25·3
0180	0·732	1·23	3·2	Absent.	0
220	0·13	4·5	7·85	Strong.	−29·6
440	0·26	3·5	7·32	Strong.	50·8
660	0·39	2·6	6·25	Weak (doubtful).	0·4
880	0·52	1·97	4·7	Moderate.	−33·8
10, 10, 0	0·650	1·47	3·7	Absent.	− 2·4
620	0·315	3·1	7·0	Strong.	−80·8
820	0·414	2·48	5·8	Strong.	76·6
401	0·325	2·99	6·9	Strong.	42·0
102	0·509	2·03	4·8	Moderate.	58·4
202	0·517	1·99	4·7	Absent.	2·3
302	0·529	1·94	4·6	Absent.	2·3
402	0·546	1·87	4·5	Moderate.	22·4
703	0·840	0·96	2·7	Moderate.	−18·6
803	0·861	0·90	2·65	Moderate.	33·2
011	0·256	3·5	7·33	Strong.	164·0
221	0·288	3·25	7·15	Strong.	−42·0
811	0·480	2·15	5·1	Moderate.	−15·0

with the corresponding structure factors, as well as the estimated and calculated intensities, are given in Table III.

* From the unpublished data of S. Sen, Dacca University.
† Observed by Caspari, Proc. Roy. Soc. A, cxxxvi. p. 82 (1932).

The projections of one molecule along the crystallographic planes are shown in figs. 4–6.

Fig. 4.

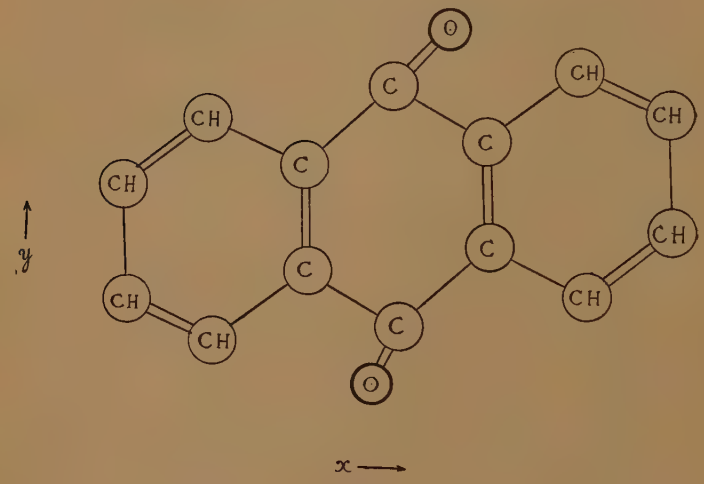

Projection of one molecule on the (001) plane.

Fig. 5.

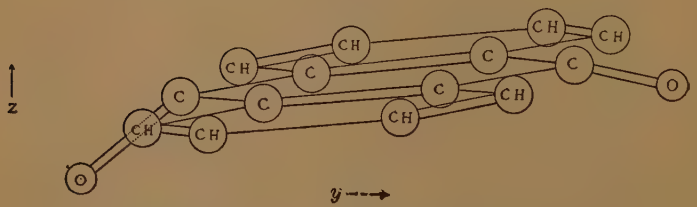

Projection of one molecule on the (100) plane.

Fig. 6.

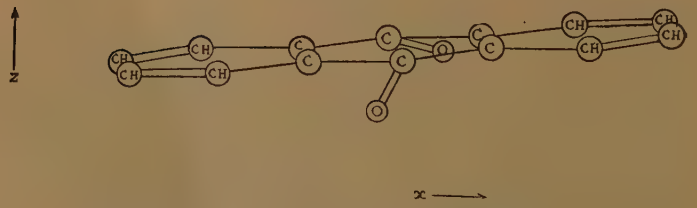

Projection of one molecule on the (010) plane.

Discussion.

The agreement between the observed intensities and the corresponding calculated structure factors as given above appears to be satisfactory. In the calculations of structure factors the values for the atomic factors for oxygen are the most uncertain elements; but there are a number of planes in which the contribution of oxygen atoms to the structure factors are small, and so any change in the atomic factors does not appreciably affect the agreement in such cases. The following is a list of planes in which the contribution of oxygen atoms in the total structure factor is less than 3 :—(800), (10, 00), (12, 00), (880), (10, 10, 0), (060), (010,0), (0120), (0140), (0180), (102), (011), (703). From the agreements in these cases, which are evidently independent of the choice of atomic factors of oxygen, we may conclude that our determination of the atomic arrangements are essentially correct. Now, since the structure factors calculated on the basis of this arrangement and Wollan's values of the atomic factors of oxygen agree with the estimated intensities of reflexion from other planes in which the contribution from oxygen atoms are considerable, it is apparent that the atomic factors of oxygen in anthraquinone do not deviate much from the values given by Wollan for magnesium oxide.

The preliminary results * of this structure determination were published in a note; much better agreement than that has, however, been obtained by the slight modification of the structure proposed there. According to the structure presented here the carbon skeleton of the anthraquinone molecule lies in one plane; the hexagons are not perfectly regular but slightly deformed. The deformation of the middle ring is similar to that in benzoquinone observed by Robertson, the hexagon angles being the same in two cases; but the C—C and C=C distances in anthraquinone are intermediate between those in anthracene and benzoquinone. All the hexagon angles in the two outer rings are 120°. This is to be expected, since here there is nothing to distinguish between these angles, as each of them is formed by a single bond and a double bond. C—C and C=C distances are the same

* B. C. Guha, ' Nature,' cxxxix. p. 969 (1937).

as the corresponding quantities for the central ring. On calculation from the parameters of the atoms these distances are found respectively to be 1·46 Å. and 1·35 Å. The shape of the carbon and oxygen skeleton of the molecule is shown in fig. 7. In benzoquinone C—C and C=C distances are 1·5 Å. and 1·32 Å. respectively. This difference of anthraquinone from benzoquinone is probably

Fig. 7.

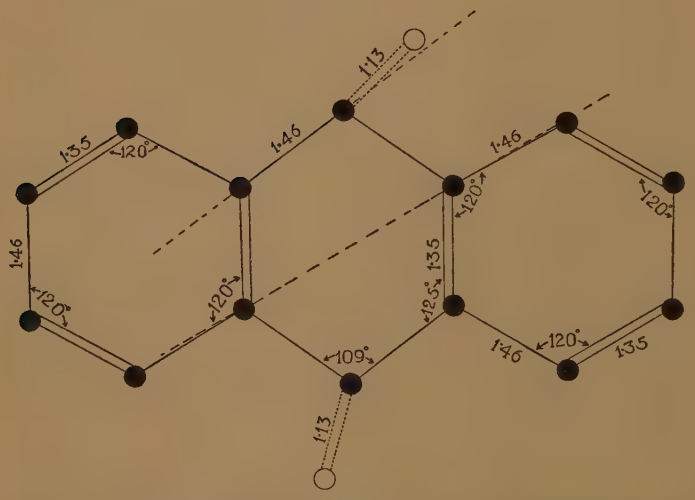

Shape of the carbon skeleton of anthraquinone molecule, showing distortion from the anthracene structure.

due to the restraining influence exerted by the outer rings on the distortion produced by the oxygen atoms.

In conclusion, I wish to express my sincere thanks to Dr. K. Banerjee for his kind interest in this work.

Summary.

The arrangement of the atoms in the anthraquinone crystal has been determined by the trial and error method. It has been found that the carbon atoms are all in one plane, and the carbon plane is tilted from the (001) plane by 6° about each of the "*a*," "*b*," and "*c*" axes. The hexagons deviate slightly from regularity; the side rings have all the internal angles equal to 120°,

but the lengths of sides are alternately 1·35 Å. and 1·46 Å. For the middle ring the internal angles differ from 120°; the angle between the two single bonds is 109°, and that between a single bond and a double bond is 125°. The C—C bonds are 1·46 Å. and the C=C bonds are 1·35 Å, as in the outer rings. The oxygen atoms are inclined to the carbon plane unsymmetrically, the C=O distances being 1·13 Å. each.

XIX. *Short Derivation of a Fundamental Probability Formula.* *By* Ludwik Silberstein, *Ph.D.**

[Received May 23, 1938.]

LET $p=1-q$ be the (constant) probability of an event in a single trial and $f(n, k)$ the probability of the event happening k times in a set of n trials. The approximate evaluation of the rigorous expression $f(n, k)=\binom{n}{k} p^k q^{n-k}$ for great n, k, $n-k$ is usually accomplished by a somewhat cumbersome method based on Stirling's formula for the factorials of great numbers.

The object of the present note is to derive that approximate value of $f(n, k)$ by a more rapid method, suggested by Rayleigh's treatment of the problem of phases at random ('Theory of Sound,' i. p. 37).

By the very meaning of p and q we have for the probability f the functional equation

$$f(n+1, k)=pf(n, k-1)+qf(n, k).$$

Instead of n, k introduce the variables n and

$$\lambda=k-np.$$

If n increases by $\Delta n=1$, then $\Delta\lambda=\Delta k-p$, and since Δk is either 1 or 0 with the probabilities p and q, we have $\Delta\lambda=1-p=q$ and $\Delta\lambda=-p$ respectively. Thus the functional equation becomes

$$f(n+1, \lambda)=pf(n, \lambda-q)+qf(n, \lambda+p), \quad . \quad . \quad (1)$$

* Communicated by the Author.

whence, treating n, λ as continuous variables, and writing $f(n, \lambda) = f$,

$$f + \frac{\partial f}{\partial n} = p\left(f - q\frac{\partial f}{\partial \lambda} + \frac{1}{2}q^2\frac{\partial^2 f}{\partial \lambda^2}\right) + q\left(f + p\frac{\partial f}{\partial \lambda} + \frac{1}{2}p^2\frac{\partial^2 f}{\partial \lambda^2}\right).$$

Since $p+q=1$, the terms in f and in $\partial f/\partial\lambda$ cancel *, and we have for f the differential equation

$$\frac{\partial f}{\partial n} = \frac{1}{2}pq\frac{\partial^2 f}{\partial \lambda^2}. \quad . \quad . \quad . \quad . \quad . \quad . \quad . \quad (2)$$

An integral of this equation, well known from the theory of heat conduction, is

$$f = \frac{a}{\sqrt{n}}e^{-\lambda^2/2pqn},$$

where a is, so far, an arbitrary constant. But since

$$\int_0^n f dk = 1,$$

it will be determined by

$$\frac{a}{\sqrt{n}}\int_{-np}^{nq} e^{-\lambda^2/2pqn}\, d\lambda = \frac{a\sqrt{2\pi pq}}{2}\left\{\Phi\left(\sqrt{\frac{pn}{2q}}\right) + \Phi\left(\sqrt{\frac{qn}{2p}}\right)\right\} = 1,$$

where $$\Phi(x) = \frac{2}{\sqrt{\pi}}\int_0^x e^{-x^2} dx,$$

the error function. Even if $\sqrt{pn}$ and $\sqrt{qn}$ amount only to a few units the bracketed error functions are practically indiscernible from 1, and we have $a = 1/\sqrt{2\pi pq}$.

Thus, $$f(n, k) = \frac{e^{-\frac{(k-np)^2}{2pqn}}}{\sqrt{2\pi pqn}}, \quad . \quad . \quad . \quad . \quad . \quad . \quad (3)$$

which is the required formula.

Rochester, N.Y.
May 10, 1938.

* This is the reason why the expansion with respect to λ had to be pushed to the next term of the Taylor series.

XX. *Molecular Force and Imperfect Gases.*

By WENG WEN-PO *.

[Received April 21, 1938.]

(1) *The Molecular Force.*

A GREAT amount of work has been done in attempts to explain the deviation of a gas from Boyle's Law The number of empirical, semi-empirical, and theoretical equations of state in common use as general representations of facts is also very large. It is practically impossible to mention them even briefly. It is, however, generally believed that the deviation of a gas from Boyle's Law is due to the finite volume of the molecules and the attraction between them.

Let us assume that the force between two spherically symmetrical molecules is composed of two independent parts, namely, a repulsion and an attraction Each part of the force is represented by an inverse power law of the distance which separates the molecules, while the causes of these forces are not at the moment specified.

Let the force between two spherically symmetrical molecules be represented by

$$f(\gamma)=-\frac{d}{d\gamma}\mathrm{E}_p(\gamma)=\frac{\mathrm{A}}{\gamma_{\mu}}+\frac{\mathrm{B}}{\gamma\lambda}, \quad . \quad . \quad . \quad (1)$$

where γ is the distance between their centres, $\mathrm{E}_p(\gamma)$ their mutual potential energy, and A, B, μ, and λ are constants. The force $f(\gamma)$ is thus determined by the four constants.

To facilitate later discussion we will introduce several auxiliary quantities. The first one is γ_0, which is defined by

$$f(\gamma_0)=0. \quad . \quad . \quad . \quad . \quad . \quad . \quad . \quad (2)$$

The quantity γ_0 may be called the equilibrium separation of the molecular force. After introducing γ_0, either the constant A or B in equation (1) can be eliminated from the expression of $f(\gamma)$. Let us eliminate B for definiteness. We have then

$$f(\gamma)=\frac{\mathrm{A}}{{\gamma_0}^{\mu}}\left[\left(\frac{\gamma_0}{\gamma}\right)^{\mu}-\left(\frac{\gamma_0}{\gamma}\right)^{\lambda}\right]$$

and

$$\mathrm{E}_p(\gamma)=\frac{\mathrm{A}}{{\gamma_0}^{\mu-1}}\left[\frac{1}{(\mu-1)}\left(\frac{\gamma_0}{\gamma}\right)^{\mu-1}-\frac{1}{(\lambda-1)}\left(\frac{\gamma_0}{\gamma}\right)^{\lambda-1}\right] \quad . \quad (3)$$

* Communicated by the Author.

A second auxiliary quantity is the potential energy required to separate a pair of molecules from γ_0 to infinity. If this is denoted by $E_p(\gamma)\Big]_{\gamma_0}^{\infty}$ it follows at once

$$E_p(\gamma)\Big]_{\gamma_0}^{\infty} = -\frac{A}{\gamma_0^{\mu-1}}\left[\frac{\lambda-\mu}{(\mu-1)(\lambda-1)}\right] \quad . \quad . \quad . \quad (4)$$

Then the constant A can also be eliminated by the introduction of $E_p(\gamma)\Big]_{\gamma_0}^{\infty}$.

Introducing yet another quantity γ_1, defined by

$$\gamma_0 = \gamma_1\left(\frac{\lambda-1}{\mu-1}\right)^{\frac{1}{\lambda-\mu}}, \quad . \quad . \quad . \quad . \quad . \quad (5)$$

we can write equation (1) as

$$E_p = -\frac{E_p(\gamma)\Big]_{\gamma_0}^{\infty}}{(\lambda-\mu)}\left[\frac{(\lambda-1)^{\lambda-1}}{(\mu-1)^{\mu-1}}\right]^{\frac{1}{\lambda-\mu}}\left\{\left(\frac{\gamma_1}{\gamma}\right)^{\mu-1} - \left(\frac{\gamma_1}{\gamma}\right)^{\lambda-1}\right\}. \quad . \quad . \quad . \quad (6)$$

(2) *The Second Virial Coefficient.*

Among the numerous equations of state for gases, Kammerlingh-Onnes's equation of state has been found to be the most successful attempt at an accurate empirical representation.

Kammerlingh-Onnes's equation can be written as

$$PV = RT\left[1 + \frac{B'(T)}{V} + \frac{C'(T)}{V^2}\left(+\frac{D'(T)}{V^3}\right) + \frac{E'(T)}{V^4} \ldots\right], \quad . \quad . \quad . \quad (7)$$

where P and V are respectively the pressure and molar volume of the gas, R is the gas constant, and T the temperature on the absolute scale. B'(T) C'(T), etc., are usually called the second and third, etc., virial coefficients respectively.

It is well known that the theoretical equation of state of a gas involving the second virial coefficient only can be represented by

$$PV = RT - \frac{f_0(T)}{V},$$

where

$$f_0(T) = 2\pi N_0 RT\int_0^{\infty} \gamma^2\left(e^{-\frac{E_p(\gamma)}{k_0 T}} - 1\right)d\gamma$$

or
$$B' = 2\pi N_0 \int_0^\infty \gamma^2 \left(e^{-\frac{E_p(\gamma)}{k_0 T}} - 1 \right) d\gamma, \quad . \quad . \quad (8)$$

where k_0 is the Boltzmann's constant and N_0 the Avogadro's number. In order to make the expression appear simpler we denote

$$\alpha = \frac{E_p(\gamma)\Big]_{\gamma_0}^{\infty}}{k_0(\lambda-\mu)} \left[\frac{(\lambda-1)^{\lambda-1}}{(\mu-1)^{\mu-1}} \right]^{\frac{1}{\lambda-\mu}} \times \frac{1}{T} \quad . \quad . \quad . \quad (9)$$

and

$$I(\alpha) = \int_0 \left(e^{\alpha \left[\left(\frac{\gamma_1}{\gamma}\right)^{\mu-1} - \left(\frac{\gamma_1}{\gamma}\right)^{\lambda-1} \right]} - 1 \right) d\left(\frac{\gamma}{\gamma_1}\right)^3 . \quad . \quad (10)$$

By substituting equations (6), (9), and (10) into (8) we obtain

$$B'(T) = \frac{2\pi}{3} N_0 \gamma_1^3 I(\alpha). \quad . \quad . \quad . \quad . \quad (11)$$

The actual evaluation of the integral $I(\alpha)$ has been effected by Jeans, Keesom *, and Lennard-Jones †. In our symbols the result can be written as

$$I(\alpha) = \alpha^{\frac{3}{\lambda-1}} \left\{ \Gamma\left(\frac{\lambda-4}{\lambda-1}\right) - \sum_{i=1}^{\infty} \frac{3\Gamma\left(\frac{i(\mu-1)-3}{\lambda-1}\right)}{i\,!\,(\lambda-1)} \alpha^{\left(\frac{\lambda-\mu}{\lambda-1}\right) i} \right\}; \quad (12)$$

when $\lambda \to \infty$ equation (12) reduces to

$$I(\alpha) = 1 - \sum_{i=1}^{\infty} \frac{3}{i\,!\,[i(\mu-1)-3]} \alpha^i \quad . \quad . \quad (12\,a)$$

Based on equations (12) and (12 *a*) graphs of the integral $I(\alpha)$ have been plotted as shown in fig. 1 for $\mu = 7$ and $\lambda = 12$, 17, 24, and ∞. A comparison between the theory and experiments has been demonstrated by Fowler ‡ for helium. The agreement is generally good, but we cannot determine the value of λ conclusively even when μ is assumed. Equally good agreement has been obtained for argon by Herzfeld § by assuming the repulsion between the molecules to be an exponential function of their separation.

* Comm. Phys. Lab. Leiden, xxiv. *b* 1912).
† Proc. Roy. Soc. A, cvi. p. 463 (1924).
‡ Fowler, ' Statistical Mechanics,' 1936.
§ Phys. Rev. lii. p. 374 (1937).

It is, however, possible by means of equation (12) to solve the equation

$$I(\alpha_b)=B'(T_b)=0 \quad . \quad . \quad . \quad . \quad . \quad (13)$$

for α_bi n terms of μ and λ alone. The temperature T_b as defined by equation (13) is usually called the Boyle point, and, therefore, α_b is the value of the parameter α corresponding to the Boyle point. By applying repeated substitution to equation (12) we obtain accordingly,

$$\alpha_b=1{\cdot}23 \quad \text{for} \quad \lambda=12 \quad \mu=7.$$

$$\alpha_b=0{\cdot}85 \quad \text{for} \quad \lambda=\infty \quad \mu=7.$$

Fig. 1.

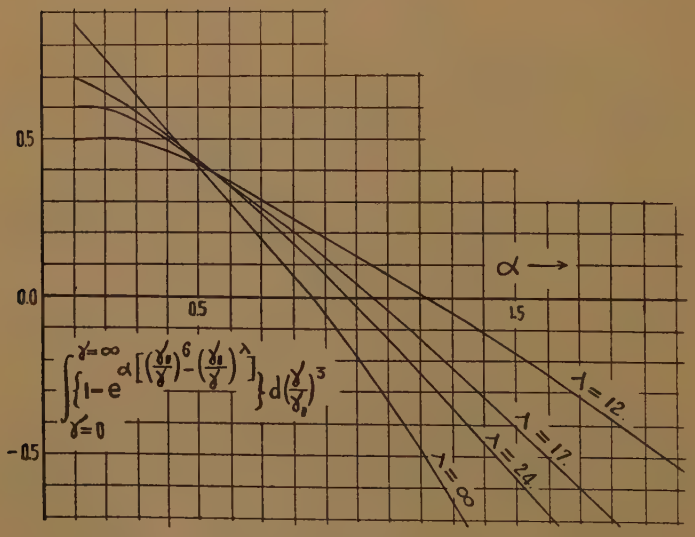

Let us take T_b as a known quantity, since it can be easily and quite accurately determined from the experimental data. By equation (9), we are thus able to calculate $E_p(\gamma)]_{\gamma_0}^{\infty}$ in terms of μ, λ, and T_b. Alternatively we can find the value of α corresponding to various temperatures in terms of μ, λ, and T_b by the following equation:

$$\alpha=\alpha_b T_b \times \frac{1}{T} \quad . \quad . \quad . \quad . \quad . \quad (14)$$

(3) *The Joule-Thomson Effect* *.

There is another physical property besides the second virial coefficient which also involves the integral $I(\alpha)$. This is the Joule-Thomson effect.

The thermodynamical formula for the Joule-Thomson effect can be written as

$$\frac{\Delta T}{\Delta P} = \left\{ T\left(\frac{\partial V}{\partial T}\right)_p - V \right\} \frac{1}{C_p}, \quad . \quad . \quad . \quad (15)$$

where $\frac{\Delta T}{\Delta P}$ is the Joule-Thomson coefficient, and C_p the specific heat at constant pressure. Taking equation (7) as the equation of state, the Joule-Thomson effect can be expressed, by means of equation (15), as

$$\frac{\Delta T}{\Delta P} = \frac{1}{C_p} \left\{ \frac{T\frac{dB'(T)}{dT} - B'(T) + \left(T\frac{dC'(T)}{dT} - 2C'(T)\right)\frac{1}{V} + \cdots}{1 + 2\frac{B'(T)}{V} + \frac{3C'(T)}{V^2} \cdots} \right\}.$$

$$. \quad . \quad . \quad (16)$$

When the virial coefficient of orders higher than the third are neglected, equation (16) reduces to

$$\frac{\Delta T}{\Delta P} = a_j(T) + b_j(T)P, \quad . \quad . \quad . \quad (17)$$

where

$$C_p a_j(T) = T\frac{dB'(T)}{dT} - B'(T), \quad . \quad . \quad . \quad (18)$$

$$C_p b_j(T) = T\frac{dC'(T)}{dT} - 2C'(T) - 2B'(T)a_j(T). \quad . \quad (19)$$

If the Joule-Thomson coefficients are plotted against pressure at different temperatures, we expect a system of straight lines with different slopes. The intercepts are $a_j(T)$ and slopes $b_j(T)$ when the pressure is low. The Joule-Thomson coefficients at constant temperature for CO_2, air, and argon show approximate linear relation with P. As a matter of fact, an empirical equation in the

* During the course of publication a part of the work in this section was published by Hirschfelder, Ewell, and Roebuck, in J. Chem. Phys. vi. p. 205 (1938).

form of equation (17) has been used to record the experimental result of the Joule-Thomson effect for air.

Substituting equation (11) into (18), the quantity $a_j(\mathrm{T})$ can be put into the theoretical expression,

$$a_j(\mathrm{T}) = \frac{2\pi}{3}\frac{\mathrm{N}_0\gamma_1^3}{\mathrm{C}_p}\left[-\mathrm{I}(\alpha)+\mathrm{T}\frac{d\mathrm{I}(\alpha)}{d\mathrm{T}}\right]. \quad . \quad . \quad (20)$$

By means of equation (14) we can easily transform the variable T into α. Equation (20) thus becomes

$$a_j(\mathrm{T}) = \frac{2\pi}{3}\frac{\gamma_1^3\mathrm{N}_0}{\mathrm{C}_p}\left[-\mathrm{I}(\alpha)-\alpha\frac{d\mathrm{I}(\alpha)}{d\alpha}\right]. \quad . \quad . \quad (21)$$

Similarity is exhibited in this equation and equation (11). Analogous to the Boyle point, at which the second virial coefficient vanishes, there is a temperature at which $a(\mathrm{T})$ vanishes. We may call this particular temperature T_j, the inversion temperature of the Joule-Thomson effect at zero pressure. Let α_j be the value of the parameter corresponding to T_j, or

$$a_j(\mathrm{T}_j) = \left[-\mathrm{I}(\alpha)-\alpha\frac{d\mathrm{I}(\alpha)}{d\alpha}\right]_{\alpha_j} = 0. \quad . \quad . \quad (22)$$

By equation (12) we obtain, by simple operations,

$$-\mathrm{I}(\alpha)-\alpha\frac{d\mathrm{I}(\alpha)}{d\alpha} = d^{\frac{3}{\lambda-1}}\left\{-\binom{\lambda-2}{\lambda-1}\Gamma\binom{\lambda-4}{\lambda-1}\right.$$
$$\left.+\frac{3}{(\lambda-1)^2}\sum_{i=1}^{\infty}\frac{i(\lambda-\mu)+\lambda+2}{i\,!}\Gamma\begin{bmatrix} i(\mu-1)-3 \\ \lambda-1 \end{bmatrix}\alpha^{\frac{\lambda-\mu}{\lambda-1}i}\right\}; \quad (23)$$

when λ approaches infinity equation (23) reduces to

$$-\mathrm{I}(\alpha)-\alpha\frac{d\mathrm{I}(\alpha)}{d\alpha} = -1+3\sum_{i=1}^{\infty}\frac{i+1}{i\,![i(\mu-1)-3]}\alpha^i. \quad (23\,a)$$

With the aid of equations (23) and (23 *a*) equation (22) can then be solved numerically by repeated substitution. We get accordingly

$$\alpha_j = 0{\cdot}66 \quad \text{for} \quad \lambda=12 \quad \mu=7.$$
$$\alpha_j = 0{\cdot}44 \quad \text{for} \quad \lambda=\infty \quad \mu=7.$$

It follows at once

$$\frac{\mathrm{T}_j}{\mathrm{T}_b} = \frac{\alpha_b}{\alpha_j} = 1{\cdot}88 \quad \text{for} \quad \lambda=12 \quad \mu=7.$$
$$\frac{\mathrm{T}_j}{\mathrm{T}_b} = \frac{\alpha}{\alpha_j} = 1{\cdot}92 \quad \text{for} \quad \lambda=\infty \quad \mu=7.$$

The early value of inversion temperature for hydrogen determined by Olszewski * at a pressure of about 20 atmospheres is −80·5° C., or approximately 193° A. By interpolating Holborn and Otto's data † of the second virial coefficients we find T_b for hydrogen to be 104° A. approximately. Then the experimental value of the ratio of $\frac{T_j}{T_b}$ is 1·9 approximately. The agreement might be merely a coincidence because the above classical deduction does not hold for helium and hydrogen molecules, for which, according to Slater ‡, quantization of energy should be considered.

Equation (21) can be applied in a very interesting way. Suppose we tabulate the observed values of $a_j(T)$ of a certain imperfect gas as a function $\frac{T_b}{T}$. Then also tabulate the calculated values of $-I(\alpha)-\alpha\frac{dI(\alpha)}{d\alpha}$ with assumed μ and λ as a function of $\frac{\alpha}{\alpha_b}$. The arguments of the two functions are equal because of equation (14). If we plot the two quantities $a_j(T)$ and $-I(\alpha)-\alpha\frac{dI(\alpha)}{d\alpha}$ against the common argument, the two sides of equation (21) can be compared by choosing a suitable ratio of the scales on which the two quantities are plotted. The better the two graphs can be made to fit each other the nearer will be the assumed values of μ and λ to the truth.

Let us take argon as an example, since the data of both $B'(T)$ and $a_j(T)$ for this gas are adequate for our purpose. Interpolating Holborn and Otto's data of $B'(T)$, the Boyle point, or T_b, for argon was found to be 345° A. The Joule-Thomson effect of argon has been measured recently by Roebuck and Osterberg § at various pressures and temperatures. In figs. 2 and 3 their data of Joule-Thomson coefficients at one atmosphere, which is practically equal to $a_j(T)$, are plotted against $\frac{T_b}{T}$ in dots. and

* ' Landolt und Bornstein Tabellen.'
† ' International Critical Tables.'
‡ Phys. Rev. xxxviii. p. 237 (1931).
§ Phys. Rev. (2) xlvi. p. 785 (1934).

are compared with the theoretical quantity $-I(\alpha)-\alpha\frac{dI(\alpha)}{d\alpha}$, which is plotted in a continuous curve. The ratio of the two scales of the ordinates is so chosen as to facilitate the comparison. In fig. 2 the quantities $-I(\alpha)-\alpha\frac{dI(\alpha)}{d\alpha}$ and

Fig. 2.

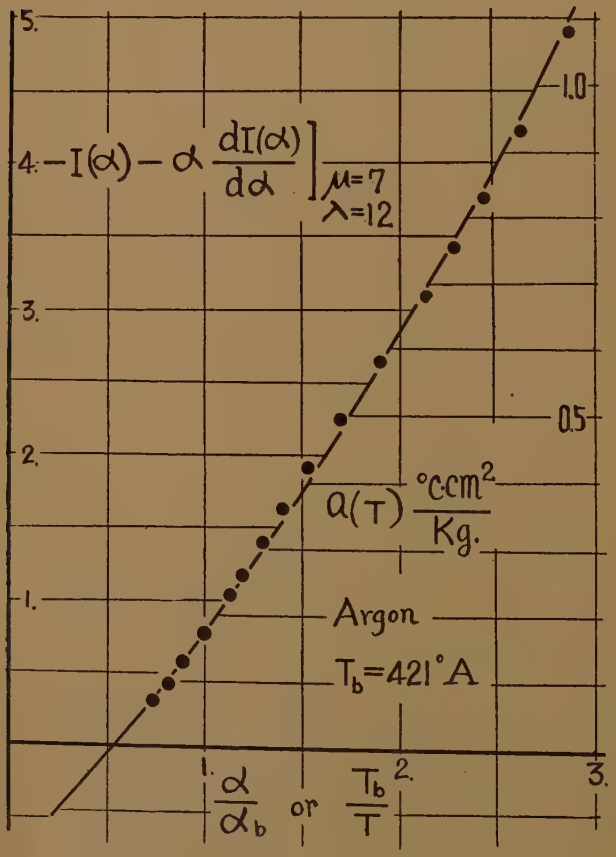

α_b are calculated by assuming $\mu=7$ and $\lambda=12$, and in fig. 3 $\mu=7$ and $\lambda=\infty$.

Judging by figs. 2 and 3 it is obvious that λ is not infinity or that the argon molecules are not incompressible.

The data of Joule-Thomson effect for air is also very complete. As a matter of fact, they are so complete that we are tempted to carry out a similar test of equa-

tion (21), although the contribution to $a_j(T)$ from the binary complexes must be neglected. In fig. 4 the experimental values * of $a_j(T)$ for air, plotted in dots, are compared with the theoretical curve for $\mu=7$ and $\lambda=\infty$. $T_b=345°$ A. for air was interpolated from Holborn and Otto's data of B′(T).

Fig. 3.

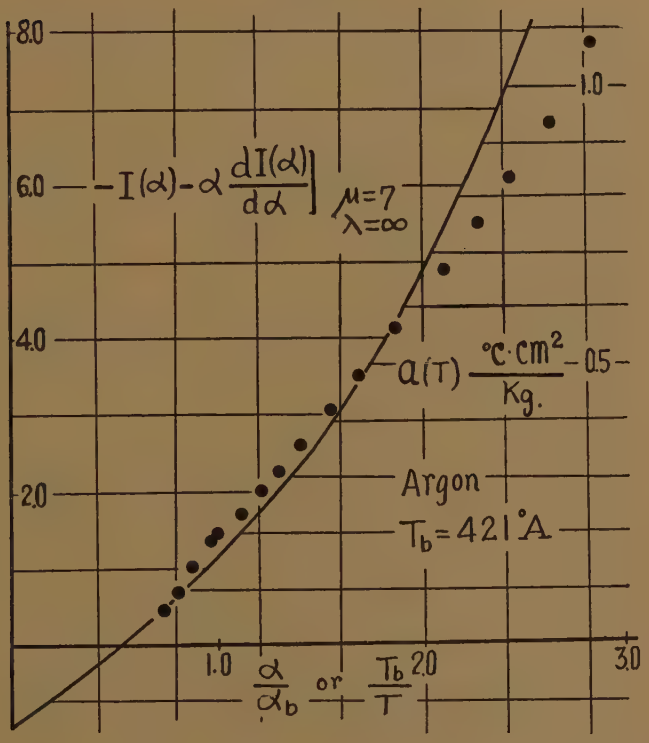

(4) *The Joule-Thomson Effect and Second Virial Coefficient.*

Dividing equation (11) by (21) we obtain

$$\frac{B'(T)}{C_p a_j(T)}=\frac{I(\alpha)}{-I(\alpha)-\alpha\frac{dI(\alpha)}{d\alpha}}, \quad . \quad . \quad . \quad (24)$$

* Hausen's data taken from ' Landolt und Bornstein Tabellen '; Noell's data from ' International Critical Tables.'

where the constant γ_1 has been eliminated. If we have accurate experimental data of B′(T), C_p, and a_j(T) there are only μ and λ remaining unknown in equation (24). Let us again take argon and air as examples. In Table I. the necessary data are tabulated. The values of B′(T)

Fig. 4.

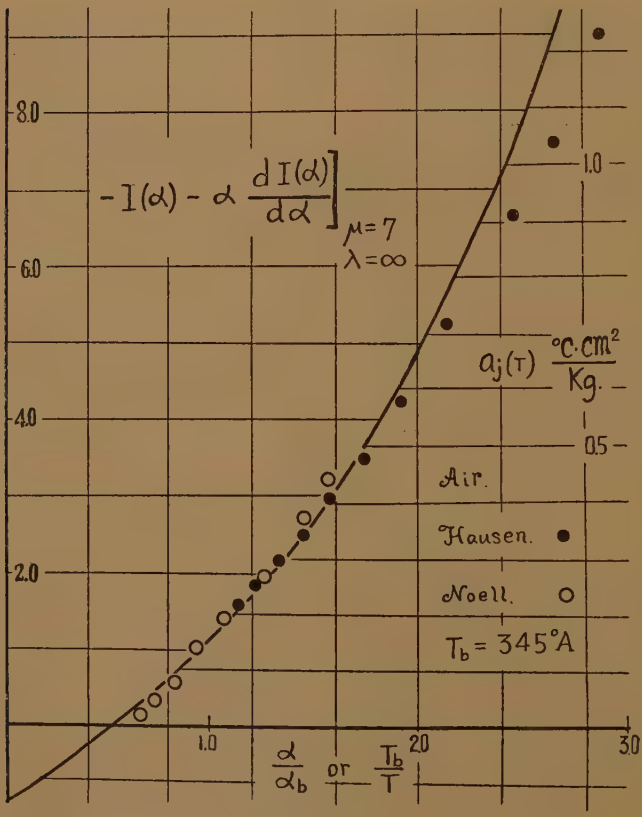

for both gases are those of Holborn and Otto. By interpolating these we got respectively $T_b=421°$ A. for argon and $T_b=345°$ A. for air. Assuming $C_p=7/2R$ for air and $C_p=5/2R$ for argon, the left-hand side member of equation (24) for these two gases as calculated in Table I. is plotted in fig. 5 in dots and circles. The continuous curve is the right-hand side member of equation (24).

The common argument is $\frac{T}{T_b}$ or $\frac{\alpha}{\alpha_b}$, which is the reciprocal of that used before. The curve for $\lambda=12$ and $\mu=7$ is so near to that for $\lambda=\infty$ and $\mu=7$ that it is practically impossible to separate the two in the part of the curve plotted. The position of the asymptote for $\lambda=12$ and $\mu=7$ is, however, plotted in a dotted line.

TABLE I.

Air.

Temp. °A.	$B'(T)10^3$ in Leiden units.	$a_j(T)$ °C./kg. cm.$^{-1}$.	$\frac{2}{7R}\frac{B'(T)}{a_j(T)}$.
273	−0·603	0·272	−0·167
323	−0·141	0·197	−0·054
373	0·159	0·138	0·087
423	0·380	0·084	0·34
473	0·550	0·052	0·80

Argon.

Temp. °A.	$B'(T)10^3$ in Leiden units.	$a_j(T)$ °C./kg. cm.$^{-1}$.	$\frac{2}{5R}\frac{B'(T)}{a_j(T)}$.
173	−2·872	0·83	−0·378
223	−1·687	0·58	−0·318
273	−0·986	0·42	−0·220
373	−0·192	0·23	−0·091
423	0·052	0·18	0·010
473	0·208	0·133	0·177
523	0·501	0·062	0·883

(5) *Further Assumptions.*

We have so far made assumptions for μ and λ only. No particular attention has been paid to the other two constants of the molecular force, namely, γ_1 and $E_p(\gamma)]_{\gamma_0}$. These have been handled as merely mathematical constants. Considering their respective definitions it is, however, natural to imagine that they can be estimated by other physical constants of the substance. The constant γ_0 is the equilibrium separation of the molecular force. We

should be able to estimate it by the lattice constant of the substance at absolute zero, at which the molecules would be resting motionless at their respective equilibrium positions when the zero-point energy is neglected. The other constant $E^{p}(\gamma)]_{\gamma_0}^{\infty}$ has been defined as the potential energy required to separate a pair of molecules at a separation of γ_0 to infinity. Similarly we should be able to estimate this constant by the latent heat of sublimation at absolute zero.

To make use of these relations effectively we will tackle the problem in a different manner. The investigation

Fig. 5.

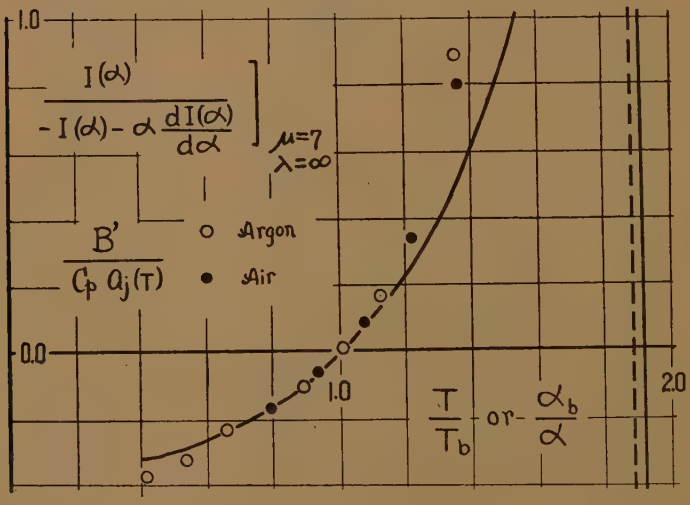

which we have so far made applies generally to any single gas. Let us now study a group of gases in a comparative manner, and start by assuming that the constants γ_0 and $E_p(\gamma)]_{\gamma_0}^{\infty}$ for each individual gas of the group are proportional to the lattice constant and latent heat of sublimation at absolute zero respectively. In other words, when one gas of the group has its lattice constant at absolute zero twice that of the other, we assume that the constant γ_0 of their respective molecular force bears the same ratio and so on.

For practical application of these assumptions it is inconvenient to use physical constants at absolute zero.

We will then use the corresponding properties at the normal boiling-points instead, as we can show later that the error so introduced would not be serious. The average molecular spacing in a liquid, which corresponds to the lattice constant of a solid, can be estimated by the density and the molecular weight of the substance. The latent heat of evaporation at the normal boiling-point will be used for the heat of sublimation in the solid state. Then the constants of the molecular force of a group of substances can be compared by

$$E_p(\gamma)\Big]_{\gamma_0}^{\infty} = \frac{\mathscr{L}M}{\Re N_0}, \quad . \quad . \quad . \quad . \quad . \quad (25)$$

$$\gamma_0 = J_e\left(\frac{M}{\rho_e N_0}\right)^{\frac{1}{3}} . \quad . \quad . \quad . \quad . \quad . \quad (26)$$

where $\mathscr{L}$ is the latent heat of evaporation per gram of substance, M the molecular weight, N_0 Avogadro's number, ρ_e the density of the substance in the liquid state at the normal boiling-point, and J_e and $\Re$ are two constants of proportionality.

Substituting equations (5) and (26) into (11), we get

$$\frac{B'(T)\rho_e}{N} = j_e^{\,3} \times \left(\frac{\mu-1}{\lambda-1}\right)^{\frac{3}{\lambda-\mu}} \times \frac{2\pi}{3} I(\alpha) \quad . \quad . \quad (27)$$

By equations (9) and (25) the parameter α can be expressed by

$$\alpha = \frac{1}{\Re(\lambda-\mu)}\left[\frac{(\lambda-1)^{\lambda-1}}{(\mu-1)^{\mu-1}}\right]^{\frac{1}{\lambda-\mu}} \times \frac{\mathscr{L}M}{RT} . \quad . \quad . \quad (28)$$

The two quantities $\frac{B'(T)\rho_e}{M}$ and $\frac{\mathscr{L}M}{RT}$ can be considered as two variables, and their relation is determined by μ and λ. Whenever μ and λ of a number of gases are the same, so will be the relation between $\frac{B'(T)\rho_e}{M}$ and $\frac{\mathscr{L}M}{RT}$. In fig. 6 these two quantities for several elementary gases are plotted against each other. The values of B'(T) used are those of Holborn and Otto.

It is obviously shown in fig. 6 that the constants μ and λ for those gases are approximately the same.

Similar treatment has been carried out for hydrogen and helium, but the relation between $\frac{B'(T)\rho_e}{M}$ and $\frac{\mathscr{L}M}{RT}$ for these two gases is not common to those plotted in fig. 6.

(6) *The Corresponding State.*

When the constants μ and λ of a group of substances are equal, there are only two other constants, namely,

Fig. 6.

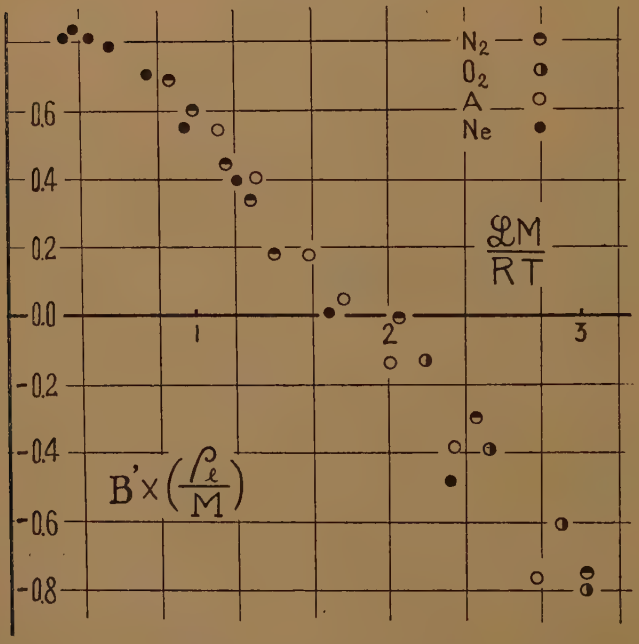

γ_0 and $E(\gamma)]_{\gamma_0}^{\infty}$, to determine the molecular force, and therefore the inter-molecular potential energy. These two characteristic constants γ_0 and $E_p(\gamma)]_{\gamma_0}^{\infty}$ will also appear in the general equation of states. It is wellknown that an equation of state which contains only two characteristic constants can be transformed into an universal equation of state in reduced variables. Hence we can get some information of molecular force by studying the corresponding states and reduced variables.

A consideration of physical dimensions will show that it must * be possible to write an equation of state with two characteristic constants only in the form

$$\frac{P}{P_0} = f\left(\frac{V}{V_0}, \frac{T}{T_0}\right) \quad . \quad . \quad . \quad . \quad . \quad (29)$$

where P_0, V_0, and T_0 are constants characteristic to each substance. These characteristic constants of each substance can be determined by any fixed points of the function defined by equation (29). Let us first take the Boyle point as a fixed point which can be defined by

$$\lim_{V \to \infty} V^2 \frac{d}{dV} PV = 0. \quad . \quad . \quad . \quad . \quad (30)$$

The solution is obviously of the form

$$T_b \alpha T_0. \quad . \quad . \quad . \quad . \quad . \quad . \quad . \quad (31)$$

In other words, $\frac{T_b}{T_0}$ is a numerical constant for this group of substances whose μ and λ are the same.

If the assumptions which we make in section (5) are true, we have by equation (28)

$$\alpha T \alpha \frac{\mathscr{L}M}{R} \quad . \quad . \quad . \quad . \quad . \quad . \quad . \quad (32)$$

when μ and λ are assumed to be constants. By equation (14) the left-hand member of equation (32) is equal to $\alpha_b T_b$. Hence it follows from equation (31) that

$$T_0 \alpha \frac{\mathscr{L}M}{R}, \quad . \quad . \quad . \quad . \quad . \quad . \quad (33)$$

since α_b is a constant whenever μ and λ are.

Another fixed point which we can make use of is the imaginary condition defined by $P=T=0$, which may be called the state of absolute zero. The volume of the substance, instead of vanishing with P and T, remains finite. Following equation (29), the ratio of the specific molar volume at absolute zero temperature and pressure to V_0 is a constant for the group of substances whose μ and λ are constant. Let us use the density of a substance in the liquid state at the normal boiling-point

* Jeans, ' The Dynamical Theory of Gases,' 1925.

for that at absolute zero, as we did before. We have, accordingly,

$$V_0 \alpha \frac{M}{\rho_e}. \quad . \quad . \quad . \quad . \quad . \quad . \quad . \quad (34)$$

Equations (33) and (34) can be tested by the virial coefficients. Suppose we write Kammerlingh-Onnes's equation in the form of equation (29) :

$$\frac{P}{P_0} = \frac{T}{T_0}\frac{V_0}{V}\left(\frac{RT_0}{P_0V_0}\right)\left[1+\frac{B'(T)}{V_0}\left(\frac{V_0}{V}\right)+\frac{C'(T)}{V_0^2}\left(\frac{V_0}{V}\right)^2+\ldots\right].$$
$$. \quad . \quad . \quad (35)$$

As equation (29) is an universal equation of state for the variables $\frac{P}{P_0}$, $\frac{T}{T_0}$, and $\frac{V}{V_0}$, all the coefficients $\frac{B'(T)}{V_0}$, $\frac{C'(T)}{V_0^2}$,

Fig. 7.

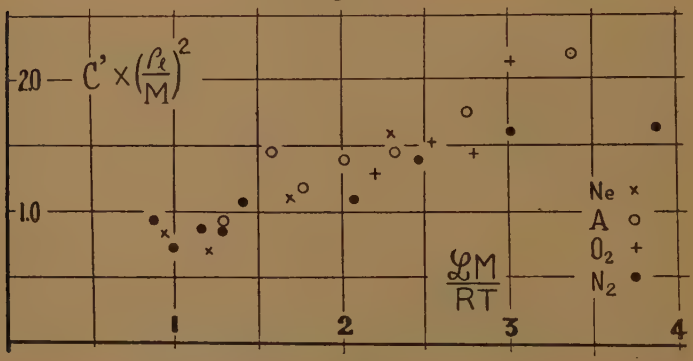

etc., should be functions of $\frac{T}{T_0}$ only. By equations (33) and (34) we can write down the relations as

$$\frac{B'(T)\rho_e}{M} = \phi_1\left(\frac{\mathscr{L}M}{RT}\right) \quad . \quad . \quad . \quad . \quad (35)$$

$$\frac{C'(T)\rho_e^2}{M^2} = \phi_2\left(\frac{\mathscr{L}M}{RT}\right). \quad . \quad . \quad . \quad . \quad (36)$$

Equation (35) has been tested in section (5) as shown in fig. 6. Equation (36) can be tested in a similar manner. In fig. 7 the quantity $C'(T)\left(\frac{\rho_e}{M}\right)^2$ for nitrogen, oxygen, hydrogen, and argon are plotted against $\frac{\mathscr{L}M}{RT}$. The values of C'(T) used in fig. 7 are these of Holborn and Otto.

It is well known that characteristic constants P_0, V_0, and T_0 can be determined by the critical condition, which may be defined by

$$\left(\frac{\partial P}{\partial \bar{V}}\right)_T = \left(\frac{\partial^2 P}{\partial \bar{V}^2}\right)_T = 0.$$

The solutions of these equations must be of the form

$$T_0 \alpha T_c, \quad \ldots\ldots\ldots \quad (38)$$

$$P_0 \alpha P_c, \quad \ldots\ldots\ldots \quad (39)$$

$$V_0 \alpha V_c \text{ or } V_0 \alpha \frac{M}{\rho_c}, \quad \ldots\ldots\ldots \quad (40)$$

where T_c, P_c, V_c, and ρ_c are the critical temperature, the critical pressure, the critical molar volume, and the critical density respectively.

TABLE II.

Elements.	T_b °A.	ρ_e.	$\frac{\rho_e}{\rho_c}$.	$\frac{T_b}{T_c}$.
Ne	121	1·204	2·49	2·72
A	421	1·402	2·64	2·78
N_2	325	0·808	2·60	2·58
O_2	423	1·14	2·65	2·75
Cl_2	—	1·557	2·72	—

Dividing equation (31) by (38), equation (40) by (34), and equation (33) by (38), we obtain

$$T_b \alpha T_c,$$

$$\rho_e \alpha \rho_c,$$

$$\mathscr{L}M \alpha R T_c.$$

In Table II. the ratios of $\frac{T_b}{T_c}$ and $\frac{\rho_e}{\rho_c}$ for some non-metallic elements are shown.

For complex molecules our conclusions will not apply strictly. We can, however, easily imagine that some physical properties are not sensitive to certain variations in the molecular force. It should not be surprising that our deduction will hold for certain complex molecules.

In Table III. the ratios $\frac{\rho_e}{\rho_c}$ and $\frac{\mathscr{L}M}{RT_c}$ for some complex molecules are shown. The ratios are, generally speaking, of the same order of magnitude.

There are quite a number of empirical rules concerning the critical conditions, latent heat, and the normal boiling. Prudhomme's * rule and Trouton's rule are among the best known. In these the normal boiling-point has all the properties of a corresponding state as the critical point.

TABLE III.

Substance.	$\frac{\rho_e}{\rho_c}$†	$\frac{\mathscr{L}M}{TR_c}$†	Substance.	$\frac{\rho_e}{\rho_c}$†	$\frac{\mathscr{L}M}{RT_c}$
H_2O	—	7·6	CH_3COCH_3	3·0	7·2
HCl	2·8	—	$HCO_2C_2H_5$	2·8	7·2
SO_3	3·0	9·7	$CH_3CO_2CH_3$	2·9	7·2
NH_3	2·6	6·9	$CH_3OC_2H_5$	2·6	—
CO.....	2·6	5·3	$C_2H_5CO_2CH_3$	2·9	7·3
$CHCl_3$	2·9	6·6	$(CH_3)_2CHCO_2H$.	—	8·1
CCl_4	2·9	6·5	$(C_2H_5)_2O$.....	2·7	6·7
CH_4.....	2·6	5·9	$(C_2H_5)_2NH$	2·9	6·8
CH_4O	2·9	8·3	$C_2H_5CO_2C_2H_5$ ...	3·0	7·6
CH_4S	2·7	—	$CH_3(CH_2)_3CH_3$ ..	2·9	—
C_2H_2	2·7	—	C_6H_5Br	—	6·8
$CH_3.CN$ ..	—	6·6	C_6H_5Cl	—	7·0
CH_3CO_2H..	3·0	6·0	C_6H_5F	2·9	—
HCO_2CH_3..	2·8	7·0	C_6H_6	2·9	6·6
C_2H_5Br....	2·8	6·5	$C_3H_7CO_2C_2H_5$ ...	—	7·9
C_2H_5OH ..	2·9	—	Toluene	3·0	6·8
C_5H_5N ...	—	6·6	$CH_3(CH_2)_3CH_3$ ..	3·0	7·2
$CH_3.S.CH_3$.	2·8	—	$C_7H_{15}CO_2C_2H_5$...	—	8·0

Judging by the definition of the normal boiling-point, however, it is evidently not a fixed point in the reduced variables. This can be explained by the fact that the critical pressure for most substances does not vary widely. and that the vapour pressure of a liquid increases very rapidly with temperature, so much so that a wide range of pressure can be obtained in a very limited temperature change. Thus the boiling-point approximates to a corresponding state. This justifies our using the density and

* *Cf.* J. Phys. Chem. p. 2307 (1930).

† Values of ρ_e taken from 'International Critical Tables,' vol. i. p. 107; $\mathscr{L}$, vol. v.; T_c, ρ_c, vol. iii.

the latent heat at the normal boiling-point for those at the absolute zero.

There are numerous illustrations to show the existence of corresponding states in the liquid state. An empirical relation between the critical data and the thermal expansion of liquids has been pointed out by Thorpe and Rucker * as early as 1884. The modified form of the empirical rule by Davis † is fairly well known. Recently an interesting and comparatively comprehensive demonstration has been devised by E. Bauer, M. Magat, and M. Surdin ‡. Plotting the molecular volumes against

TABLE IV.

Temp. °A.	B′(T) c.c.	$B'(T)+\frac{1}{2}Ra_j(T)$ c.c.	$T\frac{\Delta B'(T)}{\Delta T}$ c.c.
573	11·2	24	
			34
473	4·66	32	
			32
423	1·17	38	
			44
373	− 4·30	43	
			47
323	−11·0	53	
			67
273	−22·1	64	
			79
223	−37·8	81	
			106
173	−64·4	106	

temperatures on the reduced scale, they were able to obtain a very neat single curve for a great number of substances.

(7) *Supplements.*

It is perhaps not out of place to show that the data of the Joule-Thomson effect and the second virial coefficients for argon which we used in sections (3) and (4) are fairly consistent. Transposing equation (18),

$$B'(T)+C_p a_j(T)=T\frac{dB'(T)}{dT}. \quad . \quad . \quad . \quad (41)$$

* Trans. Chem. Soc. xlv. p. 135 (1884).
† Phil. Mag. xxiii. p. 657 (1912).
‡ *Jour. de Phys. et Rad.* vii. p. 441 (1936).

From a series of values of B′(T) one can calculate $T\frac{\Delta B'(T}{\Delta T}$ which can be considered as an approximation of the right-hand side of equation (41). In Table IV. the left-hand side member of equation (41) for argon is shown with $T\frac{\Delta B'(T)}{\Delta T}$ for the same gas. The figures are quite satisfactory.

Thanks are due to Dr. J. Bruckshaw, of the Imperial College, for his help during the preparation of this paper.

Imperial College,
London.

XXI. *Effect of a Longitudinal Magnetic Field on the Conductivity and Refractive Index of Ionized Air.* *By* B. N. Singh, *M.Sc.*, *Demonstrator in Physics, Benares Hindu University* *.

[Received March 23, 1938.]

Introduction.

THE magneto-ionic theory of the ionosphere, which has recently acquired a considerable importance, has necessitated the experimental investigation of the properties of an ionized gas in the presence of a magnetic field. Several investigations have been made in this direction by different authors during recent years, but a complete and quantitative experimental verification of the magneto-ionic theory in the laboratory seems to have not been made as yet. A brief reference to the experiments made by the previous authors is given below.

Shortly after the establishment of the magneto-ionic theory by Appleton and others [1], Benner [2], in 1929, published the results of his investigations on the refractive index and conductivity of space containing free electrons in the presence of a transverse magnetic field. By varying the magnetic field he showed that near about the gyro-frequency of the incident wave the values of refractive index and conductivity changed abruptly. In 1930 Appleton and Childs [3] found that the space containing

* Communicated by S. S. Banerjee, D.Sc.

free electrons exhibited the inverse Zeeman effect. Gutton [4] and Jonescu and Mihul [5] have also observed the phenomenon of magnetic resonance in an ionized gas with the transverse magnetic field. Appleton and Boorhariwalla [6] have recently studied experimentally the relation between the conductivity and pressure of the ionized air under the influence of an imposed transverse magnetic field.

It will be observed that the experiments with the ionized gas mentioned above were carried out in the presence of a transverse magnetic field, and in most of the cases cited above the main aim of the authors appears to be to show the existence of a magnetic resonance. Very few investigations have, however, been made with longitudinal magnetic field, and with a view to verify quantitatively the various results predicted by the magneto-ionic theory. Keck [7], for instance, has shown the existence of Faraday effect in ionized gas in presence of the longitudinal magnetic field with a wave-length of 4 cm. of the incident wave. Mitra and Ghosh [8] have recently been able to detect the double refraction phenomenon with a longitudinal magnetic field. In almost all the cases of the above investigations approximate equations obtained by neglecting the collisional frequency of the electrons have been used for finding out the values of refractive index and conductivity. But for the thorough verification of the magneto-ionic theory the values of collisional frequency, however small, cannot be always neglected, as has been shown in later sections. In the present communication the author has recorded the results of his study on the variation of the conductivity and refractive index of ionized air for different values of longitudinal magnetic field. Complete equations, including the collisional frequency, have been employed for the calculation of the above constants.

List of Symbols used.

c = velocity of electromagnetic waves in free space.
e = charge of electrons in e.s.u.
H_L = longitudinal component of the magnetic field.
H_T = transverse component of the magnetic field.
$i = \sqrt{-1}$.
k = absorption coefficient.

m = mass of electron.
N = electron density.
p = angular frequency of the impressed wave.
$p_0^2 = 4\pi Ne^2/m$.
$p_L = H_L e/mc$.
$p_T = H_T e/mc$.
$\alpha = -p^2/p_0^2$.
$\beta = p\nu/p_0^2$.
$\gamma_L = pp_L/p_0^2$.
$\gamma_T = pp_T/p_0^2$.
μ = refractive index.
ν = collisional frequency of electrons.
σ = conductivity in e.s.u.

Theory.

The dispersion equation of an ionized gas in the presence of a magnetic field is given by

$$\left(\mu - \frac{ick}{p}\right)^2 = 1 + \frac{2}{2(\alpha+i\beta) - \gamma_T^2/(1+\alpha+i\beta) \pm [\gamma_T^4/(1+\alpha+i\beta)^2 + 4\gamma_L^2]^{1/2}}. \quad \ldots (1)$$

In the case of a purely longitudinal magnetic field $\gamma_T = 0$, and the above equation reduces to

$$\left(\mu - \frac{ick}{p}\right)^2 = 1 + \frac{1}{(\alpha+i\beta) \pm \gamma_L}. \quad \ldots (2)$$

Separating the real and imaginary parts of both the sides and equating them, we get

$$\mu^2 - \frac{c^2k^2}{p^2} = 1 + \frac{\alpha \pm \gamma_L}{(\alpha \pm \gamma_L)^2 + \beta^2} \quad \ldots (3)$$

and

$$\frac{2ck}{p}\mu = \frac{\beta}{(\alpha \pm \gamma_L)^2 + \beta^2}. \quad \ldots (4)$$

From equations (3) and (4) we get

$$\sigma = \mu \frac{kc}{2\pi} = \frac{\beta p}{4\pi\{(\alpha \pm \gamma_L)^2 + \beta^2\}} \quad \ldots (5)$$

and

$$\mu^2 = \frac{1}{2}\left[1 \pm \frac{\alpha \pm \gamma_L}{(\alpha \pm \gamma_L)^2 + \beta^2} + \sqrt{1 + \frac{2(\alpha \pm \gamma_L) + 1}{(\alpha \pm \gamma_L)^2 + \beta^2}}\right]. \quad (6)$$

Substituting the values of α, β, and γ_L in the equations (5) and (6) we finally get

$$\sigma = \frac{{p_0}^2 \nu}{4\pi\{(p \pm p_L)^2 + \nu^2\}} \quad \ldots\ldots\ldots\ldots \quad (7)$$

and

$$\mu^2 = \frac{1}{2}\left[1 - \frac{(p \pm p_L){p_0}^2}{p\{(p \pm p_L)^2 + \nu^2\}} + \sqrt{\frac{\{{p_0}^2 - p(p \pm p_L)\}^2 + p^2\nu^2}{p^2\{(p \pm p_L)^2 + \nu^2\}}}\right]. \quad (8)$$

The positive and negative signs in the above equations correspond to the so-called "ordinary" and "extraordinary" waves respectively. The reason for using the above equations in preference to the approximate ones, which are more commonly used and are obtained by neglecting the collisional frequency ν, will be apparent from the following considerations. If ν be much smaller than p it can be safely neglected in the case of ordinary wave for all values of p_L, since ν has to be compared with $p+p_L$. In the case of the extraordinary wave, however, ν cannot be always neglected, even when it is considerably smaller than p, as ν has to be then compared with $p-p_L$, the value of which attains zero when p_L happens to be equal to p.

Experimental Arrangement and Observations.

The experimental arrangement for determining the conductivity and refractive index of ionized air in presence of longitudinal magnetic field was a modification of that adopted by Mitra and Banerjee [9] for studying the dielectric constant of ionized air without magnetic field. A discharge-tube T (fig. 1), about 75 cm. long and of external diameter 3 cm., containing the ionized air was placed along the length of a Lecher wire system LL, and was completely surrounded by a coil to produce the required longitudinal magnetic field. The air inside the tube was ionized by high frequency discharge obtained from a valve oscillator. Two external electrodes EE were connected to the secondary coils, coupled to the tank inductance of the valve oscillator (not shown in diagram). The waves propagating through the ionized medium were generated by an ultra-short wave oscillator 0, producing

waves of lengths 2 to 4 metres. As the intensity of the wave emerging out from the discharge-tube is considerably reduced due to absorption, a system of Hertzian dipole aerial AA was used in the output of the ultra-short wave oscillator, as well as at the input end of the Lecher wires. B denotes the sliding metal bridge. The conductivity was determined from the knowledge of leakance per unit length of the Lecher wires, which was measured by the method employed by Banerjee [10] in connexion with the measurement of radiation resistance of transmission lines. The refractive index was found by the usual method from the values of wave-lengths in air and in the ionized medium. The values of collisional

Fig. 1.

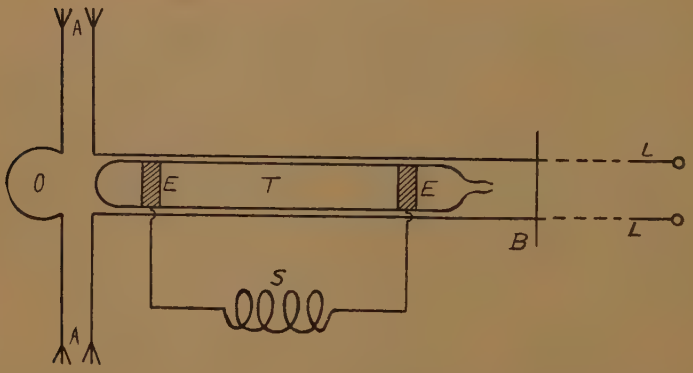

frequency (ν) and the electron density (N) were determined experimentally by the probe method of Mott-Smith and Langmuir [11] with the later modification by Banerji and Ganguli [12]. A separate tube was used for this purpose with the same dimensions as the former, fitted with two electrodes and containing inside it one hollow iron bobbin to measure the " collector " current. Frequency of the impressed wave was 81 megacycles per sec. The collisional frequency (ν) was $1{\cdot}2\times10^8$ per sec., and the electron density (N) was $2{\cdot}0\times10^7$ per c.c.

Table I. below gives the observed and calculated values of the conductivity and the square of the refractive index for the ordinary wave for different values of the magnetic field. Table II. gives the same for the extra-ordinary wave. The calculated values of the above

constants have been obtained from equations (7) and (8) in the previous section.

Curves A and B in fig. 2 show the variation of the conductivity of ionized air with the longitudinal magnetic field for the ordinary and extraordinary waves respectively. The curves with dotted lines are drawn from experimental

TABLE I.

Magnetic field in gauss.	Conductivity (σ) in e.s.u.		Square of the refractive index (μ^2).	
	Observed.	Calculated.	Observed.	Calculated.
0	$0{\cdot}28\times10^7$	$0{\cdot}22\times10^7$	0·81	0·77
9·6	0·26 „	0·13 „	0·82	0·83
21·7	0·20 „	0·07 „	0·84	0·86
28·9	0·17 „	0·06 „	0·86	0·88
43·4	0·15 „	0·04 „	0·87	0·89

TABLE II.

Magnetic field in gauss.	Conductivity (σ) in e.s.u.		Square of the refractive index (μ^2).	
	Observed.	Calculated.	Observed.	Calculated.
0	$0{\cdot}28\times10^7$	$0{\cdot}22\times10^7$	0·81	0·77
9·6	0·52 „	0·47 „	0·70	0·68
18·1	1·31 „	1·19 „	0·61	0·57
21·7	2·08 „	1·97 „	0·60	0·59
23·5	2·60 „	2·57 „	0·66	0·65
27·1	3·65 „	3·92 „	0·97	0·97
28·9	3·84 „	4·19 „	1·18	1·23
34·3	2·50 „	2·57 „	1·63	1·57
43·4	1·16 „	0·76 „	1·46	1·41

values and those with continuous lines from calculated ones. Fig. 3 represents similar curves for the square of refractive index of ionized air.

The following facts will be observed from the above curves. In the case of the ordinary wave (fig. 3, A) the square of the refractive index of ionized air increases slowly with the increase of magnetic field, and would assume its

maximum value of unity when the magnetic field attains infinite value. The conductivity for the corresponding wave, however (fig. 2, A), shows a gradual decrease when the magnetic field is increased, and it tends to become zero when the magnetic field approaches infinity. It may be added here that the general form of the above curves for an ordinary wave will not alter even if the approximate equations for the conductivity and refractive index,

Fig. 2.

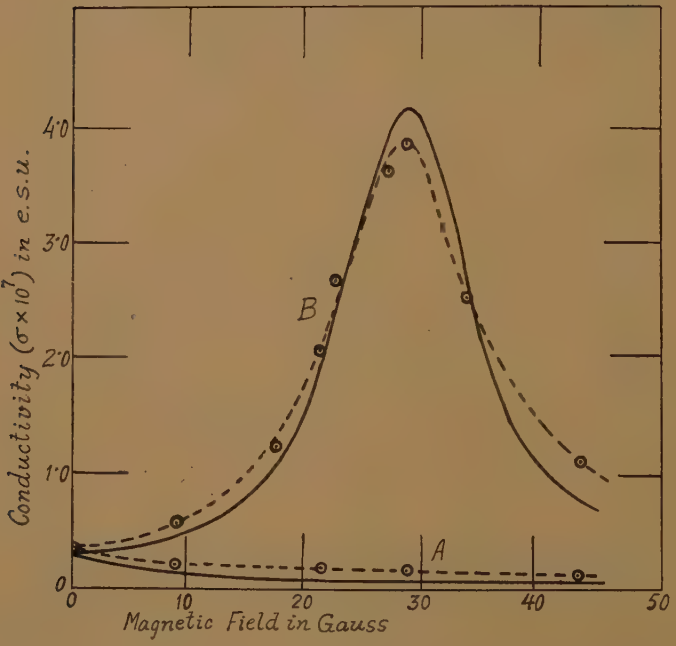

obtained by neglecting the collisional frequency, are employed for calculating their values. In the case of the extraordinary wave, on the other hand, it will be seen from fig. 3, B that the square of the refractive index decreases as the magnetic field increases, and, as the latter approaches the value of gyro-frequency of the wave, the former assumes a minimum value and then suddenly increases to a maximum. With further increase of magnetic field the square of refractive index

again gradually decreases, and would ultimately reach a value of unity when the magnetic field becomes infinity. The conductivity, as shown in fig. 2, B, gradually increases with the magnetic field, and attains a maximum value at gyro-frequency of the wave and then falls down. The nature of the curve on both the sides of gyro-frequency is identical. The important point which is to be noted in this case is that neither of the curves reaches infinity near about gyro-frequency of the wave. It may be

Fig. 3.

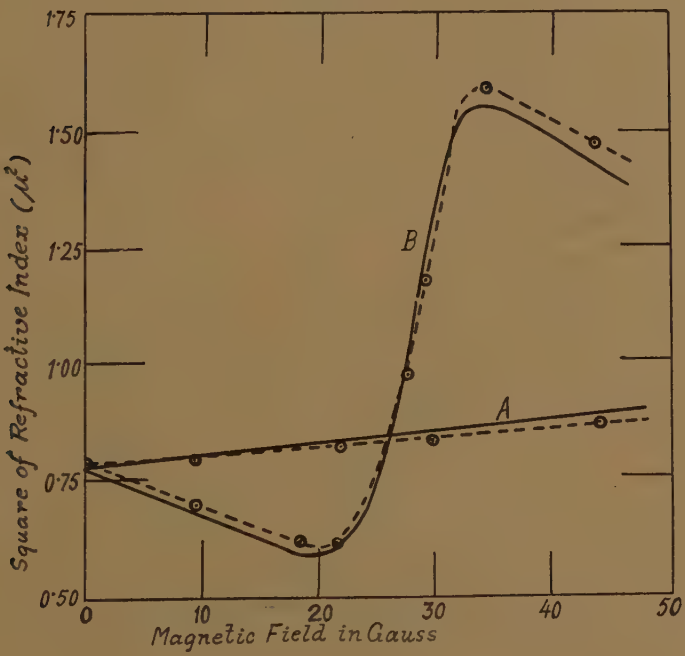

mentioned that for the extraordinary wave the values of the refractive index and conductivity should become infinity near the gyro-frequency of the wave if the collisional frequency be neglected and approximate equations be used. If, however, the complete equations be employed without neglecting the collisional frequency the observed curves agree fairly well with those drawn from theoretically calculated values.

Summary and Conclusion.

Conductivity and refractive index of ionized air have been determined in the presence of applied longitudinal magnetic field. The measurements were made with ultra short waves of frequency $8{\cdot}1 \times 10^7$ cycles per sec. passing through a discharge-tube containing the ionized air. Variations of the above constants were found as the magnetic field was increased. Complete dispersion formula of the ionized gas in the presence of the magnetic field has been employed for the purpose of verifying the experimentally observed values of the above constants. The values of electron density (N) and collisional frequency (ν) were determined by "probe" method of Mott-Smith and Langmuir. It has been found that the values of conductivity and refractive index do not reach infinity near about gyro-frequency of the incident wave when the magnetic field is increased, as is generally expected, from the approximate formulæ obtained by neglecting the collisional frequency.

In conclusion, the author wishes to express his deep sense of gratitude to Principal P. K. Dutt, M.A. (Cantab.), for giving him the facilities for carrying out the above work. He is also very grateful to his colleague Dr. S. S. Banerjee, D.Sc., for the keen interest which he took in the preparation of the present paper.

References.

(1) Appleton, E. V., Inst. Elec. Eng. lxxi. p. 642 (1932); Hartree, D. R., Proc. Camb. Phil. Soc. xxvii. p. 143 (1931); Goldstein, S., Proc. Roy Soc. A, cxxi. p. 259 (1928).
(2) Benner, S., *Naturwiss*, xvii. p. 120 (1929).
(3) Appleton, E. V., and Childs, E. C., Phil. Mag. x. p. 982 (1930).
(4) Gutton, H., *Ann. de Physique*, xiii. p. 62 (1930).
(5) Jonescu, V., and Mihul, C., *Jour. de Phys.* vi. p. 35 (1935).
(6) Appleton, E. V., and Boohariwalla, D. B., Proc. Phys. Soc. xlvii. p. 1074 (1935).
(7) Keck, P., *Ann. der Physik*, xv. p. 903 (1932).
(8) Mitra, S. K., and Ghosh, A. C., 'Nature,' cxxxvii. p. 68 (1936).
(9) Mitra, S. K., and Banerjee, S. S., 'Nature,' cxxxvi. p. 512 (1935).
(10) Banerjee, S. S., Phil. Mag. xix. p. 787 (1935).
(11) Mott-Smith, H. M., and Langmuir, I., Phys. Rev. xxviii. p. 727 (1926).
(12) Banerji, D., and Ganguli, R., Phil. Mag. xi. p. 410 (1931).

Physics Laboratory, College of Science,
Benares Hindu University.
March 14, 1938.

XXII. *Acoustical Insulation afforded by Double Partitions constructed from Dissimilar Components.*

By J. E. R. Constable, *M.A., Ph.D., B.Sc., Physics Department, National Physical Laboratory, Teddington, Middlesex* *.

[Received May 10, 1938.]

In a previous paper † the author has described a theoretical and experimental investigation of the sound transmission through a double partition constructed from similar components. It was shown there that the insulation at frequencies greater than the fundamental resonance frequency of the components is at first decreased as the separation is increased, but afterwards increases continuously up to a point at which the separation is approximately a quarter wave-length. After this point the insulation decreases to a second minimum, and thereafter minima occur at successive increases of a half wave-length in the separation. The first minimum, at which the insulation can be less than that of one component alone, arises from air coupling effects. The experiments, which were made with a double window glazed with 21 oz. glass, amply confirmed the theoretical results. Other investigators ‡ have made similar theoretical investigations, and Hurst has extended the theory to the case of a multiple partition constructed from a number of equally spaced similar components.

The properties of a double partition constructed from dissimilar components do not seem to have been examined except by Renault §, who has made an experimental and theoretical study of the particular case of a double partition used in railway coaches and constructed from two sheets of iron, one of which was twice as heavy as the other. He has demonstrated resonance effects which arise from air coupling and are similar to those obtained with partitions constructed from similar components.

It is often recommended that dissimilar components should be used in the construction of sound-insulating

* Communicated by Dr. G. W. C. Kaye.

† Phil. Mag. ser. 7, xviii. p. 321 (1934).

‡ E. Wintergerst, ‘ Schalltechnik,’ iv.–v. (1931); D. Hurst, Canadian J. of Research, xii. p. 398 (Mar. 1935); A. L. Kimball, J. Acoustical Soc. of America, vii. p. 222 (1936).

§ L. Renault, ‘ Revue d’Acoustique,’ vi. p. 69 (1937).

double partitions (particularly double windows), and it is of some importance therefore to investigate this point. In this paper is given the results of a theoretical investigation of such partitions. An experimental investigation has not been attempted as there are so many possible variables. The agreement between theory and experiment obtained by Constable in the case of double partitions made from similar components and by Renault in the special case in which one component was twice as heavy as the other encourage the belief that the theoretical results obtained below should be sufficiently accurate for practical purposes.

Calculation of Sound Transmission through a Double Partition constructed from Dissimilar Components.

In the following calculation of the sound transmission through a double partition constructed from dissimilar components the simplification is adopted of neglecting wave motion in the interspace between the two components. This is justified by the dimensions of the air spaces commonly met with and also by the fact that the additional minima arising from this wave motion appear to be experimentally negligible.

The two components are assumed to be connected by the air interspace only. They are treated as if each is a rigid piston having a single resonance, although, as is known experimentally * in practice, each leaf has a large number of resonance frequencies. The justification for this assumption is (1) that as far as causing pressure variations in the interspace is concerned the fundamental mode of vibration is likely to be very much more effective than the other modes, in which the panel vibrates in a form consisting of a number of areas separated by nodal lines, adjacent areas vibrating in opposite phase; (2) that this assumption has led to results which have been experimentally confirmed in the special cases of double partitions studied by Constable and by Renault.

For the purposes of the calculation the double partition (see figure) is supposed to be of infinite area, and the sound is supposed to consist of plane waves falling at normal incidence upon it.

* J. E. R. Constable and G. H. Aston, Proc. Phys. Soc. xlviii. p. 919 (1936); J. E. R. Constable, Proc. Phys. Soc. xlviii. p. 914 (1936).

Let

σ_1, σ_2 be the masses per unit area of the two leaves of the partition.

ω_1, ω_2 be the resonance pulsatances ($=2\pi\times$frequency) of the two leaves.

$\alpha_1=\sigma_1(\omega_1^2-\omega^2)$.

$\alpha_2=\sigma_2(\omega_2^2-\omega^2)$.

x_1, x_2 be the displacements of the two leaves.

$\beta=\Pi\gamma/d$=stiffness of air layer per unit area.

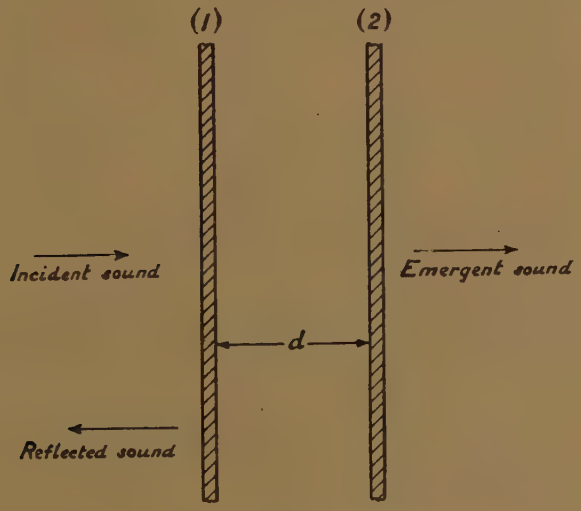

Π=atmospheric pressure.

γ=ratio of the two specific heats for air.

d=separation between the two leaves.

ρ=density of air.

c=velocity of sound in air.

y=displacement in the incident sound wave.

ω=pulsatance of incident sound.

The equations of motion of the two leaves are :—

Leaf 1.

$$\sigma_1\ddot{x}_1-2\rho c\dot{y}+\rho c\dot{x}_1+(x_1-x_2)\beta+x_1\omega_1^2\sigma_1=0. \quad . \quad (1)$$

Leaf 2.

$$\sigma_2\ddot{x}_2+\rho c\dot{x}_2+(x_2-x_1)\beta+x_2\omega_2{}^2\sigma_2=0. \quad . \quad . \quad . \quad (2)$$

Put $y=y_0e^{i\omega t}$, $x_1=X_1e^{i\omega t}$, $x_2=X_2e^{i\omega t}$,

we have

$$X_1\sigma_1(\omega_1{}^2-\omega^2)-2i\rho c\omega y_0+i\rho c\omega X_1+(X_1-X_2)\beta=0, \quad . \quad (3)$$

$$X_2\sigma_2(\omega^2{}_2-\omega^2)+i\rho c\omega X_2-(X_1-X_2)\beta=0; \quad . \quad (4)$$

whence $$X_1=\left(\frac{\beta+i\rho c\omega+\alpha_2}{\beta}\right)X_2. \quad . \quad . \quad . \quad . \quad (5)$$

Substituting (5) in (3), and reducing, the sound reduction factor R of the partition is given by

$$R=\frac{y_0{}^2}{|X_2|^2}$$

$$=1+\frac{\{\beta(\alpha_1+\alpha_2)+\rho^2c^2\omega^2+\alpha_1\alpha_2\}^2+\rho^2c^2\omega^2(\alpha_1-\alpha_2)^2}{4\rho^2c^2\omega^2\beta^2}, \quad (6)$$

which reduces to the formula obtained by Constable * for a double partition constructed from similar components if $\alpha_1=\alpha_2=\alpha$.

By differentiating it appears that the sound reduction factor passes through a minimum when the separation, d, has a value given by the formula

$$d=-\frac{\Pi\gamma(\alpha_1+\alpha_2)(\rho^2c^2\omega^2+\alpha_1\alpha_2)}{(\rho^2c^2\omega^2+\alpha_1{}^2)(\rho^2c^2\omega^2+\alpha_2{}^2)} \quad . \quad . \quad . \quad (7)$$

This value of d is positive provided

$$(\alpha_1+\alpha_2)(\rho^2c^2\omega^2+\alpha_1\alpha_2)$$

is negative, *i. e.*, α_1 and α_2 are both negative or, under certain conditions, that at least one of these quantities is negative. It cannot be positive if both quantities are positive. In other words, the sound reduction factor will pass through a minimum as the separation is increased provided the test frequency is greater than both resonance frequencies or, in certain circumstances, provided it is greater than at least one of the frequencies. There will not be a minimum if the test frequency is less than both resonance frequencies.

* J. E. R. Constable, *loc. cit.*

The actual value of the minimum is of some interest. By substituting in equation (6) it appears that the minimum value of the sound reduction factor is

$$R_{min}=1+\frac{(\alpha_1^2-\alpha_2^2)^2}{4(\rho^2c^2\omega^2+\alpha_1^2)(\rho^2c^2\omega^2+\alpha_2^2)} \quad . \quad . \quad . \quad (8)$$

It appears therefore that, in contradistinction to the behaviour of a double partition constructed from similar components, the insulation does not fall to unity when it passes through its minimum value. The minimum value is greater the greater the differences between the values of α for the two leaves. The values of α can, of course, differ either because the weights of the two leaves are different or because their resonance frequencies (*i. e.*, their stiffnesses) are different.

The above results indicate a possible advantage in using dissimilar components for the construction of a double partition. There is, however, another factor to be considered. The design of a double partition is usually subjected to overriding considerations of weight and thickness. The weight may be limited either for structural reasons or on account of cost; for example, it may be that the total sum which can be spent upon the glazing of a double window is limited, or, speaking roughly, the total weight of glass which can be used is limited. Similarly the thickness of a double window is often limited by practical considerations, for example, the thickness of the wall into which it is to be built. In the following calculation is determined the optimum relation between the weights of the two leaves of a double partition for a given thickness and total weight.

To simplify the mathematics various approximations have been used. These are:

1. that $\rho^2c^2\omega^2$ can be neglected in comparison with $\sigma_1^2(\omega_1^2-\omega^2)^2$ and $\sigma_2^2(\omega_2^2-\omega^2)^2$; and

2. that ω_1^2 and ω_2^2 are small compared with ω^2.

Both of these approximations seem to be justifiable save in exceptional circumstances.

(a) *Determination of the Relation between the Weights of the Components which make the Frequency of the Resonance due to Air Coupling a Minimum.*

Obviously one feature to aim at in the design of a sound-insulating double partition is that the frequency of the

air-coupling resonance should be low and, if possible, outside the range of frequencies against which insulation is required.

By using the approximations referred to above equation (7) can be reduced to

$$d=\frac{(\sigma_1+\sigma_2)\Pi\gamma}{\sigma_1\sigma_2\omega^2}.$$

If $\sigma_1+\sigma_2=\sigma$ (a constant), differentiation of the above expression shows that the minimum value of ω occurs when

$$\sigma_1=\sigma_2=\sigma/2,$$

i. e., when the two leaves are similar.

(b) *Determination of the Relation between the Weights of the Components which make the Insulation a Maximum for any particular Frequency and Separation.*

The other feature to aim at is that the insulation afforded by the partition shall be a maximum.

Equation (6) becomes, when the approximations referred to are used,

$$R=1+\frac{\{\beta\sigma\omega^2-(\sigma_1\sigma-\sigma_1^2)\omega^4\}^2+\rho^2c^2\omega^6(2\sigma_1-\sigma)^2}{4\rho^2c^2\omega^2\beta^2}.$$

By differentiation it can be shown that for frequencies greater than the frequency of the air-coupling resonance R has a maximum value when $\sigma_1=\sigma_2$, *i. e.*, when the two leaves are similar. For frequencies equal to or less than the air-coupling resonance frequency $\sigma_1=\sigma_2$ gives a minimum value of the insulation. Therefore, if insulation is particularly required at these low frequencies dissimilar partitions are advisable. The dissimilarity is only advisable, however, if insulation at higher frequencies is unimportant, and the extent of the dissimilarity depends upon the extent to which insulation at the higher frequencies can be dispensed with. If insulation at the higher frequencies is of no importance then the maximum dissimilarity is required, *i. e.*, a single leaf having the total allowable weight, if insulation at very low frequencies is necessary.

For overall insulation, however, it seems that a double partition is best constructed from similar components,

since this should give not only the maximum insulation at frequencies above the air-coupling resonance frequency, but also should make the air-coupling resonance occur at the lowest possible frequency.

These conclusions hold whether the intervening layer is air (as has been assumed for the purposes of the calculation) or any other elastic material. In this connexion mention may be made of experiments with double windows reported by Kreuger and Sager *, who were unable to find any advantage either in glazing the two components with different weight glass or in subdividing differently the component windows with glazing bars.

It should perhaps be pointed out that the calculations in this paper have been concerned only with the transmission of sound of air-borne origin. It is possible that the conclusions would need to be modified if impact sounds had to be taken into consideration.

Summary.

A theoretical investigation is made of the sound transmission through a double partition constructed from dissimilar components. It is shown that the insulation is to be expected to pass through a minimum as the separation between the components is increased, just as happens in the case of double partitions constructed from similar components. The sound reduction at the minimum increases as the dissimilarity between the components increases. On the other hand, for a given separation the frequency at which the minimum occurs is smallest, and the minimum, consequently, of least importance, when the components are similar. It is shown that at frequencies for which the resonances of the components and the air-coupling resonance can be neglected the insulation obtainable from a double partition of given total weight and thickness is greatest when the components are similar. It is concluded that double partitions are best constructed from similar components, and some experimental evidence in support of this is quoted.

* H. Kreuger and J. H. Sager, ' Proceedings of Royal Swedish Institute for Engineering Research,' no. 132 (1934). An abridged translation of this paper was given by J. E. R. Constable and K. M. Constable in ' Building,' March, 1937.

XXIII. *The Nernst Heat Theorem and Irreversible Processes at Low Temperatures.* *By* A. R. Ubbelohde, *M.A., B.Sc.(Oxon), Dewar Fellow of the Royal Institution* *.

[Received May 17, 1938.]

In a discussion of the "Thermodynamics of Irreversible Processes" (Ubbelohde, Trans. Far. Soc. xxxiii. pp. 599 & 1198 (1937)) it was suggested that the Nernst Heat Theorem might be extended to include physical processes which are irreversible in the thermodynamic sense. In view of the confirmation of this statement by the recently published experiments on the viscosity of liquid helium (Allen and Misener, 'Nature,' cxli. p. 75 (1938), *cf.* Kapitza, *ibid.*) it seems desirable to examine the suggested extension of the Heat Theorem in some detail.

The Application of Thermodynamics to Spontaneous Change.

According to the second law of thermodynamics a change can only take place spontaneously in an isolated system if it results in a decrease of free energy or an increase in entropy. The free energy dissipated in a spontaneous change ultimately appears as heat. From the Gibbs-Helmholtz equation

$$G-H=T\frac{dG}{dT}$$

(G is the change in free energy of a system in passing from one state to another, and H is the change in heat content), H may be measured in any process, whether reversible or irreversible, but unless G is measured in a reversible process some loss of free energy will take place. Inspection of the Gibbs-Helmholtz equation shows, however, that at 0° K G=H, so that there can be no free energy loss at 0° K., *i. e.*, no spontaneous change can take place in a system maintained at 0° K. This conclusion would in itself be rather trivial, on account of the unattainability of the absolute zero, but in the case of systems to which the Heat Theorem applies G∼H over

* Communicated by the Author.

a range of temperatures in the neighbourhood of 0° K., since for such systems

$$\mathrm{Lt}_{T\to 0}\frac{dG}{dT}=0.$$

This suggests that for such systems irreversible processes involving the conversion of free energy to heat must become highly improbable towards absolute zero.

An equivalent way of stating this conclusion is that since the entropy of systems obeying Nernst's Heat Theorem tends to a constant value towards absolute zero (this constant may be zero in certain methods of computing entropy, *cf.* Ubbelohde, 'Introduction to Modern Thermodynamical Principles,' p. 57) the probability of a spontaneous increase in entropy in such systems must become vanishingly small towards absolute zero.

The same conclusion may be reached by less direct but somewhat more informative reasoning. From the standpoint of thermodynamics a system is in equilibrium when small local fluctuations of density, average kinetic energy per molecule, or analogous quantities do not lead to a spontaneous change throughout the whole system. Quantitatively this is expressed by the equations

$$dG=0 \quad \text{or} \quad dS=0,$$

which state that at equilibrium the free energy of the system is a minimum, or the entropy is a maximum, with respect to small changes in the independent variables. In order to follow the application of thermodynamic reasoning to spontaneous changes it is essential to note that equilibrium is dynamic. Small local fluctuations are taking place all the time, but when these equations are satisfied the fluctuations do not on a time average lead to any change in the system. When the system is only slightly displaced from equilibrium these fluctuations will be practically the same in magnitude and in their time of relaxation. It follows from the second law of thermodynamics, however, that the result of a series of fluctuations in any one region must now be on a time average to lead to a decrease in free energy or increase in entropy of the system. The rate at which spontaneous changes of free energy or entropy can take place will depend both on the probability of finding a given fluctuation in the system and on its time of relaxation. Although

this time of relaxation can only be determined by the kinetic theory of the system, and not by thermodynamics, the probability of local fluctuations can be readily calculated as follows, from the entropy of the system :—

According to Einstein (*Ann. der Physik*, xxxiii. p. 1275 (1910)) the probability W′ of a local fluctuation of magnitude ΔS entropy units in any element of the system is given by the equation

$$W' = We^{\Delta S/k},$$

where the value of W is obtained from Boltzmann's equation for the entropy of the system,

$$S = k \ln W.$$

In systems which obey the Heat Theorem $S \sim 0$ over a range of temperatures in the neighbourhood of absolute zero, *i. e.*,

$$W \sim 1.$$

(It may be added that the H.T. zero (*cf.* Ubbelohde, *l. c.*) for entropy is correct in this instance, since in the theory of fluctuations only differences of entropy which can be measured are significant.)

In the neighbourhood of absolute zero the probability of a fluctuation of magnitude ΔS will thus be

$$W' = e^{\Delta S/k}$$

for systems obeying the Heat Theorem. Owing to the nature of the exponential function W increases very rapidly with small increases of S above zero, so that W′ likewise increases very rapidly. In other words, the probability of fluctuations in the neighbourhood of absolute zero is vanishingly small compared with the probability at temperatures where the entropy S is appreciable, and spontaneous processes involving an increase in entropy should become less and less probable as the entropy tends towards zero.

This point can be made clearer by a numerical illustration. Suppose we consider the fluctuations in a small region of a system containing 100 molecules. At temperatures where the entropy of the system is appreciable a convenient representative value for S may be taken to be $S = R \ln 2$ cals/°/mole $= 1{\cdot}37$ entropy units, *i. e.*, $S = k \ln 2$ entropy units per molecule, where k is Boltzmann's constant.

For this region the value of W would thus be

$$W = e^{100 \ln 2} = e^{69} \text{ approx.}$$

At a temperature where S has sunk to 1/100th of the above value, viz., 0·137 entropy units, the value of W will be $e^{0 \cdot 69}$. It follows that the probability of a fluctuation of magnitude ΔS will have sunk by the factor $e^{68 \cdot 3} = 10^{30}$ approx. No plausible increase in relaxation time with falling temperature can compensate for this enormous decrease in probability. The conclusion is again that the rate of spontaneous increase of entropy in systems whose entropy tends towards zero must likewise tend to zero. If the Nernst Heat Theorem applies to the system when in equilibrium it also applies to irreversible processes in the system, for which the displacement from equilibrium is small.

The use of Thermodynamic Variables in describing Irreversible Processes.

Before discussing experimental examples of the suggested extension of the Nernst Heat Theorem it is necessary to consider at least two limitations in its applicability. The first of these arises whenever attempts are made to calculate numerically the rate of dissipation of free energy or of increase of entropy, and is due to the fact that the relaxation time of a fluctuation is not in general independent of its magnitude. For example, in the conduction of heat in gases, the " hotter " molecules in any region lead to relatively more heat transport, and a numerical solution of the rate of increase of entropy has only been achieved by the kinetic theory of Chapman and Enskog. This limitation to thermodynamic reasoning has been referred to in previous papers, and does not affect its utility in indicating the general dependence of irreversible processes upon temperature and other thermodynamic variables. In particular it does not affect the applicability of the Heat Theorem at low temperatures, at which the decrease in probability of fluctuations would seem to outweigh any possible decrease of relaxation time.

A more important limitation in the applicability of the Heat Theorem arises from the fact that the use of thermodynamic variables, such as temperature, in describing

irreversible processes is never quite exact, in spite of the fact that some of the most precise secondary methods of measuring temperature depend on irreversible processes, as in platinum resistance thermometry. The scope of this limitation can only be discussed quantitatively in terms of the statistical mechanics of the various systems considered, but for the present purpose it is sufficient to illustrate it from practical examples in the measurement of temperature in irreversible processes.

One of the simplest of these arises in the conduction of heat in a gas at reduced pressures. The gas may be supposed to be bounded by two very large parallel walls at different temperatures, so as to secure a uniform flow of heat perpendicular to the walls. According to the usual analysis planes at any point in the gas parallel to the walls will be planes of "equal temperature." Owing to the fact that the conduction of heat is an irreversible process measurements of the "temperature" in any such plane will not in general be independent of the means selected for measurement. For example, the minimum disturbance of the heat conduction might be realized by using thin metal plates and measuring their lattice parameter accurately with X-rays, so as to infer the temperature in any one plane. The temperature such a plate would take up depends, however, on the accommodation coefficient a of its surface. Using the simple theory of Knudsen (*Ann. der Physik*, xxxiv. p. 593 (1911)), if T_1 is the "temperature" of molecules approaching the plate and T_2 the "temperature" of molecules leaving it, the temperature of the plate will be T_a, where

$$T_1-T_2=a(T_1-T_a).$$

For another plate with accommodation coefficient a'

$$T_1'-T_2'=a'(T_1'-T'_a).$$

Solving these equations,

$$T_a-T_a'=\frac{(T_1'-T_2')}{a'}-\frac{(T_1-T_2)}{a}+T_1-T_1'.$$

Furthermore, the heat transfer per unit area parallel to the walls is

$$Q=NC_v(T_1-T_2)=NC_v'(T_1'-T_2'),$$

where N is the number of molecules travelling toward

or away from the plate per unit area per second and C_v is the specific heat per molecule. Thus

$$T_a - T_{a'} = \frac{Q}{NC_v}\left(\frac{1}{a} - \frac{1}{a'}\right) + T_1 - T_1'.$$

Since a is not necessarily equal to a', the " temperature " observed at the plane will not be independent of the method of measurement except when $Q \to 0$ and $T_1 \sim T_2$, or alternatively when N becomes very large. In either case it follows that $T_a - T_{a'}$ only tends to zero, *i. e.*, the measurement of temperature in an irreversible process such as heat conduction only becomes independent of the means of measurement when the effective gradient per unit number of molecules is sufficiently small.

This conclusion cannot be avoided by selecting more refined measurements of " temperature." For example, it might be supposed that a measurement of the intensity distribution in the infra-red emission spectrum of the molecules could be used as a measurement of temperature with a minimum disturbance to the system, but in this case it would be necessary to assume that a sufficiently large number of molecules were approximately at the same temperature to make the temperature/intensity distribution formulæ valid in application. In general, the only valid measurement of temperature depends on the construction of a Kelvin heat-engine working between the two regions whose relative temperature is to be measured. Since the minimum amount of working substance in a heat-engine is a single molecule, the number of molecules in a region whose temperature is to be measured must be sufficiently large not to be appreciably disturbed by such a method of measurement. In general the use of temperature as a variable in describing any irreversible process is only justified when the displacement from equilibrium is sufficiently small. When the use of temperature is justified it becomes pertinent to enquire whether other thermodynamic variables can likewise be used in discussing the system with reasonable accuracy.

Experimental Examples of the Application of the Heat Theorem to Irreversible Processes.

Whenever it is possible to formulate an irreversible process as a spontaneous dissipation of free energy or

increase of entropy at a steady rate it becomes possible to verify the suggested extension of the Nernst Heat Theorem. Up to the present only a limited number of such processes have become of importance in low temperature physics, and may be briefly discussed as follows (*cf.* also other examples in Trans. Faraday Soc. xxxiii. pp. 599 & 1198 (1937)) :—

Electrical Resistance.

When a current C passes through a conductor the free energy dissipated per unit volume in unit time is C^2R, where R is the specific resistance. If the suggested extension of the Heat Theorem applies, this quantity should tend to zero at absolute zero. The quantity C is arbitrary, so that the specific resistance should tend to zero. As is well known, three types of behaviour are observed experimentally :—

(1) The resistance of pure strain-free metals decreases to zero in accordance with the above conclusion.

(2) The resistance of solid solutions and of cold-worked pure metals reaches a limiting value, and as far as is known does not decrease further. Such systems therefore fail to obey the suggested extension of the Heat Theorem. Although the reason for this can only be adequately discussed in terms of kinetic theory, it is interesting to note that the breakdown in the extension of the Heat Theorem is in parallel with the breakdown of the Heat Theorem applied to reversible processes in such systems. As is well known neither solid solutions nor glasses (a limiting case of cold-worked lattices) obey the Nernst Heat Theorem (*cf.* Ubbelohde, *l. c.* p. 42).

(3) Superconducting systems obey the proposed extension of the Heat Theorem by ceasing to dissipate electrical free energy altogether below a certain temperature. The nature of the fluctuations in such systems has been previously discussed.

Thermal Conductivity.

The relation between the coefficient of thermal conduction and the rate of increase of entropy per unit volume is in the simplest case (Ubbelohde, *l. c.* p. 605)

$$\frac{\partial S}{\partial t} = \frac{K}{T^2}\left(\frac{dT}{dx}\right)^2 = K\left(\frac{d \ln T}{dx}\right)^2.$$

This equation can only be expected to hold so long as the rate of increase of entropy per unit volume is small compared with the total entropy S, so that at low temperatures it may be expected to break down at progressively smaller values of $d \ln T/dx$. When it holds the extension of the Heat Theorem suggests the conclusion that $\frac{\partial S}{\partial t}$ must tend to zero towards absolute zero. In practice this could be realized in one of two ways. If $K \to \infty$ towards 0° K., it becomes impossible to establish finite temperature gradients in the system, so that the Heat Theorem might be obeyed. If, as is more likely, K does not tend to infinite values, then the conclusion is that for any process of heat conduction for which a " temperature gradient " has a physical meaning and for which the simple equation for heat conduction still applies K must tend to *zero* at absolute zero. The results described by de Haas (' Physica,' v. p. 321 (1938)) have hardly been carried to sufficiently small values of ln T to test this rather surprising conclusion.

Viscosity.

Although a quantitative theory of the viscosity of fluids is only possible on the basis of a kinetic theory of molecular motion, thermodynamic considerations (*cf.* Ubbelohde, *l. c.* p. 605) suggest that the dissipation of available energy as heat as the result of viscous drag must become highly improbable towards absolute zero in systems obeying the Heat Theorem.

In the simplest case the equation for the dissipation of available energy is $\frac{\partial A}{\partial t} = \eta \left(\frac{dV}{dx} \right)^2$, where $\frac{dV}{dx}$ is the velocity gradient. Since for solids by definition $\left(\frac{dV}{dx} \right) = 0$, solids automatically obey the extension to the Heat Theorem. If the system remains fluid, so that $\frac{dV}{dx}$ can be given finite values down to the lowest temperatures, the conclusion is that when the extension to the Heat Theorem applies η must tend to zero towards absolute zero. This behaviour would probably be shown by helium I, since, according to Simon (*Ergbniesse d. Exact. Naturwissenschaften*, p. 222

(1929)), liquid helium obeys the Nernst Heat Theorem. On changing to helium II the liquid practically ceases to dissipate energy by viscous drag, and is thus in complete accord with the extension of the Heat Theorem. Two points of interest in connexion with this behaviour are :

(1) When the flow becomes turbulent it is no longer possible to define the temperature of the system with accuracy, and the use of other thermodynamical variables is equally questionable.

(2) The thermodynamic behaviour of the system suggests some sort of regular structure in liquid helium II (*cf.* Simon, *l. c.*). If this suggestion is correct the fluctuations in this liquid must become cooperative, and the abrupt decrease in the rate of dissipation of available energy on changing from helium I to helium II is in complete accord with the general tendency of irreversible processes to decrease in rate in cooperative systems (*cf.* Ubbelohde, *l. c.* p. 1210).

Although further experimental evidence is required before the scope of the proposed extension of the Nernst Heat Theorem can be properly estimated, the conclusions are sufficiently interesting to support the attempt to classify irreversible processes at low temperatures from this point of view.

The Davy Faraday Laboratory,
The Royal Institution.

XXIV. *Kirchhoff Constraints and Sagittal Graphs.* *By* W. H. Ingram *.

[Received April 8, 1938.]

FROM the dynamical view-point the graph (*i. e.*, the topological diagram) of an electric net is regarded as a representation either (1) of the constraints on, or (2) of the orthogonality of, the coordinates according as they are, or are not, subject to conditions of constraint.

In the first case the line-segments of which the graph is composed have sense, in contradistinction to the second case. The two cases imply each other and usually are not distinguished ; however, we shall distinguish them by the adjectives *sagittal* and *neutral* respectively.

* Communicated by the Author.

The sagittal graph is not transformable to a geometrically different graph by any non-singular transformation of the dynamical variables (local currents), and does not exist for most variables thus related to the original, *e. g.*, variables related to the original by linear equations with irrational coefficients *.

On the other hand, the neutral graph may be transformed under certain circumstances to a geometrically different figure. For example †, the neutral graph N of the resistance matrix

$$R=\begin{bmatrix} 3 & -1 & 0 & -1 \\ -1 & 4 & -1 & -1 \\ 0 & -1 & 3 & -1 \\ -1 & -1 & -1 & 4 \end{bmatrix}$$

Fig. 1.

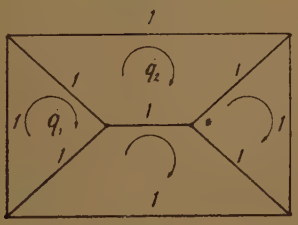

Fig. 2.

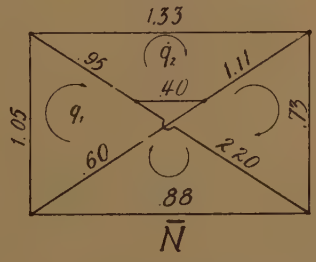

is transformed into the graph $\bar{N}$ of the resistance matrix $\bar{R}=A_t R A$ by the transformation of variable of matrix

$$A=\begin{bmatrix} 1 & 0 & 0 & 0 \\ 0 & 1 & 0 & 0 \\ 0 & 0 & 1 & 0 \\ 0 & 0{\cdot}35 & -0{\cdot}4 & 1 \end{bmatrix}.$$

* Corresponding to every sagittal graph there is an *incidence matrix* (Veblen, ' Analysis Situs,' p. 11) or *incidence table* (Tucker, ' Electrical Engineering,' May 1937, p. 619), but not every incidence table has a graph, *e. g.*, the incidence table resulting from a change of terminal-basis almost always has no graph. Hence any mathematical treatment so broad as to be free of specific coordinates (*i. e.*, a tensor treatment) is correspondingly devoid of physical meaning.

† I am indebted to Dr. Ronald M. Foster for this example. No similar example exists for neutral garphs of nullity 3 or less.

The forces exerted by the environment on any dynamical system have a sign agreeing with or opposite to the signs of the local velocities according as they are active or reactive; in the sagittal graph the external forces may be represented by auxiliary arrows as in fig. 3 or fig. 4*, where the sagittal graph of a Wheatstone bridge is represented.

Forces of constraint are represented in a similar way in the *extended graph* obtained by arbitrarily selecting one vertex of a sagittal graph, then called the *ground point* or *ground*, and connecting all remaining vertices thereto by *Lagrangean connexions*, thought of as perfect conductors without inductance or capacity, in which the forces of constraint may be assumed to act. The extended graph of fig. 4 is shown in fig. 5.

Fig. 3.

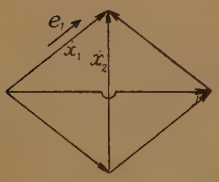

Fig. 4.

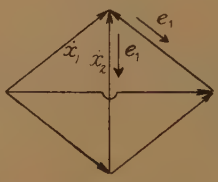

Fig. 5.

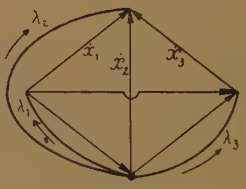

By reference to Listing's formula † for the cyclomatic number ‡ it is seen that the number of Lagrangean connexions is exactly the number of constraints. The constraints represented by the vertices have the form $\Sigma\alpha_{jk}\dot{x}_k=0$ $(k=1,\ 2\ldots n)$, where the α's are 1, -1, or 0 according as the kth current enters, leaves, or avoids the jth vertex. The corresponding forces of constraint $\frac{\partial}{\partial\dot{x}_j}\left(\sum_k \lambda_k\left(\sum_l \alpha_{kl}x_l\right)\right)$ may be thought of as acting in the

* The theorem that a plurality of forces each of magnitude e_1 acting as indicated in fig. 4 are equivalent to the force e_1 acting as indicated in fig. 3 is due to T. H. Blakesley, Phil. Mag. cciii. p. 448 (1894). If we call this a *Blakesley step* and cancel arrows meeting head on, we have the theorem that in any graph V forward steps are necessary and kV sufficient to restore any original force regime, V being the number of vertices and k any natural number.

† Listing, 'Census räumliche Komplexe,' Göttingen, 1862; also Dehn-Heegaard, 'Encyklopädie,' iii. AB, 3, p. 171.

‡ *I. e.*, "nullity," in the terminology of Hassler Whitney; *vide* "Geometric Circuits of Electrical Networks," by R. M. Foster, Trans. Am. Inst. El. Engrs. li. p. 309 (1932).

Lagrangean connexions to preserve the Kirchhoff conditions at the vertices. The Lagrangean multipliers λ_k come out, numerically at least, the potentials of the vertices with respect to ground.

That the independent currents (dynamically generalized velocities) associated respectively with the chords to any tree in the sagittal graph are circuital has been understood since the time of Kirchhoff and Listing. With the extended graph in mind, we have the more general THEOREM: *All currents are circuital.* *Proof*: We need only note that the Lagrangean connexions form a tree with respect to which the sagittal graph is a system of chords, n in number. Hence there are n, one for each chord *, independent circuits in the extended graph, and currents represented in the sagittal graph are circuital.

Suppose that the current x_1 does not appear in any of the equations of constraint. We introduce the redundant variables y_1 and z_1 and write down, as is always possible,

$$\left.\begin{aligned} \dot{x}_1 - \dot{y}_1 &= 0 \\ \dot{y}_1 - \dot{z}_1 &= 0 \\ \dot{z}_1 - \dot{x}_1 &= 0 \end{aligned}\right\},$$

a system of constraints whose sagittal graph is a triangle. Since, in this case, the cyclomatic number is unity, we have

$$\left.\begin{aligned} \dot{x}_1 &= \dot{q}_1 \\ \dot{y}_1 &= \dot{q}_1 \\ \dot{z}_1 &= \dot{q}_1 \end{aligned}\right\},$$

a non-singular transformation to the current $\dot{q}_1$ flowing in the closed circuit of the triangle. The equations of constraint are seen to be identities, hence $\dot{x}_1$ flows in a closed circuit.

Our more fundamental viewpoint thus leads to a proof of a proposition generally accepted as a postulate, namely, that currents not subject to Kirchhoff's law flow in circuits.

* *Cf.* Ahrens, *Math. Annalen*, xlix. p. 311 (1897). By *chord* is meant any one of a system of line-segments left after the abstraction of a tree.

XXV. *Sensitivity of the Immersed Venturi-Pitot Head at Low Speeds.* *By* C. Salter, *M.A., of the Aerodynamics Department, National Physical Laboratory* *.

[Received April 29, 1938.]

Introduction.

THIS paper deals with experiments designed to improve the sensitivity of a small-size Venturi combined with a total head tube, and to discover whether such an instrument would prove satisfactory as a standard low-speed anemometer.

The lack of sensitivity of the Pitot static tube at speeds below about 12 feet per second makes it an instrument inconvenient to use at those speeds, although it is a suitable laboratory standard against which low-speed anemometers can be calibrated. The low-speed vane anemometer calibrated in this way is extremely useful, but, unfortunately, somewhat delicate, and is damaged if subjected to an excessive wind speed. Consequently a more robust instrument would prove most useful provided it fulfilled the demands of consistency and convenience and its calibration were not appreciably affected by slight changes in wind direction.

The simple Venturi combined with a total head tube is not so convenient as the vane anemometer in that it requires the use of a Chattock or similar gauge, but it can be made to give a pressure difference of many times that of the Pitot static tube at speeds of the order of 10 feet per second.

Unfortunately the immersed Venturi is subject to a considerable scale effect such that at low Reynolds numbers there is a tendency for the air to flow round it instead of through it, but this effect depends not only on overall size, but also very largely on particular dimensions. It has long been known that a small Venturi is much less sensitive than a large one at a given wind speed.

Previous investigations into the characteristics of immersed Venturis are somewhat limited, and mainly confined to comparatively high wind speeds. The experi-

* Communicated by E. F. Relf, F.R.S.

ments of Piercy and Mines[1] at 40–45 feet per second showed

(*a*) that straight-tapered cones were better than those having a conoidal internal shape ;
(*b*) that external streamlining was undesirable ;
(*c*) that the contraction ratio of the entry was critical, with a value of about four for straight-tapered cones ;
(*d*) that the venturi should be short.

In the experiments described below it has not been assumed that all these deductions apply at low wind speeds although, owing to the large number of variables involved, some limitation had to be placed on the range of the investigation.

Bourdon[2] in 1882 described a triple venturi for use in measuring wind speeds of ventilation in mines.

Further information was obtainable from Messrs. Reid and Sigrist, who provided the venturis used for the tests. They were able to point out that the reduction in pressure at the throat depended largely on the sharpness of the edge just upstream of the suction gap at speeds of 60–10 miles per hour. Also that a Townend ring fitting round the entry had a considerable effect on the sensitivity, although its position was critical.

Range of Investigation.

Experiments were carried out on a series of Venturi-Pitot heads fitted with detachable inlets, and it was decided that the overall size of the venturi should not be more than about one inch in maximum diameter and about four inches in length, while wind speeds were confined to the range 0–10 feet per second, all speeds referred to in the paper being equivalent dry-air speeds at normal temperature and pressure (15·6° C. and 760 mm.).

The sensitivity of the instruments with the various modifications is expressed in terms of the readings of a 13-inch Chattock gauge, which are proportional to the pressure difference arising between the total head tube and the venturi throat. These readings can be converted to inches of water by multiplying by the factor 0·00065.

Fig. 1 (*a*) is a sectional drawing of the instrument finally constructed, and designated V.P.H. 6. In this figure some

of the dimensions are indicated by letters in order that the dimensions of the other two instruments V.P.H. 1 and V.P.H. 5, which, with V.P.H. 6, were used for all except the preliminary experiments, might be conveniently tabulated. This is done on the same figure.

Fig. 1.

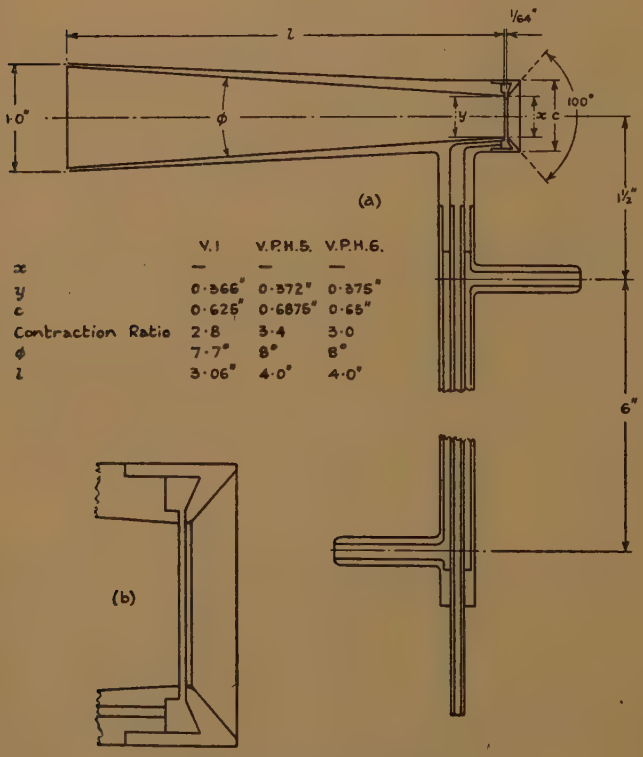

	V.1	V.P.H.5.	V.P.H.6.
x	—	—	—
y	0·366"	0·372"	0·375"
c	0·625"	0·6875"	0·65"
Contraction Ratio	2·8	3·4	3·0
ϕ	7·7°	8°	8°
l	3·06"	4·0"	4·0"

Sectional drawing of V.P.H. 6.

Fig. 2 is a sectional drawing of a typical Venturi, drawn on an exaggerated scale to illustrate those dimensions, changes of which were considered in so far as they affected the pressure at the throat. These may be listed as follows :—

1. Width of annular suction gap at the throat, g.
2. Sharpness of the leading edge of the inlet, f.

3. Sharpness of the edges adjacent to the suction gap, e and h.
4. Angle of inlet cone—θ.
5. Shape of inlet cone.
6. Contraction ratio of inlet.
7. Length of expansion, l.
8. Angle of taper of the expansion, ϕ.
9. Relation of diameters at the throat, x and y.

Experiments were also made to examine the effect of fitting a Townend ring round the forward portion of the venturi and of inclining the instrument at various angles to the wind direction. Finally, an attempt was made to examine the consistency over a long period of the pressure differences generated from day to day as the prevailing air density varied with atmospheric conditions.

Fig. 2.

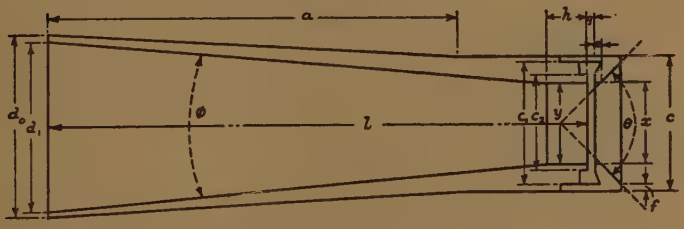

Typical Venturi.

Results.

Width of Suction Gap at Throat.

Preliminary tests showed that the width of this gap, if small, was not critical; it was therefore standardized at 1/64 inch.

Sharpness of Leading Edge of Inlet: Characteristic of Edges adjacent to Gap.

It was found and confirmed on several occasions that the leading edge of the inlet should be fairly sharp in order to ensure the greatest reduction of pressure at the throat. On the other hand, a thin cylindrical extension fitted round this edge so as to project upstream resulted in no improvement whatever.

The form of the edge e on the upstream side of the gap is a most important factor in affecting the sensitivity

of the instrument. The suction at the throat is greatest when this is a sharp knife-edge. As, however, such edges are undesirable in an instrument of this type, it is better

Fig. 3.

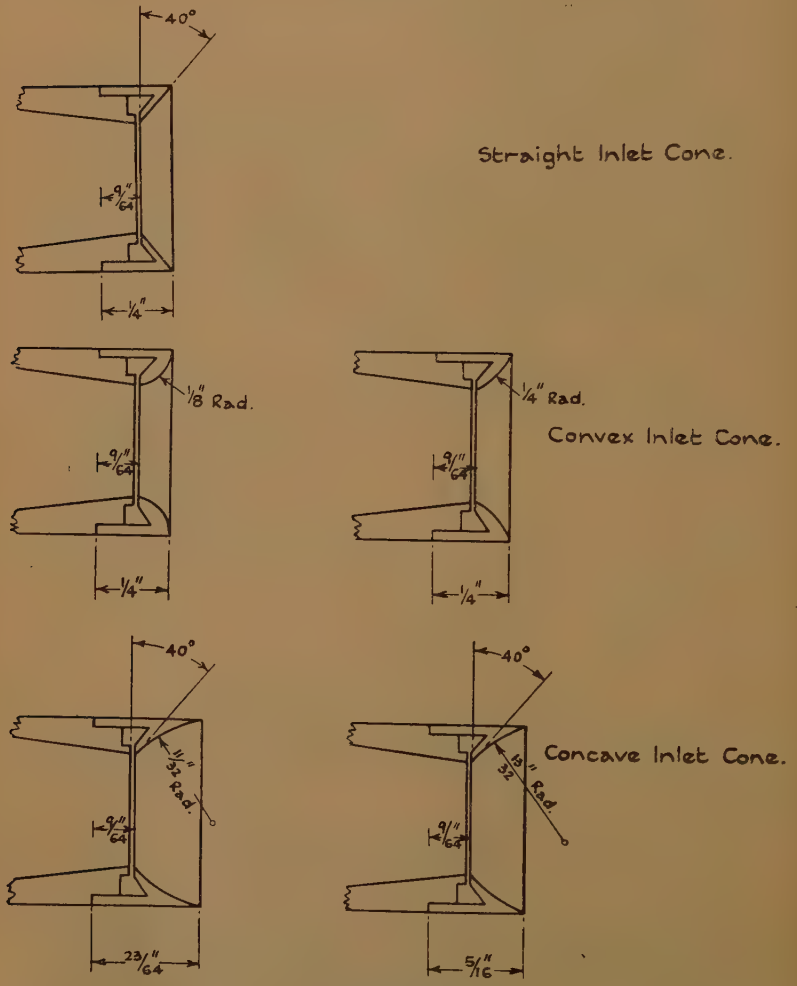

Twice full scale.
Details of inlets,

to turn down these parts to a thickness of about 0·003 inch, the angle between the inlet taper and the short cylindrical face just upstream of the gap being then

rounded off. The shape of the inlet then becomes something like that drawn in fig. 1 (*b*) to an exaggerated scale. Although the net result is an appreciable decrease in sensitivity from the best obtainable, this decrease is not excessive.

On the downstream side the expansion should commence immediately after the throat, in which case the dimension h in fig. 2 will be zero.

Angle of Inlet Cone.

The angle of the inlet cone in cases where the conical surface has a constant taper depends to some extent on the diameters x and y immediately upstream and downstream of the suction gap respectively. In general where e is sharp and $x > y$, θ should be about 110° ; if $x = y$, θ should be about 100° ; and if $x < y$, θ should be about 90°. These angles, however, are only approximate, and if the edge e is not quite sharp are even less critical.

Curvature of Inlet.

It was originally intended to confine the investigation to cases where both the internal inlet and expansion

TABLE I.

Radius.	1/8 in. convex.	1/4 in. convex.	Straight.	13/32 in. concave.	11/32 in. concave.
Ft./sec.					
8	70	78	105	92	90½ divisions.
10	125	143	176½	165	160½ „

cones were straight-sided. Other inlets were, however, made and tested on the head V.P.H. 1. These have the sections shown in fig. 3, in which are illustrated one with a straight inlet cone, two with cones having convex radii of curvature of 1/8 and 1/4 inch respectively, and two with concave radii of 11/32 and 13/32 inch. In each case the loss of sensitivity compared with that obtained with the straight-sided cone was very considerable, and is indicated in Table I. at the two speeds of 8 and 10 feet per second. It is deduced therefore that it is unlikely that the straight inlet can be improved upon.

Contraction Ratio of Inlet.

Using Venturi-Pitot head V.P.H. 1 three sets of curves were obtained, and are given in fig. 4 to illustrate the

Fig. 4.

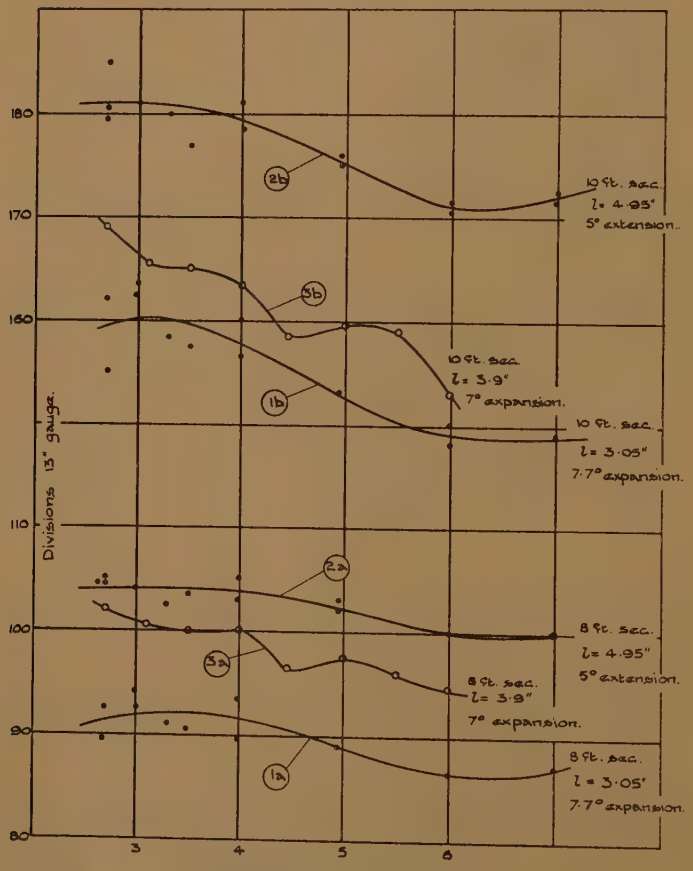

Contraction ratio of inlet.

Effect of varying contraction ratio of inlet.

effect of variations in the contraction ratio $\left(\frac{C^2}{x^2}\right)$. In order to obtain these curves detachable inlets were made of large outside diameter which could be reduced step by step by turning off surplus material in a lathe. These inlets were faired into the body of the Venturi with

plasticine, and contraction ratios varying from 2·7 to 7 were easily obtained.

In the figure curves 1 *a* and 1 *b* show at 8 and 10 feet per second respectively the variation of sensitivity with contraction ratio for the otherwise unmodified instrument,

Fig. 5.

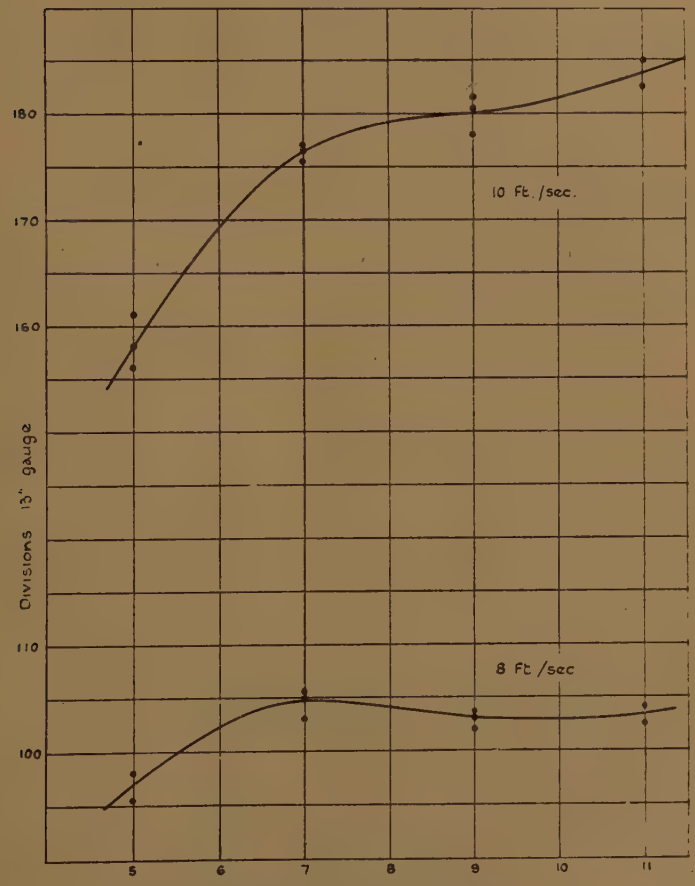

Effect of varying angle of expansion.

the length l of the head measured from the suction gap to the tail being 3·06 inches and the angle of expansion being 7·7°. Curves 2 *a* and 2 *b* are similar curves when l=4·95 inches, an extension of 5° taper being in this case

fitted to the tail in order to increase the value of l. 3 *a* and 3 *b* refer to the case where $l = 3{\cdot}9$ inches, the original expansion cone being removed and replaced by another with a 7° internal taper. Although these curves show no very critical value of the variable, a contraction ratio

Fig. 6.

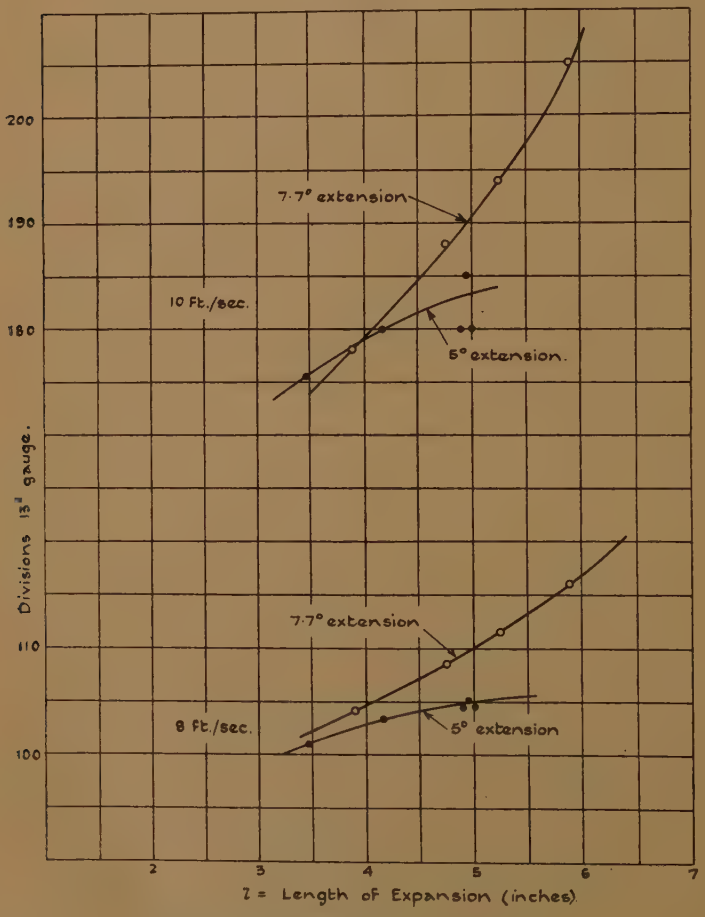

Effect of varying length of expansion.

of 3 is probably as good as any. It is, incidentally, not convenient to construct such an instrument with a ratio much less than this. It is, furthermore, found that at lower speeds still the actual ratio is even less important.

The curves can also be used to confirm that a long expansion is advantageous in respect of improvement of sensitivity.

Angle of Taper of Expansion.

After removing the original expansion cone of V.P.H. 1, others were fitted having various lengths and tapers in order to find the optimum values, if any, of these two variables.

TABLE II.

V.P.H. 5.

x....	·370	·371	·372	·373	·374	·375	·376	·377	·378
Ft./sec.									
2·5	5·3	5·5	5	5	5	5	5	5	5
3	8	8	7·5	7·5	7·5	7·5	7	7	7
4	17·3	17	16·5	16	16·5	15	14·5	14	14
6	47·5	49	48	48	47·5	46	44·5	42·5	42
8	91·5	98	98·5	100	100	99	96	91·5	92
10	145·5	159	163	169	170	174	170	163	167·5

TABLE III.

V.P.H. 6.

x.....	·372	·373	·374	·375	·376	·377	·378	·379
Ft./sec.								
2·5	5·5	5·3	5	5	5	5	5	5
3	8·5	8	8	8	7·5	7·5	7·5	7
4	17·5	16·5	16·5	15·5	15·5	15	15	14·3
6	47	48·7	49	47	47	46	46	44·7
8	89·5	96	101	99	100	101	100	98·5
10	140	152·7	164	168	170	176	177·5	177·5

The relative importance of the taper of the expansion is illustrated in fig. 5, where sensitivity is plotted against this taper in degrees, the total length of the Venturi in this case being kept approximately constant at about 4 inches. There is little variation over the range 7° to 11°, although a considerable drop occurs at 5°, this applying both at 8 and 10 feet per second. It is found, however, that the pressure differences are rather less steady at large angles, so that one might suggest 8° as being the best total included angle of expansion.

Length of Expansion.

In fig. 6 are drawn curves to show the effectof lengthening the Venturi V.P.H. 1 by extending the tail. In one

Fig. 7.

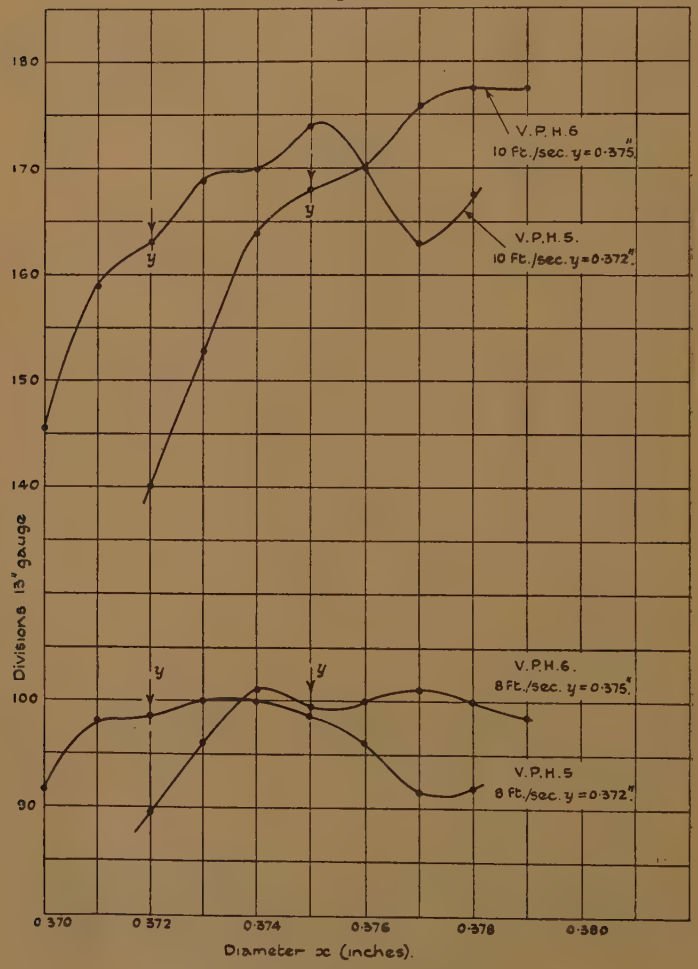

Effect of varying throat-diameters.

case the extension had an internal taper of 5°, in the other 7·7°, and lengths plotted as abscissæ refer to the length of the expansion measured from the suction-gap. It is seen that the sensitivity increases continuously with

the value of l, slowly in the case of the 5° extension, and rapidly when this has a taper of 7·7°. The expansion cone should therefore be made as long as possible. In addition, it was found that the sharpness of the trailing edge was not critical, so that this may be made sufficiently thick to be safe from accidental damage.

Relation of Diameters at the Throat.

A series of experiments was carried out on heads V.P.H. 5 and V.P.H. 6, with the form of inlet illustrated in fig. 1 (*b*), where the edge is not quite sharp and is rounded as explained above, in order to determine the best relation between the two diameters at the throat immediately upstream and downstream of the gap. The results of these experiments are very interesting, and are given in Tables II. and III. (p. 281) and fig. 7.

In fig. 7 curves are drawn as usual for the two speeds of 8 and 10 feet per second, giving the variation in sensitivity with this relation. x is the diameter in inches at the throat of the nearly sharp edge just upstream of the gap, and y is the diameter on the downstream side. In the two cases $y=0{\cdot}372$ inch and 0·375 inch respectively and x is the variable. At 10 feet per second the best value of x is about 0·003 inch greater than y for both heads. At 8 feet per second the corresponding relation is x greater than y by 0·001 inch for V.P.H. 5, although with the other head the relation is doubtful but not critical. The tables, however, show that at lower speeds this relation is no longer true, and x should be less than y by about 0·001 or 0·002 inch. As the sensitivity, therefore, is already ample at the two higher speeds, it is suggested that x should be made less than y by about 0·001 inch in order to get better overall performance, but the values actually employed must evidently depend largely on the speed range in which one is interested.

The curves of fig. 7 also show that the maximum sensitivity obtainable with V.P.H. 6 (contraction ratio 3·0) is slightly greater than that given by V.P.H. 5 (contraction ratio 3·4).

Effect of Townend Rings.

Fig. 8 illustrates two approximately streamlined rings which were supported in turn in various positions around

and upstream of the forward end of the Venturi V.P.H. 1. The dimensions of the rings were respectively :

7/8 in. inside diameter ; 1/16 inch thick ; 1/4 in. long.
3/4 „ „ „ ; 3/64 „ „ ; 3/16 „ „

Fig. 8.

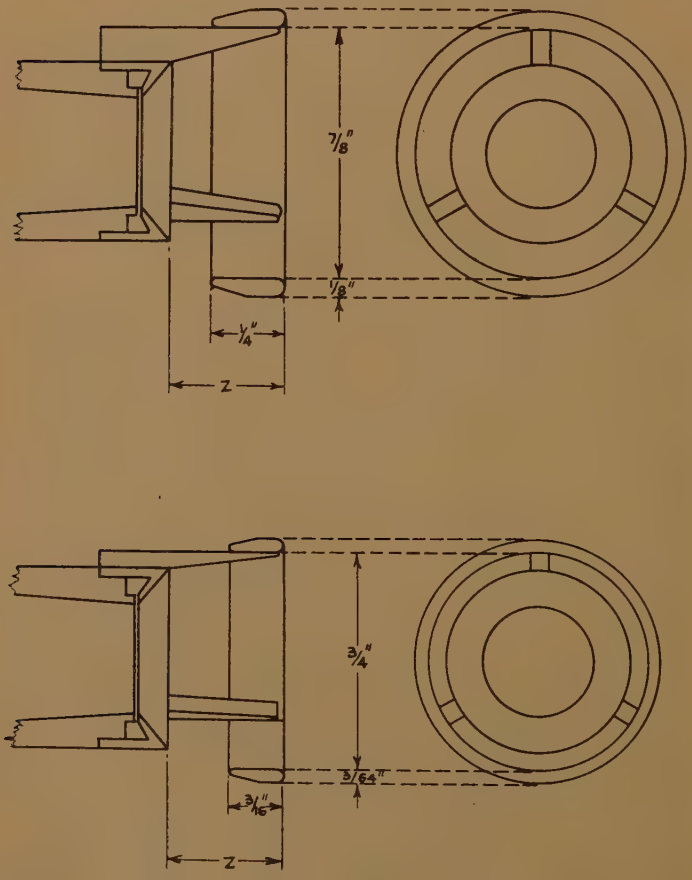

Twice full scale.

Details of Townend ring.

They were held in position by three prongs as shown, soldered to the detachable inlet, these prongs being suitably reduced in length as the rings were drawn backwards. The position of the rings was defined by

the distance z between the leading edges of the ring and of the venturi, and sensitivities, obtained at 8 and 10 feet per second, are plotted in fig. 9, on which is also indicated the result when the rings and prongs were removed. These curves show that the gain due to the

Fig. 9.

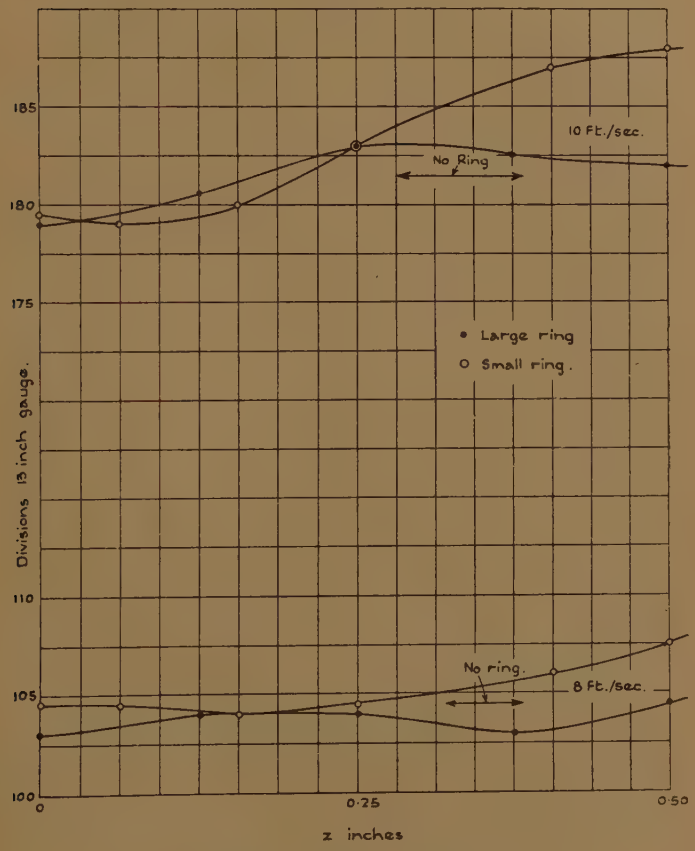

Effect of fitting Townend rings

rings, although small, is appreciable, but is only obtained by fitting the ring at an inconvenient distance (about $\frac{1}{2}$ inch) ahead of the inlet in a position, where it is, of course, liable to be damaged or distorted. It is therefore considered that the Venturi head cannot be satisfactorily improved by the employment of such a ring.

Further experiments with V.P.H. 6 related to the variation of sensitivity when the axis of the head was rotated

Fig. 10.

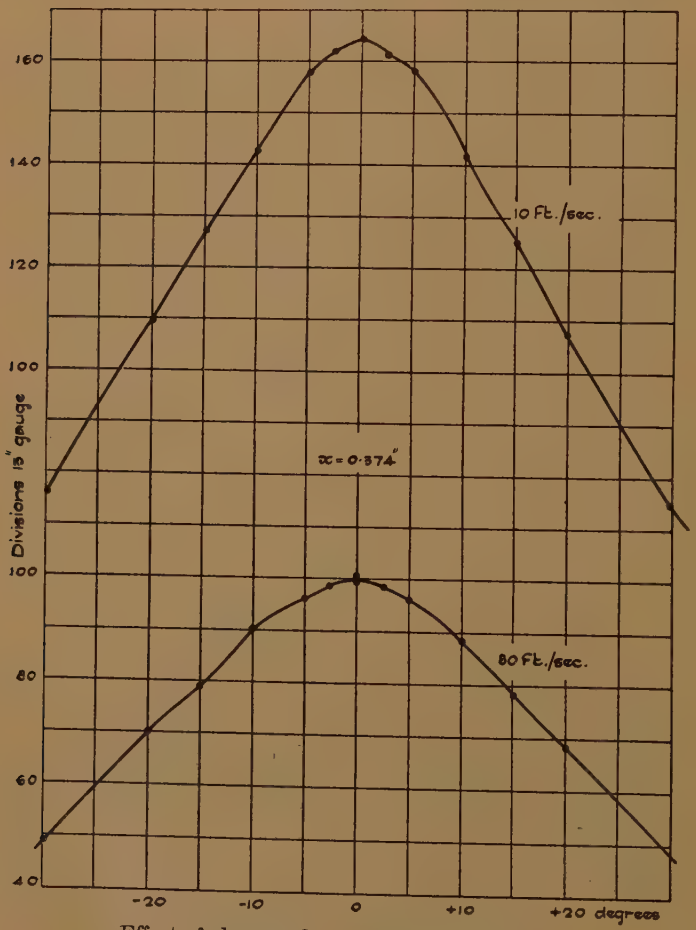

Effect of change of wind-direction, V.P.H. 6.

so as to be inclined to the direction of the air-stream. Typical curves are given in fig. 10 for a value of the diameter x of 0·374 inch, and other observations gave similar results. It is seen that the wind-direction is of considerable importance and the permissible tolerance

TABLE IV.

V.P.H. 6.

Ft./sec.	13-inch gauge and Pitot static tube.	$x=0{\cdot}375$	Approximate relative sensitivity.
2·5	2·2	5·1	2·3
3	3·15	7·6	2·4
4	5·6	15·5	2·8
6	12·6	47·2	3·7
8	22·4	99·75	4·4
10	35	167·75	4·8

Fig. 11.

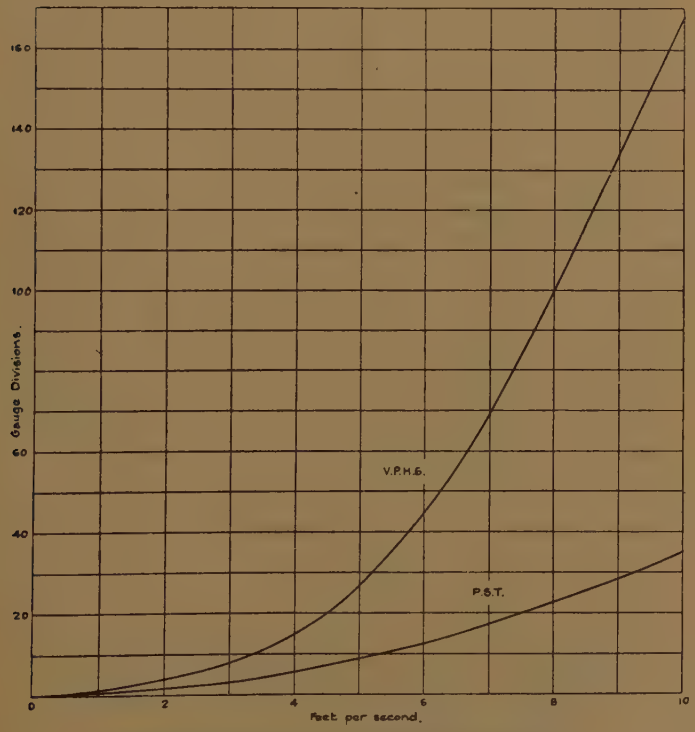

Comparison of V.P.H. 6 with Pitot static tube.

in the alignment of the head is very small. This constitutes a serious weakness in respect of the use of the instrument as a low-speed anemometer.

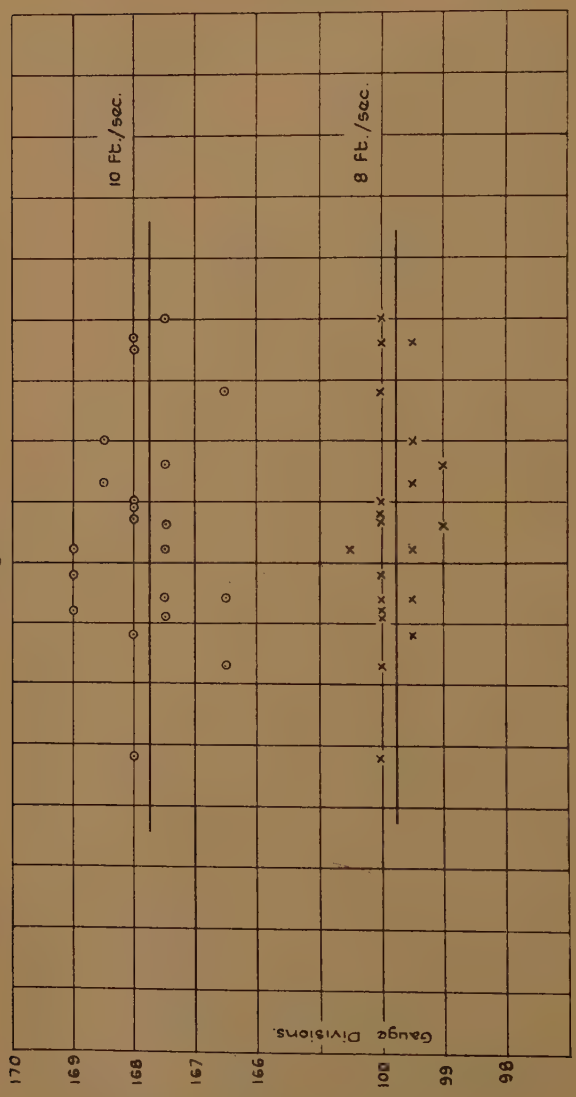

Fig. 12.

Comparison with Pitot Static Tube.

Table IV. indicates the approximate relative sensitivities of the Venturi-Pitot head V.P.H. 6 ($x=0{\cdot}375$ inch) and the Standard Pitot static tube. At 10 feet per second the

former gives nearly five times the pressure difference generated by the latter. The ratios become, however, progressively less at lower speeds, but could be increased at all speeds by the modifications indicated above, only, however, at the expense of compactness and robustness. The gain is further illustrated in fig. 11.

Consistency of Pressure Differences.

It was fortunately found convenient to check the calibration of instrument V.P.H. 6 over a fairly long period during which air-densities varied from 0·974 to 1·01 relative to dry air at 15·6° C. and 760 mm. pressure. In this case the value of the diameter x was 0·375 inch.

The readings obtained are plotted in fig. 12, whence the mean readings at 8 and 10 feet per second can be estimated at 99·75 and 167·75 gauge divisions, with maximum variations of 0·7 and 0·75 per cent. respectively. At lower speeds the variations were greater, but the accuracy of measurement with the apparatus available considerably less. There seems to be no consistent change which could be said to depend on air-density, and the variations are of the same order as for the Standard Pitot static tube at these speeds. It was on one occasion found that a slight smear of grease on part of the face of the inlet cone caused quite a large decrease in sensitivity, but no other likely cause of the variations was noticeable during the tests.

Although it must finally be concluded that the instrument is not really suitable for use as an accurate standard low-speed anemometer, the information obtained during the course of the experiments may prove useful in other directions.

References.

(1) Piercy and Mines, "On the Immersed Venturi, with Special Reference to its use on Aircraft for Purposes of Power Transmission." R. & M. 664.

(2) E. Bourdon, " Sur un Anémomètre Multiplicateur applicable à la Mesure de la Vitesse du Vent dans les Galeries des Mines." *Comptes Rendus de l'Académie des Sciences* (Paris), 1882, p. 229.

(3) M. L. Aguillon. " Note sur les Appareils de Contrôle et de Surveillance de l'Aérage des Mines." *Annales des Mines*, 7 Série Tome xx. 1881.

(4) Stewart, ' Aircraft Instruments.'

XXVI. *Generalization of the Theory of Electrical Discharges.* *By* J. S. Townsend, *Wykeham Professor of Physics, Oxford, and* E. W. B. Gill, *Fellow of Merton College, Oxford* *.

[Received June 13, 1938.]

1. ACCORDING to the general theory † of the actions of electrons and positive ions in discharges which was given many years ago, the supply of electrons required to maintain a direct current discharge between electrodes in a gas is provided by the ionization of molecules of the gas by the collisions of electrons and positive ions and by the emission of electrons from the negative electrode by the impacts of positive ions.

In direct currents of positive electricity from points or the positive corona discharges from wires, where the positive ions approach the negative electrode under the action of a small electric force there is no appreciable emission from the negative electrode when the ratio of the force to the pressure of the gas is below a certain limit.

In oscillatory discharges the current may be maintained by the ionization of molecules by the collisions of electrons, when the force is so small in all parts of the gas that there is no appreciable supply of electrons by actions of positive ions.

This general theory was originally based on the results of a large number of experiments which were made to determine the coefficients of ionization of electrons and positive ions, and it has since then been confirmed by other direct experiments ‡.

Other theories have also been proposed, but it has been shown that they are not in accordance with many properties of the currents §.

2. In direct currents between electrodes it is necesssary in order to start the discharge to have a certain minimum potential between the electrodes which is the sparking

* Communicated by the Authors.

† 'Electricity in Gases,' Chapters IX. and X.

‡ J. S. Townsend and F. Llewellyn Jones, Phil. Mag. xii. p. 282 (Feb. 1933). J. S. Townsend and G. D. Yarnold, Phil. Mag. xviii. p. 594 (Oct. 1934).

§ J. S. Townsend, Phil. Mag. xiv. p. 444 (March 1923), and xx. p. 242 (Aug. 1935).

potential, but in order to start or maintain a high frequency discharge it is necessary to have a certain minimum amplitude of the force depending on the pressure of the gas and the dimensions of the vessel containing it.

With oscillatory forces of very small amplitude a few electrons may acquire sufficient energy to ionize the molecules of the gas, but the rate at which electrons disappear from the gas, by diffusion to the surface of the containing vessel, and by the oscillatory motion of electrons near the surface, exceeds the rate of ionization by collision.

As the force is increased the oscillatory motion increases, also the rate of diffusion to the boundary since the energy of agitation is increased, but the rate of ionization increases more rapidly than the motions to the boundary, and a critical point is reached where the rate of ionization is equal to the rate at which electrons arrive at the surface of the vessel containing the gas *.

With a very small increase of the force above the critical point there is a rapid increase in the number of electrons and a glow appears in the gas. Also, since the rate at which positive ions move towards the surface is less than that of the electrons, a positive charge accumulates in the gas and the force due to this charge retards the motion of the electrons from the gas, so that the force required to maintain a small current is less than the critical force required to start the discharge.

In these respects there is a close resemblance between the oscillatory discharges and the uniform positive columns of direct currents in long tubes where that part of the current is maintained with a very small electric force equal to the mean force in the uniform column of the oscillatory current †.

In the following investigation it is proposed to extend this theory to cover different kinds of discharges in gases at low pressures, and to show under what conditions the electric forces required to maintain the discharges may be effected by a magnetic force. Some of the problems involved in determining the energy of agitation of the electrons are similar to those which occur in the theory

* J. S. Townsend, *Comptes Rendus*, t. clxxxvi. p. 55 (Jan. 1928) and Phil. Mag. xiii. p. 745 (April 1932).

† J. S. Townsend and W. Nethercot, Phil. Mag. viii. p. 600 (March 1928).

of the effect of the earth's magnetic field on the transmission of electromagnetic waves in the upper atmosphere such as that given by Appleton *, and more recently by Bailey †, and Martyn ‡. An interesting account of these investigations has been given by Mitra §, but the methods of solving the problems that occur in the theory of the absorption or refraction of electromagnetic waves are not the most suitable for determining the conditions under which discharges are maintained in a gas.

3. The most convenient method is to compare the motion of electrons or the rate of ionization under various conditions with the motion or rate of ionization in a uniform electric field when there is no magnetic force.

The simplest case is that of the motion of electrons in a magnetic field under the action of a direct electric force of constant intensity. In the theory || of the motion which has already been given it has been shown that the coefficient of diffusion and the mean velocity of the electrons in the direction of the electric force depends on the sum of a series of terms of the form $\cos \omega s$ or $\sin \omega s$ where s is a free path of an electron and ω a constant. In order to find the sum of a series of this form it is essential to take into consideration the distribution of the free paths about the mean free path l, since the sum of the series is not obtained even approximately by substituting l for s in each term.

In order to calculate the mean energy of the electrons moving under the action of an oscillatory force it will be seen that the mean energy is determined by the same trigonometrical series.

A simple ¶ method of finding the sum of such a series in the cases where ωl is small (less than the value $\omega l = 1$) has just been given in another paper, but since there are several calculations in the theory of the motion of electrons, depending on these series, it is of interest to explain the

* E. V. Appleton, Proc. Phys. Soc. xxxvii. p. 16 (1925).

† V. A. Bailey, Phil. Mag. xviii. p. 516 (1934), xxiii. p. 774 and p. 929 (1937).

‡ D. F. Martyn, Phil. Mag. xix. p. 376 (1935).

§ S. K. Mitra, "Report on The Present State of our Knowledge of the Ionosphere." Proc. Nat. Inst. of Sciences of India, i. no. 3 (1935).

|| 'Electricity in Gases,' p. 97.

¶ J. S. Townsend, Phil. Mag. xxv, p. 459 (March 1938).

original * method of finding the solution for any values of ωl.

4. It has been found that an electron, moving with energies less than the energy required to ionize molecules or to excite radiation, loses a very small proportion of its energy in the collisions of electrons with molecules and that an electron traverses a large number of free paths with approximately the same velocity.

Let l_1, l_2 . . . . lc, be the lengths of a large number c of consecutive paths traversed by an electron moving with the velocity U in the time lc/U, l being the mean free path ; t_1, t_2 etc., the intervals of time l_1/U, l_2/U etc., between collisions, and T the mean interval between collisions.

There are large inequalities in the lengths of the free paths and it has been shown † that in a large number c of free paths the number that exceed the length s is $c\epsilon^{-s/l}$ and the number of lengths between s and $s+ds$ is $c\epsilon^{-s/l}\,ds/l$. These paths contribute the amount

$$c \cos(\omega s)\epsilon^{-s/l}\,ds/l$$

to the sum of the cosines $(\cos \omega l_1 + \cos \omega l_2 \ldots . \cos \omega lc)$, and the total sum of all the cosines is

$$c\int_0^\infty \cos(\omega s)\epsilon^{-s/l}\,ds/l.$$

This expression may be integrated by parts and the total sum is thus found to be $c/(1+\omega^2 l^2)$.

By a similar method the sum of the sines is found to be $c\omega l/(1+\omega^2 l^2)$. Also where an electron traverses a large number c of free paths with the same velocity the sum of the series $(\cos \omega t_1 + \cos \omega t_2 \ldots . \cos \omega t_c)$, is obtained by substituting l_1/u for t_1, l_2/u for t_2 etc. The sum of these cosines is thus found to be $c/(1+\omega^2 T^2)$.

The series which are required in the calculations of the motions of the electrons are therefore

$$\cos \omega t_1 + \cos \omega t_2 \ldots . \cos \omega t_c = c/(1+\omega^2 T^2), \quad . \quad . \quad (1)$$

and

$$\sin \omega t_1 + \sin \omega t_2 . \ldots \sin \omega t_c = c\omega T/(1+\omega^2 T^2). \quad . \quad (2)$$

It has already been shown by these equations that both the velocity W in the direction of an electric force and the

* J. S. Townsend, Proc. Roy. Soc. A, lxxxvi. p. 571 (1912).
† J. S. Townsend, Proc. Roy. Soc. A, lxxxvi. p. 197 (1912).

coefficient of diffusion K are reduced by the factor $1/(1+\omega^2T^2)$ by the action of a magnetic force of intensity H, the constant ω being He/m.

5. When electrons move in a gas under a direct electric force of uniform intensity F it has been found that for large ranges of forces and pressures of the gas a state of motion is attained where the mean velocity of the electrons in the direction of the force is small compared with the mean velocity of agitation *. Under these conditions † the mean velocity W in the direction of the force of a group of electrons moving with the same energy of agitation $mU^2/2$ is $2Fel/3mU$.

[The expression Fel/mU which is usually given for the velocity W is an approximation, obtained by assuming that the mean displacement in the direction of the force when electrons move in free paths of length l_1 is $(Xe/2m)(b_1^2/U^2)$.]

The increase in the energy of the electrons per second due to the motion in the direction of the force is W.Fe and the number of collisions of an electron with molecules is U/l. If the mean loss of energy $\lambda mU^2/2$ of an electron in a collision be small, the loss of energy per second is $\lambda mU^3/2l$ and in the steady motion where the mean energy E of the electrons is constant the mean value of W.Fe is equal to the mean value of $\lambda mU^3/2l$. In order to obtain an accurate expression for the energy E by equating these two quantities, it is necessary to take into consideration the distribution of the velocities of agitation about the mean E velocity. For the Maxwellian distribution of the velocities, the mean energy deduced by this method is given by the equation

$$E=Fel/\sqrt{2\cdot7\times\lambda} \quad . \quad . \quad . \quad . \quad . \quad (3)$$

l and λ being taken to be constant.

If V^2 be the mean of the squares of the velocities of agitation the mean energy E is $mV^2/2$, and for this distribution the mean velocity of agitation is $\cdot92\times V$. When the electrons move in a magnetic field, the effect of the magnetic force may be indicated by comparing the energy acquired in the steady state of motion, with that acquired when there is no magnetic force. For this

* 'Motion of Electrons in Gases,' Clarendon Press, Oxford (1925).
† Phil. Mag. xxii. p. 145 (July 1936).

purpose it will be sufficient to make approximate calculations in which it is assumed that all electrons moving with the same energy $mU^2/2$ after collisions with molecules traverse free paths of the same length l_x in the same time l_x/U, and the velocity U may be is taken as the mean velocity of agitation.

With these simplifications the velocity W is FeT/m, T being the mean interval between collisions l/U, and the mean energy in the steady motion is given by the equation

$$E=Fel/\sqrt{2\lambda}. \quad . \quad . \quad . \quad . \quad . \quad (4)$$

6. In a magnetic field of intensity H the electrons move in spirals with the angular velocity He/m about axes parallel to the direction of the electric force. When the electric force is in the direction of the magnetic force the velocity W is independent of the magnetic force, and the mean energy acquired by the electrons under the action of a direct force is given approximately by equation (4).

But if the magnetic force be in a direction perpendicular to the electric force the velocity W is reduced from FeT/m to $FeT/m(1+\omega^2T^2)$ where ω is the angular velocity He/m.

The increase in the energy of the electrons per second due to the displacement in the direction of the force is therefore reduced from W.Fe to $W.F.e/(1+\omega^2T^2)$ which is approximately $F^2e^2T/m(1+\omega^2T^2)$ and in the steady motion where this gain of energy is equal to the loss of energy $\lambda E/T$ in collisions the equation for the mean energy becomes

$$E(1+\omega^2T^2)^{\frac{1}{2}}=Fel/\sqrt{2\lambda}. \quad . \quad . \quad . \quad . \quad (5)$$

For large values of ωT the expression for E becomes

$$E=F^2e^2/\lambda m\omega^2 \quad . \quad . \quad . \quad . \quad . \quad . \quad (6)$$

which is independent of the pressure of the gas.

In equations (4), (5), and (6) for the energy E, the numerical factors depending on the distribution of the energies of the electrons about the mean energy E are omitted.

In direct current discharges between electrodes most of the energy acquired by the electrons in moving in the direction of the force is lost in large amounts in collisions with molecules of the gas, and in the collisions with the positive electrode, and there are large inequalities in the

energies of the electrons. Under these conditions the preceding investigations may be taken as showing the general effect of a magnetic force, and the expressions for the mean energy in the form given by equations (4), (5), and (6) may be taken as approximations.

7. When there is no magnetic force an electron acquires the energy $Fe\delta$ in moving a small distance δ in the direction of the electric force F, and the number of collision of the electron with molecules of the gas is $U\delta/Wl$. With the magnetic force H acting in a direction perpendicular

TABLE I.

(Potentials V required to start a discharge in air between a cylinder 4·2 cm. in diameter and a co-axial wire one millimetre in diameter.)

p.	H=0 V.	H=44 V.	H=88 V.
·74	395	395	395
·47	380	380	380
·20	465	425	385
·14	610	530	385

to the electric force the velocity W is reduced to $W/(1+\omega^2T^2)$ and in moving the distance δ in the direction of the electric force the number of collisions of the electron with molecules is $U\delta(1+\omega^2T^2)/Wl$. Thus a magnetic force has the same effect as an increase in the pressure which diminishes the mean free path from l to $l/(1+\omega^2T^2)$.

This may be seen by the effect of a magnetic force on the sparking potential between electrodes in a gas. The sparking potential is diminished by the action of a magnetic force when the gas is at pressures less than that corresponding to the minimum sparking potential, and is increased by the magnetic force when the gas is at larger pressures.

The former effect may be shown with comparatively small magnetic forces, since the interval T between collisions is large at the lower pressures. It is shown by the following observations of the potential required to start a discharge from a wire one millimetre in dia-

meter to a coaxial cylinder 4·2 cm. in diameter containing air at different pressures. The magnetic force in the direction of the axis was obtained by a current in a solenoid wound round the cylinder. The potentials V between the wire and the cylinder required to start a discharge are given in the preceding table. The pressures p of the air are given in millimetres in the first column of the table. The potentials are in volts. The numbers in the second column are the potentials required to start a discharge when there is no magnetic force, those in the third column the potential with a magnetic force of 44 e.m. units and in the fourth column with a magnetic force of 88 e.m. units.

8. A magnetic force in the direction of the electric force has no effect on the energy acquired by the electrons, but the coefficient of diffusion in directions perpendicular to the magnetic force is reduced from the value $lU/3$ to $lU/3(1+\omega^2T^2)$.

In discharge-tubes where the electric and magnetic forces are in the direction of the axis of the tube, the rate of diffusion of electrons to the surface of the tube is diminished by the action of the magnetic force so that the electric force is diminished since the rate of ionization required to balance the loss due to diffusion is diminished.

The effect is most noticeable in gases at low pressures and may be observed either in the positive columns of direct current discharges, or in oscillatory discharges when the electric force is in the direction of the axis of the tube.

9. It has already been shown * that the mean energy acquired by electrons under the action of an oscillatory force $X \sin(qt+\alpha)$ is equal to the energy acquired under the action of a direct force of intensity $X/\sqrt{2}$ for a large range of pressures of the gas. This condition is realized in the uniform luminous columns of oscillatory discharges where the pressure of the gas is the same as in the uniform positive columns of direct current discharges.

In monatomic gases in tubes about 4 centimetres in diameter these pressures are of the order of 10 millimetres and in diatomic gases about one millimetre.

* J. S. Townsend, Phil. Mag. (7) xiii. p. 745 (April 1932).

At lower pressures the mean energy of the electrons acquired under the action of a direct force increases as the inverse of the pressure, equation (4), but under the action of an oscillatory force the increase in the energy is not so great. This may be shown by the following simple method of comparing the energies.

When there is no magnetic force acting on the electrons the acceleration of an electron in the direction of the force is $(Xe/m) \sin (qt+\alpha)$, and if u_0 be the velocity of the electron in the direction of the force at the time $t=0$, the velocity in a free path at the time t is

$$(u_0 - Xe\ (\cos qt+\alpha) - \cos \alpha)/mq).$$

If a large number of electrons collide with molecules the mean value of u_0 is zero after the collisions at the time $t=0$, and the mean increase in the energy of the electrons at the time t is $2mf^2 \sin^2 (qt/2) \sin^2 (qt/2+\alpha)/q^2$ where f is the acceleration Xe/m.

Thus the energy depends on the phase α of the electric force at the time $t=0$ at the beginning of the free paths, and since all values of α are equally probable the mean value of $\sin^2(qt/2+\alpha)$ is $1/2$; and the mean increase E in the energy of electrons at the time t after collisions with molecules is $mf^2 \sin^2 (qt/2)/q^2$ which may be written in the form

$$E_t = mf^2(1-\cos qt)/2q^2. \quad . \quad . \quad . \quad . \quad (7)$$

If there were no collisions with molecules for a long interval (t) there would be large fluctuations in the energy E_t from $E_t=0$ to $E_t=mf^2/q^2$ as t increases. There is therefore a limit to the energy an electron may acquire when moving freely under the action of an oscillatory force.

10. But when the electrons collide with molecules all directions of motion are equally probable after each collision, and the mean energy increases in the free paths after the collisions. The mean energy therefore continues to increase until the energy acquired by the action of the electric force is equal to the loss of energy in the collisions.

At the time t_1 when the electron has traversed the free path of length l_1 the increase in the energy E_t equation (7) is $mf^2(1-\cos qt_1)/2p^2$ and after traversing a large number c of free paths of lengths $l_1, l_2 \ldots l_c$ the total increase is

$$\Sigma E_t = mf^2(c - \cos qt_1 - \cos q_2t_2 \ldots \cos qt_c)/2q^2. \quad . \quad (8)$$

If the change in the energy of an electron in an interval between collisions be small compared with the mean energy $m\mathrm{U}^2/2$, the intervals t_1, t_2 etc., between collisions may be taken to be proportional to the free paths, and the series of cosines in equation (8) is given by equation (1). The total increase in the energy $\Sigma\mathrm{E}$ in the time $c\mathrm{T}$ is thus found to be

$$\Sigma\mathrm{E}_t=c\mathrm{X}^2e^2\mathrm{T}^2/2m(1+q^2\mathrm{T}^2) \quad . \quad . \quad . \quad (9)$$

X being the amplitude of the oscillatory force and T the mean interval between collisions.

In the steady motion this increase is equal to the mean loss of energy in collisions $c\lambda\mathrm{E}$ and the equation for the mean energy E becomes

$$\mathrm{E}(1+q^2\mathrm{T}^2)^{\frac{1}{2}}=\mathrm{X}el/2\sqrt{\lambda}. \quad . \quad . \quad . \quad . \quad (10)$$

Comparing equations (5) and (10) it is seen that the mean energy acquired by electrons in a magnetic field of intensity H under the action of a direct electric force of intensity F depends on the frequency $\omega/2\pi$ of the free oscillations of the electrons in the magnetic field, in the same way as the energy acquired under the action of an oscillatory force X sin $(qt+\alpha)$ depends on the amplitude X and the frequency $q/2\pi$ when there is no magnetic force.

11. In electrodeless discharges in large vessels or in wide tubes where the electric force is parallel to the axis of the tube, the loss of conductivity due to electrons coming into contact with the surface of the vessel is principally due to diffusion which depends on the energy of agitation of the electrons and on the pressure of the gas. In all cases the rate of diffusion diminishes as the pressure increases so that the rate of ionization required to maintain a discharge also diminishes. In order to estimate the changes in the force required to maintain a discharge due to changes in the pressure of the gas, it is necessary to consider the energy of agitation of the electrons as given by equation (10).

From a theoretical point of view the simplest cases are those in which the product $q\mathrm{T}$ is small (less than ·3) and those in which $q\mathrm{T}$ is large (greater than 3).

The former condition is obtained in discharges in gases at pressures greater than one millimetre. At one millimetre pressure the mean free path of an electron in air may be taken to be about ·03 cm., and the mean velocity

of agitation of the electrons in these discharges to be about 10^8 cms. per second.

Under these conditions the product qT in equation (10) is less than ·3 when the frequencies of the oscillations are less than 3×10^7 cycles per second, and the term q^2T^2 may be neglected in the factor $(1+q^2T^2)$. The expression for the mean energy thus becomes

$$E=Xel/2\sqrt{\lambda} \quad . \quad . \quad . \quad . \quad . \quad (11)$$

which is independent of the frequency of the oscillation, and since the mean free path is inversely proportional to the pressure p of the gas, the energy E is proportional to X/p.

The rate of diffusion is also independent of the frequency, so that the high frequency force required to maintain a small current in a gas is independent of the frequency when the gas is at pressures not less than one millimetre.

In the discharges in gases at these pressures the rate of ionization required to maintain a current is comparatively small.

This is indicated by the value of the coefficient of ionization α which is the same as in a direct current where the intensity F of the force is $X/\sqrt{2}$. With small values of X/p the change in the coefficient α due to a change in the amplitude X is comparatively large. Thus when the pressure of the gas is increased the rate of ionization is reduced to the required value by a small reduction in ratio X/p.*

The amplitude X of the oscillatory force therefore increases with the pressure, but the ratio X/p diminishes.

12. In discharges where the frequencies are greater than 3×10^7 cycles per second and the pressure is a small fraction of a millimetre the product (q^2T^2) becomes large and may be taken as the value of the factor $(1+q^2T^2)$ in equation (9).

Equation (10) for the mean energy thus becomes

$$\lambda E=X^2e^2/2mq^2 \quad . \quad . \quad . \quad . \quad . \quad . \quad (12)$$

Thus with the lower pressures and higher frequencies, the amplitude of the force required to maintain a given energy is independent of the pressure of the gas and proportional to the frequency. And since the rate of

* J. S. Townsend, Phil. Mag. xi. p. 1112 (May 1931).

ionization and the rate of diffusion depend only on the pressure of the gas and the energy of agitation of the electrons, the amplitude of the force required to maintain a discharge is proportional to the frequency when the pressure is constant. This result is independent of the numerical factor depending on the distribution of the energies of agitation of the electrons which is omitted in the equation (12).

It may also be seen that in oscillatory discharges of the same frequency, a large increase in the amplitude of the force is required in order to maintain a discharge when the pressure is reduced.

With a given oscillatory force the mean energy of agitation of the electrons is independent of the pressure, but the rate of ionization is proportional to the pressure and the rate of diffusion is inversely proportional to the pressure. When the pressure is reduced the loss of conductivity due to diffusion is increased, and in order to increase the energy of agitation and make the increase in the rate of ionization which is required to maintain a discharge, it is necessary to make a large increase in the amplitude of the force.

13. The results of these calculations are shown diagrammatically by the curves (fig. 1), where the ordinates are proportional to the amplitudes of the forces and the abscissæ proportional to the pressure. The amplitudes given by Curve 1, are for oscillations of the same frequency, and those given by Curve 2 for oscillations of twice the frequency. In the part AB where the curves coincide the product (qT) is small (less than ·3), in the parts CD and C′D′ the product (qT) is large (greater than 3) and the ordinates of Curve 2 are double the ordinates of Curve 1.

14. The mean energy acquired by electrons in a magnetic field under the action of an oscillatory force may also be found by the same method.

In this case in order to take into consideration the phase α at the time $t=0$ when an electron begins to move in a free path, it is convenient to calculate the increase in the energy of the electrons for the cases in which the phase is zero and for that in which the phase is $\pi/2$.

In the former case the force is $X \sin qt$ and if the magnetic force H be in the direction of the axis of y and u and w the velocities of an electron in the directions

of the axes x and z the accelerations are given by the equations

$$\left.\begin{aligned} m\,du/dt &= Xe \sin qt + Hew \\ \text{and} \qquad m\,dw/dt &= -Hew \end{aligned}\right\} \quad . \quad . \quad (13)$$

and the velocities in a free path are :

$$\left.\begin{aligned} u &= w_0 \sin \omega t + u_0 \cos \omega t + fq(\cos qt - \cos \omega t)/(\omega^2 - q^2) \\ \text{and} \qquad w &= w_0 \cos \omega t - u_0 \sin \omega t + f(q \sin \omega t - \omega \sin qt)/(\omega^2 - q^2), \end{aligned}\right\} \quad . \quad . \quad . \quad (14)$$

Fig. 1.

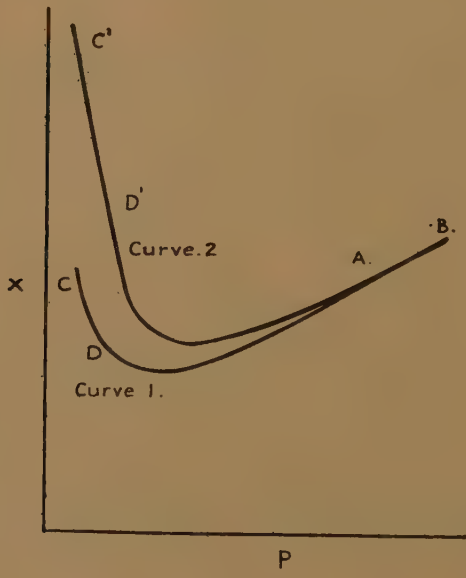

f being the acceleration Xe/m, ω the angular velocity He/m and u_0 and w_0 the velocities at the time $t=0$.

15. The case of resonance where the frequency $q/2\pi$ is equal to $\omega/2\pi$ is of particular interest. As q approaches ω, $(q-\omega)$ becomes small compared with ω and equations (14) may be simplified by substituting $(\omega t+(q-\omega)t)$ for qt, and 2ω for $(q+\omega)$. The following expressions are thus obtained for $\cos qt$ and $\sin qt$,

$$\left.\begin{aligned} \cos qt &= \cos \omega t - (q-\omega)t \sin \omega t \\ \text{and} \qquad \sin qt &= \sin \omega t + (q-\omega)t \cos \omega t, \end{aligned}\right\} \quad . \quad (15)$$

neglecting terms involving higher powers of $(q-\omega)t$, and equations (14) for the velocities reduce to

$$\left.\begin{aligned} u&=(w_0+ft/2)\sin\omega t+u_0\cos\omega t,\\ \text{and}\quad w&=(w_0+ft/2)\cos\omega t-u_0\sin\omega t-(f/2\omega)\sin\omega t,\end{aligned}\right\}\quad(16)$$

for any values of t when q is equal to ω.

When q is between the limits $(1\pm\cdot01)\omega$ the higher powers of $(q-\omega)t$ may be neglected in the expressions for $\cos qt$ and $\sin qt$ in equations (15), and the velocities are given by equations (16) for large values of t which may be several multiples of the periodic time $2\pi/\omega$.

The coefficient $(w_0+ft/2)$ of the first term on the right of equations (16) increases continuously with the time, and for values of t greater than π/ω this coefficient becomes much greater than the coefficient $f/2\omega$ of the last term in the second equation, and for an approximate estimate of the energy of the electron this term may be neglected.

With this simplification the energy $m(u^2+w^2)/2$ at any time t within the above limits is given by the equation

$$m(u^2+w^2)/2=m((w_0+ft/2)^2+u_0^2)/2. \quad . \quad . \quad (17)$$

This is the energy acquired by a electron in the time t moving under the action of a direct force of intensity X/2 in the direction of the axis of z.

16. The motion of an electron in the case where the phase α is $\pi/2$ at the time $t=0$ is obtained by substituting $X\cos qt$ for $X\sin qt$ in equations (13). Following the same method of simplifying the calculations the expressions obtained for the velocities when ω is equal to q are

$$\left.\begin{aligned} u&=(w_0+f/2\omega)\sin\omega t+(u_0+ft/2)\cos\omega t\\ \text{and}\quad w&=w_0\cos\omega t-(u_0+ft/2)\sin\omega t,\end{aligned}\right\}\quad.\quad(18)$$

and omitting the term $f/2\omega$ as in the first calculation the equation for the energy at the time t after a collision is thus found to be

$$m(u^2+w^2)/2=m((u_0+ft/2)^2+w_0^2)/2, \quad . \quad . \quad (19)$$

which is the energy acquired by an electron under the action of a direct force of intensity X/2 in the direction of the axis of x.

The increase in the energy in the interval between two collisions is independent of the phase α. The energy increases continuously with the time t and there are no

periodic fluctuations about the mean in the intervals between collisions which are obtained when there is no magnetic force.

Thus in a gas at low pressures the electrons moving under the electric force $X \sin (qt+a)$ and a magnetic force of intensity qm/e the kinetic energy acquired by the electrons in the steady state of motion is equal to the energy acquired under the action of a direct force F of intensity $X/2$ when there is no magnetic force acting on the electrons.

This condition is obtained for a large range of small pressures when the mean interval T between the collisions of electrons with molecules is greater than half the periodic time π/q of the oscillatory force.

The energy thus acquired is much greater than that acquired by the same oscillatory force when there is no magnetic force, the latter being the energy acquired under the action of a direct force of amplitude $X/\sqrt{2(1+q^2T^2)}$ as given by equation (10).

17. The amplitude X of the electric force required to maintain a discharge in a gas at a low pressure when there is no magnetic force is much greater than the amplitude X_h of the force required to maintain a discharge in a magnetic field where the intensity H of the magnetic force is adjusted to the value qm/e. If the mean energy of the electrons were the same in the two cases the ratio of the amplitudes X/X_h would be $\sqrt{(1+q^2T^2)/2}$, but since the coefficient of diffusion in directions perpendicular to the magnetic force is reduced from K to $K/(1+q^2T^2)$ the rate at which the electrons disappear from the gas by diffusion is diminished, and there is a corresponding reduction in the rate of ionization and in the force required to maintain the discharge.

It would be difficult to calculate to what extent the force X is diminished by the change in the rate of diffusion, as the calculation would involve the determination of numerical constants depending on the distribution of the energies of the electrons about the mean energy E.

The effect of the magnetic force on the rate of diffusion is clearly shown by the values of X_h obtained experimentally for oscillatory discharges of different frequencies in a gas at low pressure. The energy of agitation of the electrons acquired under the action of the oscillatory

force is independent of the frequency, being the same as the energy acquired under the action of a direct force of intensity $X_h/2$, but the magnetic force ($H=qm/e$) being proportional to the frequency, the rate of diffusion diminishes as the force H increases. There is a corresponding reduction in the rate of ionization required to maintain the discharge which is indicated by the reduction in the amplitude X_h as the frequency increases.

Thus while the electric force X required to start a discharge in a gas at a low pressure increases with the frequency when there is no magnetic force, the force X_h required to start a discharge in a magnetic field diminishes as the frequency ($q/2\pi$) is increased when the intensity H of the magnetic force is adjusted to the value qm/e.

18. In order to find the effect of the magnetic force when He/m is equal to q and the gas is at higher pressures where qT is less than π it is necessary to take in the terms $(f/2\omega)\sin\omega t$ in the expressions (14) and (16) for the velocities.

The mean increase E_{ht} in the energy of an electron at the time t after a collision with this term included is

$$E_{ht}=mf^2(q^2t^2+\sin^2 qt)/8q^2. \quad . \quad . \quad . \quad (20)$$

The increase in the energy ΣE_{ht} of an electron after a large number c of collisions is obtained by substituting l_1/u, l_2/u &c. for t in equation (20) and proceeding in the same manner as in the calculation of ΣE_t, equation (7). The mean increase E_{hT} of the energy for a large number of free paths is thus found to be

$$E_{hT}=mf^2T^2(1+1/(1+4q^2T^2))/4. \quad . \quad . \quad (21)$$

and the mean increase E_T when there is no magnetic force as given by equation (9) is

$$E_T=mf^2T^2/2(1+q^2T^2). \quad . \quad . \quad . \quad . \quad (22)$$

It is thus seen that in gases at low pressures where qT is greater than 1/2 the mean energy E_{hT} acquired by the electrons in the magnetic field of intensity H equal to mq/e is greater than the energy E_T acquired under the action of the same electric force when there is no magnetic force. At higher pressures where qT is less than 1/2 the

energy E_{kT} is less than E_T. The ration of these energies for small values of qT is given in the following Table :—

TABLE II.

q^2T^2	·25	·5	·75	1·0
E_{kT}/E_T ...	·94	1·0	1·10	1·2

19. These results of the theoretical investigation have been tested experimentally by measuring the electric force required to start a discharge in dry air in a large spherical bulb B, 13 centimetres in diameter. The bulb was of pyrex and connected as shown in fig. 2, through a tube immersed in liquid air, to an air pump and a McLeod

Fig. 2.

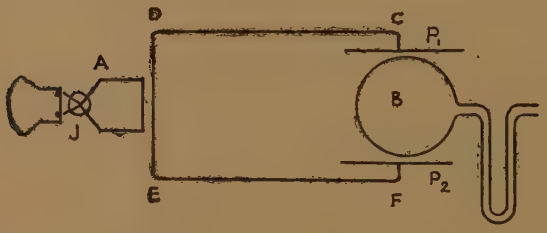

gauge. This prevented the diffusion of mercury vapour and other impurities into the bulb. The oscillatory force was maintained by two large parallel plates P_1 and P_2 which formed the condenser of a secondary circuit CDEF loosely coupled to a high frequency continuous wave generator.

The amplitude of the current in the secondary circuit was adjusted either by altering the coupling or making a small change in the lengths of the wires CD and EF.

The current in the line DE was indicated by a small aperiodic circuit A containing a vacuo-junction J connected to a galvanometer. This current was gradually increased until a faint discharge appeared in the bulb.

For oscillations of the same frequency the amplitude of the electric force in the space between the plates P_1 and P_2 is accurately proportional to the square root of the

galvanometer deflexion. The force in volts per centimetre for one reading of the galvanometer was determined approximately by a measurement of the potential between the plates. Thus the ratio of the amplitude of forces of the same frequency required to start discharges under different conditions is given accurately by the galvanometer, but the actual values in volts per centimetre and the ratio of the amplitudes of oscillations of different frequencies have only been determined approximately. The magnetic force in a direction perpendicular to the electric force was maintained by a current in a large pair of Helmholtz coils.

Fig. 3.

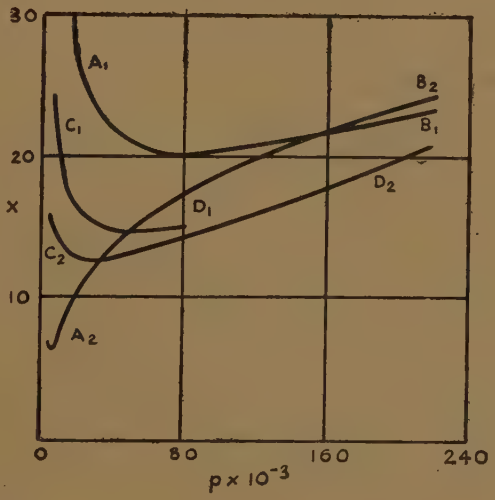

20. The oscillatory electric forces required to start discharges in air at different pressures are given by the curves (fig. 3).

The ordinates are the amplitudes of the forces, the unit being approximately one volt per centimetre, and the abscissæ the pressures in thousandths of a millimetre. The curve $A_1 B_1$ gives the amplitudes of forces oscillating with the frequency $4{\cdot}8 \times 10^7$ cycles per second when there is no magnetic force. At the lower pressures the force diminishes as the pressure increases and at the higher

pressures the force increases with the pressure, as in the curves (fig. 1) deduced from theoretical considerations.

21. The oscillatory force required to start a discharge in a magnetic field depends on the intensity H of the magnetic force, and a minimum amplitude of the electric force is obtained with a certain value of H when the gas is at pressures less than one-tenth of a millimetre. This value of H is independent of the pressure and is near the theoretical value qm/e where the frequency $He/2\pi m$ of the free oscillations in the magnetic field is equal to the frequency $q/2\pi$ of the electric force. The minimum values of the amplitudes of the electric force oscillating with the frequency $4{\cdot}8 \times 10^7$ cycles per second, obtained in a magnetic field, are given by the curve $A_2 B_2$ (fig. 3). The large difference between the ordinates of the curves $A_1 B_1$ and $A_2 B_2$ at the lower pressures is due partly to the increased efficiency of the electric force in maintaining the energy of agitation of the electrons, and partly to the decrease in the rate of diffusion in the magnetic field as explained in Section 17.

At the higher pressures, greater than ·14 mm., the electric force required to start the discharge when there was no magnetic force was slightly less than that required in a magnetic field of intensity H of the order qm/e. This is in accordance with the values of the ratio of the energies E_{hT}/E_T given in Table II., where it is shown that the mean energy of the electrons acquired under the action of an electric force is diminished by the action of the magnetic force when the product qT is less than ·5.

22. The curves $C_1 D_1$ and $C_2 D_2$ are the corresponding curves for oscillations of the frequency 3×10^7 cycles per second. With this frequency the change in the amplitude of the oscillatory force required to start the discharge due to the magnetic force as shown by the difference between the ordinates of the two curves is much less than the change in the amplitude with oscillations of the higher frequency. A similar result is indicated by the theory as it is seen (Sections 16 and 17) that with the lower frequency the change in the efficiency of the electric force in maintaining the energy of agitation and also the change in the rate of diffusion due to the action

of a magnetic force H increase with the frequency, when H is equal to qm/e.

It will also be observed that the ordinates of the curve $A_1 B_1$ for the lower pressures are greater than the ordinates of the curve $C_1 D_1$. The ratio of these ordinates as has already been mentioned has not been determined very accurately, and the ratio as shown by the curves is somewhat greater than the ratio indicated by the theory. As explained in Section 12, the ratio of the forces required to start a discharge in gas at very low pressures, is equal to

Fig. 4.

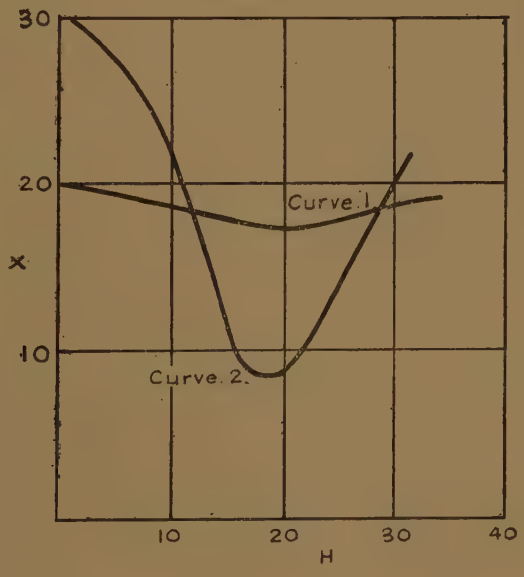

the ratio of the frequencies, where there is no magnetic force.

A comparison of the ordinates of the curves $A_2 B_2$ and $C_2 D_2$ is also of interest. In this case the ordinates of the curves $A_2 B_2$ for the lower pressures are less than the ordinate of the curve $C_2 D_2$. In these discharges the magnetic force is proportional to the frequency and the energy of agitation of the electrons depends only on the amplitude of the electric force, and since the rate of diffusion increases as the magnetic force diminishes, the

amplitude of the electric force increases as the frequency diminishes (as explained in Section 17).

23. The effect of a magnetic force on the electric force required to start a discharge in air at two different pressures is shown by the curves (fig. 4). The ordinates of the curves are the amplitudes of the electric force in volts per centimetre and the abscissæ the magnetic force in e.m. units. The frequency of the oscillations was $4{\cdot}8 \times 10^7$ cycles per second. Curve 1 gives the amplitudes of the forces required to start discharges in air at ·08 mm. pressure, and curve 2 gives the amplitude in air at ·016 mm. pressure.

The minimum electric force in a discharge in air at ·016 mm. pressure is at the point where the magnetic force is 17 e.m. units and $He/2\pi m$ is $4{\cdot}75 \times 10^7$, which is almost exactly the frequency of the electric force.

24. The mean energy of agitation of the electrons may also be estimated from the form of the curve 2 (fig. 4), and it is of interest to show by a simple calculation that the mean energy deduced from these experiments is in general agreement with the theory of ionization by collision, and with the investigations of the motion of electrons from which the mean free paths and the mean energy of agitation of the electrons have been determined.

In the theory * of ionization by collision the changes in the coefficient of ionization with the electric force F and pressure p of the gas are explained on the hypothesis that electrons moving with small velocities of agitation lose only a small proportion of their energies in collisions with molecules, but when the energy increases and approaches the amount required to ionize molecules the electrons lose a large proportion of their energies in collisions, and some acquire sufficient energy to ionize the molecules.

The mean energy of the electrons depends on the ratio X/p and in the discharges under consideration the mean energy is much less than the energy required to ionize molecules of the gas.

The mean energy of electrons moving in gases under the action of a uniform electric field has been determined experimentally by measurements of the lateral diffusion

* ' Ionization of Gases by Collision,' p. 28 (1910).

of a stream of electrons, also the mean free paths of the electrons. In air * the mean energy expressed in volts is approximately 6 when the ratio X/p is 100, and the mean free path in air at one millimetre pressure is ·027 cm.

Thus in air at ·016 mm. pressure the mean free path is 1·7 cm. and the mean interval T between collisions is 1·7/U, U being the mean velocity of agitation. The velocity U when the kinetic energy is 6 volts, is $1{\cdot}47\times10^8$ cm. per second.

Also as is shown by curve 2, fig. 4, the force X required to start a discharge in air at ·016 mm. pressure is 30 volts per cm., when there is no magnetic force, and it follows from the theory of the motion the mean energy E of the electrons in the discharge is proportional to $X/\sqrt{2(1+q^2T^2)}$. The force X_h in the magnetic field when H is adjusted to the value qm/e is 8·5 volts per centimetre and the mean energy E_h in this discharge is proportional to $X_h/2$. Thus the ratio E/E_h of the energies in the two discharges is $5/\sqrt{(1+q^2T^2)}$.

Since the loss of conductivity by diffusion is reduced by the magnetic force, the mean energy E_h required to maintain the necessary rate of ionization is less than the mean energy E. The factor $\sqrt{(1+q^2T^2)}$ is therefore less than 5. And the value of u given by the equation $\sqrt{1+q^2T^2}=5$ is a lower limit to the velocity of agitation of the electrons. Since $q/2\pi$ is $4{\cdot}8\times10^7$ cycles per sec. and l is 1·7 cm. the lower limit to the mean velocity of agitation in the discharge when there is no magnetic field is $1{\cdot}03\times10^8$ cm. per second. The most probable value is about $1{\cdot}6\times10^8$ cm. per second, which corresponds to an energy of about 7 volts.

XXVII. *Notices respecting New Books.*

The Fine Structure of Matter.—Part II. *Molecular Polarization.* Part III. *The Quantum Theory and Line Spectra.* By C. H. Douglas Clark. (London: Chapman and Hall, 1938. Price 15*s.* each part.)

WITH the publication of these two substantial books, Dr. Clark completes the second volume of his 'Comprehensive Treatise on Atomic and Molecular Structure.' The

* J. S. Townsend and V. A. Bailey, Phil. Mag. xlii. p. 872 (1921).

introductory volume is already well known and appreciated, and the first part of the second volume on 'X-rays and the Structure of Matter' has recently been reviewed in this Journal. These two new parts do not fall below the standard we have come to expect from the author.

Part II. is concerned in the main with the Debye theory of polarization, Fajan's theory of deformation, and the derivation and meaning of dipole moments; with an introductory chapter on dielectric constants and a concluding one on the Kerr effect. The subject is a comparatively new one, and has grown with great rapidity. The author's main concern is with the information which the phenomena furnish as to the structure of organic and inorganic compounds, and he has made a very complete and well-documented summary of the material available. Sufficient theory is, however, included to make the book self-explanatory.

In Part III. we are on the rather more generally familiar ground of Line Spectra and their interpretation in terms of the quantum theory. The treatment, in the main, follows the outlines of the Bohr-Sommerfeld theory; the spinning electron being later introduced to explain the multiple structure of the spectral lines. No attempt is made to expound the quantum mechanical theory of spectra, but the relation between the symbolisms of the two theories is clearly indicated. The relationship between line spectra and electronic configuration is considered in detail. The book forms an admirable introduction to the subject, and, like its predecessors, it abounds in references to the relevant literature.

It is difficult to know whether to admire most the industry which Dr. Clark has shown in collecting such a vast amount of data, or the skill with which he arranges and presents it. The research worker proposing to undertake investigations either theoretical or practical on any subject within its purview will find the whole volume a valuable addition to his library.

J. A. Crowther.

[*The Editors do not hold themselves responsible for the views expressed by their correspondents.*]

THE

LONDON, EDINBURGH, AND DUBLIN

PHILOSOPHICAL MAGAZINE

AND

JOURNAL OF SCIENCE.

[SEVENTH SERIES.]

SEPTEMBER 1938.

XXVIII. *On the Molecular Weights of the Globular Proteins.*

By D. M. WRINCH, *M.A., D.Sc. Oxon., D.Sc. Lond., Mathematical Institute, Oxford* *.

[Plates I. & II.]

[Received June 16, 1938.]

SUMMARY.

THE further consideration of the cyclol theory shows th at its predictions and general point of view are in good accord with the findings of Svedberg. The shape of the C_n cyclols and the nature of the cyclol network suggest that compound cyclols may exist, and it is found that the actual numbers given by Svedberg for fourteen different molecular weight classes may all be represented by simple or compound cyclols on the assumption that the corresponding apparent residue weights lie between 121 and 128.

The consideration of compound cyclols suggests a simple interpretation of the reversible dissociation characteristic of many proteins, and explains in particular the effect of dilution and changes in pH on the molecular weights of such proteins. A cage-colony structure is proposed for the virus proteins and other heavy proteins.

* Communicated by the Author.

1. *Introduction.*

ANY theory of the structure of proteins must necessarily take into account the vast body of facts regarding their physico-chemical behaviour which have been established by Svedberg and his school. Previous communications (Wrinch, 1937, *b*, *d*) were therefore devoted to considering the cyclol theory of protein structure in relation to some of Svedberg's findings, an investigation which seemed to be of interest, especially in view of the fact that no attempt has so far been made to explain or interpret these fundamental facts in terms of the polypeptide chain hypothesis (Rimington, 1931).

The cyclol hypothesis, it was found, predicts the existence of space-enclosing protein molecules whose skeletons comprise certain specific numbers of residues. Protein molecules having definite molecular weights may therefore be expected. The actual shape of the closed or space-enclosing cyclols is in accord with and offers an interpretation of the nature of the "globularity" which Svedberg attributes to these proteins. The fact that proteins fall into a number of molecular weight classes was interpreted to mean that the proteins falling into any one of these classes have the same number of amino acid residues, so that each class may be regarded as connoting one closed cyclol or an association of a certain number of such units. The variation within one class is then accounted for by the different selections of residues in the various proteins which can yield an average residue weight varying about mean values such as 115 to 124, and which may also entail the presence of different numbers of water molecules in the molecule.

The fundamental result of the enquiry was to show that there exist only certain sequences of space-enclosing cyclols (possibly only one); that, in fact, only a certain small number of molecular weight classes is to be expected in any range of weights. Some of these connote single cyclols. The polyhedral character of closed cyclols in general, however, suggests that "compound" structures consisting of certain numbers of cyclols in association may also exist. The striking phenomenon of the reversible dissociation and association of certain proteins discovered by Svedberg allows of simple interpretation and explanation on these lines. We suggest, then,

that the proteins which exhibit this behaviour are compound structures in the sense explained above.

On the present occasion we discuss first the order of magnitude of molecular weight classes predicted by the cyclol hypothesis, as at present developed. The feasibility of identifying some of these with those actually found by Svedberg is then considered. These tentatively proposed identifications at once rivet attention upon certain compound structures, and a later division of the paper is devoted to investigating the kind of compound structures to be expected. On the basis of Svedberg's figures, especially those for Helix hæmocyanin and other very heavy blood proteins, suggestions are made as to possible cage-colony structures on the basis of which proteins having molecular weights of any size can be built, simply by the association of the requisite numbers of units: these units may even be of only two types, C_1 and C_2. Specific ways of arranging the units, we presume, are conditioned by stability requirements; they yield definite implications as to the ways in which such a compound structure can break up: moreover, the stimulus under which the dissociation takes place in general affords some indication of the type of coordination which is being attacked. As a result, we have a general picture of the "globular" proteins in substantial agreement with that to which Svedberg has been led by his researches. "Probably the protein molecule is built up by successive aggregation of definite units," says Svedberg (1937), "but that only a few aggregates are stable. The higher the molecular weight the fewer are the possibilities of stable aggregation. The steps between the existing molecules therefore become larger and larger as the weight increases. These statements are borne out by the data for various constants of protein molecules as determined at Uppsala. An examination shows that the individual molecular weights within the groups differ considerably, but, on the other hand, it cannot be denied that a random distribution of molecular weights would give an entirely different picture."

2. *Molecular Weight Classes of Cyclols.*

It has been established that closed cyclols fall into one or more sequences, and that in any one sequence the

number of amino acid residues per molecule forms a quadratic function of the natural numbers. So far it has proved possible to construct only one sequence (see Pl. I. figs. 1*a* & 1*b*, and Pl. II. figs. 2*a* & 2*b*), C_1, C_2, . . . C_n, . . . We do not yet know whether this is the only possible one. If only amino residues are present, these contain 72, 288, . . . $72n^2$, . . . residues in their skeletons. If certain numbers of imino acid residues are present, these numbers may be correspondingly modified.

The predictions of the cyclol theory are thus, it would seem, perfectly definite in the sense that the theory implies that only certain residue numbers are permissible in protein skeletons. The number $72n^2$ for simple structures has already been arrived at by means of the actual geometrical construction of structures containing these numbers of residues: correspondingly a compound structure consisting of m such C_n cyclols in association, if it exists, will give the number $72n^2m$. All the residue numbers derivable from the one sequence found are thus mathematically determinate, and although we do not yet know whether or not simple structures other than the C_n structures exist, we do know that there cannot be more than a very small number of sequences. Furthermore, as we have previously emphasized, the part played by geometrical considerations in an investigation of the structure of proteins is purely permissive. These considerations when fully developed yield information as to the only space-enclosing cyclols which can exist, and so (on the cyclol theory) restrict the proteins to a certain set of possible structures. We cannot make the deduction that every structure which is geometrically possible actually exists.

To make a beginning, however tentative, in relating theory to fact, we may consider the case of a protein which has the C_n structure and consists of $72n^2$ amino acid residues, whose average weight is r together with γ water molecules per residue. Its molecular weight M is then given by

$$M=72n^2\,(r+18\gamma)=72n^2r_a,$$

where r_a may be called the apparent residue weight.

Molecular weight classes associated with compound structures consisting of m C_n cyclols in association will correspondingly be given by

$$M=72n^2m\,r_a.$$

The values of r_a for all proteins presumably lie within certain limits r_a^- and r_a^+. It is difficult or impossible to prescribe these limits at all narrowly. All estimates of r_a are based upon more or less incomplete chemical analyses, and take no account of the number of water molecules present.

So far, therefore, as the cyclols already constructed are concerned, the molecular weight classes of proteins may be expected to be multiples of one single range of values ($72\,r_a^-$ to $72r_a^+$). If values 120 and 150 be adopted for r_a^- and r_a^+, this range is 8640 to 10,800, and molecular weight classes represented by some of the following may be expected :—

8640 to 10,800—C_1,
17,280 to 21,600—$2C_1$,
25,920 to 33,200—$3C_1$,
35,560 to 43,200—$4C_1$ or C_2,

and so on.

Now the predictions of the theory are perfectly clear as to the residue numbers and structures to be expected of the globular proteins, and the theory suggests that proteins should in the future be classifiable on the basis of the numbers of residue in their skeletons rather than molecular weight. Owing to the limitations of the experimental methods, it is unfortunately impossible at present to test these predictions quantitatively, since the appropriate values for r_a in general are at present unknown. In particular cases, where there is considerable information about the hydration of protein, *e. g.*, in the cases of egg albumin, serum albumin, and serum globulin, it is possible to narrow down the values r_a^- and r_a^+ and so subject the theory to more rigorous testing. On the present occasion, however, we would stress the fact that the theory shows how molecular weight classes which are related to one another by simple proportions may be explained. We also note for future consideration the assumptions concerning values for r^- to r_a^+ which are necessary in order to identify Svedberg's classes with those already predicted. These assumptions appear not unplausible, but we would rather emphasize the great need for information as to r_a for the globular proteins in general under the particular conditions in which their molecular weights have been obtained (*cf.* McBain, Dawson and

Baker, 1934; McBain, 1936). Hydration values of proteins, which in any case are only available for a small proportion of the proteins studied by Svedberg, have been found to be enormously different for one and the same protein under different conditions (Adair and Adair, 1936). Hydration values have been investigated mostly for protein crystals, and it seems to be difficult, if indeed it is legitimate, to derive from these hydration values information as to the degree of hydration of proteins in the state in which they have been studied in the ultracentrifuge.

3. *Svedberg's Molecular Weight Classes.*

In a recent review Svedberg (1937) gives fourteen molecular weight classes. These comprise eleven numbers which are multiples of 17,600 (the multiples are 1, 2, 4, 8, 16, 24, 48, 96, 168, 192, and 384) and three others representing each a single protein, namely 26,000 (gliadin), 77,800 to 82,800 (yellow ferment), and 628,000 to 650,000 (thyroglobulin). The number 17,600 corresponds to the compound structure consisting of two C_1 units if $r_a = 17{,}600/144 = 122{\cdot}2$. Correspondingly all the multiples of this number correspond to simple or compound cyclol structures with $r_a = 122{\cdot}2$.

The other three numbers fall into the same sequence. Thus 26,000 corresponds to 3 C_1 units with $r_a = 120{\cdot}4$: the numbers 77,800 to 82,800 to 9 C_1 units with $r_a = 120{\cdot}1$ to $127{\cdot}8$, and the numbers 628,000 to 659,000 to 72 C_1 units with $r_a = 121{\cdot}7$ to $125{\cdot}4$. Evidently many of these numbers permit alternative cyclol structures. Thus the compound structure $4C_1$ is replaceable by the simple structure C_2, $9C_1$ by C_3, and $16C_1$ by C_4, and so on.

We therefore suggest the modification of Svedberg's unit 17,600, which excludes three of his molecular weights, into a unit half the size, interpretable as a 72 amino acid residue structure. We can then interpret all his molecular weights as compound C_1 structures or alternatively we can interpret some as higher cyclols, C_2, C_3, and C_4, and some as compound C_2, C_3, or C_4 structures. The complete set of alternatives is covered by the following structures :—

(2, 3, 4, 8, 9, 16, 32, 48, 72, 96, 192, 336, 384, 768) C_1 units,
(1, 2, 4, 8, 12, 18, 24, 48, 84, 96, 192) C_2 units,
(1, 8) C_3 units,

(1, 2, 3, 6, 12, 21, 24, 48) C_4 units,

(2) C_6 units,

(3, 6, 12) C_8 units.

It thus appears that Svedberg's figures do, as he suggested, indicate that many proteins are built up by the successive aggregation of definite units, and that the number of units which can be associated in a compound structure is limited rather severely, presumably by stability requirements. The limitation is seen in the absence of such factors as 5, 7, 11 . . . (except in the one case of $168 \times 17{,}600$, which appears to be rather anomalous), and, in fact, is implicit in Svedberg's observation, already quoted, to the effect that steps between actual molecular weights increase with the weight. If every multiple of any simple structure could occur the step from one molecular weight to the next need never exceed the weight of the simple structure however large the molecular weights themselves might be. This, according to Svedberg, proves not to be the case.

We would again emphasize the provisional and tentative nature of the suggested identification of Svedberg's molecular weights with cyclol structures. Mention has already been made of the fundamental difficulty that little is as yet known as to the degree of hydration of the proteins in the state in which their molecular weights have been measured in the ultra centrifuge. The position is that if the value 122·2 is acceptable for r_a for the eleven classes which are multiples of 17,600, then the structures proposed can stand as a basis for future discussion. Similarly, if the value 120·4 is acceptable for gliadin, 120·1 to 127·8 for yellow ferment, and 121·1 to 125·4 for thyroglobulin, then the structure proposed for these three proteins can also stand provisionally.

In the investigation we have taken Svedberg's figures strictly as given; but it should be pointed out that they are only approximations. Thus, the figure $2 \times 17{,}600 = 35{,}200$ represents a class of nine different proteins for which M_s values range from 35,000 to 45,800 and M_c values from 33,600 to 40,500. Again, the figure $24 \times 17{,}600 = 48 \times 8800 = 422{,}000$ represents a class of six proteins for which M_s values range from 379,600 to 503,000 and M_c values from 379,000 to 447,000.

We proceed now to investigate the compound cyclol

structures which have molecular weights of the right order of magnitude.

4. *Compound Cyclol Structures.*

It has already been suggested (Frank, 1936) that the cyclol fabric (fig. 3) depends for its stability upon the hydration of its peptide hydroxyls. Whether this is in fact the case or not, a study of known structures containing hydroxyls (Bernal, 1933 ; Megaw, 1934 ; Bernal and Megaw, 1935) and tertiary nitrogens possessing lone pairs of electrons (Hendricks, Wulf, Hilbert, and

Fig. 3.

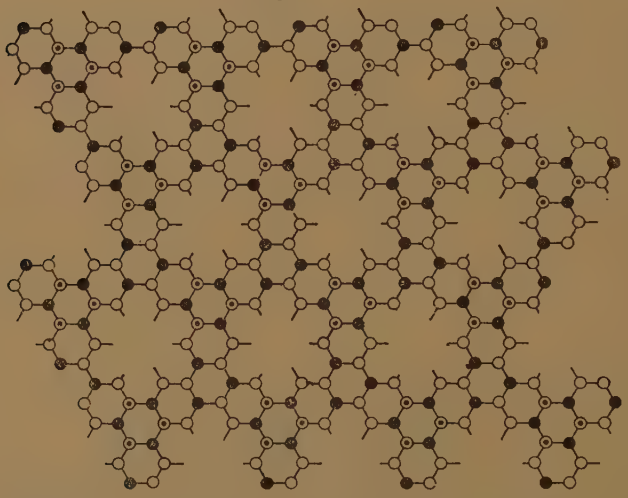

The cyclol fabric. The median plane of the lamina is the plane of the paper. The lamina has its " front " surface above and its " back " surface below the paper.—[From Proc. Roy. Soc. A, clx. (1937) p. 69, fig. 9.]

● =N.
O =C(OH), peptide hydroxyl upwards.
⊙ =C(OH), peptide hydroxyl downwards.
O— =CHR, direction of side chain initially outwards.
O— =CHR, direction of side chain initially upwards.

Liddel, 1936) makes it probable that some proportion of such constituents of a cyclol network are linked by hydrogen or hydroxyl bonds to water molecules or to other foreign molecules or ions capable of forming such links. This suggestion has been worked out in detail in connexion with the hydration of proteins (Wrinch,

1938 *b*). For the moment we are concerned rather to emphasize (Wrinch, 1936) that cyclol networks are admirably adapted to interlinking with one another, and that it is possible that cyclols can exist both independently with adequate complements of foreign constituents built into the fabric or so associated with each other that an adequate proportion of their peptide hydroxyls and tertiary nitrogens are interlinked. This idea provides a suggestion for a mechanism by which compound cyclols can be built. Other suggestions will present themselves at a later stage of the argument.

Now a cyclol molecule has a polyhedral frame (fig. 4) consisting of four hexagonal faces and four triangular faces, joined by twelve edges over which the network

Fig. 4.

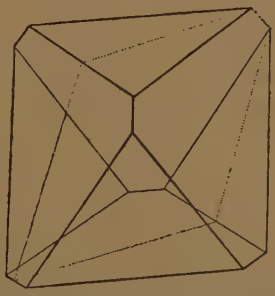

The polyhedral frame of the C_2 molecule.—[' Transactions of the Faraday Society,' xxxiii. 1368 (October 1937), p. 1373.

is bent; there are also six slits representing a special type of lacuna which differentiates globular proteins from proteins consisting of open cyclols (Wrinch, 1937, *d*). The association of two cyclols can therefore be of a variety of geometrical types, including apposition of faces, apposition of edges, and apposition of slits. Examples are shown of two cyclols with hexagonal faces (fig. 5), with edges (fig. 6), and with slits (fig. 7) in apposition. A structure known to be of $2C_1$ type (*e. g.*, possibly erythrocruorin *Lampetra*, cytochrome C, lactalbumin α, myoglobin) then belongs definitely to one or another of a fixed number of different varieties, of which those illustrated are examples.

In the same way a structure known to be of $3C_1$ type (*e. g.*, possibly gliadin) may belong to a fixed number of different varieties, including that shown in fig. 8, in

Fig. 5.

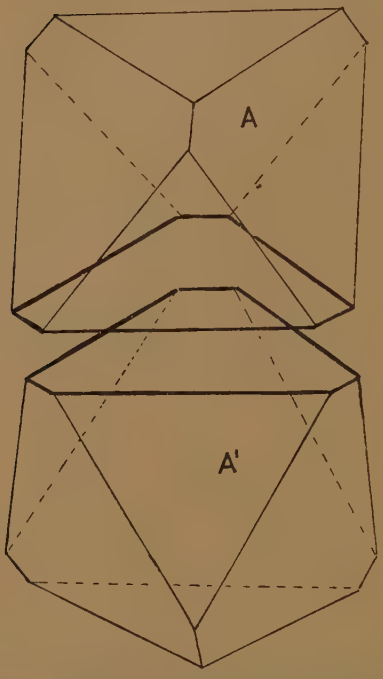

A compound structure consisting of a pair of C_n units, A and A′ (drawn for $n=1$), with hexagonal faces apposed. Each unit may be compared with fig. 1 *a* (Pl. I.) and fig. 2 *a* (Pl. II.) for $n=1$ and $n=2$ respectively.

Fig. 6.

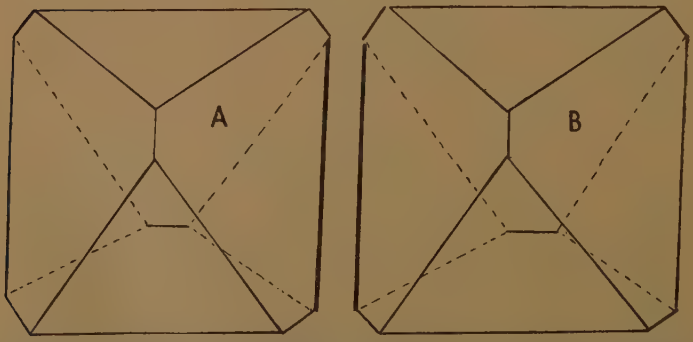

A compound structure consisting of a pair of C_n units, A and B (drawn for $n=1$), with edges apposed. Each unit may be compared with fig. 1 *a* (Pl. I.) and fig. 2 *a* (Pl. II.) for $n=1$ and $n=2$ respectively.

Fig. 7.

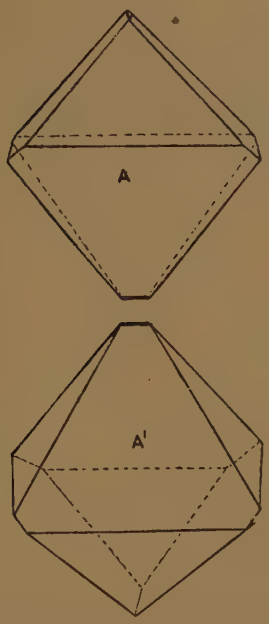

A compound structure consisting of a pair of C_n units, A and A′ (drawn for $n=1$), with slits apposed. Each unit may be compared with fig. 1 *b* (Pl. I.) and fig. 2 *b* (Pl. II.) for $n=1$ and $n=2$ respectively.

Fig. 8.

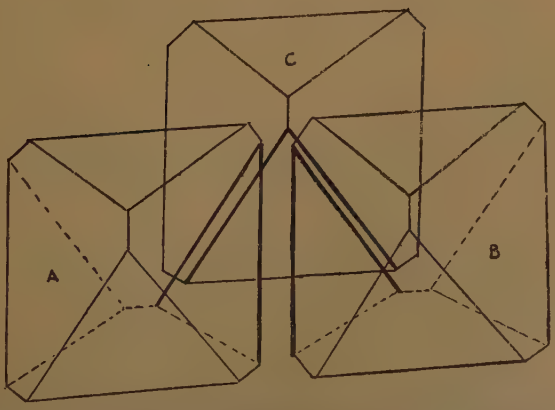

A compound structure consisting of a trio of C_n units, A, B, and C (drawn for $n=1$). Each pair AB, BC, CA is arranged as in fig. 6.

which each two C_1 units are linked by a pair of apposed edges. A structure with a number of residues corresponding to $4C_1$ again belongs to one of a fixed number of varieties. Included in this set is the example shown in fig. 9, in which four C_1 units are interlinked by pairs of edges; the simple cyclol C_2 also comes into consideration. All these possibilities have to be considered

Fig. 9.

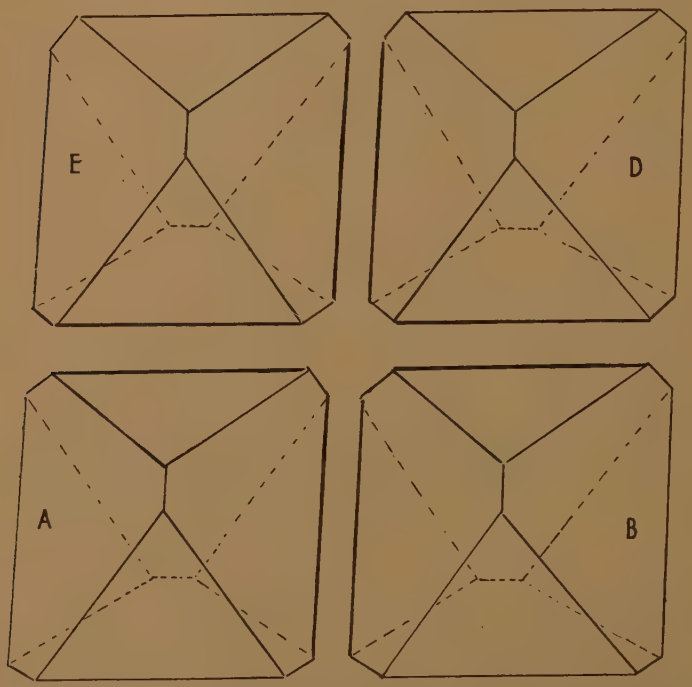

A compound structure consisting of a quartette of C_n units, A, B, D, and E (drawn for $n=1$). Each pair AB, BD, DE, EA is arranged as in fig. 6.

in connexion with the 35,000 molecular weight class, which includes zein, erythrocruorin (*Arca* and *Chironomos*), lactoglobulin, pepsin, insulin, Bence-Jones protein, and egg albumin. We have already suggested that these proteins may be 288 amino acid residue structures (Wrinch, 1937, *b*, *d*), and have considered how far a C_2 structure is satisfactory, in particular, for insulin (Wrinch, 1937, *c*, *e*) and for pepsin (Wrinch, 1937, *f*); when there

is reason to suppose that any of the class are compound structures, *e. g.*, possibly in the case of egg albumin (Williams and Watson, 1937), the various structures made up of four C_1 units must be considered.

It will be noticed that figs. 6, 8 and 9 all show cyclols associated in the same way, by means of pairs of edges. This arrangement is essentially that in a face-centred cubic lattice, and as such can be continued indefinitely.

Fig. 10.

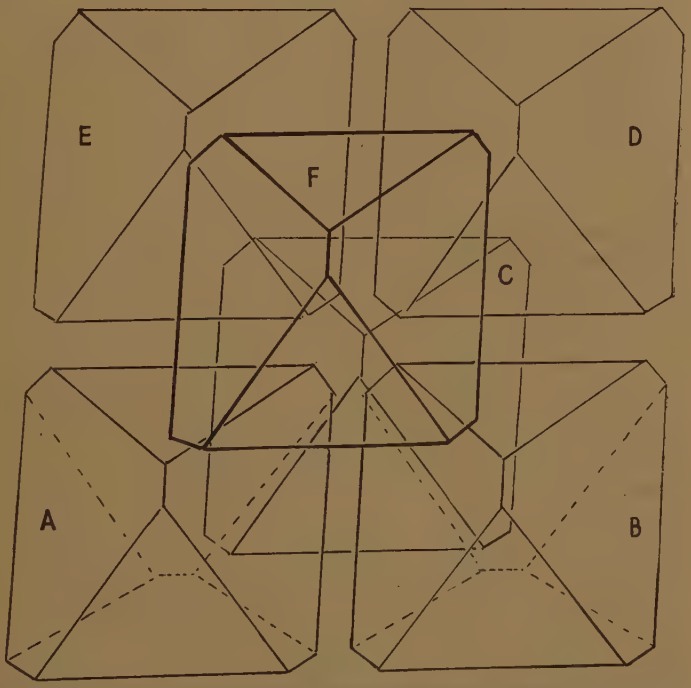

A compound structure consisting of a sextette of C_n units, A, B, C, D, E and F (drawn for $n=1$). Each pair AB, AC, AE, AF, BC, BD, BF, CD, CE, DE, DF, EF is arranged as in fig. 6; each trio ABC, ABF, ACE, AEF, BCD, BDF, CDE, DEF is arranged as in fig. 8. The quartette ABDE is arranged as in fig. 9.

We suggest (Wrinch, 1938*c*) that certain proteins, notably those with very high molecular weights, such as the hæmocyanins, virus proteins, etc., may consist of cage-colonies, one example of which is sketched in fig. 10. The tobacco virus protein has been shown in 'X-ray Studies' (Bernal and Fankuchen, 1936) to be built on the plan of a

hexagonal unit of dimensions 20 A. and 20 A. in the *c*-planes and normal to these planes to have a repeat of $3 \times 22{\cdot}2$ A. These dimensions fit with those of C_1 cages. In order to make more detailed suggestions regarding this cage-colony structure, we await informatiou regarding the nature of the association between the protein and nucleic acid components.

In building cage-colony structures in general all other ways in which numbers of cyclols can be packed, by apposition of faces, slits, etc., also come into consideration. Mixed types of coordination are also a possibility in which, as for example in fig. 11, certain units are linked by edges and others by slits.

It is of interest to notice the symmetry characteristic of compound cyclols in relation to those of the simple cyclols. The symmetry of all C_n cyclols, apart from their R group (in the case for example when all R groups are simply hydrogens and all the amino acids are glycine), is the same. They have no centre of symmetry; they have four trigonal axes, three dyad axes, and no tetrad axes. Some or all of these symmetry characteristics can be destroyed by suitable distributions of R groups. A cyclol can be simply trigonal if (as has been suggested in the study of the possibility that insulin is a C_2 structure) one hexagonal face and the opposite trigonal face have trigonal arrangements of R groups and the other three hexagonal faces and triangular faces have identical, non-trigonal distributions of R groups. By destroying the trigonal character of the R group distribution on either hexagonal or triangular face the trigonality of the molecule can be destroyed. Compound cyclols, however, can be built in which the structure, even apart from R groups, has as low a symmetry as we please. Thus the structure shown in fig. 5 has one trigonal axis and that shown in fig. 6 no symmetry elements at all. On the other hand, it is of interest to notice that a compound structure can conserve just those symmetry characteristics associated with the simple cyclols of which it is formed. An example is shown in fig. 10.

5. *The Reversible Dissociation of Compound Structures.*

The suggestion that cyclol networks can interlink by forming hydroxyl or hydrogen bonds allows a development of the idea of compound cyclols on the lines

indicated by the figures 5–11. The dissociation of a compound molecule in which interlinking is of this type will occur when there is in the solution a sufficient concentration of hydroxyl or hydrogen bond forming molecules. (This behaviour is found to occur in the case

Fig. 11.

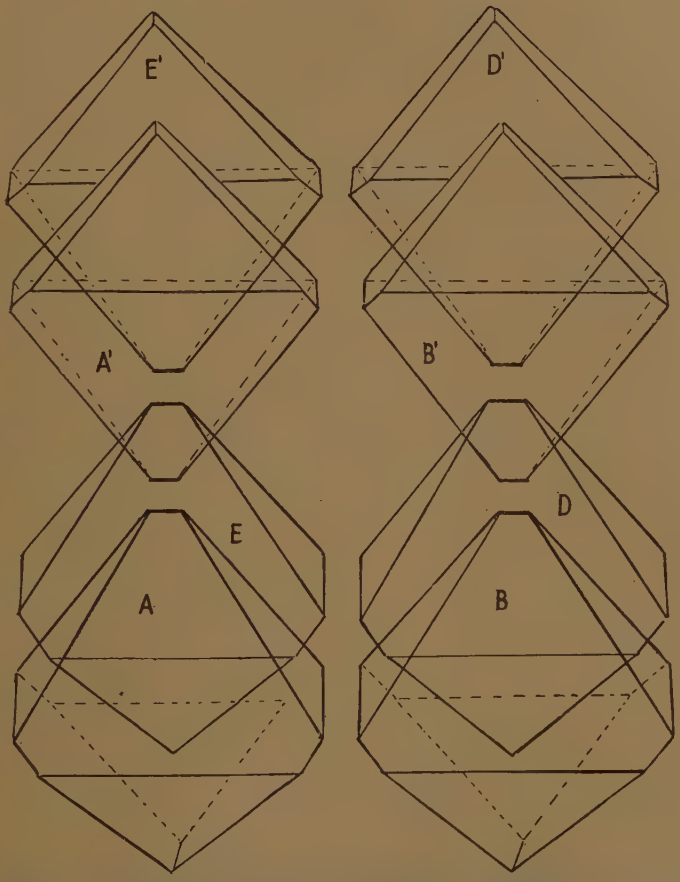

A compound structure consisting of an octette of C_n units, A, B, D, E, A′, B′, D′, E′ (drawn for $n=1$). Each pair AA′, BB′, DD′, EE′ is arranged as in fig. 7; each quartette ABDE, A′B′D′E′ is arranged as in fig. 9.

of benzoic acid. In benzene it is associated, but on the addition of phenol it dissociates. The accepted explanation (Barger, 1905) is that molecules of phenol combine

with the solute.) Two sets of facts regarding proteins become relevant in this connexion—the break-up of protein molecules on dilution (*cp.* the interesting findings of Beale (1937) with regard to the tobacco virus protein) and on the addition of urea and certain other molecules. Horse hæmoglobin, for example, is partly dissociated into half-molecules upon dilution (Svedberg, 1937); thyroglobulin (Heidelberger and Pedersen, 1937) also shows several dissociation products when diluted (Lungren, 1936). Again, horse hæmoglobin dissociates into half-molecules under the action of urea, acetamide, and formamide (Steinhardt, 1936). Egg albumin also exhibits similar behaviour (Williams and Watson, 1937).

We suggest that the explanation of these phenomena resides in the capacity of water and of urea and of certain other molecules to form hydrogen or hydroxyl bonds with the protein networks; a sufficient concentration of these molecules therefore breaks down the association of protein networks in favour of a situation in which each is associated with an adequate number of foreign molecules and not with another protein network. An interesting precedent is afforded by the clay minerals such as montmorillonite (Pauling, 1930; Nargelschmidt, 1934; Hofmann, 1934 *a*) and by graphitic oxide (Hofmann, 1934 *b*). In the anhydrous state montmorillonite has hydroxyl links between its layers; in the hydrated state those hydroxyls are linked to foreign water molecules which form a new layer between layers previously interlinked. The water molecules, we may say, split the laminate structure. In providing this interesting precedent for the dissociation phenomena exhibited by certain proteins, the clay minerals are again seen to be of the greatest relevance for the problem of protein structure (Wrinch, 1936).

The suggestion that hydroxyl and hydrogen bonds provide the mechanism for interlinking of individual cyclols into compound structures followed from a consideration of the cyclols network itself. The presence of the constituent residues also may play a part. The R groups of two cyclols may hold them together in various ways. In the case of R groups containing hydroxyls, such as serine, tyrosine, and hydroxyproline, it may again be by some means of hydrogen and hydroxyl bonds. If the R groups are ionizable, then basic and acidic groups

may form salt linkages (Astbury and Woods, 1933). Finally, in the case of cystine (Astbury and Woods, 1933) disulphide linkages may make two or more single cyclols into what is essentially one covalent unit; this may also be the case if and when covalent peptide linkages are formed between R groups, *e. g.*, between arginine and glutamic acid (Astbury, 1933).

Interlinking by means of salt linkages, and also presumably by hydrogen and hydroxyl linkages, depends essentially upon the acidity of the medium. It thus explains many cases of reversible dissociation and association of protein molecules caused by changes in pH, for in such cases the state of greatest association is always in a pH range which includes the isoelectric point of the protein. This phenomenon is widespread amongst the proteins (Svedberg, 1937). It is characteristic of serum albumin and serum globulin and also of the seed globulins, excelsin, amandin, and edestin, belonging to the class at about 282,000 (Burk, 1937). The most striking cases are perhaps those of the respiratory proteins (Eriksson-Quensel and Svedberg, 1936.) Helix hæmocyanin, for example, of weight 6,740,000 dissociates step-wise into halves, eighths, and sixteenths under the stimulus of pH changes. The pH dissociation products represent perfectly homogenous components.

Still another mechanism for holding together compound structures is suggested by further researches on Helix hæmocyanin (Svedberg, 1937). It is found that upon addition of 0·01 molar calcium chloride the dissociation on the alkaline side of the isoelectric point, which normally starts at pH 7·4, does not become noticeable until a pH of about 9·5 is reached, where splitting into halves and eighths takes place. We may, perhaps, deduce that divalent calcium ions link together certain R^- groups in different parts of the compound structure, and that these components, securely held together by salt linkages between R^+ and R^- groups when the pH is near the isoelectric point, tend to fall apart as an increase in pH causes the suppression of more and more of the positively ionized groups. Calcium ions, we presume, link together R^- groups which for lower pH values had R^+ partners; all calcium ions having been used in this way, and the pH being still further increased, the submolecules fall apart when the number of $R^-Ca^{++}R^-$ links

is not sufficient to counterbalance the repulsions between R^- groups which have lost their partners.

The actual detailed suggestions regarding the nature of the compound structures made above are tentative. The interesting point is this: it appears possible to understand many aspects of protein behaviour which have been brought to light in the ultra-centrifuge, by assuming that certain definite protein units can exist associated in pairs, in trios, in quartettes, even in groups of eight and higher numbers.

The proteins on this view would seem to fill the gap between two well-established types of phenomena; they are on the one hand to be regarded simply as associated molecules like formic acid dimers (Pauling and Brockway, 1935) where the number of units is comparatively large, on the other hand as crystals where the number of units is comparatively small. The cyclol hypothesis explains this characteristic behaviour in terms of the specific nature of the cyclol protein fabric and the special geometrical shape of space-enclosing cyclols determined by the valency angles of the atoms of which the fabric consists.

A number of other results obtained by Svedberg are concerned with the splitting of proteins by specific molecules. These may prove to be understandable in terms of the hypothesis that the foreign molecules form links to protein network, previously linked with each other. As instances we may cite the results (Svedberg, 1937) that serum albumin and Helix hæmocyanin are split by clupein. The fact that the former is split by arginine and ammonium chloride but not by lysine and ammonium chloride, and the latter by lysine and ammonium chloride but not by arginine and ammonium chloride, shows that the ultra centrifuge provides new methods for the study of the specificity of individual proteins.

6. *Conclusion.*

The further consideration of the cyclol theory shows that its predictions and general point of view are in good accord with the findings of Svedberg. This hypothesis entails the deduction that in any range of molecular weights there is only a definite number of globular protein structures comprising specific numbers of amino

acid residues. The geometrical shape of these units and the nature of the cyclol network of which they are made both suggest that such units may build compound structures. It follows that structures having molecular weights of all orders of magnitude may be built from a few different units, or even from one single unit.

The actual numbers given by Svedberg for all fourteen different molecular weights classes may be represented by simple or compound C_1, C_2, C_3, C_4, C_6 units or even C_1 and C_2 units alone, on the assumption that the apparent residue weights of the molecules lie between 121 and 128. A cage-colony structure is proposed for the heavier proteins. On the basis of these results it is claimed that the cyclol hypothesis offers general interpretation in qualitative terms of Svedberg's results, many of which prove readily understandable in terms of the idea of the compound structure built up of one or more fundamental units. Quantitative testing of the hypothesis requires data regarding the degree of hydration of the molecules during the ultra centrifugal analysis which are not yet available.

Pending the results of quantitative tests we wish to emphasize the general point of view upon which our enquiry into the structure of proteins is based. Given that protein molecules are polycondensation products of amino acids which are interlinked by bonds between the nitrogen of one and the terminal carbon of another, there are only a certain mathematically determinate number of possible structures. The cyclol hypothesis gives precise expression to this general point of view by postulating that the C—N polycondensation of amino acids are built on the two-dimensional scheme exemplified by the cyclol network, and we find that this logically implies the existence of simple and compound space-enclosing structures, which moreover have only certain molecular weight ranges, and that these cover Svedberg's figures. This particular postulate has been developed in considerable detail since it was hardly feasible to show the potentialities of the geometric method by general statements alone. The important point is, however, that the number of possible structures which conform to the metrical conditions imposed by the constituent atoms is mathematically determinate. If and when quantitative tests dispose of the cyclol hypothesis it will

be necessary to investigate other alternative ways of building protein molecules. In any case, our final objective (Wrinch, 1938 *a*, *c*) is the full and exhaustive formulation of all geometrically possible C—N polycondensation products of the amino acids and imino acids, since these alone can provide a firm foundation for theories as to the structure of proteins.

The thanks of the author are offered to Dr. Irving Langmuir, to Professor Niggli and Professor W. L. Bragg, to Professor E. H. Neville, to H. D. Megaw, to G. F. Adair, M. Dixon, and R. Hill, and to many other colleagues. She is once again greatly indebted to M. F. Howson for the drawings.

References.

Adair and Adair, Proc. Roy. Soc. B, 819, p. 422 (1936).
Astbury, Trans. Faraday Soc. xxix. p. 193 (1933).
Astbury and Woods, Phil. Trans. Roy. Soc. A, p. 716 (1933).
Barger, J. Chem. Soc. lxxxvii. p. 1042 (1905).
Beale, Contrib. Boyce Thompson List, viii. p. 413 (1937).
Bernal, Ann. Rep. Chem. Soc. p. 401 (1933).
Bernal and Fankuchen, ' Nature,' cxxxviii. p. 1051 (1936).
Bernal and Megaw, Proc. Roy. Soc. cli. p. 384 (1935).
Burk, J. Biol. Chem. cxx. p. 63 (1937).
Eriksson-Quensel and Svedberg, Biol. Bull. lxxi. p. 498 (1936).
Frank, ' Nature,' cxxxviii. p. 242 (1936).
Heidelberger and Federson, J. Exp. Med. lxv. p. 393 (1937).
Hendriks, Wulf, Hilbert, and Liddell, J. Am. Chem. Soc. lviii. p. 1991 (1936).
Hofmann, *Kolloid Z.* lxix. p. 120 (1934 *a*).
Hofmann, Liebig's *Ann.* 510, p. 1 (1934 *b*).
Lungren, ' Nature,' cxxxviii. p. 122 (1936).
McBain, J. Am. Chem. Soc. lviii. p. 315 (1936).
McBain, Dawson, and Baker, J. Am. Chem. Soc. lvi. p. 1021 (1934).
Megaw, *Z. Krystallogr.* lxxxvii. p. 185 (1934).
Nargelschmidt, *Z. Krystallogr.* lxxxvii. p. 120 (1934).
Pauling, Proc. Nat. Acad. Sci. Wash. xvi. pp. 123, 578 (1930).
Pauling and Coryell, Proc. Nat. Acad. Sci. Wash. (1936).
Pauling and Brockway, Proc. Nat. Acad. Sci. Wash. xx. p. 336 (1934).
Rimington, Trans. Faraday Soc. xxvii. p. 1 (1931).
Steinhardt, ' Nature,' cxxxviii. p. 800 (1936).
Svedberg, ' Nature,' cxxxix. p. 1051 (1937).
Williams and Watson, ' Nature,' cxxxvi. p. 506 (1937).
Wrinch, ' Nature,' cxxxvii. p. 411 (1936).
Wrinch, Proc. Roy. Soc. A, clx. p. 59 (1937 *a*).
Wrinch, ' Nature,' cxxxix. p. 972 (1937 *b*).
Wrinch, ' Science,' lxxxv. p. 566 (1937 *c*).
Wrinch, Proc. Roy. Soc. A, clxi. p. 505, (1937 *d*).
Wrinch, Trans. Faraday Soc. xxxiii. p. 1368 (1937 *e*).
Wrinch, Phil. Mag. xxiv. p. 940 (1937 *f*).
Wrinch, Proc. Phys. Soc. l. p. 141 (1938 *a*).
Wrinch, Phil. Mag. xxv. p. 705 (1938 *b*).
Wrinch, Cold Spring Harbor Symposium (in the press) (1938 *c*).

XXIX. *Operational Solution of the Wave Equation.* *By* Louis A. Pipes, *Ph.D., Electrical Engineering Department, The University of Wisconsin* *.

[Received April 8, 1938.]

Introduction.

IT is the purpose of this paper to obtain the general solution of the inhomogeneous wave equation by an operational process. As is well known the wave equation is of the utmost importance in physics, particularly in the fields of electromagnetism and sound.

The inhomogeneous wave equation has been dealt with successively by L. Lorenz, Lord Rayleigh, H. A. Lorentz, Beltrami, and Poincare. In the last few years, with the growing practical importance of high-frequency electromagnetic fields, this equation has assumed a central position in the theory of electricity, because both the scalar and vector potentials are propagated in accordance with it.

The method to be employed in this paper is the Laplace Transform point of view of the " Operational Calculus."

The Inhomogeneous Wave Equation.

The equation to be considered may be written in the form

$$\frac{1}{a^2}\frac{\partial^2 u}{\partial t^2} = \nabla^2 u + 4\pi w(x, y, z, t). \quad . \quad . \quad . \quad (1)$$

This equation is also known under the name of D'Alembert's or Lorenz's equation.

A solution of this equation will be obtained subject to the initial boundary conditions

$$(u)_{t=0} = \mathrm{F}(x, y, z), \quad . \quad . \quad . \quad . \quad . \quad . \quad (2)$$

$$(\partial u/\partial t)_{t=0} = \mathrm{G}(x, y, z), \quad . \quad . \quad . \quad . \quad (3)$$

that is, we specify the initial value of u and its time derivative at $t=0$.

The Laplacian Transformation.

Following van der Pol (Phil. Mag. viii. p. 861 (1929)), we will regard $g(p)$ as the operational equivalent of $h(t)$ if $g(p)$ and $h(t)$ are related by the fundamental equation

$$g(p) = p\int_0^\infty e^{-pt} h(t)\, dt, \quad . \quad . \quad . \quad . \quad (4)$$

* Communicated by the Author.

where p is a complex number whose real part is greater than zero, and the integral is supposed to converge.

If the above relation is satisfied, we write

$$g(p) \doteqdot h(t). \quad . \quad . \quad . \quad . \quad . \quad . \quad . \quad (5)$$

Now, by the Fourier-Mellin theorem, we have the inversion formula

$$h(t) = \frac{1}{2\pi i} \int_{c-i\infty}^{c+i\infty} \frac{g(p)e^{pt}dp}{p}, \quad i = \sqrt{-1}, \quad . \quad . \quad (6)$$

where c is a positive constant such that the path of integration in the complex p plane lies to the right of the singularities of the integrand.

The Operational Solution.

If we take

$$\frac{\partial^2 u}{\partial t^2} = a^2 \nabla^2 u + 4\pi a^2 w(x, y, z, t), \quad . \quad . \quad . \quad (1)$$

multiply by $pe^{-pt}dt$, and integrate from 0 to infinity, and suppose the integrals to converge, we obtain

$$p^2\mathrm{U} - p^2\mathrm{F}(x, y, z) - p\mathrm{G}(x, y, z) = a^2 \nabla^2 \mathrm{U} + 4\pi a^2 \mathrm{W}(x, y, z, p), \quad . \quad . \quad . \quad (7)$$

where we have set

$$\mathrm{U} \doteqdot u \quad . \quad . \quad . \quad . \quad . \quad . \quad . \quad . \quad (8)$$

and

$$\mathrm{W} \doteqdot w, \quad . \quad . \quad . \quad . \quad . \quad . \quad . \quad . \quad (9)$$

and have integrated

$$p \int_0^\infty e^{-pt} \frac{\partial^2 u}{\partial t^2} dt$$

by parts, making use of the initial conditions. We may therefore write the transformed equation in the form

$$\nabla^2 \mathrm{U} - (p^2/a^2)\mathrm{U} + (p^2/a^2)\mathrm{F} + (p/a^2)\mathrm{G} + 4\mathrm{W} = 0 \, . \quad (10)$$

If we let

$$p^2/a^2 = -k^2 \quad . \quad . \quad . \quad . \quad . \quad . \quad . \quad (11)$$

and

$$4m = (p^2/a^2)\mathrm{F} + (p/a^2)\mathrm{G} + 4\pi\mathrm{W} \quad . \quad . \quad . \quad (12)$$

we have to solve the equation

$$\nabla^2 \mathrm{U} + k^2 \mathrm{U} + 4m = 0 \quad . \quad . \quad . \quad . \quad . \quad (13)$$

for the operational equivalent of u. This equation is known as Helmholtz's Equation.

Solution of Helmholtz's Equation.

We have succeeded by means of the Laplacian Transformation in eliminating all dependence on time and have obtained a new equation in which the functions depend only on the coordinates and on the parameter p. To solve the equation (13) we employ one of the forms of Green's Theorem, which may be stated in the form

"If U and V are two arbitrary scalar space functions of suitable differentiability, then

$$\iiint_{\text{Vol.}} (\text{V}\nabla^2\text{U}-\text{U}\nabla^2\text{V})dv=\iint (\text{V}\nabla\text{U}-\text{U}\nabla\text{V}).\bar{ds}, \quad (14)$$

where the surface of integration on the right is such as to enclose the volume of integration on the left side of the equation."

Consider the equation

$$\nabla^2\text{V}+k^2\text{V}=0\,; \quad . \quad . \quad . \quad . \quad . \quad (15)$$

this equation has a particular integral,

$$\text{V}=\frac{\exp(\mp ikr)}{r}, \quad . \quad . \quad . \quad . \quad . \quad (16)$$

where r is the distance from some fixed point p.

Let us draw a sphere of radius a about P, and let the volume of integration be taken throughout the space outside this sphere included by a sphere of arbitrarily large radius b.

Let $\text{V}=\frac{\exp(\pm ikr)}{r}$, and substitute into (14). We then obtain

$$\iiint_{\text{Vol.}} \frac{e^{\pm ikr}}{r}(\nabla^2\text{U}+k^2\text{U})dv=\iint_{\text{S.}}\left[\frac{e^{\pm ikr}}{r}\nabla\text{U}-\text{U}\nabla\frac{(e^{\pm ikr})}{r}\right].d\bar{\text{S}}$$

$$+\iint_{\text{S.}}\left[\text{U}\frac{\partial}{\partial a}\frac{(e^{\pm ika})}{a}-\frac{e^{\pm ika}}{a}\frac{\partial\text{U}}{\partial a}\right]a^2dw, \quad . \quad (17)$$

where the first integral on the right is taken over the surface of the large sphere and the second integral over the surface of the small sphere, and $(\nabla\text{U}).d\bar{\text{S}}=\frac{\partial\text{U}}{\partial n}ds$. Letting the sphere about P shrink to zero and letting the outer sphere become infinitely large, then if U vanishes

for large r at least as strongly as $1/r$ the first integral will vanish. The second integral may be written as

$$-\iint \mathrm{U}e^{\pm ika}\,dw \pm ik\iint a\mathrm{U}e^{\pm ika}\,dw - \iint a\,\frac{\partial \mathrm{U}}{\partial a}\,e^{\pm ika}\,dw,$$

where $$ds = a^2 dw.$$

Now as a approaches zero the only term that remains is the first. It becomes $-4\pi \mathrm{U}_p$, the value of U at the point p.

Hence

$$\iiint_{\text{Vol.}} \frac{e^{\pm ikr}}{r}\,(\nabla^2\mathrm{U} + k^2\mathrm{U})\,dv = -4\pi \mathrm{U}_p. \quad . \quad . \quad (18)$$
$$\text{All space.}$$

But

$$\nabla^2\mathrm{U} + k^2\mathrm{U} = -4\pi m, \quad . \quad . \quad . \quad . \quad (13)$$

and consequently

$$\mathrm{U} = \iiint \frac{m(x_1, y_1, z_1)\epsilon^{\pm \frac{p}{a}r}}{r}\,dv \quad . \quad . \quad . \quad (19)$$

is the solution required.

Interpretation of the Operational Equivalent.

We have now succeeded in obtaining an explicit solution for the operational equivalent of the function $u\,(x, y, z, t)$. Since

$$m(x, y, z, p) = \frac{p^2}{2\pi a^2}\mathrm{F} + \frac{p}{4\pi a^2}\mathrm{G} + \mathrm{W}(x, y, z, p), \quad (12)$$

it is seen that the solution is composed of three parts.

Now, directly from the contour integral (6) we have the results

$$e^{-p(r/a)} \doteqdot \left\{ \begin{array}{l} 0 \text{ if } t \text{ is less than } r/a \\ 1 \text{ if } t \text{ is greater than } r/a \end{array} \right\} . \quad . \quad . \quad (20)$$

and

$$e^{+p(r/a)} \doteqdot \left\{ \begin{array}{l} 0 \text{ if } t \text{ is less than } -r/a \\ 1 \text{ if } t \text{ is greater than } -r/a \end{array} \right\} . \quad . \quad (21)$$

Now since (at) and r are both positive, the condition that (at) be greater than $-r$ is automatically satisfied, and the condition that (at) be greater than r only must be considered.

First let the term

$$\frac{1}{4\pi a^2}\iiint_{\text{All space.}} G(x_1, y_1, z_1)e^{pr/a}\,dv \quad . \quad . \quad . \quad (22)$$

be considered.

To carry out the integration let us consider the introduction of spherical coordinates with the origin at (x, y, z) :

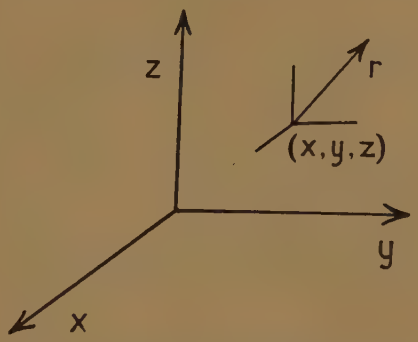

$$\left.\begin{aligned} x_1 &= x + r\sin(\theta)\cos(\phi), \\ y_1 &= y + r\sin(\theta)\sin(\phi), \\ z_1 &= z + r\cos(\theta), \\ dv &= r^2\sin(\theta)dr\,d\theta\,d\phi. \end{aligned}\right\} \quad . \quad . \quad . \quad . \quad (23)$$

Hence

$$\frac{1}{4\pi a^2}\iiint_{\text{All space.}} \frac{G(x_1, y_1, z_1)e^{\pm(pr/a)}\,dv}{r}$$

$$= \frac{1}{4\pi a^2}\int_0^\infty r\,dr\int_0^\pi\int^{2\pi} G(x + r\sin\theta\cos\phi,\ y + r\sin\theta\sin\phi,\ z + r\cos\theta)\sin\theta\,dr\,d\theta\,d\phi. \quad . \quad . \quad . \quad . \quad (24)$$

Since this expression is zero unless r is less than at by the conditions (20) and (21), we can replace the infinite limit in the integration with respect to r by the limit at, and hence write

$$\frac{1}{4\pi a^2}\iiint_{\text{All space.}} G(x_1, Y_1, z_1)\,e^{\pm pr/a}\,dv$$

$$\doteqdot \frac{1}{4\pi a^2}\int_0^\infty r\,dr\int_0^\pi\int_0^{2\pi} G(x + r\sin\theta\cos\phi,\ Y + r\sin\theta\sin\phi,\ z + r\cos\theta)\sin\theta\,d\theta\,d\phi. \quad . \quad . \quad . \quad . \quad (25)$$

We now recall the well-known operational theorem that if

$$g(p) \doteqdot h(t) \quad . \quad . \quad . \quad . \quad . \quad . \quad . \quad (26)$$

then $$pg(p) \doteqdot \frac{d}{dt}h(t) \quad \text{if} \quad h(0)=0.$$

Hence

$$\frac{p}{4\pi a^2}\iiint_{\text{All space.}} \frac{G(x_1, y_1, z_1)e^{\pm pr/a}\,dv}{r}$$

$$\doteqdot \frac{1}{4\pi a^2}\frac{d}{dt}\int_0^{at} r\,dr \int_0^{\pi}\int_0^{2\pi} G(x+r\sin\theta\cos\phi, y+r\sin\theta, \sin\phi, z+r\cos\theta)\sin\theta\,d\theta\,d\phi.$$

$$. \quad . \quad . \quad . \quad (27)$$

Or, differentiating the expression with respect to the upper limit, one obtains

$$\frac{t}{4\pi}\int_0^{\pi}\int_0^{2\pi} G(x+at\sin\theta\cos\phi,\ y+at\sin\theta\sin\phi,\ z+at\cos\theta)\sin\theta\,d\theta\,d\phi.$$

$$. \quad . \quad . \quad . \quad (28)$$

In this integral we have a point function integrated throughout the surface of a sphere. The element of spherical surface is

$$dS=(at)^2\sin\theta\,d\theta\,d\phi. \quad . \quad . \quad . \quad . \quad (30)$$

By definition the mean value of a function on a sphere is

$$\bar{F}=\frac{1}{4\pi r^2}\int_0^{\pi}\int_0^{2\pi} Fr^2\sin(\theta)\,d\theta\,d\phi. \quad . \quad . \quad . \quad (31)$$

Hence, placing $r=at$, we have

$$\frac{p}{4\pi a^2}\iiint_{\text{All space.}} \frac{G(x_1, y_1, z_1)\,e^{\pm pr/a}\,dv}{r} \doteqdot t\bar{G}(at), \quad . \quad (32)$$

where $\bar{G}(at)$ means the mean value of the function $G(x, y, z)$ upon a sphere of radius at about (x, y, z).

Now considering

$$\frac{1}{4\pi}\iiint_{\text{All space.}} \frac{(p/a)^2F(x_1, y_1, z_1)e^{-\pm pr/a}\,dv}{r}, \quad . \quad . \quad (33)$$

and going through the same argument, with the exception that in this case the second derivative with respect to

t must be taken because of the presence of the factor p^2, we obtain

$$\frac{p^2}{4\pi a^2}\iiint \frac{\mathrm{F}(x_1, y_1, z_1)e^{\pm pr/a}\,dv}{r} = \frac{d}{dt}[t\overline{\mathrm{F}}(at)], \quad . \quad (34)$$

where $\overline{\mathrm{F}}(at)$ means the mean value of $\mathrm{F}(x, y, z)$ upon a sphere of radius about at and centre at z, y, x.

We must now consider the term

$$\iiint_{\text{All space.}} \frac{\mathrm{W}(x_1, y_1, z_1)e^{\pm pr/a}\,dv}{r} \quad . \quad . \quad . \quad . \quad (35)$$

Now we have the well-known theorem :

If $g(p) \doteqdot h(t)$, then

$$e^{pk}g(p) = h(t+k), \quad k \text{ greater than } 0 \text{ if } h(t)=0, \quad (36)$$

for $0<t<k$, and

$$e^{-pk}g(p) \doteqdot \left\{ \begin{array}{ll} 0 & \text{for } t \text{ less than } k, \\ h(t-k) & \text{for } t \text{ greater than } k,\ k \text{ positive.} \end{array} \right\} \quad . \quad . \quad . \quad (37)$$

Hence we have the result

$$\iiint_{\text{All space.}} \frac{\mathrm{W}(x_1, y_1, z_1)e^{\pm pr.a}\,dv}{r} \doteqdot \iiint_{\text{All space.}} \frac{w(x_1, y_1, z_1\, t \pm r/a)\,dv}{r} . \quad . \quad . \quad . \quad (38)$$

The choice of the plus sign in the argument $t+r/a$ corresponds to an advanced potential in the theory of electricity, and the minus sign to a retarded potential. It is the retarded potential that has physical interest.

Conclusion.

By using Laplacian Transform or operational methods the solution

$$u(x, y, z, t) = \frac{d}{dt}[t\overline{\mathrm{F}}(at)] + t\overline{\mathrm{G}}(at) + \iiint_{\text{All space.}} \frac{w[x_1, y_1, z_1\, t \pm r/a]\,dv}{r} \quad (39)$$

has been obtained for the equation

$$\frac{\partial^2 u}{\partial t^2} = a^2 \nabla^2 u + 4\pi a^2 w(x, y, z, t), \quad . \quad . \quad . \quad (1)$$

subject to the boundary conditions

$$(u)_{t=0}=\mathrm{F}(x, y, z) \quad . \quad . \quad . \quad . \quad . \quad . \quad (2)$$

and

$$(\partial u/\partial t)_{t=0}=\mathrm{G}(x, y, z). \quad . \quad . \quad . \quad . \quad . \quad (3)$$

If comparison be made between this treatment and the older classical treatments the greater simplicity of the operational method will be apparent.

Bibliography.

B. Van der Pol, Phil. Mag. viii. p. 861 (1929).

XXX. *On Wave-motion for Infinite Domains.*

By Dr. Arnold N. Lowan, *Brooklyn College* †.

[Received April 2, 1938.]

THE object of this paper is the integration of the general differential equation of wave-motion :

$$\text{(I.)} \quad \nabla^2 u(\mathrm{P}, t)=2b\frac{\partial}{\partial t}u(\mathrm{P}, t)+\frac{1}{a^2}u(\mathrm{P}, t)+\Phi(\mathrm{P}, t)$$

for one, two, and three dimensions ; the solution satisfying the initial conditions :

$$\text{(II.)} \quad \lim_{t\to 0} u(\mathrm{P})=f(\mathrm{P}),$$

$$\text{(III.)} \quad \lim_{t\to 0}\frac{\partial}{\partial t}u(\mathrm{P})=g(\mathrm{P}).$$

The appended bibliography covers the solution of the differential equation (I.) for certain special cases of infinite, semi-infinite, or finite domains; in the latter case additional boundary conditions are prescribed. This paper will be divided into four sections, beginning with the simplest case of wave-motion in a one-dimensional, non-resisting medium and ending with the non-homogeneous, differential equation of wave-motion for a three-dimensional, resisting medium.

† Communicated by the Author.

Section I.

Vibration of an Infinite String.

In this case the displacement $u(x, t)$ must satisfy the following system :

$$\frac{\partial^2}{\partial t^2}u(x, t)=c^2\frac{\partial^2}{\partial x^2}u(x, t), \quad . \quad . \quad . \quad . \quad (1)$$

$$-\infty<x<\infty\,;\ t>0,$$

$$\lim_{t\to 0}u(x, t)=f(x), \quad . \quad . \quad . \quad . \quad . \quad . \quad . \quad (2)$$

$$\lim_{t\to 0}\frac{\partial}{\partial t}u(x, t)=g(x), \quad . \quad . \quad . \quad . \quad . \quad . \quad (3)$$

Let

$$\mathrm{L}\{u(x, t)\}=\int_0^\infty \exp(-pt)u(x, t)\,dt=u^*(x, p), \quad . \quad (4)$$

whence

$$\mathrm{L}\left\{\frac{\partial}{\partial t}u(x, t)\right\}=pu^*(x, p)-u(x, 0)$$

$$=pu^*(x, p)-f(x) \quad . \quad . \quad . \quad . \quad . \quad (5)$$

and

$$\mathrm{L}\left\{\frac{\partial}{\partial t^2}u(x, t)\right\}=p^2u^*(x, p)-pu(x, 0)-\left(\frac{\partial u}{\partial t}\right)_{t=0}$$

$$=p^2u^*(x, p)-pf(x)-g(x). \quad . \quad . \quad (6)$$

It is then seen that the function $u^*(x, p)$ must satisfy the ordinary differential equation :

$$\frac{\partial^2}{\partial x^2}u^*(x, p)-\frac{p^2}{c^2}u^*(x, p)=-\frac{p}{c^2}f(x)-\frac{1}{c^2}g(x)$$

$$=-\mathrm{F}(x, p) \quad (\text{say}). \quad . \quad (7)$$

In view of the identity

$$\Phi(x)=\frac{1}{\pi}\int_{-\infty}^{+\infty}\Phi(\xi)\,d\xi\int_0^\infty \cos\alpha(x-\xi)\,d\alpha, \quad . \quad . \quad (8)$$

it is readily seen that

$$u^*(x, p)=\frac{1}{\pi}\int_{-\infty}^{\infty}\mathrm{F}(\xi, p)\,d\xi\int_0^\infty\frac{\cos\alpha(x-\xi)}{\left(\frac{p}{c}\right)^2+\alpha^2}\,d\alpha$$

$$= \frac{1}{\pi}\int_{-\infty}^{\infty} f(\xi)\, d\xi \int_0^{\infty} \frac{p\cos\alpha(x-\xi)}{p^2+c^2\alpha^2}\, d\alpha$$

$$+ \frac{1}{\pi}\int_{-\infty}^{\infty} g(\xi)\, d\xi \int_0^{\infty} \frac{\cos\alpha(x-\xi)}{p^2+c^2\alpha^2}\, d\alpha$$

$$= u_1^*(x, p) + u_2^*(x, p) \quad \text{(say)} \quad . \quad . \quad . \quad . \quad (9)$$

is the solution of (7). The problem now reduces to that of obtaining the inverse Laplace transform of the functions $u_1^*(x, p)$ and $u_2^*(x, p)$.

In view of the identity

$$\int_0^{\infty} \exp(-pt)\cos\lambda t\, dt = \frac{p}{p^2+\lambda^2}, \quad . \quad . \quad (10)$$

it follows at once

$$u_1(x, t) = \frac{1}{\pi}\int_{-\infty}^{\infty} f(\xi)\, d\xi \int_0^{\infty} \cos\alpha(x-\xi)\cos c\alpha t\, d\alpha$$

$$= \frac{1}{2\pi}\int_{-\infty}^{\infty} f(\xi)\, d\xi \int_0^{\infty} \cos\alpha(x-\xi+ct)\, d\alpha$$

$$+ \frac{1}{2\pi}\int_{-\infty}^{\infty} f(\xi)\, d\xi \int_0^{\infty} \cos\alpha(x-\xi-ct)\, d\alpha. \quad (11)$$

If in the first term of (11) we make the substitution $\xi - ct = \eta$ and in the second term the substitution $\xi + ct = \eta$, and take into account the identity (8), we get at once

$$u_1(x, t) = \tfrac{1}{2}\{f(x+ct) + f(x-ct)\}. \quad . \quad . \quad . \quad (12)$$

Consider now the expression $u_2^*(x, p)$. This may be conveniently transformed with the aid of the identity

$$\int_0^{\infty} \frac{\cos r\alpha}{p^2+\alpha^2}\, d\alpha = \left\{ \begin{array}{ll} \dfrac{\pi}{2p}\exp(-pr) & \text{for } r>0, \\ \dfrac{\pi}{2p}\exp(pr) & \text{for } r<0. \end{array} \right\} \quad (13)$$

In view of (13) $u_2^*(x, p)$ becomes

$$u_2^*(x, p) = \frac{1}{2c}\int_{-\infty}^{x} g(\xi)\, \frac{\exp\left[-\frac{p}{c}(x-\xi)\right]}{p}\, d\xi$$

$$+ \frac{1}{2c}\int_{x}^{\infty} g(\xi)\, \frac{\exp\left[\frac{p}{c}(x-\xi)\right]}{p}\, d\xi. \quad (14)$$

In order to obtain the inverse Laplace transform of $u_2^*(x, p)$ we make use of the identity

$$\frac{\exp(-\lambda p)}{p} = \int_\lambda^\infty \exp(-pt)\, dt. \quad . \quad . \quad . \quad (15)$$

This can be rewritten in the form :

$$L^{-1}\left\{\frac{\exp\left[-p\left(\frac{x-\xi}{c}\right)\right]}{p}\right\} = k(t) = \left\{\begin{array}{l} 0 \text{ if } t < \dfrac{x-\xi}{c}, \\ \\ 1 \text{ if } t > \dfrac{x-\xi}{c}. \end{array}\right\}$$

$$. \quad . \quad . \quad (16)$$

In view of (16) the first term in (14) becomes

$$\frac{1}{2c}\int_{x-ct}^{x} g(\xi)\, d\xi.$$

Similarly the second term becomes

$$\frac{1}{2c}\int_{x}^{x+ct} g(\xi)\, d\xi.$$

Thus, collecting our results we get the well-known result

$$u(x, t) = \tfrac{1}{2}f(x+ct) + \tfrac{1}{2}f(x-ct) + \frac{1}{2c}\int_{x-ct}^{x+ct} g(\xi)\, d\xi. \quad (17)$$

Section II.

In this section we will now consider the case of the non-homogeneous differential equation of wave-motion,

$$\frac{\partial^2}{\partial x^2}u(x, t) = 2b\frac{\partial}{\partial t}u(x, t) + \frac{1}{a^2}\frac{\partial^2}{\partial t^2}u(x, t) + \phi(x, t), \quad (1)$$

$$-\infty < x < \infty\,;\ t > 0,$$

where

$$\lim_{t\to 0} u(x, t) = f(x) \quad . \quad . \quad . \quad . \quad . \quad (2)$$

and

$$\lim_{t\to 0}\frac{\partial}{\partial t}u(x, t) = g(x). \quad . \quad . \quad . \quad . \quad (3)$$

Let us make the substitution

$$u(x, t) = \exp(-kt)v(x, t), \quad . \quad . \quad . \quad . \quad (4)$$

where $k=a^2b$.

Then the function v satisfies the system

$$\frac{\partial^2}{\partial x^2}v(x,t)+\frac{k^2}{a^2}v(x,t)=\frac{1}{a^2}\frac{\partial^2}{\partial t^2}v(x,t)+\phi_1(x,t), \quad . \quad (5)$$

where $$\phi_1(x,t)=\exp(kt)\phi(x,t),$$

$$\lim_{t\to 0} v(x,t)=f(x), \quad . \quad . \quad . \quad . \quad . \quad . \quad . \quad . \quad . \quad . \quad (6)$$

$$\lim_{t\to 0}\frac{\partial}{\partial t}v(x,t)=g(x)+kf(x)=h(x), \quad \text{(say)}. \quad . \quad (7)$$

Acting on (5) (Section II.) with the Laplace operator defined in Sect. I. (4) we get

$$\frac{d^2}{dx^2}v^*(x,p)-\frac{1}{a^2}(p^2-k^2)v^*(x,p)$$

$$=-\frac{1}{a^2}\{pf(x)+h(x)\}+\phi_1^*(x,p)$$

$$=-\mathrm{F}(x,p) \quad \text{(say)}. \quad . \quad . \quad . \quad . \quad (8)$$

The solution of (8) (Sect. II.) is given by the integral

$$v^*(x,p)=\frac{1}{\pi}\int_{-\infty}^{\infty}\mathrm{F}(\xi,p)\,d\xi\int_0^{\infty}\frac{\cos\alpha(x-\xi)}{\alpha^2+\dfrac{p^2-k^2}{a^2}}d\alpha$$

$$=\frac{a}{2}\int_{-\infty}^{x}\mathrm{F}(\xi,p)\frac{\exp\left[-\sqrt{p^2-k^2}\left(\dfrac{x-\xi}{a}\right)\right]}{\sqrt{p^2-k^2}}d\xi$$

$$+\frac{a}{2}\int_{x}^{\infty}\mathrm{F}(\xi,p)\frac{\exp\left[\sqrt{p^2-k^2}\left(\dfrac{x-\xi}{a}\right)\right]}{\sqrt{p^2-k^2}}d\xi. \quad (9)$$

Remembering the definition of the function $\mathrm{F}(x,p)$ from (8) (Sect. II.) the last equation becomes

$$v^*(x,p)=\frac{1}{2a}\int_x^{\infty}f(\xi)\frac{p.\exp\left[\sqrt{p^2-k^2}\left(\dfrac{x-\xi}{a}\right)\right]}{\sqrt{p^2-k^2}}d\xi$$

$$-\frac{1}{2a}\int_{-\infty}^{x}f(\xi)\frac{p.\exp\left[-\sqrt{p^2-k^2}\left(\dfrac{x-\xi}{a}\right)\right]}{\sqrt{p^2-k^2}}d\xi$$

$$+\frac{1}{2a}\int_x^\infty h(\xi)\frac{\exp\left[\sqrt{p^2-k^2}\left(\frac{x-\xi}{a}\right)\right]}{\sqrt{p^2-k^2}}\,d\xi$$

$$-\frac{1}{2a}\int_{-\infty}^x h(\xi)\frac{\exp\left[-\sqrt{p^2-k^2}\left(\frac{x-\xi}{a}\right)\right]}{\sqrt{p^2-k^2}}\,d\xi$$

$$-\frac{a}{2}\int_x^\infty \phi_1^*(\xi,p)\frac{\exp\left[\sqrt{p^2-k^2}\left(\frac{x-\xi}{a}\right)\right]}{\sqrt{p^2-k^2}}\,d\xi$$

$$+\frac{a}{2}\int_{-\infty}^x \phi_1^*(\xi,p)\frac{\exp\left[-\sqrt{p^2-k^2}\left(\frac{x-\xi}{a}\right)\right]}{\sqrt{p^2-k^2}}\,d\xi$$

$$=v_1^*(x,p)+v_2^*(x,p)+v_3^*(x,p)$$
$$+v_4^*(x,p)+v_5^*(x,p)+v_6^*(x,p) \quad \text{(say)} \qquad \ldots \quad (10)$$

Consider the expression

$$v_3^*(x,p)=\frac{1}{2a}\int_x^\infty h(\xi)\frac{\exp\left[-\sqrt{p^2-k^2}\left(\frac{x-\xi}{a}\right)\right]}{\sqrt{p^2-k^2}}\,d\xi, \quad (11)$$

if we make the substitution

$$x-\xi=-a\eta, \qquad \ldots \quad (12)$$

then (11) becomes

$$v_3^*(x,p)=\frac{1}{2}\int_0^\infty h(x+a\eta)\frac{\exp\left(-\eta\sqrt{p^2-k^2}\right)}{\sqrt{p^2-k^2}}\,d\eta. \quad (11')$$

In view of the identity

$$\frac{\exp\left(-\eta\sqrt{p^2-k^2}\right)}{\sqrt{p^2-k^2}}=\int_0^\infty \exp(-pt)\mathrm{G}(\eta,t)\,dt, \quad (13)$$

where $$\mathrm{G}(\eta,t)=\begin{cases}0 & \text{if } t<\eta,\\ \mathrm{J}_0(k\sqrt{\eta^2-t^2}) & \text{if } t>\eta,\end{cases}$$

(11′) becomes, after an obvious transformation,

$$v_3^*(x,p)=\int_0^\infty \exp(-pt)\,dt\int_0^\infty h(x+a\eta)\mathrm{F}(\eta,t)\,d\eta$$
$$=\int_0^\infty \exp(-pt)\,dt\int_0^t h(x+a\eta)\mathrm{J}_0(k\sqrt{\eta^2-t^2})\,dt$$

$$= \mathrm{L}\left\{\int_0^t h(x+a\eta)\mathrm{J}_0(k\sqrt{\eta^2-t^2})\,d\eta\right\}, \quad . \quad (11'')$$

whence

$$v_3(x,t) = \frac{1}{2}\int_0^t h(x+a\eta)\mathrm{J}_0(k\sqrt{\eta^2-t^2})\,d\eta. \quad . \quad (14)$$

Returning again to the variable ξ defined by (12), the last equation becomes

$$v_3(x,t) = \frac{1}{2a}\int_x^{x+at} h(\xi)\mathrm{J}_0\left(k\sqrt{\left(\frac{x-\xi}{a}\right)^2-t^2}\right)d\xi. \quad (14')$$

In an entirely similar manner we obtain

$$v_4(x,t) = \frac{1}{2a}\int_{x-at}^{x} h(\xi)\mathrm{J}_0\left(k\sqrt{\left(\frac{x-\xi}{a}\right)^2-t^2}\right)d\xi. \quad (15)$$

The last two equations may be combined into

$$v_3(x,t)+v_4(x,t) = \frac{1}{2a}\int_{x-at}^{x+at} h(\xi)\mathrm{J}_0\left(k\sqrt{\left(\frac{x-\xi}{a}\right)^2-t^2}\right)d\xi.$$

$$. \quad . \quad . \quad (16)$$

Consider now

$$v_1^*(x,p) = \frac{1}{2a}\int_x^\infty f(\xi)\frac{p\exp\left[\sqrt{p^2-k^2}\left(\frac{x-\xi}{a}\right)\right]}{\sqrt{p^2-k^2}}d\xi. \quad (17)$$

With (17) let us associate

$$w_1^*(x,p) = \frac{1}{2a}\int_x^\infty f(\xi)\frac{\exp\left[\sqrt{p^2-k^2}\left(\frac{x-\xi}{a}\right)\right]}{\sqrt{p^2-k^2}}d\xi. \quad (18)$$

In view of (11) and (14), (18) yields

$$w_1(x,t) = \frac{1}{2}\int_0^t f(x+a\eta)\mathrm{J}_0(k\sqrt{\eta^2-t^2})\,d\eta. \quad . \quad (19)$$

Now, since

$$\mathrm{L}\left\{\frac{\partial}{\partial t}w_1(x,t)\right\} = p\mathrm{L}\{w_1(x,t)\} - w_1(x,0)$$

$$= pw_1^*(x,p) = v_1^*(x,p), \quad . \quad (20)$$

it follows that

$$v_1(x,t) = \frac{\partial}{\partial t} w_1(x,t)$$

$$= \frac{1}{2}\frac{\partial}{\partial t}\int_0^t f(x+a\eta) J_0(k\sqrt{\eta^2-t^2})\, d\eta$$

$$= \frac{1}{2} f(x+at) + \frac{1}{2}\int_0^t f(x+a\eta)\, \frac{\partial}{\partial t} J_0(k\sqrt{\eta^2-t^2})\, d\eta. \quad \ldots \quad (21)$$

If in the second term we return to the variable of integration ξ given by (12), we get

$$v_1(x,t) = \tfrac{1}{2} f(x+at) + \frac{1}{2a}\int_x^{x+at} f(\xi)\frac{\partial}{\partial t} J_0\left(k\sqrt{\left(\frac{x-\xi}{a}\right)^2 - t^2}\right) d\xi. \quad (21')$$

In an entirely similar manner we get

$$v_2(x,t) = \tfrac{1}{2} f(x-at) + \frac{1}{2a}\int_{x-at}^{x} f(\xi)\frac{\partial}{\partial t} J_0\left(k\sqrt{\left(\frac{x-\xi}{a}\right)^2 - t^2}\right) d\xi. \quad (22)$$

The last two equations may be combined into

$$v_1(x,t) + v_2(x,t) = \tfrac{1}{2} f(x+at) + \tfrac{1}{2} f(x-at) + \frac{1}{2a}\int_{x-at}^{x+at} f(\xi)\frac{\partial}{\partial t} J_0\left(k\sqrt{\left(\frac{x-\xi}{a}\right)^2 t^2}\right) d\xi. \quad \ldots \quad (23)$$

Consider now

$$v_5^*(x,p) = -\frac{a}{2}\int_0^\infty \phi_1^*(\xi,p)\frac{\exp\left[\sqrt{p^2-k^2}\left(\frac{x-\xi}{a}\right)\right]}{\sqrt{p^2-k^2}} d\xi$$

$$= -\frac{a^2}{2}\int_0^\infty \phi_1^*(x+a\eta,p)\frac{\exp\left[-\sqrt{p^2-k^2}\eta\right]}{\sqrt{p^2-k^2}} d\eta. \quad (24)$$

By Borel's Theorem,

$$L\left\{\int_0^t f_1(\tau) f_2(t-\tau)\, d\tau\right\} = f_1^*(p) f_2^*(p),$$

(24) yields at once

$$v_5(x,t) = -\frac{a^2}{2}\int_0^\infty d\eta \int_0^t \phi_1(x+a\eta,\, t-\tau)\mathrm{G}(\eta,\,\tau)\,d\tau$$

$$= -\frac{a}{2}\int_0^t d\eta \int_0^t \phi_1(x+a\eta,\, t-\tau)\mathrm{J}_0(k\sqrt{\eta^2-\tau^2})\,d\tau$$

$$= -\frac{a}{2}\int_x^{x+at} d\xi \int_0^t \phi_1(\xi,\, t-\tau)\mathrm{J}_0\left(k\sqrt{\left(\frac{x-\xi}{a}\right)-\tau^2}\right)d\tau. \quad \ldots \quad (25)$$

In an entirely similar fashion

$$v_6(x,t) = -\frac{a}{2}\int_{x-at}^x d\xi \int_0^t \phi_1(\xi,\, t-\tau)$$

$$.\mathrm{J}_0\left(k\sqrt{\left(\frac{x-\xi}{a}\right)^2-\tau^2}\right)d\tau, \quad (26)$$

and therefore

$$v_5(x,t)+v_6(x,t) = -\frac{a}{2}\int_{x-at}^{x+at} d\eta \int_0^t \phi_1(\xi,\, t-\tau)$$

$$.\mathrm{J}_0\left(k\sqrt{\left(\frac{x-\xi}{a}\right)^2-\tau^2}\right)d\tau. \quad (27)$$

In view of (4), (16), (23), (27), and (5) our final solution of the system (1), (2), and (3) becomes

$$u(x,t) = \tfrac{1}{2}\exp(-ba^2t)\{f(x+at)+f(x-at)\}$$

$$+\frac{1}{a}\int_{x-at}^{x+at} f(\xi)\frac{\partial}{\partial t}\mathrm{J}_0\left(ba^2\sqrt{\left(\frac{x-\xi}{a}\right)^2-t^2}\right)d\xi$$

$$+\frac{1}{a}\int_{x-at}^{x+at}[g(\xi)+ba^2f(\xi)]$$

$$.\mathrm{J}_0\left(ba^2\sqrt{\left(\frac{x-\xi}{a}\right)^2-t^2}\right)d\xi$$

$$-a\int_{x-at}^{x+at} d\xi \int_0^t \exp[ba^2(t-\tau)]\phi(\xi,\, t-\tau)$$

$$.\mathrm{J}_0\left(ba^2\sqrt{\left(\frac{x-\xi}{a}\right)^2-\tau^2}\right)d\tau.$$

$$\ldots \quad (28)$$

For $\phi(x,t)=0$ (28) reduces to the solution given by Riemann-Weber †.

† ' Differenzialgleichungen der math-physick,' vol. ii.

For $\phi(x, t)=0$ and $b=0$ (28) yields the solution for the infinite vibrating string.

Section III.

Two-dimensional Case.

We will now consider the case of the two-dimensional non-homogeneous differential equation of wave-motion. The statement of the problem is now given by the following system of equations :

$$\nabla^2 u(x, y; t)=2b\frac{\partial}{\partial t}u(x, y; t)+\frac{1}{a^2}\frac{\partial^2}{\partial t^2}u(x, y; t)+\phi(x, y; t), \quad \ldots (1)$$

where

$$\operatorname*{Lim}_{t\to 0} u(x, y; t)=f(x, y), \quad \ldots (2)$$

and

$$\operatorname*{Lim}_{t\to 0}\frac{\partial}{\partial t}u(x, y; t)=g(x, y). \quad \ldots (3)$$

Let

$$\left.\begin{aligned} u(x, y; t)&=\exp(-kt)v(x, y; t),\\ \phi_1(x, y; t)&=\exp(-kt)\phi(x, y; t),\end{aligned}\right\} \quad \ldots (4)$$

where $k=a^2b$; then

$$\nabla^2 v(x, y; t)+\frac{k^2}{a^2}v(x, y; t) =\frac{1}{a^2}\frac{\partial^2}{\partial t^2}v(x, y; t)+\phi_1(x, y; t). \quad \ldots (5)$$

Acting on (3) with the Laplace operator we get

$$\begin{aligned}\nabla^2 v^*(x, y; p)-\frac{1}{a^2}(p^2-k^2)v^*(x, y; p) &=-\frac{1}{a^2}\{pf(x, y)+h(x, y)\}+\phi_1^*(x, y; p)\\ &=-\mathrm{F}(x, y; p) \quad \text{(say)}. \quad \ldots (6)\end{aligned}$$

In this case we use the following identity, which is a generalization of the Fourier Integral in two dimensions:

$$\mathrm{F}(x, y)=\frac{1}{4\pi^2}\overline{\int_{-\infty}^{\infty}\int\int\int}\mathrm{F}(\xi, \eta)\cos\{\alpha(x-\xi)+\beta(y-\eta)\}\,d\xi\,d\eta\,d\alpha\,d\beta. \quad \ldots (7)$$

In view of (7) it can be readily seen that the solution of (6) is given by

$$v^*(x, y; p) = \frac{1}{4\pi^2} \iint_{-\infty}^{\infty} F(\xi, \eta, p)\, d\xi\, d\eta \cdot \iint_{-\infty}^{\infty} \frac{\cos\{\alpha(x-\xi)+\beta(y-\eta)\}}{\alpha^2+\beta^2+\frac{p^2-k^2}{a^2}}\, d\alpha\, d\beta. \quad (8)$$

Let

$$\left.\begin{aligned} &\alpha = \rho\cos\theta\,;\ \beta = \rho\sin\theta\,; \\ &x-\xi = \mathrm{R}\cos\phi\,;\ y-\eta = \mathrm{R}\sin\phi\,; \\ &d\alpha\, d\beta = \rho\, d\rho\, d\theta\,; \end{aligned}\right\} \quad . \quad . \quad (9)$$

whence

$$\alpha(x-\xi)+\beta(y-\eta) = \mathrm{R}\rho\cos(\theta-\phi). \quad . \quad . \quad (10)$$

With these substitutions equation (8) becomes

$$v^*(x, y; p) = \frac{1}{4\pi^2} \iint_{-\infty}^{\infty} F(\xi, \eta; p)\, d\xi\, d\eta \int_0^{\infty} \frac{\rho\, d\rho}{\rho^2+\frac{p^2-k^2}{a^2}} \cdot \int_0^{2\pi} \cos[\mathrm{R}\rho\cos(\theta-\phi)]\, d\theta. \quad (11)$$

But

$$\int_0^{2\pi} \cos[\mathrm{R}\rho\cos(\theta-\phi)]\, d\theta = 2\pi \mathrm{J}_0(\mathrm{R}\rho). \quad . \quad . \quad (12)$$

If we make the further substitutions

$$\left.\begin{aligned} x-\xi &\to a\xi, \\ y-\eta &\to a\eta, \\ \rho &\to \frac{\rho}{a}, \end{aligned}\right\} \quad . \quad . \quad . \quad . \quad . \quad . \quad (13)$$

and make use of (12), then (11) becomes

$$v^*(x, y; p) = \frac{a^2}{2\pi} \iint_{-\infty}^{\infty} F(x+a\xi, y+a\eta; p)\, d\xi\, d\eta \cdot \int_0^{\infty} \frac{\rho \mathrm{J}_0(\rho\sqrt{\xi^2+\eta^2})}{\rho^2+p^2-k^2}\, d\rho. \quad (14)$$

Remembering the definition of $F(x, y ; p)$ from (6), we get

$$v^*(x, y ; p) = \frac{1}{2\pi} \overline{\iint_{-\infty}^{\infty}} f(x+a\xi, y+a\eta)\, d\xi\, d\eta \cdot \int_0^\infty p \frac{\rho J_0(\rho\sqrt{\xi^2+\eta^2})}{\rho^2+p^2-k^2} d\rho$$

$$+ \frac{1}{2\pi} \overline{\iint_{-\infty}^{\infty}} h(x+a\xi, y+a\eta)\, d\xi\, d\eta \cdot \int_0^\infty \frac{\rho J_0(\rho\sqrt{\xi^2+\eta^2})}{\rho^2+p^2-k^2} d\rho$$

$$- \frac{a^2}{2\pi} \overline{\iint_{-\infty}^{\infty}} d\xi\, d\eta \cdot \int_0^\infty \frac{\phi_1^*(x+a\xi, y+a\eta ; p)\rho J_0(\rho\sqrt{\xi^2+\eta^2})}{\rho^2+p^2-k^2} d\rho$$

$$= v_1^*(x, y ; p) + v_2^*(x, y ; p) + v_3^*(x, y ; p) \quad \text{(say)}. \quad \ldots \quad (15)$$

Consider the integral

$$w_2^*(\xi, \eta ; p) = \int_0^\infty \frac{\rho J_0(\rho\sqrt{\xi^2+\eta^2})}{p^2+\rho^2-k^2} d\rho. \quad \ldots \quad (16)$$

In view of the identity

$$\int_0^\infty \exp(-pt) \frac{\sin \lambda t}{\lambda} dt = \frac{1}{p^2+\lambda^2} \quad \ldots \quad (17)$$

it follows that

$$w_2(\xi, \eta ; t) = \int_0^\infty \rho \frac{J_0(\rho\sqrt{\xi^2+\eta^2}) . \sin t\sqrt{\rho^2-k^2}}{\sqrt{\rho^2-k^2}} d\rho. \quad (18)$$

Making use of the fact that

$$J_{\frac{1}{2}}(x) = \sqrt{\frac{2}{\pi x}} \sin x,$$

(18) becomes

$$w_2(\xi, \eta ; t) = \sqrt{\frac{\pi t}{2}} \int_0^\infty \frac{\rho J_0(\rho\sqrt{\xi^2+\eta^2}) J_{\frac{1}{2}}(t\sqrt{\rho^2-k^2})}{(\rho^2-k^2)^{\frac{1}{4}}} d\rho. \quad (19)$$

Thus

$$v_2(x, y; t) = \frac{1}{2\pi}\sqrt{\frac{\pi t}{2}}\iint_{-\infty}^{\infty} h(x+a\xi, y+a\eta)\, d\xi\, d\eta$$
$$\cdot \int_0^\infty \rho J_0(\rho\sqrt{\xi^2+\eta^2}) J_{\frac{1}{2}}(t\sqrt{\rho^2-k^2}) \frac{d\rho}{(\rho^2-k^2)^{\frac{1}{4}}}$$
$$= \frac{1}{2\pi}\sqrt{\frac{\pi t}{2}} \int_0^\infty \mathrm{R}\, d\mathrm{R}$$
$$\cdot \int_0^{2\pi} h(x+a\mathrm{R}\cos\phi, y+a\mathrm{R}\sin\phi)\, d\phi$$
$$\cdot \int_0^\infty \rho J_0(\mathrm{R}\rho) J_{\frac{1}{2}}(t\sqrt{\rho^2-k^2}) \frac{d\rho}{(\rho^2-k^2)^{\frac{1}{4}}}. \quad (20)$$

In the identity (G. N. Watson, 'Theory of Bessel Functions,' p. 415)

$$\int_0^\infty J_\mu(\mathrm{R}\rho) \frac{J_\nu(t\sqrt{\rho^2-z^2})\rho^{\mu+1}}{(\rho^2-z^2)^{\frac{1}{2}\nu}}\, d\rho$$
$$= \begin{cases} 0 \text{ if } t<\mathrm{R}, \\ \dfrac{\mathrm{R}^\mu}{t^\nu}\left\{\sqrt{t^2-\mathrm{R}^2}\right\}^{\nu-\mu-1} J_{\nu-\mu-1}(z\sqrt{t^2-\mathrm{R}^2}) \text{ if } t>\mathrm{R}. \end{cases}$$
$$\left\{z\right\} \quad . \quad . \quad . \quad (21)$$

If
$$\mu=0,\ z=ki,\ \nu=\tfrac{1}{2},$$
we obtain

$$\int_0^\infty \frac{\rho J_0(\mathrm{R}\rho) J_{\frac{1}{2}}(t\sqrt{\rho^2-k^2})}{(\rho^2-k^2)^{\frac{1}{4}}}\, d\rho$$
$$= \begin{cases} 0 \text{ if } t<\mathrm{R}, \\ \dfrac{1}{\sqrt{t}}\left(\dfrac{ki}{\sqrt{t^2-\mathrm{R}^2}}\right)^{\frac{1}{2}} J_{-\frac{1}{2}}(ki\sqrt{t^2-\mathrm{R}^2}) \text{ if } t>\mathrm{R}. \end{cases}$$
$$. \quad . \quad . \quad (22)$$

In view of (22) and of the identity

$$J_{-\frac{1}{2}}(x) = \sqrt{\frac{2}{\pi x}}\cos x, \quad . \quad . \quad . \quad . \quad (23)$$

(20) becomes

$$v_2(x, y; t) = \frac{1}{2\pi}\int_0^t \frac{\mathrm{R}\,d\mathrm{R}}{\sqrt{t^2-\mathrm{R}^2}}\cosh(k\sqrt{t^2-\mathrm{R}^2})\,dt \cdot \int_0^{2\pi} h(x+a\mathrm{R}\cos\phi,\ y+a\mathrm{R}\sin\phi)\,d\phi. \quad (24)$$

Now consider the expression

$$v_1^*(x, y; p) = \frac{1}{2\pi}\overline{\iint_{-\infty}^{\infty}} f(x+a\xi,\ y+a\eta)\,d\xi\,d\eta \cdot \int_0^\infty \frac{p\rho \mathrm{J}_0(\rho\sqrt{\xi^2+\eta^2})}{\rho^2+p^2-k^2}\,d\rho. \quad (25)$$

With (22) let us associate

$$w_1^*(x, y; p) = \frac{1}{2\pi}\overline{\iint_{-\infty}^{\infty}} f(x+a\xi,\ y+a\eta)\,d\xi\,d\eta \cdot \int_0^\infty \frac{\rho \mathrm{J}_0(\rho\sqrt{\xi^2+\eta^2})}{\rho^2+p^2-k^2}\,d\rho. \quad (26)$$

In view of (15) and (20), (26) yields

$$w_1(x, y; t) = \frac{1}{2\pi}\int_0^t \frac{\mathrm{R}\,d\mathrm{R}}{\sqrt{t^2-\mathrm{R}^2}}\cosh k\sqrt{t^2-\mathrm{R}^2} \int_0^{2\pi} f(x+a\mathrm{R}\cos\phi,\ y+a\mathrm{R}\sin\phi)\,d\phi. \quad (27)$$

Since

$$\mathrm{L}\left\{\frac{\partial}{\partial t} w_1(x, y; t)\right\} = p\mathrm{L}\{w_1(x, y; t)\} - w_1(x, y; 0) = v_1^*(x, y; p),$$

it follows that

$$v_1(x, y; t) = \frac{\partial}{\partial t} w_1(x, y; t) \frac{1}{2\pi}\frac{\partial}{\partial t}\int_0^t \frac{\mathrm{R}\,d\mathrm{R}}{\sqrt{t^2-\mathrm{R}^2}}\cosh k\sqrt{t^2-\mathrm{R}^2} \cdot \int_0^{2\pi} f(x+a\mathrm{R}\cos\phi,\ y+a\mathrm{R}\sin\phi)\,d\phi. \quad (28)$$

Finally, turning to the expression for $v_3(x, y; p)$, the corresponding inverse Laplace transform may be obtained with the aid of Borel's Theorem in the form

$$v_3(x, y; t) = -\frac{a^2}{2\pi}\int_0^t \mathrm{R}\, d\mathrm{R}\int_0^{2\pi} d\phi \cdot \int_0^t \phi_1(x+a\mathrm{R}\cos\phi,\ y+a\mathrm{R}\sin\phi;\ t-\tau) \cdot \frac{\cosh k\sqrt{\tau^2-\mathrm{R}^2}}{\sqrt{\tau^2-\mathrm{R}^2}}\, d\tau. \quad . \quad . \quad . \quad . \quad . \quad . \quad (29)$$

Collecting our results, we get as the final solution

$$v(x, y; t) = v_1(x, y; t) + v_2(x, y; t) + v_3(x, y; t), \quad . \quad (30)$$

where $v_1(x, y; t)$, $v_2(x, y; t)$, and $v_3(x, y; t)$ are given by (28), (20), and (29).

Section IV.

Three-dimensional Case.

In this case we have to solve the system

$$\nabla^2 u(x, y, z; t) = 2b\frac{\partial}{\partial t}u(x, y, z; t) + \frac{1}{a^2}\frac{\partial^2}{\partial t^2}u(x, y, z; t) + \phi(x, y, z; t), \quad (1)$$

$$\lim_{t\to 0} u(x, y, z; t) = f(x, y, z), \quad . \quad . \quad . \quad . \quad (2)$$

$$\lim_{t\to 0}\frac{\partial}{\partial t}u(x, y, z; t) = g(x, y\, z). \quad . \quad . \quad . \quad . \quad (3)$$

If, as before, we make the substitutions

$$u(x, y, z) = \exp(-ba^2 t)v(x, y, z; t) = \exp(-kt)v(x, y, z; t) \text{ (say)}, \quad . \quad (4)$$

$$\phi_1(x, y, z; t) = \exp(kt)\phi(x, y, z; t), \quad . \quad . \quad . \quad (5)$$

the function $v(x, y, z; t)$ must satisfy the system

$$\nabla^2 v(x, y, z; t) + \frac{k^2}{a^2}v(x, y, z; t) = \frac{1}{a^2}\frac{\partial^2}{\partial t^2}v(x, y, z; t) + \phi_1(x, y, z; t), \quad (6)$$

$$\lim_{t\to 0} v(x, y, z; t) = f(x, y, z) \quad . \quad . \quad . \quad . \quad . \quad (7)$$

$$\lim_{t\to 0}\frac{\partial}{\partial t}v(x, y, z; t)=g(x, y, z)+kf(x, y, z)$$

$$=h(x, y, z) \quad \text{(say)}, \quad . \quad . \quad . \quad (8)$$

and, therefore, we obtain for the Laplace transform of $v(x, y, z; t)$

$$\left(\nabla^2-\frac{p^2-k^2}{a^2}\right)v^*(x, y, z; p)$$

$$=-\frac{1}{a^2}\{pf(x, y, z)+h(x, y, z)\}+\phi_1^*(x, y, z; p)$$

$$=-\mathrm{F}(x, y, z; p) \quad \text{(say)}. \quad . \quad . \quad . \quad . \quad . \quad . \quad . \quad (9)$$

In view of the identity (this is the three-dimensional generalization of the Fourier Integral identity)

$$\mathrm{F}(x, y, z)=\frac{1}{8\pi^3}\overline{\overline{\iiint}}_{-\infty}^{\infty}\mathrm{F}(\xi, \eta, \zeta)\,d\xi\,d\eta\,d\zeta$$

$$\cdot\overline{\overline{\iiint}}_{-\infty}^{\infty}\cos\left[\alpha(x-\xi)+\beta(y-\eta)+\gamma(z-\zeta)\right]d\alpha\,d\beta\,d\gamma, \quad (10)$$

the solution of (9) is obtained in the form

$$^*v(x, y, z; p)=\frac{1}{8\pi^3}\overline{\overline{\iiint}}_{-\infty}^{\infty}\mathrm{F}(\xi, \eta, \zeta; p)\,d\xi\,d\eta\,d\zeta$$

$$\cdot\overline{\overline{\iiint}}_{-\infty}^{\infty}\frac{\cos\{\alpha(x-\xi)+\beta(y-\eta)+\gamma(z-\zeta)\}}{\alpha^2+\beta^2+\gamma^2+\dfrac{p^2-k^2}{a^2}}d\alpha\,d\beta\,d\gamma. \quad (11)$$

If we make the substitutions

$$\left.\begin{aligned} x-\xi &\to -a\xi,\\ y-\eta &\to -a\eta,\\ z-\zeta &\to -a\zeta,\\ \alpha, \beta, \gamma &\to \frac{\alpha}{a}\cdot\frac{\beta}{a}\cdot\frac{\gamma}{a}, \end{aligned}\right\} \quad . \quad . \quad . \quad . \quad . \quad (12)$$

(11) becomes

$$v^*(x, y, z; p) = \frac{a^2}{8\pi^3} \overline{\overline{\iiint}}_{-\infty}^{\infty} \mathrm{F}(x+a\xi, y+a\eta, z+a\zeta; p)\, d\xi\, d\eta\, d\zeta \cdot \overline{\overline{\iiint}}_{-\infty}^{\infty} \frac{\cos(\alpha\xi+\beta\eta+\gamma\zeta)}{\alpha^2+\beta^2+\gamma^2+(p^2-k^2)}\, d\alpha\, d\beta\, d\gamma. \quad (13)$$

It is convenient to transform the second triple integral appearing in (13). We make use of the following important theorem (see G. N. Watson, 'Theory of Bessel Functions,' p. 452):

If $\nabla^2\phi = -\lambda^2\phi$, then

$$\overline{\overline{\iiint}}_{-\infty}^{\infty} \phi(\alpha, \beta, \gamma) f(\sqrt{\alpha^2+\beta^2+\gamma^2})\, d\alpha\, d\beta\, d\gamma = \frac{4\pi}{\lambda}\phi(0, 0, 0)\int_0^\infty rf(r)\sin kr\, dr. \quad (14)$$

Let

$$\phi(\alpha, \beta, \gamma) = \cos(\xi\alpha+\eta\beta+\zeta\gamma, \quad . \quad . \quad . \quad (15)$$

$$f(\sqrt{\alpha^2+\beta^2+\gamma^2}) = \frac{1}{\alpha^2+\beta^2+\gamma^2+p^2-k^2}, \quad . \quad (16)$$

whence

$$\phi(0, 0, 0) = 1, \quad . \quad . \quad . \quad . \quad . \quad . \quad . \quad . \quad (17)$$

$$\lambda = \sqrt{\xi^2+\eta^2+\zeta^2}, \quad . \quad . \quad . \quad . \quad (18)$$

$$f(r) = \frac{1}{r^2+p^2-k^2}, \quad . \quad . \quad . \quad . \quad (19)$$

and, therefore,

$$\overline{\overline{\iiint}}_{-\infty}^{\infty} \frac{\cos(\alpha\xi+\beta\eta+\gamma\zeta}{\alpha^2+\beta^2+\gamma^2+p^2-k^2}\, d\alpha\, d\beta\, d\gamma = \frac{4\pi}{\sqrt{\xi^2+\eta^2+\zeta^2}}\int_0^\infty \frac{r\sin kr}{r^2+p^2-k^2}\, dr. \quad (20)$$

In view of (20), (13) becomes

$$v^*(x, y, z; p) = \frac{a^2}{2\pi^2} \overline{\overline{\iiint}}_{-\infty}^{\infty} \frac{\mathrm{F}(x+a\xi, y+a\eta, z+a\zeta; p)}{\sqrt{\xi^2+\eta^2+\zeta^2}}\, d\xi\, d\eta\, d\zeta \cdot \int_0^\infty \frac{r\sin\lambda r\, dr}{r^2+p^2-k^2}. \quad (21)$$

The last simple integral in (21) may be evaluated. Making use of the identity (Gray and Mathews, 'Bessel Functions,' p. 78)

$$\int_0^\infty \frac{r \sin kr \mathrm{J}_0(xr)}{r^2+a^2} dr = \frac{\pi}{2} \exp(-ka)\mathrm{I}_0(kx) \quad . \quad (22)$$

for $x=0$, the last integral in (21) becomes

$$\frac{\pi}{2}\exp(-\lambda\sqrt{p^2-k^2}),$$

and, therefore,

$$v^*(x, y, z; p) = \frac{a^2}{4\pi}\overline{\iiint_{-\infty}^{\infty}} \frac{\mathrm{F}(x+a\xi, y+a\eta, z+a\zeta)}{\sqrt{\xi^2+\eta^2+\zeta^2}} \cdot \exp(-\lambda\sqrt{p^2-k^2})\, d\xi\, d\eta\, d\zeta. \quad (23)$$

Bearing in mind the significance of $\mathrm{F}(x, y, z; p)$ from (9) we get

$$\begin{aligned} v^*(x, y, z; p) = {} & \frac{1}{4\pi}\overline{\iiint_{-\infty}^{\infty}} f(x+a\xi, y+a\eta, z+a\zeta)p \\ & \cdot \exp(-\lambda\sqrt{p^2-k^2}) \frac{d\xi\, d\eta\, d\zeta}{\sqrt{\xi^2+\eta^2+\zeta^2}} \\ & + \frac{1}{4\pi}\overline{\iiint_{-\infty}^{\infty}} h(x+a\xi, y+a\eta, z+a\zeta) \\ & \cdot \exp(-\lambda\sqrt{p^2-k^2}) \frac{d\xi\, d\eta\, d\zeta}{\sqrt{\xi^2+\eta^2+\zeta^2}} \\ & - \frac{a^2}{4\pi}\overline{\iiint_{-\infty}^{\infty}} \phi_1^*(x+a\xi, y+a\eta, z+a\zeta; p) \\ & \cdot \exp -(\lambda\sqrt{p^2-k^2}) \frac{d\xi\, d\eta\, d\zeta}{\sqrt{\xi^2+\eta^2+\zeta^2}} \\ = {} & v_1^*(x, y, z; p) + v_2^*(x, y, z; p) + v_3^*(x, y, z\, p), \\ & \quad . \quad . \quad . \quad (24) \end{aligned}$$

We proceed to the evaluation of the inverse Laplace transform of (24).

We start with the identity

$$\frac{\exp(-\lambda\sqrt{p^2-k^2})}{\sqrt{p^2-k^2}} = \int_\lambda^\infty \exp(-pt) J_0(k\sqrt{\lambda^2-t^2})\, dt$$

$$= \int_0^\infty \exp(-pt) H(\lambda, t)\, dt, \quad . \quad . \quad (25)$$

where $$H(\lambda, t) = \begin{cases} \text{if } t<\lambda, \\ J_0(k\sqrt{\lambda^2-t^2}) \text{ if } t>\lambda. \end{cases}$$

This yields

$$\exp(-\lambda\sqrt{p^2-k^2})$$

$$= \exp(-p\lambda) - \int_\lambda^\infty \exp(-pt) \frac{\partial}{\partial\lambda} J_0(k\sqrt{\lambda^2-t^2})\, dt. \quad (26)$$

Consider the contribution $v^*_{2,1}(x, y, z; p)$ to $v^*_2(x, y, z; p)$ arising from the first term in (26).

Using spherical polar coordinates this contribution can be written

$$v^*_{1,2}(x, y, z; p) = \int_0^\infty \exp(-p\rho)\rho\, d\rho$$

$$\cdot \frac{1}{4\pi} \int_{\phi=0}^{2\pi} \int_{\theta=0}^{2\pi} h(x+a\rho\sin\theta\cos\phi, y+a\rho\sin\theta\sin\phi,$$

$$z+a\rho\cos\theta) \sin d\phi\, d\theta, \quad (27)$$

If we introduce the function

$$\Phi_1(x, y, z; t) = \frac{1}{4\pi} t \int_{\phi=0}^{2\pi} \int_{\theta=0}^{\pi} h(x+at\sin\theta\cos\phi,$$

$$y+at\sin\theta\sin\phi, z+at\cos\phi) \sin\theta\, d\phi\, d\theta, \quad (28)$$

we obtain at once

$$v_{2,1}(x, y, z; t) = L^{-1}\{v^*_{2,1}(x, y, z; p)\} = \Phi_1(x, y, z; t). \quad (29)$$

The second contribution, $v^*_{2,2}(x, y, z; p)$ to $v^*_2(x, y, z; p)$, arising from the second part of (25), can be written

$$v^*_2(x, y, z; p) = -\frac{1}{4\pi} \int_0^\infty \exp(-pt)\, dt \int_0^t \lambda\, d\lambda$$

$$\cdot \int_{\phi=0}^{2\pi} \int_{\theta=0}^{\pi} h(x+a\lambda\sin\theta\cos\phi, y+a\lambda\sin\theta\sin\phi,$$

$$z+a\lambda\cos\theta) \frac{\partial}{\partial\lambda} J_0(k\sqrt{\lambda^2-t^2}) \sin\theta\, d\phi\, d\theta. \quad . \quad (30)$$

Comparison with (26) and (27) shows clearly that

$$v_{2,2}(x, y, z; t) = -\int_0^t \Phi_1(x, y, z; \tau) \frac{\partial}{\partial \tau} J_0(k\sqrt{\tau^2 - t^2})\, d\tau, \quad (31)$$

Thus finally

$$v_2(x, y, z; t) = \Phi_1(x, y, z; t) - \int_0^t \Phi_1(x, y, z; \tau) \frac{\partial}{\partial \tau} J_0(k\sqrt{\tau^2 - t^2})\, d\tau, \quad (32)$$

where $\Phi_1(x, y, z; t)$ is given by (28).

Consider now

$$v_1^*(x, y, z; p) = \frac{1}{4\pi} \overline{\iiint_{-\infty}^{\infty}} f(x+a\xi, y+a\eta, z+a\zeta) p \cdot \exp(-\lambda\sqrt{p^2 - k^2}) \frac{d\xi\, d\eta\, d\zeta}{\sqrt{\xi^2+\eta^2+\zeta^2}}. \quad (33)$$

With (33) let us associate

$$w_1^*(x, y, z; p) = \frac{1}{4\pi} \overline{\iiint_{-\infty}^{\infty}} f(x+a\xi, y+a\eta, z+a\zeta) \cdot \exp(-\lambda\sqrt{p^2 - k^2}) \frac{d\xi\, d\eta\, d\zeta}{\sqrt{\xi^2+\eta^2+\zeta^2}}. \quad (34)$$

Comparing the expression $w_1^*(x, y, z; p)$ in (34) with $v_2^*(x, y, z; p)$ as defined in (24), and taking into account (31), we obtain at once

$$w_1(x, y, z; t) = \Phi_2(x, y, z; t) - \int_0^t \Phi_2(x, y, z; \tau) \frac{\partial}{\partial \tau} J_0(k\sqrt{\tau^2 - t^2})\, d\tau, \quad (35)$$

where

$$\Phi_2(x, y, z; t) = \frac{1}{4\pi} t \int_{\phi=0}^{2\pi} \int_{\theta=0}^{\pi} f(x+at\sin\theta\cos\phi, y+at\sin\theta\sin\phi, z+at\cos\phi) \sin\theta\, d\phi\, d\theta. \quad (36)$$

In other words, the expression $\Phi_2(x, y, z; t)$ is obtained from $\Phi_1(x, y, z; t)$ by replacing $h(x, y, z)$ by $f(x, y, z)$.

Since

$$\mathrm{L}\left\{\frac{\partial}{\partial t} w_1(x, y, z; t)\right\} = p w_1^*(x, y, z; t) - w_1(x, y, z, 0) = p w_1^*(x, y, z) = v_1^*(x, y, z; p),$$

it follows that

$$v_1(x, y, z; t) = \frac{\partial}{\partial t} w_1(x, y, z; t)$$

$$= \frac{\partial}{\partial t} \left\{ \Phi_2(x, y, z; t) - \int_0^t \Phi_2(x, y, z; \tau) \frac{\partial}{\partial \tau} J_0(k\sqrt{\tau^2 - t^2}\, d\tau \right\}. \quad (37)$$

Finally, turning to the expression for $w_3^*(x, y, z; p)$, the corresponding inverse Laplace transform may be obtained with the aid of Borel's Theorem in the form

$$v_3(x, y, z; t) = -\frac{a^2}{4\pi} \overline{\iiint_{-\infty}^{\infty}} \frac{d\xi\, d\eta\, d\zeta}{\sqrt{\xi^2+\eta^2+\zeta^2}} \int_0^t \phi_1(x+a\xi, y+a\eta, z+a\zeta; t-\tau) H(\lambda, \tau)\, d\tau.$$

Bearing in mind the definition of $H(\lambda, \tau)$ in (25), the last expression becomes, after transforming to polar coordinates

$$v_3(x, y, z; t) = -\frac{a^2}{4\pi} \int_0^t \lambda d\lambda \int_{\phi=0}^{2\pi} \int_{\theta=0}^{\pi} \int_{\tau=0}^{t} \phi_1(x+a\lambda \sin\theta \cos\phi, y+a\lambda \sin\theta \sin\phi, z+a\lambda \cos\phi; t-\tau) \sin\theta \frac{\partial}{\partial \tau} . J_0(k\sqrt{\tau^2 - t^2})\, d\phi\, d\theta\, d\tau. \quad (38)$$

The final solution of the systems (1) to (3) can now be written in the form

$$u(x, y, z; t) = \exp(-ba^2 t)\{v_1(x, y, z; t) + v_2(x, y, z; t) + v_3(x, y, z; t)\}, \quad . \quad . \quad . \quad (39)$$

where the terms in brackets in (39) are given by (37), (32), and (38), the functions Φ, Φ_1, and Φ_2 in the latter formulæ being defined in (5), (28), and (36).

References.

(1) H. Poincaré, *Comptes Rendus*, cxvii. (1893).
(2) E. Picard, *Comptes Rendus*, cxviii. (1894).
(3) Riemann-Weber, ' Die Differenzial- und Integralgleichungen der Mechanik und Physik,' chap. 18 (1925).
(4) W. Ignatowsky, C. R. Acad. Ser. U.R.S.S. ser. 2, p. 59 (1935).
(5) Sbrana, Mem. del Acad. dei Lincei, ser. 6, v. pp. 221–51 (1933).
(6) A. Korn, *Sitzungsberichte Berlin Math. Ges.* xxvi. (1927).
(7) W. Machler, *Commentarii Math. Helv.* v. p. 256 (1933).
(8) Tokyo Sakuray, Proc. Phys. Math. Soc. Japan, ser. 3, xix. pp. 297–328 (1937).
(9) A. N. Lowan, " On the Operational Treatment of certain Mechanical and Electrical Problems," Phil. Mag. xvii. p. 1134 (1934).

Brooklyn College.
Yeshiva College.

XXXI. *The Measurement of the Velocity of Light over a Single Journey.* *By* R. J. Clark *.

[Received January 4, 1938.]

Abstract.

It is shown that if two clocks, previously synchronized by using the known velocity of any signals over the double journey between them, are used to measure the velocity of those signals over a single journey, the result will necessarily be that the velocity over a single journey is equal to that over a double one.

It is also shown that when wave trains are employed for signals, and also that the standard length employed, depends on waves of the same kind as the signals, the result may be that the measured velocity of the waves is the same in every direction.

If the dimensions of material bodies depend on a mechanism involving electromagnetic waves, and if the frequency of a moving clock alters according to the classical theory of Larmor and Lorentz, then measurements made in a physical system may be as required by the restricted theory of relativity.

The possibility of measuring the velocity of light over a single journey is discussed, and an outline is given of a possible method.

THE usual methods of measuring the velocity of light give the time taken by a short flash to travel a measured distance and to return to its starting-point after reflexion at one or more mirrors. (1) The accuracy in the more recent of the double-journey experiments is about 2 or 3 parts in 100,000. (2), (3) To be of real interest a single-journey experiment should be equally precise.

Roemer's method gives, ostensibly, the difference between the times for two single journeys of different lengths, over different paths, and by difference, the time for a single journey over a fictitious path, the length of which is equal to the difference in length of the paths traversed. Unless the velocity be constant, it is difficult to say exactly what is measured, but whatever it be, the

* Communicated by A. S. Eve, F.R.S.

uncertainty in the solar parallax makes the method useless for a precise determination.

To do a single-journey experiment, we need a source of light, a lens or a mirror to make a nearly parallel beam, some means of making flashes, and two clocks A and B, fixed a measured distance s, apart, to find the times t_1 and t_2, shown when the flashes reach them. The velocity is $s/(t_2-t_1)$. In order that we may properly subtract t_1 from t_2, we must keep the clocks in synchronism by some system of signalling, the alternative method of transport of chronometers being insufficiently accurate. In the double-journey experiment, which can always be done, this difficulty does not arise.

Correctly to synchronize the clocks, we require the time of transmission of the signals from A to B, or from B to A. Since we can always measure any velocity over the double journey AB BA, these times of transmission can be found, if we know, or can find, the ratio or the difference of the velocities over the single journeys. We must find this ratio, or difference, by a separate experiment, which, as we shall now show, must not involve synchronization of the clocks by the signals, of which the velocity over a single journey is to be measured.

If by using the velocity of light over the double journey, we synchronize the clocks A and B, we can then use them to measure its velocities over the single journeys AB and BA. Even though all three velocities differ in magnitude, this procedure always leads, without inconsistency, to the result that the three are equal. To prove this it is convenient to consider the various cases separately.

Let the velocities over the single journeys, AB and BA, be c_1 and c_2 and the velocity over the double journey be c. Let an observer at A synchronize the clocks by Einstein's method, sending out a flash which illuminates them in succession, and, returning reflected from B, illuminates A again. He adjusts A so that

$$t_2=\tfrac{1}{2}(t_1+t_3),$$

where t_1 and t_3 are the times shown on A, and t_2 the time shown on B. The clocks will now appear synchronous when observed from either station. The time taken by the flash to go from A to B and back is

$$s\left(\frac{1}{c_1}+\frac{1}{c_2}\right);$$

this is correctly measured by clock A, therefore

$$\tfrac{1}{2}(t_3-t_1)=\frac{s}{2}\left(\frac{1}{c_1}+\frac{1}{c_2}\right).$$

The fraction of this time taken on the outward journey is

$$\frac{s}{c_1}\div s\left(\frac{1}{c_1}+\frac{1}{c_2}\right)=\frac{c_2}{c_1+c_2},$$

and clock A is set slow or fast

$$\pm\left(\frac{1}{2}-\frac{c_2}{c_1+c_2}\right)\left(t_3-t_1\right)=\pm\frac{s}{2}\left(\frac{1}{c_2}-\frac{1}{c_1}\right)\text{ seconds,}$$

according as $c_1>$ or $<c_2$.

If the clocks be continuously illuminated so that they are synchronized by signals making a single journey, the error is the same. Observers at A and B will each suppose the clocks to be synchronous, when the distant one appears s/c seconds slow. A will set his near clock $s(1/c_2-1/c)$ seconds slow if $c_1>c_2$, and $s(1/c-1/c_2)$ seconds fast if $c_1<c_2$. B will set his near clock $s(1/c-1/c_1)$ seconds fast if $c_1>c_2$, and $s(1/c_1-1/c)$ seconds slow if $c_1<c_2$. But

$$s\left(\frac{1}{c_2}-\frac{1}{c}\right)=\frac{s}{2}\left(\frac{1}{c_2}-\frac{1}{c_1}\right)=s\left(\frac{1}{c}-\frac{1}{c_1}\right),$$

so that both observers agree, and the error is the same as before.

The observer now finds the time for the journey AB. It is s/c_1, but if $c_1>c_2$ the clock A at the start is

$$\frac{s}{2}\left(\frac{1}{c_2}-\frac{1}{c_1}\right)$$

seconds slow, and the time is measured as

$$\frac{s}{c_1}+\frac{s}{2}\left(\frac{1}{c_2}-\frac{1}{c_1}\right)=\frac{s}{2}\left(\frac{1}{c_1}+\frac{1}{c_2}\right)$$

seconds, half the time for the double journey. It is easy to see that this is the case if $c_1<c_2$, and that it does not matter if the time is taken for the journey BA.

If the observer assume for the single journey AB a velocity c_1' and by it synchronize the clocks, then the velocity over AB must be measured as c_1'. But measurement of the velocity over BA will give a different result, c_2'.

If he make a second approximation by assuming the new velocity c', such that

$$\frac{s}{c'}=\frac{s}{2}\left(\frac{1}{c_1'}+\frac{1}{c_2'}\right)$$

to synchronize the clocks, the measurements will become consistent as before. Such a process of successive approximation therefore leads to the result that the velocities over AB and BA are equal.

Let the velocities for the signals U, V, W, etc., be respectively u_1, u_2, and u, v_1, v_2, and v, w_1, w_2, and w etc. Let the clocks A and B be synchronized by the system U ; the error is

$$\pm\frac{s}{2}\left(\frac{1}{u_2}-\frac{1}{u_1}\right).$$

Then on measuring the velocities v_1 and v_2 we shall find for the times of passage, not $\frac{s}{v_1}$ and $\frac{s}{v_2}$ but

$$\frac{s}{v_1}\pm\frac{s}{2}\left(\frac{1}{u_2}-\frac{1}{u_1}\right)=t_1$$

and

$$\frac{s}{v_2}\mp\frac{s}{2}\left(\frac{1}{u_2}-\frac{1}{u_1}\right)=t_2.$$

Therefore

$$(t_1+t_2)=s\left(\frac{1}{v_1}+\frac{1}{v_2}\right),$$

which is correct. When we use the measured times of passage t_1 and t_2 to synchronize the clocks, we apply them directly and the error is unaltered. If the clocks be synchronized by the different signals in turn and the results are the same, then although

$$\frac{s}{2}\left(\frac{1}{u_2}-\frac{1}{u_1}\right)=\frac{s}{2}\left(\frac{1}{v_2}-\frac{1}{v_1}\right)=\frac{s}{2}\left(\frac{1}{w_2}-\frac{1}{w_1}\right),$$

we neither know that these times are zero, nor know which to choose if they all differ.

The preceding arguments apply to all signals. Therefore we cannot find the ratio of the backward and forward velocities of any signals, by measuring, on clocks synchronized by those signals, the times taken on the two journeys, for such an experiment will show that they are equal. As we cannot properly synchronize two clocks without knowing the backward and forward velocities

of the synchronizing signals, and as we cannot measure these velocities by single-journey methods without synchronizing clocks, it follows that, unless we can find either their ratio or their difference without synchronizing clocks, the result of every precise measurement of velocity over a single journey will be doubtful or perhaps meaningless. For example, if we synchronized by acoustic signals, we could find no difference between the velocities of sound, up and down wind, even though it blew a hurricane.

The velocity v, wave-length λ, and frequency ν of some systems of progressive waves are connected by the relation $v=\nu\lambda$. If we have a train of such waves (undamped) moving in the direction AB, we can, by reflexion at B, superpose on it a reversed train of the same frequency. Putting $x=0$ at B and $\nu=1/\tau$, the direct and reflected trains may be represented by equations like

$$R_1=R_0 \sin 2\pi\left(\frac{x}{\lambda}+\frac{t}{\tau}\right)$$

and

$$R_2=R_0 \sin 2\pi\left(\frac{x}{\lambda}-\frac{t}{\tau}\right)$$

if, and only if, the velocities of the waves are equal and opposite. The equation for the resultant,

$$R=2R_0 \sin 2\pi\frac{x}{\lambda}\cos 2\pi\frac{t}{\tau}, \quad . \quad . \quad . \quad . \quad (1)$$

represents a system of standing waves in which the phase is independent of x.

If the velocity change on reflexion the two waves have the same period τ, but different lengths λ and λ', therefore the trains will be represented by equations of the type

$$R_1=R_0 \sin 2\pi\left(\frac{x}{\lambda}+\frac{t}{\tau}\right)$$

and

$$R_2'=R_0 \sin 2\pi\left(\frac{x}{\lambda'}-\frac{t}{\tau}\right).$$

The sum of these is

$$R'=2R_0 \sin\pi\left(\frac{x}{\lambda}+\frac{x}{\lambda'}\right)\cos 2\pi\left[\frac{t}{\tau}+\frac{x}{2}\left(\frac{1}{\lambda}-\frac{1}{\lambda'}\right)\right]. \quad (2)$$

which represents a wave system with the phase dependent on x. The amplitude is

$$2R_0 \sin \pi x \left(\frac{1}{\lambda}+\frac{1}{\lambda'}\right),$$

therefore the distance between successive nodes is

$$\frac{\lambda''}{2}=\frac{\lambda\lambda'}{\lambda+\lambda'}.$$

Let the change of phase be ϵ, then

$$\cos\left(2\pi\frac{t}{\tau}+\epsilon\right)=\cos\left[2\pi\frac{t}{\tau}+2\pi.\frac{x}{2}\left(\frac{1}{\lambda}-\frac{1}{\lambda'}\right)\right]$$

and

$$\epsilon=2\pi.\frac{x(\lambda'-\lambda)}{2\lambda\lambda'}.$$

Therefore between one node and the next the phase changes by

$$\eta=\pi\frac{\lambda'-\lambda}{\lambda'+\lambda},$$

and by one complete period between points $\lambda_p=\dfrac{2\lambda\lambda'}{\lambda'-\lambda}$ apart. We may take λ_p as the length of the phase wave. The phase velocity is λ_p/τ, which is clearly infinite when $\lambda=\lambda'$. If we could measure the phase velocity over a double journey we could tell whether or not $\lambda=\lambda'$. Unfortunately the phase velocity cannot be reversed on one of two parallel paths. We must therefore measure λ and λ' in order to see if they are equal. It is doubtful if we could do this with a grating, but if we could it would solve the problem of finding the equivalent of a signal of infinite velocity.

In a moving non-dispersive medium we have

$$\lambda=v_1\tau, \quad \lambda'=v_2\tau,$$

where v_1 and v_2 are constants. Therefore

$$\frac{\lambda_p}{\tau}=\frac{2v_1v_2}{v_2-v_1}=\text{constant}.$$

In a dispersive medium we do not double λ and λ' on doubling τ, but presumably change both v_1 and v_2. Therefore $\dfrac{\lambda_p}{\tau}$ is not constant, unless $\left(\dfrac{1}{v_2}-\dfrac{1}{v_1}\right)$ is either

zero or has the same finite value, whatever the frequency. If keeping τ constant we change the medium for another either dispersive or not, then $\frac{\lambda_p}{\tau}$ will change unless $\left(\frac{1}{v_2} - \frac{1}{v_1}\right)$ either is always zero, or has the same finite value in every medium. The velocities in different media vary greatly; on substituting electromagnetic waves for those of sound, the velocity ratio is nearly 10^5. Although the wave velocities be so different, the phase velocities in standing systems in different media may be equal and probably are nearly so. If the phase velocity is the same in all systems of standing waves, then it is almost certainly infinite, and the backward and forward wave velocities in each system are almost certainly equal.

One object in measuring the velocity of light over a single journey is to see whether it is affected by the motion of the earth. If this affects no measurement, then for all signals U, V, W, ...

$$\left(\frac{1}{u_2} - \frac{1}{u_1}\right) = \left(\frac{1}{v_2} - \frac{1}{v_1}\right) = \text{etc.} = \text{a constant}$$

which should be zero, for as a signal we use nothing of which the velocity might depend on direction from any cause except the motion of the earth. Therefore if there be a number of differences between the signals, it is possible that some are affected by the motion. If the differences change with the seasons, the possibility becomes a probability. But it is possible that all signals are equally changed. The signals least likely to be affected would be those made acoustically.

The Michelson-Morley experiment is said to prove that the velocity of light is the same in every direction and independent of the motion of its source. The analogous acoustic experiment will show that the velocity of sound is affected by the wind, because the dimensions of the apparatus are variable in terms of an acoustic standard of length, but constant in terms of the length of a standard bar. If we adopt an acoustic standard of length, and keep the dimensions constant by this new standard, the result will be very different.

The most natural way of making an acoustic standard of length is to set up a linear system of standing waves of sound, maintained at constant frequency ν_0 by a generator which is controlled by a clock. We adopt the

distance between consecutive nodes as the standard of length.

Let V be the velocity of sound, measured by ordinary clocks and standard bars. In still air the distance between consecutive nodes in the standing wave system is

$$\frac{\lambda''}{2}=\frac{1}{2}\frac{V}{\nu_0}=\frac{1}{2}V\tau_0 \text{ cm.}$$

In a wind of velocity v, whose direction makes an angle θ with the path of the system, the wave velocities v_1 and v_2, referred to the generator, are given by the equations

$$V^2=v^2+{v_1}^2-2vv_1\cos\theta,$$

$$V^2=v^2+{v_2}^2+2vv_2\cos\theta,$$

showing that where $\theta=0$, $v_1=V+v$ and $v_2=V-v$, and that where $\theta=\pi/2$, $v_1=v_2=\sqrt{V^2-v^2}$. The distance from node to node is

$$\frac{\lambda''}{2}=\frac{\lambda_1\lambda_2}{\lambda_1+\lambda_2}=\frac{v_1v_2}{v_1+v_2}\tau_0=\left(\frac{1}{v_1}+\frac{1}{v_2}\right)^{-1}\tau_0 \text{ cm.}$$

Let the acoustic interferometer be set up in still air, let the two paths for the sound be at right angles, and the length of one C be S_C cm. or N_C acoustic units Let the other D be S_D cm. or N_D acoustic units long. Then

$$S_C=\frac{N_C}{2}V\tau_0,$$

$$S_D=\frac{N_D}{2}V\tau_0.$$

The times required for sound to travel the length of the paths and back are

$$\frac{2S_C}{V}=N_C\tau_0=t_1,$$

and

$$\frac{2S_D}{V}=N_D\tau_0=t_2.$$

Therefore no change in the interference pattern will be produced by rotating the interferometer in still air.

If the interferometer be put in a steady wind of velocity v, then, as ordinarily measured, its dimensions are unchanged, but measured acoustically they are altered; we adjust them to the values they had when there was

no wind, and keep them so adjusted. Let the wave velocities backwards and forwards along C be v_1 and v_2, and along D v_3 and v_4 cm. per second, then the new lengths are

$$S'_C = N_C\left(\frac{1}{v_1}+\frac{1}{v_2}\right)^{-1}\tau_0 \text{ cm.}$$

and

$$S'_D = N_D\left(\frac{1}{v_3}+\frac{1}{v_4}\right)^{-1}\tau_0 \text{ cm.}$$

The times for the double journeys along the paths are

$$S'_C\left(\frac{1}{v_1}+\frac{1}{v_2}\right) = N_C\tau_0 = t_1,$$

and

$$S'\left(\frac{1}{v_3}+\frac{1}{v_4}\right) = N_D\tau_0 = t_2,$$

which are the same as before and do not depend on the values of the wave velocities. Therefore the experiment carried out in this way shows that the velocity of sound is the same in every direction and is unaffected by the wind. It is clear also that it is independent of the motion of the source. Therefore when lengths are measured in terms of an acoustic standard, we shall be able to derive for sound a series of propositions corresponding to those derived in the theory of relativity from the constant velocity of light.

Let us now suppose (*a*) that the equation for the addition of velocities is of the classical form $V = V_1 + V_2$ and (*b*) that the dimensions of a crystal lattice are proportional to the distance between the nodes of a system of standing electromagnetic waves of constant frequency which accompany the crystal. This is practically equivalent to saying that the atoms in a crystal are at the nodes or loops of a system of standing waves, and that the waves in the spaces between the atoms are substantially waves in free space. For simplicity assume that the waves are in an isotropic medium and travel in it with a constant speed c as in the classical theory. The frequency may depend on the kind of crystal; let it be ν_1 and the period be τ_1. Let the crystal have an arbitrary velocity v through the medium.

In the direction of motion the distance between nodes is

$$\frac{\lambda''}{2} = \left(\frac{1}{v_1}+\frac{1}{v_2}\right)^{-1}\tau_1 = \left(\frac{1}{c+v}+\frac{1}{c-v}\right)^{-1}\tau_1 = \frac{c^2-v^2}{2c}\tau_1;$$

when $v=0$

$$\frac{\lambda''}{2} = \frac{1}{2} c\tau_1.$$

Therefore the crystal contracts in the direction of motion in the ratio

$$1 : \left(1 - \frac{v^2}{c^2}\right).$$

Perpendicular to the motion the wave velocities are

$$v_1' = v_2' = (c^2 - v^2)^{\frac{1}{2}}$$

and the distance between nodes is

$$\left(\frac{1}{v_1'} + \frac{1}{v_2'}\right)^{-1} \tau_1 = \frac{1}{2}\left(c^2 - v^2\right)^{\frac{1}{2}} \tau_1.$$

Therefore at right angles to the motion the crystal contracts in the ratio

$$1 : \left(1 - \frac{v^2}{c^2}\right)^{\frac{1}{2}}.$$

The ratio between the length l parallel to the velocity and the breadth b at right angles to it is

$$\frac{l}{b} = \frac{l_0}{b_0}\left(1 - \frac{v_2}{c_2}\right)^{\frac{1}{2}},$$

where l_0 and b_0 refer to the crystal at rest. This is the same as the Fitzgerald-Lorentz contraction. With this internal wave mechanism all dimensions contract.

If we cut from a crystal at rest a standard bar of length l_0, then when moving longitudinally with velocity v the length is

$$l_0\left(1 - \frac{v^2}{c^2}\right).$$

The time taken for light to make the journey along the stationary bar and back is

$$t = \frac{2l_0}{c}.$$

When the bar is moving the journey takes

$$t' = l_0\left(1 - \frac{v^2}{c^2}\right)\left(\frac{1}{c+v} + \frac{1}{c-v}\right) = \frac{2l_0}{c} = t.$$

The bar and any wave-length of light are therefore mutually consistent standards of length. The experimental

evidence that this is so is conclusive. In all the methods of counting the number of wave-lengths in a metre the light makes a double journey.

If the dimensions of crystals change with their motion so will the dimensions of bars composed of them. In the Michelson-Morley experiment and all its modifications there will be the same compensating changes as in the acoustic experiment imagined above. Therefore if our surmise concerning the internal wave-mechanism in a crystal is correct in principle, neither the original nor the modified experiments can show any effect of motion on the velocity of light, provided that the experiment is done *in vacuo* and the waves between the atoms are substantially unaffected by the presence of the atoms themselves.

Let an interferometer and source of light move with velocity v; let the velocities of light backwards and forwards along the optical paths C and D be v_1, v_2 and v_3, v_4 respectively. Let C and D be at right angles for example. For path C, the length

$$S_C = N_C \left(\frac{1}{v_1} + \frac{1}{v_2}\right)^{-1} \tau_1,$$

and for path D,

$$S_D = N_D \left(\frac{1}{v_3} + \frac{1}{v_4}\right)^{-1} \tau_1.$$

The times for the double journeys of light along the paths are

$$t_1 = S_C \left(\frac{1}{v_1} + \frac{1}{v_2}\right) = N_C \tau_1,$$

$$t_2 = S_D \left(\frac{1}{v_3} + \frac{1}{v_4}\right) = N_D \tau_1,$$

which do not depend on the wave velocities. But if the experiment be done in air there will not be complete compensation. If the path C be along the direction of motion

$$t_1' = N_C \left(\frac{1}{c+v} + \frac{1}{c-v}\right)\left(\frac{1}{c/\mu + kv - v} + \frac{1}{c/\mu - kv + v}\right)\tau_1$$

$$= N_C \tau_1 \mu \left(1 - k\frac{v^2}{c^2}\right),$$

$$t_2' = N_D \tau_1 \frac{\sqrt{c^2 - v^2}}{2} \cdot \frac{2}{\sqrt{\frac{c^2}{\mu^2} - (k-1)^2 v^2}}$$

$$= N_D \tau_1 \mu \left(1 - \frac{k}{2}\frac{\mu^2}{c^2}\right),$$

approximately, where $k = (1 - 1/\mu^2)$, μ being the refractive index. These times are different. The shift of the fringes to be expected is of the order of 0·1 per cent. of the full shift which might, on the original theory, be shown. Should it be necessary to allow for this dragging effect on the velocity of the standing waves, the shift might be larger, but one could hardly expect more than a few per cent. of the full amount. In this case the measured velocity calculated as from a fringe shift will have the wrong sign[4].

All the relativity experiments which depend on the existence of a contraction for their null results will be approximately accounted for by this hypothesis, provided that the transverse contraction does not matter. This means actually that, in addition to the Lorentz contraction, there is a general shrinkage all round. But we have so far assumed that the frequency of the waves between the atoms is unchanged whether the crystal be moving or not. Now according to the classical theory of Larmor and Lorentz the frequency ν of a clock moving with velocity v through the luminiferous ether should be

$$\nu = \nu_0 \left(1 - \frac{v^2}{c^2}\right)^{\frac{1}{2}},$$

where ν_0 is the frequency when at rest. On making this correction we find that the transverse contraction in a moving bar reduces to zero, and the results deduced from our hypothesis agree with those deduced from the theory of relativity. We have only to write for the distance between nodes in a standing wave system transverse to the direction of motion

$$\frac{\lambda''}{2} = \left(\frac{1}{v_1'} + \frac{1}{v_2'}\right)^{-1} \tau_1 = \tfrac{1}{2}(c^2 - v^2)^{\frac{1}{2}} \tau_1$$

$$= \tfrac{1}{2}(c^2 - v^2)^{\frac{1}{2}} c (c^2 - v^2)^{-\frac{1}{2}} \tau_0 = \tfrac{1}{2} c \tau_0,$$

the same as at rest. Similar corrections apply in the other cases which we have worked out above. On this

point of view the restricted theory of relativity is a consequence of a simple mechanism which determines the dimensions of moving material bodies. The validity of the physical theory is not denied by adopting such an hypothesis, which is only the adoption of a mechanism which itself not relativistic shows how relativistic mechanics comes about.

If this view be justified the only way of measuring the velocity of light over a single journey which is at all likely to succeed is to use sound waves as synchronizing signals for the clocks. Actually this is hardly practical, so that a better way would be to compare the phase velocities of various standing waves, electrical waves on wires, waves of sound in air, etc. If all such standing wave systems have the same phase velocity then that is almost certainly infinite. However, it is not certain or even likely that it is the same in every case, and the only way to proceed is to examine a number of systems, which must therefore be the first step in the experiment. If all synchronizing signals which we can employ to synchronize a pair of clocks give the same result, the only practical conclusion is that motion of translation in a straight line produces no observable effects. The condition for this is that for all signals $s\left(\frac{1}{v_2}-\frac{1}{v_1}\right)=$ a constant, but not $s\left(\frac{1}{v_1}+\frac{1}{v_2}\right)=$constant.

To compare phase velocities in standing systems we set up two on near and parallel paths, and measure, by oscillographs or otherwise, the phase relationship between them at suitable pairs of points. If this phase relationship is the same at all pairs of points which lie on a common perpendicular to the paths, then the phase velocities are the same.

An experiment like this probably could be done; it would be easiest and most interesting if the synchronizing signals were electrical waves on a transmission line, for, to show that their speed is independent of direction would be important. To do the experiment one would measure the distance between two stations A and B and join them by a transmission line, having constant inductance, capacity, resistance, and leakance per unit length, the two

quantities last named being as small as possible in order to minimize attenuation.

On considering experiments like those of Laville [5], it seems that, for continuous waves on a transmission line with a parallel return, the attenuation constant γ is given very approximately by the formula

$$\gamma = \frac{1}{c}\frac{\sqrt{\rho c/\lambda_0}}{2d \log 2D/d},$$

where c = the ratio of the units,
ρ = the specific resistance of the conductor,
λ_0 = the wave-length in free space,
d and D = the diameter of, and distance between, the conductors.

Since γ is small we can replace λ_0 by λ, the wave-length on the line, and putting $\rho = 1{\cdot}6 \times 10^3$ (for Cu), $d=1$, $D=100$, $\lambda = 3 \times 10^3$, we find $\gamma = 1{\cdot}3 \times 10^{-8}$ approximately. This is for a line of two straight conductors on which the wave velocity is nearly 3×10^{10} cm./sec. By using helical conductors we can reduce γ further and make the velocity more or less what we please.

In practice it is impossible to make $\gamma = 0$, therefore equations for actual waves on a transmission line will be of the type

$$R_1 = R_0 e^{\gamma x} \sin 2\pi\left(\frac{x}{\lambda} + \frac{t}{\tau}\right),$$

$$R_2 = R_0 e^{-\gamma x} \sin 2\pi\left(\frac{x}{\lambda} - \frac{t}{\tau}\right),$$

of which the sum is

$$R = 2R_0\left[\cosh \gamma x \sin 2\pi\frac{x}{\lambda}\cos 2\pi\frac{t}{\tau} + \sinh \gamma x \cos 2\pi\frac{x}{\lambda}\cos 2\pi\frac{t}{\tau}\right].$$

representing two systems of standing waves in quadrature. If the line be 1·2 km. long, *i. e.*, 40 wave-lengths for $\nu = 10^7$, and $\gamma = 10^{-7}$, the amplitude of the second system will be 1·2 per cent. of the first, at the generator end of the line, and zero at the other. In comparing phases between standing wave systems on different paths, each one, unless they are electrical waves in the air, will have these two

components. We may either balance out the smaller by a suitable auxiliary generator or resolve into components. When the wave system is used for synchronizing it appears best to balance one out.

If the signals be used to synchronize a pair of shutters, the method of measurement is like that used by Fizeau to find the velocity of light. To do this experiment we might make two electro-optical shutters and two amplifiers to work them, with as nearly as possible the same characteristics. We might next place the shutters a short distance δs apart, drive them by one oscillator of adjustable frequency, and sending light through A and B in this order, find r_2, the ratio of the light incident on B to that transmitted through it. Next, passing light through B and then A we find for A, the corresponding ratio, r_1.

We now set up the shutters near the ends of the transmission line, and on it establish a system of standing waves. If there be $2n$ nodes between the points at which the amplifiers are connected to the line, the shutters will open and close with the phase difference which they had when connected directly to the oscillator. The second system of standing waves we suppose neutralized by an auxiliary generator, supplying the necessary e.m.f. at some stage in the amplifier, rather than to the line itself.

Let the source of light be near A ; let s be the distance between the shutters, and let them open ν_s times per second. When ν_s has been adjusted so that for shutter B the ratio of incident to transmitted light is r_2, then flashes are transmitted as if the shutters were δs apart, and the time for the journey must be an integral number N_1 of complete periods. Therefore

$$\frac{s-\delta s}{c_1} = \frac{N_1}{\nu_{s_1}}.$$

By putting the source at B we shall find, similarly,

$$\frac{s-\delta s}{c_2} = \frac{N_2}{\nu_{s_2}}.$$

As in Fizeau's Method, N_1 and N_2 take in succession the values 1, 2, 3 ... N ...

It is difficult to estimate the accuracy of the experiment. If we could detect a change in r_1 or r_2 for one degree change in phase of the shutter, it would be considerable. For instance, with $\nu_s = 10^7$ cycles per second and $s = 1{\cdot}2$ km.

N will be about 80 and the accuracy about 4 parts in 100,000. N might be made about 100.

This experiment might directly determine the time of passage over a single journey. It is feasible if we can set up standing waves of the kind represented by equation (1), or of the kind represented by (2), if we allow for change of phase. The fundamental difficulty is to find a method of comparing velocities which are parallel and oppositely directed.

References.

(1) Fizeau, *Comptes Rendus*, xxix. p. 90 (1849). Foucault, *Comptes Rendus*, xxx. p. 551 (1850).
(2) Michelson, Astrophysical Journal, xl. p. 1 (1927).
(3) Mittelstadt, *Ann. der Phys.* ii. p. 285 (1929).
(4) Miller, 'Nature,' cxxiii. p. 162 (1934).
(5) Laville, Thèse: Paris, Masson éditeur (1924).

XXXII. *Co-existence of Normal and Supra-conductive Regions.* *By* K. Mendelssohn *and* J. G. Daunt, *Clarendon Laboratory, Oxford* *.

[Received June 9, 1938.]

Abstract.

It has been shown that an isothermal co-existence of supra-conductive and normal material can occur in the same specimen. The time effects in supraconductors have been discussed with regard to such a co-existence.

SINCE the discovery of the diamagnetic behaviour of supraconductors various attempts have been made to link their properties of zero resistance (R) and zero induction (B) causally by electrodynamic equations, but so far all theories have failed in this respect and the two phenomena have still to be treated as entirely independent[1]. The thermodynamical treatment[2] which differentiates between the supraconductive and the normal metal as between two "phases" only requires that in the supra-conductive "phase" B should be 0 and that in the normal 'phase" B should have the same value as the external

* Communicated by the Authors.

field H. The electrical resistance does not appear at all in these considerations. So far all experimental evidence seems to indicate that whenever the condition $B=0$ is fulfilled, R also is equal to zero. A great number of experiments show, however, that in cases where $B\neq 0\neq H$, $R\neq 0$.

The most conclusive experiments are those in which the setting up and subsequent destruction of a persistent current in a ring by an external magnetic field can be observed by the change of induced magnetic moment in a varying external field. Such experiments have been carried out by Grayson Smith and Wilhelm[3], Shoenberg[4], and Schubnikow and Chotkewitsch[5]. The general features of the results are essentially the same in all three investigations. It was found that the induced current first increased with rising field, passed through a sharp maximum and became zero before the threshold field (H_c) was reached. By accurate calculation of the electrical data of the ring and by allowing for the diamagnetic susceptibility of the specimen without a persistent current, Schubnikow and Chotkewitsch could show that when the external field reached 1/2 H_c (*i. e.*, H_c at the surface of the ring) the persistent current became zero or at least very small *. This means that as soon as lines of force enter the material of the conductor and its induction begins to deviate from the value zero, it is no longer supra*conductive*, although its diamagnetism only disappears entirely when the external field has reached the value H_c.

This important result suggests immediately the possible conception that quite in general the resistance may cease to be zero in a supraconductive body as soon as B deviates from zero *anywhere* in the volume. This possibility has in fact already been pointed out by Schubnikow and Chotkewitsch. Experiments on specimens of an irregular shape[6], [7], on the other hand, have led us to the assumption that persistent currents (other than diamagnetic ones) can exist although the total induction of the specimen is not zero. In fact, we see no other possibility of explaining the hysteresis phenomena in ,*e. g.*, a short

* The correction for the magnetic moment of the ring was assumed to be proportional to H (formula 2), it has to be remembered, however, that this relation only holds up to 1/2 H_c, and that at higher fields the moment falls with increasing H, *i. e.* the correction ceases to be valid at the same value at which the persistent current becomes zero.

cylinder of a pure supraconductive metal (fig. 6, ref. 6, fig. 1; ref. 7) otherwise than by assuming such currents and therewith zero resistance. Our explanation of the time effects in supraconductors[8] also relies on the isothermal co-existence of supraconductive and normal regions in the metal and on the assumption of persistent currents in the boundary surface.

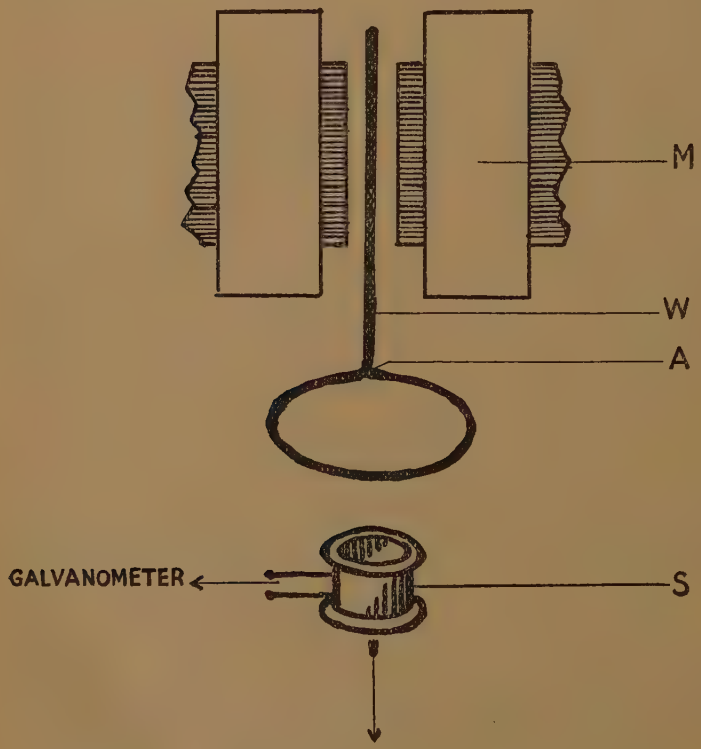

Although from these and other reasons it did not appear likely that local penetration of magnetic flux should destroy zero resistance in the whole specimen, it seemed desirable to decide this question by a direct experiment.

A single crystal wire of tin of high purity of 1 mm. ϕ was bent to form a circular loop of 0·9 cm. radius, having a 9 cm. long bit of the wire left over. The loop was welded at A autogeneously and the remaining length of the

wire W bent perpendicular to the plane of the loop. The specimen was immersed in liquid Helium II at 1·875° K. The magnetic moment of the ring could be determined by the search coil S. A small electromagnet M was so arranged that supraconductivity could be destroyed locally in W.

With the aid of an external magnetic field a persistent current was set up in the ring and the resulting moment determined in zero field. Then supraconductivity in W was destroyed by switching on M. If the resistance in the ring would have ceased to be zero, the persistent current would have been annihilated and the magnetic moment fallen to zero. No change, however, was observed, which means, that the resistance in one part of the specimen remained zero while the induction was different from zero in another part. This result and the experiments on short cylinders mentioned above show quite definitely that there can be an isothermal co-existence of regions distinguished by normal and by zero resistance in the same specimen and that while, as was clearly shown by Schubnikow and Chotkewitsch the penetration of a specimen by magnetic flux and reappearance of resistance may coincide, this need not necessarily be the case in a specimen of different shape.

A word might be added concerning the time-effects. The slow change of induction observed after a sudden variation of external field or temperature was ascribed by Mendelssohn and Pontius[7], [8] to a gradual expansion or contraction of macroscopic supraconductive regions and a dying-out of persistent currents in a boundary surface between the two states which has a small but finite resistance. It seems convenient for these considerations to distinguish between two kinds of supra-currents : " diamagnetic currents," which are set up and annihilated at the reversible establishment and destruction of the supraconductive state in a solid body and the existence of which is entirely dependent on the external magnetic field, and " persistent currents," which are set up by changes of the external field in annular supraconductive regions and which carry their own field. Whereas the annihilation of a diamagnetic current is a reversible process, the annihilation of a persistent current occurs irreversibly. It is evident that if the time-effects are caused by a " dying-out " of currents these currents must

be " persistent " ones, as the annihilation of a current in a region with finite resistance will be accompanied by the development of Joule heat and will therefore be irreversible. It seems thus that time-effects, " persistent currents " and the co-existence of macroscopic supraconductive and normal regions are causally connected. These questions will be discussed in detail in a later communication.

References.

(1) *Cf.* K. Mendelssohn, Proc. Roy. Soc. A, clii. p. 34 (1935).
(2) C. J. Gorter and H. Casimir, *Physica*, i. p. 305 (1934).
(3) H. Grayson Smith and J. O. Wilhelm, Proc. Roy. Soc. A, clvii. p. 132 (1936).
(4) D. Shoenberg, Proc. Roy. Soc. A, clv. p. 712 (1936).
(5) L. W. Schubnikow and W. T. Chotkewitsch, Phys. Sow. x. p. 231 (1936).
(6) K. Mendelssohn, J. Daunt and R. B. Pontius, *VIIe Int. Congr. du Froid, La Haye*, i. p. 445 (1936).
(7) K. Mendelssohn and R. B. Pontius, ' Nature,' cxxxviii. p. 29 (1936).
(8) K. Mendelssohn and R. B. Pontius, *Physica*, iii. p. 327 (1936).

XXXIII. *On the Fluorescent Ion of Chromium in Ruby.*

By B. V. Thosar, *M.Sc., College of Science, Nagpur, India* *.

[Received February 7, 1938.]

IT has been a well-known observed fact that ruby, the hard refractory red precious stone, fluoresces with a bright red colour when excited with light of shorter wave-lengths. The spectrum of the fluorescent light of ruby, among other solid phosphors, has recently been investigated with great thoroughness by Deutschbein[1], who has photographed and measured the wave-lengths of a number of lines and bands of ruby at room-temperature, also at −190° C. The spectrum contains an intense red doublet which becomes very sharp at low temperatures, the wave-lengths being λ 6920 and λ 6934. Ruby is nothing but corundum, *i. e.*, crystalline Al_2O_3, with a small percentage of chromium as an impurity, probably in the form of Cr_2O_3. It has been pointed out by previous observers, and reaffirmed by Deutschbein, that the intense red doublet is due to the chromium ion, Cr^{+++}, corresponding to the transitions between the energy

* Communicated by the Author.

levels of the ion in the ^2G and ^4F states. It will be seen from fig. 1 that the transitions [2] which give rise to these lines involve a change in the value of J from $4\frac{1}{2}$ to $4\frac{1}{2}$ and from $3\frac{1}{2}$ to $3\frac{1}{2}$ respectively, *i. e.*, $\Delta J=0$.

It is to be noted that the transitions in question are between doublets and quartets, and are really forbidden by the usual selection rules, and should be shown, if at all, as very weak lines. Actually the red doublet of ruby is remarkably intense. The origin of other weaker lines and bands of the fluorescence spectrum yet remains obscure, though it has been pointed out that some of

Fig. 1.

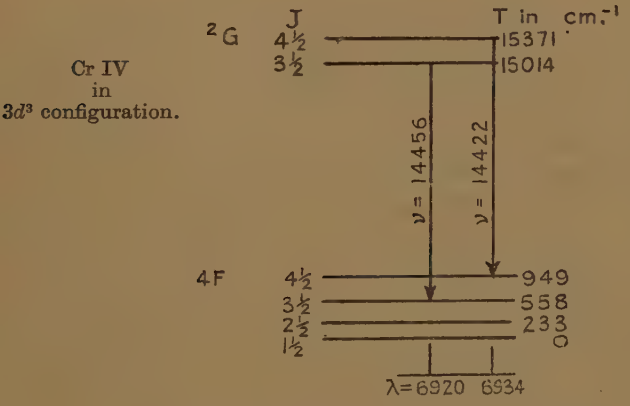

Energy level diagram of red doublet of ruby.

these may be due to a kind of inter-molecular Stark effect. We will, however, confine our attention here only to the sharp intense lines at λ 6920 and λ 6934.

Now, crystalline salts of rare-earths show similar sharp lines in absorption and emission, and a complete review of the explanations offered, with some mathematical theory, has been recently given by Van Vleck[3]. In this paper on rare-earths reference has been made to similar phenomena shown by crystals of the first transitional series. The case of ruby, however, is quite different from all these, in that here the fluorescent material chromium occurs only as an impurity and in very small proportion within the ground-material corundum. The actual physical state of the fluorescent ion Cr^{+++} in

relation to the surrounding crystalline material does not seem to have received much attention. The view tacitly taken seems to be that stray molecules of chromium oxide or the Cr^{+++} ions are scattered as an impurity throughout the ground-material of ruby, the ionized chromium atom giving rise to the red doublet. While offering an explanation of the effect of a magnetic field on this red doublet of ruby a suggestion regarding the nature of inclusion of the fluorescent chromium ion within the body of the ground-material corundum has been put forward in the following paragraphs.

Effect of Magnetic Field on the Ruby Doublet.

An old and interesting paper of Mendenhall and Wood[4] dealing with the effect of magnetic and electric fields on the fluorescent lines of solids has not received much attention. In this the observers have described the Zeeman pattern shown by the two intense red lines at $-180°$ C., the longitudinal effect due to a field-strength of 22,000 gauss being observed by means of a concave grating. As depicted in fig. 2 each line of the doublet splits into four lines unsymmetrically placed, the outermost components being 5·0 Å.U. apart and the distance from the centre of middle pair to long wave-length outer components being 0·25 Å.U. more than the distance to the short wave-length components. It is to be noted that both the lines of the doublet give an exactly similar Zeeman pattern.

Before coming to the interpretation of this Zeeman pattern it will be seen that this case of Zeeman effect in question is of unique interest and of special importance, since, here, the radiating ion of chromium Cr^{+++} occurs as a constituent in the formation of a solid crystalline material. In the usual experimental mode of investigating the Zeeman effect, *e. g.*, an arc, a spark in air or a discharge-tube placed in a magnetic field, the radiating atoms or ions are in the gaseous form and are therefore independent of one another. Hence the pattern obtained is not likely to be influenced in its main characteristics by the relationship between the radiating ion and its surrounding atoms. In the present case, however, the emitting ion placed in a magnetic field is still a part of solid crystalline matter, and the ions and fields surrounding

it will profoundly affect the Zeeman pattern shown. In the case of the line of the doublet due to the transition

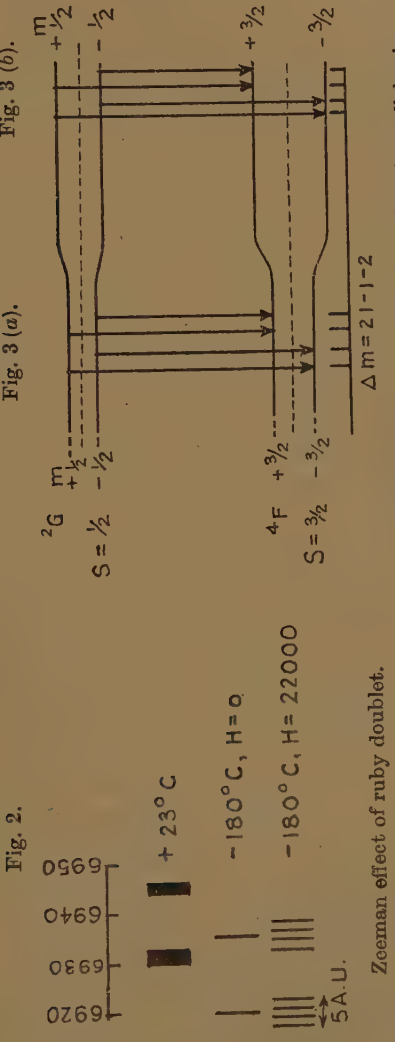

$^2G_{7/2} \rightarrow {}^4F_{7/2}$ the usual theory of the Zeeman effect will predict the splitting of each one of the two levels for which $J = 7/2$ into eight sub-levels where "m" will take the

half-integral values from $+3\frac{1}{2}$ to $-3\frac{1}{2}$. For longitudinal effect, which involves the transitions governed by $\Delta m = \pm 1$, the pattern would thus consist of no fewer than fourteen components. Actually it is seen to consist of only four components. Similarly the other line of the doublet due to the transition $^2G_{9/2} \rightarrow {}^4F_{9/2}$ should, according to usual theory, show 18 Zeeman lines, as, here, each of the levels would split up into 10 sub-levels corresponding to "m" taking the half-integral values from $+9/2$ to $-9/2$. Here, as before, there are only four Zeeman lines shown in the pattern. As already stated above, this must be a result of the fluorescing ion not being free from the influence of the surrounding ions and fields. The phenomenon at once becomes intelligible if it is assumed that only the resultant spin-vector S of the three $3d$ electrons of the Cr^{+++} ion responds to the external magnetic field, the resultant orbital moment L of the ion remaining unaffected. Assuming that the L-vector is not free to orientate itself in the field, the higher ^2G-state as well as the lower ^4F-state in the magnetic field will have two energy levels according as the resultant spin $S = 1/2$ for ^2G-state and $S = 3/2$ for ^4F-state is parallel or anti-parallel to the direction of the field H. There will thus be four transitions possible (fig. 3 (a)) from the two levels in the upper to the two levels in the lower state. This idea that only the resultant spin-moment and not the orbital moment contributes to the energy of the chromium ion in a magnetic field is identical with the idea introduced by D. M. Bose[5] and elaborated by Stoner[6], that only the S-moment (and L-moment only partially in some cases) of the ion is quantized in an external field and contributes to the paramagnetic susceptibility of the crystals of the elements of the first transition series. Stoner[6] has shown that in the case of the rare-earth crystals the orbital moment L coupled with the spin moment S is quantized in the external field, as the electrons which contribute to the susceptibility are in an inner incomplete shell and are shielded by the outer electrons. In the case of the elements of the transition series, however, the incomplete group of d-electrons is on the outside of the ion, and on account of interaction with the surrounding ions the L moment in this case is not free to orientate in an external field, the S moment alone being free.

The application, as put forward above, of the ideas of Bose and Stoner regarding the paramagnetic behaviour of the ions of the first transition series to the case of the Zeeman pattern of the ruby doublet due to the Cr^{+++} ion is thus seen to be successful in explaining the occurrence of only four lines in the pattern. This result is deeply interesting and significant in two ways. In the first place, unlike the considerations of paramagnetic susceptibility which are of a statistical nature, this Zeeman pattern of Cr^{+++} ion in solid crystalline state can be regarded as the most direct evidence in favour of the suggestion that only the spin-moment is free to orientate in an external field when the ions are in solid state. Zeeman effect as usually studied yields little information about the interatomic or the interionic relationship since the atoms or ions are in the gaseous state and are independent of one another. In this fortunate instance, however, we have the emitting ion still a component part of the crystalline state, and the characteristics of the Zeeman pattern obtained are at least qualitatively in very good accord with the basic assumptions of the theory of paramagnetic behaviour of the ion in question.

Nature of Inclusion of the Cr^{+++} Ion.

Secondly, the uncertain question of the exact nature of inclusion of Cr^{+++} ions throughout the mass of the ground-material corundum admits of elucidation in a striking manner. The supposition that only the S-moments and not the L-moments are capable of orientation in an applied field is really equivalent to supposing that the L-moment of the ion (if it is due to electrons in the group of highest total quantum number as it is in this case of Cr-ion) tends to assume a definite orientation with respect to neighbouring ions or atoms or molecules. Now this means that every Cr-ion embedded within the ground-material has its L-vector orientated in identical manner with respect to its surrounding ions. This would be possible if we assume that the ions of chromium are scattered within the ground-material not merely as stray impurity causing undefined local disturbance of the regular crystal lattice, but are all proper constituents of the lattice substituting in places the Al-ions in the body of the ground-material Al_2O_3. As shown in fig. 4 the structure of crystalline corundum as revealed by X-ray

examination[7] contains groups of two Al-atoms and three O-atoms, the latter forming an equilateral triangle while the two metal atoms are symmetrically situated with respect to the centre of this triangle, one above and the other below it. Davey[8] has shown that the structures of crystalline Al_2O_3 and Cr_2O_3 are very similar, both having three molecules per unit prism, and both are molecular or valence compounds. It is therefore reasonable to assume that the fluorescent ions of chromium in ruby substitute the Al-ions in the crystal lattice, thus becoming regular component ions in the crystalline state, with their L-vectors all orientated in like manner with respect to the neighbouring ions. This would secure equivalent inability of the L-moment in all the fluorescent ions to respond to the applied magnetic field, and would thus lead to identical energy value for all the ions in the

Fig. 4.

○ = metal ion, Al or Cr.

● = oxygen atom.

Distance AB = 2·726 Å.U. for Al_2O_3.
2·754 Å.U. for Cr_2O_3.

X-ray structure of Al_2O_3 and Cr_2O_3.

same spectroscopic state. The definition and sharpness of the Zeeman lines obtained in the pattern can then be understood.

Quantitative Consideration.

From the values reported by Mendenhall and Wood for the Zeeman pattern, for the line λ 6920, the interval between the two outermost of the four components is seen to be equal to $\Delta\nu = 10{\cdot}4$ cm. $^{-1}$. As shown in fig. 3 corresponding to these two shifts $m = +2$ and -2 respectively. For spin-moments the Landé g-factor has the value 2. Where ν_0 is the normal Zeeman shift the interval between the two outermost components will, by theory, be given by the following calculation:

$$\Delta\nu = (\Delta m - \Delta m').g.\nu_0.\mathrm{H}$$

$$\therefore \quad = 4 \times 2 \times 4{\cdot}674 \times 10^{-5} \times 22000$$

$$= 8{\cdot}23 \text{ cm.}^{-1}, \text{ taking } g = 2.$$

This value is certainly rather removed from the observed interval 10·4 cm.$^{-1}$, but it is of the same order of magnitude and lends support to the main idea developed above.

A clue to the probable explanation of the numerical disagreement, and also of the asymmetry of the Zeeman pattern, is found in the consideration that in both the ^{2}G- and the ^{4}F-states of the ion the surrounding crystalline field in which the ion is situated will greatly influence the energy of the ion, the change in energy due to this cause being more in the higher, *i. e.*, ^{2}G-state. If, further, in a magnetic field, the two sub-levels of each state corresponding to the parallel and anti-parallel positions of the spin-vectors are affected to a different extent by the superposition of the crystalline field on the ion, then, as depicted in fig. 3(*b*), an asymmetric Zeeman pattern would result. This explanation is rendered acceptable on noting that a temperature change from 23° C. to −180° C. shifts the ruby doublet through as large an interval as from λ6932–46 to λ6920–34, and this is presumably brought about by the change in the crystalline field in which the emitting ion is situated.

Ruby and Sapphire.

It was known to previous workers, and has been lately confirmed by Venkateswaran[9], that sapphire, when exposed for a sufficiently long time, shows a fluorescent spectrum almost identical with that of ruby. This means that it is again the Cr^{+++} ions occurring as impurity in the ground-material Al_2O_3 of sapphire that are the emitters of light. The intensity of the red doublet in this case is very much feebler. In terms of the explanation offered above this will be so on account of very few Cr-ions from the Cr_2O_3 impurity actually replacing the Al-atoms of the crystal lattice in this case, unlike ruby. Those which have become proper ionic constituents of the lattice are in a position to absorb light in the blue end of the spectrum, according to the transition $^4F \rightarrow {}^2H$. Such ions must be much fewer in sapphire than in ruby, and this fact, combined with the effect of other impurities like ferric and titanium oxides, may be the reason why sapphire is blue and ruby is red. It is interesting to note in this connexion the work of Saha[10] and others on the colours of inorganic salts. In the case of chromic chloride

it has been shown that the colour arises due to interaction of light with Cr^{+++} ions, the reaction consisting in changing the spins only of the electrons in the incomplete d^3-shell. The energy required for this change is small and falls in the visible region. In ruby also Cr^{+++} ions which have entered the crystal lattice will change their spins only by absorption of light (the blue end) and give rise to red colour, and the number of such ions being larger in ruby than in sapphire they will also account for much greater intensity of the red emission doublet in ruby.

The Forbidden Transition.

It is noteworthy that the transitions which give rise to such intense red doublet in ruby $^2G_{7/2,\,9/2} \rightarrow {}^4F_{7/2,\,9/2}$ are really forbidden by the usual selection principles, since they are transitions from doublets to quartets. Such forbidden lines occur with great intensity whenever the atom excited in the metastable state is in such attenuated condition that collisions are rare, and the atom has nothing else to do than to revert back to its normal state by running its usual life. Three intense lines of highly ionized iron atom Fe VI in $3d^3$ configuration corresponding to the forbidden transitions $^4F \rightarrow {}^2G$ occur in the spectrum of Nova Pictari[11] and are a case in point. Analogous to the highly ionized iron atoms in the above star, the ionized chromium atoms in this case are excited by absorption of short-wave light, and have to return to the normal state through the forbidden transitions, since mutual collisions are as rare and inadmissible in the crystalline state as in the attenuated stellar atmosphere. Besides this the following statement of H. C. Bowen[12] also furnishes a clue to this curious phenomenon of two very strong emission lines shown by chromium ions in a solid phase: "In the higher stages of ionization the excited potentials of the forbidden transitions between the terms of the very low $3d^n$ configurations are very much lower than that of any permitted line—their forbidden lines may be very strong in comparison with the permitted lines."

The author hopes to be able soon to present other lines of evidence in support of the idea put forward above, namely, the fluorescent ions of chromium in ruby actually

enter the lattice of the crystalline ground-material, substituting in random places the Al-ions of corundum.

In conclusion, I wish to thank Prof. Sir C. V. Raman for inspiration and the opportunity I had to study the fluorescence of ruby at liquid-air temperature in his laboratory at Bangalore during the years 1935–36.

Summary.

The Zeeman pattern of the red fluorescence doublet of ruby at −180° C. has been explained on the supposition that the fluorescent Cr^{+++} ions enter the crystal lattice of Al_2O_3, substituting in places the Al-ions, and that it is the spin-moment only and not the orbital moment that responds to the magnetic field. This is shown to be in entire agreement with the theory of paramagnetism of the ions of the transition series, as developed by Bose, Stoner, and others. Taking the Landé factor $g=2$, the calculated Zeeman interval is shown to be of the same order of magnitude as the observed one, but numerically different. A possible explanation of this disagreement and of the asymmetry of the pattern has been indicated. Reasons for the difference in intensity of the red doublet for ruby and sapphire and in their colour have been offered. The curiously great intensity of this forbidden doublet has also been explained.

References.

(1) O. Deutschbein, *Ann. der Phys.* xiv. p. 712 (1932); *Zeit. für Phys.* lxxvii. p. 489 (1932); and *Physik. Zeitsch.* xxxii. p. 874 (1932).
(2) Bacher and Goudsmit, 'Atomic Energy States,' p. 166 (International Series in Physics).
(3) Van Vleck, Journ. Phys. Chem. xli. p. 67 (1937).
(4) Mendenhall and Wood, Phil. Mag. xxx. p. 316 (1915).
(5) D. M. Bose, *Zeit. für Phys.* lxiii. p. 864 (1927).
(6) E. C. Stoner, Phil. Mag. viii. p. 250 (1929).
(7) Pauling and Hendricks, Journ. Amer. Chem. Soc. xlvii. p. 781 (1925).
(8) W. P. Davey, Phys. Rev. xxi. p. 716 (1923).
(9) C. S. Venkateswaran, Journ. Ind. Acad. Sci. ii. p. 459 (1935).
(10) M. N. Saha, 'Spectroscopy in Service of Chemistry,' p. 301 (Sir P. C. Ray commemoration volume of Ind. Chem. Soc.).
(11) H. S. Jones, Month. Not. Roy. Astron. Soc. xcii. p. 728 (1932).
(12) H. C. Bowen, Rev. Mod. Phys. viii. p. 55 (1936).

XXXIV. *A Note on Riemannian Tensors.*

By V. V. Narlikar *.

[Received April 11, 1938.]

Abstract.

It is shown how non-null tensors can be represented by vectors with reference to an orthogonal system of basic tensors called R-tensors. The transformation of vectors is discussed and some new inequalities are deduced from the vector representation.

1. *Null Tensors.*

A NULL tensor is one whose quadratic invariant is identically zero. If Ui is a null vector $UiU=0$; also if $Tij=AUiUj$, $TijT^{ij}=0$. Tij is thus a null tensor. In what follows we will be considering only non-null tensors with real components, and the results will be obtained, specifically, for a Riemannian space of four dimensions, the method being applicable for a space of n dimensions in general.

2. *Representation of Tensors by Vectors.*

The representation of tensors by orthogonal ennuples is well known. Owing to the rule of lowering suffixes by the use of the fundamental tensor g^{ij}, there is no loss of generality if we confine our attention here to covariant tensors. Consider a tensor of the mth order, $a_{s_1 s_2 \ldots s_m}$. Its representation in terms of an orthogonal ennuple and the associated invariants is, in the usual notation given by

$$a_{s_1 s_2 \ldots s_m} = \sum_{h_1 \ldots h_m} C_{h_1 h_2 \ldots h_m} e_{h_1} \ldots e_{h_m} \lambda_{h_1 | s_1} \ldots \lambda_{h_m | s_m}. \quad (1)$$

If the 4^m components are all independent, the above representation is equivalent to

$$a_{s_1 s_2 \ldots s_m} = \sum_{1}^{4^m} \alpha^r R_{(r)\, s_1 s_2 \ldots s_m}, \quad \ldots\ldots (2)$$

where the 4^m independent tensors are all provided by $\lambda_{h_1 [s_1} \ldots \lambda_{h_m | s_m}$. These R-tensors satisfy the conditions

$$R_{(r)\, s_1 \ldots s_m} R^{s_1 - \ldots s_m}_{(s)} = 0 \text{ or } 1, \quad \ldots\ldots (3)$$

* Communicated by the Author.

according as $r \neq s$ or $r = s$ respectively. It is obvious from (3) that we cannot have an identity of the form

$$\sum_{(r)} p^r \mathrm{R}_{s_1 s_2 \ldots s_m} = 0 \quad . \quad . \quad . \quad . \quad . \quad . \quad (4)$$

unless all the p's vanish. The R-tensors may be said to constitute an orthogonal set of normalized tensors.

If, however, all the components of a tensor $a_{s_1 s_2 \ldots s_m}$ are not independent, let only n of them be so. It is clear from the representation by orthogonal ennuples that the independent R-tensors will also be n. By way of illustration we will give the representation for the curvature tensor R_{ihkj}. Let the unit vectors of the ennuple be u^i, v^i, w^i, and x^i, and let their indicators be e_1, e_2, e_3, e_4, respectively. We have then six R-vectors of the form

$$\tfrac{1}{2}[u^i u^j v^h v^k + u^h u^k v^i v^j - u^i u^k v^h v^j - u^h u^j v^i v^k], \quad . \quad . \quad (5)$$

twelve more of the form

$$\frac{e_2 e_3}{\sqrt{8}}[u^i u^j (v^h w^k + v^k w^h) + u^h u^k (v^i w^j + v^j w^i) - u^i u^k (v^h w^j + v^j w^h) - u^h u^j (v^i w^k + v^k w^i)], \quad (6)$$

while only two more independent ones remain of the form

$$\frac{e_1 e_2 e_3 e_4}{\sqrt{8}}[u^i v^j w^h x^k + u^j v^i w^h x^k + u^k v^h w^j x^i + u^h v^k w^i x^j - u^h v^j w^i x^k - u^j v^h w^k x^i - u^i v^k w^h x^j - u^k v^i w^j x^h]. \quad (7)$$

The conditions for an orthogonal set of normalized tensors such as (3) are satisfied by the twenty R-tensors, and so we have

$$\mathrm{R}_{ihkj} = \sum_{r=1}^{20} \alpha^r \mathrm{R}_{(r)ihkj}. \quad . \quad . \quad . \quad . \quad . \quad (8)$$

Similarly, we can express the contracted curvature tensor by

$$\mathrm{R}_{ij} = \sum_{r=1}^{10} \alpha^r \mathrm{R}_{(r)ij}; \quad . \quad . \quad . \quad . \quad . \quad . \quad (9)$$

for $r = 1$ to 4, $\mathrm{R}_{(r)ij}$ is of the form $e_1 u_i u_j$, while for the remaining six values of r it is of the form $\frac{e_1 e_2}{\sqrt{2}}(u_i v_j + u_j v_i)$.

Thus

$$g_{ij} = \sum_{r=1}^{4} {}_{(r)}\mathrm{R}_{ij}. \quad . \quad . \quad . \quad . \quad . \quad . \quad (10)$$

In this manner R_{ij} can be represented as a vector α^r in a 10-space, R_{hijk}, as a vector in a 20-space, while the general tensor $a_{s_1 s_2 \ldots s_m}$, not subject to spatial identities, as a vector in a 4^m-space.

3. *The Vector-Transformations.*

The vector-representation is with reference to the R-tensors, and the system of R-tensors depends upon the orthogonal ennuple chosen. There is a six-fold arbitrariness about the orthogonal ennuple, since its sixteen components are subject only to the ten restrictions,

$$g_{ij} = e_1 u_i u_j + e_2 v_i v_j + e_3 w_i w_j + e_4 x_i x_j. \quad . \quad . \quad (11)$$

There is thus a six-fold arbitrariness even about the choice of the basic R-tensor system. A tensor referred to two different R-tensor systems will be represented by two different vectors, and it is the transformation connecting these vectors and, incidentally, the R-tensor systems, that will be considered now.

Let
$$\mathrm{R}_{ihkj} = \sum_{s=1}^{20} \lambda_r^s \, {}_{(s)}\mathrm{R}'_{ihkj}, \quad . \quad . \quad . \quad . \quad . \quad (12)$$

so that if

$$\mathrm{R}_{ihkj} = \sum_{r=1}^{20} \alpha^r \, {}_{(r)}\mathrm{R}_{ihkj} = \sum_{r=1}^{20} \alpha'^r \, {}_{(r)}\mathrm{R}'_{ihkj}, \quad . \quad . \quad . \quad (13)$$

the vector-transformation is

$$\sum_{r=1}^{20} \alpha^r \lambda_r^s = \alpha'^s. \quad . \quad . \quad . \quad . \quad . \quad . \quad (14)$$

The fourteen scalar differential invariants of R_{ihkj} bring out the restrictions on λ_r^s. Thus the quadratic invariant gives

$$\mathrm{R}_{ihkj}\mathrm{R}^{ihkj} = \sum_{r=1}^{20} (\alpha^r)^2 = \sum_{s=1}^{20} \left\{ \sum_{r=1}^{20} \alpha^r \lambda_r^s \right\}^2. \quad . \quad . \quad (15)$$

The values of λ_r^s can be inferred for the four-dimensional case from the following two-dimensional representation :

$$\mathrm{R}_{ij} = l_1^2 \, {}_{(1)}\mathrm{R}'_{ij} + m_1^2 \, {}_{(2)}\mathrm{R}'_{ij} + \sqrt{2}\, l_1 m_1 \, {}_{(3)}\mathrm{R}'_{ij},$$

$$\underset{(2)}{R_{ij}}=l_2^2\underset{(1)}{R'_{ij}}+m_2^2\underset{(2)}{R'_{ij}}+\sqrt{2}\,l_2m_2\underset{(3)}{R'_{ij}},$$

$$\underset{(3)}{R_{ij}}=\sqrt{2}\,l_1l_2\underset{(1)}{R'_{ij}}+\sqrt{2}\,m_1m_2\underset{(2)}{R'_{ij}}+(l_2m_1+l_1m_2)\underset{(3)}{R'_{ij}}.$$

Here (l_1, m_1) and (l_2, m_2) are unit vectors satisfying the conditions of orthogonality in the Euclidean space S_2.

It will be found that

$$g_{ij}=\underset{(1)}{R_{ij}}+\underset{(2)}{R_{ij}}=\underset{(1)}{R'_{ij}}+\underset{(2)}{R'_{ij}}.$$

4. *Tensor Invariants.*

A necessary and sufficient condition that a tensor be zero is that its representative vector be zero. The magnitude of the vector is given by the quadratic invariant A_2. For

$$A_2=A_{s_1s_2\ldots s_m}A^{s_1\ldots s_m}=\Sigma(\alpha^r)^2. \quad . \quad . \quad . \quad (18)$$

Hence $A_2=0$ is a necessary and sufficient condition that the components $A_{s_1\ldots s_m}$ be all zero. A tensor equation can thus be represented by a scalar invariant equation. It is interesting to find that if we denote for the curvature tensor R_{ihkj}, $R_{ihkj}R^{ihkj}$ by R_2, and $R_{ij}R^{ij}$ by G_2 the ten equations of gravitation, viz.,

$$R_{ij}-\tfrac{1}{2}Rg_{ij}+\lambda g_{ij}=-kT_{ij}, \quad . \quad . \quad . \quad . \quad (19)$$

can be represented by the single equation

$$(R_{ij}-\tfrac{1}{2}Rg_{ij}+\lambda g_{ij}+kT_{ij})(R^{ij}-\tfrac{1}{2}Rg^{ij}+\lambda g^{ij}+kT^{ij})=0$$

or

$$G_2+k^2T_2+2kT_{ij}R^{ij}-2R\lambda+4\lambda^2+2k\lambda T-kRT=0, \quad (20)$$

and the Weyl condition for a Riemannian space V_n to be conformal to a Euclidean space Sn by its equivalent, viz.,

$$R_2-\frac{4G_2}{n-2}+\frac{2R^2}{(n-1)(n-2)}=0. \quad . \quad . \quad (21)$$

If $A_{s_1\ldots s_m}$ and $B_{s_1\ldots s_m}$ have representative vectors α^r and β^r we have, from the inequalities,

$$\text{(i.)} \quad \Sigma(\alpha^r)^2+\Sigma(\beta^r)^2\geqslant 2\Sigma\alpha^r\beta^r,$$

$$\text{(ii.)} \quad \Sigma(\alpha^r)^2\Sigma(\beta^r)^2\geqslant(\Sigma\alpha^r\beta^r)^2,$$

$$A_2+B_2\geqslant 2A_{s_1\ldots s_m}B^{s_1\ldots s_m}, \quad . \quad . \quad . \quad . \quad (22)$$

and $$A_2B_2 \geqslant (A_{s_1 \ldots s_m}B^{s_1 \ldots s_m})^2. \quad . \quad . \quad . \quad . \quad (23)$$

If we replace $A_{s_1 \ldots s_m}$ by R_{ihkj} and the other tensor by $\lambda(g_{ij}g_{hk}-g_{ik}g_{hj})$ we deduce

$$R_{ihkj}R^{ihkj}=R_2 \geqslant \tfrac{1}{6}R^2 \quad . \quad . \quad . \quad . \quad . \quad (24)$$

and, similarly,

$$G_2 \geqslant \tfrac{1}{4}R^2. \quad . \quad . \quad . \quad . \quad . \quad . \quad (25)$$

Similar results can be deduced about any tensor $A_{s_1 \ldots s_m}$ for which there exists a tensor of the same type involving only functions of g_{ij}.

Another inequality obtained by us from the vector-representation is, for V_4,

$$G_2-\tfrac{1}{4}R^2 \leqslant \tfrac{1}{2}R_2. \quad . \quad . \quad . \quad . \quad . \quad (26)$$

This is obvious when we express each of the terms as a function of α^r where α^r is defined by (8).

Benares Hindu University.
April 5, 1938.

XXXV. *Operational Forms and Contour Integrals for Bessel Functions with Argument* $a\sqrt{t^2-b^2}$. *By* N. W. McLachlan, *D.Sc.**

[Received July 4, 1938.]

1. *Introduction.*

BESSEL functions with argument $a\sqrt{t^2-b^2}$ were used by Heaviside in the solution of submarine cable transmission problems about half a century ago. Herein it is not intended to deal with practical applications of such functions, but to derive a number of O.F.'s and the corresponding contour integrals. The latter are obtained from the O.F.'s by using a modified version of the Mellin inversion theorem. Some of the O.F.'s in § 2 were obtained by Niessen † using a different procedure. To avoid breaking the continuity of the text,

* Communicated by the Author.
† Phil. Mag. xx. p. 977 (1935).

Niessen's forms have not merely been quoted. For convenience the following abbreviations are used :

$$y=\sqrt{t^2-b^2},\ r=\sqrt{p^2+a^2},\ s=\sqrt{p^2-a^2},\ v=\sqrt{p^2-ia^2},$$
$$\mathrm{P}=p+\sqrt{p^2+a^2},\ \mathrm{Q}=p+\sqrt{p^2-a^2},\ \mathrm{T}=p+\sqrt{p^2-ia^2}.$$

A new symbol.—During the past few years I have made the symbol $\doteqdot$, which designates O.F., some thousands of times (!), and submit that it has disadvantages. First, it has been used by engineers for half a century to represent "is approximately equal to." Secondly, four separate operations are required to form it, namely, two strokes and two dots. This necessitates one's pen being lifted three times. It is suggested that the sign $\Rightarrow$ made fairly heavy with one stroke of the pen is preferable. On the average, three of these signs can be made in the same time as that required for one of the other. The round end always points to the O.F., *e. g.*,

$$t^2 \Rightarrow 2\,!/p^2, \quad \text{or} \quad 2\,!/p^2 \Leftarrow t^2.$$

2. *The* J *Functions.*

We commence with the known integral

$$p\int_b^\infty e^{-pt}\mathrm{J}_0(a\sqrt{t^2-b^2})\,dt = \frac{pe^{-b\sqrt{p^2+a^2}}}{\sqrt{p^2+a^2}}, \quad . \quad \text{(M)} \quad (1)$$

$$= \sqrt{2b/\pi}\,\frac{p\mathrm{K}_{\frac{1}{2}}(br)}{r^{\frac{1}{2}}}, \quad \text{(M)} \quad (2)$$

$t>b$, real and positive. Dividing (1) throughout by p and differentiating with respect thereto, we obtain

$$p\int_b^\infty e^{-pt}t\mathrm{J}_0(a\sqrt{t^2-b^2})\,dt = \frac{p^2be^{-br}}{r^2} + \frac{p^2e^{-br}}{r^3}, \quad . \quad (3)$$

so
$$t\mathrm{J}_0(ay) \Rightarrow (p/r)^2e^{-br}\left(b+\frac{1}{r}\right) . . \quad . \quad \text{(M)} \quad (4)$$

Differentiating (1) with respect to b, we have

$$p\int_b^\infty e^{-pt}\frac{\mathrm{J}_1(a\sqrt{t^2-b^2})}{\sqrt{t^2-b^2}}\,dt = \frac{p}{ab}(e^{-bp}-e^{-br}), \quad \text{(M)} \quad (5)$$

$$\Leftarrow \frac{\mathrm{J}_1(ay)}{y} . . \quad . \quad . \quad . \quad . \quad (6)$$

The term $\frac{pe^{-bp}}{ab}$ represents an infinite impulse at $t=b$. It is neutralized by an equal but opposite term in the expansion of $-\frac{pe^{-br}}{ab}$. This must be so, for $\frac{J_1(ay)}{y}=\frac{1}{2}a$ at $t=b$.

Using the integration rule of the operational calculus with lower limit $t=b$, (5) yields

$$\int_b^t \frac{J_1(ay)}{y}\,dt \supset \frac{1}{ab}(e^{-bp}-e^{-br}). \quad . \quad (M) \quad (7)$$

Differentiating (1) with respect to a gives

$$p\int_b^\infty e^{-pt}\sqrt{t^2-b^2}\,J_1(a\sqrt{t^2-b^2})\,dt=\frac{pae^{-br}}{r^2}\left(b+\frac{1}{r}\right),$$

$$. \quad . \quad . \quad (M) \quad (8)$$

$$\subset yJ_1(ay). \quad . \quad . \quad (9)$$

Dividing (5) throughout by p and differentiating with respect thereto, we have

$$t\frac{J_1(ay)}{y} \supset \frac{p}{a}\left(e^{-bp}-\frac{pe^{-br}}{r}\right). \quad . \quad (M) \quad (10)$$

Since $\frac{d}{dt}J_0(a\sqrt{t^2-b^2})=-at\frac{J_1(a\sqrt{t^2-b^2})}{\sqrt{t^2-b^2}}$, we get

$$-\int_b^t d[J_0(a\sqrt{t^2-b^2})]=1-J_0(a\sqrt{(t^2-b^2)})=a\int_b^t t\frac{J_1(ay)}{y}\,dt.$$

$$. \quad . \quad . \quad (11)$$

Now $t>b$, so from (1) and (11), we obtain

$$\int_b^t t\frac{J_1(ay)}{y}\,dy \supset \frac{1}{a}\left(e^{-bp}-\frac{pe^{-br}}{r}\right). \quad (M) \quad (12)$$

This result could have been obtained from (10) by applying the integration rule with lower limit b, but the above procedure is of interest, as owing to the origin being shifted to $t=b$, unity in (11) is interpreted by e^{-bp}. By altering the limits in (11), we have $(t>b)$

$$a\int_t^\infty t\frac{J_1(ay)}{y}\,dt=J_0(ay), \quad . \quad . \quad . \quad . \quad (13)$$

and by (1)

$$\int_t^\infty t\frac{J_1(ay)}{y}\,dt \supset \frac{pe^{-br}}{ar}. \quad . \quad . \quad (M) \quad (14)$$

For the sake of generality we shall derive the differentiation rule for functions of the type $f(a\sqrt{t^2-b^2})$. By definition

$$\phi(p)=p\int_b^\infty e^{-pt}f(a\sqrt{t^2-b^2})\,dt=-\int_b^\infty f(a\sqrt{t^2-b^2})d(e^{-pt}). \quad . \quad . \quad . \quad (15)$$

After repeated integration by parts we find that

$$\phi(p)=e^{-bp}\sum_{r=0}^{n-1}p^{-r}\left[\frac{d^r}{dt^r}f(a\sqrt{t^2-b^2})\right]_{t=b} + p^{-n+1}\int_b^\infty e^{-pt}\frac{d^n}{dt^n}[f(a\sqrt{t^2-b^2})]\,dt, \quad (16)$$

so $$\frac{d^n}{dt^n}[f(a\sqrt{t^2-b^2})]$$

$$\supset p^n\phi(p)-e^{-bp}\sum_{r=0}^{n-1}p^{n-r}\frac{d^r}{dt^r}[f(a\sqrt{t^2-b^2})]_{t=b}, \quad (17)$$

$$=p^n\phi(p), \quad . \quad . \quad . \quad . \quad . \quad . \quad . \quad . \quad . \quad . \quad . \quad (18)$$

provided $f(0)=\frac{d}{dt}f(0)=\frac{d^{n-1}}{dt^{n-1}}f(0)=0$.

As an illustration let $f(a\sqrt{t^2-b^2})=\mathrm{J}_0(a\sqrt{t^2-b^2})$, then by (1), (17)

$$\frac{df}{dt}=-at\frac{\mathrm{J}_1(a\sqrt{t^2-b^2})}{\sqrt{t^2-b^2}}\supset\frac{p^2e^{-br}}{r}-pe^{-bp}, \quad (\mathrm{M}) \quad (19)$$

which is identical with (10). In this case $f(0)=1$, which accounts for the second term on the r.h.s. of (19).

By aid of recurrence formulæ for Bessel functions and the rules of the operational calculus, many O.F.'s may be derived from those in various sections herein. If desired, those forms having an exponential factor can be expressed in terms of $\mathrm{K}_{\frac{1}{4}}$ as at (2).

The O.F. of $\mathrm{J}_\mu(t)\mathrm{J}_\nu(t)$.

Taking the known formula

$$\mathrm{J}_\mu(t)\mathrm{J}_\nu(t)=\frac{2}{\pi}\int_0^{\frac{1}{2}\pi}\mathrm{J}_{\mu+\nu}(2t\cos\theta)\cos(\mu-\nu)\theta\,d\theta, \quad (20)$$

we obtain

$$p\int_0^\infty e^{-pt}\mathrm{J}_\mu(t)\mathrm{J}_\nu(t)\,dt = \frac{2p}{\pi}\int_0^{\frac{1}{2}\pi}\cos(\mu-\nu)\theta\,d\theta\int_0^\infty e^{-pt}\mathrm{J}_{\mu+\nu}(2t\cos\theta)\,d\theta, \quad (21)$$

or

$$J_\mu(t)J_\nu(t) \supset \frac{2^{\mu+\nu+1}}{\pi} p \int_0^{\frac{1}{2}\mu} \frac{\cos^{\mu+\nu}\theta \cos(\mu-\nu)\theta \, d\theta}{\sqrt{p^2+4\cos^2\theta}\,(p+\sqrt{p^2+4\cos^2\theta})^{\mu+\nu}}. \quad . \quad . \quad . \quad (22)$$

Writing $\cos^2\theta = 1-\sin^2\theta$, (22) gives

$$J_\mu(t)J_\nu(t) \supset \frac{pk^{\mu+\nu+1}}{\pi} \times \int_0^{\frac{1}{2}\pi} \frac{\cos^{\mu+\nu}\theta \cos(\mu-\nu) d\,d\theta}{\sqrt{1-k^2\sin^2\theta}(\frac{1}{2}pk+\sqrt{1-k^2\sin^2\theta})^{\mu+\nu}}, \quad (M) \quad (23)$$

$$R(\mu+\nu) > -1,$$

where $k = 2/\sqrt{p^2+4}$, $R(p) > 0$. When $\mu = \nu$, (23) becomes

$$J_\nu^2(t) \supset \frac{pk^{2\nu+1}}{\pi} \times \int_0^{\frac{1}{2}\pi} \cos^{2\nu}\theta \, d\theta / \sqrt{1-k^2\sin^2\theta}\,(\tfrac{1}{2}pk+\sqrt{1-k^2\sin^2\theta})^{2\nu}, \quad . \quad . \quad . \quad (M) \quad (24)$$

$R(\nu) > -\frac{1}{2}$. When $\nu = 0$, (24) gives

$$J_0^2(t) \supset \frac{pk}{\pi} \int_0^{\frac{1}{2}\pi} d\theta/\sqrt{1-k^2\sin^2\theta}, \quad . \quad . \quad . \quad (25)$$

$$= \frac{pk}{\pi} E(k, \tfrac{1}{2}\pi), \quad . \quad . \quad . \quad . \quad . \quad (M) \quad (26)$$

where E is the first complete elliptic integral of modulus k, $k^2 < 1$.

3. *The I Functions.*

Since $I_\nu(x) = i^{-\nu}J_\nu(ix)$, the following formulæ can be deduced from those given in § 2.

$$tI_0(ay) \supset (p/s)^2\left(b+\frac{1}{s}\right)e^{-bs}, \quad . \quad (M) \quad (27)$$

$R(p) > a^*$,

$$I_1(ay)/y \supset (p/ab)(e^{-bs}-e^{-bp}), \quad . \quad (M) \quad (28)$$

$$yI_1(ay) \supset (pa/s^2)\left(b+\frac{1}{s}\right)e^{-bs}, \quad . \quad (M) \quad (29)$$

$$tI_1(ay)/y \supset (p/a)[(p/s)e^{-bs}-e^{-bp}], \quad (M) \quad (30)$$

$$\int_b^t tI_1(ay)\frac{dt}{y} \supset (1/a)[(p/s)e^{-bs}-e^{-bp}], \quad (M) \quad (31)$$

* This condition applies to (27)–(31) inclusive to ensure convergence of the Laplace integral.

and

$$I_\mu(t)I_\nu(t) \supset \frac{pk_1^{\mu+\nu+1}}{\pi}\int_0^{\frac{1}{2}\pi} \frac{\cos^{\mu+\nu}\theta\cos(\mu-\nu)\theta\,d\theta}{\sqrt{1-k_1^2\cos^2\theta}\,(\frac{1}{2}+\sqrt{1-k_1^2\cos^2\theta})},$$

. . . (M) (32)

$R(\mu+\nu)>-1$, where $k_1=2/p$, $R(p)>2$. When $\mu=\nu$, (32) can be expressed in the form

$$I_\nu^2(t) \supset \frac{pk_1^{2\nu+1}}{\pi}$$

$$\times\int_0^{\frac{1}{2}\pi}\sin^{2\nu}\theta\,d\theta/\sqrt{1-k_1^2\sin^2\theta}\,(\tfrac{1}{2}+\sqrt{1-k_1^2\sin^2\theta})^{2\nu},$$

. . . (M) (33)

$R(\nu)>-\frac{1}{2}$. When $\nu=0$ in (33), we obtain

$$I_0^2(t) \supset \frac{2}{\pi}\int_0^{\frac{1}{2}\pi} d\theta/\sqrt{1-k_1^2\sin^2\theta}, \quad . \quad . \quad . \quad (34)$$

$$= \frac{2}{\pi}E(k_1, \tfrac{1}{2}\pi). \quad . \quad . \quad . \quad . \quad (M) \quad (35)$$

We know that

$$e^{-t}I_0(t) \supset p/\sqrt{p^2+2p} = \phi(p). \quad . \quad (M) \quad (36)$$

Using one of the rules *, we have

$$e^{-t^2}I_0(t^2) \supset \frac{p}{\sqrt{\pi}}\int_0^\infty e^{-p^2v^2/4}\phi(1/v^2)\,dv, \quad . \quad . \quad (37)$$

$$= \frac{p}{\sqrt{\pi}}\int_0^\infty e^{-p^2v^2/4}\,dv/\sqrt{2v^2+1}. \quad . \quad (38)$$

Substituting $v=\frac{1}{\sqrt{2}}\sinh\theta$ in (38), we obtain

$$e^{-t^2}I_0(t^2) \supset pe^{p^2/16}K_0(p^2/16)/2\sqrt{2\pi}. \quad . \quad . \quad . \quad (39)$$

4. *The Y Functions.*

We commence with the definition

$$Y_\nu(ay) = [\cos\nu\pi J_\nu(ay) - J_{-\nu}(ay)]/\sin\nu\pi, \quad . \quad (40)$$

* Humbert, 'Le calcul symbolique,' Paris (1934). This integral may also be written in the form

$$\frac{\nu p}{2\sqrt{\pi}}\int_0^\infty e^{-\frac{1}{4}p^2s^\nu}\phi(s^{-\nu})s^{\frac{1}{2}\nu-1}\,ds,$$

$R(\nu)\neq 0$. When $R(\nu)<0$, the sign of the integral is unaltered.

and the known O.F.*

$$\left(\frac{t-b}{t+b}\right)^{\frac{1}{2}\nu} J_\nu(a\sqrt{t^2-b^2}) \supset (p/r)(a/\mathrm{P})^\nu e^{-br}, \quad (\mathrm{M}) \quad (41)$$
$$\mathrm{R}(\nu)>-1.$$

Substituting from (41) into (40), we obtain

$$\left(\frac{t-b}{t+b}\right)^{\frac{1}{2}\nu} Y_\nu(a\sqrt{t^2-b^2}) \supset \frac{pe^{-br}}{r\sin\nu\pi}[(a/\mathrm{P})^\nu\cos\nu\pi-(\mathrm{P}/a)^\nu],$$
$$\ldots \quad (\mathrm{M}) \quad (42)$$

$-1<\mathrm{R}(\nu)<1$. When $\nu=0$, the r.h.s. of (42) takes the indeterminate from 0/0. Differentiating the denominator and numerator independently with respect to ν, and taking the limit $\nu\to 0$, we find that

$$p\int_b^\infty e^{-pt}Y_0(a\sqrt{t^2-b^2})\,dt=-(2/\pi)(p/r)e^{-br}\log(\mathrm{P}/a),$$
$$\ldots \quad (\mathrm{M}) \quad (43)$$

$$\subset Y_0(ay)=a\int_t^\infty t\,\frac{Y_1(a\sqrt{t^2-b^2})\,dt}{\sqrt{t^2-b^2}}.$$
$$\ldots \quad (43)$$

Proceeding as in § 2, we get

$$tY_0(ay)\supset(2/\pi)(p/r^2)e^{-br}\left[1-p\log(\mathrm{P}/a)\left\{b+\frac{1}{r}\right\}\right],$$
$$\ldots \quad (\mathrm{M}) \quad (44)$$

and

$$yY_1(ay)\supset-(2/\pi)(p/r^2)e^{-br}\left[(p/a)+a\log(\mathrm{P}/a)\left\{b+\frac{1}{r}\right\}\right].$$
$$\ldots \quad (\mathrm{M}) \quad (45)$$

Writing $b=0$ in (44) and (45) gives

$$tY_0(at)\supset(2/\pi)(p/r^2)\left[1-\frac{p}{r}\log(\mathrm{P}/a)\right], \quad (\mathrm{M}) \quad (46)$$

and
$$tY_1(at)\supset-(2/\pi)(p/r^2)[(p/a)+(a/r)\log(\mathrm{P}/a)].$$
$$\ldots \quad (\mathrm{M}) \quad (47)$$

Since $Y_0(x)=-\frac{2}{\pi}\int_0^\infty \cos(x\cosh\theta)\,d\theta$, we have

$$p\int_0^\infty e^{-pt}Y_0(a\sqrt{t})\,dt/\sqrt{t}$$
$$=-\frac{2p}{\pi}\int_0^\infty\int_0^\infty e^{-pt}\cos(a\sqrt{t}\cosh\theta)\,d\theta\,dt/\sqrt{t} \quad (48)$$

* McLachlan & Meyers, Phil. Mag. xxiii. p. 918 (1937).

$$=-2\sqrt{p/\pi}\int_0^\infty e^{-a^2\cosh^2\theta/4p}\,d\theta, \quad . \quad . \quad . \quad . \quad . \quad (49)$$

by using a known exponential/cosine integral. The r.h.s. of (49) may be expressed in the form

$$-2\sqrt{p/\pi}\int_0^\infty e^{-a^2(1+\cosh 2\theta)/8p}\,d\theta=-\sqrt{p/\pi}\,e^{-a^2/8p}\mathrm{K}_0(a^2/8p),$$

$$. \quad . \quad . \quad (50)$$

so $$\mathrm{Y}_0(a\sqrt{t})/\sqrt{t}\supset-\sqrt{p/\pi}\,e^{-a^2/8p}\mathrm{K}_0(a^2/8p). \quad (\mathrm{M}) \quad (51)$$

5. *The Hankel Functions.*

These are defined to be

$$\mathrm{H}_\nu^{(1)\,(2)}(x)=\mathrm{J}_\nu(x)\pm i\mathrm{Y}_\nu(x). \quad . \quad . \quad . \quad (52)$$

Applying this to §§ 2, 4, we obtain the following formulæ:

$$\left(\frac{t-b}{t+b}\right)^{\frac{1}{2}\nu}\mathrm{H}_0^{(1)\,(2)}(ay)$$

$$\supset(p/r)(a/\mathrm{P})\,e^{-br}\left[1\pm\frac{i}{\sin\nu\pi}\{\cos\nu\pi-(\mathrm{P}/a)^{2\nu}\}\right].$$

$$. \quad . \quad . \quad (\mathrm{M}) \quad (53)$$

$-1<\mathrm{R}(\nu)<1.$

$$\mathrm{H}_0^{(1)\,(2)}(ay)\supset(p/r)e^{-br}\left[1\mp\frac{2i}{\pi}\log(\mathrm{P}/a)\right], \quad (\mathrm{M}) \quad (54)$$

$$t\mathrm{H}_0^{(1)\,(2)}(ay)\supset(p/r^2)e^{-br}\left[p\left(b+\frac{1}{r}\right)\left\{1\mp\frac{2i}{\pi}\log(\mathrm{P}/a)\right\}\pm\frac{2i}{\pi}\right],$$

$$. \quad . \quad . \quad (\mathrm{M}) \quad (55)$$

and

$$y\mathrm{H}_1^{(1)\,(2)}(ay)$$

$$\supset(p/r^2)e^{-br}\left[a\left(b+\frac{1}{r}\right)\left\{1\mp\frac{2i}{\pi}\log(\mathrm{P}/a)\right\}\mp\frac{2ip}{\pi a}\right].$$

$$. \quad . \quad . \quad (\mathrm{M}) \quad (56)$$

By writing $b=0$ in (53), (55), (56), we get

$$\mathrm{H}_\nu^{(1)\,(2)}(at)\supset(p/r)(a/\mathrm{P})^\nu\left[1\pm\frac{i}{\sin\nu\pi}\left\{\cos\nu\pi-(\mathrm{P}/a)^{2\nu}\right\}\right],$$

$$. \quad . \quad . \quad (\mathrm{M}) \quad (57)$$

$-1<\mathrm{R}(\nu)<1.$

$$tH_0^{(1)\,(2)}(at) \supset (p/r^2)\left[(p/r)\left\{1 \mp \frac{2i}{\pi}\log(P/a)\right\} \pm \frac{2i}{\pi}\right],$$

. . . (M) (58)

and

$$tH_1^{(1)\,(2)}(at) \supset (p/r^2)\left[(a/r)\left\{1 \mp \frac{2i}{\pi}\log(P/a)\right\} \mp \frac{2ip}{\pi a}\right].$$

. . . (M) (59)

Since $J_0(a\sqrt{t})/\sqrt{t} \supset \sqrt{\pi p}e^{-a^2/8p}I_0(a^2/8p)$, we have, by aid of (51),

$$H_0^{(1)\,(2)}(a\sqrt{t})/\sqrt{t} \supset \sqrt{\pi p}e^{-a^2/8p}\left[I_0(a^2/8p) \mp \frac{i}{\pi}K_0(a^2/8p)\right].$$

. . . (M) (60)

6. *The K Functions.*

By definition

$$K_\nu(ay) = \tfrac{1}{2}\pi i^{\nu+1}H_\nu^{(1)}(aiy). \quad . \quad . \quad . \quad (61)$$

Using formulæ in § 5, we get the following :

$$p\int_b^\infty e^{-pt}K_0(a\sqrt{t^2-b^2}) = (p/s)e^{-bs}\log(Q/a) \quad (M) \quad (62)$$

$$\subset K_0(ay). \quad . \quad . \quad . \quad (M) \quad (63)$$

$$tK_0(ay) \supset -(p/s^2)e^{-bs}\left[1 + p\log(Q/a)\left\{b - \frac{1}{s}\right\}\right],$$

. . . (M) (64)

$$yK_1(ay) \supset -(p/s^2)e^{-bs}\left[(p/a) + a\log(Q/a)\left\{b + \frac{1}{s}\right\}\right],$$

. . . (M) (65)

$$\left(\frac{t-b}{t+b}\right)^{\frac{1}{2}\nu}K_\nu(ay) \supset (\pi/2\sin\nu\pi)(p/s)e^{-bs}[(Q/a)^\nu - (a/Q)^\nu],$$

. . . (M) (66)

$$-1 < R(\nu) < 1.$$

$$tK_0(at) \supset (p/s^2)[(p/s)\log(Q/a) - 1], \quad . \quad . \quad (M) \quad (67)$$

and $$tK_1(at) \supset -(p/s^2)[(p/a) + (a/s)\log(Q/a)]. \quad (M) \quad (68)$$

Also

$$p\int_0^\infty e^{-pt}K_0(a\sqrt{t})\frac{dt}{\sqrt{t}} = p\int_0^\infty e^{-px^2}K_0(ax)\,dx \quad . \quad (69)$$

or $$\frac{\mathrm{K}_0(a\sqrt{t})}{\sqrt{t}} \supset \tfrac{1}{2}\sqrt{\pi p}e^{a^2/8p}\mathrm{K}_0(a^2/8p) \quad \text{(M)} \quad (70)$$

by a known integral. Combining the results in (51) and (70) we obtain

$$[\mathrm{K}_0(a\sqrt{t})+\tfrac{1}{2}\pi\mathrm{Y}_0(a\sqrt{t})]/\sqrt{t} \supset \sqrt{\pi p}\sinh(a^2/8p)\mathrm{K}_0(a^2/8p), \quad \text{(M)} \quad (71)$$

and

$$[\mathrm{K}_0(a\sqrt{t})-\tfrac{1}{2}\pi\mathrm{Y}_0(a\sqrt{t})]/\sqrt{t} \supset \sqrt{\pi p}\cosh(a^2/8p)\mathrm{K}_0(a^2/8p). \quad \text{(M)} \quad (72)$$

7. *Ber, Bei, Ker, and Kei Functions.*

Substituting $ai^{3/2}$ for a in (1), (4), (6), (10), (41), we get

$$\operatorname{ber} ay+i\operatorname{bei} ay \supset (p/v)e^{-bv}, \quad \text{(M)} \quad (73)$$

$$t(\operatorname{ber} ay+i\operatorname{bei} ay) \supset (p/v)^2\left(b+\frac{1}{v}\right)e^{-bv}, \quad \text{(M)} \quad (74)$$

$$(\operatorname{ber}_1 ay+i\operatorname{bei}_1 ay)/y \supset \frac{pe^{-\frac{3}{4}\pi i}}{ab}[e^{-bp}-e^{-bv}], \quad \text{(M)} \quad (75)$$

$$y(\operatorname{ber}_1 ay+i\operatorname{bei}_1 ay) \supset (pa/v^2)\left(b+\frac{1}{v}\right)e^{-bv+\frac{3}{4}\pi i}, \quad \text{(M)} \quad (76)$$

$$t(\operatorname{ber}_1 ay+i\operatorname{bei}_1 ay)/y \supset \frac{pe^{-\frac{3}{4}\pi i}}{a}\left[e^{-bp}-\frac{pe^{-bv}}{v}\right], \quad \text{(M)} \quad (77)$$

and

$$\left(\frac{t-b}{t+b}\right)^{\frac{1}{2}\nu}(\operatorname{ber}_\nu ay+i\operatorname{bei}_\nu ay) \supset (p/v)(a/\mathrm{T})^\nu e^{-bv+\frac{3}{4}\nu\pi i}. \quad \text{(M)} \quad (78)$$

$$\mathrm{R}(\nu)>-1.$$

Substituting $ai^{\frac{1}{2}}$ for a in (62)–(68), we get

$$\ker ay+i\operatorname{kei} ay \supset (p/v)\log(\mathrm{T}/ai^{\frac{1}{2}})e^{-bv}, \quad \text{(M)} \quad (79)$$

$$t(\ker ay+i\operatorname{kei} ay)$$

$$\supset -(p/v^2)e^{-bv}\left[1+p\log(\mathrm{T}/ai^{\frac{1}{2}})\left\{b-\frac{1}{v}\right\}\right], \quad \text{(M)} \quad (80)$$

$$y(\operatorname{ker}_1 ay+i\operatorname{kei}_1 ay)$$

$$\supset -(p/v)e^{-bv-\frac{1}{4}\pi i}\left[(p/ai^{\frac{1}{2}})+ai^{\frac{1}{2}}\log(\mathrm{T}/ai^{\frac{1}{2}})\left\{b+\frac{1}{v}\right\}\right], \quad \text{(M)} \quad (81)$$

$$t(\ker at+i\,\mathrm{kei}\,at)\supset(p/v^2)[(p/v)\log(\mathrm{T}/ai^{\frac{1}{2}})-1], \quad \text{(M)} \quad (82)$$

$$t(\ker_1 at+i\,\mathrm{kei}_1 at)\supset-(p/v^2)e^{-\frac{1}{2}\pi i}\left[(p/ai^{\frac{1}{2}})+\frac{ai^{\frac{1}{2}}}{v}\log(\mathrm{T}/ai^{\frac{1}{2}})\right],$$

. . . (M) (83)

and

$$\left(\frac{t-b}{t+b}\right)^{\frac{1}{2}\nu}(\ker_\nu ay+i\,\mathrm{kei}_\nu ay)$$

$$\supset(\pi/2\sin\nu\pi)(p/v)e^{-bv-\frac{1}{2}\nu\pi i}[(\mathrm{T}/ai^{\frac{1}{2}})^\nu-(ai^{\frac{1}{2}}/\mathrm{T})^\nu],$$

. . . (M) (84)

$$-1<\mathrm{R}(\nu)<1.$$

8. *Expansions of O.F.'s in terms of the K Function.*

We have

$$p\int_b^\infty e^{-pt}(t^2-b^2)^\mu\,dt=b^{2\mu+1}p\int_0^\infty e^{-pb\cosh\theta}\sinh^{2\mu+1}\theta\,d\theta$$

or

$$(t^2-b^2)^\mu\supset\frac{2^{\mu+\frac{1}{2}}\Gamma(\mu+1)b^{2\mu+1}}{\sqrt{\pi}\,p^{\mu-\frac{1}{2}}}\mathrm{K}_{\mu+\frac{1}{2}}(bp), \quad \text{(M)} \quad (85)$$

$$\mathrm{R}(\mu)>-1, \quad t>b.$$

Since

$$\mathrm{J}_\nu(a\sqrt{t^2-b^2})=\sum_{r=0}^\infty\frac{(-1)^r(\frac{1}{2}a)^{\nu+2r}(t^2-b^2)^{\frac{1}{2}\nu+r}}{r!\;\Gamma(\nu+r+1)},$$

it follows from (85) that

$$\mathrm{J}_\nu(a\sqrt{t^2-b^2})$$

$$\supset\frac{1}{\sqrt{\pi}}\sum_{r=0}^\infty\frac{(-)^r(ab)^{\nu+2r}b\Gamma(\frac{1}{2}\nu+r+1)}{r!\;\Gamma(\nu+r+1(2p)^{\frac{1}{2}\nu+r-\frac{1}{2}}}\mathrm{K}_{\frac{1}{2}\nu+\frac{1}{2}+r}(bp),$$

. . . (M) (86)

R $(\nu)>-1$. When $\nu=0$ in (86), we have by (1)

$$\frac{pe^{-b\sqrt{p^2+a^2}}}{\sqrt{p^2+a^2}}=\frac{1}{\sqrt{\pi}}\sum_{r=0}^\infty\frac{(-1)^r(ab)^{2r}b}{r!\;(2p)^{r-\frac{1}{2}}}\mathrm{K}_{\frac{1}{2}+r}(bp). \quad (87)^*$$

As another example, using (5) and (85), we obtain

$$e^{-bp}-e^{-b\sqrt{p^2+a^2}}=\frac{1}{\sqrt{\pi}}\sum_{r=0}^\infty\frac{(-1)^r(ab)^{2r+2}}{(r+1)!\;(2p)^{r+\frac{1}{2}}}\mathrm{K}_{\frac{1}{2}+r}(bp). \quad (88)$$

* This result can also be obtained from Watson's 'Theory of Bessel Functions,' formula 11, p. 141, by taking $\nu=\frac{1}{2}$ and writing K for Y.

Other expansions can be written down using formulæ herein.

9. *Contour Integrals.*

These can be found by applying a modification of the Mellin inversion theorem to the operational forms herein. The particular case of this theorem which we require is as follows :

$$\text{If} \qquad \phi(p)=p\int_b^\infty e^{-pt}f(a\sqrt{t^2-b^2})\,dt, \quad . \quad . \quad . \quad (89)$$

then will

$$f(a\sqrt{t^2-b^2})=\frac{1}{2\pi i}\int_{c-i\infty}^{c+i\infty}e^{zt}\phi(z)\frac{dz}{z}, \quad . \quad . \quad (90)$$

and *vice versa*, provided conditions (*a*), (*b*), (*c*), (*d*), (*f*) given in a former paper * are satisfied when $t>b$. Condition (*e*) in that paper requires some modification, which we shall now determine. Substituting for $f(a\sqrt{t^2-b^2})$ from (90) into (89), we have

$$\frac{p}{2\pi i}\int_b^\infty e^{-pt}\,dt\int_{c-i\infty}^{c+i\infty}e^{zt}\phi(z)\,dz/z \quad . \quad . \quad . \quad . \quad (91)$$

$$=\frac{p}{2\pi i}\int_{c-i\infty}^{c+i\infty}\phi(z)\frac{dz}{z}\int_b^\infty e^{-(p-z)t}\,dt \quad . \quad . \quad (92)$$

$$=-\frac{p}{2\pi i}\int_{c-i\infty}^{c+i\infty}e^{-(p-z)b}\frac{\phi(z)\,dz}{z(z-p)}, \quad . \quad . \quad . \quad (93)$$

the changed order of integration in (92) being permissible, since $\mathrm{R}(p)>\mathrm{R}(z)$ on the contour and the conditions mentioned above are assumed to be fulfilled.

Consider the closed contour of the figure (p. 406), comprising $c\pm i\mathrm{R}$ and the semicircle C, the point $z=p$ being within the contour. By hypothesis all the singularities of $\phi(z)/z$ lie to the left of $c\pm i\mathrm{R}$. The only singularity of the integrand in (93) within the contour is a simple pole at $z=p$ (complex, but $\mathrm{R}(p)>0$) †. The value of the integral (93) taken clockwise round the *closed* contour is $\phi(p)$. For this to represent the value of the integral taken along $c\pm i\mathrm{R}$ *only*, that round C must $\to 0$ as $\mathrm{R}\to\infty$. Since p is finite, this obviously happens if $|e^{zb}\phi(z)/z|\to 0$ uniformly as $|z|\to\infty$ in the angle range

* Phil. Mag. xxv. p. 259 (1938).

† For convenience p may be taken as the real axis at a point $x>c$.

$-\frac{1}{2}\pi \leqslant$ phase $z \leqslant \frac{1}{2}\pi$. When this is so, integral (90) is zero for $t<b$. When $b=0$, the above condition degenerates to that required for argument *at* (condition (*e*) in the former

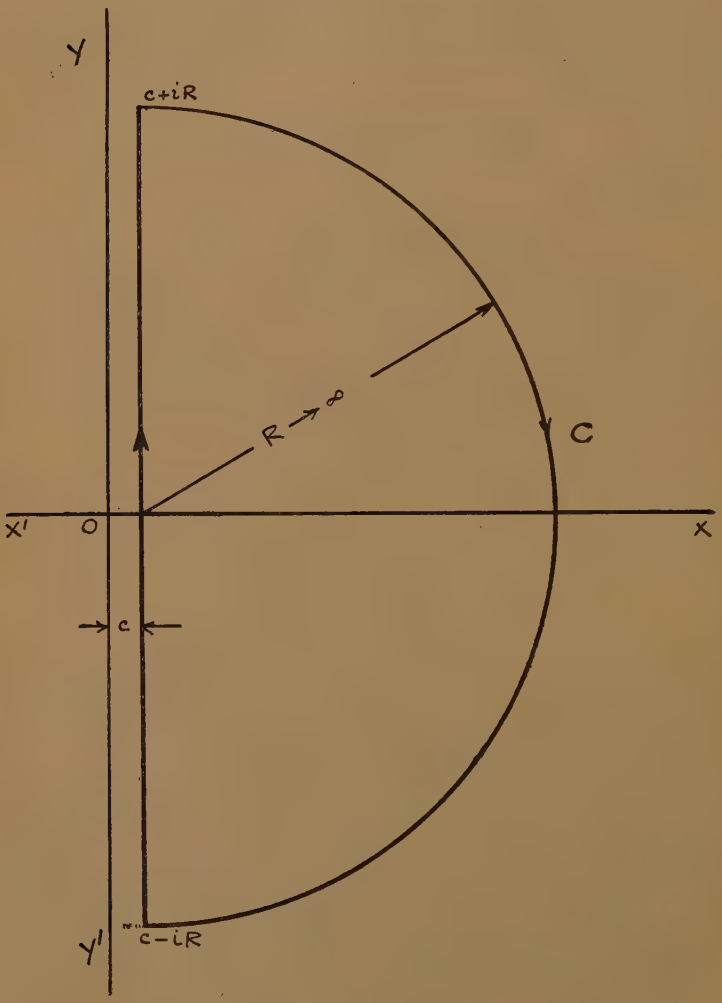

paper). As an example of the application of the above condition, we cite the case of

$$f(a\sqrt{t^2-b^2})=J_0(a\sqrt{t^2-b^2}) \supset \frac{pe^{-b\sqrt{p^2+a^2}}}{\sqrt{p^2+a^2}} = \phi(p). \quad (94)$$

Writing z for p in (94), the necessary condition for validity of (89), (90) as applied to (94), is that

$$\left| \frac{e^{xb}\phi(z)}{z} \right| = \left| \frac{e^{b(z-\sqrt{z^2+a^2})}}{\sqrt{z^2+a^2}} \right| \to 0 \quad . \quad (95)$$
$$|z| \to \infty \qquad |z| \to \infty$$

uniformly. Obviously this condition is satisfied, so the Mellin theorem can be applied to (94). The O.F.'s herein which fall into this category are distinguished by the letter M. Using these and formula (90), fifty-seven contour integrals can be written down. For example, from (51) and (90) we get

$$\mathrm{Y}_0(a\sqrt{t})/\sqrt{t} = \frac{-1/\sqrt{\pi}}{2\pi i} \int_{c-i\infty}^{c+i\infty} e^{zt-a^2/8z} \mathrm{K}_0(a^2/8z) \frac{dz}{z^{\frac{1}{2}}} . \quad (96)$$

Some of the integrals may be transformed and/or referred to the contour $-\infty$, $(0+)$, $-\infty$, as shown elsewhere *.

10. *Dimensional checking of O.F.*

In integrals like (89) where $b \geqslant 0$, if t has dimension d (in a physical application, say), that of p is to be regarded as d^{-1}. Consequently, if f and ϕ are expansible in absolutely convergent series, and if $f \supset \phi$, term by term, the dimensions of corresponding terms must be identical. For instance, in the case of

$$\mathrm{J}_0(t) \supset p/\sqrt{p^2+1}, \quad . \quad . \quad . \quad . \quad . \quad (97)$$

we have

$$1 - \frac{t^2}{2^2} + \frac{t^4}{2^2.4^2} - \frac{t^6}{2^2.4^2.6^2} + \ldots$$
$$= 1 - \frac{1}{2p^2} + \frac{1.3}{2^2.2!\,p^4} - \frac{1.3.5}{2^3.3!\,p^6} + \ldots, \quad (98)$$

the dimensions of the corresponding terms being d^0 (no dimension), d^2, d^4, etc. For mere checking purposes it is often sufficient to consider the dimensions of the first pair of terms. In the case of

$$\mathrm{J}_\nu^2(2a\sqrt{t}) \supset e^{-2a^2/p} \mathrm{I}_\nu(2a^2/p), \quad . \quad . \quad . \quad (99)$$

we may (if we please) consider a^2 to have dimension d^{-1}, so that $2a\sqrt{t}$ and $2a^2/p$ are dimensionless. Alternatively a can be dimensionless. If the exponential index were written $2a^2p$, a dimensional check would reveal an error.

* Phil. Mag. xxiii. p. 761 (1937); Math. Gazette, xxii. p 37 (1938).

The contour integral (90) can be regarded in a similar way. Writing $\phi(z)/z=\chi(z)$, since z * has dimension d^{-1} (to make zt dimensionless), the first term of $f(t)$ must have dimension d^{-1} times that of the corresponding term of $\chi(z)$. Thus in the integral

$$J_0(t)=\frac{1}{2\pi i}\int_{c-i\infty}^{c+i\infty} e^{zt}\,dz/\sqrt{z^2+1}, \quad . \quad . \quad (100)$$

the first term of $1/\sqrt{z^2+1}=\chi(z)$ is $1/z$, having dimension d^1, whereas that of $J_0(t)$ is 1 (dimensionless and therefore d^{-1} times d^1). In $\sqrt{t^2-b^2}$ b has the same dimension as t.

XXXVI. *Generalized Fractional Integration and Differentiation.* *By* W. Fabian, *M.A., Ph.D.**.

[Received March 7, 1938.]

HAVING, in our previous work on the Fractional Calculus, dealt with fractional integration and differentiation along continuous arcs, we shall now give a method of integrating and differentiating fractionally over sets of points which do not necessarily form continuous arcs, and shall give some applications of these generalized fractional integrals and differential coefficients.

The Lebesgue Fractional Integral and Generalized Fractional Differential Coefficient.

Let L be a simple curve, defined by

$$z=x+iy=x(t)+iy(t)$$

for values of $t\geqslant t_0$, and which is such that L can be broken up into a finite number of curves, for each of which $x(t)$ and $y(t)$ are monotonic functions of t. Let G(L) be a fixed measurable set of points on L, and E(L) the set consisting of all points of G(L) on that arc of L which corresponds to (t_0, t). Let Γ be the curve in the w-plane, which is traced out by the point

$$w=m_0[E(L)],$$

* Although $z=x+iy$ is complex, it has the same dimensions as either x or y, since i is dimensionless.

† Communicated by the Author.

where $m_0[\mathrm{E(L)}]$ is as defined previously * under the heading "Generalized Differentiation, Generalized Taylor Series."

We define a λth integral of a function $f(z)$ over E(L), or a $(-\lambda)$th differential coefficient of $f(z)$ with respect to E(L), by

$$\mathrm{D}^{-\lambda}\{\mathrm{E(L)}\}f(z)=\frac{1}{\Gamma(\lambda+\gamma)}\left(\frac{d}{dw}\right)^{\gamma}\int_0^w (w-\tau)^{\lambda+\gamma-1}\mathrm{F}(\tau)d\tau,$$

where the integration and differentiation are along $\overline{\frown}$, the integration being in the sense of Lebesgue †, and $f(z)=\mathrm{F}(w)$; λ is any number, real or complex, and γ is the least integer greater than or equal to zero such that ‡ $\mathrm{R}(\lambda)+\gamma>0$.

Applications.

The equivalence § of $\int_{\mathrm{E(L)}} f(z)dz$ and $\int_0^w \mathrm{F}(w)dw$ (along $\overline{\frown}$) and of $\mathrm{D}\{\mathrm{E(L)}\}f(z)$ and $\dfrac{d\mathrm{F}(w)}{dw}$ (along $\overline{\frown}$) enables us, with our work on this subject, to extend a large part of our work on the Fractional Calculus and apply it to the Lebesgue fractional integral. Thus we can deduce the *Generalized Riemann Series* ‖ :—

Let $\mathrm{D}^n\phi\{\mathrm{E(L)}\}\equiv\mathrm{D}^n\{\mathrm{E(L)}\}f(z)$, *for all positive integral and zero values of* n, *be one-valued continuous measurable functions of* E(L) *in the measurable set* G(L). *Let* e(L) *be one of the sets* E(L), *of non-zero measure, different to that of* G(L). *Let*

$$\lim_{n\to\infty}\mathrm{D}^{-\lambda-n}\{\mathrm{Ge(L)}\}\mathrm{D}^{\lambda+n}\{\mathrm{G(L)}\}f(z)$$

$$+\lim_{n\to\infty}\frac{1}{\Gamma(\lambda-n)}\int_{e(\mathrm{L})}[\{m_0[\mathrm{G(L)}]$$

$$-m_0[\mathrm{E(L)}]\}^{\lambda-n-1}\mathrm{D}^{\lambda-n}\{\mathrm{E(L)}\}f(z)]\,dz=0,$$

* Fabian, Phil. Mag. (7) xxii. p. 533 (1936).
† Fabian, Phil. Mag. (7) xxii. p. 525 (1936).
‡ $\mathrm{R}(\lambda)$ stands for the real part of λ.
§ Fabian, Phil. Mag. (7) xxii. pp. 531–533 (1936); see also the footnote in our paper in Phil. Mag. (7) xxiv. p. 813 (1937).
‖ Fabian, Phil. Mag. (7) xx. pp. 786–787 (1935).

where Ge(L) *is the set of points in* G(L) *which are not points of* e(L). *Then*

$$\phi\{G(L)\}=\sum_{n=-\infty}^{\infty}\frac{D^{\lambda+n}\{e(L)\}f(z)}{\Gamma(\lambda+n+1)}\{m_0[G(L)]-m_0[e(L)]\}^{\lambda+n}.$$

Similarly we have the expansion

$$f(z)=\frac{1}{\Gamma(-\lambda)}\sum_{n=0}^{\infty}(-1)^n\frac{D^{n-\lambda}\{E(L)\}f(z)}{n\,!\,(n-\lambda)}\{m_0[E(L)]\}^{n-\lambda},$$

under conditions analogous to those for which the expansion

$$f(z)=\frac{1}{\Gamma(-\lambda)}\sum_{n=0}^{\infty}(-1)^n\frac{f_{\lambda-n}(z)}{n\,!\,(n-\lambda)}(z-a)^{n-\lambda}$$

was established *.

XXXVII. *A Criticism of the Special Theory of Relativity.*

By Albert Eagle, *B.Sc., A.R.C.Sc., Lecturer in Mathematics in the University of Manchester* †.

[Received June 16, 1938.]

IF x and t denote the position and time in one system, S, at rest relatively to a fixed ether throughout space; and if x' and t' denote the same quantities in a system S′, moving in the directions of x and x' with a velocity u, Lorentz's well-known transformation connecting the two sets of variables is

$$x'=k(x-ut), \quad . \quad . \quad . \quad . \quad . \quad . \quad . \quad (1)$$

and

$$t'=k(t-ux/c^2), \quad . \quad . \quad . \quad . \quad . \quad . \quad (2)$$

where c is the velocity of light and $k=(1-u^2/c^2)^{-\frac{1}{2}}$.

As is well known, x and t, and x' and t', may be interchanged in these equations if the sign of u is changed.

Now let the systems S and S′ consist of graduated scales, identical when S and S′ are at relative rest, together with a "clock," placed at every unit graduation of both systems, to indicate t and t'—an electrically

* Fabian, Quarterly Journ. of Math. vii. no. 28, pp. 252–5 (1936).

† Communicated by the Author.

maintained vibrating quartz-rod will do, or even atomic electrons emitting a sharp spectrum line, if we are only interested in the *rates* of the clocks and not their readings. All the clocks must be such that if they were transferred to the same system their behaviour would be indistinguishable.

When the zero mark of S′ is passing the zero mark of S both clocks there read zero time. At this moment, by S's clock at $x=1$, the graduation $x'=k$ on S′'s scale coincides with the unit mark on S's scale; so that, since $k>1$, S′'s scale seems to an observer on S to be contracted.

But also at the same moment, by S′'s two clocks at $x'=0$ and $x'=1$, the readings on S's scale coincident with these two marks are $x=0$ and $x=k$, as is seen from (1) and (2); so that, just as clearly, to an observer on S′, S's scale seems to have become contracted.

It is likewise when they compare the respective *rates* of the clocks in the two systems. When S′'s clock at $x'=1$ (which agreed with S's clock at $x=0$) has reached S's clock at $x=1$, S's clock reads $t=1/u$; while S′'s clock facing it reads $t'=1/ku$. So that (since $k>1$) the observer on S, who knew that it was the *same* clock on the system S′ which was being checked against two *known* synchronous clocks in his own system, would declare that the clocks on the system S′ were going more slowly than his own.

Again, if an observer on S′ notes the times when his two clocks, at $x'=1$ and at $x'=0$, pass S's clock at $x=0$, he finds that at the first instant $t=-1/ku$ and $t'=-1/u$, while both times are zero at the second moment; so that, to him, it seems that S's clocks are going more slowly than his own since $|t|<|t'|$.

The observers on both systems would also agree that the magnitude of their relative velocity was the same, namely, u.

These well-known results have led some relativitists to deny that there was such a thing as absolute size, or absolute rate of time-flow, or absolute velocity through the ether. Everything they said was relative, and is seemingly quite the same for different observers no matter how they are moving; and there is no possibility of them finding out, by observing each other's systems, which is moving through the ether fastest and which is (perhaps)

stationary. This result led many relativitists to deny that there was any such thing as a fixed medium that was at rest throughout space to which all velocities could be referred.

Nevertheless, it has not been pointed out sufficiently plainly, I think, that the only reason *why* the observers on S and S′ cannot detect their motion through the ether is because the method of synchronising their clocks has been skilfully chosen to *prevent* this motion from revealing itself. For the set of clocks on both systems are supposed to be adjusted to synchronism by sending light-signals from one clock to another and setting the reading on the second clock when a light-signal arrives there as the mean of the starting and return times shown by the first clock. This, which is quite right for a system at rest in the ether, is quite wrong for a system which is moving through a stationary ether. This method if setting the clocks in synchronism begs the whole question by *assuming*—what may be in complete disagreement with the physical facts—that light travels with the same speed in both the positive and negative directions of x'. If this assumption is made the basis of our ideas of simultaneity in different localities of a moving system, obviously the experiments described above could not possibly detect motion through the ether.

It might be thought that S″'s clocks could be correctly synchronised by synchronising them in the same neighbourhood and then slowly moving them into position along the x' axis. But this is not so. For S″'s clocks are going at $(1-u^2/c^2)^{\frac{1}{2}}$ of the rate of S's clocks; and, if now u is increased by du [$\approx dx'/dt$], the rate is further reduced by $(1-u^2/c^2)^{-}\, u.du/c^2$; which means that by the time the clock has travelled unit distance along the axis of x' (which is really a distance of $(1-u^2/c^2)^{\frac{1}{2}}$ it will be in retardation by just u/c^2. Against this, the error committed by S′ sending light-signals to and fro is $(1-u^2/c^2)^{\frac{1}{2}}\{1/(c-u)-\frac{1}{2}/(c-u)-\frac{1}{2}/(c+u)\} = (1-u^2/c^2)^{-\frac{1}{2}}u/c^2$, on S's clocks (or u/c^2 on S″'s clocks). So that the two errors are the same if u^3/c^4 is negligible.

The only correct method of synchronising S″'s clocks which I can see is as follows: two clock-dials, at $x'=0$ and at $x'=1$, in planes normal to the x' axis, must be connected by a shaft and the hands set to exactly the same readings. These dials must then be driven by a master clock,

at $x'=\frac{1}{2}$, driving the shaft at its exact centre through a gear-wheel or crank.

When this is done the connexion between the pairs of variables x and t, and x' and t', is as follows:

$$x'=k(x-ut) \quad . \quad . \quad . \quad . \quad . \quad . \quad . \quad (3)$$

and

$$t'=t/k, \quad . \quad . \quad . \quad . \quad . \quad . \quad . \quad . \quad (4)$$

since it is well known from classical electromagnetic theory that the dimensions of the system S′, parallel to x', are reduced in the ratio k to 1; and that the time of oscillation of "clocks," or elastic vibrations, or molecular rotations, is increased in the ratio of 1 to k *.

The relation between the two pairs of variables in (3) and (4) is by no means reciprocal. These equations also show that the time variable, when multiplied by $c(-1)^{\frac{1}{2}}$, is *not* mathematically indistinguishable from a space variable. It will also readily be found, by eliminating u from (3) and (4), that $x^2-c^2t^2$ does *not* transform into $x'^2-c^2t'^2$. (Or, for three dimensional space, that $x^2+y^2+z^2-c^2t^2$ does not transform into $x'^2+y'^2+z'^2-c^2t'^2$.) It will be found that there is *no* invariant function of x and t which will transform into the same function of x' and t'. Hence Minkowski's idea that what really exists in the universe is not either time or space separately, but a combination of them usually known as the space-time-continuum, is seen to be simply due to a mathematical accident or coincidence which happened when synchronism in a moving system was erroneously defined. Minkowski's space-time-continum must, therefore, be entirely discarded; and this means that we must give up any belief that Einstein's General Theory of Relativity—which depends upon bodies moving so as to take the shortest path through this space-time-continuum—can have any value or importance, despite the agreement which it gives with a few minute physical phenomena.

We further see that the Special Theory of Relativity

* If we regard a solid body as made up of, virtually, point electric charges held together by the electric and magnetic forces between them, the *very nature* of these forces makes the Lorentz-FitzGerald contraction an absolute necessity; so the author cannot appreciate the view of some mathematical physicists who regard this contraction as merely a fact of appearance and not of reality. It is also untrue to regard the Lorentz-FitzGerald contraction as an *ad hoc* suggestion put forward to explain the null result of the Michelson-Morley experiment.

really affords no grounds for doubting whether motion through the ether is a physical reality or not, since the theory does nothing but inform us that if we define synchronism in such a way that motion through the ether cannot possibly be detected by light-signals, it will remain impossible for us ever to detect its existence in this manner.

Relativitists, with everyone else, now admit that the apparently regular elliptic orbits of binary stars at a great distance away, proves that the light-waves, which left the two stars at the same moment when they happened to be equidistant from us, reach us at the same moment, even though one star was receding, and the other approaching, with a velocity of perhaps several dozen kilometers a second. Now how can light, emitted from stars moving with pretty large velocities in opposite directions, travel many billion of miles through space with a velocity which is absolutely independent of the velocity of the source *unless* it travels through a fixed medium in space with a velocity which depends only on the properties of the medium ? This consideration also shows that the former contention of relativitists, that light always travels with the same speed relative to its source (and even relative to any and every particle in the universe), cannot be a physical fact. And if relativitists make it appear to be a fact, it can only be because its velocity is measured in a system of variable space and time units (which are also based on erroneous ideas of synchronism) which are designed to make the velocity always come the same. The fact that a measured velocity, in variable units, should always come the same when, physically, the velocity *is variable*, is not a matter of any importance—or interest.

The fact that I insist on a fixed medium filling space in no way implies that the medium must be pictured as having the properties of an elastic solid, as in the nineteenth century, or be contradictory to the " photon " properties which physicists now require light to possess. Light-waves may well travel through the ether in such a way that a disturbed ether particle transmits the *whole* of its disturbance to one, and only one, neighbouring particle ; so that the amplitude of the disturbances need not decrease at all with distance, distance merely causing there to be fewer disturbed particles per unit area of cross-section per unit time.

XXXVIII. *The Complete Solution of the Differential Equation for the Confluent Hypergeometric Function.* *By* W. J. Archibald, *M.A., Rouss Physical Laboratory, University of Virginia* *.

THE complete solution of the differential equation

$$z\frac{d^2y}{dz^2}+(b-z)\frac{dy}{dz}-ay=0 \quad . \quad . \quad . \quad . \quad (1)$$

for the case in which "b" is a positive integer has been stated several times in the literature †. However, the solution which is given is correct only when $b=1$. For other integral values of "b" there are terms in $1/z$ which have been omitted. In view of the fact that this equation has arisen in connexion with the problem of the distribution of concentration in a dilute solution in a centrifugal field of force ‡, it is important to discover a complete solution, valid for any positive integral value of "b."

The simplest solution of (1) is

$$\mathrm{F}(a\,;\,b\,;\,z)=1+\frac{a}{1.b}z+\frac{a(a+1)}{1\cdot 2\,b(b+1)}z^2+\ldots.$$

This function can also be expressed as a contour integral §, viz. :—

$$\mathrm{F}(a\,;\,b\,;\,z)=\frac{\Gamma(b)}{2\pi i}\int_C\left(1-\frac{z}{t}\right)^{-a}e^t t^{-b}\,dt,$$

where the contour C is any closed path which encircles the points $t=0$ and $t=z$. The path of integration may be deformed § in such a manner that $\mathrm{F}(a\,;\,b\,;\,z)$ can be expressed as the sum of two integrals. Thus

$$\mathrm{F}(a\,;\,b\,;\,z)=\mathrm{W}_1(a\,;\,b\,;\,z)+\mathrm{W}_2(a\,;\,b\,;\,z),$$

where

$$\mathrm{W}_1(a\,;\,b\,;\,z)=\frac{\Gamma(b)}{2\pi i}\int_{-\infty}^{(0+)}\left(1-\frac{z}{t}\right)^{-a}e^t\,t^{-b}\,dt.$$

$\mathrm{W}_2(a\,;\,b\,;\,z)$ is given by the same integrand, and a path

* Communicated by the Author.

† H. A. Webb and J. R. Airey, Phil. Mag. xxxvi. p. 132 (1918). H. Bateman 'Partial Differential Equations,' p. 457 (1932).

‡ O. Lamm, *Arkiv. for Mat., Astr. och Fysik*, xxi. no. 2 (1929). H. Faxen, *ibid.* xxi. no. 3 (1929). S. Oka, *Proc. Physico-Mat. Soc. Japan*, xix. p. 1094 (1937).

§ N. F. Mott and H. S. W. Massey, 'Atomic Collisions,' p. 36 (1933).

that encircles the point $t=z$. It can be shown * that W_1 and W_2 are two independent solutions of (1).

Let us consider the function $W_s(a\,;\,b\,;\,z)$, where

$$W_s(a\,;\,b\,;\,z)=(-1)^{a+b}\,W_1(a\,;\,b\,;\,z).$$

It is possible to express $W_s(a\,;\,b\,;\,z)$ as a contour integral of the Mellin-Barnes type. One can easily show (by the method employed by Whittaker and Watson †) that

$$W_s(a\,;\,b\,;\,z)=(-1)^b\frac{\Gamma(b)}{\Gamma(b-a)}\frac{z^{-a}}{2\pi i}\int_{-\infty i}^{+\infty i}\frac{\Gamma(s)\,\Gamma(-s+a)\,\Gamma(-s+a-b+1)z^s ds}{\Gamma(a)\,\Gamma(a-b+1)}, \quad . \quad (2)$$

where the contour has loops if necessary so that the poles of $\Gamma(s)$ and those of $\Gamma(-s+a)\,\Gamma(-s+a-b+1)$ are on opposite sides of it. In the right-hand side of the s-plane the integrand of (2) has simple poles at $s=a-b+1+n$ $(n=0,\,1,\,2,\,\ldots.\,(b-2))$ and double poles at $s=a+n$ $(n=0,\,1,\,2,\,\ldots.)$. Therefore ‡

$$W_s(a\,;\,b\,;\,z)=(-1)^{b+1}\frac{\Gamma(b)}{\Gamma(b-a)\,\Gamma(a)\,\Gamma(a-b+1)}\times\left[\sum_{n=0}^{b-2}R'_{s=a-b+1+n}+\sum_{n=0}^{\infty}R''_{s=a+n}\right],$$

where $R'_{s=a-b+1+n}$ denotes the residue of

$$f(s)=\Gamma(s)\,\Gamma(-s+a)\,\Gamma(-s+a-b+1)z^s$$

at the simple poles, and $R''_{s=a+n}$ denotes the residue of $f(s)$ at the double poles.

It is evident immediately that

$$R'_{s=a-b+1+n}=\frac{\Gamma(n+a-b+1)\,\Gamma(b-n-1)(-1)^{n+1}z^{n+a-b+1}}{n}.$$

To evaluate $R''_{s=a+n}$ we proceed as follows: using the relation

$$\Gamma(\chi)\,\Gamma(1-\chi)=\frac{\pi}{\sin\pi\chi},$$

we may express $f(s)$ as

$$f(s)=\frac{\pi^2}{(-1)^{b+1}\sin^2\pi(s-a)}\phi(s),$$

where

$$\phi(s)=\frac{\Gamma(s)z^s}{\Gamma(1-a+s)\Gamma(b-a+s)}.$$

* Whittaker and Watson, ' Modern Analysis,' p. 343 (1927).
† ' Modern Analysis,' p. 345.
‡ ' Modern Analysis,' p. 346

Now, utilizing the well known relation

$$\frac{\pi^2}{\sin^2 \pi(s-a)} = \sum_{n=-\infty}^{+\infty} \left[\frac{1}{(s-a-n)^2}\right],$$

and the Taylor expansion of $\phi(s)$ about the point $s=a+n$, we get for $f(s)$ the following :

$$f(s) = \ldots \frac{(-1)^{-b-1}}{(s-a-n)^2}$$
$$\{\phi(s)_{s=a+n} + \phi'(s)_{s=a+n}(s-a-n) + \ldots\} + \ldots,$$

from which it is evident that the residue of $f(s)$ at the double pole $s=a+n$ is

$$(-1)^{-b-1}\phi'(s)_{s=a+n}.$$

Writing $s=\sigma+n$, we have

$$\phi'(s)_{s=a+n} = \frac{d}{d\sigma}\left[\frac{\Gamma(\sigma+a)z^{\sigma+a}}{\Gamma(\sigma+1)\Gamma(\sigma+b)}\right]_{\sigma=n}.$$

The expression on the right of the above equation can be easily evaluated with the help of the following relations *

$$\left[\frac{d}{d\sigma}\Gamma(\sigma+a)\right]_{\sigma=n} = \Gamma(n+a)\left\{\frac{1}{a} + \frac{1}{a+1} + \ldots + \frac{1}{a+n-1} + \frac{\Gamma'(a)}{\Gamma(a)}\right\}, \quad \frac{\Gamma'(1)}{\Gamma(1)} = -\gamma,$$

where γ=Euler's constant=·5772 .... Carrying through the differentiation one finds

$$\phi'(s)_{s=a+n} = \frac{\Gamma(a)}{\Gamma(b)} A_n z^{a+n}\left\{\log z + B_n + \psi(a) - \psi(b) + \gamma\right\},$$

where

$$A_n = \frac{\Gamma(n+a)}{\Gamma(a)} \cdot \frac{\Gamma(b)}{\Gamma(n+b)} \frac{1}{\lfloor n},$$

$$B_n = \left(\frac{1}{a} + \frac{1}{a+1} + \ldots + \frac{1}{a+n-1}\right) - \left(\frac{1}{b} + \frac{1}{b+1} + \ldots. + \frac{1}{b+n-1}\right)\left(-\left(1 + \frac{1}{2} + \ldots. + \frac{1}{n}\right)\right),$$

$$B_0 = 0, \quad \psi(a) = \frac{\Gamma'(a)}{\Gamma(a)}.$$

(Extensive tables of the psi function are available †.)

* Courant and Hilbert, *Methoden der Mathematischen Physik*, i. p. 406 (1924).

† ' Tables of the Higher Mathematical Functions.' (1933)

Combining these results we obtain

$$W_s(a\,;\,b\,;\,z)=\frac{\sin\pi a}{\pi}\Big[(-1)^{b+1}F(a\,;\,b\,;\,z)\{\log z+\psi(a)$$

$$-\psi(b)+\gamma\}+\sum_{n=0}^{b-2}\frac{\Gamma(b)\,\Gamma(n+a-b+1)\,\Gamma(b-n-1)(-1)^{n+1}}{\Gamma(a)\,\underline{n}\;z^{b-n-1}}$$

$$+(-1)^{b+1}\sum_{n=1}^{\infty}A_nB_nz^n\Big],$$

which may be taken as the second solution of (1). However, a solution with more convenient properties is the following:

$$W(a\,;\,b\,;\,z)=(-1)^{b+1}\Big[\frac{\pi}{\sin\pi a}W_s(a\,;\,b\,;\,z)$$

$$+(-1)^{b+1}\pi\cot\pi aF(a\,;\,b\,;\,z)\Big].$$

Expressing the W_s and F functions in terms of W_1 and W_2 we have

$$W(a\,;\,b\,;\,z)=\pi\cot\pi aW_2(a\,;\,b\,;\,z)-i\pi W_1(a\,;\,b\,;\,z).$$

Since the contour integrals for W_1, W_2, and F have the same integrands, and since $\cot\pi a$ does not change its sign when "a" is increased or decreased by unity, it follows that any properties of F which can be derived from its contour integral will hold equally well for W. Furthermore, the asymptotic expansion of W can easily be obtained, since the asymptotic expansion of W_1, and W_2 are known *. The following are a few of the properties which $W(a\,;\,b\,;\,z)$ and $F(a\,;\,b\,;\,z)$ have in common (no doubt many others can be found):

$$\frac{d}{dz}F(a\,;\,b\,;\,z)=\frac{a}{b}F(a+1\,;\,b+1\,;\,z)$$

$$aF(a+1\,;\,b+1\,;\,z)=(a-b)F(a\,;\,b+1\,;\,z)+bF(a\,;\,b\,;\,z)$$

$$aF(a+1\,;\,b\,;\,z)=(z+2a-b)F(a\,;\,b\,;\,z)+(b-a)F(a-1\,;\,b\,;\,z).$$

Since $$\psi(1-a)=\psi(a)+\pi\cot\pi a$$

* Mott and Massey, 'Atomic Collisions,' p. 39.

the expression for $W(a\,;\,b\,;\,z)$ is

$$W(a\,;\,b\,;\,z)=F(a\,;\,b\,;\,z)\{\log z+\psi(1-a)-\psi(b)+\gamma\}$$
$$+(-1)^b\sum_{n=0}^{b-2}\frac{\Gamma(b)\,\Gamma(n+a-b+1)\,\Gamma(b-n-1)(-1)^n}{\Gamma(a)\,\lfloor n\, z^{b-n-1}}$$
$$+\sum_{n=1}^{\infty}A_nB_nz^n.$$

For the case in which $b=1$, this reduces to the second solution given by Webb and Airey (except for a constant multiple of $F(a\,;\,b\,;\,z)$ If $b>1$ (b is a positive integer) there are terms in $1/z$ which arise from the residues at the simple poles.

XXXIX. *Notices respecting New Books.*

Perspectives in Biochemistry. Thirty-one Essays presented to Sir Frederick Gowland Hopkins by past and present members of his Laboratory. Edited by Joseph Needham and David E. Green. (Cambridge University Press, 1937. Price 15*s.* net.)

THE universal recognition which has been accorded to the work of the Cambridge school of biochemistry, the personal distinction of its director, the well-known names of the essayists, and the rapid development which is at present taking place in this branch of science all combine to give to these "Perspectives" a peculiar attractiveness. To anyone who has had the privilege of working in the stimulating atmosphere of the Tennis Court Road Institute this volume must be invaluable not only as a survey of present-day research, but as bearing unmistakable marks of the personalities of the director and his colleagues. The aim of the writers has been to indicate the most promising lines of advance in the various fields which they survey, and even on those who have followed research in only a few sections of biochemistry, the extent of the progress made and the implications for the future revealed by these essays must produce a deep impression.

The field covered includes physiology and zoology, embryology and genetics, medicine, microbiology, and nutrition, while the two concluding essays deal with various hygienic and social aspects of the science.

It is, of course, impossible here to touch upon more than a few of the essays, and the choice has been decided by the reviewer's personal interests. The reader who approaches biochemistry from the organic side will find a special attraction

in the series of chapters which include Respiratory Carriers, Intermediate Hydrogen Transport in Biological Oxidations, Oxidation and Fermentation, and Chemical Cycles in Muscle Contraction.

The first of these essays includes a brief survey of the function of lactoflavin as the hydrogen carrier in a complex enzyme system. That this substance, isolated from milk and from white of egg, should have been proved to be identical with the growth-promoting factor of the Vitamin B_2-complex is of great interest. That it should now turn out to be an ingredient of two co-enzymes, including that of alcoholic fermentation, and to be concerned with several other well-known dehydrogenation processes is of profound significance. A further instance of the close relation between some vitamins and some enzymes is afforded by the discovery that aneurin (Vitamin B_1) when combined with two molecules of phosphoric acid as pyrophosphate possesses the properties of co-carboxylase. Since the carboxylase system effects the decarboxylation of pyruvic acid in alcoholic fermentation the astounding fact emerges that this process involves the participation of both Vitamin B_1 and the lactoflavin ingredient of the B_2 complex.

The establishment of the relation of aneurin to carboxylase is an interesting extension of the work of Peters and his colleagues at Oxford, who have demonstrated the part played by aneurin in the oxidation of pyruvic acid in the brain. A disturbance in carbohydrate breakdown, due to absence of Vitamin B_1, brings about a serious disturbance in the function of the nervous system.

In this connexion an interesting comparison is drawn between the mental effects produced by narcotics and by an atmosphere deficient in oxygen (as at high altitudes), and these are shown to have much in common with the characteristic symptoms of Vitamin B_1-deficiency in which oxidative reactions in the brain are partially inhibited.

The new methods for the treatment of certain types of mental disorder involving either prolonged narcosis combined with glucose-insulin treatment, or the administration of insulin to the point where coma ensues are briefly outlined, and also the scientific grounds on which these treatments are based.

The chapter entitled "Tendencies in Microbiological Chemistry" has many points of interest. It contains an account of some compounds recently isolated from mould cultures which, owing to their unusual composition, are of particular importance. Foremost among these are the chlorinated aromatic compounds geodin and erdin isolated from cultures of *Aspergillus terreus*. These are the first halogenated organic compounds to be detected as products of microbiological action. Their formation by the living cell

recalls that of thyroxine, the iodo-derivative of tyrosine, occurring in the thyroid gland. Another instance is " Tyrian purple " contained in a certain marine gastropod from the Mediterranean, which has been shown to be a dibromo-derivative of indigo. Compounds of this type are, however, of rare occurrence, even in animals, and the mechanism of their formation extremely obscure.

Readers of this chapter will be grateful to its author for having raised certain questions regarding current tendencies in biochemical research. All chemists and biologists will agree when he urges that investigation of the products of microbiological actions should not be confined to such organisms as common yeast and *Bacterium coli*. Again, he agrees with Kluyver that results obtained by the use of " fixation agents," inhibitors, and cell-free preparations in the study of micro-organisms, while of considerable interest, must be interpreted with the greatest caution owing to the abnormal conditions which obtain when such methods are employed. Few will disagree here, but it is not to be expected that these methods will be discarded as yet. They have rendered great service especially in the study of carbohydrate metabolism in muscle and yeast, although in the latter case results obtained by their aid have occasionally been incorrectly interpreted.

The author states " I maintain most forcefully that so far as microbiological and particularly mycological chemistry are concerned attempts to elucidate mechanisms are somewhat premature and might well await the accumulation of more experimental facts." Here he is of course, anxious to stimulate that vigorous discussion so necessary to the development of a young science. " The impression . . . that there is something *infra dig.* in the mere accumulation of facts " to which the author refers, is a natural, though over emphasized and extreme, reaction to the methods of the older preparative and descriptive schools of chemistry and biology. Progress will be made along the middle way between the two extremes of view which the author discusses.

Combustion, Flames, and Explosions of Gases. By Bernard Lewis and Guenther von Elbe. [Pp. xiii=415.] (The Cambridge Series of Physical Chemistry, 1938. Price 21*s.* net.)

The authors have attempted a " co-ordination and critical appraisal " of the recorded observations and theoretical investigations in the field of gaseous combustion. They display immense enthusiasm for their subject and have produced a most readable book of much usefulness. It should be pointed out, however, that to a considerable extent it is an expression of the authors' personal views, and calls for a critical reading.

The book is in four parts: the first relates to the chemistry and kinetics of the reactions between fuel gases and oxygen, the second to the propagation of flames, the third to the state of the burnt gases, and the fourth to technical problems, mainly those relating to the internal combustion engine. Much ground is therefore covered, but there are noticeable omissions which should be taken into account in any attempt at comprehensive co-ordination. The high pressure researches of Bone and his collaborators are not taken into their scheme, nor do they appear very seriously to have considered the flame photographs taken by many observers from the point of view of the state of the burnt gases. It seems probable that a full examination of these would lead to a profound modification of some of the views they express and to a less strained interpretation of flame temperature, soap bubble, and explosion experiments.

The authors have done much service in collecting and systematizing thermo-chemical data, and the value of their work is greatly enhanced by the incorporation of them in Appendix A. These they have used throughout the first three parts of their book, but in Part IV. they give ideal internal combustion engine efficiencies based upon data now known to be incorrect. This is to be regretted, as the work of Hershey, Eberhardt, and Hottel, based upon correct data, was available. Indeed, the general thermodynamic treatment of internal combustion engines leaves much to be desired, but on the other hand the present state of knowledge in regard to the combustion processes in spark-ignition engines and in compression-ignition engines is excellently summarized.

A Text Book on Crystal Physics. By W. A. Wooster. [Pp. 295+xxii.] (Cambridge University Press, 1938. Price 15*s.* net.)

Physicists were interested in the properties of crystals long before the discovery of X-ray methods of analysis, but in the 25 years which have elapsed since the first analysis was made, attention has been directed almost exclusively to structural analysis and relatively little attention, particularly on the experimental side, has been given to other aspects of the subject. The appearance of this book is perhaps an indication that the centre of interest is now moving back to the older problems which have to be re-examined in the light of the results obtained in the last 25 years.

All who are concerned with the study of crystal properties will heartily welcome the appearance of this book, for it is the first to be written in English devoted entirely to this subject. Most of the physical properties of crystals depend on the direction relative to the crystallographic axes in which they

are measured. The neatest way of dealing with this dependence on direction is by the use of a tensor notation ; this is explained in the first chapter of the book. The average reader may find it a difficult opening, especially if he is only vaguely acquainted with the elements of crystal symmetry, but having surmounted this obstacle he will find the succeeding chapters considerably easier. Among the properties treated by the method are thermal expansion, plastic deformation, conduction, piezo-electricity and elasticity.

It is clear that much original work still remains to be done. The physical properties of relatively very few crystals have been examined at all fully. Thus, in the introduction to the chapter on conduction, the author states that " The classical theory of conduction was completed 50 years ago, but up to the present there are no more than a dozen non-cubic crystals for which the absolute principal thermal conductivities are known." The author gives no account of quantum-mechanical theories of the various physical properties which he considers, for this is clearly outside the scope of the book. In many cases he is unable to correlate the physical properties with the details of the crystal structures ; the work of W. L. Bragg on the birefringence of calcite is a notable exception. For the most part, however, he is able to make a useful correlation between the physical properties and the type of structure ; *e. g.*, in treating thermal expansion he discusses the available data for non-cubic crystals in relation to the following lattice types : isosthenic lattices, layer lattices, chain lattices and three-dimensional frameworks. In addition to systematizing such data as are available, the author also gives short accounts of the main experimental methods which are used ; this side of the book would have been more useful if a few well-chosen references had been given to assist the reader desiring to know more of the experimental techniques. This, however, is a minor criticism, and in all other respects the book is excellent and the author is to be congratulated on its opportune appearance. The reviewer can thoroughly recommend it to all interested in the subject.

G. W. Brindley.

The Evolution of Physics. By Albert Einstein and Leopold Infeld. [Pp. x+320.] (Cambridge : at the University Press, 1938. Price 8*s.* 6*d.*)

" In the whole history of science from Greek philosophy to modern physics," state the authors, " there have been constant attempts to reduce the apparent complexity of material phenomena to some simple fundamental ideas and relations."

It is with the evolution of the fundamental ideas which underlie the larger part of physics that this book is concerned.

It is written for readers with " a complete lack of any concrete knowledge of physics and mathematics," and the field of discourse is so bounded that such readers would barely suspect the elaboration of technique, experimental and mathematical, which have given those ideas significance. The idealized reader might well wonder how physicists spend their time. For the student and investigator, however, each too often seeing little beyond the complexities of the problem of the moment, a severely non-technical survey of the growth of fundamental ideas may be of the greatest service, especially when, as here, profound knowledge and insight combine with expository skill in its making.

The rise is first described of that essentially simple mechanical picture of the physical world as a world of particles exerting forces on each other according to their distances apart; a picture whose range of application for long seemed limitless. The phenomena of electromagnetism and light, however, do not adapt themselves naturally to the simple scheme, as is shown in the second section, sweepingly entitled " The decline of the mechanical view." All the difficulties of the " medium " become prominent. In connexion with electromagnetism a new concept is developed, that of the " field." From field problems arises relativity. The development of the special and general theories is described, and their coordinating power is indicated. This part of the book will be read with especial interest as giving an indication of what, to the inventor of those theories, seem their essential underlying ideas. The last section deals with " Quanta." The apparent wave-particle contradictions are made clear, and quantum mechanics is presented as a formulation of statistical laws giving the change in time probabilities for large congregations of individuals.

The theme underlying the survey may be indicated by a quotation: " Science is not just a collection of laws, a catalogue of unrelated facts. It is a creation of the human mind, with its freely invented ideas and concepts. Physical theories try to form a picture of reality and to establish its connexion with the wide world of sense impressions." This is an attitude which would not, perhaps, at present, gain universal assent. A monograph may yet appear on the economic causes and effects of relativity. There are few physicists, however, who would not accept this book as a masterly survey of some of the great steps which have led to their present outlook on the physical world. To students and others who wish to gain an impression, with a minimum of technicalities, of how the fundamental ideas have developed there is no book which could be more strongly recommended. E. C. S.

[*The Editors do not hold themselves responsible for the views expressed by their correspondents.*]

FIG. 1 *a*.

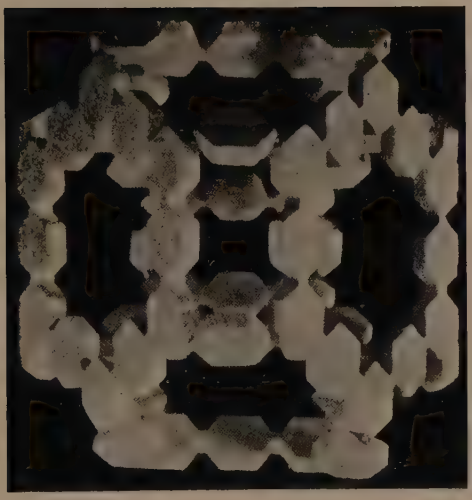

FIG. 1 *b*.

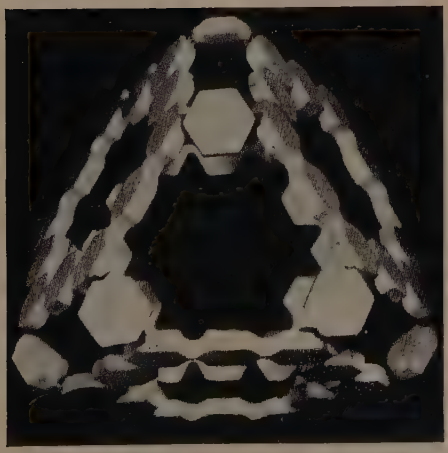

The C_1 molecule whose skeleton comprises 72 amino acid residues.
[From Proc. Roy. Soc. A, clxi. pl. 15.]

THE

LONDON, EDINBURGH, AND DUBLIN

PHILOSOPHICAL MAGAZINE

AND

JOURNAL OF SCIENCE.

[SEVENTH SERIES.]

OCTOBER 1938.

XL. *On some Effects caused in the Ionosphere by Electric Waves.*—Part II.

By V. A. BAILEY, *M.A.*, *D.Phil.* (*Oxon.*), *F.Inst.P.*, *Professor of Experimental Physics, University of Sydney* *.

[Received May 18, 1938.]

1. *Introduction.*

THIS communication contains the second part of an investigation the first part of which has already been published under the same title †.

In Part I. a new mathematical theory of radio interaction was developed which was found to be in good agreement with previously known facts, and which also led to interesting new conclusions ‡ that were subsequently largely verified by experiment §.

An earlier investigation ‖ to which reference will occasionally be made here will for brevity be denoted by (A).

For convenience the definitions of the principal symbols used are collected together in the following table :—

* Communicated by the Author.

† V. A. Bailey, Phil. Mag. xxiii. p. 929 (May 1937).

‡ Also see V. A. Bailey, ' Nature,' cxxxix. p. 68 (Jan. 9, 1937).

§ V. A. Bailey, ' Nature,' cxxxix. p. 838 (May 15, 1937).

‖ V. A. Bailey, Phil. Mag. xxiii. p. 774 (April 1937).

Notation.

ω=angular frequency of a wave.

$\breve{\mathrm{E}}$=electric vector.

Z=r.m.s. value of E=E/$\sqrt{2}$.

θ=angle between the direction of propagation and the earth's magnetic field.

N=concentration of electrons.

ν=collision frequency of an electron.

$\tau=e^2/m=2{\cdot}5\times10^8$, where e is the electronic charge in e.s.u.

$\Omega=-\mathrm{H}e/mc$, where H is the total intensity of the earth's field and c is the velocity of light.

$p_0^2=4\pi\tau\mathrm{N}=3{\cdot}19\times10^9\,\mathrm{N}$.

$\omega_0=p_0^2/\omega$.

$\gamma=\Omega/\omega_0$.

$\alpha=\tan^{-1}\cos\theta$.

$\Theta=2\cos\theta/\sin^2\theta=\tan 2\alpha$.

$x=\Theta x'$, where $x'=\nu/\Omega$.

$y=\Theta y'$, where $y'=(\omega-\omega_0)/\Omega$.

$z=x+\iota y$.

$\zeta=z^{-1}=\xi+\iota\eta$.

$\rho^2=x^2+y^2$.

R=$r+\iota s$=polarization number of a wave.

μ=index of refraction.

χ=index of absorption=$\kappa c/\omega$, where

κ=coefficient of absorption.

$q=\mu-\iota\chi$.

$\zeta_1=q^2-1=\xi_1+\iota\eta_1$.

$\bar{w}$=mean work, in ergs, done on an electron per collision.

2. *Calculation of the Polarization Number* R, *Refractive Index* μ, *and Absorption Index* χ.

The well-known method commonly used for computing the values of μ, χ, and R is extremely unwieldy, so an alternative method is given here which is not only much

more compact, but also lends itself more readily to other purposes. It is based on the formulæ (19) and (14) of Part I.*, when expressed as follows † :—

$$R+R^{-1}=2\zeta, \quad . \quad . \quad . \quad . \quad . \quad . \quad (1)$$

$$\zeta_1 Z_1=1, \quad . \quad . \quad . \quad . \quad . \quad . \quad . \quad (2)$$

where $$Z_1=X+\iota Y=(z'+R\cos\theta)\gamma\iota-1. \quad . \quad . \quad . \quad (3)$$

For known values of γ, θ, x', and y' we deduce from (1) the values of R and then from (2) the values of μ and χ.

The actual computation is easily carried out by means of the following formulæ, used in succession :

$$\rho^2=x^2+y^2, \quad . \quad . \quad . \quad . \quad . \quad . \quad . \quad (4)$$

$$\xi=x/\rho^2, \ \eta=-y/\rho^2, \quad . \quad . \quad . \quad . \quad . \quad (5)$$

$$A=\xi^2-\eta^2-1, \ B=2\xi\eta, \quad . \quad . \quad . \quad . \quad (6)$$

$$C=+\sqrt{A^2+B^2}, \quad . \quad . \quad . \quad . \quad . \quad (7)$$

$$F=+\sqrt{\tfrac{1}{2}(C+A)}/\xi, \quad . \quad . \quad . \quad . \quad . \quad (8)$$

$$r=\xi(1\pm F), \ s=\eta(1\pm F^{-1}), \quad . \quad . \quad . \quad (9)$$

$$X=-(y'+s\cos\theta)\gamma-1, \ Y=(x'+r\cos\theta)\gamma, \quad . \quad (10)$$

$$L^2=X^2+Y^2, \quad . \quad . \quad . \quad . \quad . \quad . \quad (11)$$

$$a'=\sqrt{1+(1+2X)/L^2}, \ b'=1+X/L^2, \quad . \quad . \quad (12)$$

$$\mu=\sqrt{\tfrac{1}{2}(a'+b')}, \ \chi=\sqrt{\tfrac{1}{2}(a'-b')}. \quad . \quad . \quad (13)$$

As a simple check on the computation up to the stage of formula (9) the following relation should be satisfied :

$$\frac{\xi}{r}+\frac{\eta}{s}=1. \quad . \quad . \quad . \quad . \quad . \quad . \quad (14)$$

Formulæ (4) to (8) are definitions, but (9) can be derived as follows :

From (1) we have

$$R=\zeta\pm\sqrt{\zeta^2-1}.$$

Also $$\zeta^2-1=\xi^2-\eta^2-1+2\xi\eta\iota=A+\iota B$$
$$=Ce^{\iota\sigma},$$

where $\tan\sigma=B/A$, *i. e.*, $\cos\sigma=A/C$.

* This pair of formulæ is equivalent to the pair of magneto-ionic formulæ given in the usual form ; *cf.* H. R. Mimno, " Physics of the Ionosphere " (Am. Inst. Phys., Jan. 1937), p. 20.

† V. A. Bailey, Phil. Mag. xviii. p. 516 (Sept. 1934).

Therefore

$$\sqrt{\zeta^2-1}=\sqrt{C}\,(\cos\tfrac{1}{2}\sigma+\iota\sin\tfrac{1}{2}\sigma)$$
$$=\sqrt{\tfrac{1}{2}(C+A)}+\iota\sqrt{\tfrac{1}{2}(C-A)}$$

in consequence of the relations

$$\cos\tfrac{1}{2}\sigma=\sqrt{\tfrac{1}{2}(1+\cos\sigma)},\quad \sin\tfrac{1}{2}\sigma=\sqrt{\tfrac{1}{2}(1-\cos\sigma)}.$$

Therefore $r+\iota s=\xi+\iota\eta\pm\xi F\pm\iota\eta F^{-1}$,

from which the formulæ (9) follow.

Formulæ (10) to (12) are definitions arising from (3), but (13) follows easily from the following pair of equations which are derived from (2):

$$\mu^2-\chi^2-1=X/L^2,$$
$$2\mu\chi=Y/L^2.$$

Formula (14) is easily seen to be satisfied by substitution from (9).

These calculations may also be carried out rapidly by means of a special link mechanism, as will be shown in another paper to be published jointly with Mr. J. M. Somerville.

The following approximate formulæ for r and s will now be deduced:

$$\left.\begin{aligned} &r=x(1\pm G)/\rho^2,\ s=-y(1\pm G^{-1})/\rho^2,\\ &\text{where}\quad \rho^2=x^2+y^2,\ G^{-1}=\sqrt{1+\rho^2},\\ &\text{provided that}\quad \rho^2\tan^2\left(\tfrac{1}{2}\sin^{-1}\frac{2x}{1+\rho^2}\right)\ll 1. \end{aligned}\right\} \quad . \ . \ (15)$$

From (4), (5), (6), and (7) we have

$$A=-(1+\xi^2+\eta^2)+2\xi^2=-(1+\rho^{-2})+2x^2\rho^{-4},$$
$$B=-2xy\rho^{-4},$$
$$C^2=A^2+B^2=\rho^{-4}[(1+\rho^2)^2-4x^2].$$

$$\left.\begin{aligned} &\text{On setting}\quad J=\frac{x}{1+\rho^2}=\tfrac{1}{2}\sin\sigma\\ &0\leqslant\sigma\leqslant\pi/2 \end{aligned}\right\} \quad . \ . \ . \ . \ (16)$$

we then obtain

$$A=(1+\rho^{-2})\tfrac{1}{2}(\rho^{-2}\sin^2\sigma-1-\cos^2\sigma),$$
$$C=(1+\rho^{-2})\cos\sigma.$$

Therefore

$$C+A=(1+\rho^{-2})\tfrac{1}{2}\rho^{-2}\sin^2\sigma.(1-\rho^2K^2),$$

where $K=\tan \frac{1}{2}\sigma$ and $0 \leqslant K \leqslant 1$,

and so from (8)

$$F=\sqrt{\frac{1-\rho^2K^2}{1+\rho^2}} \quad . \quad . \quad . \quad . \quad . \quad . \quad (17)$$

When $$\rho^2K^2 \ll 1 \quad . \quad . \quad . \quad . \quad . \quad . \quad (18)$$

we have $$F \doteqdot \frac{1}{\sqrt{1+\rho^2}} = G,$$

and so from (9) we obtain the formulæ (15).

Any one of the following relations satisfies (18) and is therefore a condition sufficient for adopting (15) :

$$x^2 \ll \rho^2,\ x^2 \ll (\rho+\rho^{-1})^2,\ \rho^2 \ll 1. \quad . \quad . \quad . \quad (19)$$

To prove that the first of these relations leads to (18) we proceed as follows :—Writing $\rho=\cot \beta$, where $0 \leqslant \beta \leqslant \pi/2$, we then have from (16)

$$\sin^2 \sigma = (x^2/\rho^2) \sin^2 2\beta,$$

i. e., $$\sin^2 \sigma \ll \sin^2 2\beta.$$

Therefore $\frac{1}{2}\sigma < \beta$, *i. e.*, $K < \rho^{-1}$,

and $$\frac{K^{-2}}{(1+K^{-2})^2} \ll \frac{\rho^2}{(1+\rho^2)^2}.$$

Therefore $$K^2+K^{-2} \geqslant \rho^2+\rho^{-2},$$

i. e., $$K^{-2} \geqslant \rho^2+(\rho^{-2}-K^2),$$

i. e., $$K^{-2} \geqslant \rho^2,$$

which at once leads to (18).

The proportional error ϵ in setting $F \doteqdot G$ is given approximately in order of magnitude (within a factor 2) by the formula

$$\epsilon = \left(\frac{x}{\rho+\rho^{-1}}\right)^2.$$

This follows from the relations

$$\epsilon = \tfrac{1}{2}\rho^2K^2,\ \tfrac{1}{4} \leqslant J^2/K^2 \leqslant 1,$$

since the latter shows that J^2/K^2 does not differ from $\frac{1}{2}$ by a factor exceeding 2.

We now consider the special case of a wave in the lower part of the E layer, with ω of the same order of magnitude as Ω, *i. e.*, we take

$$\left.\begin{array}{l} \omega=(1+\epsilon)\Omega \\ |\ \epsilon\ | < 0{\cdot}5, \end{array}\right\} \quad . \quad . \quad . \quad . \quad . \quad (20)$$

$$N \ll 3\times 10^4,\ \nu \leqslant 10^6,\ \Omega = 10^7,$$

and so $\nu \ll \omega$ and Ω, $\omega_0 \ll \omega$ and Ω. . . . (21)

Then $x' \leqslant 0{\cdot}1$, $y' = 1+\epsilon$,

and so . . . $x = x'\Theta$, $y = (1+\epsilon)\Theta$,

where*

$$\Theta = \tan 2\alpha \text{ and } \tan\alpha = \cos\theta.$$

Clearly the first relation in (19) is satisfied, and so (15) is applicable.

Also $1+\rho^2 \doteqdot \sec^2 2\alpha + (2\epsilon+\epsilon^2)\tan^2 2\alpha$,

and so $G^{-1} \doteqdot \sec 2\alpha\sqrt{1+(2\epsilon+\epsilon^2)\sin^2 2\alpha}$

$\doteqdot \sec 2\alpha(1+\epsilon\sin^2 2\alpha + \frac{1}{8}\epsilon^2 \sin^2 4\alpha)$,

provided that $|\, 2\epsilon+\epsilon^2 \,|\, \sin^2 2\alpha \ll 1$,

i. e., $|\,\epsilon\,| \ll \sqrt{1+\operatorname{cosec}^2 2\alpha} - 1$.

This condition is always satisfied when

$$|\,\epsilon\,| \ll 0{\cdot}41. \quad . \quad . \quad . \quad . \quad . \quad . \quad . \quad (22)$$

We have then

$$\left.\begin{aligned} G^{-1} &\doteqdot \sec 2\alpha(1+\epsilon\sin^2 2\alpha), \\ G &\doteqdot \cos 2\alpha(1-\epsilon\sin^2 2\alpha). \end{aligned}\right\} \quad . \quad . \quad . \quad (23)$$

Hence by (15)

$$r = x' \cot 2\alpha . (1+\epsilon)^{-2}(1 \pm \cos 2\alpha \mp \epsilon \cos 2\alpha \sin^2 2\alpha),$$
$$s = -\cot 2\alpha . (1+\epsilon)^{-1}(1 \pm \sec 2\alpha \pm \epsilon \sec 2\alpha . \sin^2 2\alpha),$$

and so

$$\left.\begin{aligned} r_e &\doteqdot x' \cos 2\alpha \cot\alpha\{1-2\epsilon(1+\cos 2\alpha \sin^2\alpha)\}, \\ r_0 &\doteqdot x' \cos 2\alpha \tan\alpha\{1-2\epsilon(1-\cos 2\alpha \cos^2\alpha)\}, \end{aligned}\right\} \quad (24)$$

$$\left.\begin{aligned} s_e &\doteqdot -\cot\alpha(1-\epsilon\cos 2\alpha), \\ s_0 &\doteqdot \tan\alpha(1+\epsilon\cos 2\alpha). \end{aligned}\right\} \quad . \quad . \quad . \quad . \quad . \quad . \quad (25)$$

It can be verified that in (24) and (25) the first formulæ give the polarization number R_e of the extraordinary wave and the others give the polarization number R_0 of the ordinary wave.

3. *Resonance in Gyro Interaction.*

In section 5 of Part I. a proof was given that when the angular frequency ω of a wave varies about Ω, the value of the local angular gyro-frequency, a notable degree of

* The auxiliary angle α is introduced because it simplifies the subsequent work to a remarkable extent.

resonance may occur in the effects caused by this wave in the ionosphere; but the range of variation of ω was there somewhat unduly restricted*, and the more complete study of the variation of the modulation M″, impressed on a second wave, was postponed. We therefore proceed here to investigate these questions more fully.

As before, on account of its predominant effect we consider here only the action of the extraordinary wave in the lower part of the E layer; then from (24) and (25) we have

$$\left.\begin{aligned} r&=x'k(1-l\epsilon),\\ s&=-m(1-n\epsilon),\end{aligned}\right\} \quad . \quad . \quad . \quad . \quad . \quad (26)$$

where

$$\left.\begin{aligned} k&=\cos 2\alpha.\cot\alpha,\ l=2\cos^2\alpha(1+2\sin^2\alpha),\\ m&=\cot\alpha,\ n=\cos 2\alpha.\end{aligned}\right\} \quad . \quad (27)$$

So from (10) and (20) it follows that

$$\mathrm{X}=-(\Omega^2/p_0^2)2\cos^2\alpha.\epsilon-1,$$

$$\mathrm{Y}=(\nu\Omega/p_0^2)2\cos^2\alpha(1+4\sin^4\alpha.\epsilon),$$

and then from (2) that

$$q^2=\frac{a-ib}{c-ib}, \quad . \quad . \quad . \quad . \quad . \quad . \quad (28)$$

where

$$\left.\begin{aligned} a&=\epsilon,\ b=b_0(1+4\sin^4\alpha.\epsilon),\ c=c_0+a,\\ b_0&=\nu/\Omega,\ c_0=p_0^2\sec^2\alpha/2\Omega^2 \quad . \quad . \quad .\end{aligned}\right\} \quad . \quad (29)$$

Also in virtue of (21) we note that

$$b_0\ll 1,\ c_0\ll 1. \quad . \quad . \quad . \quad . \quad . \quad . \quad (30)$$

On writing

$$\left.\begin{aligned} b/a&=\tan\phi,\ b/c=\tan\psi,\\ \delta&=\phi-\psi,\ \mathrm{Q}=\left(\frac{a^2+b^2}{c^2+b^2}\right)^{\frac{1}{2}},\end{aligned}\right\} \quad . \quad . \quad . \quad . \quad (31)$$

(28) becomes

$$q^2=\mathrm{Q}^2e^{-\iota\delta},$$

and so in succession we find

$$\mu-\iota\chi=\mathrm{Q}e^{-\frac{1}{2}\iota\delta},$$

$$\mu=\mathrm{Q}\cos\tfrac{1}{2}\delta,\ \chi=\mathrm{Q}\sin\tfrac{1}{2}\delta. \quad . \quad . \quad . \quad (32)$$

* I am indebted to Mr. Somerville for pointing this out.

We now study the variation with ϵ of $\bar{w}$, the mean work done on an electron per collision. In Part I. (equation (49)) this was shown to be given by the formula

$$\bar{w}=\tau Z^2\beta\Gamma a_s, \quad \ldots\ldots \quad (33)$$

where β, Γ, and a_s are defined respectively by the equations (48), (50)*, and (46) in Part I., namely,

$$\beta=\left|\frac{R_p-R_0}{R_e-R_0}\right|^2 \frac{1+|R_e|^2}{1+R_p^2}, \quad \ldots \quad (34)$$

where R_p is the polarization number of the original plane wave,

$$\left.\begin{aligned}&\Gamma=S/\nu\omega_0,\\ \text{where}\quad &S=2\mu_e\chi_e/(\mu_e^2+\chi_e^2),\end{aligned}\right\} \quad \ldots \quad (35)$$

Fig. 1.

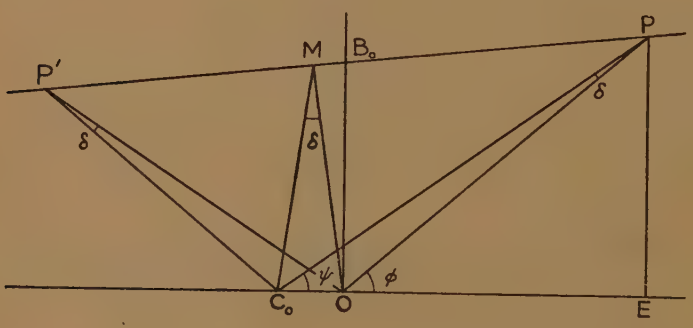

and

$$\log a_s=-2\int_0^s \kappa\, ds, \quad \ldots\ldots \quad (36)$$

where s is the length of the ray-trajectory up to the point under consideration.

Following a procedure similar to that given in Part I. (p. 945), we set in fig. 1 $OB_0=b_0$, $OC_0=c_0$, $OE=\epsilon$, and make the slope of $P'B_0P$ equal to $4b_0\sin^4\alpha$.

We have then

$$OE=a,\ C_0E=c,$$
$$EP=OB_0+OE(4b_0\sin^4\alpha)=b,$$

and so in virtue of (31)

$$\delta=\text{the angle } C_0PO.$$

* We here use Γ in place of the symbol γ in (50) Part I.

From (35) and (32) we have

$$\Gamma = \frac{\Omega}{\nu p_0^2}(1+\epsilon)\sin\delta, \quad \ldots \quad (37)$$

so on account of (22) it follows that as ϵ varies Γ varies proportionately nearly like $\sin\delta$.

Clearly δ has a maximum value at the point M, where a circle through O and C_0 touches the line P'P, *i. e.*, where $\epsilon = \frac{1}{2}OC_0$. It follows that Γ passes through a maximum value when ω is nearly equal to $\Omega(1+\frac{1}{2}c_0)$, *i. e.*, by (30) nearly equal to Ω.

To find the variation of β with ϵ we have by (24), (25) and the condition $x' < 0{\cdot}1$

$$R_0 = \iota \tan\alpha(1+\epsilon\cos 2\alpha),$$
$$R_e = -\iota\cot\alpha(1-\epsilon\cos 2\alpha).$$

Fig. 2.

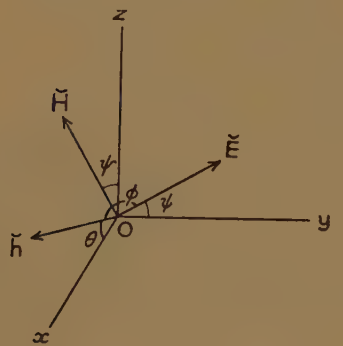

Also $R_p = \cot\psi$, where ψ is the angle between the z-axis and the magnetic vector of the original plane wave as shown in fig. 2.

Therefore

$$|R_p - R_0|^2 = R_p^2 + \tan^2\alpha + 2\epsilon\tan^2\alpha\cos 2\alpha.$$

$$|R_e - R_0|^2 = (\cot\alpha + \tan\alpha - \epsilon\cos 2\alpha.\ \overline{\cot\alpha - \tan\alpha})^2$$
$$= 4\,\mathrm{cosec}^2 2\alpha(1-2\epsilon\cos^2 2\alpha)$$

$$1+|R_e|^2 = 1+\cot^2\alpha - 2\epsilon\cot^2\alpha\cos 2\alpha$$
$$= \mathrm{cosec}^2\alpha(1-2\epsilon\cos^2\alpha.\cos 2\alpha).$$

Therefore $$\beta = \beta_r(1+B\epsilon), \quad \ldots \quad (38)$$

where
$$\beta_r = \frac{(R_p^2+\tan^2\alpha)\operatorname{cosec}^2\alpha}{4\operatorname{cosec}^2 2\alpha(1+R_p^2)}$$
$$=\cos^2\alpha\cos^2\psi+\sin^2\alpha\sin^2\psi$$

and
$$B=\frac{2\tan^2\alpha.\cos 2\alpha}{\cot^2\psi+\tan^2\alpha}+2\cos^2 2\alpha-2\cos^2\alpha\cos 2\alpha$$
$$=2\cos 2\alpha\left(\frac{1}{1+\cot^2\alpha.\cot^2\psi}-\sin^2\alpha\right).$$

It is convenient now in place of the angle ψ to use the angle ϕ between the electric vector $\breve{E}$ of the original plane wave and the earth's magnetic vector $\breve{h}$.

The direction cosines of $\breve{E}$ are $(0, \cos\psi, \sin\psi)$ and those of $\breve{h}$ are $(\cos\theta, 0, \sin\theta)$. Therefore

$$\left.\begin{aligned}&\cos\phi=\sin\psi\sin\theta,\\ \text{and so}\quad&\sin^2\phi=\cos^2\psi+\tan^2\alpha\sin^2\psi,\end{aligned}\right\}\quad\ldots\quad(39)$$

and
$$1+\cot^2\alpha.\cot^2\psi=\tan^2\theta\tan^2\phi.$$

Thus we find that
$$\beta_r=\cos^2\alpha.\sin^2\phi\quad\ldots\quad(40)$$

and
$$B=2\sin^2\alpha(\cot^2\phi-\cos 2\alpha).\quad\ldots\quad(41)$$

It is easy to verify that the formulæ for β_r and B are in agreement with those given in Part I., so the conclusion arrived at there still holds true, namely, where a_s is not much less than unity the quantity $\bar{w}$ passes through a notable maximum as ω passes through the value Ω.

A simple formula for the product $\beta\Gamma$ can be obtained as follows :

From (31) we have
$$\tan\delta=\frac{c-a}{b+ac/b},$$

and from (29)
$$c-a=c_0$$

and
$$b+\frac{ac}{b}=b_0(1+4\sin^4\alpha.\epsilon)+\frac{\epsilon(c_0+\epsilon)b_0^{-1}}{1+4\sin^4\alpha.\epsilon}$$
$$\doteqdot b_0(1+p\epsilon+q'\epsilon^2),$$

where
$$p=4\sin^4\alpha+p_0^2\sec^2\alpha/2\nu^2,\ q'=\Omega^2/\nu^2.\quad\ldots\quad(42)$$

Therefore
$$\left.\begin{aligned}&\tan\delta=\frac{C}{1+p\epsilon+q'\epsilon^2},\\ \text{where}\quad&C=p_0^2\sec^2\alpha/2\nu\Omega.\end{aligned}\right\}\quad\ldots\quad(43)$$

From (37) and (38) we have

$$\beta\Gamma=(\beta,\Omega/\nu p_0^2)(1+B\epsilon)(1+\epsilon)\sin\delta,$$

so, on using the formulæ (40), (41) and the relation

$$\sin\delta=\frac{\tan\delta}{\sqrt{1+\tan^2\delta}},$$

we obtain the following result:

$$\left.\begin{aligned}\beta\Gamma&=\frac{\sin^2\phi}{2\nu^2}\cdot\frac{1+A\epsilon}{\sqrt{(1+p\epsilon+q'\epsilon^2)^2+C^2}},\\ \text{where}\quad A&=\cos^2 2\alpha+2\sin^2\alpha.\operatorname{cosec}^2\phi.\end{aligned}\right\}\quad\ldots\quad(44)$$

The formula for $\beta\Gamma$ becomes even simpler when the following additional restriction exists:

$$\omega_0^2\ll\nu^2.\quad\ldots\quad(45)$$

For then, since $1\leqslant\sec^2\alpha\leqslant 2$, we have $C^2\ll 1$, and so (44) reduces to

$$\left.\begin{aligned}\beta\Gamma&=\frac{\sin^2\phi}{2\nu^2}\cdot\frac{1}{1-p'\epsilon+q'\epsilon^2},\\ \text{where}\quad p'&=\frac{\tan^2\theta+2\cot^2\phi}{\tan^2\theta+2}-\frac{p_0^2(1+\cos^2\theta)}{2\nu^2},\\ q'&=\Omega^2/\nu^2.\end{aligned}\right\}\quad\ldots\quad(46)$$

The first term in p' must lie between 0 and 3 because of the relation

$$0\leqslant\cot^2\phi\leqslant\tan^2\theta,$$

which necessarily follows from (39).

The formula (33) now takes the form

$$\bar{w}=\tau Z^2 a_s\left(\frac{\frac{1}{2}\sin^2\phi}{\nu^2+(\omega-\Omega)^2-\nu^2p'\epsilon}\right).\quad\ldots\quad(47)$$

When the electron concentration N is sufficiently small we have $a_s=1$ and $p'\epsilon\ll 1$, and then this formula for $\bar{w}$ is in close agreement with the formula (27) of Part I. As the latter was derived without reference to the fundamental equations of Maxwell and Lorentz or to Poynting's theorem on which the above formula for $\bar{w}$ is ultimately based, we may take this agreement to constitute a valuable check on the whole investigation.

In order to be able to calculate a_s we now proceed to derive formulæ for μ and χ in terms of ϵ.

From (29) and (30) we have

$$a^2+b^2=b_0^2(1+8\sin^4\alpha.\epsilon+q'\epsilon^2),$$
$$c^2+b^2=b_0^2(1+C^2+2p\epsilon+q'\epsilon^2),$$

so from (31) it follows that

$$Q=\left(\frac{1+8\sin^4\alpha.\epsilon+q'\epsilon^2}{1+C^2+2p\epsilon+q'\epsilon^2}\right)^{\frac{1}{2}}. \quad . \quad . \quad . \quad (48)$$

Under the restriction (45) this simplifies to the formula

$$Q=1-\frac{p_0^2\sec^2\alpha}{4}.\frac{\epsilon}{\nu^2+\Omega^2\epsilon^2}.$$

Also, on account of (45) we have from (43) that $\tan^2\delta \ll 1$, and so

$$\cos\tfrac{1}{2}\delta \doteqdot 1, \sin\tfrac{1}{2}\delta \doteqdot \tfrac{1}{2}\tan\delta.$$

Consequently (32) yields the formulæ

$$\mu \doteqdot 1-\frac{1}{4}p_0^2\sec^2\alpha.\frac{\epsilon}{\nu^2+\epsilon^2\Omega^2} \quad . \quad . \quad . \quad (49)$$

and

$$\chi \doteqdot \frac{1}{4}\mu.\frac{p_0^2\sec^2\alpha}{\nu\Omega}.\frac{1}{1+p\epsilon+q'\epsilon^2}. \quad . \quad . \quad (50)$$

When

$$N<800 \quad . \quad . \quad . \quad . \quad . \quad . \quad . \quad (51)$$

then $p_0^2\epsilon \ll \nu^2$, and so

$$\left.\begin{aligned}\mu &\doteqdot 1,\\ \chi &\doteqdot \frac{1}{2}C'.\frac{\nu}{\nu^2+\epsilon^2\Omega^2},\end{aligned}\right\} \quad . \quad . \quad . \quad . \quad (52)$$

where $C'=p_0^2\sec^2\alpha/\Omega$.

Since $\kappa=\omega\chi/c$, therefore

$$\kappa=K\sec^2\alpha.\frac{N\nu}{\nu^2+\sigma^2}, \quad . \quad . \quad . \quad . \quad (53)$$

where

$$\left.\begin{aligned}K&=0{\cdot}0266,\\ \sigma&=\epsilon\Omega.\end{aligned}\right\} \quad . \quad . \quad . \quad . \quad . \quad (54)$$

With the physical conditions given in Part I., namely a vertical magnetic field and a wave incident on the E layer at an angle i_0, and with y denoting the height of a point above the lowest part of the E layer, we have

$$\theta=i_0,\ s=y\sec i_0.$$

Therefore

$$\tan\alpha=\cos i_0,$$

and so from (36) and (53) we obtain

$$\log a_s=-2K(\cos i_0+\sec i_0)I, \quad . \quad . \quad . \quad (55)$$

where
$$\mathrm{I}=\int_0^{\nu}\frac{\mathrm{N}\nu}{\nu^2+\sigma^2}\,dy. \quad . \quad . \quad . \quad . \quad . \quad (56)$$

We may now adopt the following relations :

$$\left.\begin{aligned}\nu&=\nu_0 e^{-ny},\\ \mathrm{N}&=f(\nu),\end{aligned}\right\} \quad . \quad . \quad . \quad . \quad . \quad (57)$$

where
$$\nu_0=1{\cdot}1\times10^6,\ n=10^{-6}.$$

Then (56) becomes

$$-n\mathrm{I}=\int_{\nu_0}^{\nu}\frac{f(\nu)d\nu}{\nu^2+\sigma^2}. \quad . \quad . \quad . \quad . \quad . \quad (58)$$

Thus for Martyn's distribution of electronic concentration we have

$$\mathrm{N}=f(\nu)=\mathrm{N}_0\nu^{-c},$$

where
$$c=10 \text{ and } \mathrm{N}_0=1,$$

and so
$$-n\mathrm{I}=\mathrm{N}\int_{\nu_0}^{\nu}\frac{\nu^{-c}d\nu}{\nu^2+\sigma^2}.$$

On writing
$$u=\tan v=\sigma/\nu \quad . \quad . \quad . \quad . \quad . \quad . \quad (59)$$

this gives the following results :

$$\left.\begin{aligned}\sigma^{c+1}n\mathrm{I}&=\mathrm{N}_0\int_{\mu_0}^{\mu}\frac{u^c.du}{1+u^2}\\ &=\mathrm{N}_0\int_{v_0}^{v}\tan^c v.dv.\end{aligned}\right\} \quad . \quad . \quad . \quad . \quad (60)$$

For any integral value of c the first integral on the right of (60) can be easily evaluated as the sum of a finite number of terms.

Thus when $c=10$ and $\mathrm{N}_0=1$ we have

$$\left.\begin{aligned}\mathrm{I}&=\frac{10^6}{\sigma^{11}}\left[\frac{u^9}{9}-\frac{u^7}{7}+\ldots+u-\tan^{-1}u\right]_{\mu_0}^{\mu},\\ \text{where}\quad u&=\epsilon\,\Omega/\nu,\quad \sigma=\epsilon\Omega.\end{aligned}\right\} \quad . \quad (61)$$

By means of the formulæ (61) and (55) we can thus compute a_s for a fixed height and different values of ϵ ; the corresponding values of $\bar{w}$ can then be determined by means of (47).

In this way the values of $\bar{w}$, resulting from a wave with an angle of incidence i_0 equal to 45°, have been computed for different values of ω in the neighbourhood of Ω, and with Ω equal to 8×10^6 the value corresponding to London. From them the values of the quantity $N\nu\bar{w}$ at each of four different levels in the E region have been determined, and are given in terms of the wave-length by means of the curves in fig. 3. This quantity has been adopted because in the absence of a specification of the second

Fig. 3.

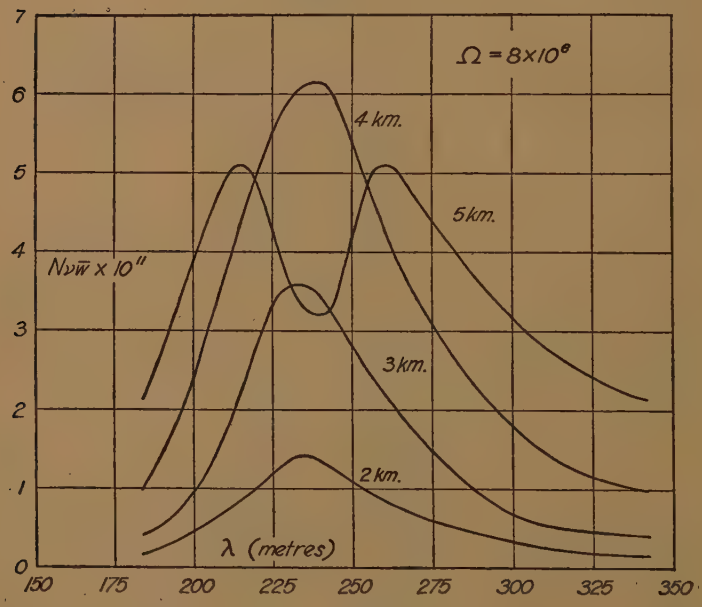

wave it gives the fullest possible information about the relative contribution of a particular level to the modulation M″ impressed on the second wave ; it may for convenience be termed the index of interaction.

It will be seen from fig. 3 that as the height increases the resonance curve relatively flattens out and ultimately changes from the dromedarian type with one hump to the bactrian type with two humps. We may therefore expect that the modulation impressed on a wave reflected at the 5 km. level of the E layer (*e. g.*, a medium wave) will show two resonance maxima as the modulating wave

has its frequency varied in the neighbourhood of the gyro-frequency *.

The value λ_{min} of the wave-length at which $N\nu\bar{w}$ is a minimum depends on the angle ϕ. When N is small λ_{min} can be determined by means of formula (27) of Part I. As examples we deduce that corresponding to the angles of incidence 0° and 35° the values of λ_{min} are respectively ∞ and $2\lambda_{gyro}$.

The index of interaction $N\nu\bar{w}$ then steadily increases with the wave-length up to about 2000 metres, when its value is about one-fifth of that which it has near the gyro wave-length. With very long waves the value of this index is still larger, but the actual interaction with broadcasting waves then diminishes because the very long waves are reflected in regions of the ionosphere much below those which reflect broadcasting waves.

All the conclusions about gyro interaction given in Part I. remain unaltered by the present method of discussion. An important conclusion is that under certain circumstances a vertical Hertzian oscillator radiating a gyro wave may cause observable interaction when its radiated power is as low as 1 or 2 kw.

It is of interest also to consider the problem of determining the least radiated power which under appropriate and practicable circumstances can influence the E layer in an observable manner.

The first step in increasing the effectiveness of the vertical Hertzian aerial mentioned above is to place it horizontally, for this increases the maximum value of the electric intensity Z at the bottom of the E layer by the factor † 2. When the ground is a conductor it may partly neutralize this gain, but if the horizontal aerial is fixed at a height $\lambda/4$ above the ground, where λ is the

* With any other distribution of electron concentration we may proceed similarly, since any arbitrary distribution can always be represented approximately by means of a Prony series of exponential functions of y, *i. e.*, we may set

$$N = \sum_m b_m \nu^{-c_m}, \text{ where } c_m > 0,$$

and so in the above discussion replace (60) by the following:

$$nI = \sum_m b_m \sigma^{-c_m - 1} \int_{v_0}^{v} \tan^{c_m} v \, dv.$$

† This is due to a change, relative to the oscillator, of the radial distance of the affected part of the E region by a factor $\sqrt{2}$, and a similar change of the zenithal angle from 45° to 90°.

gyro wave-length, the effect of the ground is, if anything, advantageous. In this way the minimum power needed to cause observable interaction can be reduced to about 0·4 kw. or less *.

With a perfectly conducting ground, or with a suitable reflecting system of conductors placed on the ground below the horizontal aerial, the maximum value of Z is further increased by the factor 2, and so with relatively simple means the least power needed is about 100 watts.

This power can be reduced to 50 watts by adding a second horizontal Hertzian oscillator with its axis at right angles to that of the first, and maintaining in the two oscillators equal currents with phases differing by one-quarter of a cycle in such a way as to cause an extraordinary wave to be radiated upwards from the aerial system.

Finally, by building up horizontal, parallel arrays of such oscillators and so concentrating the radiation in an upward beam, it appears easily possible to reduce the power needed to cause observable radio interaction to a value as low as 1 watt †.

4. *Some Effects caused by a Powerful Gyro Wave.*

As the intensity of a gyro wave is increased to large values the primary effect is to increase u, the mean velocity of agitation of the electrons, until velocities of collision with molecules are attained which cause the molecules to emit light or fresh electrons or both.

It is therefore of interest to determine the minimum power W_m which may need to be radiated from an appropriate system of aerials in order to maintain a steady electrical discharge in the E layer at night.

We consider first the aerial system, which consists of a horizontal half-wave Hertzian oscillator placed at a height $\lambda/4$ above a highly reflecting ground, and for simplicity again take the terrestrial magnetic field to be vertical.

* Since λ is usually of the order of 200 m. we see that the aerial masts need be little more than 50 m. tall and the horizontal aerial about 100 m. long.

† The corresponding aerial system, consisting of 98 half-wave aerials in all, would require an area of about 0·36 km.^{2} for its erection, and would, of course, cost much more than is needed to generate 1 watt of gyro radiation.

If the radiated power be W kilowatts, the r.m.s. electric intensity Z at the lower part of the E layer vertically above the oscillator is given by the formula *

$$Z^2 = 5{\cdot}8 \times 10^{-9} W \quad . \quad . \quad . \quad . \quad . \quad (62)$$

when Z is expressed in volts/cm.

As the vertically radiated wave is plane it may be analysed into two circularly polarized waves of equal intensities, one of which imparts only relatively negligible energy to the electrons ; thus the effect on the electrons may be attributed entirely to an extraordinary circular wave with a rotating constant vector of magnitude E′ equal to $\frac{1}{2}(\sqrt{2}\,Z)$, *i. e.*, to $Z/\sqrt{2}$.

Such a circular wave can be generated alone by adding to the Hertzian oscillator an orthogonal one, such as was described in the last section, and radiating the power $\frac{1}{2}W$ from each. In this way a vertical circularly polarized gyro beam with rotating constant vector of magnitude E (equal to Z) may be produced by means of an aerial system radiating the power W kilowatts where

$$E^2 = 5{\cdot}8 \times 10^{-9} W, \quad . \quad . \quad . \quad . \quad (63)$$

E being expressed in volts/cm.

It is shown in Appendix I. that at a given pressure p a rotating constant force E yields the same value of u as an equal stationary constant force X or a stationary alternating force of equal r.m.s. value Z.

The experiments of H. A. Wilson † and D. M. Myers ‡ show that electric discharges can occur in air when, in the uniform column X/p or Z/p, the ratio of the electric force to the gas pressure p is approximately as low as 16. We may therefore conclude that two of the necessary conditions for producing a glow discharge, namely the generation of fresh electrons and light, are satisfied when

$$E/p \geqslant 16, \quad . \quad . \quad . \quad . \quad . \quad . \quad (64)$$

i. e., by (63) when

$$W \geqslant 4{\cdot}4 \times 10^{10} p^2. \quad . \quad . \quad . \quad . \quad . \quad (65)$$

As shown by Table IV. in Part I. the maximum effects caused by a low-powered gyro wave occur at that level

* *Cf.* A. L. Green, A. W. A. ' Technical Review,' iii. p. 130 (Jan. 1938). The lower part of the E layer is taken to be 90 km. high.

† Proc. Camb. Phil. Soc. xi. pp. 249 & 391 (1902).

‡ Unpublished experiments with high-frequency discharges made in Sydney on the lines developed by J. S. Townsend and his associates.

in the E layer which corresponds to $y=2{\cdot}7$ km., $\nu=8{\cdot}4\times10^5$, $a_s=0{\cdot}84$, and $N=15$. It is easy to deduce that at that level, with an assumed temperature of about 15° C., the gas pressure p is approximately 2×10^{-3} mm. of mercury.

We then conclude from (65) that both light and fresh electrons are generated at collisions when the power radiated from our simple polarizing aerial system is not less than W_m, where

$$W_m=2\times10^5 \text{ kilowatts.}$$

The supply of electrons needed for initiating and maintaining this glow discharge is provided by those natural processes which are normally responsible for maintaining throughout the night the well-established notable concentrations of electrons in the E layer.

But the generation of electrons by collisions under the influence of the above gyro wave will also serve to maintain the discharge if it supplies electrons at a rate not slower than the rate at which electrons disappear from the scene of action through the combined effect of

(*a*) Diffusion, (*b*) Drift under a constant electric force, (*c*) Attachment, and (*d*) Recombination.

Townsend * has shown that only the first two of these processes are important in the uniform column of discharge-tubes, the diffusion being towards the wall of the tube and the drift tending to reduce the disappearance of electrons by diffusion. So to compare the rates of artificial supply and disappearance of electrons in the E region it will suffice to determine the size of a part of this region for which the above processes are quantitatively similar to those occurring in an air-discharge-tube with Z/p equal to 16.

In the E region, where $\nu^2\leqslant0{\cdot}01\Omega^2$, the coefficient K of diffusion along the earth's magnetic field and the coefficient K_h of transverse diffusion are related as follows :

$$K_h\leqslant0{\cdot}01\,K \quad . \quad . \quad . \quad . \quad . \quad . \quad (66)$$

in consequence of the formula †

$$K_h=K/(1+\Omega^2/\nu^2).$$

* J. S. Townsend, Phil. Mag. p. 1112 (May 1931).

† See J. S. Townsend, ' Electricity in Gases,' p. 99 (Clarendon Press, 1915).

Also $K=lu/3$, where l is the mean free path, and at the level of the E region under consideration the gas pressure is about 2×10^{-3} mm.

From (66) it follows that transverse diffusion is negligible in comparison with longitudinal diffusion, and so our problem simplifies to determining that thickness of a horizontal slab of the E region which corresponds to the diameter of the air-discharge-tube for which Z/p has the value 16. In Myer's experiments he found this value of Z/p with a tube of diameter 5 cm. and an air pressure of about 1 mm.

So it follows by a simple argument*, involving mean free paths, that the corresponding slab must have a thickness of about 25 metres.

In this slab the electronic concentration will increase from the natural value 15 until at the slab's upper boundary the gyro wave is too weak to generate fresh electrons by collision at an adequate rate. Consequently the concentration of electrons in this slab could ultimately exceed fifty times the natural concentration.

Thus a relatively strong discharge can be maintained in the E layer by means of the circular gyro wave radiated with a power $W_m=2\times10^5$ kw.

By adopting in place of two orthogonal horizontal Hertzian oscillators two orthogonal arrays of such oscillators the effective power gain in the vertical direction can easily be increased by a large factor g, and then a sufficient radiated power to produce a glow discharge in the E layer is

$$W_m=2\times10^5/g \text{ kw.}$$

If each array consists of n adjacent parallel rows, each containing n parallel half-wave oscillators spaced $\lambda/2$ metres apart, the factor g and the total area A occupied by the aerial system are given by the following formulæ:

$$g=n^2,\ A=n\times10^{-2} \text{ km}^2.$$

The following table gives the calculated values of the total number $(2n^2)$ of oscillators and the area A corresponding to several values of the radiated power W_m.

From the first column it follows that, with a system of 800 half-wave aerials and on the local gyro frequency,

* *Cf.* F. B. Pidduck, 'A Treatise on Electricity,' p. 505. Camb. Univ. Press (1925).

the stations of 500 kw. at Cincinnati and Moscow could each generate a celestial glow at night; from the fourth column it follows that, with 2700 aerials, each of the following stations of 150 kw. could produce a similar but less extensive glow: Droitwich, Hilversum, Luxembourg, Lahti, Motala, Radio-Romania *.

Radiated power (kw.). ..	500	320	220	150	100
Number of oscillators....	800	1250	1800	2740	4050
Area occupied (km.^{2}) ...	4	6·2	9	13·7	20

A glow produced in this way would have great scientific value, as it would allow the nature of the upper atmosphere to be examined by means of controllable spectroscopic and other observations.

Where only small arrays can be provided, or where adequate power cannot be generated continuously, it may nevertheless perhaps be generated in a series of short pulses †.

The more complete discussion of the distribution of the additional ionization produced by the gyro wave will be postponed to a future occasion, but we can here without undue labour determine upper and lower limits to that part of the ionosphere which may be the seat of a glow discharge at night when E/p has the value 16 at a level about 90 km. high.

At the height 70 km. the values of p and E are respectively about 7·4 and 1·28 times as large as the corresponding values at 90 km. high, and so the value of E/p is about 2·8. Also it is known that in air with $X/p=2·5$ the value of the attachment ‡ coefficient α'/p is 5×10^{-4} and the value of the electronic ionizing § coefficient α/p is less than 3×10^{-5}, *i. e.*, $\alpha'\gg\alpha$. It follows therefore that at 70 km. and lower the free electrons disappear far more rapidly than they appear through generation by the wave with the value of E/p adopted above, and then that a glow discharge cannot be maintained below 70 km.

* The margin of error in our calculations is such that stations of 120 kw. may well be included in this list.

† *Cf.* M. A. Bontch Bruewitch, 'Nature,' cxxxiii. p. 175 (1934).

‡ V. A. Bailey, Phil. Mag. p. 840 (Oct. 1925).

§ F. H. Sanders, Phys. Rev. xli. (5) p. 667 (Sept. 1932).

Also Table IV. in Part I. shows that even without additional ionization the wave becomes so weak after traversing 6 km. of the E layer that the value of E/p becomes too low for maintaining a discharge.

We may thus conclude that the circular gyro wave emitted with the power W_m can generate a glow only in those regions of the ionosphere which lie between 70 and 96 km. high.

It is now of interest to determine the brightness of such a glow and the degree of illumination at the ground which it may provide.

It can be shown that with the aerial system containing 800 oscillators about half the radiated energy lies within a vertical cone of vertical angle equal to 6°, so the glow may be taken to lie within a cylinder of length about 20 km. and diameter 9 km. with its centre at a height of about 85 km.

The luminous intensity of such a glow discharge in air may be roughly estimated by means of the following facts :—

(*a*) A typical 15 mm. cold-cathode neon sign tube, excited with potentials having a frequency of 60 cycles/sec., has a luminous intensity of 2 candles per watt of energy used *.

(*b*) A high frequency electrodeless discharge in a bulb containing mercury and argon can have a luminous intensity of 10 candles/watt †.

(*c*) A discharge through nitrogen in a tube of 2 cm. diameter and at a pressure of 0·5 mm. of mercury requires an electric force of 5 volts/cm., and can have a luminous intensity of about 0·5 candle/watt ‡.

We may therefore, without serious error in the order of magnitude, assign to our high frequency discharge in air a luminous intensity of 1 candle per watt.

With a radiated power of 500 kw. the total intensity would be about $2{\cdot}5 \times 10^5$ candles, and the corresponding brightness of the glow to an observer on the ground immediately below it would therefore be about 4×10^{-7} candles/cm.^{2}. This is about 50 times as bright as the

* See ' Standard Handbook for Electrical Engineers,' p. 1665 (6th ed., 1933).

† *Id.* p. 1668.

‡ See Engel u. Steenbeck, ' Elektrische Gasentladungen,' vol. ii. p. 250 (J. Springer, 1934).

sky on a moonless night * and about one-twentieth as bright as radioluminous material which contains 1 part in 10^5 of radium. So we may conclude that the celestial glows which the 500 kw. stations at Cincinnati and Moscow could generate would be easily visible.

The corresponding degree of illumination at the ground would then be 4×10^{-5} lux, which is much smaller than the minimum illumination of 0·22 lux required to light roadways †.

An illumination of 0·22 lux at the ground immediately below may, however, be obtained by radiating a power of 10^6 kw. ‡. So to illuminate roadways over an area of 10,000 km.^{2} up to its boundary it would be sufficient to radiate a power of about 2×10^6 kw. §.

The corresponding brightness of the celestial glow would be about 5×10^{-3} candles/cm.^{2}, *i. e.*, about 1/50 that of the full moon, and its apparent diameter would be about ten times that of the moon. It would be surrounded by one or more faint rings corresponding to the loops of the vertical polar diagram of the aerial system.

With this power and aerial system the glow discharge may extend down to levels about 60 km. above the ground, where the air pressure is about 0·1 mm. and the normal value of ν is about 4×10^7. Thus a possible effect of such a powerful and concentrated beam is to set up processes in regions where the value of ν is at least as great as that of Ω, and so we need to reconsider the problem of selecting the most advantageous frequency for generating the glow.

At least in the initial stages, when N is small, the formula (47) for $\bar{w}$ is here applicable with

$$\nu\geqslant4\times10^7 \quad \text{and} \quad \Omega=10^7.$$

We then see that $\bar{w}$, and so u, has a value nearly independent of the frequency ω when $\omega<2\times10^7$. Thus the glow could be maintained at the 60 km. level almost equally well with any wave-length down to 100 metres ;

* *Cf.* Ch. Fabry, ' Introduction Générale à la Photometrie,' p. 41 (1927).

† *Cf.* ' Standard Handbook for Electrical Engineers,' p. 1724.

‡ On account of the corresponding large values of E/p we have here adopted a luminous efficiency of 3 candles/watt.

§ This method of producing useful illumination by means of gyro waves was described by the author in a patent specification filed on 27th November, 1936 (Australian Patent Application no. 4982/36, and British Patent Application no. 32940/37).

resonance at the gyro wave-length λ_g would give only a trifling advantage.

The adoption of a wave-length appreciably greater than λ_g would on the whole be disadvantageous, in particular with regard to the associated aerial system.

The adoption of wave-lengths appreciably less than λ_g would offer some advantages in regard to the aerial system, and these would be greatest at the lowest wave-length 100 metres ; but they would be more than offset by the following disadvantages :—

(*a*) The normal absence of free electrons below the E layer at night may make it impossible with a power of 2×10^6 kw. to *initiate* a discharge in regions as low as the 60 km. level *.

(*b*) It would be necessary to keep the beam concentration as high as possible in order to initiate and maintain a discharge in such low regions ; with much lower beam concentrations the glow would be generated in regions much nearer to the E layer, and then the most effective wave-lengths would be near λ_g ; moreover, with a gyro wave the fact that a low concentration is adequate allows the best possible concentration to be determined empirically with relatively little trouble.

(*c*) With wave-lengths much lower than λ_g a notable amount of the radiation would be reflected down by the E or F layers, and so would be liable to disturb radio receivers over a large area. On the other hand, with the wave-length λ_g nearly all the radiation emitted by our polarizing aerial system is absorbed in the E layer ; for, as shown in the Appendix II., a ray emitted at any angle θ with the vertical has very nearly that polarization which belongs to an extraordinary gyro wave which is propagated in the E layer at the same angle θ to the earth's field, and it is well known that such a wave is almost completely absorbed in the E layer †.

The following experiment, carried out by E. W. B. Gill

* Unless the power is switched on before sunset, when the D layer at 55 km. (reported by Mitra, Syam, and others) may perhaps serve to provide the initial ionization.

† In northern Europe and the U.S.A., where the earth's field is inclined about 20° to the vertical, even with gyro waves there would be some small amount of radiation reflected down again.

and recently published by him *, gives strong support to some of our main conclusions :—

A bulb containing air at a low pressure was placed between two plates connected to a tuned circuit coupled to a medium power generator of 6-metre waves, and a magnetic field of 18 gauss perpendicular to the electric field was applied to the bulb. The effect of the magnetic field on the potential difference V required to start an electrodeless discharge in the bulb with different air pressures p was observed. Above 0·1 mm. there was no appreciable effect, but at lower pressures the potential V was reduced by the factor F as follows :—

p (mm.) ...	0·02,	0·01,	$<0·002$.
F	5,	40,	large.

The last entry indicates that with $p<0·002$ the discharge was easily started with the magnetic field present, but could not be started at all with that field absent.

In recent publications † Dr. Huxley has presented mathematical theories of the action of electric fields on free electrons in a gas and of the propagation of waves through a gas containing free electrons both in the presence of a constant magnetic field, which make a closer study of the approximations involved, and is led to formulæ the exact consequences of which for the theory of radio interaction may require considerable investigation. This problem is in hand, and a preliminary examination suggests that no serious modification of the conclusions in Parts I. and II. is likely to be made. For example, Huxley's formulæ, like ours, lead to resonance in interaction near the gyro frequency, but with a broader maximum in the resonance curve.

In conculusion, I would like to acknowledge the considerable benefit I have derived from the assistance and criticisms of Mr. J. M. Somerville, from discussions with Dr. G. Builder, Dr. A. L. Green, and Professor O. U. Vonwiller; I am also indebted to Mr. C. S. Davis for assistance with the drawing of figs. 1–3, and to Mr. L. Goddard for some computations concerning aerial systems.

* ' Nature,' cxl. p. 1061 (Dec. 18, 1937).

† L. G. H. Huxley, Phil. Mag. xxiii. p. 442 (March 1937), and xxv. p. 148 (Jan. 1938).

SUMMARY.

Following on Part I. of a general investigation, the present publication (Part II.) contains a more complete study of resonance in gyro interaction, and shows that :

1. The resonance curves may have either one or two maxima depending on the height at which the auxiliary wave is reflected.

2. With an appropriate and simple aerial system observable interaction can be caused by radiating, in the form of a directed gyro wave, a power as low as 50 watts.

It is also shown that in latitudes distant from the equator an easily visible electric discharge can be produced in the ionosphere, at levels between 70 and 96 km. high, by means of a suitable aerial system radiating 500 kilowatts of power in the form of a concentrated gyro wave, and that by increasing this power to 2×10^6 kilowatts it is probable that at the least the minimum illumination 0·02 foot-candles prescribed for roadways would be produced over an area of about 10,000 km.^{2}.

APPENDIX I.

Theorem.

The mean work done on an electron per collision by the rotating electric field $\breve{\mathrm{E}}$ of a circularly polarized extraordinary gyro wave, propagated in the direction of the terrestrial magnetic field, is the same as the corresponding work done by a stationary constant field $\breve{\mathrm{X}}$ alone, and with the same gas pressure, when the rotating force E is equal to the stationary force X.

To establish this we have recourse to the formula (13) in (A), namely *

$$w=(\tau/\nu)\sum_{m,\,n}\mathrm{E}_m\mathrm{E}_n\mathrm{T}_m\mathrm{O}_{mn}\mathrm{T}, \quad . \quad . \quad . \quad . \quad (67)$$

where $\breve{\mathrm{E}}$, the vector doing the work w, is given by

$$\breve{\mathrm{E}}=\sum_n \mathrm{E}_n\breve{n}\mathrm{T}_n,$$

E_n is a constant, $\breve{n}$ a unit vector, T_n a function of the time t,

$$\mathrm{O}_{mn}=\breve{m}\breve{n}\mathrm{P}-\breve{h}\mathrm{V}\breve{m}\breve{n}\mathrm{Q}+(\breve{h}\breve{m})(\breve{h}\breve{n})\mathrm{R},$$

$$\mathrm{P}=\partial/(\partial^2+\Omega^2),$$

* On neglecting the transient term w_0.

$$Q=\Omega/(\partial^2+\Omega^2),$$
$$R=\partial^{-1}-P,$$
$$\partial=\nu+D, \quad D=d/dt,$$

and $\breve{h}$ is a unit vector in the direction of the magnetic field.

For the field $\breve{X}$ we have only one value of n, $E_1=X$, $T_1=1$, and $\Omega=0$.

Therefore

$$P=\partial^{-1}, \quad Q=0, \quad R=0,$$
$$O_{11}=P=\partial^{-1},$$
$$T_1O_{11}T_1=\nu^{-1},$$

and so by (67)

$$w(\nu/\tau)=X^2\nu^{-1},$$

i. e.,

$$\bar{w}=\tau X^2/\nu^2. \quad . \quad . \quad . \quad . \quad . \quad . \quad . \quad (68)$$

For the circular gyro field we have

$$\breve{E}=E_1\breve{n}_1T_1+E_2\breve{n}_2T_2,$$

where $\breve{n}_1$, $\breve{n}_2$, and $\breve{h}$ form a right-handed, orthogonal system of vectors, $E_1=E_2=E$, $T_1=\cos\Omega t$, $T_2=\sin\Omega t$.

Applying to this formula (21) in (A), we find that

$$\bar{w}/\tau=Z_1^2\left(\frac{1}{\nu^2}+\frac{1}{\nu^2+4.\Omega^2}\right)\frac{1}{2}+Z_2^2\left(\frac{1}{\nu^2}+\frac{1}{\nu^2+4\Omega^2}\right)\frac{1}{2}$$
$$+Z_1Z_2\left(\frac{1}{\nu^2}-\frac{1}{\nu^2+4\Omega^2}\right),$$

since

$$\breve{n}_1\breve{n}_2=0, \; s^2_{\breve{h}n}=1, \; c^2_{\breve{h}n}=1,$$

and

$$\breve{h}V\breve{n}_1\breve{n}_2=\breve{h}\breve{h}=1.$$

Since also $Z_1=Z_2=E/\sqrt{2}$, it follows that

$$\bar{w}=\tau E^2/\nu^2. \quad . \quad . \quad . \quad . \quad . \quad . \quad . \quad (69)$$

From the formulæ (68) and (69) the theorem clearly follows.

For a stationary alternating field alone the same formula (21) shows that

$$\bar{w}=\tau Z^2/(\nu^2+\omega^2),$$

and so when

$$\omega^2 \ll \nu^2 \text{ and } Z=X$$

the constant and alternating fields do approximately the same mean amount of work on an electron.

In the steady state we have $\overline{w}$ equal to η, the energy lost at a collision, and so

$$\eta(\nu/p)^2=\tau\mathscr{L}^2,$$

where $$\mathscr{L}=\mathrm{X}/p \text{ or } \mathrm{E}/p \text{ or } \mathrm{Z}/p.$$

For a given species of molecule, however, we have also necessarily the fact that η and ν/p are functions of u (the velocity of agitation) alone. It then follows that for a given species u is a function of $\mathscr{L}$ alone.

Experiments * show that with a given gas the velocity u is a single-valued monotonic function of X/p. It follows therefore that at a given pressure the same value of u is produced by each of the forces E, X, and Z.

Appendix II.

Taking a rectangular system of axes with Ox and Oy in the directions respectively of two horizontal oscillating current elements $i_1 l$ and $i_2 l$ at a place in the southern hemisphere, and the axis Oz vertically upwards, *i. e.*, in the same general sense as the earth's magnetic field there, we put a positive electric charge q at the origin O and allow a negative charge $-q$ to rotate around it anti-clockwise in the xy plane† at a fixed distance from O and with the constant angular velocity ω.

At time t the components of the electric moment $-ql$ along Ox and Oy are respectively M_1 and M_2, where

$$\mathrm{M}_1=-ql\cos\omega t, \quad \mathrm{M}_2=ql\sin\omega t.$$

To identify the oscillating electric moment M_1 with the oscillating current element $i_1 l$ we may regard M_1 as due to variable charges $\pm q_1$ on small spheres placed on the x axis and joined by a straight wire of length l. Then

$$i_1=\frac{dq_1}{dt}=\frac{1}{l}\frac{d\mathrm{M}_1}{dt}=\omega\, q\sin\omega t.$$

Similarly $i_2=\omega q\cos\omega t$.

Thus the pair of orthogonal oscillators, each with a current of amplitude I, may be replaced by the equivalent rotating charge q, where $q=\mathrm{I}/\omega$.

* See J. S. Townsend, ' Motion of Electrons in Gases ' (Clarendon Press, 1925).

† *I. e.*, in the sense which would turn Oy through the angle $\pi/2$ and make it coincide with Ox.

According to H. A. Lorentz * the magnetic field vector $\breve{\mathrm{H}}$ at a point P is now given by

$$\breve{\mathrm{H}} = -\frac{q}{c^2 r} \mathrm{V} \breve{\mathrm{A}} \breve{u},$$

where

$\breve{\mathrm{A}}$ is the acceleration vector of the charge $-q$,

$\breve{u}$ is a unit vector in the direction of OP, and

r is equal to OP.

The polarization number is R, where

$$\mathrm{R} = \mathrm{H}'/\mathrm{H}'',$$

and H′, H″ are the components of $\breve{\mathrm{H}}$ respectively in and perpendicular to the magnetic plane zOP.

To find H′ and H″ we first note that

$$\breve{\mathrm{A}} = -\omega^2 \breve{l},$$

where $\breve{l}$ is the position vector of the charge $-q$.

Thus $$\breve{\mathrm{H}} = \mathrm{C} \mathrm{V} \breve{l} \breve{u},$$

where $$\mathrm{C} = q\omega^2/c^2 r,$$

i.e., $\breve{\mathrm{H}}$ lies in the plane N normal to OP and is perpendicular to the projection of $\breve{l}$ on N.

Consequently the end of the vector $\breve{\mathrm{H}}/\mathrm{C}$ describes the ellipse obtained by projecting the circular orbit of $-q$ on the plane N and turning this projection through a right angle.

The major and minor axes of this ellipse are equal to l and $l \cos\theta$ respectively. and so the projections of $\breve{\mathrm{H}}/\mathrm{C}$ on these axes are respectively $-l \cos(\omega t - \phi)$ and $l \cos\theta \sin(\omega t - \phi)$, where θ and ϕ are respectively the zenithal and azimuthal coordinates of P. Since the major axis lies in the magnetic plane the minor axis must be perpendicular to that plane, and so we have

$$\mathrm{H}' = -\mathrm{C} l e^{\iota(\omega t - \phi)}, \quad \mathrm{H}'' = \mathrm{C} l \cos\theta . e^{\iota(\omega t - \phi - \pi/2)}.$$

This at once yields the relation

$$\mathrm{R} = \mathrm{H}'/\mathrm{H}'' = l/\iota \cos\theta,$$

from which †, by comparison with the first formulæ in

* ' The Theory of Electrons,' p. 51 (Teubner, Leipzig, 1909).

† The above formula for R can also be obtained by adding the fields of the two oscillators $i_1 l$ and $i_2 l$ when expressed by means of the standard formula for the distant magnetic field of a Hertzian oscillator.

(24) and (25), we conclude that the wave radiated along OP by the orthogonal pair of oscillators has approximately the same polarization as an extraordinary gyro wave propagated at the angle θ to the earth's magnetic field in a medium for which

$$\nu \ll \Omega(\cot^2\theta + \mathrm{cosec}^2\theta),$$

such, for example, as the E layer.

This conclusion is true also for any array of such orthogonal pairs of oscillators, for the optical interference between waves from different sources travelling in the same direction affects the total intensity but not the polarization. The presence of a reflecting ground also makes no difference when the oscillators are parallel to it.

Corrigenda to Part I.

Page 930, line 9, replace $\Omega = \mathrm{H}e/m$ by $\Omega = -\mathrm{H}e/mc$.
Page 934, line 17, in equation (26) *replace* $|\mathrm{H}|^2$ *by* $|\mathrm{H}_y|^2$.
Page 938, line 8, add $\frac{1}{2}\mathrm{M}^2 w_0$ to R.H.S. of the formula for Δw.
Page 948, line 32, should be $\gamma = \mathrm{S}\omega/\nu p_0^2 = (1+\epsilon)f\mathrm{S}/\mathrm{S}_T\nu^2$.
Page 954, line 4, add $\frac{1}{2}\mathrm{M}^2\bar{w}_e$ to R.H.S. of the formula for $\Delta\bar{w}$.
Page 958, line 31, *replace* footnote * *by* the following :—For a heterogeneous medium this formula still holds true.

XLI. *Electrodynamic Volume and Porosity of Metallic Particles.* *By* H. Löwy, *Dr.Phil.**.

[Received May 13, 1938.]

THE dielectric constant $\bar{\epsilon}$ of a mixture of insulating substances, containing in 1 ccm. $\bar{n}$ molecules of the component h with the polarizability α_h, is given by the equation

$$\frac{\bar{\epsilon}-1}{\bar{\epsilon}+2} = \frac{4\pi}{3}\sum_h \bar{n}_h\alpha_h \quad . \quad . \quad . \quad . \quad . \quad (1)$$

This equation is fundamental in H. A. Lorentz's theory of dielectrics †.

Supposing that this equation is valid also in the case when metallic particles are dispersed in the dielectric, we write (1) in the form

$$\frac{\bar{\epsilon}-1}{\bar{\epsilon}+2} = \frac{4\pi}{3}\left(\sum_i \bar{n}_i\alpha_i + \sum_m \bar{n}_m\alpha_m\right), \quad . \quad . \quad . \quad . \quad (2)$$

* Communicated by the Author.
† H. A. Lorentz. 'Theory of Electrons,' § 117 (Leipzig 1909, Teubner).

designating by index i the insulating substances, by index m the metallic particles.

Applying formula (1) to a volume filled out with the insulating substance i, we have $\bar{\epsilon}=\epsilon_i$ and $\bar{n}_i=n_i$, where n_i is the number of molecules in 1 ccm. of the component i and

$$\frac{\epsilon_i-1}{\epsilon_i+2}=\frac{4\pi}{3}n_i\alpha_i. \quad . \quad . \quad . \quad . \quad . \quad . \quad (3)$$

Designating by v_i the volume which in 1 ccm. of the mixture is filled out with the component i, we have

$$\bar{n}_i=n_i v_i \quad . \quad . \quad . \quad . \quad . \quad . \quad . \quad . \quad (4)$$

and

$$\frac{4\pi}{3}\sum_i \bar{n}_i\alpha_i=\frac{4\pi}{3}\sum_i n_i v_i\alpha_i=\sum_i v_i\frac{\epsilon_i-1}{\epsilon_i+2} \quad . \quad . \quad . \quad (5)$$

If the metallic particles are spheres of radius a_m, the polarizability is

$$\alpha_m=a_m^3 \quad . \quad . \quad . \quad . \quad . \quad . \quad . \quad (6)$$

and equation (2) reduces to

$$\frac{\bar{\epsilon}-1}{\bar{\epsilon}+2}=\sum_i v_i\frac{\epsilon_i-1}{\epsilon_i+2}+\sum_m v_m, \quad . \quad . \quad . \quad . \quad (7)$$

where v_m is the volume, which in 1 ccm. of the mixture is filled out with metal and

$$\sum_i v_i+\sum_m v_m=1 \quad . \quad . \quad . \quad . \quad . \quad . \quad . \quad (8)$$

(7) *and* (8) *are the general equations for metallic suspensions.*

In this deduction we have supposed that the metallic spheres are compact; only in this case we can put

$$\frac{4\pi}{3}\sum_m \bar{n}_m a_m^3=\sum_m v_m. \quad . \quad . \quad . \quad . \quad . \quad (9)$$

We will now consider the following cases of *non compact structure* of the metallic particles:—

1. *The metallic particles are hollow bodies* (for instance spheres). In this case we have

$$\frac{4\pi}{3}\sum_m n_m\alpha_m=\frac{4\pi}{3}\sum_m n_m a_m^3=\sum_m V_m>\sum_m v_m, \quad . \quad (10)$$

V_m being the total volume of the metal spheres in 1 ccm. and v the total volume of the metal in 1 ccm. Instead of (7) and (8) we have the equations

$$\frac{\bar{\epsilon}-1}{\bar{\epsilon}+2}=\sum_i v_i\frac{\epsilon_i-1}{\epsilon_i+2}+\sum_m V_m \quad . \quad . \quad . \quad . \quad (11)$$

$$\sum_i v_i+\sum_m V_m=1 \quad . \quad . \quad . \quad . \quad . \quad . \quad (12)$$

2. *The metallic particles have sponge structure. In this case we put quite generally*

$$\frac{4\pi}{3}\sum_m \bar{n}_m \alpha_m=\sum_m V_m \quad . \quad . \quad . \quad . \quad . \quad (13)$$

and call V_m the "*electrodynamic volume*" which, in general, is different from the *volume filled out with matter*, v_m.

In the case when the insulating substances i are exclusively outside the metal sponge, equations (11) and (12) remain valid, together with (13), instead of the more special equation (10).

In the case when the insulating substances i are *not* exclusively outside the metal sponge, but fill out partially or totally its interstices, the summation $\sum_i$ in both equations (11) and (12) must be restricted to the space outside the metal sponge. The modification of equation (11) is necessitated by *Faraday's cage effect.*

For $i=1$, $m=2$ (two-substances-problem), equations (11) and (12) reduce to one

$$\frac{\bar{\epsilon}-1}{\bar{\epsilon}+2}=(1-V_2)\frac{\epsilon_1-1}{\epsilon_1+2}+V_2 \quad . \quad . \quad . \quad (14)$$

for all the special cases we have considered, the case of the hollow metal body as well as the case of the metal sponge with the insulating substance being exclusively or *not* exclusively outside.

In the case of the two-substances-problem the porosity p_2 of the metallic particles is given by the simple formula

$$p_2=\frac{V_2-v_2}{V_2}, \quad . \quad . \quad . \quad . \quad . \quad . \quad (15)$$

V_2 being the electrodynamic, v_2 the matter-volume of the particles.

TABLE I.

Dry Silt—Cu, $v_2=0{\cdot}05$.

ϵ_1	4·1	4·6	5·2	6·0
$\bar{\epsilon}$ measured.....	4·8	5·4	6·0	6·8
V_2 according to (14)...	0·10	0·11	0·12	0·09
p_2 according to (15) ..	0·50	0·55	0·58	0·44?

TABLE II.

Dry Silt—Brass, $v_2=0{\cdot}06$.

ϵ_1	3·7	4·0	4·5	5·1
$\bar{\epsilon}$ measured.....	7·6	8·8	9·8	14·0
V_2 according to (14)...	0·41	0·44	0·45	0·56
p_2 according to (15) ..	0·86	0·87	0·87	0·89

TABLE III.

Dry Silt—Brass, $v_2=0{\cdot}06$.

ϵ_1	4·1	4·7	5·2	5·9
$\bar{\epsilon}$ measured.....	10·6	11·3	13·1	14·9
V_2 according to (14)...	0·50	0·50	0·53	0·53
p_2 according to (15) ..	0·88	0·88	0·89	0·89

TABLE IV.

Dry Silt—Fe, $v_2=0{\cdot}077$.

ϵ_1	3·0	3·3	3·6	3·8
$\bar{\epsilon}$ measured	3·9	4·8	5·2	5·3
V_2 according to (14)...	0·15	0·23	0·23	0·21
p_2 according to (15) ..	0·49 ?	0·67	0·67	0·63

The measurements of the dielectric constant of metallic suspensions I have made with Dr. M. Mahmoud Ghali * can be used for the determination of the electrodynamic volume V_2 and the porosity p_2 of the metal particles and for the proof of formula (14). For a given concentration v_2 of the metal, the value V_2, calculated according to (14), must be independent of ϵ_1. In each of the following Tables I., II., III., IV., which correspond to Tables V., VI., VII., VIII. in the quoted paper *, the different values of ϵ_1 have been obtained by varying the density of the sand.

The great values of p_2 seem to indicate that we are concerned with the case of hollow bodies. This pseudo-porosity occurs when the metal particles have the shape of leaves which can roll together.

Cairo, May 5, 1938.

XLII. *Operational Forms and Contour Integrals for Struve and other Functions.* *By* N. W. McLachlan, *D.Sc.*†

[Received July 4, 1938.]

1. *Introduction.*

STRUVE'S function is defined to be

$$\mathbf{H}_\nu(t) = \sum_{r=0}^{\infty} \frac{(-1)^r(\frac{1}{2}t)^{\nu+2r+1}}{\Gamma(r+\frac{3}{2})\Gamma(\nu+r+\frac{3}{2})}, \quad . \quad . \quad . \quad (1)$$

from which we find immediately that

$$t^{-\frac{1}{2}}\mathbf{H}_{\frac{1}{2}}(t) = \sqrt{2/\pi}\left[1-\frac{d}{dt}(\sin t)\right]\Big/t. \quad . \quad . \quad . \quad (2)$$

Using the recurrence formula

$$t^{-n+\frac{1}{2}}\mathbf{H}_{n+\frac{1}{2}}(t) = \frac{\sqrt{2/\pi}}{2^n n!} - \frac{d}{dt}[t^{-n+\frac{1}{2}}\mathbf{H}_{n-\frac{1}{2}}(t)], \quad . \quad (3)$$

* H. Löwy and M. M. Ghali. *Gerlands Beiträge zur Geophysik* liii. p. 334, 1938. In this paper the Faraday effect has been ignored and the equations must be modified as indicated in the present paper.

† Communicated by the Author.

we ultimately obtain the relationship

$$t^{-n-\frac{1}{2}}\mathbf{H}_{n+\frac{1}{2}}(t)=\sqrt{2/\pi}\left[\frac{t^{-1}}{2^n n!}+\sum_{r=1}^{n}\frac{(-1)^r}{2^{r-1}(r-1)!}\left(\frac{1}{t}\frac{d}{dt}\right)^r(t^{-1})\right.$$
$$\left.+(-1)^{n+1}\left(\frac{1}{t}\frac{d}{dt}\right)^{n+1}(\sin t)\right], \quad (4)$$

n being a positive integer. The sigma term in (4) may be expressed in the form

$$4\sum_{r=1}^{n}\frac{(2r)!\,(2t)^{-2r-1}}{r!\,(r-1)!}, \quad . \quad . \quad . \quad . \quad . \quad (5)$$

and the last term (including $\sqrt{2/\pi}$) may be replaced by

$$t^{-n-\frac{1}{2}}\mathbf{Y}_{n+\frac{1}{2}}(t)=(-1)^{n+1}\left(\frac{1}{t}\frac{d}{dt}\right)^{n+1}t^{\frac{1}{2}}\mathbf{J}_{\frac{1}{2}}(t). \quad . \quad . \quad (6)$$

From (1) we also get

$$t^{-\frac{1}{2}}\mathbf{H}_{-\frac{1}{2}}(t)=\sqrt{2/\pi}\frac{\sin t}{t}. \quad . \quad . \quad . \quad . \quad . \quad (7)$$

Using the recurrence formula

$$t^{-n+\frac{1}{2}}\mathbf{H}_{-n-\frac{1}{2}}(t)=\frac{d}{dt}[t^{-n+\frac{1}{2}}\mathbf{H}_{-n+\frac{1}{2}}(t)], \quad . \quad . \quad . \quad (8)$$

we find that

$$t^{-n-\frac{1}{2}}\mathbf{H}_{-n-\frac{1}{2}}(t)=\sqrt{2/\pi}\left(\frac{1}{t}\frac{d}{dt}\right)^n\left(\frac{\sin t}{t}\right) \quad . \quad . \quad . \quad . \quad (9)$$

$$=t^{-n-\frac{1}{2}}\mathbf{Y}_{-n-\frac{1}{2}}(t)=(-1)^n t^{-n-\frac{1}{2}}\mathbf{J}_{n+\frac{1}{2}}(t), \quad (10)$$

n being a positive integer.

2. *Operational Forms for Struve Functions of Half Odd Integral Order.*

By virtue of (10) it follows that *

$$\mathbf{H}_{-n-\frac{1}{2}}(t)\supset(-1)^n p/\sqrt{p^2+1}\,(p+\sqrt{p^2+1})^{n+\frac{1}{2}}, \quad (\mathrm{M}) \quad (11)$$

n being a positive integer.

When $n=0$ in (4) we have

$$t^{\frac{1}{2}}\mathbf{H}_{\frac{1}{2}}(t)=\sqrt{2/\pi}\,(1-\cos t) \quad . \quad . \quad . \quad . \quad . \quad . \quad . \quad . \quad . \quad (12)$$

* The new sign $\supset$ for O.F. introduced in a former paper (Phil. Mag. xxvi. p. 395 (1938) is used throughout.

$$\supset \sqrt{2/\pi}\left(1-\frac{p^2}{p^2+1}\right)=\sqrt{2/\pi}/(p^2+1). \quad \text{(M)} \quad (13)$$

Since $\mathbf{H}_{\frac{1}{2}}(t)=\sqrt{2/\pi}t-\mathbf{J}_{-\frac{1}{2}}(t)$, we get

$$\mathbf{H}_{\frac{1}{2}}(t)\supset\sqrt{2p}-\frac{p(p+\sqrt{p^2+1})^{\frac{1}{2}}}{\sqrt{p^2+1}} \quad \text{(M)} \quad (14)$$

By (12)

$$t^{-\frac{1}{2}}\mathbf{H}_{\frac{1}{2}}(t)=\sqrt{2/\pi}\,(1-\cos t)/t \quad (15)$$

$$\supset\sqrt{2/\pi}\,p\int_p^\infty dp/p(p^2+1) \quad (16)$$

$$=\sqrt{2/\pi}\,p\log\left(\frac{\sqrt{p^2+1}}{p}\right). \quad \text{(M)} \quad (17)$$

When $n=1$ in (4) we get

$$t^{\frac{1}{2}}\mathbf{H}_{\frac{3}{2}}(t)=\sqrt{2/\pi}\,[\tfrac{1}{2}t-\sin t+(1-\cos t)/t] \quad (18)$$

$$\supset\sqrt{2/\pi}\left[\frac{1}{2p}-\frac{p}{p^2+1}+p\log\left(\frac{\sqrt{p^2+1}}{p}\right)\right] \quad \text{(M)} \quad (19)$$

by (15) and (17). From (18)

$$t^{-\frac{1}{2}}\mathbf{H}_{\frac{3}{2}}(t)\supset\sqrt{2/\pi}\,p\int_p^\infty\left[\frac{1}{2p^2}-\frac{1}{p^2+1}+\log\left(\frac{\sqrt{p^2+1}}{p}\right)\right]dp \quad (20)$$

$$=\sqrt{2/\pi}\left[\tfrac{1}{2}-p^2\log\left(\frac{\sqrt{p^2+1}}{p}\right)\right]. \quad \text{(M)} \quad (21)$$

Multiplying (18) by t we have

$$t^{\frac{3}{2}}\mathbf{H}_{\frac{3}{2}}(t)=\sqrt{2/\pi}\,[\tfrac{1}{2}t^2-t\sin t+1-\cos t] \quad (22)$$

$$\supset\sqrt{2/\pi}\left[\frac{1}{p^2}+p\frac{d}{dp}\left(\frac{1}{p^2+1}\right)+1-\frac{p^2}{p^2+1}\right]. \quad (23)$$

$$=\sqrt{2/\pi}\left[\frac{3p^2+1}{p^2(p^2+1)^2}\right]. \quad \text{(M)} \quad (24)$$

If $n=0$ in (9) we obtain

$$t^{-\frac{1}{2}}\mathbf{H}_{-\frac{1}{2}}(t)=\sqrt{2/\pi}\,\frac{\sin t}{t} \quad (25)$$

$$\supset \sqrt{2/\pi}\, p \int_p^\infty \frac{dp}{p^2+1} \quad . \quad . \quad . \quad . \quad . \quad . \quad . \quad . \quad . \quad (26)$$

$$= \sqrt{2/\pi}\, p(\tfrac{1}{2}\pi - \tan^{-1} p) = \sqrt{2/\pi}\, p \tan^{-1}(1/p).$$

$$. \quad . \quad . \quad (\mathrm{M}) \quad (27)$$

From (25)

$$t^{\frac{1}{2}}\mathbf{H}_{-\frac{1}{2}}(t) = \sqrt{2/\pi} \sin t \quad . \quad . \quad . \quad . \quad . \quad (28)$$

$$\supset \sqrt{2/\pi}\, p/(p^2+1). \quad . \quad . \quad (\mathrm{M}) \quad (29)$$

Also by (10)

$$\mathbf{H}_{-\frac{1}{2}}(t) = \mathbf{J}_{\frac{1}{2}}(t) \supset p/\sqrt{p^2+1}\,(p+\sqrt{p^2+1})^{\frac{1}{2}}. \quad (\mathrm{M}) \quad (30)$$

From (9) with $n=1$

$$t^{\frac{1}{2}}\mathbf{H}_{-\frac{3}{2}}(t) = \sqrt{2/\pi}\left(\cos t - \frac{\sin t}{t}\right) \quad . \quad . \quad . \quad . \quad . \quad (31)$$

$$\supset \sqrt{2/\pi}\, p\left[\frac{p}{p^2+1} - \tan^{-1}(1/p)\right], \quad (\mathrm{M}) \quad (32)$$

by aid of (27).

Using the known integral

$$\sqrt{\pi/2t}\, \mathbf{H}_\nu(t) = \int_0^{\frac{1}{2}\pi} \mathbf{J}_{\nu+\frac{1}{2}}(t \sin\theta) \sin^{\frac{1}{2}-\nu}\theta \, d\theta. \quad . \quad (33)$$

we get

$$\sqrt{\pi/2}\, p \int_0^\infty e^{-pt} \mathbf{H}_\nu(t)\, dt/t^{\frac{1}{2}}$$

$$= p \int_0^{\frac{1}{2}\pi} \sin^{\frac{1}{2}-\nu}\theta \, d\theta \int_0^\infty e^{-pt} \mathbf{J}_{\nu+\frac{1}{2}}(t \sin\theta)\, dt \quad . \quad . \quad . \quad . \quad (34)$$

$$= p \int_0^{\frac{1}{2}\pi} \sin\theta \, d\theta / \sqrt{p^2+\sin^2\theta}\,(p+\sqrt{p^2+\sin^2\theta})^{\nu+\frac{1}{2}}, \quad (35)$$

$$\mathrm{R}(\nu) > -\tfrac{3}{2}. \quad (\mathrm{M})$$

Writing $y = \sqrt{p^2+\sin^2\theta}$, (35) gives

$$t\mathbf{H}_\nu^{-\frac{1}{2}}(t) \supset \sqrt{2/\pi}\, p \int_p^{\sqrt{p^2+1}} dy/(p+y)^{\nu+\frac{1}{2}}\sqrt{(p^2+1)-y^2}, \quad (36)$$

$$\mathrm{R}(\nu) > -\tfrac{3}{2}. \quad (\mathrm{M})$$

Using formulæ given above, we find that

$$\sqrt{2/\pi}\, p \int_0^{\frac{1}{2}\pi} \sin\theta \, d\theta / \sqrt{p^2+\sin^2\theta}\,(p+\sqrt{p^2+\sin^2\theta})$$

$$= \sqrt{2/\pi}\, p \int_p^\infty dp/p(p^2+1) \quad . \quad . \quad . \quad . \quad . \quad . \quad . \quad (37)$$

$$=\sqrt{2/\pi}\,p\int_p^{\sqrt{p^2+1}} dy/(p+y)\sqrt{(p^2+1)-y^2}. \quad . \quad (38)$$

the value of the integral being given at (17). Also

$$\sqrt{2/\pi}\,p\int_0^{\frac{1}{2}\pi} \sin\theta\, d\theta/\sqrt{p^2+\sin^2\theta}\,(p+\sqrt{p^2+\sin^2\theta})^2\, d\theta$$

$$=\sqrt{2/\pi}\int_p^{\sqrt{p^2+1}} dy/(p+y)^2\sqrt{(p^2+1)-y^2}, \quad (39)$$

these integrals being equal to that at (20), whose value is given at (21).

By expansion and integration term by term we find that

$$\sqrt{2t/\pi}\int_0^{\frac{1}{2}\pi} \mathbf{H}_\nu(t\sin\theta)\sin^{1-\nu}\theta\, d\theta$$

$$=\frac{(\frac{1}{2}t)^{\nu-\frac{1}{2}}}{\Gamma(\nu+\frac{1}{2})}-\mathbf{J}_{\nu-\frac{1}{2}}(t), \quad . \quad . \quad . \quad . \quad . \quad . \quad (40)$$

$$=\frac{1}{(2p)^{\nu-\frac{1}{2}}}-\frac{p}{\sqrt{p^2+1}(p+\sqrt{p^2+1})^{\nu-\frac{1}{2}}}, \quad (41)$$

$$\mathrm{R}(\nu)>-\tfrac{1}{2}. \quad (\mathrm{M})$$

3. *Modified Struve Function.*

This function is defined as

$$\mathbf{L}_\nu(t)=i^{-\nu-1}\mathbf{H}_\nu(t)=\sum_{r=0}^{\infty}\frac{(\frac{1}{2}t)^{\nu+2r+1}}{\Gamma(r+\frac{3}{2})\Gamma(\nu+r+\frac{3}{2})}. \quad . \quad (42)$$

Proceeding as in § 1 we obtain the following formulæ :

$$t^{-n-\frac{1}{2}}\mathbf{L}_{n+\frac{1}{2}}(t)=\sqrt{2/\pi}\left[\frac{-t^{-1}}{2^n n!}+\sum_{r=1}^{n}\frac{1}{2^{r-1}(r-1)!}\left(\frac{1}{t}\frac{d}{dt}\right)^r(t^{-1})\right.$$

$$\left.+\left(\frac{1}{t}\frac{d}{dt}\right)^{n+1}\sinh t\right]. \quad (43)$$

$$t^{-n-\frac{1}{2}}\mathbf{L}_{-n-\frac{1}{2}}(t)=\sqrt{2/\pi}\left(\frac{1}{t}\frac{d}{dt}\right)^n\left(\frac{\sinh t}{t}\right)=\left(\frac{1}{t}\frac{d}{dt}\right)^n[t^{-\frac{1}{2}}\mathbf{I}_{\frac{1}{2}}(t)],$$

$$. \quad . \quad . \quad (44)$$

$$\mathbf{L}_{-n-\frac{1}{2}}(t)=\mathbf{I}_{n+\frac{1}{2}}(t)=\frac{(2t)^{n+\frac{1}{2}}}{\sqrt{\pi}}\frac{d^n}{d(t^2)^n}\left(\frac{\sinh t}{t}\right) \quad . \quad (45)$$

$$=\frac{2(\frac{1}{2}t)^{n+\frac{1}{2}}}{n!\sqrt{\pi}}\left[1-\frac{d^2}{dt^2}\right]^n\left(\frac{\sinh t}{t}\right), \quad . \quad . \quad (46)$$

$$\mathbf{L}_{n+\frac{1}{2}}(t)=(-1)^{n+1}\sum_{r=0}^{n}\frac{(\frac{1}{2}t)^{2r-n-\frac{1}{2}}}{r!\,\Gamma(r-n+\frac{1}{2})}+\mathrm{I}_{-n-\frac{1}{2}}(t). \quad (47)$$

4. *Operational Forms of* **L** *Function of Half Odd Integral Order.*

By virtue of the relationship (45) between $\mathbf{L}_{-n-\frac{1}{2}}(t)$ and $\mathrm{I}_{n+\frac{1}{2}}(t)$ it follows that

$$\mathbf{L}_{-n-\frac{1}{2}}(t)\supset p/\sqrt{p^2+1}\,(p+\sqrt{p^2+1})^{n+\frac{1}{2}}, \quad (\mathrm{M}) \quad (48)$$

n being a positive integer.

We also have

$$t^{\frac{1}{2}}\mathbf{L}_{\frac{1}{2}}(t)=\sqrt{2/\pi}\,(\cosh t-1) \quad . \quad . \quad . \quad . \quad (49)$$

$$\supset 1/(p^2-1) \quad . \quad . \quad . \quad . \quad (\mathrm{M}) \quad (50)$$

$$\mathbf{L}_{\frac{1}{2}}(t)=\sqrt{2/\pi t}\,(\cosh t-1)=-\sqrt{2/\pi t}+\mathrm{I}_{-\frac{1}{2}}(t) \quad . \quad (51)$$

$$\supset -(2p)^{\frac{1}{2}}+\frac{p(p+\sqrt{p^2-1})^{\frac{1}{2}}}{\sqrt{p^2-1}} \quad . \quad . \quad . \quad (\mathrm{M}) \quad (52)$$

$$t^{-\frac{1}{2}}\mathbf{L}_{\frac{1}{2}}(t)=\sqrt{2/\pi}\,(\cosh t-1)/t \quad . \quad . \quad . \quad . \quad (53)$$

$$\supset \sqrt{2/\pi}\,p\log\left(\frac{\sqrt{p^2-1}}{p}\right) \quad . \quad . \quad (\mathrm{M}) \quad (54)$$

$$t^{\frac{1}{2}}\mathbf{L}_{\frac{3}{2}}(t)=\sqrt{2/\pi}\left[\sinh t-\left(\frac{\cosh t-1}{t}\right)-\tfrac{1}{2}t\right] \quad . \quad . \quad . \quad . \quad (55)$$

$$\supset \sqrt{2/\pi}\left[\frac{p}{p^2-1}-p\log\left(\frac{\sqrt{p^2-1}}{p}\right)-\frac{1}{2p}\right]. \quad (\mathrm{M}) \quad (56)$$

$$t^{-\frac{1}{2}}\mathbf{L}_{\frac{3}{2}}(t)=\frac{\sqrt{2/\pi}}{t}\left[\sinh t-\left(\frac{\cosh t-1}{t}\right)-\tfrac{1}{2}t\right] \quad . \quad (57)$$

$$\supset \sqrt{2/\pi}\left[p^2\log\left(\frac{\sqrt{p^2-1}}{p}\right)-\tfrac{1}{2}\right]. \quad (\mathrm{M}) \quad (58)$$

$$t^{\frac{3}{2}}\mathbf{L}_{\frac{3}{2}}(t)=\sqrt{2/\pi}\,[t\sinh t-\cosh t+1-\tfrac{1}{2}t^2] \quad . \quad . \quad . \quad (59)$$

$$\supset \sqrt{2/\pi}\left[-p\frac{d}{dp}\left(\frac{1}{p^2-1}\right)-\frac{p^2}{p^2-1}+1-\frac{1}{p^2}\right] \quad (60)$$

$$=\sqrt{2/\pi}\left[\frac{3p^2-1}{p^2(p^2-1)^2}\right]. \quad . \quad . \quad . \quad . \quad . \quad (\mathrm{M}) \quad (61)$$

$$t^{-\frac{1}{2}}\mathbf{L}_{-\frac{1}{2}}(t)=\sqrt{2/\pi}\sinh t/t \quad . \quad . \quad . \quad . \quad (62)$$

$$\supset \sqrt{2/\pi}\, p \coth^{-1} p. \quad . \quad . \quad (\mathrm{M}) \quad (63)$$

$$t^{\frac{1}{2}}\mathbf{L}_{-\frac{1}{2}}(t) = \sqrt{2/\pi}\sinh t = t^{\frac{1}{2}}\mathrm{I}_{\frac{1}{2}}(t) \quad . \quad . \quad . \quad (64)$$

$$\supset \sqrt{2/\pi}\, p/(p^2-1). \quad . \quad . \quad (\mathrm{M}) \quad (65)$$

$$\mathbf{L}_{-\frac{1}{2}}(t) = \mathrm{I}_{\frac{1}{2}}(t) \supset p/\sqrt{p^2-1}\,(p+\sqrt{p^2-1})^{\frac{1}{2}}. \quad (\mathrm{M}) \quad (66)$$

$$t^{\frac{1}{2}}\mathbf{L}_{-\frac{3}{2}}(t) = \sqrt{2/\pi}\,(\cosh t - \sinh t/t) \quad . \quad . \quad . \quad . \quad (67)$$

$$\supset \sqrt{2/\pi}\, p\left(\frac{p}{p^2-1} - \coth^{-1} p\right). \quad (\mathrm{M}) \quad (68)$$

$$\sqrt{\pi/2t}\,\mathbf{L}_\nu(t) \supset p\int_0^{\frac{1}{2}\pi} \sin\theta\, d\theta/\sqrt{p^2-\sin^2\theta}\,(p+\sqrt{p^2-\sin^2\theta})^{\nu+\frac{1}{2}},$$

$$\quad . \quad . \quad . \quad (69)$$

$$\mathrm{R}(\nu) > -\tfrac{3}{2}.$$

Writing $v = \sqrt{p^2-\sin^2\theta}$, (69) becomes

$$\sqrt{\pi/2t}\,\mathbf{L}_\nu(t) \supset \sqrt{\pi}/2\, p\int_0^\infty e^{-pt}\mathbf{L}_\nu(t)\, dt/t^{\frac{1}{2}} \quad . \quad . \quad . \quad . \quad (70)$$

$$= p\int_p^{\sqrt{p^2+1}} dv/(p+v)^{\nu+\frac{1}{2}}\sqrt{v^2-(p^2-1)},$$

$$\quad . \quad . \quad . \quad (\mathrm{M}) \quad (71)$$

$$\mathrm{R}(\nu) > -\tfrac{3}{2}.$$

Also

$$\sqrt{2t/\pi}\int_0^{\frac{1}{2}\pi} \mathbf{L}_\nu(t\sin\theta)\sin^{1-\nu}\theta\, d\theta$$

$$= \mathrm{I}_{\nu-\frac{1}{2}}(t) - \frac{(\frac{1}{2}t)^{\nu-\frac{1}{2}}}{\Gamma(\nu+\frac{1}{2})} \quad . \quad . \quad . \quad . \quad . \quad . \quad (72)$$

$$\supset \frac{p}{\sqrt{p^2-1}\,(p+\sqrt{p^2-1})^{\nu-\frac{1}{2}}} - \frac{1}{(2p)^{\nu-\frac{1}{2}}}, \quad (73)$$

$$\mathrm{R}(\nu) > -\tfrac{1}{2}. \quad (\mathrm{M})$$

5. *Circular Functions.*

By a well-known formula

$$e^{\pm it}t^\nu \supset \Gamma(1+\nu)\, p/(p\mp i)^{\nu+1}, \quad . \quad . \quad . \quad (74)$$

$$\mathrm{R}(\nu) > -1,$$

so $$t^\nu \sin t \supset \frac{\Gamma(1+\nu)\, p}{2i(p^2+1)^{\nu+1}}[(p+i)^{\nu+1} - (p-i)^{\nu+1}], \quad (\mathrm{M}) \quad (75)$$

$$\mathrm{R}(\nu) > -1,$$

and

$$t^{\nu}\cos t \supset \frac{\Gamma(1+\nu)p}{2(p^2+1)^{\nu+1}}[(p+i)^{\nu+1}+(p-i)^{\nu+1}], \quad \text{(M)} \quad (76)$$

$$\mathrm{R}(\nu)>-1.$$

When $\nu=n$, a positive integer

$$t^n\left\{\begin{matrix}\sin t\\ \cos t\end{matrix}\right\} \supset \frac{n!\,p}{(p^2+1)^{\frac{1}{2}n+\frac{1}{2}}}\left\{\begin{matrix}\sin\\ \cos\end{matrix}\right\}[(n+1)\tan^{-1}(1/p)], \quad \text{(M)} \quad (77)$$

By aid of a known integral

$$t^{-\frac{1}{2}}\cos bt^{\frac{1}{2}} \supset \sqrt{\pi p}\, e^{-b^2/4p}. \quad . \quad . \quad \text{(M)} \quad (78)$$

Differentiating with respect to b gives

$$\sin bt^{\frac{1}{2}} \supset \sqrt{\pi/p}\, b\frac{e^{-b^2/4p}}{2}. \quad . \quad . \quad \text{(M)} \quad (79)$$

Applying one of the rules of the operational calculus to (78) yields

$$t^{\frac{1}{2}}\cos bt^{\frac{1}{2}} \supset \frac{\sqrt{\pi/p}}{2}\, e^{-b^2/4p}\left(1-\frac{b^2}{2p}\right). \quad \text{(M)} \quad (80)$$

For the range $0<t<1$,

$$p\int_0^1 e^{-pt}(1-t^2)^{\nu}\,dt \supset (1-t^2)^{\nu} \quad . \quad . \quad . \quad . \quad . \quad . \quad . \quad . \quad . \quad (81)$$

$$=\tfrac{1}{2}\sqrt{\pi}\,\Gamma(\nu+1)\left(\frac{2}{p}\right)^{\nu-\frac{1}{2}}[\mathrm{I}_{\nu+\frac{1}{2}}(p)-\mathbf{L}_{\nu+\frac{1}{2}}(p)], \quad . \quad . \quad . \quad (82)$$

$$\mathrm{R}(\nu)>-1.$$

When $\nu=-\frac{1}{2}$ in (82), we have

$$1/\sqrt{1-t^2} \supset \tfrac{1}{2}\pi p[\mathrm{I}_0(p)-\mathbf{L}_0(p)], \quad . \quad . \quad . \quad (83)$$

$$0<t<1,$$

and since $\dfrac{d}{dt}(\sin^{-1}t)=1/\sqrt{1-t^2}$, by the integration rule it follows that

$$\sin^{-1}t \supset \tfrac{1}{2}\pi[\mathrm{I}_0(p)-\mathbf{L}_0(p)], \quad . \quad . \quad . \quad . \quad (84)$$

$$0<t<1.$$

Using another rule, (83) and (84) yield

$$t/\sqrt{1-t^2} \supset \tfrac{1}{2}\pi p[\mathbf{L}_1(p)-\mathrm{I}_1(p)]+p, \quad . \quad . \quad (85)$$

$$0<t<1,$$

and $$t\sin^{-1}t \supset \tfrac{1}{2}\pi\left[\frac{\mathbf{L}_0(p)-\mathrm{I}_0(p)}{p}+\mathbf{L}_1(p)-\mathrm{I}_1(p)\right]+1, \quad (86)$$
$$0<t<1.$$

6. *Hyperbolic Functions.*

By definition, $\operatorname{cosech} t = 2/(e^t-e^{-t})$

$$=2\sum_{r=0}^{\infty} e^{-(2r+1)t}; \quad . \quad . \quad . \quad . \quad (87)$$

also $$\frac{2e^{-(2r+1)t}t^{\nu-1}}{\Gamma(\nu)} \supset 2p/(p+2r+1)^{\nu} = \frac{2^{-\nu+1}p}{\left(\frac{p+1}{2}+r\right)}. \quad (88)$$

Hence from (87) and (88)

$$\frac{(2t)^{\nu-1}}{\Gamma(\nu)}\operatorname{cosech} t \supset p\sum_{r=0}^{\infty}\frac{1}{\left(\frac{p+1}{2}+r\right)^{\nu}} \quad . \quad . \quad (89)$$

$$=p\zeta\left(\nu,\frac{p+1}{2}\right), \quad . \quad (\mathrm{M}) \quad (90)$$
$$\mathrm{R}(\nu)>1,$$

ζ signifying the zeta function. In like manner we find that

$$\frac{(2t)^{\nu-1}}{\Gamma(\nu)}\coth t \supset p\sum_{r=0}^{\infty}\frac{1}{\left(\frac{p}{2}+r\right)^{\nu}}-\left(\frac{2}{p}\right)^{\nu-1} \quad . \quad (91)$$

$$=p\zeta(\nu,p/2)-(2/p)^{\nu-1}, \quad . \quad (\mathrm{M}) \quad (92)$$
$$\mathrm{R}(\nu)>1.$$

Writing unity for i in (74), we get

$$t^{\nu}\left\{\begin{matrix}\sinh t\\ \cosh t\end{matrix}\right\} \supset \frac{\Gamma(1+\nu)p}{2(p^2-1)^{\nu+1}}[(p+1)^{\nu+1}\pm(p-1)^{\nu+1}],$$
$$. \quad . \quad . \quad (\mathrm{M}) \quad (93)$$
$$\mathrm{R}(\nu)>-1.$$

By definition

$$\tanh t=\frac{e^t-e^{-t}}{e^t+e_{-t}}=1+2\sum_{r=1}^{\infty}(-1)^r e^{-2rt} \quad . \quad . \quad (94)$$

$$\supset 1+2p\sum_{r=1}^{\infty}\frac{(-1)^r}{(p+2r)} \quad . \quad . \quad . \quad . \quad . \quad (95)$$

$$= \tfrac{1}{2}p\left[\psi\left(\frac{p+2}{4}\right) - \psi\left(\frac{p}{4}\right)\right] - 1, \quad \text{(M)} \quad (96)$$

$$= p\left[\psi\left(\frac{p}{2}\right) - \psi\left(\frac{p}{4}\right)\right]^{*} - 1, \quad \text{(M)} \quad (97)$$

where ψ represents the logarithmic derivative of the gamma function. Since $\tanh 0 = 0$, by the differentiation rule we obtain

$$\operatorname{sech}^2 t \supset \tfrac{1}{2}p^2\left[\psi\left(\frac{p+2}{4}\right) - \psi\left(\frac{p}{4}\right)\right] - p \quad (98)$$

$$= p^2\left[\psi\left(\frac{p}{2}\right) - \psi\left(\frac{p}{4}\right)\right]. \quad (99)$$

Proceeding as at (94)–(96), we find that

$$\operatorname{sech} t \supset \tfrac{1}{2}p\left[\psi\left(\frac{p+3}{4}\right) - \psi\left(\frac{p+1}{4}\right)\right]. \quad \text{(M)} \quad (100)$$

By aid of known integrals, we get

$$t^{-1}\tanh t \supset p\log(p/4) + 2p\log\left[\Gamma(p/4)\Big/\Gamma\left(\frac{p+2}{4}\right)\right] \quad (101)$$

and $t^{-1}(1 - \operatorname{sech} t)$

$$\supset -p\log(p/4) + 2p\log\left[\Gamma\left(\frac{p+3}{4}\right)\Big/\Gamma\left(\frac{p+1}{4}\right)\right]. \quad (102)$$

Since $$p\int_0^\infty \frac{e^{-pt}\,dt}{\sqrt{1+t^2}} = \tfrac{1}{2}\pi p[\mathbf{H}_0(p) - \mathrm{Y}_0(p)], \quad (103)$$

$$1/\sqrt{1+t^2} \supset \tfrac{1}{2}\pi p[\mathbf{H}_0(p) - \mathrm{Y}_0(p)]; \quad (104)$$

and since $\dfrac{d}{dt}\sinh^{-1} t = 1/\sqrt{1+t^2}$, we have

$$\sinh^{-1} t \supset \tfrac{1}{2}\pi[\mathbf{H}_0(p) - \mathrm{Y}_0(p)]. \quad \text{(M)} \quad (105)$$

Applying one of the rules to (104) and (105), we obtain

$$t/\sqrt{1+t^2} \supset \tfrac{1}{2}\pi p[\mathbf{H}_1(p) - \mathrm{Y}_1(p)] - p \quad (106)$$

and $$t\sinh^{-1} t \supset \tfrac{1}{2}\pi\left[\frac{\mathbf{H}_0(p) - \mathrm{Y}_0(p)}{p} + \mathbf{H}_1(p) - \mathrm{Y}_1(p)\right] - 1. \quad \text{(M)} \quad (107)$$

* This alternative expression was found independently by Prof. P. Humbert, who communicated it to the author.

By a simple transformation we have

$$p\int_1^\infty e^{-pt}\frac{\cosh(\nu\cosh^{-1}t)\,dt}{\sqrt{t^2-1}}=p\int_0^\infty e^{-p\cosh u}\cosh\nu u\,du, \quad (108)$$

so
$$\frac{\cosh(\nu\cosh^{-1}t)}{\sqrt{t^2-1}}\supset pK_\nu(p), \quad . \quad (M) \quad (109)$$
$$t>1.$$

Applying the integration rule to (109) gives

$$\int_1^t\frac{\cosh(\nu\cosh^{-1}t)}{\sqrt{t^2-1}}dt\supset K_\nu(p), \quad . \quad (M) \quad (110)$$
$$t>1.$$

The integral in (110) can be expressed in the form

$$\frac{1}{\nu}\int_1^t\cosh(\nu\cosh^{-1}t)d(\nu\cosh^{-1}t)=\frac{1}{\nu}\sinh(\nu\cosh^{-1}t), \quad (111)$$

so
$$\sinh(\nu\cosh^{-1}t)\supset\nu K_\nu(p), \quad . \quad (M) \quad (112)$$
$$t>1,$$

or
$$\int_0^\infty e^{-p\cosh\theta}\sinh\theta\sinh\nu\theta\,d\theta=\frac{\nu}{p}K_\nu(p), \quad . \quad (113)$$

$\cosh\theta$ being written for t in the Laplace integral which corresponds to the l.h.s. of (112).

Corresponding to formulæ (78), (79), (80), we have

$$t^{-\frac{1}{2}}\cosh bt^{\frac{1}{2}}\supset\sqrt{p\pi}\,e^{b^2/4p}, \quad . \quad . \quad (M) \quad (114)$$

$$\sinh bt^{\frac{1}{2}}\supset\frac{\sqrt{\pi/p}}{2}.be^{b^2/4p}, \quad . \quad (M) \quad (115)$$

and
$$t^{\frac{1}{2}}\cosh bt^{\frac{1}{2}}\supset\frac{\sqrt{\pi/p}}{2}e^{b^2/4p}\left(1+\frac{b^2}{2p}\right). \quad (M) \quad (116)$$

Combining the two sets of formulæ yields

$$t^{-\frac{1}{2}}(\cosh bt^{\frac{1}{2}}\pm\cos bt^{\frac{1}{2}})\supset 2\sqrt{\pi p}\left\{\begin{matrix}\cosh\\ \sinh\end{matrix}\right\}b^2/4p, \quad (M) \quad (117)$$

$$\sinh bt^{\frac{1}{2}}\pm\sin bt^{\frac{1}{2}}\supset\sqrt{\pi/p}\,b\left\{\begin{matrix}\cosh\\ \sinh\end{matrix}\right\}b^2/4p, \quad (M) \quad (118)$$

and $t^{\frac{1}{2}}(\cosh bt^{\frac{1}{2}} \pm \cos bt^{\frac{1}{2}})$

$$\supset \sqrt{\pi/p}\left[\begin{Bmatrix}\cosh\\ \sinh\end{Bmatrix}\frac{b^2}{4p} + \frac{b^2}{2p}\begin{Bmatrix}\sinh\\ \cosh\end{Bmatrix}\frac{b^2}{4p}\right]. \quad . \quad . \quad (\mathrm{M}) \quad (119)$$

7. *Exponential Functions.*

Proceeding as at (94)–(96), we readily find that

$$1/(1+e^{-t}) \supset \tfrac{1}{2}p\left[\psi\left(\frac{p-1}{2}\right) - \psi\left(\frac{p}{2}\right)\right]; \quad (\mathrm{M}) \quad (120)$$

and that

$$(1-e^{-at})/(1-e^{-t}) \supset p[\psi(p+a)-\psi(p)], \quad (\mathrm{M}) \quad (121)$$
$$\mathrm{R}(a)>0, \ \mathrm{R}(p+a)>0.$$

By a known integral

$$\frac{(1-e^{-at})(1-e^{-bt})}{t(1-e^{-t})}$$
$$\supset p\log[\Gamma(p)\Gamma(p+a+b)/\Gamma(p+a)\Gamma(p+b)], \quad (\mathrm{M}) \quad (122)$$
if $\mathrm{R}(p)>0$, $\mathrm{R}(p+a)>0$, $\mathrm{R}(p+b)>0$, $\mathrm{R}(p+a+b)>0$.

Applying one of the rules to (122) gives

$$\frac{(1-e^{-at})(1-e^{-bt})}{(1-e^{-t})}$$
$$\supset p[\psi(p+b)+\psi(p+a)-\psi(p+a+b)-\psi(p)], \quad (\mathrm{M}) \quad (123)$$

with the restrictions below (122).

By a known integral

$$\frac{t^{\nu-1}}{\Gamma(\nu)(1-e^{-t})} \supset p\zeta(\nu, p), \quad . \quad . \quad . \quad (\mathrm{M}) \quad (124)$$

$\mathrm{R}(p)>1$, $\mathrm{R}(\nu)>1$. When $\nu=2$ by aid of the shift rule we obtain

$$\frac{te^{-t}}{(1-e^{-t})} = 1-\tfrac{1}{2}t-\sum_{n=1}^{\infty}(-1)^n \mathrm{B}_n\frac{t^{2n}}{(2n)!} \supset p\zeta(2, p+1),$$
$$. \quad . \quad . \quad (\mathrm{M}) \quad (125)$$

B_n being the nth Bernoullian number. Using another known integral, we have

$$e^{-t^2}t^{\nu-1} \supset \frac{\Gamma(\nu/2)}{\sqrt{\pi}}\, p\int_0^{\infty} e^{-x^2}\,dx \Big/ \left(1+\frac{p^2}{4x^2}\right)^{\nu/2} \quad . \quad (126)$$

$$= \frac{\Gamma(\nu)}{2^{\nu/2}}\, p e^{p^2/8} D_{-\nu}(p\sqrt{2}), \quad . \quad . \quad . \quad . \quad (127)$$

$$R(\nu) > 1,$$

D signifying Weber's parabolic cylinder function.

8. *Product Bessel Functions.*

In the Phil. Mag. xxi. p. 308 (1936) J. C. Costello introduced series relating to products of ber and bei functions. Using Costello's notation, we have

$$t^{\frac{1}{2}} W_\nu^{(b)}(2t^{\frac{1}{2}}) = t^{\frac{1}{2}}(\mathrm{ber}_\nu 2t^{\frac{1}{2}}\, \mathrm{bei}'_\nu 2t^{\frac{1}{2}} - \mathrm{bei}_\nu 2t^{\frac{1}{2}}\, \mathrm{ber}' 2t^{\frac{1}{2}}) \quad (128)$$

$$= \sum_{r=0}^{\infty} t^{\nu+2r+1}/r!\, \Gamma(\nu+r+1)\, \Gamma(\nu+2r+2) \quad (129)$$

$$\supset \sum_{r=0}^{\infty} 1/r!\, \Gamma(\nu+r+1)\, p^{\nu+2r+1} \quad . \quad . \quad . \quad (130)$$

$$= \frac{1}{p} I_\nu(2/p), \quad . \quad . \quad . \quad . \quad . \quad . \quad . \quad (M) \quad (131)$$

$$R(\nu) > -?.$$

$$X_\nu^{(b)}(2t^{\frac{1}{2}}) = \sum_{r=0}^{\infty} t^{\nu+2r}/r!\, \Gamma(\nu+r+1)\, \Gamma(\nu+2r+1) \quad (132)$$

$$= \frac{d}{dt}[t^{\frac{1}{2}} W_\nu^{(b)}(2t^{\frac{1}{2}})] = \mathrm{ber}_\nu^2 2t^{\frac{1}{2}} + \mathrm{bei}_\nu^2 2t^{\frac{1}{2}} \quad . \quad (133)$$

$$\supset I_\nu(2/p), \quad . \quad . \quad . \quad . \quad . \quad . \quad . \quad . \quad (M) \quad (134)$$

since $f(0) = [t^{\frac{1}{2}} W_\nu^{(b)}(2t^{\frac{1}{2}})]_{t=0} = 0, \quad R(\nu) > -1.$

This form was obtained for $\mathrm{ber}_\nu^2 2t^{\frac{1}{2}} + \mathrm{bei}_\nu^2 2t^{\frac{1}{2}}$ by McLachlan and Meyers *, whilst Humbert † has given the form for argument $-2\sqrt{2ti}$.

$$t^{-\frac{1}{2}} Z_\nu^{(b)}(2t^{\frac{1}{2}}) = 2t^{-\frac{1}{2}}(\mathrm{ber}_\nu 2t^{\frac{1}{2}}\, \mathrm{bei}'_\nu 2t^{\frac{1}{2}} + \mathrm{bei}_\nu 2t^{\frac{1}{2}}\, \mathrm{ber}' 2t^{\frac{1}{2}})$$

$$= \frac{d}{dt}[X_\nu^{(b)}(2t^{\frac{1}{2}})] \quad . \quad . \quad (135)$$

$$= \sum_{r=0}^{\infty} t^{\nu+2r-1}/r!\, \Gamma(\nu+r+1)\, \Gamma(\nu+2r) \quad . \quad (136)$$

$$\supset p I_\nu(2/p), \quad . \quad . \quad . \quad . \quad . \quad . \quad . \quad . \quad (M) \quad (137)$$

since $[X_\nu^{(b)}(2t^{\frac{1}{2}})]_{t=0} = 0, \quad R(\nu) > 0.$

* Phil. Mag. xxiii. p. 761 (1937); xxiii. p. 918 (1937).
† Phil. Mag. xxiv. p. 888 (1937).

$$V_\nu^{(b)}(2t^{\frac{1}{2}}) = \sum_{r=0}^{\infty} (\nu+2r)\, t^{\nu+2r+1}/r!\, \Gamma(\nu+r+1)\, \Gamma(\nu+2r) \quad (138)$$

$$= \frac{d}{dt}[t^{\frac{1}{2}} Z_\nu^{(b)}(2t^{\frac{1}{2}})] = \mathrm{ber}_\nu' 2t^{\frac{1}{2}} + \mathrm{bei}_\nu' 2t^{\frac{1}{2}} \quad . \quad . \quad . \quad (139)$$

$$\supset p^2 I_\nu(2/p), \quad . \quad . \quad . \quad . \quad . \quad . \quad . \quad . \quad . \quad (\mathrm{M}) \quad (140)$$

since $[t^{\frac{1}{2}} Z_\nu^{b)}(2t^{\frac{1}{2}})]_{t=0} = 0, \quad \mathrm{R}(\nu) > +1.$

9. *Miscellaneous Functions.*

Using known integrals, we obtain the three forms at (141)–(143), namely,

$$(1-t^2)^{\nu-\frac{1}{2}} \supset \sqrt{\pi}\, \Gamma(\nu+\tfrac{1}{2}) p (2/p)^\nu I_\nu(p), \quad . \quad (141)^*$$
$$-1<t<1, \quad \mathrm{R}(\nu) > -\tfrac{1}{2},$$

$$(t^2-1)^{\nu-\frac{1}{2}} \supset \frac{\Gamma(\nu+\frac{1}{2})}{\sqrt{\pi}} p (2/p)^\nu K_\nu(p), \quad (\mathrm{M}) \quad (142)$$
$$t>1, \quad \mathrm{R}(\nu) > -\tfrac{1}{2};$$

and $$(1+t)^{-\nu} \supset p\mathrm{S}(\nu, p) = p^{\frac{1}{2}\nu} e^{\frac{1}{2}p} \mathrm{W}_{-\frac{1}{2}\nu, \frac{1}{2}-\frac{1}{2}\nu}(p), \quad . \quad (143)$$

where S represents Schlömilch's function and W the confluent hypergeometric function. By aid of one of the rules we obtain from (143)

$$t(1+t)^{-\nu} \supset 1-(p-\nu+1)\,\mathrm{S}(\nu, p) \quad . \quad . \quad . \quad . \quad . \quad (144)$$

$$= 1 - p^{\frac{1}{2}\nu-1}(p-\nu+1)\, e^{\frac{1}{2}p} \mathrm{W}_{-\frac{1}{2}\nu, \frac{1}{2}(1-\nu)}(p). \quad (145)$$

To determine the O.F. of $(2bt-t^2)^{\nu-\frac{1}{2}}$ we proceed as follows:—

$$\phi(p) = p \int_0^{2b} e^{-pt}[b^2-(b-t)^2]^{\nu-\frac{1}{2}} dt \quad . \quad . \quad (146)$$

$$= p e^{-pb} b^{2\nu} \int_{-1}^{+1} e^{pbx}(1-x^2)^{\nu-\frac{1}{2}} dx, \quad . \quad . \quad (147)$$

where $x = (1-t/b)$.

Consequently

$$(2bt-t^2)^{\nu-\frac{1}{2}} \supset \sqrt{\pi}\, \Gamma(\nu+\tfrac{1}{2})\, p . (2b/p)^\nu e^{-pb} I_\nu(pb), \quad (\mathrm{M}) \quad (148)$$
$$\mathrm{R}(\nu) > -\tfrac{1}{2}, \quad 0<t<2b.$$

For $(t^2+2bt)^\nu$ we have

$$\phi(p) = p \int_0^\infty e^{-pt}[(t+b)^2-b^2]^\nu dt \quad . \quad . \quad (149)$$

* This form belongs to system B; the form for system A is given at (82). See Phil. Mag. xxv. p. 259 (1938).

$$=pe^{\frac{1}{2}pb}b^{2\nu+1}\int_1^\infty e^{-pbx}(x^2-1)^\nu\,dx, \quad . \quad (150)$$

so $$(t^2+2bt)^\nu \supset \frac{\Gamma(\nu+1)}{\sqrt{\pi}}p(2b/p)^{\nu+\frac{1}{2}}e^{pb}\mathrm{K}_{\nu+\frac{1}{2}}(pb), \quad . \quad (151)$$

$t>0$, $\mathrm{R}(\nu)>-1$.

10. *Contour Integrals.*

The operational forms given herein are based upon what was designated system A (the Laplace transform) in a former paper *, but the majority of them are in accordance with system E (the Mellin inversion theorem with lower limit 0 or 1 as the case may be). The forms valid on system E are distinguished by the letter M. Moreover, corresponding to each O.F. $[\phi(p)\subset f(t)]$ so marked, we have the contour integral

$$f(t)=\frac{1}{2\pi i}\int_{c-i\infty}^{c+i\infty}e^{zt}\phi(z)\frac{dz}{z}. \quad . \quad . \quad . \quad (152)$$

There are sixty-three integrals of this type, many of which can be transformed and/or referred to the contour $-\infty$, $(0+)$, $-\infty$, as shown in another paper †.

11. *Three additional Rules.*

1. We know that

$$\frac{d}{dt}f(t)\supset p\,\phi(p) \quad . \quad . \quad . \quad . \quad . \quad (153)$$

if $f(0)=0$; and by a known rule

$$\left(\frac{1}{t}\frac{d}{dt}\right)f(t)\supset p\int_p^\infty\phi(p)\,dp; \quad . \quad . \quad . \quad (154)$$

also

$$\frac{d}{dt}\left(\frac{1}{t}\frac{d}{dt}\right)f(t)\supset p^2\int_p^\infty\phi(p)\,dp \quad . \quad . \quad . \quad (155)$$

if $\left[\frac{1}{t}\frac{d}{dt}f(t)\right]_{t=0}=0$. Ultimately we get

$$\left(\frac{1}{t}\frac{d}{dt}\right)^n f(t)\supset p\int_p^\infty p\int_p^\infty\ldots p\int_p^\infty\phi(p)\,(dp)^n; \quad . \quad (156)$$

* Phil. Mag. xxv. p. 259 (1938).
† Phil. Mag. xxiii. p. 761 (1937).

provided $\left[\left(\frac{1}{t}\frac{d}{dt}\right)^r f(t)\right]_{t=0} = 0, \quad r=0, 1, 2, \ldots (n-1).$

2. We know that

$$tf(t) \supset -p\frac{d}{dp}[\phi(p)/p], \quad . \quad . \quad . \quad . \quad (157)$$

and by a known rule

$$\int_0^t tf(t)\,dt \supset -\frac{d}{dp}[\phi(p)/p]; \quad . \quad . \quad . \quad (158)$$

also by another rule

$$t\int_0^t tf(t)\,dt \supset p\frac{d}{dp}\left\{\frac{1}{p}\frac{d}{dp}[\phi(p)/p]\right\}. \quad . \quad (159)$$

Ultimately we obtain the rule

$$\int_0^t t\int_0^t \ldots t\int_0^t tf(t)\,(dt)^n \supset (-1)^n p\left(\frac{1}{p}\frac{d}{dp}\right)^n\left\{\frac{\phi(p)}{p}\right\}. \quad . \quad . \quad . \quad (160)$$

3. By a known rule *

$$\int_0^\infty e^{-pt}f(t^2)\,dt = \frac{1}{\sqrt{\pi}}\int_0^\infty e^{-p^2v^2/4}\,\phi(1/v^2)\,dv. \quad . \quad (161)$$

If we write $v^2=s^\nu$, where $R(\nu)\neq 0$, (161) becomes

$$\int_0^\infty e^{-pt}f(t^2)\,dt = \frac{\nu}{2\sqrt{\pi}}\int_0^\infty e^{-p^2s^{\nu/4}}\,\phi(s^{-\nu})\,s^{\frac{1}{2}\nu-1}\,ds. \quad . \quad (162)$$

Differentiating both sides of (162) with respect to p, n times, and multiplying by p throughout, we get

$$p\int_0^\infty e^{-pt}t^n f(t^2)\,dt$$

$$= (-1)^n\frac{\nu p}{2\sqrt{\pi}}\int_0^\infty\left(\frac{d}{dp}\right)^n[e^{-p^2s^{\nu/4}}]\,\phi(s^{-\nu})\,s^{\frac{1}{2}\nu-1}\,ds. \quad (163)$$

Since

$$\left(\frac{d}{dp}\right)^n e^{-p^2s^{\nu/4}} = (-1)^n\left(\frac{s^\nu}{2}\right)^{\frac{1}{2}n}e^{-\frac{1}{8}p^2s^\nu}\,D_n\left(\frac{ps^{\frac{1}{2}\nu}}{\sqrt{2}}\right) \quad . \quad (164)$$

$$= (-1)^n\left(\frac{s^{\nu/2}}{2}\right)^n e^{-\frac{1}{4}p^2s^\nu}\,He_n(ps^\nu/2), \quad (165)$$

* Humbert, 'Le calcul symbolique,' Paris (1934).

where D_n and He_n are Weber's parabolic cylinder function and Hermite's polynomial of order n, respectively, (163) can be expressed in the forms

$$t^n f(t^2) \supset \frac{\nu p}{2^{\frac{1}{2}n+1}\sqrt{\pi}} \int_0^\infty e^{-\frac{1}{8}p^2 s^\nu} D_n\left(\frac{p s^{\frac{1}{2}\nu}}{\sqrt{2}}\right) \phi(s^{-\nu})\, s^{\frac{1}{2}n\nu+\frac{1}{2}\nu-1}\, ds \quad \ldots \quad (166)$$

$$= \frac{\nu p}{2^{n+1}\sqrt{\pi}} \int_0^\infty e^{-\frac{1}{8}p^2 s^\nu} He_n\left(\frac{p s^{\frac{1}{2}\nu}}{2}\right) \phi(s^{-\nu})\, s^{\frac{1}{2}n\nu+\frac{1}{2}\nu-1}\, ds. \quad \ldots \quad (167)$$

Any convenient value of ν may be used. The signs of (162), (163), (166), (167) are independent of that of $R(\nu)$.

XLIII. *Some Problems in the Mathematical Theory of the Conduction of Heat.* *By* H. S. Carslaw, *Emeritus Professor of Mathematics, University of Sydney, and* J. C. Jaeger, *Lecturer in Mathematics, University of Tasmania* *.

[Received April 6, 1938.]

Part I.

RECENT papers in this Journal by Lowan † and the work of Doetsch ‡, and Churchill § lead us to illustrate by the solution of some problems a similar method which we have for some time applied in the Conduction of Heat and elsewhere. It will be seen (§ 3) that it throws some light on the Heaviside operational method of attacking such questions.

In Part I. we take some problems of linear flow, and in Part II. we deal with radial flow, the surface (internal or external) being a circular cylinder and the distribution symmetrical about its axis.

The principle of the method will be seen from the

* Communicated by the Authors.

† Phil. Mag. (7) xxiv. pp. 62–70 (1937); *ibid.* pp. 410–424.

‡ Doesch, G., 'Theorie u. Anwendung der Laplace-Transformation,' being Bd. xlvii. of the *Grundlehren der Mathematischen Wissenschaften*, Berlin (1937); and many papers in the mathematical journals.

§ (1) *Math. Zs.* xlii. pp. 567–579 (1937); (2) *Math. Ann.* cxiv. pp. 591–613 (1937).

simple example in the next section*. It is solved by "Operational Methods" in Jeffreys' Tract †, and the solution given below should be compared with his.

§ 2. *Linear Flow. Rod of length l. End $x=0$ kept at a constant temperature v_0. End $x=l$ kept at zero. Initial temperature of the rod v_0.*

Here we have to solve

$$\frac{\partial v}{\partial t}=\kappa\frac{\partial^2 v}{\partial x^2}, \quad 0<x<l, \quad t>0, \quad . \quad . \quad . \quad (1)$$

$$\left.\begin{aligned} &v\to v_0, \text{ when } x\to 0,\\ &v\to 0, \text{ when } x\to l,\end{aligned}\right\} t>0, \quad . \quad . \quad . \quad . \quad (2)$$

$$v\to v_0, \text{ when } t\to 0, \quad 0<x<l. \quad . \quad . \quad . \quad (3)$$

Multiply (1) by e^{-pt}, where $p>0$, and integrate with respect to t from 0 to ∞.

Then
$$\int_0^\infty e^{-pt}\frac{\partial v}{\partial t}\,dt=\kappa\int_0^\infty e^{-pt}\frac{\partial^2 v}{\partial x^2}\,dt. \quad . \quad . \quad . \quad (4)$$

But
$$\int_0^\infty e^{-pt}\frac{\partial v}{\partial t}\,dt=[e^{-pt}v]_0^\infty+p\int_0^\infty e^{-pt}\,v\,dt$$
$$=-v_0+p\mathrm{V},$$

where
$$\mathrm{V}=\int_0^\infty e^{-pt}v\,dt. \quad . \quad . \quad . \quad . \quad . \quad . \quad (5)$$

Thus, assuming that v is such that we can change the order of integration and differentiation in the right-hand side of (4), we have

$$\kappa\frac{d^2\mathrm{V}}{dx^2}-p\mathrm{V}=-v_0, \quad 0<x<l. \quad . \quad . \quad . \quad . \quad (6)$$

Also
$$\left.\begin{aligned} &\mathrm{V}\to\frac{v_0}{p}, \text{ when } x\to 0,\\ &\mathrm{V}\to 0, \text{ when } x\to l,\end{aligned}\right\} \quad . \quad . \quad . \quad . \quad . \quad (7)$$

assuming that v is such that, at $x=0$ and l,

$$\lim\int_0^\infty e^{-pt}v\,dt=\int_0^\infty e^{-pt}\lim v\,dt.$$

* Reference may be made to a paper by Carslaw, 'Mathematical Gazette,' xxii. no. 250 (July 1938).

† Jeffreys, H., 'Operational Methods in Mathematical Physics' (Cambridge Tract, no. 23, 2nd ed. p. 63 (1931)).

From (6) and (7) we find that

$$V = \frac{v_0}{p}\left\{1 - \frac{\sinh q(l-x)}{\sinh ql}\right\}, \quad . \quad . \quad . \quad . \quad (8)$$

writing

$$q = \sqrt{\frac{p}{\kappa}}. \quad . \quad . \quad . \quad . \quad . \quad . \quad . \quad (9)$$

Then we find v from equation (5).

Now, if

$$F(p) = \int_0^\infty e^{-pt} f(t)\, dt,$$

$F(p)$ is said to be the Laplace Transform of $f(t)$, and a table of Laplace Transforms would form part of the apparatus of this method. If V (p) in (8) occurred in this table we would write down $v(x, t)$ at once *.

But, if V (p) in (8) is not found in the table we use the "inversion formula †," that, under very general conditions, the equation

$$\left.\begin{aligned} F(p) &= \int_0^\infty e^{-pt} f(t)\, dt \\ \text{is satisfied by} \qquad f(t) &= \frac{1}{2i\pi}\int_{c-i\infty}^{c+i\infty} e^{\lambda t} F(\lambda)\, d\lambda, \end{aligned}\right\} \quad . \quad . \quad . \quad (10)$$

where c is a positive constant.

Applying this formula to the value of V given in (8), we have

$$v = \frac{v_0}{2i\pi}\int_{c-i\infty}^{c+\infty} e^{\lambda t}\left(1 - \frac{\sinh\sqrt{\frac{\lambda}{\kappa}}(l-x)}{\sinh\sqrt{\frac{\lambda}{\kappa}}l}\right)\frac{d\lambda}{\lambda} \quad . \quad (11)$$

Consider the closed circuit of fig. 1, formed by the line AB parallel to the imaginary axis in the λ-plane and at a distance c from it, and the circle Γ of radius R with centre at 0.

* It is known that there can only be one continuous solution $f(t)$ of this equation between $F(p)$ and $f(t)$. *Cf.* Lerch, *Acta Math.* xxvii. pp. 339–352 (1903).

† A purely formal "proof" of this theorem can be derived from Fourier's Integral. For a not too difficult proof see Churchill, *Math. Zs.* xlii. pp. 567–579 (1937). One of the conditions to be satisfied by $F(p)$ is that there is a real positive constant, say α, such that $F(\lambda)$ is regular when the real part of $\lambda > \alpha$ (*i. e.*, $R(\lambda) > \alpha$), and the constant c is to be greater than α. Further, $F(\lambda)$ is to be bounded when $R(\lambda) \geqslant c$.

We choose $\mathrm{R}=\kappa(n+\frac{1}{2})^2\frac{\pi^2}{l^2}$,

so that it does not pass through a zero of $\sinh\sqrt{\frac{\lambda}{\kappa}}l$.

It can be shown that the integral in (11) over the circle Γ in the diagram tends to zero as $n\to\infty$.

It follows that we can replace the integral in (11) by the limit of the integral over this closed circuit as $n\to\infty$.

Fig. 1.

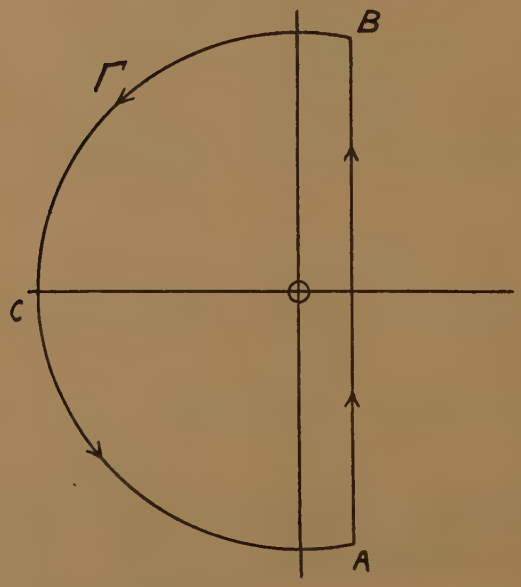

Then, from the Theory of Residues *, we have at once

$$\frac{v}{v_0}=\frac{x}{l}-\sum_{n=1}^{\infty}e^{-\kappa\frac{n^2\pi^2}{l^2}t}\frac{\sinh i\frac{n\pi}{l}(l-x)}{\left[\lambda\frac{d}{d\lambda}\sinh\sqrt{\frac{\lambda}{\kappa}}l\right]_{\lambda=-\kappa\frac{n^2\pi^2}{l^2}}}. \qquad (12)$$

* $\dfrac{\sinh\sqrt{\frac{\lambda}{\kappa}}(l-x)}{\sinh\sqrt{\frac{\lambda}{\kappa}}l}$ is a single-valued function of λ, as may be seen by writing down the series for $\sinh\sqrt{\frac{\lambda}{\kappa}}(l-x)$ and $\sinh\sqrt{\frac{\lambda}{\kappa}}l$.

But $$\lambda \frac{d}{d\lambda} \sinh \sqrt{\frac{\lambda}{\kappa}} l = \frac{1}{2} \sqrt{\frac{\bar{\lambda}}{\kappa}} l \cosh \sqrt{\frac{\bar{\lambda}}{\kappa}} l. \quad . \quad (13)$$

Therefore $$\frac{v}{v_0} = \frac{x}{l} - \frac{2}{\pi} \sum_1^\infty e^{-\kappa \frac{n^2\pi^2}{l^2} t} \frac{\sin \frac{n\pi}{l}(l-x)}{n \cos n\pi}$$

$$= \frac{x}{l} + \frac{2}{\pi} \sum_1^\infty e^{-\kappa \frac{n^2\pi^2}{l^2} t} \frac{\sin \frac{n\pi}{l} x}{n} \quad . \quad . \quad . \quad . \quad . \quad (14)$$

§ 3. If we had multiplied (1) by pe^{-pt} instead of e^{-pt}, and proceeded as above, writing now

$$V = p \int_0^\infty e^{-pt} v \, dt, \quad . \quad . \quad . \quad . \quad . \quad (15)$$

the equations for V would have been

$$\left.\begin{aligned} &\kappa \frac{d^2V}{dx^2} - pV = -pv_0, \\ &V \to v_0, \text{ when } x \to 0, \\ &V \to 0, \text{ when } x \to l, \end{aligned}\right\}, \quad . \quad . \quad . \quad . \quad (16)$$

giving $$V = v_0 \left(1 - \frac{\sinh q(l-x)}{\sinh ql}\right), \quad . \quad . \quad . \quad (17)$$

where $q = \sqrt{\frac{p}{\kappa}}$, as in Jeffreys' solution.

And the "interpretation" of this function $V(p)$ by Bromwich's Rule gives

$$v = \frac{v_0}{2i\pi} \int_{c-i\infty}^{c+i\infty} e^{\lambda t} \left(1 - \frac{\sinh \sqrt{\frac{\bar{\lambda}}{\kappa}}(l-x)}{\sinh \sqrt{\frac{\bar{\lambda}}{\kappa}} l}\right) \frac{d\lambda}{\lambda},$$

as in § 2 (11).

The justification of Bromwich's Rule for such partial differential equations, even as the theory is developed by Jeffreys in his Tract, is far from being established. The advantage of the method of this paper is that, after multiplying the equation by e^{-pt} and integrating, the solution is obtained, either from a table of Laplace Transforms, if $V(p)$ occurs there, or by reduction of the inversion formula.

It will be noticed that the "subsidiary equation" for V in § 2 differs from that in Jeffreys' Tract, but that with $V = p\int_0^\infty e^{-pt} v\,dt$ they agree *.

Assumptions as to the nature of v have been made. Such seem to be inevitable. They are to be found even in the elaborate discussion in Titchmarsh's 'Fourier Integrals' †, where the Laplace and other transforms are rigorously treated with the Lebesgue Integral ‡ instead of the Riemann.

It should be remarked that for a complete proof we should verify that the solution found by this method does, in fact, satisfy the given partial differential equation and the initial and boundary conditions.

In these problems this verification is possible, and the assumptions made as to the nature of the unknown function are not required. This verification follows from the possible deformation of the path $\int_{c-i\infty}^{c+i\infty}$ into a path beginning at infinity in the third quadrant and, after passing to the right of the origin, ending at infinity in the second. Such a path corresponds to the "path P" used in 'Conduction of Heat,' chapters x. and xi.

§ 4. This section contains the solution of the problem of *a unit source at x' in the semi-infinite solid ($x>0$), radiation taking place at $x=0$ into a medium at zero* ‡. Here we have to solve

$$\frac{\partial v}{\partial t} = \kappa \frac{\partial^2 v}{\partial x^2}, \quad x>0,\ t>0 \ldots \quad (18)$$

* In the "Symbolical Calculus," as developed by van der Pol (*e. g.*, Phil. Mag. (7) vii. pp. 1153–1162 (1929), and viii. pp. 861–898 (1929), the relation between the unknown function $h(x)$ and its operational representation $f(p)$ is

$$f(p) = p\int_0^\infty e^{-px} h(x)\,dx.$$

† Titchmarsh, E. C., 'Introduction to the Theory of Fourier Integrals,' (1937). Notice especially chapter x. In this connexion it may also be remarked that the proof of the uniqueness of the solution as given, for example, in Carslaw's 'Conduction of Heat' (§ 8) is defective. This was pointed out by Doetsch in *Math. Zs.* xxii. pp. 293–306 (1925) (§ 2), and xxv. pp. 608–626 (1926) (footnote (10) on p. 614). In all such "proofs" further assumptions as to the nature of v have been made.

‡ This is the problem discussed by Lowan in Phil. Mag. (7) xxiv. pp. 62–70 (1937). It is solved by contour integration in 'Conduction of Heat,' § 82.

$$-\frac{\partial v}{\partial x}+hv=0, \text{ when } x\to 0,\ t>0 \quad . \quad . \quad . \quad (19)$$

$$v=\frac{1}{2\sqrt{(\pi\kappa t)}}e^{-\frac{(x-x')^2}{4\kappa t}}+w, \quad . \quad . \quad (20)$$

where w satisfies (18) and $\lim_{t\to 0} w=0$ for $x>0$.

Let $$u=\frac{1}{2\sqrt{(\pi\kappa t)}}e^{-\frac{(x-x')^2}{4\kappa t}} \quad . \quad . \quad . \quad . \quad . \quad . \quad (21)$$

and $$\mathrm{U}=\int_0^\infty e^{-pt}u\,dt, \text{ where } p>0. \quad . \quad . \quad . \quad (22)$$

V and W are defined by similar equations *.

Then $$\mathrm{V}=\mathrm{U}+\mathrm{W}, \text{ since } v=u+w. \quad . \quad . \quad . \quad (23)$$

Also, on multiplying $\frac{\partial w}{\partial t}=\kappa\frac{\partial^2 w}{\partial x^2}$ by e^{-pt} and integrating from 0 to ∞, we obtain, with similar assumptions to those made in § 2,

$$\kappa\frac{d^2\mathrm{W}}{dx^2}-p\mathrm{W}=0, \quad x>0 \quad . \quad . \quad . \quad . \quad (24)$$

$$-\frac{d\mathrm{W}}{dx}+h\mathrm{W}=\frac{d\mathrm{U}}{dx}-h\mathrm{U}, \text{ when } x\to 0. \quad . \quad (25)$$

But it is known † that

$$\mathrm{U}=\frac{1}{2\sqrt{(\kappa p)}}e^{-\sqrt{\frac{p}{\kappa}}|x-x'|}$$

$$=\frac{1}{2\sqrt{(\kappa p)}}e^{-q|x-x'|}. \quad . \quad . \quad . \quad . \quad (26)$$

Thus we can replace (25) by

$$-\frac{d\mathrm{W}}{dx}+h\mathrm{W}=\frac{1}{2\sqrt{(\kappa p)}}(q-h)e^{-qx'}, \text{ when } x\to 0. \quad (27)$$

It follows from (24) and (27) that

$$\mathrm{W}=\frac{1}{2\sqrt{(\kappa p)}}\frac{q-h}{q+h}e^{-q(x+x')}. \quad . \quad . \quad . \quad (28)$$

* *E. g.*, $$\mathrm{V}=\int_0^\infty e^{-pt}v\,dt.$$

† This follows at once from the integral

$$\int_0^\infty e^{-x^2-\frac{a^2}{x^2}}dx=\frac{\sqrt{\pi}}{2}e^{-2|a|}.$$

Hence

$$V=\frac{1}{2\sqrt{(\kappa p)}}\left\{e^{-q|x-x'|}+e^{-q(x+x')}-\frac{2h}{q+h}e^{-q(x+x')}\right\}. \quad (29)$$

But the first and second terms are the Laplace Transforms of

$$\frac{1}{2\sqrt{(\pi\kappa t)}}e^{-\frac{(x-x')^2}{4\kappa t}} \quad \text{and} \quad \frac{1}{2\sqrt{(\pi\kappa t)}}e^{-\frac{(x+x')^2}{4\kappa t}}$$

respectively.

We have thus only to find the part of v corresponding to the third term, using the inversion formula.

Fig. 2.

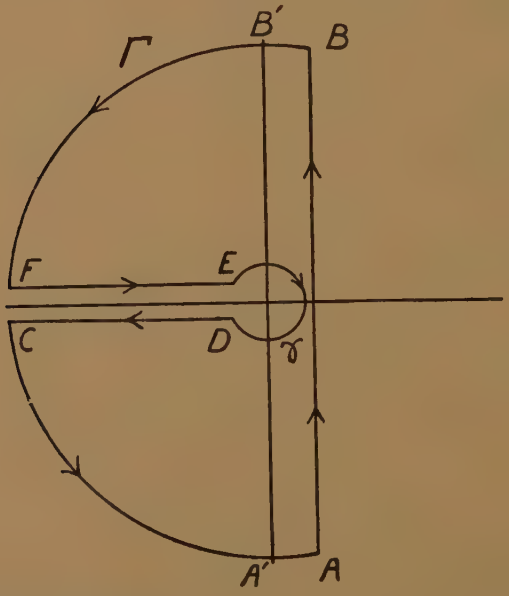

Consider the integral

$$\int e^{\lambda t}\frac{e^{-\sqrt{\frac{\lambda}{\kappa}}(x+x')}}{\sqrt{\frac{\lambda}{\kappa}}+h}\frac{d\lambda}{\sqrt{\lambda}}$$

over the closed circuit of fig. 2, AB being at a distance c from the imaginary axis; a cut has been made in the λ-plane along the negative real axis to make the integrand single-valued within the circuit, and $-\pi \leqslant \arg\lambda \leqslant \pi$.

It is not difficult to show that when the radius of the

circle Γ tends to ∞, the integrals over the arcs A′A, B′B, and the two quadrants CA′, B′F each tends to zero.

Thus we can replace

$$\int_{c-i\infty}^{c+i\infty} e^{\lambda t} \frac{e^{-\sqrt{\frac{\lambda}{\kappa}}(x+x')}}{\sqrt{\frac{\lambda}{\kappa}}+h} \frac{d\lambda}{\sqrt{\lambda}}$$

by the limit of the integrals over the line CD (arg $\lambda=-\pi$), the line EF (arg $\lambda=+\pi$), and the small circle γ, the radius of this circle tending to zero, and C, F moving off to $-\infty$.

It is clear that the circle γ gives zero.

Also from CD, on putting $\lambda=\rho e^{-i\pi}$, we have

$$-i\int_0^\infty e^{-\rho t} \frac{e^{i\sqrt{\frac{\rho}{\kappa}}(x+x')}}{h-i\sqrt{\frac{\rho}{\kappa}}} \frac{d\rho}{\rho}.$$

And from EF, on putting $\lambda=\rho e^{i\pi}$, we have

$$i\int_0^\infty e^{-\rho t} \frac{e^{-i\sqrt{\frac{\rho}{\kappa}}(x+x')}}{h+i\sqrt{\frac{\rho}{\kappa}}} \frac{d\rho}{\rho}.$$

Adding these we obtain

$$2i\int_0^\infty e^{-\rho t} \frac{h\cos\sqrt{\frac{\rho}{\kappa}}(x+x')-\sqrt{\frac{\rho}{\kappa}}\sin\sqrt{\frac{\rho}{\kappa}}(x+x')}{h^2+\frac{\rho}{\kappa}} \frac{d\rho}{\sqrt{\rho}}. \quad \ldots \quad (30)$$

Thus the part of v corresponding to the third term of (29), namely

$$-\frac{h}{2i\pi\sqrt{\kappa}}\int_{c-i\infty}^{c+i\infty} e^{\lambda t} \frac{e^{-\sqrt{\frac{\lambda}{\kappa}}(x+x')}}{\sqrt{\frac{\lambda}{\kappa}}+h} \frac{d\lambda}{\sqrt{\lambda}},$$

is

$$-\frac{h}{\pi\sqrt{\kappa}}\int_0^\infty e^{-\rho t} \times \frac{h\cos\sqrt{\frac{\rho}{\kappa}}(x+x')-\sqrt{\frac{\rho}{\kappa}}\sin\sqrt{\frac{\rho}{\kappa}}(x+x')}{h^2+\frac{\rho}{\kappa}} \frac{d\rho}{\sqrt{\rho}},$$

or

$$-\frac{2h}{\pi}\int_0^\infty e^{-\kappa\alpha^2 t}\frac{h\cos\alpha\,(x+x')-\alpha\sin\alpha(x+x')}{h^2+\alpha^2}d\alpha. \quad (31)$$

Using the integrals

$$\left.\begin{aligned}\int_0^\infty e^{-h\xi}\cos\alpha\xi\,d\xi&=\frac{h}{h^2+\alpha^2},\\ \int_0^\infty e^{-h\xi}\sin\alpha\xi\,d\xi&=\frac{\alpha}{h^2+\alpha^2},\end{aligned}\right\} \quad . \quad . \quad . \quad (32)$$

and reversing the order of integration in the repeated integral, we replace (31) by

$$-\frac{2h}{\pi}\int_0^\infty e^{-h\xi}\left[\int_0^\infty e^{-\kappa\alpha^2 t}\cos\alpha\,(x+x'+\xi)\,d\alpha\right]d\xi, \quad (33)$$

i. e.,

$$-\frac{h}{\sqrt{(\pi\kappa t)}}\int_0^\infty e^{-h\xi-\frac{(x+x'+\xi)^2}{4\kappa t}}d\xi. \quad . \quad . \quad . \quad (34)$$

Then from (29) and (34)

$$v=\frac{1}{2\sqrt{(\pi\kappa t)}}\left\{e^{-\frac{(x-x')^2}{4\kappa t}}+e^{-\frac{(x+x')^2}{4\kappa t}}-2h\int_0^\infty e^{-h\xi-\frac{(x+x'+\xi)^2}{4\kappa t}}d\xi\right\}. \quad (35)$$

§ 5. Now take the case of a *unit source at* x' *in* $0<x<l$, *the ends* $x=0$ *and* $x=l$ *being kept at zero.*

Here we have to solve

$$\frac{\partial v}{\partial t}=\kappa\frac{\partial^2 v}{\partial x^2}, \quad 0<x<l, \quad t>0, \quad . \quad . \quad . \quad (36)$$

$$\left.\begin{aligned}v&\to 0 \text{ when } x\to 0,\\ v&\to 0 \text{ when } x\to l,\end{aligned}\right\} t>0, \quad . \quad . \quad . \quad . \quad (37)$$

$$v=\frac{1}{2\sqrt{(\pi\kappa t)}}e^{-\frac{(x-x')^2}{4\kappa t}}+w, \quad . \quad . \quad . \quad (38)$$

where w satisfies (36) and $\lim_{t\to 0} w=0$, for $0<x<l$.

With the same notation as in § 4 the equations for W are

$$\kappa\frac{d^2\mathrm{W}}{dx^2}-p\mathrm{W}=0, \quad 0<x<l, \quad . \quad . \quad . \quad (39)$$

$$\mathrm{W}=-\mathrm{U} \text{ when } x\to 0 \text{ and } x\to l. \quad . \quad . \quad . \quad (40)$$

Thus

$$\left.\begin{aligned} W &= -\frac{1}{2\sqrt{(\kappa p)}} e^{-qx'}, \text{ when } x \to 0, \\ &= -\frac{1}{2\sqrt{(\kappa p)}} e^{-q(l-x')}, \text{ when } x \to l. \end{aligned}\right\} \quad . \quad . \quad (41)$$

From (39) and (41) we find that

$$W = -\frac{1}{2\sqrt{(\kappa p)}} \frac{e^{-q(l-x')} \sinh qx + e^{-qx'} \sinh q(l-x)}{\sinh ql}. \quad (42)$$

$$= \frac{1}{2\sqrt{(\kappa p)}} \frac{e^{-ql} \cosh q(x-x') - \cosh q(l-x-x')}{\sinh ql} \quad . \quad (43)$$

But $V = U + W$.

Therefore

$$V = \frac{1}{2\sqrt{(\kappa p)}} \left\{ e^{q(x-x')} + \frac{e^{-ql} \cosh q(x-x') - \cosh q(l-x-x')}{\sinh ql} \right\},$$

when $x < x'$.

Thus

$$V = \frac{1}{2\sqrt{(\kappa p)}} \left\{ \frac{\cosh q(l+x-x') - \cosh q(l-x-x')}{\sinh ql} \right\}, \quad (44)$$

when $x < x'$.

And when $x > x'$, we have to interchange x and x' in (44).

It follows that, when $x < x'$,

$$v = \frac{1}{4i\pi\sqrt{\kappa}} \times \int_{c-i\infty}^{c+i\infty} e^{\lambda t} \frac{\cosh \sqrt{\frac{\lambda}{\kappa}}(l+x-x') - \cosh \sqrt{\frac{\lambda}{\kappa}}(l-x-x')}{\sinh \sqrt{\frac{\lambda}{\kappa}} l} \frac{d\lambda}{\sqrt{\lambda}},$$

. . . (45)

x, x' being interchanged when $x > x'$.

In this case we use fig. 1, the radius of the circle Γ being $\kappa(n+\frac{1}{2})^2 \frac{\pi^2}{l^2}$, as in § 2, and the integral $\int_{c-i\infty}^{c+i\infty}$ can be replaced by the integral over the closed circuit when $n \to \infty$, since it will be found that the integrals over the circular arcs tend to zero when $n \to \infty$.

Then the Theory of Residues gives at once

$$v=\frac{1}{2\sqrt{\kappa}}\sum_{n=1}^{\infty}e^{-\kappa\frac{n^2\pi^2}{l^2}t}\frac{\cos\frac{n\pi}{l}(l+x-x')-\cos\frac{n\pi}{l}(l-x-x')}{\left[\sqrt{\lambda}\frac{d}{d\lambda}\sinh\sqrt{\frac{\lambda}{\kappa}}l\right]_{\lambda=-\kappa\frac{n^2\pi^2}{l^2}}}. \quad . \quad . \quad . \quad (46)$$

It follows that

$$v=\frac{2}{l}\sum_{1}^{\infty}e^{-\kappa\frac{n^2\pi^2}{l^2}t}\sin\frac{n\pi}{l}x\sin\frac{n\pi}{l}x'. \quad . \quad . \quad . \quad (47)$$

This has been obtained for $x<x'$, and as the result for $x>x'$, is got by interchanging x and x', it will be seen that it holds for both cases *.

§ 6. As a final example we take the same problem as in § 5, but with *radiation at* $x=0$ *and* $x=l$ *into a medium at zero.*

The equations for v are as follows:

$$\frac{\partial v}{\partial t}=\kappa\frac{\partial^2 v}{\partial x^2}, \quad 0<x<l, \quad t>0 \quad . \quad . \quad . \quad (48)$$

$$\left.\begin{aligned}-\frac{\partial v}{\partial x}+hv=0, \text{ when } x\to 0,\\ \frac{\partial v}{\partial x}+hv=0, \text{ when } x\to l,\end{aligned}\right\} t>0 \quad . \quad . \quad (49)$$

$$v=\frac{1}{2\sqrt{(\pi\kappa t)}}e^{-\frac{(x-x')^2}{4\kappa t}}+w, \quad . \quad . \quad . \quad . \quad (50)$$

where w satisfies (48) and $\lim_{t=0} w=0$ for $0<x<l$.

With the same notation as before, it will be found that

$$W=A\sinh qx+B\sinh q(l-x) \quad . \quad . \quad . \quad (51)$$

where

$$A=\frac{q-h}{2\sqrt{(\kappa p)}}\frac{qe^{-qx'}+(q\cosh ql+h\sinh ql)e^{-q(l-x')}}{\sinh ql((q^2+h^2)\sinh ql+2qh\cosh ql)} \quad (52)$$

and

$$B=\frac{q-h}{2\sqrt{(\kappa p)}}\frac{(q\cosh ql+h\sinh ql)e^{-qx'}+qe^{-q(l-x')}}{\sinh ql((q^2+h^2)\sinh ql+2qh\cosh ql)}. \quad (53)$$

* *Cf.* ' Conduction of Heat,' § 75, ii. and § 84.

Then

$$8\sqrt{(\kappa p)}\sinh ql((q^2+h^2)\sinh ql+2qh\cosh ql)\,\mathrm{W}$$
$$=2(q^2-h^2)(\sinh q(x+x')+\sinh q(2l-x-x'))$$
$$+(q-h)^2\{2\cosh q(x-x')+\sinh q(2l+x-x')$$
$$+\sinh q(2l-x+x')-\cosh q(2l+x-x')$$
$$-\cosh q(2l-x+x')\}. \quad . \quad . \quad . \quad . \quad . \quad . \quad . \quad . \quad (54)$$

It will be seen that W is unaltered when we interchange x and x'. But $\mathrm{V}=\mathrm{U}+\mathrm{W}$, where

$$\mathrm{U}=\frac{1}{2\sqrt{(\kappa p)}}e^{-q|x-x'|}.$$

Then, after some reduction, it will be found that

$$\mathrm{V}=\frac{1}{\sqrt{(\kappa p)}}$$
$$\times\frac{(q\cosh qx+h\sinh qx)(q\cosh q(l-x')+h\sinh q(l-x'))}{(q^2+h^2)\sinh ql+2qh\cosh ql}$$
$$. \quad . \quad . \quad (55)$$

when $x<x'$.

And when $x>x'$, we interchange x and x' in (55).

Now the roots of the equation

$$\left(\frac{\lambda}{\kappa}+h^2\right)\sinh\sqrt{\frac{\lambda}{\kappa}}l+2h\sqrt{\frac{\lambda}{\kappa}}\cosh\sqrt{\frac{\lambda}{\kappa}}l=0$$

are known to be

$$-\kappa\alpha_1^2, \quad -\kappa\alpha_2^2, \ldots .$$

where $\pm\alpha_1, \pm\alpha_2, \ldots .$ are the roots (all real) of

$$\tan\alpha l=\frac{2\alpha h}{\alpha^2-h^2}. \quad . \quad . \quad . \quad . \quad . \quad . \quad (56)$$

We can thus write down v from (55) in the form

$$v=\frac{1}{2i\pi\sqrt{\kappa}}\int_{c-i\infty}^{c+i\infty}e^{\lambda t}$$
$$\times\frac{\mathrm{N}}{\left(\frac{\lambda}{\kappa}+h^2\right)\sinh\sqrt{\frac{\lambda}{\kappa}}l+2h\sqrt{\frac{\lambda}{\kappa}}\cosh\sqrt{\frac{\lambda}{\kappa}}l}\frac{d\lambda}{\sqrt{\lambda}},$$

where N is the product of

$$\sqrt{\frac{\lambda}{\kappa}}\cosh\sqrt{\frac{\lambda}{\kappa}}x+h\sinh\sqrt{\frac{\lambda}{\kappa}}x$$

and $$\sqrt{\frac{\lambda}{\kappa}}\cosh\sqrt{\frac{\lambda}{\kappa}}(l-x')+h\sinh\sqrt{\frac{\lambda}{\kappa}}(l-x'). \quad (57)$$

Using fig. 1, and choosing Γ so that it does not pass through one of the roots $\lambda=-\kappa\alpha^2$—it is sufficient to take its radius as $\kappa\left(\left[n+\frac{1}{2}\right)^2\frac{\pi^2}{l^2}\right]\Big)$,—we find that we can replace $\int_{c-i\infty}^{c+i\infty}$ by the closed circuit of fig. 1 when $n\to\infty$.

Thus the Theory of Residues gives

$$v=\frac{1}{\sqrt{\kappa}}\sum_{s=1}^{\infty}e^{-\kappa\alpha_s^2t}\frac{(\alpha_s\cos\alpha_sx+h\sin\alpha_sx)(\alpha_s\cos\alpha_s(l-x')+h\sin\alpha_s(l-x'))}{\left\{\sqrt{\lambda}\frac{d}{d\lambda}\left[\left(\frac{\lambda}{\kappa}+h^2\right)\sinh\sqrt{\frac{\lambda}{\kappa}}l+2h\sqrt{\frac{\lambda}{\kappa}}\cosh\sqrt{\frac{\lambda}{\kappa}}l\right]\right\}_{\lambda=-\pi\alpha s^2}} \quad . \quad . \quad . \quad (58)$$

when $x<x'$.

This reduces to

$$v=2\sum_{s=1}^{\infty}e^{-\kappa\alpha_s^2t}\frac{(\alpha_s\cos\alpha_sx+h\sin\alpha_sx)(\alpha_s\cos\alpha_sx'+h\sin\alpha_sx')}{l(\alpha_s^2+h^2)+2h}, \quad . \quad . \quad . \quad (59)$$

and in this form it holds for $x\gtrless x'$.

This result is obtained by contour integration in ' Conduction of Heat,' § 85.

Part II.

In this part some problems in conduction of heat with radial flow are discussed by the method explained in § 2 of Part I.*

§ 1. *Circular cylinder of radius a. Surface kept at constant temperature (unity). Initial temperature zero.*

Here we have to solve :

$$\frac{\partial v}{\partial t}=\kappa\left(\frac{\partial^2v}{\partial r^2}+\frac{1}{r}\frac{\partial v}{\partial r}\right), \quad 0\leqslant r<a, \quad t>0, \quad . \quad . \quad (1)$$

$$v\to1 \text{ when } r\to a, \quad t>0, \quad . \quad . \quad . \quad . \quad . \quad . \quad (2)$$

$$v\to0 \text{ when } t\to0, \quad 0\leqslant r<a. \quad . \quad . \quad . \quad . \quad (3)$$

* See p. 474.

Multiply (1) by e^{-pt}, $(p>0)$, and integrate with regard to t from 0 to ∞.

Then $$\int_0^\infty e^{-pt}\frac{\partial v}{\partial t}dt=\kappa\int_0^\infty e^{-pt}\left(\frac{\partial^2 v}{\partial r^2}+\frac{1}{r}\frac{\partial v}{\partial r}\right)dt,$$

and with assumptions as to the nature of v similar to those in Part I., we have, on putting

$$\mathrm{V}=\int_0^\infty e^{-pt}v\,dt, \quad \ldots\ldots \quad (4)$$

$$\kappa\left(\frac{d^2\mathrm{V}}{dr^2}+\frac{1}{r}\frac{d\mathrm{V}}{dr}\right)=p\mathrm{V}, \quad 0\leqslant r<a \quad \ldots \quad (5)$$

$$\mathrm{V}\to\frac{1}{p} \quad \text{when } r\to a. \quad \ldots\ldots \quad (6)$$

Thus we are led to

$$\mathrm{V}=\frac{1}{p}\frac{\mathrm{I}_0\left(\sqrt{\frac{p}{\kappa}}r\right)}{\mathrm{I}_0\left(\sqrt{\frac{p}{\kappa}}a\right)}, \quad \ldots\ldots \quad (7)$$

and we have to find v from (4).

Now it is known that the zeros of $\mathrm{I}_0\left(\sqrt{\frac{\lambda}{\kappa}}a\right)$ are at

$$-\kappa\alpha_1^2, \quad -\kappa\alpha_2^2, \ldots.$$

where $\pm\alpha_1, \pm\alpha_2, \ldots$ are the roots (all real *) of

$$\mathrm{J}_0(\alpha a)=0.$$

Also

$$\frac{\mathrm{I}_0\left(\sqrt{\frac{\lambda}{\kappa}}r\right)}{\mathrm{I}_0\left(\sqrt{\frac{\lambda}{\kappa}}a\right)}$$

is a single-valued function of λ.

Hence, using the inversion formula—Part I., equation (10),—we have

$$v=\frac{1}{2i\pi}\int_{c-i\infty}^{c+i\infty}e^{\lambda t}\frac{\mathrm{I}_0\left(\sqrt{\frac{\lambda}{\kappa}}r\right)}{\mathrm{I}_0\left(\sqrt{\frac{\lambda}{\kappa}}a\right)}\frac{d\lambda}{\lambda}, \quad \ldots \quad (8)$$

where c is a positive constant.

* *Cf.* Watson, ' Theory of Bessel Functions,' § 15.25. This will be referred to in future as " T.B.F."

Now using fig. 1, where the radius * of the circle Γ is

$$\kappa\left[(n+\tfrac{1}{2})\frac{\pi}{a}\right]^2,$$

Fig. 1.

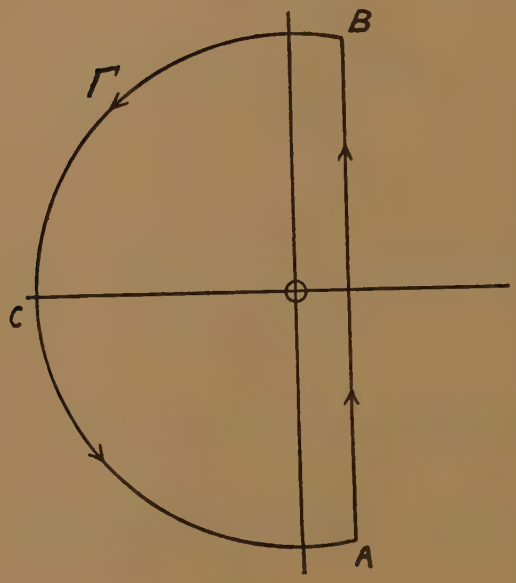

it will be found that when $n\to\infty$ the integral over Γ,

$$\int e^{\lambda t}\frac{I_0\left(\sqrt{\frac{\lambda}{\kappa}}r\right)}{I_0\left(\sqrt{\frac{\lambda}{\kappa}}a\right)}\frac{d\lambda}{\lambda},$$

tends to zero.

It follows that we can replace the right-hand side of (8)

* In this case the circle does not pass through a zero of $I_0\left(\sqrt{\frac{\lambda}{\kappa}}a\right)$ for any value of n. See T.B.F. §15.32.

by the integral over this closed circuit. Then, from the Theory of Residues *, we have

$$v=1+\frac{2}{a}\sum_{s=1}^{\infty}e^{-\kappa\alpha_s^2 t}\frac{J_0(\alpha_s r)}{\alpha_s J_0'(\alpha_s a)}. \quad . \quad . \quad . \quad (9)$$

If the constant surface temperature is v_0, we must multiply this by v_0.

This result is, of course, well-known †. It has been worked out here as a simple illustration of this method.

§ 2. *The solid bounded internally by the circular cylinder $r=a$, and otherwise unbounded. The surface $r=a$ kept at constant temperature (unity). The initial temperature zero.*

Here we have to solve

$$\frac{\partial v}{\partial t}=\kappa\left(\frac{\partial^2 v}{\partial r^2}+\frac{1}{r}\frac{\partial v}{\partial r}\right), \quad r>a, \quad t>0, \quad . \quad . \quad (10)$$

$$v\to 1 \quad \text{when} \quad r\to a, \quad t>0, \quad . \quad . \quad . \quad (11)$$

$$v\to 0 \quad \text{when} \quad t\to 0, \quad r>a. \quad . \quad . \quad . \quad (12)$$

With the same notation as before

$$V=\frac{1}{p}\frac{K_0\left(\sqrt{\frac{p}{\kappa}}r\right)}{K_0\left(\sqrt{\frac{p}{\kappa}}a\right)}, \quad . \quad . \quad . \quad . \quad (13)$$

and

$$v=\frac{1}{2i\pi}\int_{c-i\infty}^{c+i\infty}e^{\lambda t}\frac{K_0\left(\sqrt{\frac{\lambda}{\kappa}}r\right)}{K_0\left(\sqrt{\frac{\lambda}{\kappa}}a\right)}\frac{d\lambda}{\lambda}. \quad . \quad . \quad (14)$$

* The zero at $\lambda=0$ gives the term 1. The zero at $\lambda=-\kappa\alpha_s^2$ gives

$$e^{-\kappa\alpha_s^2 t}\frac{J_0(\alpha_s r)}{\left[\lambda\frac{d}{d\lambda}\left(I_0\left(\sqrt{\frac{\lambda}{\kappa}}a\right)\right)\right]_{\lambda=-\kappa\alpha_s^2}}$$

But $$\lambda\frac{d}{d\lambda}\left(I_0\left(\sqrt{\frac{\lambda}{\kappa}}a\right)\right)=\frac{1}{2}\sqrt{\frac{\lambda}{\kappa}}a\,I_0'\left(\sqrt{\frac{\lambda}{\kappa}}a\right),$$

Thus $$\left[\lambda\frac{d}{d\lambda}\left(I_0\left(\sqrt{\frac{\lambda}{\kappa}}a\right)\right)\right]_{\lambda=-\kappa\alpha_s^2}=\frac{1}{2}\alpha_s a\,J_0'(\alpha_s a).$$

† *Cf.* Carslaw, " Conduction of Heat," § 110, where several other problems in this paper are discussed by another method.

Now consider the closed circuit of fig. 2 formed by the line AB at distance c from the imaginary axis, the circle Γ of radius R, the circle γ of radius ϵ, and CD, EF on which $\arg \lambda = -\pi$ and π, respectively. The integrand is regular inside and upon this circuit, there being no zeros of

$$K_0(z) \text{ in } |\arg z| \leqslant \frac{\pi}{2} *.$$

Fig. 2.

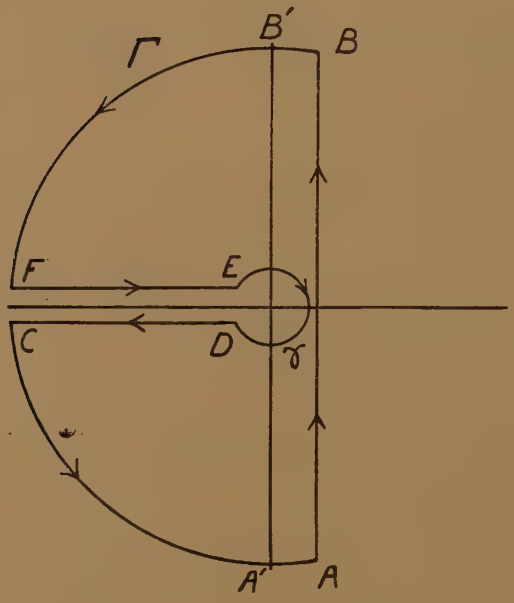

The approximations for $K_0\left(\sqrt{\frac{\lambda}{\kappa}}r\right)$ and $K_0\left(\sqrt{\frac{\lambda}{\kappa}}a\right)$ show that the integral over Γ tends to zero when $R \to \infty$.

Then we can replace

$$\frac{1}{2i\pi}\int_{c-i\infty}^{c+i\infty} e^{\lambda t}\frac{K_0\left(\sqrt{\frac{\lambda}{\kappa}}r\right)}{K_0\left(\sqrt{\frac{\lambda}{\kappa}}a\right)}\frac{d\lambda}{\lambda}$$

by the limit of the integrals over CD, γ (in the counter-clockwise direction) and EF.

* T.B.F. §15.7.

On CD we put $\lambda=\rho e^{-i\pi}$, and we obtain for the integral when $R\to\infty$ and $\epsilon\to 0$,

$$-\frac{1}{2i\pi}\int_0^\infty e^{-\rho t}\frac{K_0\left(\sqrt{\frac{\rho}{\kappa}}re^{-\frac{i\pi}{2}}\right)}{K_0\left(\sqrt{\frac{\rho}{\kappa}}ae^{-\frac{i\pi}{2}}\right)}\frac{d\rho}{\rho},$$

$$i.\,e.,\quad -\frac{1}{2i\pi}\int_0^\infty e^{-\rho t}\frac{J_0\left(\sqrt{\frac{\rho}{\kappa}}r\right)+iY_0\left(\sqrt{\frac{\rho}{\kappa}}r\right)}{J_0\left(\sqrt{\frac{\rho}{\kappa}}a\right)+iY_0\left(\sqrt{\frac{\rho}{\kappa}}a\right)}\frac{d\rho}{\rho}. \quad (15)$$

On EF we put $\lambda=\rho e^{i\pi}$, and we obtain for the integral

$$\frac{1}{2i\pi}\int_0^\infty e^{-\rho t}\frac{K_0\left(\sqrt{\frac{\rho}{\kappa}}re^{\frac{i\pi}{2}}\right)}{K_0\left(\sqrt{\frac{\rho}{\kappa}}ae^{\frac{i\pi}{2}}\right)}\frac{d\rho}{\rho},$$

$$i.\,e.,\quad \frac{1}{2i\pi}\int_0^\infty e^{-\rho t}\frac{J_0\left(\sqrt{\frac{\rho}{\kappa}}r\right)-iY_0\left(\sqrt{\frac{\rho}{\kappa}}r\right)}{J_0\left(\sqrt{\frac{\rho}{\kappa}}a\right)-iY_0\left(\sqrt{\frac{\rho}{\kappa}}a\right)}\frac{d\rho}{\rho}. \quad (16)$$

Adding (15) and (16) we have

$$\frac{1}{\pi}\int_0^\infty e^{-\rho t}\times\frac{J_0\left(\sqrt{\frac{\rho}{\kappa}}r\right)Y_0\left(\sqrt{\frac{\rho}{\kappa}}a\right)-J_0\left(\sqrt{\frac{\rho}{\kappa}}a\right)Y_0\left(\sqrt{\frac{\rho}{\kappa}}r\right)}{J_0^2\left(\sqrt{\frac{\rho}{\kappa}}a\right)+Y_0^2\left(\sqrt{\frac{\rho}{\kappa}}a\right)}\frac{d\rho}{\rho}. \quad (17)$$

The small circle γ gives 1 in the limit.

Thus

$$v=1+\frac{1}{\pi}\int_0^\infty e^{-\rho t}\times\frac{J_0\left(\sqrt{\frac{\rho}{\kappa}}r\right)Y_0\left(\sqrt{\frac{\rho}{\kappa}}a\right)-J_0\left(\sqrt{\frac{\rho}{\kappa}}a\right)Y_0\left(\sqrt{\frac{\rho}{\kappa}}r\right)}{J_0^2\left(\sqrt{\frac{\rho}{\kappa}}a\right)+Y_0^2\left(\sqrt{\frac{\rho}{\kappa}}a\right)}\frac{d\rho}{\rho} \quad (18)$$

or

$$v=1+\frac{2}{\pi}\int_0^\infty e^{-\kappa u^2 t}\frac{J_0(ur)Y_0(ua)-J_0(ua)Y_0(ur)}{J_0^2(ua)+Y_0^2(ua)}\frac{du}{u}\ *\quad . \quad (19)$$

§3. *When the surface temperature is cos ωt*, the problem of §1 requires the solution of (1) and (3), with

$$v\to\cos\omega t \quad \text{when} \quad r\to a, \quad t>0. \quad . \quad . \quad . \quad (20)$$

With the same notation as before,

$$V=\int_0^\infty e^{-pt}v\,dt,$$

we have the following equations for V,

$$\kappa\left(\frac{d^2V}{dr^2}+\frac{1}{r}\frac{dV}{dr}\right)=pV, \quad 0\leqslant r<a, \quad . \quad . \quad (21)$$

$$V\to\frac{p}{p^2+\omega^2} \quad \text{when } r\to a. \quad . \quad . \quad . \quad . \quad (22)$$

Thus

$$V=\frac{I_0\left(\sqrt{\frac{p}{\kappa}}r\right)}{I_0\left(\sqrt{\frac{p}{\kappa}}a\right)}\frac{p}{p^2+\omega^2} \quad . \quad . \quad . \quad . \quad (23)$$

and

$$v=\frac{1}{2i\pi}\int_{c-i\infty}^{c+i\infty}e^{\lambda t}\frac{I_0\left(\sqrt{\frac{\lambda}{\kappa}}r\right)}{I_0\left(\sqrt{\frac{\lambda}{\kappa}}a\right)}\frac{\lambda\,d\lambda}{\lambda^2+\omega^2}. \quad . \quad . \quad (24)$$

Using, as before, fig. 1, we replace this integral by the limit when $n\to\infty$ of the integral over the closed circuit, since it will be found that the integral over the circular part of the circuit vanishes in the limit.

In this case there are poles at $\lambda=\pm i\omega$ in addition to those at $-\kappa\alpha_1^2, -\kappa\alpha_2^2, \ldots$.

The Theory of Residues then gives the result

$$v=\frac{1}{2}e^{i\omega t}\frac{I_0\left(\sqrt{\frac{\omega}{\kappa}}e^{\frac{i\pi}{4}}r\right)}{I_0\left(\sqrt{\frac{\omega}{\kappa}}e^{\frac{i\pi}{4}}a\right)}+\frac{1}{2}e^{-i\omega t}\frac{I_0\left(\sqrt{\frac{\omega}{\kappa}}e^{-\frac{i\pi}{4}}r\right)}{I_0\left(\sqrt{\frac{\omega}{\kappa}}e^{-\frac{i\pi}{4}}a\right)}$$

* *Cf.* Goldstein, Proc. London Math. Soc. (2) xxxiv. p. 53 (1932). This problem had previously been considered by Rayleigh, Phil. Mag. (6), xxii. pp. 381–396 (1911), ' Scientific Papers,' vi. p. 64 ; and by Nicholson, Proc. Roy. Soc. (A), c. pp. 226–240 (1921). Rayleigh's solution is not complete. Nicholson's, though the result is correct, seems faulty. See also Titchmarsh, ' Theory of Fourier Integrals,' 10.10, p. 287.

$$+\sum_{s=1}^{\infty} e^{-\kappa\alpha_s^2 t}\frac{J_0(\alpha_s r)}{\left[\lambda\frac{d}{d\lambda}I_0\left(\sqrt{\frac{\lambda}{\kappa}}a\right)\right]_{\lambda=-\kappa\alpha_s^2}}\frac{\kappa^2\alpha_s^4}{\kappa^2\alpha_s^4+\omega^2}. \quad (25)$$

Writing *

$$\left.\begin{aligned}\text{ber } z+i\,\text{bei } z&=I_0\left(ze^{\frac{i\pi}{4}}\right)\\ \text{ber } z-i\,\text{bei } z&=I_0\left(ze^{-\frac{i\pi}{4}}\right)\end{aligned}\right\}, \quad \ldots \quad (26)$$

the first two terms in v reduce to

$$\frac{\text{ber}\sqrt{\frac{\omega}{\kappa}}r\,\text{ber}\sqrt{\frac{\omega}{\kappa}}a+\text{bei}\sqrt{\frac{\omega}{\kappa}}r\,\text{bei}\sqrt{\frac{\omega}{\kappa}}a}{\text{ber}^2\sqrt{\frac{\omega}{\kappa}}a+\text{bei}^2\sqrt{\frac{\omega}{\kappa}}a}\cos\omega t$$

$$+\frac{\text{ber}\sqrt{\frac{\omega}{\kappa}}r\,\text{bei}\sqrt{\frac{\omega}{\kappa}}a-\text{ber}\sqrt{\frac{\omega}{\kappa}}a\,\text{bei}\sqrt{\frac{\omega}{\kappa}}r}{\text{ber}^2\sqrt{\frac{\omega}{\kappa}}a+\text{bei}^2\sqrt{\frac{\omega}{\kappa}}a}\sin\omega t, \quad \ldots \quad (27)$$

and the third term gives

$$\frac{2\kappa^2}{a}\sum_{s=1}^{\infty}e^{-\kappa\alpha_s^2 t}\frac{J_0(\alpha_s r)}{J_0'(\alpha_s a)}\frac{\alpha_s^3}{\kappa^2\alpha_s^4+\omega^2}. \quad \ldots \quad (28)$$

Thus adding (27) and (28) we are led to the solution †

$$v=\frac{(\ldots.)\cos\omega t+(\ldots.)\sin\omega t}{\text{ber}^2\sqrt{\frac{\omega}{\kappa}}a+\text{bei}^2\sqrt{\frac{\omega}{\kappa}}a}$$

$$+\frac{2\kappa^2}{\alpha}\sum_{s=1}^{\infty}e^{-\kappa\alpha_s^2 t}\frac{J_0(\alpha_s r)}{J_0'(\alpha_s a)}\frac{\alpha_s^3}{\kappa^2\alpha_s^4+\omega^2}. \quad \ldots \quad (29)$$

§4. *In the corresponding problem for the solid bounded internally by* $r=a$, the equations for V are

$$\left.\begin{aligned}&\kappa\left(\frac{d^2V}{dr^2}+\frac{1}{r}\frac{dV}{dr}\right)=pV, \quad r>a\\ &V\to\frac{p}{p^2+\omega^2} \quad \text{when } r\to a\end{aligned}\right\}, \quad \ldots \quad (30)$$

* T.B.F., p. 81. There is an obvious mistake in the series for ber z and bei z.

† The $(\ldots.)$ and $(\ldots.)$ are as in (27).

and we have

$$V=\frac{K_0\left(\sqrt{\frac{p}{\kappa}}r\right)}{K_0\left(\sqrt{\frac{p}{\kappa}}a\right)}\frac{p}{p^2+\omega^2}, \quad . \quad . \quad . \quad . \quad (31)$$

giving

$$v=\frac{1}{2i\pi}\int_{c-i\infty}^{c+i\infty}e^{\lambda t}\frac{K_0\left(\sqrt{\frac{\lambda}{\kappa}}r\right)}{K_0\left(\sqrt{\frac{\lambda}{\kappa}}a\right)}\frac{\lambda}{\lambda^2+\omega^2}d\lambda. \quad . \quad (32)$$

If we write

$$\left.\begin{aligned}\ker z+i\,\mathrm{kei}\,z&=K_0\left(ze^{\frac{i\pi}{4}}\right)\\ \ker z-i\,\mathrm{kei}\,z&=K_0\left(ze^{-\frac{i\pi}{4}}\right)\end{aligned}\right\}, \quad . \quad . \quad . \quad (33)$$

and use fig. 2, we obtain *

$$v=\frac{\left(\ker\sqrt{\frac{\omega}{\kappa}}r\ker\sqrt{\frac{\omega}{\kappa}}a+\mathrm{kei}\sqrt{\frac{\omega}{\kappa}}r\,\mathrm{kei}\sqrt{\frac{\omega}{\kappa}}a\right)}{\ker^2\sqrt{\frac{\omega}{\kappa}}a+\mathrm{kei}^2\sqrt{\frac{\omega}{\kappa}}a}\cos\omega t$$

$$+\frac{\left(\ker\sqrt{\frac{\omega}{\kappa}}r\,\mathrm{kei}\sqrt{\frac{\omega}{\kappa}}a-\ker\sqrt{\frac{\omega}{\kappa}}a\,\mathrm{kei}\sqrt{\frac{\omega}{\kappa}}r\right)}{\ker^2\sqrt{\frac{\omega}{\kappa}}a+\mathrm{kei}^2\sqrt{\frac{\omega}{\kappa}}a}\sin\omega t$$

$$+\frac{1}{\pi}\int_0^\infty e^{-\rho t}\times\frac{J_0\left(\sqrt{\frac{\rho}{\kappa}}r\right)Y_0\left(\sqrt{\frac{\rho}{\kappa}}a\right)-J_0\left(\sqrt{\frac{\rho}{\kappa}}a\right)Y_0\left(\sqrt{\frac{\rho}{\kappa}}r\right)}{J_0^2\left(\sqrt{\frac{\rho}{\kappa}}a\right)+Y_0^2\left(\sqrt{\frac{\rho}{\kappa}}a\right)}$$

$$\times\frac{\rho\,d\rho}{\rho^2+\omega^2}. \quad . \quad . \quad . \quad (34)$$

§ 5. The corresponding problems when radiation takes place at the surface $r=a$ into a medium at constant temperature (v_0) can be solved in the same way.

* *Cf.* Goldstein, *loc. cit.* §17 (228).

For the first ($0 \leqslant r < a$) the solution is

$$v = v_0\left(1 - \frac{2h}{a}\sum_{s=1}^{\infty} e^{-\kappa\alpha_s^2 t}\frac{J_0(\alpha_s r)}{J_0(\alpha_s a)}\frac{1}{h^2+\alpha_s^2}\right), \quad . \quad (35)$$

and for the second ($r > a$), the solution is

$$v = v_0\left(1 - \frac{2h}{\pi}\int^{\infty} e^{-\kappa u^2 t} \times \frac{C_0(ur)}{[uJ_1(ua)+hJ_0(ua)]^2+[uY_1(ua)+hY_0(ua)]^2}\frac{du}{u}\right). \quad (36)$$

where *

$$C_0(ur) = [uJ_1(ua)+hJ_0(ua)]Y_0(ur) - [uY_1(ua)+hY_0(ua)]J_0(ur). \quad . \quad . \quad . \quad (37)$$

The case of the solid bounded by the cylinders $r=a$ and $r=b$, with constant surface temperatures v_0 and v_1 respectively, and initial temperature zero can be solved in this way. The same remark applies to the corresponding problems with radiation at the surfaces.

XLIV. *Optical Resolution and the Visual Examination of two Overlapping Photographic Images.* *By* J. K. Robertson, *F.R.S.C., and* R. H. Hay, *M.Sc., Queen's University, Kingston, Canada* †.

[Received July 5, 1938.]

[Plate III.]

IN a note on optical resolution Buxton [1] has suggested the substitution of a "less arbitrary criterion" for the one in general use due to the late Lord Rayleigh. It will be recalled that Rayleigh [2], having observed that, when the centre of the diffraction pattern due to a narrow source falls on the first minimum of an adjacent source, the two images can just be separated visually, considered this to be "the limit of closeness at which there could be any decided appearance of resolution." Although experiment confirmed this conclusion, and led to the adoption of the Rayleigh criterion as a means

* *Cf.* Goldstein, *loc. cit.* §16 (222).

† Communicated by Prof. J. K. Robertson.

of expressing resolving power numerically, it is possibly not always realized that there is nothing absolute about the test. To quote Rayleigh : " this rule is convenient on account of its simplicity, and it is sufficiently accurate in view of the necessary uncertainty as to what exactly is meant by resolution."

It is difficult to see why there is anything " less arbitrary " in Buxton's suggestion that limiting resolution be considered as reached when the amplitude curves for the diffraction patterns of each image intersect at their points of inflexion. As Buxton points out, the angular separation of two point sources, when just separated according to his proposal, is about 20 per cent. greater than the separation given by the Rayleigh criterion ; or the resolving power is that much less.

Fig. 1.

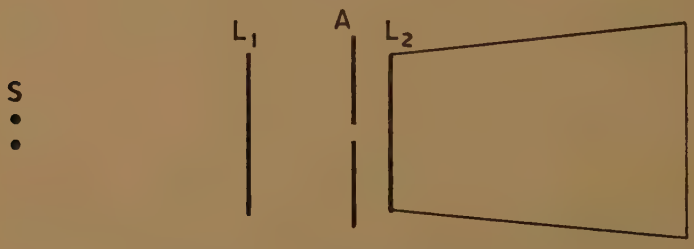

S, precision double-slit ; L_1, collimating lens ; A, adjustable aperture ; L_2, 54 cm. camera lens.

It would seem, therefore, that the only justification for a change in present procedure would be an experimental proof that the use of Buxton's suggestion predicts limiting values more nearly in agreement with those actually observed. Past experience and tests by Ditchburn and Power-Steele [3], as well as those reported in this paper, indicate, however, that with modern methods of observation resolving powers exceeding those given by the Rayleigh criterion may be obtained.

Experimental Results.

In an investigation, whose original object was the comparison of resolution observed visually and photographically, a precision double slit, S, in fig. 1, illuminated by a sodium flame, was placed in the focal

plane of a collimating lens L_1 removed from a Hilger constant deviation spectroscope. Images were observed in the focal plane of the objective lens L_2 of the camera attachment of the same instrument. The original slit of the spectroscope served as an adjustable narrow rectangular aperture A placed before the objective. For varying widths of this aperture the images were either observed visually by means of an eye-piece or photographed on Ilford hypersensitive panchromatic plates.

The precision double slit supplied by the manufacturer was not all that could be desired. Measurements of the width of each component at three different places showed a lack of uniformity from end to end, with a slight difference in the average widths of the two components, a difference which is revealed by the microphotometer trace of the under-exposure in Pl. III. fig. 2 (*a*). Fortunately the main argument of this paper is not seriously altered by the lack of uniformity of the slits. The centre-to-centre distance between the two components showed less variation, having a mean value of 0·222 mm., with an accuracy of about 2 per cent. Since the focal length of the collimating lens L_1 was 283 mm., application of the Rayleigh criterion for sodium light gives 0·75 mm. as the aperture width at the limit of resolution. A check measurement using the centre-to-centre separation of the photographic images obtained with full aperture of the objective gave an average value slightly greater than 0·76 mm. The error, therefore, in adopting 0·76 mm. for *b*, the "Rayleigh width," cannot be much greater than 1 per cent.

Visual Observations.

Two sets of visual observations were made, each by two observers. In the first the aperture was *narrowed* until the limit of resolution had been passed—that is, until the observer *just* ceased to be able to tell that there were two images. In a second set the aperture, originally too narrow, was *widened* until a lowering of intensity at the middle of the diffraction pattern could first be observed—that is, until it could be stated definitely that there were two images. The results of these observations are given in Table I. It will be noted that 0·76 mm., the average value of the critical

width when a minimum can be detected at the centre of the diffraction pattern, is in satisfactory agreement with the Rayleigh width.

Photographic Observations.

For each of the five apertures given in Table II. three or four photographs of the superimposed images were made on the same plate. For aperture no. 1 the exposures were 15, 30, and 60 sec. ; for no. 2, 10, 30, 60, and 120 sec. ; for the remaining three, 15, 30, 60, and 120 sec. The first was an under-exposure, the last either a normal or an over-exposure. The photographic images were examined in the following ways :—(1) by micro-

TABLE I.

	Aperture narrowed.		Aperture widened.	
	R.H.H.	J.K.R.	R.H.H.	J.K.R.
	·665	·667	·752	·784
	·669	·679	·774	·756
	·681	·665	·778	·735
	·673	·674	·772	·760
	·653	·668	·770	·761
	·653	·679	·753	·753
	·658	·674		·752
	·791	·670		·747
				·747
				·752
Mean ..	·669	·672	·766	·753
	·67		·76	

photometer traces ; (2) by observation with an eye-piece used as a magnifier ; and (3) by viewing enlarged positives on bromide paper.

In agreement with the work of Ditchburn and Power-Steele [3] the microphotometer traces show a detectable minimum indicating the presence of two components, for apertures whose widths were considerably less than b, the critical Rayleigh width. For example, the reproductions shown in Pl. III. fig. 2 correspond to aperture no. 2, of width 0·69 mm. or 0·91 b. Traces for aperture no. 3, of width 0·66 mm. or 0·87 b, are not reproduced, but in some of the exposures show just enough of a minimum to justify taking this as the limiting width for microphotometer detection of two components. This means

that two small objects can be separated by the microphotometer when their angular separation is some 10 per cent. less than that given by the Rayleigh criterion.

It is interesting to note that the microphotometer tracing readily detects in the diffraction pattern of two overlapping images a minimum whose theoretical intensity is only a few per cent. less than that of the maxima on either side. (In the Rayleigh criterion, it will be recalled, the minimum has a dip of about 20 per cent.) If, for example, we have two narrow sources of equal intensity, and an aperture (like no. 2) of width 0·91 *b*, a plot of the theoretical resultant diffraction pattern gives a minimum whose intensity is 94 per cent. of the maxima. This 6 per cent. dip can readily be observed in the tracings of Pl. III. fig. 2, although the objection

Table II.

Plate. no.	Aperture. (mm.)	Appearance of image.
1.....	0·703	Two components for all exposures.
2.....	0·687	Two components for three exposures, doubtful for fourth.
3.....	0·657	Two components for three exposures, doubtful for fourth.
4.....	0·631	On or just past the limit.
5.....	0·600	Definitely past the limit.

may be made that in this case the actual sources are not quite of equal intensity. To test this point further use was made of the microphotometer traces for apertures 0·89 *b* and 0·92 *b*, reproduced in the Ditchburn and Power-Steele [3] paper. Theoretical intensity patterns for these apertures give minima with intensities 96 and 93 per cent. of the maxima. Not only did the microphotometer traces published in their paper give marked evidence of these minima, but, if the traces are accurately reproduced, they actually accentuate the theoretical dip.

The results obtained when the photographic images were examined by a magnifier are given in the third column of Table II. It will be noted that, apparently at least, this means of examination is nearly as sensitive

in detecting two components as the microphotometer. As it is known from the work of G. P. Thomson [4] and others that, under certain conditions, an illusory subjective minimum may be seen at the centre of an image which according to the microphotometer is uniform in density, a careful examination was made to find out to what extent the minimum observed at the centre of the image was real.

In some respects the evidence is contradictory. If a plate such as no. 2 is taken and the images are viewed through a low-power microscope minima are undoubtedly seen, but if the region surrounding an image is completely covered by two pieces of black paper the minimum disappears in whole or in part. This suggests that the effect is an illusion, and yet the microphotometer traces for plate no. 2 show that a minimum is actually present—and, it may be added, traces were made at two different laboratories. Moreover, if plate no. 5 is taken, where the images according to the microphotometer are single, no minima are observed on viewing either through the magnifier or the low-power microscope, even when the surrounding field is not covered. The weight of the evidence, therefore, seems to be in favour of the reality of the minima observed visually in plate no. 2.

The third method of observing the photographic images by positive enlargements presents the same problem in a slightly different manner. This will be clear by a comparison of the photographs of Pl. III. fig. 2 with those of fig. 3. If the reproductions are at all faithful to the original enlargements, the reader will observe in fig. 2, especially in (*a*) and (*b*), faint minima running down the centre of the image, whereas in neither (*a*), (*b*), nor (*c*) of fig. 3 is any minimum observed. Again, it will be noted that the microphotometer traces of fig. 2, which correspond to plate 2, show a real dip, but no such dip exists for any of the traces of fig. 3, which corresponds to plate 5. There would seem no doubt, therefore, about the reality of the minima observed in the enlargements of fig. 2. But if the reader will take two pieces of dark paper, and cover all but the actual image in (*a*) or (*b*) of fig. 2, he will observe that the minimum will either be much less marked or it may possibly seem to disappear altogether. A similar effect is illustrated by the lower part of the enlargements, where the background

of the image is white, because during exposure black paper covered the bromide paper up to the edge of the image. It will be noted that the minimum is less marked in this part of the reproduction.

Falling back on the microphotometer traces, we may again maintain that the faint minima observed in the enlargements of plate 2 are real, just as when the images were viewed through a magnifier. If this is granted, then the disappearance of the minima under the conditions specified must be considered an illusory phenomenon resulting from the lack of conditions favourable for the eye to detect very slight gradations in density. Or it may be that when the minimum has a pronounced appearance, we have to deal with the combination of a real effect, as shown by the microphotometer, and an illusory effect of the kind described by Thomson [4]. In any case there seems little doubt that visual observation of a photographic image is about as sensitive a test for the presence of two components as the microphotometer.

The authors wish to acknowledge their indebtedness to Professor E. F. Burton and Professor H. J. C. Ireton, of the McLennan Laboratory, University of Toronto, and to Dr. L. E. Howlett and Dr. Jones, of the National Research Laboratories, Ottawa, for their kindness in making microphotometer traces.

Summary.

An examination of resolving power has shown that microphotometer traces of photographic diffraction images are at least 10 per cent. more effective than visual observation, the microphotometer detecting a minimum whose theoretical intensity is only a few per cent. less than that of the neighbouring maxima.

Evidence is given that observation of the photographic images either visually through a magnifier or by enlarged positives is nearly as sensitive a test of resolution as the microphotometer, although in these methods it is necessary to guard against a possible illusory effect.

References.

(1) Phil. Mag. xxiii. p. 440 (1937).
(2) Collected works, i. p. 420.
(3) Proc. Roy. Irish Acad. xli. p. 137.
(4) Camb. Phil. Soc. xxiii. p. 419 (1927).

XLV. *Some Aspects of Nitrogen Afterglows.* *By* D. B. McNeill, *Ph.D.*, *and* K. F. Harvey, *M.Sc.*, *Queen's University, Belfast* *.

[Received July 2, 1938.]

[Plate IV.]

In a previous paper [1] some phenomena connected with active nitrogen and nitrogen afterglows were described. In this an account was given of the action of impurities in the discharge and a hypothesis was advanced to explain the production of the intercombination (Vegard–Kaplan) bands. These bands have not yet been produced with the intensity required for their rotational structure to be analysed [2]. In the present paper, some attempts to develop strong sources of the bands are described. These failed in their original purpose, but other observations were made, which are described together with experiments on the diffusion of the Lewis–Rayleigh form of the afterglow and its behaviour in a magnetic field.

1. *Argon-Nitrogen Mixtures.*

It was shown by Johnson [3] that the spectrum of nitrogen underwent considerable modification if it were excited in the presence of excess argon. More recently Bernard [4] has obtained a number of intercombination bands by electron beam excitation of a similar mixture. The spectra obtained by Johnson included the first positive bands of nitrogen, the final level of which is the initial level ($A^3\Sigma$) of the intercombination bands. It might therefore be anticipated that by using a modification of his technique a good source of the intercombination bands would be obtained.

It has been found that the effects of metastable atoms and molecules are enhanced in two types of positive column discharges. The first is the constricted discharge described by Seeliger [5]. In this the main part of the current is carried through an axially constricted channel. This is surrounded by an aureole wnich, at least in the case of oxygen-argon mixtures, contains large concentrations of metastable atoms [6]. Unfortunately, addition of pure nitrogen does not give a marked

* Communicated by Prof. K. G. Emeléus.

constriction of the positive column in argon [5]. The second type of tube is one in which the current density is kept extremely low. Discharges of this type were therefore used, but it was found necessary to work at very reduced pressure if the current density was to be kept low. At the pressures used (less than 0·1 mm.) there must have been considerable loss of metastable molecules by diffusion to the walls. To minimise diffusion a π-shaped tube of soda-glass was constructed with its horizontal arm 4 cm. in diameter. A quartz window was attached by a graded seal to one end of the tube so that the positive column could be viewed end on. The tube was provided with short wire electrodes in the vertical arms and the current limited by a thermionic diode. It was degassed at high temperature under vacuum, but as in previous work [1] it was found impossible to remove hydrogen completely. The argon contained about 0·1 per cent. nitrogen. It was used at pressures between 0·01 and 0·06 mm., with rectified currents of 0·01–0·04 milliamp.

Even with this small range of conditions the discharge took several forms. When the pressure was less than 0·01 mm. and the current less than 0·02 milliamp. it consisted of a small diffuse glow 2 cm. long at the centre of the tube near the anode. As the pressure increased with a simultaneous slight increase in current, the glow increased in size, until at 0·04 mm. it filled most of the tube. Above 0·05 mm. the appearance of the discharge altered abruptly, the current increased some five-fold, and the tube became filled with a bluish light, with a bright spot near the anode. These changes resemble some which have been described for oxygen [7] and helium [8], and probably represent a transition from the Townsend type of discharge to the ordinary glow discharge.

With 50 hours exposure spectrograms were obtained of a discharge through the gas at 0·03–0·05 mm. pressure, with a current of 0·01 to 0·04 milliamp. A number of bands were obtained, in addition to argon lines and the spectrum of hydrogen. The band heads were at 2977, 2937, 2761, 2560, 2509, 2423, and 2333 A, and may be identified as 8–6, 7–0, 6–0, 6–2, 5–1, 5–2, and 3–6 inter-combination bands. They were not strong, and it could not be decided with the low dispersion used if the bands

found by Bernard in the visible were present amongst the argon lines there.

2. *High Frequency Discharges.*

High frequency discharges (10^7 cycles per second) through nitrogen have been investigated by Kern [9]. He found that the light from the first positive bands showed little variation, whereas that from the negative bands fluctuated with the voltage. This anomalous behaviour of the positive bands can be regarded as the result of a short-period afterglow. It suggested that the discharge might be capable of development as a source of the intercombination bands, since it shows that the molecules persist in the $A^3\Sigma$ state.

To investigate this possibility, electrodeless tubes 25 cm. long and either 1 or 5 cm. diameter were set up with a quartz window at one end. Discharges were excited in them from a coaxial solenoid passing currents of up to 20 amps. at 10^6 cycles. No attempt was made to separate the different phases of the discharge. The appearance of the discharge depended in a marked way on the pressure of the nitrogen. Three principal types of discharge were observed. Below 0·03 mm. a feeble purple glow occurred which filled only that part of the tube surrounded by the solenoid. Above 0·04 mm. the discharge was of a reddish colour and filled the tube and pumping leads. It was noticed that it traversed bends in the leads by making distinct angular turns. In the intermediate pressure region the discharge again filled the tube and pumping lead, but was much more intense than at either higher or lower pressures ; there was also considerable generation of heat. The optimum discharge condition is probably related to the minimum of a Paschen sparking curve. In addition, at a pressure below 10^{-3} mm., fluorescence of the glass similar to that noticed in plasmoidal discharges by Wood [10] was obtained. The spectrum of the discharge at various pressures was photographed, but did not contain any intercombination bands. Both positive and negative bands were excited, the negative bands increasing in relative intensity with decrease in pressure.

3. *Auroral Afterglows.*

By very prolonged running of an intermittent discharge through nitrogen Kaplan was able to produce " auroral "

afterglows, the spectra of which contained the intercombination bands. Cario and Stille [11] have failed to reproduce Kaplan's conditions by using more orthodox technique and running a discharge for comparatively short periods through nitrogen which was initially pure.

A tube similar to that used by Kaplan was built by the authors. After rigorous degassing, a heavy discharge was passed through oxygen in the tube to remove possible residual carbon. The pumping lead was heated in a current of oxygen for the same purpose. After this the tube was re-evacuated and a charge of nitrogen, prepared from Kahlbaum's sodium azide, circulated through it to remove residual oxygen. The tube was finally pumped down and degassed once more. Nitrogen was then again admitted and an intermittent discharge passed.

Fig. 1.

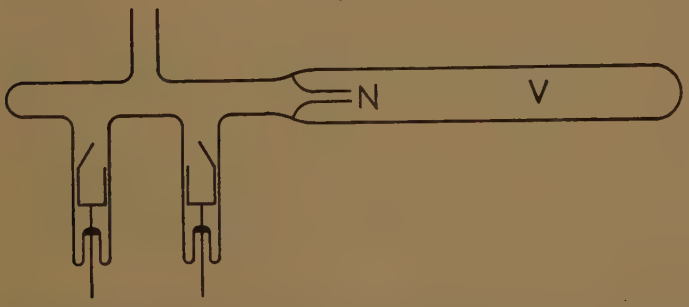

An afterglow was observed whose spectra did not contain the intercombination bands. This is in agreement with the findings of Cario and Stille, and confirms that Kaplan's conditions can be obtained only by his method. A possible explanation of this has been advanced in a previous paper [1].

4. *Lewis–Rayleigh Afterglow.*

A number of observations on the properties of the Lewis–Rayleigh afterglow have been made. The tube used (fig. 1) was π-shaped and had a "viewing chamber" (V) connected at one end through a nozzle (N), 2 cm. long and 0·4 cm. in diameter. The nitrogen was activated by a condensed discharge. An afterglow filled the whole of the viewing chamber, even behind the nozzle, and appeared to have an equal intensity

everywhere. A photograph of the glow in the viewing chamber is shown in Pl. IV., A (exposure 10 hours). The nozzle is seen at the left of the tube. The horizontal bright lines arise from stray reflections. The bright patch in front of the nozzle is where the afterglow was viewed end on in a side tube, not shown in fig. 1. Pl. IV., B is a similar photograph (12 hours exposure) of the glow in a larger viewing chamber, width 5 cm., with a nozzle 4 cm. long and 2 cm. in diameter.

The afterglow lasted for some 20 seconds after the activating discharge had been switched off, distinguishing it from a stray discharge. When the afterglow died away it faded out near the nozzle first, and the rather indefinite dark boundary moved away from this with a speed of approximately 8 cm./sec. The afterglow was also observed to travel up the pumping lead. Its speed, which was greater than in the viewing chamber, could not be measured exactly as the glow faded out too rapidly as it moved away from the exciting discharge.

A somewhat analogous effect was noticed when working with low current density discharges through the nitrogen-argon mixtures. In these, when the discharge was switched off, the tube became dark. About half a second later a very faint blue glow was seen to " pour " from the pumping lead into the discharge-tube and then diffuse through it. This appearance persisted for about three seconds.

A short length at the middle of the viewing chamber was held in a magnetic field which was varied from 1,500–4,500 gauss. No difference could be detected in the behaviour of the afterglow either when the magnetic field was applied continuously or intermittently.

References.

(1) McNeill, Phil. Mag. xxv. p. 471 (1938).
(2) Hamada, Phil. Mag. xxiii. p. 25 (1937). Kaplan, Phys. Rev. xlviii. p. 800 (1935); Pub. Astron. Soc. Pacific, xlvii. p. 257 (1935).
(3) Johnson, Phil. Mag. xlviii. p. 1069 (1924).
(4) Bernard, *Comptes Rendus*, cc. p. 2074 (1936).
(5) Seeliger, *Phys. Zeits.* xxxiii. p. 313 (1932).
(6) Unpublished work carried out in this laboratory.
(7) Greeves and Johnson, Phil. Mag. xxi. p. 659 (1936).
(8) Emeléus, Greeves, and Montgomery, Proc. Roy. Irish Acad. xliii. p. 35 (1936).
(9) Kern, *Ann. de Phys.* xxviii. p. 169 (1937).
(10) Wood, Phys. Rev. xxxv. p. 673 (1930).
(11) Cario and Stille, *Zeits. f. Physik.* cvii. p. 396 (1937).

XLVI. *The Effects of Stray Admittances in Four-Arm Bridge Networks.*

By N. F. Astbury, *M.A.*, *F.Inst.P.* (From the National Physical Laboratory.) *.

[Received July 28, 1938.]

Abstract.

When one or more of the arms of a bridge consists of two or more components in series, the stray admittances between the junctions of these components affect the conditions of balance. Two fundamental results are obtained, referring to cross admittances between junctions in adjacent arms and in opposite arms. It is shown that in general the equations of balance are unsymmetrical, and that in consequence the presence of such admittances is shown by a change in balance point when the components in any one arm are interchanged. For certain cases of circuit symmetry the effects vanish. The lack of symmetry distinguishes the effects from those arising from capacitances to earth. The application of the results to certain practical cases is considered, and suggestions as to treatment by circuit arrangement and by screening are made.

1. *Introduction.*

Workers concerned with precision alternating current bridge measurements are familiar with the frequently recurring necessity of evaluating small correcting terms which find their origin in the imperfections of the circuit components and in the inadequacy of control of stray magnetic and electric fields. Such correcting terms may conveniently be regarded as falling into three classes. There are first the familiar "residual" effects, which can be regarded as characteristic of each component and which can be determined as such. Into this group fall the small phase-angles of "non-reactive" resistors, power factors of capacitors and inductors, and phase defects of mutual inductors; allowance can be made for these quantities in any practical case by a simple extension of the circuit equations. In the second group we must consider possible corrections to the circuit

* Communicated by the Author.

equations arising from the effects of capacitance between the circuit components and neighbouring bodies at earth potential. When such capacitances are localized at the vertices of a bridge network they can be rendered nugatory by the use of a Wagner earthing arm[1]; if they operate from points other than the vertices then a Wagner arm is inadequate as a means of suppressing their effects, and the impedances of the bridge arms must be modified to establish balance under these conditions. This problem has been discussed by Butterworth[2], while a general discussion on the significance of effective impedance values in a.c. bridge circuits has been given by Hartshorn and Astbury[3].

The third group of corrections arises from the linkages between the electric fields of the bridge components. This question does not appear to have been discussed to any extent, possibly because on the whole the errors arising from it are likely to be less than those arising from the other causes discussed. Nevertheless it cannot be disregarded, and when measurements of the highest precision are being made it is important that one should at least know the order of magnitude of any possible error.

The problem does not seem capable of any complete theoretical solution, and its practical solution, which is usually to be sought in a careful use of electrostatic screens, must necessarily be incomplete. The problem most frequently arises in practice when one arm of a four-arm network consists of two or more components in series. The difficulties of screening the junctions—and, in fact, in many cases the complete neglect of any such precaution—lead to the existence of small capacitances between these junctions and other parts of the network. If the components forming the arm are individually screened this simplifies but does not remove the problem, for the screening is usually incomplete, while if the components are unscreened the problem is considerably complicated by the introduction of distributed effects. In seeking a solution, however, it will be assumed that the stray capacitances associated with any component may be considered as acting at its terminals, an approximation with which most experimenters would agree and which most nearly represents the general practical case. In what follows the equations

of balance of a four-arm network will be deduced on the assumption that the junctions of components in any one arm are linked to other points in the circuit by capacitance (or, in fact, an admittance of any sort), and one or two practical illustrations will be discussed.

2. *Equations of Balance in the presence of Cross-admittances.*

In deducing the equations of balance the following transformations will be used. The star O, ABC and the delta ABC (fig. 1) are equivalent when the following relations exist between their component impedances [4]:

$$a, b, c = \frac{YZ, ZX, XY}{X+Y+Z}, \quad . \quad . \quad . \quad . \quad (2.1)$$

$$X, Y, Z = \frac{ab+bc+ca}{a, b, c}. \quad . \quad . \quad . \quad . \quad (2.2)$$

Fig. 1.

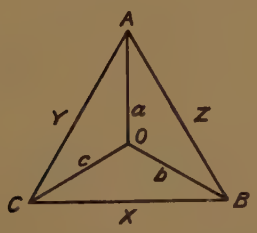

The second transformation [5] may be stated as follows. A star of n rays, OP_1 $OP_2 \ldots OP_n$ may be replaced by a pair mesh of $\frac{1}{2}n(n-1)$ impedances joining every pair. If the ray impedances are denoted by $Z_1, Z_2, \ldots Z_n$, and the pair impedances by Z_{rs}, etc., then

$$Z_{rs} = Z_r Z_s \Sigma\left(\frac{1}{Z_n}\right). \quad . \quad . \quad . \quad . \quad . \quad (2.3)$$

Equation (2.2) is clearly a special case of this.

In what follows it will be assumed that the cross-admittance is small compared with the admittances of the bridge arms. Then the necessary practical results can be deduced from a consideration of two problems only: first, the case of a four-arm bridge in which points

on *adjacent* arms are linked by a cross-admittance, and second, the case of a bridge in which points on *opposite* arms are so linked.

These are illustrated diagrammatically in figs. 2 and 3, in which the vertices of the bridge are denoted by S_1, S_2, D_1, D_2—S_1, S_2 being the points of application of the supply and D_1, D_2 the points of application of the detector. The impedances of the arms are denoted by Z_1, Z_2, Z_3, and Z_4. The cross-admittance, Γ, acts between the points P_1 and P_2, or P_1 and P_3. In practicc the points P_1, P_2, P_3 would be the junctions between components forming the arms. Suppose P_1 divides Z_1 in the ratio $p_1/(1-p_1)$, so that $S_1P_1=p_1 . Z_1$. Similarly, let $D_1P_2=p_2Z_2$, $S_2P_3=p_3Z_3$, etc., and let $\xi_1=\Gamma Z_1$, $\xi_2=\Gamma Z_2$,

Fig. 2.

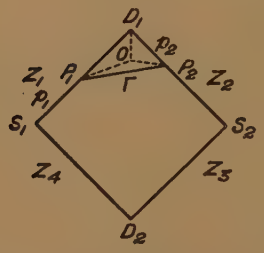

Fig. 3.

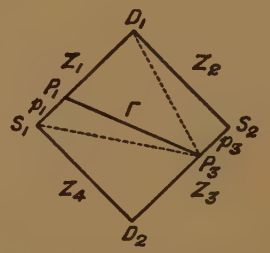

etc.* In the absence of any cross-admittance the condition of balance will obviously be

$$Z_1Z_3=Z_2Z_4. \quad . \quad . \quad . \quad . \quad . \quad . \quad (2.4)$$

In the presence of a cross-admittance the values of the effective impedances of bridge arms will be modified, and denoting the values of such modified effective impedances by dashed letters, the condition of balance is

$$Z_1'Z_3'=Z_2'Z_4'. \quad . \quad . \quad . \quad . \quad . \quad (2.5)$$

In the adjacent arm case, that of fig. 2, the effective values can be found as follows. The delta $P_1D_1P_2$ can be transformed into a star O, $P_1D_1P_2$, in which one ray (OD_1) will become part of the detector lead, and so will not enter into the equations of balance, while the

* It should be noted that all the symbols represent complex quantities, and that ξ_1, etc., will be quantities of the first order of smallness.

other rays become part of Z_1 and Z_2. We have, applying (2.1),

$$\begin{aligned} Z_1' &= S_1P_1+P_1O \\ &= p_1Z_1+(1-p_1)Z_1/[1+\Gamma\{(1-p_1)Z_1+p_2Z_2\}] \\ &\doteq Z_1[p_1+(1-p_1)\{1-\xi_1(1-p_1)-\xi_2p_2\}] \\ &= Z_1\{1-\xi_1(1-p_1)^2-\xi_2p_2(1-p_1)\} \quad . \quad . \quad . \quad (2.6) \end{aligned}$$

Similarly we find

$$Z_2' = Z_2\{1-\xi_1p_2(1-p_1)-\xi_2p_2^2\}. \quad . \quad . \quad (2.7)$$

The modified equation of balance thus becomes

$$\begin{aligned} Z_1Z_3\{1-\xi_1(1-p_1)^2-\xi_2p_2(1-p_1)\} \\ = Z_2Z_4\{1-\xi_1p_2(1-p_1)-\xi_2p_2^2\}, \end{aligned}$$

which may be written

$$\begin{aligned} Z_1Z_3\{1-\xi_1(1-p_1)(1-p_1-p_2)\} \\ = Z_2Z_4\{1+\xi_2p_2(1-p_1-p_2)\}. \quad (2.8) \end{aligned}$$

If $p_2=0$ we have the case of an admittance shunting part of Z_1, and the result given by (2.8) in this case is clearly correct. If $p_2=1$, we have the case of only one series arm (Z_1), and we get

$$Z_1Z_3\{1+\xi_1p_1(1-p_1)\} = Z_2Z_4\{1-p_1\xi_2\}. \quad . \quad (2.9)$$

This form will be referred to later.

The case of the opposite arms, shown in fig. 3, can be dealt with by transforming the star P_1, S_1 D_1 P_3 to the delta $S_1D_1P_3$. A new value of Z_1 is obtained and a four-rayed star P_3, $S_1D_1S_2D_2$ is left which, by (2.3), transforms into a mesh of six impedances, of which two, S_1S_2 and D_1D_2, are in shunt with supply and detector, and so do not appear in the equations of balance. Of the remaining four, one, S_2D_2, becomes the modified value of Z_3, while the others are thrown in shunt with Z_2, Z_4, and the modified value of Z_1.

Applying (2.2), we find

$$S_1D_1 = Z_1(1+u_1), \quad . \quad . \quad . \quad . \quad . \quad . \quad (2.10)$$

$$P_3D_1 = (1+u_1)/p_1\Gamma, \quad . \quad . \quad . \quad . \quad . \quad (2.11)$$

$$P_3S_1 = (1+u_1)/(1-p_1)\Gamma, \quad . \quad . \quad . \quad (2.12)$$

in which

$$u_1 = \xi_1p_1(1-p_1). \quad . \quad . \quad . \quad . \quad . \quad (2.13)$$

Applying (2.3), and writing σ for the sum of the ray admittances, we get

$$S_1D_1=\sigma(1+u_1)^2/p_1(1-p_1)\Gamma^2, \quad . \quad . \quad . \quad (2.14)$$

$$D_1S_2=p_3Z_3\sigma(1+u_1)/p_1\Gamma, \quad . \quad . \quad . \quad . \quad . \quad (2.15)$$

$$S_2D_3=p_3(1-p_3)Z_3{}^2\sigma, \quad . \quad . \quad . \quad . \quad . \quad . \quad (2.16)$$

$$D_3S_1=(1-p_3)Z_3\sigma(1+u_1)/(1-p_1)\Gamma. \quad . \quad (2.17)$$

We have also, if $u_3=\xi_3p_3(1-p_3)$,

$$\sigma=\Gamma(1+u_1+u_3)/(1+u_1)u_3$$
$$=\Gamma(1+u_3)/u_3 \quad . \quad . \quad . \quad . \quad . \quad . \quad (2.18)$$

retaining only first order terms.

The effective value of Z_1 is the parallel combination of the two values of S_1D_1 given by (2.10) and (2.14). Thus

$$Z_1'=Z_1(1+u_1)\{1-u_1u_3(1+u_1)/(1+u_3)\}$$
$$=Z_1(1+u_1) \quad . \quad . \quad . \quad . \quad . \quad . \quad . \quad . \quad (2.19)$$

to first order accuracy. We have also

$$Z_3'=Z_3(1+u_3), \quad . \quad . \quad . \quad . \quad . \quad . \quad (2.20)$$

$$Z_2'=Z_2\{1-\xi_2p_1(1-p_3)\}, \quad . \quad . \quad . \quad (2.21)$$

$$Z_4'=Z_4\{1-\xi_4p_3(1-p_1)\}. \quad . \quad . \quad . \quad (2.22)$$

The condition of balance is thus

$$Z_1Z_3\{1+\xi_1p_1(1-p_1)+\xi_3p_3(1-p_3)\}$$
$$=Z_2Z_4\{1-\xi_2p_1(1-p_3)-\xi_4p_3(1-p_1)\}. \quad (2.23)$$

It should be noted that when p_2 is put equal to unity in (2.8), and p_3 is put equal to zero in (2.23), the resulting expressions are identical, each reducing to the form given in (2.9).

3. *General Considerations arising from the Foregoing.*

In the fundamental expressions (2.8) and (2.23) the maximum value possible for the coefficients of ξ_1, ξ_2, etc., is unity. The maximum possible errors likely to arise in practice are therefore of the same order as ξ_1, ξ_2, etc., but of course it is not possible to discover by inspection from the above equations whether the in-phase or quadrature components are likely to be affected. This can only be done by expanding the equations in their complex forms for any particular case.

It will be observed that if $1-p_1-p_2=0$ the effect of a cross-admittance between adjacent arms is zero. Physically this means that there is never any potential

difference between the junctions connected by the admittance.

A most important point arising from the equations is that the conditions of balance are not in general symmetrical with regard to p_1, p_2, p_3, and p_4. The presence of the effects under consideration will therefore be detected in any practical case by a change in balance point when the components in any arm are interchanged, so that any p becomes replaced in the equations by its complement $1-p$. For the adjacent arm case we have

$$Z_1Z_3\{1-\xi_1(1-p_1)(1-p_1-p_2)\} = Z_2Z_4\{1+\xi_2p_2(1-p_1-p_2)\}. \quad (2.8)$$

When the components of Z_1 are interchanged we have

$$Z_1'Z_3\{1-\xi_1p_1(p_1-p_2)\}=Z_2Z_4\{1+\xi_2p_2(p_1-p_2)\}, \quad (3.1)$$

in which Z_1 has been changed to Z_1' to indicate that a change is necessary in order to restore balance. We then find

$$(Z_1-Z_1')/Z_1=(1-2p_1)\{p_2\xi_2+(1-p_2)\xi_1\}, \quad (3.2)$$

and the fractional change in Z_1, given on the left-hand side of this equation, will always be finite unless the arm is perfectly symmetrical to start with (*i. e.*, $p_1=\frac{1}{2}$), which is not very probable in practice, since p_1 will in general be complex. Similar considerations can be applied to (2.23). These results are of considerable importance, since they allow discrimination between the particular effects under consideration and those arising from either of the other sources of error discussed in the introduction. In particular they are distinguished by their lack of symmetry from any effects arising from earth-capacitance effects associated with the mid-arm junction points. Thus it has been shown elsewhere [2] that if, in a four-arm bridge with a Wagner earth, an admittance Γ connects a point such as P_1, fig. 2, to earth, then the effective value of Z_1 becomes

$$Z_1'=Z_1\{1+\xi_1p_1(1-p_1)\}, \quad (3.3)$$

ξ_1 being written for ΓZ_1 as before. This expression is symmetrical in p_1, and therefore no change is to be expected if the components are interchanged. Now expression (3.3) may be deduced by a simple application of equation (2.9) to the case of a six-arm network (*i. e.*, a bridge with Wagner arms), and when this is done it appears

that although for this case the main bridge balance is symmetrical the Wagner arm balance is not. In fig. 4 is shown a four-arm bridge $Z_1Z_2Z_3Z_4$ with Wagner arms Z_5 and Z_6. It is known that the necessary and sufficient conditions for the balance of such a network are given by [6]

$$\frac{Z_1}{Z_4}=\frac{Z_2}{Z_3}=\frac{Z_5}{Z_6}. \quad . \quad . \quad . \quad . \quad . \quad (3.4)$$

When an admittance Γ connects P_1, say, with E, we may apply equation (2.9), adjusting the suffices to fit fig. 4. We find then as modified conditions of balance

$$\frac{Z_1\{1+\xi_1 p_1(1-p_1)\}}{Z_3}=\frac{Z_2}{Z_3}=\frac{Z_5\{1-p_1\xi_5\}}{Z_6}, \quad . \quad (3.5)$$

showing that the main bridge balance is symmetrical and the Wagner arm balance unsymmetrical.

It may be concluded, therefore, that in any four-arm bridge, whether used with Wagner arms or not, in which one or more arms consist of components in series, the

Fig. 4.

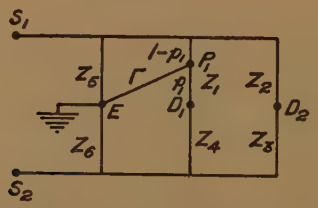

presence of any effects due to cross-admittances between the junctions of any such arms may be detected by a change in the main balance following an interchange of components in the arms. This interchange must clearly be carried out in such a way as not to affect the existing cross-admittance, but this should present no practical difficulty.

Finally, it may be pointed out that, although the equations have been worked out for only one junction in each arm, their application to the case of arms with several junctions follows very simply so long as the convention as to the first order magnitude of ξ_1, etc., is maintained. For any term involving a ξ in the equations given above a summation of similar terms would be substituted. The extension to the case of uniformly distributed admittance can be easily obtained by integration, although this is hardly a case likely to be met with in practice.

4. *Some Practical Applications.*

It is impossible to give more than a passing reference to the many practical cases to which the foregoing results can be applied. In almost every bridge using self or mutual inductors the situation must arise, since in such bridges an inductive coil always shares an arm with another component, usually a resistance. The Campbell-Heaviside self-inductance bridge [8] provides a good example for the application of equation (2.8), while the Heydweiller modification of the Carey Foster capacitance bridge [8] provides an example of (2.23). The application of the results to the design of the new capacitance testing set at the National Physical Laboratory has been given elsewhere [7].

The Rosa-Wien capacitance bridge [8], shown in fig. 5,

Fig. 5.

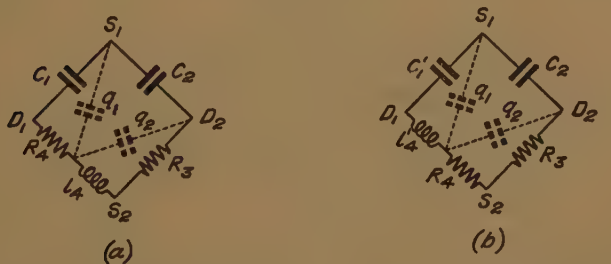

provides a simple illustrative example. The difference between the power factors of the condensers C_1 and C_2 is balanced out by the inclusion of a small variable self-inductance, l_4, in one or other of the resistance arms. If γ_1 and γ_2 be the power factors, we have

$$C_1/C_2=R_3/R_4 \quad \text{and} \quad \gamma_1-\gamma_2=\omega l_4/R_4, \qquad . \quad (4.1)$$

where $\omega/2\pi$ is the frequency of the supply current. In practice we may assume, in the absence of perfect shielding, cross-admittances to exist as represented by the capacitances q_1 and q_2. In order to simplify the arithmetic, let us put $R_3=R_4=R$. Then we may write, for fig. 5 (*a*), if $j=\sqrt{-1}$,

$$Z_1=R+j\omega l_4 \quad Z_2=(1+j\gamma_1)/j\omega C_1,$$
$$Z_3=(1+j\gamma_2)/j\omega C_2 \quad Z_4=R,$$
$$p_1=j\omega l_4/(R+j\omega l_4),\ p_2=p_3=1,\ \xi_1=jwq_1R,\ \xi_2=q_1/C_1.$$

Considering first the effect of q_1 we find, on applying (2.8), (2.9), or (2.23), and separating in-phase and quadrature parts,

$$C_1(1-\omega^2 l_4 q_1)=C_2, \quad . \quad . \quad . \quad . \quad . \quad . \quad . \quad (4.3)$$

$$\gamma_1-\gamma_2=\frac{\omega l_4}{R}\left(1+\frac{q_1}{C_1}\right). \quad . \quad . \quad . \quad (4.4)$$

When the components of Z_1 are interchanged, as in fig. 5 (*b*), we find $p_1=R/(R+j\omega l_4)$, and development of the equations gives

$$C_1(1-\omega^2 l_4 q_1)=C_2\left(1-\frac{q_1}{C_1}\right), \quad . \quad . \quad . \quad (4.5)$$

$$\gamma_1-\gamma_2=\frac{\omega l_4}{R}\left(1-\frac{q_1}{C_1}\right). \quad . \quad . \quad . \quad (4.6)$$

We find the effect of q_2 in an exactly similar way. For the arrangement of fig. 5 (*a*) we have

$$C_1=C_2, \quad . \quad . \quad . \quad . \quad . \quad . \quad . \quad . \quad . \quad (4.7)$$

$$\gamma_1-\gamma_2=\frac{\omega}{R}(l_4+R^2 q_2), \quad . \quad . \quad . \quad . \quad (4.8)$$

while for the interchanged arrangement (fig. 5 (*b*))

$$C_1=C_2\,(1+2\omega^2 l_4 q_2) \quad . \quad . \quad . \quad . \quad (4.9)$$

$$\gamma_1-\gamma_2=\frac{\omega l_4}{R}. \quad . \quad . \quad . \quad . \quad . \quad . \quad (4.10)$$

The reversal effect is shown very strikingly in equations (4.3) and (4.5) and in (4.8) and (4.10). For audio-frequencies and reasonable values of q_1 and q_2 the effects in the other cases are not marked. The results given by equations (4.5) and (4.8) approximate closely to those which would arise if the stray capacitance were thrown directly across C_2 or R_3. The effects are easily demonstrated experimentally, and the results have been checked for the case in which $R_3=R_4=1000$ ohms and $C_1=C_2=0{\cdot}01$ μF. A small variable air condenser was connected in turn between the junctions of R_4 and l_4, and the vertices S_1 and D_2 and the readings of capacitance and power factor at balance were recorded as a function of the added cross-capacitance. The results corresponding to equations (4·3) and (4.5) and (4.8) and (4.10) were plotted, giving pairs of intersecting lines, the points of intersection of which correspond to the residual values of q present in the circuit. In the case quoted the residual value of q_1 was found to be 5 $\mu\mu$F and the residual

value of q_2 was found to be 10 $\mu\mu$F. The results are shown in fig. 6.

The Owen bridge [8] for the measurement of self-inductance provides another interesting example. The diagrams in fig. 7 show two arrangements of this bridge, with a small capacitance q joining the junctions in the adjacent arms. As was pointed out in section 3 (p. 512) such a capacitance will have no effect if the points it

Fig. 6.

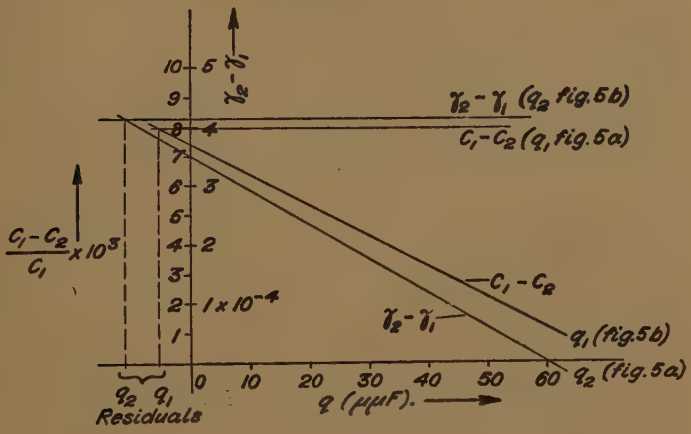

Fig. 7.

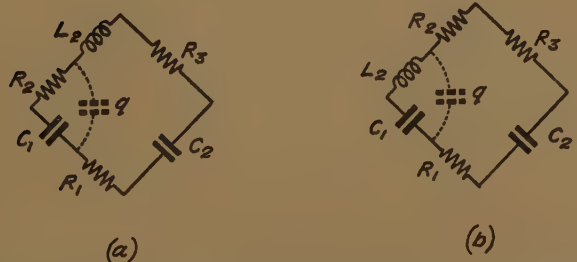

connects are at the same potential, *i. e.*, if $1-p_1=p_2$ or $1-p_2=p_1$. The Owen bridge possesses these properties for certain arrangements. In the arrangement shown in fig. 7 (*a*) we have

$$1-p_1=1/(1+j\omega C_1R_1) \quad \text{and} \quad p_2=R_2/(R_2+j\omega L_2).$$

Thus $1-p_1=p_2$ if $L_2=C_1R_1R_2$, which is the case for an equal arm bridge, provided that L_2 has a very low resistance compared with R_1. When the components of both arms are interchanged the complementary

condition $1-p_2=p_1$ must obviously hold, and again there will be no effect. If, however, only one arm is reversed, as shown in fig. 7 (*b*), the equalities no longer hold, and the cross-admittance will be operative to the extent given by equation (2.8).

Conclusion.

The effects discussed in the foregoing are likely to be of interest only in work of high precision in the audio-frequency range, and in general need be considered only when an accuracy of 1 in 10,000 or greater is sought. However, the growing tendency to develop bridge methods of measurement for carrier and radio frequencies necessitates a fuller understanding of the many sources of error to which such measurements are liable, and it is hoped that the results given in this paper will prove helpful in this respect.

It will be apparent from what has been said that the treatment of cross-admittance effects may be made to depend not only on the more obvious method of screening but also on the arrangement of the circuits to produce the symmetry which leads in some cases to the self-balancing of the effects, as was illustrated very simply by the case of the Owen bridge. With regard to the screening of the components, it is recommended that this should be carried out so that stray capacitances are localized at the terminals. The screening of an arm containing components in series can then be carried out, theoretically, by surrounding each junction by a screen at the potential of the junction, which can be done in bridge circuits by making use of tapping points on the Wagner arms for supplying the auxiliary screen potentials. To make the arrangement complete the junction screens must be enclosed in earthed screens, so that all stray capacitances finally appear in the Wagner arms. A simpler and more practicable scheme, adopted in the N.P.L. capacitance testing set already mentioned, is to throw the capacitances associated with the junctions in shunt with part of the arm by surrounding the whole arm by a screen connected to one end of the arm. This alters the characteristics of the arm, but it does so in a perfectly definite way which is easily calculated (see, for example, equation (2.8) with $p_2=0$).

It perhaps need hardly be pointed out that it is useless

to lay down a rule for the replacement of series combinations of impedances by equivalent parallel groups in order to avoid the effects under discussion. While obviously this does eliminate the possibility of any such effects, it must be borne in mind that certain series combinations have the advantage of being perfectly aperiodic, while their "equivalent" shunt circuits are not. The experimenter must decide every case on its merits, and consider which particular circuit defect he is best able to tolerate or eliminate.

References.

(1) Wagner, 'Electrician,' lxviii. p. 483 (1911).
(2) Butterworth, Proc. Phys. Soc. xxxiv. p. 8 (1922).
(3) Hartshorn and Astbury, Phil. Trans. Roy. Soc. A, ccxxxvi. no. 769, p. 423 (1937).
(4) Kennelly, Elec. World, xxxiv. p. 413 (1899).
(5) Rosen, J. I. E. E., lxii. p. 916 (1924).
(6) Dye and Jones, J. I. E. E. lxxii. no. 434, p. 181 (1933).
(7) Astbury and Ford, Proc. Phys. Soc. (pending).
(8) Campbell and Childs, 'The Measurement of Inductance, Capacitance, and Frequency' (Macmillan, London, 1935), chaps. 13 and 18.

XLVII. *Capillary Ascent in Cylindrical Tubes.*

By Alfred W. Porter, *D.Sc., F.R.S.*

[Received August 30, 1938.]

In the 'Proceedings of the Royal Society,' xcii. pp. 184 and 195, the late Lord Rayleigh dealt with the theory of the rise of liquids in a capillary tube. In the important case for which the angle of contact equals zero, and for which the capillary constant equals

$$\beta^2=\frac{\text{surface tension}}{g\,(\text{effective density})},$$

he derives the formula $\beta^2=\frac{1}{2}r\,(h_0+r/3-0{\cdot}1288r^2/h_0)$, which is equivalent to that given by Poisson in his theory of capillary action published in 1831 (*i. e.*, more than a century ago). He then proceeds to show that in the particular case for which the angle of contact is zero another term needs to be added giving

$$\beta^2=\tfrac{1}{2}r\left(h_0+\tfrac{1}{3}r-0{\cdot}1288\frac{r^2}{h_0}+0{\cdot}1312\frac{r^3}{{h_0}^2}\right).$$

Unfortunately he does not indicate the range of the

* Communicated by the Author.

variables for which these equations are respectively adequate, so that the experimentalist is left with no guidance in selecting the equation to be adopted. To proceed further it is best to write the equation in a non-dimensional form. The three terms formula becomes

$$\frac{\beta^2}{r^2} = \frac{1}{2}\frac{h_0}{r} + \mathrm{R}_1 = \frac{1}{2}\frac{h_0}{r} + \frac{1}{6} - \cdot 0322\frac{r}{h_0},$$

while the four term formula is

$$\frac{\beta^2}{r^2} = \frac{1}{2}\frac{h_0}{r} + \frac{1}{6} - \cdot 0322\frac{r}{h_0} + \cdot 0328\frac{r^2}{{h_0}^2}$$
$$= \frac{1}{2}\frac{h_0}{r} + \mathrm{R}_2.$$

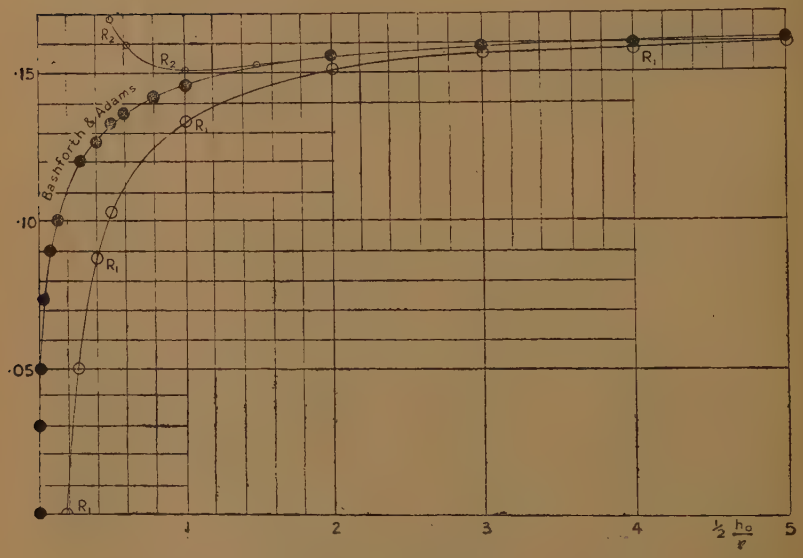

Fortunately we also have the values calculated by means of Bashforth and Adams's Tables. These are correct to at least five significant figures. They are shown on the diagram by means of black disks and serve as an ultimate standard of reference by comparison with which any formula may be tested. Hence inspection of the figure shows that Poisson's formula is always in defect of the true value, while Rayleigh's is in excess for values of $\frac{1}{2}\frac{h_0}{r}$ less than about 2.

XLVIII. *An Original Method of Comparison of Capacities at Radio Frequencies.* *By* W. Vaughan, *B.Sc., Ph.D.**

[Received June 1, 1938.]

Part I.

THE comparison of capacities of condensers at audio frequencies is almost invariably carried out by some form of bridge employing a fixed standard capacity and variable resistances. Such an arrangement as for example the Schering Bridge with a Wagner earth connexion is capable of yielding results of a very high order of accuracy. For measurements at radio frequencies, however, substitution methods are more common, since the adaptation of a bridge method for use at these frequencies is difficult, calling as it does for considerable elaboration of the apparatus. The principle of most of these substitution methods is well known. It usually depends upon the change in frequency of an oscillatory circuit when the unknown capacity is added. The frequency is then restored to its original value by the reduction of the capacity of a standard variable condenser, this reduction representing the magnitude of the unknown added to the circuit. Providing that a suitable standard variable is available, this method combines the advantages of ease and rapidity of operation with a considerable range of adaptability. The accuracy of such a determination is, however, rarely of a very high order.

It is obvious that in any substitution method the limit of accuracy is fixed absolutely by the reliability of the readings of the standard variable, and hence by the accuracy of its calibration and the degree of fineness to which its scale can be read. Furthermore, the accuracy obtainable with any particular variable is greatest when its maximum value is only slightly in excess of the unknown. This does not appear to have been always fully realized in many determinations of large dielectric constants using only one standard variable. Indeed, the measurement of even small dielectric constants to an accuracy of 1 per cent. by such methods requires a very accurate and costly standard variable condenser.

A critical examination of a considerable number of

* Communicated by Dr. S. Marsh.

substitution measurements has shown that in many cases the system of adjusting the standard variable to give exact substitution was far more accurate than the subsequent ability to interpret the adjustment merited. This was noticeably the case when a calibration curve had to be used. The use of heterodyne methods whilst giving very accurate settings has, at times, been confused with the accuracy of reading the condenser and has consequently led to very optimistic claims for the accuracy of the determination. Further difficulties always arise in substitution methods from the difficulty of estimating stray capacities. In all radio frequency methods some form of screening is necessary and capacities to earth are in parallel with the standard variable. On adding the unknown to the oscillatory circuit these capacities undergo a redistribution, whilst the unknown itself may introduce further stray capacities in parallel with itself. The determination of lead capacity and inductance effects, and of the capacity of the switch for introducing the unknown, is practically impossible.

At the commencement of the research about to be discussed a considerable amount of experience of these methods had been obtained, and it had been found that the difficulties mentioned above always constituted a very real barrier in work of any precision. Accordingly it was sought to develop an entirely new method which, in removing these disadvantages, should neither lead to undue complication of the apparatus nor restrict its adaptability. The method eventually devised represents in some respects a simplification of the foregoing practice and includes the following unique features :—

(*a*) Use of a fixed standard capacity in place of the variable needed for substitution methods. The former is far less costly and much more reliable than the latter. In the determination of dielectric constants the fixed standard may be of the simplest form since a knowledge of its absolute capacity is not required.

(*b*) Neither the unknown nor the standard condenser need be removed from the circuit at any stage of the operation, so that switching difficulties do not arise.

(*c*) Capacities to earth, unless large, may be ignored, so that screening is a matter of simplicity. This further facilitates the design of test-condensers for dielectric

constant measurements, and, if desired, guard-rings may be used.

(*d*) Capacities ranging from the order of a few up to several hundreds of $\mu\mu$F. may be measured without modification to the apparatus, beyond the provision of a standard of the same order of magnitude as the unknown if the maximum degree of accuracy is to be realized.

(*e*) Considerable leakage in the unknown condenser does not affect the procedure nor to any great extent the accuracy obtainable.

Experimental Circuit.

The admittance of the circuit shown in fig. 1, at a frequency n cycles per second, assuming C_a and C_b to be

Fig. 1.

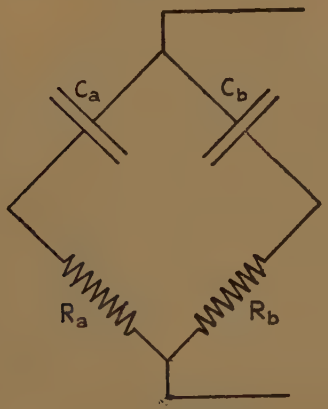

pure capacitances and R_a and R_b to be strictly non-inductive, is given by,

$$Y=\frac{1}{R_a+\frac{1}{j\omega C_a}}+\frac{1}{R_b+\frac{1}{j\omega C_b}},$$

where $\omega=2\pi n$. *I. e.*,

$$Y=j\omega\left\{\frac{C_a}{1+R_a^2\omega^2C_a^2}+\frac{C_b}{1+R_b^2\omega^2C_b^2}\right\}$$
$$+\omega^2\left\{\frac{R_aC_a^2}{1+R_a^2\omega^2C_a^2}+\frac{R_bC_b^2}{1+R_b\omega^2C_b^2}\right\}.$$

In practice the term $\frac{R^2C^2\omega^2}{2M2}$ will be kept small in

comparison with unity ; *e. g.*, consider the use of a 500 $\mu\mu$F. condenser in series with a resistance of 10 ohms at a frequency of 10^6 cycles/sec., then the term $R^2C^2\omega^2$ will be about 10^{-3}. Actually this will be shown to represent an extreme case, and since the experimental procedure is such that R_a has its maximum value when R_b is zero, and *vice versa*, the simplification

$$Y=j\omega(C_a+C_b)+\omega^2(R_aC_a^2+R_bC_b^2)$$

will be true to within 0·1 per cent. for all circumstances subsequently to be examined.

This network is connected in parallel with an inductance L and a tuning condenser C_t, oscillations being generated in the latter by connecting it across the grid and filament of a triode oscillator (fig. 3). Assuming that the stray

Fig. 2.

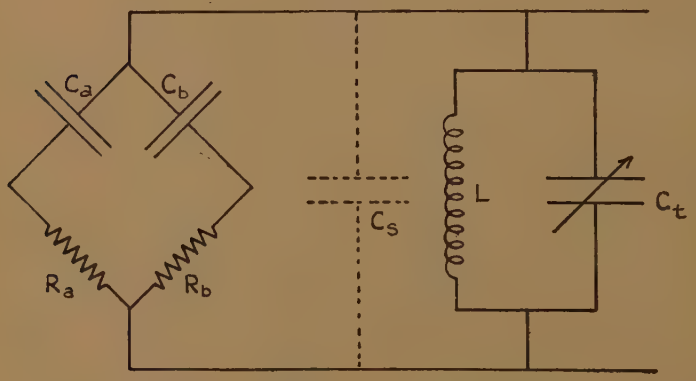

capacities across L and C_t are represented by C_s, and neglecting for the moment the effect of stray capacities across the resistances, the total admittance now becomes

$$Y_T=j\omega\left[(C_a+C_b)+C_t+C_s-\frac{1}{\omega^2L}\right]+\omega^2[R_aC_a^2+R_bC_b^2]. \quad (1)$$

It may now be shown that, subject to the restrictions already imposed upon the term $R^2C^2\omega^2$, the frequency of self oscillations generated in this circuit will be

$$n=\frac{1}{2\pi\sqrt{L\times[(C_a+C_b)+C_t+C_s]}},$$

i. e., it is independent of the values of R_a and R_b. As this is a matter of some importance if the method is to yield

highly accurate results, a more complete theoretical and experimental investigation of this statement will be included at a later point.

The theory of the simple comparison of the capacities C_a and C_b will now be dealt with. Suppose the resistance R_a in series with C_a to be given a definite value, whilst R_b is reduced to zero. The admittance expression now becomes

$$Y_a = R_a C_a^2 \omega^2 + \text{imaginary terms independent of } R_a.$$

R_a is now reduced to zero, and a resistance R_b joined in series with C_b. The admittance in this case will be

$$Y_b = R_b C_b^2 \omega^2 + \text{imaginary terms independent of } R_b.$$

Assuming, however, that the value of R_b was such that

Fig. 3.

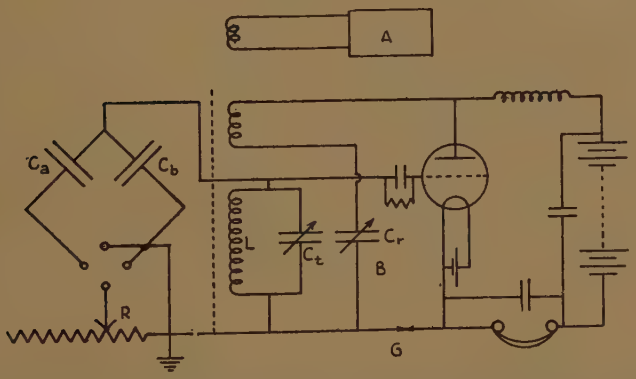

its addition exactly restored the original admittance, then

$$R_a C_a^2 \omega^2 = R_b C_b^2 \omega^2,$$

i. e.,

$$\left(\frac{C_a}{C_b}\right)^2 = \frac{R_b}{R_a} \quad \ldots \ldots \quad (2)$$

If therefore, experimental means of judging this equality of admittance can be applied, the capacities C_a and C_b can readily be compared in terms of two resistances. Actually, several methods suggest themselves when it is remembered that changes in the real admittance term for an oscillatory circuit such as this alter the amplitude of the oscillations set up in it.

In the initial attempt to compare capacities in this way the arrangement shown in fig. 3 was used. Circuit B

shows the practical form of the arrangement just described, A representing a Sullivan heterodyne wavemeter. The variable resistance R must have negligible self inductance and capacity, and to meet these requirements a metre bridge wire was used, a thin wire of high specific resistance being chosen in order to minimize the effects of slider contact resistance. Since only ratios of resistances are required, the absolute value for any particular setting could be taken as proportional to the length of wire. The method of operation was as follows :—

With the full length of R joined in series with C_a the larger of the two condensers, and C_b earthed, the circuit B (now in self oscillation) was tuned to the required frequency by comparison with the wavemeter A. Slight mistuning now gave a heterodyne note in the phones, and this was used as an indication of self oscillation in circuit B. The reaction condenser C_r was then adjusted until self oscillation just disappeared. On reducing the resistance R slightly, oscillations recommenced, the exact position of the slider at which this occurred being noted. This represents the resistance R_a. Condenser C_a was now earthed and R joined in series with C_b. Without disturbing the setting of C_r, a setting R_b was then found, at which self oscillation again disappeared. The ratio of the capacities may now be calculated from

$$\frac{C_a}{C_b} = \sqrt{\frac{R_b}{R_a}}.$$

Additional results could be obtained by resetting the reaction condenser, and these showed a very reassuring degree of constancy. On account of the extreme simplicity of the method, and of the satisfactory results obtained, some time was spent in exploring its full possibilities. The results of this investigation are summarized below :—

(*a*) The pitch of the heterodyne note remained satisfactorily constant during the adjustment of the slider. In order to obtain complete freedom from hand-capacity effects, the complete circuit, with the exception of the resistance R, was placed in a metal screening box. For convenience, a loud-speaker and amplifier replaced the phones in later experiments.

(*b*) As might be expected, an anode-bend detector

gave less satisfactory results than a leaky-grid detector on account of the difficulty in deciding the exact point of disappearance of the heterodyne note.

(*c*) It was found, especially when anode voltages of more than 75 were used, that oscillations did not commence at the same point on the wire at which they had previously ceased. This, however, introduced no difficulty, providing adjustments were made with reference to one of these points only. The point of cessation was in all cases found to be the more sharply defined.

(*d*) In order to test the method under the most favourable conditions the condensers chosen had approximately equal capacities. As has already been pointed out, a variety of results could be obtained by slight readjustments of the condenser C_r. Under the conditions stated, results agreeing among themselves to within 1·5 to 2 per cent. were easily obtainable, and this may therefore be taken as some indication of the accuracy of the method. Approximately the same degree of agreement was obtained with pairs of condensers of the order of 100 $\mu\mu$ F., as with condensers of about 1000 $\mu\mu$ F., at various frequencies between 150 Kc./sec. and 1200 Kc./sec. In the latter case it was found advisable to couple the test network to the oscillator by means of a small variable condenser in order that it should not add excessively to the grid circuit damping.

The first modification of the method gave an improved method of detecting the exact point of cessation of oscillation. For this purpose a galvanometer was included in the grid circuit at the point G (fig. 3). It is now possible to dispense with the wavemeter except as a means of determining the frequency of operation. If circuit B is in a state of self oscillation, the galvanometer shows grid-current. At the point at which oscillations cease the grid-current falls sharply to zero, the point of disappearance being very well defined. An alternative method is to find values of R_a and R_b which give equal grid-currents, circuit B remaining in self oscillation throughout the experiment. Equality of grid-current is an indication of equality of amplitude of oscillation. This can only occur providing the substitution R_b for R_a has left the decrement of the circuit, and hence the admittance of the network unchanged. The method as

it now appears represents perhaps one of the simplest ways of comparing capacities at radio frequencies.

As it now stands, the method clearly has the greatest accuracy when C_a and C_b are approximately equal. The following modifications to the network show how its range may be extended :—

(a) *Comparison of Capacities of widely differing Magnitudes.*

Suppose condenser C_b has a capacity several times that of C_a. In the first stage of the comparison C_a is connected directly to earth whilst a resistance R_b is joined in series with C_b (fig. 4 *a*). The real part of the admittance expression is now

$$Y_b = C_b^2 R_b \omega^2.$$

Fig. 4 *a*.

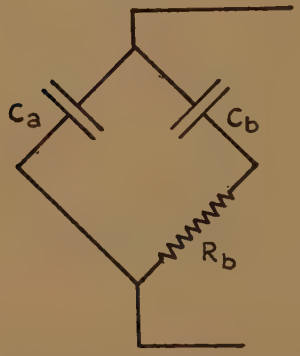

Fig. 4 *b*.

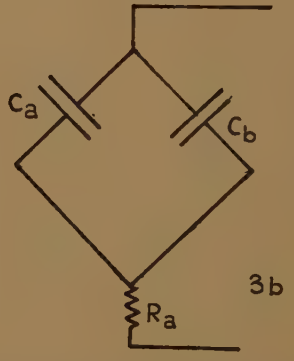

C_a is now connected in parallel with C_b (fig. 4 *b*) and a resistance R_a found which leaves the admittance unchanged. The real admittance term is now

$$Y_a = (C_a + C_b)^2 R_a \omega^2,$$

so that

$$(C_a + C_b)^2 R_a = C_b^2 R_b,$$

i. e.,

$$\frac{C_a}{C_b} + 1 = \sqrt{\frac{R_b}{R_a}}. \quad \ldots\ldots \quad (3)$$

Applying this method it was found possible to make use of quite a large proportion of the resistance wire for both R_a and R_b. When C_b was about twice as large as C_a it was found possible to obtain results agreeing among themselves to within about 3 to 4 per cent., and when C_b

was about four times as large as C_a the results agreed to within about 5 per cent. The form of the expression shows that comparisons with larger capacity ratios would not be very accurate, and in such cases it is probably preferable to use an intermediate standard.

(b) *Comparison of approximately Equal Capacities.*

If C_a and C_b differ by only a very small amount their capacities may be compared with even greater accuracy than is obtainable in the general method already discussed. A fixed resistance X, which may well be one or more units of a P.O. Box, is connected in series with C_a and C_b is earthed. A resistance R_b is now found which shall have exactly the same effect in series with C_b as X in series with C_a. The capacity ratio is now

$$\left(\frac{C_a}{C_b}\right)^2 = \frac{R_b}{X}. \quad . \quad . \quad . \quad . \quad . \quad . \quad . \quad (4)$$

The experiment is now repeated with X in series with C_b, and a new resistance R_a is found to give the same effect in series with C_a as X in series with C_b. This gives the capacity ratio

$$\left(\frac{C_a}{C_b}\right)^2 = \frac{X}{R_a}. \quad . \quad . \quad . \quad . \quad . \quad . \quad . \quad (5)$$

Combining the expressions 4 and 5 it follows that

$$\frac{C_a}{C_b} = \sqrt[4]{\frac{R_b}{R_a}}. \quad . \quad . \quad . \quad . \quad . \quad . \quad . \quad (6)$$

Using this method for the comparison of two condensers of nominal capacity 500 $\mu\mu$ F. a series of results showing agreement to within 1 per cent. was obtained. This method is of value principally for capacities which do not differ by more than about 25 per cent.

(c) *Radio-frequency Bridge.*

If a key is placed at the point K (fig. 5) the circuit becomes an exceedingly simple form of radio-frequency bridge. When the key is open the real admittance term becomes

$$Y_1 = \omega^2\{C_a^2 R_a + C_b^2 R_b\}.$$

On closing the key this becomes

$$Y_2 = \omega^2 \left\{ (C_a + C_b)^2 \frac{R_a R_b}{R_a + R_b} \right\}.$$

The condition of balance, *i. e.*, that the closing of the key shall not affect the admittance of the circuit, is

$$C_a^2R_a+C_b^2R_b=(C_a+C_b)^2\frac{R_aR_b}{R_a+R_b},$$

i. e.,

$$\frac{C_a}{C_b}=\frac{R_b}{R_a} \quad . \quad . \quad . \quad . \quad . \quad . \quad . \quad . \quad (7)$$

Unfortunately this arrangement is of more theoretical than practical interest. In the first place it is not a null method, since the condition of balance is determined by the equality of grid-current before and after closing the key. Secondly, although the slider contact resistance has no effect on the balance point if the slider is connected to earth, the fact that it does contribute to the total

Fig. 5.

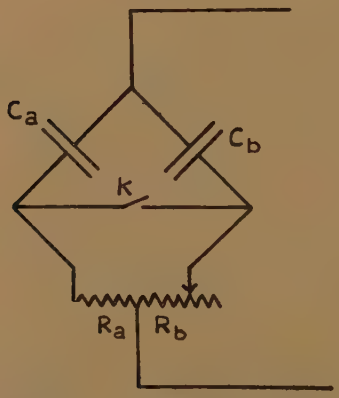

admittance makes adjustment somewhat difficult and the balance point cannot be easily found.

(d) *Improvement in Sensitivity.*

In each of the following methods whenever very small capacities were being compared, even a reflecting galvanometer was found to be scarcely sensitive enough to indicate the small changes in grid-current. The change in grid-current, however, produces a change in the bias voltage developed across the grid leak, and this in turn gives rise to a proportionately larger change in anode current. To make use of this magnified effect the galvanometer was transferred to the anode circuit and arrangements were made to balance out the steady anode current so

that small changes could be readily observed with the galvanometer. (The circuit chosen was that shown in fig. 6.) In order to compensate for the effects of drift of battery potential, attempts were made to balance out the anode current by a bridge arrangement using a second valve of the same type as that in the oscillator circuit, both valves being fed from the same batteries. The results of these experiments were disappointing on account of the one valve being in a static condition whilst the other was generating oscillations. Later experience showed, however, that with the simpler circuit shown in fig. 6, drift due to battery variation was not serious over the duration of an experiment providing that H.T. was derived from accumulators maintained in satis-

Fig. 6.

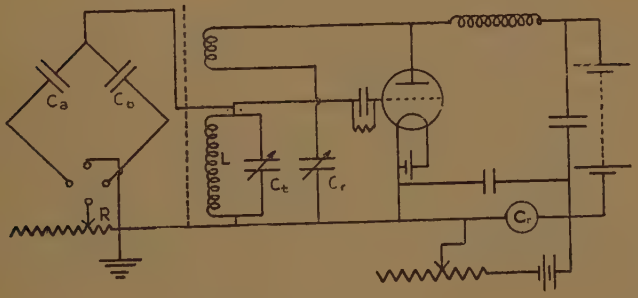

factory condition. To facilitate rapid balancing of the anode current the galvanometer was shunted by a suitable variable resistance so that it could be rendered insensitive until the final stage of the experiment. With this form of circuit it was found that sensitivity was greater than the adjustment of the type of resistance used for R really justified.

Summary of Initial Investigations.

The circuits developed and the results obtained with them indicate that with this method quite a satisfactory order of accuracy is obtainable with the simplest of apparatus. Not the least interesting feature of the method is its ability to yield results which require no subsequent correction for stray capacities to earth. The most serious limitation of the method in its present

form arises from the unsatisfactory form of the variable resistance R.

The second part of this paper deals with improvements in this direction.

Part II.

The first part of this paper gave an account of a very simple method of comparing capacities at radio frequencies. The most serious difficulties in the way of its development were shown to arise from the provision of suitable variable resistances The restrictions on the choice of this resistance are indicated below :—

(*a*) The resistance must be non-inductive and of low self capacity. The first requirement calls for a narrow loop, whilst the second limits the design even of this.

(*b*) It must have a fairly high value, say 20 ohms or over, for two distinct reasons. Firstly, large resistance variations are necessary in order to give reasonable current changes when comparing small capacities. Secondly, the effects of contact resistance must be negligible.

Finally, after much speculation on a variety of differing designs, it was decided to adopt a system in which the resistance could be varied in steps, and to study the variations in galvanometer deflexions which they produced with a view to interpolating the exact values of resistance necessary to produce compensation in any particular case. Before attempting this, a more complete examination of the theoretical aspect of the method was undertaken in order to ascertain whether it was really capable of yielding more accurate results.

In the simple treatment several simplifications and certain assumptions were made. These are examined in detail below.

The term $R^2C^2\omega^2$.

It was shown on page 523 that the real part of the admittance expression was

$$Y_r=\omega^2\left\{\frac{R_aC_a^2\omega^2}{1+R_a^2C_a^2\omega^2}+\frac{R_bC_b^2\omega^2}{1+R_b^2C_b^2\omega^2}\right\}, \quad . \quad (8)$$

and subsequently the term $R^2C^2\omega^2$ was assumed to be

sufficiently small to be neglected. If, however, this term had been retained, the expression for the capacity ratio would have been

$$\frac{C_a}{C_b} = \sqrt{\frac{R_b}{R_a} + R_b R_a C_a^2 \omega^2 - R_b^2 C_b^2 \omega^2},$$

i. e.,

$$\frac{C_a}{C_b} = \sqrt{\frac{R_b}{R_a}\left\{1 + C_a^2 \omega^2 R_a^2 \left(1 - \frac{R_b}{R_a}\right)\right\}} \quad . \quad . \quad (9)$$

instead of the simplified form

$$\frac{C_a}{C_b} = \sqrt{\frac{R_b}{R_a}}.$$

Thus the error introduced will depend upon the magnitude of

$$\sqrt{\left\{1 + C_a^2 \omega^2 R_a^2 \left[1 - \frac{R_b}{R_a}\right]\right\}}$$

compared with unity.

There will be no loss of generality if C_a is assumed to be less than C_b, so that both R_b/R_a and the term $\left[1 - \frac{R_b}{R_a}\right]$ will always be somewhat less than unity. Therefore the greatest error will occur when C_a is very much smaller than C_b. Taking a specific case, suppose that a resistance of 100 ohms is used in series with a capacity of 100 $\mu\mu$ F. at a frequency of 1000 Kc./sec., then the value of $R_a^2 C_a^2 \omega^2 \left[1 - \frac{R_b}{R_a}\right]$ will be only about 4×10^{-3}, consequently, in assuming the simplified form of expression 2 an error of less than 0·2 per cent. is introduced. In the majority of cases C_b will not be more than twice C_a, so that the assumption implies an error of less than one part in a thousand.

Suppose, however, that no restrictions are placed on the magnitude of resistances or capacities and that the experiment previously described yields two ratios R_b/R_a and R_d/R_c for two separate determinations, then equation (9) gives two expressions for the capacity ratio, viz.:

$$\left(\frac{C_a}{C_b}\right)^2 = \frac{R_b}{R_a}\left\{1 + C_a^2 \omega^2 R_a^2 \left[1 - \frac{R_b}{R_a}\right]\right\}$$

and

$$\left(\frac{C_a}{C_c}\right)^2 = \frac{R_d}{R_c}\left\{1 + C_a^2 \omega^2 R_c^2 \left[1 - \frac{R_d}{R_c}\right]\right\},$$

and combining these, the following gives a general solution of the problem

$$\left(\frac{C_a}{C_b}\right)^2 = \frac{R_b}{R_a}\left\{1+\frac{\left(\frac{R_d}{R_c}-\frac{R_b}{R_a}\right).R_a^2}{R_b\{R_a-R_b\}-R_d\{R_c-R_d\}}\cdot\left[1-\frac{R_b}{R_a}\right]\right\}. \quad . \quad . \quad . \quad (10)$$

In no case was it found necessary to use this cumbersome expression, since within the limits of accuracy of the experiment the ratios R_d/R_c and R_b/R_a were always found to be equal. In any particular determination where this is found to be the case there is, therefore, ample justification for using the simplified expression

$$\left(\frac{C_a}{C_b}\right)^2 = \frac{R_b}{R_a}.$$

Effect of Frequency Variations.

Since the apparatus is almost entirely screened, frequency variations can arise only from variations in battery supply conditions or from the effects of adding resistance to the oscillatory circuit. The general effect of a frequency variation can be examined as follows :—

Suppose that the frequency change during a particular determination is such that ω becomes $(\omega+\delta\omega)$. Then the equation

$$R_aC_a^2\omega^2 = R_bC_b^2\omega^2$$

should be written

$$R_aC_a^2\omega^2 = R_bC_b^2(\omega+\delta\omega)^2,$$

so that the capacity ratio becomes

$$\frac{C_a}{C_b} = \left(1+\frac{\delta\omega}{\omega}\right)\sqrt{\frac{R_b}{R_a}}. \quad . \quad . \quad . \quad . \quad (11)$$

Clearly the error introduced will be of the same order of magnitude as the change in frequency, and since most of this work was carried out at frequencies of about 1000 Kc./sec. the heterodyne wavemeter immediately reveals errors from this cause of greater than 0·1 per cent. It must be pointed out, however, that the wavemeter should not be left in operation throughout the experiment on account of the danger of direct pick-up of radiations from it.

Variation in frequency arising from the addition of resistances to the oscillatory circuit can be estimated by comparison of the experimental circuit (fig. 7 *b*) with the simple basic circuit (fig. 7 *a*). These circuits will be equivalent if

$$C=C_t+C_a,$$

$$R=R_a\cdot\frac{C_a^2}{(C_t+C_a)^2}$$

Applying the well-known relation

$$n=\frac{1}{2\pi}\sqrt{\frac{1}{LC}-\frac{R^2}{4L^2}},$$

the frequency of oscillation is given by

$$n=\frac{1}{2\pi}\sqrt{\frac{1}{L(C_t+C_a)}-\frac{R_a^2}{4L^2}\cdot\frac{C_a^4}{(C_t+C_a)^4}}. \quad . \quad (12)$$

Fig. 7 *a*.

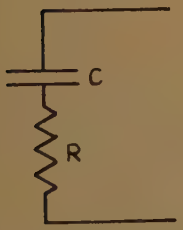

Fig. 7 *b*.

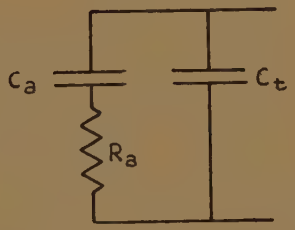

When R_a is zero this reduces to

$$n_0=\frac{1}{2\pi}\sqrt{\frac{1}{L(C_t+C_a)}},$$

so that

$$n=n_0\sqrt{1-\frac{R_a^2C_a^4}{4L(C_t+C_a)^3}}$$

$$=n_0\sqrt{1-\frac{n_0^2\pi^2R_a^2C_a^4}{(C_t+C_a)^2}}. \quad . \quad . \quad . \quad (13)$$

The ratio C_t/C_a is scarcely ever likely to be less than 2, and in most cases will be far greater than this, so that at a frequency of 1000 Kc./sec., a value of R_a of 100 ohms with C_a equal to 100 $\mu\mu$F., gives the expression

$$\frac{n_0^2\pi^2R_a^2C_a^4}{(C_t+C_a)^2},$$

a value of about 4×10^{-4}. The addition of R_a therefore produces a change in frequency of no more than 0·02 per cent. even under the most extreme conditions.

This conclusion was tested experimentally in the following manner. The resistance box described later in this paper was used to add resistances up to about 225 ohms in series with a 200 $\mu\mu$F. condenser connected across the oscillator circuit. This was loosely coupled to a heterodyne wavemeter, the frequency of which was adjusted to give a beat note which could be compared against that emitted by a sonometer wire so that small changes in frequency could be readily estimated. The changes in frequency

Fig. 8.

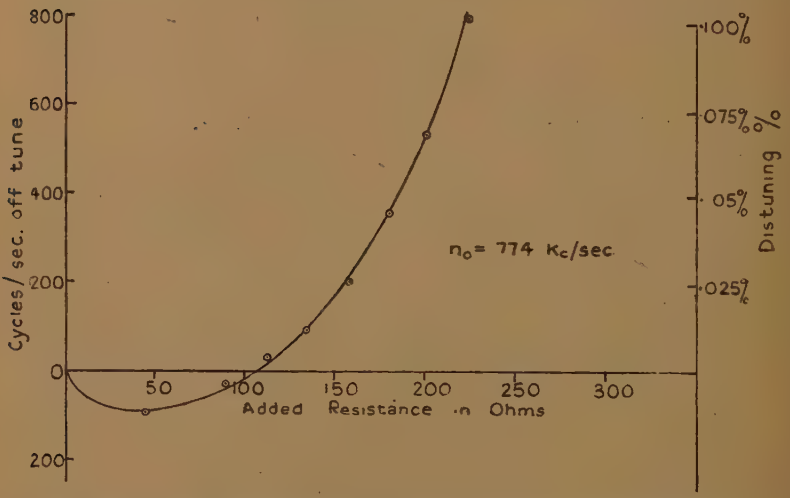

resulting from the addition of various resistances are shown in fig. 8. It is interesting to note that until about 150 ohms has been added, the frequency does not vary by more than 0·025 per cent. of its original value, viz., 774 Kc./sec. This further indicates that the type of resistance used is comparatively free from undesirable effects due to self capacity and inductance.

Effects due to the Presence of Harmonics.

The wave-form used in the experiment is probably anything but sinusoidal, and it is very likely that quite large harmonics are generated. The experimental procedure requires the observation of rectified currents by

means of a galvanometer, and any harmonics will contribute to these currents. If, however, the proportion of harmonic to fundamental is unchanged by the addition of resistance to the oscillatory circuit, the effects of harmonics will be of no consequence, since they merely add a constant fraction to the fundamental rectified current.

Replacing once more the experimental circuit of fig. 7*b* by the basic circuit of fig. 7*a*, it is seen that the application of an alternating potential E produces a current

$$I=\frac{E}{\sqrt{R^2+\left(L\omega-\frac{1}{C\omega}\right)^2}}.$$

At resonance,

$$I_0=\frac{E_0}{R}$$

and

$$L\omega_0=\frac{1}{C\omega_0},$$

where ω_0 corresponds to the resonant frequency.

At any other frequency designated by ω, the current will be

$$I=\frac{E}{R\sqrt{1+\frac{1}{R^2}\left(\frac{\omega}{C\omega_0}-\frac{1}{C\omega}\right)^2}}, \quad . \quad . \quad (14)$$

so that for the harmonic which has a frequency k times that of the fundamental the current will be

$$I_k=\frac{E_k}{R}\frac{1}{\sqrt{1+\frac{1}{R^2C^2}\left\{\frac{k\omega_0}{{\omega_0}^2}-\frac{1}{k\omega_0}\right\}^2}}$$

$$=\frac{E_k}{R}\frac{1}{\sqrt{1+\frac{1}{R^2C^2{\omega_0}^2}\left\{k-\frac{1}{k}\right\}^2}}$$

$$=\frac{E_k}{R}\frac{1}{\sqrt{1+\frac{\pi^2}{\delta^2}\left\{k-\frac{1}{k}\right\}^2}}, \quad . \quad . \quad . \quad . \quad (15)$$

where δ is the logarithmic decrement of the circuit at the fundamental frequency.

Thus the ratio of harmonic to fundamental current will be

$$\frac{I_k}{I_0}=\frac{E_k}{E_0}\frac{1}{\sqrt{1+\frac{\pi^2}{\delta^2}\left\{k-\frac{1}{k}\right\}^2}} \quad . \quad . \quad . \quad . \quad (16)$$

The value of E_k/E_0 will depend upon the wave-form generated by the valve, and hence upon the conditions of operation. Now it is obvious that the principle of adjustment of the variable resistance is the restoration of the decrement of the circuit to its original value, and, further, that the method of adjustment brings either the anode current or the grid current to its initial value, so that both the decrement and the operating conditions of the valve remain unchanged. Thus it is seen that in changing from resistance R_a there is no change in the amplitude of either the fundamental or the harmonics. The effects of the latter may therefore be ignored.

Effects due to Condenser Losses.

The principal causes of condenser losses are dielectric absorption and dielectric leakage. The former is generally represented by a perfect condenser in series with a resistance, whilst leakage is usually represented by a shunting resistance. It may be shown, however, that except in the case of poor dielectrics, condenser losses may be conveniently represented by a large parallel resistance R_p across a perfect condenser C. The reactance of the condenser is $\frac{1}{j\omega C}$, so that the power factor Δ is $\frac{1}{\omega CR_p}$.

If a resistance R is added in series with the arrangement as in fig. 9, the impedance of this part of the circuit will be

$$Z=\frac{1}{j\omega C+\frac{1}{R_p}}+R$$

$$=\frac{(R_p+R)+Rj\omega CR_p}{j\omega CR_p+1},$$

so that the admittance expression becomes

$$Y=\frac{j\omega CR_p+1}{(R_p+R)+Rj\omega CR_p}$$

$$=\frac{j\omega C}{\left(1+\frac{R}{R_p}\right)^2+R^2C^2\omega^2}+\frac{\left(\frac{1}{R_p}+\frac{R}{R_p^2}\right)+\omega^2C^2R}{\left(1+\frac{R}{R_p}\right)^2+R^2C^2\omega^2}. \quad (17)$$

The addition of a resistance R_b in series with the standard condenser C_b, which will be assumed to show negligible dielectric losses, will therefore result in the same change

Fig. 9.

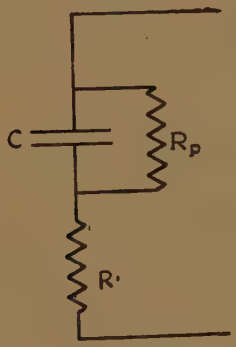

in admittance as the addition of a resistance R_a in series with the leaky condenser C_a if

$$\omega^2C_b^2R_b=\frac{\omega^2C_a^2R_a-\frac{R_a}{R_p^2}\left(1-\frac{R_a}{R_p}\right)}{\left(1+\frac{R_a}{R_p}\right)^2}. \quad . \quad . \quad (18)$$

This leads to the following relation for the capacity ratio,

$$\left(\frac{C_b}{C_a}\right)^2=\frac{R_a}{R_b}\frac{1}{\left(1+\frac{R_a}{R_p}\right)^2}\left\{1-\frac{1}{\omega^2C^2R_p^2}\left[1+\frac{R_a}{R_p}\right]\right\},$$

i. e.,

$$\left(\frac{C_b}{C_a}\right)^2=\frac{R_a}{R_b}\frac{1}{\left(1+\frac{R_a}{R_b}\right)^2}\left\{1-\Delta^2\left[1+\frac{R_a}{R_p}\right]\right\}. \quad . \quad . \quad (19)$$

The power factor Δ will always be sufficiently small to justify the omission of the term $\Delta^2\left[1+\frac{R_a}{R_b}\right]$ in comparison with unity, so that the capacity ratio is given by

$$\frac{C_b}{C_a}=\frac{1}{\left(1+\frac{R_a}{R_p}\right)}\sqrt{\frac{R_a}{R_b}} \quad . \quad . \quad . \quad . \quad . \quad (20)$$

This indicates that the error introduced will be about the same as R_a/R_p. A series of different determinations using different values of R_a and R_b will at once show the presence of large errors arising from condenser losses. Such a series of results may also be used to compute a fairly accurate result for the capacity ratio.

Fig. 10.

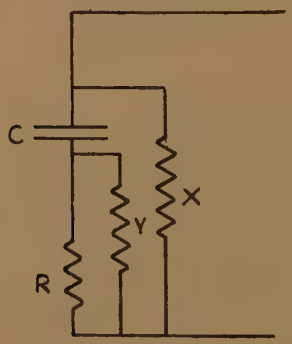

Effects of Leakage to Earth.

In the construction of test condensers for dielectric measurements earthed screens and supports are frequently used. The leakage to these from both the condenser plates is indicated by the resistances X and Y (fig. 10). The presence of X merely adds a term 1/X to the admittance expression, no matter what the value of R. In calculating change in admittance its effect may therefore be entirely ignored. The resistance Y shunts R, and since the latter is always a very small fraction of the former, its effect will be inappreciable.

Effects of Stray Capacities.

The effects of all stray capacities may be included in the three additional capacities C_h, C_{la}, and C_{lb} (fig. 11), C_h representing all stray capacities from the high potential side of the condensers, whilst C_{la} and C_{lb} represent the stray capacities across the resistances R_a and R_b. Since in the experiment R_a and R_b are alternatively zero, C_{la} and C_{lb} never appear together, and each may be taken in turn to represent the self capacity of the resistance together with the cross capacity between the points A and B.

C_h cannot affect the results in any way, since it adds an imaginary term $j\omega C_h$ to each of the admittance expressions,

Fig. 11.

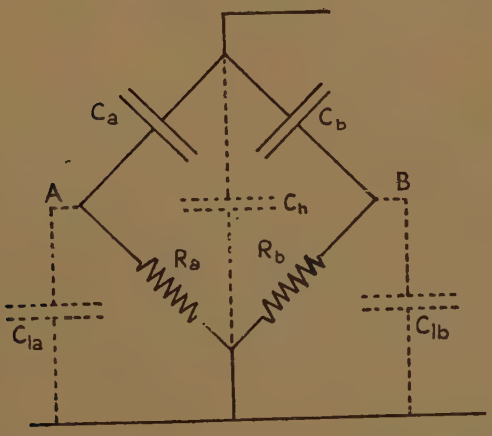

and so vanishes when terms for change in admittance are considered.

The effects of C_{la} and C_{lb}, however, appear in both real and imaginary parts of the expressions for change in admittance. The impedance of the C_a branch of the circuit now becomes

$$Z_a = \frac{1}{j\omega C_{la} + \frac{1}{R_a}} + \frac{1}{j\omega C_a}$$

$$= \frac{{}_a j w C_a + j\omega C_{la} R_a + 1}{j\omega C_a (j\omega C_{la} R_a + 1)},$$

so that the admittance is

$$Y_a = \frac{j\omega C_a - \omega^2 C_{la} C_a R_a}{j\omega R_a (C_a + C_{la}) + 1}$$

$$= j\omega C_a \cdot \frac{1 + \omega^2 R_a^2 C_a^2 \frac{C_{la}}{C_a}\left(1 + \frac{C_{la}}{C_a}\right)}{1 + \omega^2 R_a^2 C_a^2 \left(1 + \frac{C_{la}}{C_a}\right)} + \frac{\omega^2 C_a^2 R_a}{1 + \omega^2 R_a^2 C_a^2 \left(1 + \frac{C_{la}}{C_a}\right)^2}. \quad (21)$$

The change in admittance on adding R_a to this branch is therefore

$$j\omega C_a \left[\frac{1 + \omega^2 R_a^2 C_a^2 \frac{C_{la}}{C_a}\left(1 + \frac{C_{la}}{C_a}\right)}{1 + \omega^2 R_a^2 C_a^2 \left(1 + \frac{C_{la}}{C_a}\right)^2} - 1 \right] + \frac{\omega^2 C_a^2 R_a}{1 + \omega^2 R_a^2 C_a^2 \left(1 + \frac{C_{la}}{C_a}\right)^2}, \quad (22)$$

and since the imaginary term contains C_{la}, there will be a change in frequency on adding R_a. It has already been shown that in all cases $\omega^2 R_a^2 C_a^2$ may be ignored in comparison with unity, and since C_{la}/C_a will usually be fractional, the change in the imaginary term may be ignored. If, however, C_a is a very small capacity so that C_{la}/C_a is not fractional, the term $\omega^2 R_a^2 C_a^2$ will be sufficiently small to justify this. It follows therefore that no serious change in frequency will occur.

Attention may now be turned to the change in the real part of the admittance. On adding R_a to the circuit, this will be

$$\frac{R_a C_a^2 \omega^2}{1 + \omega^2 R_a^2 C_a^2 \left(1 + \frac{C_{la}}{C_a}\right)^2}.$$

Similarly, on short-circuiting R_a and adding R_b in series with C_b the change will be

$$\frac{R_b C_b^2 \omega^2}{1 + \omega^2 R_b^2 C_b^2 \left(1 + \frac{C_{lb}}{C_b}\right)^2}.$$

Equating these as before,

$$R_a C_a^2 + \omega^2 R_a R_b^2 C_a^2 C_b^2 \left[1 + \frac{C_{lb}}{C_b}\right]^2 = R_b C_b^2 + \omega^2 R_b R_a^2 C_a^2 C_b^2 \left[1 + \frac{C_{la}}{C_a}\right]^2, \quad (23)$$

so that the capacity ratio is given by

$$\left(\frac{C_a}{C_b}\right)^2 = \frac{R_b}{R_a}\left\{1 + \omega^2 C_a^2 R_a^2 \left[\left(1 + \frac{C_{la}}{C_a}\right)^2 - \frac{R_b}{R_a}\left(1 + \frac{C_{lb}}{C_b}\right)^2\right]\right\}. \quad . \quad . \quad . \quad (24)$$

The accuracy of the simplification

$$\left(\frac{C_a}{C_b}\right)^2 = \frac{R_b}{R_a}$$

now depends upon whether the expression

$$\left[\left(1 + \frac{C_{la}}{C_a}\right)^2 - \frac{R_b}{R_a}\left(1 + \frac{C_{lb}}{C_b}\right)^2\right] \quad . \quad . \quad . \quad (25)$$

can be ignored in comparison with unity. The analysis loses nothing of its generality if C_a be assumed to be the smaller of the two capacities, in which case R_b/R_a is fractional. Furthermore, C_{la}/C_a and C_{lb}/C_b will also be fractional unless very small capacities are being compared. In the latter case, however, the reduction in $\omega^2 R_a^2 C_a^2$ will compensate for the larger term within the bracket, so that it is very unlikely that under any circumstances expression (25) will be large enough to introduce serious error.

As in previous cases, a series of determinations of the ratio R_a/R_b at once indicates the presence of such errors. The foregoing investigation has indicated that whilst screening of the parts of the apparatus at high R.F. potential may be unrestricted, care must be taken to minimize stray capacities across the resistances. This, however, introduces no complication, since with the type of resistance used in these experiments the self capacity was small and well distributed, and, in addition, screening of the resistance elements was found to be quite unnecessary.

Effect of Inductance of Leads.

In substitution methods, account must be taken of inductance of leads, since in the switching necessary small inductances as well as the unknown capacity are added or removed. In the method under examination, the lead inductance remains in the oscillatory circuit throughout the experiment. Suppose L_a represents the lead inductance of the C_a branch of the circuit, then the impedance of this part of the network will be

$$Z_a = j\left\{\omega L_a - \frac{1}{\omega C_a}\right\} + R_a.$$

The value of L_a will never be greater than about 1 μH, so that ωL_a will always be a negligible fraction of the condenser reactance $\frac{1}{\omega C_a}$. Lead inductances may therefore be completely ignored.

This examination of the conditions under which the method operates has made it evident that its extension to determinations of a high order of accuracy presents only one major problem, namely, the provision of suitable resistances. It is clear from the difficulties already enumerated that there is little possibility of designing a continuously variable resistance for this purpose, so that attention is now turned to resistances variable in steps.

Moullin * has given a complete analysis of the design of units suitable for inclusion in resistance boxes for use at radio frequencies, and this was made the basis of design in the present case. The wire used was No. 47 S.W.G. Manganin, which, on account of its extremely small skin-effect, gives resistance units which may be calibrated by means of steady currents, whilst at the same time its small cross-section permits long narrow loops having small self inductance and capacity to be constructed. These loops, which were about 3·5 cm. in length and only 1 mm. in width, were mounted on paxolin strip. Ten such units, each having a resistance of about 23 ohms, were connected to a dial switch on the

* E. B. Moullin, ' Radio Frequency Measurements.'

top of the resistance box. A further set of resistances having about half the value of the first was connected to a second switch in the same box. The whole was carefully calibrated with steady currents. This formed a calibrated resistance box having a total resistance of about 356 ohms, the smallest unit being about 12 ohms.

Using this set of resistances, the possibility of interpolating between the fixed values was next investigated. For this purpose the circuit shown in fig. 13 was used. As pointed out on page 532 (Part I.), the addition of resistance R in series with C produces changes in anode

Fig. 12.

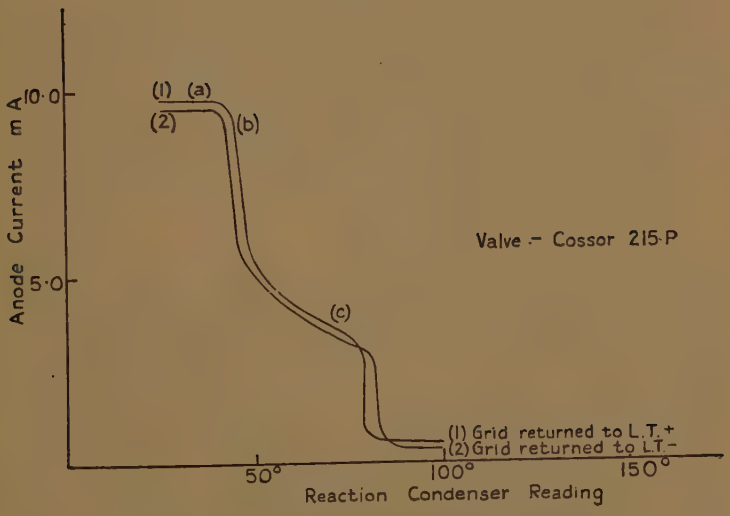

current when the valve is generating oscillations. The changes could be observed by measuring the potential across the resistance A. The initial potential across this resistance due to the anode current when R was zero was first of all balanced out by means of the auxiliary battery B and the set of resistances X, so that actual changes in potential could be determined by means of a Tinsley potentiometer connected at P. The variations in potential resulting from adding different values of R were then observed.

Although the results of this investigation were at first confusing, it was soon found that when R produced

comparatively small changes in anode current the relation between changes in R and the resulting change in potential across A was approximately linear. In this connexion the setting of the condenser C was found to have a marked effect on the relation obtained. If, for example, C_r was set to give feeble self oscillation, a very sensitive condition resulted, and large changes in anode current resulted from variations in R. In this condition the circuit was very sensitive to drift in battery potentials, and the relation between R and P, the potential across A, was far from linear. If, on the other hand, the capacity of C_r was increased to give a larger amplitude of oscillation, sensitivity decreased, the effects of battery drift became relatively unimportant, and an approximately linear relation was found between R and P. The effect (on the anode current) of the setting of C_r is shown in fig. 12. At (*a*) the capacity of C_r is not great enough to cause self oscillation. If the working-point is adjusted to the region of (*b*) where the amplitude of oscillation is small, the results shown in Table I. are obtained.

TABLE I.

Working-point at (*b*), fig. 12.
Addition of a resistance of 227·8 ohms to grid circuit changes the anode current from 4·1 to 6·4 *m*A.
Anode resistance A=585 ohms.

R ohms.	log R.	P volts.	log P.	log R/P.	R/P.
22·71	1·3562	0·0687	$\bar{2}$·8369	2·5193	330·4
45·08	1·6540	0·1513	$\bar{1}$·1798	2·4742	298·0
67·85	1·8315	0·2451	$\bar{1}$·3893	2·4412	276·2
90·40	1·9562	0·3506	$\bar{1}$·5448	2·4124	258·5
113·7	2·0557	0·4686	$\bar{1}$·6708	2·3849	242·6
135·1	2·1326	0·6001	$\bar{1}$·7782	2·3544	226·1
158·5	2·2001	0·7539	$\bar{1}$·8773	2·3228	210·3
181·4	2·2586	0·9281	$\bar{1}$·9680	2·2906	195·2
204·5	2·3107	1·1116	0·0457	2·2650	184·0
227·8	2·3575	1·3526	0·1313	2·2262	168·5

Table II. gives results for a working-point in the region (*c*) where the amplitude of oscillation is greater. In all subsequent investigations a working-point similar to (*c*) was invariably found to be the more satisfactory. Similar results to the above were obtained for a

number of different types of 2 volt receiving valves, and it may therefore be concluded that any valve yielding a curve similar to fig. 12 may be used.

TABLE II.

Working-point at (*c*), fig. 12.
Addition of a resistance of 227·8 ohms to grid circuit changes anode current from 2·25 to 2·45 *m*A.
Anode resistance A=1022 ohms.

R ohms.	log R.	P volts.	log P.	log R/P.	R/P.
22·71	1·3562	0·01920	$\bar{2}$·2833	3·0433	1105
45·08	1·6540	0·03983	$\bar{2}$·6002	3·0438	1106
67·85	1·8315	0·06122	$\bar{2}$·7869	3·0446	1108
90·40	1·9562	0·08140	$\bar{2}$·9106	3·0456	1110
113·7	2·0557	0·1019	$\bar{1}$·0080	3·0477	1116
135·1	2·1326	0·1210	$\bar{1}$·0828	3·0498	1121
158·5	2·2001	0·1409	$\bar{1}$·1489	3·0512	1125
181·4	2·2586	0·1606	$\bar{1}$·2057	3·0529	1130
204·5	2·3107	0·1800	$\bar{1}$·2553	3·0554	1136
227·8	2·3575	0·1991	$\bar{1}$·2991	3·0584	1144

Method of Interpolation.

Examination of Table II. shows that there is only an approximately linear relation between R and P, since the ratio R/P increases slightly with P. If, however, the values of R/P are plotted against P it becomes a simple matter to calculate the value of R necessary to produce any particular potential change P across A. From the point of view of ease of calculation it is more useful to plot the value of log R/P against P, especially as this is found to give approximately a straight line. Examples of the calculation are given later.

The Final Form of the Circuit.

Fig. 13 shows the circuit in its final form. It will be noticed that the condenser network is now coupled to the oscillator by a variable condenser C_c. By setting this to a suitable value at the commencement of the experiment, it is possible to keep the changes in anode current within any desired limits. The amplifier and loud-speaker, which were fed from separate batteries, could be switched into the circuit as desired and were

used in conjunction with the wave-meter W to check the frequency at the beginning and end of each experiment. A Tinsley potentiometer in conjunction with a sensitive mirror galvanometer provided the means of measuring potential changes across A, which was a resistance of 1000 ohms. The latter together with the resistance X were arms of a P.O. box, whilst Z, the resistance by which the steady potential across A was balanced out at the commencement of each experiment, was an ordinary rheostat. A suitable shunt could be placed across the galvanometer G whilst the approximate setting of Z was being obtained.

The whole of the oscillator was built into an earthed screening box, the condensers to be compared being

Fig. 13.

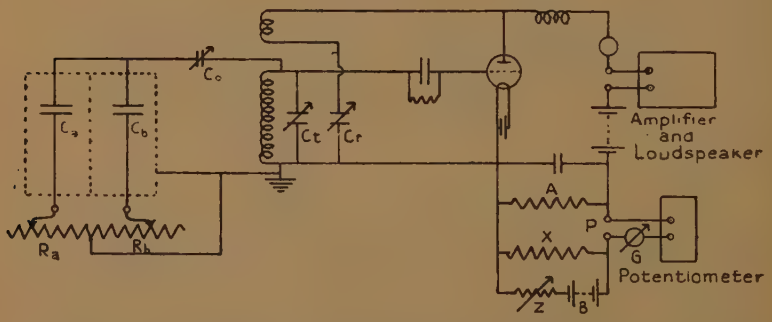

placed in separate compartments. Screening of the resistance units and their connecting leads was quite unnecessary, even at the highest frequencies, providing the earthing arrangements were satisfactory. Movements of the operator were then found to have no effect either on frequency or upon the reading of the potentiometer.

Tests of Accuracy of the Method.

The accuracy of the results obtainable by this method was tested in three different ways. Two of these were purely comparisons between capacities, whilst the third was the determination of the dielectric constant of a standard liquid. Benzene was chosen for this purpose, and an account of the procedure and the results obtained form the subject of a later paper. The principle of the

former methods was the determination of the ratio of a pair of unknown capacities, the result being checked by the determination of their capacity when joined in parallel. In the first instance two condensers of nominal capacity 100 $\mu\mu$ F. and 200 $\mu\mu$F. respectively were employed, whilst in the second case the interelectrode capacities of a pair of valves of the order of 5 $\mu\mu$ F. were compared. Thus the method could be tested over the entire range of its application, and since these determinations give an important insight into the operation of the method they will be described in detail.

Comparison of Large Capacities.

The condensers used were two ordinary fixed condensers of the type common in ordinary radio practice, and having capacities of 100 and 200 $\mu\mu$ F. respectively. To eliminate stray capacities as much as possible, they were mounted in separate compartments of a copper screening box. Using the form of circuit of fig. 13, the procedure was as follows :—

(a) *Preliminary Adjustments.*—These include the setting of the tuning condenser C_t, the variation of the reaction condenser C_r until the anode current has been reduced to rather less than half its static (non-oscillating) value, reduction of the coupling condenser C_c until the addition of the largest value of R does not reduce the anode current by more than about 20 per cent. These adjustments must be followed by the variation of the resistance Z to make the potential difference across P approximately zero. It will now be necessary to make a further slight alteration in C_t to bring the frequency back to the desired value (about 1000 Kc./sec.).

(b) *Frequency Change and Battery Drift.*—With the amplifier and wave-meter connected, the variation in the pitch of the heterodyne note as R is increased from zero to its maximum is observed. If the change in pitch is excessive, further reduction in C_c is necessary. The effects of battery drift may be observed by noting the drift of the potential P for several minutes.

(c) *Determination.*—The above adjustments being completed, the main determination may now be carried out. In the first stage the resistance box is joined in series

with C_a whilst C_b is earthed. A series of potential measurements P_a, as R_a is varied from zero to its maximum value, is now taken. R_a is then reduced to zero and the frequency and potential across P again observed as a check on troubles due to battery drift. A second set of observations is now obtained by adding resistances in series with C_b, the other condenser C_a being connected to earth. The whole range of operations rarely took more than about half an hour, whilst in most cases the principal observations set out under (*c*) could be completed in 10 to 15 minutes.

TABLE III.

Resistances added in Series with Condenser C_a.

R_a ohms.	log R_a.	P_a volts. $\times 10^{-2}$.	log P_a.	log R_a/P_a.	log R_b/P_b.	log R_b/R_a.	C_a/C .
12·29	1·0899	1·652	$\bar{2}$·2180	2·8717	3·4540	0·5823	1·955
25·11	1·3998	3·354	$\bar{2}$·5256	2·8742	3·4553	0·5811	1·953
38·04	1·5803	5·058	$\bar{2}$·7040	2·8763	3·4585	0·5825	1·955
50·92	1·7069	6·723	$\bar{2}$·8276	2·8793	3·4607	0·5814	1·953
63·78	1·8047	8·398	$\bar{2}$·9242	2·8805	3·4622	0·5817	1·954
76·92	1·8860	10·079	$\bar{1}$·0034	2·8826			
89·90	1·9538	11·724	$\bar{1}$·0691	2·8847			
103·1	2·0133	13·399	$\bar{1}$·1270	2·8863			
116·3	2·0655	15·028	$\bar{1}$·1769	2·8886			
129·4	2·1119	16·677	$\bar{1}$·2221	2·8898			

TABLE IV.

Resistances added in Series with Condenser C_b.

R_b ohms	log R_b.	$P_b$volts $\times 10^{-2}$.	log P_b.	log R_b/P_b.	log R_a/P_a.	log R_b/R_a.	C_a/C_b.
22·71	1·3562	0·801	$\bar{3}$·9035	3·4527	2·8710	0·5813	1·953
45·08	1·6540	1·586	$\bar{2}$·2002	3·4538	2·8717	0·5821	1·954
67·85	1·8315	2·380	$\bar{2}$·3766	3·4549	2·8730	0·5819	1·954
90·40	1·9562	3·16[0]	$\bar{2}$·5008	3·4554	2·8739	0·5815	1·953
103·7	2·0557	3·970	$\bar{2}$·5988	3·4569	2·8748	0·5821	1·954
135·1	2·1326	4·727	$\bar{2}$·6745	3·4581	2·8760	0·5821	1·954
158·5	2·2001	5·550	$\bar{2}$·7404	3·4597	2·8770	0·5827	1·956
181·4	2·2586	6·287	$\bar{2}$·7985	3·4601	2·8780	0·5821	1·954
204·5	2·3107	7·076	$\bar{2}$·8498	3·4609	2·8793	0·5816	1·954
227·8	2·3575	7·865	$\bar{2}$·8957	3·4618	2·8800	0·5818	1·954
	Mean value of C_a/C_b (15 results) 1·9540.						

Calculation of Results.

In order to indicate clearly how results may be calculated from the above observations, a complete computation is shown in Tables III. and IV. For the first set of results, viz., the variation of P with R_a the value of log R_a/P has been calculated and in fig. 14 is shown plotted against P. From this curve the value of R_a necessary to produce any potential change may be determined. The results

Fig. 14.

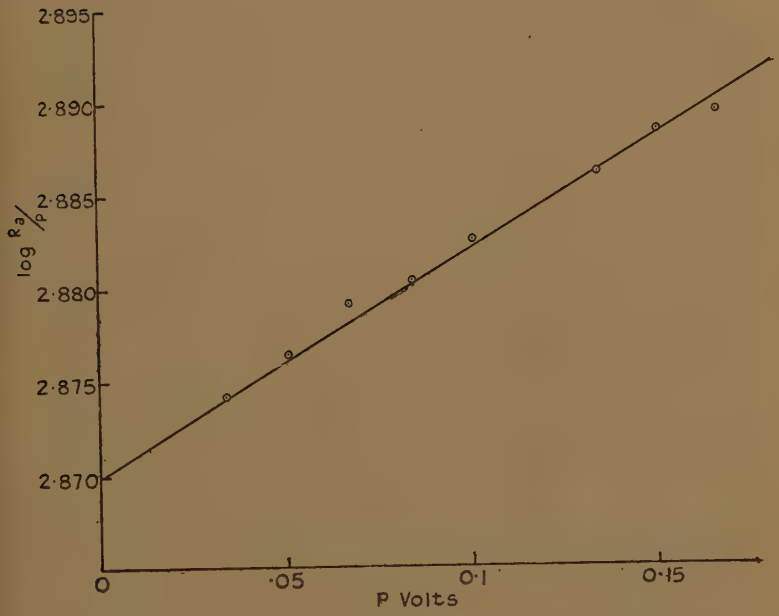

for condenser C_b show that a resistance of $R_b=158{\cdot}5$ ohms added in series with C_b produces a potential change of $5{\cdot}500\times10^{-2}$ volts. The above curve gives the value of log R_a/P corresponding to this potential change as $2{\cdot}8770$, so that the resistance in series with C_a, which gives a potential change of $5{\cdot}500\times10^{-2}$ volts, will be given by

$$\begin{aligned}\log R_a &= \log R_a/P + \log P\\ &= 2{\cdot}8770 + \bar{2}{\cdot}7404\\ &= 1{\cdot}6174\end{aligned}$$

Now, from the relation

$$\frac{C_a}{C_b}=\sqrt{\frac{R_b}{R_a}},$$

$$\therefore \quad \log C_a/C_b=\tfrac{1}{2}(\log R_b-\log R_a)$$
$$=\tfrac{1}{2}(2{\cdot}2001-1{\cdot}6174)$$
$$=0{\cdot}2913.$$

Thus $C_a/C_b=1{\cdot}956$.

Obviously with the large array of results available a considerable number of determinations can be obtained. It is, of course, desirable to plot the relation $\log R_b/P$ against P as well as that indicated above, since this yields a further set of results. The method of calculation may be summarized as follows:—From the experimental observations determine the value of $\log R_b/P_b$ and $\log R_a/P_a$ corresponding to any definite value of P (one of these values can be obtained by direct calculation, and the other from the curve connecting P and log R/P). Subtracting these, the value of $\log R_b/R_a$ is obtained. Half this value gives $\log C_a/C_b$. This calculation is shown completely in Table IV.

The results are seen to yield in all 15 determinations of the capacity ratio. These show no systematic variation with R, and the maximum deviation from the mean is only slightly greater than 0·1 per cent.

In order to verify the above results the experiment was carried a stage further by joining the condensers C_a and C_b in parallel without disturbing any other part of the circuit and taking a further set of observations with R added in series with the pair. Examination of the circuit diagram shows that this can be done by altering only a single connexion on the low potential side, and that no change in frequency results from this operation. The results obtained from this experiment are shown in Table V. These may now be used in conjunction with the results of Table IV. in order to calculate a series of values for $(C_a+C_b)/C_a$.

Now, since

$$C_p=C_a+C_b,$$

$$\therefore \quad \frac{C_p}{C_a}=1+\frac{C_a}{C_b}.$$

From Table IV.

$$C_a/C_b = 1{\cdot}9540,$$
$$C_b/C_a = 0{\cdot}51177.$$

Thus the value of C_p/C_a calculated from Table IV. is 1·5118.

In this case it is possible to obtain five determinations. Comparing the results of Table IV. with the mean value obtained from Table V.,

$(C_a+C_b)/C_a$ calculated from Table IV. $=1{\cdot}5118$,

$(C_a+C_b)/C_a$ calculated from Table V. $=1{\cdot}5125$,

the agreement is seen to be rather closer than 0·2 per cent.

TABLE V.

Condensers C_a and C_b in parallel.

$$C_p = C_a + C_b.$$

Resistances added in Series with C_p.

R ohms.	log R.	P_p volts $\times 10^{-2}$.	log P_p.	log R_p/P_p.	log R_a/P_a.	log R_a/R_p.	C_p/C_a.
12·29	1·0897	3·757	$\bar{2}$·5749	2·5148	2·8748	0·3600	1·514
25·11	1·3998	7·580	$\bar{2}$·8797	2·5201	2·8800	0·3599	1·513
38·04	1·5803	11·331	$\bar{1}$·0542	2·5261	2·8842	0·3581	1·510
50·92	1·7069	15·062	$\bar{1}$·1778	2·5281	2·8876	0·3595	1·512
63·78	1·8047	18·829	$\bar{1}$·2747	2·5300	2·8898	0·3598	1·513
76·92	1·8860	22·503	$\bar{1}$·3522	2·5338			
89·90	1·9538	26·141	$\bar{1}$·4173	2·5365			
103·1	2·0133	29·842	$\bar{1}$·4748	2·5385			
116·3	2·0655	33·505	$\bar{1}$·5251	2·5404			
129·4	2·1119	37·193	$\bar{1}$·5704	2·5415			

Mean value of C_p/C_a (5 results) 1·5125.

There is hence justification for assuming that the method may be employed for the comparison of capacities of the order of a few hundreds of micromicrofarads with an accuracy of one or two parts in a thousand. This compares very favourably with the more elaborate of the substitution methods.

Comparison of Small Capacities.

Apart from the more general interest, the choice of interelectrode capacities of valves for this experiment has much to recommend it. The electrode system of the

modern thermionic valve is sufficiently rigid and has a small enough capacity to provide a suitable standard for this purpose. Moreover, the entire valve may be easily screened so that stray capacities can be eliminated. Three valves were chosen, one being a screen-grid tetrode. It was originally intended to attempt the measurement of the control-grid-anode capacity of the latter, but it was found impossible to reduce parallel capacities sufficiently to render the method sensitive enough for this purpose, The valves used and the capacities determined were

(A) Cossor 215 S.G. ..... Screen to anode capacity;

(B) Marconi H 210 ..... Grid to anode capacity;

(C) Mazda L. 2 ..... Grid to anode capacity.

In all cases the remaining electrodes were earthed. In the first stage of the experiment the ratios A/B, A/C, and B/C were determined; then, by joining the capacities in pairs, the values of (B+C)/C, (A+C)/A, and (B+A)/B were found. The experimental values of the latter were then compared with results calculated from the former.

Experimental Procedure.

The principle of the method was exactly similar to that used in the comparison of larger capacities, except that the coupling condenser C_c was short circuited and the reaction condenser adjusted to give a somewhat smaller amplitude of oscillation than before. Each valve was mounted rigidly inside a copper tube, the valve pins being separately screened by means of a copper strip. The method therefore gives the capacity of the electrode system together with the stray capacity in the valve base. The frequency at which the determination was carried out was about 1500 Kc./sec. This permitted a small value of C_t to be used and resulted in increased sensitivity.

In the first stage of the experiment capacities B and C were connected to earth whilst resistances were added in series with A and the corresponding potential changes noted. It is not surprising to find when using such small capacities that the relation between R and P is sufficiently linear to enable the previous process of interpolation to be omitted, and a mean value of R_a/P to be calculated

directly. In a similar way the mean value of R_b/P and R_c/P could be obtained by adding resistances in series with B and C respectively.

Results.

Tables VI. and VII. show in detail the determination of R_a/P and R_b/P respectively, and from these it will be

TABLE VI.

Resistances added in Series with Capacity A.

R_A ohms.	log R_A.	P_A volts $\times 10^{-2}$.	log P_A.	log R_A/P_A.	R_A/P_A.
22·71	1·3562	3·086	$\bar{2}$·4894	2·8668	735·8
45·08	1·6540	6·131	$\bar{2}$·7875	2·8665	735·3
67·85	1·8315	9·208	$\bar{2}$·9645	2·8670	736·2
90·40	1·9562	12·28	$\bar{1}$·0889	2·8673	736·7
113·7	2·0557	15·44	$\bar{1}$·1886	2·8671	736·3
135·1	2·1326	18·41	$\bar{1}$·2650	2·8676	737·2
158·5	2·2001	21·51	$\bar{1}$·3326	2·8675	737·0
181·4	2·2586	24·59	$\bar{1}$·3908	2·8678	737·5
204·5	2·3107	27·87	$\bar{1}$·4451	2·8656	733·8
227·8	2·3575	31·06	$\bar{1}$·4922	2·8653	733·1
			Mean (10 results).		735·89

TABLE VII.

Resistances added in Series with Capacity B.

R_B ohms.	log R_B.	P_B volts. $\times 10^{-2}$.	log P_B.	log R_B/P_B.	R_B/P_B.
22·71	1·3560	1·625	$\bar{2}$·2108	3·1452	1397
45·08	1·6540	3·221	$\bar{2}$·5080	3·1460	1400
67·85	1·8315	4·845	$\bar{2}$·6852	3·1463	1401
90·40	1·9562	6·475	$\bar{2}$·8112	3·1450	1396
113·7	2·0557	8·150	$\bar{2}$·9112	3·1445	1395
135·1	2·1326	9·734	$\bar{2}$·9883	3·1443	1394
158·5	2·2001	11·356	$\bar{1}$·0556	3·1445	1395
181·4	2·2586	12·959	$\bar{1}$·1127	3·1459	1399
204·5	2·3107	14·625	$\bar{1}$·1653	3·1454	1397
227·8	2·3575	16·264	$\bar{1}$·2111	3·1464	1401
			Mean (10 results).		1397·3

$$\text{(Capacity A)/(Capacity B)} = (R_B/P_B \div R_A/P_A)^{\frac{1}{2}}.$$
$$= (1397 \div 735{\cdot}9)^{\frac{1}{2}}.$$
$$= 1{\cdot}378.$$

seen that the various values in each case differ from the mean by only a few parts in a thousand. The method of calculating the capacity ratio from these results is also shown. Table VIII. gives a general summary of the values of R/P for each separate capacity and for pairs joined in parallel. From these the capacity ratios A/B, (A+B)/B, etc., are calculated and are shown in Table VIII. Clearly the simple ratio A/B enables a value of (A+B)/B to be calculated, and this is shown in the final column of this Table. The agreement between these two columns is seen to be as close as a few parts in a thousand, and

TABLE VIII.

General Summary of Results.

Capacity.	R/P (mean).	Capacity.	R/P (mean).
A	735·9	A+B	248·8
B	1397·3	B+C	249·8
C	746·7	C+A	185·5

Capacity ratio.	Experimental result.	Calculated result.
A/B	1·378	
(A+B)/B	2·373	2·378
B/C	0·7311	
(B+C)/C	1·729	1·7311
C/A	0·9926	
(C+A)/A	1·994	1·9926

this may therefore be taken to indicate the accuracy of the method. The largest capacity used in this determination was of the order of $5\mu\mu$F., so that the method may be used to show differences in capacity as small as about $0{\cdot}01\ \mu\mu$F.

Conclusion.

An original method of comparing capacities ranging between $5\mu\mu$F. and $500\mu\mu$F. at frequencies between 10^5 and 2×10^6 cycles/sec. has been developed and has been found to give results agreeing to within 0·2 to 0·3 per cent. The method offers many advantages over the substitution methods usually used over this range, and most of the components employed are readily available in the average laboratory. Furthermore, results are

obtained directly without necessity for subsequent correction for stray capacity effects. The method has been used successfully in the determination of the dielectric constants of benzene and 1 : 4 dioxane, and in a modified form for the estimation of the radio-frequency resistance of straight wires. The results of these investigations will be presented in later papers.

The use of continuously variable resistances would simplify the method considerably and would almost bring it into the category of an ordinary bridge method. Of the resistance devices already available for this purpose the type 602 decade box of the General Radio Co. merits special attention. Using three of these boxes having decade steps of 0·1, 1·0, and 10·0 ohms respectively, a resistance unit having a maximum value of 111·0 ohms may be built up, and with such an arrangement it should be possible to obtain direct comparisons of capacities to an accuracy of closer than 1 per cent. at frequencies of about 1000 Kc./sec. Apart from many other advantages, the total cost of apparatus for this method is only a fraction of that of a standard variable condenser capable of giving results of the same degree of accuracy in a substitution method.

In conclusion, the author wishes to express his gratitude to Dr. S. Marsh for his most helpful guidance and assistance throughout the progress of this investigation.

XLIX. *Finite Strain : Dislocation Solutions.* *By* S. T. Newing, *B.Sc., A.R.C.S., D.I.C., and* W. M. Shepherd, *D.Sc.**

[Received June 16, 1938.]

I. *Introduction.*

SOLUTIONS of problems in the theory of elasticity, using the hypothesis of finite strain, have been obtained in two previous papers †. Owing to the complexity of the equations involved, it seems probable that

* Communicated by the Authors.

† B. R. Seth, Phil. Trans. Roy. Soc. A, ccxxxiv. pp. 231–64 (1935), hereafter referred to as " S." ; W. M. Shepherd and B. R. Seth, Proc. Roy. Soc. A, clvi. pp. 171–192 (1936), hereafter referred to as " S.S."

only a very limited range of problems is amenable to analysis without labour out of proportion to the value of the results obtained.

In this paper is considered the analogue in "finite strain" of what is called by Coker and Filon* "the dislocation of the first order."

A uniform circular cylindrical tube is considered to undergo one of two types of distortion. In the first, the portion of the tube bounded by two axial planes is removed, and the surfaces so formed are brought together and cemented. In the second the tube is slit longitudinally in an axial plane and the two surfaces of the slit are forced apart by the insertion of a wedge, in such a way that each surface remains in an axial plane. In addition the internal and external surfaces of the tube may be subjected to uniform, but not necessarily equal, tractions.

In all the examples considered the tube is supposed to be constrained by end tractions to remain in a state of plane strain. The particular instance in which the cylindrical surfaces are free from tractions is considered in some detail. It concerns an initially curved plate which is bent by edge couples so that its initial curvature is either increased or decreased. The uniqueness of the solutions is considered and a somewhat curious result is obtained in this connexion.

II. *General Formulæ.*

Let (u, v, w) be the components of the displacement of a point whose coordinates in the strained state are (x, y, z). The strains are then given by equations of the types †

$$S_x = \frac{\partial u}{\partial x} - \frac{1}{2}\left\{\left(\frac{\partial u}{\partial x}\right)^2 + \left(\frac{\partial v}{\partial x}\right)^2 + \left(\frac{\partial w}{\partial x}\right)^2\right\}$$

$$\sigma_{yz} = \frac{\partial v}{\partial z} + \frac{\partial w}{\partial y} - \left\{\frac{\partial u}{\partial y}\frac{\partial u}{\partial z} + \frac{\partial v}{\partial y}\frac{\partial v}{\partial z} + \frac{\partial w}{\partial y}\frac{\partial w}{\partial z}\right\}.$$

The stress-strain relations are the same as those holding when the strains are small, viz.,

$$\widehat{xx} = \lambda\delta + 2\mu S_x,$$
$$\widehat{yz} = \mu\sigma_{yz}, \text{ etc.}$$

* 'Photoelasticity,' p. 319, hereafter referred to as C.F.P

† C.F.P. p. 188.

III. *The Method of Solution.*

Take rectangular Cartesian axes, Ox, Oy, Oz, such that Oz is the axis of the cylindrical surface considered, and let (ρ, θ, z) be cylindrical coordinates related to the Cartesian coordinates by the equations

$$x=\rho\cos\theta,\quad y=\rho\sin\theta.$$

Let the coordinates of a particle P of the material be denoted by (ρ, θ, z) after strain, while the corresponding quantities before strain are denoted by $(Q\rho, A\theta, z)$, where A is an assigned constant and Q is a function of ρ. Then the displacements parallel to the coordinate axes are (u, v, w), where

$$u=\rho\cos\theta-Q\,\rho\cos A\theta,$$
$$v=\rho\sin\theta-Q\rho\sin A\theta,$$
$$w=0.$$

After some reduction, using the formulæ of § II., stresses are obtained which are given by

$$\widehat{xx}=\frac{\lambda}{2}\left\{2-\left(Q+\rho\frac{dQ}{d\rho}\right)^2-A^2Q^2\right\}$$
$$+\mu\left\{1-\left(Q+\rho\frac{dQ}{d\rho}\right)^2\cos^2\theta-A^2\,Q^2\sin^2\theta\right\}. \quad (3.11)$$

$$\widehat{yy}=\frac{\lambda}{2}\left\{2-\left(Q+\rho\frac{dQ}{d\rho}\right)^2-A^2Q^2\right\}$$
$$+\mu\left\{1-\left(Q+\rho\frac{dQ}{d\rho}\right)^2\sin^2\theta-A^2Q^2\cos^2\theta\right\} \quad (3.12)$$

$$\widehat{xy}=-\mu\left\{\left(Q+\rho\frac{dQ}{d\rho}\right)^2-A^2Q^2\right\}\sin\theta\cos\theta \quad (3.13)$$

$$\widehat{zz}=\eta\,(\widehat{xx}+\widehat{yy}) \quad (3.14)$$

$$\widehat{yz}=\widehat{zx}=0, \quad (3.15)$$

where η is Poisson's Ratio.

One of the "body-stress" equations is identically satisfied, while the other two each gives

$$\rho\left[\left(Q+\rho\frac{dQ}{d\rho}\right)\left(2\frac{dQ}{d\rho}+\rho\frac{d^2Q}{d\rho^2}\right)(\lambda+2\mu)+\lambda A^2Q\frac{dQ}{d\rho}\right]$$
$$+\mu\left[\left(Q+\rho\frac{dQ}{d\rho}\right)^2-A^2Q^2\right]=0 \quad (3.21)$$

On making the substitutions

$$\frac{\rho}{Q}\frac{dQ}{d\rho}=U,\ \frac{2\lambda+5\mu}{2(\lambda+2\mu)}=G,$$

this equation becomes

$$U(1+U)Q\frac{dU}{dQ}=(2G-2)A^2+(4G-5)A^2U-U(1+U)^2 -(2G-2)(1+U)^2 \quad . \quad . \quad . \quad (3{\cdot}22)$$

from which is obtained

$$-\log LQ=\int\frac{U(1+U)dU}{U^3+2GU^2+U\{2+(5-4G)(A^2-1)\}-2(A^2-1)(G-1)}. \quad . \quad . \quad . \quad (3{\cdot}31)$$

If the equation $U=\frac{\rho}{Q}\frac{dQ}{d\rho}$ is used to eliminate Q from the left-hand side of equation (3.22), then it follows that

$$-\log M\rho=\int\frac{(1+U)\,dU}{U^3+2GU^2+U\{2+(5-4G)(A^2-1)\}-2(A^2-1)(G-1)}. \quad . \quad . \quad . \quad (3.32)$$

These equations (3.31) and (3.32) give the relation between ρ and Q in terms of the parameter U and the constants L and M.

The radial stress is obtained by putting $\theta=0$ in (3.11), and after the substitution for $\frac{\rho}{Q}\frac{dQ}{d\rho}$, is given by

$$\widehat{\rho\rho}=(\lambda+\mu)-\tfrac{1}{2}Q^2\{(\lambda+2\mu)(1+U)^2+\lambda A^2\}.$$

If we write

$$R=1-\frac{\widehat{\rho\rho}}{\lambda+\mu},$$

then

$$R=Q^2\{(1-\eta)(1+U)^2+\eta A^2\}. \quad . \quad . \quad (3.33)$$

It follows therefore that

$$\log(L^2R)=2\log(LQ)+\log\{(1-\eta)(1+U)^2+\eta A^2\}, \quad . \quad . \quad . \quad (3.34)$$

an equation which gives the radial stress in terms of U and the constant L. No further progress can be made

with the solution unless specific values are assigned to η and A.

For example, with $\eta=0{\cdot}25$ and $A^2=0{\cdot}94$ the cubic expression in the denominators of the integrands in (3.31) and (3.32) becomes

$$U^3+7U^2/3+1{\cdot}98U+0{\cdot}02.$$

This, in common with the other similar cubic expressions occurring in this paper, has only one real linear factor. On performing the integrations in (3.31) and (3.32), these equations yield

$$\log_{10}(LQ)=B_1\log_{10}(U+0{\cdot}01022)+B_2\log_{10}\{(U+1{\cdot}16155)^2+(0{\cdot}77913)^2\}+B_3\tan^{-1}\left(\frac{U+1{\cdot}16155}{0{\cdot}77913}\right). \quad . \quad . \quad (3.41)$$

$$\log_{10}(M\rho)=C_1\log_{10}(U+0{\cdot}01022)+C_2\log_{10}\{(U+1{\cdot}6155)^2+(0{\cdot}77913)^2\}+C_3\tan^{-1}\left(\frac{U+1{\cdot}16155}{0{\cdot}77913}\right), \quad . \quad . \quad (3.42)$$

where the logarithms have been converted to base 10 for facility in computation, and the constants have the following values :—

$B_1=\ 0{\cdot}0052360 \quad B_2=-0{\cdot}50262 \quad B_3=\ 0{\cdot}21274$

$B_2=-0{\cdot}51215 \quad C_2=0{\cdot}25607 \quad C_3=-0{\cdot}52668.$

Equation (3.34) becomes

$$\log_{10}(L^2R)=2\log_{10}(LQ)+\log_{10}\{(1+U)^2+0{\cdot}31333\}+\log_{10}(0{\cdot}75). \quad (3.43)$$

In the above group of three equations the logarithm of a negative number is to be interpreted as the logarithm of its modulus.

Using these equations it is possible to construct Table I., which gives the values of $\log_{10}(LQ)$, $\log_{10}(M\rho)$, $\log_{10}(L^2R)$, $\log_{10}(LMQ\rho)$, corresponding to values of U. As in S.S., $U>-1$ unless the tube is turned inside out, and only this range of values, $U>-1$, will be considered. If ρ is the distance of a particle of the material from the axis of the tube in the strained state and ρ' its distance in the unstrained state, then

$$\rho'=Q\rho. \quad .$$

Hence $\log_{10}(LMQ\rho)=\log_{10}(LM\rho')$, which gives ρ' in terms of U directly, when the constants L and M have

been determined. To determine the stresses we proceed as follows :—

By writing $\theta=0$ in (3.11) and (3.12) we obtain directly, expressions for $\widehat{\rho\rho}$ and $\widehat{\theta\theta}$, namely

$$\widehat{\rho\rho} = \frac{\lambda}{2}\left\{2-\left(Q+\rho\frac{dQ}{d\rho}\right)^2 - A^2Q^2\right\} + \mu\left\{1-\left(Q+\rho\frac{dQ}{d\rho}\right)^2\right\}$$

$$\widehat{\theta\theta} = \frac{\lambda}{2}\left\{2-\left(Q+\rho\frac{dQ}{d\rho}\right)^2 - A^2Q^2\right\} + \mu\{1-A^2Q^2\}.$$

TABLE I.

U.	$\mathrm{Log}_{10}(LQ)$.	$\mathrm{Log}_{10}(M\rho)$.	$\mathrm{Log}_{10}(L^2R)$.	$\mathrm{Log}_{10}(LM\rho')$.
∞	$-\infty$	−0·3594	+0·1653	$-\infty$
10	−0·9104	−0·3186	+0·1383	−1·2290
6	−0·7229	−0·2942	+0·1223	−1·0171
4	−0·5870	−0·2664	+0·1045	−0·8534
3	−0·4995	−0·2411	+0·0886	−0·7406
2	−0·3910	−0·1968	+0·0622	−0·5878
1	−0·2500	−0·0974	+0·0099	−0·3474
0·7	−0·1988	−0·0364	−0·0169	−0·2352
0·5	−0·1620	+0·0257	−0·0401	−0·1363
0·3	−0·1231	+0·1253	−0·0693	+0·0023
0·2	−0·1030	+0·2066	−0·0871	+0·1036
0·1	−0·0830	+0·3454	−0·1081	+0·2624
0	−0·0664	+0·8699	−0·1393	+0·8036
−0·1	−0·0390	+0·3829	−0·1563	+0·3439
−0·2	−0·0146	+0·2135	−0·1750	+0·1989
−0·3	+0·0090	+0·1177	−0·2021	+0·1267
−0·6	+0·0741	−0·0344	−0·3015	+0·0398
−0·8	+0·1060	−0·0807	−0·3648	+0·0253
−1·0	+0·1186	−0·0953	−0·3917	+0·0233

It follows then that

$$\frac{\widehat{\rho\rho}+\widehat{\theta\theta}}{\lambda+\mu} = \frac{2}{\lambda}\{\widehat{\theta\theta} - \mu\,(1-A^2Q^2)\}.$$

Whence with $\lambda=\mu$ and $\widehat{\rho\rho}=1-R$

$$\frac{\widehat{\theta\theta}}{\lambda+\mu} = \tfrac{1}{3}\{1-R\}+\tfrac{2}{3}\{1-A^2Q^2\}.$$

For the end tractions we have

$$\frac{\widehat{zz}}{\lambda+\mu} = \frac{\eta}{\lambda+\mu}(\widehat{\theta\theta}+\widehat{\rho\rho}) = \frac{1}{4}\frac{(\widehat{\theta\theta}+\widehat{\rho\rho})}{\lambda+\mu}.$$

Thus when R and Q are known as functions of ρ', we can determine $\frac{\widehat{\theta\theta}}{\lambda+\mu}, \frac{\widehat{\rho\rho}}{\lambda+\mu}, \frac{\widehat{zz}}{\lambda+\mu}$ for the values of ρ' in which we are interested.

IV. *The Solution in Particular Cases.*

The relation between $\log_{10}(LM\rho')$ and $\log_{10}(L^2R)$ is shown graphically in fig. 1 for $A^2=0{\cdot}94$ and in fig. 2 for

Fig. 1.

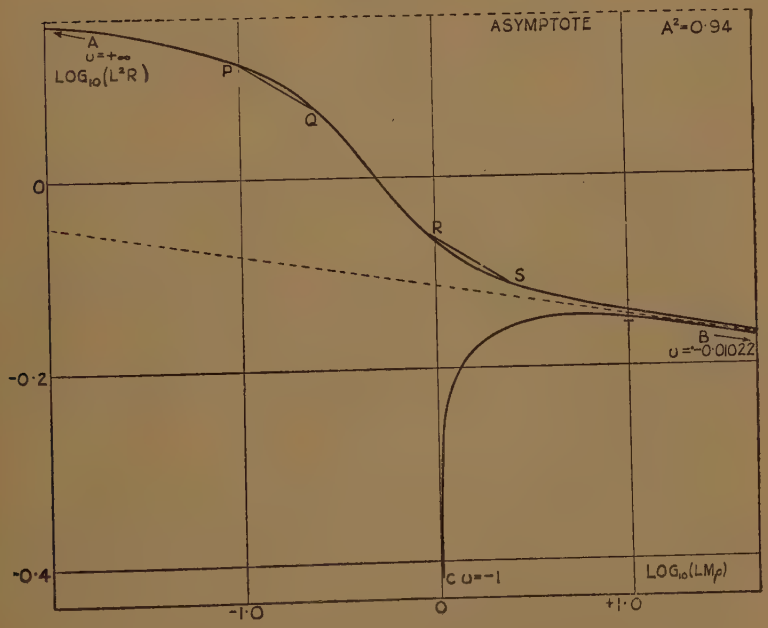

$A^2=1{\cdot}21$. It will be seen that the two graphs differ in that the slope of the asymptote is positive for the former value of A and negative for the latter. Generally when $A<1$ the asymptote has a positive slope and when $A>1$ a negative one.

In fig. 1 the portion AB of the curve corresponds to $U>-0{\cdot}01022$, and in fig. 2 to $-1<U<+0{\cdot}032602$. The portion BC of the curve in fig. 1 corresponds to $-1<U<-0{\cdot}01022$, and in fig. 2 to $-1<U<+0{\cdot}032602$. On each curve there is a turning-point T, but whereas in

fig. 1, T is within the part BC, in fig. 2 it is within the part AB.

The method of solution follows closely that used in S.S. except that the unstrained dimensions of the tube are used instead of the final dimensions. This does not change the procedure, but brings to light some points unnoticed in the previous paper (S.S.). Suppose that for a certain value of A the values of R are given, corresponding to a pair of values of ρ' ; *e. g.*,

$$\rho' = a \quad R = R_a,$$
$$\rho' = b \quad R = R_b.$$

Fig. 2.

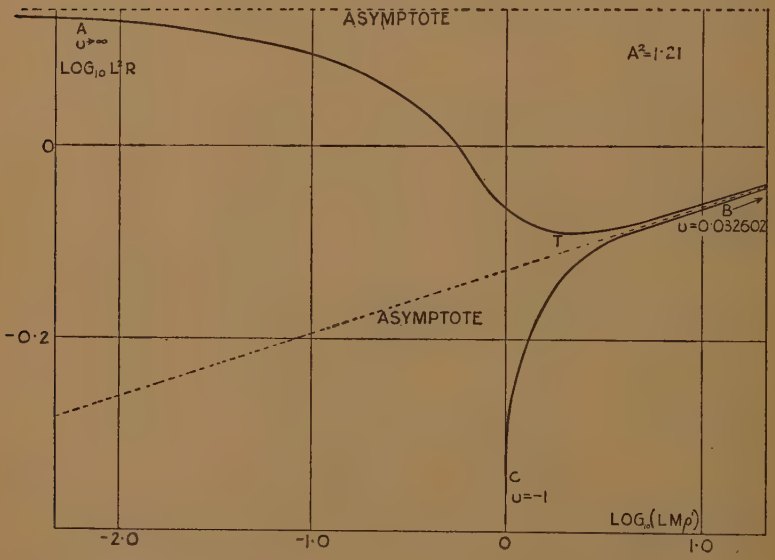

Then the corresponding segment can be constructed from the quantities $\log_{10}(R_a/R_b)$ and $\log_{10}(a/b)$, and adjoined as a chord to the appropriate curve. The solutions belong to three types according as the gradient of the chord is (i.) positive, (ii.) negative, (iii.) zero.

Type 1.—*Gradient Positive.*

If $A<1$ we have a graph of the type in fig. 1, and the chord must have its extremities in BC. It is clear that at the most the chord can be adjoined in one position so that the solution is unique.

If $A>1$ we have a graph of the type in fig. 2, and the chord may be adjoined either within BC; or within AB with at least one extremity in the portion BT. Again, the solution is unique. The surface loading in this case is such that $R\left(=1-\frac{\widehat{\rho\rho}}{\lambda+\mu}\right)$ is greater on the outer surface than upon the inner surface of the tube. A particular case of this occurs when the tube is free from traction on the inside surface but is subject to pressure on its outer surface. No example of this type is considered in detail as the solution presents no new features.

Type 2.—*Gradient Negative.*

If $A<1$ and the graph is of the type shown in fig. 1, the chord must be either within AB, or, within BC, with at least one extremity in the portion BT.

If $A>1$ and the graph is as in fig. 2, the chord must lie in the range AB with at least one extremity in the portion AT. In either case, since there is a point of inflexion in AB, if a solution exists there are two possible positions in which the chord may be adjoined to the graph.

A particular instance will illustrate this. Suppose that, with $A^2=0{\cdot}94$, the following boundary conditions apply :—

$$R_A=1{\cdot}000 \quad R_B=1{\cdot}143 \text{ so that } \log_{10}(R_B/R_A)=0{\cdot}0580$$
$$\rho'_A=2{\cdot}512 \quad \rho'_B=1{\cdot}000 \text{ so that } \log_{10}(\rho'_A/\rho'_B) \ =0{\cdot}400.$$

There are two possible positions in which the chord may be adjoined to the graph, viz., PQ and RS in fig. 1, giving the following two sets of values, obtained from the two chords.

(a) *First Position*, PQ.

$$\left.\begin{aligned}\log_{10}(ML\rho'_B)&=-1{\cdot}000\\ \log_{10}(ML\rho'_A)&=-0{\cdot}600\end{aligned}\right\} \quad \left.\begin{aligned}\log_{10}(L^2R_B)&=0{\cdot}1215\\ \log_{10}(L^2R_A)&=0{\cdot}0637\end{aligned}\right\}.$$

These, with the known values of R_A and R_B, give $\log_{10}L^2=0{\cdot}0637$.

Proceeding to the graph in fig. 3 which connects $\log_{10}(LM\rho')$ with $\log_{10}(LQ)$, and using the above value of L, it is found that, corresponding to our boundary values of $\log_{10}(LM\rho')$, $Q_B=0{\cdot}185$, $Q_A=0{\cdot}370$, so that from the relation $\rho'=\rho Q$, $\rho_B=5{\cdot}39$, $\rho_A=6{\cdot}77$.

These values make it evident that a displacement far beyond the elastic limit is involved.

(b) *Second Position* RS.

$$\left.\begin{aligned}\log_{10}(ML\rho'_B) &= -0{\cdot}035\\ \log_{10}(ML\rho'_A) &= \ \ 0{\cdot}365\end{aligned}\right\} \quad \left.\begin{aligned}\log_{10}(L^2R_B) &= -0{\cdot}0607\\ \log_{10}(L^2R_A) &= -0{\cdot}1187\end{aligned}\right\}.$$

These give $\log_{10}L^2=\bar{1}.8813$, and using fig. 3 as before, it is found that $\rho_B=1{\cdot}190$, $\rho_A=2{\cdot}600$, a quite reasonable result.

It is possible that these two solutions may correspond, in some way, to the reduction in elastic resistance after the yield point is attained.

Fig. 3.

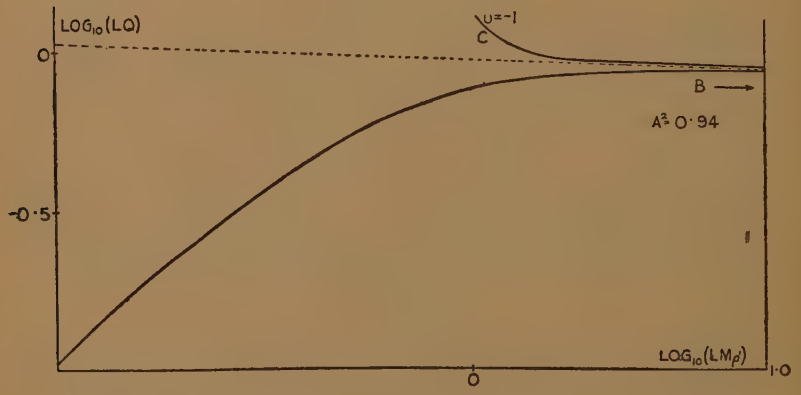

This type of solution arises when the gradient is negative, and, in particular, when the tube is free from surface loading on the outer surface, but is subjected to pressure inside.

Type 3.—*Gradient Zero.*

If $A<1$ a graph of the type shown in fig. 1 is used, and the chord can be adjoined only in the part BC. If, however, $A>1$, a graph of the type shown in fig. 2 is used, and then the chord can appear only in the part AB. The most interesting example giving rise to this solution is that of the tube under no internal or external traction, but subjected to a dislocational strain of the type we have been considering.

From statical considerations it is seen that the tractions across any axial plane reduce to a couple. This solution,

then, may be interpreted as that for a plate of constant initial curvature, bent by edge couples so that its curvature is either increased ($A<1$) or decreased ($A>1$). One example has been worked out in detail. It is supposed that in the unstrained state the plate has two cylindrical surfaces of radii 1·0 and 1·2. The portion of the curves corresponding to the neighbourhood of the points T in figs. 1 and 2 have been constructed for the values

$A^2=1{\cdot}4641,\ 1{\cdot}21,\ 1{\cdot}102,\ 0{\cdot}94,\ 0{\cdot}901,\ 0{\cdot}802.$

TABLE II.

ρ'.	ρ.	$\widehat{\rho\rho}/(\lambda+\mu)$.	$\widehat{\theta\theta}/(\lambda+\mu)$.	$\widehat{zz}/(\lambda+\mu)$.
1·0000	1·2308	0·0000	0·0224	0·0056
1·0080	1·2387	0·0011	0·0207	0·0054
1·0244	1·2551	0·0034	0·0176	0·0052
1·0405	1·2711	0·0052	0·0145	0·0049
1·0579	1·2884	0·0066	0·0108	0·0044
1·0761	1·3066	0·0075	0·0071	0·0036
1·0952	1·3257	0·0078	0·0031	0·0027
1·1152	1·3457	0·0075	−0·0012	0·0016
1·1364	1·3670	0·0065	−0·0057	0·0002
1·1586	1·3892	0·0048	−0·0106	−0·0015
1·1822	1·4129	0·0024	−0·0159	−0·0034
1·2000	1·4309	0·0000	−0·0198	−0·0049

TABLE III.

(1−A).	Mean radius after strain.	$\frac{\widehat{\theta\theta}}{(\lambda+\mu)}$ (inside).	$\frac{\widehat{\theta\theta}}{(\lambda+\mu)}$ (outside).	$\frac{\text{Couple}\times 10^4}{(\lambda+\mu)}$.
−0·210	1·3308	+0·0224	−0·0198	+1·54
−0·100	1·2098	+0·0117	−0·0104	+0·70
−0·050	1·1546	+0·0062	−0·0054	+0·39
+0·030	1·0665	−0·0040	+0·0036	−0·25
+0·051	1·0443	−0·0071	+0·0061	−0·43
+0·114	0·9854	−0·0152	+0·0132	−0·91

The stresses and displacements for the particular value $A^2=1{\cdot}21$ are shown in Table II. Table III. shows the values of the stress $\widehat{\theta\theta}$ at the outer and inner surfaces for the various values of (1−A) considered and the couples required to produce the given changes in curvature. The changes in the mean radius, given in Table III., are illustrated graphically in fig. 4.

The solution of the corresponding problem using the formulæ of the ordinary theory of infinitesimal strain is given by Coker and Filon *. The solution given is for generalized plane stress, but the transformation to plane strain is easy. It appears from the small strain theory that the hoop stress on the inner and outer surfaces is given by

$$\frac{\widehat{\theta\theta}}{\lambda+\mu}(\text{inside}) = -(1-A)\,0{\cdot}1289,$$

$$\frac{\widehat{\theta\theta}}{\lambda+\mu}(\text{outside}) = (1-A)\,0{\cdot}1142.$$

Fig. 4.

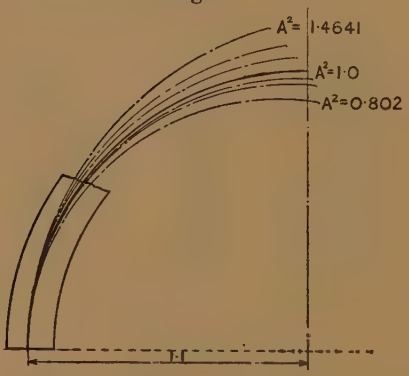

FIG. 4
CHANGE IN MEAN RADIUS FOR DIFFERENT VALUES OF A

The couple per unit length of edge is found to be given by

$$\frac{\text{couple} \times 10^4}{\lambda+\mu} = 8{\cdot}1(1-A).$$

For purposes of comparison with the results shown in Table III. the values of the corresponding quantities calculated from the small strain theory have been shown in Table IV.

The comparison is more easily made by reference to the graphs in fig. 5. The values of $\widehat{\theta\theta}$ and of the couple are in good agreement in the regions for which (A—1) is negative, *i. e.*, when the curvature is increased, but the divergence is more marked when (A—1) becomes positive. It is found that, according to the finite strain theory, the

* C.F.P. p. 320.

TABLE IV.

(1−A).	Mean radius after strain.	$\frac{\widehat{\theta\theta}}{(\lambda+\mu)}$ (inside).	$\frac{\widehat{\theta\theta}}{(\lambda+\mu)}$ (outside).	$\frac{\text{Couple}}{(\lambda+\mu)} \times 10^4$.
−0·210	1·3303	+0·0271	−0·0240	+1·70
−0·100	1·2097	+0·0129	−0·0114	+0·81
−0·050	1·1546	+0·0064	−0·0057	+0·41
+0·030	1·0666	−0·0039	+0·0034	−0·24
+0·051	1·0443	−0·0066	+0·0058	−0·41
+0·114	0·9854	−0·0147	+0·0130	−0·92

Fig. 5.

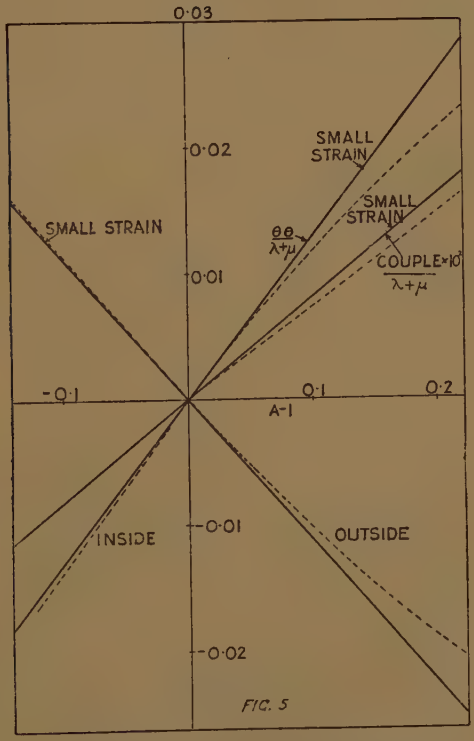

couple required to produce a given decrease in curvature is less than that calculated from the small strain theory. This is a point where experimental verification of the theory would be of interest.

L. *Field Distribution and Graphical Ray Tracing in Electron Optical Systems.* *By* L. Jacob, *M.Sc.*, *A.R.C.Sc.I.** (Communication from the Staff of the Research Laboratories of The General Electric Company, Limited, Wembley, England.)

[Received June 24, 1938.]

[Plate V.]

Summary.

1. The electrolytic trough method is applied to the case of an electron optical lens system for mapping out its field distribution to an accuracy of 2–3 per cent.

2. The approximate electron trajectory for an electron entering the field in a direction parallel to the axis is calculated, using the axial potential distribution and its derivatives.

3. Errors as large as 50 per cent. are introduced in this step-by-step process of approximation which restricts its usefulness.

4. Use is made of the axial " geometric plot " to derive a simple method for the graphical construction of the ray-paths which gives a good approximation.

The cases of widely spaced as well as closely spaced surfaces are separately considered.

1. *Introduction.*

SINCE the pioneer theoretical work of Bush † in 1926, who worked out the focussing properties of electric and magnetic fields, much further work in connexion with electron trajectories through such fields and the imperfections inherent in electron-optical systems generally has been done.

Particular mention must be made to the work of Picht ‡, who treated the electron lens as a " thick " lens, and of Maloff and Epstein §, who treated the problem of the electron path through such fields by a step-by-step

* Communicated by C. C. Paterson.

† *Ann. der Physik*, lxxxvi. p. 974 (1926); *Arch. für Elektro*, xviii p. 583 (1927).

‡ *Ann. der Physik*, xv. p. 56 (1932).

§ P. I. R. E. xxii. p. 1386 (1934).

method of approximation which gave a good idea of the electron motion.

Fundamentally, these calculations are based on an experimental determination of the axial potential distribution of the electron optical system. The accuracy with which such a distribution can be obtained is of prime importance for the later evaluation of ray-paths in the field, since the calculation involves the second and higher derivatives of the potential function.

The plotting of such electric fields of which the axial is a particular case, has long been recognized as of great value in the case of all types of dielectric stress, and its application to problems in electron optics has further opened a wide field of work.

The experimental method of McArthur *, which incorporates many improvements as regards apparatus and technique, has yielded results to within an accuracy of 5 per cent. for such field models.

In the present investigation two separate methods for obtaining the axial potential distribution in electron-optical systems of any complexity are described. These give results, to an accuracy of 2–3 per cent. Use is then made of the electron-optical equivalent of Snell's law of sines to trace out graphically the electron trajectories through such fields of force.

2. *Experimental Method.*

The method of experiment consisted in plotting the equipotential lines for the system in an electrolytic tank after the method of McArthur. As we are dealing with axially symmetrical fields it is only necessary to make a two-dimensional plot of the field, since the field in every plane through the axis will have the same configuration as that obtained from this plot. This is done by immersing a large-scale model ($\times 4$ in the present case) of the electrode system, half-sectioned along the axis, in distilled water in a large glass or porcelain tank, and exploring the field in the inter-electrode space by means of a fine wire probe. The model is suitably insulated on an ebonite base by vertical ebonite pillars of adjustable height which can slide along the groove G of the base, so that any required separation between the electrodes E can be obtained

* 'Electronics,' iv. p. 192 (1932).

(fig. 1). Great care is necessary on first setting up the system to see that it is properly aligned in both horizontal and vertical planes, and that the various electrodes in the system are truly coaxial. In order to prevent strong surface tension effects when the probe is in the near vicinity of the electrodes, the latter are extended 2–3 mm. above the actual half section, so that while the level of the distilled water in the tank is exactly on a horizontal diametral plane, the edges of the electrodes project above the surface to this extent. If this is not done the probe, when about $\frac{1}{2}$–1 mm. from the edge, is found to be pulled in towards the edge, and the potential readings fluctuate and become unreliable within this region. The use of distilled water was found to be necessary principally because of its very low conductivity. Ordinary tap-water when tried in its place was found to draw too

Fig. 1.

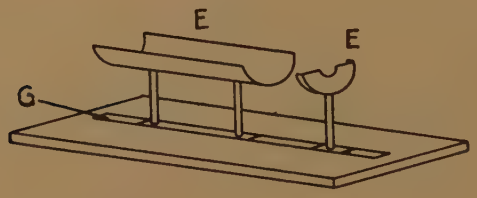

much load from the voltage supply, and was thus unsatisfactory.

Two distinct methods of measurement were used :

In the first, the axial potential distribution alone was explored by using a fine wire probe as the exploring electrode. The probe was mounted vertically from an arm attached to a rigid framework surrounding the tank. The probe holder could be moved along horizontally in a V groove by turning a screw at one end of the arm. In this way it was possible to make the probe traverse the axis of any system of suitable size from one end to the other. This will be referred to as the axial traverse method. As before, great care was necessary in mounting up the framework to see that the probe moved along the axis of the system. This was done by a method of approximations. The probe was traversed along the axis several times in succession, between each of which,

adjustments to the relative positions of tank and framework were made, using four adjusting screws bearing on the four sides of the tank. As is quite clear, the necessary adjustments were in directions approximately at right angles to the direction of the axis. When the probe traverse is truly axial, a small alternating voltage at 400 cycles obtained from a valve oscillator is then applied across the electrode system, and the P.D. between the exploring probe and either electrode is picked up on a sensitive valve voltmeter which has been previously carefully calibrated. The whole electrical system is really a potential divider which is working under its best possible conditions, *i. e.*, little or no current flow to and from the probe. In this way effects due to space charge of conducting ions are minimized, and results are readily repeatable, provided care is taken to avoid local variations of concentration of the water by contamination.

It must be emphasized that the method depends on the existence of no appreciable current flow to or from the probe so that the field distribution may not be disturbed. This is a primary condition and is fulfilled in these circumstances, since the valve voltmeter takes little or no current.

A most important factor in getting consistent results is the constancy of the applied voltage. Mains variations and consequent fluctuating output voltage from the oscillator must be eliminated. If this is not seen to, it is found that the positions of one or more equipotential surfaces become displaced backwards or forwards along the axis, and results are thus most unreliable and unrepeatable. It was finally possible by careful control and check on the output voltage to keep this constant to $\frac{1}{4}$ per cent. The voltage was kept constant to this value for each point on the equipotential plot, and results agreed when the points were repeated.

After several trials it was found best to silver-plate the electrodes and use a 0·2 mm. silver wire probe immersed to a depth of 3–4 mm. below the surface of the distilled water in the tank. If the probe is immersed further down than this the readings picked up on the valve voltmeter tend to fluctuate. The effect of silver plating all the electrodes avoided contact potential effects as well as any serious oxidation. Further, it enabled consistent results to be obtained on the same system

even though immersed for several days in the tank, provided one further precaution was taken, namely, as regards the freedom of the surface of the water from dust particles or bits of floating fluff. These, when caught by the probe disturbed the field and caused the valve voltmeter needle to jerk unsteadily at all times. It was practically impossible to avoid the presence of both these disturbing particles even with the most stringent precautions for cleanliness. They seemed to get into the tank overnight, in spite of the use of a dust-proof paper cover (in which a mica window had been inserted for observation and guide purposes) which always covered the whole tank idle or in use, and which overlapped by several inches all round the edges. It was necessary

Fig. 2.

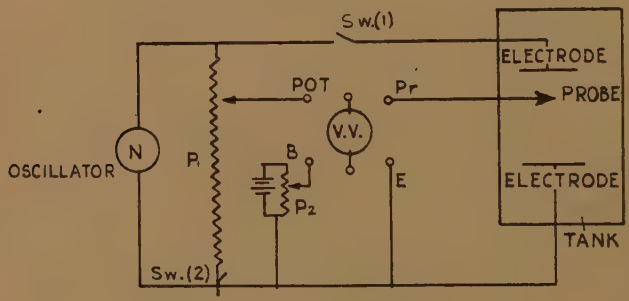

before starting work on any system, to comb out thoroughly the surface of the water with a fine glass nozzle attached to a vacuum supply. The use of a powerful torch was a great help in finding this fluff.

A further precaution against the accumulation of particles of dust or other interfering bodies was to keep a gentle air blast on the surface of the water at one end of the tank, so as to keep the surface continuously in a state of very gentle motion. This also was most helpful.

A second and more refined method of measurement was to use a null method in place of the calibrated voltmeter. This is illustrated in fig. 2.

The potential difference between probe and electrode was balanced out each time, using a D.C. potentiometer source, so that by keeping the valve voltmeter VV at a

fixed reading on its scale, a plot along any equipotential line could be quickly and conveniently followed through.

The actual order of operations was as follows :—

(*a*) Close Switch (1).
Close Pr.
Close E. VV is now across probe and one electrode. Bring probe to high potential electrode and note P.D. between electrodes.

(*b*) Open Switch (1).
Close Switch (2).
Close Pot.
Close E. Valve voltmeter is now across main potentiometer P_1. Adjust main potentiomter P_1 to some known fraction of the total applied P.D., and read this value on VV.

(*c*) For the null method, open E and close B and balance out reading on VV by adjusting bias potentiometer P_2, or, alternatively, keep VV at some known reading.

(*d*) Open Switch (2).
Close Switch (1), close E.
Close Pr and adjust the position of the probe in the tank till VV is balanced out or picks up the known reading decided in (*c*).

(*e*) Trace out the equipotential corresponding to this known volt reading.

(*f*) Repeat for other equipotentials.

By suitably guiding the probe in the tank the whole of the intra- and extra-electrode space can be explored in this way. The method of recording the various equipotentials is quite simple. Reference to fig. 3, which shows a diagrammatic view of the apparatus, will make this clear. Both probe and pencil are connected mechanically to the gate-arm A, which is pivoted at B and C and allows them to move rigidly together and freely in all directions along and parallel to the plane of the water in the tank, so that the various motions of the probe are copied exactly by the pencil, but are transferred to a different plane—that of the drawing-board immediately below the pencil.

By pressing a small hand key the pencil is actuated electromagnetically and records a pin-point on the drawing-board for every equipotential point picked up by the probe. Before setting up the framework, great care was taken and suitable tests carried out to make sure that the probe moved truly parallel to the surface of the water in the tank for every direction of motion.

Fig. 3.

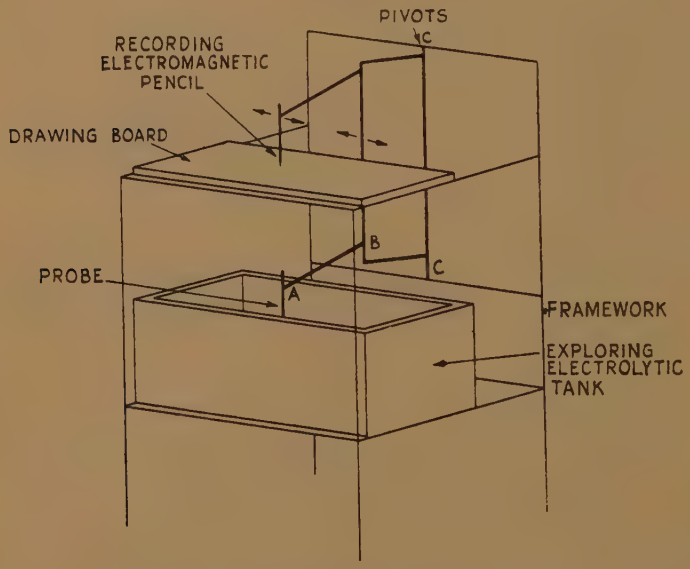

3. *Experimental Results of Field Plots.*

In order to test out the accuracy of the method a known field such as that between coaxial right circular cylinders was first introduced and studied.

As outlined above, a section of this combination by a plane through and containing the axis was set up in the electrolytic tank, and the field between the two cylinders was plotted out experimentally with the axial traverse apparatus, but in this case, the probe was arranged to move at right angles to the axis at all points along the length of the system. This gave the field transverse to the axis.

If a = radius of outer cylinder which is kept at potential V_A;

b=radius of inner cylinder which is kept at potential V_B;

V_x=potential at any point distant x from the axis, then

$$V_x = \frac{V_A \log b/x + V_B \log x/a}{\log b/a}$$

Fig. 4.

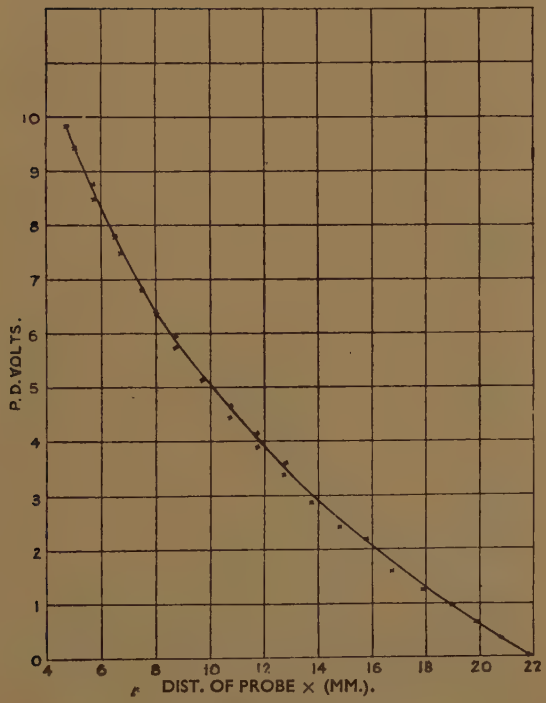

Co-axial cylinders. Voltage distribution. Inner diam. 9·5 mm.; outer diam. 45 mm. Thickness of metal 0·75 mm. ×, experimental points. Full line curve theoretical distribution.

In our particular case $V_A=0$, since the outer cylinder was tied to earth potential;

$$\therefore \quad V_x = \frac{V_B \log x/a}{\log b/a}.$$

The theoretical values of V_x for various values of x between the cylinders are shown plotted in fig. 4, together with

the experimental values ($\times$) obtained in the exploring tank.

It will be seen that there is good agreement between both sets of values over the best part of the range, and that an accuracy of 2–3 per cent. could be expected for any field plot.

Having obtained satisfactory agreement for this simple and calculable system, the work on field distributions for electron-optical systems was next proceeded with.

In the present instance, the latter consists of two elements—a cylindrical barrel of diameter 20 mm. and length 80 mm., spaced 5 mm. away from a capped disk containing a 5 mm. aperture as shown in fig. 1.

These constitute the main electron lens of a cathode ray tube. The electrons from the cathode, after acceleration by the first anode, enter this field from the left as a diverging beam of small angle, and are focussed by the action of the radial electrostatic forces as the electrons cross the various equipotentials in turn. On the optical analogy the refractive index increases all the way from the low voltage end to the high voltage end of the field, since the electron velocity is directly proportional to the refractive index. It is inevitable that, with this particular arrangement, the field extends quite considerably towards the cathode end, *i. e.*, into the region of low velocity. This part of the field is very important because of the low electron velocity and consequent comparatively large bending of the path by the field.

As before, a four-scale sectioned model was introduced into the electrolytic tank, and the field was plotted using both the valve voltmeter method previously employed for the axial traverse and also the more precise null method. Good agreement was again obtained by both methods. The result of the equipotential plot is shown in fig. 5.

Some 2000 points were taken on this set of 40 equipotential curves to complete the plot, which, as will be seen, is now capable of giving both the radial and longitudinal extra-axial equipotential distribution.

The extension of the more strongly curved equipotential surfaces well towards the low voltage end is a marked feature of the plot, and the refractive effect of the field on the electron beam should be greatest in that part of this field where the radial force has its maximum value.

A further point in support of this is the progressive increase in axial spacing in going from the high to the low potential end of the field.

This, in effect, means that for the same equipotential step, the electron spends a considerably longer time at

Fig. 5.

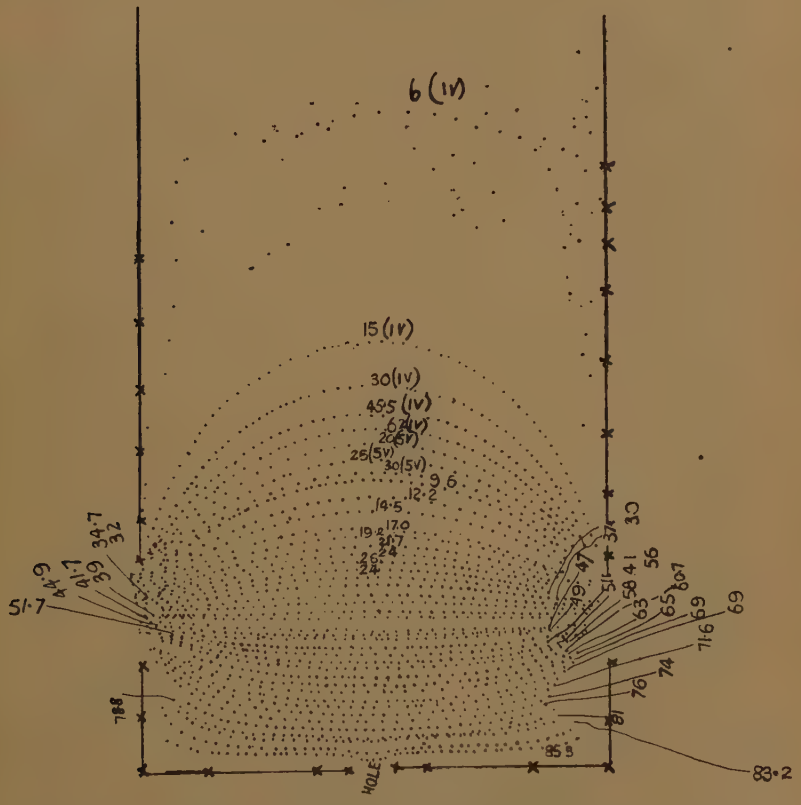

the low voltage end than at the high voltage end—the radial forces have a longer time to act, and as an additional factor the electron velocity is lowest, so that the refractive effect is much more pronounced. The graphical treatment outlined later gives an excellent realization of this theory.

For most purposes of calculation the axial potential distribution is sufficient provided care is taken to ensure

the necessary accuracy of 2–3 per cent. The axial potential distribution obtained from this plot by the null method is shown in fig. 6. Use of the two-dimensional complete field plot was made to build up the three-dimensional model of the field shown in fig. 7 (Pl. V.).

This was done by cutting out from sheet linoleum the shape of the various equipotentials in turn, the heights

Fig. 6.

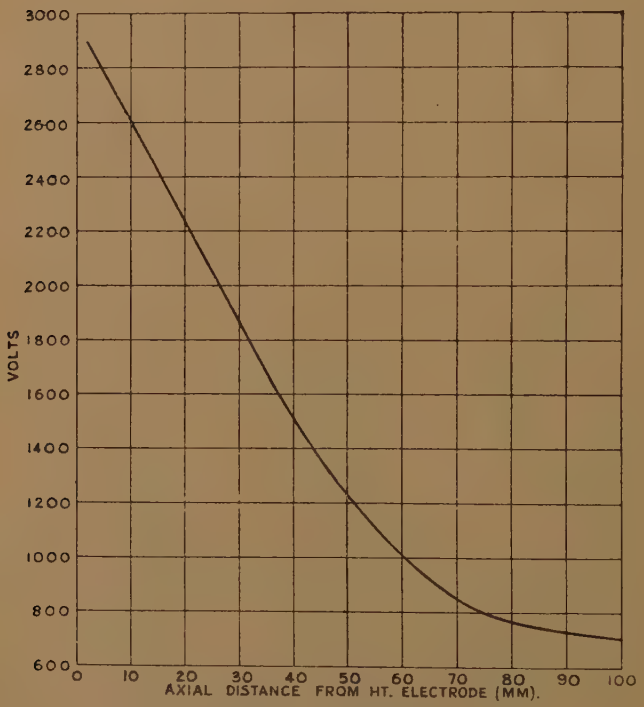

Axial potential distribution for electron-optical lens system. Bias method.
Low voltage electrode at 600 volts.
High „ „ „ 3000 volts.

of the laminæ being proportional to the potential on some arbitrary scale. The discontinuities at the edges of the curved portions were next smoothed out with plasticene, and a plaster cast then made of the model. The line A at the bottom, which is really the high potential end of the lens element, defines the aperture in the capped

disk E of fig. 1. It must be pointed out that the height of this model rather exaggerates the action of the field on any smooth ball released from the platform at the top. A much more gradual slope would have allowed of better realization of the actual trajectory, since there is then little chance of the ball leaving the surface, as no bumping can occur in the actual motion of the electron through the field. The motion on the model to be exact must follow variations in acceleration not only along the axis and along all lines parallel thereto, but also along the various radii, so that the " banked " effect on the model may have the correct influence on the motion. Allowance must be made for the rotational energy of the true ball, which is some 2/7 of the total kinetic energy, so that the velocity at all points of the motion must be multiplied by $\sqrt{7/5}$ in order to give the true velocity This is necessary, since it would require a point mass sliding without friction (an impossible requirement in the present practical case) down the model to produce an exact replica of the actual electron motion.

It is interesting to note in connexion with types of models representing electrostatic fields, that a rubber membrane stretched in such a way that the surface tension is constant over the whole surface, has been used by Kleynen * and also by Pierce † to investigate the motion of charged particles in a two-dimensional field such as that in a radio valve, where one electrode dimension has no influence on the field. The membrane is displaced vertically at the necessary points to correspond with the potential of the electrodes, and the slope is kept small with respect to unity, so that the two-dimensional Laplace equation $\frac{\partial^2 h}{\partial x^2}+\frac{\partial^2 h}{\partial y^2}=0$ is approximately satisfied. The paths traced out by a smooth ball rolling down the membrane then give a good approximation to the electron path. The use of the rubber model is of course restricted to the two-dimensional case, and the present electron-optical symmetrical field cannot be explored by its use. Bearing these limitations in mind we can, by rolling smooth ball-bearings representing the electrons down from the point 0 in our model, get a rough approximation

* Philips, Tech. Rev. ii. no. 11, p. 338 (Nov. 1937).
† Bell, Lab. Record, xvi. no. 9, p. 305 (May 1938).

to the ray-paths. The focussing action due to the curvature of the field can be simply demonstrated if the initial motion is inclined at small angles to the axis.

In this case, the trajectory is such that the balls finally emerge through the aperture A. If the initial direction of motion is inclined at too large an angle to the axis, in our case some 10°, the balls will strike the solid portion of the apertured disk, and will consequently no longer appear in the final emerging beam. It is possible in this way to obtain some idea of limiting angles as well as efficiency of the lens system (gun efficiency).

Finally, by shooting in the balls parallel to the axis at small distances from it (so as to simulate the paraxial condition) the positions of the principal planes of the lens system can be very approximately obtained.

4. *Axial Potential Distribution and its Derivatives.*

For purposes of calculation of the paraxial electron path through any axial symmetrically situated field all that it is necessary to know are both the first and higher derivatives of the axial potential distribution. It is not essential to have a complete plot of the field. In general, it is not possible to find any simple analytical expression for the axial distribution, though a method based on purely algebraic notions can be successfully applied to express its equation to any degree of accuracy: this is dealt with later.

Of course, by the use of the complete experimental plot of the field as shown in fig. 5, it is possible to map out the longitudinal and radial gradients for all points off the axis, and use these values and their higher derivatives to compute the forces acting on the electron and its subsequent displacements in its passage through the field. The complete field plot, however, can be dispensed with provided the axial potential distribution alone has been accurately determined and its higher derivatives calculated That this is so follows from the fact that the potential at any point of the field off the axis is given by the expansion *

$$V_{(z,r)}=V_z-\frac{r^2}{2^2}\cdot V''(z)+\frac{r^4}{2^2.4^2}\cdot V^{iv}(z)+\ldots.$$

* Maloff and Epstein, 'Electron Optics in Television,' p. 77. McGraw-Hill.

The radial and axial gradients are got from this expression by simple partial differentiation—thus

$$\frac{\partial V}{\partial r} = -\frac{r}{2}V''(z) + \frac{r^3}{16}V^{iv}(z) - \frac{r^5}{4.6.16}V^{vi}(z) + \ldots$$

$$\frac{\partial V}{\partial z} = V_z' - \frac{r^2}{2^2}.V'''(z).$$

Thus, knowing V′(Z) and V″(Z) etc., the electron motion can be calculated from simple dynamical considerations, treating the electron as a particle of mass m and charge e.

The radial force is $-\frac{\partial V}{\partial r}.e$, hence the radial acceleration

$$\frac{d^2r}{dt^2} = \frac{\partial V}{\partial r}.\frac{e}{m} = \frac{r}{2}.\frac{e}{m}V''(Z).$$

Maloff and Epstein * have proceeded from this, and built up an expression for r, the radial distance at any point off the axis

$$r = \int\int \frac{1}{4}r\frac{1}{V}\frac{d^2V}{dZ^2}.dz.dz - \int\int_z \frac{1}{2}\frac{1}{V}.\frac{dr}{dz}.\frac{dV}{dz}dz.dz,$$

which lends itself to calculation provided the values of the first and second derivatives at all points along the axis are known. These derivatives can be obtained in two ways—(1) method of differences using the axial plot, (2) equation to the axial plot.

Taking (1), the curve representing the axial potential distribution is smoothed out as follows, using the method of differences. Taking an interval of 5 mm. along the axis of the axial potential distribution curve, the values of the potential as read from this curve for the various successive intervals are tabulated, and the first, second, third, etc. order of differences are taken until, as in the present case, at the fourth order the figures have so evened out that it is not necessary to go any further (Table I.). With the usual notation these differences are applied to the necessary expansions.

Thus, to use the method of differences to get the first differential at the point where Z=10 mm., we have

$$f_z = f_{10},$$

$$\Delta V(f_{10}) = \mu\delta_0(f_{10}) = \tfrac{1}{2}(-179-169) = -174.$$

* *Loc. cit.*

$\Delta^2 V(f_{10}) \equiv \delta^2 f_{10} = -10,$

$\mu\delta^3 f_{10} = \frac{1}{2}(+1-4) = -\frac{3}{2},$

$\delta^4 f_{10} = +5.$

TABLE I.

Table of Differences.

Z (mm.).	V (volts).	ΔV.	Δ^2V.	Δ^3V.	Δ^4V.
0	2923				
		−163			
5	2760	..	− 6		
		−169	..	−4	
10	2591	..	−10	..	+5
		−179	..	+1	
15	2412	..	− 9	..	+4
		−188	..	+5	
20	2224	..	− 4	..	+2
		−192	..	+7	
25	2032	..	+ 3	..	−0
		−189	..	+7	
30	1843	..	+10	..	−2
		−179	..	+5	
35	1664	..	+15	..	−3
		−164	..	+2	
40	1500	..	+17	..	−2
		−147	..	0	
45	1353	..	+17	..	0
		−130	..	0	
50	1223	..	+17	..	0
		−113	..	0	
55	1110	..	+17	..	0
		− 96	..	0	
60	1014	..	+17	..	−1
		− 79	..	−1	
65	935	..	+16	..	−1
		− 63	..	−2	
70	872	..	+14	..	−1
		− 49	..	−3	
75	823	..	+11	..	0
		− 38	..	−3	
80	785	..	+ 8	..	0
		− 30	..	−3	
85	755	..	+ 5		
		− 25			
90	730				

From the expansion

$$f(a+\theta z) = f(a) + \theta\mu\delta_0 f(a) + \frac{1}{2}\theta^2\delta^2 f(a) + \frac{1}{6}(\theta^3-\theta)\mu\delta^3 f(a) + \frac{1}{24}(\theta^4-\theta^2)\delta^4 f(a) + \ldots;$$

$$\therefore \frac{df_{10}}{d\theta}=\mu\delta_0 f_{10}+\theta\delta^2 f_{10}+\frac{1}{6}.3\theta^2\mu\delta^3 f_{10}-\frac{1}{6}\mu\delta^3 f_{10}$$
$$+\frac{4}{24}.\theta^3\delta^4 f_{10}-\frac{\theta}{12}\delta^4 f_{10}.$$

Now $\theta=0$;

$$\therefore \quad \frac{df_{10}}{d\theta}=-174+0+0-\left(\frac{1}{6}.-\frac{3}{2}\right)+0-0=-\frac{695}{4};$$

$\therefore$ first differential coefficient at

$$f_{10}=\frac{1}{5}.\frac{df_{10}}{d\theta}=-\frac{139}{4}.$$

Fig. 8.

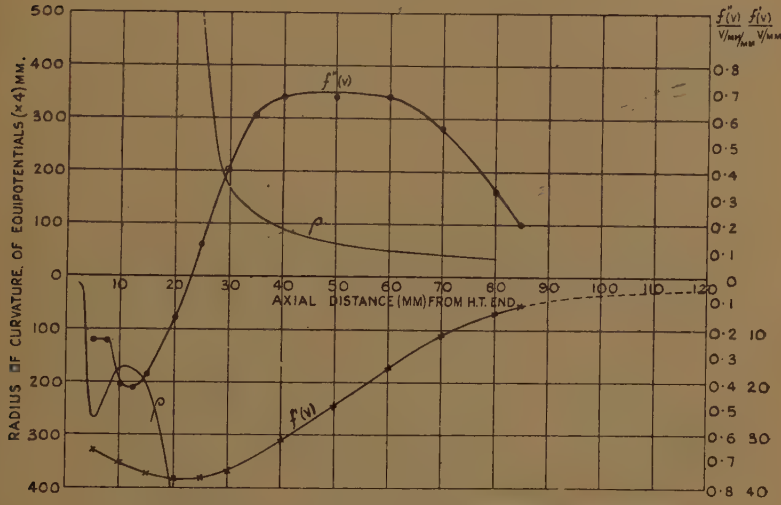

First and second derivatives of axial potential distribution as well as radii of curvature ρ of equipotentials.

Also

$$\frac{d^2f_{10}}{d\theta^2}=\delta^2 f_{10}+\frac{1}{6}.6\theta.\mu\delta^3 f_{10}+\frac{1}{24}.12\,\theta^2\delta^4 f_{10}-\frac{2}{24}\delta^4 f_{10}+\ldots$$
$$=-10+0+0-\frac{5}{12}=-\frac{125}{12};$$

$\therefore$ second differential coefficient at

$$f_{10}=\frac{1}{5^2}.-\frac{125}{12}=-\frac{5}{12}.$$

In this way the first and second derivatives can be calculated, using the coefficients of the difference table for all the intervals along the axis. In order to get a closer approximation it may be necessary to take points in between two intervals—for example, at $f_{12\cdot5}$, the value of θ is $\frac{2\cdot5}{5\cdot0}=\frac{1}{2}$, so that substitution of $\theta=\frac{1}{2}$ in the above equations will give the required derivatives at the point $Z=12\cdot5$. Fig. 8 gives the curves obtained for the first and second derivatives of the axial potential distribution. A check on their accuracy was got by comparing the values of the radii of curvature ρ of the equipotential surfaces given by $\rho=\frac{2f'(V_z)}{f''(V_z)}$ with the actual radii of curvature measured from the complete plot. Good agreement was found in all cases where this was practicable.

5. *Approximate Calculation of Electron Trajectories.*

The field plot of the main lens is useful as a guide in its design. Variations of geometry and configuration are immediately reflected in a modification of the field which in turn modifies the electron paths. An attempt was made to see how far the electrostatic lens described, treated as a thick lens, could be made to focus paraxial rays.

The method of attack was that introduced by Maloff and Epstein *, who gave a simple method of direct approximation for calculating the trajectories between closely spaced equipotentials throughout the field.

Briefly, the method is as follows :—

$$\text{Force on electron} = \text{gradient} \times \text{charge} = \frac{dV}{dx}.e.$$

If θ=angle between direction of field and axis, and resolving, then

$$m\frac{d^2r}{dt^2}=\frac{dV}{dx}.e.\sin\theta,$$

then

$$m\frac{d^2x}{dt^2}=\frac{dV}{dx}.e.\cos\theta,$$

where also $\sin\theta=\frac{r}{R}$, since

* *Loc. cit.*

r=radial height above axis,

R=average radius of curvature of both equipotentials.

A first integration gives

$$\frac{dr}{dt} = \left(\frac{e}{m} \cdot \frac{dV}{dx} \cdot \frac{r}{R}\right)t + \left(\frac{dr}{dt}\right)_0 = C_1 t + v_{r_0},$$

$$\frac{dx}{dt} = \left(\frac{e}{m} \cdot \frac{dV}{dx} \frac{\sqrt{R^2 - r^2}}{R}\right) \cdot t + \left(\frac{dx}{dt}\right)_0 = C_2 t + v_{x_0},$$

where C_1, C_2 are constants, and v_{r_0} and v_{x_0} are initial radial and longitudinal velocities.

Integrating again :

δr=change in radial height$=\frac{1}{2}C_1 t^2 + v_{r_0} . t$,

δx= ,, ,, axial position $\frac{1}{2}C_2 t^2 + v_{z_0} . t$.

It is thus possible to calculate both δr and δx throughout the whole field. The paraxial case is simplified, since it is only necessary to calculate δr for each pair of adjacent equipotentials.

The following example, Table II., shows how the method has been applied to the case of the equipotential plot of fig. 5. Every third surface only is taken, and the result obtained is some 10 per cent. below that obtained by working through all the surfaces. The initial ray is assumed to be parallel to the axis, and enters the lens at the H.T. end at a height of 5 mm. from the axis.

A glance at fig. 9 shows that at first the ray diverges and is thrown out from the axis, and progressively continues so until it is about halfway through the field. This, of course, is due to the direction of the curvature of the field. When the curvature reverses, the direction of the displacement reverses with it, and somewhere later on in the field, the radial height is the same as the initial height, *i. e.*, 5 mm. After this point the converging effect alone occurs, and the electron has lost about $2\frac{1}{4}$ mm. in height by the time it has passed through the field. The large refractive effects of the low potential end of the field are very marked, since the electron velocity is comparatively small.

If the electron were projected in a straight line from its direction of emergence from the field, then the point at which this line meets the axis defines one of the focal points of this thick electron lens. The other focal points

Table II.

Surface no.	Distance from H.T. element (mm.).	$C \times 10^{16}$.	Average time $t \times 10^{-8}$.	$Ct \times 10^{8}$.	$\frac{1}{2}Ct^2 \times 10^{-3}$.	$\left(\frac{dr}{dt}\right) \times 10^{8}$.	$\left(\frac{dr}{dt}\right) t \times 10^{-3}$.	$\delta r \times 10^{-3}$ (cm.).	$\Sigma \delta r \times 10^{-3}$ (cm.).
4 ..	7·5	2·67	0·0178	0·0475	0·425	0·0475	....	0·425	0·425
7 ..	12	1·74	0·0148	0·0258	0·192	0·0733	0·703	0·895	1·32
11 ..	17·8	1·24	0·02	0·0247	0·248	0·098	1·466	1·714	3·03
14 ..	22	0·289	0·015	0·0043	0·032	0·102	1·47	1·50	4·53
18 ..	26·7	0·40	0·0174	0·007	0·060	0·109	1·77	1·83	6·36
21 ..	32·5	−1·41	0·0226	−0·032	− 0·361	0·077	2·46	2·1	8·46
24 ..	37	−2·76	0·0181	−0·05	− 0·45	0·02	1·26	0·81	9·27
27 ..	41·5	−3·0	0·0193	−0·058	− 0·558	−0·038	0·386	− 0·172	9·09
30 ..	46·5	−3·12	0·0226	−0·0718	− 0·795	−0·11	− 0·86	− 1·65	7·44
33 ..	56	−2·96	0·0462	−0·137	− 3·15	−0·247	− 5·08	− 8·23	− 0·79
36 ..	63	−2·97	0·0368	−0·109	− 2·01	−0·356	− 9·0	− 11	− 11·8
39 ..	74·5	−2·43	0·065	−0·158	− 5·1	−0·514	− 23·1	− 28·2	− 40
41 ..	125	−0·484	0·31		−23		−159	−182	−222

could be found in a similar way by tracing the electron path for a ray parallel to the axis but entering the lens from the opposite direction, *i. e.*, the low voltage end of the main lens. The principal planes for the system are then defined as in optics by the intersection of the original parallel direction and the direction of emergence to the focal points.

In the actual approximate tracing these were found to be low by as much as 50 per cent. Such a difference

Fig. 9.

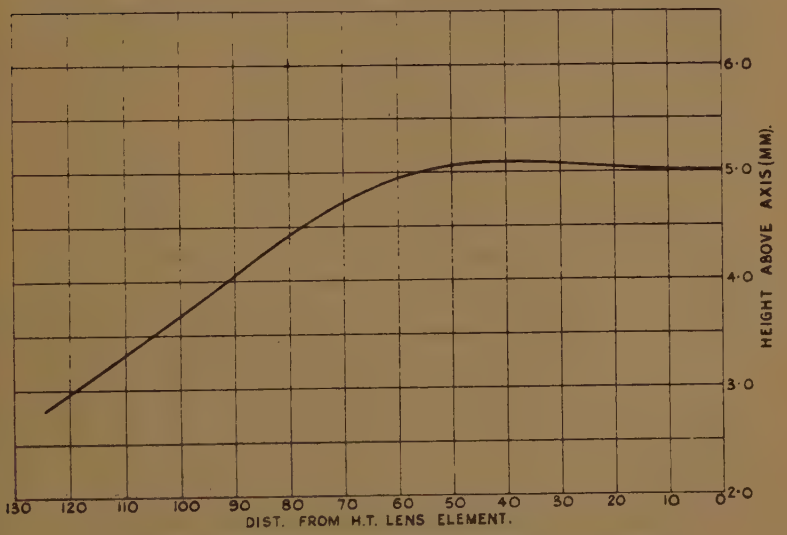

Showing approximate calculation for electron trajectory.

can arise from errors introduced by the finite steps necessary as well as by the aberrations produced by the lens.

6. *Focal Lengths of Electron Lens.*

Although it is possible to obtain the cardinal points of the electron lens from the axial potential distribution plot by the method of approximation to the electron paths, between adjacent equipotential surfaces such as has been outlined in the previous section, it was found that the results were inaccurate when obtained in this way.

At best it gives an approximate picture of the electron trajectory through the field, since comparison of the experimental values of the focal lengths with those obtained by calculation using Scherzer's * formulæ (in which the field is integrated mathematically) shows a large discrepancy.

This is partly due to the step-by-step method of approximation. Fig. 10 shows the cardinal points of the field obtained by this method.

The focal lengths of the electron lens were found to be 65 and −37·5 mm. as against 123 and −54 mm. by calculation. The calculation involves a knowledge of the

Fig. 10.

Principal planes.

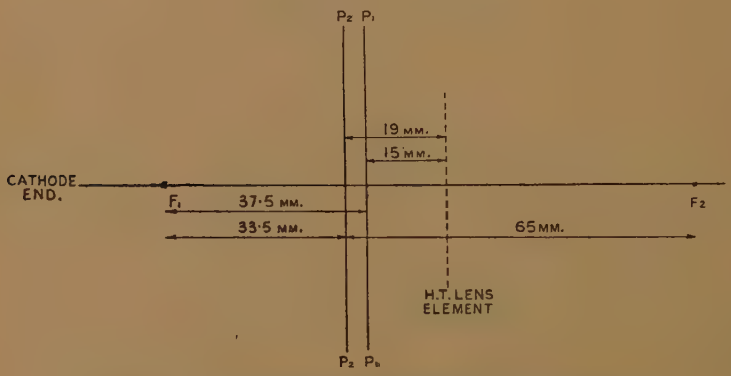

Cardinal points of electron lens (method of approximations).

first derivative of the axial potential distribution only. This was obtained previously. The focal lengths are then given by

$$\frac{1}{f'} = \frac{1}{8\sqrt{3000}} \int_{-\infty}^{+\infty} \frac{\{f'(V_z)\}^2}{\sqrt{V_z^3}}$$

and

$$f = -\sqrt{\frac{600}{3000}} f',$$

where 600 V. and 3000 V. are the voltages on the lens elements. Table III. illustrates the method of calculation.

* *Zeits. f. Physik.* lxxx. p. 193 (1933).

The function $\frac{\{f'(V_z)\}^2}{\sqrt{V_z^3}}$ is plotted in fig. 11, and the graphical integration between the axial limits is carried out, and is shown in the same figure.

It will be seen that

$$\int_{-\infty}^{+\infty} \frac{f'(V_2)^2}{\sqrt{V_z^3}} = \frac{21{\cdot}7 \times 40}{10^3}.$$

TABLE III.

Z (mm).	V_z.	V_z^3.	$\sqrt{V_z^3}$.	$f'(V_z)$.	$\{f'(V_z)\}^2$.	$\left\{\frac{[f'(V_z)]^2}{\sqrt{V_z^3}}\right\}$.
		$\times 10^6$.	$\times 10^3$.	volts/ mm.		$\times 10^{-3}$.
5	2770	21200	146	33	1090	7·45
10	2590	17400	132	34·8	1210	9·15
15	2410	14000	118	36·8	1350	11·4
20	2230	11100	105	38·2	1460	13·9
25	2040	8470	92	38·4	1470	16
30	1860	6440	80·2	37	1370	17·1
35	1670	4650	68·2	34·4	1180	17·3
40	1500	3370	58	31	960	16·6
45	1350	2460	49·6	27·6	765	15·4
50	1220	1820	42·6	24·4	595	14
55	1110	1370	37	20·8	432	11·7
60	1010	1020	32	17·6	310	9·7
65	930	803	28·4	14·2	202	7·1
70	860	637	25·2	11	121	4·8
75	810	530	23	8·6	74	3·22
80	780	474	21·8	6·6	43·6	2
82·5	765	447	21·2	6·0	36	1·7

This gives values of

$$\left.\begin{aligned} f' &= \ \ 492 \\ f &= -216 \end{aligned}\right\} \text{mm.},$$

and since these apply to a four-scale model the focal lengths of the electron lens are 123, −54 mm. respectively.

Using the same method of calculation and for the same model system, it is interesting to follow through the variations in focal length and magnification (lens to screen distance kept constant at 358 mm.) with voltage ratio. As is to be expected, an increase in the latter decreases the focal lengths and consequently increases the magnification of the system. Table IV. shows the calculated results.

Fig. 11.

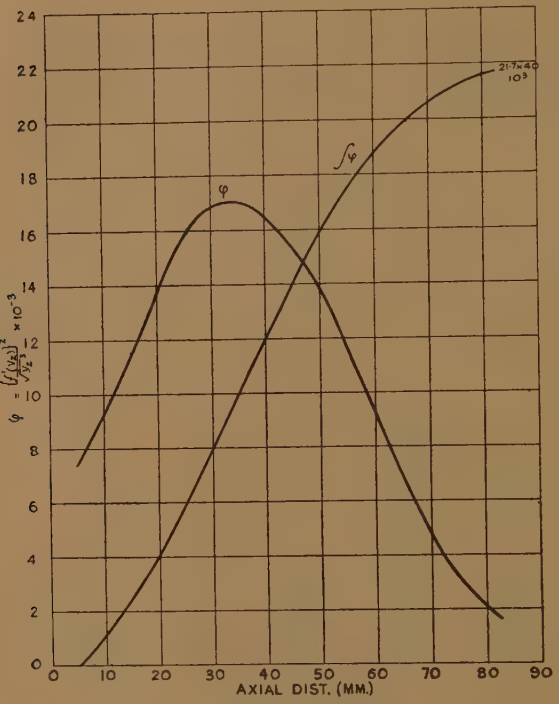

Electron lens ($\times 4$ model).
Computation of focal lengths from axial potential distribution found by the biassing method.

Graphical integration $\dfrac{\{f'(V_z)\}^2}{\sqrt{V_z^3}} = \phi.$

TABLE IV.

Voltage ratio.	V image dist. (mm.).	U object dist. (mm.).	f'.	f.	Magnification.
7·5	271	10·1	87	31·4	3·11
6·0	254	17·4	104	42·6	2·34
5·0	235	28·3	123	54	1·91
4·0	200	62	158	79	1·26
3·0	129	234	229	132	0·56

7. *Graphical Method of Ray Tracing.*

A sound and accurate knowledge of the focussing properties of electron lenses is very important in the design of all types of tube which depend for their action on electron optical principles.

As in the optical analogy, three methods of attack are available. These differ in their sphere of usefulness, depending on several factors connected with the problem on hand. They are (*a*) direct experiment, (*b*) computation, (*c*) graphical methods. While (*a*) is entirely empiric, it yields results based on very broad foundations, and there is much to recommend it, particularly when dealing with complex systems. In the case of (*b*) the computation by a step-by-step method of approximation, as already stated, can give rise to serious inaccuracies. Further, neglect of such important factors as space charge makes matters worse.

The recent work of Gabor * and Langmuir †, who have constructed ingenious mechanical devices for giving a direct trace as an approximation to the electron path through the symmetrical electrostatic field of such lens systems, should, in the author's opinion, give much greater accuracy, since a null method can be used when working through the entire field. In addition to these methods, the graphical construction so commonly used in all optical design can be similarly used to deal with electron rays in electron optics. Such a method is as follows :—Imagine an electron ray originating at the source S to enter the symmetrical electrostatic field of the electron lens E.L. with vel v_0 and at a small angle ϕ to the axis of symmetry SY (see fig. 12).

Then if this ray is inclined at an angle α to the normal N_1P_1 of the first equipotential layer V_1, it will suffer a refraction given by $\mu_1 = \dfrac{\sin \alpha}{\sin \beta} = \dfrac{v_1}{v_0}$, where β is the angle of refraction, and v_0 and v_1 are the respective initial and final velocities on either side of the equipotential V_1.

Similarly, if the refracted ray is inclined at an angle γ to the normal N_2P_2 of the equipotential layer V_2, it will

* ' Nature,' Feb. 27th, p. 373 (1937).
† ' Nature,' June 19th, p. 1066 (1937).

be further refracted, so that $\mu_2 = \frac{\sin\gamma}{\sin\delta} = \frac{v_2}{v_1}$, where μ_1, μ_2 are the refractive indices of the respective electric layers.

We can thus write down the following conditions of the refractive or focussing effect of the field:

$$\mu_1 = \frac{\sin\alpha}{\sin\beta} = \frac{v_1}{v_0} = \frac{\sqrt{V_1}}{\sqrt{V_0}},$$

$$\mu_2 = \frac{\sin\gamma}{\sin\delta} = \frac{\sqrt{V_2}}{\sqrt{V_1}},$$

$$\mu_3 = \frac{\sin\theta}{\sin\eta} = \frac{\sqrt{V_3}}{\sqrt{V_2}},$$

Fig. 12.

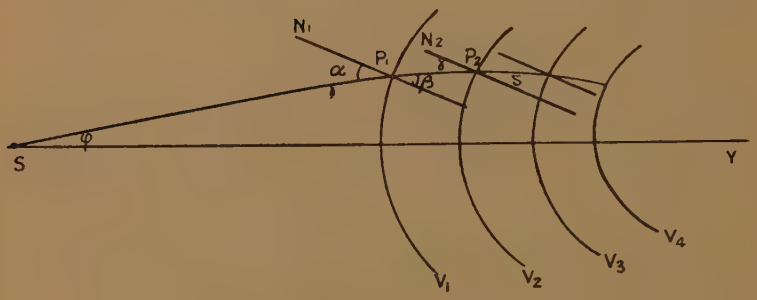

where V_1 and V_0 are the electron velocity in equivalent volts, and after the nth refraction

$$\mu_n = \frac{\sin\phi}{\sin\psi} = \frac{\sqrt{V_n}}{\sqrt{V_{n-1}}}.$$

If now the equipotentials are so drawn that $\mu_1 = \mu_2 = \mu_3 = \mu_n$,

$$\frac{\sin\alpha}{\sin\beta} = \frac{\sin\gamma}{\sin\delta} = \frac{\sin\phi}{\sin\psi},$$

i. e., that

$$\frac{\sqrt{V_1}}{\sqrt{V_0}} = \frac{\sqrt{V_2}}{\sqrt{V_1}} = \frac{\sqrt{V_3}}{\sqrt{V_2}} = K,$$

$$\therefore \quad \frac{V_1}{V_0} = K^2 = \frac{V_2}{V_1} = \frac{V_3}{V_2},$$

$$\therefore \quad V_1 = K^2 V_0,$$
$$V_2 = K^2 V_1 = K^4 V_0,$$
$$V_n = (K^2)^n V_0.$$

The value of the constant K is thus obtained from the values of V_0 and V_n, the initial and final values of the equipotential surfaces, and "n" the number of surfaces through which it is desired to trace the path. The graphical ray trace is then carried out as follows. The axial equipotential plot is first obtained by either of the methods outlined in section 2, and the "geometric plot" conditions stated above are picked off the curve. The radii of curvature are then calculated where necessary, and an enlarged copy of these equipotentials is drawn, assuming they are parts of spherical surfaces (an assumption justified in the circumstances, at least, for paraxial rays).

The following example, applicable to the present plot, will make this clear.

Since $V_n = (K^2)^n V_0$:

If we take $V_n = 3000$, the voltage on the H.T. lens element;

If we take $V_0 = 700$, the voltage of the L.T. last equipotential;

If we take $n = 30$, *i. e.*, working through 31 surfaces;

$$\therefore \quad 3000 = (K^2)^{30} \times 700;$$

$$\therefore \quad \log \left\{ \frac{3000}{700} \right\} = 30 \log K^2 = \log 4{\cdot}285 = 0{\cdot}632;$$

$$\therefore \quad \log K^2 = 0{\cdot}02106;$$

$$\therefore \quad K^2 = 1{\cdot}05;$$

$$\therefore \quad K = 1{\cdot}024 = \frac{\sin \alpha}{\sin \beta}.$$

Since
$$V_1 = K^2 V_0 = 1{\cdot}05 \times 700,$$
$$V_2 = K^2 V_1 = (1{\cdot}05)^2 \times 700,$$
$$V_3 = K^2 V_2 = (1{\cdot}05)^3 \times 700,$$

and proceeding in this way we get the whole series of equipotentials on the geometric plot. All the data required are given in Table V.

A point is now taken on the axis of this centred system, which represents the position of the electron source S,

Table V.

n.	$\log (K^2)^n$.	$(K^2)^n$.	$(K^2)^n V_0$.	Distance from H.T. electrode. (mm.).	$f'(V)$.	$f''(V)$.	$R=\frac{2f'(V)}{f''(V)}$.	
1	0·02106	1·05	735	89	− 5	+0·10	−100	
2	0·04212	1·102	771	79·5	− 7	+0·335	− 42	
3	0·06318	1·1157	809	73·5	− 9·5	+0·485	− 39	
4	0·08424	1·1214	850	70	−11	+0·56	− 39	
5	0·10530	1·27	889	67	−13	+0·615	− 42·2	
6	0·12636	1·338	937	64	−15	+0·655	− 45·7	
7	0·14742	1·404	983	61·5	−16·3	+0·675	− 48·3	
8	0·16848	1·474	1032	59	−18	+0·68	− 53	
9	0·18954	1·547	1083	56·3	−19·7	+0·68	− 58	
10	0·2160	1·62	1134	54	−21·5	+0·68	− 63	
11	0·23166	1·705	1193·5	51·5	−23·3	+0·68	− 68·5	
12	0·2527	1·79	1253	49	−25	+0·68	− 73·5	
13	0·2738	1·878	1314·6	46·5	−26·5	+0·68	− 77·8	
14	0·29484	1·972	1380·4	44·5	−28	+0·68	− 82·2	
15	0·3159	2·07	1449	42	−29·5	+0·68	− 86·8	
16	0·3369	2·17	1519	40	−31	+0·675	− 91·5	
17	0·35802	2·28	1596	37·5	−32·8	+0·66	− 99·4	
18	0·37908	2·394	1676	35·3	−34	+0·625	−108·5	
19	0·40014	2·51	1757	33	−35·5	+0·525	−135	
20	0·4212	2·638	1847	30·5	−36·7	+0·425	−173	
21	0·44226	2·769	1938	28	−37·7	+0·28	−269	
22	0·46332	2·906	2034	25·5	−38·2	+0·165	−462	
23	0·48438	3·05	2135	23	−38·4	+0·015	−5120	
24	0·50544	3·202	2241	20	−38	−0·15	+506	
25	0·5265	3·361	2353	17·5	−37·5	−0·29	+258	
26	0·54756	3·528	2470	14	−36·5	−0·4	+183	
27	0·56862	3·704	2593	10·5	−35	−0·412	+170	
28	0·5897	3·887	2721	6·7	−33·5*	−0·24*	+ 50	Measured.
29	0·6107	4·08	2856	3	....	....	+ 28·5	,,
30	0·6318	4·283	2998	0	....	....	+ 12	,,

* Doubtful.

and the initial direction of the electron bundle is then drawn to meet the first incident refracting equipotential layer at the point P_1 (fig. 13).

The normal at the point of incidence gives the angle of incidence α. The refracted ray due to the equipotential layer V_1 is drawn out by the neat method of Bloch*, which depends on a simple geometrical construction. A paper scale AB is divided at C, so that

$$\frac{BA}{BC} = \frac{\sin \alpha}{\sin \beta} = K \text{ (const.)} = 1{\cdot}024,$$

Fig. 13.

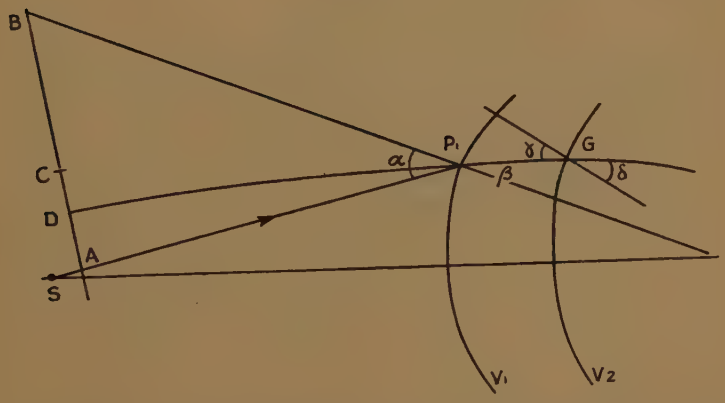

and is laid along the incident ray and the normal, so that when its extremities A and B are on these lines the perpendicular bisector of AC, *i.e.*, DP_1, passes through P_1 to G; P_1G is then the refracted ray at the surface V_1, and thus becomes the incident ray for the surface V_2. The same procedure is adopted at V_2, V_3 etc. in turn, giving an approximation to the focussing effect of the field on the ray. This method was carried out in the above case for a ray parallel to the axis and entering the system from the cathode end. The focal length found from the graphical trace was 108 mm., as against 123 mm. by calculation. The method is thus capable of giving a good approximation to the path.

Of course the paths between equipotentials are drawn in as straight lines, which is a reasonable approximation

* Journal Sc. Inst. xiii. no. 9, p. 302 (1936).

when K is quite small, *i. e.*, the equipotential surfaces are closely bunched together. For larger values of K it is possible to get a second approximation to the electron path between equipotential surfaces from the following considerations, which are based on simple geometry.

It must be remembered that in actual fact the electron traces a curved path in the field owing to the radial force which is always acting on the electron during its time of transit between the equipotentials.

In fig. 14 let KH be the axis, E the centre of curvature

Fig. 14.

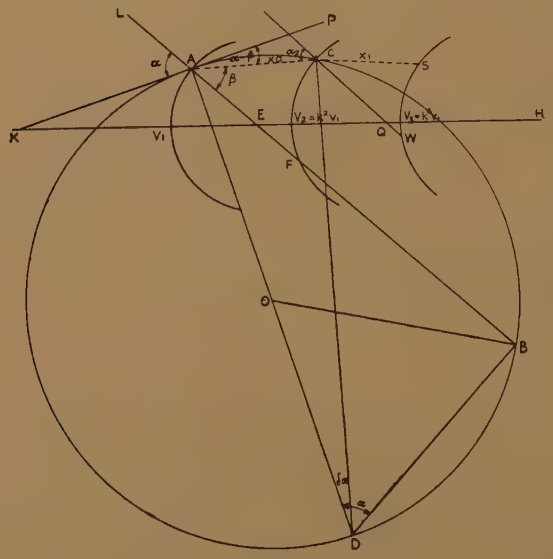

of equipotential V_1, and BFEAL be the normal to V_1 at A.

Let KAP be the incident ray, *i. e.*, $\widehat{LAK} = \alpha$.

Let AC be the refracted ray, *i. e.*, $\widehat{CAE} = \beta$.

The electron at A experiences a force tending to pull it in towards the normal LA. This force acts through the gradient $\frac{V_2 - V_1}{AF} = \frac{kV_1 - V_1}{AF}$ in the field in the direction $\rightarrow$ AE.

Average gradient in direction

$$A \rightarrow E = \frac{V_1(k-1)}{p}, \text{ where } AF = p. \quad . \quad . \quad (1)$$

Average force on electron = F = average gradient $\times e$

$$= \frac{V_1(k-1)}{p} . e. \quad . \quad . \quad . \quad . \quad . \quad . \quad (2)$$

This force can be resolved along and perpendicular to the electron path. The component along KAP simply speeds up the electron, and does not affect its subsequent path, while the component $\perp$ KAP in the direction

$$AD = \frac{V_1(k-1)}{p} . e . \sin \alpha. \quad . \quad . \quad (3)$$

This component causes the refraction to AC.

Since the electron is acted on by a force perpendicular to its motion, it can be taken to describe an arc of a circle (in the small interval between V_1 and V_2) of radius ρ and whose centre O lies in AD. The centre of this circle is found as follows:

$$\text{Centrifugal force } \frac{mv^2}{\rho} = \frac{V_1(k-1) . e . \sin \alpha}{p}, \quad . \quad . \quad . \quad (4)$$

$$\text{and since } \quad \tfrac{1}{2}mv^2 = V_1 e \quad \therefore \quad mv^2 = 2eV_1 ; \quad . \quad . \quad . \quad (5)$$

$$\therefore \quad \frac{2V_1 e}{\rho} = \frac{V_1(k-1) . e . \sin \alpha}{p} ; \quad . \quad . \quad . \quad (6)$$

$$\therefore \quad \frac{2p}{k-1} = \rho \sin \alpha = \rho . \frac{AB}{2\rho} ; \quad . \quad . \quad (7)$$

$$\therefore \quad \frac{4p}{k-1} = AB. \quad . \quad . \quad . \quad . \quad . \quad . \quad . \quad (8)$$

Now $AF = p$; $\therefore$ $AB = \frac{(4)}{(k-1)} \times AF$, and is thus known.

Hence, produce AE to B such that $AB = \frac{4}{k-1} . AF$. Draw BD $\perp$ AB to meet AD, which is $\perp$ initial direction KAP. This gives $AD = 2\rho$. Bisect AD at O, and describe the arc AC with O as centre. The latter is the better approximate electron path between equipotentials.

It will have been realized that it is not necessary to work with a fixed value of K, *i. e.*, with a fixed sliding

scale, through the whole field. In fact, by far the best procedure is to grade out the field, *i. e.*, work with different values of K, and thus with different sliding scales in different parts of the field, depending on how closely the equipotentials are spaced apart. A refinement for more accurate work when dealing with very closely spaced equipotentials, *i. e.*, with very small values of the angles of incidence and refraction, is as follows. Taking fig. 14, since KAP is a tangent to the path, and AC a chord,

$$< \mathrm{PAC} = \alpha - \beta = < \mathrm{ADC}.$$

Now, for small angles

$$\beta = \alpha - \delta\alpha; \quad \therefore \quad < \mathrm{ADC} = \delta\alpha.$$

Now
$$\frac{\mathrm{AC}}{\mathrm{AD}} \doteqdot \sin \delta\alpha \doteqdot \delta\alpha;$$

$$\therefore \quad \mathrm{AC} = x_0 = \mathrm{AD}.\delta\alpha = 2\rho_0\delta\alpha. \quad . \quad . \quad . \quad . \quad (9)$$

Similarly, for the next surface

$$\mathrm{CS} = x_1 = 2\rho_1\delta\alpha_1; \quad . \quad . \quad . \quad . \quad . \quad (10)$$

$$\therefore \quad \frac{x_0}{x_1} = \frac{\rho_0}{\rho_1} \cdot \frac{\delta\alpha_1}{\delta\alpha} \quad . \quad . \quad . \quad . \quad . \quad . \quad (11)$$

Since

$$\frac{\sin\alpha}{\sin(\alpha - \delta\alpha)} = k,$$

$$\sin\alpha = k\sin\alpha - k\cos\alpha.d\alpha;$$

$$\therefore \quad \frac{\sin\alpha}{\cos\alpha} = \frac{k}{k-1}.d\alpha = \tan\alpha;$$

$$\therefore \quad d\alpha = \frac{k-1}{k}.\tan\alpha \doteqdot \frac{k-1}{k}.\sin\alpha \quad . \quad . \quad (12)$$

when α is small;

$$\therefore \quad \frac{x_0}{x_1} = \frac{\rho_0}{\rho_1} \cdot \frac{\sin\alpha}{\sin\alpha_1} \quad . \quad . \quad . \quad . \quad . \quad . \quad (13)$$

From equation (7)

$$\rho_0 \sin\alpha = \frac{2p_0}{k-1} \quad \text{and} \quad \rho_1 \sin\alpha_1 = \frac{2p_1}{k-1},$$

where $p_1 = \mathrm{CW}$;

$$\therefore \quad \frac{x_0}{x_1} = \frac{p_0}{p_1} \quad . \quad . \quad . \quad . \quad . \quad . \quad . \quad (14)$$

Now x_0 is known ; p_0 and p_1 are known, hence x_1 can be calculated, so that by means of the compass the point S can be marked off on V_3 and the length and direction of the path between the close equipotentials V_2, V_3, V_4 etc. can be obtained in a similar way.

LI. *On the Equation to the Axial Potential Distribution in Electron Optical Systems.* *By* L. Jacob, *M.Sc.*, *A.R.C.Sc.I.* (Communication from the Staff of the Research Laboratories of The General Electric Company, Limited, Wembley, England) *.

[Received June 24, 1938.]

ATTEMPTS have been made from time to time to find an analytical solution to the field distribution in electron optical systems, but with no success. It is true that Picht † has worked out a particular solution for one special case, where the field is given by a simple expression of the form $A+Bz$, but such a simplification does not in itself correspond with what usually occurs in practice, and is hence not readily applicable. Generally, the field distribution between two equal coaxial right circular cylinders, separated by a gap, appears to be the simplest case amenable to analytical treatment, and the specialized case of an electron lens made up of such components with infinitely small separation can be solved analytically by means of a Fourier integral. Hansen and Webster ‡ have deduced the focal properties of such lens systems, in terms of simple algebraic equations involving the field distribution E and a factor γ defined as the ratio between the P.D. across the lens to the sum of the P.D.'s of its components. With symmetrical lenses, such, for instance, as the " Einzellinse " type, where the index of refraction is the same on both sides, they give the well-known optical formula in the form

$$\frac{1}{v}+\frac{1}{\mu}=\frac{1}{f}=\frac{3}{4}\gamma^2\int_{-\infty}^{+\infty}\mathrm{E}^2\,dz.$$

* Communicated by C. C. Paterson.
† *Ann. der Physik*, xv. p. 56 (1932).
‡ Rev. Sc. Inst. vii. p. 17 (Jan. 1936).

In the case of the "immersionlinse" type, where the index of refraction varies continuously through the lens, the formula becomes

$$\frac{1+\gamma}{\mu}+\frac{1-\gamma}{v}=3\gamma^2\int_{-\infty}^{+\infty}\mathrm{E}^2\,dz,$$

and defines the focal properties of the lens.

To make use of these formulæ all that is required is the value of E. This can be obtained from a plot of the field as outlined in the previous paper. This, however, is not absolutely essential, since an empirical relationship obtained from a number of field-plots with different values of ρ, the ratio of gap-width to diameter, has been worked out by Kirkpatrick and Beckerley*, who found that a good approximation to the distribution for values of ρ up to 1·75 is given by

$$\mathrm{V}_z=\mathrm{V}_0+\Delta\mathrm{V}/b\int_0^z e^{-(\pi/b^2)z^2}\,dz,$$

where

V_0=potential at middle of the gap.

V=potential across the gap.

b=experimental parameter proportional to the slope of the curve at $(o,\ \mathrm{V}_0)$, and given by $b=2\mathrm{R}\,(0{\cdot}73+0{\cdot}53\,\rho^2)$.

The integral $\int_{-\infty}^{+\infty}\mathrm{E}^2\,dz$ is then given in terms of R and ρ by the expression

$$\frac{1}{\mathrm{R}(2{\cdot}06+1{\cdot}50\rho^2)},$$

which involves only R and ρ, both of which can be varied at will. Thus, in the case of coaxial cylindrical electron-lens components, the cardinal points of any lens system can be readily calculated from the dimensions of the system, subject to the limitation as regards the value of the ratio ρ. This simplification is very helpful in design of multisection X-ray or positive-ray tubes, where such forms of lenses are extensively employed.

In the case of cathode-ray tubes, the electron-lens, although still of simple geometry, usually involves a much more complicated form of field function, which so far has not been expressible in terms of simple parameters

* Rev. Sc. Inst. vii. p. 24 (Jan. 1936).

of the system. For purposes of strict analysis it is necessary, as a first step, to obtain a very accurate field plot from which the first and higher derivatives are obtained, and these are then used as outlined in a section of the previous paper for evaluating the whole field.

Both radial and longitudinal gradients are readily calculable, and the electron motion can be rigidly calculated through the field. In order to extend the accuracy where derivatives higher than the second are called for, it has been found possible to obtain the actual equation to the axial equipotential plot in terms of Z, the distance along the axis from some fixed origin, to an accuracy as great as we please, by the following method. This is based on the use of Legendre polynomials for obtaining an approximation to the equation of a complicated function, and has been used by Seynsche and Walther * with much success.

The function $f(Z)$ is represented through the interval from $Z=a$ to $Z=b$ by a polynomial of the nth degree, $\phi(Z)$, so that the mean least square error,

$$\frac{1}{b-a}\int_a^b \{f(z)-\phi(z)\}^2\,dz,$$

is a minimum. In order to fulfil this condition practically, the interval is taken from $a=-1$ to $b=+1$, and the function $\phi(Z)$ is set in the form

$$\phi(Z)=C_0P_0(Z)+C_1P_1(Z)+C_2P_2(Z)+C_nP_n(Z),$$

where

$$P_n(Z)=\frac{1}{2^n\lfloor n}\cdot\frac{d^n(Z^2-1)^n}{dZ^n}.$$

Thus

$$P_0(Z)=1,$$

$$P_1(Z)=Z.$$

$$P_2(Z)=\frac{3}{2}Z^2-\frac{1}{2},$$

$$P_3(Z)=\frac{5}{2}Z^3-\frac{3}{2}Z,$$

$$P_4(Z)=\frac{35}{8}Z^4-\frac{15}{4}Z^2+\frac{3}{8}.$$

* *Acta Mathematica*, 57 ; i.–ii. p. 77 (1931).

$$P_5(Z)=\frac{63}{8}Z^5-\frac{35}{4}Z^3+\frac{15}{8}Z,$$

$$P_6(Z)=\frac{231Z^6-315Z^4+105Z^2-5}{16},$$

$$P_7(Z)=\frac{429Z^7-693Z^5+315Z^3-35Z}{16},$$

etc., etc.

The coefficients C_0, C_1, C_2 . . . . C_n are then given by the simple formula

$$C_V=\frac{2V+1}{2}\int_{-1}^{+1}f(Z)P_V(Z)\,dZ \quad (V=0,\ 1,\ 2\ .\ .\ .\ .\ n).$$

To apply this method in the present case it is necessary to divide the base-line (Z-axis) of the axial equipotential plot into small intervals, starting, say, at the high-potential end and calling it (-1), and then working towards the middle of the base (0), and finally towards the low-voltage end, which is now $(+1)$. The values of $P_1(Z)$, $P_2(Z)$, $P_3(Z)$, etc., are then calculated for each value of the interval Z, and the products, $f(Z)P_1(Z)$, $f(Z)P_2(Z)$, $f(Z)P_3(Z)$, etc., are further calculated, where $f(Z)$ is the ordinate (volts) for each interval.

The integral $\int_{-1}^{+1}f(Z)\,P_n(Z)$ is then obtained, using Simpson's rule over the whole interval from -1 to $+1$.

Where the slope of the curve is critical, and greater accuracy is required, the integration can be carried out over several stages of small intervals within the main interval. The following table will make this clear. The values of $f(Z)$ are taken from the equipotential plot of fig. 6 (previous paper).

The evaluation of the constants C_0, C_1, C_2, C_3, etc., is then carried out as follows, using Simpson's rule, *i. e.*,

$$\text{Area}=\frac{\text{interval}}{3}[\text{First}+\text{last ordinate}+4\Sigma\text{even}+2\Sigma\text{odd}].$$

To evaluate C_1 we have

$$\int_{-1}^{+1}P_1(Z)f(Z)\,dZ$$

$$=\frac{0{\cdot}1}{3}[-2950+700+4(-2466-1610-902{\cdot}5$$

$$-420-108+86+228+360+497$$
$$+634)+2(-2000-1242-644-244$$
$$+0+160+296+429+564)]$$
$$=\frac{0\cdot1}{3}[-2250-14806-5362]=-747\cdot266\,;$$

$$\therefore\quad C_1=\frac{3}{2}(-747\cdot266)=\underline{-1120\cdot899.}$$

Again, taking the evaluation of C_4,

$$\int_{-1}^{+1}P_4(Z)f(Z)dZ=\int_{-1}^{-0\cdot8}P_4(Z)f(Z)\,dZ$$
$$(a)$$
$$+\int_{-0\cdot8}^{+0\cdot8}P_4(Z)f(Z)\,dZ+\int_{+0\cdot8}^{+1}P_4(Z)f(Z)\,dZ.$$
$$(b)\qquad\qquad(c)$$

$$(a)\ =\frac{0\cdot02}{3}[2950-582\cdot5+4(2345\cdot69+1343\cdot53+569\cdot75$$
$$-14\cdot149-432\cdot96)$$
$$+2(1815\cdot78+936\cdot94+253\cdot71-242\cdot24)]$$
$$=\frac{1}{3\times50}\times23143\cdot32.$$

$$(b)\ =\frac{0\cdot05}{3}[-582\cdot5-164\cdot5+4(-843\cdot56-929\cdot49-692\cdot79$$
$$-348\cdot32-28\cdot16+205\cdot13+339\cdot62+376\cdot87$$
$$+332\cdot7+241\cdot54+123\cdot08-13\cdot93-149\cdot57$$
$$-258\cdot45-306\cdot26-248\cdot52)$$
$$+2(-947\cdot74-844\cdot56-521\cdot79-181\cdot93$$
$$+102\cdot11+283\cdot04+364\cdot97+361\cdot88+290\cdot63$$
$$+185\cdot6+55\cdot43-83\cdot62-208\cdot12-291\cdot72$$
$$-292\cdot56)]$$
$$=\frac{1}{3\times20}\times-13003\cdot06.$$

$$(c)\ =\frac{0\cdot02}{1}[-164\cdot5+700+4(-118\cdot94-3\cdot75+145\cdot97$$
$$+334\cdot57+566\cdot2)$$
$$+2\,(-65\cdot154+66\cdot46+235\cdot32+444\,74)]$$

Table.

Z.	$f(Z)$.	$P_1(Z)$.	$P_2(Z)$.	$P_3(Z)$.	$P_4(Z)$.	$f(Z)P_1(Z)$.	$f(Z)P_2(Z)$.	$f(Z)P_3(Z)$.	$f(Z)P_4(Z)$.
−1	2950	−1	+1	−1	+1	−2950	+2950	−2950	+2950
−0·98	2900	..	..	..	0·808860	..	..	..	2345·694
−0·96	2860	..	..	..	0·634890	..	..	..	1815·78
−0·95	2830	..	0·85375	−0·718437	0·554094	..	2416·1125	−2033·2	
−0·94	2815	..	..	..	0·477276	..	..	..	1343·53
−0·92	2795	..	..	..	0·335219	..	..	..	936·94
−0·90	2740	−0·9	0·715	−0·4725	0·207937	−2466	1959·1	−1294·65	569·75
−0·88	2680	..	..	..	0·094667	..	..	..	253·71
−0·86	2650	..	..	..	−0·0053393	..	..	..	−14·149
−0·85	2640	..	0·58375	−0·260312	−0·0505927	..	1541·1	−687·22	
−0·84	2610	..	..	..	−0·0928128	..	..	..	−242·24
−0·82	2570	..	..	..	−0·168467	..	..	..	−432·96
−0·80	2500	−0·8	0·460	−0·0800	−0·233000	−2000	1150	−200	−582·50
−0·75	2410	..	0·34375	+0·070313	−0·350023	..	828·43	169·45	−843·56
−0·70	2300	−0·7	0·2350	+0·1925	−0·412063	−1610	540·5	442·75	−947·74
−0·65	2170	..	0·13375	0·288438	−0·428335	..	290·23	625·91	−929·49
−0·60	2070	−0·6	0·04	0·3600	−0·4080	−1242	82·8	745·20	−844·56
−0·55	1930	..	−0·04625	0·409063	−0·358960	..	−89·263	789·49	−692·79
−0·50	1805	−0·5	−0·125	0·4375	−0·289062	−902·5	−225·625	789·69	−521·76
−0·45	1700	..	−0·19625	0·447188	−0·204897	..	−333·62	760·22	−348·32
−0·40	1610	−0·4	−0·260	0·44	−0·11300	−644	−418·60	708·40	−181·93
−0·35	1510	..	−0·31625	0·41782	−0·0186476	..	−477·53	630·90	−28·158
−0·30	1400	−0·3	−0·365	0·3825	+0·0729375	−420	−511	535·50	102·11
−0·25	1300	..	−0·40625	0·335938	+0·157789	..	−528·13	436·72	205·13
−0·20	1220	−0·2	−0·44	0·28	+0·232	−244	−536·8	341·6	283·04
−0·15	1160	..	−0·46625	0·216562	+0·292778	..	−540·85	251·21	339·62
−0·1	1080	−0·10	−0·485	0·1475	0·337937	−108	−523·8	159·3	364·97
−0·05	1030	..	−0·49625	0·074687	0·365898	..	−511·14	76·93	376·87

0	965	0	−0·5	0	0·375	0	−482·5	0	361·88
+0·05	910	..	−0·49625	−0·074687	+0·365898	..	−451·59	−67·97	332·97
+0·10	860	0·1	−0·485	−0·1475	+0·337937	86	−417·1	−126·85	290·63
+0·15	825	..	−0·46625	−0·216562	0·292778	..	−384·66	−178·66	241·54
+0·20	800	0·2	−0·44	−0·28	0·232	160	−352·0	−224	185·6
+0·25	780	..	−0·40625	−0·335938	0·157789	..	−316·88	−262·03	123·08
0·30	760	0·3	−0·365	−0·3825	0·0729375	228	−277·4	−290·70	55·433
0·35	747	..	−0·31625	−0·417812	−0·0186476	..	−236·24	−312·11	−13·93
0·40	740	0·4	−0·260	−0·44	−0·113	296	−192·4	−325·6	−83·62
0·45	730	..	−0·19625	−0·447188	−0·204897	..	−143·26	−326·45	−149·57
0·50	720	0·5	−0·125	−0·4375	−0·289062	360	−90	−315·0	−208·12
0·55	720	..	−0·04625	−0·409063	−0·35896	..	−33·3	−294·52	−258·45
0·60	715	0·6	+0·04	−0·36	−0·408	429	28·6	−257·4	−291·72
0·65	715	..	0·13375	−0·288438	−0·428335	..	95·631	−206·23	−306·26
0·70	710	0·7	0·235	−0·1925	−0·412063	497	166·85	−136·68	−292·56
0·75	710	..	0·34375	−0·070313	−0·350023	..	244·06	−49·92	−248·52
0·80	706	0·8	0·46	0·08	−0·233	564	324·76	56·48	−164·5
0·82	706	..	..	..	−0·168467	..	..	..	−118·94
0·84	702	..	..	..	−0·0928128	..	..	..	−65·154
0·85	702	0·85	0·58375	0·260312	−0·0505927	..	409·79	182·74	..
0·86	702	..	..	..	−0·053393	..	..	..	−3·748
0·88	702	..	..	..	0·094667	..	..	..	66·456
0·90	702	0·9	0·715	0·4725	0·207937	634	501·93	331·7	145·97
0·92	702	..	..	..	0·335219	..	..	..	235·323
0·94	701	..	..	..	0·477276	..	..	..	334·57
0·95	701	..	0·85375	0·718437	0·554094	..	598·478	503·62	..
0·96	700·5	..	..	..	0·63489	..	..	..	444·74
0·98	700	..	..	..	0·80886	..	..	..	566·2
+1	700	1·0	+1	+1	+1	700	700	700	700

$$= \frac{1}{3 \times 50} \times 5594{\cdot}44\,;$$

$$\therefore \quad C_4 = \frac{9}{2} \times -25{\cdot}132 = -113{\cdot}094.$$

In a similar way the values of

$$\int_{-1}^{+1} P_5(Z\ f(Z)\,dZ, \quad \int_{-1}^{+1} P_6(Z) f(Z)\,dZ, \quad \int_{-1}^{+1} P_7(Z) f(Z)\,dZ,$$

give the coefficients C_5, C_6, C_7.

The values obtained were as follows :—

$$\left.\begin{aligned} C_0 &= \ \ 1310{\cdot}5\ , \\ C_1 &= -1120{\cdot}90, \\ C_2 &= \ \ 608{\cdot}93, \\ C_3 &= \ \ -19{\cdot}53, \\ C_4 &= -113{\cdot}09, \\ C_5 &= \ \ 21{\cdot}62, \\ C_6 &= \ \ -3{\cdot}94, \\ C_7 &= \ \ 14{\cdot}7\ . \end{aligned}\right\}$$

Substituting these values, as well as the functions $P_0(Z)$, $P_1(Z)$, $P_2(Z)$, etc., in

$$\phi(Z) = C_0P_0(Z) + C_1P_1(Z) + C_2P_2(Z) + C_3P_3(Z) + \ldots\ ,$$

we get the resulting equation :

$$\phi(Z) = 964{\cdot}86 - 1083{\cdot}23Z + 1311{\cdot}64Z^2 + 51{\cdot}44Z^3 - 416{\cdot}86Z^4 - 466{\cdot}47Z^5 - 56{\cdot}87Z^6 + 394{\cdot}14Z^7.$$

This, then, is the equation of the axial equipotential plot when the origin is at the middle of the base, *i. e.*, at $f(Z) = 965$.

Substitution of $Z = \pm 1$ gives a value for $f(Z)$ which is 0·2 and 1 per cent. too low at the ends when compared with the experimental plot.

To transform this equation for values of Z in cm., we must divide Z by 6·25, which represents one unit (positive or negative) where Z is now in cms. measured from the point $Z = 0$, $\phi(Z) = 965$ to right or left, *i. e.*, half-way along the Z-axis of the potential distribution curve. Further, to transfer these coordinates to the low-voltage end of the field, the new value of Z must be $(6{\cdot}25 + Z)$.

where Z is now measured in the negative direction, *i. e.*, from the low-voltage end to the high-voltage end, so that, in order to get $f(Z)$, the negative value of Z must be substituted in the above formula. We thus get

$$y=\phi(Z)=965-1083{\cdot}23\left\{\frac{6{\cdot}25+Z}{6{\cdot}25}\right\}+1311{\cdot}64\left\{\frac{6{\cdot}25+Z}{6{\cdot}25}\right\}^2$$
$$+51{\cdot}44\left\{\frac{6{\cdot}25+Z}{6{\cdot}25}\right\}^3-416{\cdot}86\left\{\frac{6{\cdot}25+Z}{6{\cdot}25}\right\}^4$$
$$-466{\cdot}47\left\{\frac{6{\cdot}25+Z)}{6{\cdot}25}\right\}^5-56{\cdot}87\left\{\frac{6{\cdot}25+Z}{6{\cdot}25}\right\}^6$$
$$+394{\cdot}14\left\{\frac{6{\cdot}25+Z}{6{\cdot}25}\right\}^7.$$

Thus, taking the 700-volt equipotential where it cuts the Z-axis as the new origin, the equation to the axial potential plot is given by

$$y=\phi(Z)=698{\cdot}65+17{\cdot}974Z+44{\cdot}134Z^2+26{\cdot}11936Z^3$$
$$+6{\cdot}679851Z^4+0{\cdot}78320805Z^5+0{\cdot}0453339Z^6$$
$$+0{\cdot}00105801151Z^7.$$

This equation gives an accuracy to within 1 per cent.

LII. *Note on Velocity of Sound in Copper.* *By* G. E. Allan, *D.Sc., Applied Physics Department, Glasgow University* *.

[Received July 1, 1938.]

DURING the measurement of the velocity of sound in some zinc-copper rods, it was found desirable to know the velocity of sound in pure copper. On referring to books of tables of recent date for this information, the values quoted varied very considerably among themselves, namely, from 3553 to 3984 metres per second (see table).

On consulting the original papers the following facts were noted. In every case the velocity in the metal was expressed as a multiple of the velocity in air. Chladni [1] used as a standard an open organ-pipe of pitch Ut 3 (C 256), and his copper rod gave a note which was nearly

* Communicated by the Author.

Sol 6 (G 3072), *i. e.*, a note nearly twelve times the frequency of Ut 3. Wertheim [2] used a copper rod of density 8·729, which contained 0·38 Ag and 0·80 Fe. Its content of copper could not therefore be more than 98·82 per cent. Masson [3] described three methods by which he obtained pure copper. The metal was drawn into wires, as he was convinced that the velocity in rods of a given diameter increased with the length of the rod. His wires had a length of 1·5 metres, and their diameters lay between 0·9 and 0·1 mm. Kundt [4] showed that his now classical dust-figure method was adapted for finding the velocity

V (metre/sec.).	Observer.	Date.
3984.....	Chladni.	1802.
3553 }	Wertheim.	1844.
3666 }		
3825.....	Masson.	1858.
3971.....	Kundt.	1866.

ratio, and he gave values of this ratio for brass, steel, glass and copper. In the last case a copper rod little more than a foot long was used, and few details are given, so that Kundt probably regarded his result for copper simply as an example of his method rather than as a standard determination.

Stone, in his text-book on sound [5], gives the value 3716 metres per second for the velocity of sound in copper, but does not state any authority.

Meantime, the processes for the extraction and manufacture of copper have been improved ; the purity of the product has been enhanced, and the elastic properties of this purer product have been investigated, so that the velocity of sound might be deduced from the elastic constants [6]. It is a matter of some interest, however, to make a direct determination of the velocity of sound in the metal.

The Material.

A cylindrical rod of copper was obtained which was guaranteed to contain 99·9 per cent. of copper. Its ends were squared, and its dimensions measured, as below :—

Length	182·97 cm.
Diameter	0·958 cm.
Weight	1175·1 gm.

The diameter was found from a number of readings with a screw-gauge, and the density of the rod from the above data was 8·91 gm./cc. Later, two short lengths were cut off and weighed in air and water, and the resulting density was 8·928 gm./cc.

Method of Measuring the Frequency.

The frequency of the note given by the rod when fixed at the middle and caused to vibrate longitudinally was determined by the monochord. The method was described some years ago [7], and is shortly as follows.

The monochord wire is tuned in unison with the fundamental tone of the rod when the end of the rod is struck with a hammer. The length of the wire is measured accurately, and the Taylor frequency is calculated in the usual way, from the tension T, and the linear density ρ_1 of the wire under the given tension. Then a correction δn is added to the Taylor frequency. It is found from

$$\log \delta n = 3{\cdot}274 + 2{\cdot}391 \log n + 2{\cdot}070 \log \rho_1 - 1{\cdot}366 \log \mathrm{T}. \quad (1)$$

If the same size of wire is always used under the same tension, the equation may be reduced to the much simpler form,

$$\log \delta n = \mathrm{A} + 2{\cdot}391 \log n, \quad \ldots \quad (2$$

where A may be calculated by substituting known values of T and ρ_1 in equation (1). Having calculated A, its value may be inserted in equation (2), and δn found for a series of convenient values of n, e. g., 200, 300, ... 2000. A graph of δn and n can then be drawn from which δn may be read off for any assigned value of n. The corrected frequency is

$$\mathrm{N} = n + \delta n.$$

Frequency of the Copper Rod.

The above method was employed in determining the frequencies of the copper rod. The fundamental frequency was measured three times, each being the result of six independent settings of the monochord. The values found were 1049·7, 1051·3, and 1051·1. Mean frequency, 1050·7 at 17·3° C.

Velocity of Sound in Copper.

The velocity is found from $V=2lN$, where l is the length of the rod. Pierce has shown [8] that no "end correction" is necessary, and that the above formula is applicable as it stands.

Hence

$$V=2\times 182{\cdot}97\times 1050{\cdot}7=384500 \text{ cm./sec.},$$

or 3845 metres per second.

After short lengths had been cut from the rod, with which to measure the density, the new length of the rod was 169·03 cm. Five tests of the frequency gave the values 1138·1, 1140·0, 1138·1, 1139·3, and 1135·0, of which the average is 1138·1 at 14·6° C.

This gives the velocity 3847 metres per second, which is in good agreement with the first measurement. The mean, 3846 m./sec. agrees best with the value given by Masson.

Condition of the Material.

The copper rod as tested was in the "work-hardened" condition. The copper, after deposition by electrolysis, had been remelted, cast, drawn into rod form, and rolled. It was necessary, therefore, to find the effect of annealing the rod.

Annealing the Copper.

The rod was encased in a glass tube to retard oxidation, and heated in an electric furnace at an average temperature of 330° C. for nearly six hours. Later the heating was repeated, but without further change in the frequency of the rod.

Effect of Annealing on Frequency.

The frequency measurements after the first period of heating were 1102·5, 1104·3, 1108·4, and 1099·6, of which the mean is 1103·7. After the second annealing the frequencies were 1106·6, 1102·3, 1099·8, and 1103·5, of which the mean is 1103·1. Hence the velocity of sound in annealed copper is

$$V=2\times 1103{\cdot}4\times 169{\cdot}03$$

$$=3730 \text{ metres per second.}$$

There was a thin coating of scale on the rod as the result of heating. This was removed before measuring the frequency. The result for annealed copper thus conforms most nearly with the value given by Stone. The effect of the hardening processes is in this case to increase the velocity of sound by 3 per cent.

Effect of Temperature on Velocity.

Wertheim's values for the effect of temperature on the velocity of sound in copper are quoted in books of reference. These are :

Temp.	Velocity.
20° C.	3560 m./s.
100°	3290
200°	2950

These figures give a decrease of velocity of over 3 metres per second per degree. No effect of this magnitude was perceptible in the copper rod.

Pierce's Measurements.

Pierce in his investigation on the effect of temperature on frequency, velocity and Young's modulus by a magneto-strictive method has shown that if a is the coefficient of linear expansion of the metal, g the temperature coefficient of frequency, and h the temperature coefficient of velocity, where $a=\delta l/l\delta\theta$, $g=\delta N/N\delta\theta$, and $h=\delta V/V\delta\theta$, then $h=g+a$, where h and g are generally negative and a book value for a is sufficiently accurate. Pierce determined the values of h and g for a large number of magnetostrictive metals, including alloys.

Effect of Temperature on Velocity in Copper Rod.

A preliminary test of the copper rod when enclosed in steam-jackets showed that there was a very small but perceptible decrease in its frequency when the rod was raised to 100° C. The rod was in its original work-hardened condition. In spite of the smallness of the change to be measured, an attempt was made to obtain the approximate value of the temperature coefficient of frequency g. The rod, clamped at the middle, had its two halves surrounded by steam-jackets through which steam passed from the middle to the ends for about three-quarters of an hour. The high conductivity of the rod

was relied on to ensure a uniform temperature along the rod.

Five determinations of the frequency of the rod in the steam-jackets gave : 1124·6, 1130·7, 1123·9, 1125·2, and 1126·3. The mean frequency at 100° C. is 1126·3, and the drop in frequency from 1138·1 is 11·8, corresponding to a fall in pitch somewhat less than a comma. The above figures give

$$g = -11{\cdot}8/1138 \times 85{\cdot}4 = -0{\cdot}00011,$$

which is about one-tenth of the value found from Wertheim's figures. The note of the rod was not so clear as that given by it at 14·6° C., and was difficult to determine with accuracy.

Temperature Coefficient of Velocity.

Assuming the above value for g, we get $h = -0{\cdot}00009$, from which it may be calculated that the speed of sound in work-hardened copper at 0° C. is about 3852 metre/sec., and at 100° C. about 3815 metre/sec.

Velocity from $\sqrt{E/d}$.

A test of the work-hardened rod to measure its Young's modulus by bending gave, as the mean of six readings, $1{\cdot}325 \times 10^{12}$ dynes/cm.^{2}, or $19{\cdot}21 \times 10^6$ lb./inch^2. From this, V is 3852 metre/sec. at room-temperature, which is in fair agreement with the results of the sound experiments.

The copper rod was provided by Messrs. Imperial Chemical Industries (Metals), Ltd., to whom I wish to express my thanks.

Literature.

(1) E. E. F. Chladni, ' Die Akustik,' Berlin (1802), and ' Traité d'Acoustique,' Paris (1809).
(2) G. Wertheim, *Ann. de chim. et de phys.* xii. pp. 385–454, 581–610, and 610–624 (1844).
(3) A. Masson, *Ann. de chim. et de phys.* 3 ser. liii. pp. 257–293 (1858).
(4) A. Kundt, *Ann. d. Phys.* cxxvii. pp. 497–523 (1866).
(5) Dr. W. H. Stone, ' Elementary Lessons on Sound.' London, Macmillan & Co., 1879.
(6) ' Copper Data.' Engineers' Note Book Series. Copper Development Association.
(7) Phil. Mag. iv. pp. 1324–1337 (Dec. 1927).
(8) G. W. Pierce, Am. Acad. Arts and Sciences, lxiii. pp. 1–48 (May 1927 to May 1928).

LIII. *Notices respecting New Books.*

An Introduction to Riemannian Geometry and the Tensor Calculus. By C. E. Weatherburn. [Pp. 191.] (Cambridge University Press. Price 12*s.* 6*d.*)

THIS is an elementary book on Riemannian geometry which can be read easily by anyone who is familiar with the fundamental ideas of the differential geometry of curves and surfaces in ordinary Euclidean space. It may be regarded as a sequel to (though it may be read independently of) the author's well-known volumes on differential geometry.

The essence of the book is to take these fundamental ideas and to show how they are affected when a Euclidean metric is replaced by a Riemannian one ; and also to note how a desire to carry over certain principles of generally accepted value demands appropriate generalizations of some definitions. Since the tensor calculus plays a basic rôle in the formulation of the theory, the opportunity is taken to teach the reader the technique of that.

The first chapter runs through a number of familiar pieces of algebra which are going to be used later, and shows how the results may be expressed concisely by means of the summation convention. Then follows a chapter on co-ordinates, vectors, and tensors, in which the ideas of covariance and contravariance are brought out. Having now created a tool in the tensor calculus, it becomes possible to begin with the discussion of a Riemannian metric. Then a pause has to be made while the Christoffel symbols and covariant differentiation are introduced. The next chapters deal with the curvature of a curve, geodesics, and parallelism of vectors ; congruences and orthogonal ennuples. Riemann's symbols and the curvature of a Riemann space come next. The last three chapters are concerned with hypersurfaces in general, hypersurfaces in a Euclidean space, spaces of constant curvature, and subspaces of a Riemannian space.

There follow a short but valuable historical note on the growth of the theory of differential geometry, and a bibliography of the principal writings which have appeared on the subject. And at the end of each chapter is a useful collection of examples.

The chief thing about the book which struck the reviewer was the contrast in style with that of, say, a modern analyst. This is, of course, largely unavoidable on account of the nature of the subject, and it reflects a tradition which still

lingers among some geometers of assuming that the conditions of validity of certain statements need not be stated explicitly. It is true that these conditions are often obvious enough, but they should be set down clearly at some stage. For example, it might break some analyst's heart to find himself reading about functions whose nature has never been fully defined ; and it would be easy to choose functions which do not satisfy the conditions required on various occasions in this book. Again, whether the reader will clearly understand what is meant by a space V_n or by a Riemannian space will depend on how far he rewords the definitions for himself. For the first chapter or so the reader may well scratch his pate to know whether a given occasion is going to demand a superscript or a suffix attached to a variable ; until he comes across co- and contra-variance only revelation will make him appreciate the author's apparent vagaries. And there seem even to be times to use a Σ; a little research is needed to recognize them. Truly these are details, but they deserve attention because they are typical of a large class of text-books which hurry over the beginnings of things in order to reach results. Surely the foundation is as important as the superstructure.

Another point is the number of times a theorem is stated but not proved, or else is stated but only the necessity or sufficiency of a condition proved. In these cases references are always made to some book like Eisenhart's. Yet readers might appreciate and learn from either an outline of the proof or a statement about the corresponding problem in ordinary space, or at least some explanation of the difficulties involved.

However, the author has certainly contrived a course which gets the reader over the ground and lets him see what Riemannian geometry is about. The book may be strongly recommended to anyone who would begin a study of the subject either for its own sake or in connexion with the theory of relativity. The Cambridge printing is similar to that in the other books by the author ; it is clear, and somehow even the mass of suffixes can be tolerated.

[*The Editors do not hold themselves responsible for the views expressed by their correspondents.*]

FIG. 2.

FIG. 3.

(a)

(b)

(c)

Microphotometer traces and photographic enlargements of diffraction patterns of two adjacent narrow slit sources: fig. 2 for an aperture of width 0·91 b, where b is the critical Rayleigh width; fig. 3 for an aperture of width 0·79 b.

A.

B.

Fig. 7.

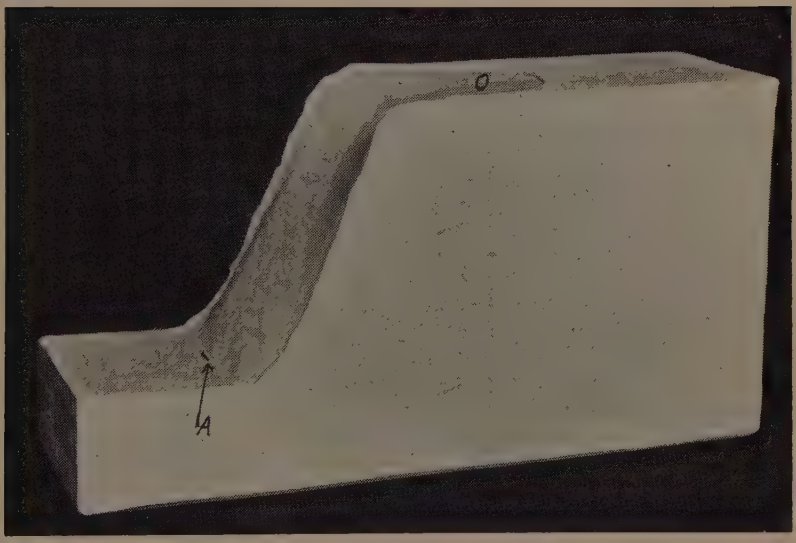

Three-dimensional model of electrostatic field of electron lens.

THE

LONDON, EDINBURGH, AND DUBLIN

PHILOSOPHICAL MAGAZINE

AND

JOURNAL OF SCIENCE.

[SEVENTH SERIES.]

NOVEMBER 1938.

LIV. *The Relations between the Energy Theorems applicable in Structural Theory.*

By D. WILLIAMS, *D.Sc., A.M.I.Mech.E.**

[Received July 21, 1938.]

Summary.

THE purpose of this article is to set out the relationships linking the various energy theorems applicable to structural problems, and to comment on their respective uses and limitations. Certain relevant proofs that may be of interest are added in an appendix.

§ 1. *Introduction.*

ON account of the increasing complexity of the structural problems that aeronautical engineers are called upon to solve, the use of energy methods, in virtue of their power and ease of application, is becoming increasingly important. Such methods cannot be fully exploited without a clear understanding of the limitations and interdependence of the various theorems upon which the methods are based; and the purpose of this report is to trace the relations linking these

* Communicated by D. R. Pye, C.B., M.A., Sc.D., F.R.S.

theorems and to indicate their several limitations as applied to practical problems. With the possible exception of the identification of the Principle of Maximum Strain Energy with that of Minimum Potential Energy, and the alternative interpretation given to Castigliano's [1] Proposition II, none of the results is claimed to be new, the object aimed at being rather to bring well-established results into a fresh perspective.

Before dealing in detail with the various theorems, it may be useful to list them here and also to indicate their place in the argument of this article. In the order in which they are later discussed the theorems (which for convenience are fully defined in the appendix) are

(A) Theorem of Virtual Work.

(B) Theorem of Minimum Potential Energy.

(C) Castigliano's [1] Theorem of the Differential Coefficients of the Internal Work—Parts I. and II. *

(D) Castigliano's [1] Theorem of Least Work. (Called by Southwell [6] "The Second Theorem of Minimum Strain Energy").

(E) Statical analogue of Bertrand's [2], [3], [4]. Theorem in Dynamics, alternatively, the Theorem of Maximum Strain Energy.

(F) Statical analogue of Kelvin's [2], [3], [4] Theorem in Dynamics (called by Southwell [6] "The First Theorem of Minimum Strain Energy").

It is shown that Theorems (A), (B) and Part I. of (C) are in their application to structural problems fundamentally identical, and capable of general application in that they are true whatever the law connecting load and deformation may be. Part II. of (C) is based on Part I. and on the assumption that the total strain energy is equal to half the sum of the products of the external forces and their respective displacements. As the latter assumption is only valid for structures that obey Hooke's Law, Part II. of (C) is only true when that law is satisfied.

Theorem (D) is deducible directly from Part II. of (C), and is therefore subject to the same limitation. In this way Theorems (B) and (D) may be regarded as the first

* Part II. is identical with what Pippard [7] and most other writers call "The First Theorem of Castigliano."

and last links in a chain of interrelated theorems. At this stage in the argument the two Theorems (B) and (D) are directly compared, and the essential features that distinguish the one from the other are analysed. Their relative usefulness in the solution of structural problems is also discussed.

Theorems (E) and (F) are next considered and the relevant proofs are included in the appendix, chiefly because they appear never to be given fully except in their dynamical form. The validity of both theorems is dependent on the operation of Hooke's Law. Theorem (E) is next enunciated in a new form, and so shown (in the appendix) to be directly related to Theorem (B), in fact to be merely a particular case of that theorem. The physical connection between Theorems (E) and (F) is then explained and their relative usefulness discussed.

Diagrammatically we may indicate the relations between the various theorems as follows (fig. 1):—

Fig. 1.

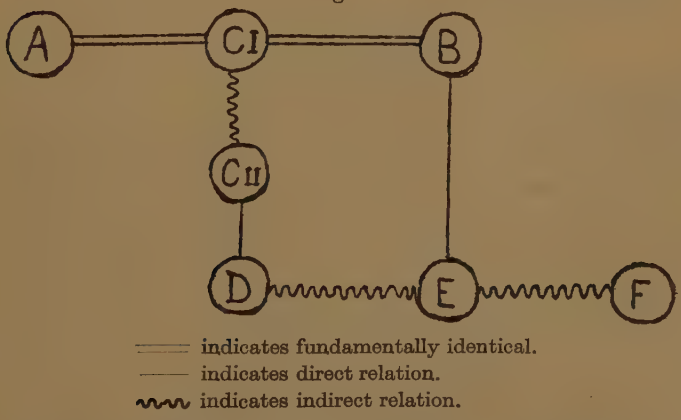

On this diagram the route followed by Castigliano was (A)—(CI)—(CII)—(D). Lamb discussed the relation between (E) and (F). The direct connexion between (B) and (E) is demonstrated in the appendix.

§ 2. *The Theorems of "Virtual Work" and "Minimum Potential Energy."*

A fundamental principle of mechanics that has an important place in the theory of structures is the

Principle of Virtual Work * (or the Principle of Virtual Velocities as it used to be called). In the form used in structural theory it states that if an elastic body is in equilibrium under external forces an infinitesimal deformation from the equilibrium configuration is accompanied by an increment of internal energy equal in value to the work done by the external forces in the course of that deformation. Thus, if U represents the internal energy, $P_1, P_2, \ldots . P_n$ the external forces, and $\delta_1, \delta_2 \ldots . \delta_n$ the corresponding displacments in the direction of those forces respectively,

$$dU = \Sigma P_r \, d\delta_r \dagger, \quad . \quad . \quad . \quad . \quad . \quad (1)$$

where the summation includes values of r from 1 to n.

If now $-P_r \, d\delta_r$ is regarded as the differential of a potential function V_r, where

$$V_r = -P_r \, \delta_r + \text{const.}, \quad . \quad . \quad . \quad . \quad . \quad (2)$$

in which P_r is a constant, (1) may be written in the form

$$d(U + \Sigma V_r) = 0. \quad . \quad . \quad . \quad . \quad . \quad (3)$$

That is to say, the total potential energy of the system, regarded as the sum of the internal energy and the potential energy of the external forces, has a stationary value for all infinitesimal displacements when the system is in equilibrium. Moreover (although this does not follow from the above argument), for stable equilibrium that stationary value may be shown to be a minimum, *i. e.*,

$$U + V = \text{minimum} \quad . \quad . \quad . \quad . \quad . \quad (4)$$

(where $V = \Sigma V_r$).

It is thus seen that the Principle of Virtual Work and the Principle of Minimum Potential Energy are essentially two different ways of saying the same thing. So long as the system is a conservative one these principles are true whatever may be the law relating deformation to resistance.

* So far, it appears that no satisfactory deduction of this principle from the elementary axioms of Statics has been made, *cf.* Reference [2] § 290, Reference [8], § 193.

† The increment dU may be imagined to be caused by small increments dP_r in the applied forces, product terms of the form $dP_r d\delta_r$ being omitted as of the second order of smallness.

§ 3. *Castigliano's Theorem of the Differential Coefficients of Internal Work.*

Castigliano presents this theorem in two parts. Part I. states that:

"If the internal work of a frame structure is expressed as a function of the relative displacements of the external forces applied to its nodes, the resulting expression is such that its differential coefficients with regard to these displacements give the values of the corresponding forces."

This is practically a reiteration of the Principle of Virtual Work of (1). In proving it Castigliano[1] merely quotes equation (1) (the right-hand side of which represents the total increment of external work), and notes that since also necessarily

$$dU = \Sigma \frac{\partial U^*}{\partial \delta_r} d\delta_r$$

(being the total increment of internal energy), it follows that

$$P_r = \frac{\partial U}{\partial \delta_r}. \quad \ldots\ldots \quad (5)$$

It is, of course, valid for any law relating displacement and resistance.

Part II. states that:

"If, on the contrary, the internal work of a frame structure is expressed as a function of the external forces, the resulting expression is such that its differential coefficients give the relative displacements of their points of application."

In proving this second part Castigliano[1] makes use of the fact that, for a structure that obeys Hooke's Law, the internal energy in the equilibrium configuration is equal to the sum of the external forces multiplied respectively by half their corresponding displacements, *i. e.*,

$$U = \tfrac{1}{2}\Sigma P_r \delta_r, \quad \ldots\ldots \quad (6)$$

and therefore

$$dU = \tfrac{1}{2}\Sigma P_r d\delta_r + \tfrac{1}{2}\Sigma \delta_r dP_r,$$
$$= \Sigma P_r d\delta_r \quad \text{(by (1))},$$

* The partial differential form is used to indicate only that while δ_r is varied, the other δ's remain constant.

from which

$$\Sigma P_r\, d\delta_r = \Sigma \delta_r\, dP_r,$$

i.e.,

$$dU = \Sigma \delta_r\, dP_r. \quad . \quad . \quad . \quad . \quad . \quad (7)$$

But necessarily, since the change of internal energy is due wholly to increments dP_r in the applied loads,

$$dU = \Sigma \frac{\partial U}{\partial P_r}\, dP_r,$$

which on comparison with (7) gives

$$\delta_r = \frac{\partial U}{\partial P_r}. \quad . \quad . \quad . \quad . \quad . \quad . \quad (8)$$

By replacing a redundant member carrying a load T by the two equal and opposite forces T to which, so far as the rest of the structure is concerned, it is clearly equivalent, we have as an immediate consequence of (8) the relation

$$\frac{\partial U}{\partial T} + aT = \lambda, \quad . \quad . \quad . \quad . \quad . \quad . \quad (9)$$

where U is the internal energy in the structure that remains after the removal of the redundant member, aT is the extension of the redundant member under the tension T, and λ is the amount by which, in the unloaded frame, the length of the redundant member is short of the distance between its end nodes. For, if the redundant member is inextensible, aT is zero, and as $\partial U/\partial T$ is by (8) the amount by which the nodes at its two ends approach each other, that amount must be equal to λ; and, moreover, when the member is extensible the gap λ is effectively reduced by the value of that extension.

By writing (9) in the form

$$\frac{\partial}{\partial T}(U + \Sigma \tfrac{1}{2} aT^2) = \lambda, \quad . \quad . \quad . \quad . \quad . \quad (10)$$

where the summation includes all the redundant members in the frame, and making λ zero, Castigliano arrived at his "Theorem of Least Work," which being derived from (8) is only true for structures obeying Hooke's Law.

It is important to note that the quantity λ in (10), obtained by differentiating the total strain energy of the system with respect to the tension T in a redundant

member, may be interpreted in two distinct though equivalent ways. It may be regarded as :

(*a*) The initial lack of fit of the redundant member, that is to say, the amount by which in the unloaded structure the length of the redundant member is less than the distance between the two nodes which that member is to connect, assuming that in the final loaded state the ends of the member coincide with the nodes ;

or

(*b*) The final lack of fit of the redundant member, that is to say, the amount by which the length of the redundant member—a dead fit in the unloaded frame—is greater than the distance in the final loaded state between the two nodes it is supposed to connect.

The definition of λ given in (*a*), and explained in the paragraph following equation (9) above, is the one given by Castigliano himself, and is invariably the one quoted by subsequent writers * on this subject. The interpretation given in (*b*), however, while equally true with that given in (*a*), is in some ways more significant. For it shows that the application in a structural problem of equation (10), when λ is made equal to zero, in other words the application of Castigliano's Theorem of Least Work, is merely a means of ensuring compatibility of displacement between the redundant member and the nodes which it connects.

§ 4. *Relation between Castigliano's Theorem of Least Work and the Theorem of Minimum Potential Energy.*

In any frame structure the conditions that have to be satisfied and that lead to a unique solution are that at each node :

(i.) The loads in the members meeting at the node are in equilibrium with the external forces applied at the node ;

(ii.) The ends of the interconnecting members suffer equal displacement, *i. e.*, there is no incompatibility of displacement at the node.

* *E. g.* by Pippard[7], who calls this definition of λ "The Second Theorem of Castigliano."

When applying Castigliano's Theorem of Least Work, condition (i.) is satisfied as soon as the loads in the members are expressed in terms of the external loads and the unknown loads in the redundant members; and the equations obtained by equating to zero the differentials of the internal energy with respect to each of these unknowns express condition (ii.). In the absence of redundant members, there cannot be any incompatibility of displacement, and there is no call for the application of the Theorem, the problem being solved by reference to the condition (i.) alone.

When applying the Theorem of Minimum Potential Energy, we begin by assuming a certain displacement (δ_r) at each node which is identical for all the members meeting at that node. Thus condition (ii.) is satisfied. Having thus stipulated the displacement at each node, the internal energy U can be written as a homogeneous quadratic function of such displacements, and the potential energy of the forces can be written as

$$W = \text{Const.} - (\delta_1 F_1 + \delta_2 F_2 + \delta_3 F_3 + \ldots + \delta_n F_n)$$
$$= -\Sigma \delta_r F_r + \text{Const.}, \quad . \quad . \quad . \quad (11)$$

where the F's stand for the external forces.

The Theorem of Minimum Potential Energy states that the displacements must be such that

$$(U+W) = \text{a minimum}, \quad . \quad . \quad . \quad . \quad (12)$$

so that equations of the type

$$\frac{\partial}{\partial \delta_r}(U+W) = 0 \quad . \quad . \quad . \quad . \quad . \quad (13)$$

are obtained, equal in number to the number of unknown displacements. But by (5)

$$\frac{\partial U}{\partial \delta_r} = P_r, \quad . \quad . \quad . \quad . \quad . \quad (14)$$

which is equal to the force, expressed in terms of the assumed displacements and the physical characteristics of the members, necessary to be applied along δ_r for equilibrium. Also, by definition,

$$\frac{\partial W}{\partial \delta_r} = -F_r, \quad . \quad . \quad . \quad . \quad . \quad (15)$$

where F_r, as already stated, is the actual force applied.

Thus (13) is really a statement of the fact that the displacements must be so chosen that P_r, the force necessary for equilibrium must equal F_r, the actual force applied, *i. e.*,

$$P_r - F_r = 0. \quad . \quad . \quad . \quad . \quad . \quad . \quad . \quad (16)$$

The satisfaction of the set of equations of which (13) is typical therefore ensures equilibrum at all the nodes and consequently the satisfaction of condition (i.).

As a concise statement of the relation between the two theorems it may be said that, in applying the Theorem of Least Work, equilibrium is assumed at each node and the satisfaction of the equations obtained by differentiating the internal energy with respect to the unknown loads in the redundant members ensures compatibility of displacement; whereas, in applying the Theorem of Minimum Potential Energy, compatibility of displacement is assumed and the satisfaction of the equations obtained by differentiating the potential energy with respect to the displacements ensures equilibrium at each node.

It may be noted that, even when the structure contains no redundant members, the theorem of Minimum Potential Energy can still be used for reaching a solution ; for in such a case the conditions that ensure compatibility of displacement, unlike the conditions that ensure equilibrium, are not by themselves sufficient to determine the loads in the members.

With regard to the relative usefulness of the two theorems it is to be noted that, whereas the Theorem of Minimum Potential Energy is true whatever may be the law relating load and extension in the members, the Theorem of Least Work is only true when that law is a linear one. Thus, if a structure does not obey Hooke's Law, there is no choice among energy methods but to use the Theorem of Minimum Potential Energy in one or other of its forms. In structures that do obey Hooke's Law the Theorem of Least Work offers the greater advantages if the structure contains clearly defined redundant members and reduces, on their removal, to a simple framework. This statement should perhaps be qualified by the condition that the number of redundant members should not be inconveniently

large * (fig. 2). In all highly redundant structures, however, there is little doubt that use of the Theorem of Minimum Potential Energy is more convenient; for in its application the assumption of compatibility of displacement is a much simpler one to deal with than the corresponding assumption of equilibrium, which is the essential preliminary to the application of the Theorem of Least Work.

Fig. 2.

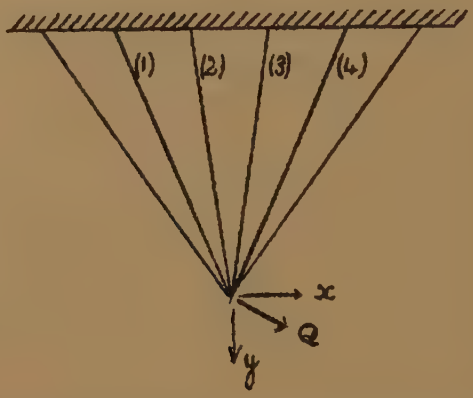

§ 5. *The Statical Analogues of the Dynamical Theorems of Bertrand and Kelvin.*

Theorems in dynamics connecting masses, impulses, velocities and kinetic energies have corresponding statical analogues connecting stiffnesses, forces, displacements and strain energy respectively. The analogy, however, only holds when the strain energy is expressible as a homogenous quadratic function of the displacements in the same way as the kinetic energy is of the velocities. In their statical form the theorems are therefore only true when there is a linear relation between load and displacement. The statical analogue of Bertrand's Theorem [2], [3], [4] states that:

"The strain energy of a structure when deformed by given forces is greater than if the freedom had been

* Clearly for the arrangement shown, where the redundant members number 4 out of a total of 6, it would be more expeditious to evaluate the x and y displacements at the common joint by the Theorem of Minimum Potential Energy rather than to evaluate the unknown loads in members (1), (2), (3), (4), by the Theorem of Least Work.

limited by the introduction of constraints." That of Kelvin's Theorem [2], [3], [4], states that:

"The strain energy of a structure corresponding to a given deformation is less than if the freedom had been limited by the introduction of constraints."

That these two theorems (which, in accordance with the list given in the appendix may be designated (E) and (F) respectively) are reasonable from a physical point of view may easily be seen from consideration of Lamb's [4] dictum that the presence of constraints increases the stiffness of an elastic body. Clearly then the work done by a given force (and hence the strain energy stored) is greatest when the stiffness is least, *i. e.*, when there are no constraints. On the other hand, the work done during a given displacement is least when the stiffness is least, *i. e.*, when the constraints are zero.

Both these theorems may be proved directly in precisely the same way as their dynamical equivalents by a mere translation of symbols, and, for the reason that such translation does not seem to be given anywhere, the proofs are added in the appendix*, where a physical proof of Theorem (F) is also given.

Since compatibility of displacement is assumed in both these theorems, it is to be expected that there is no direct connexion between either of them and Castigliano's Theorem of Least Work, but that there may be such connexion with the Theorem of Minimum Potential Energy. As, however, it is the strain energy of a system under given forces that is considered in the latter theorem and not the strain energy under given displacements, the direct connexion contemplated is with Theorem (E) rather than with Theorem (F).

Theorem (F), in fact, has little practical application in the Theory of Structures apart from its use in certain problems of elastic stability, for the usual problem is to determine the stresses in a structure set up by given forces and not by given displacements. Theorem (E), however, may be shown to be identical with the Theorem of Minimum Potential Energy for structures that obey Hooke's Law, and for such structures is therefore equally applicable.

* A proof of Theorem (F) on quite different lines is given in reference [5], § 119, *cf.* also reference [6], §§ 81, 82.

In order to demonstrate this identity it is convenient to restate Theorem (E) in the following rather different form :—

" Of all the deformations possible to a (conservative) system under given external forces the actual deformation is the one which renders the strain energy a maximum subject to equality of the strain energy to the work done on the system by the external forces."

Although the statical equivalent of Bertrand's Theorem has not (to the writer's knowledge) been previously stated in this form, it will be clear on a little consideration that the principle enunciated is the same. For in Theorem (E) as first stated, although there is equilibrium at all points, it is only maintained at certain points (where the constraints are applied) by the constraining action of hypothetical fixed smooth surfaces ; and as such constraints do no work they can be operative without affecting the equality of the total strain energy to the external work performed by the applied forces. In the second form of the theorem we have this same equality between total strain energy and total external work, but although there is no specific mention of constraints it is obvious that any deformation other than the true one can only be produced through the action of constraints and, because of the equality just mentioned, such constraints must take the form of fixed smooth surfaces.

In virtue of the second form in which Theorem (E) may be enunciated it may appropriately be called the Theorem of Maximum Strain Energy.

§ 6. *Taylor's*[9] *Relation between the Theorems of Bertrand and Kelvin.*

An interesting relation between Bertrand's and Kelvin's Theorems has been proved by G. I. Taylor. The statement in which Taylor defines this relation between the two dynamical theorems may be quoted without modification for the purpose of defining the corresponding relation between their statical analogues. It reads :

" The reduction in energy due to the imposition of constraints in the Bertrand case is less than the increase in energy due to the imposition of the same constraints in the Kelvin case."

The statical analogue of the proof given by Taylor for the dynamical case is included in the appendix.

Appendix.

(1) *Statements of the Theorems listed in* § 1.

(A) The Theorem of Virtual Work states that when an elastic * body is in equlibirium under the action of external forces, the work done by these forces in an infinitesimal displacement is equal to the increment of strain energy.

(B) The Theorem of Minimum Potential Energy states that when an elastic body is in stable equilibrium under the action of external forces the total potential energy (*i. e.* the sum of the strain energy of the body and the potential energy of the external forces) is a minimum.

(C) Part I. of Castigliano's Theorem of the Differential Coefficients of the Internal Work states that if the internal work of a frame structure is expressed as a function of the relative displacements of the external forces applied to its nodes, the resulting expression is such that its differential coefficients with regard to the several displacements give the corresponding forces.

Part II. of Castigliano's Theorem states that if, on the contrary, the internal work of a frame structue obeying Hooke's Law is expressed as a function of the external forces, the resulting expression is such that its differential coefficients give the relative displacements of their points of application.

(D) Castigliano's Theorem of Least Work states that if the strain energy of a structure obeying Hooke's Law is expressed in terms of the external loads and the (unknown) loads in the redundant members, the true values of the latter are those which render the strain energy a minimum.

(E) The Theorem of Maximum Strain Energy (statical analogue of Bertrand's Theorem) states that when a structure obeying Hooke's Law is subjected to the action of given external forces the strain energy is a maximum when the structure is unconstrained.

* The term " elastic body " covers all conservative systems.

(F) The statical analogue of Kelvin's Theorem (another theorem of minimum strain energy) states that when a structure obeying Hooke's Law is subjected to given displacements (at certain points) the strain energy is a minimum when the structure is unconstrained.

(2) *Proofs of the Statical Analogues of Bertrand's and Kelvin's Theorem* *.

Statical Analogue of Bertrand's Theorem.

Let the deformation of an elastic body under external forces be represented by generalized coordinates q_1, q_2, q_3, ... q_n. As the body obeys Hooke's Law the strain energy U is a homogenous quadratic function of these coordinates and we have

$$q_1\frac{\partial U}{\partial q_1}+q_2\frac{\partial U}{\partial q_2}+\ldots+q_n\frac{\partial U}{\partial q_n}=2U,$$

or
$$q_1Q_1+q_2Q_2+\ldots+q_nQ_n=2U, \quad . \quad . \quad . \quad (17)$$

where Q_1, Q_2, etc., stand for $\frac{\partial U}{\partial q_1}$, $\frac{\partial U}{\partial q_2}$, etc., and represent generalized components of force.

If two distinct equilibrium configurations of the structure are considered, the first being represented by forces Q and displacements q and the second by forces Q′ and displacements q', then

$$\begin{aligned} U-U' &= \tfrac{1}{2}\Sigma_r(Q_rq_r-Q_r'q_r') \text{ by (17) above} \\ &= \tfrac{1}{2}\Sigma_r(Q_r-Q_r')(q_r+q_r')-\tfrac{1}{2}\Sigma_r(Q_rq_r'-Q_r'q_r) \text{ identically} \\ &= \tfrac{1}{2}\Sigma_r(Q_r-Q_r')(q_r+q_r'), \quad . \quad . \quad . \quad . \quad . \quad . \quad . \quad . \quad (18) \end{aligned}$$

since, by the reciprocal theorem,

$$\Sigma_r(Q_rq_r'-Q_r'q_r)=0.$$

It is now required to prove that if the applied forces are the same for the two configurations, the strain energy corresponding to the first configuration, in which the structure is allowed to deform freely, is greater than that in the second configuration, in which the structure is subjected to the action of constraints. Such constraints may take the form of a relation between the

* These proofs follow Lamb's corresponding proofs for the dynamical cases.

various coordinates, but it is always possible by a change of coordinates (obtained from the original ones by a linear transformation) to represent the constraints by the vanishing of certain of the coordinates. We may write (18) in the different form

$$U-U'=\tfrac{1}{2}\Sigma_r(Q_r-Q_r')(q_r-q_r')+\Sigma_r(Q_r-Q_r')q_r'. \quad . \quad (19)$$

Now the forces applied to the structure are identical in the two cases considered for all points except those points where the constraints are applied and, therefore, it follows that at all the former points (Q_r-Q_r') vanishes, whereas at all the latter the displacement q_r' vanishes. Thus the second term of the R.H.S. of (19) disappears and we have

$$U-U'=\tfrac{1}{2}\Sigma_r(Q_r-Q_r')(q_r-q_r'), \quad . \quad . \quad . \quad (20)$$

and, as the R.H.S. of this equation is essentially positive (being the product of a force into the displacement produced by that force), U is greater than U′ and the proposition is proved.

Statical Analogue of Kelvin's Theorem.

Here we consider the strain energy stored in an elastic body as the result, not of given external forces, but of given displacements ; and it is to be proved that, subject to such displacements (*i. e.*, subject to given changes in certain of the coordinates), the strain energy stored is less when the body is (otherwise) free to distort than when it is subjected to the action of constraints.

As before, let the accented symbols relate to the case where the constraints are operative. As before also

$$\begin{aligned}U-U' &= \tfrac{1}{2}\,\Sigma_r(Q_rq_r-Q_r'q_r') \\ &= \tfrac{1}{2}\,\Sigma_r(Q_r+Q_r')(q_r-q_r')+\tfrac{1}{2}\,\Sigma_r(Q_rq_r'-Q_r'q_r) \\ &= \tfrac{1}{2}\,\Sigma_r(Q_r+Q_r')(q_r-q_r') \\ &= \Sigma_rQ_r(q_r-q_r')-\tfrac{1}{2}\,\Sigma_r(Q_r-Q_r')(q_r-q_r') \text{ identically.}\end{aligned}$$

The only points where Q_r is not zero are the points where the displacements have been fixed or where the constraints have been applied. At the former points (q_r-q_r') is zero, and at the latter Q_r is zero (the constraints as before being represented by the vanishing of the

corresponding coordinates), so that $\Sigma_r Q_r(q_r - q_r') = 0$. Hence

$$U' - U = \tfrac{1}{2}\Sigma_r(Q_r - Q_r')(q_r - q_r'), \quad . \quad . \quad . \quad (21)$$

and as the R.H.S. of this equation is essentially positive U is less than U'.

A simple physical proof of this theorem was indicated by Lamb[4]. According to this if the strain energy stored in the body as the result of given displacements is U_0, then, so long as those displacements are maintained unchanged, any further deformation of the body (such as would have been imposed by constraints operating while the given displacements were produced) must (by the principle of superposition) increase the total strain energy.

(3) *Proof of the Identity of the Theorem of Maximum Strain Energy* (i. e., *the Statical Analogue of Bertrand's Theorem*) *and the Theorem of Minimum Potential Energy, for Structures that obey Hooke's Law.*

Considering Theorem F in its second form, as given in § 5, let the deformation of the structure be represented by the displacements δ_1, δ_2, δ_3, etc. Since the body obeys Hooke's Law, the strain energy induced by the action of the external forces can be expressed as a homogeneous function V' of these displacements. Moreover, the external work performed by the applied forces in deforming the body may be expressed as a homogeneous linear function V'' of the same displacements. Now, according to the Theorem of Maximum Strain Energy, V' is a maximum subject to being equal to V'', *i. e.*, subject to being equal to V'''/2 where V''' is the loss of potential energy of the forces. Such a case of conditional maximum is most conveniently treated by the introduction of an undetermined multiplier λ, by the use of which the theorem may be converted into the equivalent statement :—

$$V' + \lambda\left(V' - \frac{V'''}{2}\right) = \text{a maximum.} \quad . \quad . \quad . \quad (22)$$

As the partial differential of the L.H.S. of this equation with respect to each of the displacements must therefore

be equal to zero, we have the following set of equations:—

$$\left.\begin{aligned}(1+\lambda)\frac{\partial V'}{\partial \delta_1}-\frac{\lambda}{2}\frac{\partial V'''}{\partial \delta_1}&=0,\\ (1+\lambda)\frac{\partial V'}{\partial \delta_2}-\frac{\lambda}{2}\frac{\partial V'''}{\partial \delta_2}&=0,\\ \cdots\cdots\cdots&\\ (1+\lambda)\frac{\partial V'}{\partial \delta_n}-\frac{\lambda}{2}\frac{\partial V'''}{\partial \delta_n}&=0.\end{aligned}\right\}\quad\ldots\quad(23)$$

If, now, the first equation of (23) is multiplied by δ_1, the second by δ_2, etc., and the resulting series of equations added together, we have

$$(1+\lambda)\left(\delta_1\frac{\partial V'}{\partial \delta_1}+\delta_2\frac{\partial V'}{\partial \delta_2}+\ldots+\delta_n\frac{\partial V'}{\partial \delta_n}\right)$$
$$-\frac{\lambda}{2}\left(\delta_1\frac{\partial V'''}{\partial \delta_2}+\delta_2\frac{\partial V'''}{\partial \delta_2}+\ldots+\delta_n\frac{\partial V'''}{\partial \delta_n}\right)=0,\quad(24)$$

which, by Euler's theorem of homogeneous functions, may be written

$$2(1+\lambda)V'-\frac{\lambda}{2}V'''=0.\quad\ldots\quad(25)$$

The value of λ may now be found by making use of the overriding condition

$$V'-\frac{V'''}{2}=0,\quad\ldots\quad(26)$$

which, in conjunction with (25), gives

$$\begin{vmatrix}2(1+\lambda), & -\frac{\lambda}{2},\\ 1, & -\frac{1}{2},\end{vmatrix}=0,$$

or
$$\lambda=-2.\quad\ldots\quad(27)$$

On substituting this value of λ in (22) we have

$$V'''-V' = \text{a maximum},$$

or
$$V'-V''' = \text{a minimum},\quad\ldots\quad(28)$$

or (strain energy of system)—(loss of potential energy of forces)
=a minimum.

i.e.

(strain energy of system) +(potential energy of forces)
=a minimum.

Thus, for a system that obeys Hooke's Law the statical analogue of Bertrand's Theorem reduces to the Theorem of Minimum Potential Energy.

(4) *Proof of the Statical Analogue of Taylor's Relation between the Theorems of Bertrand and Kelvin.*

Let U_0 represent the strain energy of a statical system due to a set of forces Q_r applied to coordinates q_r, another set of coordinates q_s being unconstrained. The resulting configuration q_r, q_s may be represented by the symbol (0).

Suppose now that the system is constrained by fixing the coordinates q_s. Under the conditions contemplated in Bertrand's Theorem forces Q_r are again applied to the coordinates q_r, and by that theorem the energy U_a of the constrained system is less than U_0, the difference, in consequence of the form of (20), being the energy corresponding to a configuration which is the difference between configurations (0) and (*a*). This configuration, which may be denoted by (0—*a*), is clearly that produced by a set of forces Q_s (equal and opposite to the constraining forces) which, applied at the coordinates q_s, produce the displacements q_s of configuration (0), *the coordinates q_r being unconstrained.*

Considering next the conditions contemplated in Kelvin's Theorem, we again hold the coordinates q_s fixed, but impose by means of forces Q_r' the displacements q_r of configuration (0). By the theorem the energy U_b of the resulting configuration is greater than U_0, the difference, in consequence of (21), being the energy corresponding to a configuration which is the difference between configurations (0) and (*b*). This configuration, which may be denoted by (*b*—0), is clearly that produced by forces Q_s' (equal and opposite to the constraining forces) which, applied at the coordinates q_s, produce the displacements q_s of configuration (0), *the coordinates q_r meanwhile remaining fixed.*

It follows directly from the statical analogue of Kelvin's Theorem that $(U_b - U_0)$ is greater than $(U_0 - U_a)$, which is the statement that required proof.

References.

(1) A. Castigliano, "Elastic Stresses in Structures" (translation by E. S. Andrews). Scott Greenwood and Co., 1919.
(2) Thomson and Tait, "Treatise on Natural Philosophy," pt. i. Cambridge University Press, 1912.
(3) E. T. Whittaker, "A Treatise on the Analytical Dynamics of Particles and Rigid Bodies." Cambridge University Press, 1927.
(4) H. Lamb, "Higher Mechanics." Cambridge University Press, 1920.
(5) A. E. H. Love, "A Treatise on the Mathematical Theory of Elasticity." Cambridge University Press, 1927.
(6) R. V. Southwell, "Theory of Elasticity." Clarendon Press, Oxford, 1936.
(7) A. J. S. Pippard, "Strain Energy Methods of Stress Analysis." Longmans, Green & Co., 1928.
(8) E. J. Routh, "Analytical Statics," vol. i. Cambridge University Press, 1909.
(9) G. I. Taylor, "A Relation between Bertrand's and Kelvin's Theorems on Impulses." Proc. Lond. Math. Soc., ser. 2, vol. xxi. pt. vi.

LV. *A new Method for determining the Uniaural Differential Threshold.* *By* J. W. Hughes, *B.Sc.**

[Received July 21, 1938.]

Theoretical Considerations.

If two notes of the same frequency giving amplitudes A_x and A_y in phase at one ear are presented to it at the same time, the total amplitude there will be (A_x+A_y). If, now, one of the notes is interrupted periodically, and the other (that of amplitude A_x, say) remains continuous, the amplitude of the note at the ear will vary from A_x to (A_x+A_y), and if the value of A_y is gradually decreased a time will come when the variation of intensity caused by the changing amplitude is only just perceptible. The amount of this variation in db. will be given by the expression $20 \log_{10} (A_x+A_y)/A_x$. This least perceptible change of intensity, denoted in what follows by δ, is the uniaural differential threshold for the particular note at the intensity corresponding

* Communicated by Dr. J. H. Shaxby.

to the amplitude A_x. If A_y gives an intensity γ db. above that due to A_x, then

$$\gamma = 20 \log_{10} \frac{A_y}{A_x}, \quad \text{or} \quad \frac{A_y}{A_x} = 10^{\gamma/20}.$$

Thus we have

$$\delta = 20 \log_{10} [1 + 10^{\gamma/20}].$$

The curve connecting δ with γ is shown in fig. 1, and it is clear that small variations in δ correspond to

Fig. 1.

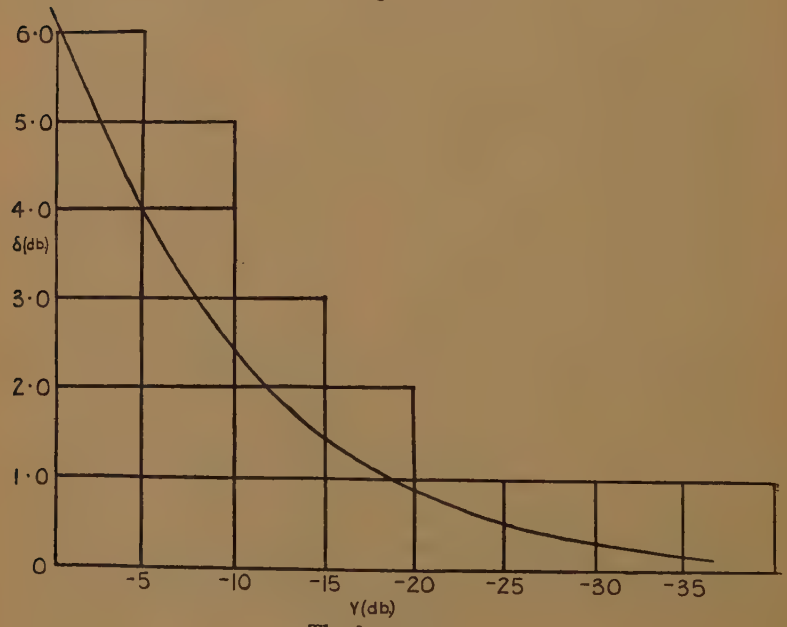

The δ—γ curve.

comparatively large changes in A_y. If, then, the postulated conditions can be realized in practice, we have a method for the determination of δ which has the advantage of a considerable "spread" in the scale of the variable quantity A_y in the region of $\delta = 0{\cdot}5$ db., the order usually found.

Before considering the means by which the conditions can be met, it is of interest to find how errors in making the two notes cophasic and in measuring the intensity difference (γ db.) between them will affect the value of δ

obtained. The effect of an error in the measurement of γ can be seen at once from the curve ; due to variations in the construction of the attenuators used such errors will occur in practice, but will certainly not amount to more than $\pm 1{\cdot}0$ db. In the region $\delta = 0{\cdot}5$ db. a variation in γ of this amount changes the value of δ deduced by approximately $\pm 0{\cdot}08$ db. ; this is negligible in comparison with the errors involved in setting the controls to give the value of γ corresponding to the differential threshold, since γ is then varied by large steps in view of the open nature of the scale.

Quite large variations in the setting of the notes to phase agreement are also permissible. If the notes differ in phase by an angle θ, the amplitude of their resultant is given by $(A_x^2 + A_y^2 + 2A_xA_y \cos\theta)^{1/2}$, corresponding to $\delta = 10 \log_{10} (1 + 10^{\gamma/10} + 2 \cos\theta . 10^{\gamma/20})$. The following table shows the values of δ corresponding to various values of γ for $\theta = 0°$ and $\theta = \pm 10°$:—

	γ (db.).	0.	−10.	−20.	−30.
δ(db.)	$\theta = 0°$	6·02	2·38	0·83	0·27
	$\theta = \pm 10°$	5·99	2·36	0·82	0·27

For the values of δ of the order usually obtained it appears that even an error of this magnitude will not appreciably affect the results, and such errors are not approached in actual practice.

Apparatus and Experimental Procedure.

One method which might be adopted to test the above calculations is as follows :—The notes are presented to the ears from two telephones mounted in a box as described later. The threshold settings of the controls are found for each 'phone (with the other silent), and the intensity of the note from each is raised, say, 50 db. ; both notes are now equal in intensity, and the reduction from equality needed in the one (γ db.) during an experiment can be read directly from its controls. The two notes are arranged to be in phase by using identical output circuits and making the voltages applied to them cophasic. With this method there would probably be errors in the phase adjustment and in the adjustment to equality of intensity, both of which might affect the value of δ deduced, though previous experiments in which these adjustments were necessary have shown that the

errors are well within the ranges already considered. But in the experiments just mentioned another fact had been noted which suggested a less troublesome and more accurate method of adjustment for equality of both phase and intensity, as the following considerations will show.

It had been found that when two currents of the same frequency and of approximately equal intensities, but opposite in phase, were passed in the proper sense through the two separate primary circuits of a special transformer, the output from the secondary circuit, which actuated a telephone, could be made to decrease to a minimum by alternate variation of the intensity and phase of one of the currents. The sharpness of adjustment to this minimum decreased with the intensity of the two notes, but it could be restored by amplification of the output from the transformer secondary. A similar effect was found when the currents passed through the two windings of a telephone in which two separate magnets were made to act on one diaphragm. Wightman and Firestone (1930), in a method devised by them for ensuring equality of output and phase from two telephones, have also observed the sharpness of this adjustment, and in a modification of their procedure used in some earlier work the effect was also present. It seemed, therefore, that this sharpness of adjustment could be utilized in the present connexion, since it could be adapted to whatever method was used to combine the amplitudes of the two notes at the ear. Once the intensities had been equalized and the notes opposed in phase, a phase reversal of one of them would give two identical notes, as in the preceding paragraph ; but besides permitting the double adjustment of phase and intensity to be carried out in one operation, it would dispense with the determination of one group of threshold settings, since the one note, fixed at a known level, could be used as the standard to which the other was thereby made equal. An investigation of the accuracy possible in this method was first undertaken, with results described later. The procedure proved very suitable for the purpose of the differential threshold experiments which are described next.

The apparatus used was that previously employed in work on the upper frequency limit for detection of binaural differences of phase. Changes of intensity

and of phase of either note could be made independently for adjustment to phase opposition, and a rotation through 180° of one of the phase-shifting transformers would then bring the notes to equality of phase and intensity. The intensity of one note could then be reduced in steps of 2·5 db., and the amount of the reduction read off on the controls. After determining the threshold settings for one note (with the other switched off), its intensity was raised to a level previously decided upon, and the other adjusted by alternate variation of its intensity and phase until the combination of the two notes became inaudible. Then a slow variation of the phase of the one note was made to find the settings (one at each end of the inaudible range) at which the combination became just audible. Setting the phase at the mean of these a similar procedure was followed with intensity variation, and the two adjustments were made alternately until two successive sets gave similar mean readings. This usually occurred after two or three trials even at the lower intensities, while at +50 db. the limits were so close together that the adjustments could be made at the first trial. The phase of the variable note was then changed by 180° and the commutator which interrupted it was started. The observer then signalled whether he heard alternations of intensity or not, and the assistant outside the "sound-proof" room in which the experiments were conducted reduced or increased the intensity of the note accordingly. The intensities at which the alternations just disappeared and just appeared were thus found; five pairs of these were taken for each intensity level of the "standard" note. The observer usually switched off the alternating combined note between signals and switched on for just long enough to decide whether alternations were perceptible or not; it was felt that their detection was easier under these circumstances. The rate of alternation was such as to give the single note for one half-second, followed by the combined note for a similar period.

It is interesting to notice that the intensity of the variable note will always be about 25 db. or so below that of the "standard" when the differential threshold is reached, so that if the intensity of the latter is, say, +20 db., the variable note would then be inaudible if acting alone, though its effect on the total amplitude

is still perceptible. This deduction is borne out by the experiments; with the one note at +15 db. and the other 5 db. below threshold, alternations were easily detected though the latter note was inaudible when the former was switched off.

Amplitude Summation.

Three methods were employed to combine the amplitudes of the two notes at the ear. In the first, two telephones mounted side by side in sponge rubber were used; they were held 6 in. from the ear at one end of a box lined with cotton-wool, and the ear was placed at the other end. The summation of the amplitudes of the notes at the ear had already been checked in the course of some previous work with this arrangment. The results obtained for the uniaural differential threshold with this apparatus agreed with those found in another way in other experiments, but with the amplifiers employed with this method of summation it was not possible to obtain notes more than 30 db. above threshold. Since the 'phones were 6 in. from the ear, the amplitudes of vibration of the diaphragms needed to produce any greater intensity would in any case involve the risk of distortion of their outputs.

A second method, which permitted greater intensities, was therefore tried, though it was not so certain that summation of amplitudes was achieved by it. The windings of an ordinary telephone receiver were broken where the coils on the two limbs of the magnet were connected together, and a third terminal was put in and arranged so that each limb could be separately energized from different sources, though the two coils still had one terminal in common. The coils were then connected to the amplifier output in the usual way, so that the intensity and phase of the current in each coil could be separately and independently controlled. The diaphragm of the telephone was therefore subjected to the action of the fields due to the two currents, and it was assumed that the resultant pressure-variations were the sum of those which would have been produced by either current acting alone. Though no direct tests were made, the results found agreed with those determined by the other methods, so that the assumption appears to be justified.

A difficulty which did not arise in the first case presented itself in the second. To produce the alternations in the one note, the corresponding telephone (in the first) or coil (in the second) was short-circuited by a mercury commutator. In the first case, when no current was passing in this 'phone, no perceptible variation of the intensity of the combined note was produced by this short-circuiting, but in the second it had the effect of making the intensity of the combined note vary even though no current passed in the short-circuited coil. Since the two coils acted on a common diaphragm, alteration of the circuit associated with one would affect the response produced by a particular current in the other, so the short-circuiting of the coil produced the alternations described. The trouble was overcome by arranging a permanent shunt of 1000 ω on the first coil (resistance 2000 ω) and, instead of short-circuiting it, the coil and its shunt were connected alternately in parallel with a 10,000 ω resistance in series with the 1 MΩ resistance of the output circuit, or with another such resistance otherwise unconnected. The impedance presented by the coil and its associated circuit was therefore subject to little variation, while the current in it alternated in the desired way. The commutator contacts were arranged to "arc" so that the 10,000 ω shunts were never out of circuit. With this arrangement no variation could be detected in the intensity of the note produced by the current in the one coil when the commutator was working and no current passed in the other.

Yet another method, in which higher intensities could also be used, was tried, in which the currents in the output circuits were mixed electrically in the telephone. The latter, a moving-coil instrument of resistance 10 ω, was arranged so that one terminal was earthed and the other connected to both output circuits, so that each output transformer was loaded with a 1 MΩ resistance in series with the 'phone. The commutator broke the connexion between one output circuit and the 'phone and substituted a direct connexion from this circuit to earth; the "arc" contact was removed to avoid short-circuiting the 'phone and giving silent intervals between the alternations. Since the telephone was presented to either output circuit with a shunt of approximately 1 MΩ, the resistance of the other, the current flowing through

the 'phone was slightly decreased, but the difference between this and the total current was too small to affect the results. The alternate removal and replacement of one of these " shunts " might tend to raise and lower the intensity from the 'phone even when no current is passing in the circuit concerned, but the variation is too small to be detected, since removal of a 1 MΩ shunt would only increase the 'phone current by 10^{-5} of its original amount.

The apparatus can be considerably simplified for use in the ordinary way. All that is necessary is a means of adjusting the amplitudes of the vibrations to various levels and to equality, an attenuator for the actual determination of the differential thresholds, and provision for producing small variations of the phase of one note and for reversing its phase by 180°. The latter is most simply accomplished by using a centre-tapped output transformer with the centre-tap earthed, and arranging that the 'phone (or coil) is connected through a 1 MΩ resistance to a reversing switch, and thence to either of the outer terminals of the transformer. The other terminal is earthed directly through a 1 MΩ resistance to balance the circuit. The small adjustments of phase can conveniently be made by a variable condenser (0·0015 μf. max.) connected across the 1 MΩ resistance and 'phone with a 0·0005 μf. condenser across the output circuit of the second amplifier if necessary. Rotation of the condenser causes intensity variations as well as changes of phase, but these do not interfere with the balancing in the position of phase opposition. Some experiments carried out with this simplified apparatus gave results similar to those found with the more complex circuit. A valve voltmeter across the output circuit showed that operation of the reversing switch varied the output by less than 0·1 db., and a cathode-ray oscillograph test indicated that the phase change produced by it was actually 180°, since the straight line trace obtained by adjustment of the phase remained a straight line when the switch was operated, though its orientation was of course changed. It is even possible to omit the phase-reversal and work with two notes in phase opposition, varying the intensity of one as already described. The amplitude of the combined note then varies from $(A_x - A_y)$ to A_x, and the relation between δ and γ becomes

$\delta = 20 \log_{10} [1 - 10^{\gamma/20}]^{-1}$. The curve practically coincides with that already discussed for values of γ below -25 db., but δ increases more rapidly with γ above this point. Experiments have shown that this procedure is quite practicable, and yields results similar to those found by the first method. The level from which the differential threshold is then measured is, of course, that corresponding to the amplitude $(A_x - A_y)$, but this, as a rule, is only about 0·5 db. below that due to A_x alone.

The results obtained by the three methods of combination are shown in the table below. Each figure represents the mean of the five pairs of values obtained at the given intensity level. Their consistency indicates that the procedure described is capable of measuring differential thresholds as accurately as others, and with a greater ease and certainty on account of the more open scale it gives.

Uniaural Differential Threshold (δ db.).

Intensity of "standard" (db. above threshold).		50.	45.	40.	35.	30.	25.	20.	15.	10.
Frequency.	Method.									
800 c./sec.	I.	..	..	..	..	0.25	..	0·33		
	II.	0·52	..	0·40	..	0·34	..	0·41		
	III. (*a*)	..	0·28	..	0·43	..	0·53	..	0·50	
	III. (*b*)	..	..	0·41	..	0·32	..	0·63		
	III. (*c*)	0·49	..	0·41	..	0·33	..	0·41		
1000 c./sec.	I.	..	..	..	..	..	..	0·41	0·46	
	II.	0·51	..	0·49	..	0·63				
	III. (*a*)	..	0·31	..	0·31	..	0·45	..	0·51	
	III. (*b*)	..	..	0·36	..	0·49	..	0·56		
	III. (*c*)	..	..	0·44	..	0·43	..	0·43	..	0·59
1200 c./sec.	I.									
	II.	..	..	..	0·32	..	0·40			
	III. (*a*)	..	..	0·33	..	0·68	..	0·35		
	III. (*b*)	..	..	..	0·30	..	0·53	0·46		
	III. (*c*)	..	..	0·23	..	0·43				

Methods :—I. two 'phones; II. twin-magnet 'phone; III. moving-coil 'phone: (*a*) original, (*b*) simplified apparatus, (*c*) phase opposition.

Adjusting the Resultant Amplitude to Zero.

It is well known that if two notes of the same frequency and $\theta°$ from phase opposition give amplitudes A_x and A_y at a point, the amplitude A of the resulting vibration is given by $A^2 = A_x^2 + A_y^2 - 2A_x A_y \cos\theta$. To appreciate

how the *loudness* of the resultant varies with θ and with the relative amplitudes of its components, it is necessary to find the difference in decibels between the intensity of the resultant and that of one component which is taken as the standard of reference. Though the variation of this difference will not represent the true variation of loudness, it will show very closely the nature of the changes to be expected, and the loudness variations could be found for any particular case from curves such as those of Fletcher and Munson (1933).

If the intensity of the resultant is D db. above that due to A_x, and that of A_y is γ db. above A_x, then

$$D=20\log_{10}\frac{A}{A_x};\quad \gamma=20\log_{10}\frac{A_y}{A_x}.$$

From the previous relation,

$$\left(\frac{A}{A_x}\right)^2=1+\left(\frac{A_y}{A_x}\right)^2-2\left(\frac{A_y}{A_x}\right)\cos\theta,$$

or $$10^{D/10}=1+10^{\gamma/10}-2.10^{\gamma/20}\cos\theta.$$

Thus we have

$$D=10\log_{10}(1+10^{\gamma/10}-2.10^{\gamma/20}.\cos\theta).$$

From this expression values of D corresponding to various values of γ at different values of θ may be calculated, or *vice versa*.

The above expression is not very suitable for computation, and a better expression is obtained as follows :— The resultant amplitude A can be obtained from the two components A_x and A_y by the usual parallelogram law, which gives a triangle of sides A, A_x, and A_y with an angle θ opposite the first. If the angles opposite A_y and A_x are α and β respectively, then

$$\frac{A}{\sin\theta}=\frac{A_x}{\sin\beta}=\frac{A_y}{\sin\alpha}.$$

Thus

$$\frac{A}{A_x}=\frac{\sin\theta}{\sin\beta}=\frac{\sin\theta}{\sin(\alpha+\theta)},\quad\text{and}\quad\frac{A_y}{A_x}=\frac{\sin\alpha}{\sin(\alpha+\theta)},$$

whence we have

$$D=20[\log_{10}\sin\theta-\log_{10}\sin(\alpha+\theta)];$$
$$\gamma=20[\log_{10}\sin\alpha-\log_{10}\sin(\alpha+\theta)].$$

To plot the curves of γ against D for fixed values of θ, the first expression is used to find $\sin(\alpha+\theta)$ for a given value of D. In general this will give two values of α to substitute in the expression for γ, corresponding to values of β greater or less than 90°. Since $\beta=\pi-(\alpha+\theta)$, the acute value β_1 can be found from the expression for D,

Fig. 2.

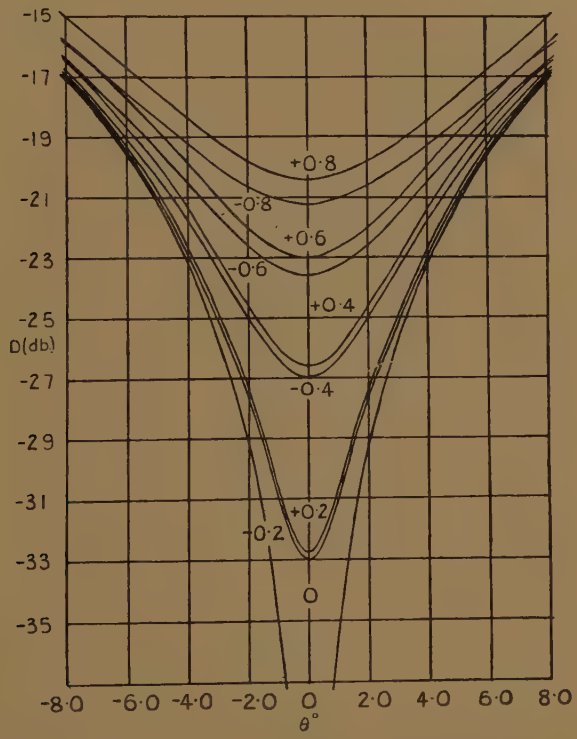

The curves γ=constant.

and then we have $\sin\alpha_1=\sin(\beta_1+\theta)$, $\sin\alpha_2=\sin(\beta_1-\theta)$ for calculation of the two values of γ for the given value of D. The curves have been drawn, and are shown in fig. 2. From them points on the curves of θ against D for fixed values of γ can be found and intermediate points can be calculated from the relation

$$\cos\theta=\tfrac{1}{2}\left[1^{\frac{2D-\gamma}{20}}-10^{\frac{\gamma}{20}}-10^{-\frac{\gamma}{20}}\right],$$

which follows from the first expression for D. The resulting curves are also shown.

There are several points of interest in these curves. In the first place the D—θ curves are symmetrical about $\theta=0°$, but the D—γ curves are not symmetrical, and have their minima displaced in the direction of negative γ.

Fig. 3.

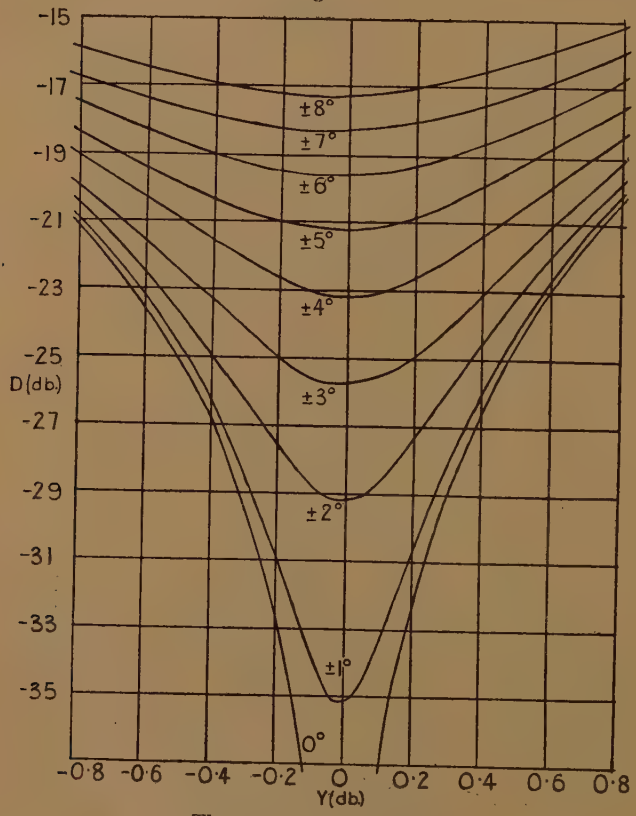

The curves θ=constant.

The triangle shows at once that the first result is to be expected, and also that the minimum resultant intensity for any particular value of θ will occur when the intensity of the variable note is less than that of the standard, since the side A has its minimum length when it is perpendicular to A_y, and the corresponding value of A_y is then less than A_x. However, for values of θ less

than 8°, the difference between the two is less than 0·1 db., and it decreases rapidly as θ approaches zero. The value of γ when D is at its minimum is given by $20 \log_{10} A_y/A_x$, or $20 \log_{10} \cos \theta$ from the triangle, and the minimum value of D is $20 \log_{10} \sin \theta$ in the same way.

The reason for the sharpness of adjustment of the intensity and phase, even for moderate intensities of the notes, is clear from the curves. Suppose the notes are each 40 db. above threshold, and that for detection of error in the adjustment the resultant needs to rise to, say, 5 db. above threshold. (With careful listening in a "sound-proof" room such a rise can easily be detected.) Then it is clear that the corresponding value of D is -35 db., and from the D—γ curves it appears that if the notes are actually in phase the value of γ may vary about 0·15 db. on either side of zero (*i. e.*, of equality of intensity). If the phase is set 1° from opposition the limits become $\pm 0{\cdot}03$ db., so that the resultant note would probably not disappear under these circumstances, but decrease to a minimum intensity as γ was varied. From the D—θ curves it is evident that at the same level the permissible variation in θ is $\pm 1°$ for $\gamma = 0{\cdot}0$ db. The effect of errors in setting both γ and θ can best be seen from the curves D = constant, which can be plotted from the other two, and are shown in fig. 4 for intervals of 2 db. from D = −20 db. to D = −34 db. Then for any intensity level, allowing an arbitrary rise of 5 db. in the resultant before its detection, the possible combinations of errors in γ and θ can be found. For example, for a level of +25 db. above threshold the curve for D = −20 db. is used, and it shows that if the phase has been correctly set ($\theta = 0°$) the intensity can be varied from equality by +0·83 db. or −0·91 db. before the resultant can be detected. If the phase-setting is 4° in error, the intensity variation is decreased to +0·57 db. or −0·68 db. and so on. A similar argument can be applied to find the phase variations detectable when there are various errors in the intensity adjustment.

The set of curves D = constant used in this way shows how the phase and intensity of the variable component can be most accurately set to the required values. Since they are symmetrical in θ, it follows that if the settings of the phase-shifting transformer are taken for the limits between which the resultant is audible the mean setting

will be that for phase opposition if the limits have been correctly determined, and this will hold whether errors are present in the intensity settings or not. If the limits are taken on the intensity controls, the mean setting (in db.) will, even for low intensities, be well within 0·1 db. of the intensity corresponding to equality. The pro-

Fig. 4.

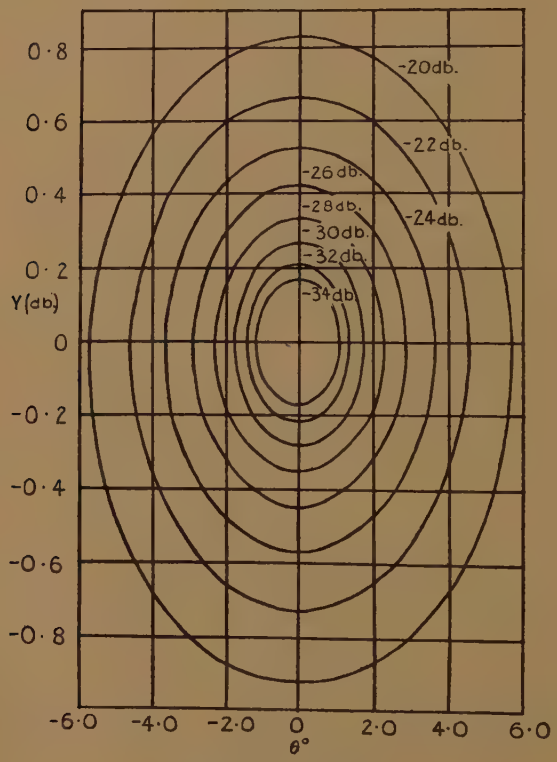

The curves D=constant.

cedure adopted in the experimental work, which has already been described, utilizes the method just outlined.

It would appear from the D—γ curves that if the phases of the two notes were set a degree or so from opposition there would be a closing-in of the limits between which the intensity of one might be varied so that the resultant remained inaudible, and a more accurate determination of the setting to equality would be possible. But greater

accuracy could not be attained in this way, as experiments showed that the limits themselves became less well defined in these circumstances. This is also indicated by the curves, since their slopes, representing the rate of change of intensity of the resultant for a steady variation in γ, are, for any particular value of D, greatest for $\theta=0°$, and decrease progressively as θ increases.

An experimental check of the curves was attempted by finding the limits between which the intensity of one component could be varied for different values of θ near phase opposition, in the expectation that a curve of the shape of the D=constant curve would result, with a maximum at the reading corresponding to $\theta=0°$. Two methods, one involving the gradual changes of intensity already described and the other using abrupt changes variable in magnitude, were tried. In the latter a part of the shunt on one coil of the special 'phone previously used could be varied, and was periodically short-circuited, and the value of this variable part when the resultant just became audible was to be found for different values of θ; the intensity and phase adjustments had previously been made in the usual way. But the experiments failed to yield any definite variation of the limits, probably for the same reason as that already given. A check of the curves is, however, provided by the experimental observation that the limits of adjustment for phase and intensity do decrease as the intensity of the standard note increases, and that the limits are approximately those which the curves for D=constant would lead one to expect.

Acknowledgments.

The author wishes to thank the Medical Research Council for grants which made the work possible, and Dr. T. S. Littler, of the University of Manchester, for the moving-coil telephone used in the experiments. Thanks are also due to Dr. J. H. Shaxby, in whose laboratory the experiments were performed, for his suggestions.

Summary.

An interrupted note variable in intensity is added to one of fixed intensity and in phase with it at the ear. It is shown that the variation required provides a very

open scale at the differential threshold. Three means of obtaining summation of the notes are described, and the accuracy of the method for ensuring that the notes are in phase is discussed.

References.

Fletcher, H., and Munson, W. A.—J. Acoust. Soc. Amer. v. p. 82 (1933).
Wightman, E. R., and Firestone, F. A.—J. Acoust. Soc. Amer. ii. p. 271 (1930).

LVI. *Surface Phenomena with Charged Spherical Particles when moving in a Solvent. Cataphoresis; Sedimentation Potential* *. *By* J. J. Hermans †.

[Received July 29, 1938.]

§1. *The Formulæ of Helmholtz-Smoluchowsky, Hückel, Henry.*

THE classical formula for the cataphoretic velocity of a charged particle in an electric field E has the form

$$U = \frac{D\zeta E}{4\pi\eta}. \quad . \quad . \quad . \quad . \quad . \quad . \quad (1)$$

Here ζ is the electrokinetic potential, D the dielectric constant, and η the coefficient of internal friction of the medium. This formula is said to apply to particles of any size or shape provided [13] (*a*) Stokes's hydrodynamical equations hold good in the electric double layer round the particle, (*b*) the external field may be superposed on that of the double layer, (*c*) the dimensions of the double layer are small compared with those of the particle, (*d*) the quantities D and η have the same value in the double layer as outside it.

Regarding the last condition, Mooney [23] called attention to the measurements of Kallmann and Dorsch [15], who determined the dielectric constant of films of a thickness of about 1μ, and, within experimental error, found no deviations. Apart from the thickness of the double layer, the electric field of the particle might change the dielectric constant. This effect, which is partly due to the inhomogeneity of the field, seems to be very small. It has at least never been found in the

---

* Communicated by the Author.

† Netherland Fellow of the Ramsay Memorial Fellowship Trust and the Hoogewerff Fund.

case of electrolytic solutions, and the electric field in the neighbourhood of an ion certainly is much less homogeneous than that in the neighbourhood of a colloid particle, the latter being much larger. As to the value of η in the double layer, no experimental data exist, but there is no reason to expect important deviations. The existence of a space charge could, of course, influence η, but this influence which, for instance, shows itself in the internal friction of electrolytic solutions, is very small[8].

It may be pointed out, however, that these conclusions are reliable only in those cases where the double layer is not too thin. As soon as the double layer becomes of molecular dimensions, we know practically nothing about its properties. The effective η may then be considerably larger, while at the same time we are up against a difficulty which is connected with the rapid drop of the electric potential in the double layer. For in electrokinetic experiments (cataphoresis, electrosmosis) the velocity gradient in the double layer has the same order of magnitude as the potential gradient. In other words, in the case of a double layer of molecular dimensions we are concerned with a velocity gradient which is never equalled in ordinary flow of liquid, and which may cause η to be very different from the macroscopic η. We want to emphasize this point because in this paper we are dealing with a double layer which is thin compared with the radius of the particle, *i. e.*, for very small particles our results must needs be accepted with great reserve.

Subsequently Debye and Hückel[6], as a result of elaborate calculations, replaced formula (1) by $U = D\zeta E/C\eta$, where C is a constant which depends on the shape of the particle. It has the value of 6π instead of 4π in the case of spheres, irrespective of the relative sizes of the double layer and the radius of the sphere. However, Mooney[23] had already pointed out that the influence of the particle on the direction of the electrical lines of force had been neglected in Hückel's calculations, and Henry[13] consistently took into account this influence. If a sphere with radius R and specific conductivity μ' is dispersed in a medium with specific conductivity μ, then an electric field E in the direction of the x-axis will set up a potential

$$\Pi = -E\left(1+\frac{\lambda R^3}{r^3}\right)x = -E\left(r+\frac{\lambda R^3}{r^2}\right)\cos\theta, \quad . \quad (2)$$

where

$$\lambda = \frac{\mu-\mu'}{2\mu+\mu'}, \quad . \quad . \quad . \quad . \quad . \quad . \quad . \quad (3)$$

r is the distance from the centre of the sphere, and $x = r\cos\theta$. Obviously the field remains unchanged only when $\lambda = 0$, *i. e.*, when the sphere and the dispersing medium have the same specific conductivity. Further, it is easily seen that the lines of force will spread around the particle if it is an insulator ($\mu' = 0$, hence $\lambda = \frac{1}{2}$). For then $\partial\Pi/\partial r = 0$ on the surface of the sphere. In all other cases the lines of force enter the sphere, and it will be shown in this

paper that this has a very pronounced effect on the mobility of the particle.

It is well known that the thickness d of the diffuse double layer is equal to $1/\chi$, χ being the reciprocal characteristic length of Debye-Hückel's theory,

$$\chi^2 = \frac{4\pi\Sigma n_\kappa e_\kappa^2}{\mathrm{D}k\mathrm{T}}.$$

The product $\chi\mathrm{R}$ is, therefore, an exact measure of the ratio between the thickness of the double layer and the radius of the particle. Now, in the case of a double layer which is very diffuse compared with the size of the particle, *i. e.*, $\chi\mathrm{R} \ll 1$, Henry finds the formula of Hückel ($\mathrm{C}=6\pi$). In the case of a double layer which is very thin compared with R, *i. e.*, $\chi\mathrm{R} \gg 1$, Henry finds for the total force on the sphere

$$(1+\lambda)\mathrm{RD}\zeta\mathrm{E} - 6\pi\eta\mathrm{RU}. \quad . \quad . \quad . \quad . \quad (4)$$

When the motion is uniform, this force must be zero, and the cataphoretic velocity becomes

$$\mathrm{U} = \frac{(1+\lambda)\mathrm{D}\zeta\mathrm{E}}{6\pi\eta}. \quad . \quad . \quad . \quad . \quad . \quad (5)$$

For non-conducting particles ($\lambda=\frac{1}{2}$) one finds, therefore, the formula of Helmholtz-Smoluchowsky ($\mathrm{C}=4\pi$), which is the same as the one obtained by Henry for a cylinder; it seems, therefore, probable that the formula applies to particles of any shape, or else that the deviations from it will be very small for particles of another shape.

This result can be tested by comparing U with the electrosmotic velocity along a plane wall which consists of the same material as the particle considered. This has actually been done by several experimenters; but there is as yet no agreement between their results. A long time before the calculations of Henry, Mooney[22] found the cataphoretic velocity of oil-droplets in water to be dependent on their radius. This dependence decreased with increasing electrolytic concentration, *i. e.*, with decreasing dimensions of the double layer, in exact agreement with the theory developed by Henry afterwards. Abramson[2], [10], however, found cataphoretic velocities which depended on neither the size nor the shape of the particles, but, as H. L. White[39] pointed out, in these experiments the electrolytic concentration

was usually too large to expect deviations. It is indeed remarkable that some striking deviations occur between cataphoretic and electrosmotic velocity even in Abramson's data[1], and exactly in those cases where the medium is distilled water without added electrolyte. The measurements of H. L. White and co-workers[37], [38] seem to leave no doubt that cataphoretic and electrosmotic velocities differ considerably with small electrolytic concentrations, but become equal with larger concentrations. Recent investigations of Abramson[25] lead to other results, but they are explained by H. L. White[37] as being due to the presence of gelatine. It seems to us that this problem has not yet been completely solved experimentally, and it will be shown in this paper that theoretical considerations regarding cataphoretic velocity tend to complicate this matter still further. For it will appear that in those cases where the electrolyte is unsymmetrical, the electrosmotic and cataphoretic velocities cannot be expected to be equal even with high electrolytic concentration, where $\chi R \gg 1$. No previous experimental evidence seems to exist for this fact. In H. L. White's results there are cases where these velocities differ by as much as 25 per cent. even with high values of χR. The number and the accuracy of the measurements are, however, still too inadequate to allow of reliable inferences. As to the accuracy of the data, P. White[35], [36] has shown recently, both by theory and experiment, that errors as large as 30 per cent. may creep into the measurements if the symmetry of the flow of liquid in the measuring cell is not fully accounted for.

In the case of conducting particles the phenomena are much more complicated, and for several reasons Henry's considerations will then break down (compare § 5 and § 7). In order to confirm the influence of the conductivity μ' as predicted by Henry, Gilford[11] determined the cataphoretic velocity of long-shaped antimony oxide crystals both in the direction of the axis and perpendicular to it. These measurements, however, were carried out in water and, though Gilford does not mention the dimensions of the crystals used, it is very unlikely that their thickness was large compared with the diffuse double layer. The velocity in a direction perpendicular to the axis would anyhow have been different from that in the direction of the axis.

§ 2. *Relaxation.*

The change in the distribution of charge round the particle considered, due to the external field, has been neglected in Henry's calculations as well as in those of earlier workers. In reality this distribution of charge will deviate from spherical symmetry, which gives rise to the so-called relaxation force. This relaxation force is well known in the theory of strong electrolytes, and this theory may be applied to colloidal particles if these particles are very small compared with the diffuse double layer, as has indeed been done by Paine[29] and by the author[14].

It is readily seen that in this case the relaxation force may play an important part in the resistance experienced by the particle. For the relaxation force is proportional to the square of the charge, while the Stokes resistance increases with the first power of the radius. The ratio between charge and radius is roughly constant[30], and, therefore, the larger the particle the greater does the influence of the relaxation force become. This simple conclusion, drawn from the theory of strong electrolytes, explains the fact, unacceptable to Pauli and Valko[30], that the decrease in the mobility of the colloid particle is much larger than that of the ions.

For two reasons Paine's calculation must be restricted to the limit of small χR. The external field is supposed to remain unaltered, and the hydrodynamical flow of liquid due to the motion of the particle is neglected[14]. Obviously this flow of liquid becomes very important with large particles; in the limit of very large χR the double layer is even carried along almost entirely by the particle. It is also obvious, however, that generally it will not be easy to calculate the influence of this flow of liquid. Mooney[23], and also Henry[13], believed the solution of this problem to be impossible. As will be shown, however, in this paper, a solution is possible for the limit of very large χR. It is readily seen that the lines of force of the external electric field will then become very important. For, if the particle is an insulator, the lines of force spread around it ($\partial\Pi/\partial r=0$ on the surface). The forces on the ions in the immediate vicinity of the surface are then directed along the surface, and the distribution of charge is not changed in this immediate neighbourhood. If, however, the particle is a conductor, the lines of force have a component perpendicular to the surface. The ions will then experience electrical forces which exert a considerable influence on the mobility of the particle.

As will be shown in § 5, one has to expect relaxation forces in this case, which may become large compared with the Stokes resistance, so that the formula (5) becomes meaningless *.

Finally, it may be mentioned that Bikerman[3] has already attempted to calculate the relaxation for the case where $\chi R \gg 1$, though his calculations are restricted to cylindrical particles, the axis of which lies in the direction of the external field. His calculation starts from the concept of surface current. This surface current conveys electricity from the one end of the particle to the other, and so causes an accumulation of charge. Bikerman then postulates that this accumulation of charge generates a potential gradient which exactly balances the transportation of electricity by setting up an electric current in the surrounding liquid. He then finds relaxation forces which may amount for up to 60 per cent. of the Stokes resistance. Bikerman's theory, however, cannot be regarded as exact because in electrolytic solutions the destruction of space charge by diffusion cannot be neglected as compared with that effected by the electric current. Moreover, Bikerman's theory does not apply to spherical particles.

§ 3. *Extreme Values in the Cataphoretic Mobility.*

In connexion with Bikerman's calculations a phenomenon may be mentioned about which opinions greatly vary. Very often maxima in the cataphoretic velocity are found when the concentration of the electrolytic solution is decreased. This maximum generally lies in the neighbourhood of 1 millimol per litre[34], and is explained by Bikerman[3] as caused by the relaxation force. In fact this force depends on the electrolytic concentration in such a way that a maximum in cataphoretic mobility is possible even when ζ increases continually. Thon[34] states that sometimes minima are found, but this statement is slightly misleading. For by a maximum in U is meant a maximum in the absolute value of U. The cataphoretic velocity being negative in the majority of cases, the maximum in $|U|$ is a minimum in U. The

* Basing himself upon Paine's calculations, Gilford[11] arrives at a very different conclusion. We have already seen, however, that Paine's results[29] only hold good for $\chi R \ll 1$, whereas Gilford applies them to the case where $\chi R \gg 1$.

minima Thon refers to are exceptional cases where the ζ-potential is positive. Plotted in the same diagram the extreme values in these cases may give an expression of being minima, though in reality they are maxima.

The problem is of considerable interest because of the question whether ζ shows a maximum or whether such a maximum is only apparent. Kruyt and van der Willigen[19] also considered the maximum as apparent, but caused by an increase in the dielectric constant when an electrolyte is added. White and Monaghan[38], however, considered the variation in the dielectric constant to be too small to be responsible for this phenomenon. Whether the relaxation force gives the correct explanation it is impossible to say without a determination of the ζ-potential independently of cataphoretic velocity. The solution of this problem might also give an answer to the question why there is not always correlation between cataphoretic velocity and coagulation rate[42].

§4. *Calculation of ζ from other Data.*

As is well known, the ζ-potential is connected with the charge e of the particle. The easiest way to find this connexion is as follows. The theory of Debye and Hückel yields the following expression for the potential in the neighbourhood of the particle :

$$\psi^0(r) = \frac{e}{D}\frac{e^{\chi R}}{1+\chi R}\frac{e^{-\chi r}}{r}. \quad . \quad . \quad . \quad . \quad (6)$$

Remembering that $\zeta = \psi^0(R)$, we find in the case of very small χR

$$e = RD\zeta, \quad . \quad . \quad . \quad . \quad . \quad . \quad (7)$$

and in the case of very large χR

$$e = \chi R^2 D\zeta. \quad . \quad . \quad . \quad . \quad . \quad . \quad (8)$$

It may be useful to remember that the latter formula is nothing but the condenser formula which expresses that the charge density $e/4\pi R^2$ is equal to $D\zeta/4\pi d$, with $d = 1/\chi$.

The formulæ (7) or (8) make it possible to compare the potential determined electrokinetically with the charge e determined by direct means. But serious discrepancies occur if this method is used[30], [16]. Rutgers and Overbeek[31] try to explain these discrepancies by distinguishing between the gegenions in the layer of water

adherent to the particle (called "Smoluchowsky-layer" by them) and the gegenions in the surrounding liquid. Rutgers[32] himself, however, mentions some very serious difficulties which have to be overcome if one accepts this model.

The author considers the discrepancies to be entirely the result of the relaxation effect during cataphoresis, as has already been suggested by Overbeek[28]. We have already seen in § 2 that the correction for relaxation becomes very large if the particle is a conductor, and this is the reason why the calculated charge, especially of gold sols*, is so markedly different from that determined by direct methods. The difference is much less important with non-conducting particles. Furthermore, it should not be forgotten that the difference is less important than suggested by Pauli and Valko[30], for these authors use the formula $U = eE/6\pi\eta R$ to calculate the charge e from the cataphoretic velocity U. This would be correct if χR could be neglected compared with unity. In most cases $\chi R \approx 1$, and the correction for relaxation and for the electrophoretic effect may then easily amount to 50 per cent.

The figures mentioned by Pauli and Valko[30] are given in the following table :—

	Albumin-chloride.	Cr_2O_3.	Fe_2O_3 (average).	Gold (average).
z_1	21	30	20·000	40·000
z_2	6	7	60	30

Here z_1 is the number of elementary charges determined by direct means and z_2 that which has been calculated from the cataphoretic velocity. One can hardly speak of a discrepancy in the first two cases if one considers that, because of the relaxation effect ,the true value of z_2 could easily have been twice as large, and further, that the value of z_1 is usually too high[30]. The cases of both iron oxide and gold are different. Even Pauli and Valko's[30] speculation that z_1 may be 10 or 100 times too large could not possibly make the values of z_1 and z_2 coincide. The measurements of Wintgen[40] with gold sols and those

* Pauli-Valko[30], p. 498: "Diese Diskrepanz erreicht gerade bei den Goldsolen einen ausserordentlichen Grad."

of Wintgen and Biltz[41] with iron oxide sols are in agreement with this conclusion.

§ 5. *Distortion of the Ion-sphere for* $\chi R \gg 1$.

In the limit of very large χR the double layer may be treated as one on a plane wall. We shall use Debye-Hückel's approximation for the potential:

$$\psi^0 = \zeta e^{-\chi y},$$

y being the distance from the wall. To give this a convenient form for the case of a sphere with radius R, we write

$$r = R(1+\sigma) \quad . \quad . \quad . \quad . \quad . \quad . \quad (9)$$

for the distance r of a point in the double layer from the centre of the sphere. Further, we abbreviate

$$h = \chi R, \quad (h \gg 1), \quad . \quad . \quad . \quad . \quad . \quad (10)$$

and find for the potential

$$\psi^0 = \zeta e^{-h\tau}. \quad . \quad . \quad . \quad . \quad . \quad . \quad (11)$$

If one wishes to account for the curvature of the surface one has to remember equation (6), which can be written as a first approximation:

$$\psi^0 = \zeta(1-\sigma)e^{-h\sigma}. \quad . \quad . \quad . \quad . \quad . \quad (12)$$

As h is large, ψ^0 diminishes very rapidly with increasing σ, and soon vanishes even for small values of σ. The influence of the curvature is, therefore, very small, and we shall only be concerned with it in those cases where the application of equation (11) yields zero as a result.

If n_κ is the average number of ions with charge e_κ in a unit of volume, the concentration of these ions in the double layer is

$$f_\kappa{}^0 = n_\kappa(1-e_\kappa\psi^0/kT). \quad . \quad . \quad . \quad . \quad (13)$$

The formulæ used here are the solution of the differential equation $\Delta\psi^0 = \chi^2\psi^0$, deduced from the original Debye-Hückel differential equation

$$\Delta\psi^0 = -\frac{4\pi}{D}\Sigma f_\kappa{}^0 e_\kappa \text{ ; with } f_\kappa{}^0 = n_\kappa \exp(-e_\kappa\psi^0/kT), \quad . \quad . \quad (14)$$

by omitting powers of ψ^0 higher than the first. Now, in the case of a plane wall an exact solution of (14) is possible[3],[4]. The theory developed in this section becomes very complicated, however, if this exact solution of (14) is introduced, and for several reasons there seems to be little advantage in doing so. For, especially in the case of large χR, we are often concerned with rather small ζ-potentials, where the difference

between the two solutions is not very important. Further, the difference is greatest in the immediate neighbourhood of the surface of the particle, and it will be shown that the points in its immediate vicinity do not contribute appreciably to the results obtained. Finally, the original differential equation (14) cannot itself be regarded as exact[12],[17],[20],[26], so that its use is not a sufficient guarantee for a correct solution.

If an external field E is applied in the direction of the x-axis, an extra potential Π is set up, given by (2) §1, which satisfies the condition $\Delta\Pi=0$. The particle acquires a velocity U in the direction of the x-axis and generates a flow of liquid, the divergence of which is zero on account of incompressibility. Following Henry, the centre of the particle will be taken as the origin of the coordinates, *i. e.*, the liquid flows in the direction of the x-axis with a velocity $-U$.

The equation of motion of an ion with charge e_κ has the form

$$\rho_\kappa v_\kappa = -kT/f_\kappa . \operatorname{grad} f_\kappa - e_\kappa \operatorname{grad}(\psi+\Pi) + \rho_\kappa q. \quad . \quad (15)$$

Here ρ_κ is a frictional factor, inversely proportional to the mobility l_κ of the ion considered, viz.[14],

$$\rho_\kappa = \frac{15.10^{-8}}{l_\kappa} \cong 2.10^{-9} \text{ c.g.s.} \quad . \quad .. \quad . \quad (16)$$

Further, ψ is the potential of the ion-sphere, q is the flow of liquid, v_κ the velocity of the ion. The first term on the right-hand side of (15) is the diffusion term, the second is due to the electric force on the ion, the third expresses the fact that the liquid transmits its motion to the ion. With the aid of the equation of continuity,

$$\frac{\partial f_\kappa}{\partial t} + \operatorname{div}(f_\kappa v_\kappa) = 0,$$

one deduces from (15) :

$$\rho_\kappa \frac{\partial f_\kappa}{\partial t} = kT\Delta f_\kappa + \operatorname{div}[f_\kappa e_\kappa \operatorname{grad}(\psi+\Pi)] - \rho_\kappa \operatorname{div}(f_\kappa q). \quad (17)$$

If there are s ion-species, there are s of these equations of motion, while, moreover, Poisson's equation has to be met :

$$\Delta\psi = -\frac{4\pi}{D}\Sigma f_\kappa e_\kappa.$$

It is clear that with uniform motion $\partial f_\kappa/\partial t=0$, as the axis of coordinates is attached to the particle. Further, we apply Debye-Hückel's approximation, which amounts

to replacing $f_\kappa \operatorname{grad} \psi$ by $n_\kappa \operatorname{grad} \psi$. The equations of motion then become

$$kT\Delta f_\kappa + n_\kappa e_\kappa \Delta\psi = -\operatorname{div}(f_\kappa e_\kappa \operatorname{grad} \Pi) + \rho_\kappa \operatorname{div}(f_\kappa q).$$

We now write

$$f_\kappa = f_\kappa^0 + \nu_\kappa\,;\ \psi = \psi^0 + \phi, \quad . \quad . \quad . \quad . \quad (18)$$

and restrict ourselves to those terms in ν_κ and ϕ which are linear in E (or U). This is permissible as long as the cataphoretic velocity is proportional to the external field, a condition which in practice is always fulfilled. This also means that $f_\kappa \operatorname{grad} \Pi$ and $f_\kappa q$ may be replaced by $f_\kappa^0 \operatorname{grad} \Pi$ and $f_\kappa^0 q$. Now $\Delta\Pi$ and div q are both zero; furthermore, f_κ^0 has spherical symmetry, and the only component of grad f_κ^0 which differs from zero lies, therefore, in the direction of r. Hence, with the aid of (2) § 1, we get

$$\operatorname{div}(f_\kappa^0 \operatorname{grad} \Pi) = \frac{df_\kappa^0}{dr}\frac{\partial \Pi}{\partial r} = -\frac{df_\kappa^0}{d\sigma}\frac{\mathrm{E}}{\mathrm{R}}\left(1 - \frac{2\lambda \mathrm{R}^3}{r^3}\right)\cos\theta,$$

$$\operatorname{div}(f_\kappa^0 q) = \frac{df_\kappa^0}{dr} q_r = \frac{df_\kappa^0}{d\sigma}\frac{q_r}{\mathrm{R}},$$

q_r being the component of q in the direction of r. Remembering equation (13), and neglecting the influence of the curvature, we finally get

$$kT\Delta\nu_\kappa + n_\kappa e_\kappa \Delta\phi = \mathrm{E}\frac{\chi\zeta}{kT} e_\kappa n_\kappa^2 \left(1 - \frac{2\lambda \mathrm{R}^3}{r^3}\right) e^{-\hbar\sigma}\cos\theta + \frac{\chi\zeta}{kT} n_\kappa e_\kappa \rho_\kappa q_r e^{-\hbar\sigma}, \quad . \quad (19)$$

$$\Delta\phi = -\frac{4\pi}{\mathrm{D}} \Sigma \nu_\kappa e_\kappa. \quad . \quad . \quad . \quad . \quad . \quad (20)$$

Introducing the quantity

$$\mathrm{S} = \Sigma \nu_\kappa e_\kappa, \quad . \quad . \quad . \quad . \quad . \quad . \quad (21)$$

i. e., the extra charge density due to distortion, it is easily deduced from (19), (20) that S satisfies the differential equation

$$\Delta\mathrm{S} - \chi^2\mathrm{S} = \frac{\mathrm{E}}{kT}\frac{\Sigma n_\kappa e_\kappa^3}{kT}\chi\zeta\left(1 - \frac{2\lambda \mathrm{R}^3}{r^3}\right)e^{-\hbar\sigma}\cos\theta + \frac{q_r}{kT}\frac{\Sigma n_\kappa e_\kappa^2 \rho_\kappa}{kT}\chi\zeta e^{-\hbar\sigma}. \quad . \quad (22)$$

Before substituting the expression for q_r we shall consider more closely the first term on the right-hand side of equation (22). As h is large, $1-2\lambda R^3/r^3$ may be expanded in powers of σ. Values of σ which are considerably larger than $1/h$ play practically no part in the calculation, because $\exp(-h\sigma)$ vanishes very rapidly with increasing σ. We get

$$\Delta S - \chi^2 S = \frac{E}{kT} \frac{\Sigma n_\kappa e_\kappa^3}{kT} \chi\zeta(1-2\lambda+6\lambda\sigma)e^{-h\sigma} \cos\theta + \frac{q_r}{kT} \frac{\Sigma n_\kappa e_\kappa^2 \rho_\kappa}{kT} \chi\zeta e^{-h\sigma}. \quad . \quad (23)$$

Now q_r is zero for $\sigma=0$. Obviously, therefore, two entirely different cases will have to be considered, according as λ is different from, or exactly equal to, $\frac{1}{2}$. In the first case the particle is a conductor; the lines of force of the external field have a component along r on the surface, and, therefore, bring about an important change in the distribution of ions close to the surface. In the second case the influence of the external field is zero in the immediate neighbourhood of the surface, and becomes different from zero only for $\sigma \neq 0$.

From the fact that only such values of σ which are of the order $\leqq 1/h$ play a part in the calculation, it is readily seen that the term with $1-2\lambda$ in (23) will exert an influence on S (and, therefore, on the relaxation), the order of which is h times that of the other terms. As will be shown, however, these other terms already lead to relaxation forces which are comparable with the Stokes resistance. The classical formula for the cataphoretic velocity becomes, therefore, meaningless in the case of conducting particles, and it is useless to correct it for relaxation by the method shown in this section. For conducting particles the theory of cataphoresis will have to be reconsidered, taking into account from the very beginning the forces on the surrounding ions. An extra complication will be introduced because of the part played by the particle itself in the motion of the ions. For, during motion in the electrolyte, both sides of the particle will act as electrodes, and a current will be set up in the surrounding solution [18].

Henceforth we shall assume $\lambda=\frac{1}{2}$. In that case we must determine the solution of (23), which is zero on the

surface of the sphere. For, both the flow of liquid and the perpendicular component of the external field are zero on the surface, *i. e.*, the distribution of ions in the immediate vicinity of the surface remains unaltered. This circumstance is also responsible for the fact that the potential gradient close to the wall is of little account in the calculation, so that the error introduced by the use of Debye-Hückel's approximation, and which, of course, is largest near the wall, becomes less serious.

The expression for q_r has been derived by Henry[13]. In the notation used by us it runs :

$$q_r=\left[-f(r)\mathrm{U}+\frac{\mathrm{DE}}{6\pi\eta}l(r)-\frac{\mathrm{DE}}{4n\eta}\left(\frac{\mathrm{R}}{r}-\frac{\mathrm{R}^3}{3r^3}\right)\int_\infty^{\mathrm{R}}\xi\,dr\right]\cos\theta, \quad \ldots \quad (24)$$

where

$$\xi=\frac{d\psi^0}{dr}+\lambda\mathrm{R}^3r\int_\infty^r\frac{\Delta\psi^0}{r^3}\,dr,$$

$$l(r)=\int_\infty^r\xi\,dr-\frac{1}{r^3}\int_{\mathrm{R}}^r r^3\xi\,dr,$$

$$f(r)=1-\frac{3}{2}\frac{\mathrm{R}}{r}+\frac{1}{2}\frac{\mathrm{R}^3}{r^3}.$$

This expression for q_r was obtained by integration of the hydrodynamical equations of Stokes. The term $-f(r)\mathrm{U}$ is the ordinary Stokes solution in the absence of an external electric field. It has been shown by Oseen[27] that the picture of the flow of liquid as given by the solution of these equations is inaccurate for large values of r ; in the immediate neighbourhood of the sphere, however (*i. e.*, for small values of σ), it holds good. The rather complicated expression (24) is considerably simplified if the formula (12) for ψ^0 is introduced. We must now take into account the influence of the curvature, because q_r is zero on the sphere ; in other words, we are concerned with quantities which are zero for $\sigma=0$. Powers of r are always expanded in terms of σ, for instance

$$\frac{\Delta\psi^0}{r^4}=\frac{\chi^2\psi^0}{\mathrm{R}^4(1+\sigma)^4}=\frac{\chi^2\zeta}{\mathrm{R}^4}(1-5\sigma)e^{-h\sigma},$$

$$\int_\infty^r\frac{\Delta\psi^0}{r^4}\,dr=\mathrm{R}\int_\infty^\sigma\frac{\Delta\psi^0}{r^4}\,d\sigma=\frac{\chi^2\zeta}{\mathrm{R}^3}\left(\frac{-1}{h}+\frac{5}{h^2}+\frac{5\sigma}{h}\right)e^{-h\sigma}.$$

The calculation is a simple one, and always makes use of similar approximations. It will, therefore, suffice to mention the result,

$$q_r = \left\{ -\frac{3}{2}\sigma^2 U + \frac{3DE\zeta}{4n\eta}\left(-\sigma + \frac{1}{h} - \frac{1}{h}e^{-h\sigma}\right)\right\}\cos\theta \quad . \quad (25)$$

In this equation U has the same order of magnitude as $DE\zeta/4\pi\eta$. Properly speaking, $\sigma^2 U$ belongs, therefore, to quantities which are neglected in (25). This term, however, is the only one which remains if no external field is applied (§ 8), and for this reason we shall retain it in the differential equation (23), which now becomes

$$\Delta S - \chi^2 S = \left\{\left(\frac{\alpha E}{h} + \beta E\sigma\right)e^{-h\sigma} - \frac{\alpha E}{h}e^{-2h\sigma} - \frac{3}{2}\gamma U\sigma^2 e^{-h\sigma}\right\}\frac{\cos\theta}{R^2}, \quad . \quad (26)$$

where we abbreviated

$$\left.\begin{aligned} \gamma &= \frac{R^2\chi^3 D\zeta}{4\pi kT}\,\frac{\Sigma n_K e_K^2 \rho_K}{\Sigma n_K e_K^2}\,; \quad \alpha = \frac{3D\zeta}{4\pi\eta}\gamma, \\ \beta &= 3\frac{R^2\chi^3 D\zeta}{4\pi kT}\,\frac{\Sigma n_K e_K^3}{\Sigma n_K e_K^2} - \alpha. \end{aligned}\right\} \quad . \quad (27)$$

In § 8 we shall be concerned with a motion without external electric field ; for the present we may neglect the last term in equation (26), which becomes

$$\Delta S - \chi^2 S = \left\{\left(\frac{\alpha E}{h} + \beta E\sigma\right)e^{-h\sigma} - \frac{\alpha E}{h}e^{-2h\sigma}\right\}\frac{\cos\theta}{R^2}. \quad (28)$$

To solve this differential equation we try

$$S = g(\sigma)\cos\theta. \quad . \quad . \quad . \quad . \quad . \quad . \quad (29)$$

Then $\Delta S = (g''/R^2 + 2g'/rR - 2g/r^2)\cos\theta$, or, in our order of approximation, $\Delta S = 1/R^2 . (g'' + 2g' - 2g)\cos\theta$. Obviously, however, the rate at which $g(\sigma)$ decreases with increasing σ has the same order of magnitude as that at which the functions ψ^0, f_K^0 decrease, viz., as $\exp(-h\sigma)$. This means that g and g' may be neglected compared with g'', the error being of the order $1/h$. Hence (28) becomes

$$g'' - h^2 g = \left(\frac{\alpha E}{h} + \beta E\sigma\right)e^{-h\sigma} - \frac{\alpha E}{h}e^{2h\sigma}, \quad . \quad (30)$$

with the boundary conditions $g(\infty)=0$; $g(0)=0$, the solution of which is

$$g(\sigma)=\left(\frac{\alpha E}{3h^3}-\frac{2\alpha+\beta}{4h^2}E\sigma-\frac{\beta E}{4h}\sigma^2\right)e^{-h\sigma}-\frac{\alpha E}{3h^3}e^{-2h\sigma}. \quad (31)$$

Remembering the nature of our approximations, it is clear that this result is accurate to within a few parts per cent. for $h=\chi R\geq 50$. It is, however, to be expected that the theory will yield a fairly good approximation even for values of h down to 25.

§ 6. *Cataphoresis.*

The charge $Sd\tau=g(\sigma)\cos\theta.d\tau$ in an element of volume $d\tau$ exerts an electric force on the particle, the resultant of which lies in the direction of the x-axis, and has the value

$$-2\pi\int_R^\infty dr\int_0^\pi d\theta\frac{eS}{Dr^2}\cos\theta.r^2\sin\theta$$
$$=-\frac{4}{3}\pi R\frac{e}{D}\int_0^\infty g(\sigma)d\sigma=\frac{4}{3}\pi R\frac{eE}{D}\frac{4\alpha+9\beta}{12h^4},$$

where $e=\chi R^2D\zeta$ is the charge of the particle. It has been assumed here that the distribution of charge in the particle itself retains its spherical symmetry. Instead of (4) § 1, the total force on the sphere becomes

$$\frac{3}{2}DR\zeta E-6\pi\eta RU+\frac{4}{3}\pi\chi\zeta ER^3\frac{4\alpha+9\beta}{12h^4}=0.$$

Hence

$$U=\frac{D\zeta E}{4\pi\eta}\left(1+\frac{8\pi}{9}\frac{\chi R^2}{D}\frac{4\alpha+9\beta}{12h^4}\right).$$

Substituting the values (27) for α and β, we get

$$U=\frac{D\zeta E}{4\pi\eta}\left\{1+\frac{\zeta}{2kT}\frac{\Sigma n_K e_K^3}{\Sigma n_K e_K^2}-\frac{5\zeta}{18kT}\frac{D\zeta}{4\pi\eta}\frac{\Sigma n_K e_K^2\rho_K}{\Sigma n_K e_K^2}\right\}. \quad (32)$$

Several conclusions may be drawn from this result :—

(1) It may be noticed that the correction terms do not depend on R or on the electrolytic concentration, if only the condition $\chi R\geq 25$ is fulfilled. We first want to examine the order of magnitude of the second correction term. In the case of water at room-temperature, $\eta=10^{-2}$,

D=80, T=300. To express ζ in mv., it may be remembered that 1 e.s.u. $=3.10^5$ mv., which gives

$$\frac{5}{18}\frac{D\rho\zeta^2}{4\pi\eta kT}=\frac{5}{18}\cdot\frac{80.2.10^{-9}}{16.3.10^{-16}}\frac{\zeta^2}{9.10^{10}}\cong 10^{-4}\zeta^2.$$

For $\zeta=50$ mv. this is a correction of 25 per cent.; it reduces the absolute value of U, and rapidly decreases with decreasing ζ-potential. The influence of the first correction term is generally far more important. This term may be negative or positive, according as ζ and $\Sigma n_\kappa e_\kappa^3$ are negative or positive. It is zero when the electrolyte is symmetrical, because then $\Sigma n_\kappa e_\kappa^3=0$. In non-symmetrical electrolytes the order of magnitude becomes

$$\frac{e\zeta}{2kT}=\frac{5.10^{-10}}{8.10^{-14}}\frac{\zeta}{3.10^5}=0{\cdot}027\,\zeta,$$

i. e., a correction of 27 per cent. for a rather small value of $\zeta=10$ mv. For larger absolute values of ζ, the cataphoretic velocity may even change its sign, while ζ does not. Secondary effects will, of course, play a part when the correction becomes so large; the imperfections in Debye-Hückel's theory and the approximate character of our calculations will then make themselves felt. In general, therefore, caution should be exercised when drawing conclusions from cataphoretic velocities in the case of non-symmetrical electrolytes.

(2) As already stated in § 1, the electrosmotic and the cataphoretic velocity will as a rule be different. The difference will only be small if the electrolyte is symmetrical and the ζ-potential not too large. In the case of electrosmosis, too, relaxation effects will occur[3] [18], at both ends of the capillary tube. But it is to be expected that, relatively speaking, the longer the capillary tube the less important will this effect be. Moyer[24], who finds the cataphoretic velocity of gelatine-coated particles to be the same as the electrosmotic velocity along a gelatine-coated wall, explains this result by assuming the "effective" χR to be the same in both cases, meaning that the "effective" value of R would be determined by the dimensions of the coating molecules and not by those of the particle. White[37], [38], however, finds the two velocities to be different, while they become equal

when χR approaches 30, which in the case of symmetrical electrolytes is in accordance with the theory developed here. For, with large values of χR, ζ generally is so small that the second correction-term in (32) amounts to less than 10 per cent., which lies within experimental error.

(3) According to the theory developed in this section, Freundlich and Abramson's [2], [10] observations that the cataphoretic velocity is independent of the shape of the particle can only hold good approximately. It is clear that relaxation forces similar to those encountered with spheres will occur with non-spherical particles. At this stage it seems impossible to foretell the extent to which the result will differ from the formula found here. Nor is the accuracy of the measurements such as to warrant a decision based on experimental data.

(4) Apparently the relaxation may be responsible for considerable differences between the particle charge determined by direct means and that calculated from cataphoretic velocity. In the case of conducting particles the cataphoretic velocity does not even yield the right order of magnitude (*cf.* § 4).

(5) The formula (32) does not throw much light on the extreme values discussed in § 3. In fact these extreme values generally occur with electrolytic concentrations where χR is no longer large compared with unity, and where the formula (32) cannot be applied. On the one hand a term with $\zeta \Sigma n_\kappa e_\kappa^3$ remains. On the other hand the Stokes's flow of liquid round the particle will now also play a part in the relaxation, which introduces a considerable negative correction in the formula for U. We have already seen, however, that Stokes's solution does not give an accurate picture of the flow of liquid except for very small distances from the particle [27]. At present an exact solution for those cases where $\chi R \approx 1$ must, therefore, be regarded as impossible. An approximate solution for the other extreme case where $\chi R \ll 1$ has been obtained by simply ignoring the flow of liquid round the particle [14], [29]. In any case, in view of the large order of magnitude of the correction terms in those cases where a calculation is possible it seems that the maximum value in U may easily be explained by the relaxation force. A definite conclusion must be delayed until further evidence has been obtained.

Appendix.

Many a reader may be surprised that the correction for relaxation sometimes becomes positive. We shall, therefore, complete our treatment by giving a rough physical picture of the process of relaxation. Let us assume the ζ-potential to be negative; our considerations, *mutatis mutandis*, will apply to a positive ζ-potential. We first remember that Debye-Hückel's approximation was used throughout the whole treatment, *i. e.*, we started with an original distribution of ions given by eq. (13), § 5, $f_K^0 = n_K - n_K e_K . \psi^0/kT$. Now in any electrolyte the value of $n_K e_K$ for the one ion is equal to that for the other with opposite sign. In other words, if we plot the concentration of the ions against the distance y from the surface of the particle, the deviation from the average concentration will be the same for both ions.

First case: the electrolyte is symmetrical (fig. 1). The original distribution of ions is given by the full curves. If an external electric field E is now applied, the positive ions tend to shift towards the left (dotted curve). The negative ions experience a force of the same magnitude towards the right. The result in first approximation will be that the

Fig. 1.

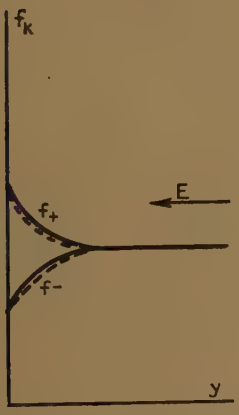

Fig. 2.

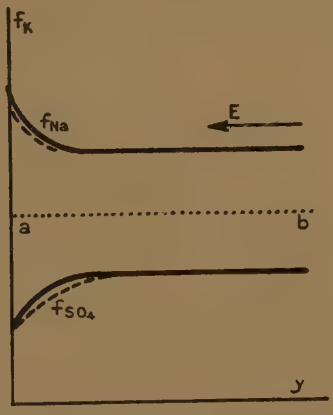

concentration of both the positive and the negative ions in the double layer is reduced to the same extent, *i. e.*, the extra charge density S is zero. This explains why the first correction term is zero in symmetrical electrolytes.

Second case: the electrolyte is of the type Na_2SO_4 (fig. 2). In this case $\zeta \Sigma n_K e_K^3$ is positive; according to formula (32) the relaxation will then enlarge the cataphoretic velocity. In fact the original distribution of the ions is given by the full curves in fig. 2. In Debye-Hückel's approximation these curves are symmetrical with respect to *ab*. If an external field E is applied, the particle will move towards the right, while at the same time the Na-ions experience a force towards the left and the SO_4-ions experience a force towards the right. The force on a SO_4-ion, however, is twice as large as that on a Na-ion, with the result that the concentration of SO_4-ions in the double layer is reduced to a larger extent than that of the Na-ions. The extra charge density will be positive, the relaxation force on the particle has the same direction as the velocity of the particle, *q.e.d.*

A similar consideration shows that the correction for relaxation is negative with electrolytes such as $BaCl_2$ ($\zeta \Sigma n_K e_K^3 < 0$).

§7. *Henry's Theory viewed in Retrospect.*

To calculate the distortion of the ion-sphere in §5 we used the expressions q and Π as found by Henry for the flow of liquid and the potential of the external field. These expressions were, however, derived by Henry, assuming that the original electric field round the particle retained spherical symmetry, and we must, therefore, investigate whether the deformation of the double layer necessitates alterations in Henry's theory. To that end we shall first examine more closely Henry's theory itself.

The expression for the external field Π as given by (3) was found by Henry as the solution of the differential equation $\Delta\Pi=0$, with the boundary conditions, $\Pi=-\mathrm{E}x$ at infinity, $\Pi=\Pi'$ and $\partial\Pi/\partial\theta=\partial\Pi'/\partial\theta$ on the sphere, while, moreover,

$$\mu\frac{\partial\Pi}{\partial r}=\mu'\frac{\partial\Pi'}{\partial r} \text{ on the sphere.} \quad . \quad . \quad . \quad (33)$$

Here Π' is the potential in the interior of the sphere. μ is the specific conductivity. The product $\mu\partial\Pi/\partial r$ is the electric current in a direction perpendicular to the surface ; equation (33) expresses the fact that this current has the same value both outside and inside the sphere. The potential Π thus found plays a rôle in Stokes's equations of motion for the liquid. Integrating these equations of motion, the flow of liquid is found, and from it the resistance experienced by the sphere.

We wish to call attention to a peculiarity which is very important to a proper understanding of cataphoresis. In the case of a very thin double layer, *i. e.*, $\chi\mathrm{R}\gg 1$, Henry finds for the total resistance $6\pi\eta\mathrm{RU}-(1+\lambda)\mathrm{RD}\zeta\mathrm{E}+e\mathrm{E}$, where $e=\chi\mathrm{R}^2\mathrm{D}\zeta$ is the charge of the sphere. Apparently the last term is about $h=\chi\mathrm{R}$ times as large as the other ones. This term $e\mathrm{E}$ is, however, cancelled by the electric force $e\mathrm{E}$ which acts on the particle ; in other words, the total force on the particle, which is zero in the case of uniform motion, is the difference between two forces which are large as compared with the resulting force itself. We may conclude that the calculated cataphoretic velocity is very sensitive towards small errors in the equations of motion. In general a relative error ξ in these equations will result in a relative error

of the order $h\xi$ in the cataphoretic velocity. This must be borne in mind in the following discussion.

When the distribution of charge loses its spherical symmetry, the equation (33) takes on a different form. From (15) it may be concluded that the electric current becomes

$$\Sigma f_\kappa e_\kappa v_\kappa = -\Sigma\left[kT\frac{e_\kappa}{\rho_\kappa}\operatorname{grad} f_\kappa + \frac{f_\kappa e_\kappa^2}{\rho_\kappa}\operatorname{grad}(\psi+\Pi) - f_\kappa e_\kappa q\right].$$

On the surface of the sphere $q=0$. Hence, condition (33) now becomes

$$\mu'\frac{\partial \Pi'}{\partial r} = \Sigma\frac{e_\kappa}{\rho_\kappa}\left[kT\frac{\partial f_\kappa}{\partial r} + f_\kappa e_\kappa\frac{\partial(\psi+\Pi)}{\partial r}\right]_{r=R} \quad . \quad (34)$$

With Henry's assumption that $f_\kappa = f_\kappa^0$ and $\psi = \psi^0$, (34) becomes identical to (33), as the factor $\Sigma f_\kappa e_\kappa^2/\rho_\kappa$ is nothing but the specific conductivity μ. Introducing the notation of § 5, equation (34) becomes

$$\mu'\frac{\partial \Pi'}{\partial r} = \Sigma\frac{e_\kappa}{\rho_\kappa}\left[kT\frac{\partial \nu_\kappa}{\partial r} + n_\kappa e_\kappa\frac{\partial \phi}{\partial r} + f_\kappa^0 e_\kappa\frac{\partial \Pi}{\partial r}\right]_{r=R}.$$

To use Henry's expression for Π amounts to neglecting the terms with ν_κ and ϕ. Obviously this means a relative error in Π of the order

$$\frac{kT\,\Sigma\nu_\kappa e_\kappa/\rho_\kappa}{\Pi\Sigma f_\kappa^0 e_\kappa^2/\rho_\kappa} \simeq \frac{kT\,\Sigma\nu_\kappa e_\kappa}{\Pi\,\Sigma n_\kappa e_\kappa^2} = \frac{4\pi S}{\Pi D\chi^2} \simeq \frac{4\pi g(\sigma)}{ERD\chi^2}.$$

To determine the order of magnitude of this expression we use (31) and successively substitute $g(\sigma)=\alpha E/3h^3$ and $g(\sigma)=\beta E/4h^3$. We then find the following order of magnitude for the relative error :

$$\frac{D\zeta^2}{4\pi\eta}\frac{\rho}{kT}\frac{1}{h^2} \text{ and } \frac{e_\kappa\zeta}{kT}\frac{1}{h^2} \text{ respectively.}$$

Expressing ζ in mv., and substituting the usual values for D, k, T, η, ρ, we get $10^{-3}\zeta^2/2h^2$ and $\zeta/30h^2$ respectively. Generally both ratios are of the order of $1/h^2$. One may therefore conclude that relative errors of the order of $1/h^2$ occur in the expression for Π, and thus in the equations of motion for the liquid. We know that a relative error of the order of $1/h$ may then occur in the cataphoretic velocity. In our order of approximation this error may be neglected. Once more, however, it appears that the

theory breaks down in the case of conducting particles; for S would then be about h times as large, the relative error in Π would be of the order of $1/h$, and that in the cataphoretic velocity of the order of unity, even irrespective of the correction for relaxation, which in this case becomes enormous.

§8. *Sedimentation Potential.*

If the particle is moving in the absence of an external electric field, for instance, under the influence of gravitation, the distortion of the double layer may be calculated in the same way as has been done in §5. The differential equation (26) for the extra charge density S now becomes

$$\Delta S-\chi^2 S=-\frac{3}{2}\gamma U\sigma^2 e^{-h\sigma}\frac{\cos\theta}{R^2}, \quad . \quad . \quad (35)$$

where

$$\gamma=R^2\frac{\chi^3 D\zeta}{4\pi kT}\frac{\Sigma n_\kappa e_\kappa^2\rho_\kappa}{\Sigma n_\kappa e_\kappa^2}. \quad . \quad . \quad . \quad . \quad (36)$$

Writing once more $S=g(\sigma)\cos\theta$, and using the same approximations as in §5, the differential equation for g becomes

$$g''-h^2 g=-\tfrac{3}{2}\gamma U\sigma^2 e^{-h\sigma}.$$

The solution must be zero on the surface of the sphere for the same reason as before, and runs

$$g(\sigma)=\left(\frac{\sigma}{4h^3}+\frac{\sigma^2}{4h^2}+\frac{\sigma^3}{6h}\right)\frac{3}{2}\gamma U e^{-h\sigma}. \quad . \quad . \quad (37)$$

The relaxation force is of the order of $1/h$ times that which has been calculated in the case of cataphoresis. It will amount to only a few parts per cent. of the Stokes resistance even in the case of a large ζ-potential, and it may therefore be neglected. It will be much more interesting to consider the direct result of the extra charge density S, which makes the particle with its double layer behave like a dipole $\mu=\int Sx\,d\tau$, where the integration has to be extended over the whole space round the sphere. We find

$$\mu=2\pi\int_R^\infty dr\int_0^\pi d\theta S.r\cos\theta.r^2\sin\theta=\frac{4}{3}\pi\int_R^\infty g(\sigma)r^3\,dr.$$

To our order of approximation this may be written

$$\mu = \frac{4}{3}\pi R^4 \int_0^\infty g(\sigma)\, d\sigma = \frac{4}{3}\pi R^4 \frac{21}{8}\frac{\gamma U}{h^5},$$

i. e., with the value (36) for γ:

$$\mu = \frac{7}{8}\frac{RD\zeta U}{\chi^2 kT}\frac{\Sigma n_\kappa e_\kappa^2 \rho_\kappa}{\Sigma n_\kappa e_\kappa^2}. \quad . \quad . \quad . \quad . \quad (38)$$

If there are n particles per unit of volume these particles generate a potential gradient $X = 4\pi\mu n/D$. This result may be applied to the case of particles of density s which fall down in a liquid of density s_0. The velocity of sedimentation is easily found to be

$$U = \frac{2}{9}\frac{g}{\eta} R^2 (s - s_0),$$

where g is the acceleration of gravity. The potential gradient X becomes

$$X = \frac{4}{3}\pi R^3 (s - s_0) n \frac{7}{12}\frac{\zeta}{\chi^2 kT}\frac{g}{\eta}\frac{\Sigma n_\kappa e_\kappa^2 \rho_\kappa}{\Sigma n_\kappa e_\kappa^2}. \quad . \quad (39)$$

If M is the mass of suspended substance per unit of volume, taking water at room-temperature as the solvent, X has the order of magnitude

$$X \cong M\frac{\zeta g \rho}{\chi^2 kT\eta} = 10^{10}\frac{M\zeta}{\chi^2}.$$

Apparently the size of the particles plays no part in this result; this size is only important in so far as χ may be the smaller the larger R, because χR must be large compared with unity. With a radius $R = 10^{-4}$ cm. χ may be taken as small as $3 \cdot 10^5$, which corresponds to an electrolytic concentration of about 10^{-4} grmol per litre. In that case X becomes $M\zeta/10$, which may amount to a few tenths of a millivolt. With macroscopic particles, distilled water with $\chi = 10^4$ may be used, in which case X may amount to some 10 millivolts.

It would seem that sedimentation potentials have seldom been determined. Dorn[7] records a few determinations with glass beads, Burton and Currie[43] used lead shot; a sand-jet in water has been under observation[33], while Billitzer[5] and Mäkelt[21] used powdered silver or a silver

coil. All these measurements, however, are only of a qualitative character, for the concentration of the powder, for instance, is nowhere stated. It would appear to us that formula (39) may be utilized in the study of sedimentation. A clear idea of the course of the sedimentation can be obtained by measuring the potential difference between various fixed points, because the volume of suspended material between these points can be calculated from this potential difference. This method seems simpler, and is probably more accurate than that of weighing[9], as the sedimentation is in no way influenced.

Summary.

When charged spherical particles move in an electrolytic solution the double layer is deformed. The theory of this phenomenon can be developed if the double layer is very thin as compared with the radius of the particle. In § 5 this is worked out for the motion under the influence of an external electric field (cataphoresis), and in § 8 for a motion in the absence of an external electric field (sedimentation potential).

The final formula for the cataphoretic velocity (§ 6) shows (1) that maxima may occur in the cataphoretic velocity with continually increasing absolute value of the ζ-potential (§ 3); (2) that the charge of the particles as calculated from the cataphoretic velocity will not as a rule tally with the charge determined by direct means (§ 4), particularly if the particle is a conductor (*cf.* also § 7); (3) that the electrosmotic and cataphoretic velocities will only be the same in special cases, and then only approximately.

From the formula for the sedimentation potential it can be concluded that sedimentation potentials of some 10 millivolts may occur when large particles fall down in distilled water under the influence of gravitation. The formula may be applied to study the process of sedimentation, and may sometimes be useful to compute the ζ-potential of large particles where no measurement of cataphoretic velocity is possible.

Finally, it may be added that the distortion of the double layer as calculated in § 5 will contribute to the dielectric constant of the systems considered. The sign of this contribution will to a large extent depend on the

sign of $\zeta \Sigma n_K e_K^3$. The author later hopes to deal with this problem in more detail.

The author is much indebted to Dr. S. Levine (Cambridge) and to Prof. D. C. Henry (Manchester) for their interest in this work; also to Dr. G. S. Hartley (London). at whose suggestions certain improvements were made in the manuscript before going to press.

References.

(1) Abramson, H. A., J. Phys. Chem. xxxv. p. 291 (1931).
(2) Abramson, H. A., *Z. phys. Chem.* cxxxiii. p. 51 (1928); J. Amer. Chem. Soc. l. p. 390 (1928).
(3) Bikerman, J. J., *Z. phys. Chem.* A, clxxi. p. 209 (1934); *Koll. Z.* lxxii. p. 104 (1935).
(4) Bikerman, J. J., *Z. phys. Chem.* A, clxiii. p. 378 (1933).
(5) Billitzer, J., *Ann. Physik*, xi. p. 937 (1903).
(6) Debye P., and Hückel, E., *Physikal. Zschr.* xxv. pp. 49, 204 (1924).
(7) Dorn, E., *Ann. Physik*, x. p. 46 (1880).
(8) Falkenhagen, H., ' Elektrolytes,' p. 249 (Leipzig, 1932).
(9) Freundlich, H., ' Kapillarchemie,' II. pp. 73, 135 (Leipzig, 1932).
(10) Freundlich, H., and Abramson, H. A., *Z. phys. Chem.* A, cxxviii. p. 25 (1927).
(11) Gilford, C. L. S., Phil. Mag. (7) xix. p. 853 (1935).
(12) Halpern, O., Chem. Physics, ii. p. 85 (1934).
(13) Henry, D. C., Proc. Roy. Soc. London, A, cxxxiii. p. 106 (1931).
(14) Hermans, J. J., Phil. Mag. (7) xxv. p. 426 (1938).
(15) Kallmann, H., and Dorsch, K. E., *Z. phys. Chem.* cxxvi. p. 305 (1927).
(16) Kemp, I., and Rideal, E. K., Trans. Far. Soc. xxxi. p. 116 (1935).
(17) Kramers, H. A., Proc. Ac. Amsterdam, xxx. p. 145 (1927).
(18) Kruyt, H. R., and Oosterman, J., Proc. Ac. Amsterdam, xl. p. 404 (1937); xli. p. 370 (1938).
(19) Kruyt, H. R., and van der Willigen, P. C., *Z. Phys. Chem.* cxxx. p. 170 (1927); *Koll. Z.* xlv. p. 307 (1929).
(20) Levine, S., Proc. Roy. Soc. London, A, clii. p. 529 (1935).
(21) Mäkelt, E., and Freundlich, H., *Z. Elektrochem.* xv. p. 161 (1909).
(22) Mooney, M., Phys. Rev. (2) xxiii. p. 396 (1924).
(23) Mooney, M., J. Phys. Chem. xxxv. p. 331 (1931).
(24) Moyer, L. S., J. Phys. Chem. xlii. p. 391 (1938).
(25) Moyer, L. S., and Abramson, H. A., J. Gen. Physiol. xix. p. 727 (1936); Bull, H. B., J. Phys. Chem. xxxix. p. 577 (1935).
(26) Onsager, L., and Fuoss, R., J. Phys. Chem. xxxvi. p. 2689 (1932).
(27) Oseen, C. W., ' Hydrodynamik,' p. 166 *et seq.* (Leipzig, 1927).
(28) Overbeek, J. Th. G., *Chem. Weekbl.* xxxv. p. 70 (1938) (Engl.).
(29) Paine, H. H., Proc. Cambr. Phil. Soc. xxviii. p. 83 (1932).
(30) Pauli, W., and Valko, E., ' Electrochemie der Kolloide,' p. 268 *et seq.*, p. 498.
(31) Rutgers, A. J., and Overbeek, J. Th. G., *Z. phys. Chem.*, A, clxxvii. p. 29 (1936).
(32) Rutgers, A. J., *Chem. Weekbl.* xxxv. p. 67 (1938) (Engl.).
(33) Stock, J., *Anz. Akad. Krakau*, A, p. 131 (1913).
(34) Thon, N., *Z. phys. Chem.*, A, cxlvii. p. 147 (1930).
(35) White, P., Phil. Mag. (7) xxiii. p. 811 (1937).
(36) White, P., and Lane, T. B., Phil. Mag. (7) xxiii. p. 824 (1937).
(37) White, H. L., and Fourt, L., J. Phys. Chem. xlii. p. 29 (1938).

(38) White, H. L., and Monaghan, B., J. Phys. Chem. xxxix. pp. 925, 935 (1935).
(39) White, H. L., Monaghan, B., and Urban, F., J. Phys. Chem. xxxix. p. 611 (1935).
(40) Wintgen, R., *Koll. Z.* xl. p. 300 (1926).
(41) Wintgen, R., and Biltz, M., *Z. phys. Chem.* cvii. p. 403 (1923).
(42) Wiegner, G., *Koll. Z.* lviii. p. 157 (1932); Tuorila, P., *Koll. Beih.* xxvii. p. 44 (1928).
(43) Burton and Currie, Phil. Mag. (6) xlix. p. 194 (1925).

The Sir William Ramsay Laboratories of
Inorganic and Physical Chemistry,
University College, London.

LVII. *Charged Colloid Particles in an Ultrasonic Field.*—II. *Particles surrounded by a Thin Double Layer*.* By J. J. Hermans †.

[Received June 29, 1938.]

§ 1. *Introduction.*

IMAGINE a suspension of spherical particles of density s in an electrolytic solution of density s_0. Let the number of suspended particles per unit of volume be n, their radius R. If a plane sonic wave with frequency ω and velocity g travels through this suspension in the direction of the x-axis the electrolytic solution at a given point x acquires a velocity

$$v_0 = b_0 e^{i\omega t}\ ;\ b_0 = a_0 \cos(\omega x/g),$$

where a_0 is the amplitude of velocity fluctuation. Let the velocity of a suspended particle at this point x be

$$v = be^{i\omega t}.$$

The greater the inertia of the particle the more b differs from b_0. It is obvious that this particle will experience a resistance in the surrounding liquid; this resistance is proportional to the relative velocity $(b-b_0)e^{i\omega t}$, say $W(b-b_0)e^{i\omega t}$, where W is a resistance factor. If, furthermore, V is the volume of the particle, it experiences a force $-V\,\partial p/\partial x$ as a result of the gradient of pressure in the sonic wave. This gradient of pressure accelerates the solvent: $dv_0/dt = -1/s_0 \cdot \partial p/\partial x$, and has, therefore,

* Communicated by the Author.

† Netherland Fellow of the Ramsay Memorial Fellowship Trust and of the Hoogewerff Fund.

the value $-s_0 dv_0/dt$. Hence the equation of motion of the particle considered:

$$\mathrm{V}s\frac{dv}{dt} = \mathrm{V}s_0\frac{dv_0}{dt} - \mathrm{W}(b-b_0)e^{i\omega t}. \quad . \quad . \quad . \quad (1)$$

We shall neglect products of velocities and their derivatives, and may therefore replace dv/dt by $\partial v/\partial t$. Equation (1) then takes the form

$$i\omega\mathrm{V}(s_0 b_0 - sb) = \mathrm{W}(b-b_0). \quad . \quad . \quad . \quad . \quad (2)$$

This equation determines b as a function of b_0; we find

$$b-b_0 = \frac{i\omega\mathrm{V}(s_0-s)}{\mathrm{W}+i\omega\mathrm{V}s}b_0. \quad . \quad . \quad . \quad . \quad (3)$$

As a result of the motion of the particle with respect to the surrounding electrolytic solution, the diffuse double layer loses its spherical symmetry, and so generates a dipole μ*. Summing up these dipoles over all the particles, and integrating for a quarter of the wave-length, a potential difference ϕ between a node and an antinode is found. The calculation of this potential difference has been carried out in a previous paper[1] in the special case where the particles are very small compared with the dimensions of the diffuse double layer. At present we shall examine the order of magnitude of ϕ for the other extreme case, *i. e.*, particles which are large as compared with the thickness of the double layer. As to the *electrical* problem, *i. e.*, the distortion of the double layer for a given flow of liquid round the particle, we shall use the method developed in the preceding article on cataphoresis and sedimentation potential; the motion of the particle affects the double layer in a way which differs considerably from that which has been discussed in a previous paper[1]. The particles may, however, also show a very different behaviour from a *hydrodynamical* point of view. Each particle carries out a vibration in the surrounding medium, the frequency of which is ω. For small particles or small frequencies the flow of liquid round the particle has practically the same form as in the case of uniform motion: the inertia of the liquid may be neglected, the velocity

* H. de Bruyn has already called attention to these dipoles, especially with regard to the resulting attractive forces between the particles: *Chem. Weekbl.* xxxv. p. 56 (1938) (Engl.).

decreases slowly with increasing distance from the surface of the particle, the reistance is given by the formula of Stokes, *i. e.*, $W=6\pi\eta R$ (η = coefficient of internal friction).

As has already been shown in a previous paper[1], these conditions are fulfilled when $s_0\omega R^2/\eta$ is small. In the present case, however, where the radius of the sphere must be large compared with the dimensions of the double layer, the value of $s_0\omega R^2/\eta$ may become of the order of unity or even larger, in which case the flow of liquid round the particle has a very different character; it decreases much more rapidly with increasing distance from the surface of the sphere, a property resulting from the inertia of the liquid.

Quantitatively the theory is as follows[2]. We take the centre of the sphere as origin of a system of polar co-ordinates: r = distance from the origin, $x=r\cos\theta$. For reasons which will become clear later we are only interested in the r-component, q_r, of the flow of liquid. If now the sphere has a velocity $(b-b_0)e^{i\omega t}$ with respect to its surroundings, q_r becomes[2]

$$q_r=(b-b_0)e^{i\omega t}\left\{-1+\left(1+\frac{3}{\gamma}+\frac{3}{\gamma^2}\right)\frac{R^3}{r^3}-\frac{3}{\gamma}\left(\frac{R^2}{r^2}+\frac{R^3}{\gamma r^3}\right)\exp\left(-\gamma\frac{r-R}{R}\right)\right\}. \quad (4)$$

The character of this flow of liquid is obviously determined by the quantity γ, which is defined by the equation

$$\gamma^2=\frac{i\omega s_0 R^2}{\eta}. \quad (5)$$

The resistance of the sphere is

$$W(b-b_0)e^{i\omega t}=(b-b_0)e^{i\omega t}.\tfrac{1}{2}i\omega V s_0\left(1+\frac{9}{\gamma}+\frac{9}{\gamma^2}\right). \quad (6)$$

It is readily seen that the resistance factor W takes the form $W=\frac{1}{2}i\omega V s_0$ for very large values of γ; the resistance is then chiefly determined by the inertia of the liquid. For very small values of γ, however, W becomes equal to $9i\omega V s_0/2\gamma^2=6\pi\eta R$. As can be seen from equation (4) the character of the flow of liquid too is very different in the two extreme cases. For our purpose it is only important to know how q_r decreases if the distance from

the surface of the sphere is increased. To that end we introduce the quantity σ:

$$r=\mathrm{R}(1+\sigma), \quad . \quad . \quad . \quad . \quad . \quad . \quad (7)$$

and expand q_r in powers of σ. In the limit where γ is very small $\exp[\gamma(r-\mathrm{R})/\mathrm{R}]=\exp(-\gamma\sigma)$ may also be expanded in powers of σ, and we get

$$q_r=-3/2\sigma^2(b-b_0)e^{i\omega t}\cos\theta. \quad . \quad . \quad . \quad (8)$$

On the other hand, in the limit where γ is very large

$$q_r=-3\sigma(b-b_0)e^{i\omega t}\cos\theta. \quad . \quad . \quad . \quad . \quad (9)$$

The velocity q_r as given by (9) changes much more rapidly with increasing σ than that given by (8). It is clear that this difference will become very important for the distortion of the electric double layer. This double layer being thin compared with R, for small values of γ the velocity of the liquid in different points of the double layer is almost the same as that of the particle itself. In other words, the double layer is carried along almost entirely by the particle, and can only give rise to a comparatively small dipolar moment μ. If, however, γ is large, the velocity of the liquid in the double layer differs considerably from that of the particle, and the distortion will become much more important.

Before proceeding to give an outline of the theory of distortion a final remark may be made concerning the hydrodynamics of the problem. We only accounted for the non-uniformity of the motion, which is governed by the value of γ. The results therefore do not apply to such velocities where Reynolds's number $s_0(b-b_0)\mathrm{R}/\eta$ is too large, because in this case the quadratic terms in the original hydrodynamic equations must also be taken into account. Using equation (3) for $b-b_0$, Reynolds's number becomes

$$\mathrm{N_R}=\frac{s_0\mathrm{R}}{\eta}\frac{\omega\mathrm{V}(s_0-s)b_0}{\mathrm{W}+i\omega\mathrm{V}s}.$$

For large values of γ, $\mathrm{N_R}$ has the order of magnitude $\mathrm{R}s_0b_0/\eta$. Taking water at room-temperature as the solvent, we have $s_0=1$ and $\eta=0{\cdot}01$. With a value of $b_0=30$ cm./sec. R may therefore amount to about 10^{-4} cm., a value which already lies in the region of rather coarse suspensions. For small values of γ, where $\omega\mathrm{V}s\ll\mathrm{W}$,

N_R has the order of magnitude $\gamma^2 R b_0/\eta$, which is always considerably below unity.

§ 2. *Outline of the Theory.*

For a given flow of liquid round the particle the deformation of the electric double layer may be calculated as follows. If the particle is at rest with respect to its surroundings the electric potential and the distribution of ions have spherical symmetry. We use Debye-Hückel's approximation

$$\psi^0 = \zeta e^{-\chi(r-R)}\ ;\ \chi^2 = \frac{4\pi}{DkT}\Sigma_\kappa n_\kappa e_\kappa^2, \quad . \quad . \quad (10)$$

where ζ is the electrokinetic potential, χ the reciprocal characteristic length of the Debye-Hückel theory, D the dielectric constant. Introducing the quantity

$$h = \chi R, \quad . \quad . \quad . \quad . \quad . \quad . \quad . \quad (11)$$

and remembering equation (7), we may also write: $\psi_0 = \zeta \exp(-h\sigma)$. The thickness of the double layer, *i. e.*, $1/\chi$, is supposed to be small as compared with R, and we have therefore $h \gg 1$. The lower limit of h for which our calculations approximately hold good may be estimated at about 25. The value of the potential ψ^0 given by the formula (10) is identical with that for a plane wall; the error thereby introduced is of the order $1/h$.

If n_κ is the average number of ions with charge e_κ per unit of volume, the concentration of these ions in the double layer is

$$f_\kappa^0 = n_\kappa\left(1 - \frac{e_\kappa \zeta}{kT} e^{-h\sigma}\right). \quad . \quad . \quad . \quad . \quad . \quad (12)$$

To calculate the distribution of ions round the *moving* particle we must know the equations of motion for the ions. Now there are three factors which exert an influence on the number f_κ of ions with charge e_κ in a unit of volume: (1) the diffusion, as a result of which f_κ changes with an amount $\partial f_\kappa^{(1)}/\partial t = kT\Delta f_\kappa/\rho_\kappa$, where ρ_κ is a frictional factor, (2) the electric field: $\partial f_\kappa^{(2)}/\partial t = \mathrm{Div}(f_\kappa \mathrm{Grad}\,\psi)/\rho_\kappa$, and (3) the flow of liquid: $\partial f_\kappa^{(3)}/\partial t = -\mathrm{Div}(f_\kappa q)$. Summing up these effects we have the equations of motion

$$\rho_\kappa \frac{\partial f_\kappa}{\partial t} = kT\Delta f_\kappa + \mathrm{Div}(f_\kappa \mathrm{Grad}\,\psi) - \rho_\kappa \mathrm{Div}(f_\kappa q).$$

The quantities q, Div, and Grad refer to a system of co-ordinates XYZ which is fixed in the liquid; we prefer a system xyz which is fixed in the centre of the particle, and write

$$z=\mathrm{Z};\ y=\mathrm{Y};\ x=\mathrm{X}-\frac{b-b_0}{i\omega}e^{i\omega t}.$$

The equations of motion then become

$$\rho_\kappa \frac{\partial f_\kappa}{\partial t}=kT\Delta f_\kappa+e_\kappa \operatorname{div}(f_\kappa \operatorname{grad}\psi)-\rho_\kappa \operatorname{div}(f_\kappa q), \quad (13)$$

where q, div, and grad now refer to the xyz-system. Besides the equations (13) the condition of Poisson,

$$\Delta\psi=-\frac{4\pi}{D}\Sigma_\kappa f_\kappa e_\kappa, \quad . \quad . \quad . \quad . \quad (14)$$

has to be met.

Using Debye-Hückel's approximation, we replace $f_\kappa \operatorname{grad}\psi$ by $n_\kappa \operatorname{grad}\psi$; further, we write

$$\psi=\psi^0+\phi e^{i\omega t};\ f_\kappa=f_\kappa{}^0+\nu_\kappa e^{i\omega t}, \quad . \quad . \quad . \quad (15)$$

and restrict ourselves to terms in ϕ and ν_κ, which are linear in q, so that $f_\kappa q$ may be replaced by $f_\kappa{}^0 q$. However, $\operatorname{div} q=0$ and $f_\kappa{}^0$ has spherical symmetry, *i. e.*, the only component of $\operatorname{grad} f_\kappa{}^0$ which differs from zero is that along r. Hence

$$\operatorname{div}(f_\kappa{}^0 q)=q_r\frac{df_\kappa{}^0}{dr}=q_r\frac{\chi\zeta}{kT}e_\kappa n_\kappa e^{-h\sigma},$$

where q_r is the component of q in the direction of r. The equations (13) (14) finally become

$$i\omega\rho_\kappa\nu_\kappa=kT\Delta\nu_\kappa+n_\kappa e_\kappa\Delta\phi-\frac{\chi\zeta}{kT}n_\kappa e_\kappa\rho_\kappa e^{-h\sigma}q_r e^{-i\omega t}, \quad (16)$$

$$\Delta\phi=-\frac{4\pi}{D}\Sigma_\kappa \nu_\kappa e_\kappa. \quad . \quad . \quad . \quad . \quad . \quad (17)$$

Though Onsager and Fuoss[3] have developed methods of matrix calculation for a system of this kind, which have been somewhat simplified by Gurjanova[4], the solution is still very complicated, and we shall only consider the specially simple case that all ρ_κ are equal, say ρ, a condition

which is met approximately for many ions. Introducing the quantities

$$K^2=\chi^2+\frac{i\omega\rho}{kT}, \quad . \quad . \quad . \quad . \quad . \quad . \quad (18)$$

$$S=\Sigma_K \nu_K e_K, \quad . \quad . \quad . \quad . \quad . \quad . \quad . \quad (19)$$

it can easily be deduced from (16) (17) that S satisfies the differential equation

$$\Delta S-K^2S=\frac{\rho}{kT}\frac{\chi^3 D\zeta}{4\pi}e^{-h\sigma}q_r e^{-i\omega t}. \quad . \quad . \quad (20)$$

As h is large, $\exp(-h\sigma)$ falls very rapidly with increasing σ, and the function q_r as given by (4) may therefore be expanded in powers of σ. Even then, however, the solution of (20) is generally very laborious and will not be carried out here. As long as no experimental data exist we shall only examine the order of magnitude in a special case, viz., where γ is of the order 1 and $\omega\rho/kT$ of the same order of χ^2. As it happens, this special case is the most interesting one in so far as it brings about the largest possible potential difference between a node and an antinode of the sonic wave, as can be shown by the following reasoning.

For a given value of R it depends on the value of ω whether the velocity of the liquid changes rapidly or otherwise with increasing σ. This change is proportional to σ^2 in the case of small γ (*cf.* eq. (8)), and becomes proportional to σ in the case of large γ (*cf.* eq. (9)). For this reason ω should be chosen large. On the other hand, when integrating the effect for a quarter of the sonic wave the result will decrease with decreasing wavelength, *i. e.*, with increasing frequency. The effect will therefore show a maximum when ω is increased; this maximum is to be found for such values of γ where the change of the velocity of liquid with increasing σ already begins to acquire the order of magnitude σ instead of σ^2, *i. e.*, when $\gamma\approx 1$. For water at room-temperature $\gamma^2=100\,\omega R^2$; with a value of γ of the order of unity $1/R$ must therefore be approximately equal to $10\sqrt{\omega}$. Moreover, $h=\chi R$ must be at least 25 if our approximations are to hold good. For a given flow of liquid round the particle the double layer is the better "stripped off" the smaller h, *i. e.*, the smaller the dimensions of the particle compared with those of the double layer.

Generally speaking the value of h should therefore be chosen as small as possible, *i. e.*, at about 25. In other words, $\chi \cong 25/R \cong 250\sqrt{\omega}$, which gives $\chi^2 = 6 \cdot 10^4 \omega$. On the other hand, in water at room-temperature the value of the frictional factor ρ for most ions lies in the neighbourhood of $2 \cdot 10^{-9}$ c.g.s., or $\rho/kT \cong 5 \cdot 10^4$; obviously χ^2 and $\omega\rho/kT$ have the same order of magnitude. A closer examination confirms these conclusions, but we shall not go into this matter further.

Expanding q_r as given by (4) in powers of σ, and assuming γ to be of the order of unity, we get in first approximation

$$q_r = (b - b_0) e^{i\omega t} \cos\theta \cdot \frac{3}{\gamma}\left(1 + \frac{1}{\gamma}\right)(1 - e^{-\gamma\sigma}).$$

To solve (20) we try $S = g(\sigma) \cdot \cos\theta$, or, if we ignore errors of the order $1/h$, $\Delta S = g''/R^2 \cdot \cos\theta$. If, furthermore, we abbreviate

$$H = KR, \quad . \quad . \quad . \quad . \quad . \quad . \quad . \quad (21)$$

the differential equation for S becomes

$$g'' - H^2 g = \alpha(1 - e^{-\gamma\sigma}) e^{-h\sigma}, \quad . \quad . \quad . \quad . \quad (22)$$

$$\alpha = \frac{3}{\gamma}\left(1 + \frac{1}{\gamma}\right) \frac{\rho}{kT} \frac{\chi^3 D\zeta}{4\pi} R^2 (b - b_0). \quad . \quad . \quad (23)$$

The solution of (22) must be zero on the surface of the sphere, because the velocity of the liquid in the immediate neighbourhood of the sphere is equal to that of the sphere itself, and the distribution of ions in this immediate vicinity must therefore remain unaltered. Taking this boundary condition into account, we get

$$g(\sigma) = \frac{\alpha e^{-h\sigma}}{h^2 - H^2} - \frac{\alpha e^{-(\gamma+h)\sigma}}{(\gamma+h)^2 - H^2} + \left[\frac{\alpha}{(\gamma+h)^2 - H^2} - \frac{\alpha}{h^2 - H^2}\right] e^{-H\sigma}. \quad . \quad (24)$$

As a result of the extra charge density $Se^{i\omega t}$ the particle with its surroundings behaves like a dipole of magnitude $\mu = e^{i\omega t} \int Sx \, d\tau$, where the integration has to be extended over the whole space outside the sphere. We find

$$\mu = 2\pi \int_R^\infty dr \int_0^\pi d\theta \, Se^{i\omega t} \cdot r^3 \cdot \cos\theta \cdot \sin\theta = \frac{4}{3}\pi \int_R^\infty g(\sigma) r^3 \, dr \cdot e^{i\omega t}.$$

To a first approximation this becomes

$$\mu=\frac{4}{3}\pi R^4\int_0^\infty g(\sigma)d\sigma\,.\,e^{i\omega t}=-\frac{4}{3}\pi R^4\frac{\alpha\gamma}{H}\frac{2h+H}{h^2(h+H)^2}\,e^{i\omega t},$$

$$\mu=-\frac{\gamma+1}{\gamma}\frac{\rho}{kT}\chi R^2 D\zeta\frac{2\chi+K}{K(\chi+K)}(b-b_0)e^{\omega t}.$$

The difference $b-b_0$ is determined by (3), where W is given by (6). In our case $\gamma\approx 1$, so W is of the same order as ωVs and $b-b_0$ of the same order as b_0, say $b-b_0=\frac{1}{3}b_0$. Furthermore, K has been assumed to be of the same order as χ, so that the order of μ becomes $\mu\simeq\rho R^2 D\zeta b_0/3\chi kT$. If there are n particles per unit of volume the potential difference between two points x and $x+dx$ is $4\pi\mu n\,dx/D$. Remembering that $b_0=a_0\cos(\omega x/g)$, and integrating for a quarter of the wave-length, we get a potential difference

$$\phi\simeq\frac{4}{3}\pi nR^3\frac{\rho}{kT}\frac{\zeta}{\chi R}\frac{g}{\omega}a_0.$$

Now the velocity g of sound in water is $1{\cdot}4\,.\,10^5$ cm./sec. Abbreviating $\frac{4}{3}\pi nR^3=p=$partial volume of suspended substance, and substituting the usual values for ρ, k, T, we get

$$\phi\simeq 0{\cdot}7\,.\,10^{10}\frac{\zeta pa_0}{\chi R\omega}.$$

We must now bear in mind that we assumed ω, R, and χ to satisfy the conditions

$$100\,.\,\omega R^2\simeq 1\,;\quad\frac{\omega\rho}{kT}\simeq\chi^2\,;\quad\chi R\geqq 25.$$

The following table gives some values of ω, R, χ which satisfy all three conditions. In this table we also calculated the values of the electrolytic concentration $c=9{\cdot}10^{-16}\,.\,\chi^2$ in gram-molecules per litre, and the approximate value of ϕ.

$10^{-7}\omega$.	10^5R(cm.)	$10^{-6}\chi$(cm.$^{-1}$).	$10^3\,c$.	ϕ.
100	0·3	8	60	$0{\cdot}3\,.\,\zeta pa_0$
10	1	2·5	6	$3\,.\,\zeta pa_0$
1	3	0·8	0·6	$30\,.\,\zeta pa_0$
0·1	10	0·25	0·06	$300\,.\,\zeta pa_0$

For $\omega=10^6$ the value of a_0 may easily amount to 35 cm./sec., so that even with the rather low value of $d=0{\cdot}001$, ϕ becomes of the order of ten times ζ. For many suspensions p may amount to 0·01, which gives,

with a usual value of $\zeta=50$ mv., the surprisingly high value of $\phi=5$ volts.

We did not go any farther than to calculate the order of magnitude in a specially favourable case. In most other cases the effect will be considerably smaller, but may nevertheless amount to values which can easily be measured. Finally, we may add that the extra charge density $Se^{i\omega t}$ gives rise to a relaxation force which enlarges the resistance of the particle. In some cases this relaxation force has the same order of magnitude as the resistance itself, and this may reduce the effect considered by 50 per cent. The accurate theory will have to take this correction into account.

Summary.

A plane sonic wave is assumed to move in a suspension of spherical particles. These particles lagging behind the solvent, their double layer is deformed, and a dipolar moment is set up. Summing up these dipolar moments for all the particles, and integrating for a quarter of the sonic wave, the potential difference ϕ between a node and an antinode is found.

The diffuse double layer round the particles is assumed to be thin as compared with their radius. It is found that the value of ϕ is maximum in the special case—interesting from both a hydrodynamical and a colloid chemical point of view—where the flow of liquid round the particle becomes different from that of uniform motion, a phenomenon which is due to the inertia of the liquid. In this case the potential difference ϕ may amount to the remarkably high value of some volts.

Measurements of ϕ may lead to a better understanding of the nature of many suspensions or colloidal solutions and their behaviour in a sonic field. Moreover, the effect may sometimes be useful to determine the ζ-potential of particles which are too large to enable a determination of cataphoretic mobility.

References.

(1) J. J. Hermans, Phil. Mag. (7) xxv. p. 426 (1938).
(2) A. B. Basset, ' Hydrodynamics ' ii. p. 260 *et seq.* (Cambridge, 1888).
(3) L. Onsager and R. Fuoss, J. Phys. Chem. xxxvi. p. 2698 (1932).
(4) J. N. Gurjanowa, *Physik. J.* ser. A, *J. exp. theor. Physik.* vii. p. 633 (1937).

The Sir William Ramsay Laboratories of
Inorganic and Physical Chemistry,
University College, London.

LVIII. *Pre-striking Conditions in a Thyratron.* By Professor E. L. E. Wheatcroft, *M.A.*, *and* T. G. Hammerton, *Ph.D.**

[Received July 27, 1938).

THE mechanism of striking of a gas-filled triode is discussed in a previous paper †. Here we describe further experimental work on the BT 1 mercury-filled thyratron, and suggest some modification of the simple theory then put forward.

The pre-striking anode current I of such a thyratron is found to obey the law

$$\log I = f(V_a + \mu V_g + \rho I), \quad . \quad . \quad . \quad . \quad (1)$$

where V_a, μ, V_g have the usual meanings for a vacuum triode, and ρ is independent of I. The form of the function f differs little from a straight line over a range of current from 0·1 to 10 microamps. ρ being positive when positive ions are present, a point is eventually reached with increasing current at which

$$\frac{dI}{dV} = \infty ,$$

where V is the controlled potential. At this point the current is no longer stable, and the tube must necessarily "strike." ρ should be expected to depend upon anode potential and upon vapour pressure.

Fig. 1 shows a plot of I against V_g for the BT 1 thyratron for an anode voltage of 270 and a wide range of condensing temperatures. The curve marked $< -10°$ represents a temperature (too low for the thermometer) where the vapour pressure can be taken as negligibly small.

I. *Experimental.*

(a) *Dependence of ρ upon Anode Potential.*—The previous paper described measurements of anode current at varying

* Communicated by the Authors.

† Phil. Mag. xxv. p. 649 (1938). Several errors were overlooked in this paper, viz. :—

P. 650, line 2, *for* cathode *read* anode.

P. 651, near bottom of page, $e^{-\frac{V_m e}{kT}}$.

P. 656, lines 10 and 11, *read* (35° C.) *and* low.

P. 656, penultimate line, *for* 2·8 *read* 2·28.

grid potential for a fixed anode voltage of 270. Subsequent measurements have been made at 210, 270, and 330 volts for condensing temperatures of less than $-10°$ C. (substantially zero vapour pressure) and 21° C. The tests were made in accordance with the technique previously described, and appear to show that ρ is independent of V_a. This unexpected result is apparently

Fig. 1.

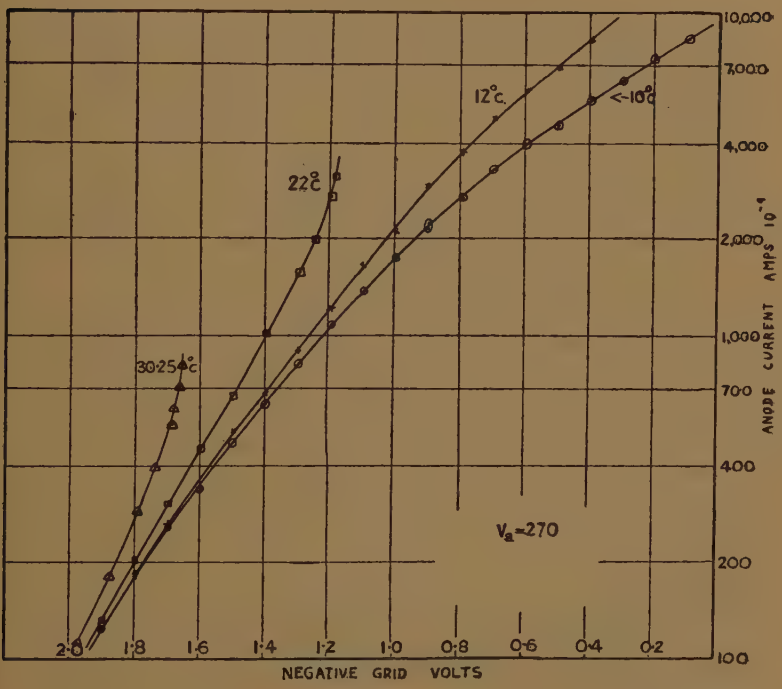

Pre-striking currents of BT1 thyratron

confirmed by the data plotted in fig. 2, where the anode potential was varied from 120 to 420 volts, while the grid potential was held at $-0·8$, $-1·0$, $-1·2$, and $-1·4$ volts. These last data are collected in fig. 3 and analysed for the constancy and value of ρ, which can in this case be determined without any foreknowledge of μ. There seems to be no systematic difference between the various sets of points.

(b) *Dependence of* ρ *upon Vapour Pressure.*—New tests were made at various condensing temperatures from below $-10°$ C. to 23° C. and the corresponding mercury vapour pressures deduced from tables. The measurements of the earlier tests were confirmed, and fig. 4, which is reproduced from the previous paper, shows the dependence of ρ upon vapour pressure for the BT 1 thyratron. The measurement of ρ is, for reasons set out

Fig. 2.

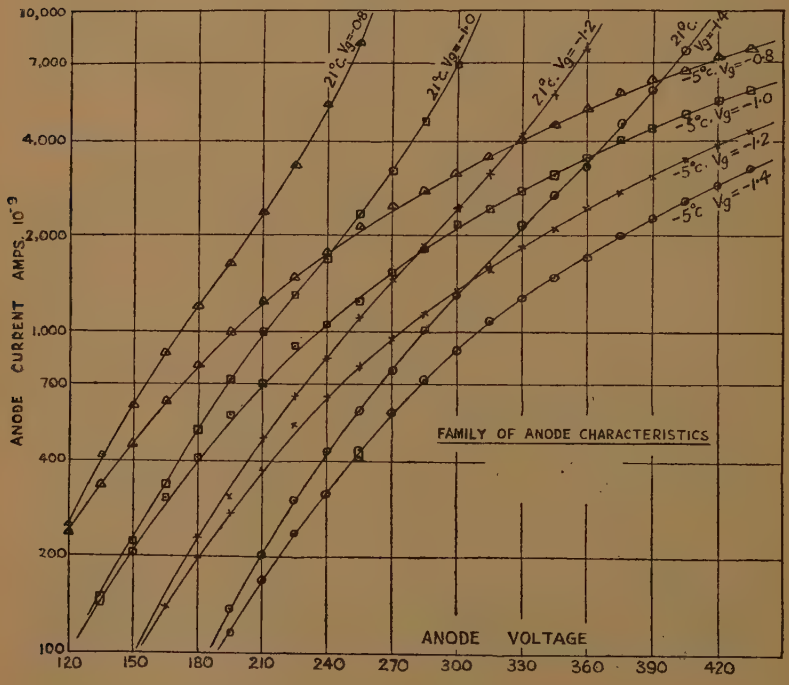

previously, always difficult, and the difference between true and calculated internal vapour pressure is, of course, still in doubt.

(c) *Pre-striking Grid Current.*—During the course of the tests described above, the current from the grid was measured and analysed after the manner of Nottingham *. The measurement was made by a resistance in the grid circuit in conjunction with a sensitive valve-voltmeter

* J. Franklin Inst. ccxi. p. 271 (1931).

having a full-scale input of some 75 millivolts and consuming a current of less than 10^{-10} amps. The instrument was somewhat troublesome, but we believe the measurements are accurate within at least ± 5 per cent. The primary object was to make the thyratron act as its own ionization pressure gauge, and so to detect any random variations of internal pressure when the external temperature was apparently constant. As was to be

Fig. 3.

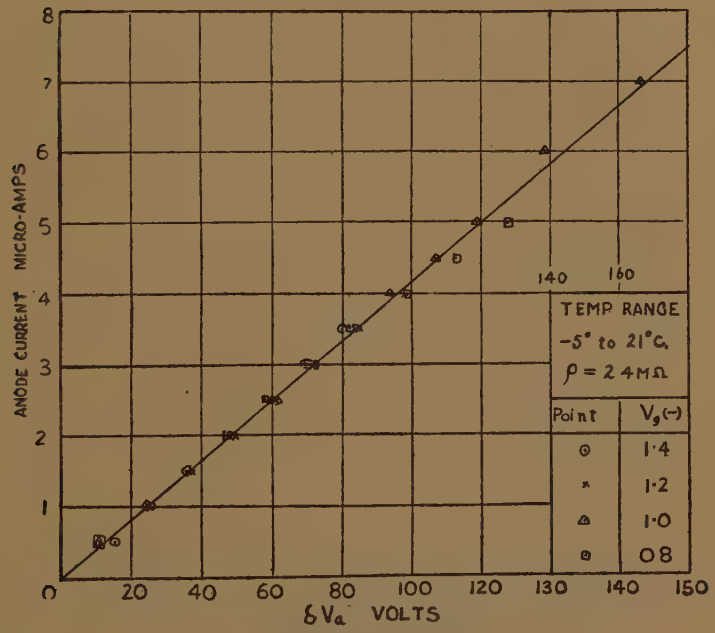

Analysis of data of fig 2.

expected, β, the number of positive ions produced per primary electron, proved to be independent of the current I, and, above a certain voltage, nearly independent of V_a. This last result follows from the fact that at high voltage and low pressure the number of collisions is few, but the electron, when a collision does occur, has nearly always adequate energy to ionize. These are typically the conditions of the Dushman and Found gauge *.

* Phys. Rev. xxiii. p. 734 (1924).

(d) *Relation between β and Vapour Pressure.*—In fig. 5 are plotted the various measurements of β against vapour pressure as calculated from the external temperature. The points are grouped well about the line drawn, but the spread is fairly large. The spread may be put down to random variations between internal pressure and external temperature.

Fig. 4.

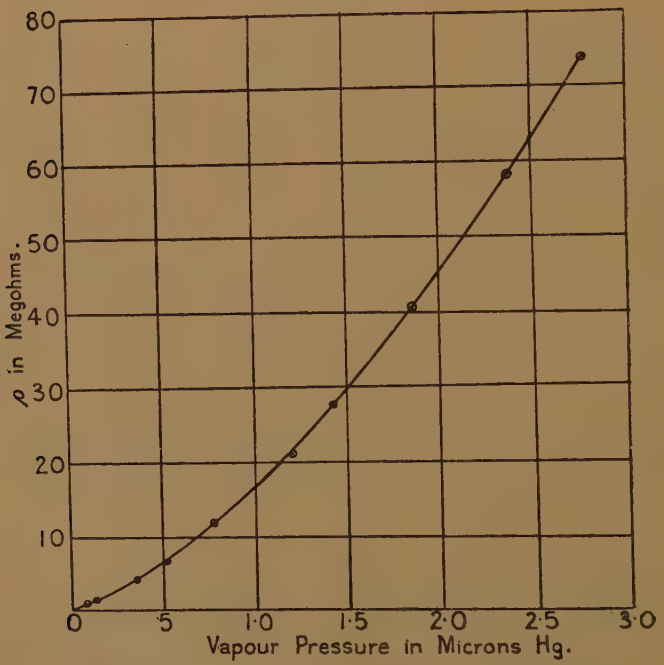

Dependence of "negative resistance due to ionization" on vapour pressure for BT 1 thyratron.

For comparison the results of Dushman and Found for mercury vapour are also shown, and are seen to agree well with the other points.

The full line represents a theoretical calculation given below.

(e) *Relation between β and ρ.*—In setting out to measure the grid current and to use the thyratron as its own pressure gauge, we hoped to eliminate the need for somewhat doubtful temperature measurements. In this we

have not entirely succeeded, for, as is shown in fig. 6, the spread when ρ is plotted against β is rather worse than that when ρ is plotted against temperature. This failure is presumably due to the inherent experimental difficulty of determining ρ, which essentially involves two different temperatures in succession and takes a considerable time. There was also, however, difficulty in measuring β,

Fig. 5.

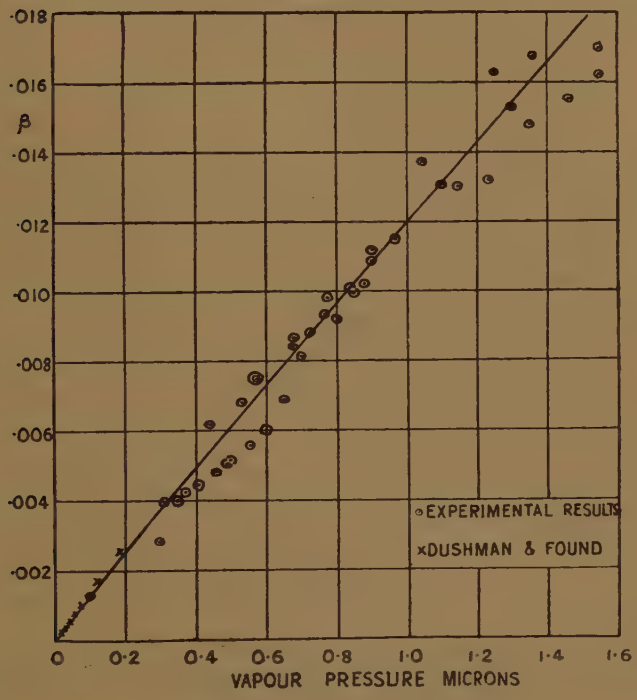

Ratio of ion to electron current.

for this involves separating the positive-ion current from the total grid current. The electron current to the grid can only be measured by creating such conditions that no positive ions are present, *e. g.*, with the anode potential zero or negative, and so, in view of the uncertainty whether the electron current is influenced by the anode potential, the determination of β was limited to the region of negative grid potential, where the electron current was negligible. This was necessarily the region

where the anode current was small and measurement of ρ very inaccurate. The spread, therefore, if disappointing, is not entirely surprising. The theoretical relation again is discussed below.

II. *Theoretical.*

(a) *Calculation of β from the Probability of Ionization.*— Data on the probability of ionization may be taken from various sources *. Let N be the number of ionizing collisions made by an electron per cm. path reduced to

Fig. 6.

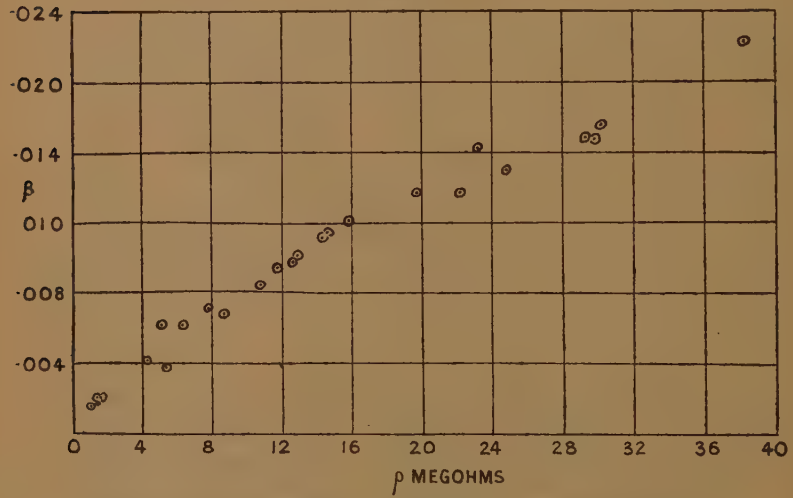

Relation between positive ion current and "negative resistance due to ionization."

1 mm. pressure at 0° C.; then at pressure p mm. and temperature T° K. the number is

$$\frac{273\mathrm{N}p}{\mathrm{T}}.$$

The total number in distance l from grid to anode is then

$$\beta = \frac{273p}{\mathrm{T}}\int_0^l \mathrm{N}\,dx$$

$$= \frac{273p}{\mathrm{T}}\int_0^{\mathrm{V_a}} \mathrm{N}\frac{dx}{d\mathrm{V}}d\mathrm{V}.$$

* Compton and Van Voorhis, Phys. Rev. xxvii. p. 729 (1926); Bleakney, Phys. Rev. xxxv. p. 139 (1930).

If we can assume that $\frac{dV}{dx}$ is constant along the path of integration, an assumption which is correct as a first approximation, we get

$$\beta = \frac{273pl}{T} \cdot \frac{1}{V_a} \int_0^{V_a} N\, dV. \quad . \quad . \quad . \quad . \quad (2)$$

From Bleakney's figures *

$$\frac{1}{V_a} \int_0^{V_a} N\, dV = 20$$

for any value of V_a above 150 volts.

For the BT 1 thyratron $l = 0{\cdot}65$ cm., so that

$$\beta = \frac{3500\, p}{T}.$$

For example, if $p = {\cdot}001$, $T = 292$, then $\beta = {\cdot}012$, as in the full line drawn in fig. 5. The line clearly agrees well with the experimental points.

(b) *Calculation of ρ in Terms of β.*—Consider first the order of magnitude of the positive-ion space charge. In an element dy of the ionization path distant y from the cathode the current of ions generated is

$$IN\, dy.$$

Consider first the region approaching zero vapour pressure, where the number of collisions made by the ions is negligibly small. Then the velocity of these ions at a plane distant x from the cathode is

$$\sqrt{\frac{2eV_a}{Ml}}\,(y-x)^{\frac{1}{2}},$$

where e is the charge and M the mass of the ions. Thus the space charge per cm. at x is given by

$$IN\sqrt{\frac{Ml}{2eV_a}} \int_x^l (y-x)^{-\frac{1}{2}}\, dy$$

$$= IN\sqrt{\frac{2Ml}{eV_a}}\,(l-x)^{\frac{1}{2}},$$

if we assume N to be independent of y.

Thus by Poisson's law

$$\nabla^2 V = 4\pi c^2 \frac{IN}{A} \sqrt{\frac{2Ml}{eV_a}}\,(l-x)^{\frac{1}{2}},$$

* *Loc. cit.*

where c is the ratio of electromagnetic to electrostatic units and A the cross-section of the discharge. Now we can only integrate this equation for a unidimensional system, but by doing so we shall at least estimate the order of magnitude correctly. From the double integration we get

$$V_a = X_0 l - \frac{16\pi c^2 IN}{15\,A}\sqrt{\frac{2M}{eV_a}}\,l^3,$$

where X_0 is a constant of integration.

From which, since $\beta = Nl$,

$$\rho = \frac{16\pi c^2 \beta}{15\,A}\sqrt{\frac{2M}{eV_a}}\,l^2 \qquad \ldots\ldots (3)$$

$$= 9{\cdot}2\times 10^7 \frac{\beta l^2}{A\sqrt{V_a}},$$

if V_a is in volts.

As stated previously, $l = 0{\cdot}65$, $V_a = 270$. Take $A = 1$ cm.^{2}. This gives

$$\rho = 2{\cdot}4\times 10^6 \beta.$$

The exact ratio at the origin of fig. 6 is not, of course, clear from the experimental points, but calculation of the effect of collisions shows that there should be no great change in the ratio up to at least 23° C., *i. e.*, over the whole of the range of the figure. We are therefore justified in taking the slope near the origin to be of the order of $\rho = 10^9\beta$, a value about 1000 times that calculated.

As a result of the foregoing calculations, it seems necessary therefore to modify previous ideas as to the mechanism by which the constant ρ depends upon positive-ion space charge. The agreement between the calculated and experimental values of β precludes the suggestion that there is a large proportion of ions generated which are not caught by the grid, and so the value of A in the calculation of ρ must at least be of the order of the area of the grid-hole, viz., ·25 cm.^{2}, and probably larger. Fig. 7 is reproduced from the previous paper, and shows a somewhat idealized potential distribution in the thyratron. It is not by any means clear from the lines of force how the ions manage, in the absence of collisions, to distribute themselves from the narrow central core along which it seems the electrons ought to be travelling,

but, as stated above, it must be supposed from the calculation of β that the majority of them do so distribute. We therefore propose to modify our theory to the extent of supposing that a small minority of the ions generated not far from the grid-hole pass through the hole to the

Fig. 7.

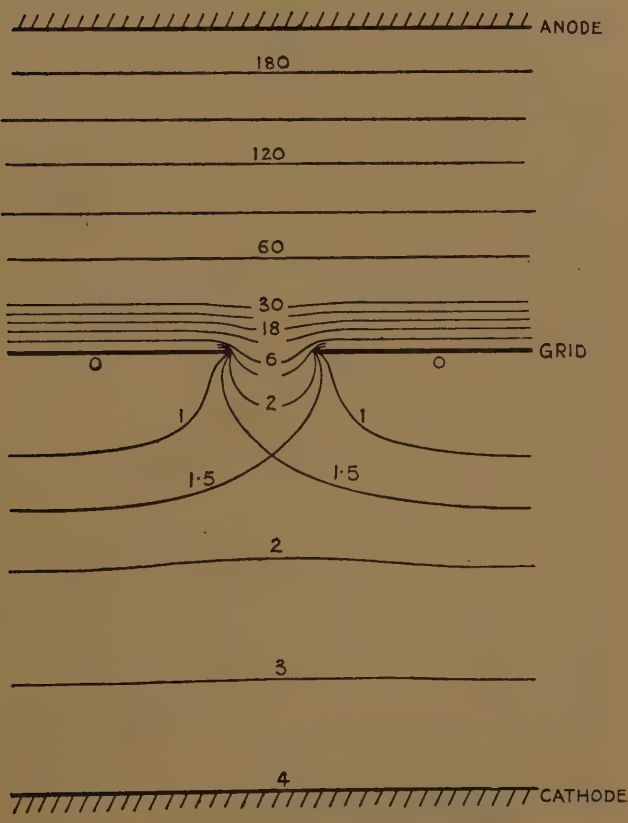

Typical potential distribution near grid-hole.

cathode, and that the magnitude of ρ depends not on the density of ions in the grid-anode space, but on the density of this smaller body of ions in the grid-cathode space. This supposition would also explain the independence of ρ and V_a, and is clearly qualitatively plausible. It is, however, difficult to make any effective quantitative

calculation, except to agree that the magnification of the effect would be at least as great as μ, which is about 200 ; actually it seems that a greater magnification still is needed to account for the experimental result.

III. *Instability.*

The implication of equation (1) is that, with perfectly steady applied potentials, the thyratron will not strike until the point is reached where dI/dV becomes infinite. In practice it is difficult to approach close to the theoretical point of instability, and in certain experiments, namely, those in which V_g was held constant, the tube struck while the slope of the curve appeared to be still a long way from the vertical. It is easily shown that resistance in the grid circuit tends to hasten the critical point, but in the experiment in question the grid resistance was only 500 ohms and the grid current known to be small. Nor do we think the effect could be entirely explained by unsteadiness in V_a or V_g, which were supposed to be constant.

It remains then to consider a further mechanism of instability, which may qualitatively be explained as follows :—The term in equation (1) which under steady conditions is written ρI is proportional to a volume charge of positive ions ; if the rate of production of these ions is proportional to I and the rate of disappearance proportional to their number, then this number will, as stated, be proportional to I under steady conditions. Actually, however, if they are produced in one part of the tube and neutralized in another, there will be a time-lag under changing conditions between generation and disappearance, and it is easy to show that this lag is of itself a cause of another form of instability. For suppose in the extreme case that the rate of disappearance could be neglected, we should have

$$\log I = (V_a + \mu V_g + \sigma \int I \, dt),$$

where σ is a constant ; and it is easily seen that I must become infinite in a finite time. This form of instability presumably explains the extreme suddenness of striking and the impossibility of stabilizing the current by high anode resistance.

LIX. *Operational Form of $f(t)$ for a Finite Interval, with Application to Impulses.* By N. W. McLachlan, *D.Sc.**

[Received August 10, 1938.]

I. *Introduction.*

THE O.F. of a function $f(t)$ usually refers to the range $t=0$ to ∞. In practical applications, however, the O.F. for a finite range of $f(t)$ may be required. Sometimes it may be written down immediately. For example, suppose we want to know the O.F. of $\sin \omega t$ for the interval $t=0$ to $2n\pi/\omega$, n being a positive integer. At $t=2n\pi/\omega$ if a sine wave of the same amplitude and pulsatance be started in opposite phase from the original, the latter is obliterated from that point onwards. Now the O.F. of $\sin \omega t$ is $\omega p/(p^2+\omega^2)$, whilst that of the wave commencing at $t=2n\pi/\omega$ is $-\dfrac{\omega p e^{-2n\pi p/\omega}}{(p^2+\omega^2)}$. The O.F. of $\sin \omega t$ over the range $t=0$ to $2n\pi/\omega$ is, therefore,

$$\phi(p)=\frac{\omega p}{p^2+\omega^2}(1-e^{-2n\pi p/\omega}). \quad . \quad . \quad . \quad (1)$$

In what follows we shall deal with the general case where the O.F. cannot always be determined so easily.

2. *Derivation of Formulæ.*

Let the interval for which the O.F. is required be $t=h_1$ to $t=h_2$, both of these quantities being real and positive. Then, by definition.

$$\phi_{h_1/h_2}=p\int_{h_1}^{h_2} e^{-pt}f(t)\,dt. \quad . \quad . \quad . \quad . \quad (2)$$

Integrating by parts and inserting the limits, we get

$$\phi_{h_1/h_2}=e^{-ph_1}f(h_1)-e^{ph_2}f(h_2)+\int_{h_1}^{h_2} e^{-pt}f^{(1)}(t)\,dt. \quad . \quad (3)$$

Repeating the integration by parts, we ultimately find that

$$\phi_{h_1/h_2}=\sum_{r=0}^{n-1} p^{-r}[e^{-ph_1}f^{(r)}(h_1)-e^{-ph_2}f^{(r)}(h_2)] + p^{-n+1}\int_{h_1}^{h_2} e^{-pt}f^{(n)}(t)\,dt. \quad (4)$$

* Communicated by the Author.

We can now obtain a number of particular cases. When $h_1=0$ and $h_2=\infty$, (4) gives

$$\phi_{0/\infty}=p\int_0^\infty e^{-pt}f(t)\,dt=\sum_{r=0}^{n-1}p^{-r}f^{(r)}(o)+p^{-n+1}\int_0^\infty e^{-pt}f^{(n)}(t)\,dt, \quad . \quad . \quad . \quad (5)$$

provided $e^{-ph_2}f^{(r)}(h_2)=0$ when $h_2=\infty$.

When $h_1=h$ and $h_2=\infty$, the O.F. of $f(t)$ from $t=h$ to ∞ is

$$\phi_{h/\infty}=p\int_h^\infty e^{-pt}f(t)\,dt$$

$$=e^{-ph}\sum_{r=0}^{n-1}p^{-r}f^{(r)}(h)+p^{-n+1}\int_h^\infty e^{-pt}f^{(n)}(t)\,dt, \quad (6)$$

$$=e^{-ph}\sum_{r=0}^{n-1}p^{-r}f^{(r)}(h)+p^{-n+1}\left[\int_0^\infty e^{-pt}f^{(n)}(t)\,dt-\int_0^h e^{-pt}f^{(n)}(t)\,dt\right], \quad (7)$$

provided $e^{-ph_2}f^{(r)}(h_2)=0$ when $h_2=\infty$.

In the case of $f(a\sqrt{t^2-b^2})$, it is easy to show that

$$\phi_{b/\infty}=p\int_b^\infty e^{-pt}f(a\sqrt{t^2-b^2})\,dt$$

$$=e^{-pb}\sum_{r=0}^{n-1}p^{-r}\left[\frac{d^r}{dt^r}f(a\sqrt{t^2-b^2})\right]_{=b}$$

$$+p^{-n+1}\int_b^\infty e^{-pt}\frac{d^n}{dt^n}[f(a\sqrt{t^2-b^2})]\,dt. \quad (8)$$

Since $$\phi_{o/h}=\phi_{o/\infty}-\phi_{h/\infty}, \quad . \quad . \quad . \quad . \quad . \quad (9)$$

we obtain from (6)

$$\phi_{o/h}=p\int_0^\infty e^{-pt}f(t)\,dt$$

$$-p^{-n+1}\int_h^\infty e^{-pt}f^{(n)}(t)\,dt-e^{-ph}\sum_{r=0}^{n-1}p^{-r}f^{(r)}(h). \quad (10)$$

Substituting from (5) for the first integral in (10), or writing $h_1=0$, $h_2=h$ in (4), we get

$$\phi_{o/h}=\sum_{r=0}^{n-1}p^{-r}\{f^{(r)}(o)-e^{-ph}f^{(r)}(h)\}+p^{-n+1}\int_0^h e^{-pt}f^{(n)}(t)\,dt. \quad (11)$$

A third formula for $\phi_{o/h}$ can be obtained by adding (10), (11) and halving the sum.

Multiplying both sides of (6) by e^{ph} and writing $t=\tau+h$, we have

$$p\int_0^\infty e^{-p\tau}f(\tau+h)\,d\tau = \sum_{r=0}^{n-1} p^{-r}f^{(r)}(h)+p^{-n+1}\int_0^\infty e^{-p\tau}f^{(n)}(\tau+h)\,d\tau. \quad (12)$$

Interpreting both sides of (12) and writing t for τ, we find that

$$f(t+h)=f(h)+tf^{(1)}(h)+\frac{t^2}{2!}f^{(2)}(h) + \ldots \frac{t^{n-1}}{(n-1)!}f^{(n-1)}(h)+\mathrm{R}_n, \quad (13)$$

which is the Taylor's expansion of $f(t+h)$ obtained for $t>0$.

Again, from (6) we get

$$\underset{h/\infty}{\phi_n} = p^n \underset{h/\infty}{\phi} - e^{-ph}\sum_{r=0}^{n-1} p^{n-r}f^{(r)}(h), \quad . \quad . \quad . \quad (14)$$

where ϕ_n is the O.F. of $f^{(n)}(t)$, and from (11)

$$\underset{o/h}{\phi_n} = p^n \underset{o/h}{\phi} + \sum_{r=0}^{n-1} p^{n-r}[e^{-ph}f^{(r)}(h)-f^{(r)}(o)]. \quad . \quad (15)$$

The sum of (14) and (15) yields

$$\underset{o/\infty}{\phi_n} = p^n \underset{o/\infty}{\phi} - \sum_{r=0}^{n-1} p^{n-r}f^{(r)}(o), \quad . \quad . \quad . \quad (16)$$

a known result.

3. *Contour Integrals for $\phi_{o/h}$ and $\phi_{h/\infty}$.*

Since $$\phi_{o/h}=p\int_0^h e^{-pt}f(t)\,dt, \quad . \quad . \quad . \quad . \quad . \quad (17)$$

then by the Mellin inversion theorem

$$f(t)=\frac{1}{2\pi i}\int_{c-i\infty}^{c+i\infty} e^{zt}\phi(z)\frac{dz}{z}, \quad . \quad . \quad . \quad . \quad (18)$$

provided the necessary conditions are fulfilled *. In (18) $\phi(p)$ is the O.F. of $f(t)$ from $t=0$ to ∞.

* Phil. Mag. xxv. p. 261 (1938) for conditions.

Inserting the value of $f(t)$ from (18) into (17), we get

$$\phi_{o\,h}=\frac{1}{2\pi i}\int_{c-i\infty}^{c+i\infty}\phi(z)\frac{dz}{z}\int_0^h e^{(z-p)t}dt \quad . \quad . \quad . \quad (19)$$

$$=\frac{p}{2\pi i}\int_{c-i\infty}^{c+i\infty}\frac{\phi(z)\,dz}{z(z-p)}\,[e^{(z-p)h}-1], \quad . \quad . \quad (20)$$

where $R(p)>R(z)$, and z is on the contour. By virtue of the conditions mentioned above being satisfied, it is permissible to change the order of integration in (19).

Consider the second integral in (20), namely,

$$-\frac{1}{2\pi i}\int_{c-i\infty}^{c+i\infty}\frac{\phi(z)\,dz}{z(z-p)} \quad . \quad . \quad . \quad . \quad . \quad (21)$$

If the contour is completed on the right of $c+i\infty$ by an infinite semicircle C there is one singularity within, namely, a simple pole at $z=p$. The value of the integral taken *clockwise* round the contour $c\pm i\infty+C$ is $\phi_{o\,\infty}$. If, however, $\left|\frac{\phi(z)}{z}\right| \to 0$ uniformly with respect to phase z, as $|z|\to\infty$, $-\frac{1}{2}\pi \leqslant$ phase $z \leqslant \frac{1}{2}\pi$, the integral along C is zero, and $\phi_{o\,\infty}$ represents the value of (21). Since

$$\phi_{o\,h}=\phi_{o\,\infty}-\phi_{h\,\infty},$$

if follows from (20), (21) that

$$\phi_{h\,\infty}=p\int_h^\infty e^{-pt}f(t)\,dt=-\frac{pe^{-ph}}{2\pi i}\int_{c-i\infty}^{c+i\infty}e^{zh}\frac{\phi(z)\,dz}{z(z-p)}, \quad (22)$$

and $$\phi_{o\,h}=\phi_{o\,\infty}+\frac{pe^{-ph}}{2\pi i}\int_{c-i\infty}^{c+i\infty}\frac{e^{zh}\phi(z)\,dz}{z(z-p)} \quad . \quad . \quad . \quad (23)$$

The evaluation of the contour integrals in (22), (23) is concerned only with those singularities of the integrand which lie to the left of $c\pm i\infty$, for since $R(p)>R(z)$ on the contour, the pole at $z=p$ is excluded.

4. *Example.*

As a simple illustration of §§ 2, 3 we shall find the O.F. of $f(t)=t^3$ from $t=0$ to h. Then, by (10) § 2, we have

$$t^3 \supset \frac{3!}{p^3}-e^{-ph}\left(h^3+\frac{3h^2}{p}+\frac{6h}{p^2}\right)-\frac{3!}{p^2}\int_h^\infty e^{-pt}dt \quad (24)$$

and $$\phi_{o\,h}=\frac{3!}{p^3}(1-e^{-ph})-e^{-ph}\left(h^3+\frac{3h^2}{p}+\frac{6h}{p^2}\right). \quad . \quad . \quad (25)$$

Using (23) and taking $\phi_{o/\infty}=3\,!/p^3$, we get

$$\phi_{o/h}=\frac{3\,!}{p^3}+3\,!\frac{pe^{-ph}}{2\pi i}\int_{c-i\infty}^{c+i\infty}\frac{e^{zh}\,dz}{z^4(z-p)} \quad . \quad . \quad . \quad . \quad (26)$$

$$=\frac{3\,!}{p^3}-3\,!\,pe^{-ph}\left(\frac{1}{p^4}+\frac{h}{p^3}+\frac{h^2}{2p^2}+\frac{h^3}{6p}\right); \quad (27)$$

on evaluating the integral at the quadruple pole at $z=0$ which is identical with (25), as it should be.

The function $y=t^3$, $0\leqslant t<h$ is shown graphically in fig. 1 *a*. It may be considered to consist of $y=t^3$ from $t=0$ to ∞ and $y_1=-t^3$ from $t=h$ to ∞. Consequently the third member of (25) represents the O.F. of $y_1=-t^3$, $h<t<\infty$. If the function $y=t^3$, $0\leqslant t<h$ is iterated to $t=\infty$, the O.F. can be found by aid of a theorem given in a former paper *, where it is shown that

$$\phi_{o/\infty}=\phi_{o/h}/(1-e^{-ph}), \quad . \quad . \quad . \quad . \quad (28)$$

h being the period and $\phi_{o/h}$ the O.F. of the zeroth period. This function is illustrated in fig. 1 *b*, its O.F. being

$$\phi_{o/\infty}=3\,!\left[1-e^{-ph}\left(\frac{p^3h^3}{6}+\frac{p^2h^2}{2}+ph+1\right)\right]\Big/p^3(1-e^{-ph}).$$

$$. \quad . \quad . \quad (29)$$

5. *Remarks on Impulses.*

In the Heaviside operational calculus and its recent developments, a function of the independent variable, say $f(t)$, is considered in the range $0<t<\infty$. When dealing with impulses a definition is frequently given to the effect that $\int_{-\infty}^{\infty} f(t)\,dt=1$, *i. e.*, the zeroth moment is unity. Take, for instance, the well-known error function

(*a*) $y=\lim_{a\to 0}\frac{1}{a}e^{-\pi t^2/a^2}$;

or (*b*) $y=\lim_{\omega\to\infty}\frac{1}{2}\omega\cos\omega t$ in the range $-\frac{\pi}{2\omega}\leqslant t\leqslant\frac{\pi}{2\omega}$.

When $a>0$ and ω is finite both of these functions are symmetrical about the y axis. Although in the limit the O.F. is taken as p, this is inconsistent with a calculus

* Phil. Mag. xxiv. p. 1055 (1937).

where $t>0$. If in the above cases the range $0<t<\infty$ is considered, the O.F. is $\frac{1}{2}p$ and the zeroth moment $\frac{1}{2}$. For $a>0$ and ω finite, both functions are now finitely

Fig. 1.

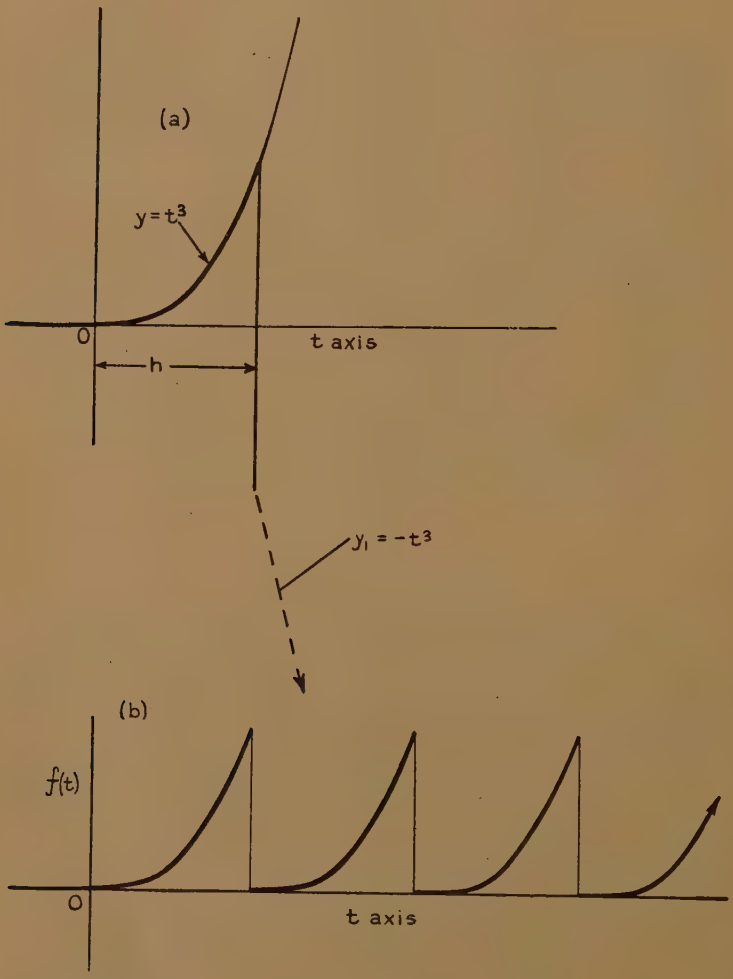

discontinuous at the origin. In practical applications where this type of function is used, the O.F. is taken as p, so the zeroth moment is tacitly doubled. Although this procedure enables the correct answer to be obtained, it is unorthodox.

6. *Impulse Theorem.*

In practical problems we are not concerned with events prior to $t=0$, so the following theorem may be useful.

Let (*a*) a function

$$\left.\begin{aligned} y=f(t),\ 0<t<h, \\ =0,\ t<0\,;\ h<t<\infty\,, \end{aligned}\right\}$$

representing an impulse of duration $t=0$ to h, be single valued and continuous between its discontinuities where it is finite; (*b*) the discontinuities, maxima and minima be limited in number; (*c*) $\int_0^h f(t)\,dt=\mathrm{A}$, a constant. Then as $h\to 0$, the O.F. of $f(t)\to \mathrm{A}p$. For

$$\phi(p)=p\int_0^h e^{-pt}f(t)\,dt, \quad . \quad . \quad . \quad . \quad (30)$$

and when h is small we may write

$$\phi(p)\simeq p\int_0^h f(t)\,dt=\mathrm{A}p. \quad . \quad . \quad . \quad . \quad (31)$$

In the limit when $h\to 0$, we get

$$\phi(p)=\mathrm{A}p, \quad . \quad . \quad . \quad . \quad . \quad . \quad (32)$$

so

$$f(t)\rightleftharpoons \mathrm{A}p, \quad . \quad . \quad . \quad . \quad . \quad . \quad (33)$$

when $h=0$. The O.F. is independent of the shape of the impulse, which may last for a short but finite time, provided all the energy is transferred to the impulsed system before it responds appreciably.

Examples.

1. Consider the first half cycle of $\frac{1}{2}\mathrm{A}\omega \sin \omega t$. This is the sum of two sine waves of equal amplitude and period, one starting at $t=0$ the other at $t=\pi/\omega$, so the O.F. is

$$\phi(p)=\tfrac{1}{2}\mathrm{A}\omega\left[\frac{\omega p}{(p^2+\omega^2)}(1+e^{-\pi p/\omega})\right]. \quad . \quad . \quad (34)$$

When $\omega\to\infty$, $|\,p\,|$ being finite,

$$\phi(p)\to \mathrm{A}p. \quad . \quad . \quad . \quad . \quad . \quad . \quad (35)$$

2. Consider the first quarter cycle of the function $\mathrm{A}\omega \cos \omega t$, which is finitely discontinuous at $t=0$. It can be regarded as a cosine wave starting at $t=0$, to which

is added a sine wave commencing at $t=\pi/2\omega$. The O.F. is

$$\phi(p)=\frac{A\omega}{(p^2+\omega^2)}\left[p^2+\omega p\, e^{-\pi p/2\omega}\right]. \quad . \quad . \quad (36)$$

When $\omega\to\infty$, $|\ p\ |$ being finite

$$\phi(p)\to Ap. \quad . \quad . \quad . \quad . \quad . \quad . \quad (37)$$

7. *Iterated Impulses.*

Sometimes in radio circuits it is necessary to consider the influence of short pulses which occur at equal time intervals, *e. g.*, a diode detector, or a heavily biassed triode in which the current flows for a short time when the applied voltage is in the neighbourhood of its positive peak. The electrical circuits can be treated analytically if we know the O.F. of the rhythmic impulses. Using the theorem already cited for iterated functions, the O.F. of the zeroth period of duration h is

$$\phi_{o/h}=Ap, \quad . \quad . \quad . \quad . \quad . \quad . \quad . \quad . \quad (38)$$

so

$$\phi_{o/\infty}=Ap/(1-e^{-ph}). \quad . \quad . \quad . \quad . \quad (39)$$

When the impulses are alternately positive and negative the O.F. of the zeroth period of duration $2h$ is

$$\phi_{o/2h}=Ap(1-e^{-ph}) \quad , \quad . \quad . \quad . \quad . \quad (40)$$

$-Ape^{-ph}$ being the negative impulse at $t=h$. Thus the O.F. of the iterated impulses is

$$\phi_{o/\infty}=Ap(1-e^{-ph})/(1-e^{-2ph})=Ap/(1+e^{-ph}). \quad . \quad (41)$$

It may be remarked that the dimension of A in a physical problem will be "force × time," force being the dimension of Ap *, p being considered real for convenience.

8. *Example.*

A voltage impulse generator is applied to the circuit shown in fig. 2 at time $t=0$. If the impulses are always positive and occur at interval h, each having the value A (which has dimensions voltage × time), find an expression for I_1, the current in the coil L. Neglect impedance of generator for simplicity.

* Force here refers to a mechanical system, or to its equivalent in an electrical, acoustical, etc. system. (See Phil. Mag. xxvi. p. 407 (1938).)

In operational form the circuital equations are

$$E-RI=pLI_1=I_2/pC, \quad . \quad . \quad . \quad . \quad (42)$$

$$I=I_1+I_2, \quad . \quad . \quad . \quad . \quad . \quad . \quad (43)$$

giving

$$I_1=E/[R(p^2LC+1)+pL]. \quad . \quad . \quad . \quad (44)$$

Introducing the O.F. of E from (39), (44) yields

$$I_1=(A/LCR)p/(p^2+ap+b)(1-e^{-ph}), \quad . \quad . \quad (45)$$

where $a=1/CR$, $b=1/LC$, and we take $b>\frac{1}{4}a^2$ for an oscillatory circuit. By the Mellin inversion theorem, the interpretation of (45) in terms of t is

$$I_1=\frac{(A/LCR)}{2\pi i}\int_{c-i\infty}^{c+i\infty} e^{zt}\,dz/(z^2+az+b)(1-e^{-zh}). \quad (46)$$

Fig. 2.

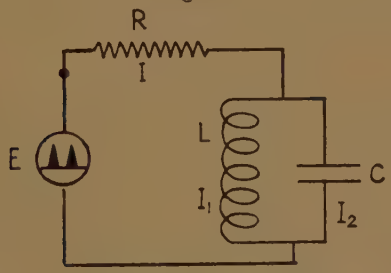

Evaluating (46) at the poles of the integrand gives

$$I_1=\frac{A}{LCR}\left[\frac{e^{-\frac{1}{2}at}\sin kt-e^{-\frac{1}{2}a(t+h)}\sin k(t+h)}{k(1+e^{-ah}-2e^{-\frac{1}{2}ah}\cos kh)}+\frac{1}{hb}\right.$$
$$\left.+h\sum_{n=1}^{\infty}\frac{\sin\left\{(2\pi nt/h)+\tan^{-1}\left(\frac{bh^2-4\pi^2n^2}{2\pi nah}\right)\right\}}{\{(bh^2-4\pi^2n^2)^2+4\pi^2n^2a^2h^2\}^{\frac{1}{2}}}\right], \quad (47)$$

where $k=\sqrt{\left(b-\frac{a^2}{4}\right)}$, The first member on the r.h.s. of (47) represents the transient which dies away rapidly in a practical circuit, after the generator is switched on. The second member A/Rh gives the constant unidirectional current, which increases as the interval h decreases. The third member represents the Fourier expansion of the current wave in inductance L during the steady state. All the harmonics are even, their frequencies being independent of the natural frequency of the circuit. The amplitudes and phases are, however, dependent upon

$a=1/CR$ and $b=1/LC$. For the nth harmonic the amplitude is a maximum when

$$C=\frac{h^2+4\pi^2n^2L^2/R^2}{4\pi^2n^2L}. \quad . \quad . \quad . \quad . \quad . \quad (48)$$

If the impulses had been alternately positive and negative (zeroth period $2h$), the current would have been

$$I_1=\frac{A}{LCR}\left[\frac{e^{-\frac{1}{2}at}\sin kt+e^{-\frac{1}{2}a(t+h)}\sin k(t+h)}{k(1+e^{-ah}+2e^{-\frac{1}{2}ah}\cos kh)}\right.$$
$$\left.-h\sum_{n=0}^{\infty}\frac{\sin\left\{(2n+1)\frac{\pi t}{h}+\tan^{-1}\left(\frac{bh^2-(2n+1)^2\pi^2}{(2n+1)\pi ah}\right)\right\}}{\{[bh^2-(2n+1)^2\pi^2]^2+(2n+1)^2\pi^2a^2h^2\}^{\frac{1}{2}}}\right]. \quad . \quad . \quad . \quad (49)$$

In this case there is no unidirectional current, whilst the harmonics are all odd. The amplitude of the nth harmonic is a maximum when

$$C=\frac{h^2+(2n+1)^2\pi^2L^2/R^2}{(2n+1)^2\pi^2L}. \quad . \quad . \quad . \quad . \quad . \quad (50)$$

Appendix.

Remainder in Taylor's Theorem obtained operationally.

By interpreting the last member of (12) § 2, we obtain a well-known formula for the remainder in Taylor's theorem. We have

$$R_n \supset p^{-n+1}\int_0^{\infty} e^{-pt}f^{(n)}(t+h)\,dt, \quad . \quad . \quad . \quad . \quad . \quad (1)$$

$$=\frac{1}{p}\ \frac{1}{p^{n-1}}\left[p\int_0^{\infty}e^{-pt}f^{(n)}(t+h)\,dt\right]. \quad . \quad . \quad (2)$$

By Borel's theorem, if $f_1(t)\supset\phi_1(p)$, and $f_2(t)\supset\phi_2(p)$, then

$$\int_0^t f_1(\lambda)f_2(t-\lambda)\,d\lambda=\int_0^t f_1(t-\lambda)f_2(\lambda)\,d\lambda\supset\frac{1}{p}\phi_1(p)\phi_2(p). \quad (3)$$

Applying (3) to (2), we have immediately

$$R_n=\int_0^t f^{(n)}(t+h-\lambda)\frac{\lambda^{n-1}}{(n-1)!}d\lambda, \quad . \quad . \quad . \quad (4)$$

$$=\int_0^t f^{(n)}(\lambda+h)\frac{(t-\lambda)^{n-1}}{(n-1)!}d\lambda. \quad . \quad . \quad . \quad . \quad (5)$$

When $h=0$, we obtain the remainder in Maclaurin's theorem. The results are deduced for $t>0$.

LX. *The Damping of the Lateral Vibration of a Mild Steel Bar.* *By* A. J. Ockleston, *B.E., Ph.D.**.

[Received June 14, 1938.]

Introduction.

VIBRATING systems in which the potential energy is due to the flexure of steel members are of common occurrence, and the damping of such systems is of considerable practical importance.

A rod vibrating laterally is one of the simplest systems of this type. The dissipative forces acting are the atmospheric resistance and the internal friction of the material. By observing the rate of decay of the free vibration of a rod in the atmosphere and in the exhausted reservoir of a vacuum pump Kelvin [1] found that in comparison with the effect of the internal friction, the air resistance was negligible.

The internal friction of solids has been studied by a number of investigators. The majority have assumed that this effect is similar to the frictional resistance of a viscous fluid, and that the internal frictional forces are proportional to the rate of change of the stresses. If this assumption is made the solution of the equation of motion for a laterally vibrating rod indicates that the decay of free vibration is logarithmic, the logarithmic decrement † for each of the various normal modes being proportional to its frequency [2].

Tests made by Hopkinson and Williams [3] and by Rowett [4] have shown that if a mild steel specimen is subjected to a cyclic variation of either direct or shear stress, the stress-strain curve is a narrow hysteresis loop, the energy dissipated per stress cycle being represented by the area of the loop. This loss of energy is independent of the speed of the cyclic variation of stress and not, as required by the viscous damping theory, proportional to it.

Measurements of the internal friction of various metals, rubber, glass, celluloid, and maple wood have been

* Communicated by Prof. W. Norman Thomas, M.A., D.Phil.

† For a damped vibration of frequency n, given by the expression

$$x = x_0 e^{-kt} \cos(2\pi nt + \theta),$$

the logarithmic decrement is, in this paper, defined as the ratio k/n.

made by Kimball and Lovell [5], [6]. The test specimen was a slender rod carried in two bearings near one of its ends. A lateral force was applied at the free end and a cyclic variation of direct stress obtained by rotating the rod. In all the materials tested the frictional loss per cycle for any particular lateral force was constant, whatever the speed of rotation. Kimball and Lovell consider that the dissipation of energy by internal friction is given, with sufficient accuracy for most purposes, by the expression

$$F = \xi f_m^2,$$

where F = the frictional loss per stress cycle per unit volume at any point,

f_m = the amplitude of the stress cycle above and below zero stress at that point,

ξ = the "internal friction constant."

From this law it follows that the decay of lateral variation is logarithmic, and that for any particular material the logarithmic decrement is independent of the frequency, and equal to ξ E, where E is the value of Young's Modulus for the material. A few observations of the lateral vibration of rods were made. For steel the decay was found to be very nearly logarithmic, but the value of ξ deduced from the logarithmic decrement was over three times that found by the revolving rod method; this was attributed to loss of energy by surface friction in the clamps at the ends of the rod [6].

In the course of an investigation by the writer of the lateral vibration of a steel frame, the logarithmic decrements of the normal modes of free vibration were determined. The values obtained could not be satisfactorily explained by either the viscous damping theory or that of Kimball and Lovell. The stress amplitudes in the frame were considerably less than those generally employed in investigations of internal friction, and the experiments described here were carried out to investigate the nature of the damping for lateral vibrations of small amplitude.

Experimental Investigation.

The majority of the tests were made on a bar of unannealed mild steel, approximately $1\frac{1}{2} \times \frac{3}{8}$ in. section,

having an effective length of about 16 in. One end of the bar was free, while the other was fixed by a massive clamp to a heavy cast iron base built into a brick pier. The six-inch length of bar held in the clamp was carefully scraped and ground so that it was, as far as possible, in contact with the clamping surfaces over the whole of its area. With this clamping the end of the bar was not perfectly rigid, but approximated thereto; the actual frequency was 1·6 per cent. less than that of a fixed free bar of the same dimensions.

A light rocker carrying a small mirror was fitted at the free end of the bar. Photographic traces of the movements of the free end during vibration were obtained by means of a beam of light reflected by the mirror and focussed on a band of film on a rotating drum. A vibrating style, operated by 50-cycle alternating current, was used to provide a time scale on the record. The point of the style bore lightly on the emulsion of the film, scratching a 100-cycle wave which, after development, was clearly visible.

By clamping weights to the bar the frequency of this vibrating system could be altered without material alteration to its configuration during vibration. For each frequency a number of photographic records of the oscillations of the free end of the bar were obtained. In all cases the fundamental mode of vibration was exited. The maximum stress-amplitudes were of the order of 1000 lb./sq. in.

From the traces the frequencies and amplitudes of vibration were determined. No difficulty was experienced in obtaining accurate values of the frequencies, the maximum discrepancy between one determination and the mean for that case being only 0·15 per cent. The smallest amplitudes could be measured to within about 1 per cent., the accuracy being greater for larger amplitudes. The "internal friction constant" is, however, proportional to the logarithmic decrement, and for small amplitudes an error of 1 per cent. in amplitude could give rise to an error of about 8 per cent. in logarithmic decrement. The scattering of the observed values about the mean curves is probably due mainly to this fact.

Contrary to both the viscous damping theory and that of Kimball and Lovell, the decay of the free

vibrations of the rod was not logarithmic. The traces were therefore divided into sections each 40 cycles and the value of the " internal friction constant " ξ calculated for each section, on the assumption that for the range considered the decay was logarithmic. For each frequency

Fig. 1.

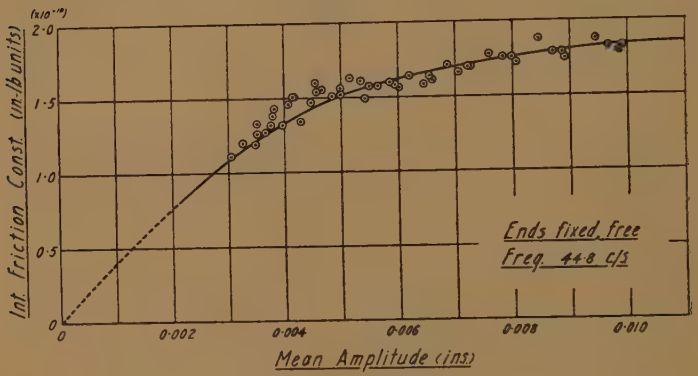

Fig. 2.

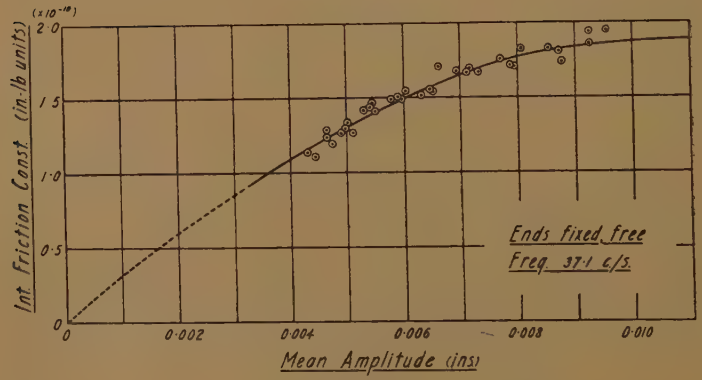

of the system the values of ξ have been plotted against the mean amplitudes of the ranges in figs. 1–6. A mean curve has been drawn through the experimental values for each frequency ; these mean curves are reproduced in fig. 7.

The preliminary observations were made on the oscillations of the mid-point of a similar bar 30 in. long, hinged

Fig. 3.

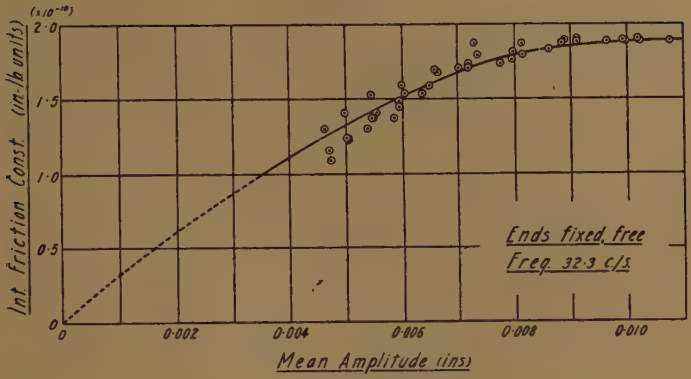

Fig. 4.

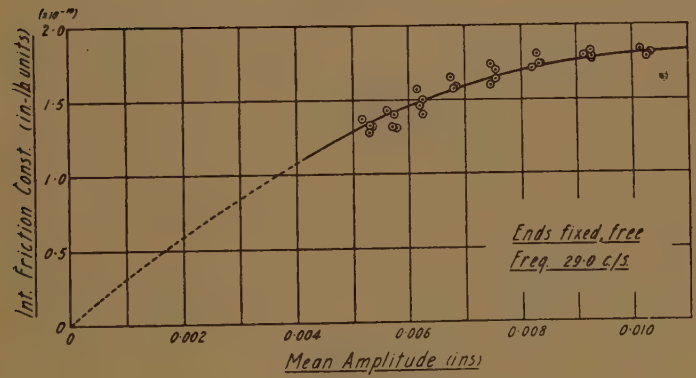

Fig. 5.

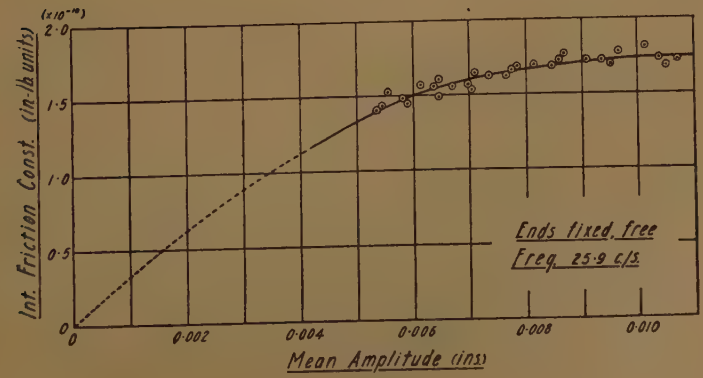

Fig. 6.

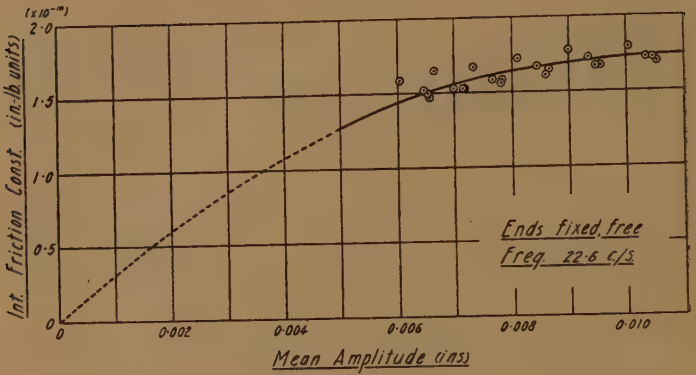

Fig. 7.

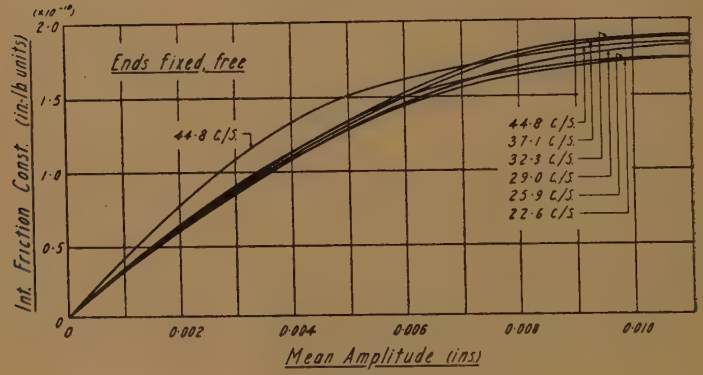

Fig. 8.

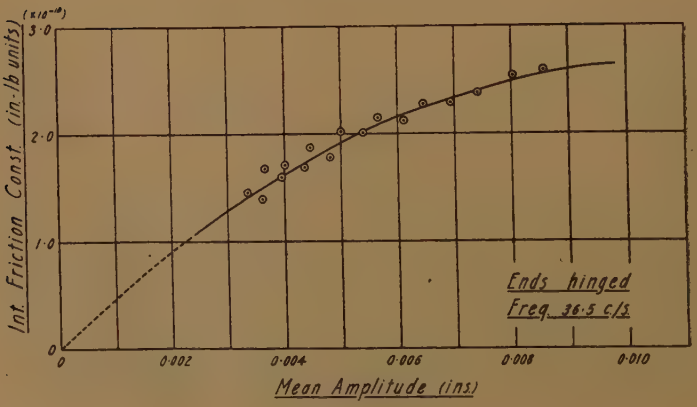

at each end, but the experiments are not considered satisfactory, as appreciable vibration of the brackets carrying the pivots occurred. It is significant, however, that the mean curve derived from these experiments is similar in shape to those subsequently obtained for the fixed free bar, and it is, therefore, included for comparison in fig. 8.

Results and Conclusions.

The plotted experimental values show that the " internal friction constant " ξ, and hence the logarithmic decrement, is not constant but decreases with decrease in amplitude. This decrease is most rapid at small amplitudes, the value of ξ for larger amplitudes being more nearly constant. As the mean curves are approximately the same for all frequencies the dissipation of energy per cycle due to internal friction appears to be independent of the frequency.

The average, for the various frequencies, of the value of ξ at the maximum amplitude of these tests, $1{\cdot}83\times10^{-10}$ in.-lb. units, agrees more closely with that determined by Kimball and Lovell [6] from the revolving rod experiments ($1{\cdot}62\times10^{-10}$) than with the value found from observations of lateral vibration ($5{\cdot}3\times10^{-10}$). It seems probable that for stress-amplitudes greater than those of the experiments described here the variation of ξ with amplitude is comparatively small. For such stress-amplitudes Honda and Konno [7] found a small decrease with decrease of amplitude in the logarithmic decrement of steel bars vibrating laterally, and a similar effect was observed for torsional vibrations by Iokibe and Sakai [8]. These variations in logarithmic decrement were attributed partly to the fact that the oscillations were large, and partly to dissipation of energy at imperfectly clamped joints; it was considered that for small amplitudes both effects would be small [7]. In the present experiments, however, the variation in logarithmic decrement is most marked when the amplitudes are small. In this connexion it may be noted that the values of ξ deduced from observations made by Quimby [9] of longitudinal vibrations of small amplitude were less than those found by Kimball and Lovell for larger amplitudes [5]. An

explanation is suggested by measurements made by Rowett [4] of the relative widths of the hysteresis loops for mild steel subject to cyclic shearing stresses. At low stresses the loops are relatively narrower than at high stresses. The hysteresis loops for direct stress are likely to be similar ; the energy dissipated per cycle will, therefore, increase more rapidly than the square of the stress, as is assumed in the expression for the " internal friction constant."

It seems likely that where the stress amplitudes are comparatively large, the decay of the lateral vibration of mild steel members is approximately logarithmic, and the dissipation of energy by internal friction is given, with sufficient accuracy for most purposes, by the law proposed by Kimball and Lovell. For small stress amplitudes, however, this law is not satisfactory. The decay is not logarithmic, the rate of decay decreasing as the amplitude decreases.

In all cases the loss of energy per cycle due to internal friction depends only on the stress amplitude, and is independent of the frequency.

References.

(1) Lord Kelvin, ' Mathematical and Physical Papers,' vol. iii. p. 23.
(2) K. Suyehiro, ' On the Damped Transversal Vibration of Prismatic Bars,' Bull. Earthquake Research Inst., Tokio Imp. Univ. vol. vi. p. 63.
(3) B. Hopkinson and G. T. Williams, ' The Elastic Hysteresis of Steel,' Proc. Roy. Soc., ser. A, vol. lxxxvii. p. 502.
(4) F. E. Rowett, ' Elastic Hysteresis in Steel,' Proc. Roy. Soc. ser. A, vol. lxxxix. p. 528.
(5) A. L. Kimball and D. E. Lovell, ' Internal Friction in Solids,' Phys. Rev., vol. xxx. 2nd ser. p. 948.
(6) A. L. Kimball and D. E. Lovell, ' Internal Friction in Solids,' Mech. Eng. vol. xlix. (5), p. 440.
(7) K. Honda and S. Konno, ' On the Determination of the Coefficient of Normal Viscosity of Solids,' Phil. Mag. vol. xlii. ser. 6, p. 115.
(8) K. Iokibe and S. Sakai, ' The Effect of Temperature on the Modulus of Rigidity and on the Viscosity of Solid Metals,' Phil. Mag. vol. xlii. ser. 6, p. 397.
(9) S. L. Quimby, ' On the Experimental Determination of the Viscosity of Vibrating Solids,' Phys. Rev. vol. xxv. 2nd ser. p. 558.

LXI. *Stresses in an Eccentrically Rotating Disk.*

By Raymond D. Mindlin, *Ph.D., Department of Civil Engineering, Columbia University, New York City* *.

[Received July 14, 1938.]

Synopsis.

The two-dimensoinal elasticity equations for small strain are solved in this paper to obtain the stresses in a circular disk which rotates about an axis normal to the plane of the disk. The axis of rotation may pass either inside or outside the disk. The unbalance introduced by the eccentricity of the axis of rotation is equilibrated by means of a concentrated force acting in the plane of the disk. The point of application of the force may be at any point in the disk along the straight line passing through the centre of rotation and the centre of the disk. The bipolar coordinate system is employed, and the solution is obtained in finite terms.

We consider a circular disk of density ρ, radius R, and of small thickness taken as unity. The disk rotates with uniform angular velocity ω about an axis normal to its plane. The point of intersection, C, of the axis of rotation and the plane of the disk is located at point $(0, c)$ of an x, y system of rectangular coordinates as shown in the figure. Point C may be anywhere along the y-axis. The coordinates axes rotate with the disk, so that the centre, D, of the disk always lies on the y-axis at a distance d from the origin.

A centripetal force F of magnitude $\rho\omega^2\pi R^2(c-d)$ is required to maintain the circular motion. This force is considered concentrated at a point A with coordinates $(0, a)$. Whereas A must lie inside the disk, C may lie inside or outside the disk.

On account of the eccentricity of the balancing force the problem is most conveniently treated in bipolar coordinates. Such a coordinate system may be obtained from the conformal transformation.

$$x+iy=ia\coth\tfrac{1}{2}(\alpha+i\beta), \quad . \quad . \quad . \quad . \quad . \quad . \quad (1)$$

* Communicated by Prof. R. V. Southwell, M.A., F.R.S.

whence $$x=\frac{a\sin\beta}{\cosh\alpha-\cos\beta},\quad y=\frac{a\sinh\alpha}{\cosh\alpha-\cos\beta},\quad\ldots\quad(2)$$

$$\alpha=\log\frac{r_1}{r_2},\quad \beta=\theta_1-\theta_2.\quad\ldots\quad(3)$$

The significance of the coordinates appearing in (2) and (3) is illustrated in the figure. It is to be observed that the positive pole $\alpha=\infty$ coincides with the point of application $(0, a)$ of the balancing force. The boundary of the disk is taken as the circle $\alpha=\alpha_1$. The centre of this

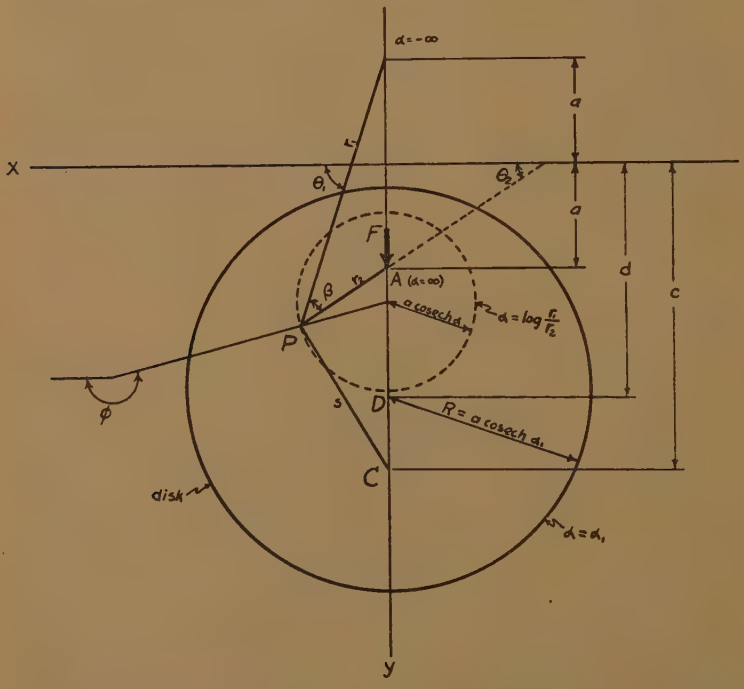

circle lies on the y-axis at a distance $d=a\coth\alpha_1$ from the origin, and its radius is $R=a\operatorname{cosech}\alpha_1$.

Important parts are taken in the ensuing solution by the stretch ratio, J, of the transformation (1) and the angle ϕ which the tangent to the curve $\beta=$constant makes with the x-axis. These are given by

$$J=\sqrt{\left(\frac{\partial x}{\partial\alpha}\right)^2+\left(\frac{\partial y}{\partial\alpha}\right)^2}=\frac{a}{\cosh\alpha-\cos\beta},\quad\ldots\quad(4)$$

$$\phi=\theta_1+\theta_2+\frac{\pi}{2}=\tan^{-1}\frac{\cosh\alpha\cos\beta-1}{\sinh\alpha\sin\beta}.\quad\ldots\quad(5)$$

The problem is treated as one of plane stress, and functions in the stresses involving the coordinate normal to the x, y-plane are neglected. The components of stress in plane curvilinear coordinates are expressed in terms of a stress function χ and a body force function Ω by[1]

$$\left.\begin{aligned}\widehat{\alpha\alpha} &= \frac{1}{J^2}\frac{\partial^2\chi}{\partial\beta^2}+\frac{1}{J^3}\left(\frac{\partial\chi}{\partial\alpha}\frac{\partial J}{\partial\alpha}-\frac{\partial\chi}{\partial\beta}\frac{\partial J}{\partial\beta}\right)+\Omega,\\ \widehat{\beta\beta} &= \frac{1}{J^2}\frac{\partial^2\chi}{\partial\alpha^2}+\frac{1}{J^3}\left(\frac{\partial\chi}{\partial\beta}\frac{\partial J}{\partial\beta}-\frac{\partial\chi}{\partial\alpha}\frac{\partial J}{\partial\alpha}\right)+\Omega,\\ \widehat{\alpha\beta} &= -\frac{1}{J^2}\frac{\partial^2\chi}{\partial\alpha\partial\beta}+\frac{1}{J^3}\left(\frac{\partial\chi}{\partial\alpha}\frac{\partial J}{\partial\beta}+\frac{\partial\chi}{\partial\beta}\frac{\partial J}{\partial\alpha}\right),\end{aligned}\right\} \quad . \quad (6)$$

where Ω is related to the x and y components of the body force per unit of volume by

$$X=-\frac{\partial\Omega}{\partial x}, \quad Y=-\frac{\partial\Omega}{\partial y}, \quad . \quad . \quad . \quad . \quad (7)$$

and χ satisfies the differential equation

$$\nabla^4\chi=-(1-\nu)\nabla^2\Omega, \quad . \quad . \quad . \quad . \quad . \quad (8)$$

in which ν is Poisson's ratio, ∇^2 is Laplace's two-dimensional operator, and $\nabla^4=\nabla^2\nabla^2$.

The body force per unit of volume at a point P distant s from C is $\rho\omega^2 s$, and it acts in the direction $\overline{CP}$. Hence, from (7),

$$\begin{aligned}\Omega &= -\tfrac{1}{2}\rho\omega^2 s^2+\text{constant},\\ &= -\tfrac{1}{2}\rho\omega^2[x^2+(y-c)^2]+\text{constant}. \quad . \quad . \quad (9)\end{aligned}$$

Considering (2) and (4), and taking the constant equal to $\frac{1}{2}\rho\omega^2(c^2-a^2)$, (9) becomes

$$\Omega=\rho\omega^2 J\sinh\alpha(c-a\coth\alpha), \quad . \quad . \quad . \quad (10)$$

and $$\nabla^2\Omega=-2\rho\omega^2.$$

Hence (8) becomes . . . . . (11)

$$\nabla^4\chi=2(1-\nu)\rho\omega^2. \quad . \quad . \quad . \quad . \quad . \quad (12)$$

The problem therefore consists in finding a solution of (12) which produces a concentrated force of magnitude $\rho\omega^2\pi R^2(c-d)$ at A, and which yields stresses according to (6) which satisfy the conditions

$$\widehat{\alpha\alpha}=\widehat{\alpha\beta}=0 \quad . \quad . \quad . \quad . \quad . \quad . \quad (13)$$

on the boundary of the disk.

It may be verified that

$$\chi_0=\tfrac{1}{8}(1-\nu)\rho\omega^2a^2\mathrm{J}^2e^{-2\alpha} \quad . \quad . \quad . \quad . \quad . \quad (14)$$

is a particular solution of (12), so that we may take our stress function to be

$$\chi=\chi_0+\chi', \quad . \quad . \quad . \quad . \quad . \quad . \quad . \quad (15)$$

where χ' is governed by

$$\nabla^4\chi'=0. \quad . \quad . \quad . \quad . \quad . \quad . \quad . \quad (16)$$

We shall now construct a convenient stress function satisfying (16) and giving a concentrated force of magnitude F acting at A in the positive y-direction. Considering polar coordinates r_2, θ_2 with origin at A, the stress function for the required single force is known to be [2]

$$\chi_a=\frac{2\pi}{\mathrm{F}}\left\{r_2\theta_2\cos\theta_2+\frac{1-\nu}{2}r_2\sin\theta_2\log r_2\right\}. \quad (17)$$

In order to express (17) in bipolar coordinates it is advantageous to first add to it the following stress function satisfying (16) and producing no singularities inside the disk :

$$\chi_b=\frac{\mathrm{F}}{2\pi}\left\{r_1\left(\theta_1+\frac{\pi}{2}\right)\cos\theta_1-\frac{1-\nu}{2}r_2\sin\theta_2\log r_1\right\}. \quad (18)$$

Then, noting that

$$r_1\cos\theta_1=r_2\cos\theta_2=x=\mathrm{J}\sin\beta,$$

$$\theta_1+\theta_2+\frac{\pi}{2}=\phi,$$

$$r_2\sin\theta_2=y-a=\mathrm{J}(\sinh\alpha-\cosh\alpha+\cos\beta),$$

$$\log\frac{r_1}{r_2}=\alpha,$$

we find

$$\chi_1=\chi_a+\chi_b=\frac{\mathrm{FJ}}{2\pi}\left\{\phi\sin\beta-\frac{1-\nu}{2}\alpha(\sinh\alpha-\cosh\alpha+\cos\beta)\right\}. \quad (19)$$

The magnitude of F is given by

$$\mathrm{F}=\rho\omega^2\pi\mathrm{R}^2(c-d),$$

$$=\rho\omega^2\pi a^2\operatorname{cosech}^2\alpha_1(c-a\coth\alpha_1). \quad . \quad . \quad (20)$$

The components of stress $\widehat{\alpha\alpha}$ and $\widehat{\alpha\beta}$ produced by Ω, χ_0 and χ_1, are found to be, from (6),

$$\left.\begin{aligned}
\widehat{\alpha\alpha} &= \rho\omega^2 \mathrm{J} \sinh\alpha(c - a\coth\alpha) \\
&\quad + \tfrac{1}{4}(1-\nu)\rho\omega^2(a\mathrm{J}e^{-\alpha} + \mathrm{J}^2 e^{-2\alpha}\sin^2\beta) \\
&\quad + \tfrac{1}{2}\rho\omega^2 \operatorname{cosech}^2\alpha_1(c - a\coth\alpha_1)[a\sinh\alpha(\cosh\alpha \\
&\qquad - \cos\beta) - \mathrm{J}\sinh^3\alpha] \\
&\quad + \tfrac{1}{4}(1-\nu)\rho\omega^2 a \operatorname{cosech}^2\alpha_1(c - a\coth\alpha_1)[\sinh^2\alpha \\
&\qquad - \sinh\alpha(\cosh\alpha - \cos\beta)], \\
\widehat{\alpha\beta} &= -\tfrac{1}{4}(1-\nu)\rho\omega^2 e^{-2\alpha}[a\mathrm{J}\sin\beta + \mathrm{J}^2\sinh\alpha\sin\beta] \\
&\quad + \tfrac{1}{2}\rho\omega^2 \operatorname{cosech}^2\alpha_1(c - a\coth\alpha_1)[a\sin\beta(\cosh\alpha \\
&\qquad - \cos\beta) - \mathrm{J}\sinh^2\alpha\sin\beta] \\
&\quad - \tfrac{1}{4}(1-\nu)\rho\omega^2 a \operatorname{cosech}^2\alpha_1(c - a\coth\alpha_1)\sin\beta \\
&\qquad \times(\cosh\alpha - \cos\beta).
\end{aligned}\right\} \quad (21)$$

These do not vanish when $\alpha = \alpha_1$, so that it is necessary to introduce further solutions of (16) in order to satisfy (13).

There exists a general method, due to Jeffery[3], for finding the required functions when the boundary stresses are expressed in the form

$$f(\alpha_1)\cos n\beta \quad \text{or} \quad f(\alpha_1)\sin n\beta.$$

In order to apply Jeffery's method in this case it would be necessary to expand in infinite series the terms in (21) which involve J. However, it is possible to avoid an infinite series treatment by introducing special functions which will remove the awkward J terms on $\alpha = \alpha_1$.

To this end we consider the simple biharmonic functions (*i. e.*, satisfying (16)) :

$$\begin{aligned}
\chi_2 &= \mathrm{G}a^{-1}y(x^2+y^2) + \mathrm{H}y^2 \\
&= \mathrm{G}\mathrm{J}^2\sinh\alpha(\cosh\alpha + \cos\beta) + \mathrm{H}\mathrm{J}^2\sinh^2\alpha, \quad . \quad (22)
\end{aligned}$$

from which

$$\left.\begin{aligned}
\widehat{\alpha\alpha} &= 2\mathrm{G}(\mathrm{J}a^{-1}\sinh\alpha + \mathrm{J}^2a^{-2}\sinh 2\alpha\sin^2\beta) \\
&\qquad + 2\mathrm{H}\mathrm{J}^2a^{-2}\sinh^2\alpha\sin^2\beta, \\
\widehat{\alpha\beta} &= 2\mathrm{G}(\mathrm{J}a^{-1}\cosh 2\alpha - \mathrm{J}^2a^{-2}\sinh 2\alpha\sinh\alpha)\sin\beta \\
&\qquad + \mathrm{H}(\mathrm{J}a^{-1}\sinh 2\alpha - 2\mathrm{J}^2a^{-2}\sinh^3\alpha)\sin\beta.
\end{aligned}\right\} \quad (23)$$

The values of the constants G and H which will remove the terms in J and J^2 from $\widehat{\alpha\alpha}$ and $\widehat{\alpha\beta}$ when $\alpha = \alpha_1$ are found to be

$$\left.\begin{aligned}
\mathrm{G} &= \tfrac{1}{4}\rho\omega^2 a[a\coth\alpha_1 - c - \tfrac{1}{2}a(1-\nu)(\coth\alpha_1 - 1)], \\
\mathrm{H} &= -\tfrac{1}{8}\rho\omega^2 a \operatorname{cosech}^2\alpha_1[2(a\coth\alpha_1 - c)\sinh 2\alpha_1 \\
&\qquad - a(1-\nu)].
\end{aligned}\right\} \quad (24)$$

The combined functions Ω, χ_0, χ_1, and χ_2 produce only the following normal and shearing stresses on the boundary of the disk :

$$\left.\begin{aligned}\widehat{\alpha\alpha}_1&=\tfrac{1}{4}\rho\omega^2 a(c-a\coth\alpha_1)[(1+\nu)(\cosh\alpha_1\\&\qquad-\cos\beta)\operatorname{cosech}\alpha_1+1-\nu],\\\widehat{\alpha\beta}_1&=\tfrac{1}{4}(1+\nu)\rho\omega^2 a(c-a\coth\alpha_1)(\cosh\alpha_1\\&\qquad-\cos\beta)\operatorname{cosech}^2\alpha_1\sin\beta.\end{aligned}\right\}. \quad (25)$$

To remove these last stresses from the boundary it is only necessary to consider a solution of (16) of the form $f_1(\alpha)+f_2(\alpha)\cos\beta$. This is known to be [3]

$$\begin{aligned}\chi_3=&J(A_0\cosh\alpha+B_0\alpha\cosh\alpha+C_0\sinh\alpha+D_0\alpha\sinh\alpha)\\&+J(A_1\cosh 2\alpha+B_1+C_1\sinh 2\alpha+D_1\alpha)\cos\beta. \quad (26)\end{aligned}$$

We require that there be no singularities inside the disk other than the single force at A as given by (17). Hence we must take

$$\left.\begin{aligned}B_0=D_0=D_1=0,\\A_1+C_1=0.\end{aligned}\right\}. \quad . \quad . \quad . \quad . \quad (27)$$

Furthermore, the term $C_0 J\sinh\alpha$ produces no stress, and $A_0 J\cosh\alpha$ produces the same stress as $B_1 J\cos\beta$, so that we may drop the terms in A_0 and C_0. (26) therefore reduces to

$$\chi_3=J[A_1e^{-2\alpha}+B_1]\cos\beta, \quad . \quad . \quad . \quad . \quad (28)$$

from which

$$\left.\begin{aligned}\widehat{\alpha\alpha}&=B_1a^{-1}+A_1a^{-1}e^{-2\alpha}+2A_1a^{-1}e^{-2\alpha}\sinh\alpha\cos\beta,\\\widehat{\alpha\beta}&=-2A_1a^{-1}e^{-2\alpha}(\cosh\alpha-\cos\beta)\sin\beta.\end{aligned}\right\}. \quad (29)$$

Setting $\alpha=\alpha_1$, and equating coefficients in (29) and (25) in the usual manner, we find

$$\left.\begin{aligned}A_1&=\tfrac{1}{8}(1+\nu)\rho\omega^2a^2e^{2\alpha_1}\operatorname{cosech}^2\alpha_1(c-a\coth\alpha_1),\\B_1&=-\tfrac{1}{4}\rho\omega^2a^2(c-a\coth\alpha_1)[(1+\nu)(\coth\alpha_1\\&\qquad+\tfrac{1}{2}\operatorname{cosech}^2\alpha_1)+1-\nu].\end{aligned}\right\}. \quad (30)$$

The complete solution is therefore given by

$$\Omega=\rho\omega^2J\sinh\alpha(c-a\coth\alpha),$$

$$\begin{aligned}\chi&=\chi_0+\chi_1+\chi_2+\chi_3\\&=\tfrac{1}{8}(1-\nu)\rho\omega^2a^2J^2e^{-2\alpha}\\&\quad+\tfrac{1}{2}\rho\omega^2a^2\operatorname{cosech}^2\alpha_1(c-a\coth\alpha_1)J[\phi\sin\beta-\tfrac{1}{2}(1-\nu)\alpha\\&\qquad\times(\sinh\alpha-\cosh\alpha+\cos\beta)]\end{aligned}$$

$$+\tfrac{1}{4}\rho\omega^2 a[a\coth\alpha_1 - c - \frac{a}{2}(1-\nu)(\coth\alpha_1 - 1)]\mathrm{J}^2\sinh\alpha \times(\cosh\alpha+\cos\beta)$$

$$-\tfrac{1}{8}\rho\omega^2 a\,\mathrm{cosech}^2\,\alpha_1[2(a\coth\alpha_1 - c)\sinh 2\alpha_1 - a(1-\nu)] \times\mathrm{J}^2\sinh^2\alpha$$

$$+\tfrac{1}{8}(1+\nu)\rho\omega^2 a^2 e^{2\alpha_1}\,\mathrm{cosech}^2\,\alpha_1(c-a\coth\alpha_1)\mathrm{J}e^{-2\alpha}\cos\beta$$

$$-\tfrac{1}{4}\rho\omega^2 a^2(c-a\coth\alpha_1)[(1+\nu)(\coth\alpha_1+\tfrac{1}{2}\,\mathrm{cosech}^2\,\alpha_1) +1-\nu]\mathrm{J}\cos\beta.$$

References.

(1) Coker and Filon, ' Photo-Elasticity,' p. 163 (Cambridge, 1931).
(2) Coker and Filon, *ibid.* p. 327.
(3) G. B. Jeffery, Phil. Trans. Roy. Soc., Series A, ccxxi. pp. 265–293.

LXII. *Note on the Electrical Discharge in Argon.*

By F. H. Newman, *D.Sc., Professor of Physics, University College, Exeter* *.

[Received July 21, 1938.]

THE theory for the use of probes in gas discharges, developed by Langmuir and his associates †, has been widely applied, and although a probe distorts the discharge to some extent, Greeves and Johnston ‡ found that the type of characteristic curve obtained was independent of the probe used, thus confirming the results of Emeléus and Brown §.

The characteristic volt-ampere curves of a probe electrode consist of three distinct parts which depend upon the potential V of the collector relative to the space in which it is placed. If V is greater than zero, the probe collects only electrons ; for V considerably less than zero, the inflowing current to the probe consists of positive ions, while for voltages slightly negative with respect to the space, both electrons and positive ions are collected. It must be remembered, however, that electron currents of considerable magnitude leave a negatively charged electrode when the latter is in the main discharge. Found

* Communicated by the Author.
† General Elect. Rev. xxvii. p. 449 (1924).
‡ Phil. Mag. xxi. p. 659 (1936).
§ Phil. Mag. vii. p. 17 (1929).

and Langmuir * produced experimental evidence for the conclusion that these currents are actually electron currents, and they also gave results which indicate that the secondary electrons originate from bombardment by metastable atoms.

The shape of the volt-ampere characteristic of a collecting electrode depends to some extent upon the intensity of the discharge and also upon the pressure of the gas. The electron emission from the collector is due to conditions in the plasma, and the increase of current is governed by the conditions in the sheath.

Emeléus and Brown † have found volt-ampere characteristics for the probe which are anomalous and are not amenable to the usual analysis. Such curves were obtained with a probe (*a*) in the cathode dark space and at its junction with the negative glow, (*b*) at the heads of striations in the positive column of a glow discharge through iodine vapour, and (*c*) throughout the greater part of a discharge tube containing oxygen or helium at a pressure of the order of 0·1 mm., passing currents of the order of a microampere per cm.^{2}, or less, with a potential difference of a few hundred volts between anode and cathode. These anomalous curves have been attributed to positive space charges.

During some investigations on the cathode fall in argon the author also found that such anomalous current-voltage curves were obtained when the probe was placed in the cathode dark space. The discharge tube was cylindrical with silver disc electrodes, half an inch in diameter and eight inches apart. The discs were well spaced from the glass walls. A probe of tungsten wires 0·14 mm. in diameter, sealed in glass, and projecting one mm. beyond the glass, was inserted parallel to, and one mm. from, the cathode. The argon gas was purified and various gas pressures used in the experiments. It was found convenient to initiate the electrical discharge by means of a high voltage "leak tester," familiar to workers with high vacuum technique. It obviates the application of an excessive potential difference across the main electrodes.

The discharge tube was thoroughly outgassed and the discharge run for several hours in order to "condition"

* Phys. Rev. xxxix. p. 237 (1931).
† Phil. Mag. xxii. p. 898 (1936).

the electrodes. The collector was maintained positive with respect to the cathode, and the current passing between the collector and cathode was measured in the usual manner by means of a galvanometer, the main discharge current being maintained constant by means of a variable liquid resistance.

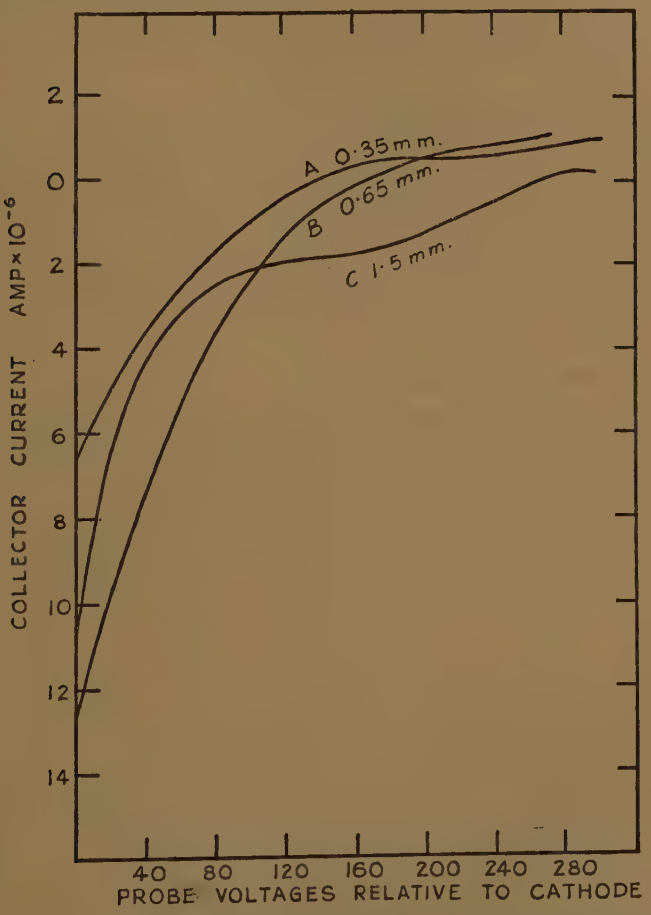

Three typical results from a large number are shown in the figure. Curve A represents the voltage-current probe characteristic at 0·35 mm. pressure, the main current density being 3×10^{-5} ampere per cm.^{2}, with the probe in the cathode dark space, the current below the zero line representing the flow of positive ions to the probe.

Curve B corresponds to 0·65 mm. pressure, a main current density of 10^{-4} ampere per cm.^{2}, with the probe again in the cathode dark space. Curve C was obtained at 1·5 mm. pressure and a main current density of 10^{-4} ampere per cm.^{2}, the probe being in the negative glow. Instead of being concave upwards, as in normal cases, the curves are concave downwards, and this anomalous characteristic must be attributed to the presence of a positive space charge.

The variation of the main discharge current with gas pressure at constant potential difference between the cathode and anode was also examined, and it was found that the current showed a maximum value at a certain pressure, the value of which depended upon the applied potential difference, *e. g.*, with 420 volts the main current was $1{\cdot}2\times10^{-3}$ ampere per cm.^{2} at 2·5 mm. pressure. As the applied potential difference was raised, the pressure at which the maximum current occurred also increased.

LXIII. *On Mean-Value Theorem in Riemann-Stieltje's Integral.* *By* D. N. Sen, *M.Sc., B.A.(Cantab.), Professor of Mathematics, Science College, Patna, India* *.

[Received June 16, 1938.]

IT is well known that for the Stieltje's integral the following property holds good :

If $\int_a^b f d\phi$ exists,

then $\int_a^b \phi df$ exists, and

$$\int_b^a f d\phi + \int_a^a \phi df = f(b).\phi(b) - f(a).\phi(a) \equiv \mathrm{K}, \text{ say.}$$

The result depends on the algebraic identity

$$\sum_1^n \phi(\xi_i)\{f(x_i)-f(x_{i-1})\} + \sum_0^n f(x_i)\{\phi(\xi_{i+1})-\phi(\xi_i)\} \equiv \mathrm{K},$$

$$(x_0 = a = \xi_0,\ x_n = b = \xi_{n+1}).$$

Pollard † remarked that he had not succeeded in proving either that the property held or that it did not hold for the Modified Stieltje's Integral. The object of

* Communicated by the Author.

† Pollard, Stieltje's Integral and its generalization, Q. J. M. vol. xlix. p. 94 (1923).

this paper is to establish the result for the Modified Stieltje's Integral.

The modified Stieltje's Integral (M) $\int_a^b f d\phi$ as defined by Pollard is more general than the ordinary Riemann-Stieltje's Integral. Having postulated that $\mathrm{LF}(s)=\mathrm{L}$, provided that for any arbitrary positive number ϵ a set Σ in (a, b) may be found such that

$$| \mathrm{F}(s)-\mathrm{L} | <\epsilon,$$

whenever s contains Σ ($\mathrm{F}(s)$ being a function of a set of points of division in (a, b)), the modified integral is defined as $\mathrm{LF}(s)$, where

$$\mathrm{F}(s)\equiv\Sigma f(\xi_i)\{\phi(x_i)-\phi(x_{i-1})\}.$$

Proof. Let $$(\mathrm{M})\int_a^b f\,d\phi=\mathrm{I}.$$

There is a set s of points of division, such that

$$\Big| \mathrm{I}-\sum_{s'} f d\phi \Big| <\epsilon,\ s'>s. \quad . \quad . \quad . \quad . \quad (1)$$

Let s be $a, a_1, a_2, \ldots, a_{n-1}, b$.

We take any $\bar{s}>s$ and consider the value of $\Sigma\phi\,df$ for $\bar{s}$ with arbitrary ξ's in the corresponding intervals.

Let the points of division of s in $a_r a_{r+1}$ be a_r, x_{r_1}, $x_{r_2}, \ldots x_{r_{m-1}}$, a_{r+1}.

Then

$$\sum_1^m \phi(\xi_{r_i}).\{f(x_{r_i})-f(x_{r_{i-1}})\}+\sum_0^m f(x_{r_i}).\{\phi(\xi_{r_{i+1}})-\phi(\xi_{r_i})\}$$
$$=f(a_{r+1}).\phi(a_{r+1})-f(a_r).\phi(a_r).$$

We shall have similar equalities for the other intervals, and adding them

$$\sum_{\bar{s}} \phi\,df+\sum_{\bar{s}_1} f\,d\phi=f(b).\phi(b)-f(a).\phi(a)$$
$$=\mathrm{K}, \quad . \quad . \quad . \quad . \quad . \quad . \quad . \quad . \quad (2)$$

where $\bar{s}_1$ consists of the points of division $a_r, \xi_{r_1}, \xi_{r_2}, \ldots \xi_{r_m}$, a_{r+1} in $a_r a_{r+1}$.

Clearly $\bar{s}_1>s$.

Therefore by (1)

$$\Big| \mathrm{I}-\sum_{\bar{s}_1} f\,d\phi \Big| <\epsilon;$$

therefore by (2)

$$\left| \sum_{\bar{s}} \phi\, df - (\mathrm{K}-\mathrm{I}) \right| < \epsilon.$$

This is true for any $\bar{s} > s$ with arbitrary ξ's. Therefore (M) $\int_a^b \phi\, df$ exists and equals K−I. Thus the result is established.

LXIV. *Notices respecting New Books.*

Fluid Mechanics. By Russell A. Dodge and Milton J. Thompson. [Pp. xi+495.] (McGraw-Hill Publishing Co., Ltd., London, 1937. Price 24*s*.)

THE study of fluid motion has undergone a great change in the last generation, due largely to the researches undertaken in connexion with aeronautics. In particular the study of the motion of viscous fluids has become of fundamental importance to aviation, to the large number of applications involving the motion of fluids through pipes, and to the resistance to ships. The mathematical formulation of the solutions so far obtained involves very complicated analysis, and in many respects it may be said that the subject is still in its primitive stage, since no definite and simple mathematical theory can yet be given, particularly when there is turbulence.

But the progress made is nevertheless considerable, and it is no exaggeration so say that the whole subject has been revolutionized during the past thirty years.

The authors of the present volume have undertaken the task of giving what might be described as a semi-mathematical treatment, suitable for engineers who are not afraid of a tolerable amount of mathematical analysis. But what distinguishes this book is that it contains a very clear and useful account of most of the important results hitherto obtained, so that while the authors may have had the engineer in mind, they have produced a book of great value to mathematical students of the subject. For, in the mathematical study of any natural problem of considerable complexity, it is often an advantage to begin by taking the analytical results for granted, coming back to them later when one has obtained some idea of the results themselves and seen a certain amount of physical justification for them.

In this sense, therefore, the book can be highly recommended not only to engineers, but also to mathematical students, especially to students of aeronautics who wish to become

acquainted with the latest results in the motion of viscous fluids.

After an account of the more or less traditional elementary hydraulics, the authors proceed to a brief account of the theory of lift, based upon circulation, with applications to aeroplane wings, lifting vanes, and air-screws. The study of the flow of viscous fluids is then treated at considerable length, including Reynolds' classical results, laminar flow in pipes, Stokes' Law. In regard to pipes, the law of distribution of velocity is deduced as the seventh-root law; the better logarithmic law is deduced later in dealing with the drag of plates. After a study of flow with free surfaces and the theory of resistance-drag coefficients, based upon the boundary layer without and with turbulence, there follows the dynamics of compressible fluids, including compressible viscous fluids.

There is a useful chapter on dynamical similarity, which the authors did well to include, although it is to a considerable extent a repetition of what is already contained in the remainder of the text. A very interesting *résumé* of methods of measuring viscosity and of the study of thin films concludes what is a remarkably useful addition to the literature of a very difficult subject. S. Brodetsky.

The Flow of Homogeneous Fluids through Porous Media. By M. Muskat and R. D. Wickoff. [Pp. xix+763.] (McGraw-Hill Publishing Co., Ltd., London, 1937. Price 45*s*.)

The importance of the subject dealt with in this volume is indicated by the fact that it is involved in problems dealing with the provision and maintenance of water-supplies, irrigation, drainage, as well as in the problems of petroleum engineering, which includes the production of gas and oil from underground reservoirs. Many industries are affected, as is made obvious by the fact that the diffusion and flow of fluids through ceramic materials, like bricks and porous earthenware, is fundamental to the ceramic industry, while the flow of gas through a sand moulding is equally fundamental to work in the foundry. The subject-matter of the book involves such problems as the construction of filter-beds for municipal water-systems, the seepage of water through, round, and beneath dams and earth reservoirs, soil erosion, tile drainage, the draining of artesian basins by means of deep wells, and of rivers and canals by wells dug near them.

The present book is therefore of great scope, and is to be welcomed as an important addition to the literature of a subject of growing importance. The authors have made it their object to produce a treatise covering every main problem,

and to give a treatment which deals with every detail of the methods used. The result is a book of very considerable size: and although it is somewhat doubtful whether the large amount of detail introduced and the considerable amount of repetition are not a disadvantage—yet this is only a minor point concerning a book of very considerable value and excellence.

The mathematical theory is interesting, and its basis can be summed up by the remark that, instead of the ordinary three equations which define the accelerations in the classical hydrodynamics, three equations are used which express the components of velocity of the fluid in terms of the pressure gradients. This follows as a generalization from the well-known Darcy's Law, of which a detailed and most interesting account is given as an introduction to the general theory. The mathematical treatment is very good, although a little garrulous, and a large number of problems are examined with the practical issues that arise in industrial, engineering, and other applications of the subject.

Beginning with incompressible fluids, the authors deal with steady motions in two-dimensional flow problems, analogous to two-dimensional problems in hydrodynamics and electricity, and involving the use of images and conjugate functions, followed by an account of steady motions in three-dimensions. Then come problems in which gravity plays an important part, like drainage from sloping sand, the seepage of water from canals and ditches, irrigation, water-logging, erosion, etc. The study of multiple well-systems occupies over a hundred pages and is of very great interest. Non-steady motions are also discussed. Then come compressible fluids in the study of the flow of gases through porous media.

In a large number of cases the results obtained are illustrated by reference to experiment and experience, thus enhancing the value of a book which is a welcome addition to technical literature.

S. Brodetsky.

The Observational Approach to Cosmology. By Edwin Hubble. [Pp. vi & 1–68.] (Oxford University Press, 1937. Price 6*s*.)

These Rhodes Memorial Lectures deal with the two sets of observational data around which centre discussions of the structure of the universe, viz.: the relationship between the red-shift of the spectral lines in the light from spiral nebulæ and their apparent magnitudes or "brightnesses," and the numbers of nebulæ per unit area of the sky which can be counted down to successive limits of brightness. Dr. Hubble points out that the only known mechanism for producing the observed red-shift is a velocity of recession proportional

to the distance of the nebula concerned, where by " distance " is meant a certain function of its apparent brightness. But he indicates that a loss of energy in the photon would have the same effect, although it is admitted that no mechanism for producing such a loss is known. Accepting that velocity is the cause of the red-shift, the expanding universes of general relativity can be applied to the observations. In this way Dr. Hubble deduces from the observed red-shift apparent-magnitude relation, and from the counts of spiral nebulæ a small closed universe with a number of rather improbable properties. Alternatively, if energy-loss produces the red-shift, the nebulæ are stationary in a large universe. Dr. Hubble presents us with the dilemma : either we must choose velocity and an unsatisfactory universe, or a credible universe with an unintelligible energy-loss in the photon.

Unfortunately, the book of necessity contains too little mathematical detail to make the reader aware that the dilemma is largely of Dr. Hubble's own creation. Assuming that red-shift is due to velocity, Dr. Hubble's conclusions rest on an arbitrary *a priori* definition of the " distance " of a nebula in terms of its apparent brightness. This definition can be shown to be incompatible with the quantity he takes for distance in his model universe and is, in any case, only one out of a number of possible definitions. Again the dimming effect of the red-shift on the apparent brightness of a nebula is calculated as if the nebula were moving in a flat Euclidean space, although the amount of the correction is used to find the curvature of space. It is possible to calculate directly the correction in each of the non-Euclidean model universes of general relativity. It then appears that Dr. Hubble's procedure is equivalent to placing very arbitrary *a priori* restrictions on the model and, in particular, to assuming that the expansion of the universe must be accelerated. In short the dilemma arises chiefly from the preliminary manipulations which the observations undergo, and not from the comparison between observation and the theoretical model universes of general relativity. By abandoning Dr. Hubble's *a priori* assumptions, it has been found possible to interpret the red-shift as velocity and, at the same time, to deduce a satisfactorily large model universe from the observations.

G. C. McVittie.

On Understanding Physics. By W. H. Watson. [Pp. xii+ 146.] (Cambridge University Press, 1938. Price 7*s.* 6*d.*)

In this book the author sets down some of the results of his reflections in clearing up his own understanding of physics. His treatment is largely influenced by Wittgenstein, whose method, it is maintained, in leading to clearness about sym-

bolism in general, should lead to clearness about physics. The philosophical problems of physics are regarded as essentially logical problems, and the author, accordingly, "offers no apology for having ignored nearly completely the history of philosophy and modern writings of scientists on the philosophy of science."

The first two chapters deal with the discipline of philosophy, and the relation between logic, psychology, and physics. As the solution of general philosophical problems may be obtained by clearing up the "grammar" of language, so a solution of the more specialized philosophical problems of physics is to be sought by a study of the symbolism of physics, and the logical structure of theories. Psychological theories are irrelevant to logic. Methods of representation, of which physics is a conglomerate, are then considered. Choices of methods are made according to our needs, and the methods are modified, or new methods are invented, as required for the incorporation of new facts. In a chapter on the nature of mechanism it is maintained that it is the logical necessity shown by absence of choice as to the result of a calculation by a given rule which underlies the usual view of causality as a compulsion on nature to go in certain way. The author's attitude to the often expressed view that quantum mechanics has abolished causality in science is that quantum mechanics merely substitutes the causality of its own laws for the causality of those of classical physics. The logic of substance and motion is fully discussed, and in a final chapter a number of special problems are considered—the logical status of physical dimensions, of force in mechanics and of electromagnetic symbolism.

That useful philosophical inquiry in connection with physics is limited, as the author seems to imply, to the investigation of logical structure, is open to serious question. It is, however, undeniable that the logical inquiry is of fundamental importance. The realization of this is not new. The novelty of the book lies in the fact that the powerful Wittgenstein technique, developed on the general philosophical side, has been brought to bear on the logical problems of physics. This is not an easy book to read, partly owing to the difficulty of the subject matter, but partly also owing to the discursiveness of the treatment. It is, however, full of illuminating points of view, and for those who consider the understanding of physics to be worth while, and do not expect it to be easy, the book may be strongly recommended as worthy of serious study. E. C. S.

[*The Editors do not hold themselves responsible for the views expressed by their correspondents.*]

THE

LONDON, EDINBURGH, AND DUBLIN

PHILOSOPHICAL MAGAZINE

AND

JOURNAL OF SCIENCE.

[SEVENTH SERIES.]

SUPPLEMENT, NOVEMBER 1938.

LXV. *Torsional Vibration in certain Mechanical Systems.* *By* W. A. TUPLIN, *M.Sc.**

[Received June 17, 1938.]

THERE are well-known methods of determining the natural frequencies of torsional vibration of systems consisting of rotors connected together by torsionally elastic members in the manner indicated in fig. 1. The

Fig. 1.

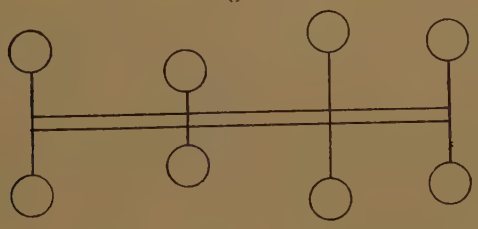

writer has previously made reference (Phil. Mag. ser. 7, xxi. p. 1097 (June 1936)) to a particular type of problem arising in investigating the characteristics of such systems.

A frequently-encountered variant of this simple system is one in which at least one of the connections between rotors contains a pair of gears. These cause the adjacent

* Communicated by the Author.

ends of the shafts which they connect to have angular velocities (relatively to the line of centres of the gears) bearing a constant ratio K to each other. The ratio of the corresponding torques (neglecting friction) is 1/K.

Simple Geared System.

The method of reducing such a system to an equivalent system of the type indicated in fig. 1 may be derived from consideration of fig. 2.

A rotor, whose moment of inertia is I_1, is connected by a shaft of torsional stiffness k_1 to a gear which meshes with another gear connected by a shaft of torsional stiffness k_2 to a second rotor. The gear assembly is regarded as rigid, and the shaft-axes fixed. The velocity

Fig. 2.

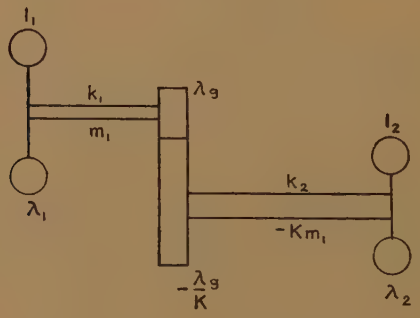

ratio of the gears is a constant K, and therefore the angular displacement of the wheel is $-\lambda_g/K$ when that of the pinion is λ_g. The torques in the shafts are m_1 and $-Km_1$. The moments of inertia of the gears are neglected.

Assuming that in the conditon of free vibration the instantaneous angular displacement of any rotor is given by an expression of the form $\theta=\lambda \sin nt$, where t represents time and n is a constant, it may be shown that the expression for the instantaneous torque in each shaft is of the form $m \sin nt$. We then have (considering the first rotor)

$$m_1 \sin nt = I_1 \frac{d^2}{dt^2}(\lambda_1 \sin nt),$$

or
$$m_1 = -n^2 I_1 \lambda_1 . \quad . \quad . \quad . \quad . \quad . \quad . \quad (1)$$

Similarly
$$-Km_1 = n^2 I_2 \lambda_2 . \quad . \quad . \quad . \quad . \quad . \quad (2)$$

Also, considering the twist in each shaft,

$$m_1 = k_1(\lambda_g - \lambda_1) \quad . \quad . \quad . \quad . \quad . \quad . \quad (3)$$

$$-\mathrm{K}m_1 = k_2\left(\lambda_2 + \frac{1}{\mathrm{K}}\lambda_g\right). \quad . \quad . \quad . \quad . \quad (4)$$

Eliminating λ_g from (3) and (4)

$$\frac{m_1}{k_1} + \lambda_1 = \mathrm{K}\left(-\frac{\mathrm{K}m_1}{k_2} - \lambda_2\right).$$

Substituting from (1) and (2) for m_1 and λ_2

$$-n^2\frac{\mathrm{I}_1\lambda_1}{k_1} + \lambda_1 = \frac{\mathrm{K}^2}{k_2}n^2\mathrm{I}_1\lambda_1 - \mathrm{K}^2\frac{\mathrm{I}_1}{\mathrm{I}_2}\lambda_1$$

whence

$$n^2 = \left[\frac{1}{\mathrm{I}_1} + \frac{\mathrm{K}^2}{\mathrm{I}_2}\right] \Big/ \left[\frac{1}{k_1} + \frac{\mathrm{K}^2}{k_2}\right]. \quad . \quad . \quad . \quad (5)$$

The natural frequency of torsional vibration of the system is $n/2\pi$.

Now if $\mathrm{K}=1$ (equivalent to no gears at all)

$$n^2 = \left[\frac{1}{\mathrm{I}_1} + \frac{1}{\mathrm{I}_2}\right] \Big/ \left[\frac{1}{k_1} + \frac{1}{k_2}\right].$$

Hence, the effect of introducing gearing is to divide I_2 and k_2 by K^2.

The same conclusion is reached after consideration of more complicated systems, and may be expressed by saying that the equivalent system of the type shown in fig. 1 is derived by multiplying each moment of inertia and each torsional stiffness by

$$\left(\frac{\text{Angular velocity in constant-velocity condition}}{\text{Corresponding angular velocity of reference shaft}}\right)^2.$$

This analysis of the system shown in fig. 2, assumes that the axes of the gears are fixed, so that their velocity-ratio is the reciprocal of the numbers of teeth in the gears. If the gears are carried in a massive mounting this assumption is justified, but cases have to be considered in which the angular displacement of the mounting under the influence of the transverse forces imposed on the shafts by gear-tooth reaction is of the same order as the twist in the shafts.

Application of External Torque at end of Straight-line System.

To examine the general case of a geared system it is necessary first to determine the effect of applying an external torque to a rotor in a system of the type shown in fig. 1. Three adjacent rotors in such a system are shown in fig 3, which also indicates that rotors and shafts are numbered from the left. The rth shaft has torsional stiffness k_r and the rotors at its ends have moments of inertia I_r and I_{r+1} Associated with the shaft are " elastic-inertia " constants,

$$a_r = \frac{k_r}{I_r} \quad \text{and} \quad b_r = \frac{k_r}{I_{r+1}}.$$

Fig. 3.

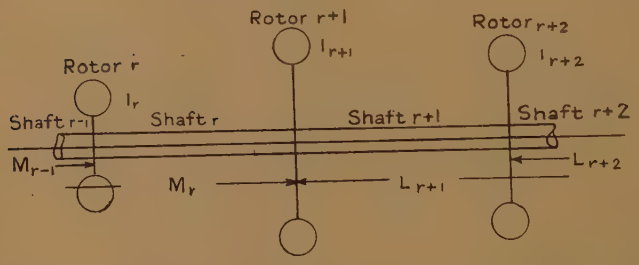

When the system is in a condition of simple harmonic torsional vibration, the angular displacement of the rth rotor is represented by $\lambda_r \sin nt$ and the instantaneous torque in the rth shaft by $m_r \sin nt$, where either the external torque maintaining the vibration is represented by $P \sin nt$ or the vibration is a free one and n depends on the elastic-inertia constants of the system.

In the communication already mentioned it is shown that (if no external torque is applied at any point to the left of the $(r+1)$th rotor),

$$m_{r+1} = \frac{M_r}{\Pi b_r} m_1 \quad \ldots\ldots\ldots \quad (6)$$

where $$\Pi b_r = b_1 b_2 b_3 \ldots . b_r$$

and M_r is a function of n and of the elastic-inertia constants of shafts 1 to r inclusive. It is the " torque function " of the system between rotors 1 and $r+1$ inclusive.

Writing $u=-n^2$, it may be shown that

$$(u+a_r+b_r)m_r=b_rm_{r+1}+a_rm_{r-1},$$

whence, by transposition and use of (6),

$$M_r=(u+a_r+b_r)M_{r-1}-a_rb_{r-1}M_{r-2}. \quad . \quad . \quad (7)$$

It is also found that

$$M_0=1 \text{ and } M_1=u+a_1+b_1.$$

Hence the expression for M_r for any value of r may be determined by repeated use of (7), starting from $r=2$.

Now if the system contains N shafts, m_{N+1} corresponds to an external torque applied to the (N+1)th rotor, and from (6),

$$m_{N+1}=\frac{M_N}{\Pi\, b_N}m_1. \quad . \quad . \quad . \quad . \quad . \quad . \quad (8)$$

Also,

$$m_N=\frac{M_{N-1}}{\Pi\, b_{N-1}}m_1. \quad . \quad . \quad . \quad . \quad . \quad . \quad (9)$$

If the system is in a state of free vibration $m_{N+1}=0$, and therefore $M_N=0$. This is an equation from which u may be determined, and it is called the "frequency equation" of the system. The degree of the equation is N, and the number of natural frequencies is therefore equal to the number of shafts.

Now the angular acceleration of the (N+1)th rotor is proportional to $m_{N+1}-m_N$, and

$$\begin{aligned} I_{N+1}\frac{d^2\lambda_{N+1}}{dt^2} &= m_{N+1}-\frac{M_{N-1}}{\Pi\, b_{N-1}}m_1 \\ &= m_{N+1}\left[1-\frac{M_{N-1}}{\Pi\, b_{N-1}}\frac{\Pi\, b_N}{M_N}\right] \\ &= m_{N+1}\left[\frac{M_N-b_NM_{N-1}}{M_N}\right]. \end{aligned}$$

Here $d^2\lambda_{N+1}/dt^2$ represents the amplitude of the angular acceleration of the (N+1)th rotor and is equal to $-n^2\lambda_{N+1}$ or $u\lambda_{N+1}$.

Hence

$$m_{N+1}=\left(\frac{M_N}{M_N-b_NM_{N-1}}\right)uI_{N+1}\lambda_{N+1}=Z\lambda_{N+1}, \quad . \quad (10)$$

where

$$Z=uI_{N+1}M_N/(M_N-b_NM_{N-1}). \quad . \quad . \quad . \quad (11)$$

Equation (10) expresses the relation between the amplitude of a harmonic torque applied to the end rotor of a " straight-line " system and the amplitude of angular displacement of that rotor.

General case of Epicyclic Gear Assembly.

A gear assembly in which not all the shaft-axes are fixed relatively to each other is known as an " epicyclic gear." (Strictly, every actual gear assembly is of this type because elasticity in mounting prevents every shaft

Fig. 4.

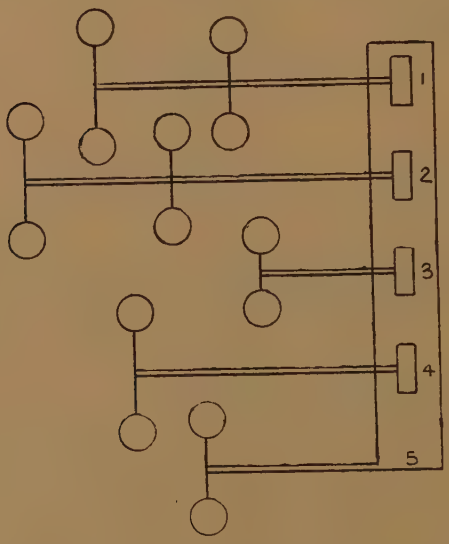

from preserving a fixed position, although there are many cases in which the assumption of fixed shaft-axes does not lead to appreciable error.)

Fig. 4 represents diagrammatically the general case. The gears 1, 2, 3, 4, etc., meshed together in any manner, are attached to correspondingly numbered " straight-line " systems. The framework on which the gear assembly is carried corresponds to another gear (5), and this may be regarded as elastically connected to the foundation on which it is mounted. In the following:

m_r=sum of amplitude of torques exerted on gear r by the other gears,

=external torque applied to system r.

λ_r=amplitude of angular displacement of gear r,
=amplitude of angular displacement of end rotor of system r.

By (10), $$m_r=Z_r\lambda_r,$$

where Z_r is the function of system r defined by (11).

Kinematic analysis of any epicyclic gear system shows that the displacement λ_r of any member may be expressed in the form

$$\lambda_r=\alpha_r\lambda_a+\beta_r\lambda_b+\gamma_r\lambda_c+\text{etc.}, \quad . \quad . \quad . \quad . \quad (12)$$

where λ_a, λ_b, etc., are the displacements of certain selected members whose number depends on the degree of complexity of the geared system, and α_r, β_r, etc., are constants depending on the numbers of teeth in the gears.

Fig. 5.

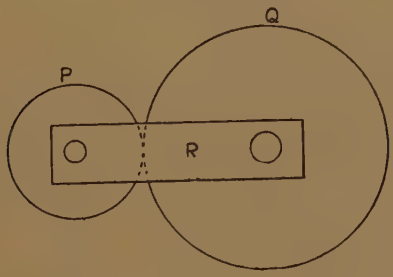

Similarly, it may be shown that the torque m_r on any member may be expressed in the form

$$m_r=A_rF_a+B_rF_b+C_rF_c+\text{etc.}, \quad . \quad . \quad . \quad (13)$$

where F_a, F_b, etc., are the torques on certain selected members or the gear-tooth reactions between certain members and A_r, B_r, etc., are constants depending on the numbers of teeth in the gears.

Writing $m_r=Z_r\lambda_r$ and making use of (12) and (13),

$$Z_r(\alpha_r\lambda_a+\beta_r\lambda_b+\gamma_r\lambda_c+\text{etc.})-(A_rF_a+B_rF_b+C_rF_c+\text{etc.})=0. \quad . \quad . \quad (14)$$

A similar relation is obtained for every member in the assembly.

Considering the simple epicyclic assembly shown in fig. 5, the total number of members is three, the angular displacement of any member may be expressed in terms of

the other two members, and the torque on any member may be expressed in terms of the tooth reaction.

Hence the number of λ's in (12) is two, and the number of F's in (13) is one. There are three equations like (14) from which λ's and F's may therefore be eliminated, leaving a relation between the Z's and the numbers of teeth in the gears. This is an equation in u, elastic-inertia constants and numbers of teeth, and it is the frequency equation for the whole system.

If a third gear S be meshed with Q, its spindle may, or may not, be carried by an extension of R. In the first case, the total number of members is four, the number of λ's remains at two, and the number of F's is increased to two by the addition of a tooth reaction between Q and S.

In the second case, an additional linkage member T, corresponding to R, is required, and the angular displacement of S will depend on that of Q and that of T. Hence, to define the displacement of S, three λ's are required, and the number of F's is increased to two by the addition of a tooth reaction between Q and S. Thus there are five members and the sum of λ's and F's is five.

In either case the number of equations obtainable is equal to the total number of λ's and F's, and similar considerations show that this applies to systems of any degree of complexity.

Considerations of inertia or elasticity are not involved in (12) or (13) and consequently, from statical principles,

$$\Sigma m_r = 0. \quad . \quad . \quad . \quad . \quad . \quad . \quad (15)$$

Also, since the total work done in a small displacement is zero,

$$\Sigma m_r \lambda_r = 0. \quad . \quad . \quad . \quad . \quad . \quad . \quad (16)$$

In dealing with certain systems, the determination of the frequency equation may be simplified by using (15) or (16) instead of one of the equations of types (12) and (13).

In general, the solution of the equations similar to (14) is most easily obtained by expressing F_a, F_b, etc., in terms of m's and so, by using $m_r = Z_r \lambda_r$, in terms of λ_a, λ_b, λ_c etc., by virtue of (12).

Method applied to Particular System.

In the system shown in fig. 6, the gear 2 rotates about a spindle supported by carrier 5, which itself rotates about XY. The effective radii of gears 1, 3, and 4 are

t_1, t_3, and t_4, and the distance between XY and the axis of 2 is t_5. The double gear 2 has two effective radii, t_{23} and t_{24}. The effective radii are proportional to the numbers of teeth.

The tooth reactions tangential to the pitch circles of the gears at the meshing points of 1, 3, and 4 are F_1, F_3, and F_4.

Then

$$\left.\begin{aligned} m_1&=F_1t_1 & m_2&=(F_1+F_3)t_{23}+F_4t_{24}\\ m_3&=-F_3t_3 & m_4&=-F_4t_4\\ m_5&=(-F_1+F_3+F_4)t_5 \end{aligned}\right\} \quad . \quad (17)$$

Fig. 6.

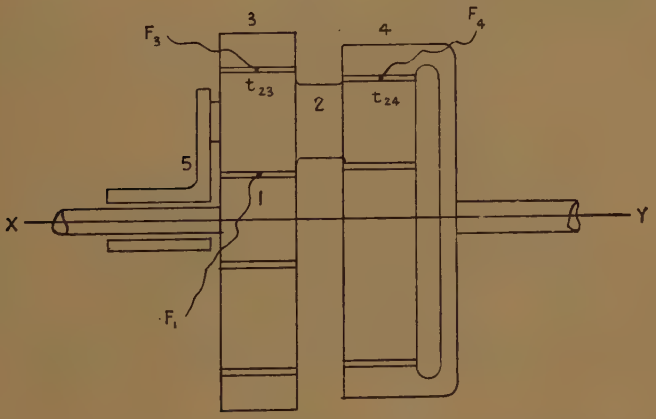

Now if 5 be assumed stationary and unit angular displacement given to 1, the corresponding displacements of of other members are those shown in line 1 of the table below. Subtraction of unity from the angular displacement of each member gives line 2, which represents another possible combination of displacements.

Member.	1.	2.	3.	4.	5.
Line 1	1	$-\frac{t_1}{t_{23}}$	$-\frac{t_1}{t_3}$	$-\frac{t_1}{t_{23}}\frac{t_{24}}{t_4}$	0
Line 2	0	$-\frac{t_1}{t_{23}}-1$	$-\frac{t_1}{t_3}-1$	$-\frac{t_1}{t_{23}}\frac{t_{24}}{t_4}-1$	-1

From this table the values of λ_2, λ_3, and λ_4 may be expressed in terms of λ_1 and λ_5, thus

$$\left.\begin{aligned}\lambda_2&=-\frac{t_1}{t_{23}}\lambda_1+\left(\frac{t_1}{t_{23}}+1\right)\lambda_5,\\ \lambda_3&=-\frac{t_1}{t_2}\lambda_1+\left(\frac{t_1}{t_3}+1\right)\lambda_5,\\ \lambda_4&=-\frac{t_1}{t_{23}}\frac{t_{24}}{t_4}\lambda_1+\left(\frac{t_1}{t_{23}}\frac{t_{24}}{t_4}+1\right)\lambda_5.\end{aligned}\right\}\quad\ldots\quad(18)$$

Any relation between m's may be expressed as a relation between λ's (by using $m_r=Z_r\lambda_r$) and, consequently, as a relation between λ_1 and λ_5. Two such relations enable λ_1 and λ_5 to be eliminated.

Substituting in the last equation of (17) the values of F_1, F_3, and F_4, taken from the other equations in that group,

$$\frac{m_5}{t_5}=-\frac{m_1}{t_1}-\frac{m_3}{t_3}-\frac{m_4}{t_4}.\quad\ldots\quad(19)$$

Also, by (15),

$$m_1+m_2+m_3+m_4+m_5=0.\quad\ldots\quad(20)$$

Denoting the coefficients of λ_1 and λ_5 in (18) by α_2, β_2, α_3, β_3, etc., as in (12), equation (19) becomes

$$\frac{Z_1\lambda_1}{t_1}+\frac{Z_3}{t_3}(\alpha_3\lambda_1+\beta_3\lambda_5)+\frac{Z_4}{t_4}(\alpha_4\lambda_1+\beta_4\lambda_5)+\frac{Z_5\lambda_5}{t_5}=0,$$

or

$$\left(\frac{Z_1}{t_1}+\frac{Z_3\alpha_3}{t_3}+\frac{Z_4\alpha_4}{t_4}\right)\lambda_1+\left(\frac{Z_3\beta_3}{t_3}+\frac{Z_4\beta_4}{t_4}+\frac{Z_5}{t_5}\right)\lambda_5=0.\quad(21)$$

In the same manner (20) becomes

$$(Z_1+Z_2\alpha_2+Z_3\alpha_3+Z_4\alpha_4)\lambda_1+(Z_2\beta_2+Z_3\beta_3+Z_4\beta_4+Z_5)\lambda_5=0.\quad\ldots\quad(22)$$

Eliminating λ_1 and λ_5 from (21) and (22), the frequency equation is found to be

$$Z_1Z_2\frac{\beta_2}{t_1}+Z_1Z_3\beta_3\left(\frac{1}{t_1}-\frac{1}{t_3}\right)+Z_1Z_4\beta_4\left(\frac{1}{t_1}-\frac{1}{t_4}\right)$$
$$+Z_1Z_5\left(\frac{1}{t_1}-\frac{1}{t_5}\right)+Z_2Z_3\left[\frac{\alpha_3\beta_2-\alpha_2\beta_3}{t_3}\right]$$

$$+Z_2Z_4\left[\frac{\alpha_4\beta_2-\alpha_2\beta_4}{t_4}\right]+Z_2Z_5\left[-\frac{\alpha_2}{t_5}\right]$$

$$+Z_3Z_4\left[\frac{1}{t_3}-\frac{1}{t_4}\right][\alpha_3\beta_4-\alpha_4\beta_3]+Z_3Z_5\alpha_3\left[\frac{1}{t_3}-\frac{1}{t_5}\right]$$

$$+Z_4Z_5\alpha_4\left[\frac{1}{t_4}-\frac{1}{t_5}\right]=0. \quad . \quad . \quad . \quad . \quad . \quad . \quad . \quad (23)$$

Special Case.

In the particular case in which one λ is expressible in terms of all the others, development of the frequency equation may proceed thus,

$$\alpha_1\lambda_1+\alpha_2\lambda_2+\alpha_3\lambda_3+\ldots+\alpha_R\lambda_R=0, \quad . \quad . \quad (24)$$

where α_1, α_2, α_3, etc., are constants and the total number of members in the assembly is R.

Also from (16),

$$m_1\lambda_1+m_2\lambda_2+m_3\lambda_3+\ldots+m_R\lambda_R=0.$$

Since the α's and λ's are independent of each other,

$$\frac{m_1}{\alpha_1}=\frac{m_2}{\alpha_2}=\frac{m_3}{\alpha_3}=\text{etc.}=Q \text{ (say)}. \quad . \quad . \quad (25)$$

Also, from (24), writing $\lambda_r=\frac{m_r}{Z_r}$,

$$\alpha_1\frac{m_1}{Z_1}+\alpha_2\frac{m_2}{Z_2}+\text{etc.}+\alpha_R\frac{m_R}{Z_R}=0. \quad . \quad . \quad . \quad (26)$$

Substituting in (26) the values of m_1, m_2, etc., from (25), and dividing throughout by Q,

$$\frac{\alpha_1^2}{Z_1}+\frac{\alpha_2^2}{Z_2}+\frac{\alpha_3^2}{Z_3}+\text{etc.}+\frac{\alpha_R^2}{Z_R}=0, \quad . \quad . \quad . \quad (27)$$

and this is the frequency equation.

Gears on Single Carrier.

The case in which a number of meshing gears run on shafts supported by a single carrier is shown in fig. 7. The diagram shows four gears and the carrier C, but the following discussion applies to any number of gears. Each gear is regarded as connected to its own straight-line vibrating system whose elastic-inertia constants are

known. The carrier is similarly connected to a straight-line system.

The numbers of teeth in the gears are t_1, t_2, etc., and the radii of the gears are proportional to the numbers of teeth. Assuming C to be fixed, the relations between angular displacements of the gears are these:

$$\lambda_2 = -\frac{t_1}{t_2}\lambda_1$$

$$\lambda_3 = -\frac{t_2}{t_3}\lambda_2 = \frac{t_1}{t_3}\lambda_1,$$

and in general

$$\lambda_r = (-1)^{r+1}\frac{t_1}{t_r}\lambda_1. \quad . \quad . \quad . \quad . \quad . \quad (28)$$

Fig. 7.

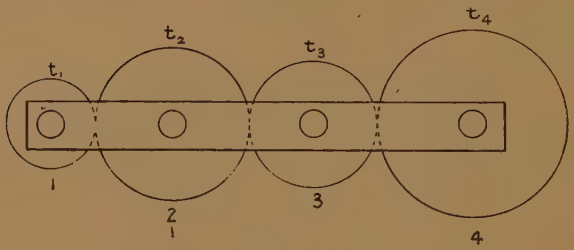

If the restriction on C's movement is relaxed, the same relation will apply between the angular displacements relatively to C, *i. e.*,

$$(\lambda_r - \lambda_c) = (-1)^{r+1}\frac{t_1}{t_r}(\lambda_1 - \lambda_c)$$

or
$$\lambda_r = (-1)^{r+1}\frac{t_1}{t_r}\lambda_1 + \left[1 - (-1)^{r+1}\frac{t_1}{t_r}\right]\lambda_c. \quad . \quad (29)$$

If the tooth reaction (normal to the line of gear centres) between gear r and gear $(r+1)$ is F_r, and if the radius of each gear be represented by its number of teeth,

$$(F_r + F_{r-1})t_r = m_r,$$

and therefore

$$F_r = \frac{m_r}{t_r} - F_{r-1} = \frac{m_r}{t_r} - \frac{m_{r-1}}{t_{r-1}} + F_{r-2} = \text{etc.}$$

$$= \left[\frac{m_1}{t_1} - \frac{m_2}{t_2} + \frac{m_3}{t_3} - \ldots + \frac{m_r}{t_r}(-1)^{r+1}\right](-1)^{r+1}. \quad (30)$$

If the total number of gears is R, then $F_R=0$, and therefore

$$\sum_1^R \frac{m_r}{t_r}(-1)^{r+1}=0 \quad \text{or} \quad \sum_1^R \frac{Z_r\lambda_r}{t_r}(-1)^{r+1}=0,$$

or

$$0=\sum_1^R \frac{Z_r}{t_r}(-1)^{r+1}\left[(-1)^{r+1}\frac{t_1}{t_r}\lambda_1+\left(1-(-1)^{r+1}\frac{t_1}{t_r}\right)\lambda_c\right]$$

$$=\sum_1^R \frac{Z_r}{t_r}\left\{\frac{t_1}{t_r}\lambda_1+\left[(-1)^{r+1}-\frac{t_1}{t_r}\right]\lambda_c\right\},$$

and therefore

$$\lambda_1 t_1 \sum_1^R \frac{Z_r}{t_r^2}-\lambda_c\sum_1^R \frac{Z_r}{t_r}\left[\frac{t_1}{t_r}+(-1)^r\right]=0. \quad . \quad . \quad (31)$$

Since $\Sigma m=0$ when the summation is effected for all members, including the carrier,

$$m_c+\sum_1^R m_r=0 \quad \text{or} \quad Z_c\lambda_c+\sum_1^R Z_r\lambda_r=0,$$

and therefore

$$Z_c\lambda_c+\sum_1^R Z_r\left\{(-1)^{r+1}\frac{t_1}{t_r}\lambda_1+\left[1-(-1)^{r+1}\frac{t_1}{t_r}\right]\lambda_c\right\}=0$$

and

$$\lambda_1 t_1 \sum_1^R \frac{Z^r}{t_r}(-1)^{r+1}+\lambda_c\left\{Z_c+\sum_1^R Z_r\left[1-(-1)^{r+1}\frac{t_1}{t_r}\right]\right\}=0.$$

$$. \quad . \quad . \quad (32)$$

Eliminating λ_1 and λ_c from equations (31) and (32),

$$Z_c\sum_1^R \frac{Z_r}{t_r^2}+\left(\sum_1^R \frac{Z_r}{t_r^2}\right)\left(\sum_1^R Z_r\left[1-(-1)^{r+1}\frac{t_1}{t_r}\right]\right)$$

$$+\left(\sum_1^R \frac{Z_r}{t_r}(-1)^{r+1}\right)\left(\sum_1^R \frac{Z^r}{t_r}\left[\frac{t_1}{t_r}+(-1)^r\right]\right)=0,$$

or

$$Z_c\sum_1^R \frac{Z_r}{t_r^2}+\left(\sum_1^R \frac{Z_r}{t_r^2}\right)\left(\sum_1^R Z_r\right)$$

$$+\left(\sum_1^R \frac{Z_r}{t_r}(-1)^{r+1}\right)\left(\sum_1^R \frac{Z_r}{t_r}(-1)^r\right)=0. \quad . \quad (33)$$

The value of the second term in (33) may be expressed by using suffix p to apply to a factor taken from the first bracket and q to apply to a factor taken from the second

bracket. The product Z_pZ_q is multiplied by one such factor and the product Z_qZ_p by a corresponding factor. The value of the second term thus becomes

$$\sum_1^R Z_pZ_q\left[\frac{1}{t_p^2}+\frac{1}{t_q^2}\right], \quad . \quad . \quad . \quad . \quad . \quad (34)$$

the summation being effected for every combination of p and q within the ranges $p=1, 2, 3, \ldots R$ and $q=1, 2, 3, \ldots R$. Similarly, the third term in (33) becomes

$$\sum_1^R Z_pZ_q\left[\frac{(-1)^{p+1}}{t_p}\frac{(-1)^q}{t_q}+\frac{(-1)^{q+1}}{t_q}\frac{(-1)^p}{t_p}\right]. \quad . \quad (34)$$

Adding (34) and (35) and re-arranging, we have

$$\sum_1^R \frac{Z_pZ_q}{t_p^2t_q^2}\{t_p^2+t_q^2+t_pt_q[(-1)^{p+1}(-1)^q+(-1)^{q+1}(-1)^p]\}$$

$$=\sum_1^R \frac{Z_pZ_q}{t_p^2t_q^2}\{t_p^2+t_q^2+2t_pt_q(-1)^{p+q+1}\}$$

$$=\sum_1^R \frac{Z_pZ_q}{t_p^2t_q^2}[t_p-(-1)^{p+q}t_q]^2.$$

Hence, (33) becomes

$$Z_c\sum_1^R\frac{Z_r}{t_r^2}+\sum_1^R\frac{Z_pZ_q}{t_p^2t_q^2}[t_p-(-1)^{p+q}t_q]^2=0, \quad . \quad . \quad (36)$$

the second summation being effected for every combination of p and q within the ranges $p=1, 2, 3, \ldots R$ and $q=1, 2, 3, \ldots R$. It will be noted that there is no term of the form $\left(\frac{Z_p}{t_p^2}\right)^2$. Equation (36) is the frequency equation.

If the carrier is very massive, its effect on the natural vibrations approximates to that of an infinitely large rotor at the point of application of the external torque to the straight-line system associated with the carrier. Hence, using (11), $Z_c=\infty$, and then (36) reduces to

$$\sum_1^R\frac{Z_r}{t_r^2}=0. \quad . \quad . \quad . \quad . \quad . \quad . \quad (30)$$

If $t_1=t_2=t_3=\ldots=t_R$, this becomes $\sum_1^R Z_r=0$. Hence the effect of the gearing is to divide each Z by the square of the number of teeth in the corresponding gear. This

result agrees with that established in connexion with the system shown in fig. 2.

Special Values of Z.

If the straight-line system attached to any particular gear consists only of a shaft and a rotor additional to the gear itself, the expression for Z is simplified. Thus, if the moment of inertia of the gear is I_g, the torsional stiffness of the shaft being k, the following substitutions may be made in (11):

$$I_{N+1}=I_g,\ b_N=k/I_g,\ M_N=u+\frac{k}{I_1}+\frac{k}{I_g},\ M_{N-1}=1.$$

Hence,
$$Z=uI_g\left(u+\frac{k}{I_1}+\frac{k}{I_g}\right)\Big/\left(u+\frac{k}{I_1}\right)$$
$$=u\left[I_g+\frac{k}{u+(k/I_1)}\right]. \quad . \quad . \quad . \quad . \quad . \quad (38)$$

From this, the following particular values of Z may be noted:

If $I_1=\infty$, $Z=uI_g+k$.

If $k=\infty$, $Z=u(I_g+I_1)$.

If $k=0$, $Z=uI_g$.

If, for example, the gears are supported in a carrier of moment of inertia I_g, mounted on a massive foundation in such a way that the torsional rigidity of the connexion is k, then $Z=uI_g+k$. If, in addition, the moment of inertia of the carrier be negligible compared with those of other members in the system, then $Z=k$.

Modification of Z by Insertion of an Elastic Element.

If the Z-value of a straight-line system ending in a gear is known, the change in the effective value of Z due to the insertion of a flexible element in the meshing of the gear may be determined by the rule developed below.

For example, distortion of gears and shafts may give P and Q in fig. 5 a relative movement corresponding to an angular displacement θ_1 of R instead of an actual value θ_2, when the torque exerted on R is m. This is equivalent to the insertion of an elastic element of torsional stiffness $m/(\theta_1-\theta_2)$ between R and R's kinematic representative used in developing the frequency equation.

This means that the straight-line system associated with R is extended by a shaft of stiffness $m/(\theta_1-\theta_2)$ or k_{N+1} (say) with a rotor of zero inertia at its outer end, *i. e.*, $I_{N+2}=0$. The elastic-inertia constants of the additional shaft are

$$a_{N+1}=\frac{k_{N+1}}{I_{N+1}}, \qquad b_{N+1}=\frac{k_{N+1}}{I_{N+2}}=\infty.$$

Now,

$$\begin{aligned} M_{N+1}&=(u+a_{N+1}+b_{N+1})M_N-a_{N+1}b_N M_{N-1}\\ &=(u+b_{N+1})M_N+a_{N+1}(M_N-b_N M_{N-1}),\end{aligned}$$

$$\begin{aligned} M_{N+1}-b_{N+1}M_N&=(u+a_{N+1})M_N-a_{N+1}b_N M_{N-1}\\ &=uM_N+a_{N+1}(M_N-b_N M_{N-1}).\end{aligned}$$

Writing Z′ for the modified value of Z,

$$Z'=uI_{N+2}\frac{(u+b_{N+1})M_N+a_{N+1}(M_N-b_N M_{N-1})}{uM_N+a_{N+1}(M_N-b_N M_{N-1})}.$$

Since $I_{N+2}=0$, the only term left in the numerator is $uI_{N+2}b_{N+1}M_N=uk_{N+1}M_N$. Then, multiplying numerator and denominator by I_{N+1}, we have

$$Z'=\frac{uI_{N+1}M_N k_{N+1}}{uI_{N+1}M_N+k_{N+1}(M_N-b_N M_{N-1})}=\frac{1}{\frac{1}{k_{N+1}}+\frac{1}{Z}}.$$

Hence $\frac{1}{Z'}=\frac{1}{Z}+\frac{1}{k_{N+1}}$, *i. e.*, the reciprocals of Z and k are additive.

Branched and Network Systems.

The "straight-line" type of torsionally vibrating system shown in fig. 1 is the simplest possible. The "branched" type of system, indicated in fig. 8, where rotors are represented by circles and shafts by straight lines, demands more elaborate treatment, and the determination of the frequency equation for this type has been discussed elsewhere.

In the following, the "network" type of system, exemplified in fig. 9, is considered. As both the branched and network systems are formed by linking up straight-line systems, it is first necessary to consider the general effect of the application of external torques to straight-line systems.

Application of External Torques to Rotors in Straight-line System.

In a freely-vibrating straight-line system, the relation between torque amplitudes in three adjacent shafts is

$$(u+a_r+b_r)m_r=b_rm_{r+1}+a_rm_{r-1}. \quad . \quad . \quad . \quad (39)$$

Fig. 8.

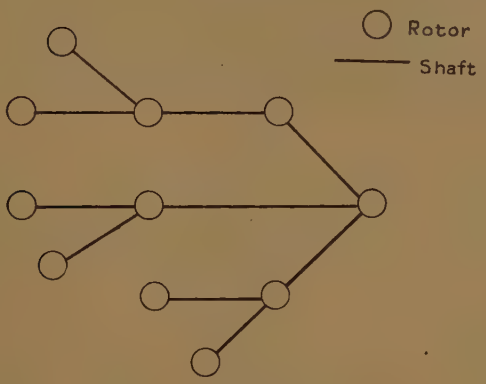

Fig. 9.

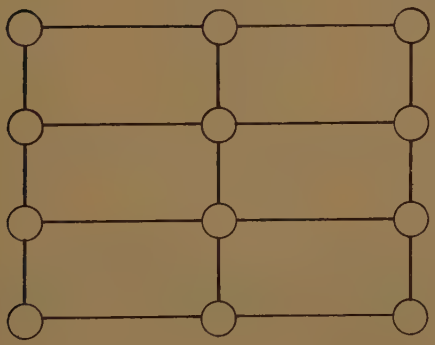

Here m_{r+1} and m_{r-1} are external to shaft r. If simple harmonic torques of amplitudes P_r and P_{r+1} and of equal frequency are applied to rotors r and $r+1$ respectively by agencies external to the system, the effect of P_{r+1} on the shaft r is added to the effect of m_{r+1}, whereas the effect of P_r is subtracted from that of m_{r-1}. (If the torques in shafts $r-1$ and $r+1$ are of equal sign and that in shaft

$r-1$ exerts a clockwise torque on rotor r, the torque in shaft $r+1$ exerts a counter-clockwise torque on rotor $r+1$.)

Modifying (39) by writing $m_{r+1}+P_{r+1}$ instead of m_{r+1}, and $m_{r-1}-P_r$ instead of m_{r-1}, and transposing, we have

$$b_r(m_{r+1}+P_{r+1})=(u+a_r+b_r)m_r-a_r(m_{r-1}-P_r). \quad . \quad (40)$$

In this equation, all the torques concerned are represented by expressions of the form $m \sin nt$, the same value of n being common to all, and $u=-n^2$.

Starting from an assumed value of m_1, repeated use of (40) gives the torque in each shaft in terms of m_1 and of the

Fig. 10.

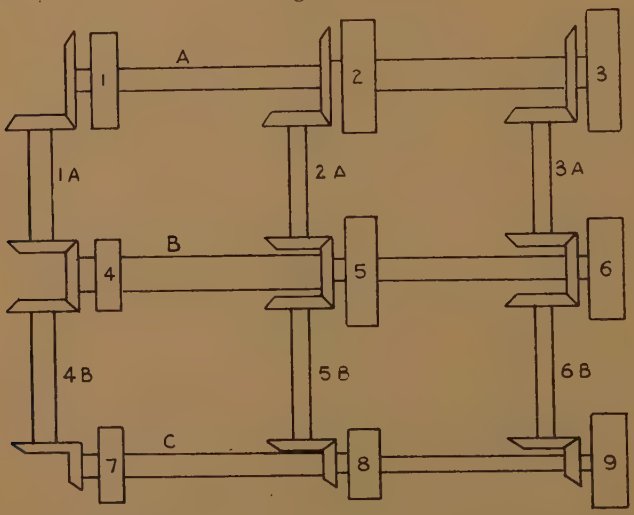

P's applied between rotor 1 and the end of the shaft remote from 1. Since $m_{N+1}=0$ (the shaft-torque on the right of the extreme right-hand rotor), and m_{N+1} is expressible in terms of m_1 and the P's, the value of m_1 is determinable in terms of the P's. Hence, the amplitude of the forced harmonic torque in any shaft may be found in terms of the external torques.

A network system may be regarded as a straight-line system whose rotors are also linked by external elastic members. These exert external torques whose amplitudes depend on the amplitudes of angular displacement at the rotors themselves.

Network Systems.

A mechanism which corresponds to a torsionally vibrating system of the " network " type is shown in fig. 10. Here each of the shafts A, B, and C carries three rotors, and this assembly in itself constitutes a straight-line system. The vertical shafts and the gears associated with them form torsionally elastic connexions between the three systems. At any instant, each vertical shaft is applying to two straight-line systems external torques depending on its angle of twist.

Fig. 11.

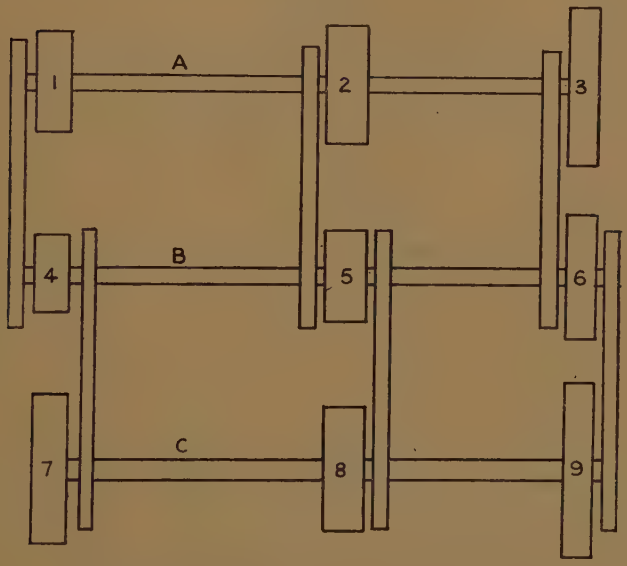

By applying the principle developed previously in connexion with simple geared systems, the system shown in fig. 10 may be replaced by an equivalent system in which all nominal velocity ratios are unity, moments of inertia and torsional stiffnesses having been modified accordingly. The effect of the vertical shafts may be represented by connexions in the form of elastic belts or chains between the horizontal shafts as shown in fig. 11.

Diagrammatically this is shown again in the left-hand part of fig. 12, where each circle represents a rotor and each straight line an elastic connexion transmitting a

torque proportional to the relative angular displacement or its ends.

It is no longer necessary to distinguish between horizontal and vertical connexions, and this may simplify analysis of the system. Thus, the left-hand diagram in fig. 12 suggests three straight-line systems connected by six members, whereas the right-hand diagram suggests a straight-line system (heavy line) whose rotors are linked by four external members.

Let the amplitude of the torque in shaft 1 be unity and of those in the vertical connexions P_{16}, P_{25}, P_{49}, and P_{58}, the corresponding torsional stiffnesses being

Fig. 12.

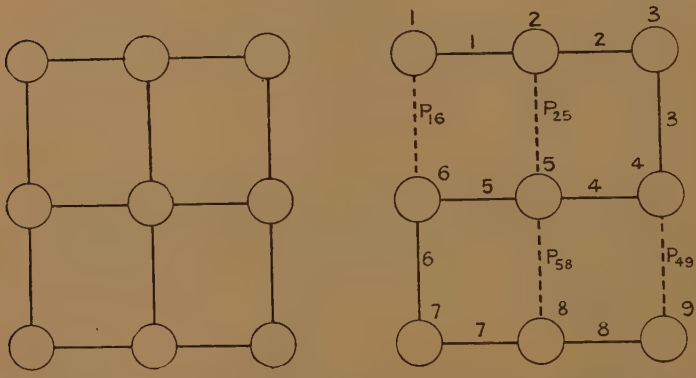

k_{16}, k_{25}, k_{49}, and k_{58}. Then, starting from shaft 1, we have from (40),

$$b_1(m_2+P_2)=(u+a_1+b_1)m_1+a_1P_1, \text{ since } m_0=0.$$

This gives m_2 in terms of P_1 and P_2 (since $m_1=1$).

Similarly,

$$b_2(m_3+P_3)=(u+a_2+b_2)m_2+a_2P_2-a_2m_1$$

and so on until, finally,

$$b_8(0+P_9)=(u+a_8+b_8)m_8+a_8P_8-a_8m_7 \quad . \quad (41)$$

($m_9=0$ since m_9 is the shaft-torque beyond the 9th rotor).

In this particular case

$$P_1=P_{16} \quad P_2=P_{25} \quad P_3=0 \quad P_4=P_{49} \quad P_5=P_{58}-P_{25}$$
$$P_6=-P_{16} \quad P_7=0 \quad P_8=-P_{58} \quad P_9=-P_{49}.$$

Since the sum of the torques acting on rotor r is equal to $I_r \frac{d^2\lambda_r}{dt^2}$,

$$(m_r+P_r)-m_{r-1}=uI_r\lambda_r,$$

or

$$\lambda_r=\frac{P_r+m_r-m_{r-1}}{uI_r}.$$

In particular,

$$\lambda_1=\frac{P_{16}+1}{uI_1}, \qquad \lambda_6=\frac{-P_{16}+m_6-m_5}{uI_6}.$$

Fig. 13.

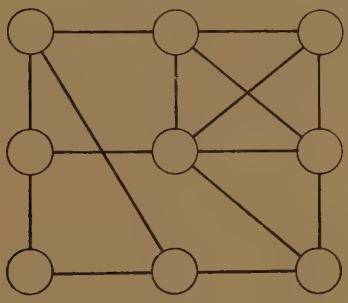

Also,

$$P_{16}=k_{16}(\lambda_6-\lambda_1)$$

$$=\frac{k_{16}}{u}\left[-P_{16}\left(\frac{1}{I_1}+\frac{1}{I_6}\right)+\frac{m_6-m_5}{I_6}-\frac{1}{I_1}\right], \quad . \quad (42)$$

where m_5 and m_6 are in terms of the P's.

Three similar equations are obtained for P_{25}, P_{49}, and P_{58}. From these four equations, the P's may be eliminated, leaving a relation between u and the elastic-inertia constants. This is the frequency equation for the system and its degree is the same as the number of flexible elements.

In dealing with network systems having many shafts, the algebraic operations involved in deriving the frequency equation by this method tend to be cumbersome.

An alternative method of carrying out the procedure is to assume a value of u so that numerical values are employed instead of $(u+a_1+b_1)$, $(u+a_2+b_2)$, etc. The first term in the first bracket of (41) is written m_9, and

after elimination of the P's a numerical value is found for m_9. This represents the ratio of m_9 to m_1, when the torques in the system are of the frequency corresponding to the assumed value of u. Since, in the condition of free vibration, $m_9=0$, the problem becomes one of finding by repeated trial values of u which make $m_9=0$.

The method is not confined to the rectangular network shown in fig. 12. It is applicable to systems in which torsionally elastic connexions between rotors are arranged in any manner whatever, *e. g.*, fig. 13.

Endless Systems.

A special case of the network system is that in which an external elastic connexion is made between the ends of a straight-line system, thus forming an endless system (fig. 14). The general form of the frequency equation for this system is easily obtainable.

Fig. 14.

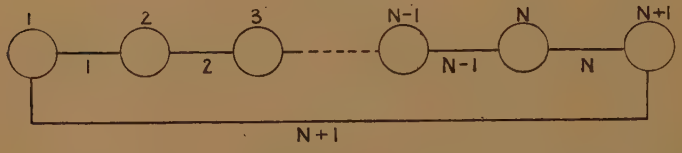

Let the torsional stiffness of the closing link (shaft N+1) be k_{N+1}. Then

$$\frac{k_{N+1}}{I_{N+1}}=a_{N+1} \quad \text{and} \quad \frac{k_{N+1}}{I_1}=b_{N+1}.$$

Let the amplitude of the torque in the (N+1)th shaft be P. Now, considering the effect on the straight-line system of the external torque P at rotor N+1, we have, from (8),

$$P=\frac{M_N}{\Pi\, b_N}m_1 \quad \text{or} \quad m_1=\frac{\Pi\, b_N}{M_N}P, \qquad . \quad . \quad (43)$$

and from (9),

$$m_N=\frac{M_{N-1}}{\Pi\, b_{N-1}}m_1=b_N\frac{M_{N-1}}{M_N}P. \qquad . \quad . \quad (44)$$

But the effect of the twist in shaft N+1 is also to exert a torque −P on rotor 1. A positive torque applied to the right-hand end of the system produces internal

torques of the same sign as does the application of a negative torque to the left-hand end of the system. Hence, by analogy with (43),

$$P=\frac{M_N}{\Pi a_N}m_N \quad \text{or} \quad m_N=\frac{\Pi a_N}{M_N}P, \quad . \quad . \quad (45)$$

and by analogy with (44),

$$m_1=\frac{L_2}{\Pi' a_N}m_N=\frac{a_1 L_2}{M_N}P, \quad . \quad . \quad . \quad . \quad (46)$$

where L_2 is the torque function of the system between rotors 2 and N inclusive, and $\Pi' a_2$ is the product $a_2 a_3 a_4 \ldots a_N$.

The true value of m_1 is the sum of those given by (43) and (46), and that of m_N is the sum of those given by (44) and (45), since the external torques P and $-P$ are applied simultaneously. Therefore,

$$m_1=\frac{P}{M_N}(\Pi b_N+a_1 L_2), \quad . \quad . \quad . \quad . \quad (47)$$

$$m_N=\frac{P}{M_N}(\Pi a_N+b_N M_{N-1}). \quad . \quad . \quad . \quad (48)$$

Now, regarding shafts N, N+1, and 1 as consecutive shafts in a straight-line system, we have

$$(u+a_{N+1}+b_{N+1})P=a_{N+1}m_N+b_{N+1}m_1,$$

and inserting in this the values of m_N and m_1 from (47) and (48), we have as the frequency equation of the system

$$(u+a_{N+1}+b_{N+1})M_N=\Pi a_{N+1}+\Pi b_{N+1}+a_{N+1}b_N M_{N-1}+a_1 b_{N+1}L_2. \quad . \quad . \quad . \quad (49)$$

Forced Vibrations in Network Systems.

If simple harmonic external torques having a common frequency are applied at various rotors in a network system, the torques produced in the shafts may be determined by a slight modification of the procedure used for deriving the frequency equation. At any rotor r in the basic straight-line system there may be an external torque of amplitude F_r, in addition to the "external" torque applied by a shaft which is not part of the straight-line system. Thus (40) becomes

$$b_r(m_{r+1}+P_{r+1}+F_{r+1})=(u+a_r+b_r)m_r-a_r(m_{r-1}-P_r-F_r). \quad . \quad . \quad . \quad (50)$$

In applying (50) to the various shafts in turn, the value used for u is that corresponding to the common frequency of the external torques. The successive shaft torques are found in terms of m_1 and the P's and F's until an equation is reached of the form $m_{r+1}=0$ or of the form $m_{r+1}=m_1$. This, in conjunction with the equations similar to (42), enables m_1 and the P's to be determined in terms of the F's. Then the torque in each shaft may be expressed in terms of the F's.

If the external torques are of different frequencies, the calculation must be repeated for each frequency.

If the frequency of an external torque coincides with a natural frequency of the system, $m_1=\infty$ and (apart from damping effects) the torque in each shaft would be infinite, unless the external torque is applied at a point which is a node in the resonant vibration-form.

LXVI. *Resonance in Truncated Cones.* *By* A. E. Bate, *Ph.D., F.Inst.P., and* E. T. Wilson, *M.Sc.**

[Received June 30, 1938.]

1. *Introduction.*

SOME years ago the effect of variation of frequency of the sound emitted by a pipe on its end-correction was the subject of an investigation [1] when the pipe was fitted with a large flange, and when unflanged. It was found that the effect, if any, was inappreciable over the range of frequencies used. The range was limited to 512 c.p.s. to keep the wave-length large in comparison with the diameter of the pipe.

A flange may be regarded as the upper limit of a cone, the lower limit being a cylinder, that is, the unflanged pipe, and it appeared probable that, with cones of various angles attached to the end of the pipe, further investigation would throw more light on this question, and that of the end-correction of conical pipes. The work to be described was therefore undertaken, and revealed the following facts :—

(*a*) The open-end correction appears to be independent of the frequency in the cylindrical pipe, but varies with it in conical pipes.

* Communicated by the Authors.

(*b*) When the cylindrical pipe terminates in a conical pipe of semi-apical angle of about 1–2°, the end-correction disappears, the actual value of the angle at which this occurs depending on the frequency.

(*c*) For cones of large angle the correction (measured along the axis) is negative, and remains so up to about 86° ; the cone of angle 90° is a plane flange with a positive end-correction.

(*d*) The conical pipes closed at the narrow end have natural resonant frequencies below about 10° semi-apical angle, the wave-length being four times the slant-height—including the appropriate correction for the unattached end.

(*e*) Conical ends above about 10° behave as conical flanges.

(*f*) The relation between frequency, slant-length, and angle for cones of small angle is obscure.

2. *Apparatus.*

The apparatus, which has been described fully in previous papers [1], consists of a cylindrical pipe of brass 5·4 cm. in diameter, which may be adjusted in length telescopically, and which is blown at one end as an organ pipe. The cones used in the first series of experiments are of a maximum slant-length of 30·5 cm., and each terminates at its narrow end in a short piece of tube 5·4 cm. diameter by which it is attached to the main pipe.

3. *Procedure.*

The wind supply was set at a suitable value, and the length of the cylindrical pipe (about one wave-length long) was adjusted to give a frequency of 4 beats per second above that of a tuning-fork. A heavy tightly fitting plunger was then placed in the pipe and adjusted until the original frequency was regained, *i. e.*, until the face of the plunger occupied a node. The second node was found in the same way, and thus the wave-length was obtained.

The cones were next attached in turn to the end of the open pipe, and the overall length of the system adjusted

to give the same frequency as before. *If* the node coincided with the junction of the conical and cylindrical pipe, the frequency of the cone would be that of the pipe, and thus may be found the frequency of a truncated cone closed at its narrow end. Invariably, however, the node was inside or outside of the cylinder, and so a series of readings was obtained giving the relationship between the frequency and the position of the node. This was repeated for each of the seven cones, and the results are given in Table I.

4. *Results.*

TABLE I.

Distance from node to open end of conical pipe (cm.)

Semi-angle of cone.		1°	5°	7½°	10°	15°	20°	25°
Frequency.	196.....	17·2	25·7	29·2	31·1	34·6	36·6	38·1
	224.....	9·8	18·1	22·1	23·9	27·5	29·8	31·2
	260.....	3·6	12·1	16·3	18·1	22·1	24·8	26·2
	292.....	−1·9	6·5	11·1	12·5	17·5	20·6	22·8
	324.....	−5·0	1·1	5·5				
	344.....	−6·7	−1·9	2·3				
	388.....	−9·6	−8·3	−6·1				

Two graphs were obtained from these results. The first gave the relationship between frequency and distance from node to junction for each cone ; when this distance is zero the corresponding frequency is the resonant frequency of that particular truncated cone closed at its narrow end. The frequencies obtained in this way are set out in Table II.

TABLE II.

Resonant frequencies.

Semi-angle of cone ..	1°	1·8°	4·3°	5°	6·1°	7·5°
Frequency	280	292	324	330	344	356

The second graph was obtained by plotting these, and the resulting curve, which could be represented closely by the equation $n=267{\cdot}5+12{\cdot}5$ A., showed that when the angle of the cone becomes zero, *i. e.*, when the

cone is a cylindrical pipe 30·5 cm. in length with a node at one end, the natural frequency is 268 c.p.s. and the quarter wave-length 32·1 cm. The end-correction is thus 1·6 cm., agreeing with the value obtained from the usual expression for an unflanged pipe, viz., 0·58 × radius, or $r/(3)^{\frac{1}{2}}$.

The end-corrections of the cones referred to in Table II. were next obtained by subtracting the axial length from the quarter wave-length, the slant-length of the conical portion being 30·5 cm. The results are :—

Semi-angle	0°	1°	1·8°	4·3°	5°	6·1°	7·3°
End-correction ..	1·6	0	−1·3	−4·0	−4·4	−5·5	−6·5 cm.

There are no readings above $7\frac{1}{2}°$ for frequencies above 292 c.p.s. This is because it was impossible to coax the node nearer the junction than the distance given, and indicates that resonance does not exist in cones of semi-vertical angle of about 10° and over. Hence, *below this angle the conical portion is to be regarded as a conical pipe, and above as a conical flange.*

An example will make this clear : when the 15° cone was attached to about 30 cm. of cylindrical pipe, the length was adjusted in an attempt to obtain a frequency of 324 c.p.s., but before this was attained the frequency jumped to about 410 c.p.s. It was then found that the anti-node was *in* the cone, and only a few cm. from its smaller end.

These conclusions were confirmed by ascertaining the positions of the nodes and antinodes in the conical pipes directly by exploring them with a small cylindrical box about 1 cm. diameter and 1 cm. deep, the ends being closed by diaphragms of gold-beater's skin The axis of the drum was at right angles to that of the cones, and was supported by two small brass tubes 40 cm. long, which communicated with a manometric flame. This arrangement was found to be very sensitive in detecting anti-nodes, but not so with nodes. These were found by placing the pipe system vertical, and lowering a horizontal paper diaphragm on which sand was placed into the pipe ; the sand ceased to " chatter " at the nodes.

The results confirmed the previous conclusions, and further evidence was obtained by finding the frequencies of the cylindrical pipe with and without the cones. The presence of the wide cones flattened the notes only slightly; this is due to an increase in the end-correction of the open cylindrical pipe in a manner similar to that when the pipe is flanged, and indicates, as stated above, that such cones act as flanges.

For the cones of smaller angle, the natural frequencies (from Table II.) are

1°.	5°.	7½°.
280	330	356

These should be equal, according to theory, as the slant-heights are the same; actually the frequency increases with angle, owing to the variation in the end-correction, which becomes increasingly negative as the angle is increased.

The resonant frequencies were confirmed by exciting resonance by a loudspeaker diaphragm attached in turn to the smaller ends of the three cones. These were found to be

1°.	5°.	7½°.
284	327	indefinite

after the necessary corrections were made.

No data concerning the end-correction of conical pipes appearing available [2], the relationship between the angle of the cones and the corrections was investigated and found to be closely represented by the expression

$$\text{Correction} = -1{\cdot}2(\text{angle}) + 1{\cdot}6,$$

as shown in the table.

Angle	0°	1°	4·3°	5°	6·1°	7 5°
Actual (cms.)	1·6	0	−4	−4·4	−5·5	−6·4
Calculated	1·6	0·25	−3·6	−4·4	−5·7	−7·4

The expression is of linear dimension, and it appeared probable that the quantity 1·2, being linear, would be proportional to the slant-length. Experiments with longer cones, however, disclosed no simple relationship.

The end-corrections vanished when the angle of the cones used (up to 50 cm. length) were about 1°, and this angle diminished with increase of length.

References.

(1) Phil. Mag. x. p. 617 (1930); also viii. p. 750 (1929), ix. p. 23 (1930).
(2) Webster, Proc. Nat. Ac. Sci. vi. p. 318 (1920).

Northern Polytechnic.
London, N.7.

LXVII. *On the Origin of Colour of Paramagnetic Ions in Solution.* *By* Prof. D. M. Bose, *M.A., Ph.D., and* P. C. Mukherji, *Research Fellow, Calcutta University* *.

[Received April 14, 1938.]

IT is well known that the inorganic salts containing paramagnetic ions of the different transition groups and the rare earth group generally show colour. Ladenburg (1) attempted to explain the origin of the colour of these salts from the standpoint of Bohr's theory of atomic structure in the following way. The first transition group of elements begin after calcium ($3s^2p^6$, $4s^2$), when the $3d$ instead of the $4p$ shell begins gradually to be filled up. It is assumed that there is very little difference in the energy of binding of the electrons attached to the $3d$ resp. $4p$ shells of such atoms, and the absorption in the visible region shown by the ions of these atoms is due to an electron transition from $3d \rightarrow 4p$ shell. For the ions of the palladium and the platinum groups, where respectively the $4d$ and $5d$ levels are being filled up, it is quite analogous to the above, while for the ions of the rare earth group the $4f$-electrons inside ($5s^2$, p^6) octet are responsible for the colours shown.

This view of the origin of colours due to electronic transitions in the paramagnetic ions was not accepted by Fajans (2) and Joos (3), who pointed out that the free ions in compounds like CuF_2 or anhydrous $CuSO_4$ do not show any colour, while the corresponding hydrated salts or their solution in water or in ammonia have a blue colour. They supposed that the colour is due to the deformation

* Communicated by Prof. D. M. Bose, M.A., Ph.D.

of the cations produced by the solvent molecules, or in other words the complexes of the type $(Cu, 4H_2O)^{++}$ or $(Cu, 4NH_3)^{++}$ are the absorbing centres instead of the free ions like Cu^{++} etc.

Another theory of the origin of colour of inorganic salts was developed by Saha [4], who postulated that the colour is due to the reaction of light on the electrons of the incomplete 3*d*-shell, but not in the way imagined by Ladenburg. In the iron group it has been established that the *l*-moments of the ions in hydrated crystals or in solution are more or less completely quenched by the interaction with the neighbouring atoms, while the spin moments are left free. Saha supposed that the process of absorption consists in the reversal of the spin of one of these electrons. In other words, the absorption bands arise from the so-called forbidden transitions in which there is a change of multiplicity of the ground term of the ion, but no change in the principal quantum number of any of the electrons present in the *d*-shell of the ion. He showed that the two principal absorption bands of Cr^{+++} ion in solution or in hydrated salts have frequencies very near those due to the transitions $^4F \rightarrow {}^2G$ and $^4F \rightarrow {}^2H$ of the free Cr IV ion.

Kato [5] made a detailed investigation of the absorption spectra of solutions containing the following paramagnetic ions: V^{+++}, V^{++}, Cr^{+++}, and Cr^{++}; she has attempted to associate each absorption band with an electron transition of the type postulated by Saha. The results obtained by her are given in Table I. It will be noticed that the frequency corresponding to the position of the centre of gravity of an absorption band is always greater than that corresponding to the postulated transition of the free ion, the amount varying from 1170 to 5099 cm.$^{-1}$. It is assumed that this displacement of frequency corresponds to the work done in overcoming the energy of coupling between the paramagnetic ion and the associated water molecules. It will be noticed that the amount of work done varies capriciously from ion to ion, and no rule can be found to account for this variation.

It is known that the susceptibilities of solutions containing ions belonging to the iron group of elements have values which deviate widely from those predicted according to Hund's rule, and they tend towards a limiting value which is obtained when the spin-moment of the ion is

TABLE I.

Cations.	λ (Å.U.).	ν (cm.$^{-1}$).	$\Delta\nu$.	Transitions.	ν (cm.$^{-1}$).	$\Delta\nu$.	Effect of surrounding atoms and molecules.
T^{+++}	5010	$200{\cdot}10^2$	..	.. ..	..	..	..
V^{++++}	7400	135	..	..	..	..	..
V^{+++}	6100	164	..	$^3F'_{2,3,4}-{}^1D_2$	11,309	..	5099
			$74{\cdot}10^2$	..	..	7429	
	4200	238	..	$^3F'_{2,3,4}-{}^1G_4$	18,738	..	5062
V^{++}	8200	122	..	$^4F'_{2,3,4,5}-{}^2P'_{1,2}$	11,030	..	1170
			9	..	..	780	
	7660	131	..	$^4F'_{2,3,4,5}-{}^2G_{4,5}$	11,810	..	1290
			48	..	..	4226	
	5600	179	..	$^4F'_{2,3,4,5}-{}^2D_{2,3}$	16,036	..	1864
			7	..	..	597	
	5400	186	..	$^4F'_{2,3,4,5}-{}^2H'_{5,6}$	16,633	..	1967
Cr^{+++}.....	5500	182	..	$^4F_{2,3,4,5}-{}^2G_{4,5}$	14,758	..	3007
			59	..	..	5960	
	4150	241	..	$^4F_{2,3,4,5}-{}^2H'_{5,6}$	20,718	..	2947
Cr^{++}.....	7300–6200	..	..	$^5D_0-{}^3D$?			
	4500	222	..	$^5D_0-{}^3F'_{2,3,4}$	19,062	..	3138
			22	..	..	2332	
	4100	244	..	$^5D_0-{}^3G_{3,4,5}$	21,394	..	3006
Mo^{+++++} ...	5400	185	..	..	..	..	..
			13				
	5800	172	..	..	..	..	..
W^{+++++}.....	6000	167	..	..	..	..	..
			$24{\cdot}10^2$				
	7000	$143{\cdot}10^2$	..	..	..	..	..

alone effective (Bose-Stoner values). The change in the magnetic susceptibilities of these solutions by light absorption has been investigated by Bose and Raha[6], and it was found that most of these ions show an increase in susceptibility on light absorption, the change being largest in those ions whose susceptibility approaches nearest to the Bose-Stoner value, *i. e.*, those in which the orbital moment is more or less effectively quenched.

To account for the magnetic, optical and photomagnetic behaviour of these solutions a theory was developed by Bose and Datta[7], whose essential points are the following :—

I. The absorbing centres are not the free ions but the hydrated complexes (Me, $n\mathrm{H_2O})^{+m}$, and if n_0 is the number of ions present a number $n=n_0(1-e^{-A/kT})$ form complexes with water molecules such that the orbital moment of the ion is completely quenched. Here A represents the work necessary to break up the complex. There are thus (n_0-n) free ions present in which both the spin and the orbital moments contribute to the susceptibility of the ion, and the deviation of the susceptibility of such a solution from the Bose-Stoner value is proportional to (n_0-n).

II. During the process of light absorption the hydrated complexes break down ; the amount of work done during this process is $A=h(\nu-\nu_0)$, when ν is the frequency of absorption of the hydrated ion and ν_0 that of the free ion. Accepting Saha's hypothesis that the spin moment of the ion is reduced by two units during the process of light absorption, the increase in susceptibility observed in such solutions on light absorption is explained by the restoration of the orbital moment in the dissociated ion. The hypothesis outlined above with certain amplifications was found capable of qualitatively accounting for the observed optical and magnetic behaviour of these solutions.

In the meantime another theory of the origin of the quenching of the orbital moment of the ion of the iron group of elements, and of the observed magnetic anisotropy in crystals containing some of these ions, was being developed by Van Vleck[8] and his co-workers. The assumption of this theory is that in a crystal the paramagnetic ion is subjected to an electric field, whose origin is due to the presence of the neighbouring atoms round

the ion, and the symmetry of the field depends upon the arrangement of these atoms in the crystal. It has been found that to account for the magnetic behaviour of the hydrated paramagnetic crystals it is necessary to assume a field of dominantly cubic symmetry with a superposed field of rhombic symmetry, the analytical expression for the energy of an ion in such a field being of the form

$$V = D(x^4+y^4+z^4)+(A+B)(x^2+y^2)-(A+B)z^2 ;$$

by a suitable choice of constants, D, A, and B, it is possible to obtain any relative values of the intensities of the cubic and rhombic fields. Van Vleck [9] has been able to account qualitatively for the difference in the magnetic anisotropy of similar crystals containing ions like Co^{++} and Ni^{++}, both of which have the same ground state. Further, Penney and Schlapp [10] have succeeded in deriving quantitative formulas to account for the temperature variation of the magnetic susceptibilities of crystals containing ions like Pr^{+++}, Nd^{+++}, Ni^{++}, etc., which are in fair agreement with experimental results. The separation between the energy levels as calculated from the magnetic data for the iron group of elements is of the order of 10^4 cm.$^{-1}$; transitions between these levels might give rise to the absorption effects in the visible and in the near infra-red part of the spectra. No attempt was, however, made by the authors of these theories to find optical evidence in support of the latter.

The present writers made an attempt to apply Van Vleck's theory to the interpretation of the absorption spectra of the Ce^{+++} ion in solution, assuming it to be due to the transition $4^2F \rightarrow 5^2D$. The value of the 5D term of Ce IV was taken from spectroscopic data, and the splitting of this term was calculated according to Jordahl's [11] investigation of the ground term of Cu^{++} ion, which is also a ^2D one. Under certain assumptions it was possible to obtain a fairly quantitative agreement with a portion of the observed data. Further attempts were made to see whether the absorption spectra of solutions containing ions like Cu^{++} and Ti^{+++}, whose ground term is ^2D, could be explained by assuming the absorption to be due to transition between the different sublevels of the latter, split up in the crystalline field. Here also a fair amount of agreement was obtained. But later, on extending the investigation to the interpretation of the absorption

spectra of ions with F as orbital number of the ground term, it was found that neither the number of absorption bands nor their relative frequencies could be deduced from the energy diagram of an F-term in a predominantly cubic field.

In the present paper we have collected together the available data on the absorption bands due to solutions containing paramagnetic ions (excluding the rare earths), and have put forward a working hypothesis to account for the number and frequencies of the principal absorption bands, ignoring for the present the subdivisions and finer structures of these bands.

The assumptions on which the interpretation is based are as follows :—

(i.) Any ion, when dissolved in a liquid containing dipole molecules, will form complexes with these molecules. The dipole molecules are polarized in the electric field of the central ion, and in turn produce a field acting on the ion which is proportional to the charge on the latter. The influence of the polarizability of the dipole molecules on the strength of the induced field will be considered in a separate paragraph at the end.

(ii.) In this electric field the ground-level of the ion is split up into a number of equidistant levels ; the number of such levels is L+1, where L is the orbital quantum number of the ground term. This is equivalent to stating that, analogous to the magnetic quantum number m_L, we can associate an electric quantum number e_L with these sublevels where $e_L = 0, 1, 2 \ldots . L$, and the energy of separation between the sublevels will be proportional to the electric quantum number e_L associated with them and to the electric charge on the central ion.

(iii.) According as the ground term is regular or inverted in the sense introduced by Van Vleck the expression for energies associated with each of the sublevels will be $h\nu_0 \pm \mathrm{Ne}.\, e_L.\kappa$, *i.e.*, the orbital quantum number associated with the lowest energy level will be 0 or L ; the magnetic moment of ions belonging to the first group will tend towards the Bose-Stoner value (*e. g.*, Cr^{+++}, Ni^{++}), while those belonging to the second group will show large deviations (*e. g.*, Co^{++}).

(iv.) The absorption bands observed in such solutions are due to transitions from the lowest of the energy levels

to the higher ones ; the probability of all such transitions appears to be of the same order of magnitude.

The mean frequencies of these absorption bands can be represented empirically by the formula

$$\Delta\nu = \mathrm{Ne}.\,\Delta e_{\mathrm{L}}.\mathrm{K},$$

where Ne = the ionic charge,

Δe_{L} = change in the electric quantum number,

K = a constant.

If this formula is correct, then $\mathrm{K}' = \mathrm{K}e = \frac{\Delta\nu}{\mathrm{N}.\,\Delta e_{\mathrm{L}}}$ will be a constant for all absorption bands, with the same solvent.

It may be mentioned here that in all solutions containing the class of paramagnetic ions considered in this paper usually broad absorption bands are observed ; only in the case of solutions and hydrated and other crystals containing Cr^{+++} ion do a large number of faint absorption lines appear in addition, whose relative intensities are of the order of 10^{-4} compared to those of the broad absorption bands. The origin of these lines can be attributed, as shown by Deutschbein * and others, as being due to transitions $^4F \rightarrow {}^2G$ and $^4F \rightarrow {}^2H$ respectively of the Cr^{+++} ion.

According to our point of view the broad absorption bands are due to transitions between the Stark levels of the ground term, while the line absorptions are due to transitions between different spectroscopic term levels of the paramagnetic ion, where both the ground and the excited level are split up according to the scheme proposed by us. Since in these transitions the multiplicity of the term alters by two units, these transitions are prohibited by the ordinary selection rules and are therefore rare.

In Table II. are collected together the absorption data for the aqueous solution of the paramagnetic ions whose ground state is a D-term. According to our assumptions the D-term is split up into three sublevels with $e_{\mathrm{L}} = 0, 1, 2$; transitions between $0 \rightarrow 1$ and $0 \rightarrow 2$ will give rise to two absorption bands whose frequency ratio will be 1 : 2, and one of them will be in the infra-red. In the table the absorption bands recorded correspond

* O. Deutschbein, *Zeits. f. Physik*, lxxvii. p. 489 (1932).

TABLE II.

Ions.	Configuration.	Ground term.	Selective Absorption. λ (Å.U.).	ν (cm.$^{-1}$).	Centre of gravity (cm.$^{-1}$).	Transitions.	$K' = \frac{\Delta\nu}{N \cdot \Delta e_L}$.	Observers.
Ti^{+++}	$3d^1$	$^2D_{3/2}$	6100 5200	16,389 19,225	17,807	0–2	2,968 cm.$^{-1}$	Bose and Datta ‡.
$(MoO)^{+++}$ ...	$4d^1$	$^2D_{3/2}$	5800 5400	17,236 18,513	17,875	0–2	2,979 ,,	Kato §.
$(WO)^{+++}$ ...	$5d^1$	$^2D_{3/2}$	7000 6000	14,282 16,662	15,472	0–2	2,579 ,,	,,
$(V.O)^{++}$	$3d^1$	$^2D_{3/2}$	7400	13,510	13,510	0–2	3,377 ,,	,,
Cr^{++}.....	$3d^4$	$^5D_0$	7300– 6200	13,695– 16,125	14,910	0–2	3,423 ,,	,,
			4500 4100	22,216 * 24,383				
Co^{+++}	$3d^6$	$^5D_4$	6120 4000	16,335 † 25,000	—	—	—	Topp ‖.
Fe^{++}	$3d^6$	$^5D_4$	10700 9500	9,343 10,523	9,933	0–2	2,483 ,,	Dreisch ¶.
Cu^{++}	$3d^9$	$^2D_{5/2}$	8200	12,192	12,192	2–0	3,064 ,,	Dreisch and Trommer**.
						Mean	=2,950 ,,	

* The doublet band is perhaps due to Cr^{+++}.
‡ *Loc. cit.*
‖ Dissert. Münster (1928).
** *Zeits. f. Phys. Chem.* xxxvii. p. 37 (1937).
† This is discussed in detail later (see Table III).
§ *Loc. cit.*
¶ *Zeits. f. Phys.* xl. p. 714 (1927).

to the transition $0 \rightarrow 2$. In our view if the absorption spectra of these solutions are carefully investigated in the infra-red region then the existence of the absorption bands representing the transition $0 \rightarrow 1$ will be established. The existence of a level corresponding to $e_L = 1$ for an ion with a D-term will be made evident when we consider the absorption spectra of Ce^{+++} ion a little below.

The position of the absorption bands of the ions $(VO)^{++}$, $(MoO)^{+++}$, $(WO)^{+++}$ are taken from Kato's paper, in which they are represented as being due to V^{4+}, Mo^{5+}, and W^{5+} ions respectively. The absorption spectra of these ions were obtained by Kato by reducing the solutions of $Na_3VO_4 . 16H_2O$, $Na_2MoO_4 . 2H_2O$, and $Na_2WO_4 . 2H_2O$ in dilute HCl either with SO_2 gas or with Bi–Hg amalgam. In these solutions a reaction of the following type takes place :

$$Na_3VO_4 + 5HCl + H \rightarrow 3NaCl + 3H_2O + VOCl_2,$$

and $VOCl_2$ dissociates into $(VO)^{++} + 2Cl^{--}$.

Therefore we are justified in attributing these absorption bands as being due to $(VO)^{++}$, $(MoO)^{+++}$, and $(WO)^{+++}$, in which there is only one free electron left in the *d*-shell of the paramagnetic ions, and the effective charges on them are two and three units respectively. We have verified this conclusion by obtaining the absorption spectra of aqueous solution of $VO(ClO_4)_2$, which is similar to that obtained by Kato.

According to the theory proposed by us the ratio of $\frac{\Delta\nu}{N . \Delta e_L}$ should be a constant " K′ " for all hydrated ions. In the last column of Table II. are given the values of K′ for all the absorbing ions. The value of K′ varies from 2,483 to 3,423 ; this variation in the value of K′ may be partly due to the rough nature of the measurements, owing to which it is not possible to determine accurately the centre of gravity of the absorption bands ; further, there may be factors on which the strength of the crystalline field depends other than those postulated by us. The elucidation of this point will be reserved for a subsequent paper.

Another point which may be noticed is that the absorption bands for the D-term are usually of a doublet nature.

We give below the difference of frequency between the doublet bands in the respective cases :—

Ion.	$\Delta\nu$ (observed).	$\Delta\nu$ (emission).
Ti^{+++}	2836 cm.$^{-1}$.	384·3 cm.$^{-1}$.
Cr^{++}	2430 „	
Fe^{++}	1180 „	
$(MoO)^{+++}$	1277 „	
$(WO)^{+++}$	2380 „	
Ce^{+++}	2408 „	2489 „
	2926 „	

The splitting effect appears not to be dependent on either the ionic charge or on the spin orbital coupling ; for the majority of the ions it is of the order of magnitude of 2400 cm.$^{-1}$. The deviations observed in the two cases may well be due to errors of observation.

Absorption due to Co^{+++} *Ion.*

From Table II. it will be seen that the absorption bands of aqueous solutions of Co^{+++}, whose ground term according to Hund is $^5D_4$, are not similar to those of other ions whose absorption spectra are given there. We give below some magnetic evidences which indicate that the ground term of Co^{+++} is not ^5D but a triplet term which may be either ^3H or ^3G ; it will also be shown that the absorption data for these ions are in agreement with the above assumptions.

If the ground term of Co^{+++} ($3d^6$) is taken to be $^5D_4$, according to Hund's rule, then the magnetic moment of such an ion according to Bose-Stoner rule will be 25·4 Weiss magnetons. Weber[12] first found that the magnetic moment of Co^{+++} ion has a value $n_W = 12·5$; but as the compound studied by him was not stable this observation did not attract much attention. Later investigations of stable compounds containing Co^{+++} ion by Ray and Sen[13] have given the following values for the effective magneton numbers for the Co^{+++} ion :—

Compounds.	n_W.
Cobaltic cyanide (blue anhydrous)	13·63
Cobaltic cyanide (red hydrated)	15·16
Cobaltic alum	14·29
Cobaltic sulphate	16·05

Table III.

	Compounds.	Centres of absorption bands. First band.	Second band.	Third band.	Ratio.	Observers.
(i.)	$[Co(NH_3)_4Cl_2]Cl$	$15{\cdot}10^3$ cm.$^{-1}$	$21{\cdot}10^3$ cm.$^{-1}$	$32{\cdot}10^3$ cm.$^{-1}$	2 : 3 : 4	Tsuchida and Kashimoto *.
	$[Co(NH_3)_4ClNO_2]Cl$	21 ,,	29·7 ,,	41 ,,	,,	Tsuchida and Kashimoto *.
	$[Co(NH_3)_4(NO_2)_2]Cl$	22·7 ,,	29 ,,	40 ,,	,,	Tsuchida and Kashimoto *.
(ii.)	$[Co(NH_3)_3(NO_2)_3]$.....	23 ,,	29 ,,	40 ,,	,,	Tsuchida and Kashimoto *.
	$[Co(NH_3)_2.(NO_2)_4]NH_4$.....	22·7 ,,	28·7 ,,	39·7 ,,	,,	Tsuchida and Kashimoto *.
	$[Co(NO_2)_6]Na_3$	21 ,,	27·3 ,,	38 ,,	,,	Tsuchida and Kashimoto *.
(iii.)	$[Co(NH_3)_6]Cl_3$.....	19·4 ,,	28·7 ,,	....	2 : 3	Samuel †.
	$[Co(H_2O)_6]Cl_3$.....	16·3 ,,	25 ,,	....	,,	Topp ‡.

(i.), (ii.), and (iii.) compounds are known to be diamagnetic.

* Bull. Chem. Soc. Jap. xi. p. 785 (1936). † *Zeits. f. Phys.* lxx. p. 43 (1931). ‡ *Loc. cit.*

The effective magneton number thus approximates to two Bohr's magneton (*i. e.*, 14·1 n_W). From this evidence the authors conclude that the ground state of Co^{+++} ion is not ^5D as expected according to Hund's rule, but is one of the metastable triplet states, the possible ones being ^{3}(H, G, F, etc.), of which ^3H will have the lowest energy value. For such a term the L-value is 5, and it will be split up into six sublevels with $e_L=0$, 1, 2, 3, 4, 5; five absorption bands are to be expected with frequency ratios 1 : 2 : 3 : 4 : 5.

In Table III. we give a list of the absorption bands observed in certain simple and complex compounds containing Co^{+++}. It is found from the table that many of these compounds give three absorption bands whose

TABLE IV.

Bands.	λ (Å.U.).	ν (cm.$^{-1}$).	C.G. (cm.$^{-1}$).	ν calc. (cm.$^{-1}$).	Transition.
I.	2970	33,660	33,660	33,282	$^4F_{5/2}\rightarrow{}^5D_{5/2}(e^L=2)$
II.	2525	39,592			
III.	2380	42,004	42,175	42,132	$^4F_{5/2}\rightarrow{}^5D_{3/2}(e_L=1)$
IV.	2225	44,930			
			—	50,982	$^4F_{5/2}\rightarrow{}^5D_{1/2}(e_L=0)$

frequency ratios are 2 : 3 : 4, showing that the ground state of the ion must be at least ^3G, if not ^3H.

The absorption spectra of these compounds raise an interesting problem. Most of these compounds are nearly diamagnetic, which implies that the ground state is ^1S, and as such should not show any Stark splitting. To account for the observed absorption bands we have to assume that the strength of the coordination bands, which produce a neutralization of the free spin moment of the Co^{+++} ion, must be very feeble, and is during the process of light absorption easily broken up, leaving the ion in the ^3H state.

Absorption Spectra due to Ce^{+++} *Ion in Solution.*

Table IV. gives the principal absorption bands of an aqueous solution of $CeCl_3$ first observed by Bose and

Datta[14]. In order to interpret the origin of these absorption bands we have assumed them to be due to a transition of the $4f^1$ electron from $4^2F \rightarrow 5^2D$. Aqueous solutions of Ce^{+++} ion show four absorption bands; band I. is weak, and diffuse, and is probably due to the superposition of two absorption bands; bands II., III., and IV. are all of nearly the same intensity, which is about twenty times that of band I. We shall consider these three bands to be subdivsions of one principal absorption band with its centre of gravity at 42,175 cm.$^{-1}$. According to our formula, if ν_0 is the mean frequency of the ^2D term of CeIV, which, according to the data of Lang[15] is 50,982 cm.$^{-1}$, then we should expect three principal absorption bands with frequencies

$$\nu = \nu_0 - \Delta\nu_i \text{ (as D-term is inverted here)}$$
$$= \nu_0 - N.K'.\Delta e_L,$$

where $N = 3$; $K' = 2950$ cm.$^{-1}$

and $\Delta e_L = 0$, 1, and 2.

The positions of these three levels above the $4^2F_{5/2}$ level, which is taken as zero, are 50,982, 42,132, and 33,282 cm.$^{-1}$ respectively, and should give rise to three corresponding bands in absorption.

So far the transitions giving rise to the absorption bands, which are presented in Table II., were between the different sublevels of the ground term (D), and they were assumed to be all of equal probability. In the present case, however, the transitions take place between the $^2F_{5/2}$ and the three sublevels of the D term. To get an estimate of the relative intensities it will be useful to introduce here the concept of an electric inner quantum number e_j compounded of e_L and e_s. In the present case for the three sublevels of the D term the values of e_j are 1/2, 3/2, and 5/2.

Then, using the ordinary rule for calculating the probabilities of transition, we obtain the relative intensities to be expected for the transitions

$$\underset{\text{(Band I.)}}{^2F_{5/2} \rightarrow {}^2D_{5/2}} \quad \text{and} \quad \underset{\text{(Bands II.–IV.)}}{^2F_{5/2} \rightarrow {}^2D_{3/2}} \text{ to be as } 1 : 14,$$

while the observed ratio of intensities is as 1 : 20, according to the investigations of Morton[17].

Bose and Datta, in their first investigation of the absorption spectra of Ce^{+++} ion, had attributed the two principal absorption bands at 2970 and 2525 Å. to transitions $^2F_{5/2} \rightarrow {}^2D_{5/2}$ and $^2D_{3/2}$. At that time this assumption had caused a certain amount of misgiving in the mind of one of us, as it was equivalent to assuming that the energy of the $5d^1\ ^2D_{5/2}$ level of Ce^{+++} was less than that of the $^2D_{3/2}$ level of the same ion, which is contrary to Hund's rule for normal terms.

Roberts, Wallace, and Pierce[16] have shown that the magnetic rotatory dispersion of $Ce(SO_4)_3$ solution can be calculated throughout the region 5780–3341 Å. by taking into account the two absorption bands at 2960 Å. and 2540 Å., and by attributing them the transitions $^2F_{5/2} \rightarrow {}^2D_{5/2,\ 3/2}$ respectively. Further, the relative intensities of these bands, calculated from the specific rotation etc., are given by

$$\left.\begin{aligned} f_{2960} &= 1{\cdot}404 \times 10^{-3} \\ f_{2540} &= 2{\cdot}291 \times 10^{-2} \end{aligned}\right\} \text{Ratio} = 1 : 16.$$

This ratio agrees well with the ratio of intensities obtained from absorption measurements.

Absorption spectra of aqueous solutions containing ions whose ground term is F are given in Table V.

For the ions V^{+++}, V^{++}, and Cr^{+++} usually two absorption bands are found, whose relative frequencies are as 2 : 3, and the K′-values vary from 2·64 to $3{\cdot}15.10^3$ cm.$^{-1}$. Each of the principal absorption bands represents a doublet, the frequency differences of which are of the order of 700 cm.$^{-1}$, which is about one-third of that obtained in the case of the splitting of the D-term :

V^{++}—859 cm.$^{-1}$	Cr^{+++}—608 cm.$^{-1}$
659 ,,	874 ,,

The absorption bands of solutions containing Co^{++} and Ni^{++} are complicated in structure. Ni^{++} contains three principal absorption bands whose frequency ratios are as 1 : 2 : 3, but the K′-values for these bands are rather high, varying from 3,640 to 4,130 cm.$^{-1}$. The infra-red band consists of four components. A similar structure can be seen in the ·67 μ band of a solution of $NiCl_2$ in HCl as measured by Datta and Deb[18]. A detailed study of the fine structure of these bands will be undertaken later.

TABLE V.

Ion.	Configuration.	Ground term.	Selective λ (Å.U.).	Absorption ν (cm.$^{-1}$).	Centre of gravity (cm.$^{-1}$).	Ratio.	Transition.	$K' = \frac{\Delta\nu}{N.\Delta e_L}$.	Observers.
V^{+++}	$3d^2$	$^3F_2$	6100	16,389	16,389	..	0–2	2,731 cm.$^{-1}$	Kato *.
			4200	23,803	23,803	2 : 3 ..	0–3	2,645 ,,	,,
V^{++}	$3d^3$	$^4F_{3/2}$	8200	12,192	12,620	..	0–2	3,155 ,,	,,
			7660	13 051		2 : 3			
			5600	17 852	18,180	..	0–3	3,055 ,,	,,
			5400	18,513					
Cr^{+++}.....	$3d^3$	$^4F_{3/2}$	6380	15,670	15,976	..	0–2	2,663 ,,	Datta and Deb †.
			6140	16,280		2 : 3			
			4470	22,365	22,807	..	0–3	2,667 ,,	Datta and Deb †.
			4300	23,249					
Co^{++}	$3d^7$	$^4F_{9/2}$	12500	8,000	8,000	..	..	....	Dreisch ‡.
			7700	12,982	12,982	..	3–1	3,245 ,,	,, ‡.
			5150	19,413	19,413	2 : 3 ..	3–0	3,235 ,,	,, ‡.
Ni^{++}.....	$3d^8$	$^3F_4$	12100	8,262	8,262	..	0–1	4,131 ,,	Houstoun §.
			6870	14,552	14,552	1 : 2 ..	0–2	3,638 ,,	,,
			4050	24,684	24,684	2 : 3 ..	0–3	4,114 ,,	,,

* *Loc. cit.*
‡ *Zeits. f. Phys.* xl. p. 714 (1927).
† *Loc. cit.*
§ Proc. Roy. Soc. Edin. xxxi. pp. 530, 538 (1910).

The absorption spectra of solutions containing Co^{++} are still more complicated, and are very susceptible to the influence of temperature and to the presence of halogen and allied anions. It is difficult to give a satisfactory interpretation of all the absorption bands observed. In Table VI. the principal absorption bands of different types of solutions containing Co^{++} ion are given together with a partial classification of their frequencies.

Influence of the nature of the associated molecules with which the paramagnetic ion forms a complex.—According to the hypothesis formulated by us the splitting of the ground term $\Delta\nu = \mathrm{Ne}.\Delta e_{\mathrm{L}}.\mathrm{K}$; here it is assumed that the paramagnetic ion is acted upon by the electric field due

TABLE VI.

$[Co(H_2O)_6]Cl_2$.		$(NH_4)_2Co(SCN)_4$.	$H_2(CoCl_4)$.	
(A).	(B).	(A).	(A).	(B).
	—			5,554 6,408
8,000		8,000	—	
	12,983			14,281
—		16,524	16,389	
	19,412			—

to polarization of the molecules associated with the ion to form a complex. The intensity of the field due to this dielectric polarization will be dependent upon the polarizability of the associated molecules. There exists a certain amount of experimental observations which are summarized in Table VII., in which the influence of the associated molecules on the positions of the absorption bands are shown.

If we compare the ratio of the absorption frequencies of the aquo to the amino compounds it is found that it is very nearly the same as the ratio of the dielectric constants of ammonia to water in gaseous states, viz., $1{\cdot}53/1{\cdot}87 = {\cdot}82$, *i. e.*, the splitting is inversely proportional to the dielectric constants of the associated molecules when they exist in the gaseous state. In view of the complicated nature of the interaction between the paramagnetic ion and its associated molecules, which in the

Table VII.

Ground state of the ion.	Substance.	Centres of selective absorption.	Ratio $\frac{\epsilon_{NH_3}}{\epsilon_{H_2O}}$.
D-state	$CuSO_4$, $5H_2O$	12,297 cm.$^{-1}$	·82
	$[Cu(NH_3)_4]Cl_2$, H_2O	14,160 „	
		Ratio ····· ·87	
F-state	$[Cr(H_2O)_6]Cl_3$	18,200 cm.$^{-1}$; 24,100 cm.$^{-1}$	
	$[Cr(NH_3)_6]Cl_3$	21,500 „ ; 23,500 „	
		Ratio ····· ·85 ·85	
	$[Ni(H_2O)_6]Cl_2$	8,497 cm.$^{-1}$; 15, 370 cm.$^{-1}$; 25,510 cm.$^{-1}$	
	$[Ni(NH_3)_6]Cl_2$	10,804 „ ; 17,200 „ ; 27,900 „	
		Ratio.. ·79 ·89 ·91	
G- or H-state	$[Co(H_2O)_6]Cl_3$	16,340 cm.$^{-1}$; 25,000 cm.$^{-1}$	
	$[Co(NH_3)_6]Cl_3$	19,460 „ ; 28,650 „	
		Ratio ····· ·84 ·87	

case of the cobaltic hexamine chloride leads to a complete suppression of the spin and orbital moment of the paramagnetic ion, it is rather surprising to find this influence should be represented by such a simple formula. Most of the amino compounds are examined when dissolved in water, and results obtained show that the dielectric properties of the associated molecules are of predominant influence in determining the intensity of the induced electric field acting on the paramagnetic ion. Taking into consideration the influence of the associated molecules our formula now takes the form

$$\Delta\nu = \frac{\mathrm{Ne}.\,\Delta e_{\mathrm{L}}.\,\mathrm{K}_0}{\epsilon},$$

where ϵ is the dielectric constant of the associated molecules when they exist in the state of vapour.

It will be of some interest to discuss here the reasons which induced us to discard the Bethe-Van Vleck's theory of splitting of the ground term as being inadequate for our purpose. According to this theory in hydrated crystals the field is of predominantly cubic symmetry. In such a field an F-term is split up into three sublevels whose relative separations are as 0 : 8 : 18 for the ions Cr^{+++} and Ni^{++}, and it is 0 : 10 : 18 for Co^{++}. The observed data, as tabulated in Table V., cannot be fitted into such a scheme. Further, in the expression for the energy of the field the ionic charge, the orbital quantum number, and the polarizability of the associated molecules do not occur in the simple form as they do in the empirical formula. Having thus established an empirical formula to correlate the absorption frequencies of the paramagnetic ions with certain properties of these ions and those of the associated molecules, it requires now a theoretical investigation to find out how the constant K_0 can be represented in terms of the properties of the ion and of the associated molecules.

Summary.

In this paper have been collected together the available data on the absorption spectra of solutions containing paramagnetic ions, excluding those due to the rare earth ions. An empirical formula has been put forward to account for the number and frequency of the principal

absorption bands, *i. e.*, without taking into consideration the subdivision and finer structure of these bands. The assumptions on which the formula is based are as follows:—

(i.) The paramagnetic ions, when dissolved in a liquid containing dipole molecules, form complexes with the latter; in the complex due to the polarization of the dipole molecules an induced electric field acts on the central ion, whose intensity is proportional directly to the charge on the ion, and inversely to the dipole moment of the associated molecule.

(ii.) In this induced field the ground term of the ion with orbital moment L is split up into L+1 equidistant sublevels, to each of which an electric quantum number e_L can be associated, such that $e_L=0, 1, 2 \ldots . L$.

(iii.) The absorption spectra is due to the transition from the lowest of these levels to the higher ones, so that in general L absorption bands are to be expected and the frequency of absorption to be given by

$$\Delta\nu=\frac{\mathrm{Ne.}|\Delta e_L|}{\epsilon}.\mathrm{K}_0,$$

where "Ne"=ionic charge,

ϵ is the dielectric constant of the associated molecules,

Δe_L is the change in electric quantum number.

(iv.) It is shown that $\mathrm{K}'=\mathrm{K}_0 e/\epsilon$ is an approximate constant whose value for aqueous solutions vary from 2,483 to 3,423 cm.$^{-1}$.

(v.) The finer structure of many of these bands have been discussed. In complex salts the influence of the polarizability of the molecules on the splitting is discussed and found to be in agreement with the empirical formula.

(vi.) The splitting of the ground-level in an electric field of predominantly cubic symmetry, as calculated according to Bethe-Van Vleck's theory, is found to be inadequate for explaining the observed data.

References.

(1) R. Ladenburg, *Naturwissenschaften*, viii. p. 5 (1920).
(2) K. Fajans, *Naturwissenschaften*, xi. p. 165 (1926).
(3) G. Joos, *Ann. der Phys.* lxxxi. p. 1076 (1926).
(4) M. N. Saha, 'Nature,' cxxv. p. 163 (1930); M. N. Saha and S. C. Deb, Bull. Acad. Sc. U. P. i. p. 1 (1931–32).
(5) S. Kato, Sc. Papers, I. P. C. R. xiii. p. 49 (1930).

(6) D. M. Bose and P. K. Raha, *Zeits. f. Phys.* lxxx. p. 361 (1933); Phil. Mag. xx. p. 145 (1935).
(7) D. M. Bose and S. Datta, *Zeits. f. Phys.* lxxx. p. 376 (1933).
(8) J. H. Van Vleck, 'Theory of Electric and Magnetic Susceptibilities' (1932).
(9) J. H. Van Vleck, Phys. Rev. xli. p. 208 (1932).
(10) Penney and Schlapp, Phys. Rev. xli. p. 194; xlii. p. 666 (1932).
(11) O. M. Jordahl, Phys. Rev. xlv. p. 87 (1934).
(12) Weber, *Ann. der Phys.* xxxvi. p. 624 (1911).
(13) P. R. Ray and D. C. Sen, Journ. Ind. Chem. Soc. xii. p. 190 (1935).
(14) D. M. Bose and S. Datta, 'Nature,' cxxviii. p. 270 (1931); *loc. cit.*
(15) R. J. Lang, Canadian J. Res. xiv. p. 127 (1936).
(16) R. W. Roberts, L. A. Wallace, and I. T. Pierce, Phil. Mag. xvii. p. 934 (1934).
(17) Morton, Phil. Mag. xvii. p. 934 (1934).
(18) S. Datta and M. Deb, Phil. Mag. xx. p. 1121 (1935).

Bose Institute,
University College of Science,
Calcutta.

LXVIII. *The Latent Heat of Fusion of Aluminium.* By J. H. Awbery, *B.A., B.Sc., F.Inst.P., Physics Department, National Physical Laboratory, Teddington, Middlesex* *.

[Received August 10, 1938.]

Introduction.

THE values for the latent heat of fusion of aluminium recorded in the literature vary by almost 50 per cent., from 64 to 94 cals. per gm.

They are set out below, together with details of the observers and an indication of the method used in each case.

The mean of these results is 82·4 cals. per gm., but the divergences from the mean are unusually great, the probable error of the mean being 2·1 cals. per degree and the probable error of an observation being 6·1. Moreover, the distribution is rather unsymmetrical, twice as many lying below as above the mean. On the other hand, if the observations are divided into two groups, a "low" group with values below 82·4 and a "high" group with values above this figure, the mean of the low group is 77·1 and of the high group 93·0. The probable errors

* Communicated by the Author.

of the means are 1·8 and 0·4 respectively, so that the means differ by more than seven times the sum of their probable errors, which suggests that they are incompatible or are not measurements of the same quantity. This conclusion is supported by the fact that the observations within either group now agree much better, the probable error of an observation being only 4·1 or 0·6 against the 6·1 found for the whole series.

TABLE I.

Latent Heat of Fusion of Aluminium.

Observers * and date.	Method.	Latent heat (cals. per gm.).
Pionchon, 1887	Calorimetric.	80
Glaser, 1904.....	,,	77
Greenwood, 1911	,,	93
Lascento, 1914	,,	64
Roos, 1916	,,	82
Roos, 1916	Cooling curve.	80
Wüst, 1922	Calorimetric.	94
Umino, 1926	,,	80
Awbery & Griffiths, 1926 ..	,,	92

TABLE II.

Observations.	Mean.	Probable error of	
		mean.	one observation.
All	84·8	1·7	4·4
Low	79·8	0·5	1·1
High	93·0	0·4	0·6
Sum	—	0·9	—
Difference	13·2	—	—

It is to be admitted that one result, that of Lascento, is so low, differing from the mean by more than three times the probable error, that it might reasonably be rejected, but if this is done the argument is but little affected. We have then Table II., showing that the means of the two groups differ by fourteen times the sum of their probable errors.

* See References at end of paper.

The position thus revealed is unsatisfactory, and demands further investigation. Assuming that the existence of two groups of measurements is established the purpose of the present investigation is to determine experimentally which group is correct.

Since eight of the nine values which vary so greatly are calorimetric, there would seem little point in repeating the determinations by that method, and an electrical method was therefore adopted. It was not anticipated that it would give results of very high accuracy, but it was

Fig. 1.

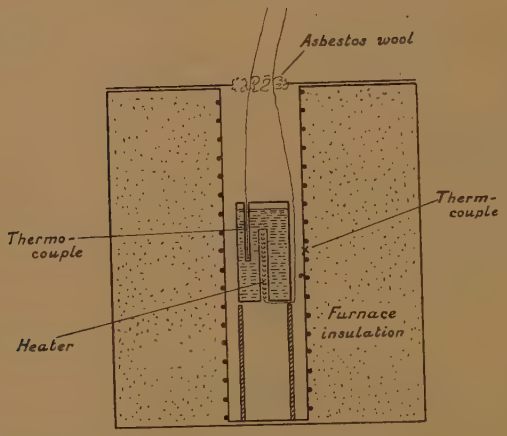

Apparatus for melting and freezing aluminium.

hoped that it would enable a decision to be made between the "high" and "low" values. It gave individual results with a good deal of scatter, but, as will be seen later, the evidence is distinctly in favour of the high value.

Method.

The aluminium is contained in a crucible provided with re-entrant tubes for an electric heater and a thermocouple, as shown in fig. 1. It is surrounded by a furnace heated electrically and provided with a thermocouple attached to the wall. The mouth of the furnace was made

as small as possible, and was closed with asbestos wool. The lower end of the furnace was closed.

By switching on current in the crucible heater and allowing conditions to become steady the rate of loss of heat from the crucible to the furnace can be determined under various conditions. Such a calibration is shown in fig. 2, in which the rate of heat loss in watts is plotted

Fig. 2.

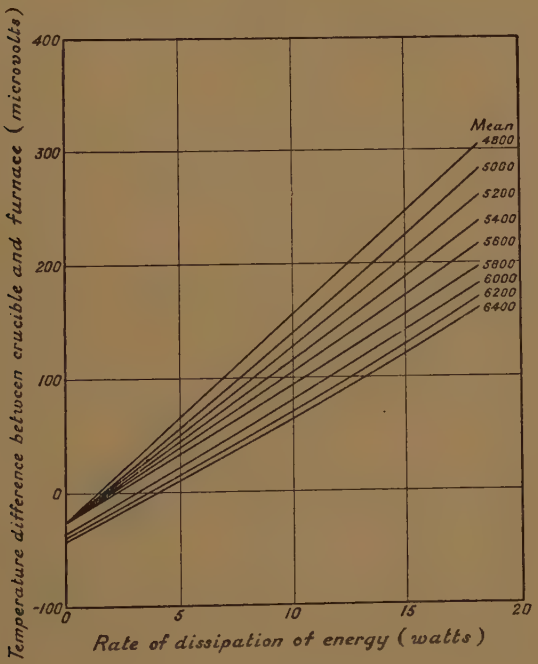

Heat loss from crucible to furnace at various temperatures.

against the temperature difference between the crucible and furnace at each of a number of mean temperatures. The temperatures are given in microvolts on the thermo-couple used, since in the calculation it is not necessary to know the temperature in degrees. The reliability of the calibration is illustrated in fig. 3, in which the rates of heat loss directly observed under various conditions are plotted against those read off from the curves in fig. 2 for the conditions in question. It should also be noted

that a calibration some months later agreed within 5 per cent. at all temperature excesses with the earlier one.

When this preliminary calibration has been completed determination of the latent heat of fusion can be carried out either by switching on the crucible heater and observing the temperatures of the furnace and crucible until melting is complete, or by commencing at a temperature above the freezing-point and determining the corresponding curves during the freeze. The duration of the process

Fig. 3.

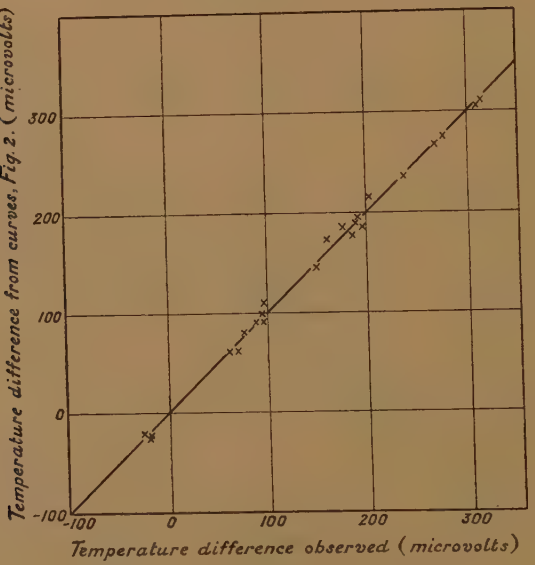

Check of calibration curves in Fig. 2.

can be read off from the curve, whilst the rate of heat loss at any instant can be deduced from the preliminary calibrations however the furnace temperature may vary. Thus the total loss of heat during the freeze or melt can be determined. In the case of freezing this quantity is the latent heat of fusion of the sample, whilst in the case of melting it has to be subtracted from the heat input (which is given as the product of the duration of the freeze and the rate of dissipation of energy). In either case the latent heat follows immediately.

Examples of the curves obtained are reproduced in figs. 4 and 5.

Fig. 4.

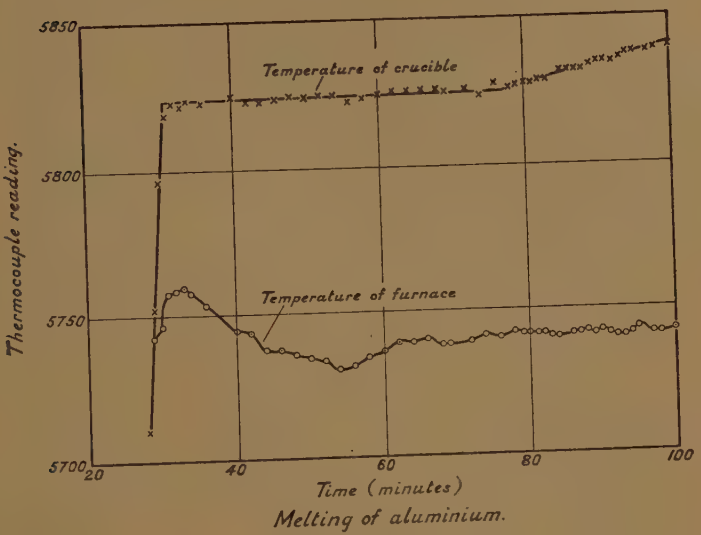

Melting of aluminium.

Fig. 5.

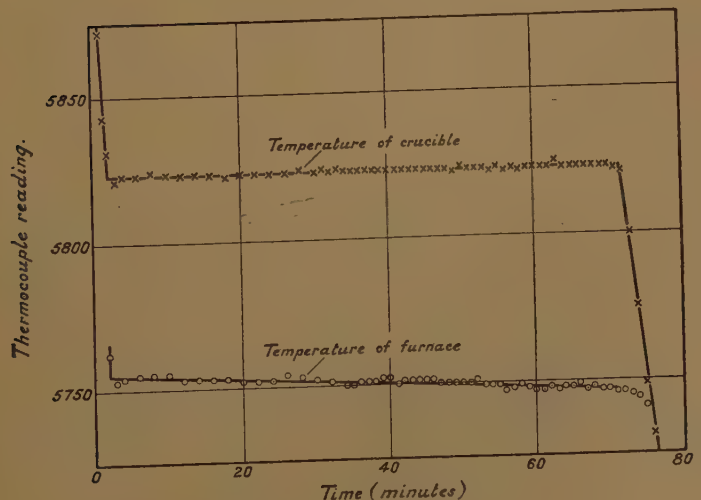

Freezing of aluminium.

Results.

In some preliminary experiments the aluminium used had less than 0·1 per cent. impurities. It was employed in an iron crucible for some time, and after the finish of the work was found to contain 0·66 per cent. iron and 0·33 per cent. oxygen in combination. The alumina should not affect the latent heat, since according to Withey * it is insoluble in molten aluminium, but the aluminium had clearly dissolved iron from the crucible, and, indeed, the melting curves in these experiments, even from the first, never gave a constant melting-point. After the technique had been worked out a fresh sample of aluminium, of purity greater than 99·99 per cent., was therefore used. The crucible was one made from

TABLE III.

Temperature of metal	Temperature of furnace.	Melting or freezing.	Latent heat (cals. per gm.).
5830 mv.	5710 mv.	M.	90·3
5825	5718	F.	90·9
5829	5789	M.	95·6
5825	5769	F.	84·0
5830	5749	M.	95·9
5825	5750	F.	90·1
		Mean..	91

sintered alumina (without any binder) in the Metallurgy Department of the Laboratory.

Six experiments were carried out in the final series, three in which the metal was melted and three in which it was frozen. The results are set out in Table III., in which details of the duration and furnace temperature are given, to show the range of variation of the conditions.

The mean agrees excellently with the " high " group referred to in the introductory paragraphs, and although there is a certain degree of scatter it is particularly to be noticed that even the lowest value is above any entries in the " low " group.

* Journ. Soc. of Chemical Industry, xlv. p. 1701 (1926).

It thus seems clear that in pure aluminium the latent heat is about 91 or 92 cals. per gm. Taking the four values now available in the high group, and giving them equal weight, the result is that the latent heat of fusion of aluminium is $92{\cdot}5 \pm 0{\cdot}4$ cals. per gm.

The existence of the low group of results is probably explained by the presence of impurities, which may in many cases have been iron. Greenwood, who obtains a value in the high group, does not give details of his observations, but states that there was a marked rise in specific heat a short distance below the melting-point, which he ignored in computing the latent heat. Presumably others who found low values encountered the phenomenon, but included this additional heat in the specific heat of the solid and not in the latent heat.

This would explain the calorimetric results, but not those obtained by the cooling curve method of Roos. This consisted in comparing the time required for solidification by the metal under examination with that required by materials of known latent heat; since, however, the freezing-points of the two materials are not the same it was necessary also to measure the rate of fall of temperature after the completion of the freeze in both cases, in order to correct the rate of heat loss from the substance under test to the value which it would have at the freezing-point of the comparison material. When determining the latent heat of aluminium he used zinc, cadmium, and tin as comparison materials, so that there was a difference of about 200° C. in the melting-points of the aluminium and the least fusible of the comparison materials. Moreover, the latent heats of the comparison materials cannot be regarded as known with any high accuracy.

Thus it is not surprising if his result was greatly in error. It appears to be confirmed by his calorimetric work, but this consisted of a single determination of the total heat of the liquid. The specific heat of the liquid was deduced on theoretical grounds, and is higher than the experimental values, whilst the total heat of the solid was taken from the results of former workers. If experimental values are taken for the former and more recent values for the latter Roos's result is raised 6 per cent., to 85 cals. per gm., which is substantially nearer to the results in the higher group.

Acknowledgments.

I desire to thank Dr. G. W. C. Kaye, Superintendent of the Physics Department, for his helpful interest in this work. The sintered alumina crucible and the exceptionally high-purity aluminium were supplied by the Metallurgy Department of the Laboratory.

Summary.

The extremes among the published values for the latent heat of fusion of aluminium differ by about 50 per cent., and the results fall into two groups, one with a mean about 92 cals. per gm. and one about 77 cals. per gm.

A method has been used in which the electrical energy required to melt a known mass is measured, and it gives a result of 91 cals. per gm

The various low values in the literature are attributed to impurities or to inherent inaccuracies in method.

It is suggested that the most probable value is $92{\cdot}4 \pm 0{\cdot}5$ cals. per gm.

References.

Pionchon, *Comptes Rendus*, Paris, xi. p. 106 (1887).
Glaser, 'Metallurgie,' i. pp. 103 & 121 (1904).
Greenwood, 'Engineering,' xcii. p. 419 (1911); Rep. Brit. Ass. (1911).
Lascento, J. Russ. Chem. Soc. xlv. p. 552 (1913); and xlvi. p. 311 (1914).
Roos, *Zs. Anorg. Chem.* xciv. p. 329 (1916).
Wüst, *Forsch. Verh. Deutsch. Ing.* no. 204 (1918); and p. 241 (1922).
Umino, Sci. Reports, Tohoku Univ. xv. p. 597 (1926).
Awbery and Griffiths, Proc. Phys. Soc.. xxxviiip. 378 (1926).

LXIX. *Note on Thermodynamics of Energy Balance Sheets of Internal Combustion Engines.* *By* A. C. Walshaw, *M.Sc., D.I.C., Lecturer in Applied Thermodynamics at the Northampton Polytechnic, London* *.

[Received July 2, 1938.]

I. *Total Energy of Working Agent at Inlet and Exhaust.*

THE accompanying diagram represents an internal combustion engine of a particular kind—a gas engine enclosed within a boundary.

* Communicated by James G. Docherty.

The working agent of all internal combustion engines at inlet or before combustion is a fuel-air mixture. In the above case the total energy of the fuel and air which enter the boundary along the streams G and A respectively is made up of :—

(i.) Potential energy (P_i) stored in the combustible constituents of the fuel.

(ii.) Total heat (H_i) of the gas and air entering the engine.

$$H_i = H_g + H_a = \left(E_g + \frac{P_g . V_g}{J}\right) + \left(E_a + \frac{P_a . V_a}{J}\right).$$

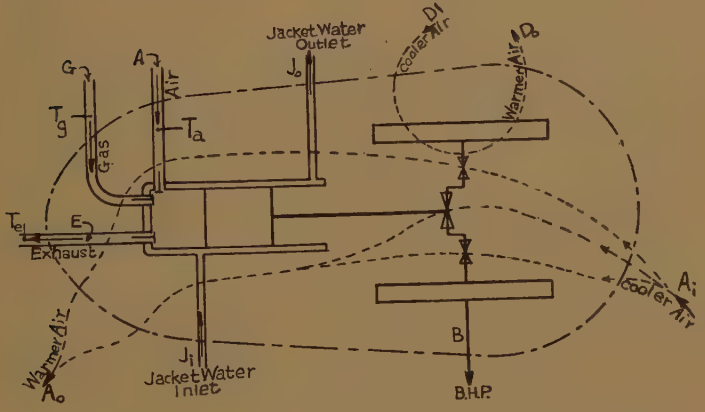

(iii.) Kinetic energy (K_i) of the gas and air which flow along the inlet-pipes with mean velocities U_g and U_a respectively.

$$K_i = K_g + K_a = \frac{m_g . U_g^2 + m_a . U_a^2}{2g . J}$$

$$= \frac{1}{2g . J}\left[\frac{P_g . V_g^3}{R_g . T_g . A_g^2} + \frac{P_a . V_a^3}{R_a . T_a . A_a^2}\right]$$

or

$$= \frac{1}{2g . J}\left[\frac{m_g^3 . R_g^2 . T_g^2}{P_g^2 . A_g^2} + \frac{m_a^3 . R_a^2 . T_a^2}{P_a^2 . A_a^2}\right]$$

heat units per second, where A represents the area of the pipe along which a volume V is flowing per second, corresponding to a mass per second of $m = \frac{PV}{RT}$.

The working agent rejected to exhaust is the products of combustion of the fuel-air mixture. These products leave the boundary along the stream E with a total energy made up of :

(i.) Potential energy (P_0) of unburnt fuel.

(ii.) Total heat (H_0) of the products of combustion, which can be divided into dry exhaust gas (of mass per second m_d) and moisture of combustion (*i. e.*, superheated steam of mass per second m_s).

$$H_0=H_d+H_s=\left[E_d+\frac{P_d.V_d}{J}\right]+m_s\left[S'.(T_e-T_s)+L+h\right]$$

heat units per second, where S′ represents the mean specific heat of superheated steam over the temperature range (T_e-T_s), and T_s, L, and h represent the saturation temperature, the latent heat, and total heat of water respectively at the pressure P_s of the steam in the exhaust products.

(iii.) Kinetic energy (K_0) of the exhaust products (dry exhaust gas and steam) flowing along the exhaust pipe with a mean velocity U_e.

$$K_0=K_d+K_s=\frac{(m_d+m_s).U_e^2}{2g.J}\text{ heat units per second.}$$

$$U_e=\frac{1}{A_e}\left(\frac{R_d.m_d.T_e}{P_d}\right),$$

where P_d represents the partial pressure of dry exhaust gas flowing at an absolute temperature T_e along the exhaust pipe of area A_e.

II. *The Energy Balance Sheet of Internal Combustion Engines.*

Internal combustion engines are energy transformers receiving energy the bulk of which is potential in a chemical form. By combustion part or the whole of this potential energy is transformed into heat, a part of which is then transformed into mechanical energy. The energy streams flowing into and out of the boundary of the diagram in section I. are indicated by means of

arrows, and if the engine has been running long enough, so that temperatures and other conditions are maintained steady, no energy will be accumulating within the boundary. It can therefore be stated that per unit of time the energy flowing into the boundary must be equal to the sum of the quantities of energy flowing out of the boundary along the various energy streams. This fact can be represented by means of the energy equation

$$G+A+J_i+A_i+D_i=B+E+J_0+A_0+D_0,$$

where the letters represent the energies per second flowing along the respective streams into and out of the boundary. Rearranged the energy equation can be written

$$(G+A)-E=B+(J_0-J_i)+(A_0-A_i)+(D_0-D_i),$$

which, when translated into words, states that the energy $[(G+A)-E]$ lost by the working agent during its passage through the engine is equal to the sum of :

(i.) The heat transformed into mechanical energy which leaves the boundary along the brake horse-power stream B.

(ii.) The heat (J_0-J_i) gained by the jacket water.

(iii.) The heat (A_0-A_i) gained by the surrounding air due to radiation, conduction and convection.

(iv.) The mechanical energy reconverted into heat (D_0-D_i) in overcoming air resistance or windage.

Also, it can be deduced from the equations of section I. that the energy lost by the working agent during its passage through the engine is :

$$\begin{aligned}(G+A)-E&=(P_i+H_i+K_i)-(P_0+H_0+K_0)\\&=P_i-[(H_0-H_i)+(K_0-K_i)+P_0].\end{aligned}$$

Thus the energy equation for the engine can be rewritten

$$\begin{aligned}P_i=B&+(J_0-J_i)+(H_0-H_i)+(K_0-K_i)+P_0\\&+[(A_0-A_i)+(D_0-D_i)],\end{aligned}$$

which means that the energy balance sheet for internal

combustion engines can be drawn up in the following way.

Energy balance sheet.	Heat units per second.	Per cent.
Potential energy in fuel supplied .	P_i	100
Heat equivalent of B.H.P.	B	
Heat gained by jacket water	(J_0-J_i)	
Gain in total heat of working agent .	(H_0-H_i)	
Gain in kinetic energy of working agent	(K_0-K_i)	
Potential energy lost in unburnt fuel	P_0	
Heat lost to surrounding air (by difference)	$[(A_0-A_i)+(D_0-D_i)]$	
Totals	P_i	100

The first three items of this balance sheet can be obtained by direct measurement in the usual way with a fair degree of accuracy. Of the next two items, namely the gain in total heat and in kinetic energy of the working agent, the former is dealt with in section III., whilst the latter can be estimated from the equation

$$\frac{1}{2g.J}\left\{\left(\frac{m_d+m_s}{A_e^2}\right)\left(m_s V_1+\frac{R_d.m_d.T_e}{P_d}\right)^2 - \left[m_g^3.\left(\frac{R_g.T_g}{P_g.A_g}\right)^2+m_a^3.\left(\frac{R_a.T_a}{P_a.A_a}\right)^2\right]\right\}$$

deduced from section I. The sixth item (P_0) representing the potential energy retained in unburnt fuel can be estimated from the analysis of dry exhaust gas, and the last item of the balance sheet representing the heat lost to the surrounding air can only be obtained by difference after the other items have been estimated.

III. *Gain in Total Heat of Working Agent.*

The gain in total heat (H_0-H_i) of the working agent during its pasaage through the engine will be seen from the equations of section I. to be

$$\left[\left(E_d+\frac{P_d.V_d}{J}\right)+m_s.[S'.(T_e-T_s)+L+h]\right] - \left[\left(E_g+\frac{P_g.V_g}{J}\right)+\left(E_a+\frac{P_a.V_a}{J}\right)\right].$$

The numerical values of the internal energies E_d, E_g, and E_a are not known, but since $dE = m.C_v.dT$ for "permanent" gases, then for the dry flue gas, $E_d = m_d.\int {}_dC_v.dT +$ a constant of integration. Or if ${}_dC_v$, the specific heat at constant volume of the dry flue gas, is expressed as a function of T (degrees absolute Centigrade)—say $f(T)$, and E for gases is reckoned from the same datum as that of steam in Callendar's Tables, namely 0° C., then

$$E_d = m_d.\int_{273}^{T_e} f(T).dT.$$

Similarly

$$E_g = m_g.\int_{273}^{T_g} \phi(T).dT, \quad \text{and} \quad E_a = m_a.\int_{273}^{T_a} \psi(T).dT,$$

where ${}_gC_v = \phi(T)$ and ${}_aC_v = \psi(T)$.

The term $\frac{P_g.V_g}{J}$ for the combustible gas and also $\frac{P_a.V_a}{J}$ for air can be estimated by direct measurement of pressure and volume, and for the dry exhaust gas $\frac{P_d.V_d}{J}$ can be estimated from results of the chemical analysis of exhaust gas; or the terms can be replaced by the substitution $\frac{R.m.T}{J}$ with the appropriate suffixes.

Thus $(H_0 - H_i)$ becomes

$$\left\{ m_d.\left[\int_{273}^{T_e} f(T).dT + \frac{R_d.T_e}{J}\right] + m_s.[S'.(T_e - T_s) + L + h] \right\}$$
$$- \left\{ m_g.\left[\int_{273}^{T_g} \phi(T).dT + \frac{R_g.T_g}{J}\right] + m_a.\left[\int_{273}^{T_a} \psi(T).dT + \frac{R_a.T_a}{J}\right] \right\}$$
$$= \left\{ m_d.\int_{273}^{T_e} f(T).dT - m_g\int_{273}^{T_g} \phi(T).dT - m_a.\int_{273}^{T_a} \psi(T).dT \right\}$$
$$+ \left\{ \frac{1}{J}(m_d.R_d.T_e - m_g.R_g.T_g - m_a.R_a.T_a) \right\}$$
$$+ \left\{ m_s.[S'.(T_e - T_s) + L + h] \right\}.$$

Since the temperatures, T_g, T_a, and T_e, and the quantities of gas and air (m_g and m_a) can be obtained by direct measurement, and $m_g+m_a=m_d+m_s$, the numerical values of the three integrals can be found when the functions $f(T)$, $\phi(T)$, and ψ (T), giving the laws of variation of specific heat at constant volume with temperature for the respective gases, are known. The terms within the second set of brackets can be found numerically when the constants R_d, R_g, and R_a for the respective gases are known. These constants can be found from gas analyses and Dalton's law of partial pressures, which results in

$$R_d=\frac{m_1R_1+m_2R_2+m_3R_3+\dots}{m_d}=\frac{\Sigma mR}{\Sigma m}$$

for the dry exhaust gas, and similarly for the combustible gas and air.

The term in the third set of brackets representing the heat carried away by the superheated steam contained in the exhaust can be estimated by use of the Steam Tables and Dalton's law of partial pressures. For since the pressure P_e in the exhaust pipe of an engine is the sum of the pressures due to dry exhaust gas (P_d) and steam (P_s), then

$$P_s=P_e-P_d=P_e-\frac{m_d.R_d.T_e}{V_e},$$

where V_e represents the volume per second of the whole of the exhaust gases flowing along the exhaust pipe.

Thus P_s can be calculated; hence the values of h, L, and S′ can be taken from the Steam Tables and used in the formula for the steam term of the equation for (H_0-H_i).

An Approximation for (H_0-H_i).

If T_i, V_i, and P_i be estimated as the absolute temperature, volume per second, and pressure of the mixture at inlet, then

$$\begin{aligned}(H_0-H_i)&=(H_s+H_d)-H_i\\&=H_s+\left(E_d+\frac{P_d.V_d}{J}\right)-\left(E_i+\frac{P_i.V_i}{J}\right)\\&=m_s.[S'.(T_e-T_s)+L+h]\\&\qquad+m_d\times{}_dC_p\times T_e-m_i\times{}_iC_p\times T_i,\end{aligned}$$

where the absolute zero of temperature is taken as the datum from which E is measured and ${}_iC_p$ is assumed constant and equal to ${}_iC_v + \frac{R_i}{J}$ for the inlet mixture, and similarly for the dry exhaust gas.

Also, since $m_i = m_d + m_s$, the equation can be written

$$(H_0 - H_i) = m_s.[S'.(T_e - T_s) + L + h - {}_vC_p \times T] + m_d.[{}_nC_p.T_e - {}_iC_p.T_i].$$

Making now the approximations that the total heat (h) of water when reckoned from absolute zero of temperature is equal to the absolute saturation temperature (T_s), and ${}_iC_p$ for m_s is equal to unity at T_i, since at inlet temperature and pressure m_s would be water, and taking a mean $C_p = \frac{{}_dC_p.T_e - {}_iC_p.T_i}{T_e - T_i}$ for the dry products, the equation can finally be reduced to

$$(H_0 - H_i) = m_s.[S'.(T_e - T_s) + L + (T_s - T_i)] + m_d \times C_p \times (T_e - T_i).$$

The above approximations which result in this less cumbersome formula may be considered good enough for the purposes of calculation of $(H_0 - H_i)$ and within the limits of accuracy of the rest of the estimated quantities involved in the testing of internal combustion engines. Thus six of the quantities of the energy balance sheet of section II. can be estimated, and the seventh obtained by difference.

The Northampton Polytechnic,
London, E.C. 1.
Oct. 1938.

LXX. *The Approximate Prediction of Skin Friction and Lift.* *By* N. A. V. Piercy, *D.Sc.*, J. H. Preston, *Ph.D.*, *and* L. G. Whitehead, *B.Sc.**

[Received July 21, 1938.]

SUCCESS in eliminating computation by applying Helmholtz's method (Schaefer, 1910) of successive approximation to the flat plate case of skin friction

* Communicated by the Authors.

(Piercy and Preston, 1936) suggests its corresponding value in more complicated problems. The application now described is to the steady part of the flow at moderately high Reynolds numbers past cylinders. There exists a number of papers on this subject, recently analysed by Howarth (1934), but whilst the methods so far employed are convenient in some connexions, in others, *e. g.*, the calculation of the position of breakaway, they involve extensive numerical work which the treatment described below obviates. Errors remaining in approximate solutions of the kind now to be derived are difficult to investigate in general terms—a common deterrent to the use of Helmholtz's method which possibly accounts for its comparative neglect in hydrodynamics. Comparison with existing solutions suggests, however, that convergence is rapid.

The formulation of the method and its application to certain problems of interest occupy the first two sections of the paper. New boundary layer equations are obtained which offer advantages in particular circumstances. For any special solution an additional assumption is necessary, as is well known, besides that of the existence of a boundary layer ; the assumption usually adopted, to avoid appeal to experiment, is that the flow exterior to the boundary layer accords with irrotational flow past the profile concerned, and this practice is followed in Section II. in order to facilitate comparison with other methods. But it is familiar that calculation diverges considerably in these circumstances from experiment, and a development of the theory, with a view to securing greater physical accuracy, is considered in Section III. The important corrections that follow are illustrated in detail for the circular cylinder and also for an elliptic cylinder whose boundary layer has been studied closely with the aid of experiment by Schubauer (1935) and others.

This development makes possible a further step described in Section IV. By taking some account of the existence of a wake it enables the circulation round a lifting cylinder to be estimated much more reliably from Betz's criterion than has formerly been possible. As an illustration the lift and stall are calculated of an elliptic cylinder which has formed the subject of wind tunnel tests at the National Physical Laboratory.

Section I.

Transformation of Exact Equations.—We begin by transforming the general equations for steady viscous flow in two dimensions,

$$\left.\begin{aligned} u\frac{\partial u}{\partial x}+v\frac{\partial u}{\partial y} &= -\frac{1}{\rho}\frac{\partial p}{\partial x}+\nu\nabla^2 u, \\ u\frac{\partial v}{\partial x}+v\frac{\partial v}{\partial y} &= -\frac{1}{\rho}\frac{\partial p}{\partial y}+\nu\nabla^2 v, \end{aligned}\right\} \quad . \quad . \quad . \quad . \quad (1)$$

to the coordinates α and β, the velocity potential and stream function respectively of potential flow past a cylinder defined by $\beta=0$, obtaining

$$\left.\begin{aligned} &\bar{q}\frac{\partial \bar{q}}{\partial \alpha}+\bar{w}\frac{\partial \bar{q}}{\partial \beta}+\frac{1}{\bar{h}}\frac{\partial \bar{h}}{\partial \alpha}(\bar{q}^2+\bar{w}^2) \\ &\quad =-\frac{1}{\rho \bar{h}^2}\frac{\partial p}{\partial \alpha}+\nu\left\{\nabla^2\bar{q}-\frac{2}{\bar{h}}\frac{\partial \bar{h}}{\partial \beta}\left(\frac{\partial \bar{w}}{\partial \alpha}-\frac{\partial \bar{q}}{\partial \beta}\right)\right\} \\ &\bar{q}\frac{\partial \bar{w}}{\partial \alpha}+\bar{w}\frac{\partial \bar{w}}{\partial \beta}+\frac{1}{\bar{h}}\frac{\partial \bar{h}}{\partial \beta}(\bar{q}^2+\bar{w}^2) \\ &\quad =-\frac{1}{\rho \bar{h}^2}\frac{\partial p}{\partial \beta}+\nu\left\{\nabla^2\bar{w}+\frac{2}{\bar{h}}\frac{\partial \bar{h}}{\partial \alpha}\left(\frac{\partial \bar{w}}{\partial \alpha}-\frac{\partial \bar{q}}{\partial \beta}\right)\right\}, \end{aligned}\right\} \quad . \quad (2)$$

$\bar{q}, \bar{w}$ being the component velocities at any point $W=\alpha+i\beta$ expressed in terms of h, the "velocity of the transformation," given by

$$h^2=\left|\frac{dW}{dz}\right|^2=\left(\frac{\partial \alpha}{\partial x}\right)^2+\left(\frac{\partial \alpha}{\partial y}\right)^2=\left(\frac{\partial \beta}{\partial x}\right)^2+\left(\frac{\partial \beta}{\partial y}\right)^2, \quad (3)$$

i. e., $\bar{q}=q/h$, etc. The equation of continuity becomes

$$\frac{\partial \bar{q}}{\partial \alpha}+\frac{\partial \bar{w}}{\partial \beta}=0. \quad . \quad . \quad . \quad . \quad . \quad (4)$$

These expressions are consistent with the corresponding equation for ψ given by Southwell and Squire (1933), and are exact. The original boundary conditions $u=0=v$ on the cylinder and $u=U, v=0$ at ∞ become in the new system $\bar{q}=0=\bar{w}$ on the cylinder and $\bar{q}=1, \bar{w}=0$ at ∞.

Boundary Layer Equations.—On examining orders of terms on the assumption that viscous effects are confined to a thin boundary layer enveloping the cylinder equations (2) reduce to

$$\bar{q}\frac{\partial \bar{q}}{\partial \alpha}+\bar{w}\frac{\partial \bar{q}}{\partial \beta}+\bar{q}^2\frac{1}{\bar{h}}\frac{\partial \bar{h}}{\partial \alpha}=-\frac{1}{\rho \bar{h}^2}\frac{\partial p}{\partial \alpha}+\nu\frac{\partial^2 \bar{q}}{\partial \beta^2}, \quad . \quad (5)$$

$$\bar{q}^2 \frac{1}{\bar{h}} \frac{\partial \bar{h}}{\partial \bar{\beta}} = -\frac{1}{\rho \bar{h}^2} \frac{\partial \bar{p}}{\partial \bar{\beta}} . \quad . \quad . \quad . \quad . \quad . \quad (6)$$

In the limit the second of these becomes $\partial p/\partial \beta = 0$, but the above form permits continuous passage, if desired, from conditions at the boundary to those at ∞. No assumption as to small curvature has been necessary, and α, β may refer to acyclic or cyclic flow. Thus the expressions may possibly be preferable to Prandtl's well-known equations when the boundary layer is rather thick, *i. e.*, at intermediate Reynolds numbers, or is sharply curved.

When the boundary layer is vanishingly thin (5) becomes

$$\bar{q} \frac{\partial \bar{q}}{\partial \bar{\alpha}} + \bar{w} \frac{\partial \bar{q}}{\partial \bar{\beta}} = (1 - \bar{q}^2) \left[\frac{1}{\bar{h}} \frac{\partial \bar{h}}{\partial \bar{\alpha}} \right]_{\beta = 0} + \nu \frac{\partial^2 \bar{q}}{\partial \bar{\beta}^2} . \quad . \quad (7)$$

We have for clearness referred α, β to the irrotational flow past the cylinder whose boundary layer flow is to be calculated, but it is important to note that actually no restriction exists to this choice.

Approximate Solution for Thin Boundary Layers.—A previous utility of the method of successive approximation in the limiting case of the flat plate suggests its adoption in this more general problem. The procedure is at once seen by writing (7) in the form

$$\bar{q}_{n-1} \frac{\partial \bar{q}_n}{\partial \bar{\alpha}} + \bar{w}_{n-1} \frac{\partial \bar{q}_n}{\partial \bar{\beta}} = (1 - \bar{q}_{n-1}^2) \left[\frac{1}{\bar{h}} \frac{\partial \bar{h}}{\partial \bar{\alpha}} \right]_{\beta = 0} + \nu \frac{\partial^2 \bar{q}_n}{\partial \bar{\beta}^2} , \quad (8)$$

and regarding the result as an equation for determining $\bar{q}_n$ and $\bar{w}_n$ from inferior approximations $\bar{q}_{n-1}$, $\bar{w}_{n-1}$ which satisfy the equation of continuity.

The first approximation assumes for $\bar{q}_1$, $\bar{w}_1$ values appropriate to wholly irrotational flow, *i. e.*, 1 and 0, respectively, when (8) becomes

$$\frac{\partial \bar{q}_2}{\partial \bar{\alpha}} = \nu \frac{\partial^2 \bar{q}_2}{\partial \bar{\beta}^2} , \quad . \quad . \quad . \quad . \quad . \quad . \quad (9)$$

an equation of the same form as was obtained in a similar manner for the corresponding step in the case of the flat plate.

To deal with (9) and subsequent approximations, it is convenient to change to the variables ξ, η, defined by

$$\xi = \left[\frac{\beta^2}{4\nu(\alpha - \alpha_1)} \right]^{\frac{1}{2}} , \quad \eta = \frac{\alpha - \alpha_1}{\alpha_2 - \alpha_1} , \quad . \quad . \quad (10)$$

where α_1, α_2 are the coordinates of the front and back stagnation points respectively. Now for the second approximation it will be shown that

$$\eta . \partial\bar{q}/\partial\eta = 0, \quad . \quad . \quad . \quad . \quad . \quad . \quad (11)$$

and terms involving the left-hand side of (11) may be neglected in the third approximation, which is sufficiently accurate for some purposes. (11) is therefore assumed in the following " first method " of solution.

First Method.—Assuming (11) and with the notation

$$\phi(\eta) \equiv 4(\alpha_2 - \alpha_1)\left[\frac{1}{\bar{h}}\frac{\partial h}{\partial \alpha}\right]_{\beta=0} . \eta, \quad . \quad . \quad . \quad (12)$$

(8) becomes in the new coordinates

$$\left[-2\xi\bar{q}_{n-1} + 2\bar{w}_{n-1}\left(\frac{\alpha_2 - \alpha_1}{\nu}\eta\right)^{\frac{1}{2}}\right]\frac{\partial \bar{q}_n}{\partial \xi}$$
$$= (1 - \bar{q}_{n-1}^2)\phi(\eta) + \frac{\partial^2 \bar{q}_n}{\partial \xi^2}, \quad . \quad . \quad (13)$$

and the equation of continuity

$$-\xi\frac{\partial \bar{q}_{n-1}}{\partial \xi} + \left(\frac{\alpha - \alpha_1}{\nu}\right)^{\frac{1}{2}}\frac{\partial \bar{w}_{n-1}}{\partial \xi} = 0. \quad . \quad . \quad (14)$$

Integrating (14), making use of the boundary conditions, and substituting in (13), gives

$$\frac{\partial^2 \bar{q}_n}{\partial \xi^2} + 2\int_0^\xi \bar{q}_{n-1} d\xi . \frac{\partial \bar{q}_n}{\partial \xi} = -(1 - \bar{q}_{n-1}^2)\phi(\eta). \quad . \quad (15)$$

It is convenient to write

$$I_n \equiv 2\int_0^\xi \int_0^\xi \bar{q}_n d\xi d\xi. \quad . \quad . \quad . \quad . \quad . \quad (16)$$

Multiplying (15) through by $e^{I_n - 1}$, and integrating twice, gives

$$\bar{q}_n = -\phi(\eta)\int_0^\xi e^{-I_n - 1}\int_0^\xi (1 - \bar{q}_{n-1}^2)e^{I_n - 1} d\xi d\xi$$
$$+ A_n \int_0^\xi e^{-I_n - 1} d\xi + C_n, \quad . \quad . \quad (17)$$

and the boundary conditions yield $C_n = 0$ and

$$A_n = \frac{1 + \phi(\eta)\int_0^\infty e^{-I_n - 1}\int_0^\xi (1 - \bar{q}_{n-1}^2)e^{I_n - 1} d\xi d\xi}{\int_0^\infty e^{-I_n - 1} d\xi} \quad . \quad (18)$$

In this solution we have immediately for the second approximation

$$A_2 = 1 \Big/ \int_0^\infty e^{-\xi^2} d\xi = 2/\sqrt{\pi}, \quad . \quad . \quad . \quad . \quad (19)$$

$$\bar{q}_2 = A_2 \int_0^\xi e^{-\xi^2} d\xi = \mathrm{erf}\,(\xi). \quad . \quad . \quad . \quad . \quad (20)$$

The denominator in the expression for A_3 has the numerical value 1·3212, whence with little further computation (18) gives for the third approximation

$$A_3 = 0{\cdot}7569 + 0{\cdot}5455\ \phi(\eta). \quad . \quad . \quad . \quad . \quad (21)$$

Fig. 1.

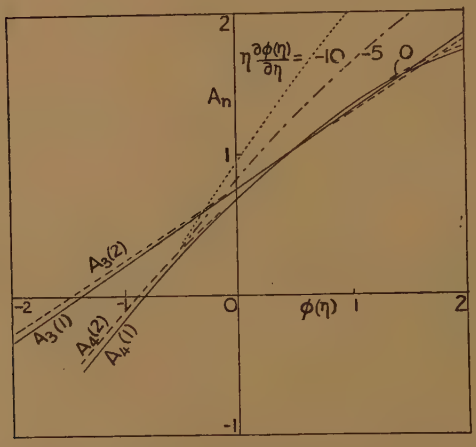

So far the computation required has been negligible, and evidence will be advanced later to show that (21) achieves considerable accuracy. It is of interest, however, to proceed to the fourth approximation, and the numerical work then increases. Values of $\bar{q}_3$ are required for $\xi = 0$ to 4. These have been calculated from (17) with the help of (21), and lead through (18) to the full line curve for A_4 marked $A_4(1)$ in fig. 1. The linear variation of A_3 with $\phi(\eta)$ according to the present solution is also shown as a full line in the figure and is marked $A_3(1)$. These curves are, of course, applicable to any cylinder.

It is by no means clear, however, that the terms involving $\partial\bar{q}/\partial\eta$ can be neglected without appreciable error in the fourth approximation. They can be included

in an extension of the above solution, but only at the expense of excessive computation, and a " second method " of approximation, as follows, becomes more convenient. Converging somewhat less rapidly than the first method, this yields a slightly less accurate expression for A_3; its advantage is associated with higher approximations.

Second Method.—In addition to the change of variables (10), we now make the substitution

$$q' = \bar{q} + 1, \quad . \quad . \quad . \quad . \quad . \quad . \quad (22)$$

and, avoiding the assumption (11), obtain in place of (13)

$$\frac{1}{2}\frac{\partial^2 q'_n}{\partial \xi^2} + \xi \frac{\partial q'_n}{\partial \xi} + \left[q'_{n-1}\xi - \bar{w}_{n-1} \left(\frac{\alpha_2 - \alpha_1}{\nu} \eta \right)^{\frac{1}{3}} \right] \frac{\partial q'_{n-1}}{\partial \xi}$$

$$-2(1+q'_{n-1})\eta \frac{\partial q'_{n-1}}{\partial \eta} = \tfrac{1}{2}\phi(\eta)[(1+q'_{n-1})^2 - 1], \quad (23)$$

and from the equation of continuity

$$\bar{w}_{n-1} = \left(\frac{\alpha - \alpha_1}{4\nu} \right)^{-\frac{1}{3}} \left(\frac{1}{2} \int \xi \frac{\partial q'_{n-1}}{\partial \xi} d\xi - \eta \int \frac{\partial q'_{n-1}}{\partial \eta} d\xi \right). \quad (24)$$

Substituting from (24) in (23), and integrating twice, gives

$$1 + q'_n = \frac{\sqrt{\pi}}{2} A_n \operatorname{erf}(\xi) - \int_0^\xi e^{-\xi^2} \int_0^\xi e^{\xi^2} . f(\xi, \eta)\, d\xi\, d\xi, \quad (25)$$

where

$$f(\xi, \eta) = 2 \frac{\partial q'_{n-1}}{\partial \xi} \left(\int q'_{n-1} d\xi + 2\eta \int \frac{\partial q'_{n-1}}{\partial \eta} d\xi \right)$$

$$-\phi(\eta)[(1+q'_{n-1})^2 - 1] - 4(1+q'_{n-1})\eta \frac{\partial q'_{n-1}}{\partial \eta}. \quad (26)$$

Finally, use of the boundary conditions yields

$$A_n = \frac{2}{\sqrt{\pi}} + \int_0^\infty e^{\xi^2} (1 - \operatorname{erf} \xi) . f(\xi, \eta) d\xi. \quad . \quad (27)$$

The second approximation is identical with that obtained by the first method of solution, *cf.* (19) and (20). Thus $\partial q_2'/\partial \eta = 0$ and (26) greatly simplifies for the third approximation, for which only one integral requires numerical evaluation. We obtain

$$A_3 = \frac{2}{\sqrt{\pi}} \left(1 - \frac{1}{\pi} \right) + 0{\cdot}52497\phi(\eta) \quad . \quad . \quad . \quad (28)$$

to compare with (21). This result is exhibited in fig. 1 as the dotted line marked $A_3(2)$.

Proceeding to the fourth approximation, values of q_3' are readily calculated with the help of (28) through the required range of ξ (0 to 4), giving for each value of ξ a linear variation with $\phi(\eta)$, and values of $\partial q'_3 d\xi$ and $\frac{\partial q'_3}{\partial \xi}$ follow. Then evaluating the integrals in the relationship

$$\frac{\partial q'_3}{\partial \eta} = \frac{\partial \phi(\eta)}{\partial \eta}\left\{\frac{\sqrt{\pi}}{2}\operatorname{erf}(\xi)\int_0^\infty e^{-\xi^2}\int_0^\xi e^{\xi^2}[1-(1+q_2')^2]\,d\xi\,d\xi - \int_0^\xi e^{-\xi^2}\int_0^\xi e^{\xi^2}[1-(1+q'_3)^2]\,d\xi\,d\xi, \quad . \quad (29)\right.$$

and collecting terms, we find for the fourth approximation

$$\frac{\sqrt{\pi}}{2}A_4 = 0{\cdot}6121 + 0{\cdot}6230\phi(\eta) - 0{\cdot}0694[\phi(\eta)]^2 - 0{\cdot}00673\,[\phi(\eta)]^3 - 4\eta\frac{\partial\phi(\eta)}{\partial\eta}[0{\cdot}00525 + 0{\cdot}01076\phi(\eta)]. \quad . \quad . \quad . \quad (30)$$

This second result for A_4 is first plotted with the last term zero as the dotted line curve marked $A_4(2)$ in fig. 1 for comparison with the first result $A_4(1)$. Two other dotted curves, for $\eta \cdot \partial\phi(\eta)/\partial\eta = -5$ and -10, exhibit the relative importance of the last term. We have not approximated further, as the numerical work, so far slight, would increase rapidly.

Skin Friction and Breakaway.—The intensity of skin friction is $\tau = -\mu\zeta_0$, the last symbol denoting the boundary value of the vorticity, and this gives

$$\tau_n = \mu\left[\frac{h^4}{4\nu(\alpha-\alpha_1)}\right]^{\frac{1}{3}}_{\beta=0} A_n. \quad . \quad . \quad . \quad . \quad (31)$$

Very simple formulæ result for the third approximation :

$$\tau_3 = \tau_2\left\{\begin{matrix}0{\cdot}6708\\0{\cdot}6817\end{matrix} + \begin{matrix}1{\cdot}9336\\1{\cdot}8608\end{matrix}\left[(\alpha-\alpha_1)\frac{1}{h}\frac{\partial h}{\partial\alpha}\right]_{\beta=0}\right\}, \quad (32)$$

the upper numbers being given by the first method and the lower by the second, whilst τ_2 follows immediately from (19) and (31). As already mentioned, the first solution to this approximation is to be preferred.

Breakaway is indicated by the skin friction vanishing. No position of breakaway occurs to the second approximation. To the third it is found by equating to zero the

expression within the curly brackets of (32), and so on for higher approximations. To the third and fourth approximations we can write shortly that for breakaway :—

$$\left.\begin{array}{ll} \text{(3rd)} & \phi(\eta) = -1{\cdot}3875 \text{ (1st method)} \\ & \quad \text{or } -1{\cdot}4654 \text{ (2nd method).} \\ \text{(4th)} & \phi(\eta) = -0{\cdot}823 \text{ (1st method).} \end{array}\right\} \quad . \quad (33)$$

A feature of the present method is the simple and direct means to determine breakaway, avoiding usually extensive computation to achieve even the accuracy now reached in the third approximation. The fourth approximation given by the first method is considered to be close because the terms neglected are unimportant in the present connexion. It may be remarked that the solution for breakaway along one side of particular cylindrical profiles is not, in some circumstances, unique ; in such cases the most upstream position of zero friction behind the front stagnation point is adopted.

Section II.

Comparison with other Methods.—The utility of the foregoing depends upon rapid convergence, so that the third or fourth approximation shall be sufficient. Investigation in general terms of the question of convergence appears to be complicated, and as an alternative we have effected comparisons with calculations by other authors in numerous special cases, covering a wide range of shape of profile. Three of these will now be described.

Following usual practice when no appeal is made to experiment, and permitting comparisons to be made directly, the flow outside the boundary layer is assumed in the present section to accord with irrotational flow past the cylinders considered. It is known that disagreement with experiment must ensue, but we are not here concerned with physical accuracy, steps towards which in *a priori* calculations are considered in subsequent sections.

Flat Plate.—An unfavourable case is provided by the flat plate. If R be the Reynolds number, τ_m the mean intensity of skin friction, and U the undisturbed velocity of a stream of fluid of density ρ, we find :—

TABLE I.—Flat Plate.

No. of approximation.		2.	3.	4.	∞.
$\frac{\tau_m R^{\frac{1}{2}}}{\rho U^2}$	1st method	1·1285	0·7569	0·687	0·664
	2nd method	,,	0·7692	0·6905	—

In this case $\partial\bar{q}/\partial\eta$ is always negligible. The errors in the fourth approximation are $3\frac{1}{2}$ and 4 per cent. respectively. It may be mentioned that the mean experimental value of the quantity calculated, for R = 14,000 to 200,000, is 0·70 (Fage, 1933).

Circular Cylinder.—From the potential function for a cylinder of radius a, viz., $W=\alpha+i\beta=U(z+a^2/z)$, where $z=x+iy$, it is found at once that

$$\frac{\tau_3(1)R^{\frac{1}{2}}}{\rho U^2}=2\left(\frac{2}{\pi}\right)^{\frac{1}{2}}0{\cdot}6708\,\frac{\sin^2\theta}{\cos\frac{1}{2}\theta}\left(1-1{\cdot}4413\,\frac{\cos\theta}{\sin^2\frac{1}{2}\theta}\right). \qquad (34)$$

Since $\eta=\frac{1}{2}(1+\cos\theta)$, we have

$$\phi(\eta)=-4\cos\theta/(1-\cos\theta)$$

and

$$\eta\,.\,\partial\phi(\eta)/\partial\eta=-4(1+\cos\theta)/(1-\cos\theta)^2,$$

whence, with the help of fig. 1, τ_4 can also be calculated quickly round the contour. Fig. 2 shows at (*a*) the right-hand side of (34); breakaway occurs at 105° from the front stagnation point according to this approximation. This simple expression gives a fair measure of agreement with the predictions of Falkner and Skan (1930), fig. 2 (*b*), and with values derived from Howarth's table, fig. 2 (*c*). But neither of these is suitable for predicting breakaway, the first for mathematical and the second for numerical reasons. τ_4 (1) is shown at (*d*) and τ_4 (2) at (*e*); the position of breakaway is seen to occur at 99°, approximately, from the front stagnation point according to the fourth approximation. It will also be noticed that the terms neglected in (18), but taken into account in (30), affect the solution over a considerable part of the contour, but only by 1° at breakaway. There remains little doubt that the mean of the latter solutions is close. Curves (*f*) and (*g*) are described later.

Elliptic Cylinders.—It is possible to obtain convenient formulæ for elliptic cylinders. For this purpose, since no confusion will arise, we employ ξ, η in their familiar connexion as denoting the elliptic coordinates related to x, y by $z=C\cosh t$, where $t=\xi+i\eta$. Then the flow past the ellipse $\xi=\xi_0$ is given by $W=CUe^{\xi_0}\cosh(t-t'_0)$, there

being no circulation since we assume the major axis to be parallel to the undisturbed stream, so that $\eta_0=0$.

On the boundary $\alpha=-CUe^{\xi_0}\cos\eta$ and h is given by

$$h_{\beta=0}=Ue^{\xi_0}\frac{\sin\eta}{(\cosh^2\xi_0-\cos^2\eta)^{\frac{1}{2}}},$$

whence

$$\frac{\tau_n R^{\frac{1}{2}}}{\rho U^2}=A_n e^{\frac{3}{2}\xi_0}\frac{\sin^2\eta}{\cosh^2\xi_0-\cos^2\eta}\left[\frac{\cosh\xi_0}{2(1+\cos\eta)}\right]^{\frac{1}{2}}. \quad (35)$$

Fig. 2.

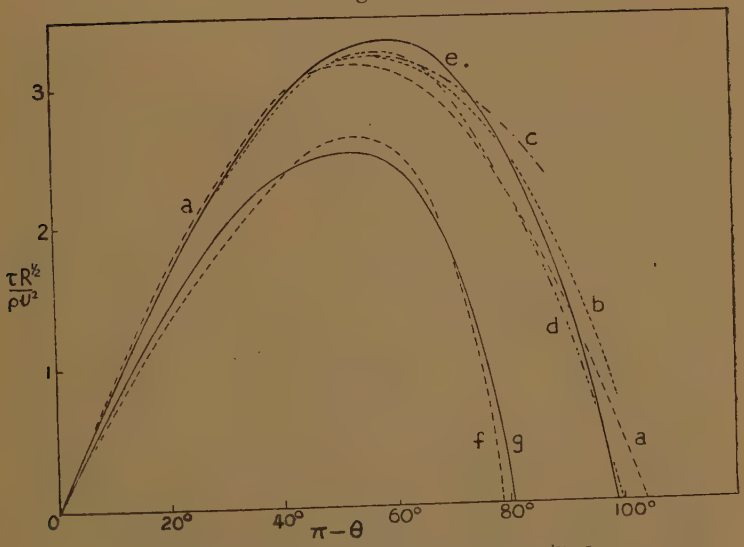

Distribution of skin friction for circular cylinder.

Present theory without wake correction :—

(*a*) Third approximation.

(*d*) Fourth approximation (first method).

(*e*) Fourth approximation (second method).

Present theory with wake correction :—

(*g*) Third approximation.

Other theories :—

(*b*) Falkner and Skan.

(*c*) From Howarth's table.

(*f*) Experimental ($R=1{\cdot}06\times10^5$).

For the third approximation by the first method of solution we have

$$A_3=0{\cdot}7569-2{\cdot}1818\,\frac{\cos\eta}{1-\cos\eta}\cdot\frac{\sinh^2\xi_0}{\cosh^2\xi_0-\cos^2\eta}. \quad (36)$$

Denoting by F the "fineness" of the section, *i. e.*, the ratio of its major to its minor axis, we note that $F=\coth \xi_0$, whence the variation of skin friction round any elliptic contour may be readily obtained. A calculation by Howarth for $F=6$ closely agrees with (36), as will be shown later.

Having sufficiently illustrated, it is hoped, the convenience and accuracy of the approximate solutions, we defer for brevity consideration of the fourth approximation for elliptic cylinders to the next section, where it can usefully be compared with experiment.

Section III.

Correction for Wake.—Although the foregoing approximations agree fairly with earlier solutions of the boundary layer equations, comparison with experiment would show serious discrepancies arising from the form assumed for the potential flow external to the boundary layer, which ignores the existence of a wake. There is, however, no restriction to this assumption. The potential function is more suitably determined as for an imaginary elongated boundary, consisting of the front part of the cylinder as far as the positions of breakaway together with the edges of an arbitrary wake joined thereto. This conception neglects various physical matters, amongst which may be mentioned the continual entry of streamlines into a real wake, which widens downstream by the diffusion of vorticity. An arbitrary thickness and configuration may be assigned to the elongation of the boundary since, except in the case of narrow cylinders, plausible variation affects the final solution in only a secondary manner.

The development involves a further system of successive approximation, which will now be described.

It is assumed that the original cylindrical contour (in the z-plane) can be transformed conformally to a circle. After such transformation to the t-plane of fig. 3 *a*, let A_1, B_1 represent the points corresponding to those of breakaway determined in the original plane by ignoring the wake, as already described. Let the elongation added take the form indicated so that in both planes the new boundary is continuous at A_1, B_1.

Flow past a boundary of this type is readily obtained by Joukowski's transformation, $t=s+a^2/s$, from that past

a boundary in the s-plane consisting of a sector of a circle together with streamlines branching from the singular points A, B (fig. 3 b). In the s-plane, therefore, AB must lie on the real axis of the transformation, and the origin O be so chosen that $OA=OB=a$.

Now an approximate solution in the s-plane can be obtained by modifying the potential function for flow past

Fig. 3 a.

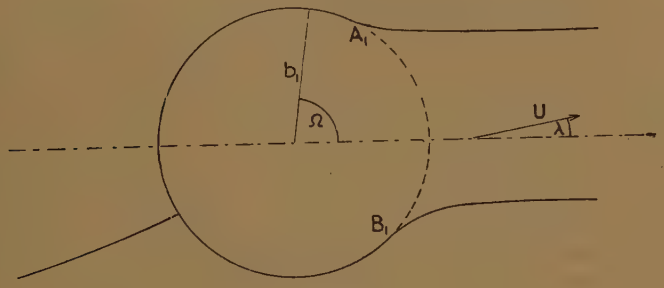

t-plane.

Fig. 3 b.

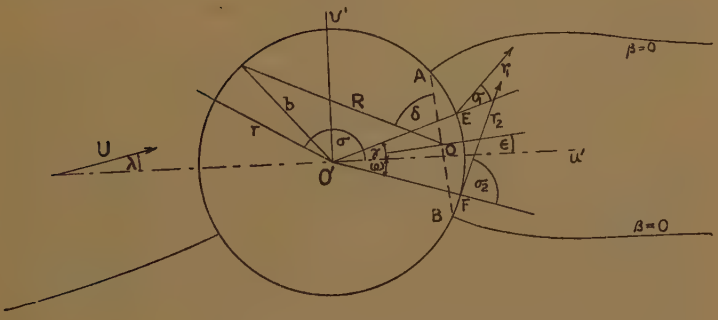

s-plane.

the circle without breakaway to include a number of sources in suitable positions behind the circle together with their image system. The simplest effective distribution consists of two sources located on the circle. Let these (E, F) be of strengths m_1 and m_2 and occupy the angular positions γ, ω, respectively (fig. 3 b). It is then easily found that in the general case with circulation K,

using the notation of the figure and referring to the axes $O'u'$, $O'v'$,

$$\alpha=U\left(r+\frac{b^2}{r}\right)\cos(\sigma-\lambda)-\frac{K}{2\pi}\sigma+\frac{m_1}{2\pi}\log\frac{r_1^2}{r}+\frac{m_2}{2\pi}\log\frac{r_2^2}{r}, \quad . \quad . \quad . \quad (37)$$

where $r_1^2=r^2+b^2-2br\cos(\sigma-\gamma)$, etc., and

$$\beta=U\left(r-\frac{b^2}{r}\right)\sin(\sigma-\lambda)+\frac{K}{2\pi}\log\frac{r}{b}+\frac{m_1}{2\pi}\left[2\sigma_1-(\sigma-\gamma+\pi)\right]$$
$$+\frac{m_2}{2\pi}[2\sigma_2-(\sigma-\omega+\pi)]. \quad . \quad (38)$$

Hence the tangential component of velocity is given by

$$q=-U\left(1+\frac{b^2}{r^2}\right)\sin(\sigma-\lambda)-\frac{K}{2\pi r}$$
$$+\frac{b}{\pi}\left[\frac{m_1\sin(\sigma-\gamma)}{r_1^2}+\frac{m_2\sin(\sigma-\omega)}{r_2^2}\right], \quad . \quad (39)$$

an expression which reduces on the circle to

$$q_{\beta=0}=-2U\sin(\sigma-\lambda)$$
$$+\frac{1}{2\pi b}\left(m_1\cot\frac{\sigma-\gamma}{2}+m_2\cot\frac{\sigma-\omega}{2}-K\right). \quad (40)$$

In proceeding to evaluate the skin friction at a point on the boundary in the z-plane it is convenient to continue to work in terms of the corresponding coordinates in the s-plane.

Considering the terms occurring in $\phi(\eta)$, $\alpha-\alpha_1$ follows immediately from (37). Also

$$\frac{1}{h}\frac{\partial h}{\partial\alpha}=\frac{1}{bq}\cdot\frac{1}{h}\frac{\partial h}{\partial\sigma}, \quad . \quad . \quad . \quad . \quad . \quad (41)$$

and since, still considering boundary values,

$$h=q\left|\frac{ds}{dt}\right|\cdot\left|\frac{dt}{dz}\right|,$$

$$\frac{1}{h}\frac{\partial h}{\partial\sigma}=\frac{1}{q}\frac{\partial q}{\partial\sigma}+\left|\frac{dt}{ds}\right|\cdot\frac{\partial}{\partial\sigma}\left|\frac{ds}{dt}\right|+\left|\frac{dz}{dt}\right|\frac{\partial}{\partial\sigma}\left|\frac{dt}{dz}\right|. \quad (42)$$

Certain terms in the last expression are common to all cases. From (40),

$$\frac{\partial q}{\partial \sigma} = -2U \cos(\sigma - \lambda)$$

$$- \frac{1}{4\pi b}\left(m_1 \operatorname{cosec}^2 \frac{\sigma-\gamma}{2} + m_2 \operatorname{cosec}^2 \frac{\sigma-\omega}{2}\right). \quad . \quad (43)$$

Also

$$\left|\frac{dt}{ds}\right| = \left\{ \left(1 - \frac{a^2}{R^2}\cos 2\delta\right)^2 + \left(\frac{a^2}{R^2}\sin 2\delta\right)^2 \right\}, \quad (44)$$

where, from fig. 3 *b*,

$$\cos\delta = \frac{b}{R}\sin(\sigma - \epsilon). \quad . \quad . \quad . \quad . \quad (45)$$

Again,

$$\frac{\partial}{\partial\sigma}\left|\frac{ds}{dt}\right| = -2\left|\frac{ds}{dt}\right|^3 \sin(\sigma-\epsilon)\left\{\frac{a^2 b\sqrt{b^2-a^2}}{R^4}\left(\cos 2\delta - \frac{a^2}{R^2}\right)\right.$$

$$\left. - \frac{2a^2b^2}{R^4}\left[\cos(\sigma-\epsilon) - \frac{b\sqrt{b^2-a^2}}{R^2}\sin^2(\sigma-\epsilon)\right]\right\}. \quad (46)$$

Finally, referring to fig. 3 *a*,

$$\frac{\cos\frac{1}{2}\Omega}{(\cos\sigma - \frac{1}{2}\Omega)} = \frac{\sqrt{b^2-a^2}}{b}. \quad . \quad . \quad . \quad (47)$$

Thus to evaluate (41) for a given case of motion in the z-plane, only two particular evaluations are required, viz.,

$$\left|\frac{dz}{dt}\right| \quad \text{and} \quad \frac{\partial}{\partial\sigma}\left|\frac{dt}{dz}\right|.$$

The modification leads to second approximations to the positions of breakaway, from which third approximations follow, and so on. Convergence is rapid, as will be illustrated.

Circular Cylinder.—The circular cylinder is especially simple because the t- and z-planes are identical, so that the skin friction may be calculated immediately from the foregoing expressions.

We have proceeded to the third approximation in calculating the modified external flow, on the assumption that the width of the wake close to the cylinder is equal to its diameter. The result is exhibited as the full line curve (*g*) of fig. 2. The dotted line curve (*f*) in that figure gives

the results of an experiment (Fage and Falkner, 1930) at the National Physical Laboratory on a cylinder of 15 cm. diameter at a Reynolds number of $1{\cdot}06\times10^5$, in which streamline flow could reasonably be expected as far as breakaway. Comparison of curve (*g*) with curve (*a*) of the same figure shows the importance of the correction now introduced, and with curve (*f*) the fair agreement with experiment. Fig. 4 shows at (*a*) the predicted pressure variation round the boundary, as modified from (*c*), that appropriate to potential flow past a circular cylinder, in comparison with (*b*) the

Fig. 4.

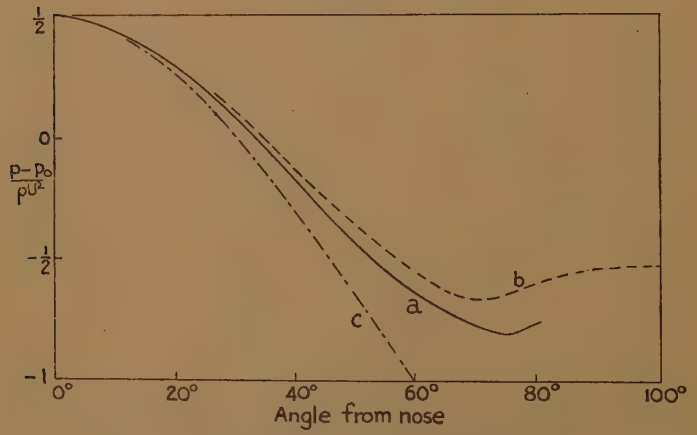

Pressure round circular cylinder.
(*a*) Present theory. (*b*) Experimental. (*c*) Potential flow.

measured values in the above test. Agreement could be improved by (1) using a higher approximation to the solution of the boundary layer equations, (2) proceeding to a higher approximation to the external flow, (3) adjusting the width of the wake. Step (1) will be illustrated shortly in the case of an elliptic cylinder; steps (2) and (3) may immediately be considered in relation to breakaway.

Breakaway is calculated directly by substitution in the expression, *cf.* (32),

$$1+2{\cdot}8826\left[(\alpha-\alpha_1)\frac{1}{\bar{h}}\frac{\partial h}{\partial\alpha}\right]_{\beta=0}=0.$$

The results obtained are given in the following table for various assumed widths of wake.

TABLE II.—Circular Cylinder.

Calculated Positions of Breakaway with Wake.

Approximation.	Width of wake/diameter of cylinder. 0·8	1·0	1·2
1st	—	105°	—
2nd	87°	85½	83½°
3rd	—	81½	—
Ultimate	—	79½	—

The table illustrates, firstly, that the process of adjusting the external flow is rapidly convergent, the third approximation being sufficiently accurate for most purposes; secondly, that variation of the width arbitrarily assigned to the wake in the vicinity of the cylinder affects the results to an unimportant extent. so that any plausible assumption is usually sufficient. We anticipate that the last remark may not apply to cylinders whose sections are very thin.

Elliptic cylinders.—The foregoing theory has also been applied to correct the breakaway predicted for elliptic cylinders. In fig. 5 the dotted curve follows from the common assumption that no wake exists; a single prediction on the same assumption, but calculated by a different method by Howarth (1935), marked 10 in the figure, is seen to be in close agreement, illustrating the mathematical accuracy achieved in the third approximation to the solution of the boundary layer equations. The chain-line curve represents the fourth approximation in the second method of solution, the wake still being ignored. Various experimental determinations of breakaway are reproduced and numbered in the figure. Observations 5, 7, and 9 by Parsons and Walker (1930) were obtained at the Reynolds numbers $2{\cdot}75$, $3{\cdot}26$, and $4{\cdot}06\times10^5$ respectively. Their fair agreement with the dotted curve is rather curious in that streamline flow presumably failed in the boundary layer before breakaway was reached. The Reynolds number for observation 3 (Fage and Falkner, 1930) was also rather high ($2{\cdot}12\times10^5$).

Observations 1 and 2 (Fage and Falkner) and 4, 6, and 8 (Parsons and Walker), however, were made at Reynolds numbers varying between $1{\cdot}06$ and $1{\cdot}80\times10^5$, and for these streamline flow is much more probable under the conditions of the experiments. This latter group all agree fairly with the full line of the figure, which is purely theoretical and represents the third approximation to the boundary layer equations with a wake of thickness equal to the distance between the points of breakaway (though any similar assumption regarding thickness would have given approximately the same result).

Fig. 5.

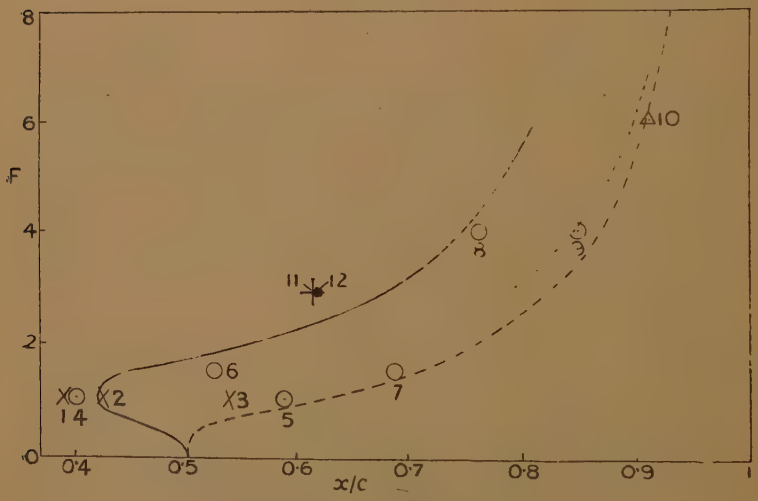

Breakaway for elliptic cylinders.

- - - Third approximation without wake.
— . — Fourth approximation without wake.
—— Third approximation with wake correction.

1–9 and 11. Experimental.
10. Howarth (calc.).
12. Fourth approximation with wake correction.

This simply determined full line curve may often be sufficiently accurate. But the single observation marked 11, made by Schubauer (1935) at the Reynolds number $0{\cdot}24\times10^5$, is believed to be reliable, whilst the theoretical estimate (marked 12) at the fineness ratio concerned according to the fourth approximation in the second method of solution with a wake assumed is in close

agreement. Thus proceeding to the fourth approximation will secure appreciably greater accuracy when this is required.

Schubauer's cylinder, having formed the subject of numerous investigations, provides a specially suitable case for detailed comparison, as follows.

In Table III. are collected estimates by various authors of the position of breakaway.

Fig. 6 relates to the same case. The curves are obtained by the present methods: (*a*) is the third and (*b*) the fourth approximation without a wake; (*c*) is the third and (*d*) the fourth approximation with a wake assumed.

TABLE III.—Elliptic Cylinder, F=2·96.

x/*c* for Breakaway as determined by Various Methods.

	Third approximation.		Fourth approximation.
Present method (potential flow without wake) ...	0·832	..	0·775
Doenhoff (1935), by Kármán and Millikan's method (potential flow without wake)	....	0·745	
Present method (with correction for wake)	0·682	..	0·620
Schubauer (direct observation)	....	0·614	
Howarth (1938) from experimental pressures)	....	0·592	
Doenhoff, as above (from experimental pressures).	....	0·590	

The points represent estimations of skin friction by Schubauer from the experimental pressures, using Polhausen's (1921) method, which fails just before breakaway is reached.

From the comparison it appears that the error in the fourth approximation to breakaway is < 5 per cent. and may be appreciably less, but it is also useful to note that the third approximation is sufficiently accurate for most purposes until breakaway is closely approached. As a final check on the latter conclusion we have calculated in this way the velocity distribution through the boundary layer at a position close behind the nose of the cylinder to compare with Schubauer's corresponding estimates from

the experimental pressures by Polhausen's method and also from direct observation. As will be seen from Table IV., where n denotes distance from the boundary, fair agreement is obtained.

Fig. 6.

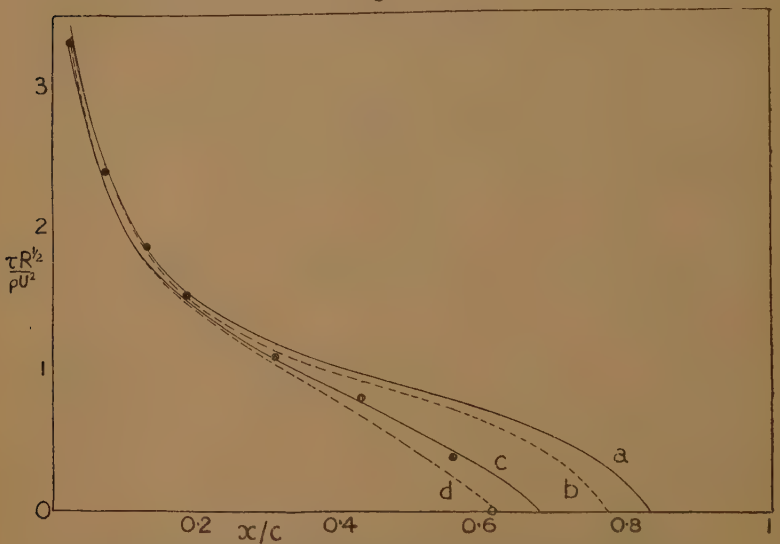

Distribution of skin friction for elliptic cylinder (F = 2·96).

(*a*) Third approximation present theory without wake corrections.
(*b*) Fourth " " " " " "
(*c*) Third " " " with " "
(*d*) Fourth " " " " " "
● Schubauer's calculations from the experimental pressures.
⊙ Schubauer's observation of breakaway at $R = 0{\cdot}24 \times 10^6$.

Table IV.—Elliptic Cylinder.
Variation of q with n for $x/c = 0{\cdot}0256$.

$n\sqrt{R}$.	Present method (third approximation).	Schubauer. From experimental pressures by Polhausen's method.	Schubauer. Observed.
0·175	0·3163	0·3144	0·275
0·345	0·5543	0·5534	0·498
0·495	0·7104	0·7141	0·673
0·660	0·8306	0·8419	0·799
0·815	0·9046	0·9275	0·892
1·09	0·9715	0·9889	0·996

The observations as given are subject to small error through their having been read from curves; those referring to positions close to the boundary are also subject to error of an experimental nature.

Section IV.

The positions of breakaway on a cylinder at velocity U about which a known circulation K exists can immediately be calculated by the methods already developed. Thus the solution for a lifting cylinder reduces to the problem of determining K.

For this purpose Howarth (1935) proposed that K be so determined as to give equal velocities (U′) outside the boundary layer at the two points of breakaway. This criterion was deduced by applying a well-known theorem of Betz, viz., that the flux of vorticity across any normal section of the boundary layer is proportional to U'^2, to the experimental fact that equal time-average vorticity is transported into the wake from the two sides of the cylinder. The deduction neglects, however, unequal contributions of vorticity to the wake from the parts of the two sides of the cylinder which are behind the positions of breakaway, which may possibly account for predictions of lift being at variance with observations; indeed, U′ and consequently the pressure, are found in experiment to differ at the two points of breakaway.

A different criterion is now advanced, whose basis is as follows. Considering an inclined cylinder whose boundary is arbitrarily extended downstream as in Section III., the extension can, from considerations of momentum, represent a wake only if it exert no force or moment. Consequently the pressures and velocities on opposite sides of the boundary-elongation representing the wake must be equal at each normal, This criterion is closely related to the requirement, studied by G. I. Taylor (1925), that the circulation round any circuit enclosing the wake only and cutting it approximately at right-angles must be zero. It can be applied in circumstances where that described above could not be satisfied, *e. g.*, in the case of a cylinder with a sharp trailing edge which is closely approached by one of the points of breakaway, as some aeroplane wings.

The new criterion is conveniently applied in the following manner, assuming for simplicity that two sources give a

sufficient approximation to the wake. Let AB, CD (fig. 7) be the intercepts of two normals (we have usually located these at distances c and $2c$, respectively, behind the cylinder, c being the maximum length of its section).

Five unknowns occur :—m_1, m_2, γ, ω, and K. These are completely determined by the following conditions :—

the thickness assigned to the wake ;
zero velocities at the two points of breakaway ;
equal velocities at A, B, and at C, D.

The resulting equations, which are complicated in the real plane, are solved conveniently by trial and error, as follows. A plausible value of K being assumed, first approximations to the points of breakaway are obtained as described in Sections I. and II. The boundary

Fig. 7.

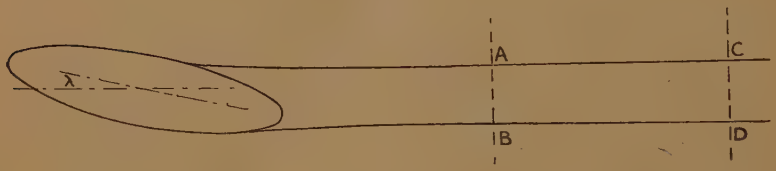

is then elongated to represent a wake, and the thickness arbitrarily assigned to this elongation (which we have usually taken as equal to the projection downstream of the distance between the points of breakaway) determines the value of m_1+m_2. With the notation of figs. 3 *b* and 6, a relation between m_1, m_2, γ, and ω, appropriate to the assumed value of K, then follows from the equations :

$$\left.\begin{aligned} &m_1+m_2=\text{const.},\\ &0=-2U\sin(\sigma_A-\lambda)-\frac{K}{2\pi b}\\ &\qquad+\frac{m_1}{2\pi_b}\cot\frac{\sigma_A-\gamma}{2}+\frac{m_2}{2\pi_b}\cot\frac{\sigma_A-\omega}{2}, \end{aligned}\right\} \quad (48)$$

together with an equation similar to the last with σ_B written for σ_A. By trial and error actual values can readily be found for the four unknowns which will make $q_A=q_B$. This condition can be satisfied for any value of K. But a particular value of K will also make $q_C=q_D$, and this

unique value, which is the circulation required, is determined by adjustment.

Finally, the lift L of unit axial length of the cylinder is given by the well-known expression : $L=\rho UK$. We shall employ the non-dimensional coefficient of lift K/Uc, c as before being the length of the section.

Inclined Elliptic Cylinder.—In order to facilitate comparison with experiment, the foregoing will now be applied to an elliptic cylinder of fineness ratio 5·4.

We first illustrate, without carrying the calculations to a high approximation, the effect of varying the thickness assumed for the wake, the cylinder being set with its

Fig. 8.

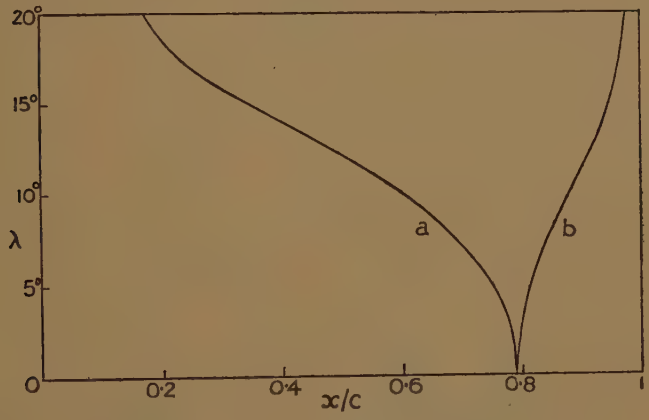

Variation of breakaway with inclination of major axis to stream for elliptic cylinder (F=5·4).
(*a*) Upper surface. (*b*) Lower surface.

major axis inclined at 12° to the undisturbed stream. We find :—

Wake thickness in terms of projected distance between points of breakaway	0·75	1·00	1·25
K/Uc	0·43	0·42	0·40

Thus the effect of varying this thickness is of secondary importance ; that appropriate to the middle column of the table is arbitrarily adopted.

Fig. 8 shows at (*a*) and (*b*) the tracks of the points of breakaway on the upper surface (that facing in the direction of lift) and the lower surface, respectively, of the

cylinder as the inclination λ of the major axis varies between 0° and 20°. This result is to the third approximation, and the positions are thus a little too far back, but the error is neglected.

Finally, fig. 9 gives at (*a*) the lift curve predicted without appeal to experiment. The curve (*b*) in this figure gives the results of experiment (Fage, 1927) at the National Physical Laboratory with an elliptic cylinder of the proportions chosen, tested under approximately two-dimensional conditions at the Reynolds number $1{\cdot}7 \times 10^5$. Differences between prediction and observation amount to about 15 per cent. with $\lambda < 12°$, and are thought to be due in part to turbulence occurring in the boundary

Fig. 9.

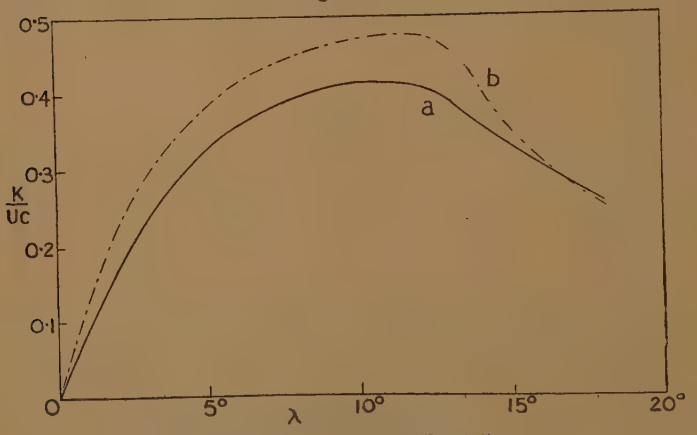

Lift of elliptic cylinder (F = 5·4).
(*a*) Present theory. (*b*) Experimental.

layer a little before breakaway in the experiment. The observed "stall," when lift begins to decrease with increase of λ, is predicted with some accuracy.

The authors are indebted to Mr. E. F. Relf for a valuable scientific suggestion. They also have pleasure in acknowledging a grant from the Department of Scientific and Industrial Research.

Conclusions.

The method of successive approximation previously developed for the flat plate case of skin friction with laminar flow can be generalized to yield a close approxima-

tion to that round the contours of cylinders appropriate to any analytical assumption regarding the irrotational flow outside their boundary layers. Computation is almost eliminated till the stage is reached when mathematical errors become small. A simple third approximation to the solution of the boundary layer equations suffices for many purposes until breakaway is approached. Explicit approximate formulæ follow for the position of breakaway and for the skin friction of elliptic cylinders.

Regarding the external flow, an appropriate assumption is obtained by recognizing the existence of a wake to the extent of elongating the cylindrical boundary from the points of breakaway to infinity. A rapidly convergent method of successive approximation is developed for its application. Any reasonable assumption regarding the thickness and configuration of this rudimentary wake secures, it appears, much closer agreement with experiment than has so far been possible by ignoring the wake.

Determining the circulation round a lifting cylinder from considerations relating to the artificial wake rather than to the points of breakaway considerably decreases earlier divergence from experiment. As an illustration, the variation of lift with inclination of section is calculated from first principles for a given elliptic cylinder, and the result is found to agree fairly with experiment, the "stall," in particular, being predicted with some accuracy.

Compared with earlier methods, those now advanced promise improved physical accuracy in predictions of skin friction, breakaway, lift, and stall which make no appeal to experimental data. Their analytical convenience will, it is hoped, facilitate investigations of associated problems for which an exceptional degree of mathematical accuracy may not be required.

References.

Doenhoff, Nat. Adv. Ctte. Aero., Tech. Note no. 544 (1935).
Fage, Aero. Res. Cttee., R. and M. no. 1097 (1927); no. 1580 (1933).
Fage and Falkner, Aero. Res. Cttee., R. and M. no. 1369 (1930).
Falkner and Skan, Aero. Res. Cttee., R. and M. no. 1314 (1930).
Howarth, Aero. Res. Cttee., R. and M. no. 1632 (1934); Proc. Roy. Soc. A, cxlix. p. 558 (1935); clxiv. p. 547 (1938).
Parsons and Walker, Nat. Adv. Cttee. Aero., Tech. Note no. 354 (1930).
Piercy and Preston, Phil. Mag. p. 995 (1936).
Polhausen, *Z. A. M. M.* i. p. 261 (1921).
Schaefer, *Ann. der Phys.* p. 33 (1910).
Schubauer, Nat. Adv. Cttee. Aero., Report no. 527 (1935).
Southwell and Squire, Phil. Trans. Roy. Soc. A, ccxxxii. p. 27 (1933).
Taylor, G. I., Phil. Trans. Roy. Soc. A, ccxxv. p. 238 (1925).

LXXI. *The Determination of the Rigidity Modulus of Nickel and some of its Alloys in the Annealed and Unannealed States.*

By D. H. Landon, *B.Sc., and* R. M. Davies, *D.Sc., University College of Wales, Aberystwyth* *.

[Received August 5, 1938.]

Contents.

	Page
I. Introduction	816
II. Theory	818
III. General Discussion of the Apparatus and the Method	821
IV. Experimental Arrangements	824
V. Experimental Procedure	827
VI. The Substances investigated	829
VII. Results	831
VIII. Possible Errors in the Quantities measured and the Effect on the Final Result	887
IX. Comparison with the Results of previous Investigations	839
X. References	840

I. *Introduction.*

THE aim of the work described in the present paper is to determine the rigidity modulus, at room-temperature, of various types of metals and alloys.

The methods available for the determination of the elastic constants are of two types—statical and dynamical methods. In the case of Young's modulus it has been shown in previous papers [(1), (2)] from this laboratory that on general grounds dynamical methods are considerably superior to statical methods both as regards accuracy and convenience. Further, it has been demonstrated that a dynamical method possesses advantages in the case of ferromagnetic substances and also in the case of annealed alloys which are " soft " and imperfectly elastic. For similar reasons it was decided to determine the rigidity modulus dynamically rather than statically.

A dynamical method of determining an elastic modulus consists essentially in determining the natural frequency or pulsatance ($=2\pi\times$frequency) of vibration of an unloaded or a loaded bar, the type of vibration being such that it involves stresses and strains corresponding to the modulus which is to be determined. Once this frequency has been determined the elastic modulus

* Communicated by the Authors.

can generally be calculated from the density of the bar and its dimensions, together with the corresponding quantities for the load. When determining the rigidity modulus a torsional vibration is clearly the appropriate type, and for reasons to be discussed later it was decided to use bars of rectangular cross-section in the present work.

In the determination of the frequency of vibration two methods are available :—

(i.) Using the natural, damped vibration of the bar.

(ii.) Setting the bar in forced vibration and determining the frequency corresponding to maximum amplitude.

The first method has been used with notable success, particularly by Goens [5], but for the present work it has the disadvantage that the duration of vibration is short, more especially with the " soft " alloys, and this makes the determination of the frequency difficult.

The second method avoids this difficulty, particularly when the forced vibrations are excited magnetically by the action of superposed steady and alternating magnetic fields on an armature attached to one end of the bar, the other end being clamped. The magnetic method of excitation has a further advantage—the alternating driving field is produced by an alternating current, and the frequency can thus be determined by some form of frequency bridge. For these reasons this method was adopted in the present work.

In the present case, since the vibrations to be excited are torsional vibrations, the armature must be subjected to an alternating couple about the axis of the bar. This couple is produced, as shown in Section III., by subjecting the ends of the armature to the action of equal and opposite alternating magnetic fields superposed on steady fields. The bar is thus set into forced torsional vibration with a pulsatance equal to that of the alternating driving field ; by varying this pulsatance it is possible to determine the apparent resonance pulsatance, ω_r, which corresponds to the maximum amplitude of the forced vibration. By an argument similar to that given in papers by Davies and James [1] it can be shown that, on account of the interaction between the armature and the magnetic fields, ω_r will not in general be equal to the true natural pulsatance, ω_0, in the absence of

magnetic fields. However, by extrapolating to zero excitation it is possible to derive the true natural pulsatance, ω_0.

II. *Theory.*

In order to calculate the rigidity modulus from quantities determined experimentally we require the expression connecting pulsatance (or frequency) with the rigidity modulus, the density, and the appropriate dimensions of the bar and its load. In this connexion it is necessary to consider the theory of the torsional vibration of bars in the form of thin strips of rectangular cross-section, since bars of this form were used in the experiments in preference to rods of circular cross-section for two reasons :—

(i.) Thin strips of *uniform* rectangular cross-section are more easily obtained than *uniform* rods of circular cross-section.

(ii.) Thin strips of rectangular section can be more easily clamped with certainty than rods of circular section.

The necessary theory has been given in a paper by Davies [4], and using the notations and assumptions of that paper the relevant results are as follows.

The bar is assumed to be of uniform cross-section and to be straight when in equilibrium. In the experiments the bar is clamped at one end and carries a load at the other : it thus comes under the category of a loaded fixed-free bar. The line passing through the centres of inertia of the normal sections of the bar is taken as axis of z, whilst the axes of x and y are the principal axes of inertia at the origin.

Then let

ρ=The density of the bar.
G=The rigidity modulus of the material of the bar.
l=The length of the bar.
A=The area of cross-section of the bar.
$M'=\rho Al$=The mass of the bar.
M=The mass of the load fixed to the free end of the bar.
K=The radius of gyration of the cross-section of the bar about Oz.
$I'=\rho AlK^2$=The moment of inertia of the bar about Oz.
I=The moment of inertia of the load about Oz.
$d=I/I'$.

n_0=The natural frequency of torsional vibration of the bar.

$\omega_0 = 2\pi n_0$=The natural pulsatance of torsional vibration of the bar.

For a thin bar of circular cross-section the velocity V of propagation of torsional waves is given by

$$V^2 = \frac{G}{\rho} \quad . \quad . \quad . \quad . \quad . \quad . \quad . \quad (2.1)$$

For a thin bar whose cross-section is not circular it can be shown that the velocity of propagation of torsional waves is equal to kV, where k is a dimensionless quantity determined by the form of the cross-section of the bar. In the case of a thin strip of rectangular cross-section, with sides $2a$ and $2b$, if $a \geqslant 3b$, and if $s = a/b$,

$$k^2 = \frac{4}{1+s^2}\left(1 - \frac{0{\cdot}63025}{s}\right) \quad . \quad . \quad . \quad . \quad (2.2)$$

to an accuracy exceeding 1 in 10,000.

In order to determine the rigidity modulus for a dynamical experiment we require a relation between the natural pulsatance of the bar and the various quantities associated with the bar, and for this purpose it is convenient to introduce a variable α', defined by the equation

$$\alpha' = \frac{\omega_0}{k\mathrm{V}} = \frac{\omega_0}{k}\sqrt{\frac{\rho}{\mathrm{G}}} \quad . \quad . \quad . \quad . \quad . \quad (2.3)$$

in the present notation.

The frequency equation for a loaded fixed-free bar in torsional vibration is

$$\alpha' l \tan \alpha' l = \frac{1}{d} = \frac{\mathrm{I}'}{\mathrm{I}} \quad . \quad . \quad . \quad . \quad . \quad . \quad (2.4)$$

If d (or the moments of inertia I and I′) in equation (2.4) has been determined, the value of $\alpha' l$ can be obtained by solving equation (2.4). For extreme values of d explicit solutions have been given (Davies, *loc. cit.* equations (1.4), (1.8), and (1.10)); for intermediate values of d it is best to draw up a table of the function $x \tan x$ [5] for small increments of the argument, and then to interpolate from such a table.

Having found the value of $\alpha' l$ in this way G can clearly be calculated from equation (2.3) if l, k, ρ, and ω_0 are determined.

Equations (2.1) and (2.4) are based on the assumption that the normal sections of the bar remain plane during vibration; this is the case when the cross-sectional dimensions of the bar are negligible in comparison with its length. When the cross-sectional dimensions are not negligible when compared with the length the normal sections become warped, and the equations will require modification. The necessary correction has been evaluated by Davies (*loc. cit.* p. 380). If ω_0 is the natural pulsatance when warping of the cross-section is neglected then ω_0 is given by equation (2.4) above in terms of the parameter α' of equation (2.3).

If ω be the natural pulsatance when warping of the cross-sections is taken into account then it is convenient to introduce a parameter β', which is similar to α' of the preceding paragraph. β' is defined by the equation

$$\beta'^2 = \frac{\omega^2}{k^2V^2} \cdot \frac{1}{1-\delta'}, \quad . \quad . \quad . \quad . \quad . \quad (2.5)$$

where

$$\delta' = \frac{\mu^2\omega^2}{k^2V^2} \quad . \quad . \quad . \quad . \quad . \quad (2.6)$$

(Davies, *loc. cit.*, equation (4.6)),

μ being a quantity determined by the size and shape of the cross-section and being of the dimensions of a length. For a thin strip of rectangular cross-section, with sides $2a$ and $2b$, if $s=a/b$ and $s \geqslant 3$ as in the present work, then

$$\mu^2 = \frac{b^2}{3(1+s^2)}\left\{ s^2 + \frac{4{\cdot}577}{s} - 4{\cdot}793 \right\}. \quad . \quad (2.7)$$

(Davies, *loc. cit.*, equation (4.21)).

For the bars used in the present work $a \doteqdot 0{\cdot}319$ cm., $b \doteqdot 0{\cdot}041$ cm., $s \doteqdot 7{\cdot}85$, giving $\mu^2 \doteqdot 5 \times 10^{-4}$ cm.^{2}.

In finding the order of magnitude of δ' we can identify ω with ω_0, since we are dealing with a small correction term, so that

$$\delta' = \frac{\mu^2\omega_0^2}{k^2V^2} \doteqdot \mu^2\alpha'^2 \quad . \quad . \quad . \quad . \quad . \quad (2.8)$$

from equation (2.3).

α' varies from one bar to another, but it is usually of the order of 10^{-1}, whence δ' is of the order of 5×10^{-6}.

From equations (2.3) and (2.5) it follows that

$$\frac{\omega^2}{\omega_0^2} = \frac{\beta'^2(1-\delta')}{\alpha'^2} \quad . \quad . \quad . \quad . \quad . \quad (2.9)$$

Now when warping of the cross-sections is permitted the frequency equation is

$$\beta' l \tan \beta' l = \frac{1+\delta'}{d} . \quad . \quad . \quad . \quad . \quad (2.10)$$

(Davies, *loc. cit.*, equation (4.6)),

which reduces to equation (2.4) when warping of the cross-sections is negligibly small.

Since δ' is so small β' cannot differ greatly from α'; to estimate the difference let $(\beta'-\alpha')l=h$. Expanding $\beta' l \tan \beta' l$ by Taylor's Theorem, we obtain

$$\beta' l \tan \beta' l = \alpha' l \tan \alpha' l + \frac{h\,\partial(\alpha' l \tan \alpha' l)}{\partial(\alpha' l)} .$$

Now from equations (2.4) and (2.10)

$$\beta' l \tan \beta' l - \alpha' l \tan \alpha' l = \frac{\delta'}{d} ,$$

whilst $$\frac{\partial(\alpha' l \tan \alpha' l)}{\partial(\alpha' l)} = \alpha' l \sec^2 \alpha' l + \tan \alpha' l.$$

Thus $$\beta'-\alpha' = \frac{\delta'}{ld} \cdot \frac{l}{\alpha' l \sec^2 \alpha' l + \tan \alpha' l} . \quad . \quad . \quad (2.11)$$

α' is of the order of 10^{-1}, l is of the order of 10 cm., and thus $\alpha' l$ is of the order of 1, whilst d is also of the order of 1.

With these values

$$\beta'-\alpha' \doteqdot \frac{\delta'}{50} \doteqdot 10^{-7};$$

the ratio $(\beta'-\alpha')/\alpha'$ is thus of the order of 10^{-6} and β'^2/α'^2 of the order of $(1+2\times10^{-6})$. It follows from equation (2.9) that $\omega^2/\omega_0^2 \doteqdot (1-3\times10^{-6})$, so that in the present work ω^2 can be identified with ω_0^2 without committing an error exceeding 3 in a million.

III. *General Discussion of the Apparatus and the Method.*

Fig. 1 represents diagrammatically the main features of the apparatus in plan and elevation. In this figure HH represent two similar rods of mild steel on which are wound (i.) two identical magnetizing coils UU and (ii.) two identical driving coils VV; the former carry the steady polarizing current I_s and the latter the alternating driving current I of pulsatance ω supplied by the

valve oscillator. R represents the bar of the material to be investigated; R is clamped at its lower end to a massive block N, whilst a suitable armature S is soldered to the upper end of R.

The coils UU are connected in series, as are also the coils VV, care being taken that the directions of the currents in the coils are such that S is subjected to a couple about the axis of the bar. Under these circumstances

Fig. 1.

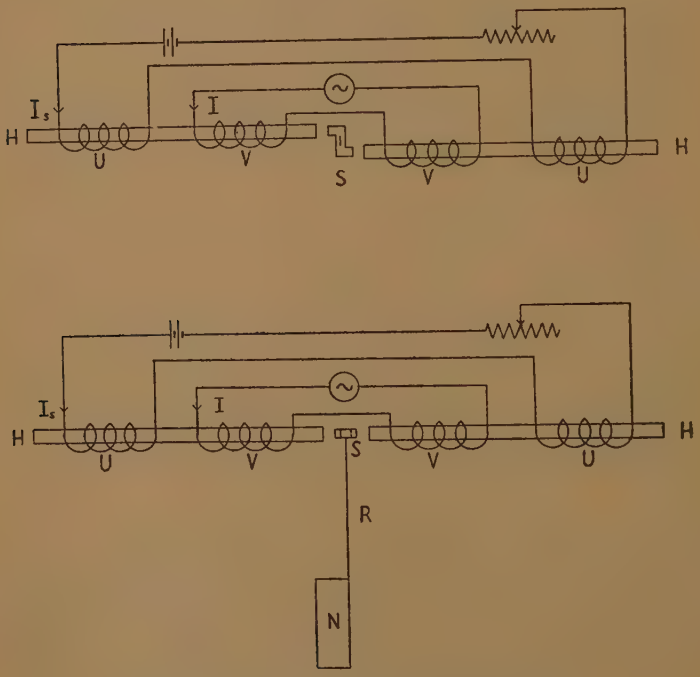

Diagrammatic representation of the apparatus.

S and R will be set into forced torsional vibration with the pulsatance ω of the driving current if ω does not differ greatly from the resonance pulsatance of the bar. The amplitude of vibration may be measured by a microscope fitted with a microscope eyepiece scale, and by varying ω the pulsatance corresponding to the maximum amplitude can be determined; this pulsatance can then be determined by measuring the frequency of the alternating current source by means of a frequency bridge.

The apparatus and experimental procedure are described in detail in later sections.

In designing the bar and armature the following points must be borne in mind :—

(i.) The resonance frequency of the system must be in the region of 1000 cycles per second in order to conform with the optimum experimental conditions.

(ii.) The system must give sharp resonance in order to determine accurately the resonance pulsatance.

(iii.) The shape of the armature must be such as to permit the bar to be excited torsionally, using the magnetizing system of fig. 1.

(iv.) The thickness of the armature must be small, since the theory given in the previous section assumes that the load is a thin lamina.

(v.) The shape of the armature must be such that its moment of inertia about Oz can be determined by experiment, or alternatively calculated from its mass and dimensions.

In connexion with the second point the sharpness of resonance of a mechanical system may be defined in a manner similar to the sharpness of resonance of an electrical circuit, *e. g.*, it may be defined as the width of the amplitude-pulsatance curve when the amplitude is equal to one-half the amplitude at resonance. The sharpness of resonance can thus be shown to be proportional to the quantity

$$\frac{\sqrt{s\mathrm{I}_e}}{r},$$

where

r=equivalent resistance coefficient of the system,
s=equivalent stiffness coefficient of the system,
I_e=equivalent moment of inertia of the system about Oz.

The equivalent resistance coefficient is determined by the various damping factors, and therefore cannot be varied. Thus, in order to obtain sharp resonance it is necessary to make I_e and s large ; this implies that the moment of inertia of the bar and load should be large and that the bar be stiff.

After trying different forms of armature in the course of preliminary experiments it was found that the above

conditions were best satisfied by using bars about 10 cm. long, 0·6 cm. wide, and 0·08 cm. thick, the bars being loaded with a rectangular piece of thin stalloy, about 2·5 cm. long, 1 cm. wide, and 0·015 cm. thick. It was found that torsional vibrations were easily excited with a system of this type, and although resonance was not so sharp as it would be if a stiffer bar and a load of greater moment of inertia were used, it was always possible to determine the resonance pulsatance to within 1 part in 2000, which is sufficiently accurate for the present purpose.

Excellent results were obtained in extrapolating to zero fields, and the moment of inertia of the armature was easily obtained from its weight and dimensions. Moreover, it was found that consistent values of the rigidity modulus were obtained with different lengths of bar, showing that condition (iv.) was satisfied and that the method of clamping the bar (described in Section IV.) was satisfactory.

IV. *Experimental Arrangements.*

The loaded bar and the details of the method of clamping the bar are shown in elevation and in plan in figs. 2 (*a*) and 2 (*b*), which have been lettered to correspond to fig. 1.

R represents the bar, to the upper end of which is soldered a rectangle of stalloy measuring 2·5 cm. in length, 0·5 to 1·0 cm. in width, and 0·015 cm. in thickness. The bar is rigidly clamped between a large steel block, N, and a strip of steel, M, which is soldered to the steel frame ABCD. For clamping purposes the frame ABCD is fitted with two steel screws, LL. The block N is 7 cm. long and is made of 2·5 cm. square section steel; the strip M is 2·5 cm. long, 0·5 cm. wide, and 0·5 cm. thick. The thickness of the frame is 0·5 cm., the length of the side AB being 4·5 cm. and that of the side BC being 3·6 cm.

Before the strip M is soldered to the frame ABCD the adjacent vertical faces of M and N are ground so that they are flat and so that the angle between these faces and the upper faces is exactly 90°. M is then soldered to the frame ABCD, and to ensure that it will be possible to adjust the upper faces of M and N to lie in the same plane the frame and N are clamped and the upper faces ground.

The method of assembly of the bar and its clamping arrangement is as follows :—The bar R is placed between M and N and adjusted so that its length is perpendicular to M. The upper faces of M and N are then adjusted until they lie in the same plane, and the screws LL are tightened.

The method of driving the bar is shown in detail in figs. 3 (*a*) and 3 (*b*), which have been lettered to correspond to figs. 1 and 2.

Referring to figs. 3 (*a*) and 3 (*b*), the steel block N is

Figs. 2 (*a*) and 2 (*b*).

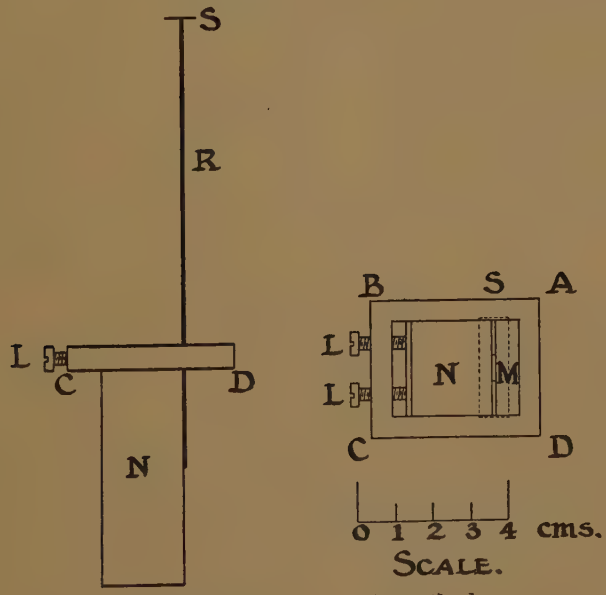

The arrangement used to damp the bar.

fitted with bolts and nuts so that it can be attached in a vertical position to an L-shaped strip of steel E which has a slot F in its vertical arm, allowing vertical movement of the block N. The horizontal arm of the L-shaped strip E is screwed down to a steel girder G, 18 in. long, 6 in. wide, and 3 in. high, which forms a base to the apparatus.

HH represent mild steel bars of circular cross-section $\frac{3}{8}$ in. in diameter. These bars, which are capable of horizontal movement in the direction of their axes, are

supported in two pairs of brass standards JJ soldered to two brass-block bases KK. One standard of each pair is fitted with a clamping screw P by means of which the steel bars H can be clamped in any desired position. The brass bases KK have a pair of slots to accommodate screws which secure the blocks to steel strips QQ, which are 6 in. long, 2 in. wide, and $\frac{1}{4}$ in. thick; these slots allow lateral movement of the blocks if necessary. The steel strips are screwed down to steel girders TT, which

Fig. 3 (*a*).

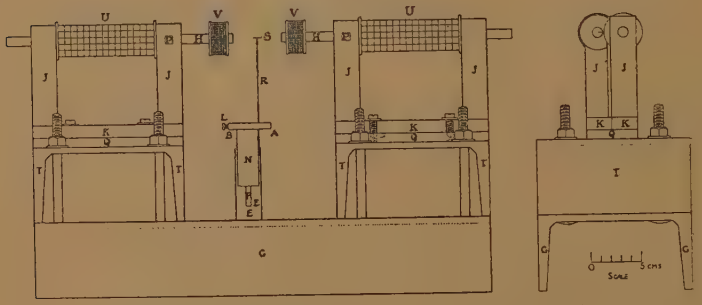

The vibrating bar and its driving arrangement.

Fig. 3 (*b*).

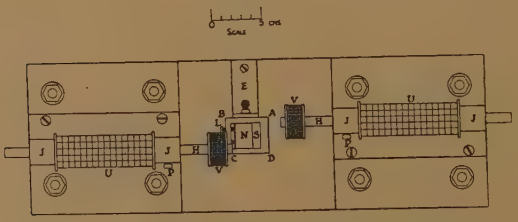

The vibrating bar and its driving arrangement.

are 6 in. square and 3 in. high; these steel girders are in turn bolted to the main girder base G.

Between the brass standards are two identical coils UU, of about 400 turns of no. 18 S.W.G., D.C.C. copper-wire wound on ebonite formers whose lengths are equal to the distance between the upright blocks, and whose inside diameters are such that they fit tightly on the steel bars HH.

Two other identical coils VV, each of 800 turns of enamelled no. 28 S.W.G. copper-wire wound on ebonite

formers fitting tightly on the steel bars, are situated at equal distances of about $\frac{1}{4}$ in. from the adjacent ends of the bars.

The coils UU are connected in series, and by passing a direct current in the appropriate direction through each coil the armature on the bar is subjected to a steady magnetic field.

The coils VV are also connected in series, and by passing an alternating current in the appropriate direction through each coil from a variable frequency valve oscillator the armature is subjected to an alternating field which is superposed on the steady field.

A microscope fitted with a 12 mm. objective is clamped rigidly to a stone slab situated above the apparatus in such a manner that the microscope may be focussed on a scratch drawn on the stalloy armature, the scratch being parallel to the long side of the armature. This scratch is illuminated by light from a small four-volt bulb, and when the bar is stationary the scratch appears as a series of sharply defined points, and as a series of lines when the bar is vibrating.

In the initial stages of the work considerable difficulty was experienced in soldering the armature to the bar in such a way that the armature would be (*a*) perpendicular to the bar, and (*b*) symmetrically placed with respect to the bar. This difficulty was overcome by using an electrical hot-plate apparatus fitted with a suitable stand.

The alternating current for the driving coils VV of figs. 3 (*a*) and 3 (*b*) was supplied by a valve oscillator similar to that described by James and Davies (*loc. cit.* p. 1058); it was, however, found convenient to use an iron-core output transformer in connexion with the amplifying valve instead of the tuned-anode arrangement previously described.

The frequency was measured by a frequency bridge described by one of the authors [6].

V. *Experimental Procedure.*

To determine the rigidity modulus the bar is clamped to its support and is set into forced torsional vibration; the amplitude is adjusted to its maximum value by varying the pulsatance of the applied alternating fields, the magnitude of the magnetizing fields and the separation between the pole-pieces and armature being kept constant.

The apparent resonance pulsatance ω_r is then measured by means of the frequency bridge. The experiment is then repeated, keeping the magnitude of the alternating fields and the separation between the pole-pieces and armature constant, but varying the steady polarizing current. This procedure is repeated for different separations, d_s, of the pole-pieces and armature, and from such a set of results the true resonance pulsatance ω_0 can be determined by extrapolation.

A typical set of results obtained in this way is shown in fig. 4. These results were obtained for an unannealed nickel bar whose length was $9{\cdot}92_8$ cm., and the moment of inertia of whose load about Oz was 0·1555 gm. cm.^{2}.

Fig. 4.

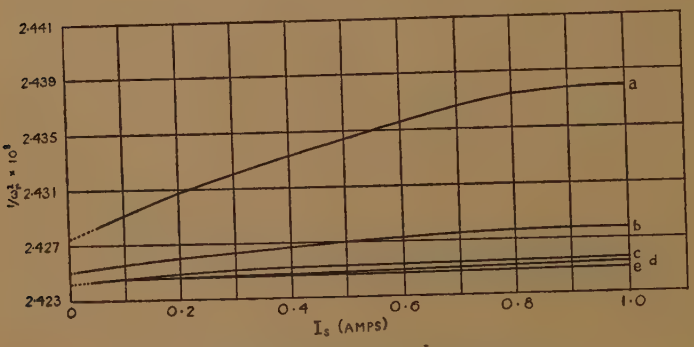

Curves showing the method of extrapolation.

The value of the driving current was maintained constant at 7·0 m.a.

Curve (*a*) represents the variation of $1/\omega_r^2$ with the magnetizing current I_s when the separation d_s is 0·1 cm. Similarly, curve (*b*) relates to d_s=0·5 cm., curve (*c*) to d_s=1·2 cm., curve (*d*) to d_s=1·5 cm., and curve (*e*) to d_s=1·8 cm.

By producing the curves to meet the $1/\omega_r^2$ axis as shown by the discontinuous lines the value of $1/\omega_r^2$ corresponding to I_s=0 can be deduced for each separation. For curve (*a*) this extrapolation gives the value $2{\cdot}427\times10^{-8}$, for (*b*) $2{\cdot}425\times10^{-8}$, and for (*c*), (*d*), and (*e*) $2{\cdot}424\times10^{-8}$.

It is clear that the value deduced in this way is independent of the separation d_s when d_s exceeds 1·2 cm., and

the value of ω extrapolated in this way is obviously the true resonance pulsatance ω_0 of the bar.

It may be interesting to add that the amplitudes at resonance are usually very small: generally the maximum amplitude of one of the extreme ends of the stalloy armature is of the order of 2×10^{-3} cm., corresponding to an angular amplitude of about 10^{-3} radian. In this way the danger of taking the bar beyond its elastic limit is avoided.

VI. *The Substances investigated.*

In the present work the substances investigated were unannealed and annealed specimens of nickel and nickel alloys. These were chosen partly because of their commercial importance and partly because they include a wide range of mechanical properties, thus allowing the method to be thoroughly tested.

The composition and previous history of the alloys investigated is given below. The heat treatment was carried out by Messrs. Henry Wiggin and Co., Ltd., who kindly presented the specimens.

Nickel.

Purity: 99·2 per cent.

(i.) Unannealed specimen: specimen 0·08 in. thick annealed for 18 min. at 860° C. and then rolled to 1/32 in. thickness. Brinell hardness = 216.

(ii.) Annealed specimen: preliminary treatment as for unannealed specimen; after rolling annealed at 860° C. for 18 min. B.H. (Brinell hardness) = 81.

Monel.

Composition: 67 per cent. Ni, 28 per cent. Cu, balance Fe and Mn.

(i.) Unannealed specimen: specimen 0·6 in. thick annealed for 20 min. at 900° C. and rolled to 1/32 in. thickness. B.H. = 212.

(ii.) Annealed specimen: specimen 0·5 in. thick annealed for 20 min. at 900° C. and rolled to 1/32 in. thickness. After rolling annealed at 900° C. for 20 min. B.H. = 115.

Ferry.

Composition: 44 per cent. Ni, 56 per cent. Cu.

(i.) Unannealed specimen: specimen 0·06 in. annealed

for 18 min. at 870° C. and then rolled to 1/32 in. B.H.=192.

(ii.) Annealed specimen: specimen 0·05 in. thick annealed for 18 min. at 860° C. and then rolled to 1/32 in. thickness. After rolling annealed at 860° C. for 18 min. B.H.=100.

Glowray.

Composition: 65 per cent. Ni, 15 per cent. Cr, 20 per cent. Fe.

(i.) Unannealed specimen: specimen 0·05 cm. thick annealed for 22 min. at 900° C. and then rolled to 1/32 in. thickness. B.H.=280.

(ii.) Annealed specimen: preliminary treatment as for unannealed specimen; after rolling annealed at 900° C. for 22 min. B.H.=169.

Brightray.

Composition: 80 per cent. Ni, 20 per cent. Cr.

(i.) Unannealed specimen: specimen 0·04 in. thick annealed for 22 min. at 900° C. and then rolled to 1/32 in. thickness. B.H.=315.

(ii.) Annealed specimen: preliminary treatment as for unannealed specimen; after rolling annealed at 900° C. for 22 min. B.H.=164.

Dullray.

Composition: 34 per cent. Ni, 4 per cent. Cr, 62 per cent. Fe.

(i.) Unannealed specimen: specimen 0·05 in. thick annealed for 18 min. at 880° C. and then rolled to 1/32 in. thickness. B.H.=218.

(ii.) Annealed specimen: preliminary treatment as for unannealed specimen; after rolling annealed at 880° C. for 18 min. B.H.=159.

48 *per cent. Nickel-Iron.*

Composition: 48 per cent. Ni, 52 per cent. Fe.

(i.) Unannealed specimen: specimen 0·05 in. thick annealed for 20 min. at 900° C. and then rolled to 1/32 in. thickness. B.H.=212.

(ii.) Annealed specimen: specimen 0·07 in. thick annealed for 20 min. at 900° C. and then rolled to 1/32 in. thickness; after rolling annealed at 900° C. for 20 min. B.H.=130.

20 per cent. Nickel-Silver.

Composition : 20 per cent. Ni, 62 per cent. Cu, 18 per cent. Zn.

(i.) Unannealed specimen : specimen 0·07 in. thick annealed for 15 min. at 740° C. and then rolled to 1/32 in. thickness. B.H.=200.

(ii.) Annealed specimen : specimen 0·06 in. thick annealed for 15 min. at 740° C. and then rolled to 1/32 in. thickness ; after rolling annealed at 740° C. for 15 min. B.H.=97.

Notes.

(i.) The annealing was done in an electric furnace (gas atmosphere) on a moving belt. The times given are the approximate times the samples were in the heating zone.

(ii.) The Brinell readings were taken on a Vickers machine, using a 1 mm. ball and 10 kgm. load.

VII. *Results.*

A number of independent experiments were carried out with each specimen. In the majority of cases it was found sufficient to keep the load of a particular bar constant and to vary the vibrating length of the bar, since a series of results with an unannealed glowray bar (see below) had shown that consistent results were obtained when both load and length of bar were varied.

The notation used in this section is identical with that of Section II., where the theory of the method is discussed.

All the results relate to room-temperature (approximately 17° C.).

(i.) *Nickel.*

(a) *Annealed specimen.*

$\rho=8{\cdot}89_1$ gm./cm.^{3} ; $2a=0{\cdot}639_1$ cm. ; $2b=0{\cdot}079_7$ cm. ; $k^2=0{\cdot}05644$; $I=0{\cdot}1046_4$ gm. cm.^{2}.

Expt.	1.	2.	3.	4.
l (cm.)	$9{\cdot}94_6$	$9{\cdot}90_0$	$9{\cdot}84_9$	$9{\cdot}81_4$
$\omega_0^2\times10^{-8}$	0·5154	0·5196	0·5231	0·5251
l/d	1·489	1·482	1·474	1·469
$\alpha'\times10^5$	9910	9944	9976	10000
$G\times10^{-11}$ (dynes/cm.^{2})	$8{\cdot}26_8$	$8{\cdot}27_5$	$8{\cdot}27_7$	$8{\cdot}26_8$

Mean value of $G=8{\cdot}27_2\times10^{11}$ dynes/cm.^{2}.

(b) *Unannealed specimen.*

$\rho = 8{\cdot}87_8$ gm./cm.^{3} ; $2a = 0{\cdot}637_3$ cm. ; $2b = 0{\cdot}082_1$ cm. ; $k^2 = 0{\cdot}05999$; $I = 0{\cdot}1555$ gm.cm.^{2}.

Expt.	1.	2.	3.	4.
l (cm.)	$9{\cdot}91_0$	$9{\cdot}96_6$	$9{\cdot}99_8$	10·50
$\omega_0^2 \times 10^{-8}$	0·4130	0·4076	0·4079	0·3830
$1/d$	1·018	1·027	1·027	1·078
$\alpha' \times 10^5$	8740	8690	8690	8420
$G \times 10^{-11}$ ..... (dynes/cm.^{2})	$8{\cdot}00_0$	$7{\cdot}99_3$	$7{\cdot}99_5$	$7{\cdot}99_6$

Mean value of $G = 7{\cdot}99_6 \times 10^{11}$ dynes/cm.^{2}.

(ii.) *Monel.*

(a) *Annealed specimen.*

$\rho = 8{\cdot}84_6$ gm./cm.^{3} ; $2a = 0{\cdot}640_1$ cm. ; $2b = 0{\cdot}077_7$ cm. ; $k^2 = 0{\cdot}05361$; $I = 0{\cdot}1051$ gm.cm.^{2}.

Expt.	1.	2.	3.	4.
l (cm.)	10·10	10·06	$9{\cdot}98_9$	$9{\cdot}96_3$
$\omega_0^2 \times 10^{-8}$	0·4139	0·4177	0·4213	0·4229
$1/d$	1·466	1·459	1·449	1·445
$\alpha' \times 10^5$	9710	9740	9786	9800
$G \times 10^{-11}$ ..... (dynes/cm.^{2})	$7{\cdot}25_1$	$7{\cdot}26_0$	$7{\cdot}26_0$	$7{\cdot}26_6$

Mean value of $G = 7{\cdot}25_9 \times 10^{11}$ dynes/cm.^{2}.

(b) *Unannealed specimen.*

$\rho = 8{\cdot}86_0$ gm./cm.^{3} ; $2a = 0{\cdot}639_1$ cm. ; $2b = 0{\cdot}080_8$ cm. ; $k^2 = 0{\cdot}05780$; $I = 0{\cdot}1066$ gm.cm.^{2}.

Expt.	1.	2.	3.	4.
l (cm.)	10·06	$9{\cdot}93_9$	10·15	10·02
$\omega_0^2 \times 10^{-8}$	0·4115	0·4174	0·4058	0·4133
$1/d$	1·491	1·476	1·505	1·485
$\alpha' \times 10^5$	9806	9872	9746	9830
$G \times 10^{-11}$ ..... (dynes/cm.^{2})	$6{\cdot}55_9$	$6{\cdot}56_4$	$6{\cdot}54_8$	$6{\cdot}55_6$

Mean value of $G = 6{\cdot}55_7 \times 10^{11}$ dynes/cm.^{2}.

(iii.) *Ferry.*

(a) *Annealed specimen.*

$\rho = 8{\cdot}89_8$ gm./cm.^{3} ; $2a = 0{\cdot}640_6$ cm. ; $2b = 0{\cdot}080_5$ cm. ; $k^2 = 0{\cdot}05722$; $I = 0{\cdot}08454$ gm. cm.^{2}.

Expt.	1.	2.	3.	4.
l (cm.)	$9{\cdot}98_1$	$9{\cdot}94_7$	$9{\cdot}90_6$	$9{\cdot}88_7$
$\omega_0^2 \times 10^{-8}$	0·4642	0·4665	0·4691	0·4708
$1/d$	1·881	1·876	1·864	1·864
$\alpha' \times 10^4$	1060	1058	1065	1067
$G \times 10^{-11}$ (dynes/cm.^{2})	$6{\cdot}42_5$	$6{\cdot}42_7$	$6{\cdot}43_0$	$6{\cdot}43_4$

Mean value of $G = 6{\cdot}42_9 \times 10^{11}$ dynes/cm.^{2}.

(b) *Unannealed specimen.*

$\rho = 8{\cdot}90_5$ gm./cm.^{3} ; $2a = 0{\cdot}639_4$ cm. ; $2b = 0{\cdot}078_5$ cm. ; $k^2 = 0{\cdot}05481$; $I = 0{\cdot}0424$ gm. cm.^{2}.

Expt.	1.	2.	3.	4.
l (cm.)	10·01	10·17	$9{\cdot}96_3$	10·04
$\omega_0^2 \times 10^{-8}$	0·5803	0·5652	0·5843	0·5769
$1/d$	3·648	3·706	3·632	3·659
$\alpha' \times 10^4$	1241	1225	1245	1241
$G \times 10^{-11}$ (dynes/cm.^{2})	$6{\cdot}12_0$	$6{\cdot}11_4$	$6{\cdot}11_9$	$6{\cdot}11_6$

Mean value of $G = 6{\cdot}11_7 \times 10^{11}$ dynes/cm.^{2}.

(iv.) *Glowray.*

(a) *Annealed specimen.*

$\rho = 8{\cdot}30_0$ gm./cm. ; $2a = 0{\cdot}636_9$ cm. ; $2b = 0{\cdot}081_3$ cm. ; $k^2 = 0{\cdot}05900$; $I = 0{\cdot}1544$ gm. cm.^{2}.

Expt.	1.	2.	3.
l (cm.)	10·11	10·26	10·11
$\omega_0^2 \times 10^{-8}$	0·4002	0·3916	0·4003
$1/d$	0·9884	1·004	0·9884
$\alpha' \times 10^5$	8475	8390	8475
$G \times 10^{-11}$ (dynes/cm.^{2})	$7{\cdot}83_6$	$7{\cdot}82_6$	$7{\cdot}83_7$

Mean value of $G = 7{\cdot}83_3 \times 10^{11}$ dynes/cm.^{2}.

(b) *Unannealed specimen.*

$\rho = 8{\cdot}30_4$ gm./cm.^{3} ; $2a = 0{\cdot}636_7$ cm. ; $2b = 0{\cdot}078_6$ cm. , $k^2 = 0{\cdot}05538$.

Expt.	1.	2.	3.	4.	5.
I (gm. cm.^{2}) ...	0·2120	0·1629	0·2103	0·2103	0·2103
l (cm.).....	$7{\cdot}91_1$	$7{\cdot}56_0$	$7{\cdot}18_7$	$7{\cdot}08_5$	$6{\cdot}98_0$
$\omega^2{}_0 \times 10^{-8}$	0·3573	0·4679	0·4017	0·4081	0·4153
$1/d$	0·5318	0·5082	0·4872	0·4803	0·4732
$\alpha' \times 10^5$	8478	9704	8990	9064	9142
$G \times 10^{-11}$ ..... (dynes/cm.^{2})	$7{\cdot}45_3$	$7{\cdot}44_9$	$7{\cdot}45_0$	$7{\cdot}45_0$	$7{\cdot}45_1$

Mean value of $G = 7{\cdot}45_1 \times 10^{11}$ dynes/cm.^{2}.

(v.) *Brightray.*

(a) *Annealed specimen.*

$\rho = 8{\cdot}42_0$ gm./cm.^{3} ; $2a = 0{\cdot}636_5$ cm. ; $2b = 0{\cdot}079_5$ cm. ; $k^2 = 0{\cdot}05661$; $I = 0{\cdot}1591$ gm. cm.^{2}.

Expt.	1.	2.	3.
l (cm.).....	10·04	10·12	10·24
$\omega_0{}^2 \times 10^{-8}$	0·3958	0·3915	0·3859
$1/d$.....	0·9214	0·9288	0·9400
$\alpha' \times 10^5$	8315	8273	8213
$G \times 10^{-11}$ ..... (dynes/cm.^{2})	$8{\cdot}51_3$	$8{\cdot}50_8$	$8{\cdot}51_0$

Mean value of $G = 8{\cdot}51_0 \times 10^{11}$ dynes/cm.^{2}.

(b) *Unannealed specimen.*

$\rho = 8{\cdot}38_4$ gm./cm.^{3} ; $2a = 0{\cdot}637_2$ cm. ; $2b = 0{\cdot}081_2$ cm. ; $k^2 = 0{\cdot}05884$; $I = 0{\cdot}1561$ gm. cm.^{2}.

Expt.	1.	2.	3.	4.
l (cm.)	$9{\cdot}99_1$	$9{\cdot}82_4$	$9{\cdot}60_8$	$9{\cdot}50_9$
$\omega_0{}^2 \times 10^{-8}$	0·3942	0·4026	0·4136	0·4192
$1/d$	0·9546	0·9386	0·9182	0·9084
$\alpha' \times 10^5$	8465	8555	8674	8732
$G \times 10^{-11}$ ..... (dynes/cm.^{2})	$7{\cdot}83_3$	$7{\cdot}83_3$	$7{\cdot}83_1$	$7{\cdot}83_1$

Mean value of $G = 7{\cdot}83_2 \times 10^{11}$ dynes/cm.^{2}.

(vi.) *Dullray.*

(a) *Annealed specimen.*

$\rho = 8{\cdot}11_4$ gm./cm.^{3} ; $2a = 0\ 639_4$ cm. ; $2b = 0{\cdot}080_5$ cm. ;
$k^2 = 0{\cdot}05746$; $I = 0{\cdot}1024$ gm. cm.^{2}.

Expt.	1.	2.	3.
l (cm.)	10·08	10·13	10·03
$\omega_0^2 \times 10^{-8}$	0·4395	0·4366	0·4436
$1/d$	1·422	1·429	1·415
$\alpha' \times 10^5$	9640	9606	9674
$G \times 10^{-11}$ (dynes/cm.^{2})	$6{\cdot}67_8$	$6{\cdot}67_9$	$6{\cdot}68_6$

Mean value of $G = 6{\cdot}68_1 \times 10^{11}$ dynes/cm.^{2}.

(b) *Unannealed specimen.*

$\rho = 8{\cdot}20_1$ gm./cm.^{3} ; $2a = 0{\cdot}633_6$ cm. ; $2b = 0{\cdot}078_7$ cm. ;
$k^2 = 0{\cdot}05606$; $I = 0{\cdot}09113$ gm. cm.^{2}.

Expt.	1.	2.	3.
l (cm.)	$9{\cdot}17_8$	$9{\cdot}33_9$	$9{\cdot}49_8$
$\omega_0^2 \times 10^{-8}$	0·4313	0·4229	0·4100
$1/d$	1·400	1·424	1·445
$\alpha' \times 10^4$	1053	1041	1028
$G \times 10^{-11}$ (dynes/cm.^{2})	$5{\cdot}68_9$	$5{\cdot}67_5$	$5{\cdot}67_8$

Mean value of $G = 5{\cdot}68_1 \times 10^{11}$ dynes/cm.^{2}.

(vii.) 48 *per cent. Nickel-Iron.*

(a) *Annealed specimen.*

$\rho = 8{\cdot}21_7$ gm./cm.^{3} ; $2a = 0{\cdot}637_5$ cm. ; $2b = 0{\cdot}081_4$ cm. ;
$k^2 = 0{\cdot}05905$; $I = 0{\cdot}06219$ gm. cm.^{2}.

Expt.	1.	2.	3.
l (cm.)	10·04	$9{\cdot}88_9$	$9{\cdot}83_8$
$\omega_0^2 \times 10^{-8}$	0·5400	0·5510	0·5561
$1/d$	2·368	2·332	2·332
$\alpha' \times 10^4$	1122	1134	1139
$G \times 10^{-11}$ (dynes/cm.^{2})	$5{\cdot}96_5$	$5{\cdot}95_7$	$5{\cdot}96_3$

Mean value of $G = 5{\cdot}96_2 \times 10^{11}$ dynes/cm.^{2}.

(b) *Unannealed specimen.*

$\rho = 8{\cdot}13_4$ gm./cm.^{3} ; $2a = 0{\cdot}637_9$ cm. ; $2b = 0{\cdot}081_0$ cm. ; $k^2 = 0{\cdot}05844$; $I = 0{\cdot}1068$ gm. cm.^{2}.

Expt.	1.	2.	3.
l (cm.)	$9{\cdot}50_9$	$9{\cdot}44_9$	$9{\cdot}34_9$
$\omega_0^2 \times 10^{-8}$	0·4168	0·4203	0·4263
l/d	1·264	1·256	1·243
$\alpha' \times 10^5$	9829	9870	9936
$G \times 10^{-11}$ (dynes/cm.^{2})	$6{\cdot}00_4$	$6{\cdot}00_4$	$6{\cdot}01_0$

Mean value of $G = 6{\cdot}00_8 \times 10^{11}$ dynes/cm.^{2}.

(viii.) 20 *per cent. Nickel-Silver.*

(a) *Annealed specimen.*

$\rho = 8{\cdot}79_6$ gm./cm.^{3} ; $2a = 0{\cdot}639_3$ cm. ; $2b = 0{\cdot}080_9$ cm. ; $k^2 = 0{\cdot}05803$; $I = 0{\cdot}07339$ gm. cm.^{2}.

Expt.	1.	2.	3.
l (cm.)	$9{\cdot}96_3$	$9{\cdot}93_0$	$9{\cdot}85_8$
$\omega_0^2 \times 10^{-8}$	0·4022	0·4042	0·4085
l/d	2·138	2·130	2·115
$\alpha' \times 10^4$	1101	1104	1110
$G \times 10^{-11}$ (dynes/cm.^{2})	$5{\cdot}02_9$	$5{\cdot}03_1$	$5{\cdot}03_2$

Mean value of $G = 5{\cdot}03_1 \times 10^{11}$ dynes/cm.^{2}.

(b) *Unannealed specimen.*

$\rho = 8{\cdot}77_5$ gm./cm.^{3} ; $2a = 0{\cdot}638_4$ cm. ; $2b = 0{\cdot}081_7$ cm. ; $k^2 = 0{\cdot}05929$; $I = 0{\cdot}1112$ gm. cm.^{2}.

Expt.	1.	2.	3.
l (cm.)	$9{\cdot}12_6$	$8{\cdot}96_8$	$8{\cdot}89_6$
$\omega_0^2 \times 10^{-8}$	0·3464	0·3545	0·3692
l/d	1·296	1·274	1·264
$\alpha' \times 10^4$	1032	1044	1050
$G \times 10^{-11}$ (dynes/cm.^{2})	$4{\cdot}80_9$	$4{\cdot}80_9$	$4{\cdot}80_7$

Mean value of $G = 4{\cdot}80_8 \times 10^{11}$ dynes/cm.^{2}.

The above results are summarized in the following table. In addition, the values of Young's modulus determined by Davies and Thomas [2] are given, as are also the values of Poisson's ratio and the bulk modulus calculated with the aid of these results. In the latter calculations it is assumed that the bars are isotropic.

Note.—The value of $23{\cdot}33\times10^{11}$ dynes/cm.^{2} for the Young's modulus of unannealed glowray, given in Davies and Thomas, was thought to be rather high, and was found to be due to an error in the determination

Substance.	Density (gm./cm.^{3}).	Young's modulus (dynes/cm.^{2}).	Rigidity modulus (dynes/cm.^{2}).	Poisson's ratio.	Bulk modulus (dynes/cm.^{2}).
Nickel (A)	$8{\cdot}89_1$	$19{\cdot}37\times10^{11}$	$8{\cdot}27_2\times10^{11}$	0·171	$9{\cdot}81\times10^{11}$
Nickel (U)	$8{\cdot}87_8$	$19{\cdot}18\times10^{11}$	$7{\cdot}99_6\times10^{11}$	0·199	$10{\cdot}62\times10^{11}$
Monel (A).....	$8{\cdot}84_6$	$14{\cdot}94\times10^{11}$	$7{\cdot}25_9\times10^{11}$	0·029	$5{\cdot}28\times10^{11}$
Monel (U)	$8{\cdot}86_0$	$15{\cdot}57\times10^{11}$	$6{\cdot}55_7\times10^{11}$	0·186	$8{\cdot}26\times10^{11}$
Ferry (A)	$8{\cdot}89_8$	$14{\cdot}54\times10^{11}$	$6{\cdot}42_9\times10^{11}$	0·130	$6{\cdot}54\times10^{11}$
Ferry (U)	$8{\cdot}90_5$	$14{\cdot}01\times10^{11}$	$6{\cdot}11_7\times10^{11}$	0·144	$6{\cdot}55\times10^{11}$
Glowray (A)	$8{\cdot}30_0$	$17{\cdot}23\times10^{11}$	$7{\cdot}83_3\times10^{11}$	0·100	$7{\cdot}17\times10^{11}$
Glowray (U) ...	$8{\cdot}30_4$	$18{\cdot}85\times10^{11}$	$7{\cdot}45_1\times10^{11}$	0·265	$13{\cdot}37\times10^{11}$
Brightray (A) ...	$8{\cdot}42_0$	$20{\cdot}17\times10^{11}$	$8{\cdot}51_0\times10^{11}$	0·185	$10{\cdot}67\times10^{11}$
Brightray (U) ...	$8{\cdot}38_4$	$18{\cdot}61\times10^{11}$	$7{\cdot}83_2\times10^{11}$	0·188	$9{\cdot}94\times10^{11}$
Dullray (A)	$8{\cdot}11_4$	$15{\cdot}38\times10^{11}$	$6{\cdot}68_1\times10^{11}$	0·151	$7{\cdot}34\times10^{11}$
Dullray (U)	$8{\cdot}20_1$	$14{\cdot}42\times10^{11}$	$5{\cdot}68_1\times10^{11}$	0·269	$10{\cdot}40\times10^{11}$
48 per cent. Nickel-Iron (A).	$8{\cdot}21_7$	$13{\cdot}65\times10^{11}$	$5{\cdot}96_2\times10^{11}$	0·145	$6{\cdot}40\times10^{11}$
48 per cent. Nickel-Iron (U).	$8{\cdot}13_4$	$15{\cdot}29\times10^{11}$	$6{\cdot}00_6\times10^{11}$	0·273	$11{\cdot}23\times10^{11}$
20 per cent. Nickel-Silver (A).	$8{\cdot}79_6$	$12{\cdot}45\times10^{11}$	$5{\cdot}03_1\times10^{11}$	0·235	$7{\cdot}82\times10^{11}$
20 per cent. Nickel-Silver (U).	$8{\cdot}77_5$	$11{\cdot}88\times10^{11}$	$4{\cdot}80_8\times10^{11}$	0·235	$7{\cdot}47\times10^{11}$

(A) denotes annealed specimen.
(U) denotes unannealed specimen.

of the thickness of the bar. On correcting this error the calculated value of Young's modulus for the bar was found to be $18{\cdot}85\times10^{11}$ dynes/cm.^{2}.

VIII. *Possible Errors in the Quantities measured and the Effect on the Final Result.*

From equation (2.3) it is seen that the value obtained for the rigidity modulus of the bar is proportional to the square of the true natural pulsatance ω_0. This pulsatance ω_0 can be determined accurately to 1 part

in 2000, hence the error involved in the final result is of the order of 1 part in 1000.

The effect on the final result of errors in other measured quantities is not immediately evident from the equation (2.3). However, this can easily be deduced by assuming a certain proportional error for a single measurement and calculating the error in the final result when all other quantities are constant.

It is possible, by means of the depth gauge method used, to measure the length of the bar to within 0·002 cm. The length of the bar is of the order of 10 cm., and so the maximum error involved in the length of the bar is of the order of 1 part in 5000. On the lines outlined above it can be calculated that an error of this magnitude in the length leads to an error of 1 part in 4000 in the value of the rigidity modulus.

The breadth of the bar, which is about 0·64 cm., can be measured to within about 0·0001 cm., which involves a maximum error of 1 part in 6000. This gives rise to an error of the same order in the final result.

The thickness of the bar, which is about 0·08 cm., can be determined to within about 0·0001 cm., which means a maximum error of 1 part in 800. The corresponding error in the value obtained for the rigidity modulus can be shown to be not more than 1 part in 500.

Considering next the measurements of the dimensions of the armature, the width, which is of the order of 0·7 cm., can be measured to within 0·0001 cm. by means of a screw-gauge. The maximum error involved is about 1 part in 8000, involving a corresponding error of 1 part in 5000 in the final result.

The length of the armature, which is about 2·5 cm., can be determined with ease to within 0·0001 cm., so that the error involved is practically negligible.

The density of the bar can be determined easily to within 1 part in 1000, and the maximum error thus involved in the final result does not exceed 1 part in 5000.

As far as the other quantities are concerned, such as the weights of the bar and armature, the errors involved are exceedingly small and may be safely neglected.

Assuming all the errors to be additive, it can be shown that the maximum error involved in the evaluation of the rigidity modulus does not exceed 0·4 per cent., the

main contribution being due to the error in the thickness of the bar.

This estimate of the error assumes uniformity of the various quantities. In practice this will not be the case, and the probable error will therefore exceed the figure estimated ; the main source of error is the non-uniformity of the thickness of the bar. Inspection of the results shows, however, that for the same substance the maximum discrepancy between individual results never exceeds 0·2 per cent.

IX. *Comparison with the Results of previous Investigations.*

With the exception of nickel it has been found very difficult to trace any previous work on the values of the

The Rigidity Modulus of Nickel.

Author.	Date.	Purity.	Heat treatment.	$G \times 10^{-11}$ (dynes/cm.^{2}).
Schaefer [7]	1901	97% Ni.	..	9·34
Grüneissen [8]	1907–8	..	Hard drawn.	7·70
			..	7·86
Guye-Schapper [9] ...	1910	..	Annealed.	7·16
Koch-Dannecker [10] .	1915	..	Annealed at 800° C.	7·23
Jokibe-Sakai [11]	1921	..	Annealed.	7·82
Kikuta [12]	1921	..	..	7·1–7·6
International Critical Tables.....	1925	..	Annealed at 990° C.	7·51
Honda-Tanaka [13] ..	1926	99·7% Ni.	..	8·0
Gutenberg- Schechtweg [14]	1930	..	Annealed at 860° C.	8·27
Present work	1938	99·2% Ni.	Unannealed.	8·00

Note.—All the above values were obtained by dynamical methods.

rigidity modulus of the substances used in the present investigation. The results of previous determinations are summarized in the above table.

It will be noted that the values given in the table cover a considerable range, and this is probably due to differences in the purity of the substances and in the previous history of the samples used.

In conclusion, the authors desire to express their indebtedness to Messrs. L. E. Sulston and D. Owen for their aid in the construction of the apparatus, to Messrs. Henry Wiggin & Co., Ltd., for the gift of the alloys, and to the Department of Scientific and Industrial Research for a maintenance grant to one of the authors (D. H. L.).

X. *References.*

(1) Davies and James, Phil. Mag. xviii. p. 1023 (1934); James and Davies, Phil. Mag. xviii. p. 1053 (1934).
(2) Davies and Thomas, Phil. Mag. xxiii. p. 361 (1937).
(3) Goens, *Ann. der Physik*, iv. p. 733 (1930).
(4) Davies, Phil. Mag. xxv. p. 364 (1938).
(5) Jahnke and Emde, Tables of Functions, etc., p. 32 (Leipzig, 1933).
(6) Davies, ' Journal of Scientific Instruments,' x. p. 274 (1933).
(7) Schaefer, *Ann. der Physik*, v. p. 220 (1901).
(8) Grüneissen, *Ann. der Physik*, xii. p. 801 (1907).
(9) Guye and Schapper, *C. R.* cl. p. 962 (1910).
(10) Koch and Dannecker, *Ann. der Physik*, xlvii. p. 197 (1915).
(11) Jokibe and Sakai, Phil. Mag. xlii. p. 397 (1921).
(12) Kikuta, Sci. Rep. Tohoku Imp. Univ. x. p. 139 (1921).
(13) Honda and Tanaka, Sci. Rep. Tohoku Imp. Univ. xv. p. 1 (1926).
(14) Gutenberg and Schlechtweg, *Phys. Zeit.* xxxi. p. 475 (1930).

LXXII. *Remarks on the Thermodynamic Scale of Temperature.*

By N. Kürti *and* F. Simon, *Clarendon Laboratory, Oxford* †.

[Received August 10, 1938.]

THE thermodynamic temperature scale has in recent years passed from the domain of purely theoretical interest to that of practical application. The reason is that, in the region of the very lowest temperatures which can be reached by the magnetic method, the usual way of realizing the temperature scale (which is based on the use of " ideal " gases), can no longer be considered owing to the non-existence of gases with appreciable pressures. In this region the magnetic susceptibility of the salts which are employed for producing these low temperatures has been used to indicate a provisional " temperature " by extrapolating Curie's Law into the unknown regions. (We shall denote these " temperatures " by T*; see also the following paper.)

† Communicated by the Authors.

Such an extrapolation is bound to give wrong results, at least at very low temperatures, as the substances cease be behave ideally on approaching the absolute zero †. It is true that, as long as the temperature is high compared with the characteristic temperature[1] of the salt, it is possible to make a rough estimate of the absolute temperature from the value of the susceptibility after demagnetization. But, in order to be certain of the real temperature, it is necessary to establish the thermodynamic scale, originally put forward by Lord Kelvin.

Essentially the method consists in carrying out a cycle between the unknown temperature and one known in the absolute scale, and calculating the unknown temperature by means of the second law of thermodynamics. When such a cycle is applied to this particular case, where the change in temperature is produced by an adiabatic process, the changes in entropy at both temperatures are equal, *i. e.*, $Q_1/T_1=Q_2/T_2$. The experiment therefore consists chiefly in measuring quantities of heat at both temperatures, either specific heats or heats of magnetization. At the temperature known in the absolute scale a measurement of the latter can be replaced by a calculation based on the laws of an ideal paramagnetic salt, as, in general, the salts used still follow these laws at the higher temperature[2]. Giauque and McDougall[3], Keesom[4], and Kürti and Simon[5] have described such and similar ways of realizing the thermodynamic scale. Some experimental determinations of the scale have been carried out by Giauque and McDougall[3], Kürti and Simon[6], and Clark[7].

De Haas and Wiersma[8] have proposed a somewhat different method, which is similar in some respects to the way in which at high temperatures the thermodynamic scale is determined using an "ideal" gas. They determine by purely magnetic measurements whether the substance behaves "ideally" in the temperature region in question, *i. e.*, whether it has a constant magnetization along an adiabatic. In this case by applying the second law they deduce that the quantity $(H_e\text{-}C)/T$ (H_e=external magnetic field) remains constant ‡. This quantity can be

† If they continued to behave ideally one would already reach absolute zero on demagnetizing from 1° and a few hundred Gauss.

‡ The constant C can be interpreted as a correction to be applied to the external field in order to obtain the internal field (see also the following paper).

determined in the temperature region of liquid helium, in which the temperature scale is known, so that it is possible to calculate the absolute temperatures along the adiabatic as long as the magnetization remains constant. Obviously this method cannot be extended to demagnetization to zero field, as in this case the substance can no longer behave "ideally." Furthermore, the method cannot be applied when starting with very high fields, for then the magnetic entropy is reduced to such small values that it is comparable with the entropy of the lattice. This means that the properties along an adiabatic are not determined solely by the magnetic behaviour, and thus the magnetization cannot remain constant. Nevertheless the method can be of great service in a certain region.

The chief difficulty of the former method consists in the determination of the heat capacities. Owing to the extremely long period of time which is necessary to establish the temperature equilibrium in such salts[9] it is not possible to apply the usual methods of heating, *e. g.*, a heating coil. This is only possible if, as has been done by Giauque and McDougall[3], the substance is heated each time from the respective lowest temperature to the starting temperature, where the transmission of heat is sufficiently quick and the specific heats are derived from the differences of such heatings. There are, however, for experimental reasons fairly large errors inherent in this method.

For this reason we carried out the heating by γ-rays or by radioactive substances mixed with the sample †. Both methods give an almost homogeneous heating. The difficulty lies in determining the absolute value of the heat absorbed by the substance. We proceeded in such a way that we did not try to determine directly the absolute value of the heats supplied to the substance at all, so that we only obtained values proportional to the absolute temperature. The factor of proportionality was then determined by introducing the necessary condition that, at high temperatures, T* and T must be equal. An uncertainty is introduced into this determination by two facts: first, the thermal insulation becomes worse at

† For instance, to heat iron alum from the lowest temperatures attainable to 1° in four hours one has either to irradiate it with the γ-rays of a 200 mCurie source placed in 5 cm. distance or to mix 10^{-2} mCurie of polonium with 1 c.c. of the substance.

temperatures above 0·7° K., as in this region the vapour pressure of the adsorbed layers of helium begins to be appreciable ; secondly, and this is still more important, the specific heats become very small in this region. The result is that calorimetric measurements are less accurate at higher temperatures, and it is just at these temperatures that measurements are necessary for determining the factor of proportionality.

It appears from what has been said in the preceding paragraphs that a method which dispenses with the necessity of determining the absolute values of the heat supplied would have several advantages. It may be asked, however, whether it is worth while improving the methods for establishing the thermodynamic scale, as recently several secondary thermometers[10] (some of which depend only slightly on the magnetic field, so that temperatures may be determined even in additional fields) have been developed in various laboratories. If such thermometers could be applied in all cases the obvious thing to do would be to calibrate them by means of a salt for which the thermodynamic scale had been established, and then bring them in thermal contact with the system under observation. It is at this point, however, that experimental difficulties arise. The chief one is that, according to our observations, the outside of the salt, where normally a thermometer would be placed, can have temperatures very different from the bulk of the material, owing to the bad heat conduction of the salt. This will be especially serious if, as in the case under discussion, the outside of the salt receives through the electrical leads an additional influx of heat †. At present therefore the thermodynamic scale must be established for each salt. For this reason we wish to describe a method in which the absolute value of the heat supplied need not be determined, and which, moreover, seems to us to be suitable in many cases on account of its simplicity.

To explain this method let us consider fig. 1, which shows the entropy of a salt, both in a zero field and in an additional field H_1, as a function of the temperature. We carry out the two following experiments :—(i.) We

† If a simple technique for cooling liquid helium by means of a paramagnetic salt is developed this difficulty will not arise, as temperature equilibrium between different substances can then easily be established.

supply the substance (in zero field) with a certain amount of heat and move from point E_0 to F. (ii.) Again we begin at E_0, but now switch on the additional field H_1, which is switched off after the same amount of heat as in (i.) is supplied to the substance. We do not reach the same point F in this case, as can easily be seen from the figure. In the entropy diagram the amount of heat supplied to the system is shown by the shaded surface on the figure

Fig. 1.

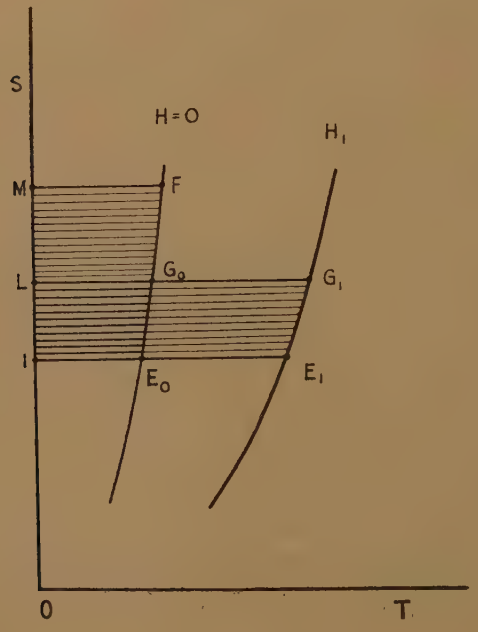

($Q=\int T dS$). Owing to the higher temperature in the additional field † we only reach a point G_0 after having switched off the field ($E_0FMI=E_1G_1LI$). It is obvious from the figure that the temperature differences are inversely proportional to the absolute temperatures ‡.

† If the change of the additional parameter (in our case the magnetic field) results in a lowering of the temperature, we end up with a higher temperature when heating in an additional field.

‡ The situation can also be expressed in the following way :—A certain influx of heat creates less increase of disorder if we allow it to flow to a body of higher temperature than to one of lower (the difference

In practice such an experiment is carried out in the following manner (fig. 2) :—To begin with, the substance (previously cooled down) is in zero field. We supply it

Fig. 2.

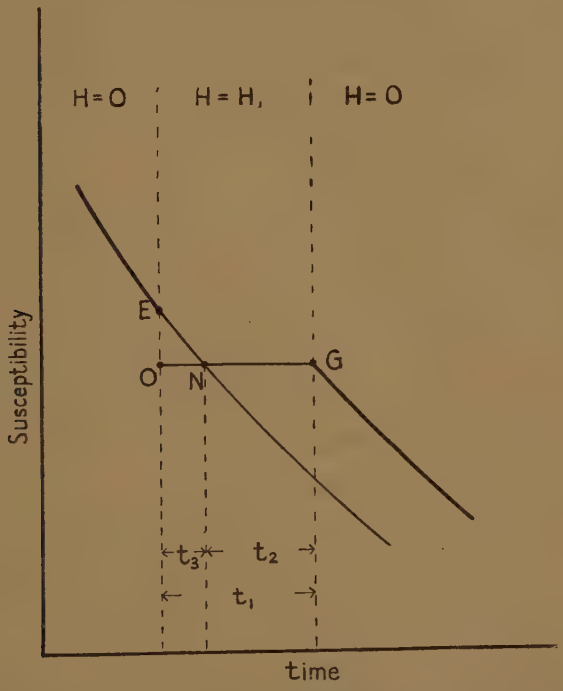

of heat content is, of course, compensated by the difference in the work done or supplied by the system). This indicates the possibility of using the following trick, which may be useful : if, for some reason or other, an experiment in which a salt has been cooled to a low temperature is interrupted, the unavoidable heating due to heat influx from the outside can be reduced by simply switching on an additional field which brings the substance to a higher temperature, *e. g.*, 0·5°. If the original temperature was, for instance, 0·05°, then after the interruption of the experiment we would find an increase in temperature only one-tenth of that which would have occurred if we had not switched on the field.

It may be helpful to illustrate these conditions by means of an " ideal " gas. For example, in one experiment we heat an ideal gas at constant volume from 10° to 11°. In a second experiment the gas, originally at the same volume and temperature, is compressed adiabatically to such an extent that it heats up to 20°. Now, the gas is supplied with the same amount of heat as in the first experiment, and heats up to 21°. After it has been expanded to its original volume again it cools to 10·5°, as equal ratios of volume correspond to equal ratios of temperature.

(for instance by means of γ-rays) with a certain amount of energy (a) per unit of time, and plot the "temperature," which is measured by any secondary thermometer (*e. g.*, the susceptibility of the salt) as a function of time. At point E the additional field H_1 is switched on while heating is continued (no measurements with the "thermometer" are necessary during that time). After a time t_1 the field is switched off again. We reach point G, and continue to heat for some time. The second part of the curve is displaced relatively to the first by an interval of time t_2.

The ratio of the average temperatures with field and without field can be obtained in the following way:— Starting from point G, we draw a line parallel to the time axis which meets the original curve produced in N. The state corresponding to the points N or G is the same, and can be supposed to have been reached in two ways: (i.) In zero field we heat from E to N, supplying a quantity of heat $a.t_3$. Thus the entropy of the substance is increased by the amount $a.t_3/T_{(0)}$. (ii.) In the additional field we heat for a time t_1, and thus increase the entropy by $a.t_1/T_{(H)}$. Both entropy changes must be equal, therefore $T_{(H)}/T_{(0)}=t_1/t_3=t_1/(t_1-t_2)$.

We have carried out several experiments, one of which we shall describe. First it is necessary to verify that the act of magnetization is really reversible, as every thermodynamic calculation depends on this fact. We have, therefore, proved this in the following way. After demagnetizing to zero field the susceptibility is measured, and the sample is then exposed to a field of the same order of magnitude as that used in the actual experiment. The field is then removed and the susceptibility again measured. If the process of magnetization or demagnetization were not reversible the sample would have a higher temperature (*i. e.*, a smaller susceptibility) at the end than at the beginning of the experiment. However, we could not find any difference at all as long as the field did not raise the temperature of the sample above 0·7° †. It was only when the temperature rose above that value that we noticed a very small difference in susceptibility, which was probably due to the fact mentioned above,

† As in these experiments we demagnetized to 0·1 only, the field that raised the temperature of the sample to 0·7 was about 3500 Gauss.

that at this temperature the thermal insulation becomes worse †.

Fig. 3 represents an experiment carried out with iron alum. The ordinate gives the galvanometer deflexions (δ), the abscissa the time in minutes. The (o) curve represents heating on zero field, the other (+), heating during which an additional field of 1440 Gauss was switched on for 588 seconds. To make the latter part of the (+) curve

Fig. 3.

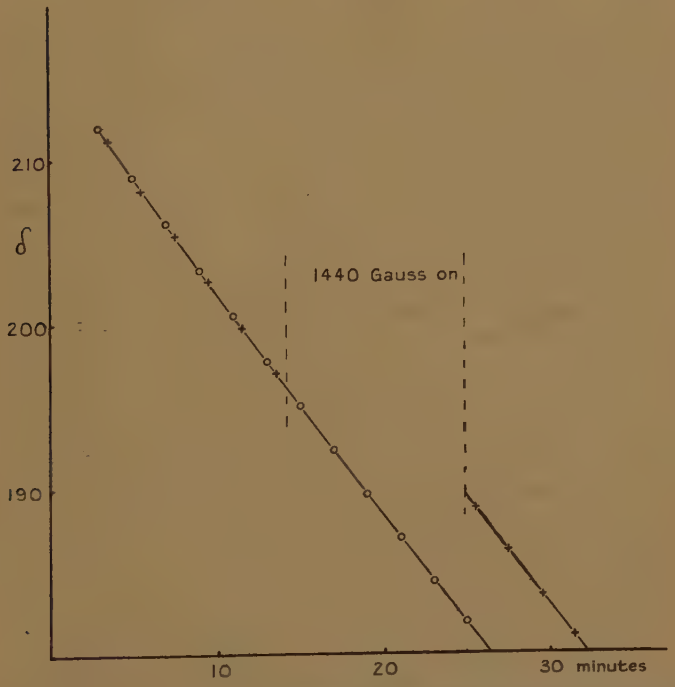

coincide with the (o) curve it has to be shifted relatively to the other by 359 seconds. According to what has been said above this means $T_{(1440)}/T_{(0)} = \dfrac{588}{588-359} = 2{\cdot}57$‡.

† The adiabatic magnetization of paramagnetic salts in this region seems to be an almost ideally reversible process. The reversibility compares favourably with any mechanical process, which is not surprising if it is remembered that the heat content of the lattice vibrations is negligible in this region. Thus there is no possibility of irreversibilities arising in temperature differences between the spin system and the lattice.

‡ In this case T_0 was about 0·12° abs.

The absolute temperature can be determined directly by taking in one such experiment as the additional field the initial field, so that the substance again reaches its initial temperature †. As one of the temperatures is now known this gives directly the absolute value of the other in zero field (or in any other which one wishes to determine).

For reasons which have been mentioned above (*i. e.*, the imperfect insulation at the initial temperature) at present this may involve some difficulty. It would be advisable therefore to proceed in the following manner, which corresponds to a certain extent to a combination with the method of de Haas and Wiersma. A series of measurements is made with rising additional fields until a temperature of about 0·7° is reached. In this way the ratio of the temperatures T_H/T_0 can be obtained, and therefore the absolute temperatures, except for an unknown factor. According to the deductions of de Haas and Wiersma the ratio $(H_e\text{-}C)/T$ approaches constancy with rising temperatures (increasing ideality of the substance). This constant region can be recognized by the fact that (T_H/T_0) is a linear function of H_e for at least three points. This function can then be extrapolated linearly to the initial field, where the temperature is known in the absolute scale and T_0 can be determined. In this way it is also possible to determine the constant ‡, which need not be found by magnetic measurements in the calibration region, as in the method of de Haas and Wiersma.

The chief advantages of this method of realizing the temperature scale are the following :—

(i.) It is not necessary to determine the absolute value of the amounts of heat supplied to the system. This of course is especially important when applying radioactive heating, which seems to be the only one which works homogeneously, a necessary condition for thermodynamic measurements.

(ii.) It is not necessary to measure any property of the salt which characterizes the state of the substance in the additional field (*i. e.*, the susceptibility of the salt) ; this

† In practice the field applied is not exactly equal to the original one, as the temperature of the salt has changed somewhat by the heating. It is, however, very simple to determine which field will bring the substance back to its original temperature by carrying out two demagnetizations from slightly different fields and finding the right field by interpolation.

‡ See also the following paper.

is important for experimental reasons, as when the additional fields are produced by a magnet with an iron core it is difficult to carry out the determination of the susceptibility.

Its chief applications seem to be the following :—

(1) To relate the absolute temperature in an additional field to that in zero field.

(2) To determine at one point the absolute temperature. This may be of interest in two cases :—(*a*) if one is interested in the absolute value of one special point (*e. g.*, the Curie point), and wishes to avoid the labour involved in determining the whole T*—T curve; (*b*) it may be preferable for purely experimental reasons to determine the proportionality factor for complete establishment of the temperature scale, mentioned in the beginning, by measuring the absolute temperature of one point instead of adjusting the T* to the T at the high temperature.

References.

(1) Kürti, N., and Simon, F., Proc. Roy. Soc. cxlix. p. 153 (1935).
(2) Kürti, N., Lainé, P., Rollin, B. V., Simon, F., VII. Congr. Int. Froid, vol. i. p. 595 (1936); Kürti, N., *Z. phys. Chem.* B, xx. p. 316 (1933).
(3) Giauque, W. F., and McDougall, D. P., Phys. Rev. xlvii. p. 885 (1935); J. Am. Chem. Soc. lx. p. 376 (1938).
(4) Keesom, W. H., *J. de Phys.* (7) v. p. 373 (1934).
(5) Kürti, N., and Simon, F., Proc. Roy. Soc. cxlix. p. 161 (1935).
(6) Kürti, N., and Simon, F., Proc. Roy. Soc. clii. p. 21 (1935); Kürti, N., Lainé, P., Simon, F., *C. R.* cciv. p. 754 (1937).
(7) Clark, C. W., Thesis, Leiden (1935).
(8) de Haas, W. J., and Wiersma, E. C., 'Physica,' iii. p. 491 (1936).
(9) Kürti, N., Rollin, B. V., Simon, F., 'Physica,' iii. p. 266 (1936).
(10) Giauque, W. F., Ind. and Eng. Chemistry, xxviii. p. 743 (1936); Giauque, W. F., Stout, J. W., Clark, C. W., J. Am. Chem. Soc. lx. p. 1053 (1938); Allen, J. F., and Shire, E. S., 'Nature,' cxxxix. p. 878 (1937); Proc. Camb. Phil. Soc. xxxiv. part ii., p. 301 (1938); de Haas, W. J., Casimir, H. B. G., van den Berg, G. J., 'Physica,' v. p. 225 (1938); van Dijk, H., Keesom, W. H., and Steller, J. P., 'Physica,' v. p. 625 (1938).

LXXIII. *Remarks on the "Curie" Scale of Temperature.* *By* N. Kürti *and* F. Simon, *Clarendon Laboratory, Oxford* †.

[Received August 11, 1938.]

IN the region attained by the magnetic method the "temperature" is usually determined by measuring the susceptibility of the salt and extrapolating it according

† Communicated by the Authors.

to Curie's law (T* scale). If this scale is regarded simply as an intermediate stage for establishing the absolute scale it obviously does not matter in what way it is defined as long as there is an unambiguous correlation between the two scales. The values are only used in order to recognize the state of the substance in further experiments.

It is not practicable, however, to establish the absolute scale in every case, as it necessitates rather painstaking experiments, nor is it yet possible in general to use secondary thermometers † which have been calibrated directly against the absolute scale, so that in most experiments the T* are the only data given. Except by the specialist there seems to be a tendency to attribute a greater significance to the T* than is warranted. Moreover, with the present method of defining the T* scale long calculations are necessary to correlate data found in different laboratories, because they have been obtained under different conditions (and sometimes the conditions are not defined at all). For these reasons we are suggesting a method of defining the T* scale satisfactorily.

The susceptibility, from which T* follows by definition, is usually determined by measuring the magnetization I of the substance produced by a homogeneous external field H_e. On account of the influence of the demagnetizing field I is, in the same external field, dependent on the shape of the sample, and it is only when the sample is in the form of an ellipsoid that I has a constant value over all of it (In the following the ratio length/diameter of the ellipsoid is denoted by p.) If κ_p represents the apparent susceptibility depending on the shape of the sample ($\kappa_p = I/H_e$), we obtain by a simple calculation [1] the following relation between the apparent susceptibilities of two samples with different p :—

$$\kappa_{p_1} = \frac{\kappa_{p_2}}{1+(N_{p_1}-N_{p_2})\kappa_{p_2}} \quad (N = \text{demagnetizing factor}).$$

The T* scale is obtained by using the relation between susceptibility and temperature given by Curie's law. It is obvious that only one definite shape (which one will be discussed later) can give a straight line in the κ_p, 1/T diagram. In the temperature region of liquid

† See the preceding paper.

helium, where calibration is carried out, the deviations from a straight line for any other shape are so small that they are normally covered by the inaccuracies of the measurement, and, for all shapes, straight lines can be

Fig. 1.

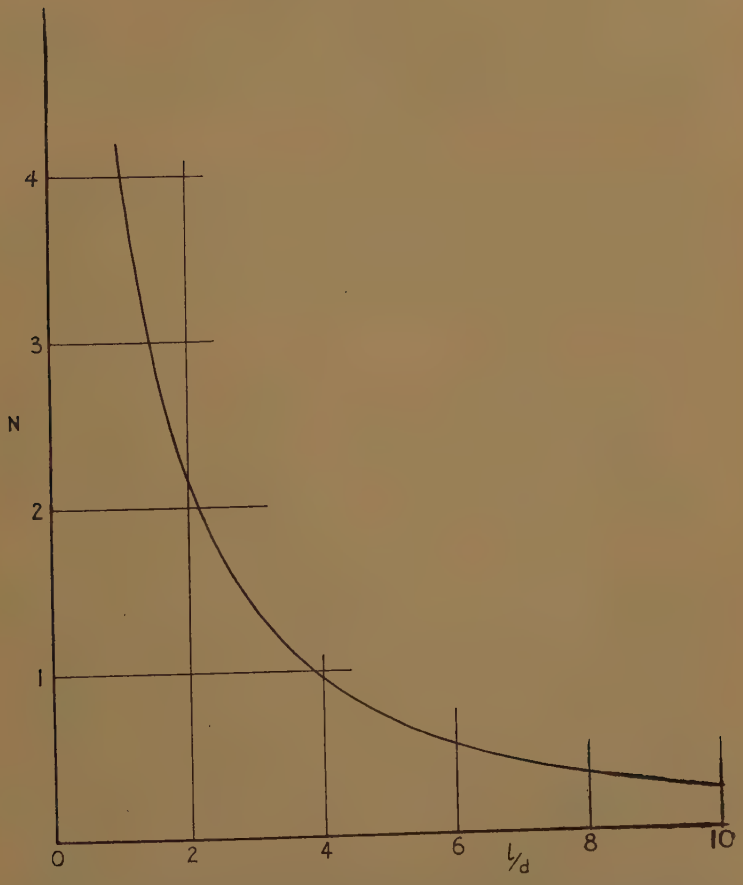

drawn through the experimental points. In using these lines to calculate the T* at very low temperatures, however, considerable differences occur.

We have calculated these differences on the assumption that the calibration curve was adjusted at temperatures T′ and T″ (which is very nearly equivalent to drawing the best straight line through the experimental points

between T′ and T″). We obtain the following formula for the difference in the T* between any two ellipsoids of shapes characterized by p_1 and p_2:—

$$T^*_{p_1}-T^*_{p_2}=\Delta-\frac{T'+T''-\Delta-T^*_{p_2}}{(T'T''/\Delta T^*_{p_2})-1}, \quad . \quad . \quad . \quad (1)$$

where

$$\Delta=(N_{p_1}-N_{p_2})c \quad . \quad . \quad . \quad . \quad . \quad . \quad (2)$$

(c = Curie-constant per c.c.).

For very low temperatures this expression reduces to

$$T^*_{p_1}-T^*_{p_2}=\Delta.$$

In fig. 1 we give the values of the demagnetizing factor $N^{(2)}$, and in the following table the Curie-constants per c.c. and the Δ (according to formula (2)) for the difference between a sphere and an ellipsoid $p=3$ for those substances which are most frequently used in the magnetic method.

Substance.	c.	$\Delta°$.
Gadolinium sulphate	$5{\cdot}85\ 10^{-2}$	0·166
Manganese ammonium sulphate ..	$2{\cdot}00\ 10^{-2}$	0·057
Iron ammonium alum	$1{\cdot}55\ 10^{-2}$	0·044
Chromium potassium alum	$0{\cdot}66\ 10^{-2}$	0·019
Titanium cæsium alum	$0{\cdot}13\ 10^{-2}$	0·0037

In fig. 2 we give the variation of $T^*_{p=1}-T^*_p$ according to formula (1) (between ellipsoids of various p's and a sphere $p=1$) with T^*_p for iron-alum, taking for T′ and T″ 2° and 4° respectively. It can be seen from these curves that while the differences are very small in the calibration region, and their relative values quite negligible, they reach very high values at low temperatures. If, for example, we were to measure a temperature for which, with an ellipsoid ($p=3$), $T^*_{p=3}=0{\cdot}01°$, and then the same temperature with a sphere, we would find in the latter case $T^*_{p=1}=0{\cdot}054°$, which means that, for the same actual temperature, the two T* would have a ratio 5·4 : 1 †. Obviously these differences will be smaller for substances with small c, *i. e.*, either substances possessing a small magnetic moment (*e. g.*, Cs-Ti-alum)

† We have verified this experimentally by demagnetizing (*a*) an ellipsoid ($p=3$) and (*b*) a sphere, of iron-alum, with the same initial conditions, so that the same actual temperatures were reached.

or systems in which the magnetic ions are highly diluted (mixed crystals). On the other hand, these substances are generally used to reach lower temperatures where the relative differences may still be important.

In addition to the question of an unambiguous definition of the T* scale we have to discuss which shape to choose. Obviously T* should be defined in such a manner that at high temperatures T* and T coincide. This means that we have to choose the shape which we expect to give a straight line in the K_p, 1/T diagram. As, according

Fig. 2.

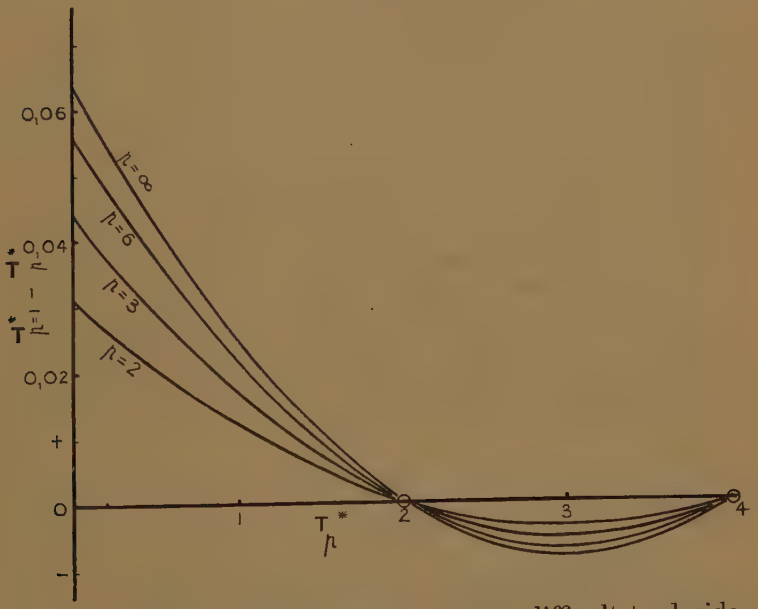

to what has been said above, it is very difficult to decide this experimentally † at present, we have to rely on

† We intend to investigate this question experimentally. This may be done in two different ways—either by measuring the susceptibility in the calibration region, or by determining C in the term $(H_e\text{-}C)/T$, which, according to de Haas and Wiersma, has to be a constant at high temperatures (see the preceding paper).

It should be mentioned at this point that, when it has been confirmed experimentally that, for a sphere, T* and T coincide at high temperatures, the best way of correlating the vapour pressure of helium with the temperature in the region below 1·5° K. seems to be the calibration against susceptibility of a salt, using, of course, a salt with a low characteristic temperature, so that the deviations arising from the interaction forces are negligible.

theoretical considerations. It is generally assumed that Curie's law will hold if the susceptibility is defined as the ratio of magnetization to the *internal* field H_i, *i. e.*, the field acting on the elementary magnets. This internal field is equal to the sum of the external field and the Lorentz field minus the demagnetizing field, and consequently that particular shape in which the demagnetizing field and the Lorentz field cancel out[1] should give a straight line in the K_p, 1/T diagram.

As one can assume[3] that at the "high" temperatures, where calibration is carried out, the expression $(4\pi/3)I$ for the Lorentz Field is correct, the required shape is that of a sphere, the demagnetizing field of which equals $-(4\pi/3)I$. We have therefore decided, some time ago, to use a $T^*_{p=1}$ scale for representing our experiments, and we should like to suggest that this procedure be adopted generally and that these "temperatures" be denoted by T⊛.

This does not mean, of course, that the measurements must be carried out with actual spheres; any ellipsoid can be used, and the corresponding T⊛ can be calculated in the following simple manner. The galvanometer deflexions in the calibration region are plotted against $1/(T-\Delta)$ (where Δ, according to formula (2), is given by $(N_{p=1}-N_p)$, instead of against 1/T. The T* derived in this manner are identical with the T⊛ which would be obtained by actually using a sphere †.

References.

(1) See, for instance, C. J. Gorter, Arch. Mus. Teyler, vol. vii. p. 194 (1933).
(2) See, for instance, Maxwell, 'Treatise,' 3rd ed. vol. ii. p. 69.
(3) Van Vleck, T. H., Tourn. Chem. Physics, vol. v. p. 320 (1937).
(4) Kürti, N., Lainé, P., Simon, F., *C. R.*, cciv. p. 675 (1937).

† This is, of course, true only in the region above the Curie point[4] Below that temperature the form of the sample affects all the magnetic properties, and therefore the properties of one form cannot be calculated in a simple way from the behaviour of another.

LXXIV. *The Diffraction of X-rays by an Age-hardening Alloy of Aluminium and Copper. The Structure of an Intermediate Phase.*

By G. D. Preston, *M.A., National Physical Laboratory* *.

[Received September 5, 1938.]

[Plates VI.–VIII.]

Introduction.

In a recent paper [1] an account was given of an effect observed in the X-ray spectrum of single crystals of an alloy of high purity aluminium with 4 per cent. by weight of copper, age-hardened at room- and elevated temperatures. The first part of the present paper contains a description of the changes observed at different stages of the age-hardening process at room-temperature and at 200° C., attention being particularly directed to correlating the changes of the X-ray spectrum with the hardness of the metal. The results described are in agreement with those published independently by Guinier[2] and his collaborators. In the second part of the paper the structure of the phase which separates from the crystal after prolonged treatment at 200° C. is described. All the experiments were carried out on the same crystal, grown by the strain-anneal method in a 1 mm. diameter wire, so that the paper forms a history of the reaction taking place in the solid. Owing to certain difficulties in the interpretation of the observed diffraction effects the contents of the first part of the paper are of a qualitative character, but it is hoped that publication of the results will direct attention to these problems and so lead to their solution. The reaction investigated is taking place in a metal, but the methods employed in its study are quite generally applicable to any material obtainable in the form of small single crystals; the results obtained suggest that the use of X-ray analysis may throw light on the mechanism of chemical reactions in the solid state.

Part I.

For the purpose of illustrating the type of experimental data obtained I have selected for description a series of

* Communicated by Dr. C. H. Desch, F.R.S.

Laue photographs of a single crystal wire orientated with a (110) direction parallel to the X-ray beam. The crystal was mounted in a small aluminium holder, which fitted the goniometer head of the X-ray spectrograph, so that X-ray examination could be carried out immediately after heat treatment of the specimen in its holder. Delay due to the necessity of re-orientating the specimen after each heat treatment was thus avoided, since the holder could be removed from and replaced in the spectrograph without disturbing the orientation of the crystal. After heat treatment at 500° C. to get the copper into solution the crystal was quenched and photographed immediately, the orientation having been previously determined. The exposure time amounted to 1·5 hours, so that the photograph records any changes which take place in that period. Similar photographs were taken after 4 hours, 24 hours, and 16 days at room-temperature. The general appearance of these photographs can be seen in fig. 2 (Pl. VI.), which is a print of that obtained from the crystal after 24 hours at room-temperature. In addition to the normal Laue spots there appear on the diagram two pairs of streaks and two short rays emerging from the central spot, one on either side of it. These are present on the photograph taken immediately after quenching, but are much fainter and much broader. Whether their presence is typical of the solid solution or whether they appear during the exposure has still to be determined. After 4 hours at room-temperature the streaks are distinctly stronger and narrower, and after 24 hours are sufficiently well developed to be reproduced. A further period of 15 days at room-temperature produces little change in the appearance of the photograph, but the streaks become narrower and more intense.

The changes of hardness which occur at room-temperature in polycrystalline material are illustrated in the left-hand side of fig. 1. As hardness tests could not be carried out on the specimen used for X-ray examination, owing to the necessity of preserving it in an undistorted state, it must be assumed for the moment that the single crystal specimen behaves in the same way as poly-crystalline material. Inspection of the figure shows that during the first day at room-temperature the hardness increases rapidly, after that more slowly, reaching a state of stability in about four days. Only small changes then occur

over prolonged periods, the rate of increase having become too small to be measurable in any reasonable time. From what has been said in the preceding paragraph it will be understood that the increase in hardness at room-temperature is accompanied by an intensification and narrowing of the streaks on the Laue photographs.

When the alloy, fully aged at room-temperature, is subjected to heat treatment at 200° C., the hardness changes in the manner shown at the right-hand of fig. 1. The effect of a few minutes heat treatment at 200° C. is to reduce the hardness to a figure nearly equal to that obtained in the alloy in the quenched condition. Further exposure at 200° C. results in a rapid increase of hardness during the first two hours, the hardness attaining a maximum in about five hours and thereafter diminishing

Fig. 1.

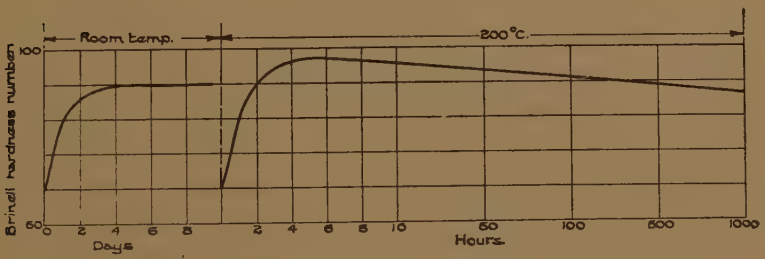

slowly over a period of the order of 500 hours. It should be noted that the time-scale in the figure has been adjusted in order to make evident the changes to which attention is here directed. The hardness changes resulting from heat treatment at 200° C. are accompanied by remarkable alterations in the appearance of the Laue photographs, which may be summarized as follows :—

(i.) 10 *minutes at* 200° C.—The hardness produced at room-temperature disappears ; both the streaks and the two central rays are almost absent from the Laue photograph. The very faint traces of the streaks which remain are quite narrow.

(ii.) 20 *minutes at* 200° C.—Hardness increasing ; the streaks begin to reappear, but are quite narrow.

(iii.) 30, 45, and 105 *minutes at* 200° C.—Hardness increasing ; streaks growing stronger. The last of these

photographs is reproduced in fig. 3 (Pl. VI.), for comparison with that obtained from the crystal aged for one day at room-temperature, fig. 2 (Pl. VI.).

(iv.) 3 *hours at* 200° C.—Hardness approaching its maximum ; the streaks show signs of resolution into a pair of ill-defined spots.

(v.) 6 *hours at* 200° C.—Hardness beginning to diminish ; the streaks now obviously showing resolution into two elongated spots. This photograph is reproduced in fig. 4 (Pl. VII.), and may be compared with one previously published, showing a crystal aged for 26 days at 150° C., a period which somewhat exceeds that necessary to

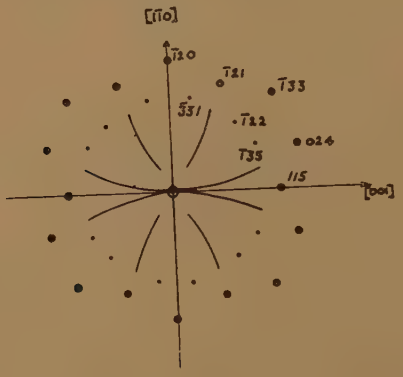

Key to figs. 2–5 (Pls. VI. & VII.).

produce maximum hardness at that temperature. It will be noticed that the pair of central rays has almost disappeared.

(vi.) 9 *hours at* 200° C.—Hardness continues to diminish slowly ; the outer of the two spots grows fainter and the inner one more intense ; the central rays disappear.

(vii.) 27 *hours at* 200° C.—Hardness diminishing slowly ; the outer spot has disappeared and the inner one is very intense and elongated ; a number of new spots have made their appearance.

(viii.) 2 *days and* 19 *days at* 200° C.—Improvement in the resolution of the newly formed spots continues ; the intense inner spot referred to above still shows distinct

signs of radial elongation even after 19 days heat treatment, as may be seen in fig. 5 (Pl. VII.).

In the previous paper it was concluded that the type of X-ray diffraction pattern obtained from this alloy was consistent with the view that in the crystal there existed regions, in the form of thin plates parallel to the (100) planes, in which copper was segregated and the spacing was slightly smaller than the normal spacing of the alloy. The question now arises as to how many planes of atoms in copper are associated with each of these regions and what is their area ?

A very rough estimate of the thickness of the diffracting elements can be formed by making use of the generally accepted fact that broadening of the X-ray diffraction spots begins to be visible when the crystal size is of the order of 10^{-4} cm., or about 10^3 crystal units of aluminium. In the state produced by 19 days annealing at 200° C. the resolution of the Laue spots is not quite perfect, so we may conclude that the newly-formed particles are of about 10^3 crystal units linear dimension. The comparative perfection of the aluminium Laue spots, which remain quite sharp throughout the process, indicates that the diffuseness of the new spots is to be ascribed to smallness of the diffracting particles rather than to the presence of strains in the crystal. In the earlier stages of the ageing process the elongation of the new spots suggests poor resolving power, such as might be associated with a grating of 100 elements or less.

A more accurate estimate of the thickness of the regions causing the streaks can be derived as follows :—In oscillation photographs taken with monochromatic copper radiation the streaks associated with the zero order reflexion are recorded. They extend from the central spot outwards to a point corresponding to $\sin\theta = 0{\cdot}183$; the corresponding value of $d = 4{\cdot}2$ Å. being approximately twice the spacing $(a/2)$ of the (100) planes of aluminium. Thus the extremities of the lines radiating from the central spot lie midway between the central spot and the first spectrum (200) from the cube-faces. If single planes rich in copper are distributed at widely separated intervals in the crystal we would expect to find a streak joining the normal spectra in rows, such as (h, k, l) $(h, k, l+2)$, etc. If the heavy planes occur in widely separated pairs, the

distance between planes of one pair being a, the spacing of aluminium, then the intensity of the streak would vanish midway between successive normal spectra in every row. If the planes occurred in groups of threes the intensity of the streak would vanish twice between the normal spectra. The observed length of the streaks is consistent with the view that the heavy planes occur in groups of two or three, the groups being separated by distances na, where n is large and varies between successive groups. A similar result can be obtained from the lines emerging from the (111) reflexions. To a point on one of these lines indices (11 z) can be assigned, where z lies between 1 and 2. Measurement of the photographs (*e. g.*, fig. 2(*a*) of the previous paper) shows that z approaches 2 at the extremity of the lines, which, therefore, disappear midway between the spectra (111) and (113).

The fact that the observed intensity distribution is not symmetrical about the normal reflexions may necessitate some modification of the above estimate. The dissymmetry has been ascribed to the presence locally of a slightly reduced spacing, the effect of which is to remove energy from one side of the maxima and to pile it up on the other. This will have the effect of making the estimated value of the number of " heavy " planes too small, by extending the streak further from the origin. In spite of this it seems that only a few planes are operative, probably less than five, and perhaps no more than two.

It is much more difficult to obtain any quantitative measure of the area of the regions rich in copper. The width of the streaks is a measure of the area, but I have not been able to make any measurements capable of quantitative interpretation. There is no doubt that the great breadth of the streaks during the first few hours of ageing at room-temperature indicates a very small area, probably of the order of 10 atomic distances. As ageing proceeds at room-temperature the streaks get narrower, revealing an increase of the areas of the regions rich in copper. Even after some weeks at room-temperature the edges of the streaks shade off gradually into the background, so that a small area is still operative. When the streaks reappear during heat treatment at 200° C. they are quite sharp at the edges and the area of the regions causing them must be large, of the order of 10^3 atomic distances.

The disappearance of the streaks produced at room-temperature after a few minutes heat treatment at 200° C. can be explained by supposing that all of the smaller regions developed at the lower temperature have re-dissolved. Further exposure at 200° C. then results in the growth of the remaining larger plates. This suggests that there may be a size of plate characteristic of the temperature at which the reaction is taking place ; when the reaction has proceeded for some time at room-temperature the effect of raising the temperature is to destroy the existing structure, and time is required for diffusive processes to build up the larger structure characteristic of the higher temperature.

Part II.

The structure present after the crystal has aged for 19 days at 200° C., illustrated in fig. 5 (Pl. VII.), is sufficiently well developed to make it possible to carry out a detailed analysis. Knowledge of the exact nature of this structure might throw light on the processes at work in earlier stages of the reaction, when the diffraction effects are difficult to interpret. Wasserman and Weerts have already reported the existence of an intermediate phase in these alloys, to which they assign a tetragonal structure with $a=8{\cdot}1$ and $c=11{\cdot}4$ Å. Although the structure of the phase described below is not the same as that reported by Wasserman and Weerts[3], the latter may exist at some earlier stage of the reaction.

The analysis of the photographs is complicated by the presence of three crystals of the new phase, one associated with each cube-face of the aluminium lattice. The specimen has been examined by the oscillating crystal method, with the axis of oscillation parallel to (001), (011), and (111) directions of the aluminium crystal. The results of these three series of experiments are summarized below.

(*a*) *Axis of Oscillation* (001).—Photographs were taken with a range of oscillation of 15° ; three photographs, in which the (100) direction of the aluminium covered the intervals 0°–15°, 15°–30°, and 30°–45° to the incident beam, were sufficient to record all the reflexions at least once. The radius of the cylindrical camera was 3 cm. ; the normal aluminium reflexions occur on the central

and the first and second layer lines corresponding to a spacing of 4·04 Å. The vertical heights, Y, of the first and second layer lines are calculated to be 1·24 and 3·53 cm., the observed values were 1·25 and 3·5 cm. In addition to the aluminium reflexions a number of other weaker reflexions were observed. These fell into two groups (*a*) lying on the aluminium layer lines, (*b*) lying on layer lines, for which Y = 0·8, 1·9, and 3·9 cm. These distances correspond, within the limits of accuracy of measurements, to a spacing of 5·8 Å., for which the calculated values of Y are 0·82, 1·87, and 3·93 cm. This spacing is a little greater than $4{\cdot}04\ \sqrt{2}=5{\cdot}71$ Å., the difference being hardly greater than the error involved in the determina-

Fig. 6.

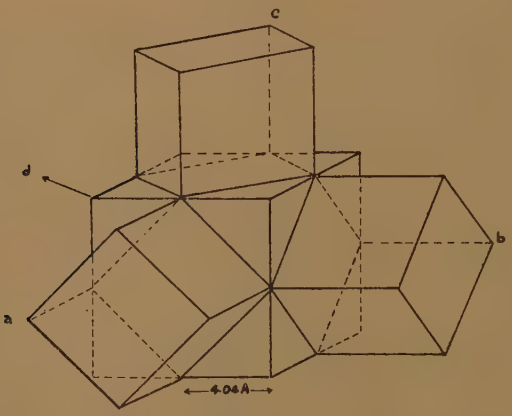

tion of the figure 5·8 Å. from the spacing of the layer lines. A possible arrangement of three crystals on the (100) faces of the aluminium is shown in fig. 6. Here the cube *d* represents 8 units of the aluminium lattice ; the cubes *a*, *b*, and *c* have a pair of their edges parallel to the face diagonals of the aluminium unit, the length of these edges is $4{\cdot}04\sqrt{2}=5{\cdot}71$ Å. The third edge is normal to the faces of the aluminium unit. This arrangement will produce spots on the layer lines observed ; the reflexions from crystals *a* and *b* rotating about their (011) axes will lie on the layer lines of a simple cube of side 4·04 Å. rotating about its (001) axis. Crystal *c* will produce layer lines corresponding with a spacing of 5·71 Å. if the units are cubic. It should be understood that fig. 6 is

diagrammatic only, and is intended to show the relative orientation of the crystals. It is not suggested that in the aluminium groups of the shape illustrated exist. The crystals *a*, *b*, and *c* are rather to be thought of as sheets extending over many units of the aluminium crystal *d*, the relative orientation being as shown.

The photographs were analysed by the usual graphical methods to ascertain whether the observed spots were consistent with a cubic unit of side 5·7 Å., attention being paid to the possibility that one edge might slightly exceed this figure. It was found that indices could be assigned to all the spots, over 70 in number, and that in every case the indices were all even or all odd. The unit is therefore face-centred. Confirmation of the fact that the unit is not quite cubic was obtained in the following way. On the central layer line of the right-hand side of the first photograph the reflexions (117) of crystal *a* and (551) of crystal *b* should appear, and they should be superimposed if the crystals are cubic, Σh^2 being 51 in each case. The spots are actually separated by about 3 mm. on the film. They were also recorded on a photograph taken with monochromatized copper radiation in which the range of movement of (100) of the aluminium crystal was 5–10° to the incident beam. Near them and on the same film is the (420) reflexion of aluminium which serves to calibrate the film in this region. The figures are as follows :—

	x cm.	sin θ.
420 Al	6·1	0·850
117 *a*	7·4	0·943
551 *b*	7·7	0·959

The axial ratio *c* is now found by the relation :—

$$\frac{\sin\theta_{551}}{\sin\theta_{117}} = \left\{\frac{50+\frac{1}{c^2}}{2+\frac{49}{c^2}}\right\}^{\frac{1}{2}} = \frac{0{\cdot}959}{0{\cdot}943} = 1{\cdot}017,$$

whence $c^2 = 1{\cdot}03$ and $c = 1{\cdot}015$.

Taking $a = 4{\cdot}04\sqrt{2} = 5{\cdot}71$ Å., $ac = 5{\cdot}80$ in agreement with the estimate made from the separation of the layer lines.

Of the possible reflexions of the face-centred cube up to and including $\Sigma h^2=51$, all were observed except (200), (222), (420), (600), (442), and (622), all the planes, in fact, for which $\Sigma h=4n+2$. Before considering the implications of this fact I will briefly summarize the observations made with (011) and (111) as axes of oscillation.

(*b*) *Axis of Oscillation* (011).—Photographs were taken with radiation from a copper target filtered through nickel and also with a monochromatic beam of copper radiation. In both cases six photographs with a range of oscillation of 15° each were taken, the whole interval of 90° covered by each set of six photographs being sufficient to record all the reflexions. The monochromatic photographs proved particularly valuable in determining the structure, owing to the absence from them of the lines into which the Laue spots are drawn out. On the other hand, they suffer from one defect due to the fact that the monochromator reflects not only the copper characteristic $\lambda=1{\cdot}54$ Å. in the first order, but also $\lambda/2=0{\cdot}77$ Å. in the second order. The photographs therefore present what are apparently half order reflexions of the aluminium crystal; reflexions of this type were obtained from a crystal of aluminium, so that there is no doubt that they arise from the presence of the half wave-length in the beam. In normal circumstances the presence of these reflexions would not matter, but in the present instance the ratio of the parameter of the aluminium and the precipitate is exactly $1:\sqrt{2}$, so that confusion may arise. For instance, the wave-length 0·77 Å. is reflected by aluminium (200) at an angle for which $\sin\theta=0{\cdot}191$ This is the angle at which a cube of side 5·7 Å. will reflect wave-length 1·54 from the (110) planes Reference to fig. 6 shows that (200) planes of aluminium are parallel to (110) planes of the new phase, so that the reflexions occur at the same orientation of the whole crystal and cannot be resolved. If the reflexion (110) of the new phase is present the structure cannot be face-centred. A decision has been effected by comparing the monochromatic photographs with those obtained with filtered radiation. The doubtful spots are part of the lines, due to the white radiation, into which Laue spots are drawn out by the oscillation of the crystal; if the spots are really due to a reflexion such as (110) from the new phase a

local intensification of the Laue streak should be observed. In no case has this happened and it has, therefore, been assumed that there is no reason for supposing that the new structure is not face-centred.

Reference to fig. 6 shows that when the axis of oscillation is parallel to a (011) direction of the aluminium, one of the other crystals is rotating about an edge (100). The reflexions from this crystal fall on layer lines at heights $Y = 0{\cdot}84$, $1{\cdot}92$, and $4{\cdot}14$ cm. above and below the central line. The other two crystals are oscillating about a line which is not a crystal edge, so that the reflexions are scattered over the films. The observed values of Y confirm the tetragonal nature of the unit. Indices were assigned to all observed reflexions, over 100 in number, with the same result as that obtained in the preceding paragraph, *i. e.*, no mixed indices are observed and all reflexions for which $\Sigma h = 4n+2$ are absent.

(*c*) *Axis of Oscillation* (111).—Photographs with filtered copper radiation were obtained with a 15° range of oscillation. Two such photographs covering a range of 30° are sufficient to record all reflexions. A set of six photographs taken with monochromatic copper radiation was also obtained with an oscillation range of 5° in each photograph. Analysis of these photographs completely confirmed the results already described. Owing to the presence of all reflexions on only two photographs, these are suitable for making an estimate of the relative intensity of the reflexions with a view to a complete determination of the structure. The results are described in the following paragraph.

(*d*) *Intensity of Reflexion.*—The relative intensities of the diffraction spots were estimated by comparison with a strip of film of which neighbouring portions had been exposed to X-rays for times t, $2t$, $3t$, $4t$, etc. The photographs with (111) as oscillation axis were used, as all planes are recorded on two photographs. The results are collected in Table I., where it will be seen that the reflexions fall into three groups. One, for which $\Sigma h = 4n+2$, is not observed ; of the others, the reflexions of planes with $\Sigma h = 4n$ are strong compared with those for which $\Sigma h = 4n \pm 1$.

Now in the calcium fluoride type of structure the reflexions are divided into three groups. If we denote

the atomic scattering factors of the two atoms by A and B then the structure factor is :—

$$\begin{aligned} &\text{when } \Sigma h = 4n \qquad F_1 = 4\,(A+2B),\\ &\quad,, \qquad 4n \pm 1 \qquad F_2 = 4\,A,\\ &\quad,, \qquad 4n+2 \qquad F_3 = 4(A-2B). \end{aligned}$$

In addition $F=0$ unless the indices are all even or all odd. The atomic scattering factors are proportional to the atomic numbers, 29 for copper and 13 for aluminium, so that if we assume a composition $CuAl_2$, F_3 will be very small compared with F_1 and F_2, and planes for which $\Sigma h = 4n+2$ will reflect too feebly to be observed. Substituting the numerical values of A and B we have

$$F_1 : F_2 : F_3 = 55 : 29 : 3,$$

and to a first approximation the intensities will be proportional to the squares of the F's, so that

$$I_1 : I_2 : I_3 = 3{\cdot}6 : 1 : 0{\cdot}01.$$

These figures are included in the last column of Table I. under F^2, and it will be seen that the observed intensities follow the variations of F^2 quite closely.

The above treatment can only be regarded as an approximation, the atomic scattering factors, A and B, have been treated as constants, whereas they should be functions of θ ; polarization, absorption, and temperature factors have been neglected, and the intensities may be affected by the shape of the diffracting particles. The effect of including these factors will be to alter the intensities, but the relative intensity of neighbouring lines will not be greatly changed. In view of the crudity of the intensity measurements, which are no more than estimates, there is little to be gained by elaborating the treatment. In spite of these omissions we may conclude that the structure of the new phase is of the calcium fluoride type, but tetragonal having $a = 5{\cdot}71$ Å. and $c = 1{\cdot}015$, and that the composition is $CuAl_2$. The structure consists of a face-centred tetragonal cell of copper atoms intermeshed with a simple cell of aluminium atoms of half the dimensions ; the copper atoms lie at the centres of cubes of aluminium atoms so that the structure may be described as body-centred, with one-half of the centre atoms missing. A similar structure has been reported[4] for $AuAl_2$. The

most interesting feature of the unit is the presence on its faces of a net of copper atoms distributed at the corners of a 4·04 Å. square, which fits exactly into the aluminium lattice. The reason for supposing that the two lattices are joined on (100) faces, as illustrated in fig. 6, is that in the earlier stages of the reaction, described in Part I., the (100) planes of the aluminium lattice are singled out as those on which something is happening. If some other set of planes were selected more than three sets of new crystals would have been produced. Even in the later

TABLE I.

h^2.	*hkl*.	I (obs.).	F^2.
3	111	2·5	1
4	200	0	0
8	220	7·0	3·6
11	311	2·2	1
12	222	0	0
16	400	6	3·6
19	331	2·0	1
20	420	0	0
24	422	5·1	3·6
27	333	2	1
	511	1·6	1
32	404	4	3·6
35	531	1	1
36	600	0	0
	442	0	0
40	620	4	3·6
43	533	1	1
44	622	0	0
48	444	4	3·6
51	711	1	1
	551	1·5	1

stages of the reaction, when the new crystals are well developed, there is evidence that the (100) planes are really in contact. The reflexions of the new crystals appear as satellites accompanying the reflexions of the aluminium, and in certain cases the two spots are joined by a bridge of reflected radiation. This is illustrated by the reproduction in fig. 7 (Pl. VIII.), which shows part of one of the photographs taken with (011) as oscillation axis. A (111) reflexion of aluminium appears on the central layer line, and diverging from it two faint lines on each of which is situated a reflexion (220) of the new crystal. Any

point on one of these lines can be given indices, referred to the aluminium lattice, of the type (11 Z), which means that the (001) plane is in some way associated with the new crystal. Although structurally different the two crystals form one diffracting unit, and the plane of union is (001). A fuller interpretation of the significance of this intensity bridge between the diffraction spots of the two crystals is much to be desired, as it might throw further light on the relation of the phases.

The presence of three crystals of the new compound, one on each cube-face of the aluminium lattice, adds considerably to the difficulty of the analysis of the X-ray photographs. It appeared, therefore, to be advisable to apply a check to the structure proposed in the preceding paragraphs. The atomic numbers of calcium and fluorine are 20 and 9, and are nearly in the same ratio as those of copper, 29, and aluminium, 13. The spacing of fluor-spar is 5·46 Å., just 5 per cent. less than that of the proposed structure of the new compound. It should therefore be possible to reconstruct the Laue photographs of the composite aluminium and $CuAl_2$ crystal from Laue photographs of CaF_2. This has been attempted, and the result is to confirm the analysis of the oscillating crystal photographs. The comparison is shown diagrammatically in fig. 8, where (*a*) and (*b*) are Laue diagrams of CaF_2 drawn from photographs taken under the same conditions as those used in obtaining a Laue photograph of the alloy. In (*a*) the X-ray beam is parallel to a (100) direction, and in (*b*) it is parallel to (110) ; in both (001) is vertical. These diagrams are now superimposed in such a way as to reproduce the relative orientations shown in fig. 6. To do this a line AB is drawn on a piece of tracing-paper and placed on the line A_1B_1 on fig. 8 *a*, which is then traced. Two tracings are now made from fig. 8 *b*, in one AB is placed on A_2B_2 and in the other on A_3B_3 : part of the composite diagram so obtained is shown in fig. 8 *c*. If the assumptions as to the orientations of the crystals made in the analysis of the oscillation photographs are correct, then this diagram should account for all the new Laue spots on the photographs of the alloy. A tracing of part of a Laue photograph of the alloy, aged for 50 days at 200° C., is shown in fig. 8 *d* ; it closely resembles fig. 8 *c*.

The resemblance is, in fact, so close that it might be

assumed that there is no difference between the reconstructed Laue diagram 8 *c* and the observed 8 *d*. There are, however, small changes in the positions of the diffraction spots, which are due to the fact that CaF_2 is cubic and the structure in the alloy is not. The most obvious of the changes of position is that of the group of four spots on the vertical and horizontal axes of fig. 8 *c* ; the reflexions (221) of aluminium, (031) of crystal (*a*), and (3$\bar{1}$3) of crystals (*b*) and (*c*). Comparison with the photograph

Fig. 8.

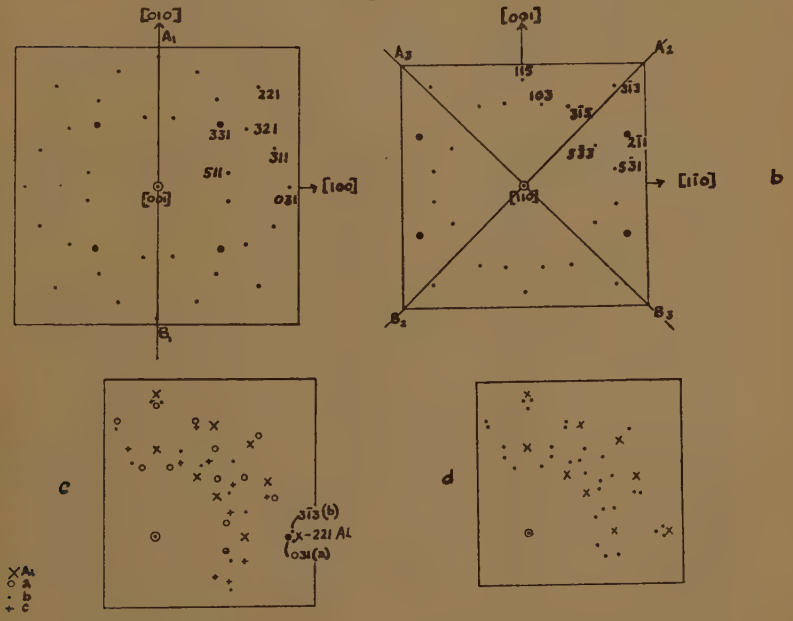

of the alloy shows that (031) is too close to the centre and (3$\bar{1}$3) too close to (221) of aluminium. Measurement of the film yielded the following figures :—

Aluminium.	S cm.	cos ϕ. Observed.	cos ϕ. Calc.
031	7·50	0·3162	0·3162
221	8·08	0·3333	0·3333
Alloy.			
031 (*a*)	7·35	0·3116	
3$\bar{1}$3 (*b*) and (*c*)	7·85	0·3267	

In this table S is the diametral distance, measured across the film, between corresponding reflexions; the photograph was taken with 5 cm. between specimen and film, so that $S=10 \tan 2\theta$ and $\phi=90-\theta$. For the aluminium spots observed values of $\cos \phi$ agree with the calculated values, $1/\sqrt{10}$ and $1/3$. The value for the reflexions of the alloy have been used to calculate the axial ratio: for the point (031) crystal (*a*) we have

$$\cos \phi = \frac{1/c}{\sqrt{9+1/c^2}},$$

and for (3$\bar{1}$3) crystals (*b*) and (*c*)

$$\cos \phi = \frac{\sqrt{2}}{\sqrt{10+9/c^2}}.$$

Substituting the observed values of $\cos \phi$ and solving, these two expressions yield values of c equal to 1·016 and 1·015 respectively in agreement with the value already deduced from the evidence of the oscillating crystal method. The analysis of the Laue photograph thus confirms the result of the other methods.

Summary.

Part I. contains an account of the changes observed in the X-ray photographs of an alloy of aluminium with 4 per cent. by weight of copper, during ageing at room-temperature and at 200° C. An attempt is made to estimate the dimension of the regions in the aluminium lattice where copper is segregating: it is concluded that these regions are thin plates involving about five, or perhaps fewer, (100) planes of atoms. The area of the plates is more difficult to estimate, but it is suggested that at room-temperature it does not exceed 100 atomic distances, and in the earliest stages of the ageing process is much smaller. When the crystal aged at room-temperature is heat-treated at 200° C., the first effect is to reduce the hardness and at the same time the effects to which the plates of copper-rich material give rise disappear from the X-ray photographs. It is suggested that the copper in the plates has gone back into solution. Further treatment at 200° C. increases the hardness, and the X-ray photographs indicate the presence of copper-rich plates still very thin, but of larger area. When the maximum hardness has been attained the diffraction effects indicate

an increase in thickness of the plates, and after prolonged exposure at 200° C. a second phase is present, giving normal three-dimensional diffraction spots.

Part II. is an analysis of the structure of this new phase. It is of the calcium fluoride type, but appears to be tetragonal, having $a=5{\cdot}71$ Å. and $c=1{\cdot}015$; the unit contains four copper and eight aluminium atoms, *i. e.*, four molecules of $CuAl_2$. The structure is different from that of $CuAl_2$ as usually obtained. Whether it is to be regarded as a metastable "intermediate" phase or the stable form of $CuAl_2$ at low temperatures is not clear. The new crystals are closely united to the aluminium lattice ; (100) planes of the aluminium unit are in contact with (001) planes of the new crystals. Three sets of the latter are present in the aluminium crystal, one on each cube-face. Analysis of a Laue photograph of the alloy confirms the result obtained from oscillating crystal photographs.

ACKNOWLEDGMENTS.

I have to thank Dr. M. L. V. Gayler for the preparation and heat treatment of the single crystals used in the investigation, and I am indebted to Professor W. L. Bragg, O.B.E., F.R.S., and to Dr. C. H. Desch, F.R.S., for their interest in and encouragement of the work.

References.

(1) Preston, G. D., Proc. Roy. Soc. A, 167, p. 526 (1938).
(2) Guinier, A., *Comptes Rendus*, ccvi. p. 1641 (1938) ; Calvet, J., Jacquet, P., and Guinier, A., *Comptes Rendus*, ccvi. p. 1972 (1938).
(3) Wasserman, G., and Weerts, J., *Metallwirtschaft*, xiv. p. 605 (1935).
(4) West, C. D., and Peterson, A. W., *Z. f. Krist.* lxxxviii. p. 93 (1934).

LXXV. *Integral Representations for Products of Whittaker Functions.* *By* A. ERDÉLYI †.

1. IT is the purpose of the present note to establish integral representations of products of Whittaker's confluent hypergeometric functions $W_{k,m}(z)$ with different arguments, by the methods of the theory of *Laplace transform*—that is to say, by operational methods. Some more general results of the author on the same subject will be published next time. Very important special

† Communicated by the Author.

cases of the results published here are those leading to integral representations for the product of Weber's parabolic cylinder functions, of modified Bessel functions of second kind, Laguerre and Hermite polynomials, error function, etc.

The function $f(s)$ is said to be the Laplace transform of $\mathrm{F}(t)$ if

$$f(s)=\mathfrak{L}_s\{\mathrm{F}(t)\}\equiv\int_0^\infty e^{-st}\mathrm{F}(t)\,dt,$$

the integral being convergent.

The composition (" Faltung ") of two functions $\mathrm{F}_1(t)$ and $\mathrm{F}_2(t)$ is to be defined as

$$\mathrm{F}_1*\mathrm{F}_2(t)\equiv\int_0^\infty \mathrm{F}_1(\tau)\mathrm{F}_2(t-\tau)\,d\tau.$$

We shall make use of the product theorem (" Faltungssatz ") †

$$f_1(s)f_2(s)=\mathfrak{L}_s\{\mathrm{F}_1(t)\}.\mathfrak{L}_s\{\mathrm{F}_2(t)\}=\mathfrak{L}_s\{\mathrm{F}_1*\mathrm{F}_2(t)\},$$

being valid if $\mathfrak{L}_s\{\mathrm{F}_1\}$ and $\mathfrak{L}_s\{\mathrm{F}_2\}$ converge absolutely.

2. We apply the product theorem to the functions

$$\mathrm{F}_1(t)=\frac{t^{-\frac{1}{2}-k+m}\left(1+\frac{t}{x}\right)^{-\frac{1}{2}+k+m}}{\Gamma(\frac{1}{2}-k+m)},$$

$$\mathrm{F}_2(t)=\frac{t^{-\frac{1}{2}-l-m}\left(1+\frac{t}{y}\right)^{-\frac{1}{2}+l-m}}{\Gamma(\frac{1}{2}-l-m)}.$$

The well-known integral representation of Whittaker functions ‡ yields, $\mathrm{W}_{k,m}(z)$ being an even function of m,

$$f_1(1)=\int_0^\infty e^{-t}\mathrm{F}_1(t)\,dt=x^{-k}e^{\frac{1}{2}x}\mathrm{W}_{k,m}(x),$$

$$f_2(1)=\int_0^\infty e^{-t}\mathrm{F}_2(t)\,dt=y^{-l}e^{\frac{1}{2}y}\mathrm{W}_{l,m}(y).$$

This is valid for

$$x\neq0,\ y\neq0,\ |\arg x|<\pi,\ |\arg y|<\pi;$$
$$\Re(\tfrac{1}{2}-k+m)>0,\ \Re(\tfrac{1}{2}-l-m)>0.$$

† G. Doetsch, ' Theorie und Anwendung der Laplace-Transformation.' Berlin, 1937, p. 161.

‡ E. T. Whittaker and G. N. Watson, ' Modern Analysis,' 4th ed. Cambridge, 1927, §16.12.

Next we compute

$$\mathrm{F}_1 * \mathrm{F}_2(t) = \frac{1}{\Gamma(\frac{1}{2}-k+m)\,\Gamma(\frac{1}{2}-l-m)} \times \int_0^t \tau^{-\frac{1}{2}-k+m}(t-\tau)^{-\frac{1}{2}-l-m}\left(1+\frac{\tau}{x}\right)^{-\frac{1}{2}+k+m} \times \left(1+\frac{t-\tau}{y}\right)^{-\frac{1}{2}+l-m} d\tau,$$

substituting $$\tau = \frac{xvt}{x+t-vt}.$$

This substitution yields

$$\mathrm{F}_1 * \mathrm{F}_2(t) = \frac{t^{-k-l}\left(1+\frac{t}{x}\right)^{-\frac{1}{2}+k-m}\left(1+\frac{t}{y}\right)^{-\frac{1}{2}+l-m}}{\Gamma(\frac{1}{2}-k+m)\,\Gamma(\frac{1}{2}-l-m)} \times \int_0^1 v^{-\frac{1}{2}-k+m}(1-v)^{-\frac{1}{2}-l-m} \times \left(1-\frac{t(x+y+t)}{(x+t)(y+t)}v\right)^{-\frac{1}{2}+l-m} dv.$$

The last integral is Jacobi's integral for the hypergeometric function †, and therefore we obtain

$$\mathrm{F}_1 * \mathrm{F}_2(t) = \frac{t^{-k-l}\left(1+\frac{t}{x}\right)^{-\frac{1}{2}+k-m}\left(1+\frac{t}{y}\right)^{-\frac{1}{2}+l-m}}{\Gamma(1-k-l)} \times {}_2\mathrm{F}_1\left[\tfrac{1}{2}-k+m,\ \tfrac{1}{2}-l+m;\ 1-k-l;\ \frac{t(x+y+t)}{(x+t)(y+t)}\right].$$

3. Applying the product theorem with $s=1$ to the functions dealt with in the preceding paragraph, we get at once the integral representation

$$\mathrm{W}_{k,m}(x)\,\mathrm{W}_{l,m}(y) = \frac{(xy)^{m+\frac{1}{2}}\,e^{-\frac{1}{2}(x+y)}}{\Gamma(1-k-l)} \times \int_0^\infty e^{-t}t^{-k-l}(x+t)^{-\frac{1}{2}+k-m}(y+t)^{-\frac{1}{2}+l-m} \times {}_2\mathrm{F}_1\left[\tfrac{1}{2}-k+m,\ \tfrac{1}{2}-l+m;\ 1-k-l;\ \frac{t(x+y+t)}{(x+t)(y+t)}\right] dt, \quad \ldots \quad (1)$$

† 'Modern Analysis,' p. 293, §14.6, Ex. 1.

valid for

$$x\neq 0,\ y\neq 0,\ |\arg x|<\pi,\ |\arg y|<\pi,\ \Re(1-k-l)>0. \quad (2)$$

Using contour integrals we can in the usual manner remove the restriction $\Re(1-k-l)>0$, and write the integral representation in the form

$$\begin{aligned} W_{k,m}(x)\,W_{l,m}(y) &= \Gamma(k+l)\,(xy)^{m+\frac{1}{2}}\,e^{-\frac{1}{2}(x+y)} \\ &\times \frac{1}{2\pi i}\int_{-\infty}^{(0+)} e^{u}\,u^{-k-l}\,(x-u)^{-\frac{1}{2}+k-m}\,(y-u)^{-\frac{1}{2}+l-m} \\ &\times {}_2F_1\left[\tfrac{1}{2}-k+m,\ \tfrac{1}{2}-l+m;\ 1-k-l;\ \frac{-u(x+y-u)}{(x-u)(y-u)}\right]du. \end{aligned} \quad . \ . \ . \quad (3)$$

The contour encircles the point $u=0$ in the positive direction, on the whole contour being $|\arg u|\leqslant\pi$. No other singularity of the integrand is to be enclosed. (3) is valid for

$$k+l\neq 0,-1,-2,\ldots;\ x\neq 0,\ y\neq 0,\ |\arg x|<\pi,\ |\arg y|<\pi. \quad . \ . \ . \quad (4)$$

4. An important special case of (3) is the Laplace integral for the product of Weber's parabolic cylinder functions, which are connected with Whittaker functions by the well-known relation †

$$D_\nu(z)=2^{\frac{1}{4}\nu+\frac{1}{4}}z^{-\frac{1}{2}}W_{\frac{1}{2}\nu+\frac{1}{4},-\frac{1}{4}}(\tfrac{1}{2}z^2).$$

Therefore we deduce

$$\begin{aligned} D_\mu(x)\,D_\nu(y) &= 2^{\frac{1}{4}(\mu+\nu+1)}(xy)^{-\frac{1}{2}}W_{\frac{1}{2}\mu+\frac{1}{4},-\frac{1}{4}}(\tfrac{1}{2}x^2)\,W_{\frac{1}{2}\nu+\frac{1}{4},-\frac{1}{4}}(\tfrac{1}{2}y^2) \\ &= 2^{\frac{1}{2}(\mu+\nu)}\,\Gamma\left(\frac{\mu+\nu+1}{2}\right)e^{-\frac{1}{4}(x^2+y^2)} \\ &\times \frac{1}{2\pi i}\int_{-\infty}^{(0+)} e^{u}\,u^{-\frac{1}{2}(\mu+\nu+1)}\left(\frac{x^2}{2}-u\right)^{\frac{1}{2}\mu}\left(\frac{y^2}{2}-u\right)^{\frac{1}{2}\nu} \\ &\times {}_2F_1\left[-\tfrac{1}{2}\mu,\ -\tfrac{1}{2}\nu;\ \tfrac{1}{2}-\tfrac{1}{2}\mu-\tfrac{1}{2}\nu;\ \frac{-2u(x^2+y^2-2u)}{(x^2-2u)(y^2-2u)}\right]du. \end{aligned}$$

† 'Modern Analysis,' §16.5.

Now we make use of the formula

$$ {}_2\mathrm{F}_1(a, b\,;\ a+b+\tfrac{1}{2}\,;\ -w^2) = 2^{a+b-\frac{1}{2}}\,\Gamma(a+b+\tfrac{1}{2})\,w^{\frac{1}{2}-a-b}\,\mathrm{P}^{\frac{1}{2}-a-b}_{a-b-\frac{1}{2}}(\sqrt{1+w^2}), $$

and obtain, putting $2u=v$,

$$ \mathrm{D}_\mu(x)\,\mathrm{D}_\nu(y) = \frac{e^{-\frac{1}{4}(x^2+y^2)}}{4i\cos\frac{1}{2}(\mu+\nu)\pi} \times \int_{-\infty}^{(0+)} e^{\frac{1}{2}v}\,(x^2-v)^{-\frac{1}{4}(-\mu+\nu+1)}\,(y^2-v)^{-\frac{1}{4}(\mu-\nu+1)} \times \left(\frac{x^2+y^2}{v}-1\right)^{\frac{1}{4}(\mu+\nu+1)} \times \mathrm{P}^{\frac{1}{4}(\mu+\nu+1)}_{\frac{1}{4}(\mu-\nu-\frac{1}{2})}\left(\frac{xy}{\sqrt{(x^2-v)(y^2-v)}}\right) dv. \quad \ldots \quad (5) $$

$$ [\tfrac{1}{2}(\mu+\nu+1)\neq 0,\ \pm 1,\ \pm 2,\ldots\ ;\ x\neq 0,\ y\neq 0, \quad |\arg x|<\tfrac{1}{2}\pi,\ |\arg y|<\tfrac{1}{2}\pi]. $$

5. Another interesting special case of (1) enables us to construct integral representations for a product of modified Bessel functions of the second kind with the same order but different arguments. Being

$$ \mathrm{K}_\nu(z) = \left(\frac{\pi}{2z}\right)^{\frac{1}{2}} \mathrm{W}_{0,\,\nu}(2z), $$

from (1) it follows at once

$$ \mathrm{K}_\nu(x)\,\mathrm{K}_\nu(y) = \pi(4xy)^\nu e^{-x-y} \int_0^\infty e^{-t}\{(2x+t)(2y+t)\}^{-\nu-\frac{1}{2}} \times {}_2\mathrm{F}_1\left[\nu+\tfrac{1}{2},\ \nu+\tfrac{1}{2}\,;\ 1\,;\ \frac{t(2x+2y+t)}{(2x+t)(2y+t)}\right] dt. $$

The hypergeometric series occurring in this integral representation reduces to Legendre's function by means of the formula †

$$ {}_2\mathrm{F}_1(a, a\,;\ 1\,;\ 1-w) = w^{-\frac{1}{2}a}\,\mathrm{P}_{-a}\left(\frac{2}{w}-1\right), $$

† 'Modern Analysis,' p. 312, §15.22, Ex. 2.

and therefore we obtain, putting $t=2v$, the integral representation

$$\mathrm{K}_\nu(x)\mathrm{K}_\nu(y)=\pi(xy)^{\frac{1}{2}\nu-\frac{1}{4}}e^{-x-y}\int_0^\infty e^{-2v}\{(x+v)(y+v)\}^{-\frac{1}{2}\nu-\frac{1}{4}} \times \mathrm{P}_{-\nu-\frac{1}{2}}\left(2\left(1+\frac{v}{x}\right)\left(1+\frac{v}{y}\right)-1\right)dv. \quad . \quad . \quad . \quad (6)$$

(6) is valid for all values of ν, and for

$$x\neq 0,\ y\neq 0,\ |\arg x|<\pi,\ |\arg y|<\pi. \quad . \quad . \quad (7)$$

A great number of other interesting special cases containing Laguerre and Hermite polynomials (in both cases the hypergeometric series in the integrand of (1) and (3) terminates and reduces to Jacobi's polynomial), the error function, the incomplete gamma function, etc. are left to the reader.

6. Our integral representations are also useful for proving certain functional relations, such as expansions, recurrence formulæ, etc., for products of Whittaker functions. Merely to set an example for this we shall prove an expansion of $\mathrm{W}_{k,m}(z)\mathrm{W}_{l,m}(z)$ in a series of Whittaker functions. For $\Re(z)>0$, $t>0$ is

$$\left|\frac{z}{z+t}\right|<1,$$

and therefore the following expansion and term-by-term integration is permissible :

$$z^{-k-l}e^z\mathrm{W}_{k,m}(z)\mathrm{W}_{l,m}(z) =\mathfrak{L}_1\left\{\frac{t^{-k-l}\left(1+\frac{t}{z}\right)^{-1+k+l-2m}}{\Gamma(1-k-l)} \times {}_2\mathrm{F}_1\left[\tfrac{1}{2}-k+m,\ \tfrac{1}{2}-l+m\ ;\ 1-k-l\ ;\ 1-\left(\frac{z}{z+t}\right)^2\right]\right\}$$

$$=\mathfrak{L}_1\left\{\frac{\Gamma(-2m)t^{-k-l}\left(1+\frac{t}{z}\right)^{-1+k+l-2m}}{\Gamma(\frac{1}{2}-k-m)\Gamma(\frac{1}{2}-l-m)}\right.$$

$$\times {}_2F_1\left[\tfrac{1}{2}-k+m,\ \tfrac{1}{2}-l+m\ ;\ 1+2m\ ;\ \left(1+\frac{t}{z}\right)^{-2}\right]\Bigg\}$$

$$+\mathfrak{L}_1\Bigg\{\frac{\Gamma(2m)t^{-k-l}\left(1+\frac{t}{z}\right)^{-1+k+l+2m}}{\Gamma(\tfrac{1}{2}-k+m)\Gamma(\tfrac{1}{2}-l+m)}$$

$$\times {}_2F_1\left[\tfrac{1}{2}-k-m,\ \tfrac{1}{2}-l-m\ ;\ 1-2m\ ;\ \left(1+\frac{t}{z}\right)^{-2}\right]\Bigg\}$$

$$=\frac{\Gamma(-2m)}{\Gamma(\tfrac{1}{2}-k-m)\Gamma(\tfrac{1}{2}-l-m)}\sum_{r=0}^{\infty}\frac{(\tfrac{1}{2}-k+m)_r(\tfrac{1}{2}-l+m)_r}{(1+2m)_r\,r!}$$

$$\times\mathfrak{L}_1\left\{t^{-k-l}\left(1+\frac{t}{z}\right)^{-1+k+l-2m-2r}\right\}$$

$$+\frac{\Gamma(2m)}{\Gamma(\tfrac{1}{2}-k+m)\Gamma(\tfrac{1}{2}-l+m)}\sum_{r=0}^{\infty}\frac{(\tfrac{1}{2}-k-m)_r(\tfrac{1}{2}-l-m)_r}{(1-2m)_r\,r!}$$

$$\times\mathfrak{L}_1\left\{t^{-k-l}\left(1+\frac{t}{z}\right)^{-1+k+l+2m-2r}\right\}.$$

Therefore, by virtue of the above used integral representation † of $W_{k,m}(z)$, it follows:

$$W_{k,m}(z)\,W_{l,m}(z)=\frac{\Gamma(1-k-l)\Gamma(-2m)}{\Gamma(\tfrac{1}{2}-k-m)\Gamma(\tfrac{1}{2}-l-m)}z^{m+\frac{1}{2}}e^{-\frac{1}{2}z}$$

$$\times\sum_{r=0}^{\infty}\frac{(\tfrac{1}{2}-k+m)_r(\tfrac{1}{2}-l+m)_r}{(1+2m)_r\,r!}z^r\,W_{k+l-m-r-\frac{1}{2},\,r+m}(z)$$

$$+\frac{\Gamma(1-k-l)\Gamma(2m)}{\Gamma(\tfrac{1}{2}-k+m)\Gamma(\tfrac{1}{2}-l+m)}z^{-m+\frac{1}{2}}e^{-\frac{1}{2}z}$$

$$\times\sum_{r=0}^{\infty}\frac{(\tfrac{1}{2}-k-m)_r(\tfrac{1}{2}-l-m)_r}{(1-2m)_r\,r!}z^r\,W_{k+l+m-r-\frac{1}{2},\,r-m}(z), \qquad \ldots\ (8)$$

$$[|\arg z|<\tfrac{1}{2}\pi;\ \Re(k+l)>0,$$
$$k+l\neq 1,\ 2,\ \ldots\ ;\ 2m\neq 0,\ \pm 1,\ \pm 2,\ \ldots].$$

When one of the two Whittaker functions occurring on the left-hand side of (8) reduces to a Laguerre or Hermite polynomial then one of the two series on the right of this relation vanishes and the other terminates.

Dřevařská 18.
Brno, Č.S.R.

† *Cf.* p. 872.

LXXVI. *The Fluorescent Chromium Ion in Ruby.* By B. V. Thosar, *M.Sc., College of Science, Nagpur, India* *.

[Received August 19, 1938.]

[Plate IX.]

In a previous communication (1) the author has discussed the effect of a magnetic field on the two intense red lines in the fluorescence spectrum of ruby. It was pointed out that the simplicity of the Zeeman pattern and the sharpness of its components can be explained on the assumption that the fluorescent chromium ions actually replace the Al-ions of the mother-lattice, and that the Cr^{+++} ions being paramagnetic, the spin-vector is free to orient in the magnetic field, but not the L-vector. Equivalent inability of the L-vector in all the ions to respond to the magnetic field thus secures the simplicity and the sharpness of the pattern. In the following paragraphs some more facts and considerations in support of this idea are presented, and some features of the fluorescence spectrum of ruby are explained with its help.

The Anti-Stokes Bands.

On the short-wave side of the two intense lines in the spectrum of ruby there are three diffuse bands of fairly large intensity and one very weak band. There are similar diffuse bands on the long-wave side of the sharp lines as well; but the anti-Stokes bands are much more intense and stand out prominently in the fluorescence spectrum. These bands naturally seemed to deserve more investigation.

It has been observed before, and can be seen from Pl. IX. (I.) *a* and *b*, that the bands are quite intense at room-temperature, but disappear completely at −190°, the liquid-air temperature. These photographs of the spectra were taken with carbon-arc light, filtered through a blue glass, as the exciting light and the red luminescence of the ruby was focussed transversely on to the slit of a Fuess spectrograph. The second photograph at −190° was taken with the ruby immersed in liquid air, in a small transparent Dewar flask. The complete disappearance

* Communicated by the Author.

of these lines at low temperatures naturally suggests that they must be attributed to infra-red vibrations in the fluorescent crystal. To test this point further the author decided to heat the ruby and to find its effect on the intensity of the anti-Stokes bands. Also, instead of using the usual blue light for exciting the ruby, a portion of the red end of the spectrum on the long-wave side of the bands and in their immediate neighbourhood was used. This red exciting band covered the positions of the two intense lines, but ended abruptly near the long-wave end of the system of bands. The use of this anti-Stokes excitation naturally gave a much feebler intensity of the fluorescent bands compared to the usual Stokes excitation by blue light. The exposure, in this case, was of the order of a few hours instead of a couple of minutes needed usually. A thousand watt tungsten filament lamp was used as the constant source of light. A combination of filters gave the required exciting band in the red end of the spectrum. The spherical bead of ruby was held in a conical glass tube and the red luminescence was observed and photographed in a transverse direction as before. A small electrical furnace was built round the glass tube holding the ruby. The fluorescence spectra of the cold (room-temperature) and hot (200°) ruby were photographed, giving exactly equal exposures and keeping all the experimental conditions scrupulously identical in the two cases. To ascertain that there was no change in the intensity of exciting light due to inconstancy of the electric lamp, several photographs of equal exposures, with the ruby alternately hot and cold, were taken. It was found that in the fluorescence of the heated ruby the intensity of the anti-Stokes bands is markedly greater than at room-temperature, as can be seen from Pl. IX. (II.), *a* and *b*.

The disappearance of the bands at low temperature and their brightening at higher temperatures point to the conclusion that they must be due to the superposition of infra-red vibrations on the sharp line radiation. But, unlike other bands in the spectrum, they are on the anti-Stokes side and are much more intense. This shows that the vibrations giving these bands must be intimately bound up with the fluorescent centre—the Cr^{+++} ion. Now, these Cr^{+++} ions are shown to replace the Al-ions in the lattice of the crystalline corundum, and hence the

vibrations in question must be due to the group Cr_2O_3 occurring in the ruby. It is interesting to note that both Al_2O_3 and Cr_2O_3 are molecular compounds[2], and the whole crystal is made up of a succession of groups of the type M_2O_3, so that the three O-atoms are somewhat closer to the two metal atoms of their own group than they are to the metal atoms of adjacent groups. Thus in the molecular group Cr_2O_3 the two Cr-ions are linked with the three O-atoms, symmetrically placed between them, by real valency bonds. The vibrations of this group of atoms will then be superposed on the sharp line radiation emitted by the Cr-ions, which are its integral components. At ordinary and higher temperatures the energy of these vibrations, which already exist in the crystal, is added to the emitted light-quantum, thus giving the bands on the short-wave side of the sharp lines. It is possible that the sharp line radiation may also be modified by superposition of the vibrations in the mother-lattice (Al_2O_3). But the probability of this and hence the intensity of the bands arising from this cause will be much less. Deutschbein[3] has explained one band on the Stokes side as due to superposition of the Raman frequency 410 cm.$^{-1}$ of corundum. He seems to have pictured the fluorescent Cr-ions as free and gas-like, evenly distributed in the body of corundum. This picture leads one to expect the Raman frequencies of corundum alone to be superposed on the monochromatic fluorescent radiation. But then the large intensity of the anti-Stokes bands and the complete lack of symmetry in the positions of the bands remain inexplicable. The author's picture of the Cr-ions as regular components of the lattice, substituting in places the Al-ions of corundum, makes the fluorescent ions integral parts of the molecular group Cr_2O_3, whose internal vibrations account for the anti-Stokes bands of large intensity. This picture does not exclude the possibility of the superposition of the vibrations in the group Al_2O_3. But the bands due to this cause will be much feebler, as indeed many bands in the spectrum on the Stokes side are.

The difficulties of calculating the proper frequencies of a polyatomic molecule like Cr_2O_3 are well known. Unfortunately no experimental infra-red or Raman data for crystalline Cr_2O_3 are available. The X-ray study of this crystal shows[4] that the three O-atoms form an

equilateral triangle with the two Cr-atoms symmetrically situated, one above and the other below the centre of this triangle. The three valencies joining a Cr-atom to the three O-atoms are therefore symmetrically split about the axis of the molecule, the line joining the two Cr-atoms. Mecke[5] has shown that a group of similar atoms joined symmetrically to a central atom by multiply-split valencies may be replaced, for the purpose of calculating the proper frequencies, by a single atom of modified weight and attached along the axis to the central atom by a valency of modified binding constant. Applying the same simplifying device to this case, the central triangle of three oxygen atoms may be regarded as a single atom of modified weight attached to the outer Cr-atoms by valency bonds lying along the axis of the molecule. Thus the group $Cr—O_3—Cr$ will vibrate like a straight "tri-atomic" molecule. It will therefore have two valency vibrations, one symmetrical and the other anti-symmetrical. In the former the outer atoms will move symmetrically, along the direction of the valency, with respect to the central atom, while in the latter they will move anti-symmetrically. There will be also two deformation vibrations, involving the motions of the three atoms perpendicular to the axis of the molecule. In the table below are given the

Anti-Stokes Bands.

No.	λ in A.U.	Intensity.	$\Delta\nu$ in cm.$^{-1}$.	Vibration type.
1....	6583 6595	6	7 65	Valence symmetrical.
2....	6692	8 diffuse	523	Valence antisymmetrical
3....	6762	4	368	Deformation.
4....	6820	faint	242	Deformation.

frequency intervals of the anti-Stokes bands measured from the centre of the sharp doublet, their intensity and the modes of vibration of the "tri-atomic" molecule described above, to which they probably owe their origin.

The occurrence of the bands due to the vibrations of the group Cr_2O_3 on the anti-Stokes side only is to be expected. For, in the usual Stokes excitation (by blue

light), a large quantum of light is incident on the group, a part of which is enough to excite the Cr-ions so as to enable them to emit the red luminescence. The remaining energy will naturally be used up in exciting all the modes of vibration of the molecule Cr_2O_3, which are, in their turn, superposed on the monochromatic radiation from the Cr-ions, thus giving the bands on the short-wave side. The excitation of the Cr-ions is invariably accompanied by the excitation of the vibrations of the Cr_2O_3 group, and hence the bands appear on the anti-Stokes side only. The group Al_2O_3 in the corundum lattice is not likely to be affected by the energy left over from the incident quantum after absorption by the Cr-ions, which are situated remote from the Al_2O_3 group. Some energy from the emitted quantum of red luminescence will have to be used in exciting the vibrations of this group. The bands corresponding to the vibration frequencies of corundum will thus occur on the Stokes side of the sharp doublet.

Magnetic Dissymmetry in Ruby.

Lehmann[6] has studied the effect of a magnetic field on the two sharp absorption lines of ruby, with different orientations of the crystal with respect to the field. It is found that there is continuous variation of the Zeeman pattern as the orientation of any principal axis of the ruby crystal is changed with respect to the direction of the field and of radiation. The pattern, in general, is simple, consisting of three or four components—at any rate, much simpler than what would obtain for a gaseous free Cr-ion in $^2G_{7/2,\,9/2}$ and $^4F_{7/2,\,9/2}$ states. The components are sharp and the variation is continuous, showing that all the fluorescent ions are subjected to identical crystalline fields through the L-interaction, while the spins are relatively free. This is, therefore, further evidence in support of the view put forward in the previous paper, namely, that the fluorescent ions of chromium actually replace the Al-ions of the corundum lattice and are subjected to definite L-interaction. Lehmann seems to have adopted the view that the Cr-ions are free and gaseous, scattered anyhow within the mother-lattice, and situated in weak crystalline fields. He has, therefore, failed to find a basis on which the variation of the Zeeman

pattern with change of orientation of the crystal can be explained. This is attempted below.

The experimental observations, classified from a different standpoint, can be summarized as follows. Here, by the "main axis" is meant the (0001) axis of the crystal, the axis of symmetry of the Cr_2O_3 group, which passes through the two Cr-ions and the centre of the triangle formed by the three oxygen atoms.

(*a*) The pattern is simplest, *i. e.*, consists of three components only when the magnetic field is parallel to the main axis.

(*b*) The pattern consists of four components when the field is perpendicular to the main axis, and any rotation of the crystal round the main axis does not change the nature of the pattern so long as the field and the axis are perpendicular to each other.

(*c*) The pattern is most complicated, for one of the sharp lines, when the main axis is inclined at about 45° to the field, and for the other line when the inclination is between 20° and 30°.

The main axis (0001) is the three-fold axis of symmetry in the molecular group Cr_2O_3 formed by the replacement of the Al-ions of the corundum lattice by the fluorescent Cr-ions. About this axis are spread symmetrically the three valencies joining the three O-atoms to the metal atom, and hence this will be the direction of L-interaction of the Cr-ions in the crystal, which are all situated along this axis. The application of a magnetic field provides another direction along which quantitization of the spin is to take place, and there is thus modification of the energy levels. In this case, on account of some spin-orbit interaction, the orbital moment must be disposed to influence the orientation of the spin-moment, so that the resultant of the magnetic and the electric fields (along L-vector-main axis) must be determining the positions of the lines in the magnetic field. Thus, it is to be expected that the nature of the Zeeman pattern will depend on the inclination of the directions of these two fields, *i. e.*, the main axis and the direction of magnetic field. It also follows that the pattern will continue to have the same features on rotating the crystal in a manner that does not alter the inclination of the main axis with

the magnetic field. This is found to be true from the results summarized above. Spedding and Nutting[7] have discussed this type of spin-orbit interaction in their work on chrome-alum. In terms of L-S coupling it may be stated that the coupling, in presence of an applied magnetic field, introduces very simple modification of the energy levels if the direction of L-vector (main axis) and the field are either (*a*) parallel or (*b*) perpendicular—in (*a*) because they are coincident in direction, and in (*b*) because, probably, the weak L-S coupling is altogether broken.

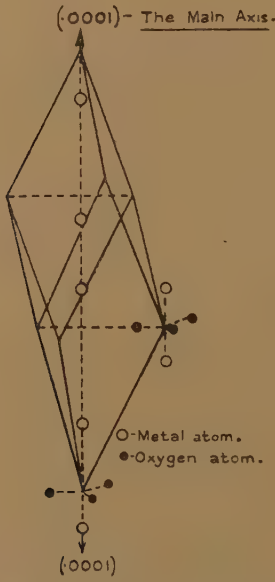

Structure unit of corundum.

But in the intermediate positions, when the field is inclined at about 45° with the L-vector, the "tussle" between the magnetic field and the L-moment to own the "allegiance" of the spin is balanced and "tense." It is in this position that the most complicated Zeeman pattern is produced. The magnetic dissymmetry in ruby thus becomes explicable if a weak L-S interaction is postulated in the paramagnetic ions of chromium, in addition to adopting the author's picture of all of them arranged regularly in the corundum lattice, in place of Al-ions, on the main axis.

The Inner Quantum Number.

The assumption of L-S interaction in the Cr-ion raises the question whether in the spectroscopic states which give the sharp lines of the fluorescence spectrum, the inner quantum number J remains "good." The explanation of the simplicity of the Zeeman pattern given previously and adapted above to the recent results of Lehmann, is based on the supposition that in spite of the weak L-S interaction, in general, the spin is free to orient in the magnetic field, while the L-moment is fixed along the main axis of the crystal. This naturally means that the inner quantum number J, arising as a result of quantization of S along L, is no longer valid in the chromium ion. The data with which this question could be decided are inadequate and even conflicting. But a discussion of the present position is attempted.

The two intense red lines of ruby have been attributed by previous workers to the transitions $^2G_{7/2} \rightarrow {}^4F_{i/2}$ and $^2G_{9/2} \rightarrow {}^4F_{9/2}$ of the trebly ionized chromium atom, as the observed frequencies are in agreement with the term values given by White[8] for Cr IV. Actually, five lines should be obtained for all the transitions possible between the ^2G and ^4F states. In fact it is found that the number and positions of the lines attributed to these transitions in the Cr^{+++} ion depend greatly on the mother-lattice[9], in which the chromium impurity is embedded. Thus, in Al_2O_3 it is a doublet with a small interval, in Ga_2O_3 the interval is greater. In a few ground-materials there is a single line in this region, while in Al_2SiO_5 there are four lines. As pointed out above, if all the multiplet levels remained good, there should be five lines. This points to the conclusion that the L-interaction greatly affects the levels and that the J-quantum number is no longer good—this would be more so in the ^2G and ^2H states, which have higher L-values. The differences in the crystalline fields of the ground-lattices will then account for the different positions of the lines. The fact that in every case the mother lattice is isomorphous with the chromium impurity is in keeping with the view that the chromium ion actually replaces the metallic atom of the ground-lattice.

That the term values determined spectroscopically for free and gaseous Cr^{+++} ions cannot often be trusted

to yield accurately the lines observed in the fluorescence of crystals is further supported by the recent determination of the term values of Cr IV by Bowen [10]. He finds that White's values are inaccurate and has also given the term values for the three ^4P states which were not recorded before. If Bowen's values for the two ^2G states are accepted, it is found that the two intense red lines of ruby cannot be accurately given by the transitions $^2G_{7/2,\ 9/2} \rightarrow {}^4F_{7/2,\ 9/2}$. In fact it seems probable that while one line of the doublet must be due to $^2G\ 9/2 \rightarrow {}^4F\ 9/2$, the other may be due to $^4P\ 5/2 \rightarrow {}^4F\ 3/2$.

But, curiously enough, the term values given by Bowen for the three newly found ^4P levels can, by transitions to ^4F state, explain remarkably well the two sharp lines at λ 7017 and λ 7049, which are next in order of intensity to the sharp doublet and which have not been explained so for. Thus,

Transition.	Bowen's values.	Fluorescence data.
$^4P_{1/2}' \rightarrow {}^4F_{1/2} =$	14293 cm.$^{-1}$	14247 cm.$^{-1}$
$^4P_{3/2}' \rightarrow {}^4F_{3/2}' =$	14177 cm.$^{-1}$	14183 cm.$^{-1}$

These rather confusing facts about the energy levels of the chromium ion in ruby can be explained on the supposition that the J quantum number and the spin-multiplicity are not valid in the higher states (^2G, ^2H), where the L-interaction must be stronger and the L–S coupling weaker. But in the lower states (^4P, ^4F) with lower values of L, the multiplicity and the number J probably remain good. It is interesting to note in this connexion that the Cr^{+++} ion is known to show anomalous paramagnetic behaviour, and it has been found that the orbital moment must be contributing to some extent to the magnetic moment of the ion. It is possible, therefore, that while in the higher states of the ion, the spin may be relatively free from the influence of the orbital moment to orient in the magnetic field, it may not be so in the lower states.

The observed facts about the anti-Stokes bands in the spectrum of ruby, the simplicity and sharpness of the Zeeman pattern of its lines and the variation of the pattern

with change in orientation of the crystal, as well as the partial invalidity of the inner quantum number, all conform nicely to the view that the fluorescent chromium ions are regular lattice constituents in corundum, replacing randomly a few Al-ions. Candler's[11] picture of the chromium impurity in ruby as evenly scattered, like "currants in a cake," does not seen to be quite accurate. The ruby is rather like a regular plum-cake, in which a few plums are replaced by currants.

Summary.

Further support is found for the author's idea put forward previously regarding the physical state of the chromium impurity in ruby, namely, that the fluorescent ions of chromium are regular lattice components and replace a few Al-ions of the corundum lattice. The intense anti-Stokes bands in the spectrum of ruby have been explained as due to the superposition of the vibrational frequencies of the molecular group Cr_2O_3, which is thus formed in the crystal. On postulating a weak L-S interaction in the ion and adopting the above structure for ruby, the magnetic dissymmetry in the crystal, in regard to the Zeeman pattern of the sharp lines, has been explained. The validity of the inner quantum number J and the spin-multiplicity have been discussed. Two sharp lines at λ 7017 and 7049 A., hitherto unexplained, are shown to arise from the transitions between the newly determined ^4P levels of Cr IV and the ^4F levels.

References.

(1) B. V. Thosar, Phil. Mag. xxvi. p. 380 (1938).
(2) Davey, Phys. Rev. xxi. p. 716 (1923); also Davey, 'Crystal Structure' (Int. Series in Phys.) p. 543.
(3) Deutschbein, *Ann. d. Phys.* xiv. p. 723 (1932).
(4) Davey, *loc. cit.*
(5) R. Mecke, "Band Spectroscopy" in the 'Structure of Molecules" (Blackie), p. 44.
(6) Lehmann, *Ann. de Phys.* xix. p. 99 (1934).
(7) Spedding and Nutting, Jour. Chem. Phys. iii. p. 369 (1935).
(8) White, Phys. Rev. xxxiii. p. 672 (1929).
(9) Deutschbein, *loc. cit.*
(10) Bowen, Phys. Rev. lii. p. 1153 (1937).
(11) Candler, 'Atomic Spectra' (Camb. Univ. Press, 1937), vol. ii. pp. 229-35.

LXXVII. *Study of the Magneto-Ionic Theory of Wave Propagation by Means of Simple Formulæ, Linkages, and Graphical Devices.* *By* V. A. Bailey, *M.A., D.Phil. (Oxon), F.Inst.P., Professor of Experimental Physics, University of Sydney, and* J. M. Somerville, *B.Sc. (Syd.), B.A. (Cantab.), Commonwealth Research Fellow in the University of Sydney* (1937) † ‡.

[Received August 8, 1938.]

1. THE general formulæ which determine the refractive index, absorption coefficient, and polarization of an electric wave in an ionized medium in the presence of a constant magnetic field, when account is taken of the effect of collisions between ions and molecules, have been given by Baker and Green §, Appleton ||, and others.

These formulæ are complex, and computation by means of them involves considerable labour. So Bailey ¶ has given a graphical procedure, using two charts (based on conformal representation) by means of which the computations may be made much more rapidly. The charts used in that method involve a large number of circles, ellipses, and parabolas.

We have found that the mode of approach adopted in Bailey's method, namely, that of determining the polarization first and then the refractive index and absorption index, has many advantages, and in this communication we give formulæ and describe linkages which depend on this mode of approach and which enable the required computations to be made very rapidly.

First we give a scheme for direct arithmetical computation of the three quantities, and also derive an approximate formula for the polarization which holds over a wide range and is useful for analytical work in that range.

Then we show how the polarization may be rapidly determined by means of a simple linkage, and how, when once the polarization is known, the refractive index and

† Now Lecturer in Mathematics and Physics, New England University College, Armidale, New South Wales.

‡ Communicated by the Authors.

§ W. G. Baker and A. L. Green, Radio Research Board Report, No. 3, Council for Scientific and Industrial Research (Aust.), Bulletin no. 60 (1932).

|| E. V. Appleton, J. I. E. E., lxxi. p. 642 (1932).

¶ V. A. Bailey, Phil. Mag. xviii. p. 516 (Sept. 1934).

absorption index may be determined by the use of either another linkage or of a chart which contains mainly two or three families of circles.

Our notation is defined in the following table :—

ω = angular frequency of the electric wave.

θ = angle between the direction of propagation and the earth's magnetic field H.

N = concentration of electrons in the medium.

ν = collision frequency of an electron.

$\Omega = -\mathrm{H}e/mc$ = the angular gyro-frequency.

e = charge on an electron in e.s.u.

m = mass of an electron.

$\omega_0 = 4\pi \mathrm{N}e/m\omega \doteq 3{\cdot}19 \times 10^9\ \mathrm{N}/\omega$.

$x' = \nu/\Omega$.

$y' = (\omega - \omega_0)/\Omega$.

$z' = x' + \iota y'$.

$\Theta = 2 \cos\theta / \sin^2\theta$.

$z = x + \iota y = \Theta z'$.

$\rho^2 = x^2 + y^2$.

$\zeta = \xi + \iota\eta = z^{-1}$.

R = polarization number of the wave.

μ = index of refraction.

χ = index of absorption $= \kappa c/\omega$, where

κ = coefficient of absorption.

c = velocity of light.

$\gamma = \Omega/\omega_0$.

2. *The Fundamental Equations.*

The polarization R is given by the equation

$$\mathrm{R} + \mathrm{R}^{-1} = 2\zeta, \quad . \quad . \quad . \quad . \quad . \quad . \quad (1)$$

and when R is known the refractive index μ and absorption index χ are given by the equation

$$\zeta_1 \mathrm{Z} = 1, \quad . \quad . \quad . \quad . \quad . \quad . \quad . \quad (2)$$

where $$\zeta_1 = \xi_1 + \iota\eta_1 = (\mu - \iota\chi)^2 - 1 \quad . \quad . \quad . \quad . \quad (3)$$

and $$\mathrm{Z} = \mathrm{X} + \iota\mathrm{Y} = (x' + \iota y' + \mathrm{R}\cos\theta)\iota\gamma - 1. \quad . \quad . \quad (4)$$

3. *The Computation of* R.

If $R=r+\iota s$, where r and s are real, then equation (1) is equivalent to the two equations

$$r^2-s^2-2\xi r+2\eta s+1=0 \quad . \quad . \quad . \quad . \quad . \quad . \quad (5)$$

and

$$\xi/r+\eta/s=1. \quad . \quad . \quad . \quad . \quad . \quad . \quad . \quad (6)$$

Also, if $r_1+\iota s_1$ and $r_2+\iota s_2$ are the two roots of (1), then

$$r_1+r_2+\iota(s_1+s_2)=2\zeta.$$

Hence the two solutions of equation (1) may be written in the form

$$r=\xi(1\pm F), \quad . \quad . \quad . \quad . \quad . \quad . \quad . \quad (7)$$

$$s=\eta(1\pm F^{-1}), \quad . \quad . \quad . \quad . \quad . \quad . \quad (8)$$

where (8) is obtained by substituting (7) in (6).

F is a real function of ξ and η which is determined by the equation obtained by substituting (7) and (8) in (5), namely

$$\xi^2(F^2-1)-\eta^2(F^{-2}-1)+1=0. \quad . \quad . \quad . \quad (9)$$

Instead of calculating F directly from ξ and η it is much better to write

$$F^2=1-K/\xi, \quad . \quad . \quad . \quad . \quad . \quad . \quad (10)$$

and to determine K.

Thus from (9) we have

$$\xi^2-(K+K^{-1})\xi+\eta^2+1=0, \quad . \quad . \quad . \quad (11)$$

and so

$$K+K^{-1}=J^{-1},$$

where

$$J=\frac{x}{1+\rho^2}. \quad . \quad . \quad . \quad . \quad . \quad . \quad (12)$$

Clearly the two possible values of K are in general respectively greater and less than 1.

Since F is real, it follows from (10) that we must have

$$K/\xi \leqslant 1.$$

It is easy to show † that if $K>1$ then $K/\xi \geqslant 1$. Hence

† If $K>1$, then $K=(1+\sqrt{1-4J^2})/2J$, and so

$$\frac{K}{\xi}=\frac{\rho^2(1+\rho^2)}{2x^2}(1+\sqrt{1-4J^2}).$$

But

$$1-4J^2=\frac{(1+\rho^2)^2-4x^2}{(1+\rho^2)^2}$$

$$\geqslant \left(\frac{1-\rho^2}{1+\rho^2}\right)^2, \quad \text{since } x^2 \leqslant \rho^2.$$

Hence

$$\frac{K}{\xi} \geqslant \frac{\rho^2(1+\rho^2)}{2x^2}\left(1+\frac{1-\rho^2}{1+\rho^2}\right)$$

$$\geq \rho^2/x^2.$$

for the value of K we must select the lesser root of (12), which is necessarily $\leqslant 1$, *i. e.*, we must have

$$0 \leqslant K \leqslant 1.$$

Values of K corresponding to different values of J are given in Table I.; also graphs of K and (K—J) as functions of J are given in fig. 1.

We may now readily derive r and s from x and y by calculating ξ, η, ρ^2, and J, then reading the value of K

TABLE I.

$K+K^{-1}=J^{-1}$.

J.	K.	J.	K.	J.	K.
0·00	0·0000	0·20	0·2087	0·40	0·5000
0·01	0·0100	0·21	0·2202	0·41	0·5215
0·02	0·0200	0·22	0·2318	0·42	0·5446
0·03	0·0300	0·23	0·2437	0·43	0·5694
0·04	0·0400	0·24	0·2557	0·44	0·5966
0·05	0·0501	0·25	0·2679	0·45	0·6267
0·06	0·0602	0·26	0·2804	0·46	0·6602
0·07	0·0703	0·27	0·2932	0·470	0·7009
0·08	0·0805	0·28	0·3063	0·475	0·7241
0·09	0·0907	0·29	0·3196	0·480	0·7500
0·10	0·1010	0·30	0·3333	0·482	0·7615
0·11	0·1114	0·31	0·3474	0·484	0·7738
0·12	0·1218	0·32	0·3619	0·486	0·7871
0·13	0·1323	0·33	0·3769	0·488	0·8016
0·14	0·1428	0·34	0·3923	0·490	0·8173
0·15	0·1535	0·35	0·4084	0·492	0·8351
0·16	0·1643	0·36	0·4250	0·494	0·8558
0·17	0·1752	0·37	0·4424	0·496	0·8808
0·18	0·1862	0·38	0·4607	0·498	0·9144
0·19	0·1974	0·39	0·4797	0·500	1·0000

from Table I. or the graph †, and finally obtaining the value of F by means of (10). With the graph more accurate values of K are found by reading the ordinates on the (K—J) curve and adding J.

Under certain conditions a simple approximate formulæ for F may be obtained; for if we solve equation (12) for K, necessarily adopting the negative sign for the radical, and expand by the binomial theorem, we readily see when J is small that J and K are approximately equal.

† Although K is introduced here purely as a computational device, it is interesting to note its geometrical significance; this is given in the Appendix.

Consequently we may write J for K in (10), and so obtain

$$F^2 \doteq 1 - J/\xi,$$

i. e.,

$$F \doteq \frac{1}{\sqrt{1+\rho^2}}. \quad . \quad . \quad . \quad . \quad . \quad (10\,a)$$

Fig. 1.

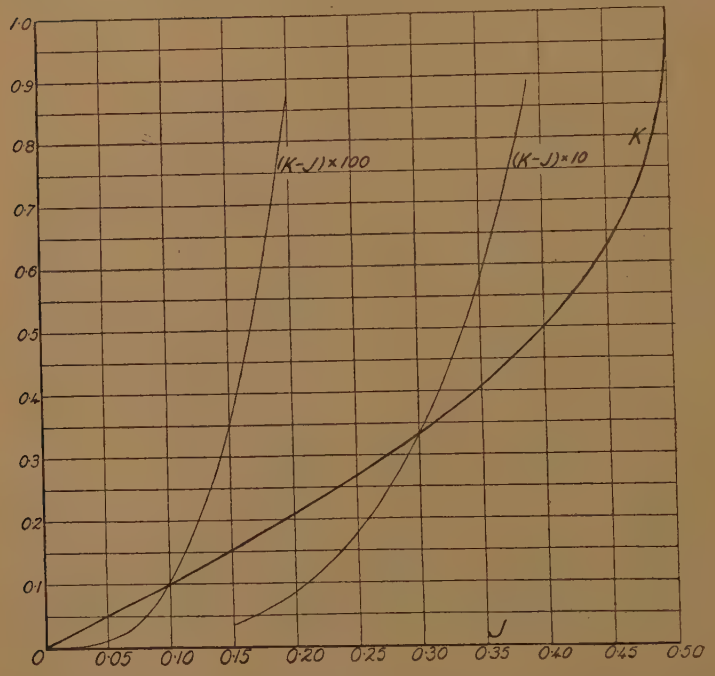

A complete discussion of the necessary conditions under which the relation (10 *a*) holds is complicated. The following condition, however, may be shown † to be necessary and sufficient for an accuracy between ½ per cent. and 2 per cent. in formula (10 *a*) :—

$$x < \frac{1}{10}(\rho + \rho^{-1}). \quad . \quad . \quad . \quad . \quad . \quad (10\,b)$$

† See V. A. Bailey, "On some Effects caused in the Ionosphere by Electric Waves."—Part II. Phil. Mag. (in the press).

4. *The Computation of μ and χ.*

From equations (2), (3), and (4) we have

$$\frac{X}{L^2}-\iota\frac{Y}{L^2}=\zeta_1=(\mu^2-\chi^2-1)-\iota(2\mu\chi),$$

where

$$\left.\begin{aligned} X&=-(y'+s\cos\theta)\gamma-1,\\ Y&=\ (x'+r\cos\theta)\gamma,\end{aligned}\right\} \quad . \quad . \quad . \quad (13)$$

$$L^2=\ X^2+Y^2. \quad . \quad . \quad . \quad . \quad . \quad . \quad . \quad . \quad (14)$$

Then

$$\mu^2-\chi^2=1+X/L^2 \quad \text{and} \quad 2\mu\chi=Y/L^2.$$

So if we write

$$a=+\sqrt{1+(1+2X)/L^2}, \quad b=1+X/L^2, \quad . \quad (15)$$

it follows that

$$\mu^2=\tfrac{1}{2}(a+b), \quad \chi^2=\tfrac{1}{2}(a-b). \quad . \quad . \quad . \quad (16)$$

Thus when R is known the values of μ and χ may be computed by means of the formulæ (13) to (16).

When χ is small it is better calculated by means of the formula

$$\chi=Y/2L^2\mu.$$

5. *Tabulated Computation.*

In Table II. a scheme is given by means of which the necessary computations may be carried out in routine fashion. The formulæ in the first column serve to calculate the corresponding quantities indicated in the second column. Two examples, worked out with a slide rule, are also given.

From (A) to (B) the data are entered.

The calculations from (B) to (C) are in essence probably necessary for any solution of the problem. Those from (C) to (D) suffice for the determination of the polarization †. The calculations from (D) to (E) are again essentially necessary, and those from (E) to (F) yield the refractive index and absorption index.

The numbers in the first column (O) of each double column correspond to the ordinary wave, and the numbers

† A check of some value can be applied to the numbers in the lines corresponding to r and s. This consists in applying the following two relations :—

$$r_1s_2+r_2s_1=0,$$
$$r_1r_2-s_1s_2=1.$$

Table II.

Computation of Polarization R, Refractive Index μ, and Absorption Index χ.

(A)	ω	2×10^6		5×10^6		
	θ	25^0		45^0		
	N	10^3		5×10^3		
	ν	10^6		5×10^5		
	Ω	10^7		10^7		
(B)	$\cos\theta$	·906		·707		
	$\sin\theta$	·423		·707		
$2\cos\theta/\sin^2\theta$	Θ	10·13		2·83		
$3\cdot19\times10^9\,N/\omega$	ω	$1\cdot595\times10^6$		$3\cdot19\times10^6$		
Ω/ω_0	γ	6·27		3·135		
ν/Ω	κ^2	·100		·050		
$(\omega-\omega_0)\,\Omega$	ζ	·0405		·181		
$\Theta x'$	x	1·013		·141		
$\Theta y'$	y	·410		·512		
(C)	x^2	1·025		·020		
	y^2	·168		·262		
x^2+y^2	ρ^2	1·193		·282		
x/ρ^2	ξ	·849		·501		
$-y/\rho^2$	η	−·3435		−1·816		
$x/(1+\rho^2)$	J	·461		·110		
From graph/Table	K	·667		·1112		
	K/ξ	·786		·2224		
$1-K/\xi$	F^2	·214		·7776		
	F	·462		·882		
	F^{-1}	2·16		1·133		
$\xi(1-F)\quad\xi(1+F)$.	r	·456	1·241	·0590	·944	
$\eta(1-F^{-1})\eta(1+F^{-1})$.	s	·398	−1·085	·242	−3·88	
(D)	$r\cos\theta$	·413	1·126	·0417	·667	
	$s\cos\theta$	·361	−·983	·171	−2·74	
$x'+r\cos\theta$	x''	·513	1·226	·0917	·717	
$y'+s\cos\theta$	y''	·401	−·942	·352	−2·56	
$-\gamma y''-1$	X	−3·51	4·90	−2·103	7·02	
$\gamma x''$	Y	3·22	7·68	·2875	2·246	
(E)	X^2	12·34	24·0	4·43	49·3	
	Y^2	10·35	59·0	·0827	5·04	
X^2+Y^2	L^2	22·69	83·0	4·51	54·3	
	X/L^2	−·1548	·059	−·466	·1293	
	$(1+2X)\,L^2$	−·266	·130	−·710	·278	
$\{1+(1+2X)/L^2\}^{\frac{1}{2}}$.	a	·857	1·062	·538	1·130	
$1+X/L^2$	b	·845	1·059	·534	1·1293	
$\frac{1}{2}(a+b)$	μ^2	·851	1·060	·536	1·130	
$\frac{1}{2}(a-b)$ or $Y^2/4L^4\mu^2$.	χ^2	·00591	·00202	·00190	·000380	
	μ	·923	1·030	·732	1·063	
	χ	·0769	·0448	·0436	·0195	
(F)		O	E			

in the second column (E) correspond to the extraordinary wave.

6. *A Link Mechanism for Determining the Polarization.*

We now show how the polarization may be immediately determined by means of a simple linkage when x and y are known, *i. e.*, we describe a linkage which in two settings automatically yields the final results of the fifteen calculations (C) to (D) of Table II.

In fig. 2 let OX, OY be the real and "imaginary" axes of an Argand diagram on which complex quantities will be represented vectorially.

Fig. 2.

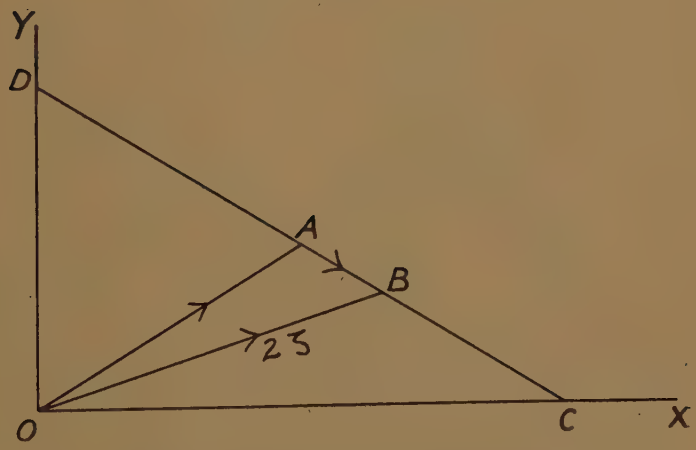

If B be the point whose coordinates are $(2\xi, 2\eta)$, then the vector $\overset{\frown}{OB}$ represents the complex number 2ζ.

We may now solve the equation

$$R+R^{-1}=2\zeta$$

by finding some point A such that

$$\left.\begin{aligned}\overset{\frown}{OA}&=R=|R|e^{i\theta},\\ \overset{\frown}{AB}&=R^{-1}=|R|^{-1}e^{-i\theta}.\end{aligned}\right\} \quad . \quad . \quad . \quad . \quad (17)$$

Thus, if AB is produced to meet the x and y axes in C and D, then

$$\angle AOC=\angle ACO=\theta,$$

and hence $$OA=AC=AD,$$

since $$\angle XOY=\pi/2.$$

Therefore A is the mid-point of CD.

Also, by equations (17)

$$OA.AB=1,$$

and so $$AB.AC=1.$$

We will now show how the point A can be determined by means of the linkage given in fig. 3.

Fig. 3.

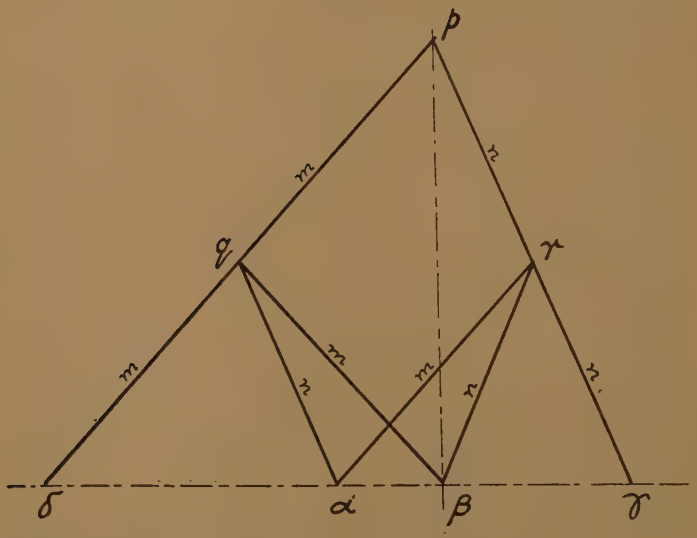

This linkage consists of six links, $p\delta$, $p\gamma$, $q\alpha$, $q\beta$, $r\alpha$, $r\beta$, where

$$pq=q\delta=q\beta=r\alpha=m,$$

$$pr=r\gamma=r\beta=q\alpha=n,$$

$$m^2-n^2=1.$$

Then clearly $p\beta$ is perpendicular to $\delta\gamma$, and therefore

$$\delta\beta^2-\beta\gamma^2=p\delta^2-p\gamma^2,$$

i. e., $$(\delta\beta-\beta\gamma)(\delta\beta+\beta\gamma)=4(m^2-n^2).$$

Since also $\delta\alpha=\alpha\gamma$, it follows that

$$4\alpha\beta.\alpha\gamma=4(m^2-n^2),$$

and so $$\alpha\beta.\alpha\gamma=1.$$

Thus the points $\alpha\beta\gamma\delta$ always bear the same relation to each other as do the points ABCD of fig. 2.

Consequently, if the point β of the linkage be placed over the point B of the Argand diagram (corresponding to 2ζ), and kept there while the points γ and δ are placed

Fig. 4 (*a*).

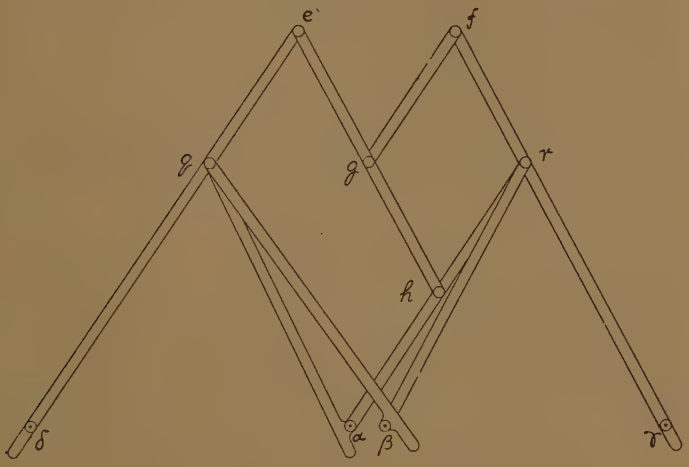

Fig. 4 (*b*).

on the real and "imaginary" axes respectively, then α will automatically take up a position such that

$$\overset{\frown}{O\alpha} = R,$$

$$\overset{\frown}{\alpha\beta} = R^{-1}.$$

In this way, when ζ is given, the linkage immediately furnishes the two solutions of equation (1).

Usually, however, we are first given z, where $z = x + \iota y = \zeta^{-1}$. But by means of the three points $\alpha\beta\gamma$ we can invert

$\frac{1}{2}z^*$, and thus obtain 2ζ. So if we plot the point $(\frac{1}{2}x, -\frac{1}{2}y)$, place α over the origin and γ over this point, then clearly β will lie over the point 2ζ, and from this point we may proceed as indicated above.

A linkage such as that described has been designed by us and constructed in the workshop of the School of Physics in the University of Sydney, and is shown diagrammatically in fig. 4. The linkage is designed with the unit of length equal to 5 inches, and with $m=3$ inches, $n=2\sqrt{2}$ inches.

To render the instrument more convenient for manipulation the two extra links *eh* and *fg* were introduced in order to obviate extending the links δq, γr to the point of intersection.

The points α and β are the centres of two sockets into which specially designed prickers may be introduced. These prickers are normally held clear of the paper by springs, but when desired they may be pushed down and locked by means of a bayonet-pin, and thus act as pivots about which the linkage may turn.

The points γ and δ are indicated by two circular sights which may be adjusted to make empirical allowance for any small inaccuracies in construction, and which allow the points γ and δ to be placed on the axes of the Argand diagram with ease.

To solve equation (1) the following procedure is adopted :—

1. The point $\frac{1}{2}z^*$ $(\frac{1}{2}x, -\frac{1}{2}y)$ is plotted on the Argand diagram.
2. α is placed over the origin, and the pricker locked down to act as a pivot.
3. The linkage is rotated about α until γ lies over $\frac{1}{2}z^*$.
4. The β pricker is locked down and the α pricker released.
5. The instrument is rotated about β until γ and δ are over the real and "imaginary" axes respectively, and a mark is made with the α pricker.

In this last position of the instrument $O\alpha$ and $\beta\alpha$ are the two roots of equation (1).

The scope of the linkage is clearly limited by the maximum and minimum extensions of $\gamma\delta$ or by those of

$\alpha\beta$. In order to enlarge this scope the auxiliary multiplier shown in fig. 4 (*b*) is used.

This multiplier is a seven-bar parallel linkage in which the lettered points always obey the relations

$$FN=FN'=2FM=2FM'=4FL=4FL'.$$

These points are the centres of sockets which may be fitted over pins concentric with the sockets at α and β. The prickers previously described fit equally well into any of the seven sockets of the multiplier, whether the sockets be free or on the pins at α and β.

It is clear that by using this multiplier the distance $\alpha\beta$ may be multiplied by 4, 2, $\frac{1}{2}$, or $\frac{1}{4}$ as desired, *i. e.*, we may obtain a point β' such that

$$\alpha\beta'.\alpha\gamma=4,\ 2,\ \tfrac{1}{2},\text{ or }\tfrac{1}{4}.$$

If on plotting $\frac{1}{2}z^*$ the corresponding vector is found to be too small (or too large) for convenient inversion by means of the instrument to yield 2ζ, we may use the multiplier first to determine $\frac{1}{2}\times 2\zeta$ (or $2\times 2\xi$), and then to determine $\frac{1}{2}$R (or 2R) by having a pricker set to give a point β' such that $\alpha\beta'.\alpha\gamma=(\frac{1}{2})^2$ (or 2^2).

This may be seen from the following discussion :—

If in fig. 2 instead of the relations

$$AB.AC=1 \quad \text{and} \quad \overset{\frown}{OB}=2\zeta$$

we have respectively

$$AB.AC=n^2 \quad \text{and} \quad \overset{\frown}{OB}=2n\zeta,$$

then the relation

$$\overset{\frown}{OA}+\overset{\frown}{AB}=\overset{\frown}{OB}$$

becomes

$$\frac{\overset{\frown}{OA}}{n}+\frac{n}{\overset{\frown}{OA}}=2\zeta,$$

since

$$\frac{\overset{\frown}{AB}}{n}=\frac{AB}{n}.e^{-i\theta}=\frac{n}{AC}e^{-i\theta}=\frac{n}{OAe^{i\theta}}=\frac{n}{\overset{\frown}{OA}}.$$

Thus we have $\overset{\frown}{OA}=n$R, and so the position of α now gives nR instead of R.

The points L′ M′ N′ may be used with advantage to locate the point β or β' when it would otherwise be necessary to turn the instrument round through 180° to work with points in another quadrant.

Using this multiplier our constructed linkage is suitable for problems in which

$$0{\cdot}25<\rho<10.$$

This instrument may be appropriately given the name Vectinvertor, since its essential property is to invert a vector.

As an example of its use and accuracy we give in the first line of the following table the values of the polarization numbers obtained by means of it for the second problem set out in Table II.

Method.	r_0.	r_e.	s_0.	s_e.
Vectinvertor.....	·060	·958	·248	−3·89
Table II.	·0590	·944	·242	−3·88

These values are seen to be in good agreement with the corresponding numbers obtained by the method of Table II., which are shown in the second line.

7. *Devices for the Determination of μ and χ.*

Having found a simple linkage which will solve equation (1), it is of interest to see whether equation (2) can be solved by similar means.

On setting

$$q=\mu-\iota\chi,$$

equation (2) becomes

$$(q^2-1)\mathrm{Z}=1,$$

i. e.,

$$2\mathrm{Z}=\frac{1}{q-1}-\frac{1}{q+1}. \quad . \quad . \quad . \quad . \quad (18)$$

This equation is illustrated on an Argand diagram in fig. 5.

The diagram is self-explanatory when it is known that the vector $\mathrm{OP}'=q^*=\mu+\iota\chi$, and that

$$\mathrm{P}'\mathrm{Q}'.\mathrm{P}'\mathrm{L}=\mathrm{P}'\mathrm{R}'.\mathrm{P}'\mathrm{M}=1.$$

This immediately suggests the use of the linkage shown in fig. 6.

The lettering of this figure is identical with that of fig. 5. LQ′P′ and MR′P′ are two Peaucellier (or other) invertors. If 2Z is plotted and R′Q′ made to coincide with this vector then when LM is adjusted to be parallel to the real axis, the vector $OP'=q^*=\mu+\iota\chi$, thus giving μ and χ.

This linkage presents several problems in design, and might perhaps be somewhat limited in scope. So we now give a graphical method for determining μ and χ which is both rapid and of a wide scope.

Fig. 5.

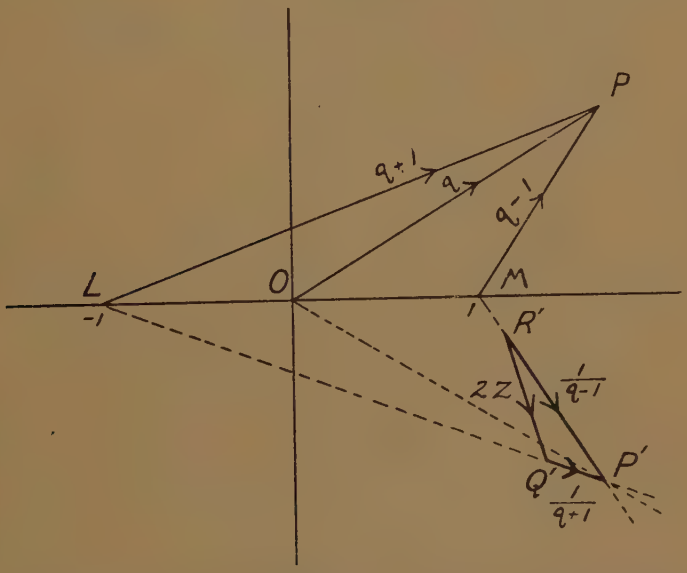

It has been shown † that from equation (2) in the form

$$(\mu-\iota\chi)^2-1=\frac{1}{X+\iota Y}=u+\iota v$$

we can derive the following equations :—

$$u^2+v^2-u/X=0, \quad . \quad . \quad . \quad . \quad . \quad (19)$$

$$u^2+v^2+v/Y=0, \quad . \quad . \quad . \quad . \quad . \quad (20)$$

$$v^2=4\mu^2(\mu^2-u-1), \quad . \quad . \quad . \quad . \quad (21)$$

$$v^2=4\chi^2(\chi^2+u+1), \quad . \quad . \quad . \quad . \quad (22)$$

and the following corresponding graphical procedure :

† See V. A. Bailey, Phil. Mag. xviii. p. 516 (1934).

With u and v measured along a pair of rectangular axes, as in fig. 7, we draw two families of coaxial circles touching at the origin the axes of v and u respectively, and label them X and Y respectively. Each label number is the reciprocal of the corresponding diameter. We also draw on the same diagram two families of confocal parabolas with the axis of u as their common axis and the point S $(-1, 0)$ as their common focus, and label them

Fig. 6.

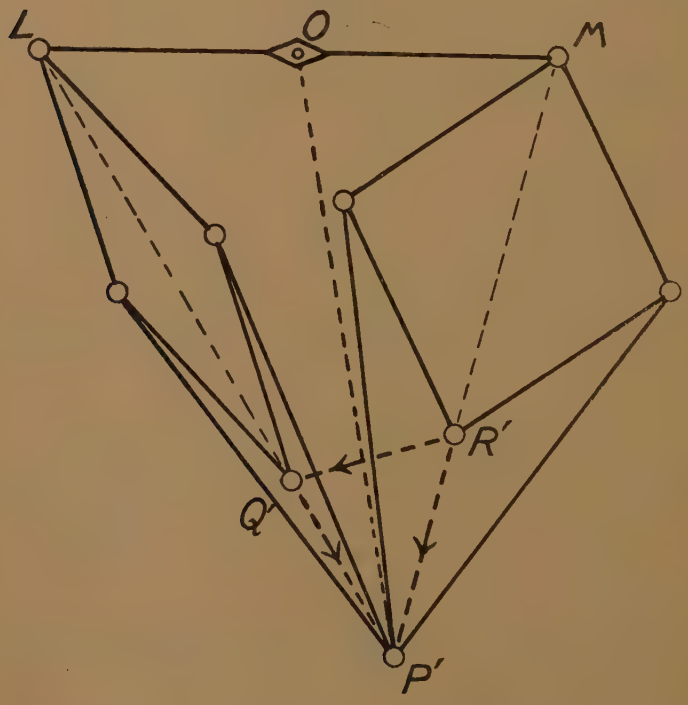

μ and χ. Each label number is equal to the square root of the distance between the focus and the vertex of the corresponding parabola.

With a large number of such circles and parabolas drawn for a range of values of X, Y, μ, and χ we can immediately determine the values of μ and χ by noting the label numbers of the two parabolas which pass through the point of intersection P of the circles labelled with the known values of X and Y.

The trouble of drawing the large number of parabolas required with this method may be avoided through the following considerations.

If r be the distance along any line through the point S $(-1, 0)$ and θ be the angle between that line and the u axis then

$$r\cos\theta=u+1 \quad \text{and} \quad r\sin\theta=v.$$

On substituting in (21) we have

$$r^2\sin^2\theta=4\mu^2(\mu^2-r\cos\theta),$$

i. e.,

$$r^2=(2\mu^2-r\cos\theta)^2,$$

and so

$$r(1+\cos\theta)=2\mu^2.$$

Fig. 7.

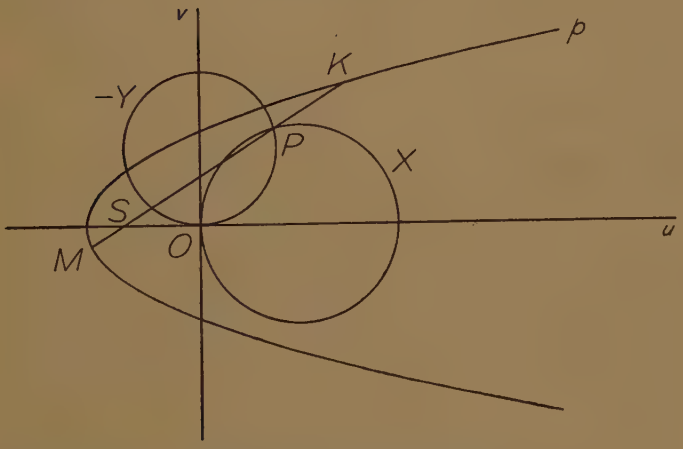

Similarly, by substitution in (22) we find

$$r(1-\cos\theta)=2\chi^2.$$

Thus for the values of μ and χ corresponding to the point P we have

$$\left.\begin{aligned} \text{SP}(1+\cos\theta)&=2\mu^2,\\ \text{SP}(1-\cos\theta)&=2\chi^2.\end{aligned}\right\} \quad . \quad . \quad . \quad . \quad . \quad (23)$$

If the standard parabola

$$r(1-\cos\theta)=2p^2$$

be drawn, as in fig. 7, and if SP intersects this parabola at the points K and M, then

$$\text{SK}(1-\cos\theta)=2p^2$$

and

$$\text{SM}(1+\cos\theta)=2p^2.$$

On combining these results with the formulæ in (23) we have

$$\mu = p\sqrt{\mathrm{SP}/\mathrm{SM}}, \quad \chi = p\sqrt{\mathrm{SP}/\mathrm{SK}}. \quad . \quad . \quad (24)$$

Thus when the point P(X, Y) has been found and the lengths SP, SM, SK have been measured we can immediately determine the values of μ and χ by means of the formulæ (24).

If squared paper be used we may substitute for the lengths SP, SM, SK respectively the ordinates of the points P, M, K, which are easily found by inspection.

The scope of this method may be extended by drawing the parabolas to three scales, say 10^{-1}, 1, and 10, with three corresponding foci; the circles will be the same, but the corresponding values of X and Y will be in the ratios $10^{-1} : 1 : 10$.

The use of parabolas can be completely avoided as follows:—

If N be the projection of P on the u axis, and if the lengths SP and SN be measured, the values of μ and χ are then easily determined by means of the formulæ

$$\mu^2 = \tfrac{1}{2}(\mathrm{SP}+\mathrm{SN}), \quad \chi^2 = \tfrac{1}{2}(\mathrm{SP}-\mathrm{SN}),$$

which follow easily from (23).

The process of adding and subtracting two lengths may be avoided by drawing the family of circles whose common centre is S; for if that member which passes through P cuts the u axis at A and B we have

$$\mu^2 = \tfrac{1}{2}\mathrm{AN}, \quad \chi^2 = \tfrac{1}{2}\mathrm{BN}.$$

To obtain the highest possible accuracy we should first determine μ or χ, whichever is the larger quantity, and then determine the smaller by using the fact that

$$\mu\chi = \tfrac{1}{2}\mathrm{PN}.$$

In conclusion, we may add that the above methods of calculation can also be applied to the formulæ recently published by Huxley *, as the forms of the latter can always be reduced to the forms of our equations (1) and (2).

We desire to express our appreciation of the excellent work done by Mr. H. Taylor in constructing our Vectinvertor, and to acknowledge the help we have received from Messrs. C. S. Davis and L. Goddard.

† L. G. H. Huxley, Phil. Mag. xxv. p. 148 (Jan. 1938).

The work of one of the authors (J. M. S.) has been made possible by a grant from the Commonwealth Government.

Summary.

Methods are given for the rapid numerical determination of the polarization R, refractive index μ, and absorption index χ of an electric wave in an ionized gaseous medium with a constant magnetic field present (*e. g.*, the ionosphere).

First is given a scheme for the arithmetical computation of R, μ, and χ.

Next a simple linkage is described by means of which R can be determined in two settings.

Finally it is shown how, when R is known, μ and χ can be determined by any one of the following means :—

1. A special linkage.
2. A chart containing two families of circles and (say) three parabolas.
3. A chart containing three families of circles.

Appendix.

The equation $x^2+y^2-ax+1=0$ represents a member of a system of coaxial circles whose centres lie on the axis of x and whose common chord is the axis of y. Moreover, the length of the tangent from the origin to any circle of the system is unity. Thus we see from equation (11) that if we select from this system the circle on which the point (ξ, η) lies (and therefore also the point (x, y), since $\zeta=z^{-1}$) then K and K^{-1} are equal to the intercepts of this circle on the axis of x.

By means of such a system we can immediately determine K when x and y are given, and then by means of (10) we obtain F. An alternative scheme is to use the system of coaxial circles passing through the two points $(\pm 1, 0)$ and the formula $F=\sqrt{1-K'/\eta}$, where K′ and K'^{-1} are the intercepts of such a circle on the axis of y.

It is also interesting to note that $1-F^2$ or K/ξ is equal to the square of the eccentricity of the corresponding ellipse in the chart based on conformal representation †.

University of Sydney,
December 1937.

† See V. A. Bailey, Phil. Mag. xviii. p. 516 (September 1934).

LXXVIII. *The Action of Soft X-rays upon Selenium Barrier-Layer Cells.* *By* Arne Eld Sandström, *D.Sc.**

[Received September 14, 1938.]

THE response of barrier-layer cells to X-rays of wave-lengths shorter than 1·5 Å. has been studied by Selenyi and Lange †, Gleason ‡, and Scharf and Weinbaum §. As regards the photo-voltaic effect in the wide range of radiation between 1·5 Å. and the near ultra-violet no investigations have hitherto been published. The author has undertaken to study the response of selenium barrier-layer cells to very soft X-rays, and some preliminary results were recently published in 'Nature' ||.

The investigation was made with ordinary commercial cells of the Falkenthal type, complicated arrangements being avoided until it could be ascertained that measurable photo-currents can be obtained with this type of photo-voltaic cells. Unfortunately these commercial cells have a protective cover of celluloid applied in such a way that it cannot be removed without severely damaging the front electrode. Naturally this cover absorbs long wave-lengths very strongly, and therefore it will practically limit the range of wave-lengths to which the cells are sensitive.

The Apparatus.

On account of the softness of the radiation the measurements necessarily had to be carried out in a vacuum. The photo-element therefore was mounted on a sort of optical bench in a high-vacuum tank. The intensity of the radiation falling on the sensitive surface of the photo-element was varied by moving the element along the optical bench. The arrangement is illustrated in fig. 1. The vacuum-receptacle consists of a brass tube A with a width of about 10 cm. and a length of 100 cm. The end pieces are square brass plates with a half-circular part removed, leaving free entrance to the upper part of the brass tube. Their lower parts serve as holders

* Communicated by Prof. A. E. Lindh.
† Selenyi, P., and Lange, B., *Naturwiss.* xix. p. 639 (1931).
‡ Gleason, P. R., Phys. Rev. xliii. p. 775, and xliv. p. 330 (1933).
§ Scharf, K., and Weinbaum, O., *Z. Phys.* lxxx. p. 465 (1933).
|| Sandström, A. F., 'Nature,' cxli. p. 873 (1938).

for the two guides C and the screw D. The gables are closed with two brass plates, one carrying the X-ray tube B, the other carrying a cone system E for the turning of the screw from the outside.

The flange-joints of the end pieces as well as between the X-ray tube and the gable are tightened with rubber packings. The circular holder K of the photo-element V is mounted on a slide H, which rests on and is held tight to the guides by two springs. The holder K is mounted at such a height that its centre is on the same

Fig. 1.

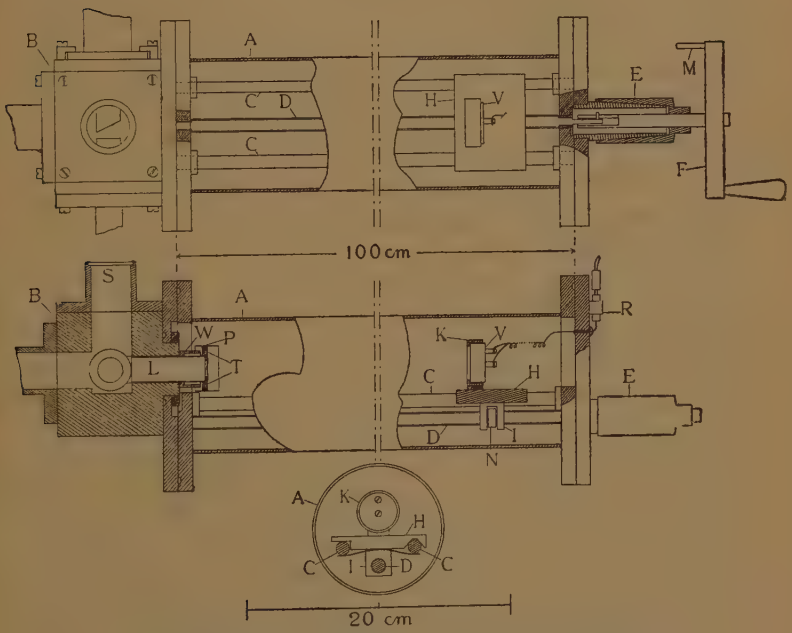

The high-vacuum optical bench with the X-ray tube and the photo-element.

level relative to the guides as is the focus spot of the X-ray tube. On the under side the slide has a fork-like extension I grasping a nut N on the screw D, and by this contrivance the slide can be moved along the guides. The receptacle is evacuated through the X-ray tube. This is of a modern Siegbahn type, with tungsten hot cathode and copper anti-cathode, both water-cooled. The latter was soon covered with a layer of tungsten,

which, to increase the continuous radiation, was not removed. Through the wall of the X-ray tube a window L with a width of 2 cm. connects the tube with the vacuum receptacle A. To prevent visible light from the cathode or the focus-spot from reaching the photo-element the contrivance P was inserted into this window. It consists of a brass tube on the inside covered with aluminium to diminish the secondary radiation. It projects into the vacuum-chamber, where it ends with an aluminium front T. In this there is a 15-mm. wide window which is covered with two aluminium foils, each $0{\cdot}5\,\mu$ thick. Behind the frontal plate T there are some holes for the evacuation. These are covered by a brass ring W, leaving a narrow space free behind the plate T. It was found that this arrangement was sufficient for a complete screening off of visible light. S is a glass window enabling observation of the interior of the tube during the running. For every turn of the crank F the small pin M closes the current through an electrical counter on which the position of the photo-element then can be read immediately.

The photo-element was connected with the galvanometer through two insulated wires which were brought through the rear end piece to the contact arrangement R. For the first measurements a Hartmann and Braun galvanometer was used, with an internal resistance of 97·7 ohms and a sensitivity of $2{\cdot}64\times10^{-9}$ amp. These measurements only aimed at determining the connexion between the photo-current and the intensity of the incident light for various external resistances. For the later measurement I used a Siemens and Halske galvanometer with a resistance, when conveniently shunted, of 35 ohms and a sensitivity of $4{\cdot}78\times10^{-9}$ amp. As the photo-current for different external resistances should be measured at the same time as the photo-electric voltage for infinite external resistance, the circuit illustrated in fig. 2 was used. A is the photo-element, B the galvanometer, and C a resistance with which the external resistance can be varied. D is a switch and F a resistance for varying the current from the source G. The potential of the photo-element is determined by measuring the voltage drop over the precision resistance E, when the current through the milliammeter H is regulated so that no current goes through the galvanometer B.

The high-tension for the X-ray tube was supplied from an aggregate in Greinacher-coupling with two 0·1 μF condensers for smoothing out the current. All galvanometer connexions were protected against disturbances from the currents for running the X-ray tube.

As already mentioned, the intensity was varied by moving the slide with the photo-element along the guides. The inverse square of the distance from the focus-spot to the sensitive layer was taken as a value of the intensity.

Naturally, precautions had to be taken to prevent secondary or reflected beams from the walls of the vacuum-receptacle A from reaching the photo-voltaic cell, and thus influencing the results. As aluminium gives only a very faint secondary radiation it ought to be possible to diminish the latter by coating the inside of A with aluminium. However, a trial showed that

Fig. 2.

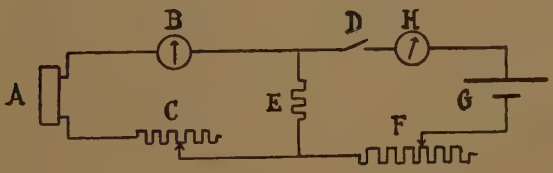

this did not affect the value of the photo-current. Then a screen just large enough to cover the photo-element was placed halfway between this and the diaphragm P. The beam could strike the wall just as well as without the screen, and thus the secondary and reflected radiations were as strong as when the element was exposed to the full intensity of the beam. Nevertheless no measurable photo-currents were obtained, and we may conclude that the influence of secondary and reflected rays certainly was negligible.

The focus-spot ought to be so small that it can be considered as a point in comparison with the distance to the cell. In the case of low voltages this is rather difficult to attain, and therefore the author considered it advisable in any case not to use shorter distances than 15 cm., and in most of the series of measurements the distance was never less than 18 cm. In addition the extension of the focus-spot may cause a systematic

error in the relative values of the intensity, especially as regards comparisons between results which were obtained with different voltages. The extension of the focus-spot also causes an uncertainty as to the true distance between the light-source and the cell. If this error in the distance is 2 mm. the relative error in the value of the intensity will be 0·4 per cent. for the lowest value and then increase to 2·7 per cent. for the highest. This is a systematic error influencing all the measured values in one and the same direction.

As slow electrons easily ionize residual gases, X-ray tubes often work unsteadily at such low voltages as those which were used for the present investigation. As the load and voltage of the tube were kept as constant as possible a change in the ionization current will cause a change in the intensity ouptut. Changes in the filament also may give rise to changes in the focus-spot, and thus to variations in the intensity. To ascertain how large these variations really were the barrier-layer cell was placed at a distance of 35 cm. from the focus-spot and readings taken during one hour with a voltage of 3·5 kv. and 105 mA. From these readings the author found that variations of ± 4 per cent. may readily be expected.

Except for the lowest intensities the errors in the galvanometer readings are far below 1 per cent., and are thus quite negligible in comparison with the errors which are discussed above. As the systematic error in the intensity for the shortest distances only may exceed 2 per cent., we will assume that the average error is less than 6 per cent. On account of this rather low accuracy the curves were always determined by as many points as could be considered reasonable. Each one of the curves in fig. 3, for example, is determined by 38 points. None of these diverges from the corresponding line more than 3 per cent. Thus the above estimated error of 6 per cent. seems to be more than large enough, and in most cases we may expect the accuracy to be higher.

If abrupt changes appear for a certain distance to the focus-spot it is always possible to ascertain if these changes are real by diminishing the current through the tube and determining the points of the curve for this new intensity. If the doubtful change appears

at the same distance to the focus-spot it certainly is caused by some reflexion or secondary radiation in the apparatus, but if it moves to a point corresponding to

Fig. 3.

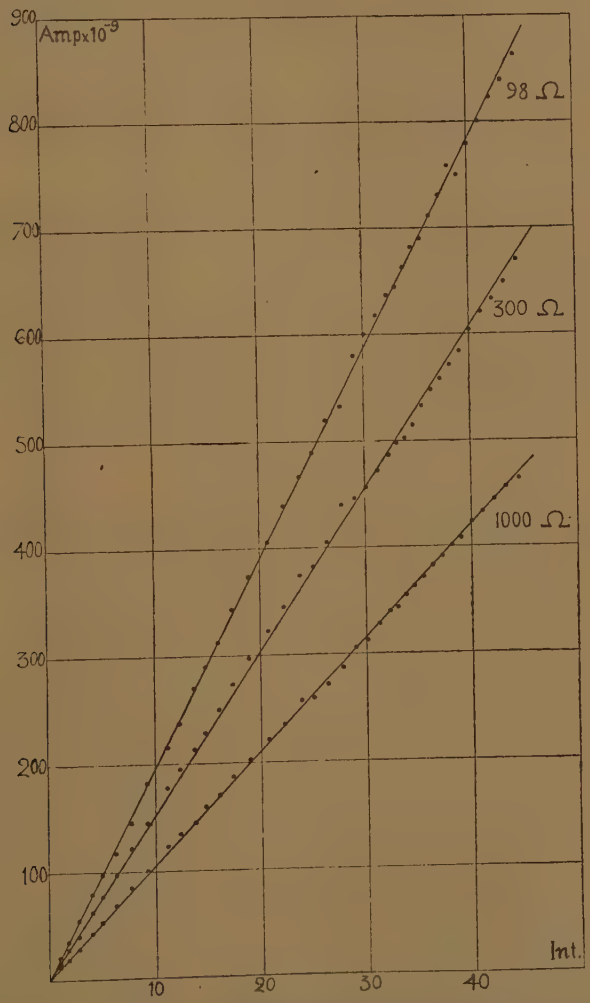

The photo-current as a function of the intensity at the external resistances 98, 300, and 1100 ohm. Wave-length range 3·5 to 20 Å.

the new output of the tube it certainly must be considered real.

The Radiation.

In most cases during the investigation the voltage of the X-ray tube was 3·5 kv. This meant that the shortest wave-length in the continuous radiation was 3·53 Å. As practically no wave-lengths longer than 20 Å. are transmitted by the Al-foils of the window L (see fig. 1), the active wave-length range may be put at 3·5–20 Å.

In some cases the short-circuit current was also measured for tube voltages of 2·5 and 1·5 kv. In the first of these cases the active wave-length range lies between 4·9 and 20 Å., and in the second between 9·3 and 20 Å.

It ought to be noted that the M-series of tungsten falls just in this region, with its strongest lines in the minimum of intensity caused by the absorption in the Al-foils. Unfortunately, the ratio between the characteristic and the continuous radiation is unknown, and, further, the whole M-series does not appear when the voltage is 2·5, and none of it when the voltage is 1·5 kv.

The Measurements.

Unit radiation intensity was taken in each separate case, as the intensity with a distance of 100 cm. between focus-spot and photo-element. This value was also used as the unit of the arbitrary scales of the figures. When curves were taken, which had to be compared, the measurements were done without any changes as regards the X-ray tube, barring the influence of letting air into it and re-evacuating. In all cases the illuminated area of the photo-element was 2 cm.^{2}. The values of the currents and voltages in figs. 3–8 all relate to this area.

As is well known, for visible light and the near ultra-violet the short-circuit current and currents for external resistances, which are small compared to the apparent internal resistance of the photo-element, are rectilinear functions of the intensity. The same obtains for X-rays of short wave-lengths. In the present case a series of observations was taken when the external resistance was 97·7, 297·7, and 1097·7 ohms. The tube voltage was 3·5 kv. and the load 30 mA. The photo-element was a Pressler cell, system Falkenthal. In fig. 3 the photo-currents are plotted against the relative intensity, and in all three cases the photo-currents are rectilinear

functions of the intensity. In this respect the conditions seem to be the same as in the case of visible light.

Observations were also made for 2·5 and 1·5 kv. voltages on the tube and with currents of 50 and 150 mA. respectively. The curve for 2·5 kv. is illustrated in fig. 4. In both cases the photo-current was found to be a rectilinear function of the intensity.

With the arrangement of fig. 2 curves were obtained for a newly bought Pressler cell and a Lange cell, as well

Fig. 4.

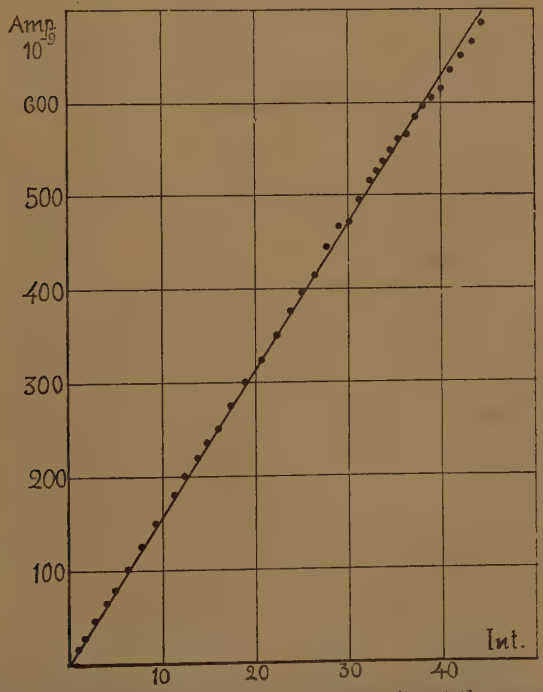

The photo-current as a function of the intensity at the wave-length range 4·9 to 20 Å. and an external resistance of 98 ohm.

as for the older Pressler cell mentioned above. In these cases the intensity of the radiation from the X-ray tube was higher than formerly, the current being 100 mA. at a voltage of 3·5 kv. The curves for the "short-circuit" currents of these three cells are illustrated in fig. 5. Here one is struck by the remarkable fact that, though in the case of the latter two cells the usual straight

lines are obtained, the photo-current of the new Pressler cell is not a rectilinear function for very small intensities. This divergence from the rectilinear curve remains when the external resistance is raised, as can be seen from fig. 6. Further, when the cell was exposed to a radiation of the wave-length range 9·3–20 Å. the same concavity of the curve appeared.

Fig. 5.

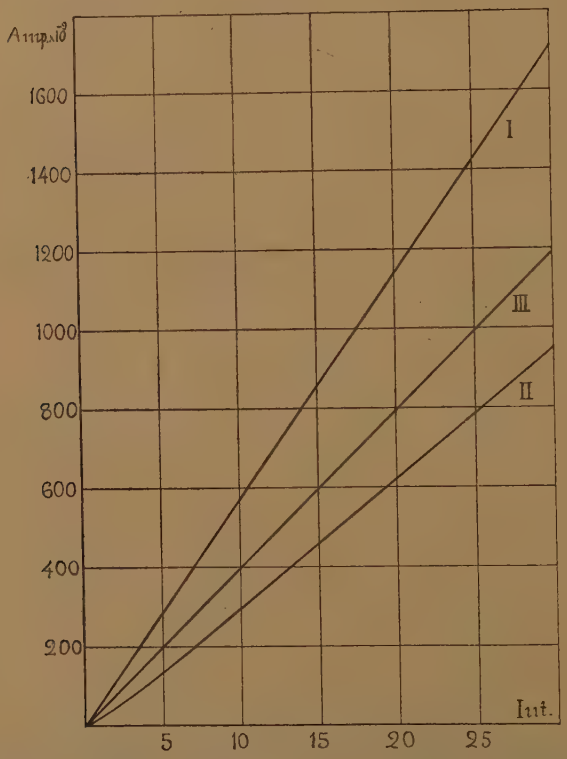

The "short" circuit current for three different photo-elements. I and II two different Pressler cells, system Falkenthal, and III, a Lange ocular-cell.

As will be more fully described below, the apparent internal resistances of the cells often show abrupt and very considerable changes. Thanks to this peculiarity it was possible to obtain curves for one and the same photo-element but with different internal resistances. It turned out, however, that the concavity of the photo-current-

intensity curve was the same when the apparent internal resistance was 2300 ohms as when it was 500 to 800 ohms.

The element was also exposed to visible light from a small electric bulb, and the intensity varied over values which gave currents of the same order of magnitude as those caused by soft X-rays. In this case no deviation from the rectilinear curve could be observed. Thus the concavity of the current-intensity curve for small intensities must be considered a characteristic feature of the action of the soft X-rays on this particular cell.

Fig. 6.

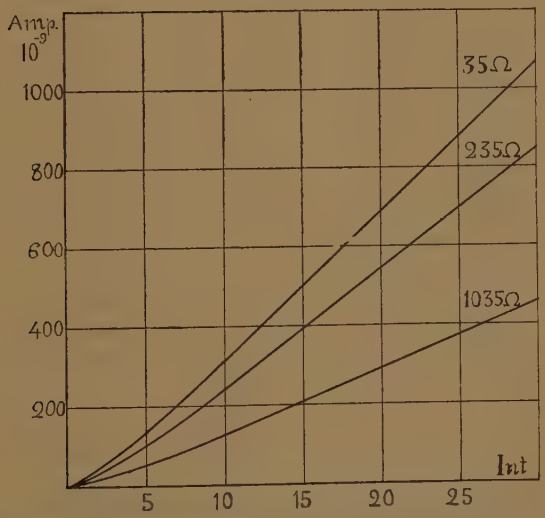

Photo-current characteristics of a photo-element showing a slight deviation from the usual conditions at small intensities.

In this place it ought to be mentioned that this peculiarity can scarcely be caused by some defect in the experimental arrangements. The observations on this element were often carried out alternately with those on the other two elements, no changes in the apparatus being made except the exchange of photo-elements. However, the curve of the last acquired element continued to show the concavity described above, while the curves of the other two elements always were straight lines.

Naturally, from the scanty material given by three elements only it is impossible to conclude as to the cause

of the observed discrepancy. However, from figs. 5 and 6 we see that the divergence from the straight line is so small that, for higher currents at least, it is possible to use the element in question on the assumption that the photo-current, as usual, is a rectilinear function of the intensity of the incident light.

On account of the specific nature of the barrier-layer cells it is impossible to measure or calculate the values of their real electromotive forces *. Failing this the elements may be characterized by their voltage for infinite external resistance. With the method of compensation illustrated in fig. 2 this voltage was determined

Fig. 7.

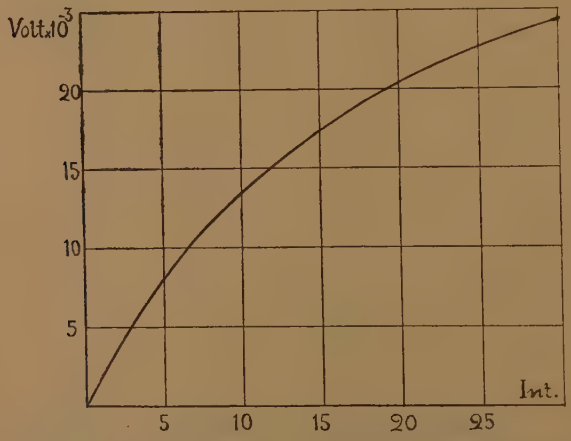

Photo-voltage of an element with a high internal resistance.

as a function of the intensity in figs. 7 and 8. However, here we also have to consider the apparent resistance of the elements. When the element has a high apparent resistance the slope of the voltage-intensity curve will decrease with increasing intensity (fig. 7), but when the element has a low resistance the slope of the curve will increase with increasing intensity (fig. 8). Thus we find here again the same condition as in the case of visible light †. It ought to be noticed that the voltages were measured at the same time as the photo-currents, so the intensity-scales in figs. 5, 7, and 8 are the same.

* B. Lange, 'Die Photoelemente,' Leipzig, 1936, part 1, p. 62.
† B. Lange, *l. c.* p. 60.

Because of the fact that the internal resistance of a barrier-layer cell can be considered as being in parallel with the electromotive forces we may write *, provided that the resistance of the electrodes and the selenium layer may be neglected, $R_i = \frac{IR_a}{I_0 - I}$, where R_i is the apparent internal resistance, R_a the external resistance at which the current is I, and I_0 the short-circuit current. The resistance of a barrier-layer cell varies not only with the intensity of the incident light, but also with the external resistance. However, Lange has pointed out

Fig. 8.

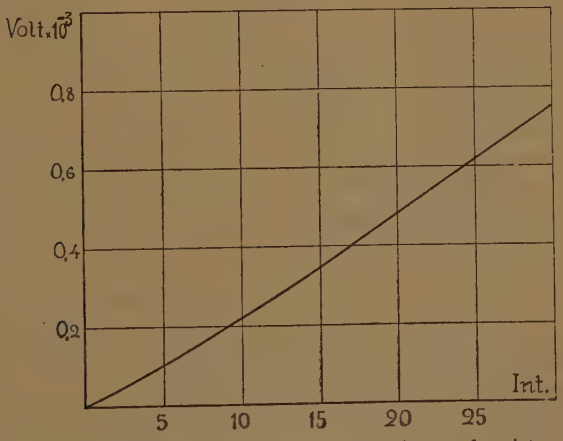

Photo-voltage of an element with a low internal resistance.

that it is possible to characterize the resistance by the resistance for $I = \frac{1}{2}I_0$, when $R_i = R_a$. To obtain this value for a given intensity the value of I was plotted against the external resistance, and from the curves the value of R_a was then found for which the current was half as much as for $R_a = 0$.

Some preliminary determinations of the resistance of the first Pressler cell indicated that its resistance had increased in a remarkable way during the course of the investigation. To ascertain if this change was accidental or not several series of observations were made during one month with a new cell. Simultaneous determinations were made of the current for four different external

* B. Lange, *l. c.* p. 64.

resistances. The values were rather crude, but the precision was still high enough to permit a comparison between the three cells at different times.

In the beginning the new cell appeared to have a very fluctuating resistance for low intensities. At the same time the voltage also varied in an unaccountable way and the characteristic of the current was not at all rectilinear. It is possible, however, that some outer disturbances caused these irregularities, because a series taken the following day did not show any abrupt changes either in the resistance or the voltage. The resistance appeared to be rather low and slightly increasing with the intensity. For each of the earlier series of observations the apparent internal resistance of this barrier-layer cell semeed to be increasing. Between the third and the fourth series the effect of visible light on this cell was studied, its resistance being found to have a mean value of 800 ohms. Still, in these observations there was nothing to indicate if the change in resistance was due to the illumination with X-rays or to certain interior changes with time.

By accident it was found, however, that when the cell had been exposed to light of wave-lengths longer than 9·28 Å. and then the resistance measured, while the cell was exposed to a radiation of the wave-length range 3·53–20 Å., a value was obtained which was three times as large as the value of the resistance at the softer radiation. At first a systematic investigation seemed to reveal that abrupt changes of the internal resistance took place when the wave-length region of the incident light was changed. A second series of observations with a rather low load on the X-ray tube gave very nearly constant values of the apparent internal resistance, the voltage of the tube being varied between 1·5 to 4·5 kv. as in the first series. Thus it is more probable that the changes in resistance are caused by more or less abrupt changes in the intensity of the incident X-radiation. With the present arrangements such changes were scarcely to be avoided when the voltage of the tube was altered during the exposure of the element to the radiation. As to an explanation of the effect of the radiation on the resistance, the main difficulty is the dual action of the X-rays. Schweickert * has found that small conducting

* Hans Schweickert, *Zeits. f. Phys.* cix. p. 413 (1938).

bridges form in the barrier-layer when the cell is stored for some time. He has also found that these bridges are easily broken up by the Joule-heat when a current is sent through the layer. Also in the present case this phenomenon may be responsible for the very low resistance of the new cell and also for the continuous increase of the resistance when photo-currents are taken from the cell with no very long interludes of rest. The abrupt changes, which sometimes seem to depend on a change in the wave-length and sometimes on a change in the intensity of the incident light cannot be directly explained in this way. But the small conducting bridges may also be found and broken up by atomic processes, which in the case of X-rays are brought about by the photo-effect itself.

The Application of Selenium Barrier-Layer Cells to Spectrophotometric Purposes in the Region of Soft X-rays.

The original object of the present investigation was to study the possibility of using commercial photo-elements for measuring intensities in long wave-length X-ray spectra. The results so far suffice to settle this question.

We will suppose that the distance between the focus-spot and the element is as short as 50 cm. We will further neglect the finite reflective power of the crystal or grating. With the aid of fig. 6 we find that in this case the best cell will give a current of $0{\cdot}286 \times 10^{-6}$ amp. for the whole unresolved wave-length region between 3·5 and 20 Å., when the voltage is 3·5 kv. and the load 100 milliamp. If we desire to resolve wave-lengths which have a separation of 0·1 XU we will have to use such a narrow slit before the element that, at the wave-length of maximum intensity, the photo-current will be only 5×10^{-12} amp. if the sensitivity is supposed to be constant in the whole wave-length region. Even with a bent crystal spectrograph the conditions will be far more unfavorable than was supposed above, and we may conclude that the commercial cells hitherto investigated are not suitable for this kind of work. This does not mean that it is impossible to make them more suitable by some alterations. The first one to suggest itself is to use cells without the protective cover of

celluloid. As yet, however, it has been impossible to procure any elements without this protective cover.

When it is only a question of measuring the intensity of soft X-rays which are not spectrally dispersed the selenium photo-elements may be very advantageous. As has been mentioned, at low voltages the intensity of the X-rays has been found to change even when voltage and load have been kept scrupulously constant. The photo-elements now afford a very convenient medium for the control of the radiation output of the tube. For example, an element may be mounted in the wall of a tube fully exposed to a part of the radiation but suitably protected from the heat. The photo-current will be strong enough for measuring with an ordinary instrument, and the contrivance can then easily be used for controlling the constancy of the intensity of the radiation from the focus-spot.

The high-vacuum optical bench as well as the X-ray tube were built with the aid of a grant from the Längmanska Kulturfonden. I am also indebted to Professor A. E. Lindh, D.Sc., Uppsala, for his kindness in allowing me to work in his laboratory as well as for the indispensable laboratory equipment he put at my disposal.

Summary.

1. As regards photo-current and photo-voltage selenium barrier-layer elements respond to soft X-rays of the wave-length region 3·5–20 Å. mainly in the same way as to visible light.

2. In one case an element showed a remarkable deviation of the current-intensity curves from the straight line for small intensities.

3. When exposed to soft X-rays the barrier-layer resistance was found to vary in a way not quite accounted for.

4. The photo-currents are too small to allow the elements to be used for intensity measurements in a spectrally dispersed radiation.

Physics Laboratory,
University of Uppsala.
September 1938.

[*The Editors do not hold themselves responsible for the views expressed by their correspondents.*]

FIG. 2.

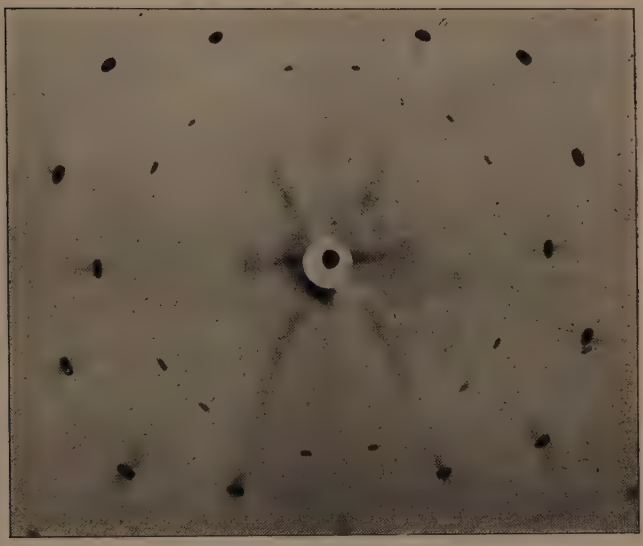

24 hours at room-temperature.

FIG. 3.

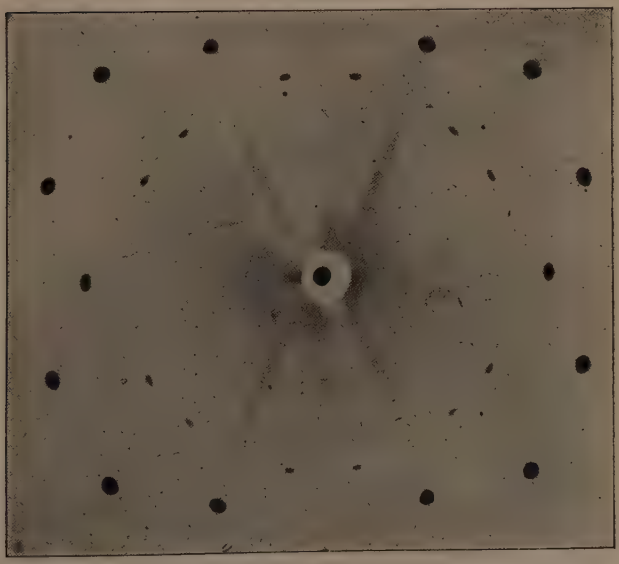

105 minutes at 200° C.

FIG. 4.

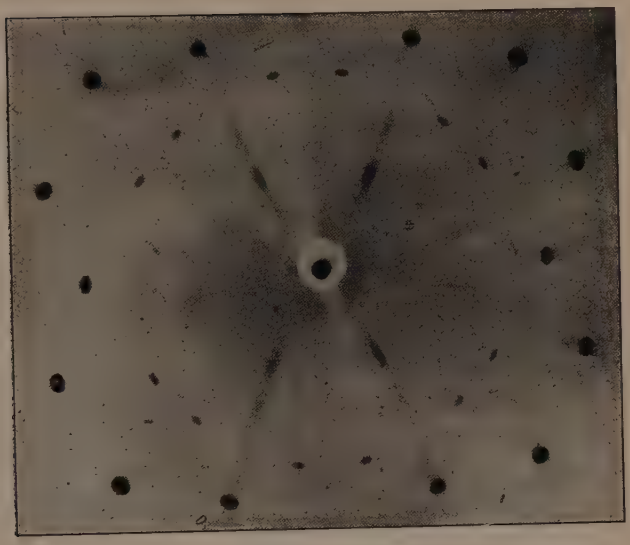

6 hours at 200° C.

FIG. 5.

19 days at 200° C.

FIG. 7.

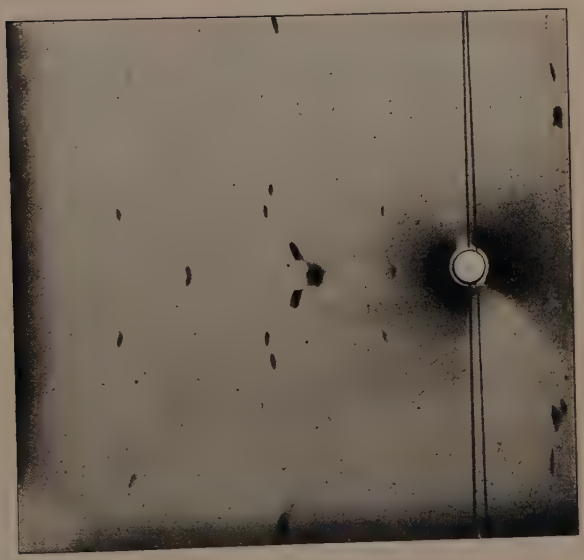

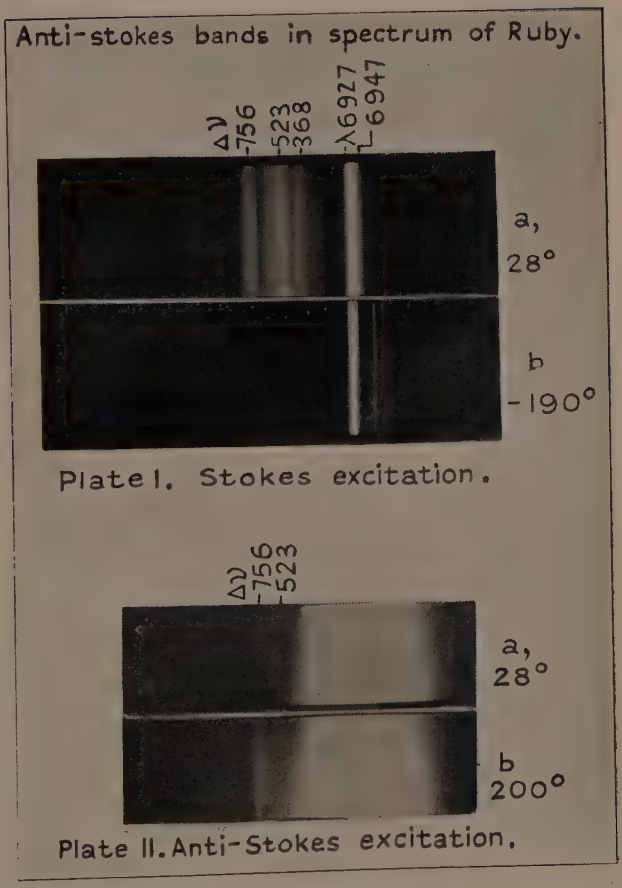
Anti-stokes bands in spectrum of Ruby.
Δν
-756
-523
-368
λ6927
L 6947
a,
28°
b
-190°
Plate I. Stokes excitation.
Δν
-756
-523
a,
28°
b
200°
Plate II. Anti-Stokes excitation.

THE

LONDON, EDINBURGH, AND DUBLIN

PHILOSOPHICAL MAGAZINE

AND

JOURNAL OF SCIENCE.

[SEVENTH SERIES.]

DECEMBER 1938.

LXXIX. *Application of the Operational or Symbolic Calculus to the Theory of Prime Numbers.*

By BALTH. VAN DER POL, *D.Sc., Natuurkundig Laboratorium der N. V. Philips' Gloeilampenfabrieken, Eindhoven, Holland* *.

[Received September 21, 1938.]

§1. IN a series of papers[1] dating back to 1929 the operational calculus, as originally developed by O. Heaviside, was extended in different directions. Whereas Heaviside applied its methods mainly to problems connected with electrical circuits with constant parameters (independent of the time) which were initially at rest, the method could be extended to arbitrary initial conditions. But also differential equations with variable coefficients could be attacked with this method and the properties of the solutions studied. Many new relations between different functions such as Bessel functions, spherical harmonics, Laguerre's and Hermite's polynomials, and others, could thus be obtained in an extremely simple way. Also the method could be extended to a " simultaneous operational calculus " where two or more variables are treated operationally. Again, following Heaviside, the method appeared a powerful weapon for evaluating integrals.

* Communicated by the Author.

It is well known that in essence Heaviside's operational calculus and the extensions obtained later on are based on the Laplace transform. This point was stressed by J. R. Carson[2] and on several occasions by ourselves[1]. But it is, perhaps, not so well known that O. Heaviside himself plainly and clearly points this out in his book 'Electromagnetic Theory,' iii. p. 236 (London, Benn Brothers, 1922).

The great heuristic value, however, of the symbolic calculus does not seem to be generally realized yet, although a set of simple rules have been developed which make the use of it a relatively simple matter.

It is the purpose of the present note to apply the symbolic calculus this time to some problems connected with the theory of prime numbers; the ease and simplicity with which the results are obtained may, we hope, again show the great heuristic power of it. But the use of the symbolic calculus in this field shows another great advantage over the usual methods in so far that the developments can most easily be depicted *graphically*, leading to a set of graphs which, we think, may considerably clarify the properties of many discontinuous functions belonging to the theory of numbers. This possibility is brought about by the fact that the operational "image" of a discontinuous "original" is a continuous function. As, moreover, the "original" fully determines the "image" and *vice versa*[3], we can deduce the properties of the discontinuous "originals" from those of their continuous "images." The great gain thus obtained will be obvious. (A further general extension of the symbolic calculus is in course of publication.)

§ 2. If we have given a function $h(x)$ which we shall call the "*original*" we obtain its "*image*" $f(p)$ with the aid of the integral

$$f(p)=p\int_0^\infty e^{-px}h(x)\,dx, \quad . \quad . \quad . \quad . \quad . \quad (1)$$

which relation we shall denote by

$$f(p)\doteqdot h(x), \quad . \quad . \quad . \quad . \quad . \quad . \quad (2)$$

assuming at the same time, as has been usual so far in the symbolic calculus, all our originals to be zero for

$x<0$. Thus, quoting some former results[1], it is easily shown with the aid of (1) that

$$\frac{p}{p-\alpha} \doteqdot e^{\alpha x}, \quad \ldots \quad (3\,a)$$

$$\frac{1}{p} \doteqdot x, \quad \ldots \quad (3\,b)$$

$$\frac{1}{p-1} \doteqdot e^{x}-1, \quad \ldots \quad (3\,c)$$

$$A \doteqdot A, \quad (A=\text{arbitrary constant}) \quad \ldots \quad (3\,d)$$

$$\log \frac{1}{p} \doteqdot \log x + C, \quad (C=\text{Euler's constant}) \quad \ldots \quad (3\,e)$$

$$-\log (p-1) \doteqdot Ei(x) = \int_{\infty}^{-x} \frac{e^{-s}}{s}\, ds, \quad \ldots \quad (3\,f)$$

to which we now add

$$\log (\alpha p+\beta) \doteqdot \log \beta + \int_{\frac{\beta}{\alpha}x}^{\infty} \frac{e^{-s}}{s}\, ds = \log \beta - Ei\left(-\frac{\beta}{\alpha}x\right), \quad (4)$$

which latter relation follows also at once from (1).

A very important function, of which we shall make considerable use further on, is the *unit function*, which we denote by $U(x-a)$ and which is zero for $x<a$, where a is a positive constant, and which equals unity for $x>a$.

Its image can, for $Re\ p>0$, at once be obtained from (1) as follows:

$$p\int_0^{\infty} e^{-px} U(x-a)\, dx = p\int_a^{\infty} e^{-px}.1.dx = e^{-ap},$$

or, for short:

$$e^{-ap} \doteqdot U(x-a). \quad \ldots \quad (5)$$

The data from the symbolic calculus here given suffice to derive not only the "Prime number theorem," but also several other relations of the theory of numbers.

§ 3. Let us first consider the step function $[x]$, where, as usual, the brackets mean the greatest integer contained in the real variable x. This function is depicted in fig. 1. As indicated by the shading it can be considered as the superposition of the unit function $U(x-1)$, jumping at

$x=1$, the unit function $U(x-2)$, jumping at $x=2$, etc. Thus, according to (5), we have

$$e^{-p}+e^{-2p}+e^{-3p}+\ldots \doteqdot [x],$$

or

$$\frac{1}{e^p-1} \doteqdot [x], \quad \mathrm{Re}\, p>0. \qquad \ldots \quad (6)$$

Fig. 1.

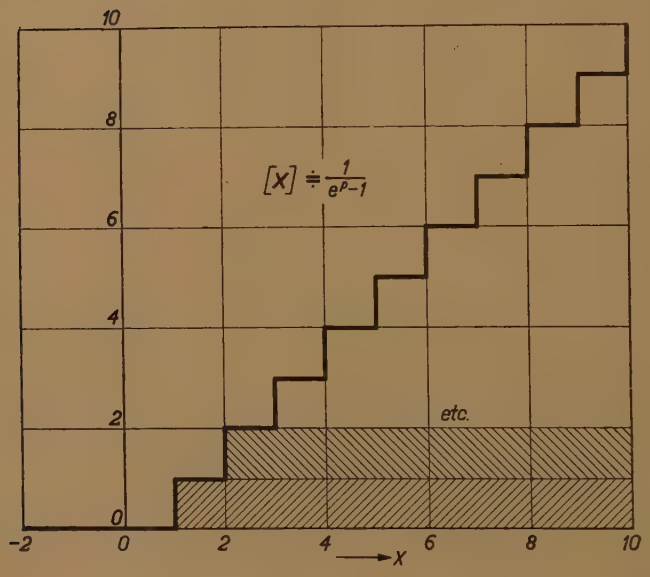

Fig. 2.

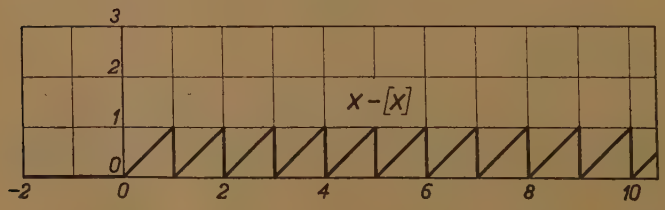

It is, further, easy to find the image of the saw-tooth function of fig. 2 given by $x-[x]$, for, with the aid of (3 b), we have at once

$$\frac{1}{p}-\frac{1}{e^p-1} \doteqdot x-[x], \quad \ldots \quad (7)$$

or, if we subtract $\frac{1}{2}$ from both sides (making the average zero),

$$x-[x]-\tfrac{1}{2} \doteqdot \frac{1}{p}-\frac{1}{e^p-1}-\tfrac{1}{2} = \frac{d}{dp}\left\{\log\left(\frac{\frac{1}{2}p}{\sinh\frac{1}{2}p}\right)\right\}, \quad (8)$$

which function of p plays an important rôle in the higher theory of the Γ functions. It is here derived, however, in an extremely simple and natural way as the image of the saw-tooth function of fig. 2.

§ 4. Consider next *the zeta function of Riemann*, $\zeta(p)$, as a function of p, and let it be the image of an original $h_1(x)$ to be obtained.

Now $\zeta(p)$ is defined for Re $p>1$ by the series

$$\zeta(p)=\frac{1}{1^p}+\frac{1}{2^p}+\frac{1}{3^p}+\ldots\ldots, \quad . \quad . \quad . \quad (9)$$

which we can write as

$$\zeta(p)=e^{-p\log 1}+e^{-p\log 2}+e^{-p\log 3}+\ldots\ldots \quad . \quad (9\,a)$$

But according to (5) $e^{-p\log n}$ is the image of $\mathrm{U}(x-\log n)$, *i.e.*, the function which jumps from zero to the value unity at $x=\log n$. Thus the original of $\zeta(p)$, see fig. 3, is the function which jumps a unit step at $x=\log 1$, $x=\log 2$, $x=\log 3$, etc., and therefore we can write down at once the very fundamental relation

$$\boxed{\zeta(p) \doteqdot [e^x]} \quad . \quad \mathrm{Re}\ p>1. \quad . \quad . \quad . \quad (10)$$

It is of interest to compare this symbolic relation with the one obtained above :

$$\boxed{\frac{1}{e^p-1} \doteqdot [x]} \quad , \quad \mathrm{Re}\ p>0 \quad . \quad . \quad . \quad (6)$$

showing that $\zeta(p)$ plays the same rôle with respect to e^x as the function $\dfrac{1}{e^p-1}$ plays with respect to x.

The fact that (10), which is here derived for the first time, could be obtained (like (6)) with the help of the symbolic calculus without practically any additional calculations again shows the great simplicity of the methods

employed. From (10) with the aid of (1) we can now write at once the integral

$$\zeta(p)=p\int_0^\infty e^{-px}[e^x]\,dx,$$

or, replacing e^x by s,

$$\zeta(p)=p\int_1^\infty \frac{[s]\,ds}{s^{p+1}}, \quad . \quad . \quad . \quad . \quad . \quad (11)$$

Fig. 3.

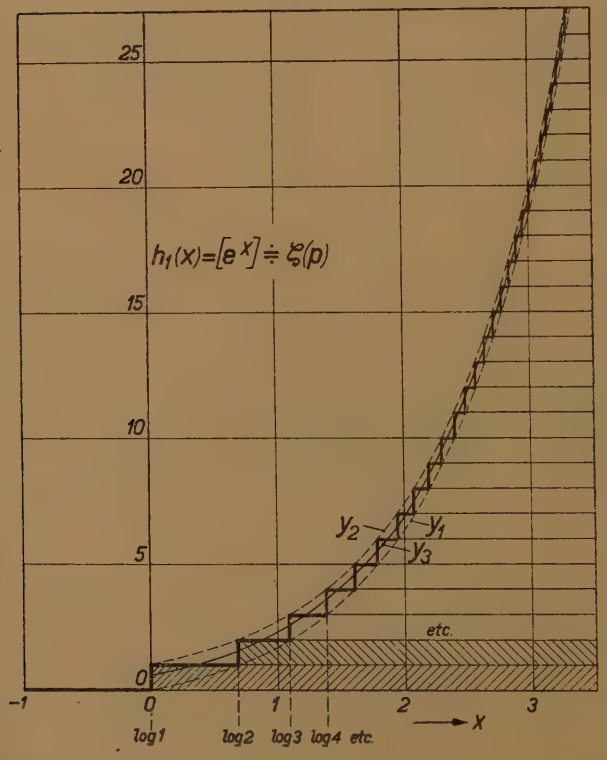

defining, like the basic series expansion (9), $\zeta(p)$ for Re $p>1$.

But again, as in (7), we can from (10) derive a saw-tooth function by subtracting from (10) the exponential (see 3 *a*)

$$\frac{p}{p-1} \doteqdot e^x,$$

and thus obtain, see fig. 4:

$$\frac{p}{p-1} - \zeta(p) \doteqdot e^x - [e^x], \quad \mathrm{Re}\, p > 1, \quad . \quad . \quad (12)$$

which is the analogue of (7). Now it is of interest to note that the natural construction of the saw-tooth function $e^x - [e^x]$ in (12), which oscillates between zero and unity, just annuls the one and only pole of $\zeta(p)$ at $p=1$, because it is known that the left-hand member of (12) has no poles[4]. Again, from (12) with the aid of (1) we can now write at once the integral

$$\frac{p}{p-1} - \zeta(p) = p \int_0^\infty e^{-px} \{e^x - [e^x]\}\, dx, \quad \mathrm{Re}\, p > 1,$$

Fig. 4.

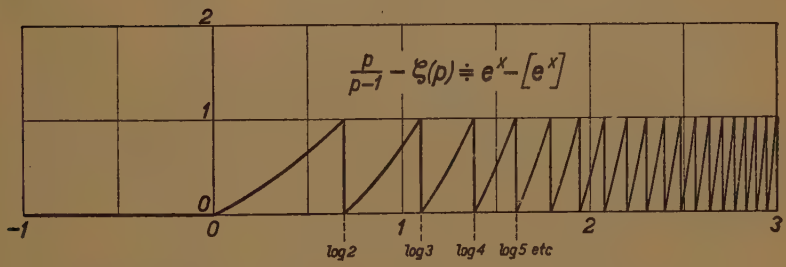

or, replacing e^x by s,

$$\frac{p}{p-1} - \zeta(p) = p \int_1 \frac{s - [s]}{s^{p+1}}\, ds, \quad . \quad . \quad (12\,a)$$

which is already valid for $0 < \mathrm{Re}\, p$, because (12 *a*) represents the analytical continuation of the left-hand function which now has no poles.

Thus (12 *a*) extends (11) in a welcome way in so far as it converges already for $\mathrm{Re}\, p > 0$. Hence (12 *a*) provides us with an integral along the real axis which defines $\zeta(p)$ also in the critical strip $0 < \mathrm{Re}\, p < 1$, in which all the much discussed zeros of the function are situated.

It is also an easy matter to construct the original of

$$\left(1 - \frac{1}{2^{p-1}}\right) . \zeta(p),$$

because it is equal to

$$\sum_{n=1,\,2,\,3\,\ldots} (-1)^{n+1} \frac{1}{n^p} = \sum_n (-1)^{n+1} e^{-p \log n}, \quad . \quad . \quad (13)$$

and therefore represents the discontinuous square-topped function of fig. 5, which jumps up unity at $x=\log(2n+1)$ and down unity at $x=\log(2n)$, and thus oscillates again between 0 and +1. Again the image in (13), representing an original which thus remains finite everywhere, remains itself finite at $p=1$.

§ 5. In order now to derive in a most simple way the "Prime number theory" and some other relations of the theory of numbers we note, fig. 3, that

$$h_1(x)=[e^x],$$

Fig. 5.

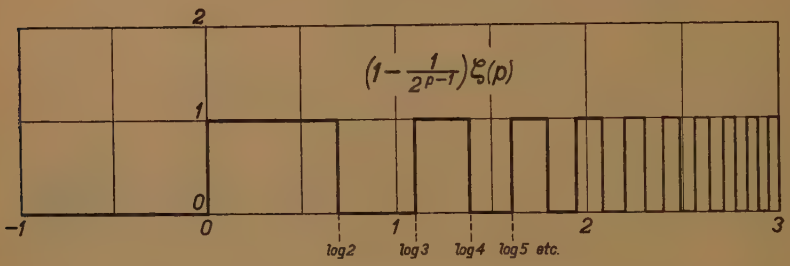

the original of $\zeta(p)$, is everywhere contained between the two limits y_1 and y_2, where

$$y_1(x)=e^x-1,$$
$$y_2(x)=e^x,$$

or operationally

$$\left.\begin{aligned} y_1(x) &\doteqdot \frac{p}{p-1}-1=\frac{1}{p-1}, \\ y_2(x) &\doteqdot \frac{p}{p-1}, \end{aligned}\right\} \quad . \quad . \quad . \quad (14)$$

which two functions of p we can consider as a first rough approximation to $\zeta(p)$, but where full account is taken of its one pole at $p=1$. The first expression, $\frac{1}{p-1}$, is also obtained when in (9) we replace the summation by an integration as

$$\int_1^\infty \frac{dn}{n^p}=\frac{1}{p-1}.$$

An even better approximation, $y_3(x)$, lying between $y_1(x)$ and $y_2(x)$, is at once evident from a consideration of the original $h_2(x)$ of $\zeta(p+1)$. For, see fig. 6, $\zeta(p+1)$, according

Fig. 6.

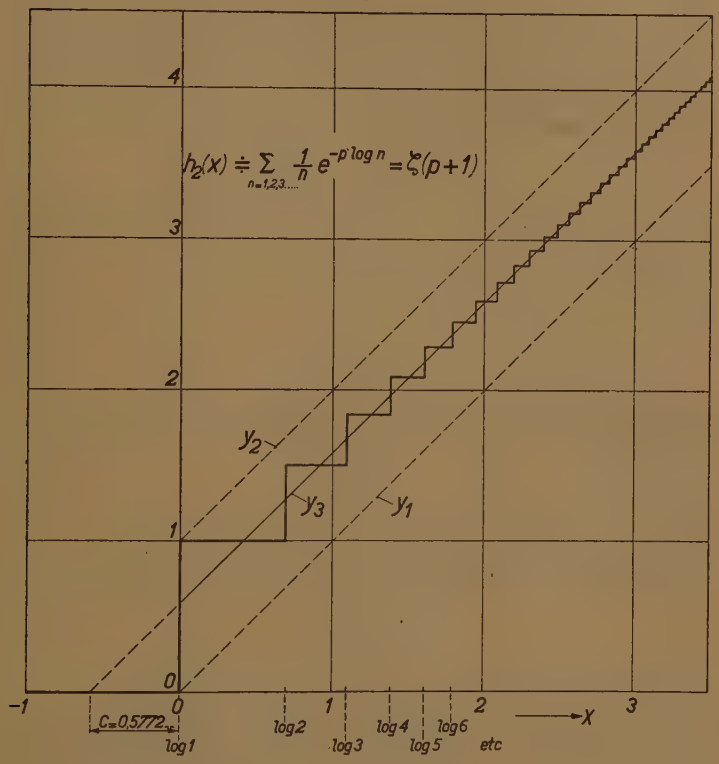

to (9), is given by

$$\zeta(p+1) = \sum_1^\infty \frac{1}{n^{p+1}} = 1e^{-p \log 1} + \tfrac{1}{2}e^{-p \log 2} + \tfrac{1}{3}e^{-p \log 3} + \ldots, \quad \ldots \quad (15)$$

the original $h_2(x)$ of which is represented by the broken line of that figure, because, according to the rules of the symbolic calculus expounded above, the original of (15) is the function which jumps unity at $x = \log 1$, one-half at $x = \log 2$, one-third at $x = \log 3$, etc. The ordinate of this function at the jump at $x = \log n$ is therefore

$1+\frac{1}{2}+\frac{1}{3}+\ldots\ldots\frac{1}{n}$. It further tends towards a straight line. Now the definition of the Euler constant C=0·5772 is

$$\lim_{n\to\infty}\left\{1+\frac{1}{2}+\frac{1}{3}+\ldots\ldots\frac{1}{n}-\log n\right\}=C,$$

and hence the function $h_2(x)$ of fig. 6 tends towards $x+C$. The two corresponding functions y_1 and y_2 belonging to fig. 6 derived from (14) are operationally

$$\frac{1}{(p+1)-1}=\frac{1}{p} \quad \text{and} \quad \frac{p+1}{(p+1)-1}=\frac{1}{p}+1,$$

the originals of which, as shown in fig. 6, are

$$y_1=x \doteqdot \frac{1}{p},$$

$$y_2=x+1 \doteqdot \frac{1}{p}+1.$$

The better approximation is therefore $y_3=x+C$, or, in the p field,

$$y_3=x+C \doteqdot \frac{1}{p}+C.$$

Thus the better approximation in fig. 3 becomes

$$y_3 \doteqdot \frac{1}{p-1}+C,$$

or

$$y_3=e^x-1+C,$$

lying, as shown in fig. 3, between y_1 and y_2.

§ 6. We have thus found two rough approximations for $\zeta(p)$, viz.,

$$y_1 \doteqdot \frac{1}{p-1} \quad \text{and} \quad y_2 \doteqdot \frac{p}{p-1}, \quad \ldots \quad (14)$$

and a better one,

$$y_3 \doteqdot \frac{1}{p-1}+C. \quad \ldots\ldots \quad (16)$$

The last expression, moreover, confirms the known result [5]:

$$\lim_{p\to 1}\left(\zeta(p)-\frac{1}{p-1}\right)=C,$$

so that the approximations used here take full account of the only pole of $\zeta(p)$. It is of great interest, as we shall see further on, that these rough approximations suffice already for the derivation of several asymptotic theorems of the prime numbers, whereas the irregularities in the functions $h_1(x)$ and $h_2(x)$ of fig. 3 and fig. 4 and of the later

Fig. 7.

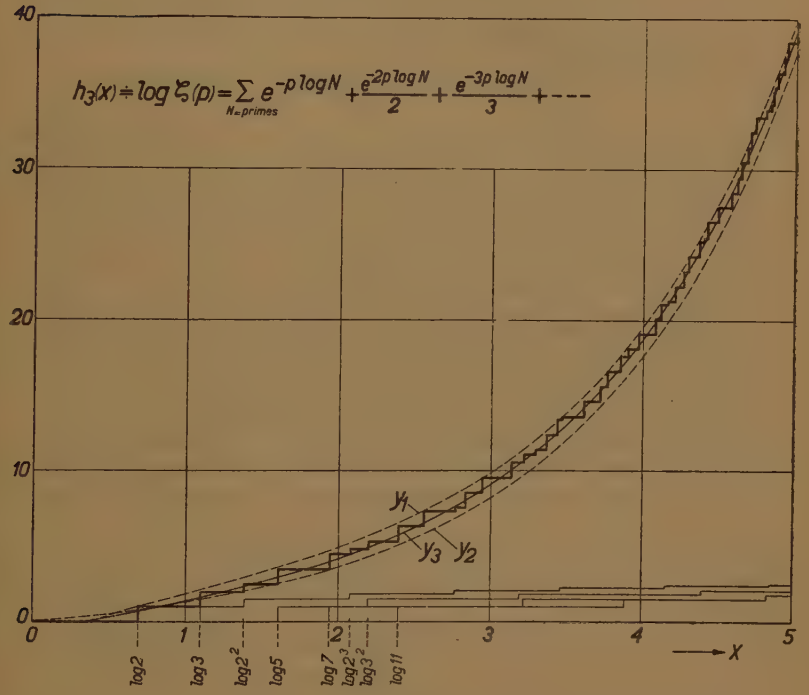

figures must therefore be produced by the more detailed properties, such as the zeros, of $\zeta(p)$.

§ 7. We are now ready to derive the prime number theory. We therefore consider $h_3(x)$, the original of $\log \zeta(p)$, for which according to (14) we have the rough approximations

$$y_1 \doteq \log\left(\frac{1}{p-1}\right) \quad \text{and} \quad y_2 \doteq \log\left(\frac{p}{p-1}\right) . \quad (17)$$

and the better one

$$y_3 \doteqdot \log\left(\frac{1}{p-1}+\mathrm{C}\right) \quad . \quad . \quad . \quad . \quad . \quad (18)$$

Now the well-known Euler expression relating $\zeta(p)$ to the *ordinary numbers* n and the *primes* N is

$$\zeta(p)=\sum_{n=1,\,2,\,3\ldots}\frac{1}{n^p}=\prod_{\mathrm{N}=2,\,3,\,5}\left(\frac{1}{1-\frac{1}{\mathrm{N}^p}}\right), \quad . \quad (19)$$

or, taking logarithms,

$$\log\zeta(p)=\sum_{\mathrm{N}=\text{primes}} e^{-p\log \mathrm{N}}+\tfrac{1}{2}e^{-2p\log \mathrm{N}}+\tfrac{1}{3}e^{-3p\log \mathrm{N}}+\ldots .$$

$$. \quad . \quad . \quad (20)$$

The original $h_3(x)$ of the second member of (20) is again easily constructed (see fig. 7); for, taking the first prime, viz. 2, first, it means, as depicted at the bottom of the figure, the function which jumps unity at $x=\log 2$, one-half at $x=\log 2^2$, one-third at $x=\log 3^3$, etc. This contributing part due to the first prime 2 is represented by the top thin curve at the bottom of fig. 7. This accounts for the first prime, viz. 2. We can again construct a similar function for the second prime, viz. 3, for the third, viz. 5, etc., and add all the results. Thus the thick curve of fig. 7 is obtained. Now, according to (17) and (18) we have for $\log\zeta(p)$ the approximations

$$\left.\begin{aligned} y_1(x) &\doteqdot \log\left(\frac{1}{p-1}\right),\\ y_2(x) &\doteqdot \log\left(\frac{p}{p-1}\right),\\ y_3(x) &\doteqdot \log\left(\frac{1}{p-1}+\mathrm{C}\right), \end{aligned}\right\} \quad . \quad . \quad . \quad (21)$$

which, with the aid of (3), are seen to be equivalent to

$$\left.\begin{aligned} y_1(x) &= \mathrm{E}i(x),\\ y_2(x) &= \mathrm{E}i(x)-\log x-\mathrm{C},\\ y_3(x) &= \log(1-\mathrm{C})-\mathrm{E}i\left\{-x\left(\frac{1}{\mathrm{C}}-1\right)\right\}+\mathrm{E}i(x). \end{aligned}\right\} \quad . \quad (22)$$

These functions are also depicted in fig. 7, which shows the very close approximation to the actual discontinuous

function, even for small values of x. Moreover, for $x \gg 1$ all three functions of (22) tend towards $\mathrm{E}i(x)$. But according to the construction of the discontinuous curve of fig. 7 the ordinate at $x_0 = \log \mathrm{N}_0$ (if we neglect for each prime all the jumps following the first one, which we shall call the subsidiary jumps) is equal to $\pi(\mathrm{N}_0)$, the number of primes smaller than N_0, because at each prime the function makes a unit jump. Hence for big values of x_0 we have

$$\pi(\mathrm{N}_0) \approx \mathrm{E}i(x_0) = \mathrm{E}i(\log \mathrm{N}_0),$$

and, as

$$\mathrm{E}i(x) = \int_{-\infty}^{-x} \frac{e^{-s}}{s}\, ds = li(e^x),$$

where

$$li(x) = \int_0^x \frac{ds}{\log s},$$

we obtain the asymptotic *prime number theorem* :

$$\pi(\mathrm{N}) \approx li(\mathrm{N}), \qquad \ldots\ldots \quad (23)$$

or, in words : *the number of primes under* N *is asymptotically given by the logarithmic integral of* N.

It may be noted that this asymptotic result is obtained from all three approximations (21). Their difference becomes only of importance at the lower end of the curve of fig. 7, where, as could be expected, y_3 shows the optimum approximation.

§ 8. In order to derive another theorem of the theory of numbers we shall next consider the original $h_4(x)$ of $\log \zeta(p+1)$.

From (20) we first obtain

$$\log \zeta(p+1) = \sum_{\mathrm{N}=\text{primes}} \log \left(\frac{1}{1 - \frac{1}{\mathrm{N}^{p+1}}} \right)$$

$$= \sum_{\mathrm{N}} \left\{ \frac{1}{\mathrm{N}} e^{-p \log \mathrm{N}} + \frac{1}{2\mathrm{N}^2} e^{-2p \log \mathrm{N}} + \frac{1}{3\mathrm{N}^3} e^{-3p \log \mathrm{N}} + \ldots \right\}, \qquad \ldots \quad (24)$$

and the contribution by each prime to the original can, as shown in fig. 8, at once again be read from (24). For, taking the prime 2 first, we obtain the upper thin curve of the upper drawing of fig. 8. It jumps unity at $x = \log 2$,

one-eighth at log 2^2, etc., and similarly for the other primes. We thus obtain the thick curve of fig. 8, where the top part of the curve is reproduced on a bigger scale in the inset.

Fig. 8.

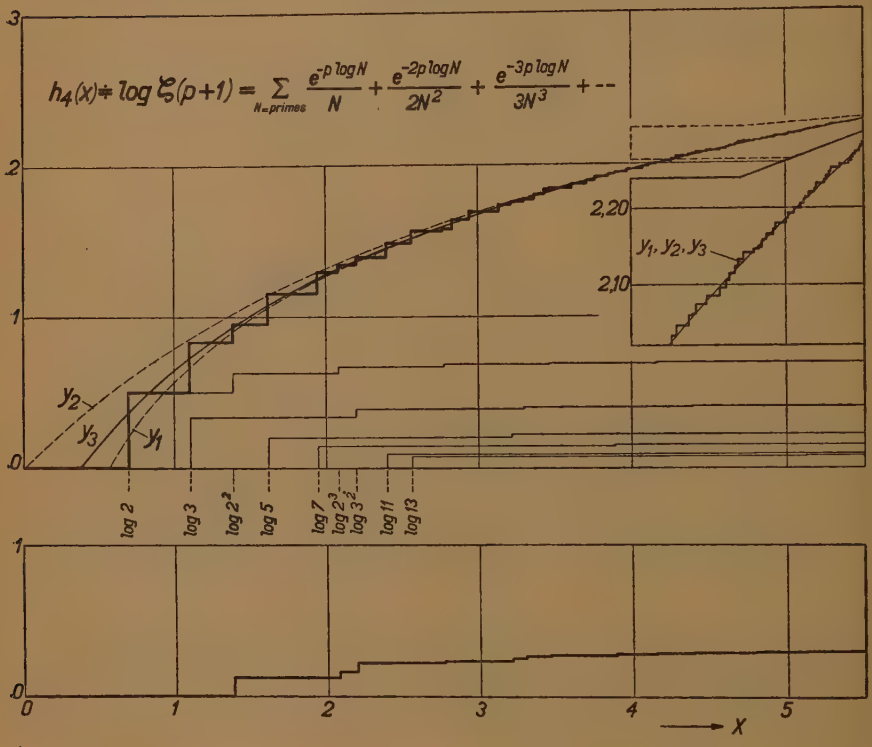

Now from our approximations (17) and (18) to $\zeta(p)$ we have as approximations for $\log \zeta(p+1)$:

$$y_1(x) \doteq \log \frac{1}{p},$$

$$y_2(x) \doteq \log \left(\frac{1}{p}+1\right),$$

$$y_3(x) \doteq \log \left(\frac{1}{p}+C\right),$$

the originals of which are easily obtained as :

$$\left.\begin{aligned} y_1(x) &= \log x + C, \\ y_2(x) &= \log x + C - Ei(-x), \\ y_3(x) &= \log x + C - Ei\left(-\frac{x}{C}\right), \end{aligned}\right\} \quad . \quad . \quad . \quad (25)$$

which three functions are drawn in fig. 8, which shows them to be again very good approximations.

If we neglect for the moment the subsidiary jumps, according to the construction of fig. 8, the value of the function at the abscissa $x_0 = \log N_0$ is $\sum_2^{N_0} \frac{1}{N}$, *i. e.*, the sum of the reciprocals of all primes up to N_0. But it follows from (25) that this value must approximately be equal to $\log x_0 + C$ or $\log(\log N_0) + C$. We have in this way neglected the contribution due to the subsidiary jumps. This total subsidiary contribution is separately depicted in the bottom figure of fig. 8, and it tends towards 0·315 . . . as a numerical summation shows.

Hence we obtain the *second prime number theorem* :

$$\sum_N^{N_0} \frac{1}{N} \approx \log(\log N_0) + C - 0{\cdot}315 \ldots ,$$

or

$$\operatorname{Lim} \left\{ \frac{1}{2} + \frac{1}{3} + \frac{1}{5} + \frac{1}{7} + \frac{1}{11} + \ldots \frac{1}{N_0} - \log(\log N_0) \right\} \approx C - 0{\cdot}315 \ldots , \quad . \quad . \quad . \quad (26)$$

where the first member contains the reciprocals of all prime numbers up to N_0. Expressed in words :

The sum of the reciprocals of all primes up to N_0 *minus the logarithm of the logarithm of* N_0 *asymptotically equals* $C - 0{\cdot}315 \ldots$, *where* C *is Euler's constant.*

It is of interest to compare (26) with

$$\operatorname{Lim} \left\{ 1 + \frac{1}{2} + \frac{1}{3} + \frac{1}{4} + \ldots . - + \frac{1}{N_0} - \log N_0 \right\} \approx C, \quad . \quad . \quad . \quad (27)$$

where the reciprocals of all integers occur. Apart from the additional constant $-0{\cdot}315 \ldots$ formula (26) is of the same form as (27), but $\log N_0$ in (27) is replaced by $\log(\log N_0)$ in (26).

§ 9. In order to derive still another theorem we shall consider the original of $-\frac{\zeta'(p)}{\zeta(p)}$. As approximations we obtain at once from (21)

$$y_1(x) \doteqdot \frac{1}{p-1},$$

$$y_2(x) \doteqdot \frac{1}{p-1} - \frac{1}{p},$$

$$y_3(x) \doteqdot \frac{1}{p-1} - \frac{1}{p+\frac{1-C}{C}},$$

the originals of which are

$$\left.\begin{aligned} y_1(x) &= e^x - 1, \\ y_2(x) &= e^x - 1 - x, \\ y_3(x) &= e^x - \frac{1}{1-C} + \frac{C}{1-C} e^{-\frac{1-C}{C}x}. \end{aligned}\right\} \quad . \quad . \quad (28)$$

Again, from (19) we obtain

$$-\frac{\zeta'(p)}{\zeta(p)} = \sum_{N=\text{primes}} \log N . \{e^{-p \log N} + e^{-2p \log N} + e^{-3p \log N} + \ldots .\}. \quad . \quad . \quad . \quad (29)$$

The original $h_5(x)$ of (29) can again at once be read from the form of (29), for the contribution to the total expression by each prime is a step function like fig. 1, the steps of magnitude log N occurring at $x = \log N$, $x = 2 \log N \ldots$, etc. The result is depicted in fig. 9, where also the approximations (28) are shown, and again a very good agreement is obtained. All three approximations (28) tend, for $x \gg 1$, towards e^x. Neglecting again the subsidiary steps, which for $x \gg 1$ is permitted, we thus obtain the asymptotic theorem

$$\sum_{N=2,\,3,\,5\,\ldots N_0} \log N \approx e^{x_0} = e^{\log N_0} = N_0,$$

or

$$\log (2, 3, 5, 7, 11 \ldots . N_0) = N_0, \quad . \quad . \quad (30)$$

or in words :

Asymptotically any prime equals the sum of the logarithms of all smaller primes.

Fig. 9.

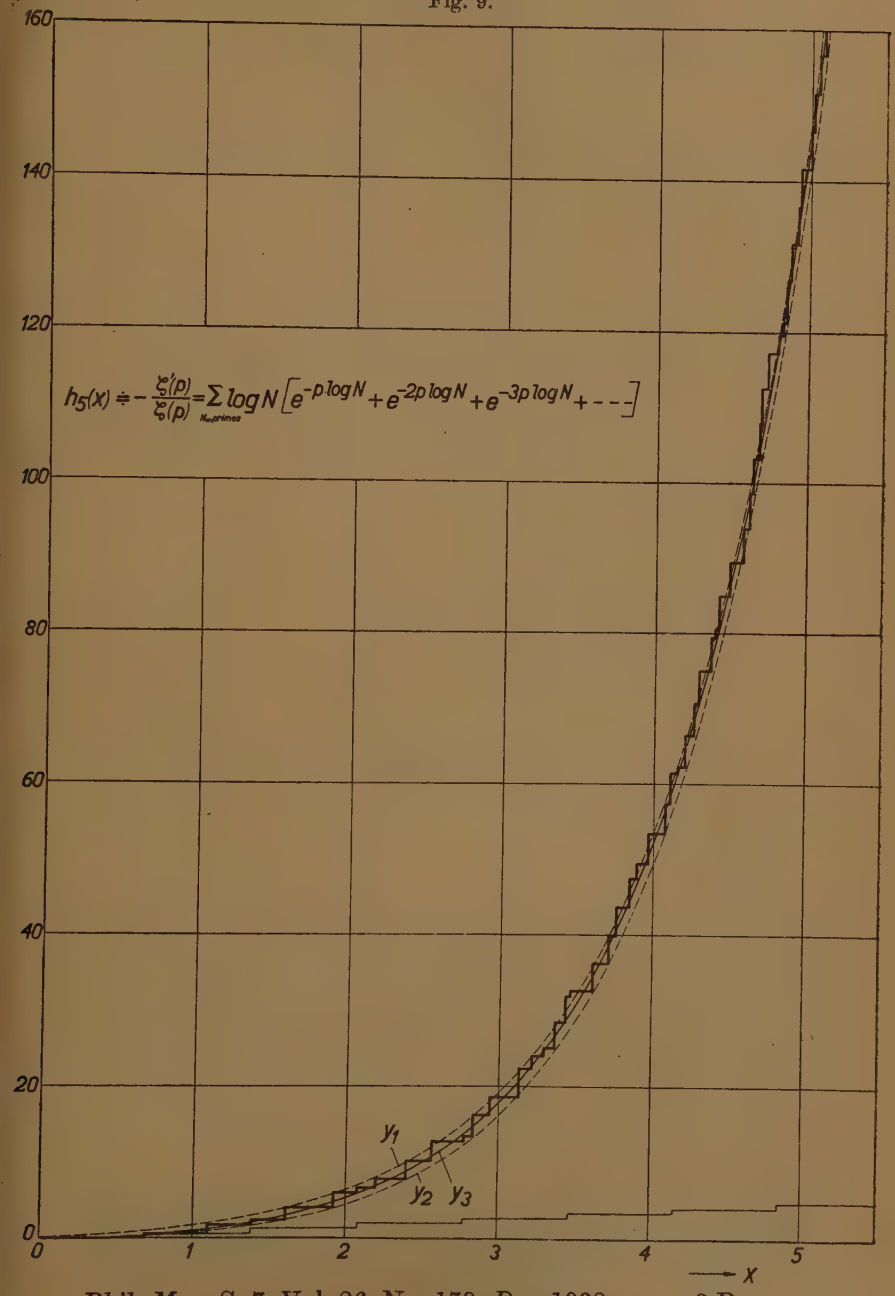
160
140
120
100
80
60
40
20
0
0
1
2
3
4
5
x
$h_5(x) \doteq -\frac{\zeta'(\rho)}{\zeta(\rho)} = \sum_{N=\text{primes}} \log N \left[e^{-p \log N} + e^{-2p \log N} + e^{-3p \log N} + \cdots \right]$
y_1
y_2
y_3

The simple construction of (29), which can also be written as

$$-\frac{\zeta'(p)}{\zeta(p)} = \sum_{N} \log N \cdot \frac{1}{e^{p \log N} - 1},$$

can be shortened with the aid of (6), yielding the operational relation

$$-\frac{\zeta'(p)}{\zeta(p)} \doteq \sum_{N} \log N \cdot \left[\frac{x}{\log N}\right] \quad . \quad . \quad . \quad . \quad (31)$$

§10. Finally we consider the original $h_6(x)$ of $-\frac{\zeta'(p+1)}{\zeta(p+1)}$.

In the same way as before we obtain as approximations

$$y_1(x) \doteq \frac{1}{p},$$

$$y_2(x) \doteq \frac{1}{p} - \frac{1}{p+1},$$

$$y_3(x) \doteq \frac{1}{p} - \frac{C}{pC+1},$$

the originals of which are

$$\left.\begin{aligned} y_1(x) &= x, \\ y_2(x) &= x + e^{-x} - 1, \\ y_3(x) &= x + C(e^{-\frac{x}{C}} - 1). \end{aligned}\right\} \quad . \quad . \quad . \quad . \quad (32)$$

Now we easily obtain

$$-\frac{\zeta'(p+1)}{\zeta(p+1)} = \sum_{N = \text{primes}} \log N \cdot \left\{ \frac{1}{N} e^{-p \log N} + \frac{1}{N^2} e^{-2p \log N} + \ldots \right\},$$

the original $h_6(x)$ of which is shown in fig. 10, which was obtained as follows :—The contribution of the first prime, viz. 2, consists as depicted again at the bottom of the figure in a jump of magnitude $\frac{1}{2} \log 2$ at $x = \log 2$, then again a jump of $\frac{1}{2^2} \log 2$ at $x = 2 \log 2$, etc., and similarly for the other primes. Thus approximately a straight line is obtained from primes only, the approximations y_1, y_2 and y_3 of (32) again being shown. An even better

approximation than y_3 is given by the linear relation $y_4 = x - C$, as indicated in the figure. Omitting again the subsidiary jumps we thus get the asymptotic relation

$$\sum_{N}^{N_0} \frac{\log N}{N} \approx x_0 = \log N_0,$$

Fig. 10.

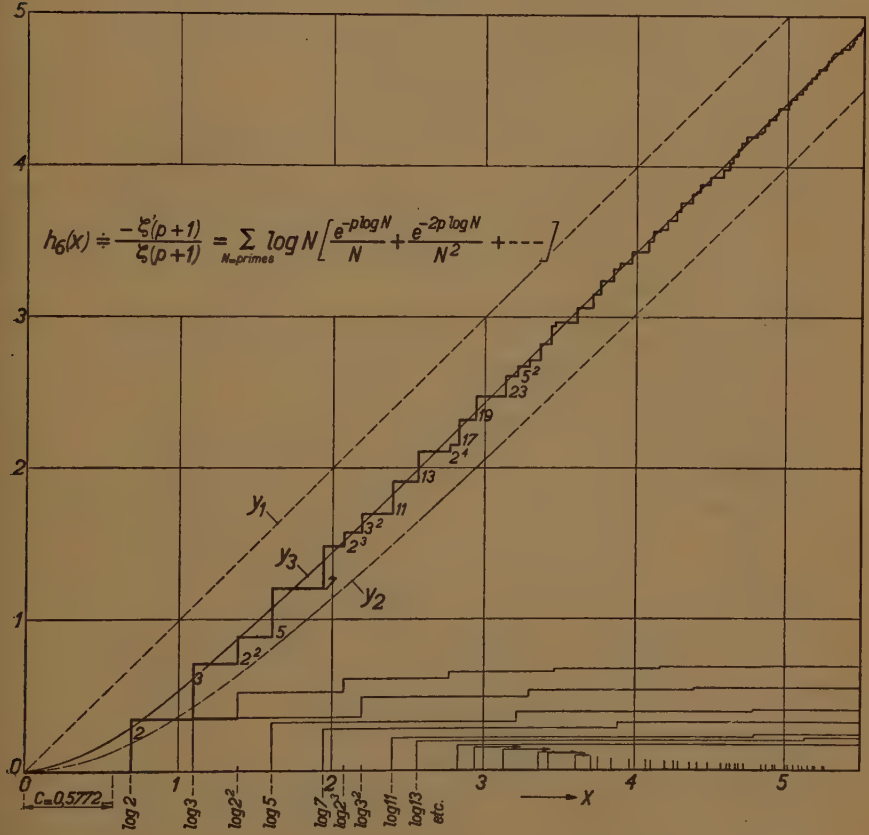

or

$$2^{\frac{1}{2}} . 3^{\frac{1}{3}} . 5^{\frac{1}{5}} . 7^{\frac{1}{7}} \ldots N_0^{\frac{1}{N_0}} \approx N_0,$$

where, again, the product contains all the primes up to N_0. In words:

Asymptotically any prime equals the product of the N*th roots of all smaller primes* N.

In conclusion, the very good fit of all the functions considered obtained from rather rough approximations of the $\zeta(p)$ function and its derivatives, wherein mainly the pole $p=1$ is considered, and derived from $\zeta(p) \doteqdot [e_i^x]$, is noteworthy. Also the fact that the asymptotic theorems can thus be derived in an extremely simple way with the aid of the symbolic calculus may again be a proof of the great heuristic value of the latter.

Finally, I wish to thank Mr. C. C. J. Addink for constructing and drawing the diagrams.

References.

(1) Balth. van der Pol, Phil. Mag. vii. p. 1153 (1929); viii. p. 861 (1929). Balth. van der Pol and K. F. Niessen, Phil. Mag. xi. p. 368 (1931); xiii. p. 537 (1932); 'Physica,' i. p. 521 (1934); *Tds. Ned. Radio Genootsch.* vii. p. 18 (1935). K. F. Niessen, Phil. Mag. xx. p. 977 (1935). P. Humbert, 'Le calcul symbolique,' Paris, 1934.
(2) J. R. Carson, 'Electric Circuit Theory and the Operational Calculus, McGraw-Hill, New York, 1926.
(3) H. Bremekamp, Proc. Acad. A'dam, xl. p. 689 (1937). G. Doetch, 'Theorie und Anwendung der Laplace Transformation' (Berlin, 1937).
(4) See, *e. g.*, E. C. Titchmarsh, 'The zeta function of Riemann,' p. 3 (Cambridge University Press, London, 1930).
(5) E. C. Titchmarsh, *l. c.* p. 3.

Eindhoven,
August 1938.

LXXX. *The Behaviour of Electrons in Iodine Vapour.* *By* R. H. Healey, *M.Sc., F.Inst.P., School of Physics, University of Sydney* *.

[Received July 20, 1938.]

Introduction.

THE behaviour of electrons in chlorine and bromine has already been described in various publications †, and the present communication gives an account of an investigation of the motion of electrons in iodine, thus extending our knowledge of the electrical properties of the halogens.

* Communicated by Prof. V. A. Bailey.

† V. A. Bailey and R. H. Healey, Phil. Mag. xix. p. 725 (1935); J. E. Bailey, Makinson, and Somerville, Phil. Mag. xxiv. p. 177 (1937).

The apparatus used will not be described here, as it was the same as that previously used in the study of chlorine, and similar to that used for a number of other gases *. A description of the methods of investigation has already been given in previous communications †.

The iodine was kindly supplied by Dr. T. Iredale of the Department of Physical Chemistry, University of Sydney. In order to remove possible traces of impurities (Br_2, Cl_2, H_2O and occluded air) the following procedure was adopted : a small quantity of concentrated KI was added to the iodine, and the mixture heated strongly in a closed vessel till the iodine melted (at about 115° C.), thus removing most of the chlorine and bromine ; then, the mixture was heated to about 110° C. *in vacuo* for half an hour, in order to allow traces of air and any other occluded gases to be pumped off ; finally, a portion of the iodine was condensed and stored in a side-tube containing P_2O_5.

Observations were made on pure iodine and on mixtures of iodine with helium or with carbon dioxide. On account of the low vapour pressure of iodine at room-temperature ($\sim$0·2 mm.), it was necessary to prepare a fresh sample of the iodine mixture each day ; however, the consistency of the experimental results was good evidence that the data so obtained were reliable. Adequate photoelectric currents were produced by illuminating a silver target with ultraviolet light.

As the Bourdon gauges previously used for chlorine and bromine were not sufficiently sensitive, it was found convenient to estimate the vapour pressure of the iodine from the data published by Baxter, Hickey and Holmes ‡.

Notation and Formulæ.

The notation used is the same as that given in previous communications, and for convenience is set out below :

p = Pressure of gas, in mm. of mercury.

Z = Electric intensity, in volts/cm.

c = The distance between successive slits of the instrument, namely, 4 cm.

* V. A. Bailey and J. D. McGee, Phil. Mag. vi. p. 1073 (1928).

† See Footnote † p. 940.

‡ Baxter, Hickey and Holmes, J. Am. Chem. Soc. xxix. p. 134 (1907).

S_1=Fraction of the stream in the first diffusion chamber which passes out of that chamber; also called the distribution ratio.

S_2=Corresponding fraction for the second diffusion chamber.

R=The distribution ratio with negative ions in either chamber.

H_0=The magnetic intensity required to make S_2 (and S_1) equal to R.

k=Mean energy of agitation of an electron in terms of the mean energy of agitation of a molecule at 15° C.

W=The drift velocity of an electron in the direction of Z, in cm./sec.

α=The probability of attachment of an electron to a molecule per unit length of its motion in the direction of Z.

u=The mean velocity of agitation of an electron, in cm./sec.$=1{\cdot}15\sqrt{k}\times 10^7$.

L=The mean free path of an electron in the gas at 1 mm. pressure, in cm.

λ=The mean proportion of its own energy lost by an electron at a collision with a gas molecule.

h=The probability of an electron's becoming attached to the molecule with which it collides.

$\omega=i_0/i_3$.

f_a=The proportion of gas A (the electronic properties of which are known) in the mixture.

g_a=The proportion in the mixture of the gas whose electronic properties have to be determined.

$q_a=\rho_a L_a^{-1}$, where $\rho_a=g_a^{-1}-1$.

$r_a=\lambda_a q_a$.

$s=gk^{-1}(1-k^{-1})^{-\frac{1}{2}}\,\sigma$.

$t=gk^{-1}(1-k^{-1})^{\frac{1}{2}}\tau$.

$\sigma=1{\cdot}25\,g^{-1}H_0/p$.

$\tau=231g^{-1}Z^2/pH_0$.

$x=k(1-k^{-1})^{\frac{1}{2}}(q_a-q_b)$.

$y=k(1-k^{-1})^{-\frac{1}{2}}(r_a-r_b)$.

For the mixtures 1 and 2, composed of iodine vapour associated with the gases A and B respectively, the following simultaneous equations are true :

$$\left.\begin{aligned} x_{12} &= \sigma_1 - \sigma_2, \\ y_{12} &= \tau_1 - \tau_2, \end{aligned}\right\} \quad . \quad . \quad . \quad . \quad . \quad (1)$$

where x_{12} and y_{12} are known functions of k determined by the properties of the known gases, and σ and τ are calculated from measurements of H_0 in the mixtures

Fig. 1.

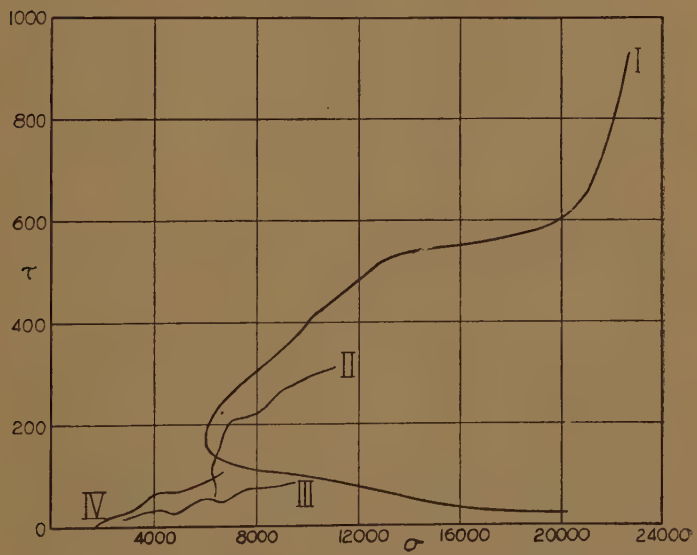

Curve I. Corresponds to $16\frac{2}{3}$ per cent. I_2 in CO_2.
Curve II. Corresponds to $33\frac{1}{3}$ per cent. I_2 in CO_2.
Curve III. Corresponds to $33\frac{1}{3}$ per cent. I_2 in He.
Curve IV. Corresponds to 100 per cent. I_2.

(see fig. 1). The graphical method previously described * enables these equations to be solved, yielding k as a function of Z/p for each mixture ; the results of such determinations are shown in figs. 2 and 3.

Next, from the curves $(Z/p, k)$ for each mixture, the

* V. A. Bailey and R. H. Healey, *loc. cit.*

values of L and λ in iodine (denoted by the subscript I) are calculated by means of the formulæ :

$$L_I = \frac{1}{s_1 g_a^{-1} - q_a} \quad . \quad . \quad . \quad . \quad . \quad . \quad (2)$$

$$\lambda_I = \frac{t_1 g_a - r^{-1}{}_a}{s_1 g_a^{-1} - q_a} \quad . \quad . \quad . \quad . \quad . \quad . \quad (3)$$

Fig. 2.

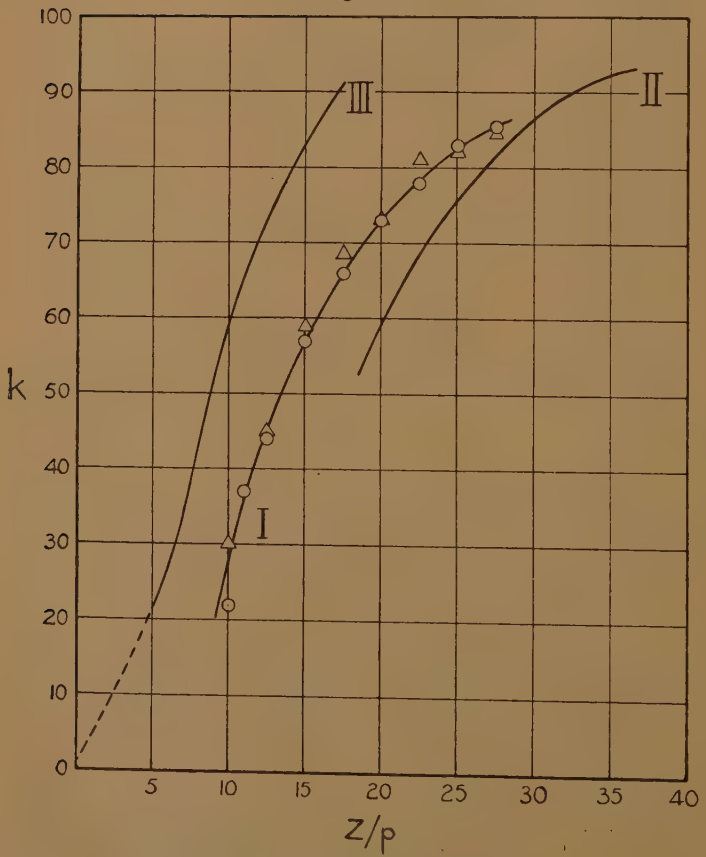

Curve I. Corresponds to 16⅔ per cent. I_2 in CO_2.
Curve II. Corresponds to 33⅓ per cent. I_2 in CO_2.
Curve III. Corresponds to 33⅓ per cent. I_2 in He.

Figs. 4 and 5 show the (L, u) and (λ, u) curves derived in this manner.

The values of W for iodine are then calculated in terms of Z/p from the expression

$$W = 0{\cdot}64\, u\lambda^{\frac{1}{2}}; \quad \ldots\ldots \quad (4)$$

the curve (Z/p, W) so obtained is shown is fig. 6.

Fig. 3.

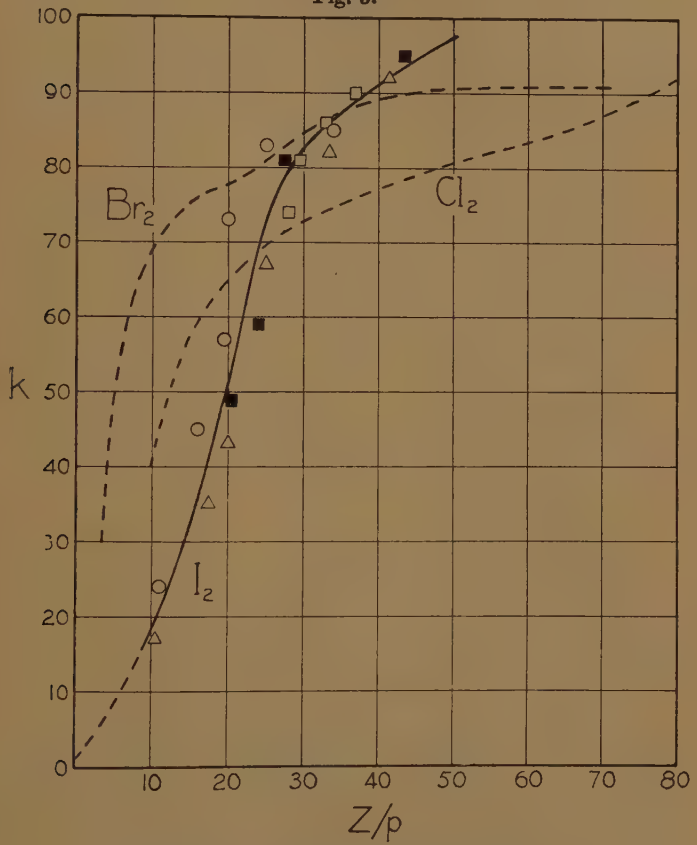

■ Corresponds to Z/p from mixtures 3 and 4.
○ Corresponds to $Z/p = \sqrt{(\sigma_1 - x)(\tau_1 - y)}/17$.
▲ Corresponds to $Z/p = \sqrt{(\sigma_2 - x)(\tau_2 - y)}/17$.
□ Corresponds to $Z/p = \sqrt{(\sigma_3 - x)(\tau_3 - y)}/17$.

From observations on S_1 and S_2 (with $H < H_0$), the values of the coefficient of attachment (α) are calculated for various mixtures by means of the formula

$$\alpha = 0{\cdot}575\{\log_{10} R(Z\phi/kc) - \log_{10} a\}, \quad \ldots \quad (5)$$

where $a=S_1(R-S_2)/(R-S_1)$,

and $(\phi-1)/(k-1)=(H/H_0)^2$.

The value of h for iodine is then computed by means of the expression

$$h_I=0{\cdot}037\ (\lambda_I+rL_I)k\alpha/Z \quad . \quad . \quad . \quad . \quad . \quad (6)$$

Fig. 4.

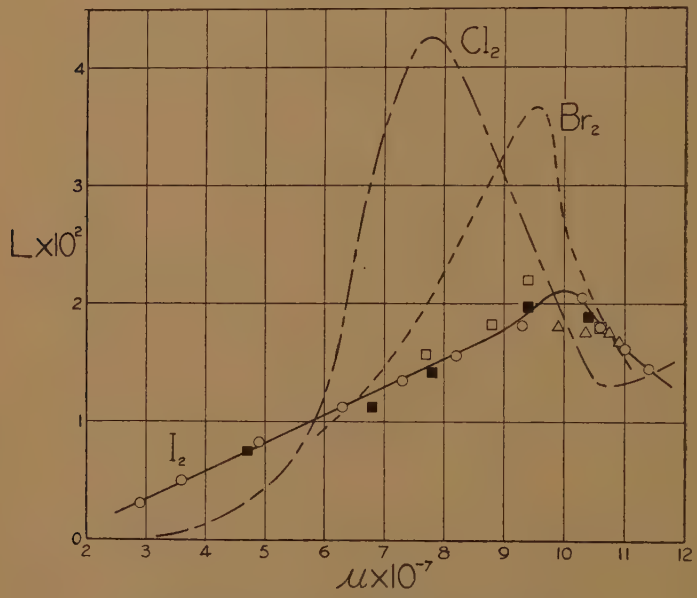

□ Computed from data obtained for mixture 1.
△ Computed from data obtained for mixture 2.
■ Computed from data obtained for mixture 3.
○ Computed from data obtained for mixture 4.

in which r and α/Z correspond to the particular mixture. Fig. 7 shows the corresponding (h, u) curve.

Finally, the (α/p, Z/p) curve, shown in fig. 8, is derived from the formula

$$\alpha/p=1{\cdot}57\ h/L\lambda^{\frac{1}{2}}. \quad . \quad . \quad . \quad . \quad (7)$$

Experimental Results.

Observations were made on four mixtures, viz. :

Mixture 1	$16\frac{2}{3}$ per cent. I_2 in CO_2.
Mixture 2	$33\frac{1}{3}$ per cent. I_2 in CO_2.
Mixture 3	$33\frac{1}{3}$ per cent. I_2 in He.
Mixture 4	100 per cent. I_2.

The (σ, τ) curves for these four mixtures are represented respectively by curves I, II, III, and IV of fig. 1. Six (x, y) curves (and the associated six (x, k) curves), one for each pair of mixtures, were computed from the known properties of CO_2 and He. The graphical method previously described makes possible three separate determinations of points on each $(Z/p, k)$ curve, by combining the results for each mixture with the results for each of the other three. Fig. 2 shows the results corresponding to mixtures 1, 2, and 3. In order to give

Fig. 5.

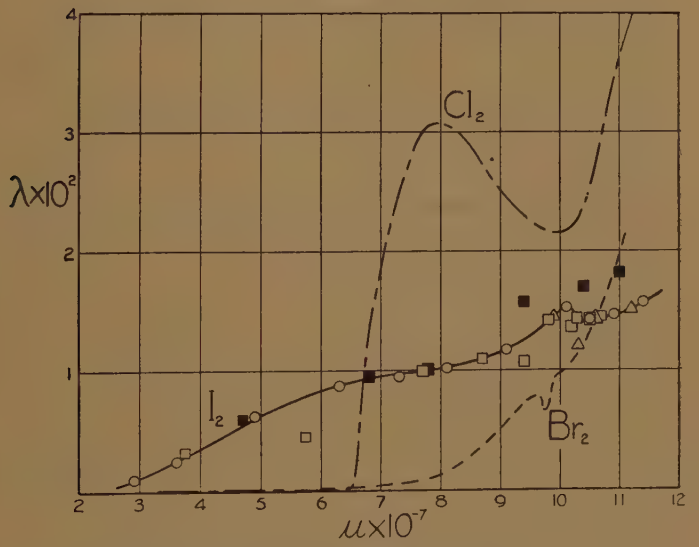

□ Computed from data obtained for mixture 1.
▲ Computed from data obtained for mixture 2.
■ Computed from data obtained for mixture 3.
○ Computed from data obtained for mixture 4 (pure I_2).

an indication of the fair agreement between the results, the points obtained for mixture 1 (curve I, fig. 2) by combining the data for this mixture with those of 3 and 4 are represented by circles and triangles respectively (the points obtained from mixtures 1 and 2 are not shown, as the similarity in shape of the two (σ, τ) curves and the (x, y) curve prevents accurate determinations of k from this combination).

Fig. 6.

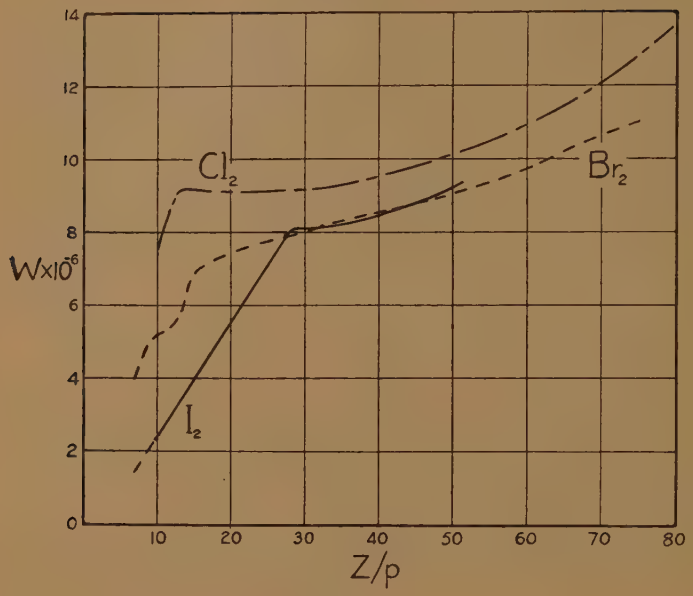

Fig. 7.

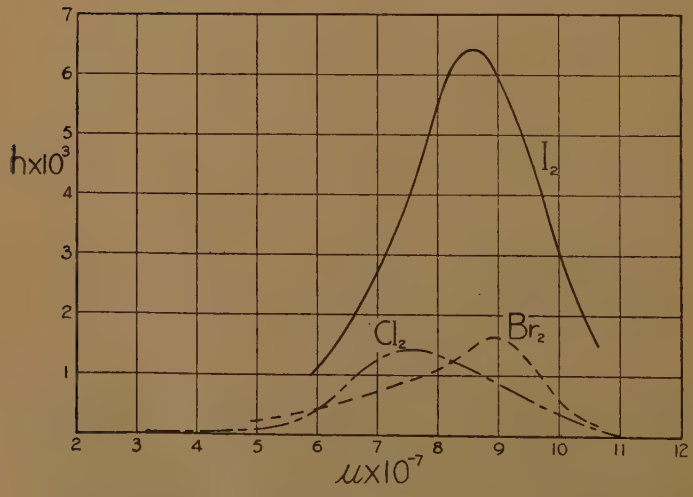

Using the graphical method, it was found that, owing to the relative shapes of the (σ, τ) and (x, y) curves, the only reliable points on the (Z/p, k) curve for pure iodine

were obtained by combining the data for mixtures 3 and 4. These points were supplemented by others obtained in the following manner * from the (Z/p, k) curves for 1, 2, and 3.

From the definitions of σ and τ it follows that

$$Z/p = g\sqrt{\sigma\tau}/17 ;$$

Fig. 8.

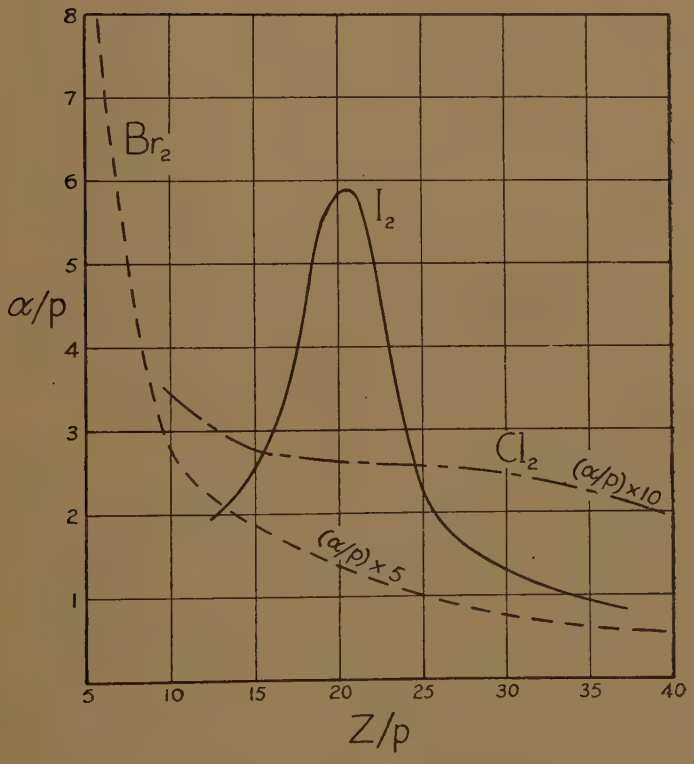

* This method of deriving the (Z/p, k) curve for pure iodine from the (Z/p, k) curves obtained for the mixtures is equivalent to the method described previously for bromine and chlorine ; there, λ and L were calculated from equations (2) and (3), Z/p then being obtained by means of the formula

$$Z/p = 4{\cdot}4 \times 10^{-16} u^2 \lambda \tfrac{1}{2}/L.$$

The more direct method is to be preferred, as the curve (Z/p, H_0/Z) for iodine is available ; and best use may be made of this curve by obtaining an accurate (Z/p, k) curve for iodine.

also $x_{\mu 4}=\sigma_\mu-\sigma_4$,

$y_{\mu 4}=\tau_\mu-\tau_4$, $\mu=1, 2, 3$.

Therefore,

$$\sqrt{\sigma_4\tau_4}/17=\sqrt{(x_{\mu 4}-\sigma_\mu)(y_{\mu 4}-\tau_\mu)}/17=(Z/p)_4.$$

Then, for a given value of k, the value of $(Z/p)_\mu$ is read from the appropriate $(Z/p, k)$ curve (I, II, or III of fig. 2); the corresponding values of σ_μ and τ_μ are readily determined from the experimental data, as σ_μ and τ_μ are functions of $(Z/p)_\mu$; also, $x_{\mu 4}$ and $y_{\mu 4}$ are known functions of k; hence the values of $(Z/p)_4$, corresponding to a given value of k, can be computed from the formula above.

The $(Z/p, k)$ curve for I_2 shown in fig. 3 is determined by the three sets of points obtained by setting $\mu=1$, 2, and 3, and the points obtained graphically by combining the data of mixtures 3 and 4. It will be seen that the various sets of points are in good agreement, and thus indicate the reliability of the methods used.

Values of L in iodine have been calculated from each of the four $(Z/p, k)$ curves (figs. 2 and 3); the four sets of points are shown in fig. 4. The curve determined by these points thus gives L for iodine as a function of u; corresponding curves for chlorine and bromine are shown in the same figure.

Four distinct sets of points can also be used to determine the λ curve. For this purpose, however, most weight must be given to the points derived from the $(Z/p, k)$ curve for pure iodine, because these are obtained more directly and are correspondingly more accurate *. Thus the (λ, u) curve for iodine, shown in fig. 5, has been obtained by drawing a smooth curve through the one set of points; it will be seen, however, that the three other sets of points, determined from observations on the mixtures, are in satisfactory agreement with this curve.

The $(Z/p, W)$ curve for iodine, shown in fig. 6, was obtained by applying formula 4 to the data given in figs. 3, 4, and 5.

A few observations were made of S_1 and S_2 in mixtures 1 and 4, and corresponding values of α/p were derived from these results by means of equation (5); values of h in iodine were then computed by means of equation (6).

* The curves $(Z/p, k)$ and $(Z/p, H_0/Z)$ for pure iodine are at least as accurate as those for the three mixtures.

The (h, u) curve, obtained by drawing a smooth curve through the points, is shown in fig. 7.

Fig. 8 gives the (Z/p, α/p) curves for chlorine, bromine and iodine. The values of α/p in iodine were obtained by making use of equation (7) and the curves (Z/p, k), (λ, u), and (L, u).

Remarks on Experimental Results.

The curves given in figs. 3–8 show a remarkable similarity in the properties of the three halogens.

From fig. 4 it will be seen that the three (L, u) curves are of the same general shape. The variation of L with u is less pronounced in iodine than in chlorine or bromine; nevertheless, as u ranges from $2{\cdot}7\times10^7$ to $10{\cdot}0\times10^7$, L_1 changes by a factor 7. The maxima of the three curves lie fairly close to one another, and, moreover, the value of $L_{max.}$ diminishes as the molecular weight increases, as is shown in the following table:—

Halogen.	Value of $L_{max.}$	Maximum occurs at $u=$
Cl_2 (71)	$4{\cdot}25\times10^{-2}$	$7{\cdot}8\times10^7$
Br_2 (160).....	$3{\cdot}65\times10^{-2}$	$9{\cdot}6\times10^7$
I_2 (254)	$2{\cdot}1\times10^{-2}$	$10{\cdot}0\times10^7$

Fig. 5 shows that the three (λ, u) curves are also of the same general form. As u increases, λ rises from small values up to a maximum, falls slightly, and then rises again. Here, as in fig. 4, the variations in the behaviour of the iodine curve are not so marked as those corresponding to chlorine and bromine. The position and value of the maxima are given below.

Halogen.	Value of $\lambda_{max.}$*	Maximum occurs at $u=$
Cl_2	$3{\cdot}08\times10^{-2}$	$8{\cdot}1\times10^7$
Br_2.....	$0{\cdot}78\times10^{-2}$	$9{\cdot}6\times10^7$
I_2	$1{\cdot}52\times10^{-2}$	$10{\cdot}1\times10^7$

* It is interesting to observe that the values of $\lambda_{max.}$ are given by

$$\lambda_{max.}=n\times0{\cdot}77\times10^{-2},$$

where

$$n=4{\cdot}00,\ 1{\cdot}01,\ 1{\cdot}97,$$

$$\doteq 4,\ 1,\ 2,$$ to within ±2 per cent.

It will be noticed that the maxima in the L and λ curves agree very closely in all three cases. The maximum in the light-absorption curve for iodine occurs at a frequency which is equivalent to $u=9{\cdot}4\times10^7$, and this agrees roughly with the maximum in the (λ, u) curve at $u=10{\cdot}1\times10^7$. There is a further interesting correlation between the light-absorption of the halogens and the corresponding (λ, u) curves: from the colours of the halogens it is evident that, as the wave-length diminishes from the infra-red, absorption would become appreciable, first in iodine, then in chlorine, and, finally, in bromine; and from fig. 5 it will be seen that, as u increases from small values, λ becomes appreciable in these gases in the same order.

As in chlorine and bromine, collisions at low electron-velocities in iodine are notably elastic; values of λ less than 3×10^{-4} have been observed.

The similarity in the properties of the three halogens is further illustrated by the (h, u) curves given in fig. 7. It should be noted that larger values of h occur in iodine than in bromine or chlorine; these values are, in fact, the largest yet recorded for any gas. The close correspondence between the variations in h and L for each vapour furnishes additional support for the conclusion that the probability of attachment increases as the electron penetrates further into the molecule.

It will be seen from fig. 8 that the value of α/p in iodine is of the order 10 times greater than the corresponding values for chlorine and bromine. The curve rises to a maximum at $Z/p=20$, then falls away; possibly, turning-points in the two other (Z/p, α/p) curves occur in the range $Z/p<5$.

In fig. 3 the (Z/p, k) curves are given, that for iodine being similar in shape to the other two. This similarity is more marked in the (Z/p, W) curves shown in fig. 6; in this case each curve rises steeply at first, then bends sharply, whereafter the gradient is considerably reduced.

In conclusion, the author desires to thank Professor V. A. Bailey for his valuable assistance and encouragement during the course of the work; also he desires to thank Mr. J. Reed for his assistance in the preparation of the paper, Mr. N. R Wilson for his aid in the construction of the apparatus, and the Colonial Sugar Refining Co., Ltd., and the Commonwealth Oxygen and

Accessories Co., Ltd., for supplying carbon-dioxide snow and liquid air respectively.

Summary.

The behaviour of electrons in iodine vapour is studied by methods similar to those previously applied to chlorine and bromine. Curves are obtained which show the variation with u of

L the mean free path of an electron in the gas at 1 mm.,

λ the mean proportion of its energy lost by an electron at a collision with a gas molecule,

h the probability of attachment of an electron to the molecule with which it collides.

The values of Townsend's energy factor k, the drift velocity of an electron W, and α/p the probability of attachment of an electron per unit length of drift at unit pressure, are given as functions of Z/p by means of another set of curves. Results deduced from independent observations on various gas mixtures containing iodine are found to be in excellent agreement.

The curves for iodine are compared with the corresponding curves for chlorine and bromine, and it is shown that the properties of these three halogens are very similar.

LXXXI. *Optical Silvering on Glass.* *By* B. Dasannacharya, *M.A., Dr.Phil., F.Inst.P., Professor of Physics, Benares Hindu University, Benares, India, and* Amar Chand Seth, *M.Sc. (Benares)* *.

[Received August 15, 1938.]

1. *Introduction and Scope.*

MANY groups of substances can precipitate silver from an ammoniacal solution of silver nitrate [1]. Whether the silver so deposited will be in the form of a bright metallic mirror sticking on any substance in contact with the mixture, the sides of the vessel in which the reaction

* Communicated by the Authors.

takes place, or will simply be deposited at the bottom in an incomplete state of reduction or in any one of the forms of silver in which it is not lustrous, depends on a number of conditions not very well investigated, namely, the nature of the reacting substances, their concentrations in the mixture, the temperature, the cleanliness of the surface, etc. It is very little realized that the formation of the film being necessarily a surface phenomenon it will depend not merely on the nature and purity of the surface, but also on the extent of surface presented in the solution to the quantity of the silver nitrate contained therein, *i. e.*, on the amount of surface presented per gram of the silver nitrate. It is the object of the present paper to demonstrate this fact and to determine the optimum conditions. The influence of the cleaning of the surface and the effect of temperature of the silvering mixture will also be investigated.

Using inverted sugar with alcohol as the reducing solution, mirrors could be obtained without having to cool the reacting mixture—as is maintained[2]—to 15° C. At the room-temperature of Benares, about 27° C., excellent mirrors could be obtained. The bloom on the silver surface, if any, does not require polishing to remove it. Rubbing with cotton soaked with soap gives a perfectly bright surface. The surface is so clean that not even a drop of water spreads on it. So far as the writers are aware this method of getting rid of the troublesome bloom is not reported anywhere in the literature. The optimum temperature for silvering has been determined as 20° C. The amount of surface to be presented is about 525 square cm. per gram of the silver nitrate present in the silvering mixture. Hence the efficiency of silvering does not depend on the concentration of the silver nitrate at all.

2. *Cleaning of the Glass Surface.*

It is essential that the surface to be silvered must be clean. How to decide, however, on the minimum amount of cleaning required for efficient silvering? Most of the papers dealing with the subject of silvering are in the form of recipes, and do not enable one to decide on suitable variations of the working conditions[3]. The following experiments were therefore carried out.

Took two glass plates $1'' \times 2''$ cut out of a piece of double the size of each plate. From their appearance one could not say that their surfaces were contaminated. Plates like these were silvered both in the same bath, after subjecting one of them to various cleaning processes. The adequacy of the cleaning was judged by the ability to produce uniform deposits. It was thus found that cleaning the surface by vigorously rubbing with cotton-wool under tap-water and subsequent washing with distilled water were not sufficient. Secondly, rubbing the glass surface with cotton and a little soap and then washing with tap-water and distilled water proved to be exceedingly efficient; but it cannot always be relied upon to remove all the impurities. Dipping the plate for three minutes in chromic acid in addition is found to give perfectly satisfactory results. Which is used first, chromic acid or soap, is found to be quite immaterial. Using these alternately once or twice should result in perfect cleaning. It is, perhaps, possible to substitute strong nitric acid in place of the chromic acid.

3. *Effect of adding an excess of Silver Nitrate or Ammonia on the Formation of the Silver Mirror.*

It is said that to a given quantity of the silver nitrate solution ammonia should be added drop by drop till the precipitated silver oxide just dissolved. To this is to be added potassium hydroxide equal to half the weight of silver nitrate used; the concentration of the solutions of the silver nitrate as well as of the potassium hydroxide is usually taken as about 7 to 10 per cent. On the addition of the potassium hydroxide a precipitate is again formed, and this should be *just* not dissolved by the addition of strong ammonia, drop by drop. If by any mistake too much ammonia is added it is suggested, by almost all workers, that dilute silver nitrate solution should be added, drop by drop, till just a little precipitate persists. *The solution is filtered*, and mixed with the reducing solution (see 5) before being poured on the glass plate. The question now is, in what way the formation of the mirror will be affected by an excess or by a deficiency of ammonia. The speck formation in the mirror as well as the speed of the deposition of silver will be influenced. These were proved as shown below.

After just dissolving the precipitate and filtering, mirrors were formed in a definite time after adding the prescribed quantity of the reducing solution and, *in addition*, 20, 10, 5, 4, 2, and 0 drops of silver nitrate and 2 and 5 drops of ammonia in beakers of the same size and taking the same amount of the mixture in each case. The change in volume due to adding varying drops of the reagents mentioned above is negligible compared to the volume of the silvering mixture. Table I. below gives the results.

TABLE I.

Influence of an excess of Silver Nitrate or Ammonia in the Mixture.

Trial.	Drops of nitrate in excess.	Drops of ammonia in excess.	Deposit.	Spots.	Black particles.
1.....	20	0	Thin.	Many, white and blue.	In plenty.
2.....	10	0	Thicker.	Less.	Fewer.
3.....	5	0	Thicker still.	Few and in corners only.	Still fewer.
4.....	4 (turbidity).	0	Similar to 3	....	In corner only.
5.....	2 (no turbidity).	0	Very thick.	Nil.	Present, not sticking to plate.
6.....	0	0	Thinner than in 5, equal to 4.	Nil.	Present.
7.....	0	2	Uniform, half thickness of 6.	Nil.	Present.
8.....	0	5	Still thinner, but uniform.	Nil.	Present.

It follows that excess of silver nitrate as well as ammonia retards the formation of the silver film. However, an excess of the silver nitrate, while it enhances the formation of white and blue spots, an excess of ammonia enables an uniform mirror deposit to be obtained. The retardation due to excess of silver nitrate is easy to understand. The excess of the nitrate combines with the ammonia and is precipitated as silver hydroxide or oxide. The ammonia, rendered thus ineffective, cannot prevent now the precipitation of the silver hydroxide from the solution which it had previously redissolved. The solution has therefore

less of the dissolved silver oxide than there was before the silver nitrate drops were added. The formation of the spots, as follows from Table I. column 5, must be attributed to the presence of the precipitated silver oxide, *i. e.*, due to the turbidity present in the solution. It may be noted that the mixture, after the addition of the last drops of silver nitrate, is filtered so that whatever precipitate is responsible for the spots must be formed after the filtration took place. When there was excess of ammonia there were no spots at all. It is possible that spots could be prevented, perhaps, if the filtration is done after allowing sufficiently long time for the precipitation to be completed. As we shall see in the next section there is a slowing down of the reaction with the addition of ammonia in excess, and if it prevents formation of spots why not add ammonia in a slight excess ?

4. *Control of the Deposition of Silver.*

We shall show that excess of ammonia only retards the process of the formation of the silver film. This can be shown by producing the film by allowing the reaction to run for different times and comparing the nature of the deposits so formed (see fig. 1).

The temperature of the reaction was 27° C., being the temperature of the room ; the strength of the silver nitrate solution was 10 per cent., and the number of drops of ammonia used in excess was five. With 3 minutes for the reaction the silver deposit was very uniform but thin. With 5 minutes it was very uniform but twice the thickness obtained in 3 minutes, as judged visually in a rough way, looking through at a cloudless part of the sky or at an illuminated white paper. With 12 minutes the deposit was again uniform and double the thickness obtained in 6 minutes. With 24 minutes the thickness was again double that with 12 minutes and uniform. With 48 minutes the thickness still further increased ; here, however, a few spots developed. With 180 minutes there was a still thicker deposit. There were some spots indicating a slightly less deposit, but due to the great thickness of the film they were noticeable only when very minutely examined. The deposit was otherwise of excellent quality after the bloom was washed off with cotton soaked in soap water and then rinsed in distilled water. While in the silvering mixture the process of the

silver deposition was allowed to go on without any shaking of the solution, lest the area presented of the glass surface to the mixture should be altered. Further, the beakers in which the silvering were observed were kept covered with glass plates to prevent evaporation of the ammonia.

We can conclude that the reaction of silvering in the above is almost linear up to about 48 minutes. The

Fig. 1.

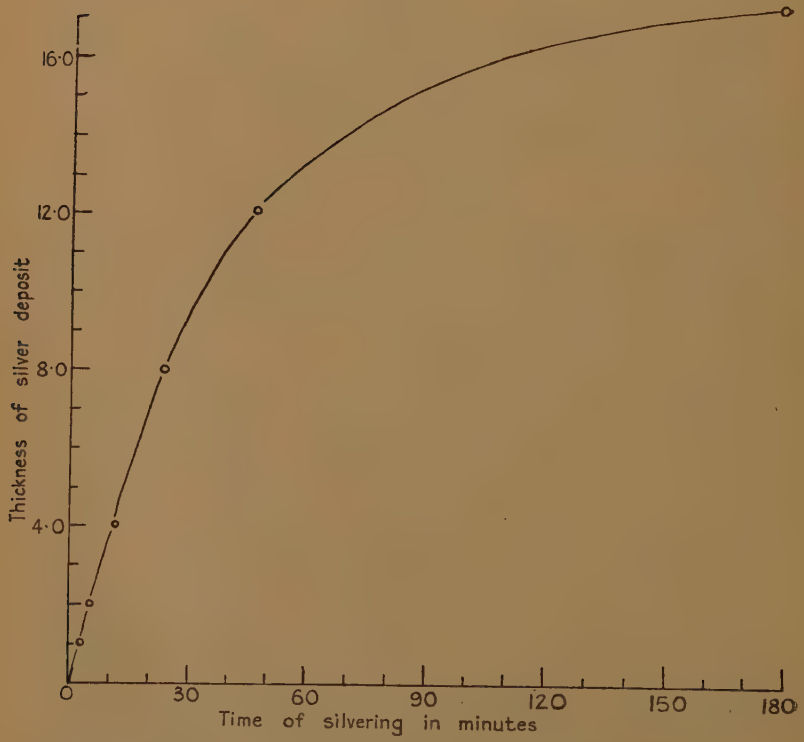

films were uniform and free from holes. The linearity is of utmost importance in enabling films to be prepared which should bear whatever ratios of thickness are desired. By noting the relatives times the reactions have been allowed to run predetermined thicknesses can be obtained.

It follows that the uniformity and freedom from holes and spots can be obtained by suitably retarding the reaction by the addition of an excess of ammonia. Liebig[4]

maintained that these results are to be obtained only by adding traces of a foreign substance like tartarate of copper, which according to him acted by increasing the adhesive forces on the surface for the silver reducing reagents. In view of our findings it is probable that the main function of the copper acetate is to suitably slow down the reaction. A subsidiary effect of the copper acetate might be the precipitation of traces of the red metallic copper along with the silver, resulting in a brighter tinge. Similar explanation could be adduced as to the influence of other substances added in small quantities, as shown by Kohlschütter and Fischmann [1].

Silverman and Howe [5] worked out a method of silvering in which both cane-sugar as well as methyl alcohol were used to slow down the action of formaldehyde in order to get films uniform and free from holes.

H. v. Wartenberg [6] has shown how $SnCl_2$ can be used to enhance the formation of the silver mirror, and in this the effect is believed to consist in the adsorption of SnO_2-sol by the glass surface and which helps in the adsorption of Ag_2O. I. Westermann [7] has shown that sodium-calcium glass at 380° C. can take considerable quantities of silver from $AgNO_3$ but not from AgBr. In the reception of silver it is made likely that Ag_2O diffuses from disintegrated $AgNO_3$ into the silica. Anyway there is no doubt that adsorption plays a great part in silvering. Hence we shall consider in the next section the function of the surface in silvering.

5. *Silvering Surface per Unit Mass of Silver Nitrate is more Fundamental than Concentration of the Silver Nitrate.*

If we take flat-bottomed glass beakers of radius r and fill each with the silvering mixture to a height h from the bottom then γ, the ratio of the area of glass surface presented per c.c. of the mixture, is given by

$$\gamma = \frac{\text{area}}{\text{volume}} = \frac{\pi r^2 + 2\pi r h}{\pi r^2 h} = \frac{1}{h} + \frac{2}{r}.$$

If the concentration of the silver nitrate in the mixture is denoted by c, then the area S presented per gram of silver nitrate is

$$S = \gamma/c = 1/c(1/h + 2/r).$$

In fig. 2 are shown the radius r against γ drawn as ordinates for different values of h. A large variation of the value for γ is easily obtained. The influence of h becomes negligible for small values of r. This is a very important point, for which we have found a very elegant application in the silvering in tubes whose one end gradually tapers to a fine capillary (see section 5 B).

Fig. 2.

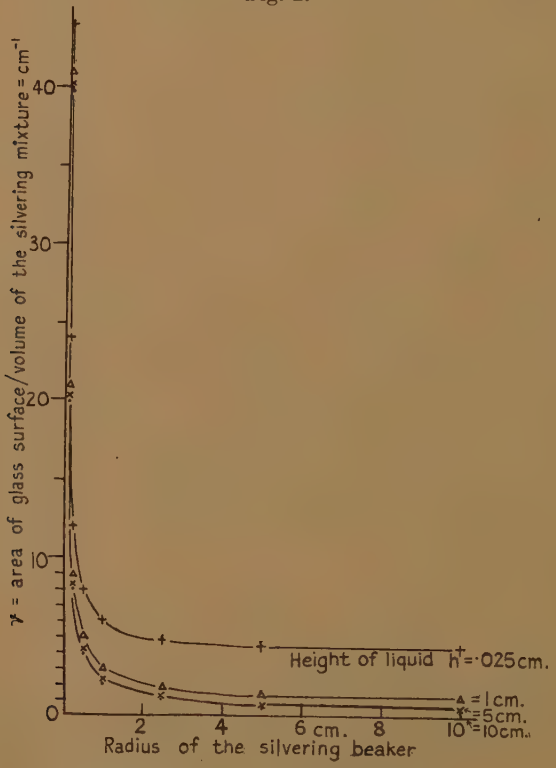

5 A. *Experiments with Beakers.*

Vessels 1 to 4 (see Table II.) were cleaned with soap and chromic acid, and the rest were filled with chromic acid and allowed to stand for half an hour ; washed all with tap-water and then with distilled water. The silvering mixture was made as follows :—

180 c.c. of 2·5 per cent. $AgNO_3$.
18 c.c. of 10 per cent. KOH.
27 c.c. of the reducing sugar solution.

Therefore the concentration c of silver nitrate in the silvering mixture is 2 per cent. The reducing solution was made as follows :—

90 gm. sugar candy.
4 c.c. nitric acid sp. gr. 1·22.
175 c.c. absolute alcohol
1000 c.c. distilled water.

The height h to which the mixture is filled is 1 cm., which was marked beforehand on each vessel with paper. The filling of the vessels took in all 15 seconds, beginning first with the vessel of the least diameter. After three

TABLE II.

Influence of Surface on the Deposition of Silver.

Vessel.	Height h (cm.).	Radius (cm.).	γ=area/vol.	γ/concentration of nitrate.	
				Conc.=2·0 per cent.	Conc.=0·477 per cent
1.....	1·0	7·1	1·28	64	268
2.....	..	4·8	1·42	71	298
3.....	..	3·0	1·67	83	350
4.....	..	1·6	2·25	117	**472**
5.....	..	0·5	5·0	250	1050
6.....	1·5	0·16	13·2	**660**	2770
7.....	2·0	0·05	40·5	2020	8500
8.....	4·0	0·02	100·3	5010	21000

The last two columns show the extent of surface per gram of the silver nitrate in the different vessels. The optimum values are shown in clarendon type for two concentrations of silver nitrate in the final silvering mixture.

minutes the vessels were emptied and the silver deposits were examined. There was not much bloom on any of the vessels, and the thickness of the deposits gradually varied from vessel 1, namely of the biggest radius, to the vessel 5, and then the thickness fell off.

The deposit in no. 2 vessel was nearly double that in vessel 1, that in 3 was double that in 2 ; in 4 it was one and a half times that in 3 ; in 5 it was slightly greater than that in 4. Deposit in the 6th was slightly thicker than that in 5. On the 7th it was slightly thinner than that on the 6th. Deposit on the 8th was less than that on the 7th. Therefore the optimum area

is for the vessel 6, with 660 sq. cm. per gram of silver nitrate.

These experiments were repeated with an initial concentration of 0·5 per cent. for the silver nitrate, for which the concentration in the silvering mixture would be 0·477 per cent., instead of 2 per cent. in the above experiment. The temperature was 26·5° C. and the time allowed for the reaction was 15 minutes. The deposits in the first and second were nearly equal, that on the third slightly thicker ; on the 4th it was thickest. On the 5th the deposit is slightly but distinctly thinner than on the 4th. On the remainder the deposits gradually diminished in thickness as the radius was decreased. The optimum value of S, *i. e.*, for the vessel 4, comes out as 472 sq. cm. per gram (see last column in Table II.).

The *mean value for* S *out of the last two experiments is* 566 *sq. cm. per gram of silver nitrate.*

One possible source of error in the last two sets of experiments is, perhaps, loss of some ammonia from the silvering dish due to evaporation from the different surfaces, which are unequal in area. This can happen in spite of the fact that the beakers were covered with glass plates. The following experiments are free from this objection, and the fact that the value of S obtained in them also agrees with the above shows that the slight and possible evaporation of ammonia is of no importance.

5 B. *Silver Deposition in Conical Tubes, and the Value of* S.

With value for S found above, supposing silvering is carried out with an initial value of silver nitrate of 0·5 per cent. concentration in a vessel whose diameter gradually varies from 1 cm. at one end to about 1 mm. at the other; the formation of the mirror should start from the end with diameter 1 cm. and proceed to the end with diameter of 1 mm. In an actual experiment the deposit started to be visible in about 3 minutes and reached up to 5 cm. from the wider end of the tube. In 5 minutes it had travelled to 7 cm., in 7 minutes up to 9 cm., and in 12 minutes up to 11 cm. After 15 minutes the solution was thrown out and washed with distilled water. Deposit was examined with transmitted light from a powerful bulb. Lest the bright light should blind the eye, and make the estimation uncertain, filter-paper was held

across the silver tube to keep off the blazing filament from direct view. The deposit was examined as seen just outside the edge of the filter-paper. Different portions of the deposited tube could be brought to the edge of the filter-paper and the variation in thickness of the film conveniently examined. The deposit gradually diminished as one proceeded from the largest to the smallest diameter. This method of observation is free from the objection referred to, namely of the evaporation of ammonia. In the present experiment there is no open surface except at the two remote ends, and near about them the deposition need not be taken into account. The heaviest deposit appeared again in vessel no. 4, as before, an experiment also simultaneously carried out as a check and connecting normal. So we may take it as confirmed that for values of S above, say, 1000—the value corresponding to 1 cm. diameter—the thickness of the silver deposit diminishes with increase of S.

If the optimum area is about 566 it follows that the position of the thickest deposit should be well defined in the conical drawn-out tube of the description used in the previous experiment if we take 6·6 per cent. silver nitrate solution in the *final* silvering mixture. On actually carrying out this test it was found that the thickest deposit appeared at a diameter equal to 1·2 mm. It follows from this that $S=2/rc=505$ sq. cm./gm. On a repetition of this experiment under identical conditions the value of S came to 467, the optimum being 1·3 mm. In both these experiments it was necessary to retard the process by the addition of 10 drops of ammonia in excess. The mean value out of these two experiments for S is 486.

In the experiments with beakers and in the conical tubes, together, the final average value for **S is 525 sq. cm./gm.**

It is appropriate to mention here that Kohlschütter and Fischmann[1] are the only people who have drawn attention to the fact that the amount of silver deposited is different according as we use a spherical flask or test-tubes, the concentration and the total amount of the silvering mixture used remaining the same. As reducing agents they used acetaldehyde as also grape-sugar (glucose). With both they found that the amount of silver deposited in the test-tubes as mirror was double that obtained in the flask. The area per unit volume of silvering mixture in the two cannot be the same, so that their findings support

our result that the amount of silver deposited as mirror is a function of the area presented per unit mass of the silver nitrate in the final silvering mixture. Whatever the amount may be that sticks as bright metallic silver on the glass, the total amount, according to Kohlschütter and Fischmann, of silver nitrate reduced—silver as mirror and silver thrown down as useless precipitate to the bottom of the silvering bath—is the same in the tubes as well as in the spherical vessel. It follows therefore that there would be a lot of bloom or mud of some variety of silver if the extent of area presented is less than the optimum.

6. *The Temperature Effect in Silvering.*

It is given in the Bureau of Standards Circular[2], no. 32, that the temperature of the silvering bath should be maintained at 15° C., and certainly not above 18°. If this is true it would involve a real hardship to do the silvering in tropical countries where the room-temperature is about 10° C. higher, in that arrangements will have to be made to specially cool the solutions. It may, however, be noted that the temperature indicated by Wadsworth—to whom we owe the description and a detailed account of the Breashear[3] method (same as the much earlier Martin's process[3]), as optimum for silvering is 21° C. In what follows we shall show, by studying silvering at different temperatures, that excellent silvering can be made at the room-temperature of Benares, namely about 27° C., though the optimum rate of deposit takes place at about 20° C. In carrying out silvering at the room-temperature we get fast-sticking films because of the fact that there is perfect uniformity of temperature between the glass and the silvering solutions.

A temperature of 50° C. is too high.

Experiment 1.—Three beakers, of diameters 6 cm., 3 cm., and 1 cm., were cleaned with soap and chromic acid. The different solutions were first maintained in a bath at 50° C., and were then mixed in the usual proportions and filled into the three vessels to the same height in all. Time allowed was 3 minutes. The initial concentration of the silver nitrate solution is 1 per cent. Results: some shining silver films were seen floating on the surface even before the reducing solution was

added, and even before the filtration could be done. The deposit obtained after the reducing solution was added was very thin in all the three beakers.

Experiment 2.—The experiment was repeated by retardation with a few drops of ammonia, with no improvement, however, in the results. We therefore conclude that 50° C. for the silvering mixture used by us is too high a temperature.

A temperature of 0° *C. is too low.*

TABLE III.

Showing Time Details for the Silvering.

Temp. °C.	Time in minutes for appearance of:			
	Colour.	Blackness.	Deposit.	Floating patches.
0	5	210	?	?
10	2	13	33	63
20	0·5	1·5	4·0	13
27	0·25	1·0	4·0	10·5
35	?	0·25	0·78	1·75
10	0·06	0·4	1·0	1·9
20	·12	·37	1·0	3·2
27	0·06	·25	1·0	2·6
35	?	·32	1·0	2·25
	0·08	0·335	1·0	2·5
	1·0	4·0	12	30

Five beakers of exactly the same size and shape were cleaned with soap and chromic acid. The height of the silvering solution in all the five beakers was kept the same, and the times allowed for the deposition, in order to be able to examine the deposits, were different. The temperature was 0° C. The solution turned slightly orange in 5 minutes and slightly brown in 10 minutes, and did not become black in even three and a half hours. There was no deposit.

Table III. gives the results of similar experiments at different temperatures. The first column gives the temperature, the second the time in minutes at which the first indication of colour takes place, the third the

time in minutes when the colour of the mixture turns black, the fourth gives the time when deposition of silver could first be noticed, and in the last column is shown the time when silver patches appear on the top surface of the silvering mixture.

The lower part of the table shows the ratios of the time with deposition time taken as unity. The values show that the ratios are independent of temperature. Therefore the average values of these are shown in the last but one row. The last row gives the value of these taking the time for the appearance of colour in the solution as unity. These in words would be that the times for the appearance of colour, for the solution to turn black, for the deposition of silver to be first noticed and the appearance of silver films floating on the free upper surface of the silvering mixture are, respectively, in *the ratios of one, four, twelve, and thirty.*

The Thickness of Deposit at Different Temperature.

As we have just seen, the higher the temperature the greater the velocity with which a chemical reaction will proceed. But in the case of silvering we have to consider further the capacity of the liberated silver to stick to the sides of the glass, and this may be assumed to vary inversely as the temperature, so that the amount Q of silver deposited will be

$$Q = \text{constant}/(a+bT)(c/T+d)$$

(a, b, c, and d are constants).

From this it follows that for smaller values of T, Q increases as T rises, it reaches a maximum, and for further rise of temperature it falls. This is exactly what is found to be the case. Table IV. shows the results (see also fig. 3, in which the result of 50° measurementis also included).

The table shows that, for equal times, the deposit at 0° C. is negligible compared to that at 20° C. At 10° it can be taken a little less than half that at 20° for 38 minutes, at 27° it is half that at 20°, at 35° it is one-fourth that at 20°. At 20° C. we get the optimum temperature (see fig. 3). At 35° the results of two experiments are shown. The time at which silver films begin to appear on the liquid surface at this temperature is not more than

1 minute and 45 seconds. The point to test is whether at this temperature of 35° the silver mirror once formed will not be redissolved into the silvering mixture. The

TABLE IV.

Thickness of Deposit in relation to Temperature and Time.

Temperature °C.	Time in minutes.		Thickness of deposit.
	Deposit commencing.	Deposit stopped.	
0	?	210	Nil.
10	33	78	Slightly thinner than at 20° C.
20	4	38	Slightly thicker than at 10°.
27	4	38	Half that at 20°.
35	0·9	38	One-fourth that at 20°.
35	0·66	15	One-eighth that at 35° and 38 minutes.

Fig. 3.

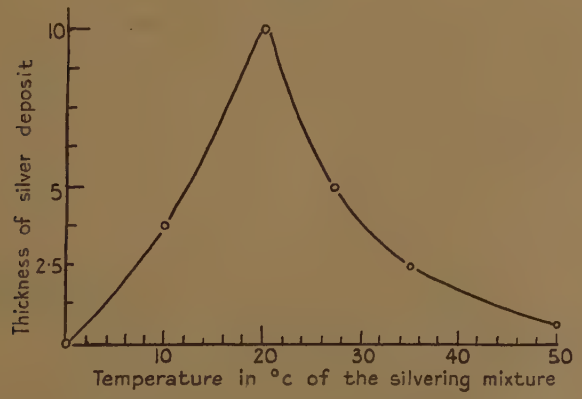

results in the last two rows of the table show that the deposit has nearly doubled itself from 15 to 38 minutes. This is important since, contrary to the usual belief, the reaction goes on usefully even long after the floating of silver films on the surface could be noted. As remarked previously, whatever bloom accumulates on the film can be easily washed off with cotton and soap.

It is possible to evaluate the constants a, b, c, and d of the equation for Q from the relative values for Q in the table.

7. *Summary and Conclusion.*

The method adopted for the study of silvering is the chemical method, in which to an ammoniacal solution of silver nitrate is added, drop by drop, a solution containing potassium hydroxide equal to half the weight of the silver nitrate used. The precipitate is redissolved by adding ammonia, drop by drop. Candy-sugar inverted with nitric acid, with the addition of alcohol, is used as the reducing agent. This process is generally referred to as the Brashear process (1883), but really it is no other than the much older Martin process (1863).

In section 2 experiments are described which enable one to decide the amount of cleaning of the glass surface necessary for proper silvering. Rubbing the plate with soap and water, and then keeping it for a few minutes dipped in chromic acid and then washing with tap-water, followed by distilled water, is found to be quite adequate.

In section 3 study has been made of the effects of adding either silver nitrate or ammonia in excess to the ammoniacal silver nitrate and KOH solution prior to the mixing of the reducing solution. Excess of silver nitrate so added leads to the development of spots in the mirror, while an excess of ammonia, while it lessens the rate of silver deposited as mirror, enables uniform deposits to be obtained (see Table I., p. 956).

Section 4 deals with the control of the deposition of silver which is got by the addition of a few drops of ammonia to the ammoniacal silver nitrate and potassium hydroxide mixture. This results in suitably slowing down the reaction, and thus enables a better control of the process of silvering.

Section 5, which is the most important, shows that *the amount of silver usefully deposited as mirror* is a function of the area of the glass surface presented to the solution to the amount of silver nitrate in the solution, and it is not determined by the concentration of the silver nitrate. This has been proved by experimenting in beakers of different ratios of area to volume, and also in a very ingenious way, namely by observing the deposition of silver in a tube whose diameter varies continuously from 1 cm.

at one end to a fraction of a millimetre at the other end. At the optimum diameter, which is different for different concentrations of the silver nitrate, the deposition of the silver film on the glass starts earliest and is also thickest at the place. The concentration of the silver nitrate in the mixture was varied from about 6 per cent. to 0·4 per cent. Irrespective of the concentration the optimum area of glass surface comes to an average of 525 sq. cm. per gram of the silver nitrate.

In section 6 a study of the deposit of the silver mirror was made at temperatures of 0, 10, 20, 27, 35, and 50° C. It is shown that the best deposition takes place at about 20° C. Very good mirrors, however, can be obtained at 27° C., being the room-temperature at Benares, it being quite unnecessary—as often maintained—to have to cool the silvering solutions to the temperature of 15° C. The amount of silver as mirror deposited in a given time is at 10° C. and 27° C. the same, being about half that at 21°. At 35° it is only about one-fourth. At zero it is very slow. While the velocity of the reaction for the reduction of silver nitrate increases with temperature almost steadily, that of the deposition of the silver as mirror on the glass surface is optimum at 20°. The relative times, namely for the silvering mixture, after the addition of the reducer, to show (1) signs of colour, (2) blackness, (3) deposition of silver film on glass, and (4) for the appearance of films of silver floating on the liquid surface, are in the ratios of 1, 4, 12, and 30 respectively, and independent of temperatures within 10 to 35° C. The absolute values of these times, however, vary inversely as the temperature, and hence are proportional to the velocity of the reduction of the silver nitrate, but not to the velocity of the deposition of silver film on the glass.

References.

(1) J. Stenhouse, Phil. Mag. (3) xxvi. pp. 233–234 (1845). H. Vogel, *J. Prakt. Chem.* lxxxvi. pp. 321–333 (1862). G. T. Morgan and M. G. Micklethwait, J. Soc. Chem. Ind. xxi. pp. 1373–1375 (1902). V. Kohlschütter and E. Fischmann, *Ann. d. Chemie*, ccclxxxvii. pp. 86–145 (1912).

(2) W. Shackleton and A. Fowler, Glazebrook, ' Dictionary of Applied Physics,' vol. iv. pp. 675–678. Physical Papers, United States Bur. of Standards, Circular no. 32, and Circular no. 389 of 1931.

(3) J. Liebig, *Annalen d. Chem.* xcviii. pp. 132–139 (1856). M. Faraday, ' Notices Royal Institution,' vi. p. 308 ; Pogg. *Annalen*, ci. p. 313 (1857). M. A. Martin, *Comptes Rendus*, lvi. pp. 1044–1045 (1863). F. Bothe, *J. Prakt. Chem.* xcii. pp. 191–193 (1864). J.

Liebig, *Annalen d. Chem.* Supplement v. pp. 257–260 (1867). R. Kayser, *Zeit. Angew. Chem.* iv. pp. 541–542 (1890). F. L. O. Wadsworth, Astrophys. J. i. pp. 252–260 (1895); *Zeit. Ang. Chem.* ix. p. 106 (1895) (this paper gives a description of the Brashear method otherwise contained only in the not easily accessible 'English Mechanic,' 1883). F. E. J. Ockenden, J. Scient. Instr. xv. pp. 206–208 (1938).

(4) J. Liebig, *Annalen d. Chem.* Supplement v. pp. 257–260 (1867).

(5) A. Silverman and R. M. Howe, J. Ind. a. Eng. Chem. ix. p. 1032 (1917).

(6) H. v. Wartenberg, *Zeit. Anorg. Allg. Chem.* cxc. pp. 185–187 (1930).

(7) I. Westermann, *Zeit. Tech. Physik*, xiii. p. 617 (1932).

Physical Laboratory,
Benares Hindu University.
11th Aug. 1938.

LXXXII. *A General Graduation Formula for the Smoothing of Time Series.* *By* T. E. W. Schumann, *M.Sc., Ph.D.**

[Received June 17, 1938.]

MANY methods for drawing a smooth curve through data spaced at equal intervals have been published from time to time, and it may appear superfluous to add yet one more to the long list. However, the method to be described in the following pages exhibits some rather attractive features, such as comparative ease of calculation, the absence of any arbitrary manipulation to include the end terms in the graduation, etc., and on this account it may prove to be of practical value to meteorologists and others who are concerned with determining trends in the analysis of statistics.

The underlying idea of this new method, which for the sake of brevity we shall refer to as the *equilibrium method*, may most conveniently be explained with the help of the accompanying diagram, fig. 1. In this figure y_1 to y_5 are the crude data, and represent the annual rainfalls for the Cape Town district during the years 1921 to 1925 inclusive. For the sake of clarity only a few points are taken, but it is to be understood that there is no limit to the number of datum points which can be included in the graduation process. Our object now is to draw a smooth curve to represent the data.

* Communicated by the Author.

In order to accomplish this we imagine an inextensible string tied to the two points u_0 and u_6, whose values are left arbitrary for the time being. Initially the string is not stretched tightly, but is supposed to exhibit a certain degree of slackness. We now imagine springs to be attached at the points y_1 to y_5 and to the string, each spring drawing the string in the positive or negative y direction with a force proportional to its own length. Unless the string is too slack at the beginning it will take up an intermediate position such as the curve u_0, u_1, u_2, u_3, u_4, u_5, u_6 in fig. 1. Evidently this is a smoothed curve of the original data.

If the original amount of slackness in the string be decreased a smoother curve is obtained, but the fit to the crude data would be inferior. By lengthening or

Fig. 1.

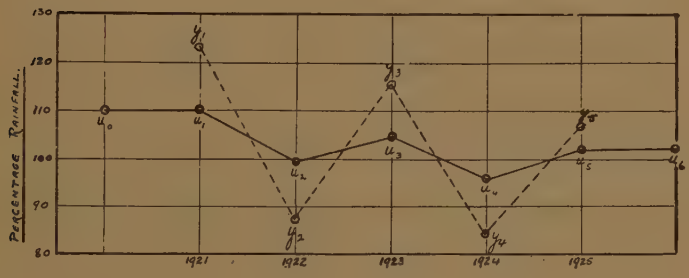

shortening the string any degree of smoothness may be obtained, but in general the closeness of fit to the original data is an inverse function of the smoothness of the fitted curve. This is a principle which is of general application, and the investigator is always obliged to decide up to what point he is prepared to sacrifice closeness of fit in order to obtain sufficient smoothness.

Subject to certain conditions it is possible to calculate quite readily the positions of the points u_1 to u_5 on the fitted curve in terms of the original data y_1 to y_5, and we now proceed towards the solution of this problem for any number of data, leaving the significance of the results obtained for later discussion.

Suppose then we have a series of n data, y_1 to y_n, spaced at equal *unit* intervals along the X-axis, *i. e.*,

at the points $x=1, 2 \ldots n$. Let u_1 to u_n be the corresponding points on the smoothed curve taken up by a string attached to the points u_0 and u_{n+1}, where the string is supposed to be drawn towards the points y_r with a force proportional to y_r-u_r.

Consider the forces acting on any point u_r of the string. The y force exerted by the spring attached at this point is $P(y_r-u_r)$, where P is a constant. The two other forces are due to the tension T of the string itself. Now, since our X scale is completely arbitrary, we may postulate that the scale intervals on the X-axis are so large that the first differences $u_{r+1}-u_r$ may all be regarded as small quantities, in which case the vertical forces reduce to $T(u_{r-1}-u_r)$ and $T(u_{r+1}-u_r)$. Hence, equating the three forces to zero, since every point on the string is in equilibrium, we obtain equations of the type

$$T(u_{r+1}+u_{r-1}-2u_r)+P(y_r-u_r)=0 \quad . \quad . \quad . \quad (1)$$

for all values of r from unity to n.

By adding these n equations together we obtain

$$T(u_0+u_{n+1})-T(u_1+u_n)+P\sum_1^n y_r-P\sum_1^n u_r=0. \quad . \quad (2)$$

If the smoothed curve is to represent the crude data correctly it is essential that the sum of the u terms should be equal to the sum of the original data, *i. e.*,

$$\sum_1^n u_r=\sum_1^n y_r, \quad . \quad . \quad . \quad . \quad . \quad . \quad . \quad (3)$$

and hence it follows that

$$u_0+u_{n+1}=u_1+u_n. \quad . \quad . \quad . \quad . \quad . \quad (4)$$

Furthermore, since u_0 and u_{n+1} are arbitrary, we assume

$$u_0=u_1 \quad . \quad . \quad . \quad . \quad . \quad . \quad . \quad (5)$$

and

$$u_{n+1}=u_n. \quad . \quad . \quad . \quad . \quad . \quad . \quad . \quad (6)$$

Proceeding, we write eq. (1) in the form

$$u_r=\frac{T}{2T+P}(u_{r-1}+u_{r+1})+\frac{P}{2T+P}y_r$$

$$=\alpha(u_{r-1}+u_{r+1})+(1-2\alpha)\,y_r, \quad . \quad . \quad . \quad (7)$$

where

$$\alpha=\frac{T}{2T+P}. \quad . \quad . \quad . \quad . \quad . \quad . \quad . \quad (8)$$

The first three equations of (7) are

$$u_1=\alpha u_0+\alpha u_2+(1-2\alpha)y_1, \quad . \quad . \quad . \quad . \quad (9\,a)$$

$$u_2=\alpha u_1+\alpha u_3+(1-2\alpha)\,y_2, \quad . \quad . \quad . \quad (9\,b)$$

$$u_3=\alpha u_2+\alpha u_4+(1-2\,\alpha)\,y_3. \quad . \quad . \quad . \quad (9\,c)$$

Remembering that $u_0=u_1$, we find from (9 a) that

$$u_1=\frac{\alpha}{1-\alpha}\,u_2+\frac{1-2\alpha}{1-\alpha}\,y_1. \quad . \quad . \quad . \quad . \quad (10)$$

For the sake of convenience the following symbols may be introduced:

$$\phi_1=1,$$

$$\phi_2=1-\alpha,$$

$$\phi_3=\phi_2-\alpha^2\phi_1=1-\alpha-\alpha^2,$$

and in general

$$\phi_{r+1}=\phi_r-\alpha^2\phi_{r-1}, \quad . \quad . \quad . \quad . \quad . \quad (11)$$

and if the value of u_1 be substituted in (9 b) we find

$$u_2=\frac{1-2\alpha}{\phi_3}\,(\alpha\phi_1y_1+\phi_2y_2)+\frac{\alpha\phi_2}{\phi_3}\,u_3. \quad . \quad . \quad (12)$$

If the same procedure is carried further step by step we arrive at the expression for the general term :

$$u_r=\frac{1-2\alpha}{\phi_{r+1}}\sum_{s=1}^{r}\alpha^{r-s}\phi_sy_s+\frac{\alpha\phi_r}{\phi_{r+1}}\,u_{r+1}. \quad . \quad . \quad (13)$$

Exactly the same procedure may now be carried out, starting at the opposite end of the series, with the result that

$$u_{r+1}=\frac{1-2\alpha}{\phi_{n-r+1}}\sum_{s=r+1}^{n}\alpha^{r-s+1}\phi_{n-s+1}y_s+\frac{\alpha\phi_{n-r}}{\phi_{n-r+1}}\,u_r. \quad . \quad (14)$$

Elimination of u_{r+1} between (13) and (14) yields

$$\frac{u_r}{1-2\alpha}=\frac{\phi_{n-r+1}\sum_{s=1}^{r}\alpha^{r-s}\,\phi_sy_s+\phi_r\sum_{r+1}^{n}\alpha^{s-r}\phi_{n-s+1}\,y_s}{\phi_{r+1}\phi_{n-r+1}-\alpha^2\phi_r\phi_{n-r}}. \quad (15)$$

This is the general solution of the system of equations (1) subject to conditions (5) and (6), and hence the problem has been formally solved.

However, it is possible to express ϕ_r in simple analytical form whereby the calculations are simplified. This we proceed to do by noting that

$$\begin{aligned}\phi_r\phi_{r-1}-\phi_r^2-\alpha^2\phi_{r-1}^2&=\phi_{r+1}\phi_{r-1}-\phi_r^2\\&=\alpha^2(\phi_r\phi_{r-2}-\phi^2{}_{r-1})\\&=(\phi_2\phi_0-\phi_1{}^2)\alpha^{2r-2}\\&=(1-2\alpha)\alpha^{2r-3}=\text{A (say)}. \quad . \quad . \quad . \quad . \quad (16)\end{aligned}$$

Put $$\theta_r=\phi_r-\frac{1}{\alpha}p^2, \quad . \quad . \quad . \quad . \quad . \quad . \quad . \quad . \quad (17)$$

where θ_r satisfies the equation

$$\theta_{r+1}=\theta_r-\alpha^2\theta_{r-1}, \quad . \quad . \quad . \quad . \quad . \quad (18)$$

which is possible provided

$$p^2-p+\alpha^2=0. \quad . \quad . \quad . \quad . \quad . \quad . \quad (19)$$

Also

$$\begin{aligned}\theta_{r+1}\theta_{r-1}-\theta_r^2&=\alpha^2(\theta_r\theta_{r-2}-\theta_{r-1}^2)\\&=\alpha^{2r-2}(\theta_2\theta_0-\theta_1{}^2)=-\frac{p}{\alpha}\text{A}. \quad . \quad . \quad . \quad (20)\end{aligned}$$

But, by virtue of (17),

$$\begin{aligned}\theta_{r+1}\,\theta_{r-1}-\theta_r^2&=\phi_{r+1}\phi_{r-1}-\phi_r^2+\frac{2}{\alpha}p^r\phi_r-\frac{1}{\alpha}p^{r-1}\phi_{r+1}\\&\qquad-\frac{1}{\alpha}p^{r+1}\phi_{r-1}\\&=\text{A}+\frac{1}{\alpha}p^{r-1}(2p\phi_r-\phi_{r+1}-p^2\phi_{r-1})\\&=-\frac{p}{\alpha}\text{A}.\end{aligned}$$

Hence $$\phi_r=p\phi_{r-1}+\frac{\text{A}(\alpha+p)}{(1-2p)p^{r-1}}. \quad . \quad . \quad . \quad (21)$$

Elimination of ϕ_{r-1} between (16) and (21) leads to the result

$$\phi_r=\frac{1}{\alpha+p}\left\{p^r+\frac{p}{\alpha}(1-p)^r\right\} \quad . \quad . \quad . \quad . \quad (22)$$

This is the general expression of ϕ_r for any value of r, where by virtue of equation (19)

$$p=\frac{1+\sqrt{1-4\alpha^2}}{2}. \quad . \quad . \quad . \quad . \quad . \quad (23)$$

As is evident from (7) and (8) α and $1-2\alpha$ are essentially positive quantities, so that the value of α always lies between 0 and 0·5. Corresponding values of α and p are given below.

TABLE I.

$p=0{\cdot}5$	0·6	0·7	0·8	0·9	0·95	1·0
$\alpha=0{\cdot}500$	0·490	0·458	0·400	0·300	0·218	0

By making use of (22) we can reduce (15) to the form

$$u_r=\frac{2p-1}{p^n-(1-p)^n}\left\{\phi_{n-r+1}\sum_1^r\alpha^{r-s}\phi_s y_s+\phi_r\sum_{r+1}^{n}\phi_{n-s+1}y_s\right\}\quad\ldots\quad(24)$$

We may now illustrate the application of the general equation (24) to the short series of five items shown in fig. 1.

Let us assume $\alpha=0{\cdot}3$,

then $p=0{\cdot}9$,

and it follows from (11) or (22) that

$\phi_1=1$, $\phi_2=0{\cdot}7$, $\phi_3=0{\cdot}61$, $\phi_4=0{\cdot}547$, and $\phi_5=0{\cdot}492$.

From equation (24) the values of u_1 to u_5 may be calculated. The values of the coefficients by which the y's have to be multiplied in order to yield the u's may be written in tabular form as follows :—

	y_1.	y_2.	y_3.	y_4.	y_5.
u_1.....	0·6667	0·2222	0·0745	0·0256	0·0110
u_2.....	0·2222	0·5188	0·1735	0·0598	0·0256
u_3.....	0·0745	0·1736	0·5040	0·1736	0·0745
u_4.....	0·0256	0·0598	0·1736	0·5188	0·2222
u_5.....	0·0110	0·0256	0·0745	0·2222	0·6667

If we apply these coefficients to the five y values we arrive at the following corresponding y and u values :—

$y_1=118{\cdot}2$	$y_2=87{\cdot}1$	$y_3=115{\cdot}5$	$y_4=83{\cdot}9$	$y_5=106{\cdot}5$,
$u_1=110{\cdot}1$	$u_2=99{\cdot}3$	$u_3=104{\cdot}6$	$u_4=95{\cdot}5$	$u_5=101{\cdot}8$,

which are shown graphically in fig. 1. If a larger value of α had been employed a smoother curve would have resulted, and it is thus evident that any series, whether short or long, may be smoothed to any desired extent by use of equation (24).

If we are dealing with a long series it is possible to introduce appreciable simplifications, and this will be the next step in our discussion.

Equation (21) may be written in the form

$$\phi_n = p\phi_{n-1} - \frac{p-\alpha}{\alpha}(1-p)^{n-1},$$

and since $(1-p)$ is always less than 0·5 it follows that for large values of n ϕ_n/ϕ_{n-1} has a limiting value equal to p. Furthermore, if n is large and r and s are small it follows from (22) that

$$\phi_{\cdot} = \frac{p^n}{\alpha+p}$$

$$\phi_{n-r+1} = \frac{p^{n-r+1}}{\alpha+p},$$

$$\phi_{n-s+1} = \frac{p^{n-s+1}}{\alpha+p},$$

and if these values are substituted in (24) we arrive at the result

$$u = \frac{2p-1}{(\alpha+p)\,p^{r+1}}\left\{\sum_{1}^{r-1}\alpha^{r-s}\phi_s y_s + \phi_r \sum_{r}^{n}\left(\frac{\alpha}{p}\right)^{s-r} y_s\right\}, \quad (25)$$

which is the expression for calculating the terms near the beginning of a long series, with a similar expression near the end of the series.

Likewise the expression which applies to the middle terms may be obtained by putting

$$\phi_r = \frac{p^r}{\alpha+p}$$

and $$\phi_s = p^s/(\alpha+p)$$

in (25), in which case

$$u_r = \frac{p-\alpha}{p+\alpha}\left\{y_r + \frac{\alpha}{p}(y_{r+1}+y_{r-1}) + \frac{\alpha^2}{p^2}(y_{r+2}+y_{r-2}) + \ldots\right\} \quad (26)$$

This expression applies to all the terms of a long series except those near the two ends of the series.

Practical Examples.

By adopting different values of α we may now, with the help of equations (25) and (26), construct tables containing the numerical coefficients for calculating the smooth curves. We here present only two such sets of tables to three places of decimals.

Case I.

$\alpha=0{\cdot}4, \quad \alpha/p=0{\cdot}5, \quad p=0{\cdot}8.$

	y_1.	y_2.	y_3.	y_4.	y_5.	y_6.	y_7.	y_8.	y_9.	y_{10}.	y_{11}.	y_{12}.
u_1	·500	·250	·125	·063	·031	·016	·008	·004	·002	·001	—	—
u_2	·250	·375	·187	·094	·047	·023	·012	·006	·003	·002	·001	—
u_3	·125	·187	·345	·172	·086	·043	·021	·011	·005	·003	·001	·001
u_4	·063	·094	·172	·336	·168	·084	·042	·021	·010	·005	·003	·001
u_5	·031	·047	·086	·168	·335	·167	·083	·042	·021	·010	·005	·003
u_6	·016	·023	·043	·084	·167	·334	·167	·083	·042	·021	·010	·005
u_7	·008	·012	·021	·042	·083	·167	·334	·167	·083	·042	·021	·010
u_8	·004	·006	·011	·021	·042	·083	·167	·334	·167	·083	·042	·021
u_9	·002	·003	·005	·010	·021	·042	·083	·167	·334	·167	·083	·042
u_{10}	·001	·002	·003	·005	·010	·021	·042	·083	·167	·334	·167	·083
u_{11}	—	·001	·001	·003	·005	·010	·021	·042	·083	·167	·334	·167

Case II.

$\alpha = 6/13, \quad \alpha/p = 2/3, \quad p = 9/13.$

	y_1.	y_2.	y_3.	y_4.	y_5.	y_6.	y_7.	y_8.	y_9.	y_{10}.	y_{11}.	y_{12}.	y_{13}.	y_{14}.	y_{15}.
u_1	·334	·223	·148	·099	·066	·044	·029	·020	·013	·009	·006	·004	·002	·002	·001
u_2	·223	·260	·173	·116	·077	·051	·034	·023	·015	·010	·007	·004	·003	·002	·001
u_3	·148	·173	·227	·151	·101	·067	·045	·030	·020	·013	·009	·006	·004	·002	·002
u_4	·099	·116	·151	·212	·141	·094	·063	·042	·028	·018	·012	·008	·006	·004	·002
u_5	·066	·077	·101	·141	·205	·137	·091	·061	·041	·027	·018	·012	·008	·005	·004
u_6	·044	·051	·067	·094	·137	·204	·135	·090	·060	·040	·026	·018	·012	·008	·005
u_7	·029	·034	·045	·063	·091	·135	·202	·134	·089	·060	·040	·026	·018	·012	·008
u_8	·020	·023	·030	·042	·061	·090	·134	·200	·134	·089	·059	·040	·026	·018	·012
u_9	·013	·015	·020	·028	·041	·060	·089	·134	·200	·134	·089	·059	·040	·026	·018
u_{10}	·009	·010	·013	·018	·027	·040	·060	·089	·134	·200	·134	·089	·059	·040	·026
u_{11}	·006	·007	·009	·012	·018	·026	·040	·059	·089	·134	·200	·134	·089	·059	·040
u_{12}	·004	·004	·006	·008	·012	·018	·026	·040	·059	·089	·134	·200	·134	·089	·059
u_{13}	·002	·003	·004	·006	·008	·012	·018	·026	·040	·059	·089	·134	·200	·134	·089
u_{14}	·002	·002	·002	·004	·005	·008	·012	·018	·026	·040	·059	·089	·134	·200	·134
u_{15}	·001	·001	·002	·002	·004	·005	·008	·012	·018	·026	·040	·059	·089	·089	·200

The figures contained in the two tables were applied towards smoothing the annual rainfall during the years 1878 to 1936 inclusive for a district in the central Cape Province. The results are shown in fig. 2, in which the small circles indicate the actual rainfall for each individual year reckoned as a percentage of the average for 1878 to 1933. The broken line is the smoothed curve when α is taken as 0·4, and the continuous curve when $\alpha = 6/13$. The latter curve gives a fairly good indication of the

Fig. 2.

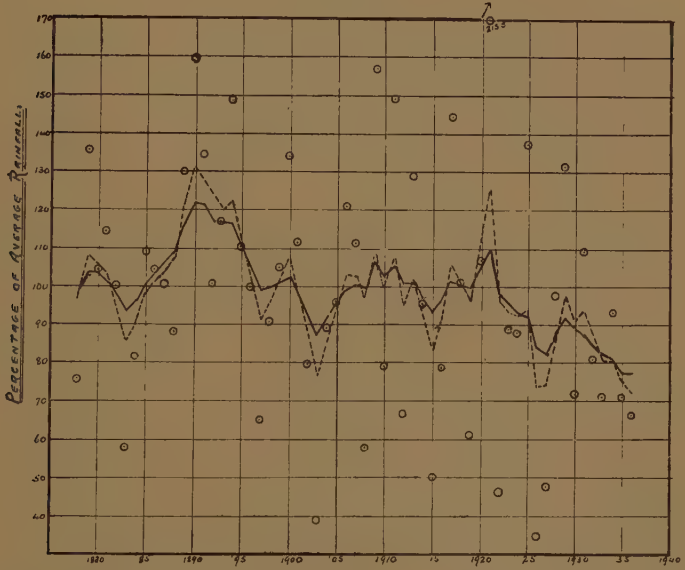

long period rainfall trend; but if greater smoothness is desired it would be necessary to assume a larger value of α and to repeat the calculation for such a value.

Theoretical Considerations.

Having explained our method of graduation and given some practical illustrations of the numerical process, we may now briefly consider its logical basis.

In 'The Calculus of Observations' * a number of

* 'The Calculus of Observations,' by Whittaker and Robinson. Blackie & Son, 1924.

graduation methods are described, and in this connexion the authors make the following statement (p. 303) :— "The methods described above (pp. 285–302) fulfil their purpose of smoothing out irregularities from observational data in a way which is on the whole efficient. From purely theoretical standpoint they are not altogether satisfactory, since each of them contains arbitrary or empirical elements whose introduction does not appear to be logically necessary." The authors then proceed to describe their own method of graduation.

With the above statement one is bound to agree, although it must be admitted that for certain purposes formulæ such as those proposed by Spencer are eminently suitable. Especially when it is desired to eliminate seasonal fluctuations from monthly data some semi-empirical formula such as proposed by Macaulay * on page 59 of his admirable mongraph leaves nothing to be desired. As a matter of fact no single method of graduation is suitable for all purposes, and the investigator is compelled to make his own choice. However, of the many methods in use there are very few which have a sound theoretical basis. This also applies to the rather elaborate method of fitting a series of parabolas to the crude data, on which a vast amount of work has been done, a comprehensive account of which is given by Sasuly †.

Although in actual practice it may not be vastly superior to others the method proposed by Whittaker and amplified by Henderson is an exception in that it has been developed on strictly logical lines.

In order to describe this method we cannot do much better than to quote from 'The Smoothing of Time Series,' p. 89 :—"In smoothing data some departure from observed facts is, of course, necessary. In any particular case the question naturally arises as to how far it is desirable to depart from the observed facts in order to obtain smoothness. If departure from the observed facts be measured by means of the sum of the squares of the deviations of the data from the graduated curve, and if roughness or lack of smoothness be measured

* 'The Smoothing of Time Series,' by F. R. Macaulay. National Bureau of Economic Research, 1931.

† 'Trend Analysis of Statistics,' by Max Sasuly. The Brookings Institution, Washington, 1934.

by the sum of the squares of the third differences of the graduated curve, the problem is to decide at what stage it is undesirable to increase the sum of the squares of the deviations of the data from the graduated curve in order to decrease the sum of the squares of the third differences of the graduated curve itself.

"Such a problem might be formulated as follows: How shall k times the sum of the squares of the deviations of the data from the graduated curve plus the sum of the squares of the third differences of that graduated curve be made a minimum? The larger the value chosen for k the more importance would be attached to closeness of fit as compared with smoothness. As the value of k approached infinity the resulting graduated curve would approach the data points. As the value of k approached zero the resulting graduated curve would approach a second degree parabola fitted to the observations by the method of least squares."

Thus the Whittaker-Henderson method does indeed rest upon a logical basis, and it will now be our object to compare their method with our equilibrium method.

Let us investigate what result would be obtained by formulating the problem in exactly the same way as Whittaker does, only substituting *first differences* for *third differences*. Our problem then is: "How shall k times the squares of the deviations of the data from the graduated curve plus the squares of the first differences of the graduated curve be made a minimum"? In this case also as k approached infinity the graduated curve would approach the data points, but when k approached zero the graduated curve would become a straight line parallel to the X-axis, because all first differences would then be zero. The expression to be made a minimum is

$$k \sum_{1}^{n} (y_r - u_r)^2 + \sum_{1}^{n-1} (u_{r+1} - u_r)^2.$$

If this expression be differentiated with respect to all the u's in turn, and the results equated to zero, we derive equations of the type

$$u_r = \frac{k}{2+k} y_r + \frac{1}{2+k} (u_{r+1} + u_{r-1})$$
$$= \alpha(u_{r+1} + u_{r-1}) + (1 - 2\alpha) y_r,$$

where $$\alpha = \frac{1}{2+k}.$$

It will be recognized that this is exactly the same equation as eq. (7), and consequently leads to identical results. The whole theory might therefore just as well have been derived from the minimum principle. There are, however, two reasons why the adopted derivation was chosen. In the first place it has an added interest in that it gives a clearer insight into what the smoothing process actually involves. In the second place it points the way towards the construction of a device whereby the smoothing of time series might be done mechanically without any lengthy calculations. It is not intended to describe such a mechanical device, but theoretically, at least, it is possible to construct one.

Evidently there is a very close relationship between the Whittaker-Henderson and the equilibrium methods of smoothing. In the first case the ultimate smooth curve becomes a parabola, and in the second it becomes a straight line, and the question arises whether there is any added merit in the more elaborate method. In the case of a long series of data this is very much to be doubted, and there seems to be little reason why the ultimate smooth curve should not be allowed to degenerate into a straight line representing the arithmetic mean of the crude data. The amount of labour involved in the practical application of the Whittaker-Henderson method will most certainly deter many workers from making use of it. This is a most important consideration which cannot be overlooked. It would therefore seem that the proposed equilibrium method might with advantage be substituted for the Whittaker-Henderson method, especially in the analysis of fairly lengthy series of data.

In conclusion, I wish to express my thanks to Prof. J. T. Morrison of Stellenbosch for his valuable criticism of this paper.

Summary.

A method of smoothing a series of equidistant observations, such as annual rainfalls, is described. The method is based upon the solution of a simple problem in statics. Equations are developed whereby the points on the graduated curve can be expressed in terms of the crude data, and a couple of numerical examples serve as illustrations.

It is also shown that the smoothing process amounts to determining a curve such that a constant times the sum of the squares of the deviations of the crude data from the smoothed curve plus the sum of the squares of the first differences of successive points on the smoothed curve is a minimum. In reality the method is a simplification of that proposed by Whittaker some fifteen years ago and later elaborated by Henderson.

LXXXIII. *The Solution of Einstein's Orbital Equation.*

By S. M. Sulaiman, *Federal Court, India* *.

[Received July 12, 1938.]

1. In the General Theory of Relativity, the equation obtained by Einstein for the motion of an infinitesimal planet is

$$\frac{d^2u}{d\phi^2}+u=\frac{\mu}{h^2}+\frac{3\mu}{c^2}u^2.$$

Sir Arthur Eddington in his 'Relativity' (§40, p. 88) has deduced its approximate solution in the following way :—

Neglecting the small term $\frac{3\mu}{c^2}u^2$, the solution is

$$u=\frac{\mu}{h^2}\{1+e\cos(\phi-\varpi)\},$$

where e and ϖ are constants.

Substituting this first approximation in the small term of the differential equation, we get

$$\frac{d^2u}{d\phi^2}+u=\frac{\mu}{h^2}+\frac{3\mu^3}{c^2h^4}+\frac{6\mu^3}{c^2h^4}.e\cos(\phi-\varpi)$$
$$+\frac{3}{2}\frac{\mu^3e^2}{c^2h^4}\{1+\cos 2(\phi-\varpi)\}.$$

It is then suggested that " of the additional terms the only one which can produce an effect within the range of observation is the term in $\cos(\phi-\varpi)$; this is of the right period to produce a continually increasing effect by

* Communicated by the Author.

resonance." Neglecting $\frac{3\mu^3}{c^2h^4}\left(1+\frac{e^2}{2}\right)$ and the term containing cos $2(\phi-\varpi)$, the solution is obtained as

$$u=\frac{\mu}{h^2}\left\{1+e\cos(\phi-\varpi)+\frac{3\mu^2}{c^2h^2}e\phi\sin(\phi-\varpi)\right\}$$

$$=\frac{\mu}{h^2}\{1+e\cos(\phi-\epsilon-\varpi)\}$$

$$=\frac{\mu}{h^2}[1+e\cos\{(1-3k^2)\phi-\varpi\}],$$

where $$\epsilon=\frac{3\mu^2}{c^2h^2}\phi=3k^2\phi.$$

From this by integration the value of the advance of the perihelion for one revolution is obtained.

2. The reverse process of differentiation of course shows that

$$\frac{d^2u}{d\phi^2}+u=\frac{\mu}{h^2}[1+6k^2e\cos\{(1-3k^2)\phi-\varpi\}]$$

neglecting k^4, while

$$\frac{\mu}{h^2}+\frac{3\mu}{c^2}u^2=\frac{\mu}{h^2}[1+3k^2+6k^2e\cos\{(1-3k^2)\phi-\varpi\}$$
$$+3k^2e^2\cos^2\{(1-3k^2)\phi-\varpi\}],$$

the extra terms being of the same order. Hence the two are not equal.

3. Taking the solution as

$$u=\frac{\mu}{h^2}[1+e\cos\{(1-3k^2)\phi-\varpi\}],$$

this is obviously the solution of

$$\frac{d^2u}{d\{(1-3k^2)\phi-\varpi\}^2}+u=\frac{\mu}{h^2},$$

or $$\frac{d^2u}{d\phi^2}+(1-3k^2)^2u=\frac{\mu}{h^2}(1-3k^2)^2,$$

or $$\frac{d^2u}{d\phi^2}+u=\frac{\mu}{h^2}(1-6k^2)+6k^2u,$$

neglecting k^4.

This differential equation is quite different from Einstein's equation, as its last term contains u and not u^2, and its coefficient also is different.

4. It is submitted that the neglect of the term containing $\cos 2\ (\phi-\varpi)$ before solving the equation is not justified on the following grounds :—

(1) The neglected term is of the same order as the term retained and should therefore not be neglected, before solving the equation. Indeed, if we combine the three constants together and compare the terms containing $\cos(\phi-\varpi)$ and $\cos 2(\phi-\varpi)$ the latter may actually be larger in magnitude when $(\phi-\varpi)$ approaches $(n+\frac{1}{2})\pi$.

(2) As a matter of fact, the solution of the equation of motion when the force varies as the inverse nth power of the distance would be of the form

$$u=\frac{\mu}{h^2}[1+\Sigma\{e\cos(n\phi-\varpi)\}],$$

and terms would not be neglected on any ground of want of resonance.

(3) The effect of neglecting terms is that instead of retaining the full equivalent of $\frac{3\mu}{c^2}u^2$, only $\frac{6\mu^3}{c^2h^4}e\cos(\phi-\varpi)$ is retained, which equals $\frac{6\mu^2}{c^2h^2}\left(u-\frac{\mu}{h^2}\right)$ nearly. The substitution of the latter term for the former in the differential equation is not justifiable, as this alters the equation to be solved from

$$\frac{d^2u}{d\phi^2}+u=\frac{\mu}{h^2}+\frac{3\mu}{c^2}u^2$$

to

$$\frac{d^2u}{d\phi^2}+u=\frac{\mu}{h^2}\left(1-\frac{6\mu^2}{c^2h^2}\right)+\frac{6\mu^2}{c^2h^2}u.$$

Hence the supposed solution is of quite a different equation altogether.

5. The new differential equation neglecting smaller terms approximately leads to a new law of acceleration :

$$-h^2u^2\left\{\frac{d^2u}{d\phi^2}+u\right\}=-\mu\left(1-\frac{6\mu^2}{c^2h^2}\right)\frac{1}{r^2}-\frac{6\mu^2}{c^2}\cdot\frac{1}{r^3}.$$

(1) Although this law also gives the same value for the advance of the perihelion per revolution

$$-\int_0^{2\pi}\frac{6\mu^2}{c^2}\cdot\frac{1}{r^3}\cdot\frac{h}{e\mu}\cos\phi\frac{r^2d\phi}{h}=\frac{6\pi\mu^2}{c^2h^2}.$$

(2) The deflexion of a light particle past the sun is

$$=-\frac{1}{c^2\mathrm{R}}\int_{-\frac{\pi}{2}}^{\frac{\pi}{2}}\left[-\mu\left(1-\frac{6\mu^2}{c^2h^2}\right)\frac{1}{r^2}-\frac{6\mu^2}{c^2}\frac{1}{r^3}\right]r^2\cos\psi d\psi$$

(where $\mathrm{R}=r\cos\psi$)

$$=-\frac{\mu}{c^2\mathrm{R}}\left[2\left(1-\frac{6\mu^2}{c^2h^2}\right)+\frac{3\pi\mu}{c^2\mathrm{R}}\right],$$

which is almost the Newtonian value, and not Einstein's.

6. It was shown by me in 1934 that the correct law of gravitation as derived from

$$\frac{d^2u}{d\phi^2}+u=\frac{\mu}{h^2}+\frac{3\mu}{c^2}u^2$$

is $$-h^2u^2\left[\frac{d^2u}{d\phi^2}+u\right]=-\frac{\mu}{r^2}-\frac{3\mu h^2}{c^2}\cdot\frac{1}{r^4},$$

which gives the same value for the advance of perihelion, and an excess value for the deflexion of light in near agreement with the value obtained by Freundlich.

7. The approximate equivalent of the equation as given in paragraph 1 may be put simply as

$$\frac{d^2u}{d\phi^2}+u=\frac{\mu}{h^2}\left\{1+3k^2\left(1+\frac{e^2}{2}\right)+6k^2e\cos(\phi-\varpi)+\frac{3}{2}k^2e^2\cos 2(\phi-\varpi)\right\}.$$

Now the following particular solutions can be easily verified by differentiation :—

If $$\frac{d^2u}{d\phi^2}+u=\frac{\mu}{h^2}\left\{1+3k^2\left(1+\frac{e^2}{2}\right)\right\},$$

then $$u=\frac{\mu}{h^2}\left\{1+3k^2\left(1+\frac{e^2}{2}\right)\right\}.\{1+e\cos(\phi-\varpi)\}.$$

If $$\frac{d^2u}{d\phi^2}+u=\frac{\mu}{h^2}.6k^2e\cos(\phi-\varpi),$$

then $$u=\frac{\mu}{h^2}.3k^2e.(\phi-\varpi)\sin(\phi-\varpi).$$

If $$\frac{d^2u}{d\phi^2}+u=\frac{\mu}{h^2}\frac{3}{2}k^2e^2\cos 2(\phi-\varpi),$$

then $$u=-\frac{\mu}{h^2}\cdot\frac{1}{2}k^2e^2\cos 2(\phi-\varpi).$$

Hence the second approximate solution is

$$u=\frac{\mu}{h^2}\Big[\Big\{1+3k^2\Big(1+\frac{e^2}{2}\Big)\Big\}\times\{1+e\cos(\phi-\varpi)\}$$
$$+3k^2e(\phi-\varpi)\sin(\phi-\varpi)-\frac{1}{2}k^2e^2\cos 2(\phi-\varpi)\Big]$$
$$=\frac{\mu}{h^2}\Big[1+(3+2e^2)k^2+\Big\{1+3\Big(1+\frac{e^2}{2}\Big)k^2\Big\}e.\cos(\phi-\varpi)$$
$$+3k^2e(\phi-\varpi)\sin(\phi-\varpi)-k^2e^2\cos^2(\phi-\varpi)\Big],$$

where $k=\frac{\mu}{ch}$.

8. It may be pointed out that the real reason why the term containing $\cos^2(\phi-\varpi)$ does not in a complete revolution contribute towards the advance of the perihelion is not any "want of resonance" with $\cos(\phi-\varpi)$ over a *large* number of complete revolutions, but the circumstance that all terms like $\cos^{2n}(\phi-\varpi)$ must equally fail to do so in *each* revolution, as in the value of the advance in one revolution the integral $\int_0^{2\pi}\cos^{2n+1}(\phi-\varpi)d\phi$ would occur and therefore vanish, while terms containing $\cos^{2n+1}(\phi-\varpi)$ would not produce any such result.

LXXXIV. *Absolute Measurements of Radiometric Action in Gases.* *By* Dr. Ernst Fredlund, *Stockholm* *.

[Received September 26, 1938.]

THE fundamental investigations of Professor Martin Knudsen [1] [2] relevant to the properties of rarefied gases have provided a basic explanation for radiometric action in the particular case where the gases are strongly rarefied. Corresponding theoretical investigations at higher pressures have also been carried out, and in

* Communicated by Prof. H. Spencer Gregory.

conjunction with experimental data on the subject it is accepted that radiometric action in the higher pressure range is due to the streaming associated with mass motions of the gas, originating from the temperature differences set up. This condition of streaming along with the resulting radiometric action is regulated by the boundary conditions at the surface where the temperature differences exist.

According to Maxwell [3] and later Hettner [4] the velocity of slip u_2 associated with the tangential gas flow is related to the temperature gradient $d\mathrm{T}/dx_2$ in the manner given by the equation

$$u_2 - \gamma . du_2/dx_1 = \frac{3\eta}{4\rho \mathrm{T}} . d\mathrm{T}/dx_2,$$

where γ denotes the coefficient of slip, η the coefficient of viscosity, ρ the density of the gas, and x_1 the normal to the surface.

Although the study of radiometric action in gases at high pressure has been mainly confined to a theoretical aspect there is by no means a dearth of experimental evidence, and two investigations in this connexion are worthy of especial consideration, viz.: (1) The exhaustive study of Brüche and Littwin [5] in regard to the general character of the radiometric action and to the effect of varying molecular weight, and (2) the particularly beautiful work of Martin Knudsen [6] on the connexion between radiometric forces and the effect of accommodation.

The number of theoretical contributions to the subject is indeed legion, and amongst such investigations the present paper confines itself to the elegant theory of radriometic action propounded by Weber [7]; this has been done by the author for two reasons—firstly, because Weber's theory is more susceptible of application to the experiments described below than any other, and, secondly, because the author considers that it offers the most accurate theoretical study of radiometric action yet attempted.

Weber deals in particular with the Knudsen guard ring radiometer [2], but his results can also be applied to the case where a circular plate is disposed between two extended plane parallel surfaces maintained at different temperatures. The theory of Weber has been developed

from an experimentally modified form of the Maxwell-Hettner boundary equation [8]

$$u_2 - k_2\gamma \cdot \frac{du_2}{dx_1} = k_1 \cdot \frac{\eta}{\rho T} \cdot \frac{dT}{dx_2} \cdot \frac{1}{1+\lambda/D} \quad . \quad . \quad (1)$$

in conjunction with a procedure analogous to the manner in which calculations associated with thermomolecular pressure gradients in tubes have been treated. The resulting equation for the radiometer pressure may be written in the form

$$\frac{dp}{dT} = \frac{1}{2} \cdot \frac{p}{T} \cdot \frac{1}{\alpha\left(\frac{D}{\lambda_1}\right)^2 \cdot p^2 + \beta\left(\frac{D}{\lambda_1}\right) \cdot p + \mu} \quad . \quad . \quad . \quad (2)$$

In these equations D denotes the distance between the movable disk and the wall, k_1 and k_2 constants approximately equal to 4/3, dp the radiometer pressure corresponding to a temperature difference dT, p the gas pressure, T the absolute temperature, and λ_1 the mean free path at a pressure of one dyne per sq. cm. and at a temperature T. The constants α and β are given by

$$\alpha = \pi/24, \quad \beta = 3\pi/8,$$

and μ is approximately equal to 2·70.

Weber's formula shows that the radiometric effect at low pressures increases with the pressure, but for complete coincidence with the Knudsen relation in this range the factor $(1+\lambda/D)$ in (1) must be replaced by a rather more complicated expression. The formula further shows that the radiometer pressure at high pressure decreases as the gas pressure increases, and also a maximum effect $(dp/dT)_M$ is attained at a pressure p_M, where

$$p_M = \frac{\lambda_1}{D} \cdot \sqrt{\frac{\mu}{\alpha}}; \quad \left(\frac{dp}{dT}\right)_M = \frac{1}{2T} \cdot \frac{\lambda_1}{D} \cdot \frac{1}{2\sqrt{\alpha\mu}+1} \quad (3)$$

and also

$$\lambda_M = D\sqrt{\frac{\alpha}{\mu}} \quad . \quad . \quad . \quad . \quad . \quad . \quad . \quad (4)$$

Formula (2) can be written in the form

$$dp = f\left(\frac{D}{\lambda}\right),$$

where f denotes a function of D/λ. Writing $p.D/\lambda_1=\chi$ we have

$$dp=R=f(x)=\frac{\Delta T}{2T}\cdot\frac{D}{\lambda_1\mu}\cdot\frac{\chi}{\frac{\alpha}{\mu}\chi^2+\frac{\beta}{\mu}\chi+1},$$

where $\Delta T=dT$ is a quantity small in comparison with T.

It is thus possible by means of a simple transformation to refer all gases with different values of λ_1 and for different values of D to one and the same radiometer pressure curve. This has been shown by Weber in an elegant manner, and the reason that his transformation has not

Fig. 1.

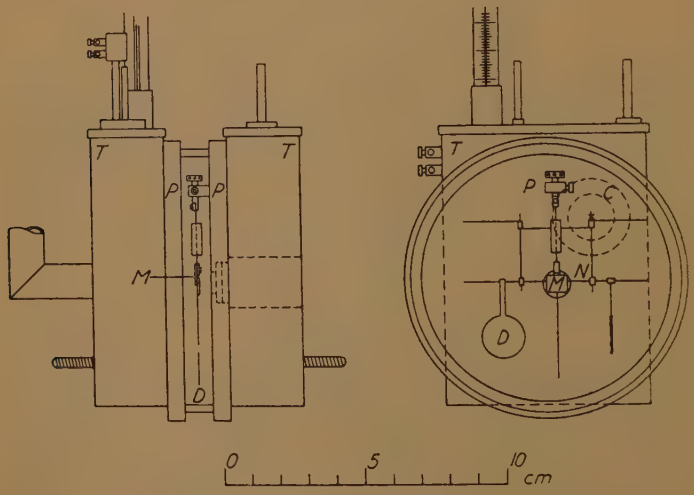

been used in the present instance is explained by reference to the experimental results detailed below.

The construction of the radiometer [9] is represented diagrammatically in fig. 1. Two circular copper plates P (diameter 100 mm.) form the boundary surfaces of the thermostats T, which are maintained during the investigation at the temperatures of melting ice and 20° C. respectively. The plates P are fixed at a distance apart of 10 mm. by means of a glass ring cemented to the plates to form a gas-tight joint.

A torsion balance carrying the circular disk D, the mirror M, and the magnetic needle N is suspended between the plates, and is designed and assembled so as to ensure

almost complete insensitivity to mechanical vibrations. Two magnetic coils C are arranged so as to occupy a position external to the plates P and within the thermostats T. The common axis of the coils passes through the upper pole of the needle N, and the passage of an electric current through the coils makes it possible to balance the radiometric forces on the disk and maintain its position midway between the plates. From a previous calibration of the phosphor-bronze suspension strip, using the method of oscillations, it was found that a compensating current of 1 m.a. through the coils corresponded to a force of $1{\cdot}763 \times 10^{-2}$ dynes acting on the disk. The distance between the plates P is 10 mm., the thickness of the disk 0·30 mm., and the magnitude D in the Weber formula 0·485 cm.

A vapour-trap immersed in liquid air is connected on one side to the radiometer, and on the other to a McLeod gauge, a gas pipette system, and the pumping arrangement. The trap is of the normal type, and consists of two concentric cylindrical tubes. It is a well known phenomenon that in using such traps the existence of a thermomolecular temperature gradient causes a pressure difference to arise between the two sides of the trap, and the author has shown [10] that such differences can be eliminated by proper design of the trap. The dimensions should be such that the difference between the inner radius of the outer tube and the outer radius of the inner tube must be equal to the inner radius of the inner tube.

Measurements of the radiometric action are carried out as follows:—The bulb of the gas pipette system is filled with the desired gas to a suitable pressure, and commencing with a known fixed low pressure the pressure in the radiometer is increased by increments (usually a total number of 20) every third minute, and for each such increment observations are made of the pressure, the compensating current, and the temperatures of the thermostats.

For slight variations of the thermostatic temperatures above or below 0·00° C. and 20·00° C. the values of the compensating current may be corrected from the rule that the radiometric action is proportional to the temperature difference between the fixed plates.

Very little experimental data in respect of investigations under well-defined conditions are available, and for this

reason measurements of radiometric forces in regard to hydrogen nitrogen, and argon are discussed in great detail, and a less exhaustive study made in the case of oxygen and air owing to the similarity of the results found in respect of nitrogen.

In Tables I., II., and III. the radiometric forces R calculated in terms of the compensating current mA are tabulated along with the corresponding values of the gas pressure p.

In fig. 2 the results have been plotted on a double logarithmic scale partly because of the question of covering

TABLE I.

Nitrogen.		Argon.		Hydrogen.	
p.	R.	p.	R.	p.	R.
0·000	0·000	0·000	0·000	0·000	0·000
0·567	1·080	0·604	1·150	0·874	1·245
1·112	2·040	1·180	2·090	1·669	2·290
1·643	2·950	1·725	3·155	2·506	3·315
2·140	3·710	1·960	3·500	3·350	4·400
2·186	3·740	2·264	4·070	3·380	4·460
2·732	4·630	2·830	4·990	4·19	5·440
3·274	5·425	3·372	5·860	4·99	6·465
3·814	6·210	3·934	6·645	5·86	7·450
4·23	6·910	4·48	7·470	6·69	8·390
4·90	7·610	5·02	8·235	7·51	9·310
5·44	8·265	5·57	8·985	8·34	10·235
5·98	8·960	6·11	9·730	9·13	11·200
6·52	9·565	6·66	10·365	9·90	12·040
7·05	10·140	7·21	11·040	10·66	12·855
7·60	10·690	7·75	11·605	11·45	13·640
8·12	11·235	8·30	12·320		

an exceptionally large range of values of R and p and partly to do justice to the relative accuracy of the measurements.

At the same time the choice of such a scale permits of a close examination of the results in the neighbourhood of the limits of the high and low pressure ranges.

At low pressure R is found to vary directly with p, fig. 2, as found by Knudsen, but for different gases the (R, p) curves in this region are not found to coincide, a result which brings out the influence of the effect of accommodation on the radiometric forces in this pressure range [9].

At high pressure R is found to decrease inversely as the square of the pressure, a result which is substantiated by

TABLE II.

Nitrogen.		Argon.		Hydrogen.	
p.	R.	*p.*	R.	*p.*	R.
0·00	0·00	0·00	0·00	0·00	0·00
2·73	4·50	3·26	5·74	4·16	5·52
5·40	8·15	6·42	10·30	8·42	10·52
8·05	11·08	8·30	12·36	12·17	14·46
8·16	11·24	9·63	13·83	12·60	14·96
10·69	13·50	12·67	16·53	16·61	18·92
13·27	15·42	16·00	18·64	20·78	22·48
14·52	16·80	19·24	20·13	25·00	25·54
18·36	17·89	22·44	21·12	29·88	28·36
21·00	18·67	25·66	21·76	32·74	30·82
23·52	19·27	28·82	22·34	36·72	32·74
26·04	19·62	32·06	22·60	40·8	34·64
28·54	19·80	35·26	22·62	48·6	37·62
31·14	19·82	38·40	22·56	56·5	39·42
33·66	19·66	41·6	22·45	64·4	40·94
36·20	19·18	44·9	22·16	72·2	41·88
38·76	18·83	48·1	21·82	80·2	42·28
43·8	17·94	..	..	99·7	42·72
48·9	17·26	..	..	119·2	41·72
54·0	16·62				
59·1	16·08				
64·1	15·23				

TABLE III.

Hydrogen.		Argon.		Nitrogen.	
p.	R.	*p.*	R.	*p.*	R.
0·384	0·61	0·265	0·47	0·358	0·59
35·50	31·52	13·03	16·54	14·74	16·18
69·6	40·68	25·64	21·87	29·44	19·73
139·4	39·75	38·72	22·59	43·45	19·35
173·0	36·25	51·3	21·66	58·95	17·56
206·2	32·71	64·0	19·94	72·10	15·67
238·8	29·51	77·2	18·10	86·8	13·75
271·4	26·34	89·1	16·35	100·5	12·10
298·4	24·07	101·8	14·66	114·5	10·67
335·8	21·73	114·5	13·15	129·0	9·45
364·6	19·88	126·8	11·84	143·6	8·34
428·0	15·22	151·7	9·65	172·0	6·67
492·0	13·12	176·2	8·08	199·7	5·40
553·0	12·22	203·6	6·66	226·6	4·47
641·0	9·29	226·0	5·68	254·8	3·76
799·0	6·99	250·8	4·87	283·4	3·20
946·0	5·21	314·4	3·48	353·6	2·24
1238·0	3·40	372·0	2·58	422·0	1·65
1527·0	2·56	492·0	1·82	561·0	1·14
1858·0	1·50	613·0	1·07	7720·0	0·00
18620·0	0·00	6720·0	0·00		

reference to fig. 3, in which R is plotted as a function of $1/p$. In this a system of curves of parabolic form is obtained in place of the system of straight lines which would have been obtained if the radiometer action in this range had varied inversely as the pressure p. These results contradict the theories of Weber [7] and others, and the same lack of agreement occurs between the present measurements and those obtained by Brüche and Littwin [5]. On the other hand, the results are in agreement with those carried out by Rasmussen [11] on the relation between the radiometer pressure, the dimensions of the apparatus, and the effect

Fig. 2.

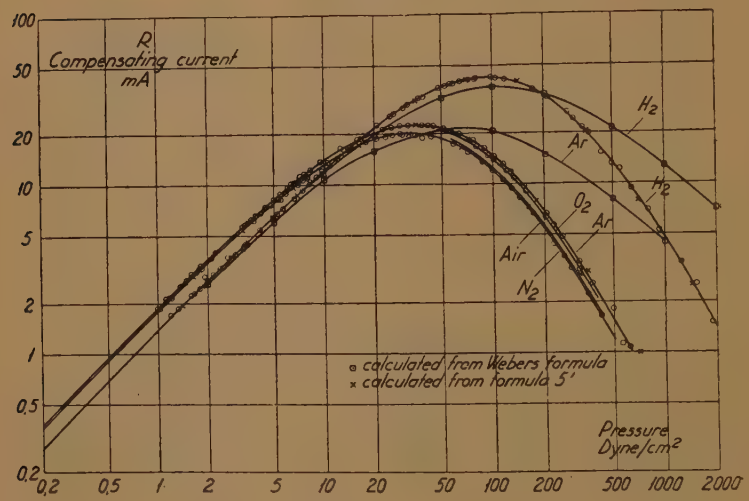

of accommodation. The reason for such discrepancy will not be discussed in the present paper, it can only be explained by recourse to further investigation.

One point of particular interest on the curves is the point at which the radiometric action is a maximum. The magnitude R_M and the position p_M of such maxima obtained from the present measurements are tabulated in Table IV. along with corresponding data for λ_1 the mean free path at a temperature 283·1° C., and also the values of $\frac{D}{\lambda_M}$ at a pressure p_M.

On examining the values given in Table IV. we find in the first place that for different gases both R_M and p_M

increase with the mean free path. With good approximation R_M/λ_1 can be said to be a constant. This coincides in the main with both Brüche and Littwin's experiments and the theoretical treatment of Weber (*cf.* formulas (3)).

Certain deviations arise, however, in particular as regards λ_M. While Brüche and Littwin found with good approximation that λ_M is constant for different gases at one and the same plate distance D, and while $D/\lambda_M = 4{\cdot}54$ according to Weber[7] (a result which closely agrees with

Fig. 3.

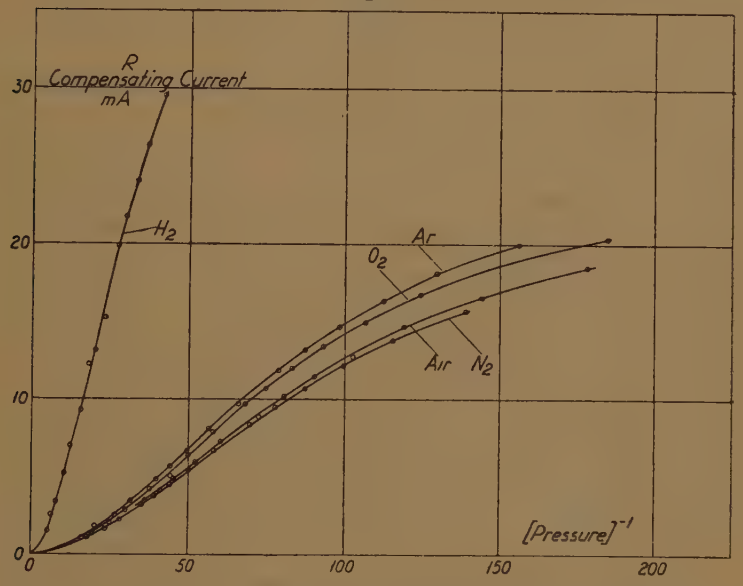

that obtained by Brüche and Littwin[5]), it is here found that λ_M for Ar, N_2, air, and O_2 is almost constant, while λ_M for H_2 is considerably lower, and also that $D/\lambda_M = 2{\cdot}51$ for the first four gases, while for H_2, $D/\lambda_M = 4{\cdot}06$. In consideration of, *inter alia*, Knudsen's investigation[6] it should not be out of place to connect this circumstance with the accommodation coefficient. We shall not go further into this matter here, but shall only establish that hydrogen where the influence of the accommodation coefficient is most marked shows the greatest deviation from the other gases within both the low and high pressure ranges.

In addition Table IV. shows R_M calculated in dynes and also R_M in mA units calculated from Weber's formula (3), starting from the fact that the surface of the movable vane is 1·80 cm.², and that 1 mA unit is equivalent to $1{\cdot}673.10^{-2}$ dynes. As one can observe, there exists in certain cases a very close agreement between Weber's theoretical value and the one experimentally determined here. In a similar way, beside the experimentally established quantity p_M, the table also shows p_M calculated from Weber's expression (3). The agreement here in regard to hydrogen is palpably good, but is satisfactory even with

TABLE IV.

Gas.	H_2.	Ar.	N_2.	Air.	O_2.	
Sensitiveness ..	1·400	1·880	1·883	1·883	1·840	$\frac{\text{mA}}{\text{dyne cm.}^{-2}}$
R_M(exper.) ...	42·64	22·67	19·83	20·32	21·78	mA
R_M(exper.) ...	0·7135	0·3786	0·3318	0·3396	0·3640	dyne
R_M (theor.)....	38·30	21·80	20·51	20·84	22·17	mA
P_M(exper.)	96·7	34·40	31·00	32·60	35·10	dyne cm.$^{-2}$
P_M(theor.)	108·0	61·53	57·87	58·82	62·55	dyne cm.$^{-2}$
λ_1	11·54	6·57	6·18	6·28	6·68	cm.
λ_M.....	0·1194	0·1912	0·1992	0·1926	0·1903	cm.
$\frac{R_M}{\lambda_M}$	3·70	3·45	3·21	3·24	3·25	$\frac{\text{mA}}{\text{cm.}}$
$\frac{D}{\lambda_M}$	4·06	2·54	2·43	2·52	2·55	

The instrumental constants used in the table are :—

1 mA = $1{\cdot}673.10^{-2}$ dynes.
Area of the disk 1·80 cm.².
Distance disk-wall 0·485 cm.

Further λ_1 has been calculated from Landolt-Börnstein, v. ed., 1923, p. 119. λ is reduced to 283·1° K. on the basis of Chapman's formula

$$\eta = \eta_0 \left(\frac{T}{273}\right)^n,$$

in which the exponent n has also been taken from Landolt-Börnstein, v. ed., p. 178.

reference to the other gases taken in order of magnitude. In this case, however, there is a systematic divergence between experiment and theory.

Even though the agreement between the experimental values given here and from Weber's theory is in many

respects far from complete, it must nevertheless be emphasized that these experiments prove Weber's investigation to be one which has been the most successful in a theoretical explanation of radiometric effect. The striking coincidence between Weber's theoretical values on the size of the maximum with those obtained here should be particularly noticed. A similar coincidence could not be obtained on the basis of any of the other radiometric theories.

A closer study of the curves given in fig. 2 shows that if they are moved to lie one over the other so that their maximum points coincide they will cover each other within the whole experimentally investigated pressure range 0 to about 10000 dynes/cm.^{2}. It can therefore be experimentally established that for the radiometer here dealt with, the radiometric force, independent of the nature of the gas, has a certain fixed course. In other words, it is, by means of a suitable transformation, possible to obtain from the radiometric curve established for a given gas the radiometric curve for any other gas.

As shown above, a similar conclusion follows directly from Weber's theory, but, in spite of this agreement, it is impossible to regard Weber's radiometric formula (2) as an adequate expression for the experiments discussed in this paper. This is illustrated by the plotted curves in fig. 2, which show the course of the radiometric effect for both hydrogen and argon according to formula (2). Too much importance must not be attached to the lack of agreement between theory and practice at low pressures, since in this range Weber's theory offers only an approximate treatment of a more complicated effect, but, on the other hand, in the pressure range beyond the maximum Weber's theory attempts to give a more rigid explanation of the phenomena. Within this range the divergence between theory and experiment becomes more and more marked, a circumstance which is founded on the fact that the reduction of the effect demanded by the theory in inverse proportion to p corresponds in the experiments to a decrease inversely proportional to p^2. It is therefore possible to attempt to represent the results of the experiments by the following formula:

$$R = \frac{ap}{1+bp+cp^2+dp^3}, \quad . \quad . \quad . \quad . \quad (5)$$

which is built up in the same way as the formula used by Rasmussen[11]. On examination this formula has been found to satisfy the present results with good approximation within the entire experimental range of pressures considered. During the tests the procedure of re-writing formula (5) to

$$R=\frac{a}{b}\cdot\frac{x}{1+x+Ax^2+Bx^3} \quad . \quad . \quad . \quad . \quad (5^1)$$

was adopted, where $p=x.b$, and the constants b, A, and B were determined from the data of the maximum points, combined with the measured values for R when $p=5p_M$. The values of the constants b, A, and B arrived at by this calculation have been collected in Table V. In addition,

TABLE V.

Gas.	H_2.	N_2.	Ar.	Air.	O_2.
$b.10^2$	1·427	3·065	2·798	3·252	3·154
$\lambda_1.b$	0·164	0·189	0·184	0·204	0·210
$b_R.10^2$.....	0·999	3·12	2·81	2·97	2·70
A	0·2957	0·9206	0·8420	0·6964	0·6475
B	0·08311	0·09860	0·1232	0·1032	0·07619

for the gases H_2, Ar, and N_2, values of R as a function of p have been calculated with the help of formula (5^1) and the constants in Table V., and then plotted in fig. 2. It proves that the agreement for all gases referred to within the entire pressure range is very good excepting for the very highest pressures. The table, in addition, gives the quantity $b.\lambda_1$, and it appears that $b.\lambda_1$, is by approximation constant and equal on an average to 0·190. Since the plate distance =0·485 cm., it follows from formula (2) that $\beta/\mu=0·392$, which approaches very closely to the value 0·436 required by Weber. Finally, the table also gives the quantity b_R, which is the quantity comparable to our b, included in Rasmussen's[11] formula, and which has been calculated from the expression $b_R=0·9660/p_M$. There is good agreement between b and b_R for the gases Ar, N_2, air, and O_2. According to Rasmussen the constants A and B are equal respectively to·1 and 1/27 for all gases.

It must now be observed, however, that the values given in Table V. for B, and in particular A, vary with the

nature of the gas. This does not agree with the result just arrived at, namely, that the curves in the double logarithmic diagram may be made to coincide through moving the one up parallel to the other, since this result requires A and B to be identical for all gases if formula (5^1) is to fulfil these obligations.

We are thus forced to form the conclusion that formula (5^1) represents in a very approximate manner only the results of actual experiments on radiometer action; at the same time it is possible, by making use of the constants in Table V., to represent the experimental results in a form similar to that given by equation (5^1).

The measurements of the radiometric effect referred to above have the advantage that it has been found possible to establish the relation between radiometric force, pressure and temperature with great accuracy. It has further been found possible, during the whole series of measurements, to keep the movable vane in the same fixed position relative to the walls of the radiometer. On the other hand, it was not possible, for experimental reasons, to construct the measuring system (the disk) in the desired simple way, *i. e.*, so that the system exposed to the radiometric force is made simply in the form of one circular disk. We hope in the very near future to be able to return to these measurements with a still more improved form of radiometer, since we are convinced that only continued investigation under well-defined conditions can lead to definite conclusions.

Summary.

Absolute measurements of the radiometric effect have been carried out with a series of different gases. At low pressure the well-known increase of the radiometric effect in proportion to the pressure of the gas was obtained, while at high pressure it appeared that the effect diminished in inverse proportion to the square of the gas pressure. If the radiometric effect is plotted as a function of the gas pressure in a double logarithmic diagram curves are obtained for the different gases which, by moving them up parallel to each other, can be made to coincide within the entire pressure range. A reduced radiometric curve therefore exists from which the curve for any gas can be obtained by means of a suitable transformation. The size and position of the maximum can

with approximation be established according to Weber's theory of radiometric action.

References.

(1) M. Knudsen, *Ann. d. Phys.* xxviii. p. 75 (1909).
(2) M. Knudsen, *Ann. d. Phys.* xxxii. p. 809 (1910).
(3) J. Clerk-Maxwell, Phil. Trans. clxx. 1, p. 231 (1879).
(4) G. Hettner, *Zeits. f. Phys.* xxx. p. 258 (1924).
(5) E. Brüche and W. Littwin, *Zeits. f. Phys.* lxvii. p. 333 (1931).
(6) M. Knudsen, *Ann. d. Phys.* vi. p. 129 (1930).
(7) Sophus Weber, *Medd. Copenhagen* xiv. p. 13 (1937).
(8) Sophus Weber, W. H. Keesom, and G. Schmidt, *Comm. Kamerlingh Onnes Lab.* Leiden, no. 246 *a*, p. 9, and Sophus Weber, *ib.* no. 246 *b*, p. 7.
(9) E. Fredlund, *Ann. d. Phys.* xiv. p. 617 (1932).
(10) E. Fredlund, *Arkiv. Mat. Astr. o. Fys.* xxvi. A, no. 6, p. 1 (1937).
(11) R. E. H. Rasmussen, *Ann. d. Phys.* xxii. p. 643 (1935).

LXXXV. *Arcs of Various Metals in Capillary Tubes.* *By* Dr. V. Voss, *University of Pretoria* *.

[Received September 3, 1938.]

[Plate X.]

UNDOUBTEDLY the easiest type of mercury arc to construct is one in which the arc is run in a capillary tube †. It seemed likely that arcs of other metals might also be run conveniently in capillary tubes. In this paper an account is given of how this was done, very simply, with seven different metals. The pressure in these arcs was equal to or greater than atmospheric pressure.

After experimenting with various forms of arc container, the one described below was finally adopted. The metal to be used was first cast in a thin rod by introducing bits of it into a pyrex tube of internal diameter about 7 mm., to one end of which had been sealed a much narrower pyrex tube, closed at the end. The pyrex tube was exhausted and heated, and when the metal was molten it was shaken down into the thin tube. The glass was then cracked away from the metal.

* Communicated by the Author.

† See, *e. g.*, Voss, Phil. Mag. xxiv. p. 312 (Aug. 1937); also xx. p. 179 (July 1935).

A piece of silica tubing about 8 cm. long, internal diameter about 0·8 mm., external diameter about 7 mm., was now sealed on to a wider silica tube, and an elongated bulb *a* was blown at the end, as shown in the figure. Two small bulbs were blown at *c* and *d*. A piece of molybdenum wire was pushed down the tube, so that one end projected well into the bulb *a* while the other end reached half-way into the bulb *c*. A short length of the metal casting was introduced into the wider silica tube, which was then connected by rubber tubing to the pump and thoroughly exhausted. The tube was now collapsed lightly on to the molybdenum wire at *b*. This will not be an airtight seal but molten metal will not be able to pass it. If the tube is heated too strongly at *b* with the oxy-gas flame, little fractures appear in the tubing when it cools. The capillary tube is next heated strongly with a bunsen flame and the metal is melted, and with

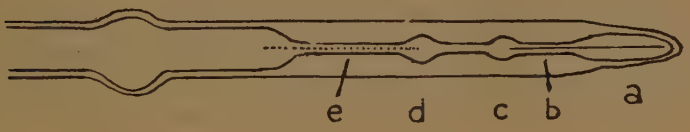

a sharp flick shaken down into the bulbs *c* and *d* and the capillary connecting them. If too much is introduced it should be distilled away again. The tube is taken off the pump and the second molybdenum wire electrode (shown dotted) introduced. The metal in *d* can be melted and the wire pushed in till it enters the bulb. The tube is again exhausted, and collapsed lightly on to the wire at *e*, a couple of cm. from *d*. The tube is then cracked off at file scratches to the left of *e* and to the right of *b*. The arc can be conveniently mounted, by means of brass strips, in a vertical position about an inch away from a board (hard asbestos sheet was used) fixed to a wooden base (see Pl. X. (*l*)). Copper wires, fused on to the molybdenum electrodes, lead to terminals on the board. Originally the arcs were started by first heating gently with a burner till the metal melted and then heating the capillary between *c* and *d* intensely till the metal vaporised. But unless the preliminary heating was done very carefully the expanding metal was liable to crack the tube.

Furthermore, in the case of metals having a high boiling-point (*e. g.* thallium, B.P. 1280° C.) they had to be vaporized with an oxy-gas flame, and this soon pitted away the tube and frosted its surface to such an extent that it could no longer be used. The use of a heating-coil is much better as the metal can be heated perfectly uniformly till it melts. The arc-holder is held in one hand and tapped down against a light hammer held in the other. This splits the thread and the arc strikes. If the arc does not strike readily it is advisable to switch off the heating current, once the metal is molten, and then to tap the arc-holder while the metal cools. The arc gap may wander along the capillary, but when it reaches a bulb it is anchored by the widening of the capillary there. Thus if the molybdenum wires do not project too far into the bulbs, neither of them can be uncovered by the arc gap. If this were to happen, the molybdenum arc lines would appear in the spectrum.

When the arc is running the molten arc-metal forms an effective seal at *b* (see figure), and if the wattage is increased the temperature and pressure may rise unduly and the capillary may swell. With care, however, the wattage may be varied within certain limits, especially in the case of metals whose boiling-point is well below the softening-point of quartz. As the external resistance is decreased the wattage and the resistance of the arc increase. But of course this is not due solely to a rise in temperature and pressure, but is caused partly by an increase in the length of the gap. When the arc is to be stopped the external resistance in the circuit is increased so that the arc gap gradually closes, the atmosphere forcing the molten metal away from *b* into the bulb *c*. While this is being done the heating current should again be switched on so as to ensure that the metal, away from the arc gap, remains molten.

No attempt is made here at a detailed analysis of the spectra, but some of the obvious features are recorded. In each spectrum some of the lines are reversed. As the temperature and pressure rise the continuous background is enhanced, also the reversals become more pronounced, and new reversals may appear. Some lines which are sharp at lower temperatures broaden out and become more and more diffuse as the temperature rises. For example, the pair of lines λ 3076 and 3072 from the zinc

arc both get more diffuse, and the former relatively weaker as the wattage is raised. Again, when a mercury arc-tube is used the group λ 2652, 2654, 2655 diffuses into one vague blur as the wattage is increased from 5 to 28.

For each arc a list of the reversed lines is given. But these lists are probably not complete. Only those reversals about which there can be no doubt are given. Larger dispersion would probably disclose more reversals among close groups of lines. Further, panchromatic plates were used, which were not very sensitive to the ultra-violet. When Kodak film was used in a smaller spectrograph, it revealed more reversals further out in the ultra-violet.

A few wave-lengths have been marked at intervals along the spectra, for identification purposes.

A 212 volt d.c. generator was used—c denotes the current in amps. before the arc was struck, i the current through the arc, r the resistance in ohms of the arc, w the watts consumed in the arc. The melting-points and boiling-points (at 760 mm. pressure) of the metals are taken from Kaye and Laby's "Physical and Chemical Constants." The atmospheric pressure in Pretoria is about 650 mm.

1. *Cadmium*: M.P. 321° C., B.P. 778° C. (see Pl. X. (*a*)).

Diameter of capillary about 1 mm., $c=1{\cdot}25$, $i=1{\cdot}05$, $r=32$, $w=35$. Spectra (*b*) and (*c*) were taken with a smaller spectrograph, using Kodak film. In (*b*) the wattage was higher than in (*c*), and (*b*) shows the reversal of λ 2288 appreciably broader than it is in (*c*).

Reversed lines: 3404, 3261, 2288 A.

2. *Zinc*: M.P. 418° C., B.P. 918° C. Spectrum (*d*).

Diameter of capillary 0·85 mm., $c=1{\cdot}05$, $i=0{\cdot}74$ $r=85$, $w=47$.

Reversed lines: 3345, 3303, 3282, 2801, 2771. With the exception of 3282 each of the above is really a close group of lines, but each group is diffused into one broad line showing a distinct reversal. The reversals cannot be seen when the arc is run at 25 watts, but are just evident at 47 watts and very distinct at 54 watts. At a low wattage the arc is purple, but gets "whiter" as the wattage is increased. It shows striking colour

effects, *e. g.* lemon-coloured paper appears rosy-red in the light of the arc, and green paper appears blue.

3. *Thallium* : M.P. 301° C., B.P. 1280° C. Spectra (*e*) and (*f*).

Spectrum (*e*) taken with tube of diameter 0·93 mm. $c=1·9$, $i=1·8$, $r=6$, $w=19$.

Spectrum (*f*) taken with a different arc. The capillary used had a diameter of 0·8 mm., but before filling with thallium the tubing between bulbs *c* and *d* (see figure) was drawn down to about half its diameter. Here $c=1·2$, $i=1·0$, $r=35$, $w=35$. Spectrum (*f*) shows how the continuous background, and the distinctness of the reversals, increase with the wattage. The thallium arc is very brilliant and of a greenish colour. At a low wattage the green line is very conspicuous in a pocket spectroscope, but at a high wattage it is quite black against an almost continuous background.

Reversed lines : 5350, 3776, 3529, 3519, 3230, 2922, 2918, 2826, 2768, 2709, 2609, 2580, 2380.

Thus all the lines that are reversed originate from the normal level, or from the adjacent level to which electrons can be raised by thermal agitations.

4. *Tellurium* : M.P. 450° C., B.P. 1390° C. Spectrum (*g*).

Diameter of capillary 0·85 mm., $c=0·46$, $i=0·25$, $r=387$, $w=24$.

This arc emits a bright white light. The visible spectrum is continuous but lines show up in the ultra-violet. The wattage could only be varied very slightly. With a current of 0·25 amp. the arc ran continuously, but if the current were made slightly less or slightly greater the arc would not burn.

Reversed lines : 2383 and 2386.

This is a much simpler form of tellurium arc than the one described by Rompe * and used subsequently by Marden, Beese, and Meister †.

5. *Bismuth* : M.P. 269° C., B.P. 1420° C. Spectrum (*h*).

Diameter of capillary 0·8 mm., $c=1·15$, $i=1·0$, $r=28$, $w=28$.

* Rompe, *Z. fur Phys.* ci. p. 214 (1936).

† Marden, Beese, and Meister, J. Franklin Inst. ccxxv. p. 45 (1938).

Some care has to be exercised in filling this arc, and always in using it, as bismuth expands on solidifying. Thus, after the arc is stopped the heating current is not shut off abruptly but is decreased very gradually until the bismuth has solidified.

Reversed lines: 3068, 3025, 2993, 2989, 2938, 2898, 2628, 2401.

6. *Antimony*: M.P. 630° C., B.P. 1440° C. Spectrum (*i*).

Diameter of capillary 0·78 mm., $c=1·8$, $i=1·45$, $r=28$, $w=59$.

Reversals: 2598, 2529, 2312.

7. *Lead*: M.P. 327° C., B.P. 1525° C. Spectrum (*j*).

The capillary was drawn down to a diameter of approximately 0·4 mm., $c=0·91$, $i=0·5$, $r=191$, $w=48$.

This, as might be expected, was the least satisfactory of the arcs, as the boiling-point of lead is too near the softening-point of silica. If great care is exercised an arc-tube will last for a long time. When the arc has been started the external resistance in the circuit must be increased to the point where the arc will only just continue to burn. If the external resistance is too small the temperature will go up above the softening-point of silica and the tube will be spoiled. Reversed lines: 4058, 3683, 3640, 3573, 2873, 2833, 2823, 2802, 2663, 2614, 2577, 2476, 2446, 2444, 2412, 2402, 2394.

The colour of the last three arcs was very similar and might be described as a pinkish-golden.

This capillary tube method of constructing arcs, while very simple in the case of certain metals, has obvious limitations. Thus magnesium cannot be used as it attacks silica at high temperatures. The same applies to sodium and potassium. It will probably also apply to lithium, cæsium and rubidium, but these were not obtainable here. Something might, however, be done with alloys containing traces of these metals. Furthermore, the method cannot be used in the case of metals whose boiling-point is greater than the softening-point of silica.

The complete reversal of some of the lines seems surprising. In spectrum (*f*) for instance, the tube had a diameter of approximately 0·4 mm. Even if the cross-

section of the arc itself were very small it would be surrounded by a sheath of unexcited vapour less than 0·2 mm. thick. And yet this produced complete reversal of the resonance lines. Two photographs (spectrum (k)) were taken of a mercury arc in a tube of diameter 1 mm. In the upper one a magnetic field deflected the arc towards the slit of the spectroscope, thus decreasing the thickness of the absorbing sheath of vapour, and in the lower one the field was reversed and deflected the arc away from the slit. It can be seen how much broader the reversal of the 2537 line is in the lower photograph.

LXXXVI. *The Large Deflexions of a Thin Circular Ring.* *By* R. A. Fairthorne, *B.Sc.**

[Received September 5, 1938.]

DURING an investigation of the approximate engineering theory of the deflexion of rings it was found necessary to calculate some exact solutions for comparison. Since no studies of the complete circular elastica seem to have been published the results are given here.

The ring is assumed to be thin and uniform, and of stiffness B. In the unstressed state it is a complete circle of radius a. It is supposed that deformation is inextensional—that is, the length of the perimeter is not altered by the loads, deformation being due to flexure alone. Under these conditions the deflexions have been calculated for certain symmetrical applications of load.

1. *Pure Bending. Four Equal Moments of Alternate Sign, equally spaced round the Circumference.*

There is no tension or compression in any part of the ring. Therefore the bending moment, and thus the curvature, is constant along the arc between consecutive loads.

Let ρ_1 = radius of curvature of quadrant whose curvature is increased.

2α = angle subtended by this quadrant after deformation.

* Communicated by the Author.

ρ_2=radius of curvature of quadrant whose curvature is decreased.
M=applied moment at junction of quadrants.
a=original radius of ring.
B=stiffness of ring.

From elastic theory

$$\left(\frac{1}{\rho_1}-\frac{1}{a}\right)-\left(\frac{1}{\rho_2}-\frac{1}{a}\right)=\frac{M}{B}. \quad . \quad . \quad . \quad (1)$$

Since deformation is inextensional,

$$\left.\begin{aligned}\rho_1\alpha&=\frac{\pi a}{4},\\ \rho_2\left(\frac{\pi}{2}-\alpha\right)&=\frac{\pi a}{4},\end{aligned}\right\} \quad . \quad . \quad . \quad . \quad . \quad (2)$$

whence

$$\left.\begin{aligned}\alpha&=\frac{\pi}{8}\left(2+\frac{Ma}{B}\right),\\ \rho_1&=2a\Big/\left(2+\frac{Ma}{B}\right),\\ \rho_2&=2a\Big/\left(2-\frac{Ma}{B}\right).\end{aligned}\right\} \quad . \quad . \quad . \quad . \quad (3)$$

The outward deflexion along the major axis of symmetry is therefore

$$\begin{aligned}u&=\rho_1(1-\cos\alpha)+\rho_2\cos\alpha-a\\ &=am(m+4\cos\alpha-2)/(4-m^2),\end{aligned}$$

where $$m=\frac{Ma}{B}, \qquad \alpha=\frac{\pi}{8}\left(2+\frac{Ma}{B}\right). \quad . \quad . \quad . \quad (4)$$

The deflexion ratio, u/a, along the major axis is shown in fig. 1.

2. *Two Diametrically Opposed Concentrated Loads.*

2.0. *Loads acting inwards.*

Let P be the value of each concentrated load. The problem is the same as that of a quadrantal arc, subjected to a radial load of P/2 at one end, whose ends are constrained to remain perpendicular to and move along the original radii at these ends.

Let T, N, and M be the tension, shear and moment at any point of the arc, and ψ the angle made by the tangent with a line perpendicular to the direction of the load. The equations of equilibrium are

$$\left.\begin{aligned} \frac{dT}{d\psi}+N&=0,\\ T-\frac{dN}{d\psi}&=0,\\ N=\frac{dM}{ds}&=\frac{1}{\rho}\frac{dM}{d\psi}, \end{aligned}\right\} \quad \ldots\ldots \quad (5)$$

where ρ is the radius of curvature and s the distance along the arc.

Fig. 1.

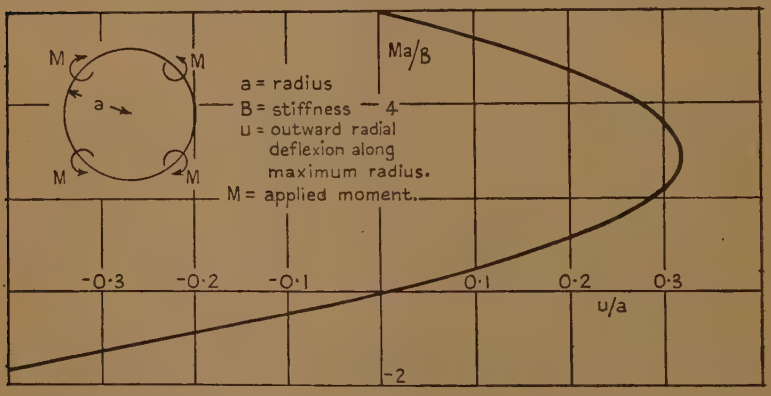

Also, from elastic theory,

$$M=B\left(\frac{1}{\rho}-\frac{1}{a}\right). \quad \ldots\ldots \quad (6)$$

From the first two equations of (5)

$$T=\alpha\sin\psi-\beta\cos\psi,$$
$$N=\beta\sin\psi-\alpha\cos\psi,$$

where α, β are constants of integration.

Here $T=0$ when $\psi=0$, and $T=-P/2$ when $\psi=\pi/2$. Therefore

$$T=-\frac{P}{2}\sin\psi, \qquad N=\frac{P}{2}\cos\psi.$$

From (5) and (6)

$$N=\frac{B}{2}\frac{d}{d\psi}\left(\frac{1}{\rho}\right)^2,$$

whence

$$\frac{1}{\rho}=\left(C+\frac{P}{B}\sin\psi\right)^{1/2}, \quad . \quad . \quad . \quad . \quad (7)$$

where C is a constant for a given value of P and equals the square of the curvature at the point of application of the load.

The length of arc is

$$s=\int_0^{\psi}\rho\, d\psi, \quad . \quad . \quad . \quad . \quad . \quad . \quad (8)$$

and the inward deflexion at the point of application of the load is

$$u=a-\int_0^{\pi a/2}\sin\psi\, ds. \quad . \quad . \quad . \quad . \quad . \quad (9)$$

Equations (7), (8), (9), and the conditions that the total length of arc is $\pi a/2$ and that ψ is zero and $\pi/2$ at the ends, are sufficient to give the deflexion ratio u/a in terms of the loading coefficient Pa^2/B. In order that tabulated elliptic functions may be used these relations are put into three different forms according to the value of the curvature at the origin and the existence of an inflexion in the deformed arc.

2.1. *No Inflexion.*

(*a*) $C \geqslant P/B$

From (7)

$$s=\int_0^{\psi}\left(C+\frac{P}{B}\sin\psi\right)^{-1/2}d\psi=\left(C+\frac{P}{B}\right)^{-1/2}\times\int_0^{\psi}\left(1-k^2\sin^2\left(\frac{\pi}{4}-\frac{\psi}{2}\right)\right)^{-1/2}d\psi$$

$$=k\sqrt{\frac{2B}{P}}\int_{\pi/4-\psi/2}^{\pi/4}\Delta\, d\phi,$$

where

$$k^2=\frac{2P}{B}\Big/\left(C+\frac{P}{B}\right)\leqslant 1, \qquad \Delta^2=1-k^2\sin^2\phi.$$

When $\psi=\pi/2$, $s=\pi a/2$.

Therefore $$\frac{\pi a}{2} = k\sqrt{\frac{2B}{P}}.F\left(\frac{\pi}{4}, k\right),$$

or $$\sqrt{\frac{Pa^2}{B}} = \frac{2\sqrt{2}}{\pi}k.F\left(\frac{\pi}{4}, k\right), \quad . \quad . \quad . \quad (10)$$

where $F(\phi, k)$ is the elliptic integral of the first kind, of amplitude ϕ and modulus k.

$$u = a - \int_0^{\pi a/2} \sin\psi\, ds = a - k\sqrt{\frac{2B}{P}} \times \int_0^{\pi/4} (1 - 2\sin^2\phi)/\triangle . d\phi$$

$$= a - k\sqrt{\frac{2B}{P}}.F\left(\frac{\pi}{4}, k\right) \times \left\{ 2k^2\left(\frac{E(\pi/4, k)}{F(\pi/4, k)} - 1\right) + 1 \right\},$$

where $E(\phi, k)$ is the elliptic integral of the second kind.

Substituting $F(\pi/4, k)$ from (10), we have

$$\left.\begin{aligned} \frac{u}{a} &= 1 + \frac{P}{k^2}\left(1 - \frac{E(\pi/4, k)}{F(\pi/4, k)}\right) - \frac{\pi}{2}, \\ \sqrt{\frac{Pa^2}{B}} &= \frac{2\sqrt{2}}{\pi}k.F\left(\frac{\pi}{4}, k\right). \end{aligned}\right\} \quad . \quad . \quad . \quad (11)$$

(*b*) $$0 \leqslant C \leqslant P/B.$$

$$s = \int_0^{\psi} \left(C + \frac{P}{B} - \frac{2P}{B}.\sin^2\left(\frac{\pi}{4} - \frac{\psi}{2}\right)\right)^{-1/2} d\psi.$$

Put $$\sin\left(\frac{\pi}{4} - \frac{\psi}{2}\right) = k\sin\phi,$$

where $$k^2 = \frac{B(C + P/B)}{2P}.$$

Then $$s = \sqrt{\frac{2B}{P}}\int_\alpha^\beta \frac{d\phi}{\triangle}, \quad . \quad . \quad . \quad . \quad . \quad (12)$$

where

$$\sin\alpha = \frac{1}{k}\sin\left(\frac{\pi}{4} - \frac{\psi}{2}\right); \quad \sin\beta = \frac{1}{k\sqrt{2}}; \quad \triangle^2 = 1 - k^2\sin^2\phi.$$

When $$\psi = \frac{\pi}{2}, \qquad s = \frac{\pi a}{2}.$$

Therefore, from (12),

$$\frac{\pi a}{2}=\frac{2B}{P}.F\left(\arcsin\frac{1}{k\sqrt{2}},\,k\right), \quad . \quad . \quad (13)$$

and

$$u=a-\int_0^{\pi a/2}\sin\psi\,ds=a\left\{1-\sqrt{\frac{2B}{Pa^2}}\right.$$
$$\left.\times\left(2E\left(\arcsin\frac{1}{k\sqrt{2}},\,k\right)-F\left(\arcsin\frac{1}{k\sqrt{2}},\,k\right)\right)\right\}.$$

Substituting $\sqrt{\frac{Pa^2}{B}}$ from (13),

$$\left.\begin{aligned}\frac{u}{a}&=1+\frac{\pi}{2}-\pi.\frac{E\left(\arcsin\frac{1}{k\sqrt{2}},\,k\right)}{F\left(\arcsin\frac{1}{k\sqrt{2}},\,k\right)},\\ \sqrt{\frac{Pa^2}{B}}&=\frac{2\sqrt{2}}{\pi}F\left(\arcsin\frac{1}{k\sqrt{2}},\,k\right).\end{aligned}\right\} \quad . \quad . \quad (14)$$

These relations hold good when k lies between 1 and $1/\sqrt{2}$, that is, when $\frac{Pa^2}{B}$ lies between 0·63 and 2·78.

2.2 *Inflexion.*

The inflexion will occur when $\sin\psi=-\frac{BC}{P}=-\sin\theta$, say.

The length of arc is always positive ; therefore the length of the perimeter of the quadrant is

$$\frac{\pi a}{2}=\left\{\int_{-\theta}^{0}+\int_{-\theta}^{\pi/2}\right\}\left(C+\frac{P}{B}.\sin\psi\right)^{-1/2}d\psi$$
$$=\left\{2\int_{-\theta}^{0}+\int_{0}^{\pi/2}\right\}\left(C+\frac{P}{B}.\sin\psi\right)^{-1/2}d\psi.$$

Putting

$$\sin\left(\frac{\pi}{4}-\frac{\psi}{2}\right)=k\sin\phi, \quad \text{where} \quad k^2=\frac{B}{2P}\left(C+\frac{P}{B}\right).$$

Then

$$\sin\theta=2k^2-1,$$

$$\sin\left(\frac{\pi}{4}+\frac{\theta}{2}\right)=k,$$

and

$$\sqrt{\frac{Pa^2}{B}} = \frac{2\sqrt{2}}{\pi}\left\{2F\left(\frac{\pi}{2}, k\right) - F\left(\arcsin\frac{1}{k\sqrt{2}}, k\right)\right\}, \quad \ldots \quad (15)$$

$$u = a - \left\{\int_{-\theta}^{0} + \int_{-\theta}^{\pi/2}\right\} \rho \sin\psi . d\psi$$

$$= a - \sqrt{\frac{2B}{P}} \cdot \left\{2\left(2E\left(\frac{\pi}{2}, k\right) - E\left(\arcsin\frac{1}{k\sqrt{2}}, k\right)\right)\right.$$

$$\left. - \left(2F\left(\frac{\pi}{2}, k\right) - F\left(\arcsin\frac{1}{k\sqrt{2}}, k\right)\right)\right\}.$$

Fig. 2.

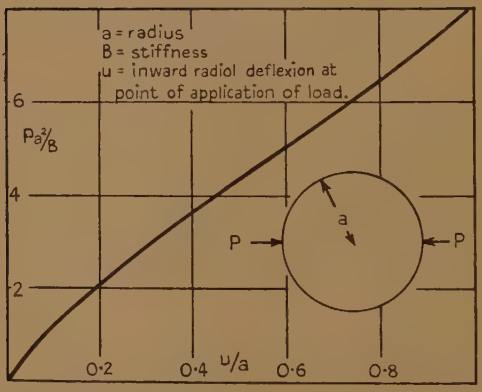

Substituting from (15),

$$\left.\begin{aligned} \frac{u}{a} &= 1 + \frac{\pi}{2} - \pi\frac{2E\left(\frac{\pi}{2}, k\right) - E\left(\arcsin\frac{1}{k\sqrt{2}}, k\right)}{2F\left(\frac{\pi}{2}, k\right) - F\left(\arcsin\frac{1}{k\sqrt{2}}, k\right)}, \\ \sqrt{\frac{Pa^2}{B}} &= \frac{2\sqrt{2}}{\pi}\left\{2F\left(\frac{\pi}{2}, k\right) - F\left(\arcsin\frac{1}{k\sqrt{2}}, k\right)\right\}. \end{aligned}\right\} \quad \ldots \quad (16)$$

The resulting curve is asymptotic to $u/a = 1 + \pi/2$, and is plotted in fig. 2.

2.3. *Loads acting outwards.*

The working is similar to that for inward loads, but there are no inflexions. The curvature at the point of

application of the load is always greater than $\sqrt{P/B}$. The entire course of the deformation is covered by the relations

$$\left.\begin{aligned} \frac{u}{a} &= \frac{\pi}{k^2}\left\{1-\frac{\mathrm{E}\left(\frac{\pi}{2},k\right)-\mathrm{E}\left(\frac{\pi}{4},k\right)}{\mathrm{F}\left(\frac{\pi}{2},k\right)-\mathrm{F}\left(\frac{\pi}{4},k\right)}\right\}-\frac{\pi}{2}-1, \\ \sqrt{\frac{Pa^2}{B}} &= \frac{2\sqrt{2}}{\pi}k\left\{\mathrm{F}\left(\frac{\pi}{2},k\right)-\mathrm{F}\left(\frac{\pi}{4},k\right)\right\}. \end{aligned}\right\} \quad (17)$$

This is asymptotic to $u/a=\pi/2-1$, u being positive outwards. The course of the deformation is shown in fig. 3.

Fig. 3.

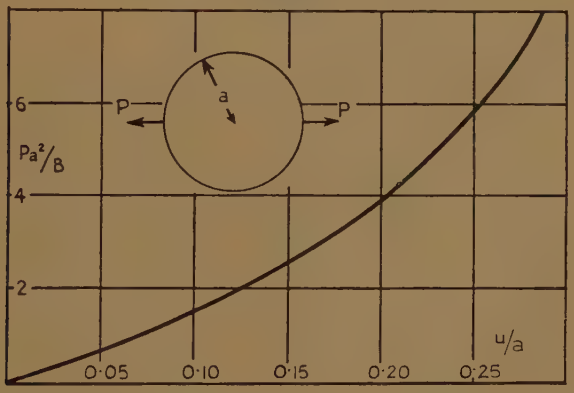

3. *Two Opposed Inward Loads along a Diameter, and Two Equal Opposed Outwards Loads along a Perpendicular Diameter.*

3.0. *Deflexion along the compressed diameter.*

If ψ is the angle of the tangent at a point of the perimeter with the tangent at the point of application of one of the compressive loads, P, the tension is given by

$$T=P/\sqrt{2}.\cos(\psi+\pi/4),$$

and the curvature

$$\frac{1}{\rho}=\left(C-\frac{P\sqrt{2}}{B}\cos\left(\psi+\frac{\pi}{4}\right)\right)^{1/2},$$

where C is the square of the curvature at the point where $\psi=\pi/4$.

3.1. *No inflexion.*

(*a*) $C \geqslant P\sqrt{2}/B$.

If the arc, s, is measured from the point of application of the compressive load

$$s = \int_0^{\psi} \rho \, d\psi = 2^{1/4} k \sqrt{\frac{B}{P}} \int_{3\pi/8 - \psi/2}^{3\pi/8} \triangle^{-1} \, d\phi,$$

where

$$\left.\begin{aligned} \phi &= \frac{3\pi}{8} - \frac{\psi}{2}, \\ k^2 &= \frac{2P\sqrt{2}}{B} \Big/ \left(C + \frac{P\sqrt{2}}{B}\right), \\ \triangle^2 &= 1 - k^2 \sin^2 \phi. \end{aligned}\right\}.$$

Therefore arc of quadrant is

$$\frac{\pi a}{2} = 2^{1/4} k \sqrt{\frac{B}{P}} \left\{ F\left(\frac{3\pi}{8}, k\right) - F\left(\frac{\pi}{8}, k\right) \right\},$$

or

$$\sqrt{\frac{Pa^2}{B}} = \frac{2^{5/4}}{\pi} k \left\{ F\left(\frac{3\pi}{8}, k\right) - F\left(\frac{\pi}{8}, k\right) \right\}. \quad (18)$$

The deflexion, u, at the origin, measured positively inwards, is

$$\begin{aligned} u &= a - \int_0^{\pi a/2} \sin \psi \, . \, ds \\ &= a - 2^{1/4} k \sqrt{\frac{B}{P}} \int_{\pi/8}^{3\pi/8} (1 + \sin 2\phi - 2 \sin^2 \phi)/\triangle \, . \, d\phi. \end{aligned}$$

Therefore

$$\begin{aligned} \frac{u}{a} &= 1 - 2^{-1/4} k \sqrt{\frac{B}{Pa^2}} \left[F(\phi, k) - \frac{2}{k^2} (F(\phi, k) - E(\phi, k) + \triangle) \right]_{\phi = \pi/8}^{3\pi/8} \\ &= 1 - \frac{\pi}{2\sqrt{2}} \left\{ 1 - \frac{2}{k^2} \right. \\ &\qquad \left. \times \left(1 - \frac{E(3\pi/8, k) - E(\pi/8, k) - \triangle(3\pi/8, k) + \triangle(\pi/8, k)}{F(3\pi/8, k) - F(\pi/8, k)} \right) \right\}. \end{aligned}$$

. . . (19)

These expressions for u/a, Pa^2/B are valid when k lies between zero and unity—that is, when Pa^2/B lies between zero and 0·842.

(*b*) $P\sqrt{2}/B \geqslant C \geqslant P/B$.

Here
$$s = 2^{1/4}\sqrt{\frac{B}{P}}\int_{\lambda}^{\alpha} \triangle^{-1}\, d\phi,$$

where
$$\sin\left(\frac{3\pi}{8} - \frac{\psi}{2}\right) = k \sin\phi,$$

$$k^2 = \left(C + \frac{P\sqrt{2}}{B}\right)\frac{B}{P2\sqrt{2}},$$

$$\triangle^2 = 1 - k^2 \sin^2\phi,$$

$$\sin\alpha = \frac{1}{k}\sin\frac{3\pi}{8},$$

$$\sin\lambda = \frac{1}{k}\sin\left(\frac{3\pi}{8} - \frac{\psi}{2}\right).$$

Therefore
$$s\left(\frac{\pi}{2}\right) = \frac{\pi a}{2} = 2^{1/4}\sqrt{\frac{B}{P}}[F(\phi, k)]_{\phi=\beta}^{\alpha},$$

where
$$\sin\beta = \frac{1}{k}\sin\frac{\pi}{8},$$

whence
$$\sqrt{\frac{Pa^2}{B}} = \frac{2^{5/4}}{\pi}[F(\phi, k)]_{\phi=\beta}^{\alpha}, \quad . \quad . \quad . \quad (20)$$

$$u = a - \int_0^{\pi a/2} \sin\psi \,.\, ds$$
$$= a - 2^{3/4}\sqrt{\frac{B}{P}}\int_{\beta}^{\alpha}\left\{k\sin\phi - \frac{k^2\sin^2\phi}{2\triangle} + \frac{\triangle}{2}\right\} d\phi.$$

Therefore
$$\frac{u}{a} = 1 - \frac{\pi}{2\sqrt{2}}[2E(\phi, k) - F(\phi, k) - 2k\cos\phi]_{\beta}^{\alpha}/[F(\phi, k)]_{\alpha}^{\beta}, \quad (21)$$

where
$$\sin\alpha = \frac{1}{k}\sin\frac{3\pi}{8}, \qquad \sin\beta = \frac{1}{k}\sin\frac{\pi}{8}.$$

The expressions (20), (21) are valid when k lies between unity and $\sin 3\pi/8$—that is, when Pa^2/B lies between 0·84 and 2·20.

3.2. *Inflexion.*

There will be an inflexion when ψ equals θ, where
$$\cos(\theta + \pi/4) = BC/P\sqrt{2}.$$

Thus the inflexion first appears at the origin when C equals P/B. It then travels along the arc until θ is $-\pi/4$ and C is $P\sqrt{2}/B$.

Since θ is negative, the absolute length of arc of the original quadrant is

$$\frac{\pi a}{2} = \left\{ \int_{\theta}^{0} + \int_{\theta}^{\pi/2} \right\} \rho \, d\psi.$$

Using the same transformation as in the preceding case, 3.1 (*b*), we obtain

$$\frac{\pi a}{2} = -2^{1/4} \left\{ \int_{\pi/2}^{\alpha} + \int_{\pi/2}^{\beta} \right\} \triangle^{-1} \, d\phi,$$

where

$$\sin \alpha = \frac{1}{k} \sin \frac{3\pi}{8}, \quad \sin \beta = \frac{1}{k} \sin \frac{\pi}{8}, \quad \cos\left(\frac{\pi}{8} + \frac{\theta}{2}\right) = k.$$

Therefore

$$\sqrt{\frac{Pa^2}{B}} = \frac{2^{5/4}}{\pi} \left\{ 2F\left(\frac{\pi}{2}, k\right) - F(\alpha, k) - F(\beta, k) \right\}, \quad (22)$$

and, as in 3.1 (*b*), but with different limits of integration,

$$\frac{u}{a} = 1 - \frac{\pi}{2\sqrt{2}} \times \frac{[2E(\phi, k) - F(\phi, k) - 2k \cos \phi]_{\phi=\alpha}^{\pi/2} + [2E(\phi, k) - F(\phi, k) - 2k \cos \phi]_{\phi=\beta}^{\pi/2}}{2F(\pi/2, k) - F(\alpha, k) - F(\beta, k)}. \quad (23)$$

The relations (22), (23) are valid when k lies between unity and $\sin 3\pi/8$—that is, when Pa^2/B is greater than 2·20. The resulting deflexion curve, shown in fig. 4, is asymptotic to $u/a = 1 + \pi/2\sqrt{2}$.

3.3. *Deflexion along the stretched diameter.*

The deflexions along the line of action of the load when P is negative are the same as the deflexions along the line of action of the perpendicular load when P is positive. Therefore they are to be found by putting

$$u = a - \int_{0}^{\pi a/2} \cos \psi \, . \, ds.$$

If u is the deflexion when P is positive, and u' the deflexion when P has an equal but negative value, it will be found that the following relations hold :—

No Inflexion.

(*a*)

$$\frac{u'+u}{a}=2+\frac{2^{7/4}}{k}\sqrt{\frac{B}{Pa^2}}\left\{\Delta\left(\frac{3\pi}{8},k\right)-\Delta\left(\frac{\pi}{8},k\right)\right\}. \quad (24)$$

(*b*)

$$\frac{u'+u}{a}=2-2^{3/4}\sqrt{\frac{B}{Pa^2}}$$
$$\times\{(4k^2-2+\sqrt{2})^{1/2}-(4k^2-2-\sqrt{2})^{1/2}\}. \quad (25)$$

Fig. 4.

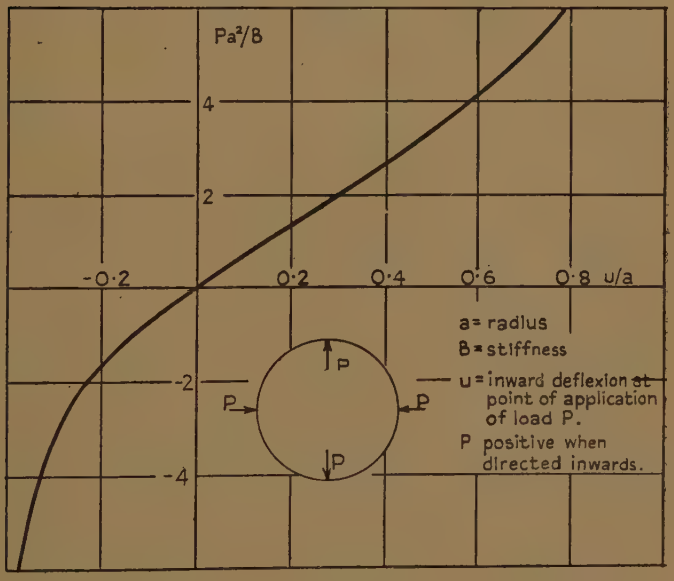

Inflexion.

$$\frac{u'+u}{a}=2-2^{3/4}\sqrt{\frac{B}{Pa^2}}$$
$$\times\{(4k^2-2+\sqrt{2})^{1/2}+(4k^2-2-\sqrt{2})^{1/2}\}. \quad (26)$$

From these and the appropriate values of u/a, k, and Pa^2/B the values of u'/a may be calculated for negative values of P. The deflexion curve, for positive and negative values of P, is shown in fig. 4. The curve is asymptotic to $u/a=1\pm\pi/2\sqrt{2}$.

LXXXVII. *The Crystalline Diamagnetism of Thallium.*

By Dr. S. Ramachandra Rao *and* A. S. Narayanaswami, *Annamalai University, Annamalainagar, South India* *.

[Received June 16, 1938.]

1. *Introduction.*

THE magnetic susceptibility of single crystals of thallium was studied recently by Rao and Subramaniam[1]. The magnetic anisotropy was found to be 2·5. On heating the single crystal it was found that the hexagonal structure of the α-thallium passed into the cubic structure of the β-variety at 235° C. These results could be explained on the assumption that in α-thallium, two of the three valence electrons have their orbits in the hexagonal plane and that their binding is homopolar. The third electron is considered as free. In the β-variety only Tl^{+1} ions are present, the remaining valence electron being considered as free. Stoner[2] has drawn attention to the significance of such observations from the point of view of the Brillouin zone theory of the metal.

Much useful information regarding the properties of metals can be obtained by the study of single crystals containing admixtures of small quantities of foreign metals[3]. Goetz and Focke[4] and Shoenberg and Uddin[5] have measured the magnetic anisotropy of bismuth crystals and shown that even 0·1 per cent. of tin or tellurium makes a large difference in the magnetic anisotropy. While tin increases the anisotropy, tellurium is found to decrease this value. Similar studies on antimony crystals were carried out by Hart[6] and on cadmium crystals by Rao and Sriraman[7].

In view of the special interest attaching to thallium because of its magnetic properties, it was thought it would be of advantage to study the magnetic properties of single crystals of thallium containing small admixtures of foreign metals. In this investigation we have studied the influence of lead, tin, cadmium and bismuth. We have also examined the influence of cold-work on thallium crystals.

* Communicated by the Authors.

2. *Experiment.*

(a) *Metal.*

The metal used was a very pure variety from Kahlbaum. Two samples were studied, one being granular and the other in the form of sticks. Spectroscopic analysis of the metal showed the presence of lead (less than 0·01 per cent.). Traces of ferromagnetic impurities were also detected and allowed for during the magnetic investigations. The specific gravity of the cast rods of thallium was determined by the hydrostatic method and was found to be 11·90[8].

The elements which were added as impurities were also of high purity and were samples of metals already investigated in this laboratory.

Thallium crystallizes at ordinary temperatures in the hexagonal close-packed structure, the a and c values being 3·47 and 5·52 A.[9].

(b) *Preparation of Single Crystals.*

Polycrystalline rods of thallium were prepared having lengths of about 10 cm. and diameters of about 3·5 mm. The tubes containing the metal were arranged to have twice the length of the metal casts within. Full details regarding the preparation of such rods are given elsewhere[10] The residual pressure at which the metal was melted and cast was arranged to be 10^{-5} mm.

Single crystals of thallium were prepared by the method of slow cooling. The tube containing the metal was lowered through an electrical heater in which the temperature was maintained at about 330° C., several degrees higher than the melting-point of thallium (300° C.). The rate of lowering of the tube containing the metal through the furnace was arranged to be 3 cm. per hour.

(c) *The Gouy Method.*

To determine the magnetic susceptibility of the polycrystalline metal, the tube containing thallium was suspended from one arm of a chemical balance by a fine wire. The specimen was arranged to have its axis vertical and the metal surface to lie symmetrically between the pole faces. The Gouy force was determined by weighing the tube containing the metal initially and then finding out the change in the balancing weight when the magnetic field was applied. The current through the electromagnet was varied from 3 to 7 amperes. The magnetic

field was found to vary in this range from 19 to 25 kilogauss. The Gouy forces in this range of field strengths were determined to one-tenth of a milligram.

Water was chosen as the standard substance. It can be shown that χ, the specific susceptibility of the metal, can be expressed in the form

$$\chi = \frac{k_a}{\rho} + \frac{k_w - k_a}{\rho} \cdot \frac{m}{m^1} \cdot \frac{d_w^2}{d_m^2},$$

where

k_a =the volume susceptibility of the surrounding air,
k_w=the volume susceptibility of water,
ρ =the relative density of the metal,
d_w=the diameter of the tube containing water,
d_m=the diameter of the metal cylinder,
m=the Gouy force on the metal,
m^1=the Gouy force on the water column.

In this investigation the tube used for the metal was initially filled to a height of about 10 cm. with freshly distilled water and the Gouy force was determined at different field strengths. Hence d_w and d_m are identical. This method of calibrating each tube separately with water before using it for the metal avoided a source of much uncertainty. We have, therefore,

$$\chi = \frac{k_a}{\rho} + \frac{k_w - k_a}{\rho} \cdot \frac{m}{m^1}.$$

The volume susceptibility k_a for air was assumed to be $0{\cdot}029$ [11] (paramagnetic) at 30° C. k_w was taken to be $0{\cdot}72$ at the same temperature.

(d) *Determination of the Principal Susceptibilities of the Single Crystals.*

The glass tube containing the single crystal was suspended from the right pan of the chemical balance in the following manner. A circular paper with its circumference graduated in degrees was pasted on the pan through the centre of which was passed a short, thick, vertical wire. A cross pointer attached to this wire and moving over the divisions of the scale gave the setting of the crystal in any measurement. The Gouy forces for any crystal were measured at different positions of the pointer on the scale. The forces were measured at intervals of 10° or 20° during

one complete rotation of the crystal, the current in the electromagnet being 5 amp. On plotting the Gouy forces against the readings on the circular scale, maxima and minima alternately occurred at intervals of 90°. The crystal was next placed in each of these positions and the Gouy forces at different field strengths were measured. On extrapolating the χ, 1/H graph in each case, the susceptibilities at infinite field strength (1/H=0) could be determined.

If χ_0 and χ_{90} correspond to the maximum and minimum specific susceptibility of the crystal during one complete rotation of the cylindrical specimen, we can show that[12]

$$\chi_{90}=\chi_\perp \quad \text{and} \quad \chi_0=\chi_\perp \cos^2\phi+\chi_{||} \sin^2\phi,$$

where $\chi_\perp$ and $\chi_{||}$ are the specific susceptibilities perpendicular and parallel to the hexagonal axis, and ϕ the angle between the hexagonal axis and the cylindrical axis. Knowing ϕ, $\chi_\perp$ and $\chi_{||}$ could be determined from the above equations.

The most accurate method of determining the angle of the crystal is by the use of X-rays. In the absence of proper equipment for this method, the method of Bridgman is adaptable. But thallium gave considerable difficulty, since the metal attained a dull surface on exposure to air. On removing the bright white crystal by cracking the glass, the entire surface became gradually covered with a dark grey film. Hence optical reflexion methods could not be used. Further, the metal got impure by the oxide layer and could be used for further work only after melting in vacuum and removing the scum.

The following method was therefore adopted in view of the above mentioned difficulties. If the single crystal sealed within the tube is converted into a perfect polycrystal, the susceptibility χ is given by $\chi=\frac{1}{3}[2\chi_\perp+\chi_{||}]$. This mean susceptibility χ is experimentally determined. Since $\chi_\perp$ is determined directly from the position of the minimum Gouy force ($\chi_{90}=\chi_\perp$), $\chi_{||}$ can be calculated. It is also possible to calculate the angle ϕ from the relation

$$\chi_0=\chi_\perp \cos^2\phi+\chi_{||} \sin^2\phi.$$

All metals, whether chill-cast or slowly cooled, are not perfect polycrystals. They have preferred orientation, and a crystal of the hexagonal structure shows maxima and minima of Gouy force on rotating it about its axis

with one of the ends lying symmetrically between the pole-pieces. The perfect polycrystal is one which will not show any tendency to twist about a vertical axis when the field is applied. The metal rod which shows preferred orientation can be converted into a perfect polycrystal by annealing at high temperature. In the case of thallium it was found that the substance became a perfect polycrystal after annealing for 10 hours at 280° C. (the melting-point of the metal = 300° C.) and cooling slowly afterwards. The only assumption we have made is that the density of the single crystal is the same as that of the polycrystal. As a matter of fact, careful experiments showed that the difference in density was definitely less than 0·2 per cent.

3. *Results.*

(a) *Polycrystalline Metal.*

The susceptibility of the pure polycrystalline metal was determined by measuring the Gouy force on a few well-

Table I.

Field current in amp.	$(1/H).10^5$.	Gouy force in mg. wt. for metal.	Gouy force in mg. wt. for water.	χ.
3	5·17	50·1	12·4	0·2446
4	4·71	59·8	14·7	0·2453
5	4·49	65·7	16·2	0·2453
6	4·34	70·1	17·3	0·2453
7	4·22	73·4	18·1	0·2456

annealed specimen rods at different field strengths in each case. The results obtained with a typical specimen are shown in Table I.

At infinite field strength the specific susceptibility of the sample works out to 0·249. This value compares favourably with 0·247 obtained by Rao and Subramaniam [1] and 0·25 of Honda [14].

(b) *Principal Susceptibilities of Thallium Single Crystals.*

In Table II. are shown the values of the Gouy force for various angles of setting (θ) of the crystal during one complete rotation. The current through the electromagnet was maintained at 5 amp. during these measurements.

Since the single crystal was suspended from one pan of the balance by a fine wire, it was observed to rotate in the presence of the magnetic field. The reading observed on the graduated scale pasted on the scale-pan would not therefore give the correct setting of the crystal. Hence the twist of the crystal was observed directly with a mirror, lamp and scale arrangement. The angle through which the crystal was rotated when the magnetic field was switched on during any setting could thus be directly

TABLE II.

Setting of the torsion head.	Twist of the crystal.	Corrected setting θ.	Gouy force in mg. wt.
0°	+14°	14°	49·0
20	+10	30	44·8
40	+ 4	44	43·4
50	0	50	43·2
70	− 6	64	44·2
90	−12	78	46·1
110	−15	95	50·3
130	− 7	123	63·1
140	0	140	64·8
160	+13	173	56·3
180	+14	194	48·1
200	+10	210	44·8
220	+ 4	224	43·6
230	0	230	43·3
250	− 6	244	45·1
270	−12	258	46·4
290	−13	277	50·6
310	−10	300	62·3
320	0	320	65·0
340	+ 9	349	58·9
360	+12	12	49·2

found, and the correction may be applied to the reading of the circular scale to get the correct setting.

These corrections do not alter the settings corresponding to the maximum and minimum Gouy forces, since at these positions the crystal shows no rotation when the magnetic field is applied. But the corrected orientations enable us to get a correct relation between the Gouy force and the angle of setting.

The rotation of the crystal could, of course, be avoided by using thicker wires, but these brought about so many complications that it was decided to use fine suspension

wires and apply the correction due to torsion to the setting readings.

Fig. 1 shows the graph between θ and the Gouy force on the specimen. The maximum force occurs when $\theta=50$ or $230°$ and the minimum when $\theta=140$ or $320°$. The crystal was placed successively in these positions, and the Gouy forces were determined in each position for different field strengths. Fig. 2 shows the graphs between χ and $1/H$ in the two cases. On extrapolating these we obtain for the susceptibilities the values of 0·163 and 0·245. Hence $\chi_{\perp}=0{\cdot}163$.

Fig. 1.

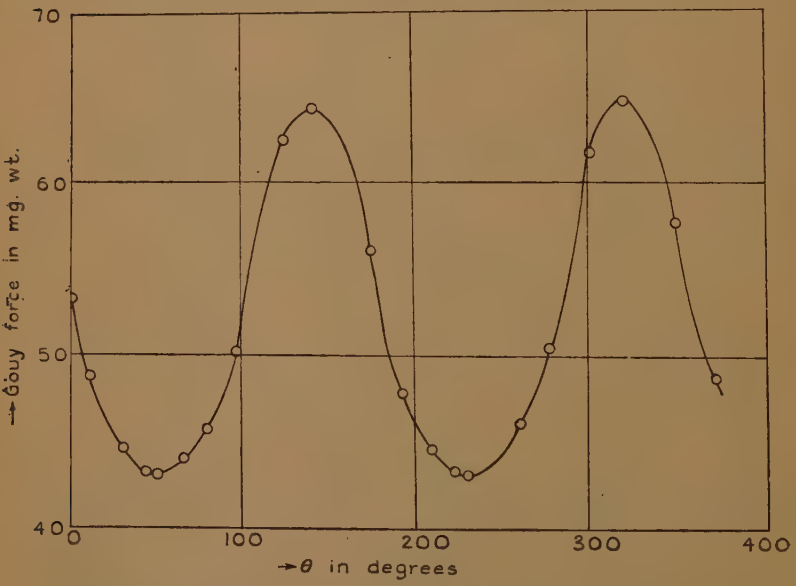

On annealing the specimen at 280° C. for several hours and slowly cooling it, the susceptibility of the polycrystalline state was found to be 0·248. Since the susceptibility of the polycrystal is given by $\chi=\frac{1}{3}[2\chi_{\perp}+\chi_{\parallel}]$ we obtain for $\chi^{\parallel}$ the value 0·418. The magnetic anisotropy $\chi_{\parallel}/\chi_{\perp}$ is hence 2·56. A calculation of ϕ gives the value 34° 32′.

The polycrystalline specimen was once again recrystallized, and the single crystal measurements could thus be repeated several times.

The mean of a number of measurements with several specimens gave $\chi_\perp = 0{\cdot}164$, $\chi_{\parallel} = 0{\cdot}420$, $\chi_{\parallel}/\chi_\perp = 2{\cdot}56$, and (mean) $\chi = 0{\cdot}2490$. Rao and Subramaniam obtained the following values :—

$\chi_\perp = 0{\cdot}165$, $\chi_{\parallel} = 0{\cdot}412$, $\chi_{\parallel}/\chi_\perp = 2{\cdot}50$ and (mean)$\chi = 0{\cdot}247$.

There is good agreement between the sets of values.

(c) *Influence of Small Quantities of Lead.*

Lead dissolves in small quantities in thallium. In fact, it is one of the common impurities in thallium. Alloys

Fig. 2.

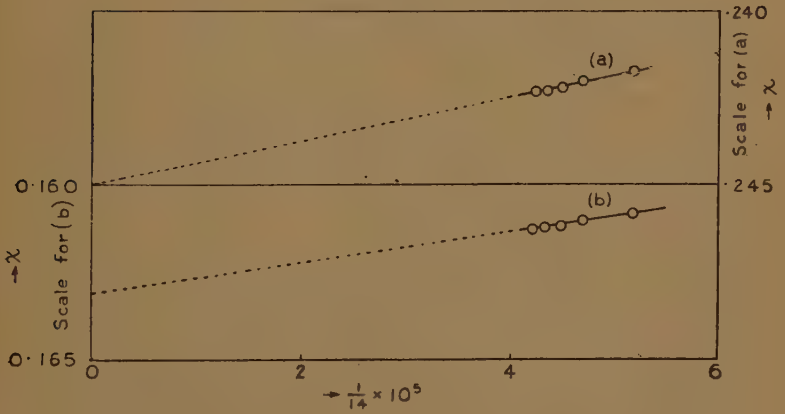

of thallium containing known quantities of lead were prepared by adding weighed quantities of the two metals in suitable proportions and melting them in vacuum. Before being cast the tube was shaken well to mix the molten metals uniformly The crystallization of the alloy and subsequent annealing were carried out just as in the case of the pure metal. The lead used was found to have a specific susceptibility of 0·107. The results for the alloys are given in Table III.

The influence of lead is definitely to lower the magnetic anisotropy. While the value of $\chi_\perp$ shows a small increase, $\chi_{\parallel}$ decreases much. The mean susceptibility shows a small decrease.

(d) *Influence of Small Quantities of Tin.*

Tin is of special interest, since it is paramagnetic while thallium is diamagnetic. The specific susceptibility of the tin used was found by Rao and Subramaniam[1] to be 0·038 (paramagnetic). Hart[6] has recorded that the effect of adding small quantities of tin to antimony is to lower the magnetic anisotropy of antimony. While $\chi_\perp$ was nearly constant, $\chi_{||}$ was found to decrease on adding tin. At concentrations of tin above 1·2 per cent. the value of $\chi_{||}$ became negative. In some respects these results are similar to those obtained here.

TABLE III.

Specimen no.	Atomic per cent. of lead.	Relative density.	Mean χ.	$\chi_\perp$.	$\chi_{||}$.	$\chi_{||}/\chi_\perp$.
1.....	0	11·90	0·248	0·163	0·418	2·56
2.....	0·49	11·92	0·254	0·178	0·406	2·28
3.....	0·99	11·91	0·246	0·175	0·388	2·22
4.....	1·97	11·89	0·232	0·174	0·348	2·00

TABLE IV.

Specimen no.	Atomic per cent. of tin.	Relative density.	Mean χ.	$\chi_\perp$.	$\chi_{||}$.	$\chi_{||}/\chi_\perp$.
1.....	0	11·90	0·248	0·163	0·418	2·56
2.....	0·86	11·81	0·249	0·201	0·345	1·72
3.....	1·71	11·79	0·228	0·204	0·276	1·30
4.....	2·56	11·77	0·210	0·210	0·210	1·00
5.....	3·39	11·73	0·206	0·211	0·196	0·93

$\chi_\perp$ is found to show a sudden increase when the concentration of tin is increased to 0·5 per cent. Thereafter the value increases gradually. $\chi_{||}$ decreases rapidly at first and thereafter slowly. The magnetic anisotropy decreases rapidly and becomes 1 at 1·5 per cent. As the percentage of tin is increased, the magnetic anisotropy measured by $\chi_{||}/\chi_\perp$ becomes smaller than 1.

(e) *Influence of Small Quantities of Cadmium.*

The specific susceptibility of the cadmium used was found to be 0·1746 by Rao and Sriraman[7]. The results are shown in Table V.

TABLE V.

Specimen no.	Atomic per cent. of cadmium.	Relative density.	Mean χ.	$\chi_\perp$.	$\chi_{\parallel}$.	$\chi_{\parallel}/\chi_\perp$.
1.....	0	11·90	0·252	0·165	0·426	2·58
2.....	0·91	11·86	0·248	0·160	0·424	2·65
3.....	1·80	11·82	0·246	0·159	0·420	2·64
4.....	3·58	11·76	0·245	0·157	0·421	2·68

It will be observed that both $\chi_\perp$ and $\chi_{\parallel}$ show a tendency to decrease as the concentration of cadmium is increased. The magnetic anisotropy shows a definite increase in value.

(f) *Influence of Small Quantities of Bismuth.*

The bismuth used had a specific susceptibility of 1·412.

TABLE VI.

Specimen no.	Atomic per cent. of bismuth.	Relative density.	Mean χ.	$\chi_\perp$.	$\chi_{\parallel}$.	$\chi_{\parallel}\ \chi_\perp$.
1.....	0	11·90	0·248	0·163	0·418	2·56
2.....	0·49	11·80	0·260	0·181	0·418	2·31

In this case $\chi_{\parallel}$ remains constant while $\chi_\perp$ shows an increase. The magnetic anisotropy definitely decreases as the bismuth is introduced.

(g) *General Conclusions.*

In fig. 3 are shown the graphs between the concentration of foreign metal and the magnetic anisotropy. It will be observed that in the case of cadmium there is a slow rise in the value of the magnetic anisotropy. In all the other cases the anisotropy decreases, this decrease being largest in the case of tin. The graphs also indicate that the rate of change of anisotropy with concentration is larger when the concentration of the added metal is lower.

(h) *Cold-working.*

To facilitate the removal of thallium single crystals from the tubes in which they were cast, the walls were covered with a trace of apiezon oil before the molten metal was poured in. The apiezon oil did not affect the pressure

inside, since its vapour pressure is known to be exceedingly low.

The process of removing the crystal by cracking the glass seems to introduce strain on the crystal. The single crystal of thallium after removal from its container was inserted immediately in a glass tube, through which it slid smoothly, and the tube was sealed in vacuum. The length of the sealed tube was arranged to be twice that of the crystal. The magnetic measurements were next carried out with this arrangement. The specimen was next removed and a tensional force of suitable magnitude was applied. The crystal was guarded against any

Fig. 3.

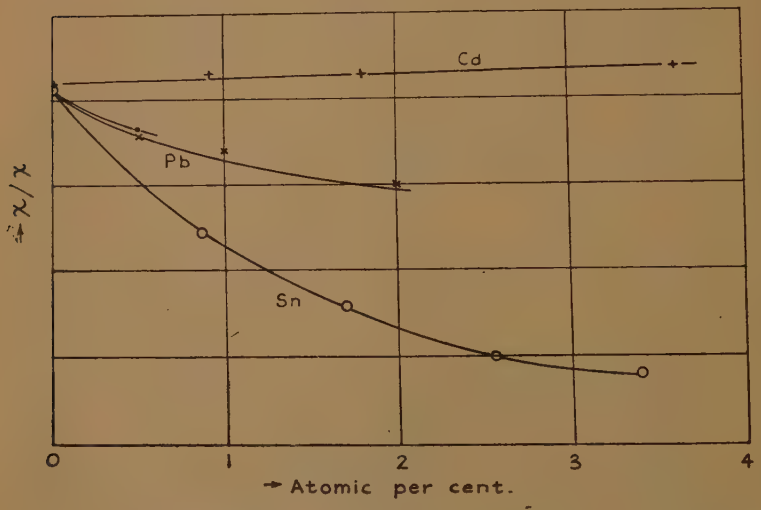

direct contact with iron during this process. The magnetic measurements were made with the strained rod sealed *in vacuo*. This was repeated after giving the crystal different tensions. The results are tabulated below. When the stress reached the value of 16 kg. wt. per sq. cm., the section of the crystal became elliptical and the crystal began to yield, showing slip bands on the surface.

From measurements on the unstrained crystal it is possible to calculate the angle ϕ between the hexagonal axis and the cylindrical axis of the crystal. This was assumed to be constant in the succeeding measurements,

and the principal susceptibilities were calculated for any strained crystal on this assumption.

The results are no doubt slightly affected by the formation of a thin layer of grey film on the surface during the experiments, but this layer could not cause variations of the magnitude observed below.

TABLE VII.

Tensional force k.g. wt.	Stress in kg. wt. per sq. cm.	Change in length per unit. length.	Relative density.	$\chi_\perp$.	$\chi_{\parallel}$.	χ.	$\chi_{\parallel}/\chi_\perp$.
Initial readings		0	11·90	0·163	0·418	0·248	2·56
After removing the crystal from the glass container.		—	11·88	0·174	0·360	0·236	2·07
0·5	4·0	0·003	11·87	0·174	0·340	0·230	1·95
1·3	10·4	0·010	11·85	0·177	0·328	0·227	1·85

The effect of cold-working is clearly to decrease the magnetic anisotropy. While $\chi_\perp$ shows a small increase, $\chi_{\parallel}$ decreases rapidly and the mean susceptibility χ also decreases. These changes are almost similar to those obtained when lead is added in small quantities to thallium (*vide* Table III.).

4. *Conclusions.*

Fig. 3 shows the graphs between concentration of the foreign metal and magnetic anisotropy. It will be noted that while cadmium increases the anisotropy, the other three metals decrease this value. Tin has the largest influence, although it has the same number of valency electrons as lead.

These results are similar to those obtained with bismuth crystals by Goetz and Focke[4] and by Shoenberg and Uddin[5]. It was found by them that while tin increased the magnetic anisotropy of bismuth, tellurium decreased this value. This observation has been attributed to the fact that while the bismuth atom contains 5 valence electrons, tin contains 4 and tellurium 6.

Thallium contains 3 valency electrons, lead or tin 4, and cadmium 2. We find that while tin or lead decreases the anisotropy, cadmium increases this value.

It will also be observed that although lead and tin contain the same number of valence electrons per atom, they affect

the anisotropy of thallium differently. The decrease of the anisotropy due to tin is uniformly two and a half times the decrease obtained by the same atomic percentage of lead. This seems to be true at all concentrations between 0 and 2 per cent. This result is in agreement with the observations of Shoenberg and Uddin[5], who find that, with bismuth crystals, tin is four times as effective as lead. We also observe that the influence of bismuth on thallium crystals is nearly the same as that of lead, although bismuth has 5 valence electrons per atom and lead has only 4. We can hence conclude that the decrease in the anisotropy of thallium crystals caused by the presence of small admixtures of foreign metals is not entirely dependent on the number of valence electrons per atom of the metal introduced.

Considering next the influence of the foreign metals on the principal susceptibilities, we observe that while lead influences the value of $\chi_{\parallel}$ more than that of $\chi_{\perp}$, tin alters both the susceptibilities considerably.

Summary.

A study is made of the principal diamagnetic susceptibilities of thallium containing small admixtures of cadmium, lead, tin and bismuth. While cadmium increases the magnetic anisotropy of thallium, the other metals decrease this value. Although lead and tin contain the same number of valence electrons, tin is two and a half times as effective as lead in reducing the magnetic anisotropy. Attention is drawn to the similarity of these observations with those on bismuth by Goetz and Focke and by Shoenberg and Uddin. Cold-working of thallium is accompanied by a reduction of its magnetic anisotropy.

References.

(1) Phil. Mag. xxi. p. 609 (1936).
(2) Sc. Rep. Tohoku Imp. Univ., Honda mem. vol., 1936, p. 299.
(3) See Mott and Jones, ' Properties of Metals and Alloys,' 1936, p. 213.
(4) Phys. Rev. xlv. p. 170 (1934).
(6) Proc. Roy. Soc. clvi. pp. 687 and 701 (1936).
(6) Phys. Rev. lii. p. 130 (1937).
(7) Proc. Roy. Soc. (in the press).
(8) For standard determinations see Mellor's Treatise, v. p. 411.
(9) Wyckoff, ' The Structure of Crystals,' 1931, p. 207.
(10) Proc. Ind. Acad. Sc., iv. p. 39 (1936).
(11) All susceptibility values are given in 10^{-6} units, and unless otherwise stated are diamagnetic.
(12) Proc. Ind. Acad. Sc. iv. p. 190 (1936).

LXXXVIII. *Classical Wave Functions for Moving Corpuscles.* *By* W. E. Benham †.

[Received July 1, 1938.]

THIS paper is written largely in the belief that the ultimate explanation of the universe will be found along the lines of classical rather than the new quantum mechanics. By this I mean more specifically that the apparent discontinuities in energy that are assumed in the quantum theory will be found to be smoothed to some extent, while the periodicity associated with energy will still be retained. Eigen values will receive explanation on the basis of inertial functions derivable on classical conceptions.

In order to avoid misconceptions, I would say at once that the achievements of quantum physicists have my profoundest admiration. The various principles which characterize wave mechanics have in most cases been for the specific purpose of explaining experimental results. Indeed, much stress is laid upon the urgency of having an explanation for experimental data, to the extent that conveys the impression (if one may be forgiven the analogy) that experimental results are like plants which if kept in darkness for a period will perish beyond repair rather than hardy annuals which can bide the pleasure of Jove.

If the urgent need for a quasi-metaphysical outlook on certain aspects of modern physics is not appreciated by those who, whether by circumstance or temperament, feel inevitably welded to the older school, the reason may be found in a difference in interpretation of the best means of achieving the end which may be assumed held in common. If physical reality is to be achieved most rapidly by neo-Newtonian methods, then undoubtedly such methods could be described as desirable. If, on the other hand, Newtonian methods should still prove capable of important advances in knowledge, these should be pursued until such time as no further advance is possible.

Those who advocate a conservative policy in Physics are to-day open to charges of " mysticism," or " obscurantism." Such an attitude is by no means confined to those

† Communicated by the Author.

who uphold quantum mechanics as superseding classical mechanics. Particularly brilliant men, like Maxwell, overshadow their contemporaries to such an extent that it may require decades to obtain a correct perspective. It required a Heaviside[1] to declare that "It is most objectionable to stereotype the work of a great man merely because it was so great an advance, and because of the great respect thereby induced." Yet, despite the "spots on the sun," Heaviside himself was still sufficiently under the influence of the "glare" to regard anti-Maxwellian methods as virtually dead. "It would be slaying the slain to attack them."

Thirty years after these words were written we find no less a person than H. A. Lorentz[2], evidently with Heaviside's remark in mind, saying, "It has been said that there are spots on the sun. I confess I am unable to stand the glare." Prof. Lorentz goes on to explain that all he was attempting to do was to lift some of the "clouds which obscure the sun."

It is probable that the first real attempt to bring the lesser lights into their right position is to be found in Prof. O'Rahilly's new book 'Electromagnetics' (Longman's). This book is of recent appearance and I have only just seen it. For the present I would content myself with noting that Prof. O'Rahilly's view seems to be that the concepts of electron theory exclude the possibility of a displacement current. This does not, in my view, mean that we cannot continue to use the displacement current in our theories, but it may mean that such a current is a fiction arising simply and solely from action at a distance between one set of charges and another.

That somewhat similar conclusions to those of Prof. O'Rahilly have been reached by myself, in the first instance through an intermediary processs in which the existence of the displacement current was taken for granted, suggests the importance of the Maxwellian conception as tiding over certain difficulties. Thus, in my published work to-date, the displacement current will everywhere be found taken for granted, though in 1936 I was beginning to concern myself with the ultimate significance of this "somewhat mysterious quantity" †. The sequel is independent of the precise nature of displacement current.

† 'Wireless Engineer,' xiii. p. 155 (August 1936).

A matter of paramount importance in the whole question as to the foundations of electron theory was Professor Fitzgerald's explicit introduction of the convection current into Maxwell's law of circuitation of currents. Fitzgerald is reported by Sir Oliver Lodge[3] to have chaffingly referred to electrostatics as "one of the most beautiful and useless adaptations of nature." Now, Fitzgerald may have realized that there was an alternative to the method of electrical images. Probably he did not, but it is noteworthy that the Fitzgerald convection current does enable us formally to dispense with image theory in simple cases. For example, the current electrostatically induced in the electrodes of a condenser due to charges moving between the electrodes may be shown, without image theory, to be $\Sigma x_1^{-1}\int_0^{x_1} i_c\,dx$ in which i_c is the convection current and x the potential function (corresponding to any part of the geometry). From this result the charges induced on each electrode may be derived in terms of the potential function associated with the geometry †.

Considerable simplification in electron theory results from the appreciation of the fact that, whereas charge is circuital, that is, is propagated unchanged, convection current is propagated according to the law $i_0dt_0=i_1dt_1=\ldots$ where $dt_0, dt_1\ldots$ correspond to the times of emission, collection of the charge i_0dt_0, on the part of surfaces normal to the direction of motion; dt_0, $dt_1\ldots$ are equal *only* in static fields.

If charge is propagated unchanged, the whole theory of moving charges can be made to depend on one, and only one, law—namely, the law of motion. We do not even need to postulate a law of force between charges. We do not need to specify any law of force, since, if charge is propagated unchanged the (total) current is circuital, and, if the total current is circuital, the current induced in a pair of electrodes must be equal to the (total) current minus the "displacement" current that would have existed in the absence of the moving charges[4]. Independently of the law of force and of whether this displacement current is real or fictitious, the latter is of the type $C\frac{dV}{dt}$, and in this way we arrive at the result

† 'Wireless Engineer,' xiii. p. 155 (August 1936).

mentioned above, namely, $i_e = x_1^{-1} \int_0^{x_1} i_i dx$. Working backwards from this result we obtain the image solution for the charges on the electrodes in the form

$$\left.\begin{aligned} e_1 &= -e\left(\frac{x}{x_1}\right), \\ e_0 &= -e\left(\frac{x_1 - x}{x_1}\right), \end{aligned}\right\} \text{(if plane or cylindrical the electrodes must be infinitely extended)}$$

which is also a way of saying that the total charge inside a closed conductor is zero, from which result the inverse square law is known to follow. Hence we obtain the result that the inverse square law must hold if charge suffers no change on propagation. But we obtain a still further result. The image solution is based on the superposition principle, namely, that the effect of any charge e_1 on charge e_2 is the same whether or no charges e_3, e_4 ...e_m are present in addition, a principle, be it noted, which is intended to apply to stationary charges only. But we have shown above that if charge suffers no change on propagation, the image solution, based on stationary charges, is still obtained. Hence, subject to the constancy of propagation of charge, not only must the inverse square law of force (electric) between charges apply, but the superposition principle must hold good even for moving charges. It is only claimed that those results necessarily apply in the case of free electrons treated as point charges. For, if the superposition principle held universally, we might be led to serious inconsistencies in solids and liquids. In particular, we might be led to infer that two similarly charged pith balls suspended near to one another would continue to repel one another if a large metal sheet were interposed, whereas, if the said plate be earthed, the pith balls will be attracted to their image charges in the plate, and the effect of the plate could be regarded as converting a repulsion to an apparent attraction.

But, I can hear it objected, if the law of force between moving charges is simply ee'/r^2, what about secondary magnetic effects and the Lienard-Schwarzchild force tormula ? My answer to this is that nothing has been left out in deriving the induced current in the condenser plates, and, consequently, secondary magnetic effects, in particular the magnetic action of one point charge on

another, must be zero in the case whether the charges are moving between a pair of plates infinitely extended †. This result is reasonable when it is remembered that magnetic effects on any given charge will tend to cancel out owing to the symmetrical placement of other charges with respect to the selected charge. In other words, the simplicity of this particular result is probably to be regarded as arising from the boundary conditions assumed. If the plates be not infinitely extended, edge effects involve magnetic forces on a selected electron near the edge due to the current carried by the core of centrally placed electrons. For a single particle the difficulty disappears automatically, but for two or three particles the difficulties of analysis are great. The extent to which two and three body problems have been studied is already considerable in astronomy, but in electron theory the two body problem is as yet unsolved.

Now, we have derived the law of electric force between point charges on the basis of the constancy of charge during propagation, so that we do not "need" Poisson's equation—we can form this for ourselves from the law of force and the conception of electric field. In other words, Poisson's equation is inherent in the invariance of electric charge. [In the case of a single electron treated as point charge Laplace's equation suffices.] There remains, then, only the law of motion to be decided, and we then have all the equations necessary to determine the behaviour of clouds of electrons under the combined influence of electric and magnetic forces, either of which may in general be varying in time, subject only to the restriction that the time variations are insufficiently rapid to necessitate the inclusion of retardation terms.

Now it may be demonstrated conclusively that the Eulerian form of Newton's second law is not only equivalent to, but gives precisely the same results (even in highly complicated problems) as the original when both are correctly applied ‡. The Hamilton-Jacobi equation is, of course, equivalent to the space integral of this equation,

† While such a simplification may be of limited interest, there is really no such thing as "free space."

‡ The equivalence is demonstrated, I fear none too neatly, in Proc. Phys. Soc. xliii. p. 1 (1935). See Appendix. Further to the concluding paragraph (p. 52), methods are now available whereby the use of Lagrangian rather than Eulerian variables may be made the more convenient choice (*q. v.*). See also 'Nature,' 3rd April, 1937.

but the introduction of a velocity potential for the purpose of integrating the equation of motion does not seem to me a helpful step, and it will now be shown that considerable information has thereby been missed.

The equation expressing Newton's second law may be written (for $\dot{r} \ll c$)

$$m\ddot{r} = m\left.\frac{\partial \dot{r}}{\partial t}\right|_{t_0} = \mathrm{F}, \quad . \quad . \quad . \quad . \quad . \quad (1)$$

and is identical with the equation, due to Euler, which may be written

$$m\left(\frac{\partial \dot{r}}{\partial t} + \dot{r}\frac{\partial \dot{r}}{\partial r}\right) = \mathrm{F}, \quad . \quad . \quad . \quad . \quad . \quad (2)$$

where F is the total force, being the sum of external and internal forces acting on a particle of mass m. Now in general $\mathrm{F} = \mathrm{X} - \frac{1}{\sigma}\frac{dp}{dx}$, where σ is the density of distribution of particles of mass m and p is the pressure. X will then be impressed force. In electron theory the term $\frac{1}{\sigma}\frac{dp}{dx}$ is commonly omitted, as it would appear to involve conceptions not strictly applicable. Thus, although it may be perfectly permissible, for example, in dealing with questions of thermionic emission, to regard the electrons as exerting a pressure on the walls of an enclosure, it is different when we come to consider the reactions of electrons on other electrons. Since, *more suo*, one electron avoids another, the kinetic theory of gases could (at best) only be regarded as applicable in the negative sense, in that, not only are collisions non-existent (probability zero), but are rendered even less possible (if possible) by virtue of mutual repulsions (probability negative). But the effect of mutual repulsions may be included in X by arranging that X is not the impressed force, but the value that force assumes as a result of mutual actions of the electrons. If X_0 be the value of X in the absence of electrons the value of p could, if desired, be represented by $\sigma\int(\mathrm{X} - \mathrm{X}_0)dx + \text{constant}$. For our purposes it is convenient to regard X as a variable rather than p. Thus it is $\epsilon\left(= -\frac{\partial \mathrm{V}}{\partial r}\right)$ that appears in Poisson's equation, which

in n space dimensions may be written

$$\frac{\partial(\epsilon r^{n-1})}{\partial r} = 4\pi\rho r^{n-1} \quad . \quad . \quad . \quad . \quad . \quad (3)$$

(for variations in the direction of θ, ϕ, ψ . . . all zero), in which, be it noted, the solid angle in n dimensions[5], given by

$$\Omega_n = \frac{2\pi^{n/2}}{\Pi\left(\frac{n}{2}-1\right)}, \quad . \quad . \quad . \quad . \quad . \quad (4)$$

has cancelled out on both sides of the equation, the 4π being merely a units constant.

Returning to Euler's equation, and writing

$$\mathrm{F}=\mathrm{X}=-e\left(\frac{\partial \mathrm{V}}{\partial r'}+[\dot{r}', \mathrm{H}]\right),$$

we have, on integration with respect to r' at t constant (the prime simply denotes that in view of the magnetic field H the path will be curved—*i. e.*, r' is not the polar co-ordinate above),

$$m\int_{r_0}^{r_1}\frac{\partial \dot{r}'}{\partial t}dr' + \left|\frac{m\dot{r}'^2}{2}\right|_{r_0}^{r_1} = |-e\mathrm{V}|_{r_0}^{r_1} - \int_{r_0}^{r_1} e([\dot{r}', \mathrm{H}]dr'). \quad (5)$$

Now

$$\dot{r}'(=\dot{r}_t') = \left.\frac{dr'}{dt}\right|_{t_0} = \frac{dr'}{d(t-t_0)} \quad \therefore \quad dr' = \dot{r}'d(t-t_0), \quad . \quad (6)$$

where t_0 corresponds to the instant at which the particle left the point r_0. t and t_0 are Lagrangian variables, to which a change from (r', t) is being made. Changing the limits to t_0 and t, (5) becomes

$$m\int_t^{t_0}\dot{r}'\frac{\partial \dot{r}'}{\partial t}d(t-t_0') + \left|\frac{m\dot{r}'^2}{2}\right|_t^{t_0} + |e\mathrm{V}|_t^{t_0} + \int_t^{t_0} e(\dot{r}'[\dot{r}', \mathrm{H}])d(t-t_0') = 0, \quad (7)$$

in which the integral term still represents a path integration in the sense that the instant t_0', at which the path was commenced, is varied continuously between t and t_0. Writing $m\dot{r}^2 = 2\mathrm{T}$, $e\mathrm{V} = \mathrm{U}$, $t-t_0' = \tau'$, we obtain (since $([\dot{r}, \mathrm{H}])=0$)

$$\int_0^{\tau}\frac{\partial \mathrm{T}}{\partial t}d\tau' + |\mathrm{T}+\mathrm{U}|_{\tau'=0}^{\tau'=\tau} = 0. \quad . \quad . \quad . \quad . \quad (8)$$

showing that the "total energy" (T+U) changes over the path by an amount equal to the integral term. If $\frac{\partial}{\partial t}$ is zero, (T+U) remains constant over the path[6]. In general, what remains conserved is not (T+U) but $\int \frac{\partial T}{\partial t} d\tau' + (T+U)$, and this represents the true total energy of the particle (be it charged or no) obtained on classical conceptions properly applied. Now, the value of integral equations for the solution of differential equations (Picard's method) is well known, but what is important here is the value of the integral equation in bringing out physical properties. There are known methods of solving (8), but at the moment let us restrict our attention to the physical significance of the integral term. This term may be interpreted as energy storage during a time equal to the transit time of a particle. The question arises "where is the energy stored"?

For the purpose of investigating this point it is convenient and legitimate to regard T as consisting of any desired number of Fourier components Thus might

$$T = T_0 + \sum_{n=1}^{\infty} T_n e^{ni\omega t} \quad . \quad . \quad . \quad . \quad . \quad (9)$$

then

$$\frac{\partial T}{\partial t} = \sum_{n=1}^{\infty} niw T_n e^{ni\omega t}, \quad . \quad . \quad . \quad . \quad (10)$$

where T_0 is independent of t. Similarly, let

$$U = U_0 + \sum_{n=1}^{\infty} U_n e^{ni\omega t} \quad . \quad . \quad . \quad . \quad (11)$$

then $| T_0 + U_0 |_{\tau'=0}^{\tau'=\tau} = 0$, and the equation becomes

$$\sum_{n=1}^{\infty} \left[\int_0^{\tau} niw T_n e^{ni\omega t} d\tau' + | (T_n + U_n) |_{\tau'=0}^{\tau'=\tau} e^{ni\omega t} \right] = 0 \quad . \quad (12)$$

So that for any order, $n=s$ say, we have ($e^{si\omega t}$ understood)

$$\int_0^{\alpha_s} T_s d\alpha_s' + | T_s + U_s |_0^{\alpha_s} = 0, \quad . \quad . \quad . \quad (13)$$

where it will be noted that $si\omega$ has been commuted (as is now permissible) and included in the imaginary angle

$$\alpha_s = si\omega\tau \quad . \quad . \quad . \quad . \quad . \quad . \quad . \quad (14)$$

α_s will be termed the transit angle of order s (the presence of i is understood when α is employed; a real transit angle is denoted by $\xi_s = s\omega\tau$).

Now for reasons which will appear shortly, it is desirable to introduce the angle $\beta_s = \alpha_s/2 [\theta_s = \xi_s/2]$, so that (13) becomes

$$\int_0^{\beta_s} 2T_s d\beta_s' + |\, T_s + U_s \,|_0^{\beta_s} = 0, \quad . \quad . \quad . \quad (15)$$

which states that as the transit half angle β_s' changes between 0 and β_s the sum of the kinetic and potential energy (of order s), together with the integral with respect to β_s of twice the kinetic energy (of order s), remains constant.

The integral term may now be regarded as potential energy arising from the storage of kinetic energy $2T_s$ over all values of the transit half angle β_s' corresponding to the path. Now, there is independent support for the contention that β_s may with advantage be regarded as a fifth (temporal) dimension expressed as an angle, but we can no more conclude from this that the stored energy resides in the fifth dimension than we could agree that the energy of a stretched spring is stored in the first dimension. We could agree, however, that the energy of a stretched spring is stored in the spring itself. A mouse caught in a trap would (if alive to tell the tale) presumably hold this view, even if it had heard of the ether.

Without committing ourselves to too concrete a picture, let us adopt the view that the integral term developed herein represents potential energy closely associated with the particle arising out of alternating components of kinetic energy which the particle may have. I was going to add "acquired," but such an addition would tend to restrict the results to cases where the possession of alternating kinetic energy is conditional on some outside source ($U_s \neq 0$). This, however, is not *essential*, since we may place $U_s = 0$ without affecting the validity of our equations. Thus we are then left with

$$|\, T_s \,|_0^{\alpha_s} + \int_0^{\alpha_s} T_s d\alpha_s' = 0, \quad . \quad . \quad . \quad . \quad (16)$$

so that

$$\frac{dT_s}{d\alpha_s} + T_s = 0,$$

$$T_s = (t)e^{-\alpha_s} = (t)e^{-2\beta_s} = (t)(\cos 2\beta_s - i \sin 2\beta_s), \quad . \quad (17)$$

where (t) represents any function of t. Alternatively, if (t) is of the type $e^{si\omega t}=e^{si\omega t_0+\alpha_s}$ then simply

$$T_s=(t_0), \quad . \quad . \quad . \quad . \quad . \quad . \quad (18)$$

where t_0 is the instant at which the particle commenced its journey. Whichever form we adopt it is evident that the past history of the particle is involved, and to this extent the result is in accordance with the findings of wave-mechanics.

The Velocity of the Waves.

In real notation

$$\begin{aligned} T_s&=(t)\ (\cos 2\beta_s - i \sin 2\beta_s) \\ &=\overline{T}_s \cos (s\omega t - 2\beta_s)\ \text{(say)}. \quad . \quad . \quad . \quad (19) \end{aligned}$$

If v is the wave velocity then must

$$\frac{\partial T_s}{\partial t}+v\frac{\partial T_s}{\partial r}=0. \quad . \quad . \quad . \quad . \quad . \quad (20)$$

Clearly if $\overline{T}_s$ varies with r we are going to get a cosine term and two sine terms. One way out of this difficulty appears to be to conclude that there must be two waves, of velocity v_1, v_2 such that

$$\left.\begin{aligned} si\omega(\overline{T}_s \cos 2\beta_s)+v_1\frac{\partial}{\partial r}(\overline{T}_s \sin 2\beta_s)=0, \\ si\omega(\overline{T}_s \sin 2\beta_s)+v_2\frac{\partial}{\partial r}(\overline{T}_s \cos 2\beta_s)=0. \end{aligned}\right\} \quad . \quad . \quad (21)$$

Now

$$\frac{\partial}{\partial r}=\frac{1}{\dot{r}}\frac{\partial}{\partial \tau}=\frac{si\omega}{2\dot{r}}\frac{\partial}{\partial \beta_s}, \text{ so that equations (21) become}$$

$$\left.\begin{aligned} \overline{T}_s \cos 2\beta_s+\frac{v_1}{2\dot{r}}\frac{\partial \overline{T}_s}{\partial \beta_s}(\sin 2\beta_s)+\frac{v_1 \overline{T}_s}{\dot{r}}\cos 2\beta_s=0, \\ \overline{T}_s \sin 2\beta_s+\frac{v_1}{2\dot{r}}\frac{\partial \overline{T}_s}{\partial \beta_s}(\cos 2\beta_s)+\frac{v_2 \overline{T}_s}{\dot{r}}(-\sin 2\beta_s)=0, \end{aligned}\right\} \quad . \quad (22)$$

giving

$$\left.\begin{aligned} v_1&=-\dot{r}\Big/\left\{1+\frac{\tan 2\beta_s}{2\overline{T}_s}\frac{\partial \overline{T}_s}{\partial \beta_s}\right\}, \\ v_2&=+\dot{r}\Big/\left\{\frac{\cot 2\beta_s}{2\overline{T}_s}\frac{\partial \overline{T}_s}{\partial \beta_s}-1\right\}. \end{aligned}\right\} \quad . \quad . \quad (23)$$

In the case where $\frac{\partial \overline{T}_s}{\partial \dot{\beta}_s}=0$, $v_1=v_2=-\dot{r}$; *i. e.*, there is no distinction between the two waves and we get a backward wave of velocity equal to the forward velocity of the particles. These conclusions break down, of course, if $\beta_s=\frac{n\pi}{4}$, where n is integral, for then either tan $2\beta_s$ or cot $2\beta_s$ is infinite. Actually $\frac{\partial \overline{T}_s}{\partial \dot{\beta}_s}\neq 0$ in general, so that it looks as though s_1 and v_2 have zeroes separated by $\pi/2$. In another case the wave fluctuates in velocity between zero and $+2\dot{r}$ in one case and between zero and $\pm\infty$ for

Fig. 1.

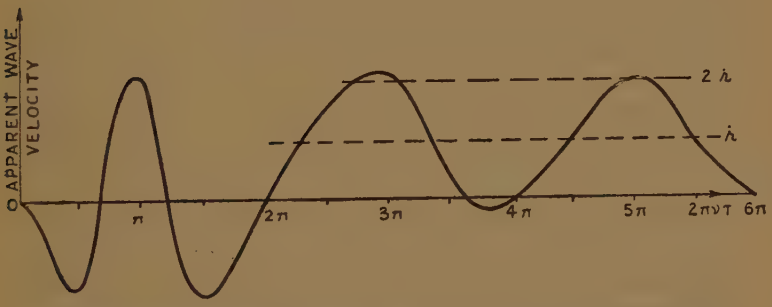

Alternating component of kinetic energy of charged particles represented in one possible way as equivalent to a plane wave, the velocity of which fluctuates between the limits $\dot{r}+\dot{r}$ and $\dot{r}-\dot{r}$, $\dot{r}$ being the particle velocity. As explained in the text, another possible interpretation would be as a five-dimensional wave of velocity $\dot{r}$ exactly.

the other, these last results being obtained by recourse to a known solution [7] in the case $s=1$, $U_s\neq 0$. The wave of immediate interest being the one which remains in the neighbourhood of the particle, this is plotted on fig. 1, with $2\pi\nu\tau$ as abscissæ. Except near the origin of $\nu\tau$ the function shown may be taken as varying in sinusoidal fashion between the values $v=0$ and $v=2\dot{r}$. Possibly the unvarying component $\dot{r}$ (see fig. 1) is to be regarded as the group velocity of the de Broglie waves.

It appears this component is the only one which remains associated with the particle, but there may be another interpretation. So far there is no sign of a wave of velocity $c^2/\dot{r}$. This limitation is probably due to the

neglect of retardation terms and of variations in m. The question of the direction and state of polarization of the waves is under investigation.

There are a variety of methods whereby the velocity of the waves may be arrived at. By one method the electrons in a space charge limited diode are possessed of spherical waves which depart from the electron with twice the velocity of the electron. By another method the waves are five-dimensional, the velocity still being twice that of the electrons. Five-dimensional waves of particle velocity would appear to occur if the problem is such that the electrons are (to a first approximation) moving with uniform velocity. The present paper must be regarded as of a provisional nature only. Clearly it will be necessary to arrive at a value for Planck's constant before real progress in the desired direction is possible. That this is by no means out of the question may be seen from Appendix I., in which a preliminary attempt shows distinct promise. It will be understood that, while there is difficulty in interpreting the factor 5, the result is arrived at purely on the basis of the experimental result $\lambda=\frac{(h)}{mv}$, Einstein's relation $(h)\nu=mc^2$, and the known laws of vacuum tube electronics under ideal boundary conditions (h) is treated as an unknown constant. The physical consequences of Appendix I. are briefly examined in Appendix II.

Transit Half Angle as Fifth Dimension.

The case for the above will be presented briefly. The electron kinetic energy may be written $T_0+mu_0u_1$, where u_1 is the electron velocity ripple, which, in a space charge limited diode of any geometry, neglecting the existence of a potential minimum in front of the cathode, is given by $u_1=|u_1|e^{-i\theta}$, where

$$|u_1|=[u_1]_{\theta=0}\frac{3}{\theta^2}\left[\frac{\sin\theta}{\theta}-\cos\theta\right]=[u]_{\theta=0}\frac{(2\pi)^{5/2}J_{3/2}(\theta)}{(8\pi^2/3)\theta_{3/2}}. \quad (24)$$

Compare this with van der Pol's solution (integrated over Ω_n) for an n-dimensional wave :—

$$u_n\frac{(2\pi)^{n/2}J_{n/2-1}(kr_n)}{(kr_n)^{n/2-1}}. \quad . \quad . \quad . \quad . \quad (25)$$

In equation (24), $8\pi^2/3$ represents the value of Ω_n in the case $n=5$, *i. e.*, is the solid angle in five dimensions; Ω_n would also have appeared in the denominator of (25), but for the particular method adopted in arriving at this result[5]. We have, therefore, the strongest reasons for regarding (24) as a five-dimensional wave function (weighted by the factor $[u]_{\theta=0}$) and, by comparison with (25) in the case $n=5$, we obtain

$$r_5=\theta/k=c_5\theta/\omega=c_5\tau/2, \quad . \quad . \quad . \quad . \quad . \quad (26)$$

where c_5 is the velocity appropriate to the waves.

Now, if θ is the fifth dimension expressed as an angle, transit angle functions, when integrated over all possible values of θ, should yield unity in the case where no weight function is involved. Now we are confined to positive values of θ, since τ cannot be negative, but there is no limit to the possible positive value of θ. In other words, our upper limit is $\underset{n\to\infty}{\mathrm{Lt}}\,(2n\pi)=\infty$. In a recent issue of 'Nature' (23. 7. 38), it was shown that the electron convection current, in our idealized problem of the Langmuir diode, when integrated for all values of θ from 0 to ∞, does, in fact, give the same answer as would also have been obtained had θ been taken as negligible. Thus †

$$\int_0^{i\infty} Y_3(2\zeta)\,d\zeta=\left|\frac{e^{-2\zeta}-1}{2\zeta}\right|_0^{i\infty}=1, \quad . \quad . \quad . \quad (27)$$

where $\zeta\equiv i\theta$.

The electron convection current ripple in a temperature limited diode is, however, dependent on the factor $\frac{\alpha}{2}Y_3(\alpha)$, or $\zeta Y_3(2\zeta)$. In order to take care of the "weight factor" ζ we must consider the value of

$$\underset{\zeta\to i\infty}{\mathrm{Lt}}\left[\zeta^{-1}\int_0^{\zeta} zY_3(2z)\,dz\right]. \quad . \quad . \quad . \quad . \quad (27)$$

We should expect the result to be zero in this case (since there is no alternating current on the "flat" part of the characteristic at low frequencies). In order to prove that this is so we take advantage of the identity

$$zY_3(2z)=Y_1(2z)-e^{-2z}, \quad . \quad . \quad . \quad . \quad (27\,b)$$

where

$$Y_1(\alpha)=\frac{1-e^{-\alpha}}{\alpha};$$

† ζ is now used as a symbol preferable to β (used earlier in the paper) to denote an imaginary half transit angle.

(27 *a*) then becomes (γ=Euler's constant)

$$\tfrac{1}{2}\operatorname*{Lt}_{\zeta\to i\infty}[\zeta^{-1}\{(\gamma+\log 2\zeta)+(e^{-2\zeta}-1)\}]=0. \quad . \quad (27\,c)$$

This last step beings out the fact that

$$\int_0^{i\infty} Y_1(\alpha)d\alpha(=\gamma+\log i\infty),$$

is a divergent integral. Fortunately, this does not upset things, since Y_1 always occurs weighted in some way. When Y_1 occurs alone (*i. e.*, not as part of Y_3 or αY_3) the weight factor is α. We thus require to find the value of

$$\begin{aligned}\operatorname*{Lt}_{\zeta\to i\infty}\left[\zeta^{-1}\int_0^{\zeta}2zY_1(2z)dz\right] &= \operatorname*{Lt}_{\zeta\to i\infty}\left[\zeta^{-1}\left|\frac{2z+e^{-2z}}{2}\right|_0^{\zeta}\right], \\ &= \operatorname*{Lt}_{\zeta\to i\infty}\left[\frac{2\zeta+e^{-2\zeta}-1}{2\zeta}\right], \\ &=1. \quad . \quad . \quad . \quad . \quad . \quad . \quad . \quad (28)\end{aligned}$$

This answer is again correct. Thus, in physics we have a term in the generalized diode impedance formula :

$$\frac{(i_c)_{0,\,t}}{id}\,\dot{x}_0\tau.\,Y_1(\alpha). \quad . \quad . \quad . \quad . \quad . \quad (29)$$

The steps leading up to the result (28) are equivalent to " borrowing " $\tau(=\alpha/i\omega)$ as weight function, and finally restoring the τ in virtue of having divided the weighted integral by α. Thus, to obtain the value of the term for small transit angles we just pick Y_1 out of the expression (its value being unity). It is important here to distinguish between small transit *angle* and small transit *time*. The latter may, indeed, be a very small quantity, but $(\dot{x}_0\tau)/d$ may not be so small compared with unity that it could be regarded as negligible. If we had had $\alpha Y_1(\alpha)$ and had obtained the result (28) (which we should have done), we should immediately have suspected an error, since at very low frequencies $\alpha Y_1(\alpha)\to 0$. In this way we see that, unlike $\tau Y(\alpha)$, $\alpha Y_1(\alpha)$ is foreign to physical applications.

So far we have encountered no result which conflicts in any way with the conception of $(-i\zeta)$ as fifth dimension. There are, however, cases where an apparent discrepancy arises. Thus, it may in some applications be difficult to assess what degree of weighting the function must have. Moreover, care must be taken to distinguish between weight factors which are truly invariant and those which,

although expressible, in any one geometry, as a function of the transit angle, are only so expressible through a space coordinate itself conditioned by the geometry. Thus, in equation (24), the weight factor $[u]_{\theta=0}$ is proportional to τ^2 *only* in a plane geometry. If the electrodes be curved the term in τ^2 would be only the first term of an infinite series in powers of τ (which may or may not be convergent). This is in contrast to the cases (αY_3) and (αY_1) previously considered, which may be shown to be truly invariant. In cases where weight functions not truly invariant occur we may try omitting the weight function. We then get (compare (24))

$$\int_{\theta=0}^{\infty} \frac{u_1}{[u_1]_{\theta=0}} d(i\theta) = \int_{\zeta=0}^{i\infty} Y_4(2\zeta) d\zeta = \tfrac{3}{2}.$$

Also

$$\int_{\theta=0}^{\infty} \frac{\tau_1}{[\tau_1]_{\theta=0}} d(i\theta) = \int_{\zeta=0}^{i\infty} Y_7(2\zeta) d\zeta = \tfrac{3}{4},$$

where τ_1 is known as the "first order variation (transit) time" and corresponds to fluctuations in path time about a mean value. The function Y_4 also corresponds to the transit angle factor for electrostatically induced current, but only is a weight function absent in the case of a plane geometry.

It may be mentioned that integration over all values of θ of the square of the modulus (or YY^*) of these wave functions gives values varying between $\pi/2$ in the case of Y_1 to $\frac{9\pi}{10}$ in the case of Y_7. While $(YY^*)<1$ in all cases, there is no question of this quantity representing a probability amplitude, as in wave mechanics, if only in view of the implicit negation of the uncertainty principle in transit time theory.

The physical quantities with which the above functions are associated in one application include those appearing below. The relation of the functions to Bessel functions of the half angle is noted in each case. By analogy with van der Pol's solution (equation (25) of this paper) the Y functions are in general mixed three and five dimensional wave-functions:—

$Y_1(\alpha)$ appears in generalized impedance formula.

$$Y_1(\alpha) = Y_1(2\zeta) = Y_1(2i\theta) = \frac{(2\pi)^{3/2}}{4\pi} \frac{J_{1/2}(\theta) e^{-i\theta}}{\theta^{1/2}}.$$

$\Upsilon_3(\alpha)$ electron convection current (ripple):

$$\Upsilon_3(\alpha)=\Upsilon_3(2i\theta)=\sqrt{\frac{\pi}{2\theta}}\,[J_{1/2}(\theta)-iJ_{3/2}(\theta)]e^{-i\theta}.$$

$\Upsilon_4(\alpha)$ electron induced current ; electron velocity (ripples):

$$\Upsilon_4(\alpha)=\Upsilon_4(2i\theta)=\frac{(2\pi)^{5/2}}{(8\pi^2/3)}\frac{J_{3/2}(\theta)}{\theta^{3/2}}e^{-i\theta}.$$

$\Upsilon_7(\alpha)$ space charge density ; transit time (ripples):

$$\Upsilon_7(\alpha)=\Upsilon_7(2i\theta)=\frac{(2\pi)^{5/2}}{(8\pi^2/3)}\{\theta J_{1/2}(\theta)-\theta iJ_{3/2}(\theta)-J_{3/2}(\theta)\}e^{-i\theta}/2\theta^{3/2}.$$

These functions are obtained in any number of space dimensions starting with an equation of the type

$$\frac{d}{d\tau}(r^{n-1}\ddot{r})=\frac{4\pi\frac{e}{m}c^2}{\Omega_n}\bar{i}, \quad . \quad . \quad . \quad . \quad (29)$$

where $\frac{d}{d\tau}$ (and the fluxions) denote differentiation following the particle, the instant t_0 being held constant during integrations ($\tau=t-t_0$), $\bar{i}$ is the total current in the case $n=3$. For $n=1$, i is the total current density. The mode of solution adopted will be published elsewhere. Solutions hitherto available in the case $n=2$ have been in such a form as to conceal the identity (and so the invariance) of the Υ functions.

Appendix I.

The connexion between the velocity of electrons and the wave-length λ of the corresponding waves, namely,

$$\lambda=\frac{h}{mv}, \quad . \quad . \quad . \quad . \quad . \quad . \quad . \quad . \quad (i.)$$

may be replaced by using Einstein's relation to replace λ, as follows :—

$$(h)=mv\lambda=mv\frac{dv}{dv}, \quad . \quad . \quad . \quad . \quad . \quad . \quad (ii.)$$

where (h) is, for the present, regarded as an unknown to be determined.

The nature of the curve of fig. 1 suggests that v changes in steps of $1/\tau$ between energy maxima. Actually, since in the space charge limited diode (with initial velocities

zero); (v=electron velocity; x_1=distance apart of plates)

$$\left.\begin{aligned} \ddot{v} &= 4\pi\frac{ec^2}{m}.\bar{\iota}, \\ \dot{v} &= 4\pi\frac{ec^2}{m}.\bar{\iota}\tau, \\ v &= 2\pi\frac{ec^2}{m}.\bar{\iota}\tau^2, \\ \iota &= \frac{3e}{\tau}.\mathrm{N}^{2/3}.\mathrm{N}^{1/3}x_1, \\ \mathrm{N} &= \left(2\pi\frac{e^2}{m}c^2\tau^2\right)^{-1}, \end{aligned}\right\} \quad . \quad . \quad . \quad . \quad . \quad \text{(iii.)}$$

we obtain by elimination of ι and partial elimination of N, writing $\mathrm{N}x_1^3=n$=number of electrons in cube of side x_1,

$$(h)=3^3.2\pi e^2c\left[\frac{d(-1/\tau^{2/3})}{d(v^{2/3})}\right]_n^{3/2}=1{\cdot}3043\times10^{-27}\left[\frac{d(-\tau^{-2/3}}{d(\ ^3(v^{2/}}\right]_n^{3/2}, \quad . \quad . \quad . \quad \text{(iv.)}$$

which is based on $e=1{\cdot}601\times10^{-20}$ (e.m.u.)†. If the constant shown is $h/5$ then $h=6{\cdot}521(5)\times10^{-27}$ erg sec., and

$$\left[\frac{d(-\tau^{-2/3}}{d(5\nu)^{2/3}}\right]_n^{3/2}=1. \quad . \quad . \quad . \quad . \quad . \quad \text{(v.)}$$

Appendix II.

The importance of Appendix I. lies in that it brings out the value, in an idealised example, of the fine structure constant $2\pi e^2c/h$ in terms of the frequency ν, the time interval τ, and n, a measure of the total number of electrons taking part.

If we take $\nu=0$ when $\tau=\infty$, and keep n constant, equation (iv.) gives, on integration and simplification,

$$\nu\tau=3^3\frac{2\pi e^2c}{(h)}n. \quad . \quad . \quad . \quad . \quad . \quad . \quad \text{(vi.)}$$

Taking $\dfrac{2\pi e^2c}{(h)}=\dfrac{1}{135}$, as before, we have

$$2\pi\nu\tau=\frac{2\pi n}{5}. \quad . \quad . \quad . \quad . \quad . \quad . \quad \text{(vii.)}$$

† H. R. Robinson, 'Nature,' vol. cxlii. pp. 159–160 (July 23, 1938).

The space charge limited diode is characterized by negative resistance regions, analogous to the eigen states of excited atoms or molecules. These regions are shown lightly shaded in fig. 2, borrowed from an earlier paper (Elec. Comm. xi., 39, p. 223, 1933 ; see also J. I. E. E. 78, p. 663, 1936).

Fig. 2.

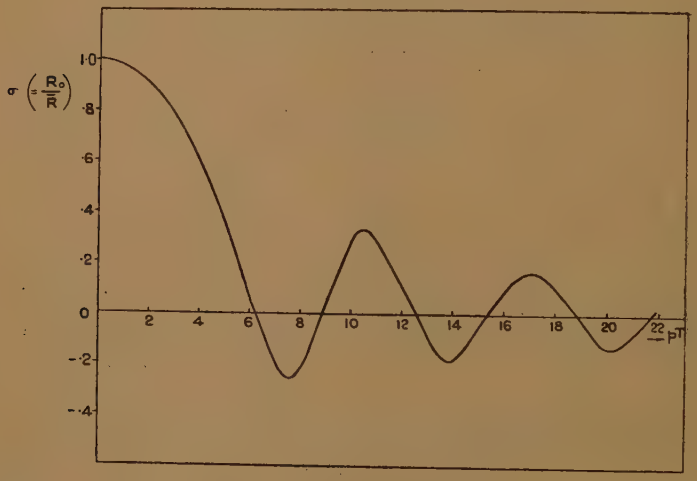

Owing to the so-called "degeneracy" of the system these regions are broad though quite clearly defined. The negative maxima are given to sufficient accuracy by

$$2\pi\nu\tau = \left(2s + \frac{1}{2}\right)\pi \quad \ldots \ (s = 1, 2, 3, \ldots). \qquad \text{(viii.)}$$

Eliminating $\nu\tau$ between equations (vii.) and (viii.), we obtain those values of n for which the electrons do work on the exciting agent (rather than *vice versâ*) :

$$n = 5s + \frac{5}{4} \quad \ldots \ (s = 1, 2, 3 \ldots). \qquad \text{(ix.)}$$

Since n is reckoned per cube of side x_1, there is no need for n to be integral. It is of interest to note that according to the above development the discontinuities hitherto associated with energy may actually be translated in terms of the discreteness of matter.

References.

(1) Oliver Heaviside, ' Electromagnetic Theory,' vol. i. (Electrician Series), pp. 68 & 69.
(2) H. A. Lorentz, ' Collected Papers ' (Rede Lecture, Cambridge, 1924).
(3) Sir O. Lodge, ' Electrons,' p. xi (Geo. Bell & Sons, 1906).
(4) This displacement current may be fictitious for the space between the condenser plates, though it exists in the circuit attached to the condenser plates, the value obtained by direct action of surface charges, one on the other, agreeing precisely with the Maxwellian value.
(5) Balth. van der Pol, ' Physica,' iii. pp. 385–392 (June 1936).
(6) Thomson and Tait, ' Natural Philosophy,' p. 279, gives the usual classical solution $T+U=$constant.
(7) W. E. Benham, Phil Mag. v. equ. (21), p. 648 (1928). See also W. E. Benham, Proc. I. R. E. 26, 9, pp. 1093–1170 (1938); Johannes Müller, Hochfreqenztechnik und Elektroakustik, 51, pp. 121–127 (1938).

LXXXIX. *The Surface Migration of Barium.* *By* M. Benjamin, *Ph.D.*, *and* R. O. Jenkins, *Ph.D.** (Communication from the Research Staff of the M.O. Valve Co., Ltd., at the G.E.C. Research Laboratories, Wembley, England.)

[Received September 21, 1938.]

[Plates XI.–XV.]

Summary.

It is found that under similar vacuum conditions barium does not migrate over tungsten, although thorium does. It is also shown that barium does not migrate over nickel.

Introduction.

A series of experiments was made by J. A. Becker (1), (2) in which he showed that barium and thorium migrate over metal surfaces. In his method the barium or thorium was fired on to one face of a tungsten strip, and the emission from both faces was recorded. The strip was then flashed at a suitable temperature, and it was found that after a time the emission from the clean side had risen whilst that from the contaminated side

* Communicated by C. C. Paterson.

had fallen to a value which indicated that the contaminating film had spread itself evenly over both faces of the strip.

We have been carrying out an electron microscope examination of the emission from barium/strontium oxide on nickel, and in the course of our experiments we have observed frequently that if a small patch of emitting material was present on a nickel surface, active material spread itself over the uncoated nickel in a non-uniform manner. It was seen that when there were irregularities in the nickel surface, those parts which were shielded from the oxide patch remained non-emitting, but that the surface surrounding such parts became covered in a way which suggested that active material was evaporating from the oxide patch.

This effect had previously been observed by Brüche[3], who came to the conclusion that the active material left the oxide in "atomic rays" and that there was no evidence of any surface migration. It is well known that the active material evolved from an oxide cathode is mainly barium, and Brüche's results, together with our observations, led us to carry out a series of experiments on the surface migration of barium.

Experimental.

Three separate experiments have been carried out for the detection of barium migration. Firstly, a nickel surface was provided with a step which acted as a barrier to any evaporating material, and the behaviour of a layer of emitting oxide was followed in the electron microscope. Secondly, barium was deposited on to one face of strips of nickel and tungsten respectively, and the thermionic emission from each side measured. Thirdly, barium and thorium respectively were thrown on to one side of a tungsten wire, and the movements of the deposited layers observed in a one-dimensional microscope.

The preliminary results of the first two experiments have already been reported[4].

I. *The Electron Microscope Experiment.*

The electron microscope and the general method of use have been described in a recent publication[5].

A nickel cathode, of rectangular section $1{\cdot}5 \times 2{\cdot}5$ mm. and 26 mm. in length, had welded across half of one flat

face a piece of nickel sheet 0·12 mm. thick. The arrangement is shown in fig. 1. Barium carbonate coating was then placed on the cathode DE so that it extended from the shoulder AD for a distance of 5 mm. to the point C. The coating thickness was 0·05 mm. The cathode was mounted with the face ECDAB facing the electron lens, and the coating was out-gassed.

The cathode was then run at 973° K., and the surfaces AB and EC were examined at frequent intervals. After two hours no movement of any emitting material beyond the edges C or A could be detected. The cathode temperature was then raised to 1073° K. and 1173° K. in turn, and the procedure repeated with similar results. At 1273° K. it was observed that in about thirty minutes the nickel adjacent to the coating edge C had begun

Fig. 1.

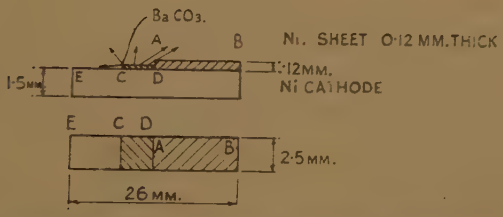

Stepped cathode for electron microscope experiment.

to emit, and in a few hours the emission had spread over the surface CE for a distance of 0·1 mm. from the coating edge, as shown in fig. 2. (Pl. XI.). During this period no sign of any emission on the surface AB was seen. The photographs in fig. 2 (Pl. XI.) indicate that evaporation of active material has occurred in a manner indicated by the arrows in fig. 1, and that the edge A has prevented any evaporated material from reaching the face AB.

If surface migration had taken place then emission should have been seen extending from A over AB, for the distance from the coating surface to A is less than 0·1 mm.

II. *The Thermionic Experiment.*

(i.) *The Tube.*

A diagram is shown in fig. 3. The tube was similar to that described by Becker and Brittain [6] for their

thorium-on-tungsten experiment. A strip S of nickel or tungsten was surrounded about its centre portion by anodes A, 10 mm. in length. Opposite the centre of each face of the strip was a source of barium B. The anodes AG acted as guard anodes, and opposite the edges of the strip were guard-plates P. The whole electrode system was supported from a pinch and glass beads, and the various anode leads were taken out through the walls of the glass envelope. A directed barium getter Q was arranged to fire into the well of the tube.

(ii.) *The Barium Source.*

If a mixture of barium and beryllium oxides in the molecular proportions of 1 : 3 is fired in hydrogen a

Fig. 3.

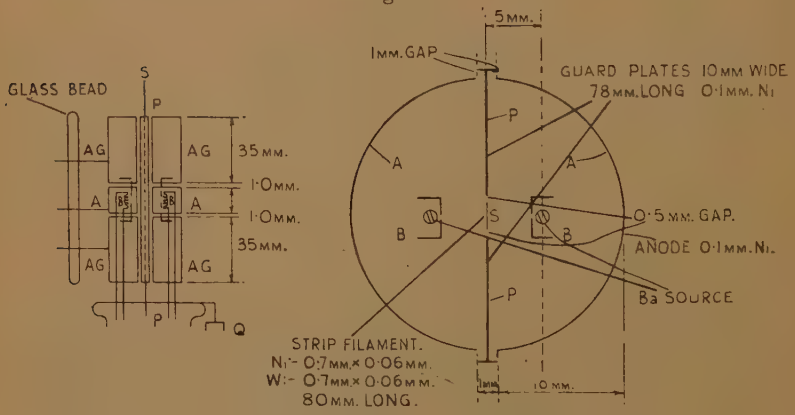

Tube for thermionic experiment.

double oxide of barium and beryllium is obtained. This compound is quite stable in air, and when heated at 1473° K. in a vacuum in contact with tantalum the compound reacts with the tantalum to give free barium and the stable beryllium tantalate. The only gas evolved during the reaction is surface gas. This can be removed by first heating the reaction mixture at about 1200° K. On raising the temperature to 1470° K. a very pure barium is obtained. In the experiment, the barium-beryllium compound was coated on to a coil of tantalum wire which could be heated by passing a current through it. The coil was surrounded by a metal shield with a 1·0 mm.

hole in it opposite the centre of the strip, so that barium could be deposited on the centre part of the strip only.

(iii.) *Experimental Procedure.*

The tube was evacuated and baked on a three-stage mercury diffusion-pump using liquid air. The electrodes and getter were out-gassed by high-frequency heating, and the tantalum coil was out-gassed by heating at 1200° K. In the case of the nickel the strip was heated at 1200° K. for one hour to clean it. The tungsten strip was heated for several hours at 2800° K. The getter was then dispersed and the tube sealed off.

The tube was set up so that the emissions to the two anodes AA could be read simultaneously. The guard anodes AG and the guard-plates P were also connected to the H.T. supply.

The strip in each case was set at about 970° K., and the emission read. Barium was then slowly dispersed on to the cold strip by heating one of the tantalum coils at 1473° K., and emission measurements were made every few seconds. The emission from the contaminated side rose until it reached a maximum. Barium was dispersed until the emission had just passed through a maximum. The barium gun on each side was then connected to the anode surrounding it, and the strip was set to run at various temperatures in turn. Emission measurements from each side of the strip were made at frequent intervals with the anodes at 350 v. After a set of observations the tungsten strip could be cleaned by flashing it, and the experiment repeated either by dispersing more barium from the first gun or by dispersing the barium from the second gun. In this way either face of the strip could be contaminated in turn. In the nickel case it was not possible to clean the strip completely without nickel evaporation occurring.

Sets of typical emission-time readings for nickel and tungsten are shown in Tables I. and II.

Referring to these tables, it will be seen that over a temperature range of 900–1100° K. no increase in the emission from the clean side takes place simultaneously with a decrease in the emission from the contaminated side even after two hours' running. The emission from the latter changes very little until the temperature exceeds 1100° K., when it begins to fall. The initial

emission from the clean side of the nickel and tungsten is considerably less than 1 per cent. of that from the contaminated side. The apparent initial emission from the clean side must be stray current from the other

TABLE I.

Variation of Emission from Ba on Ni with Time of Flashing.

I_1=current from contaminated side.
I_2= ,, ,, clean side.

Flashing temperature 830° K.			Flashing temperature 910° K.		
Time mins.	$I_1 \cdot 10^{-8}$ amps.	$I_2 \cdot 10^{-10}$ amps.	Time mins.	$I_1 \cdot 10^{-6}$ amps.	$I_2 \cdot 10^{-9}$ amps.
0	1·5	<1	0	2·0	4·2
20	1·5	<1	20	1·4	3·5
50	1·5	<1	50	1·2	3·2
80	1·5	<1	80	1·0	3·2
120	1·5	<1	120	1·0	3·2

Flashing temperature 960° K.			Flashing temperature 1100° K.		
Time mins.	$I_1 \cdot 10^{-5}$ amps.	$I_2 \cdot 10^{-8}$ amps.	Time mins.	$I_1 \cdot 10^{-4}$ amps.	$I_2 \cdot 10^{-7}$ amps.
0	1·5	2·2	0	1·6	3·3
30	2·0	4·0	10	1·8	3·3
60	2·2	3·5	20	1·8	3·2
120	2·3	2·8	40	1·6	2·5
240	2·0	2·2	60	1·1	1·9

side reaching the anode in spite of precautions taken. This view is supported by the fact that the emissions from both sides rise and fall together.

From Becker's (1932) results, assuming initially 0·8 monomolecular layers of barium on the contaminated side, migration would be complete in about two hours at 1000° K. During this time the emission of the contaminated side should fall, while that of the other side should rise until both are equal. The final covering at this point would be 0·4 layers on each side, and would give an emission

according to Becker's curves of only 1/3000 of its initial value.

In our experiments it is possible that the stray emission masked the small rise in emission to be expected from

TABLE II.

Variation of Emission from Ba on W with Time of Flashing.

I_1 = current from contaminated side.

I_2 = „ „ clean side.

Flashing temperature 870° K.			Flashing temperature 970° K.		
Time mins.	$I_1 \cdot 10^{-6}$ amps.	$I_2 \cdot 10^{-9}$ amps.	Time mins.	$I_1 \cdot 10^{-5}$ amps.	$I_2 \cdot 10^{-9}$ amps.
0	1·6	1·0	0	1·0	1·2
10	1·7	1·0	20	1·8	1·2
20	1·8	1·0	40	2·1	1·2
40	1·7	1·0	70	2·3	1·2
60	1·7	1·0	100	2·4	1·2

Flashing temperature 1020° K.			Flashing temperature 1120° K.		
Time mins.	$I_1 \cdot 10^{-5}$ amps.	$I_2 \cdot 10^{-9}$ amps.	Time mins.	$I_1 \cdot 10^{-4}$ amps.	$I_2 \cdot 10^{-7}$ amps.
0	9·5	5·6	0	2·4	9·0
20	9·4	5·4	20	2·4	9·0
40	9·3	5·1	40	2·4	9·0
70	9·2	4·7	70	2·4	9·0
100	9·2	4·5	100	2·4	9·0

the clean side, but, on the other hand, the emission from the contaminated side never fell by more than 40 per cent. of its original value, and then only at the higher temperature where evaporation must have been occurring. It therefore appears that a barium film is stable on nickel and tungsten until the temperature is such that appreciable evaporation can occur. Below this temperature no surface migration takes place.

III. *The Round Wire Experiment.* W–Ba *and* W–Th.

The two previous experiments were carried out on strips. The following experiment with a tungsten wire was

suggested to us by Dr. I. Langmuir. The tube used is shown in fig. 4, and is similar to that described by Johnson & Shockley[7] in their thoriated tungsten experiments.

A tensioned tungsten wire W, 0·12 mm. in diameter and 110 mm. in length, was mounted on a pinch, and was surrounded by a spiral nickel wire anode A, 35 mm.

Fig. 4.

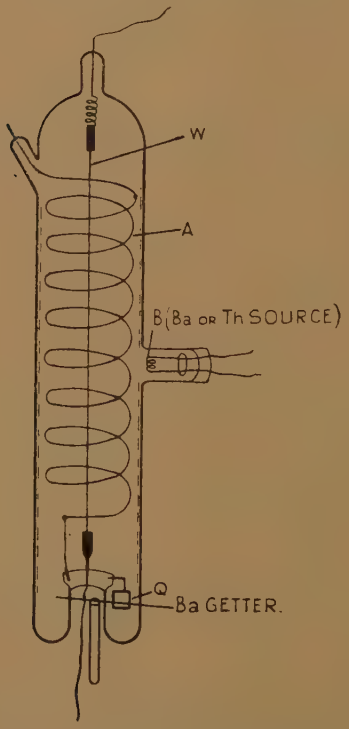

Tube for round wire experiment.

in diameter. In a side tube opposite the centre of the filament was a coated tantalum coil as a source of barium, or a piece of thorium * wire as a source of thorium.

The inside wall of the bulb was coated with a thin film of willemite, W. Attached to the pinch was a directed barium getter, Q.

* We are indebted to the Director of the Westinghouse Laboratories for this wire.

If the filament in such a tube is run at a temperature such that its emission is saturated by a high voltage applied to the anode an electron image of the wire surface is thrown on to the fluorescent walls of the tube. The device magnifies only across the diameter of the wire, and not along the length, and with the arrangement described a magnification of about 300 is obtained. If now barium or thorium is fired from the side-tube on to one side of the filament, the extent of the deposit and the intensity of emission due to it can be seen. Also any movement of the contaminating film can be seen.

The experimental procedure was as follows :—

The tube was baked and the getter and barium or thorium source out-gassed.

The tungsten filament was run at 2800° K. for several hours, the getter dispersed, and the tube sealed off. The filament was then run at 2800° K. until its emission, measured at 1873° K., was steady and of the order to be expected from a clean tungsten surface. (By switching on the H.T. it could be seen by an examination of the image whether the tungsten was emitting uniformly and whether it was free from any traces of barium from the getter.)

The barium or thorium was then evaporated on to the cold filament, and the emission measured at a reduced filament temperature with 2000 v. applied to the anode. The deposition was continued until just more than an optimum layer was obtained.

The emission was recorded and the electron image photographed. The tungsten filament was set to run at a fixed temperature, with no anode volts applied, for several hours, and emission and photographic records were made at frequent intervals at the reduced measuring temperature. The temperature of the filament was then raised and the process repeated.

The experimental results obtained are set out below.

Thorium on Tungsten.

The tungsten filament was flashed until at 1823° K. its emission was stable and equal to 190 μA. The temperature of the filament was reduced to 1250° K. and the emission measured. Thorium was then dispersed by heating the thorium wire at 1650–1700° K., and the

emission from the contaminated tungsten filament was measured frequently at 1250° K. during the process. The change in the tungsten emission is shown in Table III.

The tungsten filament was then set at 1535° K. and at frequent intervals the emission and images recorded. After 13½ hours the tungsten filament was raised to 1650° K. and the procedure repeated. In Table IV. are

Table III.

Showing Change in Tungsten Emission as Thorium Deposited. Measurements at 1250° K., E_A =2000 v.

W emission	μA.	0	0	10	14	17	14
Time of deposition at 1650° K...	hrs.	0	1	5	7	20	22

Table IV.

Change in W–Th Emission with Time of Flashing.

Emission at 1250° K. .	μA.	14	15	18	16	14	11·5	10·5		10·5	10	
Flashing temperatures.....	1535° K.	..	..	..	..	..	..	..	1655° K.			
Time of flash.	hours.	0	0·3	0·5	1·5	2·5	6·5	13·5	..	0	3	7
Fig. 5 (Pls. XII. & XIII.)	..	1	..	2	3	4	5	6	..	6	7	8

shown the emissions, and in fig. 5 (Pls. XII. & XIII.) the photographic record is shown.

Referring to fig. 5, no. 1 (Pl. XII.), it will be seen that initially half the filament is covered with thorium. After ½ hour at 1535° K. migration is obviously proceeding over one crystal. After 1½ hours thorium is seen moving over the crystals, and migration then proceeds at a continuously decreasing speed for the next 12 hours. On raising the tungsten temperature to 1655° K. the migration is speeded up, and is complete in 7 hours. During the flashing the filament emission at first rises and then commences to fall, and the changes in emission are those

that are to be expected from the results of Becker and Brittain if just more than an optimum layer was originally deposited and migration has occurred. The results leave no doubt that thorium migrates exactly in the way described by Becker and Brittain.

Barium on Tungsten.

The same pumping and flashing treatment as for the thorium tube was used.

Barium was then evaporated on to the cold tungsten filament by flashing the tantalum coil at 1473° K. The evaporation was stopped when the emission of the tungsten had just passed its maximum value.

The details are given in Table V.

TABLE V.

Showing Change in Tungsten Emission as Barium Deposited.

Tungsten emission at 1013° K.	μA.	0	50	80	94	72	60
Time of flashing of barium source at 1473° K.	sec.	0	45	55	56	71	86

The tungsten filament was then run at 923° K. for several hours, and the emission and electron image recorded at various periods. The temperature was then steadily increased in steps, and the procedure repeated. The emission results are given in Table VI. and the photographic record is shown in fig. 6 (Pl. XIV.).

Referring to fig. 6 (Pl. XIV.) it is clear that after 18 hours at 923° K. very little change to the extent of the barium deposit has occurred, and there is no evidence of migration (Pl. XIV. fig. 6, nos. 1 and 2). (The streaky fluorescence on the clean side of the tungstenis due to charges on the willemite.)

The emission figures show that some slight evaporation of the deposited layer has occurred, for the emission has passed through an optimum. At 1013° K. after 5½ hours (Pl. XIV. fig. 6, no. 3) there is evident evaporation from the hot centre of the filament, but apart from one spot marked with an arrow A there is no sign of migration. After 21½ hours (Pl. XIV. fig. 6, no. 4), evaporation is

more marked, and apart from the spot A and a second spot B no migration is evident.

After $2\frac{1}{2}$ hours at 1063° K. (Pl. XV. fig. 6, no. 5) marked evaporation is occurring, and spot A has also disappeared.

Table VI.

Variation of Emission of W–Ba with Time of Flashing.

Tungsten emission at 1013° K...	μA.	60	90	89	80	72
Temp. of flash	923° K.					
Time	hrs.	0	0·1	2	4	18
Fig. 6 (Pl. XIV.)	1	..	..	..	..	2

Tungsten emission at 1013° K.	..	72	68	67	50	34
Temp. of flash	1013° K.					
Time of flash	hrs.	0	0·9	2	5·5	21·5
Fig. 6 (Pl. XIV.)	..	2	..	..	3	4

Tungsten emission at 1013° K....	..	34	24	22	16	..	16	12	7
Temperature of flash	1063° K.	..	..	..	..	1133° K.			
Time of flash	..	0	2	2·5	7	..	0	0·5	1
Fig. 6 (Pl. XV.)	..	4	..	5	6	..	6	..	7

After 7 hours (Pl. XV. fig. 6, no. 6) spot B has also gone and evaporation is still more evident. After 1 hour at 1133° K. evaporation is very marked, and apart from a new spot at C, not related to the previous spots A and B, there is still no evidence of migration. Over this period of 50 hours flashing the emission has fallen from a maximum of 90 μA. to 7 μA., a change of 13 : 1, whereas a change of the order of 3000 : 1 is to be expected from Becker's curve (*loc. cit.*).

Pseudo Migration of Barium Atoms.

The spots A, B, and C, which have been mentioned as appearing at different times, are, we believe, due to evaporating barium condensing on the filament. We have observed that when the bariated filament is flashed at such a temperature that evaporation of barium is occurring, and the H.T. volts are applied, barium returns to the filament.

This effect is illustrated by the following experiment.

The filament, after barium deposition, was flashed at 1323° K. for a few seconds with H.T. on the anode. Various emitting spots appear over the tungsten, and on lowering the tungsten temperature to 1013° K. barium appears at various points on the filament and the filament appearance gives the impression of barium having migrated. The appearance of the filament after treatment in the way described is shown in fig. 6 (Pl. XV. no. 8).

We believe that evaporating barium atoms, ionized by the field due to the anode voltage, are returned as ions to the filament. In fig. 6 (Pls. XIV. & XV. nos. 3, 4, 5, 7) the spots A, B, and C only occur when evaporation is present, and in our experiments it is possible that a few evaporating barium atoms were present when the anode voltage was switched on for recording purposes; or, alternatively, evaporating barium atoms simply recondensed on the filament when the temperature of the filament was lowered to the measuring temperature.

Discussion.

The foregoing results show that under various conditions such that thorium migrates over tungsten no surface migration of barium is observed.

The barium film appears to be quite stable until evaporation occurs.

This latter result is in accordance with the results of the thermionic experiment on nickel and tungsten.

The electron microscope experiment leads to a similar conclusion, although in this case the barium is derived from barium oxide.

These results for barium do not accord with Becker's observations, although the thorium result is in complete agreement with Becker and Brittain's results. We

believe that in thermionic and wire experiments the barium source yielded a very pure barium; and since the vacuum technique used was that applied to thermionic valves the sealed-off pressure was at most 10^{-7} mm. Hg. In the electron microscope experiment no getter was used, but the tube was continuously evacuated, and a pressure of 10^{-5} mm. Hg. was being obtained. In the latter experiment the appearance of the emitting nickel surface (which shows up the crystal structure of the nickel) is exactly what would have been seen had a monatomic film of barium been deposited on the nickel from an independent source. It is a difficult matter, however, to prove that the emitting nickel is covered by a monatomic film of barium and not by a film of barium and/or barium oxide.

The experimental results lead to the conclusion that barium, whether obtained from barium oxide or from a pure barium source, does not migrate over the surface of nickel or tungsten.

The fact that barium derived from an oxide cathode does not migrate has a practical application. In the manufacture of oxide cathodes for electron optical devices it is sometimes necessary to confine the emitting area to a given surface. This condition can be assured during operation of the device by either shielding the uncoated cathode from the coating, so that no deposition of active material occurs, or by operating the cathode at such a temperature that no appreciable evaporation of barium occurs.

Acknowledgments.

In conclusion, we desire to tender our acknowledgments to the General Electric Co. and the Marconiphone Co., on whose behalf the work which has led to this publication was done.

References.

(1) J. A. Becker, J. Am. Electric Chem. Soc. lv. p. 153 (1929).
(2) J. A. Becker, Trans. Far. Soc. xxviii. p. 152 (1932).
(3) E. Brüche, *Zeit. f. Phys.* xcviii. p. 93 (1935–36).
(4) M. Benjamin and R. O. Jenkins, ' Nature,' cxl. no. 3534 (1937).
(5) M. Benjamin, R. J. Huck, and R. O. Jenkins, Proc. Phys. Soc. l. (1938).
(6) J. A. Becker and W. H. Brittain, Phys. Rev. xliii. (1933).
(7) R. P. Johnson and W. Shockley, Phys. Rev. xxxvi. (1936).

XC. *Paraboloidal Coordinates.*

By H. Bateman, *Ph.D., F.R.S.*†

[Received August 12, 1938.]

§1. LET $x=w\cos\phi$, $y=w\sin\phi$, $w=2\alpha\beta$, $z=\alpha^2-\beta^2$, so that w, z, ϕ are cylindrical coordinates and α, β, ϕ paraboloidal coordinates. When the functions $f(t)$, $G(s)$, $F(u)$. $V(z)$ have suitable properties the well-known integrals

$$V=\int_0^\infty [(z+t)^2+w^2]^{-\frac{1}{2}}f(t)\,dt, \quad . \quad . \quad . \quad (1.1)$$

$$V=\int_0^\infty e^{-sz}J_0(sw)G(s)\,ds, \quad . \quad . \quad . \quad . \quad (1.2)$$

$$V=2\int_0^\infty K_0(2\alpha\sqrt{u})J_0(2\beta\sqrt{u})F(u)\,du, \quad (1.3)$$

$$V=(1/\pi)\int_0^\pi V(z+iw\cos\theta)\,d\theta, \quad . \quad . \quad . \quad (1.4)$$

represent symmetrical potential functions, and the functions are connected by the usual integral equations

$$G(s)=\int_0^\infty e^{-st}f(t)\,dt, \quad . \quad . \quad . \quad . \quad . \quad . \quad . \quad (1.5)$$

$$sG(s)=\int_0^\infty \exp.(-u/s)F(u)\,du, \quad . \quad . \quad . \quad . \quad (1.6)$$

$$F(u)=\int_0^\infty J_0(2\sqrt{tu})f(t)\,dt, \quad . \quad . \quad . \quad . \quad . \quad (1.7)$$

$$V(z)=\int_0^\infty e^{-sz}G(s)\,ds=\int_0^\infty (z+t)^{-1}f(t)\,dt, \quad . \quad (1.8)$$

$$V(z)=2\int_0^\infty K_0(2\sqrt{zu})F(u)\,du, \quad . \quad . \quad . \quad . \quad (1.9)$$

which are discussed in some detail in Titchmarsh's recent book on the Fourier integral. In the cases to be considered here the changes in the order of integration involved in the derivation of these equations do not generally present any difficulty.

§2. The integral equation (1.6) is suggested by the well-known formula

$$2K_0(2\alpha\sqrt{u})J_0(2\beta\sqrt{u})=\int_0^\infty \exp.(-sz-u/s)J_0(sw)\,ds/s \quad (2.1)$$

† Communicated by the Author.

for a potential function with the axial value $2K_0(2\sqrt{zu})$, where the function $K_0(t)$ is defined by the equation [2]

$$2K_0(2\sqrt{zu}) = \int_0^\infty \exp.\,(-sz - u/s)\,ds/s \quad z>0,\ u>0. \qquad (2.2)$$

The relation (1.7) is suggested by the known relation [3]

$$[(z+t)^2+w^2]^{-\frac{1}{2}} = 2\int_0^\infty K_0(2\alpha\sqrt{u})J_0(2\beta\sqrt{u})J_0(2\sqrt{tu})\,du. \qquad (2.3)$$

The symmetrical potential V of §1 can also be expressed in the form

$$V = \int_0^\infty K_0(sw)\cos(sz)C(s)ds - \int_0^\infty K_0(sw)\sin(sz)S(s)\,ds, \qquad (2.4)$$

where the usual expressions for $C(s)$, $S(s)$ are

$$C(s) = (2/\pi)\int_0^\infty \cos(st)f(t)\,dt, \qquad (2.5)$$

$$S(s) = (2/\pi)\int_0^\infty \sin(st)f(t)\,dt. \qquad (2.6)$$

The functions $f(\mu)$, $G(s)$, $F(u)$, $V(z)$, $C(s)$, $S(s)$ will now be assembled in some interesting cases.

§3. *Case* 1.

$$f(t) = (1+t)^{-1}P_n\left(\frac{t-1}{t+1}\right) = f_n(t), \qquad (3.1)$$

say, $P_n(\mu)$ being the Legendre polynomial. The integral (1.1) may be evaluated by putting $\mu(t+1)=t-1$. If $r^2=z^2+w^2$, $R^2=(z-1)^2+w^2$, $R\bar{u}=r+1$, $R\bar{v}=r-1$, we have

$$V = (2/R)Q_n(\bar{u})P_n(\bar{v}), \qquad (3.2)$$

where $Q_n(u)$ is the Legendre function of the second kind.

The formula (1.7) gives $F(u)=S_n(0, 4u)$, where

$$S_n(a, b) = \int_0^\infty J_0[(a+bt)^{\frac{1}{2}}]f_n(t)\,dt. \qquad (3.3)$$

The formula (1.5) gives $G(s)=V_n(s)$, where $V_n(s)$ is a function used in some former papers [4], [5], [6]. The relation (1.6) now gives the new representation

$$sV_n(s) = \int_0^\infty \exp.\,(-u/s)S_n(0, 4u)\,du. \qquad (3.4)$$

By a known formula or by (3.2) the function $V(z)$ is

$$V(z)=\int_0^\infty e^{-sz}V_n(s)\,ds=\frac{2}{z-1}Q_n\left(\frac{z+1}{z-1}\right)=g_n(z), \text{ say,} \quad (3.5)$$

and the relation (1.9) becomes

$$g_n(z)=2\int_0^\infty K_0(2\sqrt{zu})S_n(0, 4u)\,du. \quad . \quad . \quad (3.6)$$

The relations (2.5), (2.6) indicate that in the present case

$$\pi C(s)=V_n(is)+V_n(-is)=\pi C_n(s), \text{ say,} \quad . \quad (3.7)$$

$$i\pi S(s)=V_n(-is)-V_u(is)=i\pi S_n(s), \text{ say.} \quad . \quad (3.8)$$

This case is of considerable interest because the potential V may be derived by inversion from a standard type of spheroidal harmonic. An interesting type of symmetrical potential may be represented by a convergent series of potentials of the present type. The associated series of functions of types $f_n(t)$, $S_n(0, 4u).C_n(s)$, $S_n(s)$, $g_n(z)$ are then of some interest.

§ 4. *Case* 2.

$$f(t)=e^{-t}F(-n, n+1\,;\,1, 1\,;\,t)=e^{-t}Z_n(t)=U_n(t), \quad (4.1)$$

where $Z_n(t)$ is the polynomial studied at the same time [4], [5], [6] as the function $V_n(s)$ and $F(a, b\,;\,c, d\,;\,z)$ is a generalized hypergeometric function, which in the notation of E. W. Barnes would have the suffixes 2, 2 before and after the symbol F.

In the present case $V(z)=V_n(z)$, $G(s)=f_n(s)$.

To find $F(u)$ we note that. with certain well-known coefficients, denoted here by $c_{n,m}$,

$$f_n(t)=\sum_{m=0}^{n} c_{n,m}(1+t)^{-m-1}, \quad . \quad . \quad . \quad (4.2)$$

and so

$$\begin{aligned} V_n(z)&=(-)^n\int_0^\infty e^{-u}(du/u)f_n(z/u)\\ &=(-)^n\sum_{m=0}^{n} c_{n,m}\int_0^\infty e^{-u}(z+u)^{-m-1}u^m\,du\\ &=(-)^n2\sum_{m=0}^{n}(c_{n,m}/m\,!)\int_0^\infty K_0(2\sqrt{zt})e^{-t}t^m\,dt\\ &=(-)^n2\int_0^\infty K_0(2\sqrt{zt})U_n(t)\,dt. \quad . \quad . \quad . \quad . \quad . \quad (4.3) \end{aligned}$$

This gives a new representation of $V_n(s)$ and indicates at the same time that $F(u)=(-)^n U_n(u)$. The formula (1.7) also gives an integral equation which has already been found by Howell [7]

$$U_n(s)=(-)^n\int_0^\infty J_0(2\sqrt{st})U_n(t)\,dt.$$

The functions $C(s).S(s)$ are now

$$\pi C(s)=f_n(is)+f_n(-is)=\pi c_n(s), \quad \text{say,} \quad . \quad . \quad (4.4)$$

$$i\pi S(s)=f_n(-is)-f_n(is)=i\pi s_n(s), \quad \text{say.} \quad . \quad (4.5)$$

A comparison of the different expressions for V when $z=0$, $w>0$ suggests the following expressions for the function $\Gamma_n(w)$, which represents V in this case,

$$\Gamma_n(w)=(1/\pi)\int_0^\pi V_n(iw\cos\theta)\,d\theta=\int_0^{\frac{1}{2}\pi} C_n(w\cos\theta)\,d\theta,$$

$$\Gamma_n(w)=\int_0^\infty (w^2+t^2)^{-\frac{1}{2}}U_n(t)\,dt,$$

$$\Gamma_n(w)=\int_0^\infty J_0(wt)f_n(t)\,dt,$$

$$\Gamma_n(w)=(-)^n 2\int_0^\infty K_0(\sqrt{2wt})J_0(\sqrt{2wt})U_n(t)\,dt,$$

$$\Gamma_n(w)=\int_0^\infty e^{-ws}(1+s^2)^{-\frac{1}{2}}P_n(a)P_n(c)\,ds, \quad . \quad . \quad . \quad . \quad (4.5)$$

where

$$a=(s+1)(s^2+1)^{-\frac{1}{2}},\ c=(s-1)(s^2+1)^{-\frac{1}{2}}. \quad . \quad (4.6)$$

The last formula may be obtained by using the known formula

$$(1+s^2)^{-\frac{1}{2}}P_n(a)P_n(c)=\int_0^\infty J_0(st)U_n(t)dt$$

to transform the third expression for $\Gamma_n(w)$.

§ 5. *Case* 3.

$$G(s)=U_n(s), \quad V(z)=f_n(z). \quad . \quad . \quad (5.1)$$

If $R'=[(z+1)^2+w^2]^{-\frac{1}{2}}$, $R'u^*=r+1$, $R'v^*=r-1$, we have

$$V=(1/R')P_n(u^*)P_n(v^*). \quad . \quad . \quad . \quad . \quad (5.2)$$

The potential V can in this case be derived by inversion from a standard type of spheroidal harmonic.

If $F_n(z)$ denotes the polynomial used in former papers [8] we have

$$F(u)=\sum_{m=0}^{\infty}(-)^m F_n(-2m-1)u^m/(m!)^2=E_n(u), \text{ say,} \quad (5.3)$$

and the formula (1.3) gives a new representation of the product of two Legendre polynomials.

The function V has a singularity at the point $z=-1$, $w=0$, and the function $f(t)$ does not exist in the ordinary sense.

When $z=0$, $w>0$ we have the formula

$$V=\int_0^{\frac{1}{2}\pi} c_n(w\cos\theta)\,d\theta=(1+w^2)^{-\frac{1}{2}}P_n(a^*)P_n(c^*), \quad (5.4)$$

where

$$a^*=(w+1)(w^2+1)^{-\frac{1}{2}}, \quad c^*=(w-1)(w^2+1)^{-\frac{1}{2}}.$$

The formula (5.2) can also be used to obtain an expression in terms of Legendre functions for the function $U_n^*(w)$ used in a former paper [5]. We have in fact

$$\begin{aligned} U_n^*(w)&=\int_0^{\infty} J_0(ws)U_n(s)s\,ds \\ &=-\lim_{z\to 0}[\partial V/\partial z] \\ &=(1+w^2)^{-\frac{3}{2}}[P_n(a^*)P_n(c^*)+a^*P_n'(a^*)P_n'(c^*) \\ &\qquad +c^*P_n(a^*)P_n'(c^*)] \end{aligned}$$

In like manner we find from (3.2) that

$$\begin{aligned} V_n^*(w)&=\int_0^{\infty} J_0(ws)V_n(s)s\,ds \\ &=-2(1+w^2)^{-\frac{3}{2}}[Q_n(a^*)P_n(c^*)+a^*Q_n'(a^*)P_n(c^*) \\ &\qquad +c^*Q_n(a^*)P_n'(c^*)]. \end{aligned}$$

§ 6. *Case* 4.

The case in which $G(s)=S_n(s^2, 2s)$ may be briefly mentioned because in this case

$$V(z)=(1+z^2)^{-\frac{1}{2}}[V_n\{(1+z^2)^{\frac{1}{2}}-z\}] \text{ for } z>0.$$

Further properties of the function $S_n(a, b)$ must be found before it can be said whether this form of $V(z)$ is valid only for $z>0$.

§ 7. Let a function $p_n(z)$ be defined by the equation

$$p_n(z)(1+z)(2+z)\ldots(n+z)=(1-z)(2-z)\ldots(n-z),$$

then in many cases the series

$$F(z)=F(1)+3p_1(z)[F(1)-F(2)]+5p_2(z)[F(1)-3F(2)+2F(3)]+7p_3(z)[F(1)-6F(2)+10F(3)-5F(4)]+\ldots$$

converges when the real part of z exceeds a certain number and gives an interpolation formula for $F(z)$. The case in which $F(z)=zV(z)$ is of particular interest for it suggests the possibility of deriving a symmetrical potential from its axial values at the points $z=1, 2, 3, \ldots$ only. In the particular case in which $V(z)=e^{-kz}$ and $k>0$ the series becomes

$$F(z)=1+3p_1(z)P_1(t)+5p_2(z)P_2(t)+\ldots,$$

where $t=1-2e^{-k}$. This is the well-known Legendre series for $(\frac{1}{2}-\frac{1}{2}t)^{z-1}z$, which is known to converge and represent this function when $4z>1$ and $-1<t<1$.

References.

(1) The formula is a particular case of one given by N. Sonine, *Math. Ann.* xvi. pp. 1–80 (1880). See p. 61.
(2) G. N. Watson, ' Bessel Functions,' p. 183.
(3) H. M. Macdonald, Proc. London Math. Soc. (2) vii. p. 142 (1909). See also G. N. Watson, ' Bessel Functions,' p. 412; J. London Math. Soc. iii. p. 22 (1928).
(4) H. Bateman, Duke Math. J. ii. pp. 569–577 (1936).
(5) H. Bateman, *Ibid.* iv. pp. 39–50 (1938).
(6) H. Bateman, Annals of Math. xxxviii. pp. 303–310 (1937).
(7) W. T. Howell, Phil. Mag. (7) xxv. pp. 622–628 (1938).
(8) H. Bateman, *Tôhoku Math. J.* xxxvii. p. 23 (1933); Annals of Math. xxxv. pp. 767–775 (1934).
(9) G. Darboux, *J. de Math.* (3) iv.; v. p. 377 (1878).

XCI. *On Gravitational Waves in Linearized Fields.*

By B. C. Mukerji, *M.A.**

[Received June 28, 1938.]

1. *Introduction.*

THE possibility of the existence of gravitational waves which move with the velocity of light was first pointed out by Einstein[1]. This was, however, proved for weak gravitational fields satisfying the linearized gravitational equations. As the system of coordinates used was Cartesian doubt has sometimes been expressed

* Communicated by the Author.

as to whether the wave phenomena are real or are only peculiar to the coordinate system used. Moreover, every solution of the linearized equations does not necessarily correspond to a solution of the rigorous equations, though the opposite is true. Hence independent corroboration of the reality of the waves or any consideration throwing additional light on the point may be welcome.

Birkhoff[2] has shown that the only central symmetric external solution of the rigorous field equations is the static Schwarzschild field. From this result it may be concluded that there cannot be any true spherical gravitational waves in free space. But though no true wave solution of the rigorous equations exists in spherical polar coordinates, it cannot be concluded the linearized equations will not admit such solutions. If they do, the doubt about the reality of the waves (gravitational) corresponding to the wave solutions in Cartesian coordinates of the linearized equations will not be unjustifiable. A close examination, however, shows that the corresponding wave solutions of the linearized equations in polar coordinates represent spurious waves, as they all can be transformed away to a flat-field. In fact our results go far deeper, and show clearly that Schwarzschild's static field is the only non-euclidean central symmetric solution of the linearized gravitational equations, every other central symmetric solution giving only a flat space. Thus the relation between the spherical wave solutions of the linearized equations and the flat-field is the same as that between the general central symmetric solutions and the Schwarzschild solution of the rigorous equations as noticed by Birkhoff.

In addition to that in the spherically symmetric field we have some definite knowledge about gravitational waves in the axial symmetric field. Einstein and Rosen[3] have recently shown that there exist real cylindrical gravitational waves represented by solutions of the rigorous field equations. A study of the linearized equations in the axially symmetric field shows, however, the complexity of the problem and how an inference from the linearized equations may sometimes be misleading; for while linearized equations admit of waves corresponding to those found by Einstein and Rosen, they have also other simple real wave solutions which, unlike in spherical symmetric field, cannot be transformed away.

The procedure in Cartesian coordinates is to start with a field $g_{ik}=\delta_{ik}+h_{ik}$, where δ_{ik} is the euclidean metric and h_{ik} is the modification due to a weak gravitational field. It can be shown that in virtue of the gravitational equations the tensor h_{ik} satisfies the wave equation in free space. An exactly similar procedure is adopted here. In section 2 we have considered gravitational fields having central symmetry, and in section 4 fields having axial symmetry.

2. *Equations of a Central Symmetric Weak Gravitational Field.*

We start with the line-element in the form

$$ds^2=-e^{\lambda}dr^2-e^{\omega}(d\theta^2+\sin^2\theta\,d\phi^2)+e^{\nu}\,.\,dt^2, \quad . \quad (1)$$

where λ, ω, and ν are functions of r and t only.

The space being empty, our field equations are[4] :—

$$-e^{-\omega}+e^{-\lambda}(\tfrac{1}{2}\omega'\nu'+\tfrac{1}{4}\omega'^2)+e^{-\nu}(-\tfrac{3}{4}\dot{\omega}^2+\tfrac{1}{2}\dot{\omega}\dot{\nu}-\ddot{\omega})=0, \quad (2)$$

$$e^{-\lambda}(\tfrac{1}{2}\omega''+\tfrac{1}{4}\omega'^2+\tfrac{1}{2}\nu''+\tfrac{1}{4}\nu'^2-\tfrac{1}{4}\omega'\lambda'-\tfrac{1}{4}\nu'\lambda'+\tfrac{1}{4}\omega'\nu')$$
$$+e^{-\nu}(-\tfrac{1}{2}\ddot{\lambda}-\tfrac{1}{4}\dot{\lambda}^2-\tfrac{1}{4}\dot{\omega}^2-\tfrac{1}{2}\ddot{\omega}-\tfrac{1}{4}\dot{\lambda}\dot{\omega}+\tfrac{1}{4}\dot{\lambda}\dot{\nu}+\tfrac{1}{4}\dot{\omega}\dot{\nu})=0, \quad (3)$$

$$-e^{-\omega}+e^{-\lambda}(\omega''+\tfrac{3}{4}\omega'^2-\tfrac{1}{2}\omega'\lambda')-e^{-\nu}(\tfrac{1}{2}\dot{\lambda}\dot{\omega}+\tfrac{1}{4}\dot{\omega}^2)=0, \quad (4)$$

$$-\dot{\omega}'-\tfrac{1}{2}\dot{\omega}\omega'+\tfrac{1}{2}\lambda\omega'+\tfrac{1}{2}\dot{\omega}\nu'=0, \quad . \quad . \quad . \quad (5)$$

where a dot denotes differentiation with respect to t and a dash differentiation with respect to r.

Let us define the weak field by

$$e^{\lambda}=1+\beta(r,t), \quad . \quad . \quad . \quad . \quad . \quad . \quad (6)$$

$$e^{\omega}=r^2\{1+\alpha_1(r,t)\}=r^2+\alpha(r,t), \quad . \quad . \quad . \quad (7)$$

$$e^{\nu}=1+\gamma(r,t), \quad . \quad . \quad . \quad . \quad . \quad . \quad (8)$$

where α, β, and γ are small quantities of the first order and limit $\alpha=\beta=\gamma=0$ leads to the euclidean metric. In the above field-equations we reject powers and products of α, β, and γ.

Equation (5) reduces to

$$-\dot{\omega}'-\tfrac{1}{2}\dot{\omega}\omega'+\tfrac{1}{2}\dot{\lambda}\omega'=0, \quad . \quad . \quad . \quad . \quad (9)$$

which on integration gives[5]

$$e^{\lambda}=\frac{e^{\omega}.\omega'^2}{4f^2(r)}, \quad . \quad . \quad . \quad . \quad . \quad . \quad (10)$$

where $f^2(r)$ is an arbitrary function of r.

Equation (10) can now replace (5) and functions α, β, γ, and $f^2(r)$ will be determined by means of the set of equations (2), (3), (4), and (10).

From (6), (7), and (10) we have

$$f^2(r)-1=\frac{\partial}{\partial r}\left(\frac{\alpha}{r}\right)-\beta. \quad . \quad . \quad . \quad . \quad (11)$$

From (2) and (3), by substitutions from (6), (7), (8), (10), and (11), we get the two following equations (in first order terms) :—

$$\ddot{\alpha}-r\gamma'+\beta-\frac{\partial}{\partial r}\left(\frac{\alpha}{r}\right)=0, \quad . \quad . \quad . \quad . \quad (12)$$

$$\ddot{\alpha}'-(r\gamma''+\gamma')+\beta'-\frac{\partial^2}{\partial r^2}\left(\frac{\alpha}{r}\right)=0, \quad . \quad . \quad (13)$$

of which equation (13) turns out to be directly obtainable from (12) by differentiating with respect to r.

From (4), with the help of (10), we get

$$1-f^2(r)=\frac{4f(r)f'(r)}{\omega'}. \quad . \quad . \quad . \quad . \quad (14)$$

If $f'(r)=0$, since $\omega'\neq 0$, $f^2(r)=1$. . . (15)

If $f'(r)\neq 0$, (14) on integration gives

$$e^{\omega/2}=\psi(t)/(1-f^2(r)), \quad . \quad . \quad . \quad . \quad . \quad (16)$$

where $\psi(t)$ is a function of t. But $\psi(t)$ must be a constant, as shown below.

From (7), (11), and (16)

$$\psi(t)=r\left\{\beta-\frac{\partial}{\partial r}\left(\frac{\alpha}{r}\right)\right\}=r\{1-f^2(r)\}$$

$$=\text{a function of } r \text{ only.} \quad . \quad . \quad . \quad (17)$$

Hence $\psi(t)$ must be a constant Further by (16) then,

$$e^{\omega}=r^2. \quad . \quad . \quad . \quad . \quad . \quad . \quad . \quad (18)$$

From (7) and (18) we find

$$\alpha=0,$$

whence further by (11)

$$\beta=1-f^2(r), \quad . \quad . \quad . \quad . \quad . \quad (19)$$

and from (17)

$$1-f^2(r)=\frac{\text{const}}{r}=+\frac{m}{r}=\beta. \quad . \quad . \quad . \quad (20)$$

Then (12) gives

$$\gamma' = \frac{m}{r^2},$$

so that $$\gamma = -\frac{m}{r} + \mathrm{F}(t); \quad \beta = +\frac{m}{r}.$$

Thus $\alpha = 0$ really corresponds to Schwarzschild's solution in empty space. We next take $\alpha \neq 0$, then $f'(r) = 0$, and $f^2(r) = 1$.

Equations (11) and (12) then give

$$\beta = \frac{\partial}{\partial r}\left(\frac{\alpha}{r}\right), \quad \ldots\ldots\ldots \quad (21)$$

$$\gamma' = \frac{\partial^2}{\partial t^2}\left(\frac{\alpha}{r}\right). \quad \ldots\ldots\ldots \quad (22)$$

We have thus only two equations to determine three functions, viz., α, β, and γ; so the equations are not sufficient to determine the functions completely.

3. *Possible Wave Solutions.*

We can get a complete wave solution by putting $\beta' = \gamma'$. Then (α/r) satisfies the wave equation

$$\left(\frac{\partial^2}{\partial r^2} - \frac{\partial^2}{\partial t^2}\right) u = 0. \quad \ldots\ldots\ldots \quad (23)$$

Equations (21) and (22) show that β and γ are also propagated as waves. These waves all travel with the fundamental unit velocity.

It should be noticed that the characteristic parts of the modified tensor are α_1, β, and γ; and α_1, (β/r), and (γ/r) are all of the form $f(t \pm r)/r$; so that while β and γ travel as "plane waves" α_1 travels as a "spherical wave": and all these waves may be convergent or divergent.

It should be noted that the above wave solution is not unique under the present circumstances. We can arrive at a wave solution by choosing a suitable relation between α and γ.

For instance, if we take

$$\gamma = \frac{\partial}{\partial r}\left(\frac{\alpha}{r}\right) + \frac{\alpha}{r}, \quad \ldots\ldots\ldots \quad (24)$$

all the three functions α/r, β, and γ satisfy the same wave equation

$$\left(\frac{\partial^2}{\partial r^2} + \frac{\partial}{\partial r} - \frac{\partial^2}{\partial t^2}\right) u = 0. \quad \ldots\ldots\ldots \quad (25)$$

This gives damped waves of the type

$$u \sim e^{-r/2} \cdot e^{\pm in\left(t - \frac{\sqrt{n^2-\frac{1}{4}}}{n} \cdot r\right)},$$

which can never be propagated with fundamental unit velocity.

The above solutions represent, however, only spurious waves. The quickest way to prove this is to calculate the Riemann-Christoffel tensor $B_{\mu\nu\sigma\zeta}$. It may be shown that this vanishes identically. Thus the following six components—

$$B_{1212},\ B_{1313},\ B_{1414},\ B_{2323},\ B_{2424},\ B_{3434},$$

which do not vanish on account of symmetry, do so in virtue of equations (21) and (22). The rest of the components vanish on account of symmetry. Thus the space-time is really flat, and the apparent gravitational field can be transformed away. It should be noticed that equations (21) and (22) are independent of any assumption of waves, and follow directly from the linearized field equations. Thus barring the Schwarzschild field every other central symmetric solution in this case represents flat-space.

The linearized equations lead to the same conclusions as can be arrived at from the rigorous equations, namely, that spherical gravitational waves cannot exist in free space.

4. *Gravitational Fields having Axial Symmetry.*

For the study of cylindrical waves Einstein and Rosen started from the line-element

$$ds^2 = A(d\omega^2 - dt^2) + Bdz^2 + Cd\phi^2, \quad . \quad . \quad . \quad (26)$$

where ϖ, ϕ, and z are the usual cylindrical coordinates.

The space being empty the rigorous field equations are

$$\frac{B_{44}}{B} + \frac{C_{44}}{C} - \frac{1}{2}\left(\frac{B_4^2}{B^2} + \frac{C_4^2}{C^2} - \frac{B_4C_4}{BC} + \frac{A_1B_1}{AB} + \frac{A_1C_1}{AC} + \frac{A_4B_4}{AB} + \frac{A_4C_4}{AC} + \frac{B_1C_1}{BC}\right) = 0, \quad . \quad (27)$$

$$\frac{A_{44}}{A} + \frac{C_{44}}{C} + \frac{1}{2} \cdot \frac{C_1^2 - C_4^2}{C^2} + \frac{A_1^2 - A_4^2}{A^2} - \frac{A_{11}}{A} - \frac{C_{11}}{C} = 0, \quad . \quad . \quad . \quad (28)$$

$$\frac{A_{44}}{A}+\frac{B_{44}}{B}+\frac{1}{2}\cdot\frac{B_1^2-B_4^2}{B^2}+\frac{A_1^2-A_4^2}{A^2}-\frac{A_{11}}{A}-\frac{B_{11}}{B}=0, \quad \ldots \quad (29)$$

$$\frac{B_{11}}{B}+\frac{C_{11}}{C}-\frac{1}{2}\left(\frac{B_1^2}{B^2}+\frac{C_1^2}{C^2}-\frac{B_1C_1}{BC}+\frac{A_1B_1}{AB}+\frac{A_1C_1}{AC}+\frac{A_4B_4}{AB}+\frac{B_4C_4}{BC}+\frac{A_4C_4}{AC}\right)=0, \quad \ldots \quad (30)$$

$$\frac{B_{14}}{B}+\frac{C_{14}}{C}-\frac{1}{2}\left(\frac{B_1B_4}{B^2}+\frac{C_1C_4}{C^2}+\frac{A_4B_1}{AB}+\frac{A_4C_1}{AC}+\frac{A_1B_4}{AB}+\frac{A_1C_4}{AC}\right)=0, \quad \ldots \quad (31)$$

where subscripts denote differentiation.

Einstein and Rosen deduced from these equations the result that $\sigma=\sqrt{g_{22}\times g_{33}}$ satisfies the wave equation

$$\left(\frac{\partial^2}{\partial\varpi^2}-\frac{\partial^2}{\partial t^2}\right)u=0. \quad \ldots \quad (32)$$

Further, by a suitable coordinate transformation it was shown $\delta=\sqrt{g_{22}/g_{33}}$ is a cylindrical wave satisfying the equation

$$\left(\frac{\partial^2}{\partial\varpi^2}+\frac{1}{\varpi}\frac{\partial}{\partial\varpi}-\frac{\partial^2}{\partial t^2}\right)u=0. \quad \ldots \quad (33)$$

To study the linearized equations we put

$$A=1+\alpha(\varpi,t)\,; \quad B=1+\beta(\varpi,t)\,;$$
$$C=\varpi^2\{1+\gamma_1(\varpi,t)\}=\varpi^2+\gamma(\varpi,t), \quad (34)$$

where α, β, and γ are small such that their squares and higher powers as well as their products may be rejected.

Equations (27) to (31), with substitutions from (34), reduce to the following set :—

$$\dot{\beta}'-(\alpha'+\beta')/\varpi+\ddot{\gamma}/\varpi^2=0, \quad \ldots \quad (35)$$

$$\ddot{\alpha}-\alpha''-\frac{1}{\varpi}\left(\frac{\partial^2}{\partial\varpi^2}-\frac{\partial^2}{\partial t^2}\right)(\gamma/\varpi)=0, \quad \ldots \quad (36)$$

$$\dot{\beta}'-\beta''+\dot{\alpha}-\alpha''=0, \quad \ldots \quad (37)$$

$$\beta''+\frac{\beta'-\alpha'}{\varpi}+\frac{1}{\varpi}\frac{\partial^2}{\partial\varpi^2}(\gamma/\varpi)=0, \quad \ldots \quad (38)$$

$$\varpi\dot{\beta}'-\dot{\alpha}+\frac{\partial^2}{\partial\varpi\,\partial t}(\gamma/\varpi)=0, \quad \ldots \quad (39)$$

where a dot denotes differentiation with respect to t and a dash differentiation with respect to ϖ.

A number of wave solutions are possible now.

The differential equations inevitably lead to the following wave solutions.

Case 1.

From (37) we see at once that $(\alpha+\beta)$ satisfies the wave equation (32).

Subtracting (35) from (38) we get

$$\beta''+\frac{2\beta'}{\varpi}-\ddot{\beta}+\frac{1}{\varpi}\left(\frac{\partial^2}{\partial\varpi^2}-\frac{\partial^2}{\partial t^2}\right)\left(\frac{\gamma}{\varpi}\right)=0, \quad . \quad (40)$$

which shows $(\beta\varpi+\gamma/\varpi)$ is a solution of the wave equation (32). This solution really corresponds to the rigorous solution $\sigma(=\sqrt{g_{22}\times g_{33}})$ of Einstein and Rosen mentioned above.

Subtracting (36) from (37) we get

$$\ddot{\beta}-\beta''+\frac{1}{\varpi}\left(\frac{\partial^2}{\partial\varpi^2}-\frac{\partial^2}{\partial t^2}\right)\left(\frac{\gamma}{\varpi}\right)=0. \quad . \quad . \quad (41)$$

Subtracting further (41) from (40), and dividing by 2, we get

$$\beta''+\frac{1}{\varpi}\beta'-\ddot{\beta}=0, \quad . \quad . \quad . \quad . \quad . \quad (42)$$

which shows that β is propagated as a cylindrical wave.

Let us now consider (39), which on integration gives

$$\varpi\beta'-\alpha+\frac{\partial}{\partial\varpi}\left(\frac{\gamma}{\varpi}\right)=\mathrm{F}(\varpi), \quad . \quad . \quad . \quad (43)$$

where $\mathrm{F}(\varpi)$ is an arbitrary function of ϖ.

Since $(\alpha+\beta)$ and $(\beta\varpi+\gamma/\varpi)$ satisfy (32), we take

$$\alpha=\phi(\varpi-t)-\beta\,; \qquad \gamma/\varpi=\psi(\varpi-t)-\beta\varpi. \quad . \quad (44)$$

Substituting these values in (43) we obtain

$$\mathrm{F}(\varpi)=\frac{\partial}{\partial\varpi}\psi(\varpi-t)-\phi(\varpi-t).$$

This relation between ψ and ϕ waves implies

$$\mathrm{F}(\varpi)=0, \text{ and } \frac{\partial}{\partial\varpi}\psi(\varpi-t)=\phi(\varpi-t),$$

whence we have by substitution from (43)

$$\alpha+\beta=\frac{\partial}{\partial\varpi}(\beta\varpi+\gamma/\varpi). \quad . \quad . \quad . \quad . \quad (45)$$

This shows the simple relation existing between the two waves $(\alpha+\beta)$ and $(\beta\varpi+\gamma/\varpi)$.

We thus find in this case there is not only a first order wave corresponding to Einstein-Rosen wave of the exact field, but there are two other wave solutions (one plane and the other cylindrical) of the linearized field equations to which there correspond no actual waves in the exact gravitational field. A calculation of the Riemann-Christoffel tensor shows that it does not vanish identically, so that these two latter wave solutions have all the appearances of real waves.

Case 2.

We can arrive at certain wave solutions of special type by assuming

$$\beta\varpi+\gamma/\varpi=0. \quad . \quad . \quad . \quad . \quad . \quad (46)$$

Equation (45) then gives

$$\alpha+\beta=0. \quad . \quad . \quad . \quad . \quad . \quad . \quad (47)$$

Equations (35), (37) to (39) are satisfied identically, while (36), by means of (46) and (47), can be reduced to

$$\left(\frac{\partial^2}{\partial\varpi^2}+\frac{1}{\varpi}\frac{\partial}{\partial\varpi}-\frac{\partial^2}{\partial t^2}\right)\left(\beta-\frac{\gamma}{\varpi^2}\right)=0. \quad . \quad . \quad (48)$$

Hence $\beta-\gamma/\varpi^2$ is a solution of (33).

This corresponds to Einstein-Rosen δ-wave of the exact field mentioned above.

From (46) and (47) we see that now all the three components of the modified tensor, viz., α, β, and (γ/ϖ^2), are propagated as cylindrical waves.

It can be verified in the manner stated above that none of these waves is spurious. A point of considerable importance to be noticed is that all waves in cases 1 and 2 travel with the fundamental unit velocity.

In conclusion, I wish to express my sincere gratefulness to Prof. N. R. Sen for the benefit of much helpful criticism.

References.

(1) Einstein, *Berl. Ber.* p. 154 (1918).
(2) Birkhoff, ' Relativity and Modern Physics,' p. 253.
(3) Einstein and Rosen, Jour. Franklin. Inst. ccxxiii. p. 43.
(4) N. R. Sen, *Zs. f. Astr. Phyk.* Bd. x. p. 291.
(5) R. C. Tolman, Proc. Nat. Acad. Sci. xx. p. 169.

Department of Applied Mathematics,
University College of Science, Calcutta.

XCII. *Calculation of the Area of Basis Metal exposed at Discontinuities in the Tin Coating of Tinplate.* By W. E. Hoare, *B.Sc.* (*Eng.*) *.

[Received September 16, 1938.]

THE results of porosity tests on tinplates are usually expressed as the number of discontinuities in the coating occurring on unit area of sheet surface. Such a method of expression is useful for the comparison of the qualities of different coatings, or for the purpose of appraisal of specimens under test against arbitrarily or empirically fixed standards. No attempt has been made previously, however, either by manipulation of existing data or by direct means, to find the area of basis metal exposed at the pore sites. The results embodied in two recent investigations have now made such a step possible.

Data obtained by the present author[1], shown in the graph (fig. 1), mathematically analysed by Taggart[2], show that the relation between number of pores per unit area and thickness of coating is given by the equation

$$\log_{10} P = 3{\cdot}653 - 2{\cdot}785 \log_{10} Y \dagger,$$

where P expresses the porosity as number of pores per 100 sq. cm. and Y expresses the thickness of coating as pounds per basis box ‡.

For the purpose of calculation, porosity is expressed as number of pores per square metre (y) and coating thickness in millimetres (x). Thus :

$$\log_{10}\left(\frac{y}{100}\right) = 3{\cdot}653 - 2{\cdot}785 \log\left(\frac{x}{0{\cdot}00154}\right),$$

* Communicated by the Author.

† The relation is more accurately expressed

$$\log_{10} P \pm 0{\cdot}505 = 3{\cdot}653 - 2{\cdot}785 \log_{10} Y,$$

the second term giving the limits between which 95 per cent. of the observations were found to lie.

‡ The amount of tin coating is usually expressed in this country as the weight of tin per basis box of sheets. The area of a basis box is 31,360 sq. in. (112 sheets 20 × 14 in.) ; 1 lb. per basis box is equivalent to 11·21 grm. per sq. metre of total surface. Except in the case of certain specially coated plates, the amount of tin in the form of intermetallic compound is approximately constant, and weight per area may be converted with negligible error into thickness. 1 lb. per basis box is equivalent to 0·0000606 in. or 0·00154 mm. thickness.

from which

$$\log_{10} y = -2{\cdot}172 - 2{\cdot}785 \log_{10} x,$$

or

$$\frac{1}{M}\log_{10} y = -\frac{2{\cdot}172}{M} - 2{\cdot}785\frac{1}{M}\log_{10} x,$$

$$\log_e y = -5 - 2{\cdot}785 \log_e x,$$

$$M = \log_{10} e = 0{\cdot}43429$$

$$\log_{10} x = M \log_e x.$$

$$\log_e y = \log\left(\frac{1}{e^5}\right) - 2{\cdot}785 \log_e x.$$

Fig. 1.

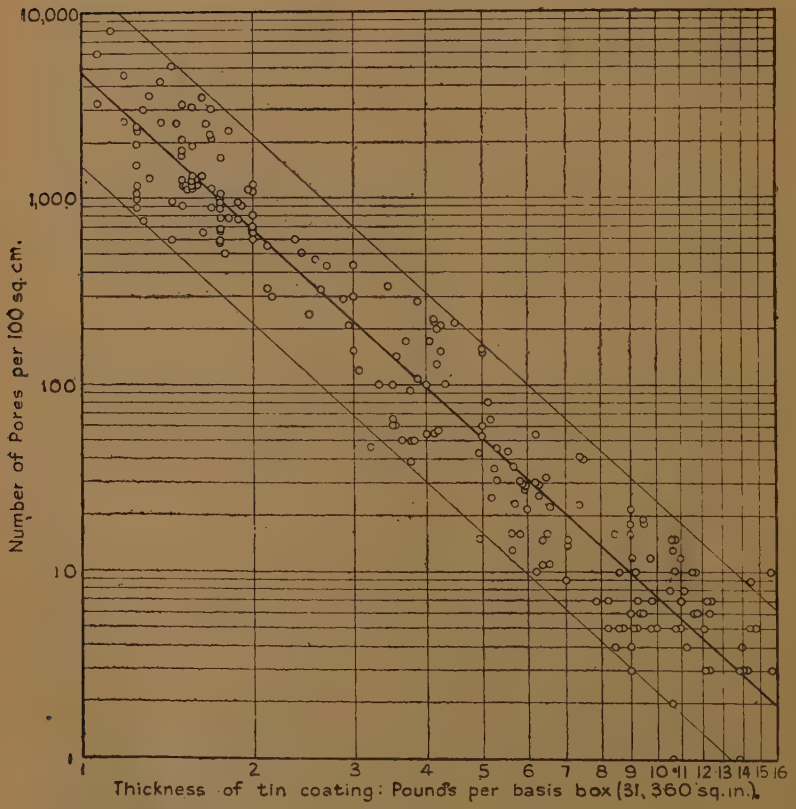

Let $e^{-5} = K$ and $2{\cdot}785 = n$. Then

$$\log y = \log K - n \log x, \quad \ldots\ldots (1)$$

and

$$yx^n = K. \quad \ldots\ldots (2)$$

Examining the effects of surface tension forces in the film of tin prior to solidification, Chalmers[3] found that non-reactive areas must be greater in diameter than a certain fraction of the local thickness of coating before they are able to cause the formation of normal pores.

Thus, if previous preparation of the steel basis sheet has been perfect and the conditions of tinning are ideally correct, the molten tin will react with the steel to form a layer of the intermetallic compound $FeSn_2$, and more tin will flow on to or " wet " this compound surface to form a continuous film. Suppose, however, that at certain regions on the basis metal this reaction between steel and molten tin does not occur. The surface at such regions is non-reactive and is in contact with tin in the molten state (see fig. 2 (*a*)). Such a state of affairs

Fig. 2.

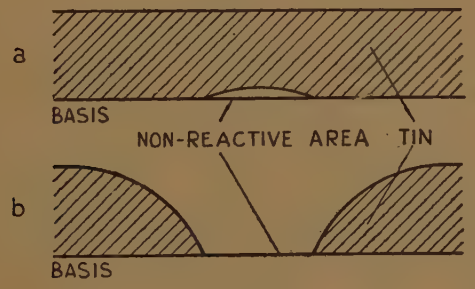

increases the total surface area of the system, which *may* then be reduced by the formation of a pore as in fig. 2 (*b*). Such an interaction can only occur if the surface area is in consequence decreased. The resultant surface is a catenoid, and it was shown mathematically that the diameter of the non-reactive area must be greater than 0·6 times the thickness of the coating in order for the above conditions to be satisfied.

Thus the minimum diameter of a normal pore at any coating thickness x is $0{\cdot}6x$, and its area $0{\cdot}09\pi x^2$. Considering an element δx in fig. 3, if the thickness of coating is $(x+\delta x)$, the diameters of all pores will be greater than $0{\cdot}6\ (x+\delta x)$, and if the thickness of coating is x, the diameters of all pores will be greater than $0{\cdot}6x$. The average diameter of pores in the group δx will therefore be $0{\cdot}6\ (x+x+\delta x)\frac{1}{2}=0{\cdot}6x$ when δx tends to zero. Similarly,

the number of pores in this group will be $y-(y-\delta y)=\delta y$. Thus the area of basis metal exposed due to the pores in this group, is given by the expression $0{\cdot}09\pi x^2 dy$, or if the total area is called A

$$dA=0{\cdot}09\,\pi x^2 dy. \quad . \quad . \quad . \quad . \quad . \quad (3)$$

Differentiate equation (1)

$$\frac{1}{y}dy+\frac{n}{x}dx=0. \quad \therefore \quad \frac{dy}{dx}=-n.\frac{y}{x},$$

Fig. 3.

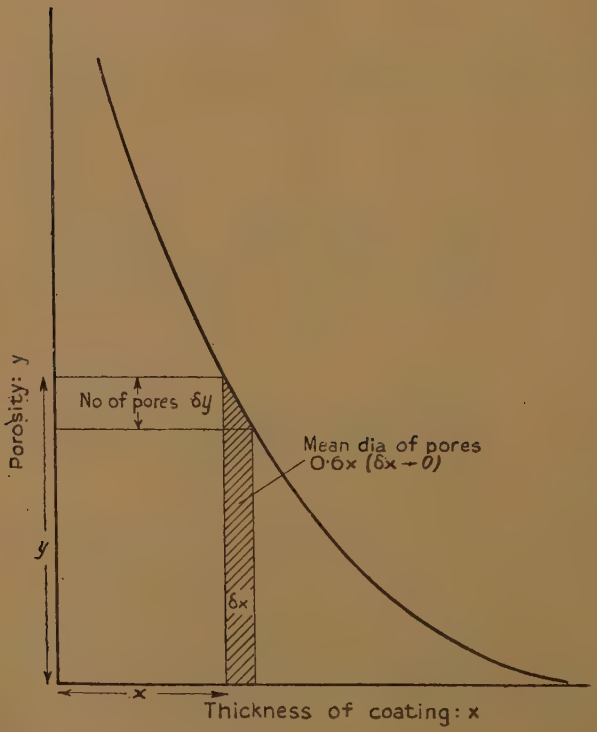

but $yx^n=K$ (equation (2)),

$$\therefore \quad \frac{dy}{dx}=-n\frac{K}{x^{n+1}},$$

and from equation (3)

$$\frac{dA}{dy}=0{\cdot}09\,\pi x^2,$$

by multiplication

$$\frac{dA}{dx} = \frac{dA}{dy} \cdot \frac{dy}{dx} = -n \frac{K}{x^{n+1}} \cdot 0{\cdot}09\pi x^2. \quad . \quad . \quad (4)$$

For the purposes of calculation, the coating thickness/porosity curve is taken to converge with the x axis at $Y=15$ lb. per basis box ($x=0{\cdot}0231$ mm.). Thus the area of basis metal exposed at any coating thickness T, is given by the expression

$$\int_{x=T}^{x=0{\cdot}0231} dA,$$

or

$$A = -0{\cdot}09\,\pi n K \int_{x=T}^{x=0{\cdot}0231} x^{1-n}\,dx,$$

$$= +0{\cdot}09\,\pi n K \left[\frac{x^{2-n}}{2-n}\right]_{x=0{\cdot}0231}^{x=T},$$

$$A = \frac{0{\cdot}09\pi n K}{2-n} \left[x^{2-n}\right]_{x=0{\cdot}0231}^{x=T} \quad . \quad . \quad . \quad . \quad (5)$$

TABLE I.

Thickness of coating.		Area of basis metal exposed sq. mm./sq. m.
lb./basis box.	mm.	
1	0·00154	0·970
1·5	0·00231	0·670
2	0·00308	0·507
2·5	0·00385	0·405
3	0·00462	0·334
4	0·00616	0·241
5	0·00770	0·180
8	0·01232	0·084
11	0·01694	0·037
15	0·02310	0

Substituting the numerical values $K=e^{-5}$ and $n=2{\cdot}785$, and evaluating, equation (5) becomes

$$A = -0{\cdot}0068\left(\frac{1}{T^{0{\cdot}785}} - 19{\cdot}2\right),$$

and if Y expresses the thickness of coating in pounds per basis box

$$A = -0{\cdot}0068\left(\frac{1}{(0{\cdot}00154\,Y)^{0{\cdot}785}} - 19{\cdot}2\right).$$

From which

$$A = 1{\cdot}1\left\{\frac{Y}{Y^{1{\cdot}785}} - 0{\cdot}119\right\} \text{ sq. mm. per sq. metre.}$$

Fig. 4.

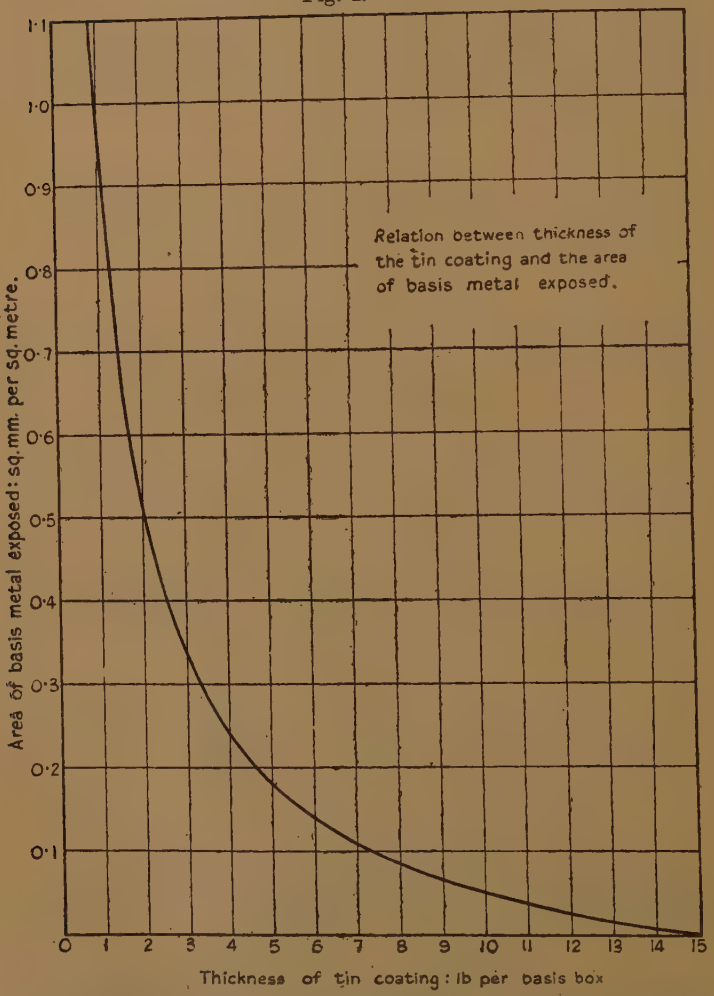

The value of the above expression for several different coating thicknesses is given in Table I. (see p. 1081), and the relation between the two variables is shown in fig. 4.

The results arrived at above may be checked by summation. As in the preceding argument the area of basis

metal exposed by any group of discontinuities between, say, thicknesses of coating x_1 and x_2 (provided x_1-x_2 is small) will be given by the expression

$$0{\cdot}09\,\pi\left(\frac{x_1+x_2}{2}\right)^{\blacksquare}.(y_1-y_2) \text{ sq. mm. per sq. metre,}$$

or if Y expresses the coating thickness in pounds per basis box and P the porosity in pores per 100 sq. cm., then

$$a=0{\cdot}09\,\pi.0{\cdot}00154^2\left(\frac{Y_1+Y_2}{2}\right)^2.100\,(P_1-P_2),$$

TABLE II.

Coating thickness lb. per basis box=Y.	Y_1+Y_2.	$(Y_1+Y_2)^2$ =B.	Pores per 100 sq. cm. =P.	P_1-P_2 =C.	B×C =K.	0·0000167 K =a.	Σa.
15	—	—	2·3	—	—	—	—
14	29	841	2·8	0·5	420	0·00702	0·00702
13	27	729	3·5	0·7	510	0·00852	0·01554
12	25	625	4·4	0·9	563	0·00925	0·02479
11	23	529	5·6	1·2	637	0·01065	0·03544
10	21	441	7·2	1·6	705	0·01180	0·04724
9	19	361	9·8	2·6	940	0·01570	0·06294
8	17	289	13·5	3·7	1070	0·01780	0·08074
7	15	225	20	6·5	1460	0·02440	0·10514
6	13	169	31	11	1860	0·03110	0·13624
5	11	121	52	21	2540	0·04240	0·17864
4	9	81	97	45	3640	0·06080	0·23944
3·5	7·5	56·25	140	43	2410	0·04030	0·27974
3	6·5	42·25	215	75	3170	0·05300	0·33274
2·5	5·5	30·25	355	140	4240	0·07080	0·40354
2	4·5	20·25	680	325	6570	0·11000	0·51354
1·5	3·5	12·25	1500	820	10050	0·16800	0·68154
1	2·5	6·25	4600	3100	19350	0·32300	1·00454

and the total area exposed at any coating thickness Y (lb. per basis box) will be

$$\Sigma_{\mathrm{Y}}^{15}a.$$

The area exposed is therefore given by the expression

$$\Sigma_{\mathrm{Y}}^{15}0{\cdot}0000167(Y_1+Y_2)^2(P_1-P_2) \text{ sq. mm. per sq. m.}$$

This sum is evaluated in Table II., and the results are seen to agree closely with those obtained by integration.

Conclusion.

Knowledge of the area of basis steel exposed at discontinuities in the coating of tinplate may be of value in researches on the corrosion of tinplate, a field of investigation which is of great importance to the food-canning industry. Recently also, attention has been drawn to certain chemical or electrochemical " reactivity " tests which may eventually succeed in providing more convenient means for determining the quality of tin coatings on steel. Standardization of these techniques, and comparison of results with the large amount of data accumulated already by routine porosity tests, would be facilitated by the ability to express the results of such tests in a less arbitrary manner.

Summary.

The calculation is based on the results of an experimental investigation of the effect of thickness of the tin coating on porosity, and on theoretical work on the size of non-reactive areas necessary to produce normal pores. The area of basis metal exposed is found to decrease regularly with increase of thickness of coating and is given by the expression

$$1{\cdot}1\left\{\frac{Y}{Y^{1{\cdot}25}}-0{\cdot}119\right\} \text{ sq. mm. per sq. m.,}$$

where Y is the thickness of coating expressed in pounds per basis box.

Acknowledgments.

Thanks are due to the International Tin Research and Development Council for permission to publish this work, and to the Council's Director of Research, Mr. D. J. Macnaughtan, for his encouragement during its prosecution. The author also desires to express his gratitude to Professor B. P. Haigh, M.B.E., D.Sc., who very kindly read the manuscript of this paper and made many most helpful suggestions; and to Mr. R. Taggart for his valued advice.

References.

(1) W. E. Hoare, J. Iron and Steel Inst. cxxxvi. pp. 99–130 (1937).
(2) R. Taggart, *ibid.* p. 123.
(3) B. Chalmers, Trans. Faraday Soc. xxxiii. pp. 1167–1176 (1937).

XCIII. *The Flow of a Viscous Fluid past a Circular Cylinder.* *By* HARISH CHANDRA GUPTA, *M.Sc., Research Scholar, University of Allahabad* *.

[Received June 20, 1938.]

FOR finding the motion of a viscous fluid near a solid obstacle the equations of motion can be simplified into what are known as Prandtl's Boundary Layer Equations †. Various attempts ‡ have been made to solve numerically these equations when the flow is past a circular cylinder and the pressure-distribution round the cylinder is known.

The method of Falkner and Skan ‡ consists in transforming the boundary layer equations by taking suitable new variables and then considering a simple approximate equation for solution. The new equation is identical with the original equations at the surface of the cylinder and on the diametral plane in the direction of the general stream; and it differs from them at other places by small amounts. This new equation is then solved by drawing nomograms for numerical values of the coefficients.

Besides making a number of approximations the authors assume that the velocity § q asymptotically tends to $\bar{q}$ as $n \to \infty$. This amounts to supposing that the boundary layer is of infinite thickness, which is objectionable.

The method of Green ‖ is more direct and more accurate. After making the variables non-dimensional he has assumed for q a power-series in n, the coefficients being functions of s; and by substitution in the boundary layer equations the series is found to be the following :—

$$\begin{aligned} q\mathrm{R} = {} & nf_0 + (n^2/2\,!)f_1 + (n^4/4\,!)f_0f_0' + (n^5/5\,!)2f_0f_1' \\ & + (n^6/6\,!)2f_1f_1' + (n^7/7\,!)\{4f_0^2f_0'' - f_0(f_0')^2\} \\ & + (n^8/8\,!)\{10f_0^2f_1'' - 13f_0f_0'f_1' + 9f_0f_0''f_1 \\ & + 9(f_0')^2f_1\} + \ldots, \quad \ldots\ldots\ldots \quad (1) \end{aligned}$$

* Communicated by Dr. Gorakh Prasad.

† Lamb's 'Hydrodynamics,' 6th edition, p. 684.

‡ (*a*) Thom, Aer. Res. Ctee. R. & M. no. 1176. (*b*) Green, Phil. Mag. (7) xii. p. 1 (1931). (*c*) Falkner and Skan, Phil. Mag. (7) xii. p. 865 (1931). For a full bibliography see Dr. Maccoll, Journ. Roy. Aero Soc. (Aug. 1930).

§ For the meanings of the various symbols see the next section.

‖ *Loc. cit.*

where $f_0 = \mathrm{R}(\partial q/\partial n)_{n=0}$, $f_1 = \mathrm{R}^2(dp/ds)$, and dashes denote differentiations with respect to s.

The numerical values of p are obtained by experiment, and those of f_1 and its differential coefficients with respect to s by graphical differentiation. The values of f_0 and its differential coefficients are obtained by a step-by-step method. Thus, if the solution at $s=45°$ is wanted when it has been carried up to $s=40°$, Taylor's series gives

$$f_{0(45°)} = f_{0(40°)} + \delta s f_0'_{(40°)} + (\delta s^2/2\,!) f_0''_{(40°)} + (\delta s^3/3\,!) f_0'''_{(40°+\theta)}, \quad \ldots\ldots (2)$$

where $0° < \theta < 5°$, and δs is the arcual measure for 5°. Here $f_{0(40°)}$, $f_0'_{(40°)}$ and $f_0''_{(40°)}$ are already known. Three values (theoretically two would do) of F, viz., $f_0'''_{(40°+\theta)}$, are now assumed, between which the correct value is supposed to lie. In each case the corresponding values of f_0, f_0', f_0'' at $s=45°$ are calculated from (2) and the similar equations for f_0' and f_0''. These are substituted in the series for $\partial q/\partial n$ obtained by differentiating (1). Thus $\partial q/\partial n$ can be tabulated for various values of n for each of the three assumed values of F.

Since $q=0$ at the surface, graphical integration gives the velocity at the end of the boundary layer. That value of F which will reproduce the known value $\bar{q}$ is found by interpolation. This value is used in (2) to give the final values of f_0, f_0', f_0'' at $s=45°$, from which the various coefficients of the power-series (1) for 45° can be evaluated; and so q can be tabulated for various values of n at $s=45°$.

The defect in Green's method is that his power-series for q is not convergent when n is of the order of the thickness of the boundary layer. Near the end of the boundary layer the series fails to give a good value of q although eight terms are retained. Fairly large alterations of values have to be made frequently to smooth out irregularities caused by the inherent defects of the method. The author himself admits that "..... large values of n were excluded and the curve smoothed off to zero by eye in such a manner that when $\partial q\mathrm{R}/\partial n$ is zero, $\partial^2 q\mathrm{R}/\partial n^2$ is also zero." The author claims that large variations in the method of smoothing have a very slight influence on the final values, but it is certain that another person using the same data and the same method will arrive at very different results.

In the present paper the boundary layer equations have been solved by a new numerical step-by-step method, the case taken up being the same as that of Green for facility of comparison. A preliminary solution showed that great accuracy * could be attained by the present method (see § 10), and so it was thought desirable to get rid of the errors of observation as far as possible. Graduation was evidently necessary for this ; but in order to keep as near to Green's values as possible the values of his dp/ds were graduated instead of those of p, although it is the latter which is directly measured in the experiments.

It is strange that symmetry has not been taken into account by Green or by Falkner and Skan in deriving values of the various coefficients at $s=0$ †. In the present paper full use has been made of the fact that the flow past a cylinder must be symmetrical about the diametral plane parallel to the stream.

2. *Notation.*

$s \equiv$ ratio of the distance along the surface, measured from the nose, to the diameter of the cylinder.

[The symbol s has thus the same meaning as in Green's paper. Following Green, we also have, however, often used s to denote the angle subtended at the centre by the distance along the surface measured from the nose. The context always makes it clear in which sense s is used at a particular place.]

$n \equiv$ ratio of the distance along the normal, measured from the surface, to the diameter of the cylinder.

$q, w \equiv$ ratios of the tangential and normal velocities at any point in the boundary layer to the velocity of the general stream.

$p \equiv$ ratio of the pressure to the product of the density of the fluid and the square of the velocity of the general stream.

$\bar{q} \equiv$ the limiting value of q at the end of the boundary layer.

* In fact the method can be made to give any desired degree of accuracy by suitably shortening the intervals along s and n.

† For example, f_1'', *i. e.*, $R^2 d^3p/ds^3$, at $s=0$ is equal to -8×10^{11} in Green's paper, although symmetry requires that it should be zero.

$k=\pi/72$, the arcual measure for 5°.

$b=1/1200$, the chosen interval along n.

$$N\equiv n/b, \quad Q\equiv 10^4 . q, \quad \bar{Q}\equiv 10^4 . \bar{q}, \quad Q'\equiv 10^4 . k . \partial q/\partial s,$$
$$Q_1\equiv \partial q/\partial n, \quad Q_2\equiv 10^{-4} . \partial^2 q/\partial n^2, \quad W\equiv -10^4 . k . w.$$

$$q_r\equiv (\partial^r q/\partial n^r)_{n=0}, \quad q_r' \equiv \partial q_r/\partial s, \quad q_r''\equiv \partial^2 q_r/\partial s^2, \text{ etc.}$$
$r=1, 2, \ldots .$

$Q(m^0, l)$ denotes the value of Q at $s=m$ degrees and $n=l.b$. Similarly for Q', Q_1, Q_2, and W. R is the Reynolds number for the motion. It is equal to $0{\cdot}943\times 10^5$ for the case under consideration. A dot placed over the last figure of a number means that the next figure is 5, thus $\dot{1}=1{\cdot}5$, $2{\cdot}\dot{5}=2{\cdot}55$.

3. *Method of Solution.*

The equations to be solved are

$$R(\partial p/\partial s+q\partial q/\partial s+w\partial q/\partial n)=\partial^2 q/\partial n^2, \quad . \quad . \quad (3)$$
$$\partial p/\partial n=0, \quad . \quad . \quad . \quad . \quad . \quad . \quad . \quad . \quad . \quad . \quad (4)$$
$$\partial q/\partial s+\partial w/\partial n=0, \quad . \quad . \quad . \quad . \quad . \quad . \quad . \quad . \quad (5)$$

the boundary conditions being

(i.) $q=w=0$ at $n=0$,

(ii.) $q=q$, $\partial q/\partial n=0$ at the end of the boundary layer.

The values of p are supposed to be known by experiment. From these $\partial p/\partial s$, $\partial^2 p/\partial s^2$, and $\partial^3 p/\partial s^3$ are calculated for all values of s. Equation (4) shows that $\partial p/\partial s$, $\partial^2 p/\partial s^2$, etc., are independent of n.

Just beyond the boundary layer Bernoulli's equation is supposed to hold, and on Prandtl's assumption w is negligibly small. Hence

$$p+\tfrac{1}{2}\bar{q}^2=C,$$

and since $\bar{q}=0$ at $s=0$, the constant $C=(p)_{s=0}$. From this equation the values of $\bar{q}$ for various values of s are calculated.

We notice that as $q=w=0$ at $n=0$ (boundary condition (i.)), equation (3) gives

$$R\, dp/ds=(\partial^2 q/\partial n^2)_{n=0}, \textit{ i. e., } q_2.$$

Differentiating, we have

$$q_2'=R\, d^2 p/ds^2 \text{ and } q_2''=R\, d^3 p/ds^3.$$

The values of q_2, q_2', q_2'' are then computed from these equations for all values of s.

For the sake of convenience we transform the equations of motion (3) and (5) into the working formulæ :

$$Q_2 = 10^{-4} \times \{q_2 + (9{\cdot}43/k)(10^{-4}QQ' - WQ_1)\}, \quad . \quad (6)$$

$$\partial W/\partial N = Q'b. \quad . \quad . \quad . \quad . \quad . \quad (7)$$

For integration Simpson's formula is quite satisfactory and convenient. Using this, (7) can be put in the form :

$$W(s, N) = W(s, N-2) + \tfrac{1}{3}.b\{Q'(s, N-2) + 4Q'(s, N-1) + Q'(s, N-2)\}. \quad . \quad . \quad . \quad (8)$$

After these preliminaries we can now proceed with the step-by-step solution. To illustrate its principle suppose that the solution has been obtained completely up to 40°, *i. e.*, the values of q have been found for the net-work of points given by $s = 0°, 5°, 10°, \ldots$ up to 40°, and $N = 1, 2, 3, \ldots$ up to the end of the boundary layer.

To obtain the values of q for various values of N at $s = 45°$ an approximate value of q_1 at 45° is first found by extrapolation. Based on this value of q_1, the known values of q_2, q_2', q_2'' at $s = 45°$ and the values of q at the previous positions, we obtain the complete solution for $s = 45°$ by the method outlined below. If this value of q_1 is smaller than the true value, q attains a maximum which is less than $\bar{q}$. If, on the other hand, this value is greater than the true value, q increases beyond $\bar{q}$. It is easy to find by interpolation the exact value of q_1 which will make q steadily tend to $\bar{q}$. q attains, in this case, the value $\bar{q}$ for a finite value of n and then practically ceases to increase or decrease because it is found * that, for this value of q_1, Q_1 and Q_2 tend to zero as $q \to \bar{q}$.

In practice an interpolation is not necessary, nor is it necessary to carry out the complete solution corresponding to the extrapolated value of q_1. It is easy to guess from the differences of Q along s, after the solution has been obtained for a few steps along n, what change should be made in the extrapolated value of q_1 which will make the computed velocities tend to the known limiting velocity.

* Equation (3) shows that Q_2 must $\to 0$ as $q \to b$. For, at the end of the boundary layer, $\partial q/\partial n = 0$. Also, Bernoulli's equation holds there. Therefore $dp/ds + \bar{q}\partial\bar{q}/\partial s = 0$. Hence, at the end of the boundary layer,

$$Q_2 = R(dp/ds + \bar{q}\partial\bar{q}/ds + w\partial q/\partial n) = 0.$$

The final value of q_1 being thus known, the complete solution at $s=45°$, viz., the values of q along n up to the end of the boundary layer, can be found by the method referred to above.

Slight alterations in the value of q_1 produce very large changes in the maximum value attained by q. Hence the skin-friction, which depends on q_1, gets very accurately determined by the present method.

We now indicate how the solution at $s=45°$ corresponding to any chosen value of q_1 is obtained.

(*a*) First, the values of q_1' and q_1'' corresponding to the chosen value of q_1 are calculated by numerical differentiation using the following formulæ * :

$$f'(s)=(1/k)\{\Delta f(s-\kappa)+\tfrac{1}{2}\Delta^2 f(s-2\kappa) +\tfrac{1}{3}\Delta^3 f(s-3k)+\ldots.\}, \quad . \quad . \quad (9)$$

$$f''(s)=(1/k^2)\{\Delta^2 f(s-2\kappa)+\Delta^3 f(s-3k) +(11/12)\Delta^4 f(s-4k)+\ldots\}. \quad . \quad (10)$$

The values of q_2, q_2', and q_2'' have already been determined. We can, therefore, calculate the coefficients of the various terms up to the one involving n^9 in the power-series

$$\begin{aligned} q=q_1 n+q_2 n^2/2\,!+\mathrm{R}q_1 q_1' n^4/4\,!+2\mathrm{R}q_1 q_2' n^5/5\,! \\ +2\mathrm{R}q_2 q_2' n^6/6\,!+\mathrm{R}^2\{4(q_1)^2 q_1''-q_1(q_1')^2\}n^7/7\,! \\ +\mathrm{R}^2[10(q_1)^2 q_2''-13q_1 q_1' q_2'+9q_2\{q_1 q_1''+(q_1')^2\}]n^8/8\,! \\ +8\mathrm{R}^2 q_1\{5q_2 q_2''-2(q_2')^2\}n^9/9\,!+\ldots, \quad . \quad . \quad . \quad (11) \end{aligned}$$

which is really Green's power-series (1) divided by R.

(*b*) This series and the series obtained from it by differentiation are used to calculate the values of Q, Q_1, Q_2 for the first step along n, i. e., for $N=1$. The corresponding value of Q′ is then found by (9). Finally, the value of W is directly obtained from (6) by substituting in it the values of Q, Q_1, Q_2, and Q′ found above and the known value of q_2.

(*c*) For the next and succeeding steps along n Green's series is not used, as the values of Q_2, etc. given by it are not good enough. The procedure now is as follows. To find Q at $N=m$, say, we (i.) extrapolate Q on the basis of its values at $N=m$, $s=40°$, 35°, etc. ; (ii.) calculate the corresponding value of Q′ by (9) ; (iii.) find W

* To make the difference-table of Q along s smooth, the values of Q have sometimes been arbitrarily changed, but never by more than 3.

by (8); (iv.) calculate Q_1 by numerical differentiation, and (v.) obtain Q_2 in the same way.

(*d*) Substituting now the values of all the quantities found above from (i.) to (iv.) in the right-hand side of (6), a new value of Q_2 is obtained. If now we were to integrate along n using this new value of Q_2, we shall get a much better value* of Q than the extrapolated value obtained in (i.) of paragraph (*c*) above with which we started. A repetition of the process once or twice would yield a value of Q in which there would be no further change by going through the above process. This evidently would be the correct value of Q at $N=m$.

But in practice it is not necessary to repeat the process. By a comparison of the value of Q_2 obtained in paragraph (*d*) above with its value obtained in paragraph (*c*) (v.), we can see at once what the correct value of Q_2 is. In general the former value of Q_2 requires but a very slight change.

(*e*) We proceed in this way till Q_1 is almost zero. If the chosen value of q_1 is correct, the value of Q_2 also will simultaneously become almost zero and Q will tend to $\bar{Q}$.

4. *Graduation.*

Those methods of graduation which do not simultaneously take into account all the values of the quantity to be graduated were not tried. Whittaker's method † did not give a sufficiently satisfactory result. A fifth-degree curve whose coefficients were found by the method of least squares gave a satisfactory graduation for dp/ds. The difference in corresponding graduated and ungraduated values of p was nowhere more than 0·008, which is well within the experimental errors. The equation for dp/ds was found to be

$$10^{-8}R^2\,dp/ds = -527{\cdot}814x + 269{\cdot}788x^3 + 9{\cdot}27672x^5, \ldots \quad (12)$$

where, for convenience, x has been put for $36s/5\pi$. The coefficients of x^2 and x^4 both are zero because of symmetry.

The values of $R^2\,dp/ds$ used by Green, as well as its graduated values and the corresponding values of p, are given in Table I.

As mentioned before, the values of q_2, q_2', q_2'' (re-

* See Appendix I.

† Whittaker and Robinson, 'The Calculus of Observations,' p. 303.

spectively equal to $R\,dp/ds$, $R\,d^2p/ds^2$, $R\,d^3p/ds^3$) are obtained from (12) and the equations obtained by differentiating it, and those of the limiting velocity q from Bernoulli's formula $q=\sqrt{(1-2p)}$. The values of $\bar{q}$ cannot be accurately determined from the given experimental values of q because of the experimental errors and the fact that q has been measured at rather large intervals along n. However, the values of $\bar{q}$ as deduced from p

TABLE I.

s (in degrees).	$-10^{-8}R^2dp/ds$.		10^3p.		Difference.
	Green's.	Graduated.	Experimental (Green).	By integrating graduated dp/ds.	
0	0	0	500	500	0
5	48·0	52·51	489	487	2
10	104·0	103·40	453	449	4
15	157·0	151·04	383	386	3
20	199·0	193·76	300	301	1
25	227·5	229·89	189	197	8
30	249·0	257·69	71	77	6
35	267·0	275·37	− 55	− 55	0
40	282·0	281·08	−189	−191	2
45	285·5	272·88	−319	−327	8
50	260·0	248·75	−457	−456	1
55	200·8	206·57	−570	−569	1
60	129·5	144·10	−655	−655	0
65	62·3	58·99	− 70(?)	−707	?
70	(−48·5)	−51·25	(−709)	−710	1

by using Bernoulli's equation do not differ from the experimental values of $\bar{q}$ (as given in Green's paper) anywhere by more than 0·022.

5. *The Solution.*

There is some difficulty (as is usual in all step-by-step methods) in finding differential coefficients with respect to s when starting the solution. Therefore, a rough solution is first found for $s=5°$, using for $\partial q/\partial s$ the quantity $(q)_{s=5°}/k$, since $q=0$ at $s=0$. The solution is then carried up to 15° by the method outlined in § 3.

Next, the solution at 5° is revised by using these computed values of q to obtain new values of Q′ by a central-

difference formula. This alters the values at 10° and 15° only slightly.

The solution can then be carried out step-by-step up to 60° by the method of § 3. After that, the interval along s has to be shortened to half its former value, *i. e.*, to $2\frac{1}{2}°$. To obtain Q′ at $62\frac{1}{2}°$, which is necessary for this, the values of Q at $57\frac{1}{2}°$ and $52\frac{1}{2}°$ are first found by interpolation.

The solution can be carried up to 70° in this way.

6. *Illustration.*

To illustrate the method the complete solution at 25° is given below. The solution up to 20° is supposed to be known. Thus, all the entries in Table IV. up to the line $s=20°$ are supposed to be known. Extrapolating the value of q_1 for $s=25°$, we get 540·0, say. The value of Q_2 at $N=0$, i. e., q_2, has already been calculated (§ 4). We know thus all the entries in the first line of Table II.

The values of q_1', q_1'' corresponding to the extrapolated value of q_1, viz., 540·0, are now calculated by (9) and (10). They are found to be $89\cdot1/k$, $-11\cdot9/k^2$ respectively. The values of q_2, q_2', q_2'' have already been determined (§ 4). At $s=25°$ they are $-24\cdot38\times10^4$, $-342\cdot0\times10^2/k$, $8825/k^2$ respectively. We are thus able now to calculate the various coefficients of the power-series (11). They are

$$\begin{aligned}
\mathrm{R}q_1q_1' &= q_4 = +2\,!(1200)^2\times10^2\times361\cdot1,\\
2\mathrm{R}q_1q_2' &= q_5 = -3\,!(1200)^3\times10^2\times77\cdot1,\\
2\mathrm{R}q_2q_2' &= q_6 = +4\,!(1200)^4\times10^2\times7\cdot2,\\
\mathrm{R}^2\{4(q_1)^2q_1''-q_1(q_1')^2\} &= q_7 = -5\,!(1200)^5\times10^2\times2\cdot8,\\
\mathrm{R}^2[10(q_1)^2q_2''-13q_1q_1'q_2'+9q_2\{q_1q_1''+(q_1')^2\}] &\\
= q_8 &= +6\,!(1200)^6\times10^2\times0\cdot9.
\end{aligned}$$

By substituting these values in the power-series (11) and the two series obtained by differentiating it successively, we get the values * of Q, Q_1, Q_2 at $N=1$. These are entered in the second line of Table II.

* We may note in passing that the interval along n, viz. 1/1200, is so small that the seventh term of (11), viz., $n^8q_8/8\,!$, has no effect on the values of Q or Q_1 at $N=1$ for any value of s, and a very slight one (viz., $<0\cdot01$) on the value of Q_2 (and that too only for a few positions). The eighth term has no sensible effect on any entry. For instance, the derivative q_8 was calculated for $s=25°$ and found to be

$$-7\,!\,(1200)^7\times12^2\times0\cdot1,$$

which does not affect the last figure in any of the entries at $N=1$.

Next, we calculate Q′ at N=1 by (9), and get

$$Q'(25°, 1)=625.$$

Substituting these values of q_2, Q_2, Q_1, Q, and Q′ in (6) we get

$$W(25°, 1)=0{\cdot}276\dot{}.$$

Thus all the entries in the second line of Table II. are known.

We calculate now the entries in the third line of Table II.

(i.) The values of Q and their differences along s for N=2, which are supposed to be known at this stage, are as follows :—

s.	Q.	Δ.	Δ^2.	Δ^3.
0°	0			
		1238		
5°	1238		−15	
		1223		−16
10°	2461		−31	
		1192		−18
15°	3653		−49	
		1142		
20°	4795			

We have now to extrapolate the value of Q at $s=25°$, N=2. We take the next third difference (Δ^3) to be −22, say. The following entries can, therefore, be written down at the bottom of the various columns of the above difference-table :

$$25°, 5868, 1072, -70, -20\dot{}.$$

The extrapolated value of Q is thus 5868.

(ii.) The corresponding value of Q′ is, therefore, by (9)

$$1072\dot{}+\tfrac{1}{2}(-70)+\tfrac{1}{3}(-20\dot{})+\tfrac{1}{4}(-2), \textit{ i. e.}, 1030.$$

(iii.) The values of Q′ at $s=25°$, N=0, 1, supposed to be known, are 0, 625.

Substituting in (8) we get

$$W=(0+4\times 625+1030)/(3\times 1200)=0{\cdot}980\dot{},$$

since W=0 at N=0.

(iv.) We have next to find Q_1 at N=2. For this we derive a formula for differentiation from Simpson's formula for integration, which is

$$Q_1(s, N)=10^{-4}(3/b)\{Q(s, N)-Q(s, N-2)\}$$
$$-\{Q_1(s, N-2)+4Q_1(s, N-1)\}. \quad (13)$$

Putting N=2, and noting that Q(25°, 2)=5868, Q(25°, 0) =0, $Q_1(25°, 0)=540{\cdot}0$, and $Q_1(25°, 1)=345{\cdot}\dot{3}$, we get

$$Q_1(25°, 2)=0{\cdot}36\times 5868-540{\cdot}0-4\times 345{\cdot}\dot{3}=191{\cdot}1.$$

(v.) Again, using a formula similar to (13), viz.,

$$Q_2(s, N)=10^{-4}(3/b)\{Q_1(s, N)-Q_1(s, N-2)\} -\{Q_2(s, N-2)+4Q_2(s, N-1)\}, \quad . \quad . \quad (14)$$

and substituting the values of the various terms, we get

$$Q_2(25°, 2)=0{\cdot}36\times(191{\cdot}1-540{\cdot}0) -\{-24{\cdot}38+4\times(-21{\cdot}38)\}=-15{\cdot}29.$$

Next, by substituting in (6) the known value of q_2 and the values of Q, Q′, W and Q_1 found above from (i.) to (iv.), we get for Q_2 a new value

$$-24{\cdot}38+(9{\cdot}43/k)(0{\cdot}5868\times 1030 -0{\cdot}980\times 191{\cdot}1), \textit{ i. e.}, -15{\cdot}36.$$

This must be almost the correct value of Q_2 at this point (see Appendix 1); but as this new value, −15·36, is numerically greater than the value, −15·29, of (v.), a value numerically slightly greater than the former, viz., −15·37, instead of −15·36, is tried. We find from this Q_1 and then Q. For this we notice that the values of Q_2 at N=0, 1, 2 are now −24·38, −21·48, −15·37. Therefore, by Simpson's formula,

$$Q_1(25°, 2)=540{\cdot}0+(\tfrac{1}{3}\times 10^4/1200) (-24{\cdot}38-4\times 21{\cdot}4\dot{8}-15{\cdot}37)=190{\cdot}9.$$

Applying the same formula once again, we have

$$Q(25°, 2)=0+(\tfrac{1}{3}\times 10^4/1200)(540{\cdot}0 +4\times 345{\cdot}\dot{3}+190{\cdot}9)=586\dot{7}.$$

Using this value in the difference-table instead of the extrapolated value 5868, the value of Q′ at N=2 comes out to be 1029, and W is found to be 0·980. These values of Q_2, Q_1, Q, Q′, and W, viz., −15·37, 190·9, 586$\dot{7}$, 1029, and 0·980 when substituted in (6) are found to satisfy it. These are, therefore, the correct values at N=2 corresponding to $q_1=540{\cdot}0$. They are entered in Table II., the third line of which is thus complete now.

The entries at N=3 are found in an exactly similar way and entered in Table II.

TABLE II.

(Corresponding to the extrapolated value of q_1, viz., 540·0.)

N.	Q_2.	Q_1.	Q.	Q′.	W.
0.....	−24·38	540·0	0	0	0
1	−21·48	345·3	3671	625	0·276
2.....	−15·37	190·9	5867	1029	0·980
3.....	− 9·52	88·4	6991	1228	1·933

The difference-table of Q along s up to 25° at N=3 is now as follows :—

s.	Q.	Δ.	Δ^2.	Δ^3.
0°	0			
		1464		
5°	1464		−14	
		1450		−17
10°	2915		−31	
		1419		−16
15°	4334		−47	
		1371		−38
20°	5705		−85	
		1286		
25°	6991			

We notice that the third-difference (Δ^3) suddenly jumps from −17 and −16 to −38. Assuming that the last third-difference should be −15, we see at once that Q(25°, 3) is too low by about 20. Hence a slightly higher value * for q_1, viz., 540·1, instead of 540·0, is tried and found to give satisfactory third-differences.

Proceeding further along N, a limiting value of Q agreeing with $\overline{Q}$ is obtained. The complete solution for this value of q_1 is given in Table III.

* After a little experience it becomes easy to guess what the change in q_1 should be. It was found that the required change in q_1 is one-third to one-sixth of the difference, at N=3 or 4, between the value of q as calculated from q_1 and the value as extrapolated from the previously completed solution, divided by the value of n.

TABLE III.

(Corresponding to the final value of q_1, viz., $540\cdot\dot{1}$.)

$q_1' = 89\cdot5/k$, $q_1'' = -11\cdot6/k^2$,
$q_4 = 2\,!(1200)^2 \times 10^2 \times 362\cdot6$,
$q_5 = -3\,!(1200)^3 \times 10^2 \times 77\cdot1$,
$q_6 = 4\,!(1200)^4 \times 10^2 \times \dot{7}\cdot2$,
$q_7 = -5\,!(1200)^5 \times 10^2 \times 2\cdot8$,
$q_8 = 6\,!(1200)^6 \times 0\cdot9$.

N.	Q_2.	Q_1.	Q.	Q′.	W.
0.....	$-24\cdot38$	$540\cdot\dot{1}$	0	0	0
1.....	$-21\cdot47$	$345\cdot\dot{5}$	3673	629	0·280
2.....	$-15\cdot3\dot{0}$	$191\cdot\dot{3}$	$5871\dot{}$	1037	0·967
3.....	$-9\cdot00$	$90\cdot\dot{8}$	$7011\dot{}$	$1268\dot{}$	1·959
4.....	$-4\cdot38$	36·7	$7514\dot{}$	1381	$3\cdot048\dot{}$
5.....	$-1\cdot7\dot{2}$	12·4	7706	1428	$4\cdot24\dot{2}$
6.....	$-0\cdot57$	3·7	$7764\dot{}$	1444	$5\cdot42\dot{1}$
7.....	$-0\cdot16$	0·8	7783	1447	6·647

The solution at 25° is now complete.

7. *Solution after* 70°.

In order to obtain the solution after 70°, the values of dp/ds for $71\frac{1}{4}°$, $72\frac{1}{2}°$, and $73\frac{3}{4}°$ are obtained by extrapolation from the graduated experimental values at the previous positions. This is easy, because a fifth degree curve has been found to represent dp/ds up to 70° (equation (12)). As a check, the corresponding values of p are calculated and compared with the experimental values. The agreement is found to be satisfactory up to 75°, where the extrapolated value of p is $-0\cdot652$ as against $-0\cdot651$, the experimental value. The values of q_2, q_2', q_2'', and $\bar{q}$ are then calculated as in § 4.

As the values of $\partial q/\partial s$, $\partial^2 q/\partial s^2$, etc. from 70° onwards get increasingly larger, the interval along s has been further reduced to $1\frac{1}{4}°$. Even then it is found difficult to extrapolate (as is required for the method of paragraph (*c*) § 3) a fairly good value of q from the values of q at the previous positions, which have been calculated. The following method is therefore adopted.

As before, a value of q_1 is extrapolated and the entries at N=1 are obtained as in paragraph (*b*), § 3. Next, at N=2 also, Q, Q_1, and Q_2 are calculated from the power-series (11) *. Suppose they are Q(?), Q_1(?), Q_2(?). The corresponding values of Q′ and W at N=2, *i. e.*, Q′(?) and W (?), are found from equations (6) and (8) by substituting in them the values of Q(?), Q_1(?), Q_2(?). This value Q′(?) is now used to obtain a new value of Q at N=2 by integration. It can be shown † that this value is nearer to the correct value than Q(?)—the three coinciding if there is no error in the extrapolated value of q_1. The correct value of q_1 can, therefore, be inferred now. It is such that the value of Q at N=2, calculated from the power-series (11), remains unaltered by going through the above process.

As q_1 is determined by examining the value it gives to q at N=2, this method does not give as exact results as the method of § 3, but it is sufficiently accurate for the purpose. The following procedure for obtaining the remaining values of Q is now more convenient.

From the values of Q at N=1 and 2 an idea can be formed about the general trend of the differences of Q along s ; and so it is easy to put down a smooth sequence of values of Q for N=3, 4, etc., tending to $\overline{Q}$ at about N=9. (The thickness of the boundary layer at $s=70°$ is about this much.) From this set of values of Q, beginning at N=0, values of Q_1 and Q_2 at N=3, 4, etc. are obtained by numerical differentiation. Values of Q′ and W are then calculated for N=3, 4, etc. successively from equations (6) and (8). Using these values of Q′ new values of Q are obtained by integrating along s. The same set of operation is performed on the new set of values, if necessary, and the process repeated till there is no further alteration in the values of Q. This completes the solution for the particular value of s under consideration.

In practice the very first operation gives values of q correct to three decimal places, which is the utmost

* The terms of the power-series for Q_1 and Q_2 at N=2 decrease rather slowly. However, as the later terms q_6, q_7, etc. are alternately positive and negative, it is evident that better values can be obtained if the last term is replaced by a fraction of itself. The run of the values of the various terms showed that the best thing would be to replace the last term (the one involving q_9) by half its actual value.

† See Appendix 2.

that the approximate value of q_1 can warrant, and so no repetition is necessary.

The values of Q obtained by the above method are given in Table IV.

It should be noted that the values of Q along n at $s=67\frac{1}{2}°$ and 70° were smoothed out (the maximum change being 0·002 when $q=1·442$) before starting the solution after 70°. Also, the values of Q at $68\frac{3}{4}°$ were found by interpolation for convenience in extrapolating the values of Q at $71\frac{1}{4}°$. The solution was then obtained at $71\frac{1}{4}°$, $72\frac{1}{2}°$, and $73\frac{3}{4}°$ by the method outlined above.

8. *Illustration of the Method of Solution after* 70°.

To illustrate the above method, the complete solution for $s=72\frac{1}{2}°$ is given below. We first extrapolate an approximate value of q_1 for $s=72\frac{1}{2}°$. We get 274·0, say. As in § 6 the first eight coefficients of the power-series corresponding to this value of q_1 can be evaluated, the values of Q, Q_1, Q_2 at N=1 obtained, and the values of Q′ and W at N=1 calculated. They are

$$Q_2=7·55,\ Q_1=-362·5,\ Q=2681,\ Q'=-2090,\ W=0·932.$$

The values of Q, Q_1, and Q_2 at N=2 also are obtained from the power-series (11). Thus,

$$Q(?)=5865,\ Q_1(?)=388·7,\ Q_2(?)=-1·11.$$

These values are substituted in equations (6) and (8), which then give

$$Q'(?)=-3188,\ W(?)=-3·208.$$

Now from the final values of Q and Q′ obtained for the previous positions we know that

$$Q'(67\tfrac{1}{2}°, 2)=-1450,\ Q'(70°, 2)=-2072,\ Q(67\tfrac{1}{2}°, 2)=8011.$$

These and the value −3188 of $Q'(72\frac{1}{2}°, 2)$, *i. e.*, Q′(?), give by substitution in Simpson's formula

$$Q(72\tfrac{1}{2}°, 2)=8011+\tfrac{1}{6}\{-1450+4(-2072)+(-3188)\}$$
$$=5857.$$

As this value is less than 5865 (the value of Q(?)), evidently the extrapolated value of q_1 is too large. We therefore try a smaller value of q_1, viz. 273·0, and get the corresponding values 5828 and 5830 for Q(?) and $Q(72\frac{1}{2}°, 2)$, the latter being the value obtained by integration along s. Since Q(?) is, in this case, the smaller of

Table IV.
Values of Q.

ε.	$q_1 \backslash N =$	1.	2.	3.	4.	5.	6.	7.	8.	9.	10.
5°	116·6	783	1238	1464	1560	1594	1604	—	—	—	—
10°	231·2	1555	2461	2915	3107	3176	3196	—	—	—	—
15°	341·5	2303	3653	4334	4626	4731	4762	—	—	—	—
20°	445·3	3013	4795	5705	6101	6246	6290	—	—	—	—
25°	540·1	3673	5871	7011	7515	7705	7764	7783	—	—	—
30°	623·6	4266	6862	8234	8855	9096	9171	9194	—	—	—
35°	693·0	4778	7745	9352	10100	10398	10495	10523	—	—	—
40°	745·3	5190	8497	10339	11224	11585	11714	11749	—	—	—
45°	777·1	5479	9082	11158	12199	12635	12804	12849	—	—	—
50°	783·9	5617	9458	11766	12983	13518	13738	13800	—	—	—
55°	760·1	5565	9568	12104	13522	14191	14482	14580	—	—	—
60°	698·7	5274	9338	12095	13745	14587	14988	15138	15200	—	—
62½°	650·7	5015	9053	11916	13698	14661	15130	15317	15400	—	—
65°	588·8	4662	8625	11584	13517	14619	15175	15415	15516	—	—
67½°	510·0	4192	8011	11044	13150	14425	15102	15415	15538	15580	—
70°	408·5	3560	7134	10204	12509	14007	14862	15290	15450	15519	—
71¼° *	346·6	3160	6556	9631	12047	13678	14647	15151	15358	15448	—
72½°	273·1	2672	5831	8885	11417	13211	14329	14938	15221	15342	15388
73¾°	180·0	2034	4828	7820	10475	12490	13832	14609	15016	15183	15257

* The last digit in the value of Q from 70° onwards is not reliable.

the two, the value 273·0 of q_1 is slightly too small. Interpolation now enables us to arrive at the final value 273·1 for q_1 at $s=72\frac{1}{2}°$. The entries in the first two lines of Table V. can now be found.

TABLE V.

Solution at $s=72\frac{1}{2}°$. Preliminary values.

$q_1'=-320\cdot8/k$, $q_1''=-319/k^2$,

$q_2=12\cdot36\dot{}\times10^4$, $q_2'=1462\cdot2\times10^2/k$, $q_2''=30875/k^2$,

$q_4=-2\,!(1200)^2\times100\times666\cdot5$,

$q_5=3\,!(1200)^3\times100\times166\cdot5$, $q_6=4\,!(1200)^4\times100\times15\cdot7$,

$q_7=-5\,!(1200)^5\times100\times19\cdot4$, $q_8=6\,!(1200)^6\times100\times4\cdot6$,

$q_9=-7\,!(1200)^7\times100\times0\cdot57$.

N.	Q_2.	Q_1.	Q.	Q′.	W.	Q, by integrating Q′.
0.....	12·36̇	273·1	0	0	0	0
1.....	7·37	361·1̇	2672̇	−2162	− 0·960	2672̇
2.....	− 2·10	384·0	5831	−3344	− 3·331	5831
3.....	− 7·54	338·4	8865	−3417	− 6·225	8890
4.....	−10·24	260·8	11375	−2954	− 8·877	11423
5.....	− 9·88	175·3̇	13190	−2252	−11·082	13208
6.....	− 7·53	101·8	14330	−1540	−12·627	14324
7.....	− 4·71̇	50·8	14950	− 994	−13·695	14938
8.....	− 2·36	22·1	15240	− 655	−14·341	15220
9.....	− 1·10	8·2	15360	− 485	−14·833̇	15342
10.....	− 0·39	2·3̇	15400	− 395	−15·171	15390

To complete the solution for $s=72\frac{1}{2}°$ we choose a smooth sequence of values of Q tending to Q, viz., 15422. These values of Q and the corresponding values of Q_1 and Q_2 obtained by numerical differentiation are entered in the fourth, third, and second columns of Table V. respectively.

The values of Q′ and W at N=3, 4, . . . successively are then found from (6) and (8). These are entered in columns 5 and 6 of Table V.

Using these values of Q′ and integrating along s we get the set of values of Q entered in column 7 of Table V.

This set of values may be taken as the final values of Q for $s=72\frac{1}{2}°$.

To show that there are no appreciable errors in these values. we repeat the same set of operations on the above set of values of Q, thus getting the complete Table VI. Comparing the values of Q in the seventh columns of Tables V. and VI., we find that the differences between the two sets are nowhere greater than 6—which hardly affects the third decimal place in the final values of q.

TABLE VI.

Solution at $s=72\frac{1}{2}°$. Final values.

N.	Q_2.	Q_1.	Q.	Q′.	W.	Q, by integrating Q′
0.....	12·36̇	273·1	0	0	0	0
1.....	7·37	361·1̇	2672̇	−2162	0·960	2672̇
2.....	− 2·10	384·0	5831	−3344	3·331	5831
3.....	− 7·82	342·4	8890	−3451	6·235	8884
4.....	−11·18	260·3	11423	−2988	8·924	11417
5.....	− 9·72	171·0	13208	−2228	11·232̇	13214
6.....	− 7·21̇	100·2̇	14324	−1518	12·651	14328
7.....	− 4·80	50·4	14938	− 998	13·815	14937
8.....	− 2·19	21·3̇	15220	− 644	14·361	15222
9.....	− 0·97	9·0	15342	− 490	14·944	15341
10.....	− 0·44	3·6	15390	− 420̇	15·201̇	15386

9. *Remarks.*

(i.) It is possible now to revise the whole solution with fresh values of $\partial q/\partial s$, derived by applying a central-difference formula to the values of q obtained above. This should give a better solution, because formerly we had necessarily to employ the Gregory-Newton formula * in deriving (9) and (10). Preliminary examination showed, however, that the alterations would not be much and hence a second approximation was not carried out.

(ii.) Solution beyond 73°—Green says that at 73° the solution fails. " The fact that the solution at 73° demands

* ' Calculus of Observations,' § 35.

a large positive value of $\partial q\mathrm{R}/\partial s$ indicates a sudden change of conditions here." His values of $10^{-6}\ \partial q\mathrm{R}/\partial s$ for $n=0{\cdot}001$, at $s=71°$, $72°$, $73°$ are $-1{\cdot}08$, $-1{\cdot}00$, $+46{\cdot}4$. But in our solution in this region at $\mathrm{N}=1$ the values of Q' at $s=71\frac{1}{4}°$, $72\frac{1}{2}°$, $73\frac{3}{4}°$ are -1760, -2162, -3030, which is a regular sequence *, showing that the method of solution does not fail. But the solution beyond 73° would be of no practical importance, because w is not now negligibly small as compared to q, and thus one of the assumptions on which the boundary layer equations are based is violated.

(iii.) It is believed that the method of the present paper is less laborious than that of Green.

10. *Comparison of Results.*

To test the comparative accuracy of the solution as given in this paper and as given by Green, the numerical values of the various terms in the first of the boundary layer equations, viz., equation (6), were calculated from the final values of q in each solution, using central-difference formulæ to find the differential coefficients of q. As regards the value of dp/ds in testing Green's solution, his own values were used to make sure that no errors were introduced on this account. As the work involves much labour, the solutions were compared only at four neighbouring points near the centre of the field, viz., at $\mathrm{N}=3, 4$; $s=30°$, $35°$. The various terms of equation (6) are shown in Table VII.

The residual errors, given by the differences between the entries in the last two rows, for the four positions are thus $5{\cdot}2\dot{1}$, $10{\cdot}06$, $3{\cdot}5\dot{5}$, $11{\cdot}04$ for Green's solution as against $0{\cdot}01$, $0{\cdot}05$, $0{\cdot}16$, $0{\cdot}01$ for our solution, showing that Green's set of values of q does not satisfy the boundary layer equations so well as ours.

It is believed that the accuracy in other parts of the field will be of the same order.

To see how far Green's solution will tally with the solution obtained by the present method on using his values of dp/ds, the work was carried out for $s=5°$, $10°$,

* The corresponding values of $10^{-6}\ \partial q\mathrm{R}/\partial s$ at $71\frac{1}{4}°$, $72\frac{1}{2}°$, $73\frac{3}{4}°$ are $-0{\cdot}38$, $-0{\cdot}47$, $-0{\cdot}66$.

Table VII.

Comparison of the solution obtained in the present paper with that of Green.

	$s=30°$, N=3.		$s=30°$, N=4.		$s=35°$, N=3.		$s=35°$, N=4.	
	Green's.	Present.	Green's.	Present.	Green's.	Present.	Green's.	Present.
$-10^{-8}R^2dp/ds$	249·0	257·7	249·0	257·7	267·0	275·5	267·0	275·5
Q	8640	8234	9831	8855	9681	9352	10386	10100
Q′.....	1090	1174	1617	1296	1062	1057	1034	1189
W.....	1·572	1·770	2·656	2·805	1·508	1·492	2·455	2·480
Q_1	147·2	110·8	160·1	45·9	145·0	131·8	19·2	56·1
Right-hand side of (6).	−11·05	−10·67	−1·24	−5·32	−10·81	−12·09	− 6·12	−6·26
Left-hand side of (6)..	− 5·84	−10·68	8·82	−5·27	−14·37	−12·25	−17·16	−6·27

15°, employing his values of dp/ds. The following values of q_1 were obtained :—

s.	5°.	10°.	14°.
q_1 of Green's solution	117·7	228·0	358·5
Our values of q_1 with Green's dp/ds	111·5	232·0	345·5

Fig. 1.

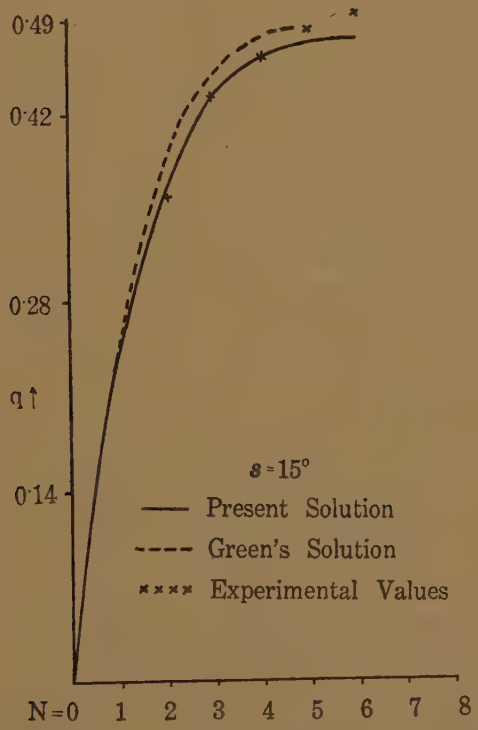

It is evident that there are fairly large differences, showing that Green's solution is different from ours mainly because his method is not very exact, and not so much because we have used graduated values of dp/ds.

In conclusion, I wish to express my best thanks to Dr. Gorakh Prasad, at whose suggestion I took up the

problem, and under whose guidance I carried out the investigation.

In figs. 1–4, the velocity-distribution curves obtained in this paper and also those obtained by Green are drawn for four equidistant values of s. The experimental values are also shown. The present values are somewhat nearer to the experimental values.

Fig. 2.

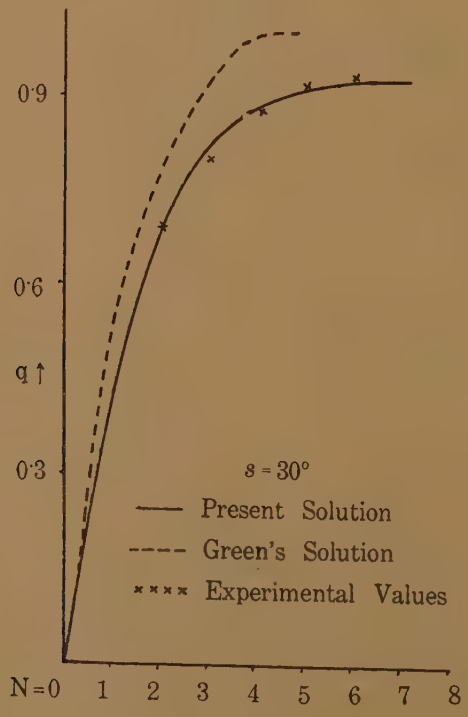

Appendix 1.

We shall prove here that if the extrapolated value of Q and the corresponding values of Q′, W, and Q_1 be substituted in the right-hand side of (6), then the value of Q_2 so obtained gives by integration a value of Q nearer to the correct one than the extrapolated value.

If the extrapolated value of the velocity be $Q+\epsilon$ instead of Q, then the corresponding values of Q′, Q_1, and W exceed the correct values by 3ϵ, $10^{-4}\times 3\epsilon/b$, and

$b\epsilon$ respectively, Simpson's rule being supposed to be used. These give for the left-hand side of (6) the value

$$Q_2+\epsilon\{10^{-4}(3Q+Q')-(3\times10^{-4}/b)W-Q_1b\}(9{\cdot}43/k).$$

Using this value we obtain, after two integrations, for the velocity the value

$$Q+\epsilon(R.b^2/9k)\{3Q+Q'-10^4bQ_1-3W/b\}.$$

Fig. 3.

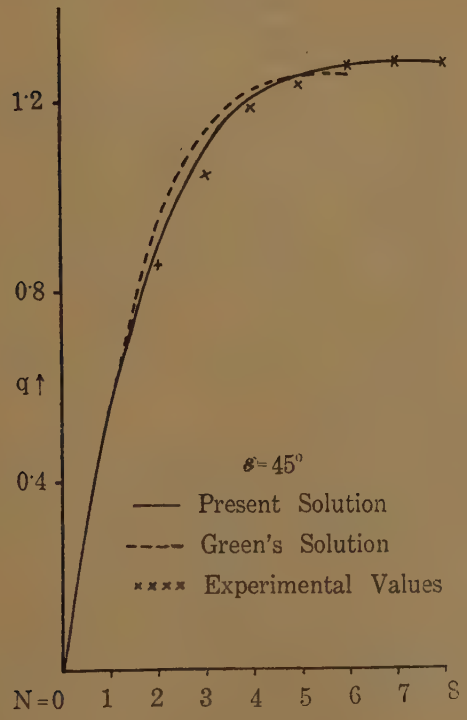

Substituting the numerical values of Q′, etc., this is found to be less than $Q+\epsilon$, even under the most unfavourable conditions, up to 60°.

After 60° this method of arriving at the correct value of Q fails towards the end of the boundary layer. However, it is easy after 60° to extrapolate for Q a value so near the exact one that we can see at once what value of Q should be taken so that Prandtl's equations may be exactly satisfied.

Appendix 2.

It will be shown here that, for positions beyond 70°, if the value of Q at N=2 be calculated from the power-series with an extrapolated value of q_1, and the corresponding values of Q_2, Q_1 be found by numerical differentiation, and these three be substituted in equations (6) and (8) so as to give values of W and Q′, then this value

Fig. 4.

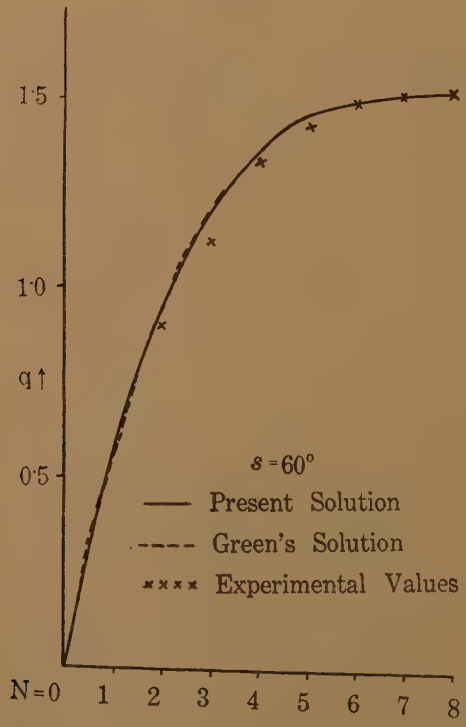

of Q′ would give on integration a value of Q nearer to the correct value than the one we started with.

Let the values of the various quantities at N=r be denoted by enclosing the quantity within brackets and attaching the suffix r. If the extrapolated value is $q_1+\epsilon$, instead of q_1, the entries in the q-table would be of the form :—

N.	Q_2.	Q_1.	Q.	Q′.	W.
0 ...	$(Q_2)_0$	$(Q_1)_0+\epsilon$	0	0	0
1 ...	$(Q_2)_1+m_1\epsilon$	$(Q_1)_1+l_1\epsilon$	$(Q)_1+k_1\epsilon$	$(Q')_1+12k_1\epsilon$	etc.
2 ...	$(Q_2)_2+m_2\epsilon$	$(Q_1)_2+l_2\epsilon$	$(Q)_2+k_2\epsilon$		

The interval along s is $\frac{1}{4}k$.

To find the coefficients k_1, l_1, m_1, and k_2 we substitute in the power-series (11) values of q_1', q_1'', ... corresponding to the value $q_1+\epsilon$. We get

$$q=\mathrm{P}+\epsilon\mathrm{F}+\ldots, \quad \ldots\ldots \quad (\mathrm{A})$$

where P is the series on the right in (11) and

$$\mathrm{F}\equiv n+\mathrm{R}(q_1'+12q_1/k)n^4/4\,!+2\mathrm{R}q_2'n^5/5\,!+\mathrm{R}^2\{8q_1q_1''-(q_1')^2+4(12q_1/k)^2-2(12q_1/k)q_1'\}n^7/7\,!+\ldots.$$

Comparing the values of Q, Q_1, ... given by (A) with the values entered in the above table, we have

$$k_1=10^4(\mathrm{F})_{n=b},\ l_1=(\partial\mathrm{F}/\partial n)_{n=b},\ m_1=10^{-4}(\partial^2\mathrm{F}/\partial n^2)_{n=b},\quad k_2=10^4(\mathrm{F})_{n=2b};$$

and using (13) and (14) we find that

$$l_2=10^{-4}(3k_2/b)-1-4l_1,\ m_2=10^{-4}(3/b)\{10^{-4}(3/b)k_2-2-4l_1\}-4m_1.$$

Let now the values of Q′ and W, which, with the values of Q, Q_1, and Q_2 as entered against N = 2 in the above table, satisfy (6) and (8), be $(Q')_2+x$ and $(W)_2+y$ respectively. Solving for x we have

$$\{10^{-4}(Q)_2-(Q_1)_2b/3\}x=\{(k\times10^8/\mathrm{R})m_2+l_2(W)_2-10^{-4}k_2(Q')_2+16bk_1(Q_1)_2\}\epsilon+\ldots.$$

Now b, k, R are known constants (§ 2); and the approximate values of k_1, l_1, and m_1 in the region $70°<s<75°$ are found to be 10, 2, 0·35, and 65 respectively. Using these and the approximate values of Q′, W, Q at N = 2 in the region, we get finally

$$x=330\epsilon.$$

Using the value of Q′, viz. $(Q')_2+330\,\epsilon$, thus obtained, we get on integration along s the value $(Q)_2+27{\cdot}5\,\epsilon$. This value is nearer to the correct value $(Q)_2$ than the value $(Q)_2+65\epsilon$ entered in the table.

XCIV. *Notices respecting New Books.*

Negative Ions. By H. S. W. Massey. *Cambridge Physical Tracts*, No. 1. [Pp. 100+18 figs.] (Cambridge University Press. Price 6*s*.)

THIS is the first of the new series of Cambridge Physical Tracts.

This is not the first time that small books of the monograph type have emanated from Cambridge, and the new series is sure of a warm welcome.

Under the general editorship of Professor Oliphant and Mr. J. A. Ratcliffe, the aim is outlined in a brief general preface which forecasts the provision of "authoritative accounts of subjects of topical interest written by those actively engaged in research . . ." so that . . . "readers will be provided with accounts of those subjects which are advancing so rapidly that a full-length book would be out of place."

There is the intention obviously that there should be no overlap with the normal text-book on the one hand or such "accounts" as are already provided on the other hand by, shall we say, Reviews of Modern Physics, Science Progress, or the useful Reports on Progress in Physics issued by the Physical Society.

An excellent topic, with the right author, is chosen for No. 1 of the new series. Dr. Massey has devoted a number of years at Cambridge and Belfast to the study of electric particles, and is particularly competent to write on the subject.

Chapters I. and II. deal with atomic and molecular ions. The application of quantum methods to certain structures is examined—electron affinity discussed and the importance of excited states stressed. The structures of certain simple negative molecular ions are described.

In Chapter III. modes of formation of ions by various collision, capture, and radiative processes are outlined and the experimental evidence set out.

The short Chapter IV. deals with the little-known matter of negative ion ionization, while Chapter V. is a stimulating *résumé* of our present knowledge in applying the ideas of ion formation and destruction to the elucidation of phenomena in the glow discharge and the upper atmosphere.

An excellent little book, well thought out and presented, it is to be thoroughly recommended. R. W.

Elliptic and Hyperelliptic Integrals and Allied Theory. By the late W. R. Westropp Roberts. With a foreword by the Rev. R. R. Hartford, B.D. [Pp. 311.] (Cambridge University Press. Price 12*s.* 6*d.*)

This book is published partly as a memorial volume to its author. Actually, the book was not completed at the time of his death in 1935 (he was eighty-five then). The duties of tutor, and later of Vice-Provost, at Trinity College, Dublin, evidently did not leave Roberts that leisure for the close application to detail which characterizes the chapters which have been written. We may be satisfied that, at any rate, only particular aspects of the theory have been omitted.

The text has an old-fashioned air about it, and one would almost expect after turning over a few pages to find the date 1898 on the title-page. Straight d's, for partial differentiation, are a sign of the times.

The first chapter, of about seventy pages, deals with a set of theorems in algebra. To begin with, these are concerned with the symmetric functions of some or all of the roots of an equation. Three differential operators, δ, $\triangle$, $\nabla(\equiv\delta\triangle-\triangle\delta)$, play fundamental parts—especially δ : if the variable z in the equation is replaced by x/y, and if x_r/y_r $(r=1, \ldots, n)$ are the roots of the equation, then $\delta\equiv-\Sigma y_r\frac{\partial}{\partial x_r}$ and $\triangle\equiv-\Sigma x_r\frac{\partial}{\partial y_r}$. Functions which vanish when operated on by δ are called O-functions and are classified. A section is also devoted to the subject of eliminants. The ordinary reader will find this a stiff chapter ; there is a lot of notation to master and the algebra is by no means light. Yet the understanding of all this is essential for what follows.

The second chapter brings us to the proper subject of the book, namely, the general integral of the type $\int\frac{\phi(z)\,dz}{\psi(z)\sqrt{f(z)}}$, where ϕ, ψ, f are polynomials in z, and f has degree $2m$. The first problem resolved is that of expressing the general integral in terms of elementary ones of the types

$$\int\frac{z^r dz}{\sqrt{f(z)}} \quad \text{and} \quad \int\frac{dz}{(z-n)\sqrt{f(z)}}.$$

Chapter III. deals with the resolution of Abel's differential equations $\sum_{i=1}^{m}\frac{z_i^r\,dz_i}{\sqrt{(fz_i)}}=0$ $(r=0, 1, \ldots, m-1)$ by means of rational integral algebraic forms. Briefly, the method is as follows. Following Jacobi, the equation for which $r=m-1$ has the

zero on the right replaced by dt, so that a new variable is introduced. Next, one takes the function $\phi(z) \equiv (z-z_1) \ldots (z-z_n)$ and deduces (the method begins curiously but seems to come right), with the help of the modified equations of Abel, an equation of the form $\left\{ \frac{\partial \phi(z)}{\partial t} \right\}^2 = \mathrm{F}(z)$, where $\mathrm{F}(z)$ is a polynomial involving $m-1$ arbitrary constants. From $\mathrm{F}(z)$ is formed (with the help of δ) a so-called square-matrix (it is really oblong, having $4m-7$ rows and $2m-4$ columns). The determinants of order $2m-4$, picked out of this matrix and put equal to 0, are the required solutions of Abel's initial equations.

Chapter IV. is concerned with an algebraic demonstration of the periodicity of the integrals and with the relations connecting the periods. The last two chapters are devoted to special consideration of the elliptic integrals and of the hyperelliptic integrals of genus 2.

There is a collection of examples at the end of each chapter but the last.

One gets the impression that Roberts was a teacher who spared no pains to be clear; and one feels that, in lectures at least, he would point out the landmarks to his class. A few sectional headings would have been correspondingly useful in this book: each step is simple enough, but there are so many steps.

The loose-cover describes this book as a striking essay in mathematical method. This is fully shown by the author's powerful command over algebraic technique and by his demonstration of what can be done by purely algebraic methods.

Gaseous Electrical Conductors. By E. L. E. Wheatcroft. [Pp. xi+265.] (Clarendon Press, Oxford, 1938. Price 21*s.* net.)

The subject of the conduction of electricity through gases (including the vacuum as a limiting case) is one of increasing importance to the Electrical Engineer; to the Physicist it has the attraction of presenting many problems which are still very far from an adequate solution. Both should welcome the very excellent survey of the subject which Professor Wheatcroft has provided in the book under review. As the author points out in his preface, it is a subject in which practice has run ahead of theory, but the theory is nevertheless essential to any proper understanding of the practice, and Professor Wheatcroft has, wisely, devoted appreciably more than half his space to a theoretical discussion of the subject. In preliminary chapters he deals briefly, but adequately, with

the various ionization processes in gases, and with the methods by which electricity is transferred from a metal to a gas. The motion of ions and electrons under electric and magnetic fields, both in vacuo and in a dense gas, is considered in detail, and further chapters deal with the breakdown of the insulating state, and with the glow, the arc, and the spark discharges. The second part of the work describes the application of the theoretical principles laid down to such practical devices as vacuum and gas-filled valves, mercury arc rectifiers, circuit breakers, and various types of commercial luminous discharge-tubes.

The book can be unreservedly recommended both to the engineer and the physicist. To those, and they are many, engaging in research on "valves" and kindred appliances it should be invaluable. Professor Wheatcroft has the enviable ability of being able to discern the essentials of a subject, and can present them vividly and clearly in a minimum number of words. The book contains far more information than one would deem possible from its length, while numerous references tell the reader where he can obtain first-hand information of any point on which he may require further details. The work, however, is much more than a mere compilation. Professor Wheatcroft is an authority on his subject, and is not afraid to point out errors and lacunæ in current theories, even when the theories have the support of eminent authorities. The book is well illustrated and excellently produced. It is a notable addition to the Oxford Engineering Science Series, to which it is the latest addition.

J. A. Crowther.

Ferromagnetism. By J. R. Ashworth, D.Sc. [Pp. xiv+97.] (London: Taylor and Francis, 1938. Price 7*s.* 6*d.*)

Dr. Ashworth has devoted the leisure of some forty years to the experimental study of ferromagnetism, and his work has been consistently guided (though he has turned aside on occasion to explore interesting bypaths) by one main consideration—the establishment of a ferromagnetic equation of state which shall closely represent and serve for an interpretation of the experimental results. The demonstration of the principle of corresponding states in the relation of ferromagnetism to temperature leads to an equation of state of the form

$$(H+H_i)\left(\frac{1}{I}-\frac{1}{I_0}\right)=R'T,$$

where H_i is an intrinsic field and I_0 the maximum intensity of magnetization. Putting $H_i=a'I^2$, we have a magnetic analogue of van der Waals's equation, the consequences of which are explored experimentally and discussed in full detail. Quantum considerations do not enter into the exposition, which is confined to the development of the ferromagnetic equation.

The investigations chronicled grew out of a technical research devoted to the improvement of magnets used in magnetic observations, and Dr. Ashworth is to be congratulated on the pertinacity with which he has pursued his theme, on the skill of his experimental work, and on the clarity with which he has discussed them in this interesting and unpretending volume.

The Physical Properties of Colloidal Solutions. By Prof. E. F. Burton. [Third edition; pp. viii+235.] (London: Longmans, Green & Co., 1938. Price 15*s.*)

One of the mildly depressing features of the rapid advances in modern science is the corresponding increase in the dimensions of the "handbooks" dealing with any particular advance, the compact little volume of some two hundred pages becoming an unwieldy and forbidding tome approaching, and sometimes exceeding, the thousand-page limit. Prof. Burton's book on colloids first appeared in 1916, and ran into a second edition in 1921. The new edition, of which more than half has been completely rewritten, is still kept within the 250-page limit, and is all the better for the author's refusal to yield to the temptation to write an encyclopædia of colloid physics. This compression has been attained by a very wise limitation of the topics discussed rather than by a skimpy treatment of a great many topics, and the reader must not seek, within its covers, for discussions of subjects that were never meant to be handled therein. In general, the author's aim has been to stress the contribution made by colloid physics to the kinetic theory of matter.

The book opens with a brief history of the subject, followed by chapters on the classification and preparation of colloidal solutions and on the forces regulating the sizes of colloidal particles. A very full section dealing with the ultra-microscope is succeeded by three chapters in which are discussed the Brownian movement, the distribution of particles in a colloidal solution, and methods for the determination of Avogadro's number. The remaining sections of the book are devoted to a consideration of the optical properties of colloidal solutions, the size of colloidal particles, electro-kinetic phenomena, and coagulation.

The treatment throughout is delightfully readable and clear, the chapters on Brownian movement and on Avogadro's number being models of their kind. Bibliographies, amounting in all to nearly 450 entries, are appended to each chapter.

The book may be warmly commended to the attention of students of chemistry and of physics in the honours grade. A.F.

[*The Editors do not hold themselves responsible for the views expressed by their correspondents.*]

INDEX TO VOL. XXVI.

ABSOLUTE measurements of radiometric action in gases, 987.
Acoustical insulation afforded by double partitions constructed from dissimilar components, 253.
Allan (G.) E., note on velocity of sound in copper, 609.
Anthraquinone, X-ray analysis of the structure of, 213.
Archibald (W. J.), the complete solution of the differential equation for the confluent hypergeometric function, 415.
Arcs of various metals in capillary tubes, 1000.
Astbury (N. F.), the effects of stray admittances in four-arm bridge networks, 507.
Atomic and ionic radii.—I. Numerical values and their bearing on the compressibilities of metals, 129; II. Application to the theory of solid solubility in alloys, 143; III. Polarization effects in alloys, 152.
Awbery (J. H.), the latent heat of fusion of aluminium, 776.
Axial potential distribution in electron optical systems, on the equation to the, 601.
Bailey (V. A.) on some effects caused in the ionosphere by electric waves.—Part II., 425.
—— and Somerville (J. M.), the graphical solution of ordinary differential equations, 1.
—— ——, study of the magneto-ionic theory of wave-propagation by means of simple formulæ, linkages and graphical devices, 888.
Band-pass effects in wave-filters terminated in negative resistances, 173.
Basis metal, calculation of the area of, exposed at discontinuities in the tin coating of tinplate, 1077.
Bate (A. E.) and Wilson (E. T.), resonance in truncated cones, 752.
Bateman (H.), paraboidal coordinates, 1063.
Benham (W. E.), classical wave functions for moving corpuscles, 1031.
Benjamin (M.) and Jenkins (R. O.), the surface migration of barium, 1049.
Books new :—E. C. Kemble, Fundamental Principles of Quantum Mechanics, 188; E. W. Strong, Procedures and Metaphysics, 189; E. C. Titchmarsh, Introduction to the Theory of Fourier Integrals, 191; C. H. D. Clark, The Fine Structure of Matter.—Part I. X-Rays and the Structure of Matter, 192; Part II. Molecular Polarization, 311; Part III. The Quantum Theory and Line Spectra, 311; Perspectives in Biochemistry, 419; B. Lewis and G. von Elbe, Combustion, Flames, and Explosion of Gases, 421; W. A. Wooster, A Text-book on Crystal Physics, 422; A. Einstein and L. Infeld, The Evolution of Physics, 423; C. E. Weatherburn, An Introduction to Riemannian Geometry and the Tensor Calculus, 615; R. A. Dodge and M. J. Thompson, Fluid Mechanics, 724; M. Muskat and R. D. Wickoff, The Floes of Homogeneous Fluids through Porous Media, 725; E. Hubble, The Observational Approach to Cosmology, 726; W. H. Watson, On Understanding Physics, 727; H. S. W. Massey, Negative Ions, 1110; the late W. R. Westropp Roberts, Elliptic and Hyperelliptic Integrals and Allied Theory, 1111; Prof. E. L. E. Wheatcroft, Gaseous Electrical Conductors, 1112; Dr. J. R. Ashworth, Ferromagnetism, 1113; Prof. E. F. Burton, The Physical Properties of Colloidal Solutions, 1114.

Bose (D. M.) and Mukherji (P. C.) on the origin of colour of paramagnetic ions in solution, 757.
Capacities at radio frequencies, an original method of comparison of, 521.
Capillary ascent in cylindrical tubes, 519.
Carslaw (H. S.) and Jaeger (J. C.), some problems in the mathematical theory of the conduction of heat, 473.
Chakravarti (S. P.), band-pass effect in wave-filters terminated in negative resistances, 173.
Charged colloid particles in an ultrasonic field.—II. Particles surrounded by a thin double layer, 674.
Clark (R. J.), the measurement of the velocity of light over a single journey, 361.
Classical wave functions for moving corpuscles, 1031.
Colloidal graphite, a study of the action of ionizing radiations on, 120.
Conduction of heat, some problems in the mathematical theory of the, 473.
Confluent hypergeometric function, complete solution of the differential equation for the, 415.
Constable (J. E. R.), acoustical insulation afforded by double partitions constructed from dissimilar components, 253.
Crowther (J. A.), Liebmann (H.), and Jones (R.), a study of the action of ionizing radiations on colloidal graphite, 120.
Crystalline diamagnetism of thallium, 1018.
" Curie " scale of temperature, remarks on the, 849.
Dasannacharya (B.) and Seth (Amar Chand), optical silvering on glass, 953.
Daunt (J. G.) and Mendelssohn (K.), co-existence of normal and supra-conductive regions, 376.
Davies (R. M.) and Landon (D. H.), the determination of the rigidity modulus of nickel and some of its alloys in the annealed and unannealed states, 816.
Diffraction of X-rays by an age-hardening alloy of aluminimum and copper. The structure of an intermediate phase, 855.
Dippy (J. F. J.), the limiting conductivities of organic acids in aqueous solutions, 93.
Eagle (A.), a criticism of the special theory of relativity, 410.
Einstein's orbital equation, the solution of, 983.
Elastic scattering of electrons by molecular hydrogen, calculation of the, 32.
Electrical discharge in argon, note on the, 719.
—— discharges, generalization of the theory of, 290.
Electrodynamic volume and porosity of metallic particles, 453.
Electrons, the behaviour of, in iodine vapour, 940.
Electrosmotic circulation in varying fields, the theory of, 49.
Energy balance sheets of internal combustion engines, note on thermodynamics of, 784.
—— theorems applicable in structural theory, the relation between the, 617.
Erdélyi (A.), integral representations for products of Whittaker functions, 871.
Fabian (W.), generalized fractional integration and differentiation, 408.
Fairthorne (R. A.), the large deflexions of a thin circular ring, 1006.
Ferguson (A.) and Kennedy (S. J.) on the surface tensions of liquid crystals, 41.
Field distribution and graphical ray tracing in electron optical systems, 570.
Finite strain; dislocation solutions, 557.
Fluorescent chromium ions in ruby, 878.
—— ion of chromium in ruby, on the, 380.
Flow of a viscous fluid past a circular cylinder, 1085.
Fredlund (E.), absolute measurements of radiometric action in gases, 987.
General graduation formula for the smoothing of time series, 970.
Generalized fractional integration and differentiation, 408.
—— hypergeometric function and certain related functions, proofs of some formulæ for the, 82.

Gill (E. W. B.) and Townsend (J. S.), generalization of the theory of electrical discharges, 290.
Globular proteins, on the molecular weight of the, 313.
Gogate (D. V.), a relativistic study of the Joule-Thomson effect and and adiabatic processes in a gas. —Part II., 166.
Graphical solution of ordinary differential equations, 1.
Gravitational waves in linearized fields, 1068.
Guha (B. C.), X-ray analysis of the structure of anthraquinone, 213.
Gupta (H. C.), the flow of viscous fluid past a circular cylinder, 1085.
Hammerton (T. A.) and Wheatcroft (E. L. E.), pre-striking conditions in a thyratron, 684.
Harvey (K. .F) and McNeill (D. B.), some aspects of nitrogen afterglows, 502.
Hay (R. H.) and Robertson (J. K.), optical resolution and the visual examination of two overlapping photographic images, 495.
Healey (R. H.), the behaviour of electrons in iodine vapour, 940.
Hermans (J. J.), charged colloid particles in an ultrasonic field.—II. Particles surrounded by a thin double layer, 674.
——, surface phenomena with charged spherical particles when moving in a solvent. Cataphoresis; sedimentation potential, 650.
Herrenden Harker (G. F.), the mechanism of synchronization in the linear time base, 193.
Hoare (W. E.), calculation of the area of basis metal exposed at discontinuities in the tin coating of tinplate, 1077.
Hughes (J. W.), a new method for determining the uniaural differential threshold, 635.
Hume-Rothery (W.) and Raynor (G. V.), atomic and ionic radii.—I. Numerical values and their bearing on the compressibilities of metals, 129; II. Application to the theory of solid solubility in alloys, 143.
Ingram (W. H.), Kirchhoff constraints,and sagittal graphs, 268.
Ionsphere, on some effects caused in the, by electric waves, 425.
Jacob (L.), field distribution and graphical ray tracing in electron optical systems, 570.
—— on the equation to the axial potential distribution in electron optical systems, 601.
Jaeger (J. C.) and Carslaw (H. S.), some problems in the mathematical theory of the conduction of heat, 473.
Jenkins (R. O.) and Benjamin (M.), the surface migration of barium, 1049.
Jones (R.), Crowther (J. A.), and Liebmann (H.), a study of the action of ionizing radiations on colloidal graphite, 120.
Joule-Thomson effect and adiabatic processes in a gas, a relativistic study of the.—Part II., 166.
Kennedy (S. J.) and Ferguson (A.) on the surface tensions of liquid crystals, 41.
Kirchhoff constraints and sagittal graphs, 268.
Kürti (N.) and Simon (F.), remarks on the thermodynamic scale of temperature, 840.
—— ——, remarks on the "Curie" scale of temperature, 849.
Landon (D. H.) and Davies (R. M.), the determination of the rigidity modulus of nickel and some of its alloys in the annealed and unannealed states, 816.
Large deflexions of a thin circular ring, 1006.
Latent heat of fusion of aluminium, 776.
Lateral vibration of a mild steel bar, the damping of the, 705.
Liebmann (H.), Jones (R.), and Crowther (J. A.), a study of the action of ionizing radiations on colloidal graphite, 120.
Limiting conductivities of organic acids in aqueous solutions, the, 93.
Linear time base, mechanism of synchronization in the, 193.
Longitudinal magnetic field, effect of, on the conductivity and refractive index of ionized air, 244.
Lowan (A. N.) on wave-motion for infinite domains, 340.
Löwy (H.), electrodynamic volume and porosity of metallic particles, 453.

McLachlan (N. W.), operational forms and contour integrals for Bessel functions with argument $a\sqrt{t^2-b^2}$, 394.
——, operational forms and contour integrals for Struve and other functions, 457.
——, operational form of $f(t)$ for a finite interval, with application to impulses, 695.
McNeill (D. B.) and Harvey (K. F.), some aspects of nitrogen afterglows, 502.
MacRobert (T. M.), proofs of some formulæ for the generalized hypergeometric function and certain related functions, 82.
Magneto-ionic theory of wave-propagation, study of the, by means of simple formulæ, linkages and graphical devices, 888.
Mean-value theorem in Riemann-Stieltje's integral, 722.
Mendelssohn (K.) and Daunt (J. G.), co-existence of normal and supra-conductive regions, 376.
Mindlin (R. D.), stresses in an eccentrically rotating disk, 713.
Molecular force and imperfect gases, 225.
Mukerji (B. C.) on gravitational waves in linearized fields, 1068.
Mukherji (P. C.) and Bose (D. M.) on the origin of colour of paramagnetic ions in solution, 757.
Narayanaswami (A. S.) and Ramachandra Rao (S.), the crystalline diamagnetism of thallium, 1018.
Narlikar (V. V.), a note on Riemannian tensors, 390.
Nernst heat theorem and irreversible processes at low temperatures, 260.
Newing (S. T.) and Shepherd (W. M.), finite strain: dislocation solutions, 557.
Newman (F. H.), note on the elecrical discharge in argon, 719.
——, note on the oxidation of the arc cathode, 187.
Nitrogen afterglows, some aspects of, 502.
Normal and supra-conductive regions, co-existence of, 376.
Ockleston (A. J.), the damping of the lateral vibration of a mild steel bar, 705.
Operational form of $f(t)$ for a finite interval, with application to impulses, 695.
Operational forms and contour integrals for Bessel functions with argument $a\sqrt{t^2-b^2}$, 394.
—— —— —— contour integrals for Struve and other functions, 457.
—— or symbolic calculus, application of the, to the theory of prime numbers, 921.
Optical resolution and the visual examination of two overlapping photographic images, 495.
—— silvering on glass, 953.
Oxidation, the parabolic law of, 65.
—— of the arc cathode, note on the, 187.
Paraboidal coordinates, 1063.
Paramagnetic ions in solution, on the origin of colour of, 757.
Piercy (N. A. V.), Preston (J. H.), and Whitehead (L. G.), the approximate prediction of skin friction and lift, 971.
Pipes (L. A.), operational solution of the wave equation, 333.
Pol (Balth. van der), application of the operational or symbolic calculus to the theory of prime numbers, 921.
Porter (A. W.), capillary ascent in cylindrical tubes, 519.
Preston (G. D.), the diffraction of X-rays by an age-hardening alloy of aluminium and copper. The structure of an intermediate phase, 855.
——, the parabolic law of oxidation, 65.
Preston (J. H.), Whitehead (L. G.), and Piercy (N. A. V.), the approximate prediction of skin friction and lift, 791.
Probability formula, short derivation of a fundamental, 223.
Radiometric action in gases, absolute measurement of, 987.
Ramachandra Rao (S.) and Narayanaswami (A. S.), the crystalline diamagnetism of thallium, 1018.
Raynor (G. V.), atomic and ionic radii.—III. Polarization effects in alloys, 152.
—— and Hume-Rothery (W.), atomic and ionic radii.—I. Numerical values and their bearing on the compressibilities of metals, 129; II. Application to the theory of solid solubility in alloys, 143.

Riemannian tensors, a note on, 390.
Rigidity modulus of nickel and some of its alloys in the annealed and unannealed states, the determination of the, 816.
Robertson (J. K.) and Hay (R. H.), optical resolution and the visual examination of two overlapping photographic images, 495.
Roscoe (R.), the calculation of the elastic scattering of electrons by molecular hydrogen, 32.
Salter (C.), sensitivity of the immersed Venturi-Pitot head at low speeds, 272.
Schumann (T. E. W.), a general graduation formula for the smoothing of time series, 970.
Sen (B.) direct determination of stresses from the stress equations in some two-dimensional problems of elasticity.—Part I., 98.
Sen (D. N.) on mean-value theorem in Riemann-Stieltje's integral, 722.
Seth (Amar Chand) and Dasannacharya (B.), optical silvering on glass, 953.
Shepherd (W. M.) and Newing (S. T.), finite strain : dislocation solutions, 557.
Silberstein (L.), short derivation of a fundamental probability formula, 223.
Simon (F.) and Kürti (N.), remarks on the thermodynamic scale of temperature, 840.
—— ——, remarks on the " Curie " scale of temperature, 849.
Singh (B. N.), effect of a longitudinal magnetic field on the conductivity and refractive index of ionized air, 244.
Skin friction and lift, the approximate prediction of, 791.
Somerville (J. M.) and Bailey (V. A.), the graphical solution of ordinary differential equations, 1.
—— ——, study of the magneto-ionic thoery of wave-propagation by means of simple formulæ, linkages and graphical devices, 888.
Special theory of relativity, a criticism of the, 410.
Stray admittances in four-arm bridge networks, the effects of, 507.
Stresses, direct determination of, from the stress equations, in some two-dimensional problems of elasticity.—Part I., 98.
—— in an eccentrically rotating disk, 713.
Sulaiman (S. M.), the solution of Einstein's orbital equation, 983.
Surface migration of barium, 1049.
—— phenomena with charged spherical particles when moving in a solvent. Cataphoresis ; sedimentation phenomena, 650.
—— tensions of liquid crystals, 41.
Thermodynamic scale of temperature, remarks on the, 840.
Thosar (B. V.) on the fluorescent ion of chromium in ruby, 380.
——, the fluorescent chromium ions in ruby, 878.
Thyratron, pre-striking conditions in a, 684.
Torsional vibration in certain mechanical systems, 729.
Townsend (J. S.) and Gill (E. W. B.), generalization of the theory of electrical discharges, 290.
Truncated cones, resonance in, 752.
Tuplin (W. A.), torsional vibration in certain mechanical systems, 729.
Ubbelohde (A. R.), the Nernst heat theorem and irreversible processes at low temperatures, 260.
Uniaural differential threshold, a new method for determining the, 635.
Vaughan (W.), an original method of comparison of capacities at radio frequencies, 521.
Velocity of light over a single journey, measurement of the, 361.
—— of sound in copper, note on, 609.
Venturi-Pitot head at low speeds, sensitivity of the immersed, 272.
Voss (V.), arcs of various metals in capillary tubes, 1000.
Walshaw (A. C.), note on thermodynamics of energy balance sheets of internal combustion engines, 784.
Wave equation, operational solution of the, 333.
—— motion for infinite domains, 340,

Wen-Po (W.), molecular force and imperfect gases, 225.
Wheatcroft (E. L. E.) and Hammerton (T. G.), pre-striking conditions in a thyratron, 684.
White (P.), the theory of electrosmotic circulation in varying fields, 49.
Whitehead (L. G.), Piercy (N. A. V.), and Preston (J. H.), the approximate prediction of skin friction and lift, 791.
Whittaker functions, integral representations for products of, 871.
Williams (D.), the relations between the energy theorems applicable in structural theory, 617.
Wilson (E. T.) and (A. E.), resonance in truncated cones, 752.
Wrinch (D. M.) on the molecular weights of the globular proteins, 313.

END OF THE TWENTY-SIXTH VOLUME.

Printed by TAYLOR & FRANCIS, Ltd., Red Lion Court, Fleet Street, E.C.4.

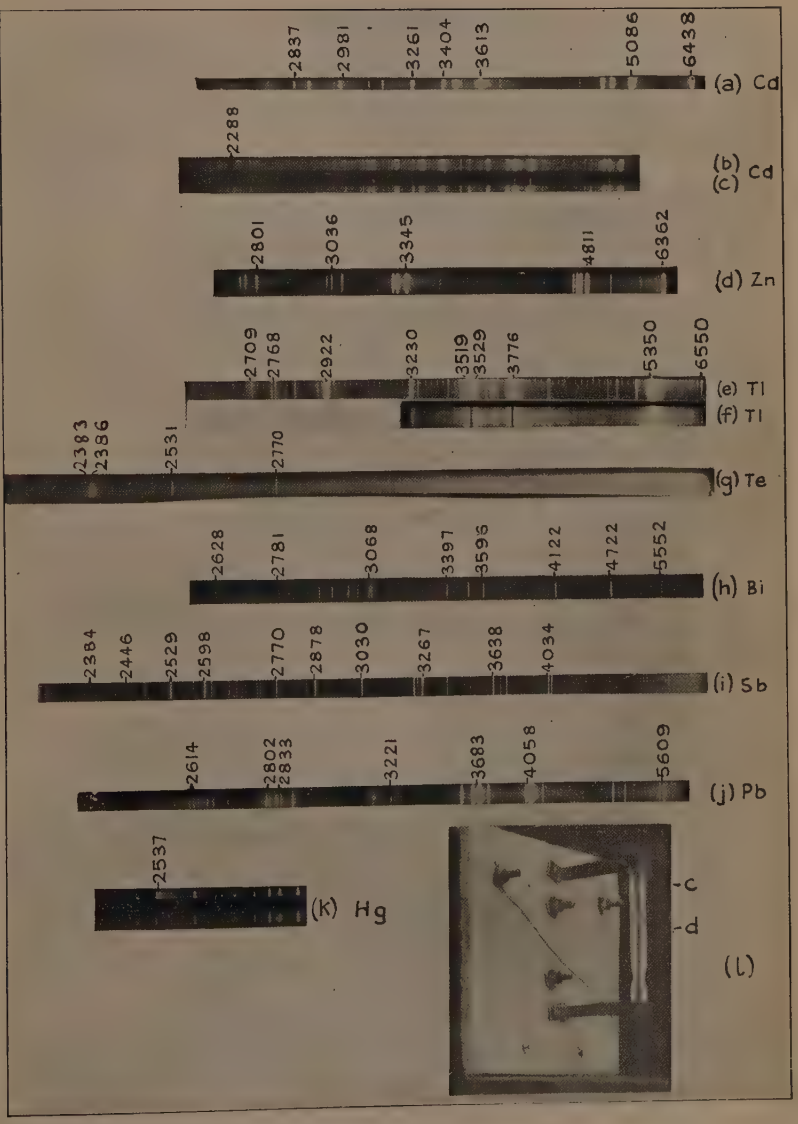
2837
2981
3261
3404
3613
5086
6438
(a) Cd
2288
(b) Cd
(c) Cd
2801
3036
3345
4811
6362
(d) Zn
2709
2768
2922
3230
3519
3529
3776
5350
6550
(e) Tl
(f) Tl
2383
2386
2531
2770
(g) Te
2628
2781
3068
3397
3595
4122
4722
5552
(h) Bi
2384
2446
2529
2598
2770
2878
3030
3267
3638
4034
(i) Sb
2614
2802
2833
3221
3683
4058
5609
(j) Pb
2537
(K) Hg
c
d
(l)

Fig. 2.

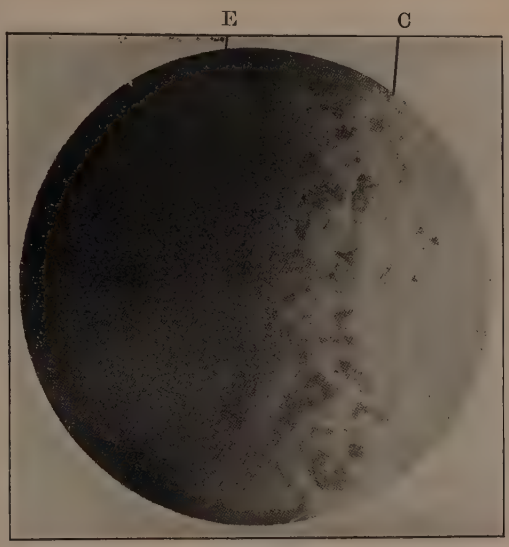

Surface ECD.

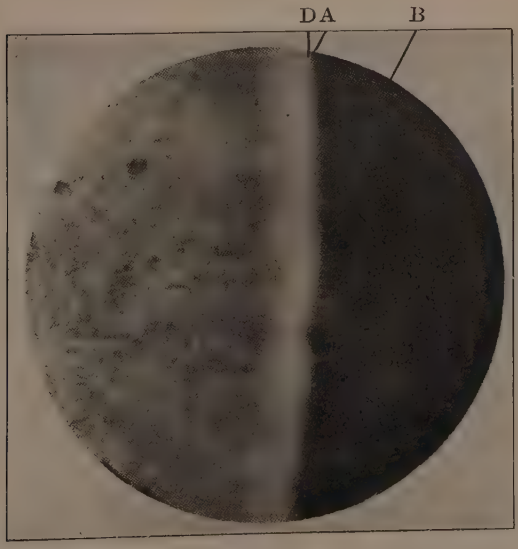

Surface CDAB.

Electron photomicrograph of stepped cathode.
Magnification ×100. Reproduction ×200.

Fig. 5.
Migration of thorium over tungsten.
(All photographs at 1250° K.)

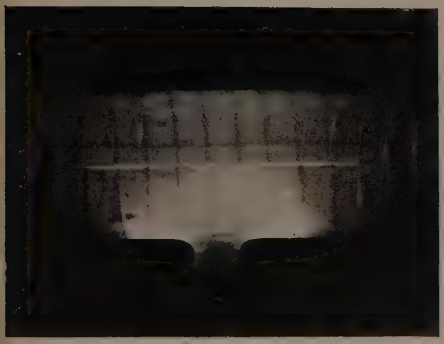

1. Initial deposit of Th.

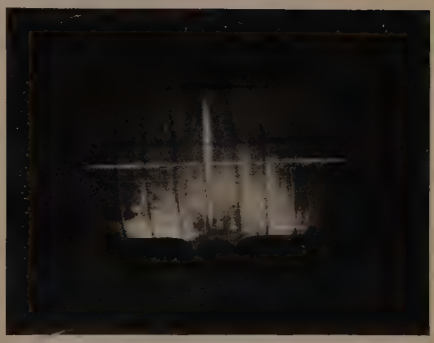

2. After ½ hour at 1535° K., showing migration along one crystal.

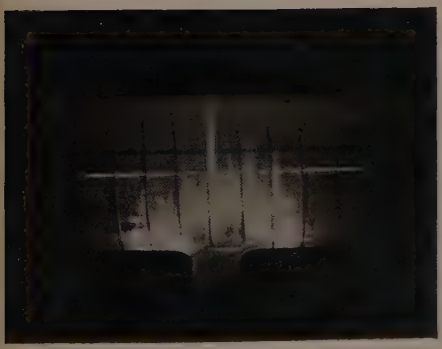

3. After 1½ hours at 1535° K., migration proceeding over other crystals.

4. After 2½ hours at 1535° K., migration proceeding slowly.

Fig. 5 (*continued*).

5. After 6 hours at 1535° K., migration still proceeding slowly.

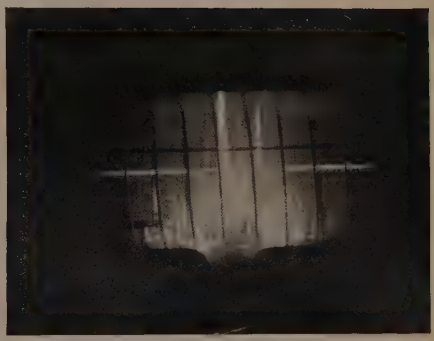

6. After 13½ hours at 1535° K., migration rate very slow.

7. After 3 hours at 1655° K., migration rapid.

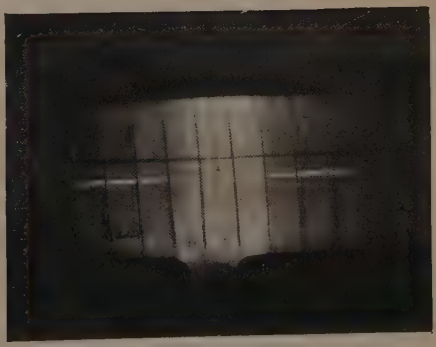

8. After 7 hours at 1635° K., migration complete.

Fig. 6.
Non-migration of barium on tungsten.
(All photographs at 1013° K.)

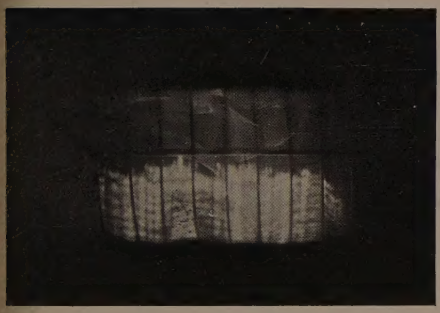

1. Original deposit of barium.

2. Deposit after 18 hours at 923° K., showing slight evaporation, no migration.

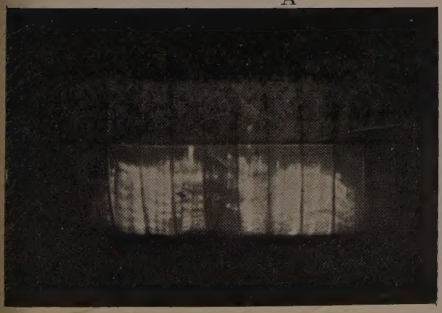

3. Deposit after $5\frac{1}{2}$ hours at 1013° K., showing evaporation but no migration.

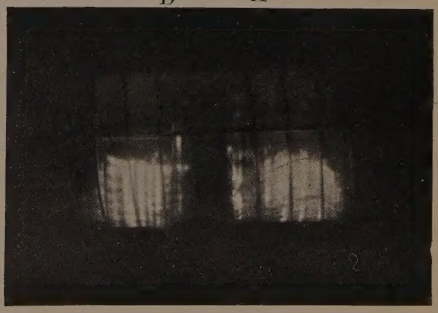

4. Deposit after $21\frac{1}{2}$ hours at 1013° K., showing marked evaporation.

FIG. 6 (*continued*).

B

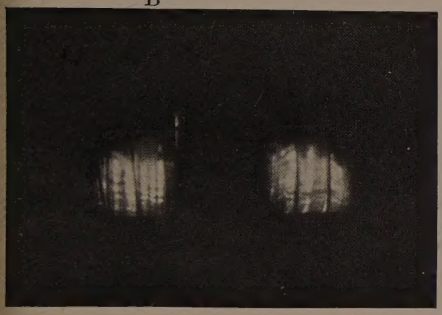

5. Deposit after $2\frac{1}{2}$ hours at 1063° K., heavy evaporation but no migration.

6. Deposit after 7 hours at 1063° K., evaporation still very heavy but no migration.

C

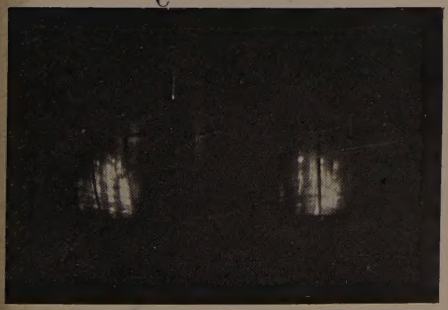

7. Deposit after 1 hour at 1133° K., extreme evaporation but no migration.

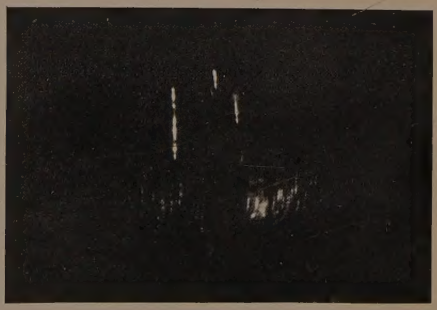

8. Spurious migration obtained by running filament at 1323° K. with H.T. on and quickly cooling filament to 1013° K.

Wool Rescael